PB-213 016

Wet Scrubber System Study

Vol. 1 scrubber handbook

A.P.T., Inc.

prepared for
Environmental Protection Agency

JULY 1972

Distributed By:

NTIS

National Technical Information Service
U. S. DEPARTMENT OF COMMERCE
5285 Port Royal Road, Springfield Va. 22151

WET SCRUBBER SYSTEM STUDY Volume 1

EPA-R2-72-118a
August 1972

PB 213 016

SCRUBBER HANDBOOK

Prepared For
ENVIRONMENTAL PROTECTION AGENCY
Control Systems Division

August, 1972

APT

Reproduced by
NATIONAL TECHNICAL
INFORMATION SERVICE
U S Department of Commerce
Springfield VA 22151

828

A.P.T., Inc. Box 71 Riverside, Ca. 92502

BIBLIOGRAPHIC DATA SHEET	1. Report No. EPA-R2-72-118a	2.	3. Recipient's Accession No. PB-213 016

4. Title and Subtitle Wet Scrubber System Study Volume I Scrubber Handbook	5. Report Date August 1972
	6.
7. Author(s) Seymour Calvert, Jhuda Goldshmid, David Leith, Dilip Mehta	8. Performing Organization Rept. No.
9. Performing Organization Name and Address A.P.T., Inc. (Ambient Purification Technology) P. O. Box 71 Riverside, California 92502	10. Project/Task/Work Unit No. 11. Contract/Grant No. CPA-70-95
12. Sponsoring Organization Name and Address ENVIRONMENTAL PROTECTION AGENCY Office of Air Programs Control Systems Division Research Triangle Park, North Carolina 27711	13. Type of Report & Period Covered 14.

15. Supplementary Notes

16. Abstracts

Previously scattered material is brought together and its applicability to scrubber technology is made clear. The various aspects of scrubber use and present engineering design methods are discussed based on a unifying concept. Actual experience on hundreds of scrubber installations is presented in a condensed form. Many related topics such as auxiliaries, materials of construction, physical and chemical data, cost estimation and optimization techniques, and the disposal of liquid and solid wastes are covered.

17. Key Words and Document Analysis. 17a. Descriptors

Air Pollution Control Equipment
Scrubbers
Manuals
Design Criteria
Expenses
Refuse Disposal
Water Pollution
Particles
Gases
Pressure

Temperature

17b. Identifiers/Open-Ended Terms

17c. COSATI Field/Group

18. Availability Statement Unlimited	19. Security Class (This Report) UNCLASSIFIED	21. No. of Pages 825
Ia	20. Security Class (This Page UNCLASSIFIED	22. Price 13.50

THIS FORM MAY BE REPRODUCED

WET SCRUBBER SYSTEM STUDY VOLUME I

SCRUBBER HANDBOOK

Seymour Calvert, Project Director
Jhuda Goldshmid
David Leith
Dilip Mehta

Prepared for

CONTROL SYSTEMS DIVISION
OFFICE OF AIR PROGRAMS - ENVIRONMENTAL PROTECTION AGENCY

CONTRACT NO. CPA-70-95

A.P.T., INC.
(Ambient Purification Technology)
P. O. Box 71, Riverside, California 92502

July, 1972

Ib

FORWARD

The Scrubber Handbook is Vol. I of a two-volume report submitted to the Office of Air Programs - Environmental Protection Agency as part of the Wet Scrubber System Study under Contract No. CPA-70-95. The second volume is entitled Final Report and Bibliography, and contains the final report, R & D recommendations and the bibliography. The two volumes are available from NTIS.

Mr. Dale Harmon of the Control System Division, Office of Air Programs, served as the contract project officer through most of the contract. He was later replaced by Dr. Leslie Sparks of the same division.

ABSTRACT

A Wet Scrubber System Study was undertaken to achieve the following objectives: (1) Evaluate current engineering technology, (2) Evaluate existing scrubber systems, (3) Investigate present usage problems, (4) Determine potential new applications, (5) Develop specific research recommendations. The products of this study are: (1) Scrubber Handbook, (2) Final Report, (3) Bibliography, (4) R & D Plan. The Scrubber Handbook brings together previously scattered material, and ~~makes~~ clear its applicability to scrubber technology. ~~It~~ discusses the various aspects of scrubber use and present engineering design methods based on a unifying concept. Actual experience on hundreds of scrubber installations is presented in a condensed form. Many related topics such as auxiliaries, materials of construction, physical and chemical data, cost estimation and optimization techniques, and the disposal of liquid and solid wastes are all covered thoroughly in the Scrubber Handbook.

The Final Report and Bibliography describes the approach and method used to achieve the objectives listed earlier. It presents two R & D plans; one at a $2 million five-year level and the second at a $7 million five-year level. The Bibliography contains about 1,700 references discussing various aspects of wet scrubbers.

IC

ENVIRONMENTAL PROTECTION AGENCY REVIEW NOTICE

This report has been reviewed by EPA and approved for publication. Approval does not signify that the contents necessarily reflect the views and policies of EPA, nor does the mention of trade names or commercial products constitute endorsement or recommendation for use.

Id

ℓ

TABLE OF CONTENTS

CHAPTER 1 INTRODUCTION 1-1
1.0 Introduction 1-2
1.1 Scope 1-3
1.2 Approach 1-4
1.3 Handbook Format 1-7
1.4 Acknowledgements 1-8
CHAPTER 2 GUIDE TO THE HANDBOOK 2-1
2.0 Introduction 2-3
2.1 Define the Problem 2-4
2.2 Explore Alternate Solutions 2-6
2.3 Decide How to Control the Problem 2-6
2.4 General Approach to Scrubbers 2-9
2.5 Detailed Considerations 2-11
2.6 Operate the System Properly 2-14
References 2-16
CHAPTER 3 SCRUBBERS AVAILABLE 3-1
3.1 Types of Scrubbers 3-2
3.2 Commercially Available Scrubbers 3-14
3.3 Scrubber Patents 3-20
CHAPTER 4 BASIC CONCEPTS 4-1
4.1 Introduction 4-4
4.2 General Concepts of Mass Transfer 4-8
Nomenclature 4-44
References 4-48
4.3 General Concepts of Particle Collection 4-50
Nomenclature 4-76

TABLE OF CONTENTS

References 4-79

4.4 Gas-Liquid Contacting 4-81

Nomenclature 4-91

References 4-93

4.5 Unit Mechanisms for Mass Transfer 4-95

Nomenclature 4-108

References 4-110

4.6 Unit Mechanisms for Particle Separation 4-112

Nomenclature 4-160

References 4-164

4.7 Effect of Pressure and Temperature on the Collection of Particles in Wet Scrubbers 4-167

Nomenclature 4-178

CHAPTER 5 DESIGN METHODS 5-1

5.1 Introduction 5-4

References 5-7

5.2 Mass Transfer 5-8

Nomenclature 5-70

References 5-75

5.3 Particle Separation 5-81

Nomenclature 5-198

References 5-203

5.4 Scrubbed Liquid Entrainment Separators 5-209

Nomenclature 5-214

References 5-216

CHAPTER 6 AUXILIARIES 6-1

6.1 Introduction 6-3

TABLE OF CONTENTS

6.2 Gas Moving 6-4

6.3 Liquid Moving 6-12

6.4 Entrainment Separation 6-16

6.5 Solvent Recycle 6-17

6.6 Sampling and Analysis 6-19

6.7 Controls 6-20

6.8 Health and Safety 6-22

References 6-25

CHAPTER 7 SCRUBBER PERFORMANCE ON INDUSTRIAL EMISSIONS 7-1

7.1 Introduction 7-2

7.2 Processes Utilizing Scrubbers 7-6

7.3 Generalizations Regarding Scrubber Use 7-123

CHAPTER 8 SYSTEM ANALYSIS, COSTS, AND OPTIMIZATION 8-1

8.1 Introduction 8-2

8.2 Design Analysis 8-3

8.3 Scrubber Cost Estimation Methods 8-15

8.4 Cost Analysis 8-32

8.5 Optimization 8-41

Nomenclature 8-49

References 8-51

CHAPTER 9 DESIGN EXAMPLES 9-1

9.1 Introduction 9-2

9.2 General Approach 9-2

9.3 Example Calculations 9-3

9-4 Trouble Shooting 9-50

References 9-61

Nomenclature 9-58

TABLE OF CONTENTS

CHAPTER 10 PHYSICAL AND CHEMICAL DATA 10-1
10.1 Introduction 10-2
10.2 Estimation Methods 10-3
10.3 Explanatory Notes 10-12
10.4 Physical and Chemical Data 10-15
Nomenclature 10-30
References 10-32
CHAPTER 11 MATERIALS DATA 11-1
11.1 Introduction 11-2
11.2 General Conditions 11-2
11.3 Plastics 11-3
11.4 Chemicals 11-4
11.5 Miscellaneous Solutions and Gases 11-8
References 11-10
CHAPTER 12 LIQUID AND SOLID WASTE DISPOSAL 12-1
12.1 Introduction 12-2
12.2 Industry Survey 12-3
12.3 Sedimentation 12.4
12.4 Coagulation and Flocculation 12-8
12.5 Filtration 12-10
12.6 Neutralization and Chemical Precipitation 12-13
12.7 Ion Exchange 12-15
12.8 Desalting 12-17
12.9 Disposal of Liquid 12-19
12.10 Disposal of Solids 12-21
12.11 Economics 12-22
References 12-26
Nomenclature 12-24
Appendix - Conversion Factors x-1

LIST OF FIGURES

FIGURE NO. Page No.

1.2-1 Schematic Diagram of Scrubber System 1-10

3.1-1 Sketches of Plates and Tower 3-4

3.1-2 Packed Tower and Packings. 3-5

3.1-3 Fiber Bed Scrubber 3-6

3.1-4 Spray Tower and Ejector. 3-7

3.1-5 Gas Atomized Spray (Venturi) Scrubber. 3-8

3.1-6 Two Kinds of Centrifugal Scrubbers 3-9

3.1-7 Zig-Zag Baffle Device. 3-10

3.1-8 Example of Impingement and Entrainment Scrubber. . . . 3-11

3.1-9 Mechanically Aided Scrubber. 3-12

3.1-10 Moving Bed Scrubber. 3-13

4.2.3-1 Typical Concentration Profiles for Gas-Liquid Mass Transfer 4-38

4.2.3-2 Typical Equilibrium Line, Showing Phase Compositions at Various Points. 4-38

4.2.3-3 Absorption from a Gas Bubble 4-38

4.2.4-1 Murphree Efficiency of Low Solubility Gases in a Plate Column Versus System Properties with Contact Factor As Parameter 4-39

4.2.6-1 Concentration Profiles for Instantaneous Reaction, Film Model 4-40

4.2.6-2 Concentration Profiles for a 2nd Order Irreversible Reaction 4-40

4.2.6-3 Enhancement Factors for Second-Order Reaction; for Quiescent Liquid or Agitated Liquid (Film or Higbie Models). 4-41

4.2.6-4 Two-Film Model: Concentration Profiles for Instantaneous Reaction with Varying Concentration of Reactant "B" 4-41

LIST OF FIGURES

4.2.7-1 Transfer Coefficient for Particle Falling in Water Vs. Particle Diameter, with Density Difference as Parameter 4-42

4.2.7-2 Resistances to Mass Transfer in a Slurry. 4-42

4.2.7-3 Transfer of Oxygen from Air Bubble to Bacterial Site. 4-42

4.2.7-4 Mass Transfer Coefficient Per Gram of Particles Falling in Water Vs. Particle Diameter, with Density Difference Parameter. 4-42

4.2.8-1 Enthalpy of Saturated Air Vs. Temperature 4-43

4.3.3-1 Cunningham Correction Factor for Particles in Air at Different Temperatures and Pressures. 4-74

4.3.3-2 Experimental Rate of Settling of Spheres and Drops in Air at 20°C and 760 mm 4-74

4.3.3-3 Calculated Diffusivity of Aerosol Particles at Different Operating Conditions. 4-74

4.3.3-4 Comparison Between Brownian Displacement and Settling Distance of Spherical Particles of Unit Density in Air, in One Second. 4-74

4.3.4-1 Change of Stearic Acid Particle Concentration with Time for Various Initial Concentrations 4-75

4.3.4-2 Coagulation Half Life Versus Initial Particle Concentration for Stearic Acid. 4-75

4.3.4-3 Saturation Ratio for Condensation on Spherical Particles at 0°C as a Function of Radius, With Surface Properties as the Parameter 4-75

4.3.4-4 Equilibrium Supersaturation as a Function of Droplet Radius for Water Droplets, each Containing Mass "m" of Solute of Molecular Weight "M" and Van't Hoff Factor "i". 4-75

4.4.1-1 Bubble Shapes in Distilled Water and Aqueous Glycerol Solutions. 4-89

4.4.1-2 Air Bubble Rise Velocity in Water Vs. Bubble Diameter, Predicted and Experimental Values. 4-89

LIST OF FIGURES

4.4.1-3 Gas Hold-up in Various Sieve-Plate Columns as a Function of F-Factor, with Water Rate As Parameter. 4-90

4.4.2-1 Drag Coefficient of a Sphere. 4-90

4.4.3-1 Plot of Phase Compositions Showing Operating and Equilibrium Lines. 4-90

4.5.1-1 Gas-Film Mass Transfer to Falling Water Drops in Air Vs. Drop Diameter 4-105

4.5.1-2 Gas-Film Mass Transfer Rate Per Gram of Falling Water Drops in Air Versus Drop Diameter. 4-105

4.5.1-3 Spray Surface Area per Unit Volume of Scrubber Vs. Air Velocity, for Counter-Current Air and Water with Drop Radius as Parameter and $Q_W/Q_A=1$. 4-105

4.5.1-4 Exposure Time for Water Drops Falling in Air 4-105

4.5.1-5 Liquid-Film Mass Transfer to Falling Water Drops in Air Versus Drop diameter with Falling Distance as Parameter. 4-106

4.5.1-6 Liquid-Film Mass Transfer per Gram of Falling Water Drops (in Air) Vs. Drop Diameter with Falling Distance as Parameter 4-106

4.5.1-7 Fractional Saturation of Sphere Vs. Dimensionless Diffusion Time 4-106

4.5.1-8 Fractional Saturation of a Sphere Vs. Dimensionless Time with "T" Parameter 4-106

4.5.2-1 Gas-Film Mass Transfer From Air Bubbles Rising in Water 4-107

4.5.2-2 Gas-Film Mass Transfer per Cubic Meter of Rising Air Bubbles 4-107

4.5.2-3 Liquid-Film Mass Transfer Coefficient From Air Bubbles Rising in Water 4-107

4.5.2-4 Liquid-Film Mass Transfer Per Cubic Centimeter of Rising Air Bubbles in Water. 4-107

4.6.2-1 Air Streamlines and Particle Trajectories around Sphere 4-113

4.6.2-2 Experimental and Calculated Collection Efficiencies for Sphere and Cylinder 4-152

LIST OF FIGURES

4.6.2-3 Theoretical Impaction Efficiency as a Function of Inertial Parameter for Different Targets. . . 4-152

4.6.2-4 Terminal Settling Velocity and Reynolds Number for Water Drops in Air at 20°C and 760 mmHg. . . 4-153

4.6.2-5 Collection of Particles by Free Falling Water Drops 4-153

4.6.2-6 Effective Capture Cross-Section Vs. Water Drop Diameter with Particle Radius as Parameter . . . 4-153

4.6.2-7 Collection Efficiency for a Unipolar Charged Aerosol on a Spherical Collector with the Opposite Charge. 4-153

4.6.2-8 Collection Efficiency of an Uncharged Aerosol on a Charged Spherical Collector 4-154

4.6.2-9 Collection Efficiency of a Charged Aerosol on an Uncharged Spherical Collector 4-154

4.6.2-10 Collection of Charged Dioctylphthalate Mist on Sphere, Theory and Experiment. 4-154

4.6.2-11 Effect of Diffusiophoresis on Collection by a Single Drop. 4-154

4.6.3-1 Single Fiber Impaction Efficiency as Function of Impaction Parameter and Reynolds Number . . . 4-155

4.6.4-1 Effect of Foam Height in a Sieve Plate Column on Maximum Penetration Diameter. 4-155

4.6.4-2 Effect of Perforation Diameter in a Sieve Plate Column on Maximum Penetration Diameter . . 4-155

4.6.4-3 Collection Efficiency in a Sieve Plate Vs. Particle Radius with Foam Height as Parameter. . 4-155

4.6.4-4 Collection of 0.4 μm Diameter Particles by Bubbles as a Function of Aerosol Inlet Concentration and Charging Field Strength. 4-155

4.6.4-5 Collection of 1 μm Diameter Particles by Bubbles as a Function of Aerosol Inlet Concentration and Charging Field Strength. 4-156

4.6.4-6 Penetration of 4 μm Diameter Particles by Bubbles as a Function of Inlet Concentration and Charging Field Strength 4-156

LIST OF FIGURES

4.6.4-7 Effect of Heat and Mass Transfer on Collection Efficiency in a Sieve Plate. 4-156

4.6.5-1 Particle Penetration Vs. Diffusion Parameter for Viscous Flow in Long Tube. 4-156

4.6.7-1 Theoretical and Experimental Collection Efficiencies of Rectangular Aerosol Jets 4-157

4.6.7-2 Two-Dimensional Representation of Impaction Stage. 4-158

4.6.7-3 Curves of $\sqrt{K}$ at an Efficiency of 0.5 as a Function of β.

4.6.7-4 Experimental Efficiency Curves for Various Values of ℓ/b for Round Jets 4-158

4.6.7-5 Experimental Curve of Variation of K_{50} with β . . 4-158

4.6.7-6 Aerodynamic Diameter Vs. Particle Diameter with Particle Density as Parameter. 4-159

4.7-1 Rate of Collection of Aerosol Particles by Diffusion at Different Operating Conditions. . . . 4-174

4.7-2 Thermophoretic Velocity as a Fraction of Temperature Gradient for Different Operating Conditions 4-174

4.7-3 Collection Efficiency of Aerosol Particles by Spheres Due to Thermophoresis at Different A/Q_G Ratios 4-175

4.7-4 Collection Efficiency of Aerosol Particles by Spheres Due to Thermophoresis at Different A/Q_G Ratios 4-175

4.7-5 Electrostatic Velocity at Different Electric Strengths and Different Operating Conditions . . . 4-175

4.7-6 Radial Velocity in a Centrifugal Collector of Diameter "D" at Different Tangential Velocities and Operating Conditions 4-175

4.7-7 Diffusiophoretic Velocity of Aerosol Particles in Air Saturated with Water Vapors at Different Operating Conditions 4-176

LIST OF FIGURES

4.7-8 Diffusiophoretic Velocity of Aerosol Particles in Air Saturated with Water Vapors at Different Operating Conditions 4-176

4.7-9 Collection Efficiency of Aerosol Particles by Liquid Drops Due to Diffusiophoresis at Different A/Q_G Ratios. 4-177

4.7-10 Collection Efficiency of Aerosol Particles by Liquid Drops Due to Diffusiophoresis at Different A/Q_G Ratios. 4-177

4.7-11 Collection Efficiency of Aerosol Particles by Liquid Drops Due to Diffusiophoresis at Different A/Q_G Ratios. 4-177

4.7-12 Collection Efficiency of Aerosol Particles by Liquid Drops Due to Diffusiophoresis at Different A/Q_G Ratios 4-177

5.2.1-1 Plate Column Material Balance. 5-57

5.2.1-2 Graphical Determination of Theoretical Plates. . . . 5-57

5.2.1-3 Schematic Diagram of Packed Column 5-57

5.2.2-1 Bubble-Cap Column Diameter 5-58

5.2.2-2 Tray Spacking Correction 5-58

5.2.2-3 Range of Liquid Rates for Trays. 5-58

5.2.2-4 Bubble-Cap Pressure Drops. 5-59

5.2.2-5 Sieve Tray Pressure Drops. 5-59

5.2.2-6 Sieve Plate Orifice Coefficient, C 5-59

5.2.2-7 Valve Tray Liquid Head 5-60

5.2.2-8 Valve Tray Dry Plate Head Loss 5-60

5.2.2-9 Number of Theoretical Plates Required for NH_3 Absorption Example 5-61

5.2.2-10 Overall Plate Efficiency. 5-61

5.3.2-1 Schematic of a Typical Packed Column 5-62

5.3.2-2 Typical Pressure Drop Vs. Velocity Plot Showing Loading and Flooding Points. 5-62

LIST OF FIGURES

5.2.3.3 Generalized Flooding and Pressure Drop Correlation 5-63

5.2.3-4 Effect of Liquid Rate on Wetted Surface 5-62

5.2.4-1 Pressure Drop Through Fibrous Packings. 5-64

5.2.4-2 Height of Transfer Unit for Typical Fibrous Packings. 5-64

5.2.5-1 Number of Transfer Units for Two Spray Devices. . 5-65

5.2.6-1 Equilibrium (Minimum)Penetration for Physical Absorption in a Cocurrent Gas-Liquid Flow 5-65

5.2.6-2 Gas and Liquid Phase Absorption Coefficient with Distance From the Point of Atomization. 5-66

5.2.6-3 CO_2 Desorption with Respect to Length of Venturi From the Point of Liquid Atomization 5-66

5.2.6-4 Penetration of a Soluble Gas Vs. "f" in a Venturi With Gas Phase Resistance Controlling and Zero Back Pressure in the Fluid 5-67

5.2.6-5 Number of Overall Transfer Units Vs. $(\hat{L}/\hat{G})$ Experimental Data of Johnstone Et Al. (1959) and Prediction by Equation 5.2.6-18 with u_G=200 ft/sec. 5-67

5.2.6-6 Values of "f" Vs. (L_M/G_M) For SO_2 Absorption by Sodium Hydroxide Solution. 5-67

5.2.8-1 Height of Transfer Unit Vs. Liquid Velocity . . . 5-68

5.2.8-2 Height of Transfer Unit Vs. Gas Velocity. 5-68

5.2.8-3 Height of Transfer Unit Vs. Static Bed Height . . 5-68

5.2.8-4 Maximum (limiting) Fraction of SO_2 Removal in Hydro-Filter. 5-69

5.2.8-5 Turbulent Contact Absorber-SO_2 Absorption Efficiencies. 5-69

5.3.1-1 Illustrative Particle Size Distribution 5-158

5.3.1-2 Illustrative Penetration-Diameter Relationship. . 5-158

5.3.1-3 Graphical Integration for Overall Penetration . . 5-158

LIST OF FIGURES

5.3.1-4 Overall Penetration Versus Cut to Mean Particle Diameter Ratio, for Log Normal Dusts, with Dust Standard Deviation as Parameter. 5-159

5.3.2-1 Impingement Baffle Wet Collector 5-160

5.3.2-2 Impingement Gas Scrubber 5-160

5.3.2-3 Grade-Efficiency Curve for Wet-Impingement Scrubber 5-160

5.3.2-4 Standard Impinjet Efficiency @ Pressure Drop of 4 mbar Per Stage 5-160

5.3.2-5 High Pressure Drop Efficiency. 5-160

5.3.2-6 Pressure Drop in a Wet Impingement Scrubber Vs. Particle Cut Diameter with Perforation Diameter as a Parameter. 5-161

5.3.2-7 Predicted Impingement Plate Performance, d_{pa50} Vs. u_o With d_h as Parameter. 5-162

5.3.2-8 Collection Efficiency Vs. Generalized Parameter in a Sieve Plate Column. 5-163

5.3.2-9 Predicted Sieve Plate Performance, d_{pa50} Vs. u_o with F and d_h as parameters, For Impaction Only. . 5-164

5.3.2-10 Comparison of Efficiency for Oil Mist in Sieve Plate Column with and Without Diffusion and Thermophoresis. 5-165

5.3.3-1 Penetration Vs. Aerodynamic Particle Diameter with Bed Height as Parameter for Packed Bed . . . 5-166

5.3.3-2 Predicted Packed Bed Performance Cut Diameter as a Function of Gas Velocity, Packing Size, Porosity, and Depth. 5-167

5.3.4-1 G(M) Versus "M" For Torgeson Theory. 5-168

5.3.4-2 Single Fiber Efficiency Due to Inertia, Interception and Diffusion, According to Torgeson . . 5-168

5.3.4-3 Single Fiber Efficiency Due to Inertia, Interception and Diffusion, According to Torgeson . . 5-168

5.3.4-4 Single Fiber Efficiency Due to Inertia Interception and Diffusion, According to Torgeson . . 5-168

LIST OF FIGURES

5.3.4-5 Single Fiber Efficiency Due to Inertia Interception and Diffusion, According to Torgeson . . . 5-168

5.3.4-6 Pressure Drop Per Unit Thickness, for Fiber Filter as Function of Gas Velocity, Fiber Diameter and Bed Porosity, According to Chen. 5-168

5.3.5-1 Predicted Counter Flow-Spray Chamber Performance Cut Diameter for Air and Water for Several Cases Impaction Only 5-169

5.3.5-2 Predicted Cross-Flow Spray Chamber Performance Cut Diameter for Air and Water for Several Cases, Impaction Only 5-170

5.3.5-3 Drop Size Distribution Curve for 12 Inch Ejector Venturi Scrubber 5-171

5.3.5-4 Drop Size Distribution Curve for Four Inch Ejector Venturi Scrubber 5-171

5.3.5-5 Observed Energy and Weight Collection Efficiency Characteristics for 12" Ejector Venturi Scrubber With Varying Inlet Fume Loading. 5-171

5.3.5-6 Observed Energy and Weight Collection Efficiency Characteristics for Ejector Venturi Scrubbers. . . 5-171

5.3.5-7 Scrubbing Performance for 12 in. Ejector Venturi Scrubber 5-171

5.3.5-8 Scrubbing Performance of Three Inch Ejector Venturi 5-172

5.3.5-9 Observed Energy Requirement for Ejector Venturi Scrubber System. 5-172

5.3.5-10 Schutte and Koerting Company Sub-Micron Scrubber System 5-172

5.3.5-11 Family of Theoretical Collection Efficiency Curves at Constant L/G and Various Motive Pressures. 5-172

5.3.5-12 Family of Theoretical Collection Efficiency Curves at Constant Motive Pressure and Various Q_L/Q_G Rates. 5-172

5.3.5-13 Carry-Over From a 4" Ejector Venturi 5-172

LIST OF FIGURES

5.3.6-1 Venturi Scrubber with Centrifugal Entrainment Separator 5-173

5.3.6-2 Optimum and Actual Drop Diameter Vs. Gas Velocity 5-173

5.3.6-3 $F(K_{Pt},f)$ Versus K_{Pt} for $f = 0.25$ 5-174

5.3.6-4 Values of "f" Versus Liquid to Gas Ratio for Dioctyl Phthalate Particles. 5-175

5.3.6-5 Values of "f" Versus Liquid to Gas Ratio for Methylene Blue Particles 5-175

5.3.6-6 Values of "f" Versus Liquid to Gas Ratio for Fly Ash. 5-176

5.3.6-7 Venturi Scrubber Penetration Vs. Aerodynamic Diameter with Gas Velocity as Parameter. 5-176

5.3.6-8 Venturi Scrubber Penetration Vs. Aerodynamic Particle Diameter with Gas Velocity as Parameter 5-177

5.3.6-9 Venturi Scrubber Penetration Vs. Aerodynamic Particle Diameter with Gas Velocity as Parameter 5-177

5.3.6-10 Venturi Scrubber Penetration Vs. Gas Throat Velocity with Liquid to Gas Ratio and Pressure Drop as Parameters 5-178

5.3.6-11 Venturi Scrubber Penetration Vs. Gas Throat Velocity with Liquid to Gas Ratio and Pressure Drop as Parameters 5-178

5.3.6-12 Venturi Scrubber Penetration Vs. Gas Throat Velocity with Liquid to Gas Ratio and Pressure Drop as Parameters 5-179

5.3.6-13 Predicted Venturi Performance, $d_{pa_{50}}$, Vs. Q_L/Q_G with "u_G" Parameter and ΔP Parameter 5-179

5.3.6-14 Predicted Pressure Drop for Venturi With Standard Air and Water 5-180

5.3.6-15 Penetration Vs. Pressure Drop with Aerodynamic Particle Diameter as Parameter, for Venturi Scrubber 5-181

5.3.7-1 Typical Cyclone Collector. 5-182

5.3.7-2 Typical Cylindrical Centrifugal Scrubber 5-182

LIST OF FIGURES

5.3.7-3 Converted Cyclone . . . 5-182
5.3.7-4 Centrifugal Spray Scrubber . . . 5-182
5.3.7-5 Generalized Cyclone Efficiency Curve . . . 5-183
5.3.7-6 Differential Volume of a Spray Centrifugal . . . 5-183
5.3.7-7 (a&b) Predicted Cyclone Performance, $d_{pa_{50}}$ Vs. "C", With Inlet Velocity as Parameter, For Several Cyclone Diameters . . . 5-184
5.3.7-7 (c&d) Predicted Cyclone Performance, $d_{pa_{50}}$ Vs. "C", With Inlet Velocity as Parameter, For Several Cyclone Diameters . . . 5-185
5.3.8-1 Shutter-Type Collector . . . 5-186
5.3.8-2 Baffle Type Separator . . . 5-186
5.3.8-3 Crescent Shape Baffle Collector . . . 5-186
5.3.8-4 Flat Louver Impingement Separator . . . 5-187
5.3.8-5 Conical Louver Impingement Separator . . . 5-187
5.3.8-6 Efficiency of Louvered Cone Collector . . . 5-187
5.3.8-7 Collector With One Baffled Wall . . . 5-188
5.3.8-8 Baffled Conduit . . . 5-188
5.3.8-9 Predicted Secondary Flow Baffles Device Performance, $d_{pa_{50}}$ Vs. "n" with "u" as Parameter at Various "α" and "h" . . . 5-189
5.3.8-10 Pressure Drop Vs. Gas Flow Rate in a Single and Double Fin Rectangular Conduit . . . 5-190
5.3.8-11 Effect of Liquid Rate on Pressure Drop in a Fin Column . . . 5-190
5.3.8-12 Friction Factor Versus Reynolds Number for Various Geometries . . . 5-190
5.3.9-1 Self-Induced Spray Wet Collector . . . 5-191
5.3.9-2 'Rotoclone' Type N Precipitator . . . 5-191

LIST OF FIGURES

5.3.9-3 Self-Induced Spray Type Scrubber. 5-191

5.3.9-4 Self-Induced Spray Wet Collector. 5-192

5.3.9-5 Self-Induced Spray Wet Collector. 5-192

5.3.9-6 Self-Induced Spray Collector Efficiency at 5 Microns-93% 5-192

5.3.10-1 Mechanically Aided Dust Precipitator. 5-193

5.3.10-2 Efficiencies of Mechanically Aided Collectors . . . 5-193

5.3.10-3 Mechanically Aided Scrubber 5-193

5.3.10-4 Mechanically Aided Collector. 5-194

5.3.10-5 Schematic Representation of the Rotating Centrifugal Operator with Continuous Dust Removal 5-194

5.3.10-6 Theoretical Curve of the Fractional Separation Efficiency of the Centrifugal Separator 5-194

5.3.10-7 Diagram of Disentegrator Gas Washer 5-194

5.3.10-8 Disintegrator Gas Washer. 5-194

5.3.10-9 Diagram of Centrifugal Collector with Centrifugal Force Acting Perpendicular to Axis. 5-195

5.3.10-10 Diagram of Centrifugal Collector with Centrifugal Force Acting Parallel to Axis 5-195

5.3.10-11 Graphical Integration of the Integral Part in Equation 5.3.10-36. 5-195

5.3.10-12 Graphical Integration of Equation 5.3.10-40. . . . 5-195

5.3.11-1 Mobile Bed Type Scrubber Hydro-Filter. 5-196

5.3.11-2 Fluidized Bed Scrubber 5-196

5.3.11-3 Collection Efficiency of Mobile Bed Scrubber . . . 5-196

5.3.11-4 Collection Efficiency in a Fluidized Bed Scrubber. 5-197

5.3.11-5 Pressure Drop in a Fluidized Bed Scrubber. 5-197

5.4.4-1 Separation Efficiency Water Droplets in Air 48 Layers .01" Dia. Wire, Droplet Sizes 1 to 20 Microns 5-213

LIST OF FIGURES

6.2-1 Typical Characteristic Curve of Fans 6-24

8.2-1 Relationship Between the Penetration Based on Mean Particle Size and the Integrated Penetration. 8-11

8.2-2 Relationship Between the Penetration Based on Mean Particle Size and the Integrated Penetration. 8-11

8.2-3 Relationship Between Average Particle Size Entering and Leaving A Collection Device 8-11

8.2-4 Integrated Penetration, Pt, Vs. d_{p50}/d_{pg}, With $B(\ln \sigma_g)$ as Parameter 8-12

8.2-5 Venturi Scrubber Integrated Penetration. 8-13

8.2-6 Venturi Scrubber Integrated Penetration 8-13

8.2-7 Venturi Scrubber Integrated Penetration 8-13

8.2-8 Predicted Integrated Penetration Vs. (d_{p50}/d_{pg}) With "σ_g" as Parameter for Secondary Flow Baffles . . . 8-14

8.3-1 Space Requirement of Dust Separators 8-19

8.3-2 Shell Thickness of Vessels Under External Pressure 8-29

8.3-3 Shell and Flat Head Weight Versus Diameter 8-29

8.3-4 Weight of Shell Including Flat Heads Versus Shell Height With Diameter as Parameter. 8-29

8.3-5 Fabrication Cost of Towers and Tanks Per "kg" Versus the Total Weight "kg" 8-29

8.3-6 Fabrication Cost of Shell Vs. Height with Diameter as Parameter, for Carbon Steel Tanks 8-30

8.3-7 Approximate Installed Cost of Steel Tower Connections 8-30

8.3-8 Tray Cost Versus Tower Height. 8-31

8.3-9 Detailed Fabrication by Method II. 8-24

8.3-10 Purchased Cost of Storage Tank (Carbon Steel) Versus Tank Volume 8-31

8.3-11 Purchase Cost per Plate or per Foot (30 cm) Height Versus Columns Diameter for Bubble Cap and Packed Tower 8-31

LIST OF FIGURES

8.4-1 Total Cost of Various Air Pollution Control Devices Vs. Efficiency on Standard Dust 8-37

8.4-2 Manufacturer's Price Vs. Gas Flow for Scrubbers 8-38

8.4-3 Manufacturer's Price Vs. Gas Flow for Scrubbers 8-38

8.4-4 Manufacturer's Price Vs. Gas Flow for Scrubbers 8-38

8.4-5 Manufacturer's Price Vs. Gas Flow for Scrubbers 8-38

8.4-6 Manufacturer's Price Vs. Gas Flow for Scrubbers 8-38

8.4-7 Survey Results Installed Cost of Packed Bed Scrubbers 8-39

8.4-8 Survey Results Installed Cost of Spray Scrubber 8-39

8.4-9 Survey Results Installed Cost of Venturi Vs. Gas Flow 8-39

8.4-10 Survey Results Installed Cost of Centrifugal Scrubber 8-40

8.4-11 Survey Results Installed Cost of Impingement and Entrainment Scrubber Vs. Gas Flow 8-40

8.4-12 Survey Results Installed Cost of Mobile Bed Scrubbers Vs. Gas Flow 8-40

8.5-1 Cyclone Geometry Nomenclature

8.5-2 Cyclone Diameter Versus CP With Inlet Velocity and Throughput as Parameters, Pressure Drop Is (3") W.C. 7.5 cm. 8-47

8.5-3 Cyclone Diameter Vs. CP With Inlet Velocity and Throughput as Parameters. Pressure Drop is 12.5 cm (5") W.C.. 8-47

8.5-4 Cyclone Diameter Vs. CP With Inlet Velocity and Throughput as Parameters. Pressure Drop: 17.5 cm (7") W.C.. .8-47

8.5-5 "C" Versus Inlet Gas Velocity With Pressure Drop as Parameter for Cyclones 8-48

8.5-6 Optimum Dimension Ratios Versus Cyclone Geometry Coefficient, "C". 8-48

LIST OF FIGURES

9.3-1 Particle Diameter Vs. Weight Percent Undersize for Asphalt Plant Dryer Dust 9-56

9.3-2 Inertial Impaction Parameter Vs. Particle Aerodynamic Diameter with Velocity/Collector Radius as Parameter. 9-56

9.3-3 Schematic Description of the Cupola Air Pollution Control System 9-57

9.3-4 Size Distributions into and From Rock Wool Cupola Scrubber. 9-57

10.2-1 Viscosity of Dry Air. 10-27

10.2-2 Reduced Viscosity of Nonpolar Gases 10-27

10.3-1 Apparent Saturation Henry's Law Constants for Gases in Distilled Water. 10-28

10.3-2 Chemical Species at Equilibrium in Aqueous H_2S Solution at 25°C. 10-29

10.4-1 Partial Pressure of HCl Over Aqueous HCl Solutions. 10-29

12-1 Cost Vs. Volume of Aerated Lagoons and Equalization Basins 12-23

12-2 Capital-Cost Relationship, Neutralization Facilities. 12-23

12-3 Capital-Cost Relationship, Oil Separators 12-23

12-4 Cost Vs. Surface Area, Primary Clarifier. 12-23

12-5 Capital-Cost Relationship for Lagoons 12-23

12-6 Capital-Cost Relationship, Vacuum Filters 12-23

LIST OF TABLES

TABLE NO. PAGE NO.

2.0-1 Steps to Follow - Solving a Pollution Problem. . . 2-4

2.4-1 Steps in Solving an Air Pollution Problem. 2-15

3.2-1 Plate Type (Category 1). 3-15

3.2-2 Massive Packings (Category 2). 3-15

3.2-3 Fibrous Packing (Category 3) 3-16

3.2-4 Preformed Sprays (Category 4). 3-16

3.2-5 Gas Atomized Spray (Category 5). 3-17

3.2-6 Centrifugals (Category 6). 3-18

3.2-7 Baffles (Category 7) 3-18

3.2-8 Impingement & Entrainment (Category 8) 3-18

3.2-9 Mechanically Aided Scrubbers (Category 9). 3-19

3.2-10 Moving Bed (Category 10) 3-19

3.2-11 Combination Scrubbers (Mixed Categories) 3-19

3.3-1 Plate Type 3-21

3.3-2 Massive Packing. 3-22

3.3-3 Fibrous Packing. 3-23

3.3-4 Preformed Sprays 3-23

3.3-5 Gas Atomized Spray 3-25

3.3-6 Centrifugal. 3-26

3.3-7 Baffle 3-26

3.3-8 Impingement & Entrainment. 3-27

3.3-9 Mechanically Aided 3-27

3.3-10 Moving Bed Scrubbers 3-27

3.3-11 Combination. 3-27

LIST OF TABLES

4.2.6-1 Rate of Absorption for Instantaneous Reversible Reactions 4-23

4.3.4.1 Experimental Coagulation Constants of Various Aerosols(Air at Ambient Conditions-760 mm Hg, 25°C) 4-63

4.3.4-2 Effect of Electrical Field on the Rate of Coagulation of Mists. 4-67

4.3.4-3 Optimum Conditioning Results for Sodium Chloride Test Suspensions. 4-73

4.6.5-1 Diffusion Through Turbulent Boundary Layer. . . . 4-137

4.6.5-2 Values of the Davies Integral $N_{Reg}=10^4$. 4-140

4.6.5-3 Values of the Davies Integral $N_{Reg}=10^5$. 4-141

4.6.5-4 Values of the Davies Integral $N_{Reg}=10^6$. 4-142

4.7-1 Effect of Increase in Temperature from 0°C to 100°C and Pressure from 1 to 10 atm on Collection Efficiency 4-173

5.1.2-1 General Origins of Design Methods in Chapter 5. . 5-4

5.2.1-1 Equations Determining Height of a Packed Column, NTUs and HTUs 5-12

5.2.2-1 Empirical Constants for Equation 5.2.2-3. 5-18

5.2.2-2 Pressure Drop Components for Plate Column Scrubbers 5-25

5.2.3-1 Packing Factors for Dumped Pieces 5-30

5.2.3-2 Packing Factors for Grids and Stacked Pieces. . . 5-31

5.2.3-3 Sources of Mass Transfer Data 5-35

5.2.3-4 Major Resistance to Mass Transfer 5-36

5.2.3-5 Liquid Distribution Points. 5-37

5.2.3-6 Sizing for Good Distribution in Packing 5-38

5.2.4-1 Values of "ψ" for Wire Mesh Mist Eliminators. . . 5-39

5.2.4-2 Constants for Equation 5.2.4-2. 5-40

5.2.4-3 Physical Characteristics of Gas Absorption Packings. 5-41

5.2.4-4 Mass Transfer Data for Spray Devices. 5-47

5.2.6-1 Equations for Mass Transfer in a Venturi. 5-53

5.3.3-1 Bed Porosity, ϵ, for Various Packing Materials. . 5-91

5.3.3-2 Experimental Values of j, Channel Width as Fraction of Packing Diameter. 5-91

LIST OF TABLES

5.3.5-1 Nozzle Pressures and Disk Speeds Resulting in the Same Liquid Discharge Velocity. 5-103

5.3.7-1 Equations for Predicting the Critical (100%) Particle Size of a Cyclone 5-125

5.3.7-2 Equations for Predicting Cyclone Pressure Drop 5-129

5.3.8-1 Performance Parameter for Baffles. 5-135

6.2-1 Operating Ranges of Fans 6-7

6.2-2 Electric Motors Prices (1970) from Godrey (1970) 6-11

7.1-1 Processes to Which Scrubbers are Frequently Applied. 7-3

7.1-2 Data Presentation Format - Explanation 7-4

7.1-3 Conversion Factors - Metric and English Units. 7-5

7.2-1 Scrubber Performance Data - Coal Drying. . . . 7-7

7.2-2 Typical Coal Dust Emissions From Thermal Coal Driers 7-9

7.2-3 Scrubber Performance Data - Stone Crushing . . 7-12

7.2-4 Characteristics of Emissions From Stone Crushing Operations. 7-13

7.2-5 Scrubber Performance Data - Clay Products. . . 7-15

7.2-6 Emissions From Clay Processing Plants. 7-16

7.2-7 Scrubber Performance Data - Lime Preparation . 7-18

7.2-8 Characteristics of Emissions from Lime Processing Industry 7-19

7.2-9 Data on Miscellaneous Mineral Processes. . . . 7-20

7.2-10 Scrubber Performance Data - Miscellaneous Mineral Processes. 7-21

7.2-11 Wet Scrubbing Processes for Removing SO_2 From Flue Gas 7-27

7.2-12 Scrubber Performance Data - Fuel Combustion. . 7-29

7.2-13 Emissions From Stationary Sources Burning Coal 7-30

LIST OF TABLES

7.2-13a Flue Gas and Particle Properties. 7-30

7.2-13b Particle Emission Factors 7-30

7.2 13c Pollutant Gas Emission Factors. 7-30

7.2-14a Stationary Sources Burning Fuel Oil 7-31

7.2-14b Stationary Sources Burning Fuel Oil 7-31

7.2-15 Stationary Sources Burning Natural Gas Emission Characteristics and Quantities 7-32

7.2-16 Scrubber Performance Data - Blast Furnaces. . . 7-37

7.2-17 Characteristics of Emissions From Blast Furnaces. 7-38

7.2-18 Scrubber Performance Data - Steel Manufacture . 7-41

7.2-19 Characteristics of Emissions From Steel Making Operations. 7-42

7.2-20 Scrubber Performance Data - Iron Foundries. . . 7-45

7.2-21 Typical Emissions From Iron Foundries 7-47

7.2-22 Scrubber Performance Data - Ferroalloys 7-50

7.2-23 Characteristics of Emissions From Ferroalloy Furnaces 7-51

7.2-24 Scrubber Performance Data - Copper Smelting and Refining. 7-53

7.2-25 Characteristic Emissions From Copper Smelting and Refining. 7-54

7.2-26 Scrubber Performance Data - Aluminum Processing. 7-58

7.2-27 Characteristic Emissions from Aluminum Processing. 7-59

7.2-28 Scrubber Performance Data - Electroplating. . . 7-62

7.2-29 Scrubber Performance Data - Nonferrous Salvage Operations. 7-65

7.2-30 Characteristic Emissions From Nonferrous Smelting. 7-66

7.2-31 Scrubber Performance Data - Chemical Cleaning Etching and Milling of Metals 7-69

LIST OF TABLES

7.2-32 Data on Miscellaneous Metallurgical Processes. 7-70

7.2-33 Scrubber Performance Data - Miscellaneous Metallurgical Industries 7-71

7.2-34 Typical Emissions From Petroleum Refineries. . 7-75

7.2-35 Scrubber Performance Data - Pulp Manufacture . 7-79

7.2-36 Particulate Emissions From Kraft Pulp Manufacturing Process. 7-80

7.2-37 Gaseous Emissions From Kraft Pulp Manufacturing Process. 7-80

7.2-38 Scrubber Performance Data - Sulfuric Acid Manufacturing. 7-84

7.2-39 Scrubber Performance Data - Hydrochloric Acid Manufacturing 7-85

7.2-40 Scrubber Performance Data - Phosphoric Acid Manufacturing. 7-88

7.2-41 Emissions from Acid Manufacturing Processes. . 7-89

7.2-42 Scrubber Performance Data - Fertilizer Manufacturing. 7-93

7.2-43 Emissions From Phosphate Fertilizer Manufacturing Processes 7-95

7.2-44 Scrubber Performance Data - Asphaltic Pavement Manufacture 7-98

7.2-45 Characteristic Emissions from Asphaltic Pavement Manufacture 7-100

7.2-46 Costs Incurred in Scrubbing Asphalt Plant Rotary Drier Effluent. 7-101

7.2-47 Scrubber Performance Data - Chlorine Gas Manufacturing. 7-104

7.2-48 Characteristic Emissions From Chlorine Gas Manufacturing. 7-105

7.2-49 Data on Miscellaneous Chemical Processes . . . 7-106

7.2-50 Scrubber Performance Data - Miscellaneous Chemical Industries. 7-108

7.2-51 Scrubber Performance Data - Food and Feed Industry 7-113

7.2-52 Particulate Emissions from Incinerators. . . . 7-117

7.2-53 Gaseous Emissions from Incineration. 7-118

7.2-54 Scrubber Performance Data - Waste Disposal Processes. 7-119

7.2-55 Data on Miscellaneous Processes. 7-121

7.2-56 Scrubber Performance Data - Miscellaneous Processes. 7-122

7.3-1 Scrubbers Used to Control Calcining Processes. 7-124

7.3-2 Scrubbers Used to Control Combustion Processes. 7-125

7.3-3 Scrubbers Used to Control Crushers and Mills . 7-127

7.3-4 Scrubbers Used to Control Driers 7-128

7.3-5 Scrubbers Used to Control Gases. 7-130

7.3-6 Scrubbers Used to Control Liquid Mists 7-131

7.3-7 Scrubbers Used to Control Smelting Operations. 7-132

7.3-8 Processes to Which Each Type of Scrubber is Applied 7-134

7.3-9 Industrial Gas Cleaning Equipment-Manufacturer's Shipments by Industry, 1967 . . 7-136

8.2-1 Particle Size Distributions. 8-6

8.3-1 Initial Cost Factors 8-15

8.3-2 Installation Cost Expressed as a Percentage of Purchase Cost 8-16

8.3-3 Expected Ranges for Installation Costs in Industrial Applications. 8-17

8.3-4 Annual Cost Factors. 8-16

8.3-5 Operating and Maintenance Cost Factors 8-18

8.3-6 Tank Fabrication Cost - Method I 8-25

8.3-7 Cost Comparison 8-25

8.3-8 Packed Columns. 8-27

LIST OF TABLES

8.3-9 Tray Towers. 8-28

8.3-10 Summary of Packed Column and Tray Tower Costs. 8-26

8.4-1 Over-All Cost of Gas Cleaning. 8-33

8.4-2 Size Distribution of Test Dust Used To Develop Efficiencies Listed in Table 8.4-1 . . 8-34

8.4-3 Price Factors for Different Fabrication Materials. 8-35

8.5-1 Optimization of Venturi Scrubber 8-43

10.2-1 Volume Contributions to Diffusivity. 10-6

10.4-1 Equilibrium Constants at 26°C After Pourbaix (1966). 10-16

10.4-2 Equilibrium Constants at 25°C. 10-18

10.4-3 Diffusivity of Ammonia in Water. 10-19

10.4-4 Equilibrium Constants at 25°C. 10-20

10.4-5 Equilibrium Constants. 10-21

10.4-6 Diffusivity of H_2SO_4 in Water at 20°C. 10-23

10.4-7 Equilibrium Constants. 10-24

10.4-8 Diffusivity of NH_3 in Water. 10-25

10.4-9 Equilibrium Constants. 10-26

12.2-1 Water Treatment Methods Used in Treating Scrubber Effluent (Industry Survey). 12-4

12.2-2 Liquid Waste Disposal Methods Applied to Wet Scrubber Effluents (Industry Survey) 12-4

12.2-3 Solid Waste Disposal Methods Applied to Wet Scrubber Effluents (Industry Survey) 12-4

CHAPTER 1

INTRODUCTION

TABLE OF CONTENTS

1.0 Introduction 1-2

1.1 Scope 1-3

1.2 Approach 1-4

  1.2.1 Design Methods 1-4

  1.2.2 Other Elements 1-5

  1.2.3 Surveys 1-6

1.3 Handbook Format 1-7

1.4 Acknowledgements 1-8

CHAPTER 1

1.0 INTRODUCTION

Wet scrubbers are defined as devices which utilize a (scrubbing) liquid in the separation of particulate or gaseous contaminants (or components) from a gas. They are used extensively for the control of air pollution emissions and also in chemical process systems. Since the term "scrubber" is rarely used to describe a dry system, we will generally refer to wet scrubbers as simply "scrubbers".

So many different scrubber configurations have been used that there is some confusion as to whether they are all in the same class, and in some writings there is a restriction of the definition according to whether they are open or packed, etc. We intend no such limitation; any device fitting the definition of the first sentence in this paragraph is a wet scrubber.

The "Scrubber Handbook" represents an effort to present the best available engineering information on scrubbers. Both theory and empiricism are employed where appropriate to the objective of providing the basis for the most effective use of scrubbers in air pollution control. This implies primarily that performance (i.e. efficiency of pollutant removal) for a given scrubber under a stated set of operating conditions be predictable within useful limits of accuracy.

Other considerations such as power requirement, equipment cost, operating cost, maintenance requirements are also important in designing the optimum pollution control system. The system designed or specified must be corrosion and erosion resistant and suited to operation with little or no attention for long periods. Nevertheless, the sine qua non requirement is that the scrubber must be capable of removing pollutant(s) to the intended degree. A cheap, simple scrubber which does not meet the efficiency requirements is not only useless but a waste of money and time. It is, therefore, of primary importance to provide as sound a basis as possible for predicting performance.

Design based on fundamental engineering concepts is the best approach to equipment and systems which perform as required and at cost. The history of engineering can be viewed as the continual evaluation of better generalized concepts of the underlying principles which govern the behavior of machines, structures, and systems. Treating each special case as being a unique, mysterious situation which can only be dealt with on the basis of long experience has given way to recognizing the underlying similarities among specific cases and to developing general principles which can be applied to all cases.

In keeping with the objective of presenting the best of present technology, we have endeavored to provide a solid base of fundamental principles and from that to build generally applicable design methods. One finds that while there is extensive, although scattered literature on basic principles of small particle behavior, the application of these to scrubber design and/or the interpretation of scrubber performance has been very infrequent. Gas absorption has received much more attention than particulate scrubbing and the literature contains a lot of rational design methods. The main gaps for gas absorber design are for devices which are or were unusual in the chemical industry and for mass transfer with chemical reaction. In general, the chemical engineer is quite used to taking a mechanistic view of mass transfer and of applying his understanding of mechanisms at the microscopic level to the design of full-scale equipment.

To a surprising extent, one encounters the attitude that particulate scrubbing is a black art which is somehow exempted from the laws of physics and can not be defined in terms of engineering principles. It may well have the appearance of a dark mystery if one does not know the mechanisms and forces at work or does not know the particle size. The easy way out is to try something and see if it works or to have blind faith in someone who works on the basis of experience, however unenlightened it may be.

With a problem as severe as air pollution we cannot afford the luxury of a primitive, cut-and-try approach to control equipment design and specification. Neither can we afford the unnecessary expense of overdesign to cover a wide range of uncertainty. Therefore, the Scrubber Handbook is an engineering text, written primarily for engineers. It does not provide easy, magical ways to design, nor does it abdicate the responsibility to apply rational principles.

1.1 SCOPE

The handbook was prepared by A.P.T. as part of the program of EPA/OAP contract CPA 70-95, "Wet Scrubber System Study".

The general concept of the study was set forth by the EPA (then NAPCA) as follows:

> "The Division of Process Control Engineering of the National Air Pollution Control Administration is developing technology and equipment for control of air pollution emissions from stationary sources. As a means of controlling air pollution emissions, a system study will be undertaken to expand the application of wet scrubbers, as both particulate collectors and chemical contactors for gaseous pollution control, by identifying gaps in current technology and defining research and development needs.
>
> A. SCOPE OF WORK
>
> The contractor selected to do this state-of-the-art study will: (1) review and assess the status of scrubber technology; (2) prepare a critical review and evaluation of existing scrubber systems and define current practices in the application of scrubbers for air pollution control; (3) define usage problems and the research and development needed to improve the performance of scrubbers as now applied; (4) identify potential new applications of wet scrubbers to additional air pollution control problems; and (5) develop specific research recommendations."

FINAL REPORT

> "The final report of this study is expected to be an authoritative and comprehensive reference source on wet scrubber technology.... This report on scrubber technology should be a comprehensive and up-to-date document that can be used for design, research, and instructional purposes. It is anticipated that this document will be reviewed periodically as new information from on-going research becomes available."

1.2 APPROACH

The approach taken was based upon first formulating the most general concept of what could possibly be involved in a scrubber system, and then determining the ranking of importance for the items involved. Since there is always a limit on what can be accomplished, it was intended that this approach would ensure that the most important things would be covered. Figure 1.2-1 is a schematic diagram of a scrubber system which has nearly everything imaginable and reasonable. It serves as a pictorial check list of what ought to be considered. Along the same vein, a detailed outline of all conceivable methods of gas purification by scrubbing was prepared and used as a guide for the study. This outline is well represented by the tables of contents for Chapters 4 and 5.

The handbook is composed of material which is the result of activity in three main areas.

1. Review and development of engineering design methods related to scrubber performance.

2. Review and development of engineering information on system elements other than the scrubber itself.

3. Acquisition and analysis of actual experience data (surveys).

1.2.1 DESIGN METHODS

Design method development was the approach to fulfilling the objective of the detailed scope of work under "Evaluate Current Engineering Technology".

> "The contractor will evaluate the status of engineering technology applicable to wet scrubbers and currently available to the designers, manufacturers, and users of scrubbers. The contractor will review and assess the published literature and unpublished information, including where appropriate information acquired through private communication with manufacturers, designers, and users of scrubbers. The contractor will determine the availability and adequacy of useful operational and design data, models, and equations and the applicability of these data for prediction of performance of the various types of scrubbers. Technology relating to the performance of scrubbers, both particulate collectors and mass transfer

> contactors, should be considered. The contractor will evaluate available technology and define research and development needed to overcome any identified deficiencies in the technology."

The general approach to this aspect of the study, and an ideal not completely realized in all cases, was to:

1. Analyze all currently known wet scrubbers of significance and define them in terms of the elemental physical and chemical mechanisms ("unit mechanisms") which are the components that can be assembled to describe any kind of scrubber.

2. Develop a set of the best available design methods (i.e. mathematical models relating design variables to performance) for each of the unit mechanisms. Utilize the best available design information but do not be limited by it. Where gaps or weak points exist, develop new or improved methods.

3. Synthesize the appropriate total design equations from the unit mechanism equations and use them to predict performance of known types of scrubbers.

4. Utilize available published and unpublished design methods, performance data, manufacturers' literature, etc. to predict performance of the systems covered in point 3, above.

5. Compare the predictions of the best methods (point 3) and the available information (point 4). Reconcile differences to firm-up the final models and to elucidate areas for further research.

6. Develop charts and tables for the reader's convenience in making design computations.

7. Present example calculations to illustrate the use of design methods.

1.2.2 OTHER ELEMENTS

As Figure 1.2-1 indicates, there are a number of elements other than the scrubber which make up the total system. Frequently the technology or cost of one of these is more significant than that of the scrubber itself. In addition, there are other considerations which may limit performance or feasibility. The kind of factors studied are as follows:

1. Equilibrium considerations and related problems such as physical solubility, chemical reaction equilibrium, rate of chemical use, solvent losses, and solvent selectivity.

2. Operating characteristics such as stability, reliability, flexibility and controllability.

3. Auxiliaries such as blowers, pumps, heat exchangers, lines, spray nozzles, controls, hooding, venting, liquid clarification for recycle,

liquid chemical treatment, crystallizers, solvent stripper, extractors, and liquid or solid waste disposal.

4. Measurement of system performance by means of manual or machine sampling and analysis of gas and liquid streams.

5. Operating and maintenance labor, materials, and other costs.

6. Health and safety considerations such as toxic gases or liquids, explosive materials, hot surfaces, and corrosive or irritant materials.

7. Materials of construction problems such as corrosion, erosion, strength, weight, ease of repair, susceptibility to stress and fatigue, and cost.

8. Economic factors and their analysis such as determining costs for investment, power, chemicals, operating labor, maintenance, and depreciation. Mathematical modeling and machine computation to determine optima costs.

1.2.3 SURVEYS

The acquisition and analysis of actual data involved several surveys followed by processing and use of the information. An outline of the general approach is as follows:

I. Acquire Information from the Following Sources
  A. Published Literature
    1. Publications - books, magazines, technical papers, etc.
    2. Government reports and publications
    3. Manufacturer's literature
    4. Bibliographies and APCA abstracts, etc.
    5. Retrieval systems - APTIC, CAES, AP Titles, D.D.C., Medlars, ACS
    6. Photographs and drawings of installations and equipment
  B. Non-Published Information
    1. Manufacturers and trade organizations for:
      a. Scrubbers
      b. Auxiliaries
    2. Users
      a. Engineering and Architect (construction) companies
      b. Ultimate customers (plant operators, etc.)
        i. Occidental Petroleum Corp. subsidiaries
        ii. Other companies
        iii. Government Agencies
    3. Air pollution control agencies
      a. Federal
      b. State
      c. Local and regional
    4. Researchers
      a. University
      b. Foundations, etc.
      c. Government agency (in-house)
      d. Government contractors
    5. APT experience and knowledge
    6. Professional societies such as APCA, AIChE, AIHA, ACS

II. Acquire Information with the Following Methods
  A. Published
    1. Library Search
    2. Search by information retrieval services (such as APTIC, etc.)
    3. Requests directed to individual researchers
    4. Requests directed to professional organizations
    5. Requests directed to governmental units
  B. Non Published
    1. Questionnaires
    2. Telephone Calls
    3. Visits and interviews
    4. Direct observations of scrubber installations

III. Analysis to Include the Following Steps
  A. Set up an information retrieval system and define all information in terms of this system. Review what is available. If inadequate, augment.
  B. Review available information in specific areas and determine whether a complete and satisfactory design method can be set up. If not, augment.
  C. Organize responses and other information relating to present usage, problems, etc. and identify patterns and conclusions, etc. If inadequate, augment or modify survey.
  D. Catalog all available scrubbers according to a classification scheme.
  E. Catalog all known uses of scrubbers.
  F. Evaluate existing systems by means of design models and knowledge.

1.3 HANDBOOK FORMAT

Some things should be mentioned concerning the format of this handbook, which is intended to serve a variety of uses, but not all conceivable readers. It is for the specialists; the full-time air pollution control engineers, or researchers, or the man with a temporary but intense interest in a specific problem. Further, the book strives to be sufficiently complete that the reader can go through at least a preliminary design computation without requiring access to a technical library. In short, this is a textbook style handbook.

As will be apparent upon reviewing the table of contents or skimming through a few chapters, this book is written for engineers. The technical level does not exceed the educational background of a representative B.S. program in chemical engineering. Comprehension of material in chapters 4 and 5, for instance, will require some study for those who are not experienced in the field. Essentially everything necessary is there, assuming the reader has access to a few standard handbooks or texts such as Perry's Handbook.

The reader will also notice that the metric system of units has been used as the primary one. In deference to long habit (for the authors as well as the readers), translations into "English units" are given at frequent intervals. An extensive table of conversion factors is given in the appendix. Actually, there are very few quantities which concern us in the scrubber field, which cause any unease in metric units. For instance, we are used to flow rates in CFM, but it is an easy conversion to get m^3/hr. Pressure drop is usually given in inches of water col., which is no problem to convert to mbars or cm W.C. Many quantities such as particle size (μm), air quality standards (μg/m^3), diffusivity (cm^2/sec), and density (g/cm^3) are generally described in metric units.

1.4 ACKNOWLEDGEMENTS

A subcontract with Garrett Research and Development Corporation was a part of the systems study, and it provided access to the various units of the Occidental Petroleum Corporation for data on scrubber use. Some of the subcontract personnel, Dr. George Preston and Mr. John Ellis, contributed to the preparation of technical material. Dr. Preston was largely responsible for Chapter 10 and several sections of Chapters 4 and 5. Mr. Ellis was largely responsible for Chapters 6 and 11, several sections of Chapter 9, and the compilation of a considerable amount of survey data for Chapter 7.

Many people and organizations contributed generously to the scrubber systems study, and their part in the preparation of this book is gratefully acknowledged. We wish especially to point out the important parts played by Mr. Dale L. Harmon, project officer for the study, and Messrs Robert Lorentz and Richard Harrington of the Environmental Protection Agency. Dr. Leslie Sparks, Project Officer, during the final period of the study contributed notably to editing the Handbook.

Some of those whose contributions were most noteworthy are the following:

Allegheney County Health Department, Bureau of Air Pollution Control, for providing information on the performance of scrubbing systems.

Professor P. H. Calderbank, papers on bubble dynamics.

County of San Bernardino Air Pollution Control District, for providing information on the performance of scrubbing systems.

Bureau of Air Quality and Noise Control, Department of Environmental Resources, Commonwealth of Pennsylvania.

Department of Environmental Control, City of Chicago, for providing information on the performance of scrubbing systems.

Department of Public Health and Welfare, Division of Air Pollution Control, City of Cleveland, for providing information on the performance of scrubbing systems.

Department of Water and Power, City of Los Angeles, for providing information on the performance of scrubbing systems.

Division of Air Pollution Control, City of Cleveland.

Environmental Protection Agency, Office of Solid Waste Management Program, incineration.

Harvard School of Public Health, for providing information on the performance of scrubbing systems.

Mr. C. B. Horsley of Braxton Corporation, for his interesting information on ultrasonic devices.

Mr. Charles S. Maneri, Chief, Federal Facilities Branch, Environmental Protection Agency, for many government scrubbers.

Mr. Charles G. Martin of Christchurch, New Zealand, for his valuable comments.

Professor Thomas T. Mercer, for his help in jet impaction.

New Jersey State Department of Environmental Protection, for providing information on the performance of scrubbing systems.

Oak Ridge National Laboratory, for description of scrubbers used in their installation, and description of their work on scrubbing of materials released due to an accident to a pressurized Water Reactor.

Tennessee Valley Authority, Division of Chemical Development.

For her tireless and careful work in the typing and reproduction of this book, we express our appreciation to Mrs. Glenna Paschal.

Figure 1.2-1

SCHEMATIC DIAGRAM OF SCRUBBER SYSTEM

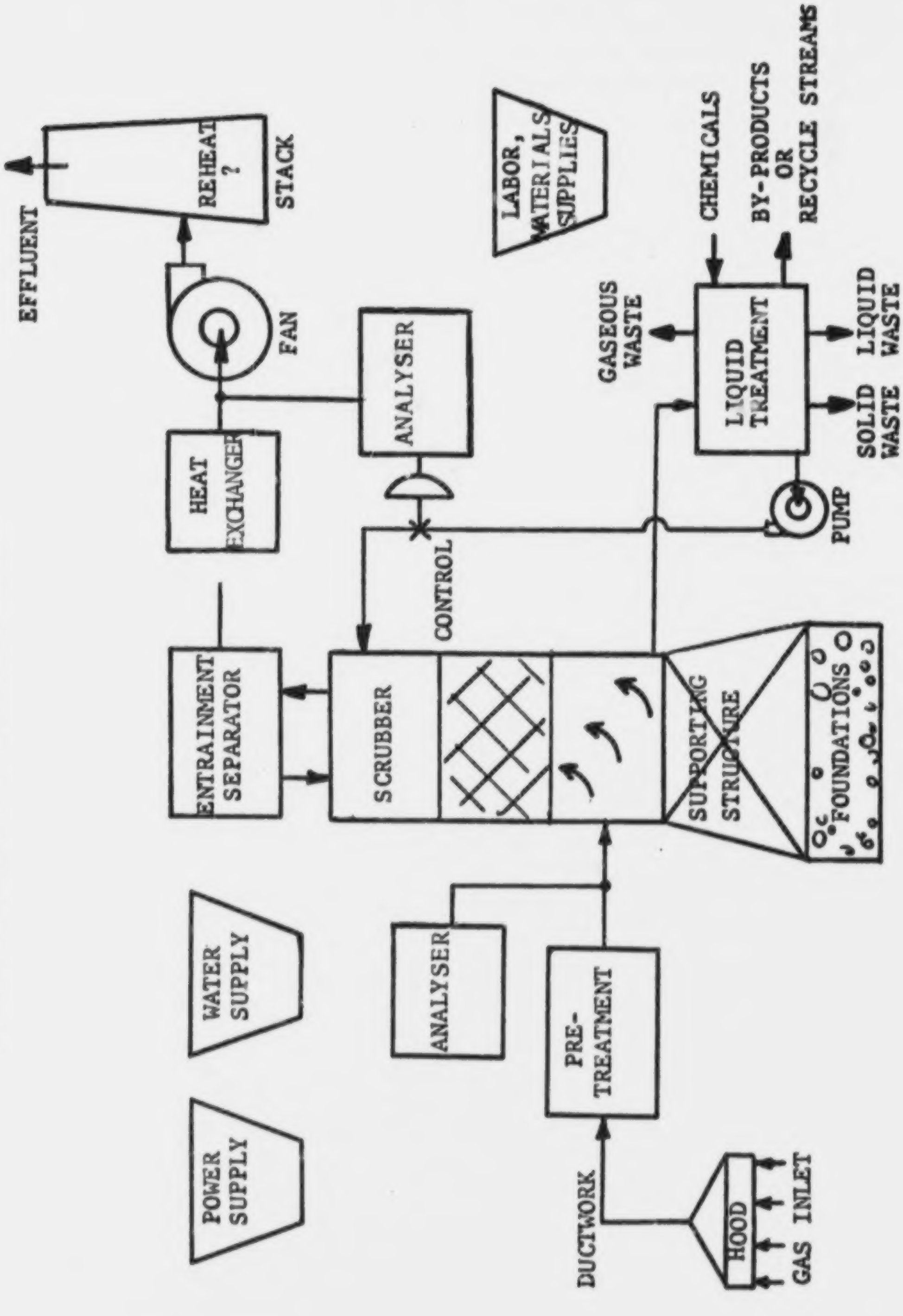

CHAPTER 2

GUIDE TO THE HANDBOOK

TABLE OF CONTENTS

2.0 Introduction 2-3

2.1 Define the Problem 2-4

2.2 Explore Alternate Solutions. 2-6

2.3 Decide How to Control the Problem. 2-6

2.4 General Approach to Scrubbers. 2-9

- 2.4.1 Define the Problem 2-10
- 2.4.2 Select the Appropriate Type of Scrubber. 2-10
- 2.4.3 Design the Scrubber. 2-11
- 2.4.4 Select Materials of Construction 2-11
- 2.4.5 Provide for Waste Disposal 2-11
- 2.4.6 Fabricate, Install, Test and Operate the Scrubber System 2-11

2.5 Detailed Considerations. 2-11

- 2.5.1 Mass Transfer. 2-11
  - 2.5.1.1 Unusual Equipment Design for Which Performance and Cost Data are Un-Available or Uncertain. 2-12
  - 2.5.1.2 Absorption with Chemical Reaction Due to Suspended Solids (Such as SO_2 by Lime Slurry) 2-12
- 2.5.2 Particle Collection. 2-12
  - 2.5.2.1 Want to Know Overall Collection Efficiency for a Typical Installation 2-12
  - 2.5.2.2 Need Data on Collection Efficiency Vs. Particle Size ("Grade Efficiency Curves") for a Specific Scrubber Under Typical Operating Conditions. 2-13
  - 2.5.2.3 Want to Define Performance in Terms of Particle "Cut Diameter" (50% Collection) for a Specific Scrubber 2-13

CHAPTER 2
TABLE OF CONTENTS

2.5.2.4 Need to Make a Detailed Computation of Predicted Collection Efficiency for a Given Application 2-13

2.5.2.5 Want to Develop a Mathematical Model for the Prediction or Correlation of Performance Relationships for an Unusual Situation 2-14

2.6 Operate the System Properly 2-14

References. 2-16

CHAPTER 2

GUIDE TO THE HANDBOOK

2.0 INTRODUCTION

For the person who consults this handbook in regard to a specific problem, the table of contents may not be enough to direct him to the appropriate section(s). To help in this situation, Chapter 2 gives an overview in terms of the steps which have to be taken in solving a problem. It begins with a brief discussion of the general air pollution problem, to ensure that all factors have been considered before getting committed to a scrubber.

The use of metric units for engineering applications will be unfamiliar to many of the readers, but it will prove to be simple to get used to. For scrubber applications, the quantities of most interest are the few given below:

Flow rate - 1,000 CFM = 28.3 m^3/min = 1,700 m^3/hr

Gas concentration - ppm = ppm

Particle concentration - 1 grain/ft^3 = 2.29 g/m^3

Pressure drop - 1 in W.C. = 2.54 cm W.C. = 2.489 mbar

Liquid to gas ratio - 1 gal/MCF = 0.134 ℓ/m^3 = 1.34×10^{-4} m^3/m^3

Power - 1 H.P. = 0.746 K.W.

Power to flow ratio - 1 H.P./MCFM = 0.438 w/m^3/hr

Temperature - 1.8°F = 1°C

Dimensions - 1 ft = 0.305 m

We are already used to metric units for such things as:

Particle size - μm (microns)	Diffusivity - cm^2/sec
Concentration - μg/m^3	Density - g/cm^3

Deciding upon the best method to control an air pollution problem requires that many alternatives should be explored and compared. Should a scrubber appear to be a technically feasible method, one then will search for the scrubber which can achieve the desired efficiency at minimum cost. How to use this handbook in such studies to evaluate scrubber manufacturers' proposals, and/or design a scrubber yourself, will be described in this chapter.

In the following sections, a method of finding and implementing the best solution to a pollution problem will be presented. The steps to follow are summarized in Table 2.0-1. First, the problem must be defined in terms useful as design criteria. Next, the various alternative methods of achieving control should be examined. Then the alternative means of control can be weighed against the criteria for solving the problem, and the most feasible solution identified. If an existing system must be upgraded, the necessary modifications can be identified and carried out. If a new system is necessary, it can be designed and built. The decision must be made whether to build the system yourself, or have a manufacturer or consultant do it. Finally, the selected means of control must be implemented, tested and operated.

A schematic diagram of a general scrubber system is presented as Figure 1.2-1. It is intended to be a visual check list of all things which might be part of a scrubber system. In most cases some components, such as a hood or pre-treatment of the gas, will be absent. There will be other instances where this reminder will spark an idea of something which could be added.

In all probability you have considered other approaches and are interested in scrubbers. No matter what the reason (i.e., you might have to design, select, or up-grade), the central task before you is how to relate scrubber performance with its configuration, size, fluid flow rates, physical and chemical properties, pressure drop, and cost. Whether one starts with performance and looks for a scrubber that will give it, or starts with a scrubber and predicts its performance, the same basic relationships and set of survey data are involved.

Table 2.0-1

Steps to Follow - Solving a Pollution Problem

Step 1	Define the Problem
Step 2	Explore Alternative Solutions
Step 3	Decide How to Control the Problem
Step 4	Decide Whether to Upgrade an Existing System or Build A New One
Step 5	Evaluate the Manufacturer's Proposals or Design the System Yourself
Step 6	Operate the System Properly

2.1 DEFINE THE PROBLEM

What needs to be done? Before attempting a solution, one must know exactly what the problem demands. It may be to conform with a legal limitation or to respond to complaints based on undesirable effects. We will presume that the reader is aware of the legal requirements or can learn of them through local, state, or federal agencies.

Limits on particulate emissions (smoke, mist, dust) are usually expressed in four ways: (1) maximum weight per hour which can be legally emitted, e.g. lb/hr; (2) maximum concentration of particulate matter in the gas stream released, e.g. g/m³, grains/cubic foot, or lb/1,000 lb gas; (3) maximum opacity of the gas stream emitted, usually measured in terms of Ringelmann number, (Ringelmann #1 equals 20% opacity, #2 equals 40%, #3 equals 60%, etc.); (4) Emission rate which is tied to an air quality standard by a formula or chart based on atmospheric dispersion considerations.

Often, several particulate emission regulations are enforced simultaneously. For example, if all four types of restrictions are employed, one might pass the regulations on weight per hour and concentration of particulate matter emitted, but still be held in violation if the emissions exceed the maximum opacity requirement. This is usually the case since large particles are the major contributors to weight while smaller particles, in the 0.1-2 μm range, are the major contributors to opacity.

The maximum allowable concentrations of pollution gases are almost always specified in terms of the maximum fraction by volume of polluting gas which may be contained in the discharged gas stream. The volume fraction is usually expressed as percent by volume, or as parts (volumes) of polluting gas per miillion parts (volumes) of gas discharged - ppm.

Emission concentration or rate limitations are clear indicators of what must be achieved. Ground level concentrations, if tied to stack emissions by a specific dispersion formula and set of atmospheric conditions, can also lead to an obvious performance requirement. If ground level concentrations are specified but dispersion relationships, buoyant rise of plume, and meteorological factors are not, emission design conditions are not so certain. Relief of symptoms, such as opacity, odor and effects on plants, animals, or materials, may also imply rather vague design objectives.

In many cases, the emission source is obvious. However, a single stack may vent several processes simultaneously. If only one of the processes vented is producing most of the pollution it may be worthwhile to isolate the emissions from this process and treat them separately, rather than treating the entire gas stream at the common stack. Emissions at or near ground level, and perhaps subject to "down wash" effects due to air flow around buildings might best be dealt with by venting through a tall stack. Knowledge of present emission rates and characteristics, plus level of emissions desired, is required to determine how difficult the clean up job will be. The effluent gas flow rate, temperature, and humidity must be known.

If particles are being emitted, knowledge of their composition, density and size distribution is necessary. If the problem is noxious gases, it is desirable to know their concentration and composition, but this is not always necessary or possible. Particle size measurement is tricky and must be done by a specially competent person if the data are to be reliable. Gas analysis is a more common procedure and is generally less prone to error than particulate measurements. To get some idea of what others have experienced and may occur in your situation, consult the tables in Chapter 7 which supply average values for particle density and size distribution, and pollutant gas concentrations for a number of processes commonly controlled by scrubbers.

2.2 EXPLORE ALTERNATE SOLUTIONS

The installation and operation of air pollution control equipment can be expensive. Alternate methods of solving the pollution emissions problem are available, and possibilities which should be considered are:

1. Modify the operation of the present process.
2. Select non-polluting raw materials or fuel.
3. Change the process or equipment.
4. Eliminate the process.
5. Apply a control device.

Assuming that the use of control equipment must be considered, one should be aware of the several possibilities available. Various kinds of control devices have been developed, and can be identified by the manner in which they operate. In most applications some types are more suitable than others. In some applications, more than one kind of device might do the job. Then deciding which device to use depends on factors such as economics, space required, availability, delivery time, maintenance required, past experience, additional facilities, etc. General categories to consider are:

1. Centrifugal collector (cyclone or multicyclone)
2. Gravity Settler
3. Electrostatic Precipitator
4. Fabric Filter
5. Wet Scrubber
6. Incineration
7. Adsorption Bed

2.3 DECIDE HOW TO CONTROL THE PROBLEM

Having in mind the alternative methods of achieving air pollution control, it is now time to evaluate all applicable methods of control, and decide which is not suitable.

1. Will it do the job? i.e.: solve the problem defined in Section 2.1.
2. Will it be reliable?
3. Will it create noise or water pollution control problems?
4. How much does it cost to install and operate?
5. Is any method good because of recycle, safety, health, etc.

Other criteria such as available space for the collector and its accessories (if a control device is selected), the availability of new material if it is decided to solve the problem by material substitution, etc., must also be evaluated. Which criteria are important and which are not must be decided case by case. The four criteria discussed below, however, will probably be important in all cases.

Will it do the job?

How to determine whether or not an alternate method of control will solve the problem may range from a simple test to a full-scale trial. One might be able to "operate the present process properly", or "select a non-polluting process material or fuel" on a test basis, to determine their influence on emissions, and get an idea of their suitability. Possibly a "change" in the "process or equipment" may be evaluated by comparisons of "before" and "after" similar changes in processes similar to yours. Trade associations may be helpful with this type of information.

If you are anticipating a hitherto untried change, it may require a pilot scale or limited full scale test if time, facilities, and resources permit. If they do not permit, and the process or equipment change is of questionable efficacy in removing the pollution, then perhaps this alternate should be passed over. There is usually an economic reason for why a process is used. "Eliminating the process" entirely is therefore primarily an economic decision, and will normally depend upon how essential the polluting process is in the overall plant operation, and the process profitability.

So far as scrubbers are concerned, the first step is to pick out some type(s) which might do the job. Even if your problem is to upgrade an existing scrubber, it may be helpful to know what kinds of related scrubbers are used, in case yours might be modified to include some of their features.

Many different kinds of scrubbers have been developed, and are discussed in Chapter 3. A description of each major kind of scrubber is given, together with its limitations. Chapter 7 gives data on the scrubbers normally used to control the emissions from a number of potentially polluting processes. All processes using scrubbers for pollution control cannot be listed in Chapter 7. However, an attempt has been made to include all processes where scrubbers are frequently applied. If a process is not listed in Chapter 7, it is probably because the process is uncommon and too little data are available, or because control is usually achieved by means other than scrubbers.

Will it be Reliable?

Reliability is an often overlooked criterion in the evaluation of alternatives. Yet if reliability is poor, a great deal of trouble and expense can be incurred. In the sense used here, reliability includes the availability of the non-polluting material or fuel, if this alternative solution is evaluated. For example, companies opting for low sulfur fuels as a solution to sulfur oxide pollution may find themselves in trouble if too many other companies make the same choice and the supply of low sulfur fuel vanishes.

Corrosion is a frequent cause of failure and Chapter 11 gives details on the properties of materials often used for scrubber construction. Proper selection of materials can preclude or solve a reliability problem. Plugging with solids either from mechanical causes or from scale precipitation is another common problem. Chapter 7 gives field data on the materials of construction and an evaluation of how well they have held up. Plugging and scaling problems are touched on in Chapter 5 for scrubber types and in Chapter 7 for various applications.

Will it Cause a Noise or Water Pollution Problem?

The whole objective of pollution control is to dispose of wastes in an unobjectionable way. One way to do this is not to make the wastes in the first place. However, if one decides to control wastes with air pollution control equipment, the ultimate disposition of the material collected must be considered.

If the collected material has value, it may be sold or recycled to the plant, otherwise it must be disposed of. In many cases, the scrubber effluent cannot be disposed of without treatment. Chapter 12 gives techniques for liquid purification, solids and sludge disposal.

If the plant is in a metropolitan area, or if workers will be in the vicinity of the control equipment,, and the equipment is noisy, then noise pollution will be a problem. One large midwestern company located in a city received complaints from citizens up to a mile away about dust emissions. The company solved the dust problem with a large, efficient scrubber. However, the scrubber used a large fan, and the fan made so much noise that the residents around the plant could not sleep at night. The complaints about the noisy scrubber system were much more severe than the previous complaints about dust. The problem was solved using acoustic insulation and cushioned scrubber mountings. The cost of remounting and enclosing the system was greater than would have been the case if the work had been done while the system was being built.

How Much Will it Cost?

When evaluating several otherwise viable alternatives, economic issues usually determine which approach will be chosen. "Operating the present process properly" will involve some sort of economic liability. This may be in terms of equipment which must be replaced or repaired, or in terms of decreasing production to the levels for which the equipment was designed,and recovering or increasing capacity by building new process equipment. Choosing to "select a non-polluting process material or fuel" will often entail a premium for the purchase of this material, otherwise it would be used in the first place. Costs of this sort and long range availability and price stability are factors which must be determined.

Electing to "change the process or equipment" is often a major decision not based on environmental matters alone. Other alternatives to pollution control usually cost less. However, if other factors enter into the decision, the environmental issue may tip the balance in favor of the new process approach. Sometimes the careful engineering study required to provide the information needed will uncover some unsuspected ways of improvement possibilities. "Eliminating the Process" is cheap and easy. However, it is seldom profitable. If shutting down one process will place an additional air pollution burden on a following process, then that burden must be evaluated.

Before deciding to "apply control devices" one naturally desires to know their installed and operating costs. Costs of scrubbers which have been installed in the past to control the emissions from certain processes are given in Chapter 7. An analysis of the factors which go into determining the costs of a scrubber system is made in Chapter 8. Chapter 8 also gives the data from which a cost estimate can be made for a scrubber which is being evaluated, according to the techniques in that chapter.

At this point, one must weigh the five alternate approaches to air pollution control against the criteria which have been posed for an acceptable solution to the problem. Under the 5th alternative, control devices, a scrubber will be one of several considered. The following sections apply only if a scrubber is selected as worthy of further consideration as a means for controlling the air pollution problem.

Handbooks comparable to this one have been prepared for electrostatic precipitators, fabric filters, afterburners, and adsorbers under E.P.A. sponsorship. No comparable handbooks are presently available on centrifugal collectors such as cyclones, multicyclones, etc. (although they are covered in part in the present handbook), or gravity collectors. A considerable amount of literature in the form of texts, sections of handbooks, and journal articles is available, however.

2.4 GENERAL APPROACH TO SCRUBBERS

The preceeding three sections have been devoted to outlining a method for deciding on how to control an air pollution problem. From here on, the discussion is concerned only with scrubbers. One may be designing a scrubber from scratch, evaluating a manufacturer's proposal, or modifying a system.

Some working knowledge of scrubber design methods is necessary to evaluate manufacturers' proposals. More knowledge is necessary to design a system from scratch. This handbook contains information at several levels of complexity ranging from broad statements summarizing the practical experience of others to very basic physical and chemical principles. We will first present an overall view of the handbook and then go into more detail. The steps in designing a scrubber are listed below and are schematically represented as related to handbook chapters in Table 2.4-1.

1. Define the Problem

2. Select the Appropriate Type of Scrubber

3. Design the Scrubber

4. Select Materials of Construction
5. Provide for Waste Disposal
6. Fabricate and Install, Test and Operate the Scrubber System

2.4.1 DEFINE THE PROBLEM

Emission standards and present emission must be evaluated to determine a design efficiency for the scrubber. The design efficiency should be higher than the efficiency necessary just to meet the emission standards. This is due to: a) variability in the amount of the emissions from day to day; b) allowance for wear and tear in the scrubber installed; c) uncertainties in the scrubber design methods used; d) possible future tightening of air pollution emission laws. To use the design methods in this handbook, the following data must be at hand: gas flowrate, temperature and humidity; particle concentration (weight per volume of gas going to the scrubber); particle density and size distribution or aerodynamic diameter distribution; pollutant gas identity and concentration (volume per volume gas going to the scrubber). The total composition of the gas should be known to protect against the possibility of side effects such as NO_x and SO_2 oxidation. Techniques of gas, particle and pollutant gas measurement are discussed in many places. A good starting point is given by Bloomfield (1968). Typical values for particle density and size distribution, plus pollutant gas concentration for numerous processes are given in Chapter 7. These values are averages. Using either these data or other generalized "emission factor" data for design purposes is risky. Actual measurements should be made.

Besides knowing the required efficiency, it is necessary to define the difficulty of separation of the pollutant from the gas. For particles this is largely dependent on particle size and density, while for gases it depends mainly on solubility in the solvent being considered.

2.4.2 SELECT THE APPROPRIATE TYPE OF SCRUBBER

Many different scrubbers have been developed for many different purposes. Chapter 3 is devoted to describing the types available and explaining the differences among them. It also gives brief descriptions of areas of applicability, lists the names of manufacturers, and briefly describes patented devices.

Chapter 7 lists the scrubbers which have been applied to various processes normally controlled by scrubbers, based on information gathered in the survey. If the process under present consideration is listed in Chapter 7, an idea can be gained of which scrubbers have operated successfully in controlling the emissions from that process.

Chapters 5 and 8 compare the limitations of various scrubbers and should be used to decide which kind or kinds of scrubbers have the capability of solving the given pollution problem. Chapter 8 also gives costs of the various types of scrubbers. After determining which types of scrubbers can perform with the desired efficiency, the least expensive scrubbing arrangement can be determined and selected for design.

2.4.3 DESIGN THE SCRUBBER

After identifying and defining the problem, and selecting the most appropriate type of scrubber to solve it, the scrubber system itself can be designed. Chapter 5 is devoted to explaining the performance and design of scrubbers. Chapter 8 describes optimized scrubber systems.

The scrubber will need a blower and ductwork. Discussion of these auxiliaries is covered in Chapter 6. Costs of components in a scrubber system are given in Chapter 8, as well as cost analyses of complete scrubber systems.

2.4.4 SELECT MATERIALS OF CONSTRUCTION

Experience with materials of construction, as reported to our survey, is described in Chapter 7. Chapter 11 deals with materials in general and discusses available materials and their applicability.

2.4.5 PROVIDE FOR WASTE DISPOSAL

The scrubber will take wastes from the gas stream and put them in the scrubbing liquid effluent. This liquid will usually have to be cleaned, transferring the pollutants to sludge form before the liquid can be discharged. Chapter 12 is concerned with methods of solid (sludge) and liquid waste treatment and disposal.

2.4.6 FABRICATE, INSTALL, TEST AND OPERATE THE SCRUBBER SYSTEM

Once the scrubber has been designed and the materials of construction selected, the scrubber must be fabricated and installed. If fabrication facilities are not available on the premises, an outside contractor can be selected to do the job and the installation. This handbook does not deal with fabrication. After scrubber has now been designed, fabricated, and installed, it must be tested to see if it meets the design objectives. Test methods are defined by EPA and various state and local agencies. If the system fails to perform up to expectations, Chapters 4 and 5 (design methods) can be consulted to search for appropriate alterations.

2.5 DETAILED CONSIDERATIONS

Any detailed study of a scrubber must take up particle collection and gas absorption separately. Consequently, this section branches into two paths to follow the course of a scrubber design. Metric units are used throughout, but English unit equivalents are also given in many places. Conversion factors are given in the Appendix.

2.5.1 MASS TRANSFER

Published literature on mass transfer adequately covers most gas absorption apparatuses and chemical systems. Some areas important in air pollution control present special problems so we have devoted more space to these. We assume that any reader interested in any further detail on usual cases has access to Perry's Handbook (1963) and other basic chemical engineering texts. Some examples of special problems are listed below:

2.5.1.1 Unusual Equipment Design for Which Performance and Cost Data are Unavailable or Uncertain

A) Basic principles of mass transfer are given in Section 4.2.

B) Gas-liquid contacting principles for drops and bubbles are in Section 4.4. More on bubble and drop size distributions and hydrodynamics is in 4.5.

C) Unit mechanisms, given in Section 4.5, are the basic building blocks for making conceptual and mathematical models of scrubbers.

D) Design methods, both those available in the literature and those developed in this study, are given in Chapter 5. Possibly the descriptions of methods developed here may serve as examples of an approach for new cases.

E) Scrubbers with some element(s) of similarity might be found by review of the catalog in Chapter 3.

F) Costs for basic vessel components can be found in Section 8.3 and these may be used as a basis for estimating the cost of a novel configuration.

2.5.1.2 Absorption with Chemical Reaction Due to Suspended Solids (Such as SO_2 by Lime Slurry)

A) Basic concepts for absorption with chemical reaction are discussed in Section 4.2.6.

B) Special considerations for transfer to slurries of reactive particles are in Section 4.2.7 along with a design example.

C) Experience with slurry scrubbing is described in Sections 7.2 and 7.3.1.2.

D) Equilibrium, physical, and chemical data which may be useful are in Chapter 10.

2.5.2 PARTICLE COLLECTION

The literature relevant to particle collection by scrubbers is quite scattered and spotty, in its coverage of the field. Most of this program's original work in design equation development was required for particulates. Because of that, the material on basic principles and unit mechanisms is comprehensive. The material one consults will depend on how precisely his interest is focused. Starting with a broad view and moving to finer detail, one might encounter problems as follows:

2.5.2.1 Want to Know Overall Collection Efficiency for a Typical Installation

A) Sketchy descriptions are given in Chapter 3.

B) Chapter 7 is the main source of this type of data.

2.5.2.2 Need Data on Collection Efficiency Versus Particle Size ("Grade Efficiency Curves") for a Specific Scrubber Under Typical Operating Conditions

A) Learn about particle size distribution from Section 4.3.2.

B) Various efficiency vs. particle size relationships are given in Section 5.3.

C) Check Chapter 9 for example calculations.

2.5.2.3 Want to Define Performance in Terms of Particle "Cut Diameter" (50% Collection) for a Specific Scrubber

A) Learn about cut diameter in Section 5.3.1.

B) Find cut diameter as a function of operating parameters in Sections 5.3 and 8.2

C) Check Chapter 9 for example calculations.

2.5.2.4 Need to Make a Detailed Computation of Predicted Collection Efficiency for a Given Application

A) Check Chapter 7 for more information about the pollution source and control approaches.

B) Define the particle size distribution and particle density from specific data, if available, or as estimated from Chapter 7, if not.

C) Find predicted performance in terms of cut diameter for the scrubber(s) being considered as discussed under Section 2.5.2.3.

D) Relate the performance cut diameter to the overall collection efficiency (or penetration) as shown in Section 5.3.1 and 8.2. Translate aerodynamic particle diameter into actual diameter and vice-versa as explained in Section 4.3.2 and 5.3.1.

E) If you know what overall efficiency you need, translate that into the necessary separation cut diameter (5.3.1) and determine whether a given scrubber could do the job under any useful set of conditions. Chapter 5.3 provides this kind of information if it is available.

F) If you want a more precise calculation of overall efficiency than the cut diameter approach gives, determine the performance vs. particle diameter relationship for the scrubber as described under Section 2.5.2.2. Then integrate this performance relationship over the inlet particle size distribution (see 5.3.1) to compute overall efficiency for that dust.

G) If you know what overall efficiency you need and want a more precise answer than the cut diameter method yields, use step "E" above to hunt for a suitable scrubber and set of operating conditions. Then make a computation as in "F", above and see whether it is suitable. If not, find a suitable solution by trial and error.

H) Check Chapter 9 for example calculations.

2.5.2.5 Want to Develop a Mathematical Model for the Prediction or Correlation of Performance Relationships for an Unusual Situation. It Might be a New Type of Scrubber or it Might be a Conventional Scrubber in an Unusual Application where Different Collecting Forces May be Intensified.

A) The overall approach would be comparable to that described under Section 2.5.1.1, above, for mass transfer. Check the table of contents for appropriate sections.

B) Thermal effects can be much more significant for particle collection than for mass transfer rates. Section 4.2.8 deals with simultaneous heat and mass transfer and Section 9.3.1 provides some example calculations involving heat and mass flux effects. Section 4.7 deals with general effects of changes of temperature and pressure on particle collection.

2.6 OPERATE THE SYSTEM PROPERLY

To continue solving the air pollution problem for which it was designed, the scrubber system must be operated and maintained properly. Clogging of spray nozzles, solid deposition on fans, clogging of packing material if used, and other maintenance problems can have a major adverse effect on efficiency. Section 9.4, on "trouble shooting", covers practical operational problems which may arise.

TABLE 2.4-1

STEPS IN SOLVING AN AIR POLLUTION PROBLEM

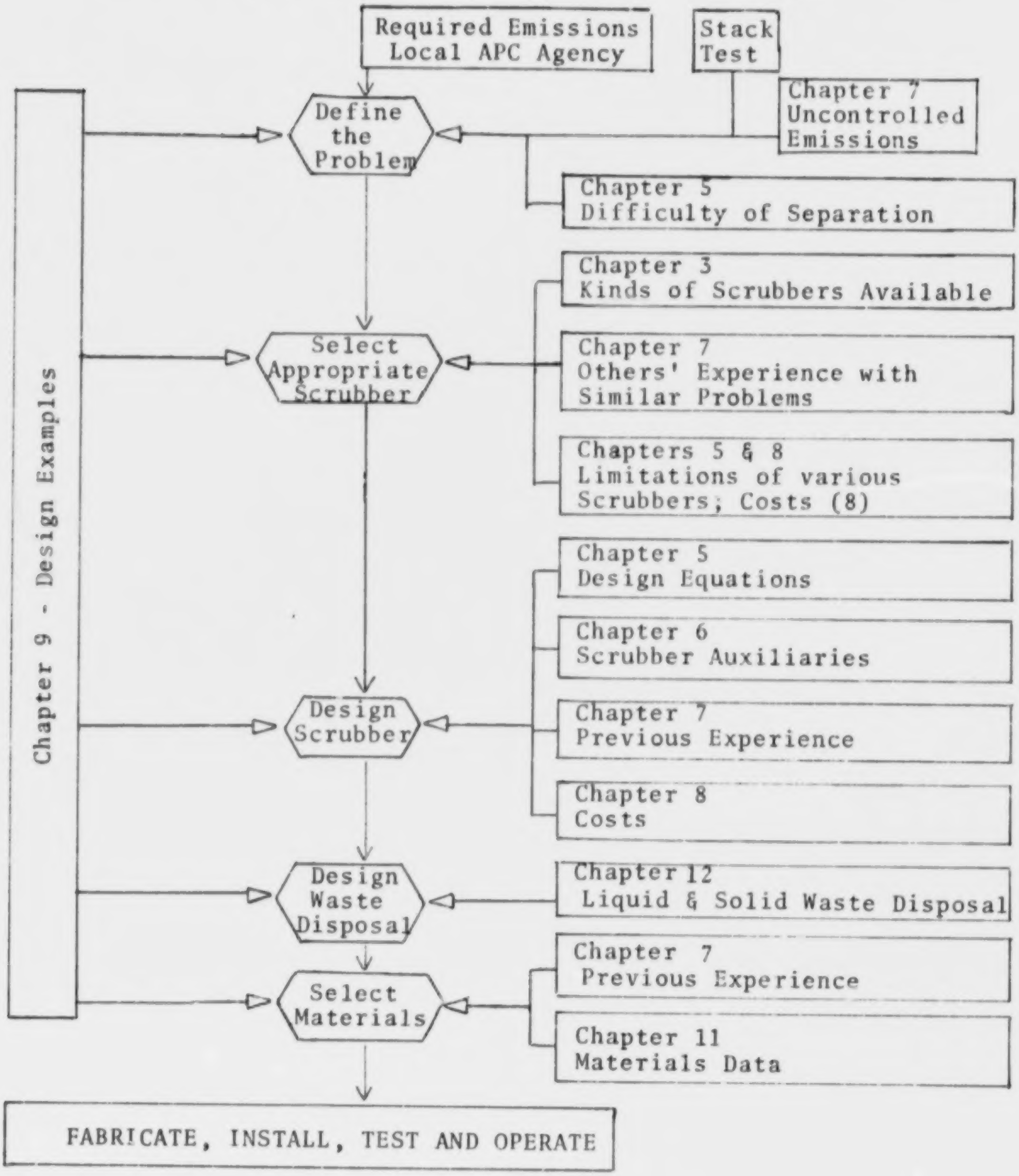

CHAPTER 2 - REFERENCES

Bloomfield, Bernard D., "Source Testing" in Air Pollution II, 2nd ed., Arthur C. Stern, editor, Academic Press, New York (1968).

National Air Pollution Control Administration (1969), Control Techniques for Particulate Air Pollutants, Publication AP-51, Public Health Service, Washington, D.C.

CHAPTER 3

SCRUBBERS AVAILABLE

TABLE OF CONTENTS

3.1 Types of Scrubbers 3-2

- 3.1.1 Introduction 3-2
- 3.1.2 Plate Scrubbers 3-3
- 3.1.3 Massive Packing Scrubbers 3-5
- 3.1.4 Fibrous Packing Scrubbers 3-6
- 3.1.5 Pre-Formed Spray Scrubbers 3-7
- 3.1.6 Gas Atomized Spray Scrubbers 3-8
- 3.1.7 Centrifugal Scrubbers 3-9
- 3.1.8 Baffle and Secondary Flow Scrubbers 3-10
- 3.1.9 Impingement and Entrainment Scrubbers . . . 3-11
- 3.1.10 Mechanically Aided Scrubbers. 3-12
- 3.1.11 Moving Bed Scrubbers. 3-13

3.2 Commercially Available Scrubbers 3-14

3.3 Scrubber Patents 3-20

CHAPTER 3

SCRUBBERS AVAILABLE

Many different scrubbers are offered for sale by many companies. Still more scrubbers have been patented, but are not currently being manufactured. Due to the diversity in scrubber design, performance, and cost, statements broad enough to apply to all scrubbers are so general that they are seldom useful. However, it is possible to divide the various types of scrubbers into homogeneous groups based largely on their operating principles. The characteristics of each group can then be discussed in more specific terms than would otherwise be the case.

The purpose of Chapter 3 is to identify ten groups, into which scrubbers can be divided. These groups will provide the framework for discussing scrubber design (Chapter 5) and experience (Chapter 7) later in the handbook. The ten scrubber groups are identified and briefly discussed in Section 3.1. Many of the scrubbers commercially available in the U.S. are categorized by group in Section 3.2. Section 3.3 contains the U.S. patent numbers assigned to various scrubbing devices, most of which are not currently being manufactured.

3.1 TYPES OF SCRUBBERS

3.1.1 INTRODUCTION

Scrubber manufacturers offer a bewildering array of products. Scrubbers are available in a wide range of designs, sizes, performance capabilities, and both capital and operating costs. Choosing the right scrubber for a particular job requires an understanding of the viable alternatives which various scrubbers may present. The purpose of this section is to organize the scrubbers currently available into homogeneous groups, and then discuss the characteristics of each group. The scrubber categories defined in this section will be used throughout the rest of the handbook.

Some scrubbers are designed primarily for the collection of particles, and others for mass transfer. As good liquid gas contact is needed for both operations, all scrubbers can collect both particles and gases to some extent. The degree to which the particle collection and mass transfer characteristics of a scrubber can be utilized, and the associated cost, will determine the applicability of the scrubber to a job with specific purification requirements.

The approach here will be to categorize scrubbers by type as follows: plate, massive packing, fibrous packing, preformed spray, gas atomized spray, centrifugal, baffle, impingement and entrainment, mechanically aided, moving bed, and combination. The operating characteristics associated with each type will be described in the following sections.

3.1.2 PLATE SCRUBBERS

A plate scrubber consists of a vertical, hollow tower with one or more plates (trays) mounted transversely inside. Gas comes in at the bottom of the tower, and must pass through perforations, valves, slots or other openings in each plate before exiting from the top. Usually liquid is introduced to the top plate, and flows successively across each plate as it moves downward to the liquid exit at the bottom. Gas passing through the openings in each plate mixes with the liquid flowing over it. Figure 3.1-1 shows several types of plates and a tower. The gas and liquid contacting causes the mass transfer or particle removal for which the plate scrubber was designed. Plate scrubbers are named for the type of plates they contain. For example, a tower containing sieve plates is called a sieve plate tower.

Plate scrubbers have been widely used for many years for mass transfer operations. Plate towers have the ability to remove gaseous pollutants to any desired concentration, if a sufficient number of plates is used.

Plate devices are also used for particle collection and several sieve (perforated) plates may be combined in a sieve plate tower. In some designs, impingement baffles are placed a short distance above each perforation on a sieve plate, forming an impingement plate. The impingement baffles are below the level of liquid on the perforated plates and for this reason are continuously washed clean of collected particles. Particle collection is aided by the atomization of the liquid flowing past the openings in the irrigated perforated plate, and the subsequent venturi effect. Particle collection efficiency is generally good for particles larger than one micron in diameter. Pressure drop is about four centimeters W.C. for each plate.

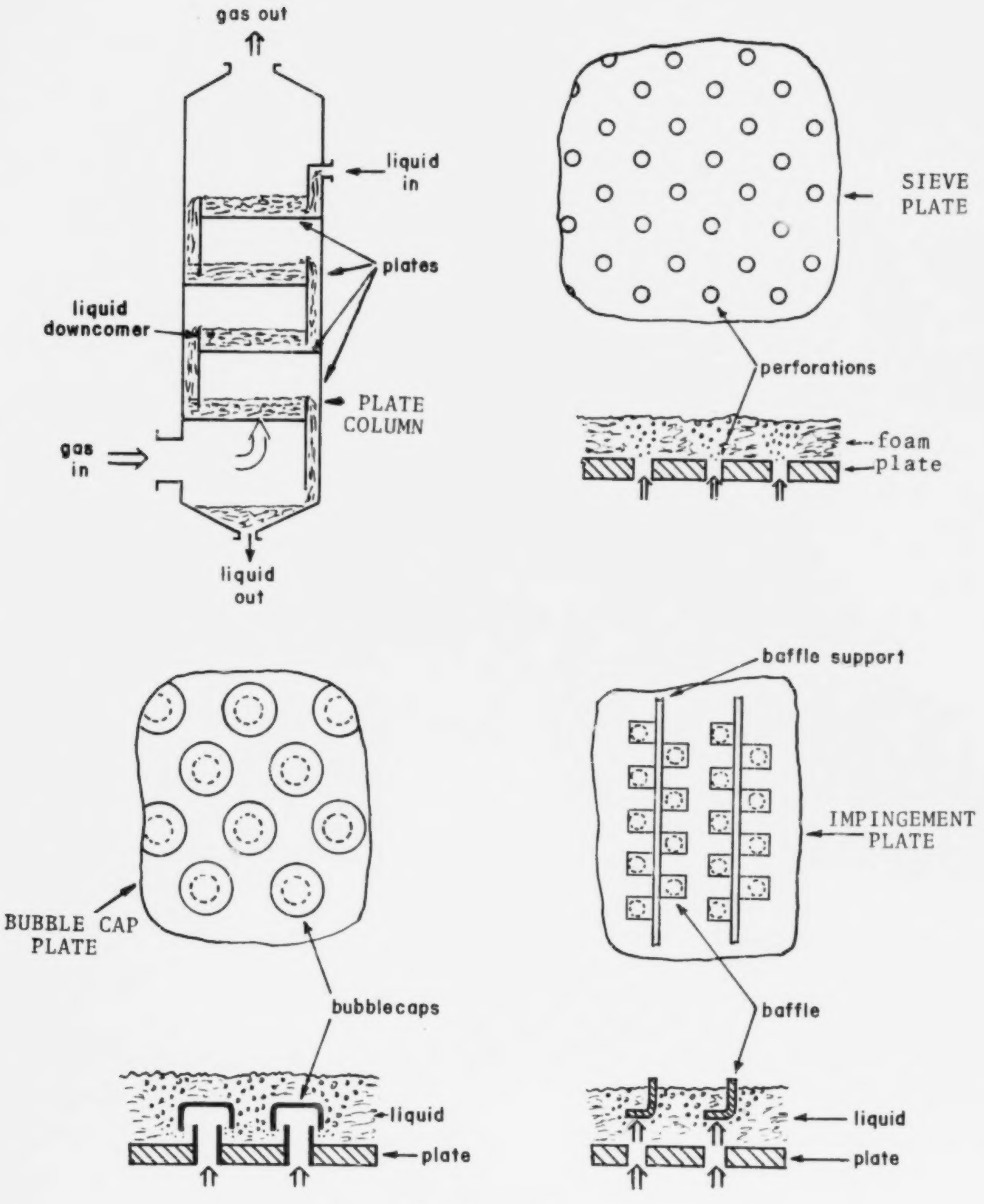

FIGURE 3.1-1
SKETCHES OF PLATES AND TOWER

3.1.3 MASSIVE PACKING SCRUBBERS

A device utilizing massive packing, consists of a hollow tower containing manufactured elements such as Raschig rings, Pall rings, Berl or Intalox Saddles, or home-made packing such as crushed rock. Liquid is usually introduced to the top of the packing, and trickles down through it. The purpose of the packing is to break down the liquid flow into a film with high surface area. The gas stream to be cleaned typically flows upward through the packing, countercurrent to the liquid. Devices of this sort are often called packed towers or packed beds. The flows can also be cocurrent or crosscurrent.

Packed beds have long been used for mass transfer operations. They are able to remove pollutant gases to any desired concentration. The only limiting factor is the economic one. As better separation is called for, beds require greater packing depth and will operate with higher pressure drop. Gases entering a packed bed should not be heavily laden with solid particles to prevent gumming and clogging of the packing material. Pressure drop is typically one cm W.C. per 10 cm bed height.

Beds can also be used for mist elimination. In this case they are usually operated without liquid passing through. The collected mist drips through the packed bed and drains from the bottom. As with mass transfer, collection efficiency can be raised indefinitely by increasing bed height. Efficiency for a bed two meters tall might be good for particles larger than several microns in diameter.

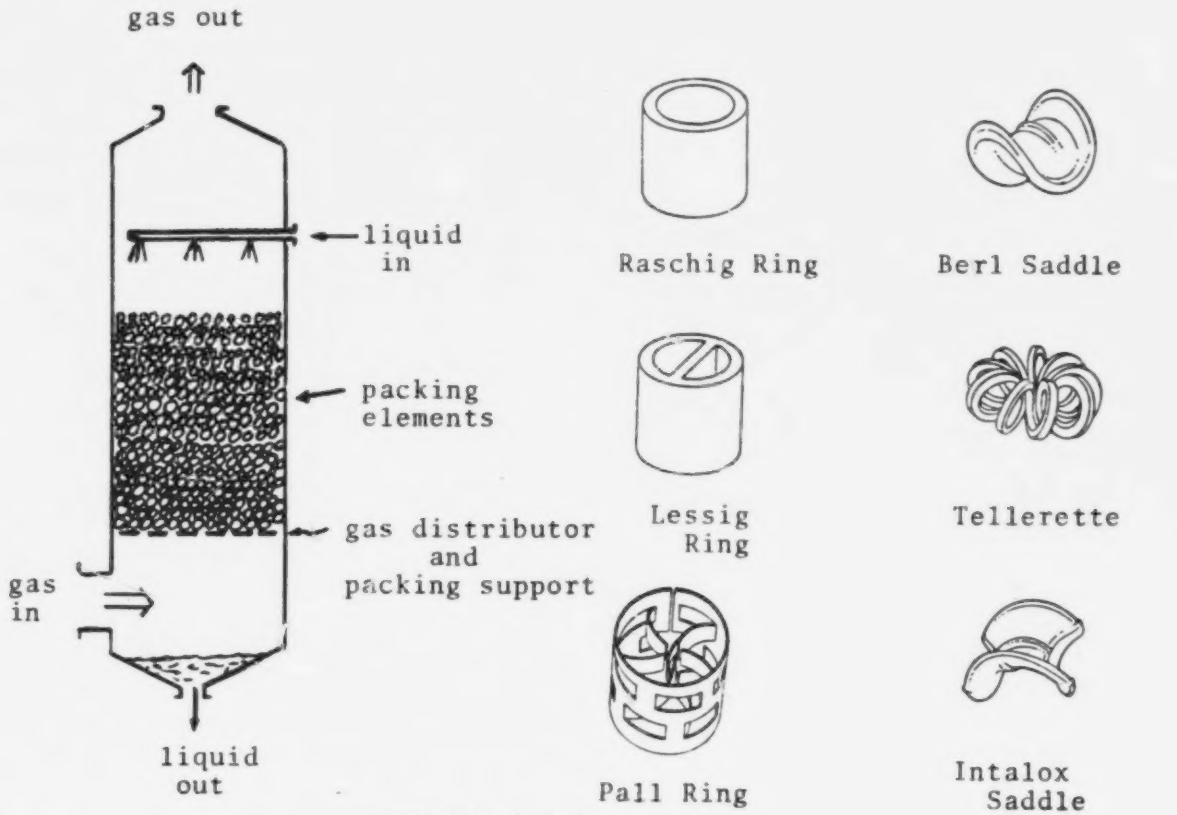

FIGURE 3.1-2
PACKED TOWER AND PACKINGS

3.1.4 FIBROUS PACKING SCRUBBERS

Fibrous packing, like massive packing, is used to provide surfaces for particle collection and gas absorption. The fibers are made from materials such as plastic, spun glass, fiberglass, or steel. Fibrous packing usually has a very large void fraction; porosities may range from 97 to 99 per cent. The packing fibers should be small in diameter for efficient operation, but strong enough to support collected particles or drops without matting together.

Fibrous packing is often used as a drop entrainment separator, following a scrubber. It can also be used to collect droplets coming from a manufacturing process. Fibrous packings are often sprayed with liquid, to aid in gas-liquid contacting for mass transfer. The wetted packing presents more liquid surface to the gas flowing through it than would the sprays alone, and when used in this way is analogous to the situation in a packed tower.

Both mass transfer and particle collection capabilities are theoretically very good. However, the low gas velocities necessary, for efficient operation, lead to large equipment size. Pressure drop is typically moderate at 10 cm W.C.

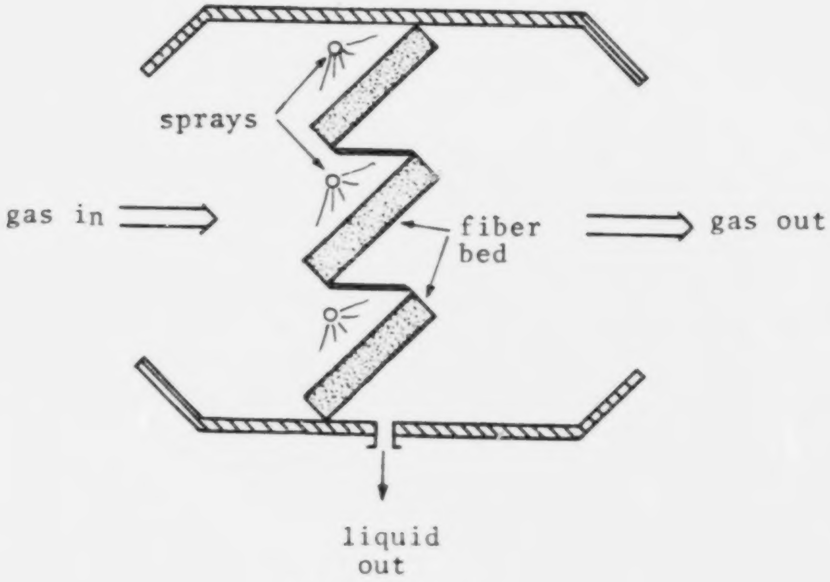

FIGURE 3.1-3

FIBER BED SCRUBBER

3.1.5 PRE-FORMED SPRAY SCRUBBERS

A pre-formed spray scrubber is a device which collects particles or gases on liquid droplets, and utilizes spray nozzles for liquid droplet atomization. The characteristics of the liquid droplets formed are determined by the properties of nozzle, liquid to be atomized, and pressure to the nozzle. The sprays are directed into a chamber suitably shaped to conduct the gas through the atomized liquid droplets. If the tower is vertical, the relative velocity between the droplets and the gas is eventually the terminal settling velocity of the droplets.

Spray towers can be used for both mass transfer and particle collection. They generally have low pressure drop, high liquid consumption, and are probably the least expensive method for achieving mass transfer. Spray chambers are most applicable to humidification or dehumidification and the removal of gases with high liquid solubilities, since the number of transfer units available is limited. Particle collection is primarily by impaction, but is usually limited by the terminal settling velocity and diameter of the spray droplets. Particle collection efficiency can be good for particles larger than several microns in diameter. Pressure drop is low, typically only a few centimeters W.C. Spray towers may provide a good solution to a problem in which the requirements are not severe.

Ejector venturis are preformed spray devices in which a high pressure spray is used both to collect particles (or for mass transfer) and to move the gas. High relative velocity between drops and gas aids particle separation. Particle collection efficiency is good for particles larger than a micron, or two, in diameter. Mass transfer is limited by the co-current nature of the gas and liquid flow. Energy consumption (as liquid pumping cost) is high.

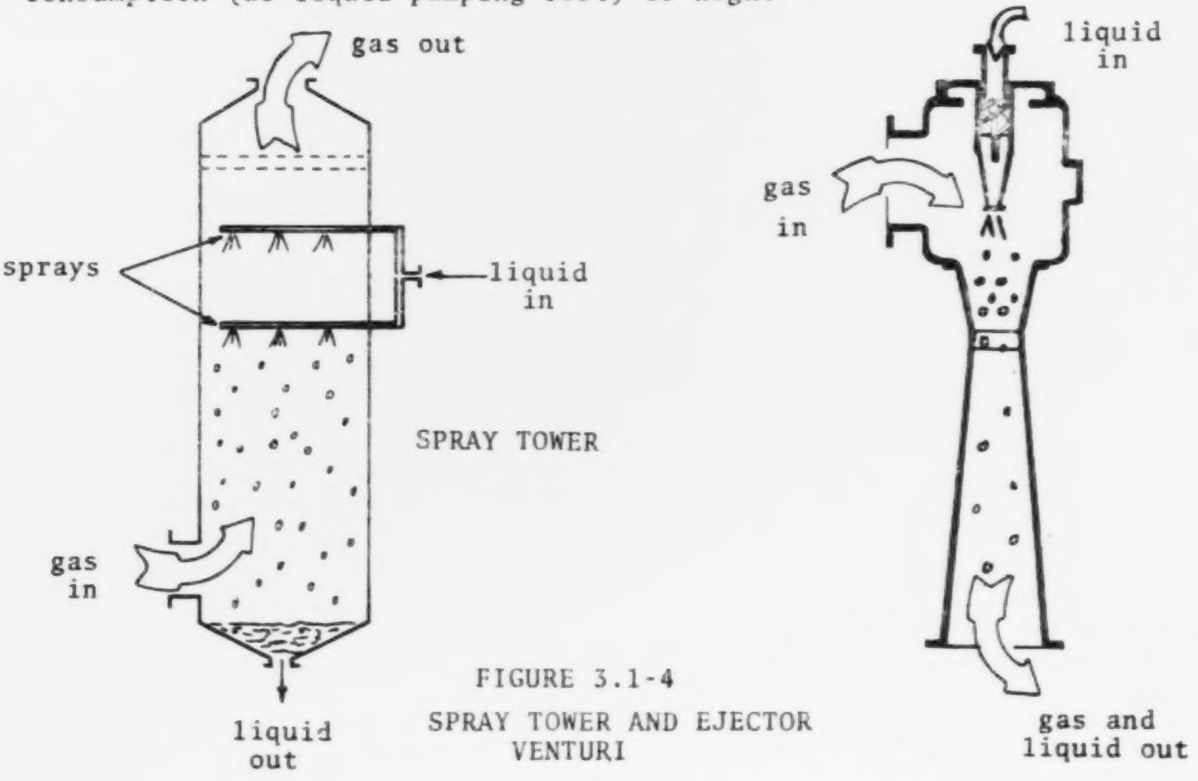

FIGURE 3.1-4

SPRAY TOWER AND EJECTOR VENTURI

3.1.6 GAS ATOMIZED SPRAY SCRUBBERS

Gas atomized spray devices utilize a moving gas stream to atomize liquid into drops, and then accelerate the drops. Typical gas atomized spray devices are the venturi scrubber and the flooded disk scrubber. High gas velocities of 60-120 m/sec (200-400 feet per second) are used in gas atomizing devices, to make the relative velocity between gas and liquid droplets high. High relative velocity promotes particle collection. Most gas atomized spray scrubbers utilize the converging and diverging sections typical of the venturi scrubber. In the venturi, liquid is introduced at the venturi throat. In the flooded disk scrubber, liquid is introduced to a disk slightly upstream of the venturi throat. The liquid flows to the edge of the disk and is atomized.

Gas atomized spray devices have been successfully used for years to remove particles and mists from gas streams. Collection efficiency generally increases with pressure drop. High pressure drop (100 cm W.G. or 40 inches W.G.) venturi scrubbers can efficiently collect submicron particles. However, mass transfer capabilities are limited due to the cocurrent nature of the gas-liquid flow.

Scrubbers of the gas atomized type have several distinct advantages. Through adjusting pressure drop by varying liquid flow rate or gas velocity, they can be made to collect even submicron fume with good efficiency. Due to the absence of moving parts, scrubbers of this type may be especially suitable for the collection of sticky particles. Disadvantages include high pressure drop for the collection of submicron particles, and limited applicability for mass transfer problems.

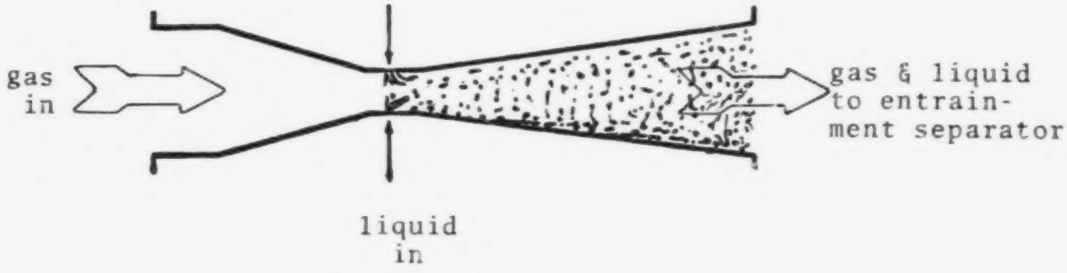

FIGURE 3.1-5

GAS ATOMIZED SPRAY (VENTURI) SCRUBBER

3.1.7 CENTRIFUGAL SCRUBBERS

Centrifugal scrubbers are usually cylindrical in shape, and impart a spinning motion to the gas passing through them. The spin may come from indroducing gases to the scrubber tangentially, or by directing the gas stream against stationary swirl vanes. Sometimes the walls of a dry centrifugal collector are wetted to hinder reintrainment of the particles which collect there. More often, sprays are directed through the rotating gas stream to catch particles by impaction upon the spray drops. Sprays can be directed outward from a central spray manifold, or inward from the collector walls. Sprays directed in from the wall are more easily serviced, as they can be made accessible from the outside of the scrubber.

Centrifugal scrubbers are generally used for particle collection and operate with a pressure drop of from 7.5 to 20 cm (3 to 8 inches) of water. They are usually inefficient for the collection of particles less than one or two microns in diameter. If a spray manifold is fitted, a centrifugal scrubber can be utilized for mass transfer. This configuration eliminates droplet carryover due to entrainment, as the droplets are impacted upon the scrubber walls by centrifugal force. The mass transfer capabilities af a centrifugal scrubber are somewhat greater than those of a comparable simple spray tower.

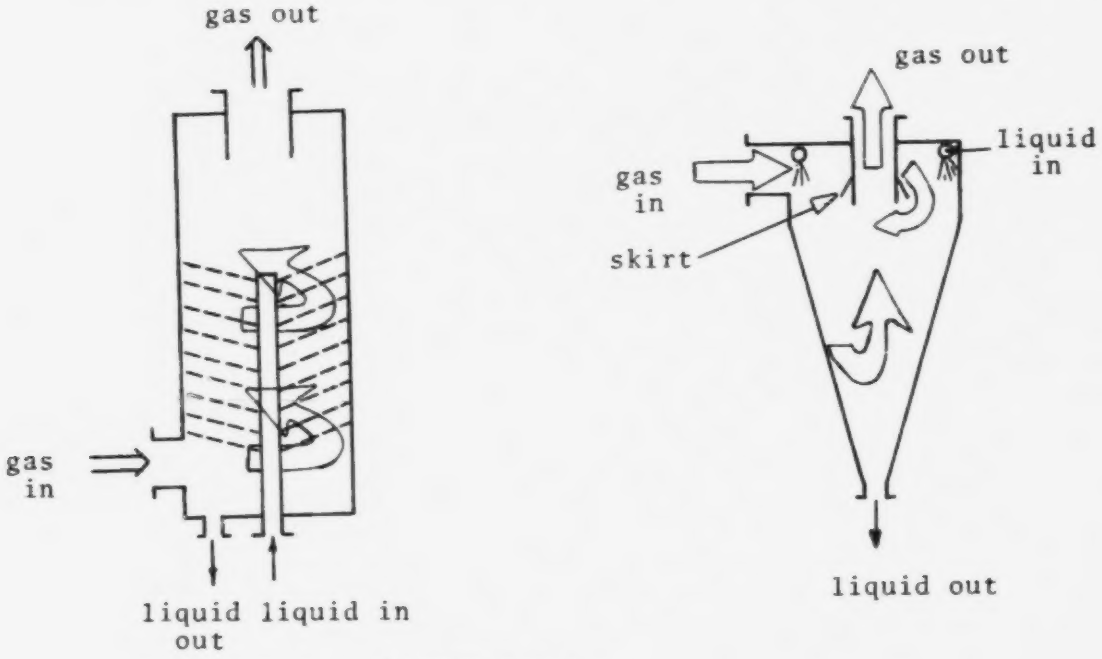

FIGURE 3.1-6
TWO KINDS OF CENTRIFUGAL SCRUBBERS

3.1.8 BAFFLE AND SECONDARY FLOW SCRUBBERS

Baffle type collection devices are designed to cause changes in gas flow direction and velocity by means of solid surfaces. The major direction of flow may be changed, or secondary flow patterns may be caused. Louvers, zig-zag baffles, and disc and donut baffles are examples of surfaces which cause changes in main flow direction. Particle deposition occurs on the targets primarily due to impaction and interception. If the material collected is liquid, it runs down the targets into a collection sump. If solid, the collected particles may be washed intermittently from the target plates.

Baffle devices are often used as entrainment separators, collecting the water droplets produced in an upstream process - often a scrubber. Baffle collectors which capture particles by changing the direction of gas flow generally have good efficiency on particles greater than 20 microns in diameter. Baffle mist eliminators, with more collecting surfaces, can have good efficiency on particles or drops down to 5 microns in diameter. Secondary flow collectors can be designed to have good efficiency on particles of 1 or 2 microns diameter. Pressure drop is usually low - on the order of 1-3 inches of water.

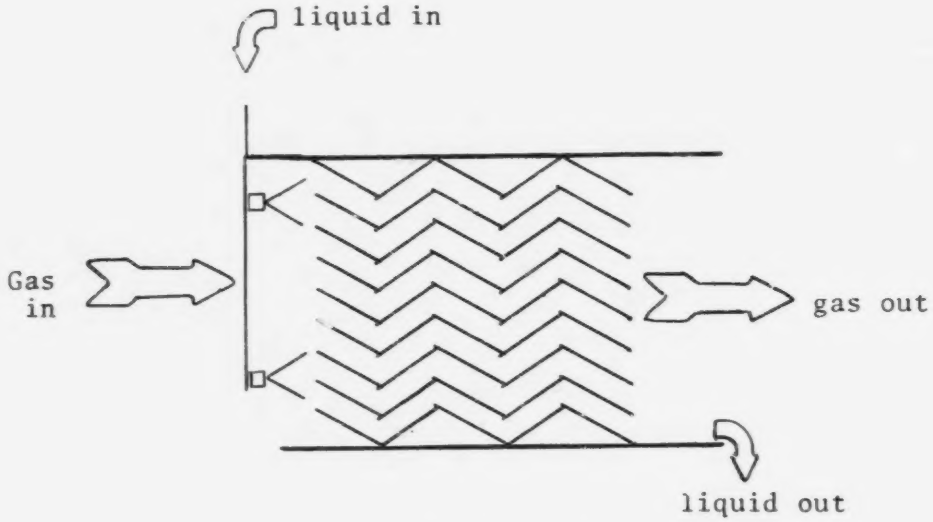

FIGURE 3.1-7

ZIG-ZAG BAFFLE DEVICE

3.1.9 IMPINGEMENT AND ENTRAINMENT SCRUBBERS

Impingement and entrainment scrubbers employ a shell which holds liquid. Gas introduced to the scrubber is made to skim over the liquid surface to reach a gas exit duct. In skimming over the liquid, the gas atomizes some of the liquid into droplets. These droplets act as the particle collecting and mass transfer surfaces which bring about gas purification in the scrubber. The gas exit duct is usually so designed as to turn the gas/droplet system flowing through it, acting as an entrainment separator.

Impingement and entrainment scrubbers are most frequently used for particle collection, although they can be used for mass transfer. They are usually used to collect particles larger than several microns in diameter. Pressure drop may range from 10-50 cm (4 to 20 inches) of water column, although the lower pressure drops are more common.

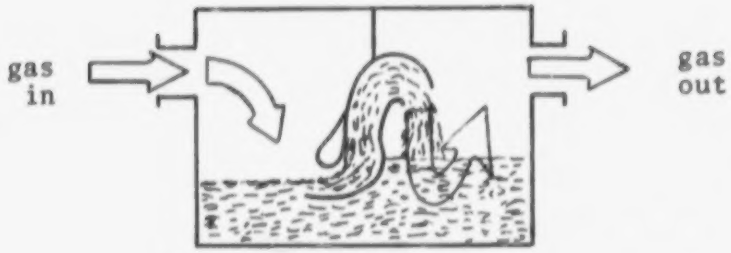

FIGURE 3.1-8

EXAMPLE OF IMPINGEMENT AND ENTRAINMENT SCRUBBER

3.1.10 MECHANICALLY AIDED SCRUBBERS

Mechanically aided scrubbers are scrubbers which incorporate a motor driven device between the inlet and the outlet of the scrubber body.

Often, the motor driven devices are fan blades, used to move the air through the scrubber. Particles are collected by impaction upon the fan blades, while the gas is moved through the device. Usually, liquid is introduced at the hub of the rotating fan blades. The liquid then runs over the blades, washing them of collected particles. The liquid is caught by the fan housing, which drains into a sump. Liquid to mechanically aided scrubbers can usually be recirculated. Particle collection efficiency is good for particles larger than one or two microns in diameter. Advantages of this type of collecting device include low space and water requirements. The main disadvantage is high operating cost.

Disintegrator scrubbers use a submerged, motor driven impellor to atomize liquid into small droplets. The drops fly from the impellor across the gas stream, collecting particles on the way. Although disintegrator scrubbers are efficient on submicron particles, they have a high operating cost due to the energy necessary to drive the impellor. Venturi scrubbers can usually achieve the same efficiency as disintegrators, but at a lower rate of power consumption.

Mechanically aided scrubbers are used almost exclusively for particle collection. Their mass transfer capabilities are generally low, due to the relatively low amount of liquid available for contacting.

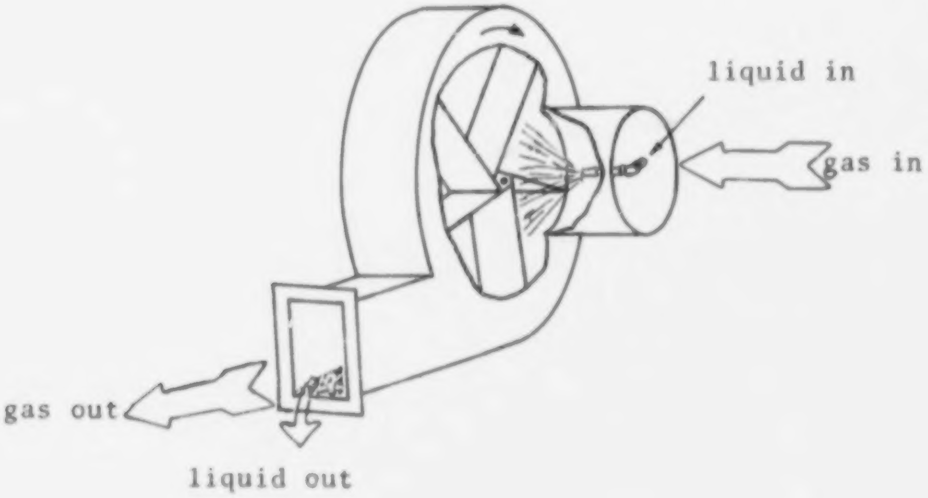

FIGURE 3.1-9
MECHANICALLY AIDED SCRUBBER

3.1.11 MOVING BED SCRUBBERS

Moving bed scrubbers provide a zone of mobile packing, usually plastic, glass, or marble spheres, where gas and liquid can intimately mix. A cyclindrical shell holds a perforated plate, on which the movable packing is placed. Gas passes upwards through the packing, while liquid is sprayed up from the bottom through the perforated plate, and/or down over the top of the moving bed. Gas velocities are sufficient to move the packing material around when the scrubber is operating. This movement aids in making the bed turbulent, and keeps the packing elements clean.

Moving bed scrubbers are used for particle collection and mass transfer - often when both must be carried out simultaneously. Particle collection efficiency can be good on one micron particles. Mass transfer and particle collection are both enhanced when several moving bed stages are used in series. Pressure drop is typically 7-15 cm W.C. per stage.

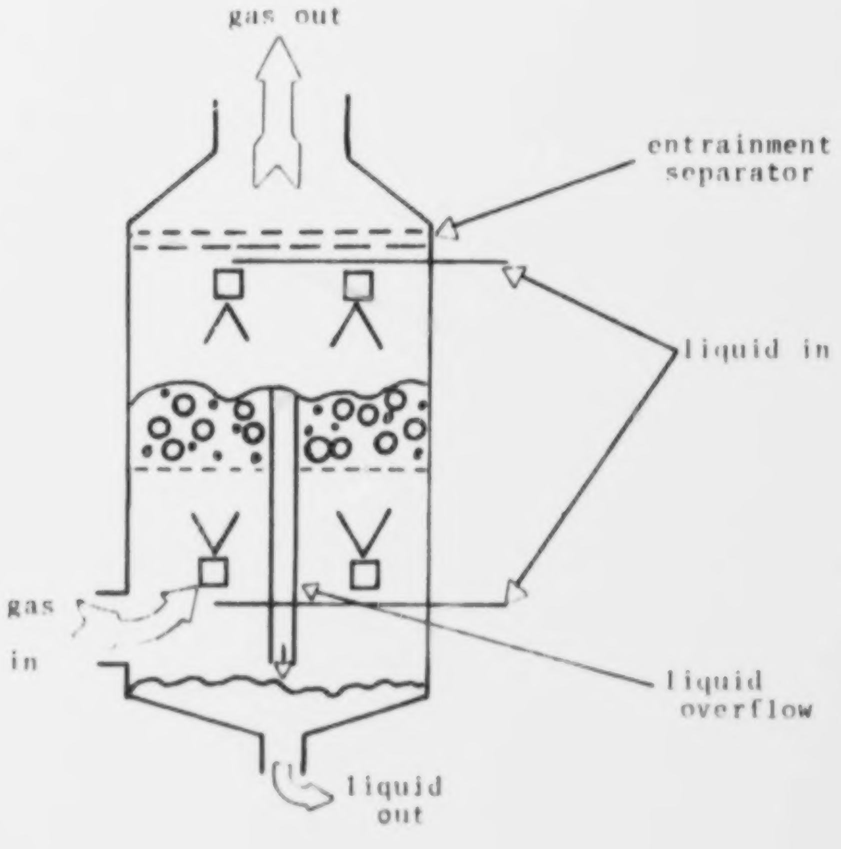

FIGURE 3.1-10

MOVING BED SCRUBBER

3.2 COMMERCIALLY AVAILABLE SCRUBBERS

A survey of scrubber manufacturers was conducted to determine what types of scrubbers are currently available and who makes them. Companies are both entering and leaving the scrubber field all the time, so at best a list of scrubber manufacturers and their products can only be accurate at the time the list is compiled.

Many companies who were thought to manufacture scrubbers and who were contacted, through oversight or neglect did not respond to our inquiries. Other companies chose not to respond to our inquiries. Although a sincere effort was made to contact all scrubber manufacturers undoubtably some oversights occurred. To the extent that scrubber manufacturers inadvertantly or deliberately chose not to participate in the survey, or were not contacted at all, this listing was incomplete at the time it was made.

The scrubbers are broken down according to the groups into which they fall, as defined in the previous section, 3.1. Added to them appears a "combination" category. This contains devices which do not fit into one of the preceeding groups. The devices in the combination group can be described as several scrubbers in series, each of which is identifiable by the number corresponding to one of the ten groups. The combination device can then be described in terms of individual, internal "scrubbers".

Before assigning a scrubber to the combination group, its components were evaluated. In many cases, one internal scrubber appeared to serve as the main particle collector, the other elements being primarily pretreaters or entrainment separators. If a main unit could be identified, the scrubber was classified under the heading of the main collector, rather than as a combination device. For example, a scrubber with a venturi throat, followed by a centrifugal demister, while strictly speaking, a combination gas-atomized spray and centrifugal scrubber would be classified here as a venturi, since the role of the centrifugal action is mainly that of mist eliminator. Devices were included in the combination category only when more than one main component scrubber was identified, or where the main component scrubber was unclear.

The catalog of available scrubbers appears in the following sections.

TABLE 3.2-1
PLATE TYPE
(CATEGORY 1)

Manufacturer	Name
Arco Industries Corporation	Type JS Impingement Scrubber
Chem-Pro Equipment Corporation	Tray Column
Combustion Equipment Associates	Tray Scrubber
Fiber Dyne	Impingement Scrubber
Johnson March Company	Incin-A-Guard
Koch Engineering Company	Flexitray Scrubber
Mass Transfer Ltd.	Tray Columns
Nutter Engineering Company	Towers & Trays
Peabody Engineering Corporation	Peabody Scrubber
Slick Corporation	Impingement Baffle Scrubber
W. W. Sly Manufacturing Company	Impinjet Scrubber
Wheelabrator Corporation	Turbulex Model HS

TABLE 3.2-2
MASSIVE PACKINGS
(CATEGORY 2)

Manufacturer	Name
Aerovent Fan Company	Type US Scrubber
Arco	Packed Beds-Types CPB and CPT
Ceilcote Company	Packed Scrubbers
Corite-Reynolds Corporation	Vertical Packed Scrubber
Corning Glass Works	Packed Towers
Corofac, Inc.	Corodraft Fume Scrubber
Dow Chemical Company	Dowpac (packing)
Dow Chemical Company	Maspac (packing)
Fluorodynamics, Inc.	Series "P" Chemtron Scrubbers
Haveg Industries, Inc.	Packed Tower
Heil	Packed Tower, Series 730 and 730 M
Koch Engineering Company	Packed Beds
Koch Engineering Company	Flexiring Separator
Maurice A. Knight Company	Packed Tower
Norton	Packed Tower + Packings

TABLE 3.2-3

FIBROUS PACKING
(CATEGORY 3)

Manufacturer	Name
ACS Industries	Mistermesh
Aget Manufacturing Company	Miskop
American Air Filter Co., Inc.	Colag
Chem-Pro Equipment Corporation	Hyperfil Packing
Hartzell Propeller Fan Company	Fume Scrubber
Knitmesh Ltd.	Knitmesh Demister
Koch Engineering Company	Sulzer Packing
Koch Engineering Company	Fleximesh Separator
Monsanto	Brink Mist Eliminator
Otto H. York Company	Demister
Packed Column Corporation	Goodloe Column Packing
Pall Trinity Micro Corporation	Filter
Wean Industries, Inc.	KSR Chemical Fume and Vapor Filter

TABLE 3.2-4

PREFORMED SPRAYS
(CATEGORY 4)

Manufacturer	Name
Antipol	Antipol "S", "W" and "L"
Ceilcote Company	Spray Tower
Ceilcote Company	Baffled Spray Tower
Commercial Fabrication and Machine	Quik-Pac
Elliot Division of Carrier Corp.	Swirl-Jet Scrub Cooler
Graham	Type 830,831,832,833,840 Counter Current Scrubber
Graham	Type 820 Scrub-Separator
Heat Systems-Ultrasonics, Inc.	Mystaire Scrubber
Heil Process Equipment Company	Fume Washer, Series 700
Heil	Water Jet Scrubber
Morse Boulger	Gas Washer System
Norton	Ejector Scrubber
Pyro Industries, Inc.	Gas Scrubber
Schutte and Koerting Company	Type 7030 Multiventuri
Schutte and Koerting Company	Type 7010, Type 7014 + Type 7015, Type 7009

TABLE 3.2-5

GAS ATOMIZED SPRAY
(CATEGORY 5)

Manufacturer	Name
Aerodyne Machinery Company	Ventri-clone
Air Pol	Venturi Scrubber
Air Pollution Industries	Flooded Wall Venturi Scrubber
American Air Filter Co., Inc.	Kinpactor
Arco Industries Corporation	Types US, USL, and USP Venturi Scrubbers
Babcock and Wilcox	Venturi
Buell Norblo	Vari-L Scrubber
Carborundum Company	Pangborne Type CV Ventri-Jet
Carter Day Company	Vortex Venturi
Ceilcote Company	Venturi
Chemical Construction Co.(Chemico)	P-A Venturi
Chemical Construction Co.(Chemico)	W A Venturi
Combustion Equipment Associates	Venturi Scrubber
*Dollinger Corporation	Model SV Submerged Venturi
Ducon Corporation	Oriclone Venturi
Ducon Corporation	Wet Approach Venturi
Fecor Industries, Ltd.	Microjet Spray Scrubber
Fluorodynamics, Inc.	Chemtron Series "V"
Heil Process Equipment Company	Venturi Scrubber, Model 720
John Zink Company	Venturi
Koch Engineering Company	Flexiventuri Scrubber
National Dust Collector Corp.	A 3 Series Ventri Rod
Peabody Engineering Corporation	Ventri-Slot
Research Cottrell	Flooded disk
Simpson	Venturi Scrubber
Slick Corporation	Series 400 Scrubber
Slick Corporation	Micro Venturi Impingement Scrubber
UOP	Aeromix Scrubber
Union Carbide	Peterson Separator
Zurn Industries	Venturi Scrubber

TABLE 3.2-6

CENTRIFUGALS
(CATEGORY 6)

Manufacturer	Name
Airetron	Cyclonic Scrubber
American Air Filter Co., Inc.	Type "R" Roto-clone
Anderson	Hief Purifier
Arco	Cyclonic Scrubber
Ceilcote Company	Wet Cyclone
Chemico	PA Cyclone Scrubber
Combustion Equipment Associates	Spray Cyclonic Scrubber
Corite-Reynolds	Vertical-Cyclindrical Centrifugal Scrubber
*Dollinger Corporation	Model WC Wet Centrifugal
Ducon Corporation	Multivane Type "L"
Ducon Corporation	UW-4 Scrubber
Ducon Corporation	UW-3 Scrubber
Koch Engineering Company	Cyclonic Scrubber
Peabody Engineering Corporation	Cyclonic Separator
Peabody Engineering Corporation	Cyclonic Scrubber
Stansteel Corporation	Centrifugal wet washing system
Wright Austin	Exhaust Head

TABLE 3.2-7

BAFFLES
(CATEGORY 7)

Detrick-Jens	Gas Scrubber
Koch Engineering Company	Baffle Separator
Peerless Manufacturing Company	Vane-type Mist Eliminator
Union Carbide	Entrainment Separator Module

TABLE 3.2-8

IMPINGEMENT & ENTRAINMENT
(CATEGORY 8)

APV Company, Inc.	Automatic Gas Washer
American Air Filter Co., Inc.	Type "N" Roto-clone
American Standard, Inc.	Leckenby Scrubber
Antipol	Antipol "T"
Carborundum Company	CPD Scrubber
Leckenby Company	Leckenby Scrubber
United Dust Collectors	Swirl Orifice
Western Precipitator Company	Turbulaire Scrubber
Zurn	Dustrator

TABLE 3.2-9

MECHANICALLY AIDED SCRUBBERS
(CATEGORY 9)

Manufacturer	Name
American Air Filter Co., Inc.	Type "W" Roto-Clone
Centri-Spray Corporation	Centri-Spray
Tri-Mer Corporation	Fan-Separator

TABLE 3.2-10

MOVING BED
(CATEGORY 10)

Buell Norblo	Polysphere Scrubber
National Dust Collector Corporation	Hydro-Filter
UOP	Floating Bed
UOP	Turbulent Contact Absorber
Vari-Systems	Hydro-Filter

TABLE 3.2-11

COMBINATION SCRUBBERS
(MIXED CATEGORIES)

Entoteler, Inc.	Centrifield Scrubber
Johnson March Corporation	Mark II, Multi Stage Scrubber
Research Cottrell, Inc.	Inano-trell
Stansteel Corporation	Model "U"
Stansteel Corporation	Model "D"
Taylor and Company	CUX Scrubber
Taylor and Gaskin, Inc.	Hydroflow Air Washer
UOP	Ventrisphere Scrubber
Western Precipitation Company	Joy Microdyne Scrubber

3.3 SCRUBBER PATENTS

3.3.1 INTRODUCTION

Many scrubbers have been patented, but are not currently being manufactured. A survey of U.S. patents was conducted, to find out information on these devices. This section presents that information.

Patents are divided into groups as defined in Section 3.1, Types of Scrubbers. For each patent, the patent number, date, and assignee are given, along with a comment on its distinguishing features.

TABLE 3.3-1

PLATE TYPE

Patent #	Date	Assignee	Comment
1,172,930	1916	H.A. Brassert and C.J. Bacon, Illinois	Perforated plates
1,794,986	1931	C.B. Schneible, to Joseph Schneible Trust	Plate has single large hole, its cover is supported by swirl vanes
1,817,778	1931	F. W. Sperr, to Koppers Co.	Single plate; high foam layer
1,844,851	1932	Peabody Engineering Corp.	Particle growth due to steam condensation aids
1,980,499	1934	G. C. Pfaff	Each plate sprayed, has baffle deflector over it
2,457,686	1948	Peabody Engineering Corp.	Baffles over plate
2,585,440	1952	Daniel T. Collins, Mich.	Special plate design
2,714,504	1955	Socony Mobil Oil Co., Inc.	Specific designs
2,747,849	1958	E. I. DuPont Company	Slotted plate
2,817,415	1957	H. B. Sykes, to Esso Research & Engineering	Continuous slotted, vertical plate
2,926,754	1960	E. G. Royatz Company	Baffle on plates for mixing
2,972,393	1961	Allied Chem. Corp, N.Y.	Water sprayed into center of truncated conical plates
3,064,955	1962	C. P. Bouette and Shell Oil Corp.	Grid bar trays
3,070,359	1962	G. P. Canevari	Gas passes through risers in plate bypassing liquid and goes to foam above plate
3,105,105	1963	W. Kittel	Kittel plate patent
3,155,472	1964	Herbert Simpson Corp.	Foam scrubber
3,215,414	1965	Shell Oil Company	
3,222,040	1965	J. Eckert	
3,225,522	1965	B. Black	Each perforation in plate is spray wetted venturi
3,233,879	1966	Socony Mobil Oil Co., Inc.	
3,245,669	1966	C. A. Huggins et al.	Valve tray
3,246,687	1966	Shell Oil Co.	
3,287,004	1966	I. E. Nutter	
3,345,049	1967	R. D. McGlothlin	Prefabricated interlocking cylinders form plate tower
3,360,247	1967	Koppers Co., Inc., Pittsburgh, Pa.	Plates are trough-shaped sectors arranged at two levels
3,394,927	1968	Houilleres du Bassin du Nord et al., France	
3,399,870	1968	Shell Oil Co., Netherland	
3,399,871	1968	Compaguire des Atchiers et Forges de la Loire France	
3,401,502	1968	P. [illegible] et al.	Utilizes counterflow pipes in series instead of plates
3,414,248	1968	M.Iwanage & H.Idemitsu,Japan	
3,410,540	1968	W.Bruckert	Each tray packed with fibers
3,425,191	1969	Heinz Butz	One plate with liquid, pull tubes and overflow
3,440,803	1969	P. M. Wechselblatt	Venturi slots in trays fed from elevated troughs
3,445,095	1969	V. Braun	Valve tray with slots
3,463,464	1969	I. E. Nutter, et al.	Trays have tapering apertures
3,467,305	1969	T. J. Webster	Trays have covered slots
3,481,115	1969	Herbert Brandt, Germany	Water is lifted on perforated plates
3,491,987	1970	Norton Company	
3,533,608	1970	E. R. McClure	4 large bubble-caps, one per tray - for smog control

TABLE 3.3-2
MASSIVE PACKING

Patent #	Date	Assignee	Comment
809,383	1906	Leon P. Lowe	Steam injector followed packed tower
1,423,696	1922	A. Evans	Gas bubbles through liq.pool & packed tower
1,543,942	1925	Walter Mathesius	Sprays separated by packing
1,625,831	1927	H. M. Stark	Variety of continuous baffle packing design
2,048,403	1934	Riley Stoker Corp.	
2,165,490	1939	Nat.Aniline & Chem.Corp.N.Y.	Several packed columns in one envelope
2,242,294	1941	Freyn Engineering Company	Gas enters tangen. to packed spray tower
2,431,455	1947	Standard Oil Develop.Co.	4-20 mesh particles collected on packing
2,587,416	1952	Pangborn Corporation	Packing material
2,653,675	1953	George E. Lynch, Cal.	Gas first supersaturated with water vapor, which later condenses on cooler pebbles.
2,661,197	1953	C. D. Patents, Ltd.	Grid packing
2,856,259	1958	A. G. Colasit Company	Activated carbon bed or other high surface material
2,867,425	1959	Harshaw Chemical Company	
2,921,776	1960	The British Oxygen Co., Ltd.	
3,006,436	1961	S & C Mfg. Co., Ohio	Cocurrent packed bed
3,010,706	1961	O.K. Atomic Energy	
3,039,749	1962	The Fluor Corp., Ltd.	Molded packings
3,109,876	1963	Dow Chemical Co.	Trickle filter type sheet packing
3,118,947	1964	Felix L. Yerzley, N.J.	Packed tower operating under flooding cond.
3,122,594	1964	Aluminum Lab Ltd., Canada	
3,167,600	1965	R. G. Worman	
3,170,969	1965	B. J. Lerner et al.	Colloidal part.of inorganic oxide coated to packing
3,192,689	1965	A. B. Smith	Spray,packing + baffles;liq.is recirculated
3,210,914	1965	U. S. Stoneware Co.,Ohio	Two packed towers one by the other, the gas makes a 180° turn
3,266,787	1966	U. S. Stoneware Co.	
3,302,372	1967	Armour Agricultural Chem. Co., Del.	Tower packed with floating spheres
3,311,356	1967	U. S. Stoneware, Inc.	
3,324,630	1967	A. J. Teller	Sprayed cross-flow packing bed
3,347,381	1967	The Mead Corporation	
3,348,825	1967	Nat. Dust Collector Corp.	Filter bed followed by packed column
3,364,656	1968	Universal Oil Prod.Co.,Ill.	Hemispherical packings
3,365,180	1968	Bernard Lerner	
3,386,798	1968	R.S. Beavans,et al. to American Standard, Inc.	Removes H_2SO_4 by reaction with $CaCl_2$
3,391,910	1968	W. H. Prahl	
3,409,279	1968	Esso Research and Engrg.Co.	
3,410,057	1968	B. J. Lerner	
3,415,502	1968	Carl George Munters	
3,430,934	1969	Linde Aktiengesellschaft Hollniegelskreuth,Germany	
3,466,019	1969	R. Priestly	Packing sheets with curved surfaces used
3,475,012	1969	Imperial Chemical Ind,Ltd. England	
3,493,218	1970	Pittsburgh Corning Corp.	
3,496,996	1970	A. Osdor	Geometric packings
3,500,615	1970	G. W. Meek	(Corregated packing) cross-flow
3,506,248	1970	United Air Specialists, Inc.	
3,528,781	1970	S. Gelfman	

TABLE 3.3-3

FIBROUS PACKING

Patent #	Date	Assignee	Comment
1,140,198	1915	H. Smith	Compressor before the filter mat.
2,881,116	1959	R. E. Siegfried	Knitted mesh
2,955,064	1960	S. H. Frohmader	Expanded mesh
2,997,132	1961	Aktiebolnget SvenskaFlaktfabriken, Sweden	Wet fibrous mats to remove Fluor.particles
3,063,216	1962	L. Silverman	Spinning disk forms fibers-clean foundry dust
3,066,462	1962	J.K. Yap et al.-Shell Oil Co.	Series of fiber pads used
3,107,986	1963	W. Plaut, et al.,to I.C.I.LTD	Best to use fibers which do not coat with collected liquid
3,218,048	1965	General Cable Corporation	
3,243,170	1966	S.R.M. Ellis, et al.	Knitted mesh
3,268,296	1966	Hooker Chemical Co.	Liquid spray over fibers
3,370,401	1968	E.I. duPont de Namours,Del.	Wet aerosol passes through fibrous pad
3,458,338	1969	Scott Paper Company	

TABLE 3.3-4

PREFORMED SPRAYS

Patent #	Date	Assignee	Comment
628,750	1899	A. Brechot (France)	Ejector venturi
1,039,008	1912	L. Anderson	Sprays in coil-clean blast furnace top gas
1,459,442	1923	Samuel C. Cutler, Mass.	Spray chamber
1,570,577	1926	A.S. Romero et al.	Sprayed spiral vanes
1,169,764	1916	Hermann A. Brassert, Ill.	Spray tower with several plates
1,734,677		H. Kreisinger, to Internat. Combustion Eng. Corp.	Sprays for capture of dust from coal driers
1,793,620	1931	Babcock and Wilcox Co.,N.J.	Several designs of spray chambers
1,818,143	1931	Harry C. Lyons, N.Y.	Spray chamber at top of chimney
1,868,632	1932	Dexter Edge, Pa.	Spray chamber
1,894,696		O.A. Lindemann to Schutte & Koerting Co.	S & K ejector venturi
2,092,305		R.B. Estes, to Nat'l Smoke Eliminator Inc.	
2,242,294	1941	Freyn Engineering Co.	Gas saturated by sprays, water condenses on particles
2,284,317	1941	E. H. Greenberg	
2,298,139	1942	St. Joseph Lead Company	Steam precond., then water spray tower
2,380,826	1943	M.I. Dorfan	Wet caps for cupola
2,498,468	1950	Hydroblast Corporation	Spray nozzles form roof over pollut.process
2,498,469		The Hydroblast Corp.	Preformed spray making a liquid curtain
2,568,875	1951	Allied Chemical & Dye Corp.	Spray, collect, respray in a tower
2,653,674	1953	Whiting Corp. Ill.	Spray chamber
2,663,382	1953	Aerosol Corp. of America	Aerosol is sprayed to catch particles
2,664,968	1954	Standard Oil Develop.Co.	Steam condensation leads to part. growth
2,709,580	1955	Chokichi Kameya	For mounting on stack
2,750,173	1956	Chemical & Dye Corporation	Plate tower type design,spray cham.in series
2,753,949	1956	Otto Construction Co.	Benzol vapor removal by sprays and resprays in tower
2,802,546	1955	C. L. Clark	
2,830,673	1955	G. Bungass	Spray & bubble through liquid,then pass through filter fabric
2,856,171	1958	Carl Otto	Benzol removal. Spray, collect it and respray in a tower

TABLE 3.3-4 (CONT'D)

PREFORMED SPRAY

Patent #	Date	Assignee	Comment
2,858,903	1958	Madeleine Fallon, L.A., Ca.	Double spray chamber
2,865,619	1958	Farbenfabriken Bayer, Ger.	Spray chamber
2,922,490	1960	So. Lightweight Aggreg. Co.	Elongated horizontal treating zone
2,938,599	1960	Shell Oil Company	Spray tower sprays, cools & condenses
3,036,417	1962	Airfilpat Holdings, Ltd. So. Africa	Spraying on a screen
3,044,235	1962	Frank Schneider	Condense steam on solids by compressing or cooling
3,105,103	1963	Solite Corporation	Preformed spray horiz. in baffled chamber
3,113,007		U.S. Atomic Energy Comm.	Add SiF_4 to condense, coag. & precipitate
3,149,935	1964	Ajem Lab, Inc., Mich. d'Aquitaine, France	Spray chamber
3,237,381	1966	Societe Nationale des Petroles	Gas comes in contact with several sprays successively
3,260,035	1966	Frank de Bellis, Gary, Ind.	Spray chamber
3,325,973	1967	The Evening News Pub.Co.,N.J.	Spraying water and surfactant on a screen
3,347,535	1967	A. J. Schimpke	
3,353,335	1967	Edward A. Caballero	Water & later chemicals are sprayed separately into duct
3,353,799	1967	E. P. Long, et al.	Sprays, packed bed demister
3,385,030	1968	Fabricating Engrg.Co., Pa.	Different ejector designs
3,395,656	1968	Steelcraft Corp., Tenn.	Special design of spray
3,475,881		Orlan Arnold, et al.	Spray humidifies,condenses on particles
3,485,012		Klockner,Humboldt,Dentz,Ga.	Sprays and baffles-for cement industry
3,487,607	1970	R. W. Cox	Heat, spray, centrifugate, condense
3,488,924	1970	Effluent Controls, Inc.	Spray, centrifugal demister
3,494,099		Electrosonic Pollution Control Corporation	Electrically charged, chemically active fog is coag. by sonics
3,518,812	1970	Ernest Kolm	Humidify to 100% saturation, condense on particles

TABLE 3.3-5

GAS ATOMIZED SPRAY

Patent #	Date	Assignee	Comment
895,790	1908	Richards Gas & Fume Conden.Co.	Venturi,spray & baffles-use in smelters
970,654	1910	Francois Sepulchre, Belgium	Injector
1,182,543	1916	B. Ferguson	
2,077,427	1937	International Precipit.Co.	Essentially venturis in series
2,579,282	1951	Pierre Georges Vicard, France	Venturi Scrubber
2,596,104	1952	C. Schneible	Liq.atomized by swirling gases, collected & reatomized in stages
2,596,105	1952	C. Schneible	Gas rotating through col.atomizes liquid
2,596,106	1952	C. Schneible	Gas rotating through col.atomizes liquid
2,746,564	1956	J. M. Humber Corporation	For removal of carbon black
3,009,687	1961	P.F.A.M., Hendricks	Sheet wetted converging throat
3,085,793	1963	Chemical Construction Co.	Venturi with conical baffle in the throat and liquid introduction design
3,116,989	1964	John W. Warren	Series of orifice plates used
3,131,237	1964	T. T. Collins	Various means to introduce liquid
3,138,441	1964	Aktiebolaget Svenska Flaktfabriken, Sweden	Varied washing liquid inlet design
3,138,442	1964	Aktiebolaget Svenska Flaktfabriken, Sweden	Venturi followed by cyclone. Venturi below liquid surface.
3,138,647	1964	Aktiebolaget Svenska Flaktfabriken, Sweden	Variable throat design
3,142,548		Aktiebolaget Svenska Flaktfabriken, Sweden	Venturi ending in liquid pool with fiber mat side openings
3,145,239	1964	Airetron Eng. Corp., N.J.	Venturi
3,170,007		Aktiebolaget Svenska Flaktfabriken, Sweden	Steam pretreatment followed by venturi
3,189,332	1965	Jones & Laughlin Steel Corp.	
3,239,999	1966	H. Price et al.	Venturi rod
3,251,174	1966	A. Ahlstrom Osakeyhtio	
3,279,156	1966	Aktiebolaget Svensk Flaktfabriken, Sweden	
3,284,435	1966	R. A. McIlroy et al.	For gas absorption
3,323,290	1967	Hans Stern, 17 Morris Crescent, Selection Pk,So.Africa	Modified multi-venturi type collector
3,332,214	1967	Nat. Dust Collec.Corp.,Chicago Illinois	Gas flows through a partially submerged modified venturi
3,339,344		Waagner-Biro Aktiengesellschaft	Spray, followed by venturi, then knockout plates
3,347,024	1967	Aktiebolaget Svenska Flaktfabriken, Sweden	Multichannel venturi
3,353,334	1967	Princeton Chemical Res.Corp.	Pyrometallic Dianhydride aerosol
3,347,024	1967	Aktiebolaget Svenska Flaktfabriken, Sweden	
3,388,897	1968	Automotive Rubber Co., Inc.	
3,396,514	1968	The Babcock & Wilcox Company	Slurry handling in a venturi system
3,405,918	1968	Airetron Engineering Corp.	
3,406,953	1968	U.S. Stoneware	Design and packed bed
3,415,039	1968	Whiting Corporation	Removes HF + SiF_4,converts to H_2SiF_6 for water treatment
3,421,692	1969	R.S. Babington et al.	Method for making monodisperse aerosol
3,439,475	1969	Nordac Ltd. (England)	Water sprayed onto series of orifice plates
3,490,204	1970	Combustion Engineering,Inc.	Aerothermocompressor principle used with venturi
3,495,813	1970	Al'Kan Research & Develop.Co.	Helical passage, gas drawing in liquid + atomizing it
3,502,308	1970	Kiyosi Simizu	Conical plug in inlet maintains constant gas velocity
3,518,816		M.M. Jolona	

TABLE 3.3-6

CENTRIFUGAL

Patent #	Date		Comment
457,493	1891	Allington & Curtis Mfg. Co.	A double cyclone
467,264	1892	A. Raymond et al.	Water & exhaust steam spray.to cyclone mist
1,483,348		Hayes et al.	Vanes in pipe providing centrifugal force
2,281,254		A.W. Anthony	Sprays from cylinder axis course across rotating gas
2,473,672	1949	G. C. Ziliotto	Horizontal cylinder, liquid on bottom-vanes to centrifugate
2,473,372	1949	Filiotte	
2,496,281		E.F. Fisher	Spray into swirl vanes
2,560,071	1951	Centrifix Corporation	Fixed centrigual devices in a tower
2,588,106	1952	G.H. Frangquist to Combust. Engineering Inc.	Coarse material injected to cyclone to agglomerate fines
2,649,291	1953	Ben Bartolucci	Detachable vane providing centrifugal force
2,684,232	1954	W. J. Caldwell	Downward whirl water spray
2,804,450	1957	Combustion Engineering,N.Y.	Liquid sprayed into gas flowing in spiral path
3,054,244	1962	Fuller Co.	
3,225,523	1965	D. Wiebe	Sprays in cyclinder walls
3,237,385	1966	A. Nutting, to American Air Filter Company	Centrifugal precleaner + wetted wall centrifugal scrubber
3,343,336	1967	Y. Broyard	Tangential inlet & outlet
3,343,346	1967	Yvon Broyard	Centrifugal
3,385,029		R.C. de Vries,to Shell Oil	Cyclone cleans,then water spray cools the gas
3,395,513	1968	Werner von Unwerth	
3,421,296	1969	F. C. Beurer, to United Aircraft	Multicyclone aircraft engine precleaners
3,443,364	1969	R.D. Saltsman, assigned to Bituminous Coal Research,Inc.	Spray in inlet duct; involuted inlet duct
3,494,107		W.J. Sackett	
3,488,924	1970	D.H. Reeve	Sprays in tangential inlet
3,492,790	1970	P. Ebert	Electrostatic aided

TABLE 3.3-7

BAFFLE

Patent #	Date	Assignee	Comment
2,074,319	1937	International Harvester Co.	Process to collect dust in air & remove
2,083,468	1937	Riley Stoker Corp	Deflecting baffles in gas passage
2,772,748	1956	Shell Development Co.	Entrainment separation design above plate
3,022,859	1962	American Air Filter Co.,Ky.	Packing for improved mass transfer
3,075,751	1963	Herand K. Najarian	Tortuous wetted wall ducts
3,122,594	1964	Aluminum Lab Ltd, Canada	Packing of floating spheres
3,133,875	1964	FHA Meister Lucius & Bruning Germany	Liquid piston type rotary blowers
3,256,001	1966	P. N. Renzi	Sprayed baffles-collecting elements rotated
3,262,682	1966	S.J.H. Bredberg	Sprayed wave type baffles
3,266,224		J.W. Todd Feretti	Apertured plates with deflector
3,273,316	1966	Sigmund L. Ross, N.Y.	Collection improved due to temperature shade
3,350,075	1967	Domtar Ltd.,Montreal,Canada	Increasing transfer area through use of light weight elements
3,390,869	1968	Howard Alliger, N.Y.	Spray nozzle simultaneously deliver compressed air saturated steam and ultrasonic vibrat. across the chimney
3,395,510	1968	General Electric Co.	Method of removing particles comprising of injecting steam and other steps.
3,404,512	1968	Universal Oil Products,Ill.	Two scrubbers in series. 1st cleans, 2nd servces as a heat exchanger
3,450,393	1969	C.G. Munters	2 superimposed sets of wetted wave type baffles
3,444,670	1969	E.C. Hangate	Removes lint from breathing air
3,467,620		Nicholas Klein	Screen in stack, cooled by water
3,486,307	1969	L.C. McDermott	Bubble Column
3,500,615	1970	Carl Munters & Co., Sweden	Special packing for a mist eliminator

TABLE 3.3-8

IMPINGEMENT & ENTRAINMENT

Patent #	Date	Assignee	Comment
2,527,450	1950	Springfield Boiler Company	Impingement on wet baffles in path of steam
2,689,715	1954	Paul Ericson, Pa.	Specially designed impingement plates
3,364,660		Societe Prat-Daniel, Paris France	
3,475,951	1969	Calif. Inst. Research Found.	Impingement and entrainment
3,514,924	1970	R. J. Flebu	Entrainment scrubber with centrifugal demister

TABLE 3.3-9

MECHANICALLY AIDED

1,132,677	1915	T.E. Murray et al.	Squirrel cage fan is close to wetted housing
2,195,707	1940	A. Nutting, to American Air Filter Co.	Sprays on fan - evolved to Rotoclone

TABLE 3.3-10

MOVING BED SCRUBBERS

3,334,470		Nat'l Dust Collector Corp.	Hydrofilter

TABLE 3.3-11

COMBINATION

3,009,538	1961	American Air Filter Co.	Baffles,venturi + plates in cylindrical shell
3,173,771	1965	Western Precipitator Co.	Joy Microdyne Scrubber
3,412,529	1968	J.P. Taylor	CUX Scrubber

CHAPTER 4

BASIC CONCEPTS

TABLE OF CONTENTS

4.1 Introduction 4
  4.1.1 General Approach to Design 4
  4.1.2 Unit Mechanisms Definition 4

4.2 General Concepts of Mass Transfer. 8
  4.2.1 Introduction 8
  4.2.2 Mass Transfer Mechanisms 8
    4.2.2.1 Mass Transfer to Molecular Diffusion. 8
    4.2.2.2 Mass Transfer by Eddy Diffusion 10
  4.2.3 Interphase Mass Transfer Theories. 10
    4.2.3.1 Mass Transfer Coefficients. 10
    4.2.3.2 Whitman - Film Theory 11
    4.2.3.3 Higbie - Penetration Theory 12
    4.2.3.4 Danckwerts - Random Surface Renewal Theory. 13
  4.2.4 Factors Affecting and/or Limiting Mass Transfer. 13
    4.2.4.1 Equilibrium Limitations 13
    4.2.4.2 System Changes - Liquid Phase 14
    4.2.4.3 System Changes - Gas Phase. 14
    4.2.4.4 Equipment Limitations 14
  4.2.5 Definitions of Efficiency. 15
  4.2.6 Mass Transfer with Chemical Reaction 17
    4.2.6.1 Reaction Kinetics 17
    4.2.6.2 Film Model Mass Transfer with Chemical Reaction .18
    4.2.6.3 Instantaneous Reaction Criteria 22
    4.2.6.4 Gas and Liquid Resistance - Film Model. 24
  4.2.7 Slurry of Sorptive or Reactive Particles 26
    4.2.7.1 Mass Transfer to Suspended Particles. 26
    4.2.7.2 Sorptive Slurries 27
    4.2.7.3 Biological Mass Slurries. 29
    4.2.7.4 Catalyst Slurries 30
    4.2.7.5 Reactive Solids Slurry. 30
    4.2.7.6 Computational Aides 31
  4.2.8 Simultaneous Heat and Mass Transfer. 33
    4.2.8.1 Introduction. 33
    4.2.8.2 General Principles. 34
    4.2.8.3 Air-Water 35
    Nomenclature. 44
    References. 48

4.3 General Concepts of Particle Collection. 50
  4.3.1 Introduction. 50
  4.3.2 Definitions and Terminology 50
    4.3.2.1 Dispersion Aerosols. 50
    4.3.2.2 Particle Size. 51
    4.3.2.3 Particle Size Distribution 52
  4.3.3 Nature of Suspension of Particles 54
    4.3.3.1 Motion of Individual Particles 54
    4.3.3.2 Brownian Motion and Diffusion. 56
    4.3.3.3 Electrostatic Properties 57

CHAPTER 4 - TABLE OF CONTENTS

4.3.3.4 Aerosols in a Magnetic Field 59
4.3.3.5 Radiometric Forces 60
4.3.4 Phenomena Leading to Change in Particle Size Distribution. 62
4.3.4.1 Brownian Coagulation 62
4.3.4.2 Coagulation of Particles in Laminar Flow 64
4.3.4.3 Coagulation of Aerosols in Turbulent Flow. . . . 65
4.3.4.4 Coagulation of Aerosols Having Electrically Charged Particles 66
4.3.4.5 Polarization Coagulation of Aerosols 66
4.3.4.6 Coagulation by Ultrasonic Vibrations 67
4.3.4.7 Kinematic Coagulation of Aerosols. 68
4.3.4.8 Condensation and Evaporation 69
4.3.4.9 Chemical Reaction. 71
4.3.4.10 Aerosol Build-up Techniques. 72
Nomenclature 76
References 79

4.4 Gas-Liquid Contacting. 81
4.4.1 Bubble Hydrodynamics. 81
4.4.1.1 Single Bubbles 81
4.4.1.2 Bubble Clouds - Sieve Plates 83
4.4.2 Drop Hydrodynamics. 84
4.4.2.1 Drop Size Distribution by Liquid Atomization. 84
4.4.2.2 Drop Steady State Motion 85
4.4.2.3 Drop Acceleration. 86
4.4.2.4 Drop Behavior in Motion. 86
4.4.3 Contacting Scheme 87
Nomenclature. 91
References. 93

4.5 Unit Mechanisms for Mass transfer. 95
4.5.1 Drops 95
4.5.2 Bubbles 98
4.5.3 Mass Transfer to Liquid Sheets. 102
Nomenclature. 108
References. 110

4.6 Unit Mechanisms for Particle Separation. 112
4.6.1 Introduction. 112
4.6.2 Collection by Drops 112
4.6.2.1 Inertial Collection. 113
4.6.2.2 Interception 115
4.6.2.3 Gravitational Collection of Particles by Drops .115
4.6.2.4 Diffusion. 116
4.6.2.5 Electrostatic Collection.. 117
4.6.2.6 Magnetic Collection. 120
4.6.2.7 Diffusiophoresis 120
4.6.3 Collection by Cylinders 120
4.6.3.1 Impaction. 120
4.6.3.2 Interception 121
4.6.3.3 Collection of Particles by a Fiber Due to Gravity 121

CHAPTER 4 - TABLE OF CONTENTS

4.6.3.4 Collection of Particles by a Fiber Due to Brownian Diffusion. 122
4.6.3.5 Electrostatic Attraction. 122
4.6.4 Collection of Particles by Bubbles 123
4.6.4.1 Inertial Collection 123
4.6.4.2 Collection by Diffusion 125
4.6.4.3 Collection of Particles by Bubbles Due to Combined Effect of Electrostatic and Inertial Forces After Bubble Formation. . . . 126
4.6.4.4 Collection of Particles by Rising Bubbles Due to the Combined Effect of Diffusion, Diffusiophoresis and Thermophoresis 129
4.6.4.5 Condensation on Particles 132
4.6.5 Deposition from a Moving Aerosol in Pipes and Ducts. . 133
4.6.5.1 Diffusive Deposition of Fine Particles in Laminar Flow. 133
4.6.5.2 Diffusion of Small Particles Through a Turbulent Boundary Layer 135
4.6.5.3 Inertial Deposition from Turbulent Flow . . . 136
4.6.5.4 Deposition of Aerosol from Turbulent Flow Due to Inertial and Brownian Motion 143
4.6.6 Collection of Particles by Liquid Jets 144
4.6.7.1 Introduction. 144
4.6.7.2 Inertial Collection 144
4.6.7.3 Combined Inertial and Diffusiophoretic Collection. 149
4.6.7.4 Combined Inertial and Thermophoretic Collection. 149
4.6.7.5 Combined Inertial and Electrostatic . . . . Collection. 150
Nomenclature. 160
References. 164

4.7 Effect of Pressure and Temperature on the Collection of Particles in Wet Scrubbers 167
Nomenclature. 178

CHAPTER 4

BASIC CONCEPTS

4.1 INTRODUCTION

4.1.1 GENERAL APPROACH TO DESIGN

Design methods are ideally based on general and rational relationships among the process variables. In other terms, it is best to understand what is going on in a scrubber and to relate scrubber performance to the basic processes or mechanisms by which particles or molecules transfer from the gas being cleaned. By using a mathematical relationship of the proper form to describe what happens physically and chemically, one can be more confident that this relationship is valid over a wide range of conditions and can be extrapolated beyond the experimental data with useful accuracy.

Empirical relationships must be resorted to in many cases where the theory has not been worked out or where the physical situation is too complicated to permit theoretical treatment within a reasonable time. Furthermore, and unfortunately, there are many cases for which we do not even have good empirical data. In these cases, a rational approach can at least give a first approximation of anticipated performance.

For reasons other than design, it is also most important to have a clear understanding of what is or may be happening and to be able to estimate probable magnitude. Whether deciding which type of equipment is best, or evolving the best operating conditions for existing equipment, or trouble shooting an operating problem, insight pays off. What may pass for engineering intuition and judgment is doubtless founded on a concept of basic mechanisms and the ability to estimate quantities.

Chapter 4 is the foundation of this presentation of knowledge of scrubbers. It is a companion to Chapter 5, and the appropriate pairs dealing with similar subject matter should be read, even if one is reading selectively, in order to obtain the total picture.

4.1.2 UNIT MECHANISMS DEFINITION

Unit mechanisms for mass transfer and particle collection are the basic physical and chemical situations in which contaminants are taken out of the gas. Analogous to the unit operations of chemical engineering, they are the elemental building blocks from which scrubbers are formed. Unit mechanisms are not the same as transport phenomena, any more than unit operations are the same as transport phenomena. They both involve the transport phenomena, but in addition, they include specific physical configurations.

Mass transfer and particle collection by single drops of liquid are unit mechanisms. Each involves, or could involve, any or several of the transport phenomena, such as molecular diffusion, turbulent diffusion, inertial impaction, electrostatic attraction, and so forth. It can also involve the interaction of these transport phenomena with the special conditions of chemical reactions in the gas or liquid phase and the evaporation or condensation of liquid.

Venturi

To illustrate the possible use of the unit mechanisms approach, let us consider mass transfer and particle collection in a venturi scrubber. If the liquid is introduced in the form of jets entering the throat, there is a region where mass and particles may be transferred to liquid jets. A complication upon the transfer to liquid jets would be the special case of unstable and disintegrating jets. In the next region downstream, drops form and the unit mechanism describing the transfer rates is transfer to drops. The subdivisions or special cases would be drops which are being formed, are stagnant, oscillating, subject to drag force, and coalescing. Some liquid would collect on the walls of the venturi and run in rivulets and sheets. Transfer to liquid sheets would be the unit mechanism describing the transfer processes and rates in this zone.

In the entrainment separator, following the venturi, there would be additional zones where drops coalesce with one another, impinge on liquid surfaces, and may exist for some period as quiescent or oscillating drops attached to liquid surfaces. There would be additional zones of liquid streams (jets) and liquid sheets.

The design engineer who must estimate transfer rates or coefficients for a venturi scrubber in situations where experimental data are not available or perhaps for a scrubber of modified design, can utilize the unit mechanisms in the following way:

1. Analyze the flow phenomena inside the scrubber and postulate the possible types of flow, geometry and patterns of flow.

2. Identify the unit mechanisms which are active in the scrubber.

3. Predict the transfer rate, per drop or per unit of liquid surface.

4. Estimate the fraction of liquid flowing as jets, drops, liquid sheets, and the flow scheme by which the liquid passes from one zone to another.

5. Compute the phase compositions as the liquid and gas pass from zone to zone, by utilizing the transfer rates predicted for the unit mechanisms and the material balance, composition, and equilibrium data which must also be provided.

Techniques for handling co-current, counter-current, and cross-flow situations will be similar to those which have been developed in chemical engineering treatment of the subject to date.

Sieve Plate

Another example of the unit mechanism approach is the analysis of the sieve or perforated plate scrubber. Contact between the gas and liquid phases will be by means of the following unit mechanisms: Jets of gas emerging from the perforations and passing into the liquid, and bubbles of gas from the time of formation through the zones of rising through the liquid and coalescing with other bubbles.

In addition to the unit mechanisms, it is also necessary to define the flow patterns (or operating line) for each of the streams. Here the customary chemical engineering approaches would be utilized. The liquid phase might be assumed to be perfectly mixed if the column is small and the liquid drips through the perforation. If the plate is large, and especially if the liquid is introduced at one side of the plate, then the liquid might be assumed to flow across the plate in plug-flow fashion. That is, the liquid would be perfectly mixed in the vertical direction, but not in the horizontal.

There are also other ways of representing the liquid flow pattern, such as residence time distribution of various degrees of mixing, ranging from plug flow to complete mixing. It will also be necessary to have equilibrium, any chemical kinetics, particle data, temperatures and pressures, and other pertinent data necessary to define the transport phenomena involved.

Impingement Plate

Further exposition of the unit mechanism approach, is given in its application to the Peabody type scrubber. This is a plate type scrubber comparable to a sieve plate except that there are solid impingement surfaces placed above the perforations. The unit mechanisms would be as follows: transfer from jets of gas, transfer from jets impinging on solid surfaces, transfer of drops formed by the atomizing action of the gas jets impinging on liquid and wetted solid surfaces, transfer to bubbles, transfer to any liquid sheets formed upon the column walls by liquid drops collecting and running down.

Additional data on flow patterns and physical and chemical conditions would have to be provided.

Mobile Packing

In the turbulent contact absorber there are plastic balls or shells which are about the same density as water, and are free to move between upper and lower constraining plates or screens. The packing and the liquid fed to the plate are violently agitated by the gas flow at the usual operating rate. The unit mechanisms involved would be as follows: transfer from gas jets emerging from the support plate, transfer to liquid jets which may be formed at the support plate at high gas velocities, transfer to liquid drops, transfer to liquid sheets formed by the impingement of drops upon pingpong or whiffle balls, transfer to liquid sheets formed by the runback of liquid along the column walls.

Mixing of the gas phase in this type of apparatus, as usually operated, is usually simple and could be assumed to be plug flow. Liquid mixing is more complex, depending as it does upon the motion of the balls as well as upon that of entrained liquid not attached to balls.

One approach would be to subdivide the column into parallel, vertical elements in which the balls are flowing either up or down. One set of elements would be for liquid and gas in cocurrent flow, and the other set would be for liquid and gas in countercurrent flow (gas moving up, balls moving down). Another approach is to define a liquid residence time distribution or mixing parameter.

Packed Column

Considerable research has been done on packed columns and much of the analysis has been along the lines of this approach. The unit mechanisms are as follows: transfer to sheets of liquid, transfer to oscillating drops of liquid supported on packing elements, transfer to curved surfaces.

If special conditions such as operating flooded or partly flooded are in effect, there may be additional mechanisms. For example, if a shallow bed of packing is operated such that flooding occurs above the packing (such as the marble bed scrubber), then in addition to transfer by the unit mechanisms listed above, there would also be jets of gas emerging from the openings in the marble bed into the liquid or froth layer: transfer to bubbles of gas, and transfer to liquid sheets formed along the column walls and perhaps other surfaces.

Here again, as in all cases, the liquid and gas mixing patterns, flow rates, and equilibria must also be known in order to define the compositions of the phases in contact at various points in the apparatus.

4.2 GENERAL CONCEPTS OF MASS TRANSFER

4.2.1 INTRODUCTION

The travel of a gas or liquid component in a mixture or solution from a region of high concentration to one of low concentration, is defined as mass transfer. A visual example of this is obtained by dropping crystals of potassium permanganate ($KMnO_4$) into a beaker of water. The $KMnO_4$ begins to dissolve in the water, and very near the crystals there is a dark purple concentrated solution. The progress of diffusion (mass transfer) can be followed by observing the growth of the purple region - dark purple where the $KMnO_4$ concentration is high and light purple where it is low.

Under stagnant conditions, the mass transfer of $KMnO_4$ would occur by molecular diffusion; whereas if the liquid were stirred, the mass transfer could also take place by eddy diffusion. Molecular diffusion is a much slower process than is eddy diffusion, where masses of the gas or liquid move as a whole. In either case, eventually the $KMnO_4$ would dissolve in the liquid and distribute itself uniformly throughout the liquid until it is saturated. At this stage it has reached the equilibrium condition (solubility limit) and no further dissolution and mass transfer can occur. Molecular diffusion, eddy diffusion, and eventual equilibrium take place in the gas phase, the liquid phase, or in a gas-liquid system.

In scrubbing processes, one or more selected components is removed from a mixture of gases by absorption into a liquid phase. The rate of interphase mass transfer is controlled largely by the diffusivities and the concentration gradients Chapters 4.5 and 5.2 analyze and discuss the rate of transfer and Chapter 10 catalogues the physico chemical constants of equilibrium and diffusion. In some cases, the gaseous components react with the liquid, following dissolution, to form a new compound. In these cases the reaction rate constant and the reaction equilibrium constant are important. These are also listed in Chapter 10.

In this section we discuss the basic mechanisms: interphase mass transfer theories, mass transfer limitations, definitions of efficiency, and mass transfer with chemical reaction. So many good texts on this subject are available that it is not necessary to go into too much detail, (see Perry's Handbook, 1963; Sherwood and Pigford, 1952; Danckwerts, 1970).

4.2.2 MASS TRANSFER MECHANISMS

4.2.2.1 Mass Transfer by Molecular Diffusion

Molecular diffusion is the process by which mass transfer takes place in a liquid or gas mixture where a component's concentration varies from point to point in the mixture. Simply because of the thermal motion of the molecules, they will move from a region of high concentration to a region of lower concentration. At a point, the mole flux of a component "A" by molecular diffusion is:

$$\hat{N}_A = -D \frac{\partial \hat{c}_A}{\partial Z} \quad \left(\frac{\text{g mol}}{\text{cm}^2 \text{ -sec}}\right) \tag{4.2.2-1}$$

where "Z" is the distance, "$\hat{C}$" is the total concentration (moles/vol), "x_A" is the mole fraction of "A" in the mixture, "N_A" is the mole flux (moles/area/time), and "D" is the diffusivity of "A" in the mixture, $cm^2\ sec^{-1}$ or similar units. Diffusivities and methods for their estimation are given in Chapter 10.

Gas-phase

At steady state, the diffusion of "A" through other components which are stagnant, is given by

$$\hat{N}_A = \frac{D_G\ P}{R_g\ T\ Z\ p_{BM}} (p_{A1} - p_{A2}) \tag{4.2.2-2}$$

where "Z" is the distance through which "A" diffuses, "p_{A1}" and "p_{A2}" are the partial pressures of "A" at the fixed planes 1 and 2 and "p_{BM}" is the log-mean partial pressure of the inerts, defined as:

$$p_{BM} = \frac{p_{B2} - p_{B1}}{\ln \left(\frac{p_{B2}}{p_{B1}}\right)} \tag{4.2.2-3}$$

For common scrubbing applications where "A", the component to be scrubbed, is very dilute in the gas, $p_{BM} \approx p$. Even for relatively high levels of "A", "p_{BM}" is negligibly different from the arithmetic mean, $(p_{B1} + p_{B2})/2$. Gas-phase diffusivities are of the order of 0.1 cm^2/sec.

Occasionally the expression for equimolal counter diffusion may apply in a wet scrubber situation, e.g. an adiabatic absorption where water replaces the contaminant in the gas stream on a mole-for-mole (or suitably modified, on a weight-for-weight) basis. This equation is:

$$\hat{N}_A = \frac{D_G}{R_g\ T\ Z} (p_{A1} - p_{A2}) \tag{4.2.2-4}$$

Liquid-phase

A precise theoretical description for diffusion in liquids is lacking but the expression usually employed for steady-state diffusion of component "A" through a solvent is:

$$N_A = \frac{D_L}{Z} (c_{A1} - c_{A2}) \tag{4.2.2-5}$$

Liquid-phase diffusivities are so much smaller than those in the gas-phase (D_L is of the order of 10^{-5} cm^2/sec) that in many scrubber applications liquid phase diffusion does not occur over a time long enough to produce a steady-state concentration profile. The starting point for several theories applicable to this unsteady-state situation is, (see Crank, 1957):

$$\frac{\partial c_A}{\partial t} = D_L \frac{\partial^2 c_A}{\partial Z^2} \tag{4.2.2-6}$$

4.2.2.2 Mass Transfer by Eddy Diffusion

Eddy diffusion occurs when a fluid phase is in turbulent motion. Mass is transferred by the circulation of eddies of fluid due to velocity fluctuations from point to point in the fluid. The mole flux of a component "A" in a turbulent fluid is

$$\hat{N}_A = -(D + \varepsilon)\frac{\partial \hat{c}_A}{\partial z} \qquad (4.2.2\text{-}7)$$

where "ε" is the eddy diffusivity. The magnitude of "ε" increases with the degree of turbulence and is usually several orders of magnitude larger than "D". At high Reynolds numbers in gas mixtures, "ε_G" can be 100 times as great as "D_G". In liquids "ε_L" can be 10^5 times as great as "D_L". The mechanism of eddy diffusion is not completely understood, but the theoretical approaches suggest "ε" should be independent of physical properties except for the dependence on Reynolds number, Treybal, (1955). However, an empirical correlation given by Emmert and Pigford, (1962), for "ε_G" in gases flowing turbulently in a duct is

$$10^5 \ \varepsilon_G \rho_G = 0.027 \ N_{Re} + 83 \qquad (4.2.2\text{-}8)$$

where "ε_G" is $cm^2 \ sec^{-1}$ and "ρ" is $g \ cm^{-3}$ and $N_{Re} = \frac{d \ u \ \rho_G}{\mu_G}$ is the Reynolds number.

Since the eddy diffusion approach is very cumbersome for design purposes, mass transfer in a turbulent fluid phase is commonly analyzed through mass transfer coefficients, discussed in Section 4.2.3.

4.2.3 INTERPHASE MASS TRANSFER THEORIES

4.2.3.1 Mass Transfer Coefficients

Section 4.2.2 on mechanisms provided a description of how mass transfer takes place within one phase. In the practical situation, a component moves to the gas-liquid phase boundary, crosses it, and moves into the bulk of the other phase.

The mass flux of component "A" from a gas-liquid interface into a liquid is described by

$$\hat{N}_A = k_L \ (\hat{c}_{Ai} - \hat{c}_A) \qquad (4.2.3\text{-}1)$$

which defines the liquid-phase mass transfer coefficient "k_L".

The mass flux from the gas to the gas-liquid interface is

$$\hat{N}_A = \hat{k}_G \ (p_A - p_{Ai}) \qquad (4.2.3\text{-}2)$$

Concentration profiles for a gas-liquid mass transfer process are shown qualitatively in Figure 4.2.3-1.

Experimental values of "k_L" and "k_G" or related coefficients have been determined and correlated for many industrially important absorptions, see for example: Treybal, (1955); Perry, (1963); Danckwerts, (1970). The designer should consult these references and many others. The following material (as well as Section 4.5 on Unit Mechanisms) is intended to give an understanding of how mass transfer coefficients depend on physical properties and operating variables.

In scrubbing of a gas by a liquid, it is normally assumed that the material is transferred in the bulk of the phases by eddies, and that the resistance to transfer is encountered in the vicinity of the interface between the phases. Hence, the material transferred from one phase to another has to cross a region in the neighborhood of the surface by molecular diffusion alone. Models based on three distinct hypotheses about the behavior of the liquid will be considered.

4.2.3.2 Whitman - Film Theory

The film theory, first proposed by Whitman in 1923, is based on the assumption that a stagnant film of fluid at the interface represents the total resistance to mass transfer and that the mass transfer takes place only by molecular diffusion through this stagnant film. The rest of the fluid is assumed to be at uniform concentration. In the gas phase, the film theory says

$$\hat{N}_A = \frac{D_G\ P}{R_g\ T\ Z\ p_{BM}} (p_A - p_{Ai}) = \hat{k}_G (p_A - p_{Ai}) \qquad (4.2.3\text{-}3)$$

and in the liquid phase

$$N_A = \frac{D_L}{Z} (c_{Ai} - c_A) = k_L (c_{Ai} - c_A) \qquad (4.2.3\text{-}4)$$

where "Z" is the thickness of the film in either phase. "k_G" and "k_L" are determined experimentally for one system and applied to predict "k_G" and "k_L" for another system with compensation for hydrodynamic conditions, knowing diffusivities for the new system.

The "two-film" concept considers interphase mass transfer as diffusion through two films in series, one in each phase. Since the mass flux must be the same in each phase, in a steady state process of absorption,

$$\hat{N}_A = \hat{k}_G (p_A - p_{Ai}) = \hat{k}_L (\hat{c}_{Ai} - \hat{c}_A) \qquad (4.2.3\ 5)$$

It is convenient to define overall mass transfer coefficients by

$$\hat{N}_A = \hat{K}_G (p_A - p_A^*) \qquad (4.2.3\text{-}6)$$

or

$$N_A = K_L (c_A^* - c_A) \qquad (4.2.3\text{-}7)$$

where "p_{Ae}" is the partial pressure of "A" which would be in physical equilibrium with "c_A" and "c_{Ae}" is the concentration of "A" which would be in physical equilibrium with "p_A". These quantities are illustrated on the equilibrium plot of Figure 4.2.3-2.

Much of the mass transfer data available in the literature is in the form of overall coefficients. In general, "K_G" and "K_L" are not constant with respect to composition as "k_G" and "k_L". If the equilibrium relation p_A (c_A) is a straight line (not necessarily with zero intercept) then "K_G" and "K_L" are constant. Henry's law is a special case of a straight equilibrium line with the intercept at the origin. When Henry's law applies:

$$\frac{1}{\hat{K}_G} = \frac{1}{\hat{k}_G} + \frac{\hat{H}}{k_L} \qquad (4.2.3\text{-}8)$$

and

$$\frac{1}{K_L} = \frac{1}{k_L} + \frac{1}{\hat{H}\ \hat{k}_G} \qquad (4.2.3\text{-}9)$$

If the equilibrium line can be regarded as straight over a limited composition range, then the above two equations hold in that range, if "H" is replaced by the slope $\Delta p/\Delta c$ of the equilibrium line.

4.2.3.3 Higbie - Penetration Theory

The penetration theory of mass transfer was first suggested by Higbie (1935), [Calvert and Kapo (1963)], as a mechanistic picture of mass transfer from a gas-liquid interface into a liquid. Higbie assumed liquid to run in a laminar flow throughout its thickness (not merely at the surface), until it is mixed upon meeting a discontinuity (e.g. in going from one packing piece to another in a packed column), or by some other cause (e.g. a liquid element slides along a gas bubble periphery, entering at the top and leaving at the bottom of the bubble, as the bubble rises through the liquid). Each element of liquid surface is assumed to be exposed to the gas for the same length of time, θ, and to absorb gas during this time at the same changing rate as though it were a stagnant layer of infinite depth. The result is expressed by Equation 4.2.3-10.

$$k_L = 2\left(\frac{D_L}{\pi\ \theta}\right)^{1/2} \qquad (4.2.3\text{-}10)$$

It is important to note that as the exposure time, θ, gets larger the absorption process approaches steady-state diffusion through a thin stagnant layer to the turbulent bulk, i.e., it approximates the film theory. Toor and Marchello (1958) have shown that the film and penetration theories are not separate, unrelated concepts but rather are limiting cases of a more general model and that the two theories, rather than being mutually exclusive, are actually complementary.

Example

Consider a liquid drop with a residence time of 10 seconds in a spray chamber. Assume the drop diameter to be 0.04 cm and the diffusivity of the gas dissolving in the liquid $D_L = 10^{-5}$

cm^2/sec. If the liquid is not circulating at the drop surface, $k_L = 2\sqrt{10^{-5}/(3.14 \times 10)} = 0.0011$ g.mol/(cm^2) (sec) (mol/cm^3). A similar example can be given for a gas bubble rising in a liquid with no surface-active agents. The gas in the bubble undergoes a toroidal circulation as shown in Figure 4.2.3-3. As the bubble rises, the liquid moves downward in relation to the bubble and leaves when it reaches the bottom of the bubble. Here, the exposure time, Θ, the time required for the liquid to slide along the bubble from top to bottom, can be approximated (Higbie, 1935) $\Theta = d_b/v_t$, in which "d_b" is the bubble diameter and "v_t" is the terminal velocity of the rising bubble. Hence,

$$k_L = 2 \left(\frac{D_L\ v_t}{d_b}\right)^{1/2} \qquad (4.2.3\text{-}11)$$

4.2.3.4 Danckwerts - Random Surface Renewal Theory

Danckwerts (1951) modified the penetration theory by assuming that the times of exposure of the surface elements are not the same and that the average rate of mass transfer depends on the distribution of the elements of surface among the various "age groups". Danckwerts assumed that there is no correlation between the time for which an element of surface has been exposed and its chance of being remixed. The rate of surface renewal (fraction per unit time) is "s". It can be shown then, that

$$k_L = (D_L\ s)^{1/2} \qquad (4.2.3\text{-}12)$$

The constant "s" must be found experimentally, so that Equation 4.2.3-12 does not provide a direct means of predicting "k_L". When a gas-film resistance occurs, Higbie and Danckwerts models, as well as the Whitman models, give rise to the conventional rule for "resistances in series".

4.2.4 FACTORS AFFECTING AND/OR LIMITING MASS TRANSFER

4.2.4.1 Equilibrium Limitations

Physical or chemical equilibria impose an upper limit on the amount of material which can be absorbed in a scrubbing process involving mass transfer. Departure from equilibrium provides the driving force for mass transfer. At equilibrium there is no concentration gradient in either phase; the concentrations in both phases are uniform; and there is not net diffusion in any direction in either phase. In the absence of chemical reactions, the driving force for mass transfer is $(p_A - p_{Ai})$ in the gas and $(c_{Ai} - c_A)$ in the liquid, where "c_A" and "p_A" are the concentrations of "A" in the bulk phases. Subscript "i" denotes values at the gas-liquid interface, and "c_Ai" and "p_{Ai}" are assumed to be at physical equilibrium with each other. Information on the physical equilibria for several mixtures of interest in scrubber applications is given in Chapter 10.

Since the absorption of a gas in a liquid is usually exothermic, the effect of higher temperatures is usually to decrease the solubility of the gas in the liquid. For the low gas and liquid concentrations encountered in most scrubbing applications, physical equilibria can often be described in Henry's law.

$$p_A = H\ \hat{x}_A\ (\text{atm/mol.fr.})\ (\text{mol.fr.}) = \hat{H}\ \hat{c}_A\ (\text{atm/g.mol/cm}^3)(\text{g.mol/cm}^3) \qquad (4.2.4\text{-}1)$$

Henry's law is not obeyed when the gaseous solute undergoes a chemical reaction or dissociation in the liquid, when partial pressures are more than about 1 atmosphere, [Treybal, (1955); Emmert and Pigford, (1963)], or when the temperature is very low. For example, NH_3 reacts to form NH_4OH in water, thus Henry's law is inapplicable; however, an "apparent" Henry's low constant can be used for very low NH_3 concentrations, $c_A \leq 2.3$ mol ℓ^{-1}(Hobler, 1966). See further discussion in Chapter 10.

4.2.4.2 System Changes - Liquid Phase

On many occasions, it is desirable to modify the system in order to improve mass transfer. One method which has been considered, is the addition of surface active agents which, in turn, increase the surface area available for mass transfer. This method was not successful in many cases because wetting agents tend to concentrate at the interface, thus suppressing rippling of the liquid film and acting as a barrier to the diffusion of the solute gas through the surface.

Where economics may permit, or out of necessity, it is best to add a chemical to the liquid phase which would react with the dissolving gas. The mass transfer coefficient will increase because of this and the equilibrium limit will increase as well. This subject is treated in detail later in Section 4.2.6.

4.2.4.3 System Changes - Gas Phase

From Henry's law, Equation 4.2.4-1, it is apparent that the equilibrium concentration of the soluble component in liquid increases as the partial pressure of the soluble component in the gas phase increases. The pressure of the gas phase may be increased intentionally or the gas may already be at high pressure as it exhausts from a process. In either case, water may be applicable to the washing of high-pressure gases where the solubility of an impurity, which is only sparingly soluble at low pressure, is brought up to an economically high level by the high partial pressure.

4.2.4.4 Equipment Limitations

A variety of equipment is used to achieve mass transfer in gas scrubbing, but plate and packed colums are most commonly used. There are many types of plates and packings in commercial use. They have been detailed in Chapter 3. New designs of plates and packings come out claiming improved mass transfer. One may evaluate these claims through the determination of the "new design" Murphree intrinsic efficiency, (see next section for a more detailed discussion of the Murphree efficiency).

Mehta and Calvert (1967)(1970) have shown that for liquid-phase-controlled systems, where mass transfer occurs from bubble rising through a column of liquid, the Murphree intrinsic efficiency can be expressed as:

$$E_{MV} = 1 - \exp - \left[\frac{3\ R_g\ T}{A\ r}\ k_L\ t_g \right] \qquad (4.2.4\text{-}2)$$

where, t_g = average residence time of a bubble in a liquid (sec)
r = radius of bubble (cm)

The liquid film mass transfer coefficient can be calculated from Higbie's penetration theory, substituting for the exposure time $\theta - 2\pi r / v_b$.

$$k_L = \left(\frac{2\ D_L\ v_b}{\pi\ r} \right)^{1/2} \qquad (4.2.4\text{-}3)$$

Substituting Equation 4.2.4-3 into Equation 4.2.4-2 gives

$$E_{MV} = 1 - \exp - \left\{ \left[\frac{3\ R_g\ T\ t_g}{r} \left(\frac{2\ v_b}{\pi r} \right)^{1/2} \right] \left[\frac{D_L^{1/2}}{H} \right] \right\} \qquad (4.2.4\text{-}4)$$

When examining the exponent it is obvious that the first part depends only upon the equipment characteristics while the second part is a function of the system properties. Mehta et al. named the equipment part the contact factor, ϕ.

$$\phi \equiv \frac{3\ R_g\ T\ t_g}{r} \left(\frac{2\ v_b}{\pi\ r} \right)^{1/2} \qquad (4.2.4\text{-}5)$$

They found by analyzing experimental data that for conventional plates, the contact factor has the limits $0.6 \times 10^5 < \phi < 3 \times 10^5$. In other words, for a given system $(D_L^{1/2}/H)$ = const. there is only a certain maximum efficiency that can be obtained in a plate column.

Figure 4.2.4-1 shows the variation of conventional plate Murphree efficiency for low solubility gases as a function of the system properties $(D_L^{1/2}/H)$ with the contact factor as parameter.

4.2.5 DEFINITIONS OF EFFICIENCY (see also 4.4.3)

The concept of an equilibrium stage is based upon the presumption that the phases leaving the stage are in thermodynamic equilibrium. However, as we have seen in the previous section, there is certain efficiency associated with an equilibrium stage. This efficiency can be expressed in many ways. Murphree (1925) expressed it as the ratio of the actual change in a vapor concentration through the tray to the change which would have occurred if the vapor had actually reached a state of equilibrium with the liquid leaving the tray.

$$E_{MV} = \frac{\hat{y}_n - \hat{y}_{n-1}}{\hat{y}^*_n - \hat{y}_{n-1}} \qquad (4.2.5\text{-}1)$$

where the subscripts "n" and "n-1" refer to the outlet and inlet vapor streams, respectively. "$\hat{y}$" is the actual gas phase concentration (mole fraction) and "$\hat{y}^*$" is the gas phase concentration in equilibrium with the actual exit liquid concentration "$\hat{x}$". The Murphree vapor efficiency, E_{MV}, is most commonly used to describe plate efficiency in a plate column.

The Murphree efficiency can also be expressed in liquid composition terms:

$$E_{ML} = \frac{\hat{x}_{n+1} - \hat{x}_n}{\hat{x}_{n+1} - \hat{x}^*_n} \qquad (4.2.5\text{-}2)$$

where "$\hat{x}^*_n$" is the liquid concentration in equilibrium with the actual exit vapor, $\hat{y}$.

The Murphree tray efficiency can represent reality only in the special case of completely mixed tray liquids, where there are only single values of "$\hat{y}_n$" and "$\hat{x}_n$". This is the reason why one may obtain greater than 100% Murphree tray efficiency under certain mixing conditions. To overcome this objection, Murphree point efficiency was defined. The equations for point efficiency are the same as 4.2.5-1 and 4.2.5-2, except that point concentrations are involved.

The tray efficiencies can be related, in turn, to the overall column efficiency, "E_o", which is defined as

$$E_o = \frac{N}{N_t} \qquad (4.2.5\text{-}3)$$

where, N = total number of equilibrium stages
N_t = total number of actual stages

Common practice also describes performance in terms of overall efficiency without regard to equilibrium limitations. While this is easy to compute as $(y_n - y_{n-1})/y_{n-1}$ or $(y_{out} - y_{in})/\hat{y}_{in}$, it can be misleading when the equilibrium limits the outlet concentration (rather than equipment performance). For example, if a gas were shaken with a liquid in a flask and the quantity of liquid were sufficient to dissolve only 1/2 of the gas, the system would eventually reach equilibrium. At that time the fractional approach to equilibrium would be 1.0 (or 100%), yet the overall efficiency would only be 0.5 (or 50%). Obviously, it is important to know how efficiency is defined before using a number which someone presents.

4.2.6 MASS TRANSFER WITH CHEMICAL REACTION

The absorption of gases is increased in transfer efficiency and in capacity when the dissolved gas reacts in the liquid phase. Enhancement of transfer efficiency will depend upon the order of the reaction, whereas that of capacity will depend upon the liquid phase reactant concentration and the stoichiometry (molecularity) of the reaction. A number of important gas scrubbing operations involve mass transfer with a chemical reaction.

The theoretical and experimental literature on chemical reactions in gas-liquid systems is abundant. Important references in the area of mass transfer with chemical reaction are the works of Danckwerts (1970), Astarita (1967), and Sherwood and Pigford (1952). Denbigh (1955) deals with the basics of reaction kinetics.

4.2.6.1 Reaction Kinetics

The rate of a chemical reaction is the rate at which the concentrations of reacting substances vary with time.

$$\hat{R}_A = -\frac{d\hat{c}_A}{dt} \qquad (4.2.6\text{-}1)$$

where "c_A" is the concentration of the gas phase component absorbed in the liquid. The dependence of this rate on the concentration of reacting substances is given by the law of mass action, which states: "the rate of any reaction is at each instant proportional to the concentrations of the reactants, with each concentration raised to a power equal to the number of molecules of each species participating in the process. Thus, for a reaction $A \xrightarrow{k_1} P$ the rate of consumption of "A" is:

$$\hat{R}_A = k_1 \hat{c}_A \qquad (4.2.6\text{-}2)$$

where "k_1" is a constant. For the reversible reaction

$$A + b\,B \underset{k_1}{\overset{k_2}{\rightleftarrows}} P \qquad (4.2.6\text{-}3)$$

The rate is given by

$$\hat{R} = k_2 \hat{c}_A \hat{c}_B^{\,b} - k_1 \hat{c}_p \qquad (4.2.6\text{-}4)$$

These equations indicate that different rate dependencies on concentrations are obtained at constant temperature for various reactions, and to distinguish these the term "order of reaction" is employed. By the order of chemical reaction is meant the sum of all the exponents to which the concentrations in the rate equation are raised. In many cases the order of reaction is identical with the molecularity of the reaction, i.e. the number of molecules involved in the step leading to reaction. However, this is not always the case since the order of reaction is confined to the dependence of the observed rate on the concentrations of the reactants.

It is evident that the order or, for that matter, the molecularity, of a reaction cannot always be predicted from the stoichiometric equations of a reaction but that each and every reaction must be investigated kinetically to ascertain both order and molecularity. Further, care must be exercised in interpreting an observed reaction order and in inferring from it the molecularity and the mechanism of the process. When the order of a reaction agrees with the rate equation obtained by applying the law of mass action to the stoichiometric equation of the reaction, it is fairly safe to assume that the reaction proceeds as given by the chemical equation. When the two are not the same, a mechanism has to be devised which is in accord both with the observed reaction order and with the overall equation of the process.

At equilibrium, the rates of forward and backward reactions are the same. For the reaction

$$A \underset{k_{-1}}{\overset{k_1}{\rightleftarrows}} P \qquad (4.2.6\text{-}5)$$

at equilibrium

$$\hat{R}_A = 0, \; k_1 \, \hat{c}_{Ae} = k_{-1} \, \hat{c}_{Pe} \qquad (4.2.6\text{-}6)$$

$$\text{and, } \left(\frac{\hat{c}_P}{\hat{c}_A}\right)_e = \frac{k_1}{k_{-1}} = K_e \qquad (4.2.6\text{-}7)$$

where "K_e" is the equilibrium constant. Note that in the case of a catalyzed reaction, since it does not change the value of "K_e", the rate of the forward and reverse reactions must be speeded up equally.

The units of the rate constant "k" for the nth order reaction are $(\text{time})^{-1}$ $(\text{concentration})^{1-n}$ which for a first-order reaction becomes simply $(\text{time})^{-1}$.

4.2.6.2 Film Model Mass Transfer with Chemical Reaction

Models predicting rates of physical gas-absorption have been discussed in Section 4.2.6. These models form the basis to arrive at the effect of a chemical reaction on the rate of absorption. Danckwerts (1970) treats various reactions using the film-model, Higbie's model and Danckwert's model, and concludes that, in most cases, all the three models lead to the same predictions. We will consider the use of the "film-model" alone in the following.

The following terms will be used to express the results of the mathematical derivations.

$E = \dfrac{\hat{N}_A}{k_L \, (\hat{c}_{Ai} - \hat{c}_A^{\circ})}$ = enhancement factor = ratio of the average rate of absorption into an agitated liquid in the presence of reaction to the average rate of absorption without reaction.

E_i = enhancement factor when reaction is instantaneous.

$\hat{N}_A$ = Average rate of absorption per unit area of interface (flux) (g.mol/cm -sec)

$\hat{c}_{Ai}$, $\hat{c}_A$, $\hat{c}_A^\circ$ = Dissolved concentrations of "A" at the interface, in the film and in the bulk respectively. (Note that in this section "c°" is bulk concentration instead of "c_A"). (g.mol/cm³)

First-order Irreversible Reaction - Film Model

$$A \xrightarrow{k_1} P \qquad (4.2.6\text{-}1)$$

$$\hat{R}_A = k_1 \ \hat{c}_A \qquad (4.2.6\text{-}2)$$

"k_1" is the first-order reaction-rate constant and "$\hat{c}_A^\circ$" is the local concentration of dissolved gas. According to the film model (Hatta, 1932) the average absorption rate is

$$\hat{N}_A = k_L \ \hat{c}_{Ai} - \left(\frac{\hat{c}_A^\circ}{\cosh\sqrt{M}}\right) \frac{\sqrt{M}}{\tanh\sqrt{M}} \qquad (4.2.6\text{-}8)$$

$$\text{where, } M = \frac{D_A \ k_1}{k_L^2} \qquad (4.2.6\text{-}9)$$

and "D_A" is the diffusivity of the gas in the liquid phase.

When $\sqrt{M}>>1$, the dissolved gas all reacts in the film and none diffuses in the unreacted state into the bulk of the liquid, then "c_A°" tends to zero and Equation 4.6.6-8 becomes:

$$\hat{N}_A = \hat{c}_A(D_A \ k_1)^{1/2} \qquad (4.2.6\text{-}10)$$

$$\text{giving: } E = (D_A \ k_1)^{1/2}/k_L = \sqrt{M} \qquad (4.2.6\text{-}11)$$

InstantaneousIrreversible Reaction - Film Model

$$A + b\ B \rightarrow P \qquad (4.2.6\text{-}12)$$

The instantaneous irreversible reaction is between one mole of "A" and "b" moles of "B" to produce one mole of "P", the solute gas "A" and reactant diffuse to the reaction phase at a distance "δ'" below the surface. Since "A" and "B" can not coexist, their concentration is zero at "δ'". See Figure 4.2.6-1.

Film-model predicts average absorption rate as (Hatta, 1928-29).

$$\hat{N}_A = k_L \ \hat{c}_{Ai} \left(1 + \frac{D_B \ \hat{c}_B^\circ}{b \ D_A \ \hat{c}_{Ai}}\right) \qquad (4.2.6\text{-}13)$$

$$E_i = \left(1 + \frac{D_B \ \hat{c}_B^\circ}{b \ D_A \ \hat{c}_{Ai}}\right) \qquad (4.2.6\text{-}14)$$

When $b\,D_A\,\hat{c}_{Ai} << D_B\,\hat{c}_B^\circ$ (in practice, when $\hat{c}_{Ai} << \hat{c}_B^\circ$);

$$\hat{N}_A \simeq k_L \frac{D_B\,\hat{c}_B^\circ}{b\,D_A} \qquad (4.2.6\text{-}15)$$

For this case the rate of absorption is independent of $\hat{c}_{Ai}$, and hence of the partial pressure of solute gas at the interface, and controlled by the rate at which B can diffuse the surface.

mth Order Irreversible Reaction - Film Model

$$\hat{R}_A = \hat{k}_m\,\hat{c}_A{}^m \qquad (4.2.6\text{-}16)$$

Hikita and Asai (1964) have solved this case assuming bulk concentration of "A" to be zero ($c_A = 0$). They arrived at a final explicit expression, for m>1, using simplifications that introduce no more than 8% inaccuracies in the answer.

$$E = (1 + M)^{1/2} \text{ for } m>1 \qquad (4.2.6\text{-}17)$$

$$\text{where } M = \frac{1}{k_L^2}\left[\frac{2\,D_A\,\hat{k}_m\,(\hat{c}_{Ai})^{m-1}}{(m+1)}\right] \qquad (4.2.6\text{-}18)$$

$$\text{when } \sqrt{M}>>1, \quad E = \sqrt{M} \qquad (4.2.6\text{-}19)$$

This may be described as "fast m'th order" regime of absorption, the rate of absorption is independent of "k_L"

Second-Order Irreversible Reaction-Film Model

$$A + b\,B \xrightarrow{k_2} P \qquad (4.2.6\text{-}20)$$

$$\hat{R}_A = \hat{k}_2\,\hat{c}_A\,\hat{c}_B \qquad (4.2.6\text{-}21)$$

See Figure 4.2.6-2.

Van Krevelen and Hofitzer (1948) have computed an approximate set of solutions assuming $c_A^\circ = 0$. They have shown that the solutions can be fitted within about 10% accuracy by the equation.

$$E = \frac{\left(M\,\frac{E_i - E}{E_i - 1}\right)^{1/2}}{\tanh\left(M\,\frac{E_i - E}{E_i - 1}\right)^{1/2}} \qquad (4.2.6\text{-}22)$$

$$\text{where:} \quad M = \frac{D_A\,\hat{k}_2\,\hat{c}_B^\circ}{k_L^2}\;; \quad E_i = \left(1 + \frac{D_B\,\hat{c}_B^\circ}{b\,D_A\,\hat{c}_{Ai}}\right)$$

Van Krevelen et al. (1948) present their results for $D_A = D_B$ but Danckwerts (1970) points out that these results are also valid for $D_A \neq D_B$. Figure 4.2.6-3 is a graphical presentation of Equation 4.2.6-22 showing "E" as a function of "M" with "E_i" as parameter. As can be seen in the figure, for a given value of "E_i" an increase in "M" brings about an increase in "E" until a limiting value is approached where $E = E_i$. This corresponds to the result in Equation 4.2.6-22 for the instantaneous irreversible reaction.

If $\sqrt{M} < 1/2\ E_i$, the reaction is pseudo-first order, and the rate of absorption is given by Equation 4.2.6-9, with $c° = 0$ and $k_2\ c_B^\circ$ replacing k_1.

m-, nth-order Irreversible Reaction-Film Model

$$A + b\ B \rightarrow P \qquad (4.2.6\text{-}12)$$

$$\hat{R}_A = \hat{k}_{mn}\ \hat{c}_A{}^m\ \hat{c}_B{}^n \qquad (4.2.6\text{-}23)$$

Assuming $\hat{c}_A^\circ = 0$, Hikita and Asai (1964) show that an approximate expression for "E" is

$$E = \sqrt{M} \left[\frac{E_i - E}{E_i - 1}\right]^{n/2} \Bigg/ \tanh \sqrt{M} \left[\frac{E_i - E}{E_i - 1}\right]^{n/2} \qquad (4.2.6\text{-}24)$$

$$\text{where,}\quad E_i = \left(1 + \frac{D_B\ c_B^\circ}{b\ D_A\ c_{Ai}}\right) \text{and}\quad M = \frac{1}{k_L^2} \left[\frac{2}{m+1}\ \hat{k}_{mn}\ D_A\ (\hat{c}_{Ai})^{m-1}\ (\hat{c}_B^\circ)^n\right]$$

First-order Reversible Reaction-Film Model

$$A \underset{k_{-1}}{\overset{k_1}{\rightleftarrows}} P \qquad (4.2.6\text{-}25)$$

The reaction has a forward rate-constant, "k_1", and a reverse rate-constant, "k_{-1}". Danckwerts and Kennedy (1954) have given the solution when $D_A = D_p$.

$$N_A = \frac{k_L\ (c_{Ai} - c_A^\circ)\ (1 + K_e)}{1 + \left[K_e \tanh \left(\frac{D_A\ k_1\ (1+K_e)}{k_L^2\ K_e}\right)^{1/2} \left(\frac{D_A\ k_1\ (1+K_e)}{k_L^2\ K_e}\right)^{1/2}\right]} \qquad (4.2.6\text{-}26)$$

Instantaneous Reversible Reactions - Film Model

Olander (1960) treats the important case of reversible reactions which are fast enough so that equilibrium is maintained at all points in the film. Danckwerts (1970) has generalized his conclusions.

$$A + b_1\ B_1 + \ldots\ \rightleftarrows\ z_1\ P + z_2\ P_2 \ldots \qquad (4.2.6\text{-}27)$$

"A" dissolves in liquid and one mole of "A" reacts stoichiometrically to destroy "b_1" moles of "B_1" etc. and to form "z_1" moles of "P_1" etc. There may be any number of reactants "B_1", "B_2", etc. and any number of products, "P_1", "P_2", etc. The concentrations at the surface are c_{Ai}, c_{Bi}, c_{Pi}, etc. and in the bulk c_A°, c_B°, c_P°, etc. Under these conditions, it can be shown that the rate of absorption, "N_A", is the sum of the rates at which unreacted and reacted "A", in the form of "P" (or any of the other products) diffuse away from the interface

$$N_A = k_L\left[\left(c_{Ai} + \frac{D_P\ c_{Pi}}{D_A\ Z}\right) - \left(c_A^\circ + \frac{D_P\ c_P^\circ}{D_A\ Z}\right)\right] \qquad (4.2.6\text{-}28)$$

When the diffusivities of the two species are equal, Equation 4.2.6-28 simplifies to

$$N_A = k_L\left[\left(c_{Ai} + \frac{c_{Pi}}{Z}\right) - \left(c_A^\circ + \frac{c_P^\circ}{Z}\right)\right] = k_L\ (c_i - c^\circ) \qquad (4.2.6\text{-}29)$$

where "c_i" and "c°" are the total concentrations, at the surface and in the bulk respectively, of "A" in both reacted and unreacted forms. "c_{Pi}", which is not known, has been shown to equal the concentration of "P" which would be obtained by saturating a liquid of the bulk concentration with the gas, the resulting concentration of unreacted gas being "c_{Ai}". Hence, in such cases where the dissolved gas dissociates in the liquids (SO_2-H_2O, H_2S-H_2O, etc.), the apparent Henry's law constant can be used to calculate the concentration gradient. The increase in gradient over the true Henry's law concentrations accounts for the enhancement in the rate of absorption due to the reaction.

Table 4.2.6-1 summarizes reactions considered by Olander (1960). The third reaction, Equation 4.2.6-36, in the table, is the same as the reaction considered above; however, the result is expressed in terms of the unreacted "A" gradient in the table. It may not always be meaningful to express the gradient in terms of the over-all concentration of "A" since "c_{Pi}" may not always be a unique function of "c_{Ai}" This is the case for the fourth reaction, Equation 4.2.6-39, given in Table 4.2.6-1.

4.2.6.3 Instantaneous Reaction Criteria

However rapid a reaction may be, it proceeds at a finite rate. Hence, whether a reaction can be treated as an instantaneous reaction depends upon the particular situation. A low value of mass transfer coefficient, "k_L", for physical absorption together with a high reaction rate of the dissolved gas promotes instantaneous behavior. This means that the rate of reaction is controlled entirely by diffusion of the reactants, the rate of reaction being sufficient to maintain equilibrium at all points. The kinetics of the reaction are then irrelevant.

The criterion for instantaneous behavior of irreversible reactions of "A" with "B" is in general

$$\frac{N_A^\circ}{k_L\ c_{Ai}} >> 1 + \frac{c_B^\circ}{b\ c_{Ai}} \qquad (4.2.6\text{-}42)$$

where N_A° is the flux if the absorbent in the neighborhood of the surface retained the bulk composition instead of becoming depleted.

TABLE 4.2.6-1

RATE OF ABSORPTION FOR INSTANTANEOUS REVERSIBLE REACTIONS (OLANDER, 1960)

Reaction $A \rightleftarrows P$ (4.2.6-25)

Equilibrium Constant $K_e = \frac{c_P}{c_A}$ (4.2.6-5)

Absorption Rate $N_A = k_L\ (c_{Ai} - c_A^\circ)\ (1 + K_e \frac{D_P}{D_A})$ (4.2.6-30)

$= k_L\ (c_{Ai} - c_A^\circ)\ \frac{[1 + K_e\ (D_P/D_A)]}{(1 + K_e)}$ (4.2.6-31)

Reaction $A \rightleftarrows 2P$ (4.2.6-32)

Equilibrium Constant $K_e = c_P^2/c_A$ (4.2.6-33)

Absorption rate $N_A = k_L\ (c_{Ai} - c_A^\circ) \left[1 + \frac{D_P}{D_A} \frac{(K_e/4)}{(\sqrt{c_{Ai}} + \sqrt{c_A^\circ})}\right]$ (4.2.6-34)

When $D_P = D_A$

$N_A = k_L\ (c_{Ai} - c_A^\circ)$ (4.2.6-35)

Reaction $A + B \rightleftarrows P$ (4.2.6-36)

Equilibrium Constant $K_e = c_P/(c_A\ c_B)$ (4.2.6-37)

Absorption rate $N_A = k_L\ (c_{Ai} - c_A^\circ) \left[1 + \frac{D_B\ D_P\ K_e\ C_B^\circ}{D_A\ (K_e\ c_{Ai}\ D_P + D_B)}\right]$ (4.2.6-38)

As $K_e \to \infty$, "N_A" tends to the value for irreversible instantaneous reaction given Equation 4.2.6-13.

Reaction $A + B \rightleftarrows P + Q$ (4.2.6-39)

Equilibrium Constant $K_e = c_P\ c_Q/(c_A\ c_B)$ (4.2.6-40)

Absorption rate $N_A = k_L\ (c_{Ai} - c_A^\circ) \left[1 + \frac{D_P}{D_A} \frac{\Phi}{(c_{Ai} - c_A^\circ)}\right]$ (4.2.6-41)

where

$$\Phi = 1/2 \left\{ \left[\left(\frac{D_Q}{D_P} - 1 \right) (K_e\ c_B^\circ\ c_A^\circ)^{1/2} + \frac{D_Q}{D_B} c_{Ai}\ K_e \right]^2 + 4 c_{Ai}\ K_e \frac{D_Q}{D_B} \left[\frac{D_B}{D_P} c_B^\circ + (K_e\ c_B^\circ\ c_A^\circ)^{1/2} \right] \right\}^{1/2} - 1/2 \left\{ \left(\frac{D_Q}{D_P} + 1 \right) (K_e\ c_B^\circ\ c_A^\circ)^{1/2} + \frac{D_Q}{D_B} K_e\ c_{Ai} \right\}$$

4.2.6.4 Gas and Liquid Resistance - Film Model

In Section 4.2.3.2 we have seen how the gas and liquid phase resistances combine yielding the overall transfer coefficient. This allows the use of the overall gradient between the gas phase and liquid phase bulk concentrations. Hence, the interfacial concentrations are not involved. Similarly, when the chemical reaction occurs in the liquid phase, one may combine the gas and liquid phase resistances. The resulting expression for "N_A" would be different in each case and needs to be derived. We will consider the case of absorption followed by instantaneous, irreversible reaction with a dissolved solute. In this case,

$$\hat{N}_A = \hat{k}_G (p - p_i) = \hat{k}_L \left(\hat{c}_{Ai} + \frac{D_B \ \hat{c}_B^\circ}{b \ D_A} \right) \qquad (4.2.6\text{-}43)$$

If Henry's law is valid, it can be shown that

$$\hat{N}_A = \left(p + \frac{D_B \ \hat{c}_B^\circ \ \hat{H}}{b \ D_A} \right) \Bigg/ \left(\frac{\hat{H}}{\hat{k}_L} + \frac{1}{\hat{k}_G} \right) \qquad (4.2.6\text{-}44)$$

Three possibilities arise, a) zero concentration of "B" at the liquid surface b) zero concentration of "A" and "B" at the liquid surface c) zero concentration of "A" at the liquid surface. These possibilities are shown in Figure 4.26-4. Thus, we see that Equation 4.2.6-44 is not valid when $\hat{k}_G \, p > (\hat{k}_L \, D_B \, \hat{c}_B^\circ / b \, D_A)$; instead, N_A remains equal to $\hat{k}_G \, p$ and the interfacial concentration of "B" is greater than zero (Figure 4.2.6-4c). Under such circumstances absorption process is entirely controlled by the transport of "A" across the gas-film, and

$$\hat{N}_A = \hat{k}_G \, p \qquad (4.2.6\text{-}45)$$

Example

Carbon dioxide, in the concentration of 2,000 ppm in air at inlet is absorbed by a saturated solution of $Ca(OH)_2$ from a bubble, of 0.4 cm diameter, rising in a 10 cm height liquid column. The total gas pressure is 1 atm. Calculate the rate of absorption of carbon dioxide.

Two reactions may occur when CO_2 is absorbed by aqueous alkaline solutions:

$$CO_2 + OH^- \rightleftarrows HCO_3^- \qquad (a)$$

$$CO_2 + H_2O \rightleftarrows HCO_3^- + H^+ \qquad (b)$$

Reaction (a) is second order whereas (b) is first order. The reaction rate constants for (a) and (b) are 6000 1/(g.mol-sec) and 0.02 (1/sec) respectively at 20°C. Solubility of $Ca(OH)_2$ is 0.184 gms/100 gms H_2O, i.e. 2.5×10^{-5} g.mol/cc. The dissociation constant for calcium hydroxide is 3.74×10^{-3} resulting in pH 12.4 when the solution is saturated with lime. Therefore, reaction (a) will be important and (b) can be neglected. Concentration of OH^- ion in the bulk of the liquid will be $c_B^\circ = 1.5 \times 10^{-6}$ g.mol/cc ($\equiv$ pH 12.4). k_L can be evaluated according to Equation 4.5.2-5.

D_{CO_2} in water $= 1.7 \times 10^{-5}$ cm²/sec. ρ_G = neglect
μ_L $= 10^{-2}$ g/cm-sec g = 980 cm/sec²
ρ_L = 1.0 g/cc

$$k_L = 0.42 \left[\frac{1.0 \times 10^{-2} \times 980}{(1.0)^2}\right]^{1/3} \left[\frac{10^{-2}}{(1.0)\ (1.7 \times 10^{-5})}\right]^{-1/2} = 0.037 \text{ cm/sec}$$

(Fig. 4.5.2-3 gives 0.04 for $D_L = 2 \times 10^{-5}$)

$$k_G = \frac{10\ D_G}{d_b\ RT} \qquad (4.5.2\text{-}2)$$

D_{CO_2} in air = 0.151 (cm²/sec) T = 293 °K
R = 82.06 (atm-cm³/g.mol-°K) d = 0.4 cm

Therefore, $k_G = 1.57 \times 10^{-4}$ (g.mol/cm²-sec-atm) (Fig. 4.5.2-1 gives 1×10^{-4} for $D_G = 0.1$)

Reaction (a) is followed instantaneously by $HCO_3^- + OH^- \rightarrow CO_3^{=} + H_2O$. Thus the overall reaction is $CO_2 + 2OH^- \rightarrow CO_3^{=} + H_2O$. The stoichiometric factor "b" is 2.

Equation 4.2.6-22 is applicable for the above reaction.

$$M = \frac{D_{CO_2}\ k_2\ c_B^\circ}{k_L^2} = \frac{1.7 \times 10^{-5} \times 6{,}000 \times 1.48 \times 10^{-6} \times 10^3}{3.7 \times 3.7 \times 10^{-4}} = .11$$

$$\sqrt{M} = .333$$

H for CO_2 in water is 18 (1,700)(atm/g.mol/cm³) at 298°K, see Chapter 10. Therefore, $c_{Ai} = p_{CO_2}/H$, i.e. $c_{Ai} = 2 \times 10^{-3}/18(1{,}700) = 6.6 \times 10^{-8}$. It is assumed that the gas phase resistance is negligible in calculating c_{Ai}. This is permissible by comparing k_G and k_L/H and finding that the gas phase resistance is quite small compared to the liquid phase resistance. Then,

$$E_i = 1 + \frac{D_B\ c_B^\circ}{b\ D_A\ c_{Ai}} = 1 + \frac{3.54 \times 10^{-5}\ 1.48 \times 10^{-6}}{2 \times 1.7 \times 10^{-5}\ 6.7 \times 10^{-8}} = 23$$

In his discussion of this reaction, Danckwerts (1970) has pointed out that if $\sqrt{M} < 1/2\ E_i$, the reaction can be considered pseudo first-order and Equation 4.2.6-9 applies with $c_A = 0$ and $k_1 = k_2\ c_B$. Accordingly, the enhancement factor is given by $\sqrt{M}/(\tanh \sqrt{M}) \approx 1$. Hence, the rate of absorption is equivalent to the rate of physical absorption. Then,

$$N_A = \frac{1}{\left(\frac{1}{k_G} + \frac{H}{k_L}\right)}\ p_{CO_2} = \frac{2 \times 10^{-3}}{\left(\frac{1}{1.57 \times 10^{-4}} + \frac{(1{,}700)\ 18}{.037}\right)} = \frac{2 \times 10^{-7}}{0.64 + 83}$$

$$\simeq 2.5 \times 10^{-9}\ \frac{\text{g.mol}}{\text{cm}^2\text{-sec}}$$

As the bubble rises, the rate of absorption will continually decrease as p_{CO_2} decreases.

4.2.7 SLURRY OF SORPTIVE OR REACTIVE PARTICLES

Often it is advantageous to use suspensions of solids in liquid (slurries) for heat or mass transfer. Gas sorption capacity can be greatly enhanced by suspending adsorptive or reactive solids in a liquid where otherwise only physical absorption might be occurring. The solids may be:

1. adsorbents (such as activated carbon).

2. biological masses (as in an activated sludge, in sewage treatment, or in penicillin manufacture).

3. catalyst (as in Fisher-Tropsch processes or polyethylene manufacture).

4. chemically reactive solids (limestone wet scrubbing of sulfur dioxide).

To abate SO_2 atmospheric pollution, much research and development is being done on scrubbing of sulfur dioxide. Of the several processes that have been proposed, use of lime or limestone slurry scrubbing is one of the more promising. This process falls in the category of "chemically reactive solid slurry". In the following reactions we shall review various aspects of slurry use in absorption practice.

4.2.7.1 Mass Transfer to Suspended Particles

One needs to know the individual mass transfer coefficients to determine the relative importance of various resistances in mass transfer to slurries. Mass transfer coefficients for transfer between gas to liquid are discussed in Section 4.5 and in Section 5.2 according to the type of equipment. The mass transfer coefficient to suspended particles is discussed here. The mass transfer coefficient, k_c, for a single sphere of diameter "d_p" at rest in a large volume of stagnant fluid is derived by equating the diffusion rate at the sphere surface to that through a shell of radius "R":

$$N_A \frac{d_p^2}{4} \quad \frac{2}{d_p} - \frac{1}{r} = -D_L \, (c_s - c) \qquad (4.2.7\text{-}1)$$

Substituting the limits $c = c_L$ at $r = \infty$, we have

$$k_c = \frac{N_A}{(c_L - c_s)} = \frac{2 \, D_L}{d_p} \qquad (4.2.7\text{-}2)$$

Any motion of the particle relative to the fluid will tend to make "k_c" larger than the value obtained by this relation. At high relative flow rates, $(N_{Sh} =)\ k_c\, d_p/D_L$ is found to be proportional, $N_{Re}^{1/2} \times N_{Sc}^{2/3}$, at very low velocities the function curves to approach the asymptote $k_c\, d_p/D_L = 2$, as given by Equation 4.2.7-2.

At low relative velocities of fluid and particle (as encountered in slurries), the mass transfer is subject to exact analysis. Friedlander (1960) reports N_{Sh} (for particles) to be a function of the Peclet number. For N_{Pe} = 500 to 10^5, his curve is represented by

$$N_{Sh} = 0.991\ N_{Pe}^{1/3} \tag{4.2.7-3}$$

Massive data collected on mass transfer from slurries have generally been taken in stirred vessels. They correlate as follows:

$$N_{Sh} = 2 + 0.6\ N_{Sc}^{0.33}\ N_{Re}^{0.5} \tag{4.2.7-4}$$

A review of the data in the literature is given by Marangozis et al. (1962).

Harriot (1962) reviewed more than 40 studies related to mass transfer to particles in stirred reactors. The reported effect of stirrer speed on mass transfer coefficient ranged from (n^0) to $(n^{0.9})$, where "n" is the stirrer revolutions per minute. The reported effects of fluid properties covered almost as wide a range of exponents. Harriot was able to explain the effects of particle diameter, diffusivity, viscosity, and density differences by using a slip velocity theory combined with a modified penetration theory. The slip velocity theories were based on the correlations for steady state transfer to particles fixed in space, with the average slip velocity used to calculate the Reynolds number.

Harriot reported that the mass transfer coefficient decreases with increasing particle size, but the coefficient is almost independent of size for particles larger than 200μ. There is no effect of volume fraction solids, in the suspension, on the mass transfer coefficient. Figure 4.2.7-1 is a plot of the transfer coefficient, k_c, for a single spherical particle settling at its terminal velocity in a liquid vs. the particle diameter with the density difference between the solid and the liquid, $\Delta\rho$, as a parameter. Diffusivity and viscosity are taken as representative values for the sake of illustration and Equation 4.2.7-5 was used to make the prediction. Because slip velocity effects are not included, the coefficients may be about 1.5 times larger than shown in Figure 4.2.7-1.

4.2.7.2 SORPTIVE SLURRIES

Gas scrubbing by suspensions of adsorbing particles may offer advantages of high capacity, easy fluid handling, and loss of inexpensive solvent. At the same time, it could offer sustained efficiency (Mehta et al. 1967). Suspensions of activated carbon in water are of special interest. The activated carbon has the capacity to absorb a range of gases while suspended in water (Mehta et al. 1967). The use of suspensions of adsorbents, in gas scrubbing applications, is not described much in the literature except in patents; however it seems to have potential.

The transfer of the solute gas from the gas phase to suspension is a combination of transfer from gas to liquid and from liquid to solid. The two processes occur simultaneously and affect the overall rate of transfer. Figure 4.2.7-2 shows resistance to mass transfer from gas to the suspension and can be viewed to take place in the following manner:

1. The solute gas diffuses from the bulk of the gas phase to the gas-liquid interface.

2. The solute gas diffuses from the gas-liquid interface to the bulk of the liquid.

3. The diffused gas mixes in the bulk.

4. The dissolved gas diffuses from the bulk of the liquid, through the liquid film surrounding the adsorbent particle, to the particle surface.

5. The dissolved gas finally diffuses through the liquid, in the pore, to the pore internal surface.

Mehta and Calvert (1967, 1969, 1969) assumed that the effect of adsorbent particles on the transfer between the gas and liquid is negligible. Hence, steps 1 to 3 are independent of the adsorbent and the transfer rate can be determined by the use of individual film mass transfer coefficients, as explained in 4.2.3.1. They have experimentally shown this to be true when the adsorbent concentration is not very high (below 5 percent by weight). Resistance to mass transfer in steps 4 and 5 depend on the pore size of the adsorbent in relation to the molecular size of the absorbate and on the particle size of the adsorbent for the intraparticle diffusion-controlled case. Dedrick and Beckmann (1966) have studied the effect of these variables and have succeeded in correlating the results based on effective diffusion coefficient and the particle diameter. Misic and Smith (1971) studied adsorption of benzene in carbon slurries and came to the same general conclusions as Mehta and Calvert.

Mehta and Calvert assumed negligible resistance for the transfer from the bulk of the liquid to the adsorbent and that at any instant they are at equilibrium. They verified this assumption for the system of pulverized activated carbon in water, which is the most suitable adsorbent for gas scrubbing by suspensions. The condition for negligible resistance was shown (Calvert et al., 1969) to be that there be sufficient carbon particles so that the requisite rate of mass transfer could be maintained by a concentration driving force, $(c_L - c_S)$, which is 10% (or less) of the maximum (see Section 4.2.7.5). They have shown the Murphree vapor efficiency, E_{MV}, for absorption and sorption to be the same.

If the adsorption isotherm can be described by the linear relationship

$$Z = K\,P\,y + C \qquad (4.2.7\text{-}5)$$

where, Z = mole fraction solute gas in adsorbent

K = constant

P = total gas phase pressure

y = mole fraction solute gas in the gas phase

C = constant

and if the Henry's Law applies for solubility of gas in liquid, Mehta et al. (1969) have shown that the number of actual plates (Section 5.2.1) required for a given separation is as follows:

$$n = \frac{\ln \left\{(1 - Ab) \left[\frac{y_o - y^*_n}{y_n - y^*_n}\right] + Ab\right\}}{- \ln \left[1 - E_{MV} + E_{MV}\, Ab\right]} \qquad (4.2.7\text{-}6)$$

where,

$$Ab = \frac{G_M}{L_M \left[s\, K\, P + (1 - s) \frac{P^2}{H}\right]} \qquad (4.2.7\text{-}7)$$

Equation 4.2.7-7 is a general equation unifying absorption, sorption and adsorption, and incorporates a number of special cases which include the Kremser equation, the Marshall and Pigford equation (1947), etc.

4.2.7.3 Biological Mass Slurries

The transfer of oxygen from the gas phase to a liquid phase is extensively employed in biological oxidants, such as a sewage waste treatment and antibiotic and yeast manufacture. It is conceivable that such a system could be used for air scrubbing where the gaseous pollutant and the oxygen are transferred from the gas phase and are converted to harmless matter by the biological masses, simultaneously solving the air and water pollution problems.

The continuous phase is often a sludge with non-Newtonian properties and the chain of consecutive reactions and transfer processes is complex and only partially understood. Nevertheless, a fair body of knowledge exists in relation to these processes. Mass transfer resistances in a typical biological oxidation are shown in Figure 4.2.7-3. A predictive method for the rate of transfer is complicated by the fact that the liquid phase properties vary widely and they can have a pronounced influence on mass transfer coefficients. The liquid phase pH can have a significant effect on the biological oxidation rate (Fair, Geyer and Okum, 1968). It has been observed that microorganisms interfere with oxygen transfer unless they are freely suspended and all clumps are smaller than 1 mm in diameter. In the latter case, mass transfer at the cell-liquid interface is rarely controlling. Eckenfelder (1956) found that the transfer coefficient (k_L A) for fresh sewage is 26-46% of that for pure water, for septic sewage 16-19% and for paper mill wastes 60-120%. Mass transfer characteristics also vary during the course of the oxidation process. Foaming is often a problem. It tends to increase during the course of the oxidation process and then to decrease again.

While no one equation can be given to compute mass transfer rates, guidelines can be given to analyze a given situation. If the biological reaction is slow compared to the absorption of gaseous components into the liquid, then the biological reaction will control the transfer under a steady state situation. The opposite is true if the biological reaction is very fast compared to the gas-liquid transfer. In such a situation the equations developed for the gas-liquid transfer can be applied.

4.2.7.4 Catalyst Slurries

There are several catalytic reactions which may be carried out in a liquid in which the reactants are dissolved, the solid catalyst being suspended in granular or powdered form. The use of slurries is common in the chemical industry, particularly for hydrogenation. Use of catalyst slurries for continuous operation appear to offer many advantages including uniform temperature control, eliminating the "hot spots" in the case of an exothermic reaction.

It is conceivable that catalyst slurries can be used to absorb pollutants and react them to harmless products although, in practice, one does not find many examples of this. The sorption of H_2S by slurries of carbon and subsequent oxidation to elemental "S" is one example and the same process using iron oxide as an intermediate reactant might be considered another. When such systems need to be considered, however, there is much literature on transfer to catalyst slurry followed by catalytic reactions. "Advances in Catalysis" published by Academic Press, New York, can serve as a guide and provide useful design data and methods.

4.2.7.5 Reactive Solids Slurry

Chemically reactive suspensions share common characteristics with adsorbent suspensions and have the additional feature of chemical reaction affecting mass transfer rates in the liquid phase. The chemical reaction can be at the surface if the particles are relatively insoluble compared to the transfer rate. In that case, adsorbent and reactive systems are identical to the extent that the transfer through the liquid is a physical process. If the solid solubility is appreciable, the reaction zone moves toward the gas-liquid interface, causing a greater concentration gradient for the absorbing gas and therefore a higher rate of transfer. Further complication is that the products may be gases or liquids, and a variety of situations may exist, each requiring a somewhat different analysis of the mass transfer phenomena involved.

The absorption of pure CO_2 by slurries of lime particles, Ca(OH), in water in a stirred flask was studied by Calvert, Mehta, and Russell (1969), who also presented a general design approach for suspensions of adsorptive or reactive particles. Their rate data showed an enhancement factor, "E", of 2.3 for lime slurry as compared to plain water. This enhancement was explained in terms of an instantaneous, irreversible reaction, Equation 4.6.2-14, which predicts the proper value of "E". However, the analysis given in 4.2.6.4 would indicate that it should be in the pseudo-first order regime and have an enhancement factor of 1.0. One can speculate that there may have been a depletion of base at the upper surface of the slurry so that the pH was <10 and the reaction therefore instantaneous (see Section 4.2.6.4) or that there may have been a trace of catalyst present, or that the presence of base at the interface changed the solubility of CO_2.

Solids concentration in the range of 1 to 10% (wt.) did not affect the mass transfer rate, k_L, so long as there was a sufficient amount of solids in the slurry. A sufficient amount was determined to be that quantity which would provide a transfer rate coefficient and surface area product, $k_c a$, which would keep pace with the CO_2 flux if the driving force, $(c_L - c_s)$, were about 10% of the solubility of $Ca(OH)_2$. In other words, only at the point where "$k_c a$" would keep the bulk concentration of base at about 90% of saturation, a decrease in absorption rate of CO_2 would be noticeable.

A similar observation was made of the sorption rates by carbon suspensions. Therefore it was concluded that the transfer process could be conveniently considered in segments as follows:

If enough solid is present to keep the solution nearly saturated in soluble solid reactants, or nearly depleted of absorbent in the case of either adsorbents or particles which react on their surfaces; the rate is controlled by the liquid-gas transfer coefficients. In other words, the function of the solid is to maintain the bulk concentration at a limiting value of either saturation or zero, depending on the case. In this case, the gas and liquid phase coefficients can be predicted independently of consideration of the slurry. Physical absorption is straightforward; the interface is assumed to be at equilibrium and the solubility relationship is that for the transferring component in the clear liquid. Chemical reaction greatly complicates matters, just as in the case of absorption into a clear liquid.

The total transfer rate is computed by means of the coefficient(s) from above, the interfacial area, and the concentration driving force. The overall driving force is the gas-phase concentration; assuming that the slurry keeps the "back pressure", or liquid bulk concentration, to zero. Individual driving forces depend on knowledge of the interfacial liquid composition.

Given the total transfer rate calculated previously, one can now compute the necessary amount of solid to satisfy the condition listed previously.

4.2.7.6 Computational Aides

For ease of computation of transfer to slurries, Figure 4.2.7-4 presents a plot of mass transfer coefficient (particle/liquid) per gram of particles as a function of particle diameter and with particle/water density difference as a parameter. This plot is based on the coefficients, k_c, given in Figure 4.2.7-1, and the surface to weight ratio = $(3/\rho_p r_p)(cm^2/g)$. The dashed line for $\Delta\rho=0$ represents a particle of density = 1.0, not moving relative to the water. For other density differences, the particles are sinking (or rising) and the mass transfer coefficient is enhanced. The solid lines are below the dashed line in the small particle region where the increase in coefficient due to particle density is not enough to compensate for the smaller number of particles per gram when density is higher.

Example: For the example in Section 4.2.6.4, it was assumed that the solution bulk concentration of $Ca(OH)_2$ is the saturated value. If lime slurry were used in a sieve plate column, about what slurry concentration would be required? We have it from 4.2.6.4 that the transfer would be liquid-phase controlled in this situation. The transfer coefficient computed was $k_L = 0.037$ (cm/sec), and the initial CO_2 flux was $N_A = 2.5 \times 10^{-9}$ (gmol/cm -sec), assuming that the interfacial solubility of CO_2 is the same as in pure water.

We will see that for this situation it is not possible to predict whether the reaction is pseudo first-order or irreversible, instantaneous second-order (as discussed in Section 4.2.7.5). However, it is possible to estimate a range of possibilities and design for it.

Assume the superficial velocity in a sieve plate column to be about 100 (cm/sec) and the foam density about 0.4 (see Section 9.3.1.1). If the foam height were 10(cm) and the plate spacing 50(cm), the volume of foam per unit area of plate would be 10 (cm^3/cm^2) and the interfacial area per unit volume of column would be:

$$a = \frac{10}{50} \left(\frac{3}{r_b}\right) (1-0.4) = \frac{0.36}{0.2} = 1.8 \ (cm^3/cm^2)$$

Since the liquid bulk concentration of CO_2 is maintained at nearly zero by the lime, the change in gas-phase composition as the bubbles rise is given by:

$$\int_1^2 \frac{dp}{p} = \frac{-K_G \ a \ Z}{G_M} = \ln \frac{p_2}{p_1} =$$

$$= - \frac{k_L \ (g.mol/cm^2\text{-}sec\text{-}g.mol/cm^3) \ a \ (cm^2/cm^3) \ Z \ (cm)}{H \ (atm/g.mol/cm^3) \ v_G \ (cm/sec) \ \rho_M \ (g.mol/cm^3)} =$$

$$= - \frac{(0.037) \ 1.8 \ (50)}{3 \times 10^4 \ (100) \ (1/24{,}600)} = -0.0273$$

So $\frac{p_2}{p_1} \simeq 0.97$, which means 3% plate efficiency for CO_2 removal if E=1.0.

If "k_L" were increased by an instantaneous, irreversible reaction, $E_i = 23$ (from Section 4.2.6.4) and "K_G" were correspondingly increased by 19.5, then, $\ln(p_2/p_1) = -19.5 \ (0.0273) = -0.46 = \ln(0.63)$. In this case, the plate efficiency would be (1-0.63) 100 = 37% based on gas phase composition change. We can not predict whether it is 3% or 37% or in between.

The rate of transfer of CO_2 per unit area of plate could range from $0.03 \ (100/24{,}600) \ (0.002) = 2.42 \times 10^{-7}$ to $0.37 \ (8.15 \times 10^{-6}) \simeq 3.0 \times 10^{-6}$ ($g.mol/cm^2$-sec). We now can look at the question of how much lime would be required to keep up with this range of absorption rates. A saturated solution of $Ca(OH)_2$ has a concentration of about 2.5×10^{-5} ($g.mol/cm^3$) so if the liquid bulk were 90% saturated and the film around the lime particle 100% saturated, the driving force for $Ca(OH)_2$ transfer from particles to liquid would be $(0.1) \times 2.5 \times 10^{-5} = 2.5 \times 10^{-6}$ ($g.mol/cm^3$). Equation 4.2.7-2 gives:

$N_A = k_c (c_s - c_L) = k_c (2.5x10^{-6})$ (gmol/cm²-sec)

The total rate of transfer is the flux, N_A, times the total surface area of particles. Since Figure 4.2.7-4 gives "k_ca'", where "a'" is particle surface area per gram of particles, it is convenient to represent particle area by the product, a'Wp; where "Wp" is the mass of particles present in the transfer volume. Thus,

N_A a' Wp = k_c a' Wp $(2.5x10^{-6})$ (gmol/sec)

We computed previously a range of CO_2 transfer rates that would require for reaction as many moles of $Ca(OH)_2$, therefore:

$2.4x10^{-7} \leq N_A a' Wp \leq 3.0x10^{-6}$ defines the lime solution rate needed.

Consequently: $0.1 \leq k_c a' Wp \leq 1.2$

If we use 100 μm diameter lime particles and their density is 2.34, $\Delta\rho \simeq 1.3$, and k_c a' ≃ 2 (cm /sec-g) from Figure 4.2.7-1. Therefore,

$0.05 \leq Wp \leq 0.6$ (g/cm² of plate) defines the lime particle holdup needed.

The liquid volume over 1 cm² of plate area is given by the froth height and density to be 4 cm³. Particle concentration on a weight basis would therefore have to range from 100(0.05/4) = 1.25% to 100(0.6/4)= 15% solids in the slurry, depending on the gas-liquid transfer rate. If the lime particle size were 30 μm diameter, the k_c a' would be about five times that for 100 μm diameter and the required slurry concentration would be 1/5 that computed above.

If a lower solids concentration were used, the transfer rate would be limited by the solid-liquid step. Also note that as the absorption goes on the solids concentration decreases, although the "k_c a'" increases because the particle diameter decreases. A most important point is that in gas absorption by slurries, the solids holdup in the column, not slurry flow rate, is the important factor in determining transfer rate. This example also points out that while there may be considerable uncertainty about the influence of a chemical reaction, it is possible to estimate maximum and minimum levels and this knowledge may suffice for design.

4.2.8 SIMULTANEOUS HEAT AND MASS TRANSFER

4.2.8.1 Introduction

In every case involving mass transfer, heat must also be transferred. In the case of solvent evaporating, the latent heat of evaporation is absorbed from the solution. There may also be sensible-heat transfer between the gas and liquid if temperature differences exist.

For the scrubbing operations where the latent-heat effects are small, heat transfer is of minor importance as a rate-limiting mechanism.

Heat effects may be neglected in gas absorption in dilute solution when the gas and liquid enter at temperature which are not too different. Because of the limited mass transfer, the latent heat transfer, due to the contaminant transfer, is limited.

Of those operations where both heat transfer and mass transfer affect the rate, humidification and dehumidification are simplest examples. Absorption of hydrochloric acid vapors from air by water is another example of simultaneous heat and mass transfer. This example will be discussed further in Chapter 9 with the other design examples. Temperature and humidity effects due to water-gas interactions can be quite important in hot gas scrubbing when they can influence diffusio- and thermophoresis and vapor-liquid equilibrium at the interface. Here we will give the underlying principles in calculation of simultaneous heat and mass transfer.

4.2.8.2 General Principles

The analogy between heat and mass transfer or penetration theory may be used to determine the relation between the coefficients of the two transfer processes. If one of these coefficients is known, the other can be calculated by assuming equality of the Chilton-Colburn "j_H" and "j_D" factors in the following equations:

$$\frac{h'}{C_p \; \rho \; v} (N_{Pr})^{2/3} = j_H \qquad (4.2.8\text{-}1)$$

$$\frac{k_G \; P_{BM} \; M_n}{\rho \; v} (N_{Sc})^{2/3} = j_D \qquad (4.2.8\text{-}2)$$

where "M_n" is the mean molecular weight.

In an adiabatic evaporation or humidification operation, the liquid attains an equilibrium temperature at which the rate of heat transfer from the gas to the liquid is balanced by the rate or heat transfer as latent heat of evaporation. The rate of heat transfer from the gas to the liquid per unit area is given by

$$q = h' (t_G - t_i) \simeq 2 \left(\frac{\rho_G \; C_{pG} \; k_G}{\pi \; \Theta}\right)^{1/2} (t_G - t_i) \text{ (by penetration theory)} \qquad (4.2.8\text{-}3)$$

and the molar rate of evaporation by

$$\hat{N}_A = \hat{k}_G (p_i - p_G) \simeq 2 \left(\frac{D_G}{\pi\Theta}\right)^{1/2} (p_i - p_G) \text{ (by penetration theory)} \qquad (4.2.8\text{-}4)$$

where "t_G" and "t_i" are the temperature of the gas and the interface, "p_G" is the partial pressure of vapor in the gas and "p_i" is the vapor pressure at temperature "t_i". At equilibrium,

$$q = \hat{N}_A \; \hat{\lambda}_M \qquad (4.2.8\text{-}5)$$

where λ_M is the molar latent heat.

From the ratio of "h'" and "k_G" expressed by Equations 4.2.8-3 and 4.2.8-4, and the relation between the vapor pressure and temperature of the liquid, it is possible to determine by trial and error the values of "t_{if}" and "p_i" which satisfy Equations 4.2.8-3, 4.2.8-4, and 4.2.8-5. Equation 4.2.8-4 then gives the rate of evaporation of the liquid into the gas stream.

4.2.8.3 Air-Water

In cooling tower or gas cooler operations the heat capacity of the water is important, and computational methods have been developed to deal with this situation, Foust (1960). The combined effects of heat and mass transfer in the gas phase can be accounted for with reasonable accuracy by using the enthalpy difference between gas and liquid as the driving force for gas-phase transfer. The equations describing the material balance (operating line) are:

For countercurrent operation;

$$G\,(i_2 - i_1) = L_2\,t_{L2}\,c_{L2} - L_1\,t_{L1}\,c_{L1} = L_m\,c_{Lm}\,(t_{L2} - t_{L1}) \qquad (4.2.8\text{-}6)$$

For cocurrent operation;

$$G\,(i_2 - i_1) = L_m\,c_{Lm}\,(t_{L1} - t_{L2}) \qquad (4.2.8\text{-}7)$$

For the gas phase, the number of transfer units can be defined in terms of enthalpy driving force as:

$$N_G = \int_{i_1}^{i_2} \frac{d_{iv}}{i_v - i_i} = \frac{\text{height}}{\text{height/tr.unit}} = Z\,\frac{k_y'\,a}{G} \qquad (4.2.8\text{-}8)$$

The relationship between bulk and interfacial conditions depends on the heat and mass transfer coefficients as shown below:

$$k_y'\,a\,(i_i - i_v) = h.\,a\,(t_L - t_{Li}) \qquad (4.2.8\text{-}9)$$

Where: G = superficial air rate per unit cross-section (g/sec-cm²)

L = superficial water rate (g/sec-cm²), L_m = mean

i = air enthalpy (cal/g dry air), i_2 = top of tower, i_1 = bottom, i_i = interface, i_v = bulk at any position, "z".

t_L = water temperature (°C), subscripts mean same as for air.

c_L = water heat capacity (cal/g-°C), c_{Lm} = mean

N_G = number of transfer units based on gas-phase

Z = height (or length) of contact zone (cm).

k_y' = gas phase mass transfer coefficient based on weight ratio driving force ≈29 k_G (g/sec-cm²)

a = interfacial area per unit volume of tower (cm^2/cm^3)

h_L = liquid phase heat transfer coefficient (cal/sec-cm^2-°C)

Figure 4.2.8-1 is a plot of air enthalpy versus water temperature for air and water at equilibrium and for air and water in contact at various conditions (operating lines) for cocurrent and countercurrent operation. The operating line for countercurrent contact (Equation 4. 4.2.8-6) is drawn for 116°C air with a 65°C dew point, water entering at 40°C, and $(Q_W/Q_A) = 1$ (ℓ/m^3). The weight ratio $(L_2/G_1) = (1/8.5x10^{-4})x10^{-3} = 1.18$, and is assumed constant through the column, so that the operating line is straight and has a slope = $L/G \simeq 1.2$. If infinite contact were possible, the dashed operating line would result and the inlet air would be in equilibrium with the outlet water. For real operation this is not possible and a condition such as represented by the solid line might be used.

In a similar way, cocurrent contact (Equation 4.2.8-7) would be represented by an operating line with a slope of $-L/G$, as shown. Infinite contact would result in outlet air being in equilibrium with outlet water, as shown by the operating line touching the equilibrium one. A real amount of contact is represented by the solid points and line. Graphical integration of Equation 4.2.8-8, with pairs of values of "i_V" and "i_i", taken from Figure 4.2.8-1 with the approximation that $h_L/k'_y \doteq \infty$, indicates that about 0.9 overall gas-phase transfer units would be required. A similar integration for the countercurrent case, if gas-phase controls, gives 0.7 overall gas-phase transfer units. The air and water would come very close to equilibrium because so few transfer units are required in the example given previously. If more water were used, more transfer would be possible and more contacting would be required.

In the above illustration, interfacial conditions were assumed to be gas-phase controlled; that is, the liquid at the interface is at the same temperature as the bulk of the liquid and the gas at the interface is in equilibrium with it. This is often approximately true, as will be shown below, following Equation 4.2.8-10. However, the interfacial conditions are governed by the ratio of liquid-phase heat transfer coefficient to gas-phase mass transfer coefficient, as Equation 4.2.8-9 shows. A line drawn from any point on the operating line, (i_V, t_L), with a slope of $-(h_L/k'_y)$ will intersect the equilibrium line at (i_i, t_{Li}).

We can estimate the ratio of coefficients for the unit mechanisms of mass transfer to drops, bubbles, and sheets, starting with "k_L" and "k_G" values for typical diffusivities of $D_L = 2x10^{-5}$ cm/sec^2 and $D_G = 0.1$ cm/sec^2 from Section 4.5. The relationship between "h_L" and "k_L" comes from penetration theory and permits computation of the heat transfer from the mass transfer coefficient. The 29 is necessary because "k'_y" is on a gram basis rather than g.mole.

For 500 μm diameter drops:

$$\frac{h_L}{k_y'} = \frac{2\left(\frac{\rho\ C_p\ k}{\pi\ \theta}\right)^{1/2}\ k_L}{2\left(\frac{D_L}{\pi\Theta}\right)^{12}\ (29)\ k_G} = \left(\frac{1.3x10^{-3}}{2x10^{-5}}\right)^{1/2}\left(\frac{k_L}{29\ k_G}\right) = 0.276\ \left(\frac{5x10^{-3}}{6x10^{-4}}\right) = 2.3 cal/(g\text{-}°C)$$

For 0.3 cm diameter bubbles rising 10 cm; $\frac{h_L}{k'} = 0.276\ \frac{4x10^{-2}}{1.3x10^{-4}} = 85.0 cal/(g\text{-}°C)$

For sheets flowing over 2 cm packing, with usual air and water rates in packed column;

$$\frac{h_L}{k_y'} = 0.276\ \left(\frac{9.2x10^{-3}}{8.4x10^{-5}}\right) = 30.0\ cal/(g\text{-}°C)$$

One can show that the ratio of $(i_v - i_i)/(i_v - i^*)$, where "i^*" is the enthalpy in equilibrium with "t_L", is given by:

$$\frac{i_v - i_i}{i_v - i^*} = \frac{(h_L/k_y')}{m+(h_L/k_y')} = \text{ratio of gas-phase to (gas-phase) driving forces} \tag{4.2.8-10}$$

The average slope of the equilibrium line, m, is about 4 between 40°C and 65°C. Thus, for drops the ratio of driving forces is (2.3/6.3) = 0.36, so only 36% of the possible driving force is available for mass transfer because the interface gets too hot. For bubbles the gas-phase driving force is 96% and for liquid sheets in packed columns it is 88% of the overall gas-phase driving force. For the example drawn on Figure 4.2.8-1, $h_L/k_y' = 4$ cal/(g-°C), (same slope as m) so the gas-phase driving force is 50% of the overall. One can see that for plate (bubble) and packed columns it is reasonable to use over-all gas-phase transfer units for simplicity in computations. While the extent of heat and mass transfer can be defined in terms of enthalpy driving force, sometimes one needs to know the gas phase conditions in terms of temperature and humidity.

Air temperature through the column can be computed by a graphical integration procedure based on Equation 4.2.8-11.

$$\frac{d\ t_v}{d\ i_v} = \frac{t_i - t_v}{i_i - i_v} \tag{4.2.8-11}$$

Starting with inlet air temperature, t_{v1}, (for countercurrent), one draws a short line segment between (i_1, t_{v1}) and (i_i, t_i). The interfacial conditions, where air and water are at the same temperature, are determined as before from Equations 4.2.8-9. A line is drawn from (i_1, t_{v1}) with a slope of $-(h_L/k_y')$ so that it intersects the equilibrium line and the point of intersection will be (i_i, t_i). Now the short line segment required can be drawn to complete the first step in the integration procedure. Another segment is drawn from the point reached (i_v, t_v) to a newly found interfacial point approximate to "i_v". A series of incremental steps are made until the outlet air enthalpy is reached. The line drawn traces the gas phase temperature from the inlet to the outlet. This procedure is illustrated in Foust (1960).

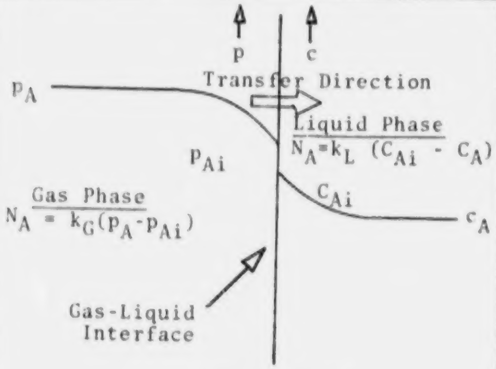

Figure 4.2.3-1
TYPICAL CONCENTRATION PROFILES
FOR GAS-LIQUID MASS TRANSFER

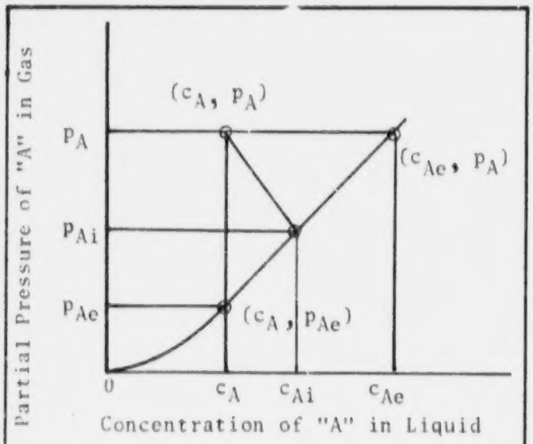

Figure 4.2.3-2
TYPICAL EQUILIBRIUM LINE, SHOWING
PHASE COMPOSITIONS AT VARIOUS POINTS

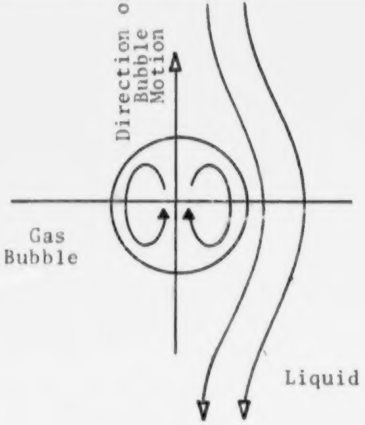

FIGURE 4.2.3-3
ABSORPTION FROM A GAS BUBBLE

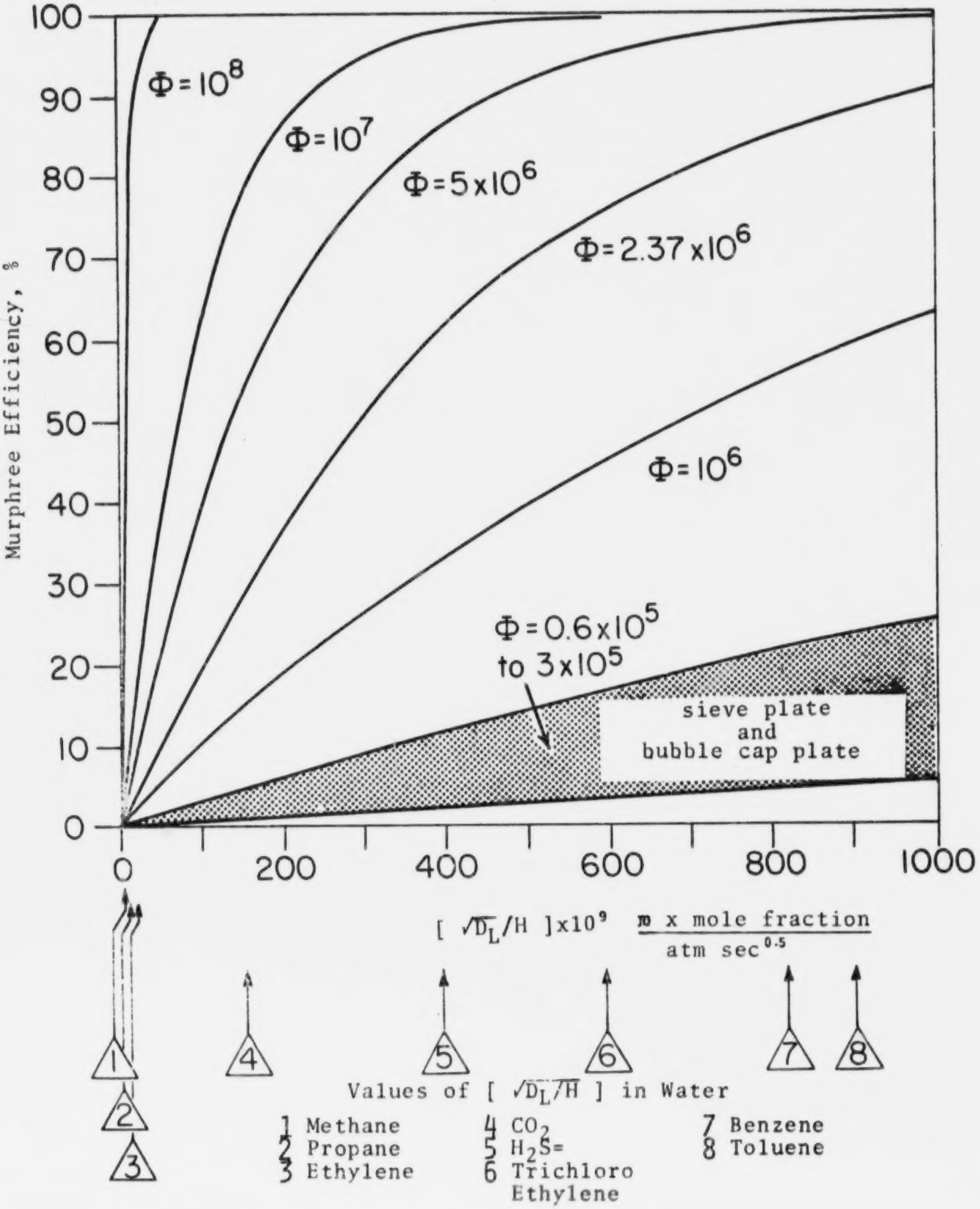

FIGURE 4.2.4-1

MURPHREE EFFICIENCY OF LOW SOLUBILITY GASES IN A PLATE COLUMN VERSUS SYSTEM PROPERTIES WITH CONTACT FACTOR AS PARAMETER

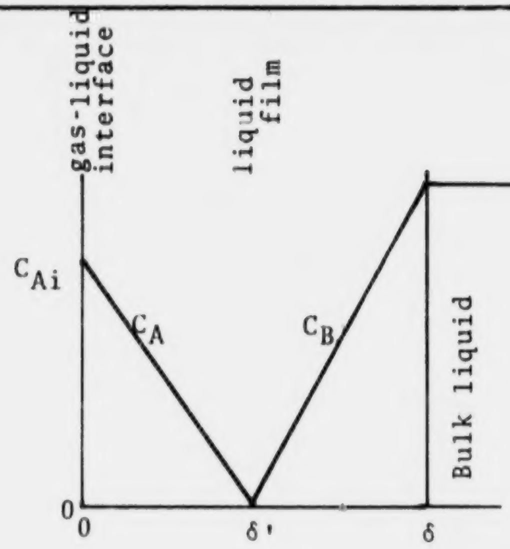

FIGURE 4.2.6-1
CONCENTRATION PROFILES FOR INSTANTANEOUS REACTION, FILM MODEL

SECOND-ORDER IRREVERSIBLE REACTION-FILM MODEL

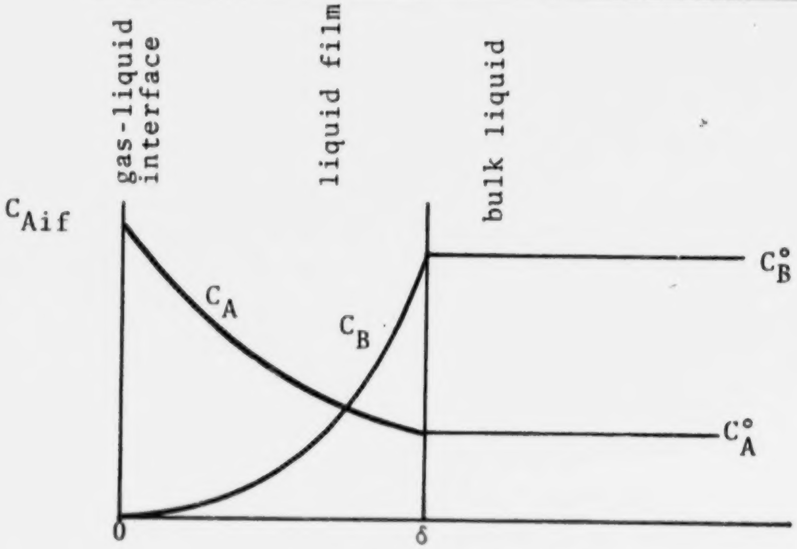

FIGURE 4.2.6-2
CONCENTRATION PROFILES FOR A 2ND ORDER IRREVERSIBLE REACTION

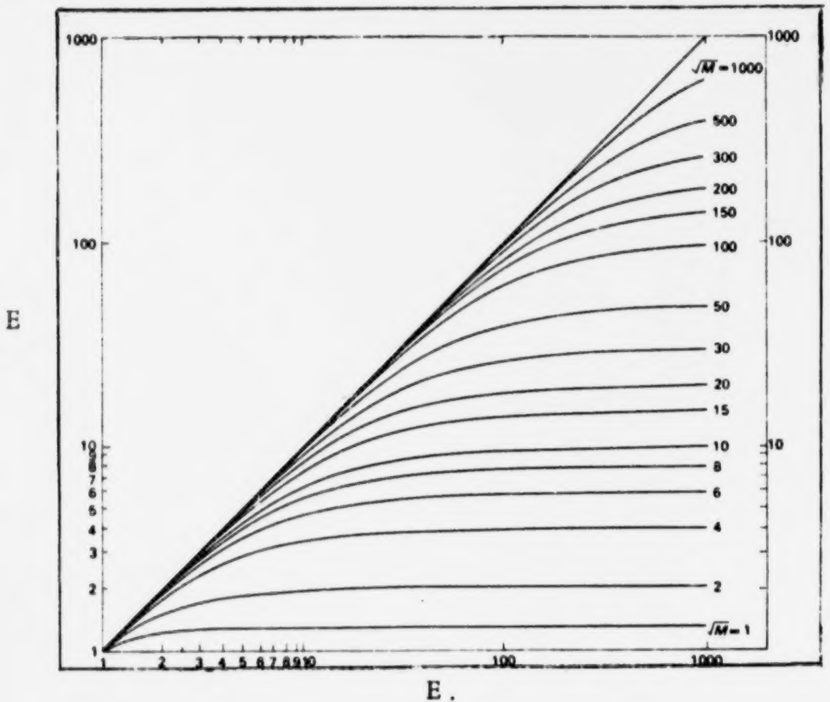

FIGURE 4.2.6-3
ENHANCEMENT FACTORS FOR SECOND-ORDER REACTION; FOR QUIESCENT LIQUID OR AGITATED LIQUID (FILM OR HIGBIE MODELS). BASED ON EQUATION 4.2.6-22

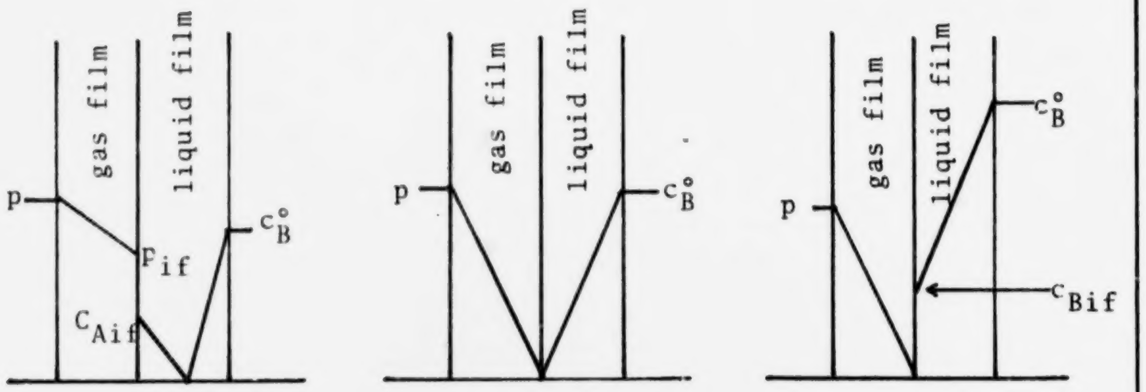

FIGURE 4.2.6-4
TWO-FILM MODEL: CONCENTRATION PROFILES FOR INSTANTANEOUS REACTION WITH VARYING CONCENTRATION OF REACTANT "B"

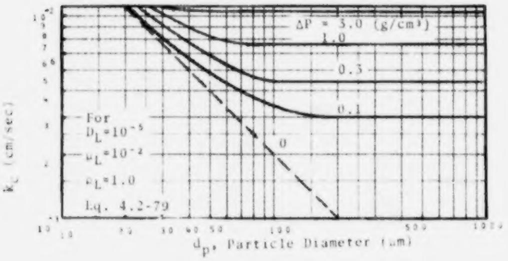

FIGURE 4.2.7-1

TRANSFER COEFFICIENT FOR PARTICLE FALLING IN WATER VS. PARTICLE DIAMETER, WITH DENSITY DIFFERENCE AS PARAMETER

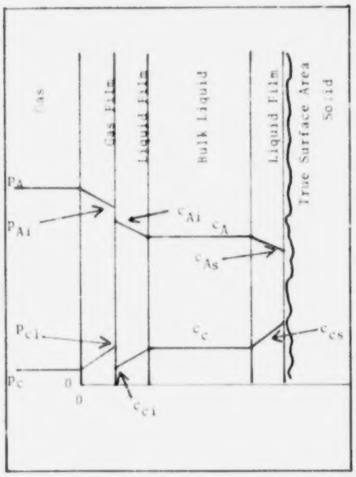

FIGURE 4.2.7-2

RESISTANCES TO MASS TRANSFER IN A SLURRY

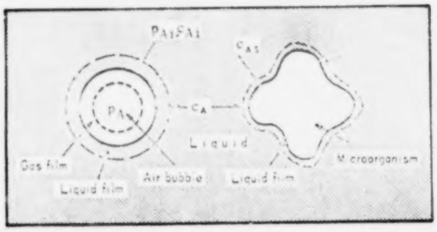

FIGURE 4.2.7-3

TRANSFER OF OXYGEN FROM AIR BUBBLE TO BACTERIAL SITE.

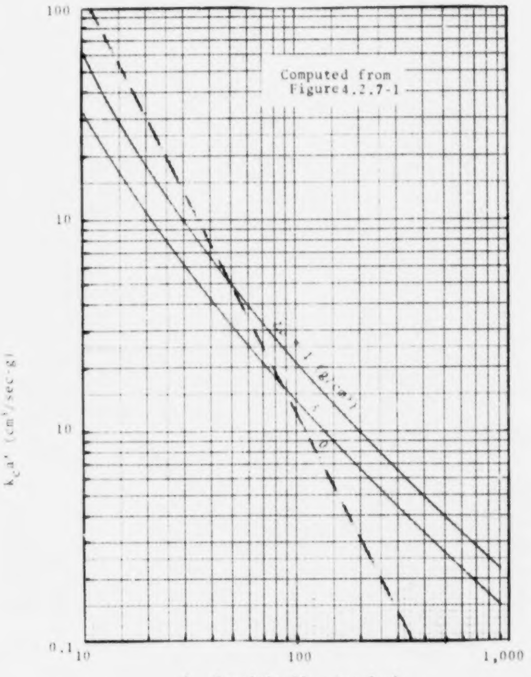

FIGURE 4.2.7-4

MASS TRANSFER COEFFICIENT PER GRAM OF PARTICLES FALLING IN WATER VS. PARTICLE DIAMETER, WITH DENSITY DIFFERENCE PARAMETER

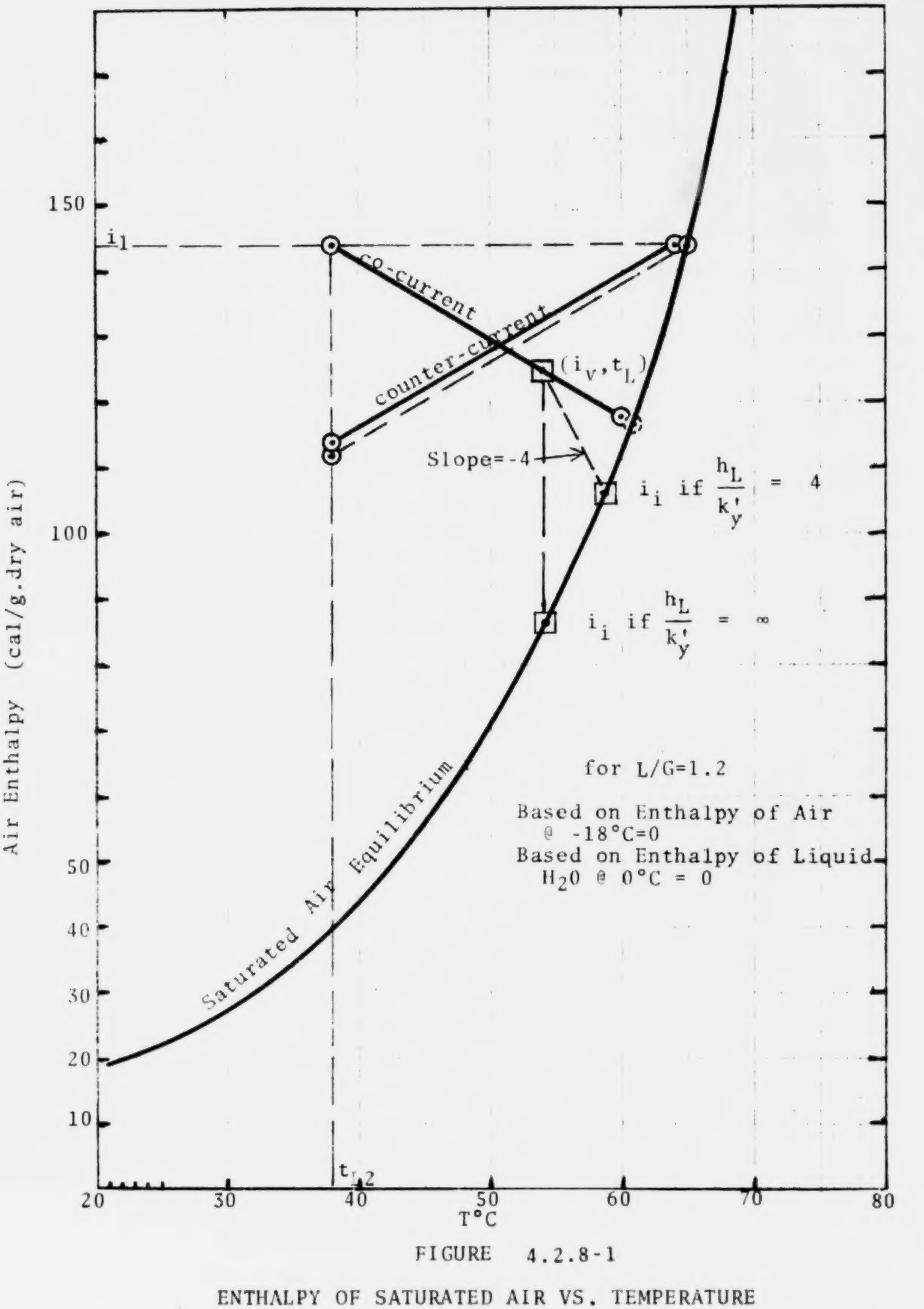

FIGURE 4.2.8-1

ENTHALPY OF SATURATED AIR VS. TEMPERATURE

SECTION 4.2 NOMENCLATURE

LATIN

a - specific surface area m^2/m^3 or cm^2/cm^3

A - component "A"

B - component "B"

c - mass concentration, Kg/m^3 or g/cm^3

$\hat{c}$ - molar concentration, $Kgmol/m^3$ or $gmol/cm^3$

C_p - specific heat, kcal/(kg°C) or cal/(g°C)

d - diameter, m or cm

D - diffusivity, cm^2/sec

E - enhancement factor

E - overall plate efficiency

E_{MV} - Murphree vapor efficiency

g - acceleration of gravity, 9.81 m/sec^2 or 981 cm/sec^2

G - gas mass flux kg/(sec m^2) or g/(sec cm^2)

$\hat{G}$ - gas molar flux, kgmol/(sec m^2) or gmol/(sec cm^2)

h' - heat transfer coefficient, cal(sec cm^2 °C)

$\hat{H}$ - Henry's law constant, atm/(kgmol/m^3), or mbar/(gmol/cm^3)

H - Henry's law constant, atm/mole fraction

i - enthalpy, cal/g

k - thermal conductivity, cal/sec cm °C)

k - first order reaction rate constant, 1/sec

$\hat{k}_G$ - gas film mass transfer coefficient, gmol/(sec cm^2 atm)

k_L - liquid film mass transfer coefficient, cm/sec

K_L - overall liquid phase transfer coefficient, cm/sec

$\hat{K}_G$ - overall gas phase transfer coefficient, gmol/(sec atm cm^2)

SECTION 4.2 NOMENCLATURE

LATIN

K_e - chemical equilibrium constant

L - liquid mass flux, kg/(sec m^2) or g/(sec cm^2)

L_M - liquid mass flowrate, kg/sec or g/sec

M - molecular weight, kg/kgmol or g/gmol

n - number of actual plates

$\hat{N}$ - molar flux, kgmol/(m^{2}sec) or gmol/(cm^{2}sec)

N - mass flux, kg/(m^{2}sec) or g/(cm^{2}sec)

p - partial pressure of solute, mbar, or atm

P - total pressure, mbar or atm

P_{BM} - log mean pressure or component B, mbar or atm

P - reaction products

q - heat flux, cal/(sec cm^2)

r - radius

Rg - ideal gas law constant

$\hat{R}$ - rate of reaction per unit volume, kgmol/cm^{3}sec) or gmol/(cm^{3}sec)

t - temperature °C

t - time, sec

T - absolute temperature, °K

u - velocity, m/sec or cm/sec

v - velocity, m/sec or cm/sec

$\hat{x}$ - mole fraction solute in liquid

$\hat{y}$ - mole fraction solute in gas

$\hat{y}^*$ - mole fraction in gas in equilibrium with $\hat{x}$

$\hat{Y}$ - moles sulute per mole inert in gas

$\hat{z}$ - mole fraction of solute in absorbent

Z - diffusion parameter

SECTION 4.2 NOMENCLATURE

DIMENSIONLESS NUMBERS

N_{Sc} ≡ $\mu_G/\rho_G D_G)$ Schmidt Number

N_{Sh} ≡ $k_G R_G Td/D_G$, Sherwood Number

N_{Pr} ≡ $C_p \mu/k$, Prandtl Number

N_{Pe} ≡ du/D, Peclet Number

N_{Re} ≡ $\rho du/\mu$, Reynolds Number

GREEK

ε - eddy diffusivity, cm^2/sec

θ - contact time, sec

$\hat{\lambda}_M$ - molar latent heat, cal/mole

ρ - density, kg/m^3 or g/cm^3

μ - viscosity, g/(cm sec)

SUBSCRIPTS

A - component "A"

b - bubble

b - number of moles of component "B" reacting with one mole of component "A"

B - component "B"

e - in equilibrium

G - gas phase

i - instantaneous reaction

i - interface

L - liquid phase

p - particle

t - teriminal velocity

SECTION 4.2 NOMENCLATURE

SUBSCRIPTS

v - vapor

1 - bottom

2 - top

SUPERSCRIPTS

$*$ - in equilibrium

^ - quantity in molar units

. - original value, i.e. without reaction

SECTION 4.2 REFERENCES

Astarita, G.,"Mass Transfer with Chemical Reaction", Elsevier Publishing Company, Amsterdam (1967).

Calvert, S., Kapo, G., Chemical Engineering, Feb. 4, March 4, (1963).

Calvert, S., Mehta, D.M., Russell, R.R., Am. Ind. Hygiene Assoc. J., 30, 57 (1969).

Crank, J., "The Mathematics of Diffusion", Oxford University Press, London (1957).

Danckwerts, P.V., "Gas Liquid Reactions", McGraw-Hill, New York (1970).

Danckwerts, P.V., Kennedy, A.M., Trans. Inst. Chem. Eng., 32, S49, (1954).

Danckwerts, P.V., Ind. Eng. Chem. 43, 1460 (1951).

Dedrick, R.L., Beckmann, R. B., "Kinetics of Adsorption by Activated Carbon from Dilute Solution", Presented at the 59th Annual Meeting, A.I.Ch.E., December (1966).

Denbigh, K.G., "The Principles of Chemical Equilibrium", Cambridge University Press, Cambridge, England (1955).

Emmert, R. E., Pigford, R. L., Am. Inst. Chem. Eng., J. 8, 170 (1962).

Fair, G.H., Geyer, J.C. and Okun, D.A., "Water and Wastewater Engineering", John Wiley, New York (1968).

Harriot, P., Chem.Eng. Sci. 17, 148 (1962).

Hatta, S., Tech. Reports, Tohoku Imp. Univ. 8, 1 (1928-9).

Hatta, S., Technol. Reports, Tohoku Imp. Univ. 10, 119 (1932).

Higbie, R., Trans. Am. Inst. Chem. Eng. 35, 365 (1935).

Hikita, H., Asai, S., Inter. Chem. Eng. 4, 5, (1964).

Hobler, T., "Mass Transfer and Absorbers", Pergamon Press, Oxford (1966).

Marangozis, J., Johnson, A.I., The Canadian J. of Chem. Eng., 231, (Dec. 1962).

Marshall, R.W., Pigford, R. L., "Applications of Differential Equations to Chemical Engineering", Univ. of Delaware (1947).

Mehta, D.M., Calvert, S., British Chem. Eng. 16, 781 (1970).

Metha, D. M., Calvert, S., Environ. Sci. & Tech. 1, 325 (1967).

Mehta, D. M., Calvert S., Brit. Chem. Eng. 14, 1563, 1969.

Murphree, E. V., Ind. Eng. Chem., 17, 747 (1925).

Olander, D. R., A.I.Ch.E.J., 6, 233 (1960).

SECTION 4.2
REFERENCES

Perry, R. H., editor, "Chemical Engineers Handbook", 4th ed., McGraw-Hill, N. Y. (1963).

Sherwood, T. K., Pigford, R. L., "Absorption and Extraction", McGraw-Hill, New York, (1952).

Toor, H. L., Marchello, J. M., A.I.Ch.E.J. 4, 98 (1958).

Treybal, R. E., "Mass Transfer Operations", McGraw-Hill, New York, (1955).

Van Krevelen, D. W., Hoftijzer, P. J., Rec. Trav. Chim. 67, 563 (1948).

Whitman, W. G., Chem. and Met. Eng. 29, 147 (1923).

4.3 GENERAL CONCEPTS OF PARTICLE COLLECTION

4.3.1 INTRODUCTION

Small dust particles are usually kept suspended in air for long times by the viscous force or drag of the air which resists any forces tending to precipitate them. Sometimes forces due to electrostatic charge, radiation flux, and other phenomena may also act to keep the particles suspended.

Dust suspensions are not a stable state and will separate in time. Separation processes and equipment are intended to make this time as short as possible. In this section we shall review some of the physical properties of aerosols, discuss the different separation and collection mechanisms and concentrate on those mechanisms which are important for dust separation by wet scrubbers.

In the scrubbing of particulate matter from gases, one is usually concerned with particles smaller than about 10 μm in diameter, since larger particles are relatively easier to separate. To design and operate a wet scrubber successfully it is important to know the properties of small particles and the dependence of these on such factors as particle composition, method of particles formation, previous treatment, etc. There are many good books, Fuchs (1964), Green and Lane (1964), Soo (1967), Davies (1966), Hidy and Brock (1970), and others which discuss the physical properties and fluid dynamics of aerosols, so this part shall be covered here only briefly. Then we shall describe the different mechanisms used for small particle collection in wet scrubbers.

4.3.2 DEFINITIONS AND TERMINOLOGY

4.3.2.1 Dispersion Aerosols

Dispersion aerosols are formed by the grinding or atomization of solids and liquids and by the transfer of powders into a state of suspension through the action of air currents or vibration. Condensation aerosols are formed when supersaturated vapors are condensed or when gases react chemically to form a non-volatile product and they are usually smaller than 1 μm in dia. Dispersion aerosols are, in most cases, considerably coarser and contain a wider range of particle sizes than condensation aerosols. When the dispersed phase is solid the dispersion aerosol usually consists of individual or slightly aggregated particles of irregular form. In condensation aerosols, solid particles are often loose aggregates of a very large number of primary particles of a regular crystalline or spherical form.

Dispersion aerosols with solid particles are called dusts. Condensation aerosols with a solid disperse phase or a solid and liquid disperse phase are called smokes or fumes. Condensation and dispersion aerosols with a liquid disperse phase are called mists. This terminology applies regardless of particle size. Distinction between smokes and condensation mists is sometimes difficult, but is preferable to calling both types of aerosols smoke. In many cases a combination of dispersion and condensation aerosols are encountered.

4.3.2.2 Particle Size

Each of the aerosol types mentioned may involve particles in a very wide range of sizes, between 10^{-3} μm and 10^{3} μm. This wide size distribution affects many of the physical properties of the dispersed system. It is convenient to subdivide the range of aerosol particle size into three groups: 10^{-3} μm to λ, λ to ≈ 1 μm, and ≈ 1 μm to 10^{3} μm, where "λ" is the mean free path of the gas molecules (0.065 μm at 20°C and 760 mm Hg). Particles in the different size groups behave differently with respect to different physical properties, like: resistance of the medium to particle movement, light scattering, rate of evaporation and cooling, and dominant mechanism of particle removal from the medium.

Examination of particles with the aid of an optical or electron microscope involves the measurement of a linear dimension of a particle. The measured "particle size" is related to the particle perimeter or to the particle projected area diameter. Particle size measurement in this manner does not account for variation in particle density or shape. All laws describing the properties of aerosols can be expressed most simply for particles of spherical shape. To accomodate non-spherical particles it is customary to define a "coefficient of sphericity" which is the ratio of the surface area of a sphere with the same volume as the given particle to the surface area of the particle.

An estimate of particle volume can be obtained from microscopic sizing, and by assuming a density, one can obtain an estimate of particle weight. Because of large variations in particle density and the aggregated nature of atmospheric particles it is useful to define another quantity as a measure of particle size based on aerodynamic behavior of the particle. The Stokes radius, r_s, is defined as the radius of a sphere having the same falling velocity as the particle and a density equal to that of the bulk material from which the particle was formed. Since dispersion and condensation aerosols are usually formed from many materials of different densities it is more useful to define another parameter called the aerodynamic diameter, d_{pa}, which is the diameter of a sphere having the same falling velocity as the particle and a density equal to 1 g/cm^3. The aerodynamic diameter will be discussed in more detail in Section 4.6.7.2.

In calculating the average size of measured particles, attention should always be given to the purpose of these calculations. It is desirable to use averages relating to definite physical properties such as surface or volume. For example, if the surface of a certain dust is to be determined, more weight should be given to finer particles. Hatch and Choate (1929) defined an average diameter as the diameter of a hypothetical particle which in some way represents the total number of particles in the sample. Their definitions are as follows:

$$\text{Mean diameter} = d_{pn} = \frac{\Sigma\, n\, d_p}{\Sigma\, n} \qquad (4.3.2\text{-}1)$$

$$\text{Mean length diameter} = d_{pln} = \frac{\Sigma\, n\, d_p^{2}}{\Sigma\, n\, d} \qquad (4.3.2\text{-}2)$$

Mean surface diameter $= d_{psn} = \left(\dfrac{\Sigma\ n\ d_p^2}{\Sigma\ n}\right)^{1/2}$ (4.3.2-3)

Mean volume diameter $= d_{pvn} = \left(\dfrac{\Sigma\ n\ d_p^3}{\Sigma\ n}\right)^{1/3}$ (4.3.2-4)

Mean volume-surface diameter $= d_s = \dfrac{\Sigma\ n\ d_p^3}{\Sigma\ n\ d_p^2}$ (4.3.2-5)
(Sauter mean diameter)

Thus for example, Equation 4.3.2-3 gives the surface area of that particle which when squared and multiplied by the total number of particles will give the total particle area.

4.3.2.3 Particle Size Distribution

The number distribution of sizes may be plotted against small equal intervals of size to derive a histogram which in the limit becomes the size frequency curve. The distribution of sizes in a particulate cloud arises from a number of chance causes, and one may expect that the distribution curve would follow the normal or Gaussian error curve. In actual fact it is rare for the sizes to be distributed equally about the mean. In general there is a skewness of the distribution and the probability curve follows a geometric or logarithmic form. By plotting the log of the particle size against frequency, the skew curve is converted into one of the symmetrical types. The log probability distribution may be expressed as:

$$f(d_p)_n = \frac{\Sigma\ n}{\log \sigma_g \sqrt{2\ \pi}} \exp\left[\frac{-(\log d_p - \log d_{pg})^2}{2 \log^2 \sigma_g}\right] \qquad (4.3.2\text{-}6)$$

where "$f(d_p)_n$" is the frequency of occurrence of diameter "d", "Σ n" the total number of particles, "σ_g" the geometric standard deviation obtained from

$$\log \sigma_g = \left(\frac{\Sigma\ [n\ (\log d_p - \log d_{pg})^2]}{\Sigma\ n}\right)^{0.5} \qquad (4.3.2\text{-}7)$$

"d_{pg}" is the geometric mean diameter defined as:

$$d_{pg} = \sqrt[n]{d_1\ d_2\ \ldots\ d_n} \qquad (4.3.2\text{-}8)$$

If the cumulative percentage of number of particles up to various stated sizes is plotted against diameter on logarithmic probability paper a straight line should theoretically be obtained as shown by Hazen (1914). The frequency distribution is related to the cumulative size frequency distribution by "ϕ", by:

$$f(d_p) = \frac{d\phi}{d(d_p)} \qquad (4.3.2\text{-}9)$$

where "$f(d_p)$" is the function defining the frequency size distribution. Equation 4.3.2-9 is multiplied and divided by "d_p" and we get after rearranging

$$\frac{d\,\phi}{d(\ln d_p)} = d_p\,\phi\,(d_p) \qquad (4.3.2\text{-}10)$$

It is usual to plot $d_p \phi\,(d_p)$ against "$\ln d_p$" for distributions extending over a wide range of particle sizes.

From the log-probability curve, the number median or 50 percent diameter, which by definition corresponds to the geometric mean, d_g, can at once be derived. The geometric standard deviation can also readily be calculated since it can be shown from the probability integral that:

$$\sigma_g = \frac{\text{84.13 percent size}}{\text{50 percent size}} = \frac{\text{50 percent size}}{\text{15.87 percent size}} \qquad (4.3.2\text{-}11)$$

Similarly, if the distribution of particles by mass is plotted on the same basis, the mass median diameter, d_{pm}, and the geometric standard deviation by mass, σ_{gm}, can be derived. Since the geometric standard deviation by mass is the same as that by number, Hatch (1933) showed that:

$$\log d_{pn} = \log d_{pg} + 6.9078 \log^2 \sigma_g \qquad (4.3.2\text{-}12)$$

An important property of the log normal distribution is, that if the number distribution is log normal, the weight distribution is also log normal and with the same log standard deviation. The generalization of the important property of the log normal distribution (also called Kapeyn's law) described above, can be formulated as follows: If the basic distribution of say particle diameter, d_p, is log normal with mean "μ" and standard deviation "σ", then the jth moment distribution (j=2 for the distribution of surface area, j=3 for that of particle volume, etc) is again log normal with the same standard deviation "σ" and mean

$$\mu_j = \mu + 2.303\, j\, \sigma^2 = \text{jth moment} \qquad (4.3.2\text{-}13)$$

This relation between the two means, that of the basic distribution and that of the moment distribution is in terms of logarithms to the "base 1°" by "base 10".

The generalization of the moment distribution property of log normal distributions proves very useful in practical work when we wish to obtain an estimate of the surface (volume) proportions from the distribution of particle size. Making use of this relation between the moment distributions of a log normal variate, both the volume and the surface mean could be immediately calculated by formula 4.2.3-13 once the basic distribution of particle diameter is given.

From a knowledge of the mean of the moment distribution in conjunction with the fact that the standard deviation for the different moment distributions is identical, the straight line representing the distribution on logarithmic probability paper can be constructed, and from it we can derive the distribution curve.

4.3.3 NATURE OF SUSPENSION OF PARTICLES

4.3.3.1 Motion of Individual Particles

Three types of forces act on an aerosol particle: external forces (gravitational, electrical, magnetic, etc.), resistance of the medium, and interaction of particles. The third is, in most cases, considerably less than the others and the particles can be considered independent of one another.

Particles in air extend over a wide range of sizes from those of size much larger, to those much smaller, than the mean free path of the gas molecules, which is 6.53×10^{-2} μm at 20°C and 760mm. The resistance of a gas to the motion of particles much larger than the mean free path, is caused by hydrodynamic forces. For rigid spherical particles where there are no inertial effects arising from fluid displaced by the moving particle and where the medium is infinite in size, this resistance is expressed by Stokes' law:

$$F = -3 \pi \mu_G d_p u_r \qquad (4.3.3\text{-}1)$$

where "F" is the resistance force and "u_r" is the relative velocity between the particle and the gas.

The terminal settling velocity of a spherical particle can be derived by equating the gravitational and resistance forces.

$$u_t = \frac{(\rho_p - \rho_G) g d_p^2}{18 \mu_G} \qquad (4.3.3\text{-}2)$$

When the particle size approaches the mean free path of the gas molecules, particles "slip" between air molecules and the resistance of the air is thought of as "discontinuous". A correction factor called the Cunningham correction factor is applied to account for the increased rate of particle fall. The particle terminal settling velocity then becomes;

$$u_t = \frac{(\rho_p - \rho_G) g d_p^2 C'}{18 \mu_G} \qquad (4.3.3\text{-}3)$$

where "C'" is the Cunningham correction factor.

The Cunningham correction factor can be calculated from:

$$C' = \left(1 + A \frac{2 \lambda}{d_p}\right) = 1 + \left[1.257 + 0.40 \exp \left(-1.1 \frac{d_p}{2 \lambda}\right)\right] \frac{2 \lambda}{d_p} \qquad (4.3.3\text{-}4)$$

where "A" is a constant and "λ" the mean free path.

From the kinetic theory of gases the mean free path is:

$$\lambda = \frac{k\ T}{\sqrt{2}\ \pi\ P\ \sigma^2} \qquad (4.3.3\text{-}5)$$

where "k" is Boltzman constant and "σ" is the molecular diameter. Thus at a constant temperature the mean free path is inversely proportional to the pressure and at a constant pressure it is directly proportional to the temperature. (When the viscosity relationship for "λ" is used, Glasstone(1946), "λ" is proporational to a fractional power of the temperature, however for small temperature changes the above approximation is valid.) For air at 20°C:

$$P\ \lambda = 6.61\text{x}10^{-3} \qquad (4.3.3\text{-}6)$$

where "P" is the pressure in mbars and "λ" is the mean free path in cm.

Inserting Equation 4.3.3-6 into Equation 4.3.3-4 one gets for the Cunningham correction factor at 20°C:

$$C' = 1 + A\,\frac{2\ \lambda}{d_p} = 1 + \frac{1.32\text{x}10^{-2}}{P\ d_p}\left[1.257 + 0.40\ \exp\left(-83.2\ P\ d_p\right)\right] \qquad (4.3.3\text{-}7)$$

For a constant pressure of 1,000 mbars one gets:

$$\lambda = 2.23\text{x}10^{-8}\ T\ \text{cm} \qquad (4.3.3\text{-}8)$$

when "T" is in °K and "λ" in cm. Substituting Equation 4.3.3-8 into Equation 4.3.3-4 gives for "C" at a constant pressure of 76 cm Hg:

$$C' = \left(1 + A\,\frac{2\ \lambda}{d_p}\right) = \left\{1 + \frac{2\ T\ 10^{-8}}{d_p}\left[2.79 + 0.894\ \exp\left(-\frac{2.47\text{x}10^7\ d_p}{T}\right)\right]\right\} \qquad (4.3.3\text{-}9)$$

Stokes' law is valid so long as there are no inertia effects arising from displacement of the air by the moving sphere, $N_{Re} \leq 0.05$. ($N_{Re} = 0.05$ corresponds to a 77 µm sphere of unit density falling through air at room temperature and pressure). At higher Reynolds numbers, the deviation becomes greater and Stokes' law tends to overestimate the velocity. From consideration of dynamical similarity the drag coefficient, C_D, which is defined as the ratio of the resistance to the product of cross-section and dynamic pressure, has been introduced. In the simple case of Stokes' law:

$$C_D = \frac{24}{N_{Re}} \qquad (4.3.3\text{-}10)$$

Since "C_D" and "N_{Re}" both contain a velocity term it is not convenient to use a graph of "N_{Re}" vs. "C_D" to calculate the velocity, the expression ($C_D\ Re^2$) which eliminates the velocity term is employed, and a direct solution for velocity can be obtained. Equation 4.3.3-10 now becomes:

$$N_{Re} = \frac{C_D \, N_{Re}^2}{24} \qquad (4.3.3\text{-}11)$$

For the inverse problem of finding the size of particles from their rate of settling, a graph which correlates "N_{Re}" and "C_D" is used. Figure 4.3.3-2 from Fuchs (1964) gives the measured rate of settling of particles and drops in air. The broken lines were calculated by Stokes' law.

When aerosol particles occupying a space confined by walls settle with a velocity, u, the medium moves in the reverse direction with a mean velocity, ψ u, where "ψ" is the volume of the disperse phase per cm^3 of the system. For most cases encountered in air pollution work, "ψ" is usually a small fraction of the total volume of the continuous phase. Since the medium is entrained in the vicinity of the particles, then in the spaces between them the velocity of the counterflow is greater than "ψ u". Thus the rate of settling of groups of particles is less than that of isolated particles in an infinite volume by a factor $(1 + \alpha \psi)$ where $\alpha > 1$. For settlement of monodispersed suspensions in water, with radii 2.4 to 4.4 μm and $\psi < 0.04 - 0.08$, values of "α" ranging from 4.8 to 6.9 were found, Fuchs (1964). Thus for aerosols settling in a confined space in the Stokes' law region, the settling velocity will be:

$$u_t = \frac{(\rho_p - \rho_G) \, g \, d_p^2}{18 \, \mu_G \, (1 + \alpha \psi)} \qquad (4.3.3\text{-}12)$$

4.3.3.2 Brownian Motion and Diffusion

The terminal settling velocities of particles much smaller than the mean free path of the gas molecules is very low, the random bombardment of air molecules deflects these particles and a random motion is superimposed on the settling motion. This random motion is called Brownian motion. Removal of these small particles is affected mainly by diffusion.

The diffusion coefficient is related to particle diameter by Fuchs (1964) by:

$$D_p = \frac{R \, T \, C'}{3 \, \pi \, \mu_G \, d_p \, N} \qquad (4.3.3\text{-}13)$$

where "N" is Avogadro's number. Figure 4.3.3-3 correlates diffusivity with particle diameter at various operating conditions.

The mean square displacement of a particle, $\overline{\Delta_x^2}$, in a given interval of time "t" along an axis "x" is:

$$\overline{\Delta_x^2} = 2 \, D_p \, t \qquad (4.3.3\text{-}14)$$

Figure 4.3.3-4 compares the root mean square displacement of a particle in one second in a given direction with the distance a spherical particle ($\rho = 1\ g/cm^3$) falls in one second in air at 76 cm Hg pressure and 20°C under gravity, calculated from Stokes' equation. It can be seen that in air, particles of unit density smaller than approximately 0.5 μm in diameter, have larger Brownian displacement than displacement due to gravitational settling.

4.3.3.3 Electrostatic Properties

Charging of aerosol particles happens in one of three ways: 1. Charging during the process of generation; 2. Charging through free ion diffusion; 3. Charging through corona discharge.

Different aerosols have different charge distributions according to their generation methods. Dust particles become charged, either by friction or separation of the particles, with the result that two groups of oppositely charged particles are formed. The dispersing medium does not become charged appreciably and any electrification detected would arise from fine particles suspended in it. The total electrification of the two sets of charged particles and the fine particles in the air accompanying them, is zero. In general, only small charges would be found on the charged particles. The average charge per particle increases, rather more slowly than the square of the diameter, but the spread of charges in relation to particle size is very large. In homogeneous systems, when the dust and the container from which it is dispersed are of the same material, the charges of opposite sign are approximately equal and there is no net charge. In an inhomogeneous system, asymmetry of charge distribution is not usually large and depends on the proportion of particles striking the surface of the containing vessel relative to those just separated.

When mists are produced by atomization, droplets from polar liquids are charged considerably more than those of non-polar liquids. The droplet charge depends upon the number of positive and negative ions which happen to be in that volume of liquid when it is released. There is then a random distribution of the charges in the droplets. In non-conducting liquids the charges produced follow a normal distribution with the average charge of zero and the mean square charge proportional to droplet volume.

Particles of condensation aerosols generated at moderate temperatures are uncharged, but they become gradually charged by gaseous ions diffusing to them, until a steady state is reached. The process is a random one and the proportion of particles becoming charged will depend on particle size, but the number of positives and negatives should be equal provided there are no extraneous effects.

Aerosol charging during generation and through free ion diffusion usually produces charges of both signs in equal quantities. Corona discharge, on the other hand, will lead to a singly charged aerosol. Corona discharge affects the aerosol through two mechanisms: Field charging and diffusion charging. Field charging predominates for particles larger than about 0.5 μm in diameter while diffusion charging predominates for smaller particles. In the intermediate range, charging is due to both mechanisms and the rate of particle charging shows a minimum at a particle diameter of about 0.3 μm.

When a conducting particle is suspended in an electric field, its charge will increase until the field caused by its own charge equals the outside field in its neighborhood. At that point the particle would not be charged further and is said to reach its saturation charge. Oglesby and Nichols (1970) give the following equation for the saturation charge of a conducting sphere:

$$q_s = 3 \pi d_p^2 \varepsilon_0 E_c \qquad (4.3.3\text{-}15)$$

For a non-conductive particle:

$$q_s = 3 \frac{\varepsilon}{\varepsilon + 2} \pi \varepsilon_0 d_p^2 E_c \qquad (4.3.3\text{-}16)$$

where "ε" is the relative dielectric constant. The charge as a function of time for a conducting and non-conducting sphere is:

$$q_{(t)} = q_s \frac{1}{1 + \dfrac{4 \varepsilon_0}{N_0 e \mu t}} \qquad (4.3.3\text{-}17)$$

where "N_0" is the number of ions per unit volume with charge, e, and mobility, μ.

For diffusion charging the same authors give the equation:

$$q_{(t)} = \frac{d_p k T}{2 e} \ln \left(1 + \frac{\pi d_p v N_0 e^2 t}{2 k T} \right) \qquad (4.3.3\text{-}18)$$

where "k" is the Boltzmann constant and "v" the root mean square thermal velocity of the ions given by:

$$v = \left(\frac{8 k T}{\pi m} \right)^{1/2} \qquad (4.3.3\text{-}19)$$

and "m" is the mass of an ion.

In the intermediate range of particle sizes both charging mechanisms contribute significant charges. In this case, it is more nearly correct to sum the rates of charging from the two mechanisms and then solve for the charge. The resulting equation is a nonlinear differential equation with no analytical solution. Oglesby and Nichols (1970) present several solutions to the combined equation.

The electrostatic force acting on a charged particle in an electric field, "E", is given by:

$$F = q E \qquad (4.3.3\text{-}20)$$

For a quasi-stationary motion, neglecting all forces except electrostatic and drag, one gets for a particle obeying Stokes' law:

$$u_{pE} = \frac{q\ E\ C'}{3\ \pi\ d_p\ \mu_G} \qquad (4.3.3\text{-}21)$$

By substituting for "q" one can derive an equation for the velocity of particle charged by diffusion, field, or both.

An aerosol consisting of particles all bearing a charge of the same sign will uniformly disperse under the action of its own bulk charge. The rate of scattering of a charged aerosol cloud is described by:

$$\frac{1}{c} - \frac{1}{c_i} = \frac{4\ q^2\ t\ C'}{3\ d_p\ \mu_G} \qquad (4.3.3\text{-}22)$$

where "c_i" is the initial particle concentration and "c" is the concentration at time "t".

Since the concentration of the aerosol is the same in all places at any instant during electrostatic scattering, motion of the medium has no effect on the scattering, so that the equation given above is valid for an aerosol experiencing either laminar or turbulent flow.

When the aerosol contains both positive and negative particles, not in equal concentrations, the particles in the minority are driven to the center of the aerosol cloud where their concentration consequently increases. Then the charge density in this central nucleus decays asymptotically, until it becomes practically neutral. At the same time scattering of the purely unipolar part of the aerosol outside the nucleus continues.

4.3.3.4 Aerosols in a Magnetic Field

When a particle with no intrinsic magnetic properties, moving with the gas at a velocity "u_G" is charged to an electric charge "q" and is then introduced into a magnetic field of strength "H", it will be acted on by a force at right angles to both the direction of the field and its direction of motion. The particle will thus be given a terminal drift velocity which may be calculated using Stokes' law:

$$u_{pM} = \frac{H\ q\ u_G\ C'}{3\ \pi\ \mu_G\ d_p} \qquad (4.3.3\text{-}23)$$

Here the drift velocity is a function of the gas velocity; the higher the gas velocity the higher the particle velocity out of the stream.

If small magnetic particles were introduced into a magnetic field they would align themselves in the magnetic field, their opposite ends being attracted to the two poles of the magnet. The net magnetic force acting on the particle can be calculated by the algebraic addition of the attractive and repulsive forces.

4.3.3.5 Radiometric Forces

If a thermal gradient is set up in an aerosol, particles will move along the gradient under the influence of the differential molecular bombardment giving rise to radiometric forces. Thus particles are driven away from a hot surface and deposited on a cold one in the vicinity. Similarly an intense beam of light will cause particles to move either in the direction of radiation flux or against it. When the radiometric force is caused by a temperature gradient in the gas it is called thermophoresis and when the cause is the illumination of particles, the force is called photophoresis.

Radiometric forces, like other interactions between particles and gas, depend essentially on the ratio of the particle radius to the mean free path of the gas molecules.

Thermophoresis

For $r << \lambda$ thermophoresis is the result of gas molecules impinging on the particle from opposite sides with different mean velocities. The net force caused by difference in momentum received by the particle from each side as calculated by Waldmann (1959) is:

$$F_T \approx - \frac{d_p^2 \ P \ \lambda}{T} \ \nabla T \qquad (4.3.3\text{-}24)$$

The thermophoretic velocity in this regime is given by:

$$u_{PT} = \frac{6 \ \mu_G}{(8 + \pi \ \alpha) \ T \ \rho_G} \ \nabla T \qquad (4.3.3\text{-}25)$$

where "α" is the fraction of gas molecules reflected diffusely by the particle. For freshly formed and very smooth surface of amorphous particles and for liquid particles $\alpha \approx 0.9$. For particles with rough surfaces obtained by mechanical working, or with aged particles, $\alpha \approx 1.0$.

When the size of a particle becomes large compared to the mean free path ($\lambda << r$) the molecule-particle interaction changes; the molecule no longer sees the particle as another molecule, but as a solid surface. In the layer of gas adjacent to the non-uniformly heated wall, approximately the same tangential temperature gradient will be established. If the temperature is higher to the left, the gas molecules impinging on the element of surface from the left have on the average, a higher velocity than those coming from the right. As a result the wall receives an impulse directed to the right, against the temperature gradient, and an equal impulse directed to the left is imparted to the gas, making it slip along the surface towards the higher temperature. From these considerations, Epstein (1929) derived the equation for the thermophoretic force:

$$F_T = - \frac{9 \ \pi \ d_p \ \mu_G^2}{2 \ \rho_G \ T} \left[\frac{k_G}{2 \ k_G + k_p} \right] \nabla T \qquad (4.3.3\text{-}26)$$

where "k_G" and "k_p" are the thermal conductivities of the gas and the particle respectively.

Under the Epstein force and the Stokes drag, a large particle at steady state, moves with the velocity:

$$u_{PT} = -\frac{3\,\mu_G}{2\,\rho_G\,T}\left[\frac{k_G}{2\,k_G + k_p}\right]\nabla T \qquad (4.3.3\text{-}27)$$

Epstein's equation agrees with experimental measurements for particles of low thermal conductivity ($k_p/k_G \lesssim 10$). However, for particles of high thermal conductivities, experimentally measured thermophoretic velocities were 30 - 100 times those predicted by the Epstein equation. Brock (1962) accounted for this discrepency by his theory which gives for the thermophoretic velocity:

$$u_{PT} = -\frac{3\,\mu_G\,C'}{2\,\rho_G\,T}\left[\frac{1}{1 + \frac{6\,C_m\,\lambda}{d_p}}\right]\left\{\frac{\frac{k_G}{k_p} + C_t\,\frac{2\,\lambda}{d_p}}{1 + 2\,\frac{k_G}{k_p} + 4\,C_t\,\frac{\lambda}{d_p}}\right\}\nabla T \qquad (4.3.3\text{-}28)$$

Brock suggests that "C_t" ranges from 1.875 to 2.48 and "C_m" from 1.00 to 1.27. He showed that his equation satisfactorily accounts for experimental results for good and poor conductors to within ≈25%. Derjaguin and Bakanov (1962) using a different approach deduced for the thermophoretic velocity of large particles:

$$u_{PT} = -\frac{(4\,k_g + 0.5\,k_p)\,\mu_G}{(2\,k_g + k_p)\,\rho_G\,T}\,\nabla T \qquad (4.3.3\text{-}29)$$

Goldsmith and May (1966) compared these three equations with experimental results for aerosol composed mainly of chromium particles and found that Derjaguin and Bakanov equation agrees best with velocities measured in air and helium. The Epstein equation modified by the addition of the Cunningham correction factor gave good agreement in helium and not such good agreement in air. Brock's equation gave better approximation in air and somewhat worse than the modified Epstein equation in helium.

Photophoresis

The motion of aerosol particles illuminated from one side-"photophoresis" - is a special case of thermophoresis. The phenomena observed depends upon the temperature distribution in the illuminated particle, which can be very different depending on particle shape, size, transparency and refractive index. In transparent particles the rear side may be heated more than the side facing the light source with the result that the particle will move towards the light. When the side facing the light is hotter than the back side, the particle will move away from the light source.

Diffusiophoresis and Stephan Flow

At the surface of bodies wetted with a volatile liquid, a dust free space is formed even when a temperature difference is lacking. This is due to the diffusiophoresis force on the particles which is the sum of the force due to Stephan flow and a force due to gas momentum transfer processes. Stephan flow is the hydrodynamic flow necessary to maintain a uniform total pressure in a diffusing gaseous system and is directed toward the liquid surface when vapor is condensing. In a binary system of a vapor and a carrier gas the velocity of the Stephan flow is:

$$u_s = -\frac{D_{vG}}{p_G}\,\frac{dp}{dx} \tag{4.3.3-30}$$

The velocity is positive when the particle moves towards the drop and negative when it moves away from the drop.

"D_{vG}" is the diffusion coefficient of the vapor in the gas, "p_g" is the partial pressure of the gas and:

$$\frac{dp}{dx} = \frac{p_o - p_v}{\Delta x} \tag{4.3.3-31}$$

"p_o" is the saturation vapor pressure of the drop liquid at the drop temperature, "p_v" is the partial pressure of the vapor of the liquid drops in the gas, "Δx" is the distance from drop surface to the gas bulk phase where the vapor pressure is "p_v". The gradient is positive for an evaporating droplet.

If the molecular mass of the diffusing vapor molecules is different than the molecular mass of the carrier gas molecules, the motion of small particles is affected by gas momentum transfer processes. Waldmann (1959) has treated this phenomenon for small particles ($r < \lambda$). When the two mechanisms, namely the Stephan flow and the difference in molecular impact are combined, one gets for a dilute vapor system, where only the vapor diffuses through the stationary gas, the following expression for the diffusiophoretic velocity:

$$u_{pDP} = -\frac{\sqrt{M_v}\;P}{p_v\sqrt{M_v} + p_G\sqrt{M_G}}\,\frac{D_{vG}}{p_G}\,\nabla p_v \tag{4.3.3-32}$$

Where "M_v" and "M_G" are the molecular weight of the diffusing vapor and stationary gas respectively, "p_v" is the vapor partial pressure and "p_G" is the gas partial pressure.

The Waldmann equation has been developed for $r < \lambda$, but, according to Waldmann and Schmitt (1960), it agrees with experimental results where (r/λ) ranged from 1 to 6 within 9%. A similar equation was also derived by Bakanov and Derjaguin (1960).

4.3.4 PHENOMENA LEADING TO CHANGE IN PARTICLE SIZE DISTRIBUTION

When aerosol particles come into contact and coalesce or adhere to one another, the process is called coagulation. The most common cause for coagulation is thermal motion which is also called Brownian coagulation. Superimposed on the Brownian motion, there may be motion produced by hydrodynamic, electrical gravitational or other forces. The velocity of approach due to such forces may be large enough to set up a rate of coagulation compared with which, that, due to Brownian motion is negligible. Thermal (Brownian) coagulation as well as coagulation of charged aerosols are spontaneous and go on continuously so that the aerosol becomes coarser.

4.3.4.1 Brownian Coagulation

Experimental data show that coagulation of very many smokes follow a simple rule. If "n" is the number of particles per cm^3 at any time, "t", and "n_o" is the number present immediately after the smoke is formed, then

$$\frac{1}{n} - \frac{1}{n_o} = k\ t \qquad (4.3.4\text{-}1)$$

where "k" is a constant. From Equation 4.3.4-1 it is easy to see that the rate at which particles disappear by coagulation is

$$-\frac{dn}{dt} = k\ n^2 \qquad (4.3.4\text{-}2)$$

This equation was originally developed by Smoluchlowski (1916, 1917) who made the following assumptions: 1. Particles adhere at every collision; 2. Particles collide due to Brownian motion; 3. Aerosol particles are spherical; 4. All particles are of the same size (monodispersed aerosol); 5. The shape and size of the particles are preserved in spite of coagulation with other particles; 6. The radius of the sphere of influence of the particles is "2r".

Making all these assumptions Smoluchowski derived the equation:

$$\frac{dn}{dt} = -k\ n^2 = -\frac{4\ R\ T}{3\ \mu_G\ N}\ n^2 \qquad (4.3.4\text{-}3)$$

Where the Cunningham correction factor is applied to Stokes' equation, Equation 4.3.4-3 should also be modified:

$$\frac{dn}{dt} = -\frac{4\ R\ T\ C'}{3\ \mu_G\ N}\ n^2 = k\ n^2 \qquad (4.3.4\text{-}4)$$

where "N" is Avogadro's number. Table 4.3.4-1 lists experimentally determined coagulation constants "k" of monodispersed aerosols in air at atmospheric pressure and 25°C.

TABLE 4.3.4-1

EXPERIMENTAL COAGULATION CONSTANTS OF VARIOUS AEROSOLS (AIR AT AMBIENT CONDITIONS - 760mm Hg, 25°C)

Green and Lane (1964)

Substance	$k \times 10^3$ cm^3/sec
Ferric oxide	0.66
Magnesium oxide	0.83
Cadmium oxide	0.80
Stearic acid	0.51
Oleic acid	0.51
Resin	0.49
Paraffin oil	0.50
p-Xylene-azo-β- naphthol	0.63
Ammonium chloride (ambient)	0.51
Ammonium chloride (46% relative humidity)	0.43
Zinc oxide formed in arc	1.9
Silica powders in electric field	2.8 - 3.7
Theoretical value	0.51

The rapidity of coagulation in particulate clouds can better be appreciated if one calculates the time taken to halve the number of particles. For stearic acid smoke $k = .51 \times 10^{-9}$ cm^3/sec. We find for a cloud of $n_o = 10^{11}$ particles/cm^3, $t_{1/2} = 0.02$ sec; for $n_o = 10^6$ particles/cm^3, $t_{1/2} = 33$ min; and for $n_o = 10^5$ particles/cm^3, $t_{1/2} = 5.5$ hours. Figure 4.3.4-1 shows the change in stearic acid aerosol concentration ($k = 0.51 \times 10^{-9}$ cm^3/sec) with time for various initial concentrations, while Figure 4.3.4-2 shows the half life, $t_{1/2}$, as a function of concentration. We see therefore that regardless of initial particle concentration, within about 1 min. all clouds of high initial concentration will have almost the same particle concentration.

If the coagulation of aerosols in a scrubber is considered, a residence time of the order of one second would be a reasonable basis for an estimate of the magnitude of the effect. For an aerosol concentration of 10^6/cm^3, which is the common concentration of industrial aerosols, the coagulation is negligible in this time interval.

Schumann (1940) gave an asymptotic solution for the mass distribution of a coagulating polydispersed system with an arbitrary initial particle mass distribution $n(m;t=0)$. He assumed "k" to be constant and $k\, n_o\, t \gg 1$ and got:

$$n(m) = \frac{c}{\bar{m}^2}\, e^{-\left(\frac{m}{\bar{m}}\right)} \qquad (4.3.4\text{-}5)$$

where "c" is the weight concentration of the aerosol and "$\bar{m}$" the mean mass of a particle at time "t":

$$\bar{m} = \frac{c}{n} = \frac{c\,(1 + 0.5\, k\, n_o\, t)}{n_o} \approx \frac{k\, c\, t}{2} \qquad (4.3.4\text{-}6)$$

4.3.4.2 Coagulation of Particles in Laminar Flow

Smoluchowski (1916) made the first attempt to account for the influence of fluid non-uniformities on coagulation rate. In laminar flow, particles may collide and agglomerate because of the various speeds with which they move, relative to one another. Neglecting Brownian diffusion and assuming no aerodynamic interaction between particles, Smoluchowski showed that the number of particles touching an absorbing sphere per second is:

$$\phi = \frac{4}{3}\, n\, (r_i + r_j)^3\, \frac{du_x}{dZ} \qquad (4.3.4\text{-}7)$$

where "r_i" and "r_j" are the radii of the absorbing sphere and the collected particle and "du_x/dZ" is the gradient of the "x" directed velocity in the "Z" direction.

If curvature of streamlines near the particles and the relative velocity are allowed for, the numerical coefficient of Equation 4.3.4-7 is reduced.

To compare the effect of Brownian and velocity gradient coagulations, the ratio of the two rates is compared. For the velocity gradient coagulation rate to be larger than the Brownian rate the condition in a monodisperse aerosol is:

$$\frac{du_x}{dZ} > \frac{\pi D_p}{r_p^{\,2}} = \frac{\pi k T C'}{3 \pi \mu_G r_p^{\,3}} \qquad (4.3.4\text{-}8)$$

Thus a small change in particle size has a large effect on the required velocity gradient.

4.3.4.3 Coagulation of Aerosols in Turbulent Flow

Turbulence can effect coagulation by two mechanisms. One is due to the difference in fluctuation velocity of the medium at two points a distance $r_i + r_j$ apart, which is similar to the mechanism described earlier for laminar flow. The second mechanism causing coagulation is the difference in the fluctuation velocity of the particles caused by unequal inertia. Both mechanisms can be envisioned only when the characteristic particle size is smaller than the characteristic length scale of the eddies in the turbulent medium. Levich (1962) and Saffman and Turner (1956) both have made estimates of the coagulation rate caused by these two mechanisms. Their results apply to cases where the particle radii are smaller by an order of magnitude than the size of the smallest eddies, Hidy and Brock (1970).

Since particle inertia depends on size, the first mechanism can give rise to collision between both equal and unequal sized particles while the second mechanism results only in encounters between particles of different sizes.

Saffman and Turner (1956) showed that the number of particles of radius "r_i" colliding with a sphere of radius "r_j" per second is given by:

$$\phi \approx 1.67 (r_i + r_j)^3 \; n \left(\frac{\varepsilon}{\nu_G}\right)^{1/2} \qquad (4.3.4\text{-}9)$$

where "ε" denotes the rate of dissipation of turbulent energy (cm^2/sec^3).

For coagulation by the second mechanism, Saffman and Turner (1956) showed that the number of particles colliding with one particle per second is:

$$\phi = 5.7 \; n \, (r_i + r_j)^2 \, (\tau_1 - \tau_2) \, \varepsilon^{3/4} \, \nu_G^{-1/4} \qquad (4.3.4\text{-}10)$$

From the limitation regarding the scale of turbulence it follows that Equations 4.3.4-9 and 4.3.4-10 hold for particles up to ≈20 μm in radius even for strong turbulence in which $\varepsilon \approx 1000$ cm^2/sec^3.

Similar equations to those presented in this section have been derived by others. However experimental evidence is unavailable as of yet to substantiate any of the equations found in the literature.

4.3.4.4 Coagulation of Aerosols having Electrically Charged Particles

Fuchs (1964) derives an equation predicting the rate of coagulation for monodisperse spherical aerosol where the particles bear charges "q_i" and "q_j". The electrostatic forces, superimposed on the Brownian motion, enhance or slow the coagulation, depending on the sign of the charge on the particles. Let us define "β" as the ratio of (ϕ/ϕ_o) where "ϕ_o" is the number of particles contacting one particle per second under Brownian coagulation and "ϕ" is the number of particles contacting one particle per second due to both forces.

For uncharged particles:

$$\phi_o = 8 \pi D r n \tag{4.3.4-11}$$

For a charged aerosol:

$$\phi = \beta \phi_o \tag{4.3.4-12}$$

For a charged aerosol Fuchs neglects induction forces and shows that in the case of bipolar charging for repulsion between particles due to equal sign charge "β" is given by:

$$\beta = \frac{\gamma}{\exp(\gamma) - 1} \tag{4.3.4-13}$$

For charge attraction:

$$\beta = \frac{|\gamma|}{1 - \exp-|\gamma|} \tag{4.3.4-14}$$

where:

$$\gamma = \frac{q_i \, q_j}{d_p \, k \, T} \tag{4.3.4-15}$$

The effect of electrical charge can be readily evaluated if we consider an example where $\gamma = 0.5$, then $\beta = 1.271$ for unlike charges and $\beta = 0.77$ for like charges, so that particles having unlike charges coagulate faster than neutral ones while those bearing like charges coagulate more slowly. The arithmetic mean of the two values is 1.02 so that in a case of a charged aerosol with no net charge the overall effect is extremely small.

4.3.4.5 Polarization Coagulation of Aerosols

When an aerosol is under the influence of an electric field the particles are inductively charged and the rate of coagulation is affected. The force field between polarized particles causes attraction between particles when they are arranged along the field direction and repulsion when they are at right angles.

The mechanism of coagulation in an electric field consists of diffusion of particles towards one another until they are close enough for electric forces to act.

Fuchs (1964) showed that "β" for this case, the ratio of "ϕ" to "ϕ_o", is a function of "α" in coagulation polarization where "α" is defined as:

$$\alpha = \left(\frac{E^2\ d_p{}^3}{32\ k\ T}\right)\left(\cos^2\Theta - \frac{1}{2}\sin^2\Theta\right)^{1/3} = \alpha_1\left(\cos^2\Theta - \frac{1}{2}\sin^2\Theta\right)^{1/3} \quad (4.3.4\text{-}16)$$

where "Θ" is the angle between the field direction and the line of centers of the particles. Table 4.3.4-2 gives the effect of electric field on the rate of coagulation of mists.

TABLE 4.3.4-2

EFFECT OF ELECTRICAL FIELD ON THE RATE OF COAGULATION OF MISTS. FUCHS (1964)

α_1	1	2	3	5	10	20	Hereafter
$\bar{\beta}$	1.0	0.95	1.07	1.7	3.4	6.8	$\bar{\beta} = \frac{1}{3}\alpha_1$

The figures show that the coagulation of mists is accelerated appreciably only by very strong electric fields.

The coagulation of solid particles in an electric field is unique. A doublet formed by the coagulation of two primary particles orientates with its long axis parallel to the field, and its dipole moment in this position is much greater, increasing the rate of coagulation.

4.3.4.6 Coagulation by Ultrasonic Vibrations

It has been known for many years that small particles suspended in a gas are readily aggregated by ultrasonic waves, particularly if standing waves are set up in a resonant enclosure. If the frequency and intensity of the vibrations are suitable, the aerosol coagulates in a few minutes or even seconds, forming annular deposits on the walls of the tube at the antinodes. A few of the finest particles usually remain suspended and coagulate extremely slowly under continued action of the ultrasonic waves.

It was shown experimentally, by Brandt and Hiedemann (1936) and St. Clair et al. (1968), that the increase in size of the particles depends upon the sound intensity. However there are indications that coarse aggregates develop only when the vibrations are not too intense since the aggregates are not strong. The addition of water or oil mists to the smoke or dust being coagulated causes the aggregates to stick together.

Two main stages can be distinguished in the coagulation process. In the first stage, the particles oscillate under the influence of the sound waves and take part in the general circulation between node and antinode increasing in size due to collision with other particles. In the second stage, the particles are so much enlarged that they can no longer follow the oscillation. During this stage coagulation continues by collisions between enlarged particles and also between enlarged and small particles.

A satisfactory theory of acoustic coagulation has yet to be developed. The behavior of suspended particles in a vibrating gas may be considered a combination of the following main factors:

a. Co-vibration of particles in the vibrating gas.

b. Hydrodynamic forces of attraction and repulsion between neighboring particles.

c. Sonic radiation pressure.

At the present time an equation relating change in particle size distribution and acoustic parameters is not available.

4.3.4.7 Kinematic oagulation of erosols

Relative motion between particles of unequal size, owing to different speeds acquired under the influence of external forces, lead to collision and coagulation. This process is called kinematic or orthokinetic coagulation. Kinematic coagulation takes place in gravitational electric and sound fields, under the action of centrifugal forces, when velocity gradients occur in a stream, etc.

The theory of kinematic coagulation is different for aerosols with large and fine particles although, in the case of coarse particles, diffusion can be neglected. Consider a coarse spherical particle falling freely with a velocity "V_s" through an aerosol consisting of finer particles. If the rate of fall of the fine particles is negligible, we can consider it equivalent to the case of an aerosol particle moving with a velocity "u_p" past a stationary sphere. The number of finer particles captured in one second by the coarse sphere of diameter "d_p" is:

$$\phi = \frac{\pi}{4} d_p^2 u_p \eta \qquad (4.3.4\text{-}17)$$

where "η" is the target efficiency.

If the sizes of the coarse and fine particles approach one another and the rate of settling of the fine particles can not be neglected, then the relative velocity and a different velocity distribution in the gas flowing around the coarse particle should be used. The gravitational coagulation of aerosols with a particle radius not exceeding 15 μm involves only a small inertial displacement. In this case the target efficiency can be calculated from Equation 4.6-12, or a similar relationship for viscous flow, neglecting the inertia of the particle and assuming that its center passes round the sphere along a streamline. The capture coefficients actually measured are usually higher than those calculated using Equation 4.6.2-11 because of inertial effects and due to changes in particle flow lines in the wake of the falling larger particle.

4.3.4.8 Condensation and Evaporation

Droplets of smoke and mist may increase or decrease in size due to condensation or evaporation. Aerosol particles when in saturated or supersaturated atmosphere may act as nuclei, enhance condensation, and grow this way. These changes in particle size and particle size distribution may have a pronounced effect on aerosol behavior.

Vapors may self nucleate and condense into drops in the absence of condensation nuclei if the degree of supersaturation "S" is great enough. The equilibrium saturation ratio over a curved surface of a pure substance is given by the Kelvin equation:

$$S = \exp\left(\frac{2\ \sigma\ M}{R\ T\ \rho_L\ r}\right) \qquad (4.3.4\text{-}18)$$

The saturation ratio, S, is the ratio of the vapor pressure at the point in question to that of a plane water surface, and "r" is the radius of curvature.

Since "S" is a decreasing function of "r", for a given concentration, water droplets grow by condensation if they are larger than a critical size, which is the condensation nuclei. Vapors reach a reasonable rate of self nucleation when saturations exceed 200-400%.

If an insoluble surface is present, as in the case of insoluble aerosol particles, drops of the critical radius will form on this surface at a higher rate than they will self nucleate since there is less condensate volume in the critical drop and fewer molecular collisions are needed. This explanation has not been found adequate, for it has been shown by Banghali and Saweris (1938) that a supersaturated vapor will not condense on a plane surface which has absorbed a liquid film. The Volmer (1939) theory of condensation on a flat surface predicts that the critical supersaturation for a given nucleation rate should rise with increasing contact angle between the liquid and the solid.

Fletcher (1958) showed that the increase in nucleation rate in the presence of aerosol particles is a function of the surface wettability of the aerosol particle by the condensing liquid and the ratio of drop radius to particle radius. His calculations of the saturations required for a given particle to nucleate a drop of critical size in one second are shown in Figure 4.3.4-3. Since for the same rate of nucleation lower saturations are required in the presence of wetted particles than in their absence, this process will dominate that of homogeneous nucleation.

When the aerosol particles are of irregular shape they may have convex and concave surfaces. From Kelvin's equation the vapor pressure on a concave surface is less than for a film on a plane surface. Hence vapor will condense more readily within a concave surface than upon a convex one. But condensation upon a concave surface would not make the particle a nuclei, it will just consume a certain portion of the vapors.

When soluble aerosol particles are present,nucleation will occur even more readily,since the equilibrium vapor pressure over a solution is less than that over pure water. Howell (1949) calculated the equilibrium supersaturation as a function of droplet radius which contains solute and Figure 4.3.4-4 is a graphical presentation of his calculations. From Figure 4.3.4-4 it is apparent that soluble particles can act as nucleation sites without having to depend on chance agglomeration of water molecules to reach a critical size. If for a given particle the ambient supersaturation is below the peak of the equilibrium saturation curve, two equilibrium drop sizes are possible. The point to the left of the peak represents stable equilibrium. Growth by condensation will occur only if the ambient saturation increases or if statistical fluctuations in size cause the drop to go over the peak. If, however, the ambient saturation is above the peak of the curve, spontaneous nucleation, condensation and growth will occur. Thus, soluble particles will serve as nucleation sites at very low supersaturation and will form drops much more readily than insoluble particles.

After a drop of critical size has been nucleated it grows at a rate determined by the vapor pressure in the gas phase and the conditions at its surface. For a spherical motionless droplet assuming stationary condensation (constant drop temperature and vapor pressure) and ideal behavior of the vapors, drop diameter can be calculated from Maxwell's equation:

$$d_d^2 - d_{do}^2 = \frac{8}{\rho_L} \frac{D\ M\ t}{R\ T} (p_\infty - p_o) \qquad (4.3.4\text{-}19)$$

where "d_d" is the drop diameter at time "t" and "d_{do}" is the drop diameter at time t=0, "D" the vapor diffusivity, "p_o" the vapor partial pressure at the drop surface calculated from drop temperature and "p_∞" the vapor pressure in the air stream.

This equation applies equally well to evaporation and condensation of vapor on droplets above about 1 μm radius and pressure above about 1 cm Hg; it holds best for 1 mm droplets at 1 atm. pressure.

For droplets condensing while moving relative to the gas and assuming all of the above conditions, Frössling's equation will best describe the rate of growth:

$$d_d^2 - d_{do}^2 = \frac{8}{\rho_L} \frac{D\ M\ t}{R\ T} (p_\infty - p_o) (1 + 0.276\ N_{Re}^{1/2}\ N_{Sc}^{1/3}) \qquad (4.3.4\text{-}20)$$

where "N_{Re}" is the Reynolds number and "N_{Sc}" is the Schmidt number.

Theoretical considerations show that the vapor pressure gradient reaches a value considerably greater than the normal value of the gradient at a distance of the order of the mean free path of the gas molecules from the droplet surface. The effect of the concentration change on the rate of evaporation and condensation can therefore be calculated to a first approximation by assuming that Maxwell's equation and a reciprocal concentration gradient $(c - c_\infty/c_0 - c_\infty) = r/\rho$ are valid only at a distance greater than "Δ" from the surface of the drop. "Δ" was found experimentally to be several times the mean free path. In the layer of thickness "Δ" adjacent to the surface the evaporation or condensation proceeds unhindered as in a vacuum. Following this line of derivation, one gets for the evaporation of droplets 2 - 20 μm radius:

$$r \frac{dr}{d\Theta} = \frac{M\ D}{\rho_L\ R\ T} (p_o - p_\infty) \left[\frac{1}{\frac{D}{r\ \nu\ \alpha} + 1} \right] \qquad (4.3.4\text{-}21)$$

where $\nu = (R\ T/2\ M)^{1/2}$ and "α" is the condensation or evaporation coefficient expressing the fraction of molecules striking a surface which condenses. For water, $\alpha = 0.034$ sec/cm², Fuchs (1959). This last equation and experimental results show (Birks and Bradley, 1949) that aerosol grows at a rate roughly proportional to the inverse of its radius. Growth continues until the ambient vapor pressure is lowered to equilibrium due to condensation of the available water vapor or due to particle movement to different regions. All of the above equations can also be used to predict evaporation rates, after the sign has been reversed.

4.3.4.9 Chemical Reaction

Aerosol build-up as well as changes in particle size and particle size distribution may result from a chemical reaction between two gaseous reacting components, between the particles and a reacting component, or between two particles reacting with one another to form a third particle.

Gillespie and Johnstone (1955) studied particle size distribution in hygroscopic aerosols and reached the following conclusions. In their work, the particle size distribution in all the aerosols studied gave straight lines on log probability paper. The particle size of the aerosol depends upon the method of formation. If the hygroscopic vapors react with water to form a new compound with the release of considerable energy, the particle size is small (< 2 μm). If the water vapors simply condense on the hygroscopic aerosol and the liquid is diluted without the release of much energy the particles are large (2 - 6 μm). Within these two classifications the particle size is directly related to the difference between the vapor pressure and the equilibrium vapor pressure of the final product. The larger this difference, the smaller the particles and the larger their number. The reaction between the hygroscopic vapors and the water vapor is very fast (less than 3×10^{-3} min as measured in this experiment).

Obviously the number concentration of the aerosol is larger, the smaller the particle size for the same aerosol loading. The larger the number concentration, the faster the agglomeration rate. Thus if enough time is allowed there is a tendency toward equalization of particle size distribution. The addition of foreign nuclei to the hygroscopic aerosol prior to the introduction of water vapors usually results in decreasing the particle size and increasing the particle number.

When particle growth takes place as a result of the diffusion of a reacting gaseous component to the particle and the growth is diffusion controlled, the equations describing condensation growth are applicable. Where reaction follows particle collision, the agglomeration equations derived earlier in this chapter will describe the changes in particle size adequately, since it was assumed that every collision was effective.

4.3.4.10 Aerosol Build-up Techniques

We have seen that many ways lead to aerosol particle growth. Some are slow but some are fast enough to be employed in commercial equipment to enhance clean-up. It will be appropriate to close this section with a short review of the work of Fahnoe, Lindroos and Abelson (1951), who studied aerosol build-up using the following techniques: 1. Steam injection utilizing direct introduction and adiabatic condensation; 2. Preconditioning by hygroscopic organic vapors, such as ethylene glycol, prior to steam injection; 3. Water spray injection; 4. Sonic agglomeration; and combinations of the above treatments. They used a NaCl aerosol with 85% of the particles smaller than 0.6 μm.

Growth was measured by the fraction collected in a cyclone (collects particles greater than 5 μm) the fraction collected by an impinger (collects particles greater than 2 μm), and the residual collected by an absolute filter or a thermal precipitator.

The optimum conditions results are given in Table 4.3.4-3. As a single treatment ethylene glycol gave best results. For a combination of two treatments in series, steam injection followed by sonic agglomeration gave best results. When three were tried there was not much difference between the different combinations. They concluded that growth of aerosol particles from 0.2 - 0.6 μm to 2 - 5 μm can be achieved using simple devices in engineering applications.

TABLE 4.3.4-3

OPTIMUM CONDITIONING RESULTS FOR SODIUM CHLORIDE TEST SUSPENSIONS [Fahnoe et al. (1951)]

Suspension: 0.60 to 0.80 grain/1,000 cu. ft.

Main Air Flow: 10 cu ft./min. at 70° to 90°F, <20% relative humidity

Type Conditioning	Extent of Conditioning	Activity Removed, % (Over-all) (>2.0μm)	 (Jet Impinger) (2.0-5.0μm)	 (Cyclone) (>5.0μm)
1. Steam	10 lb./1,000 cu.ft.	99.2	78.5	20.7
2. Water fog	92,000 grains/1,000 cu.ft. at 30 lb./sq.inch	87.3	26.7	60.6
3. Steam + water fog	As above.	99.3	21.4	77.9
4. Ethylene glycol	600 grains/1,000 cu.ft.	96.5	65.0	31.5
5. Ethylene glycol + water fog	As above.	99.2	23.8	75.4
6. Ethylene glycol + steam	As above.	99.85	64.5	35.3
7. Ethylene glycol + steam + water fog	As above.	99.85	23.3	76.5
8. Water fog + sonic agglomeration	As above, 600 cycles/sec. (12-sec.)	97.3	3.7	93.6
9. Steam + sonic agglomeration	As above, 1,900 cycles (12-sec.)	99.3	10.0	89.3
10. Steam + water fog + sonic agglomeration	As above, 2,600 cycles (12-sec.)	99.8	2.7	97.1
11. Ethylene glycol + water fog + sonic agglomeration	2,600 cycles (12-sec.)	98.9	3.2	95.7
12. Ethylene glycol + steam + water fog with sonic agglomeration	2,000 cycles (12-sec.)	99.7	2.7	97.0
13. Water fog + sonic agglomeration (double pass)	186,000 grains/1,000 cu.ft., 800 cycles (6-sec.)	98.2	3.8	94.4

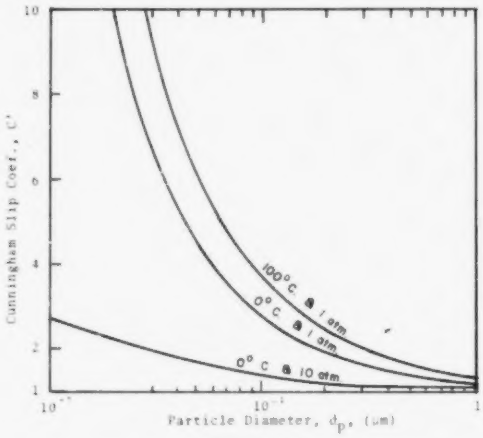

FIGURE 4.3.3-1

CUNNINGHAM CORRECTION FACTOR FOR PARTICLES IN AIR AT DIFFERENT TEMPERATURES AND PRESSURES

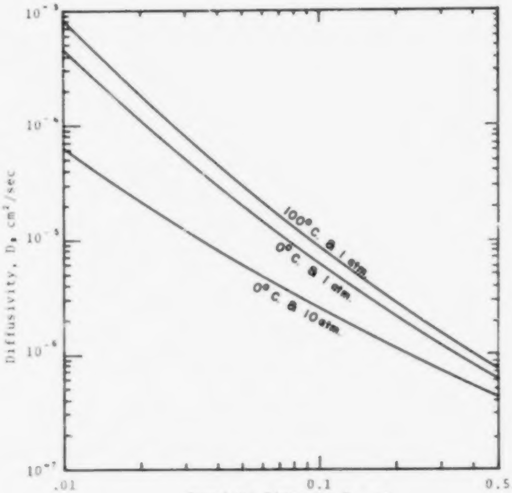

FIGURE 4.3.3-3

CALCULATED DIFFUSIVITY OF AEROSOL PARTICLES AT DIFFERENT OPERATING CONDITIONS

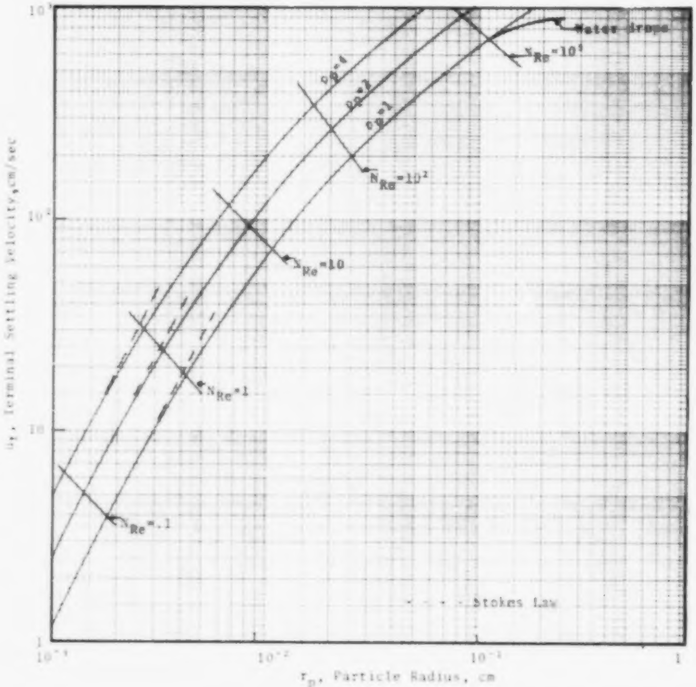

FIGURE 4.3.3-2

EXPERIMENTAL RATE OF SETTLING OF SPHERES AND DROPS IN AIR AT 20°C and 760 mm (FUCHS 1964)

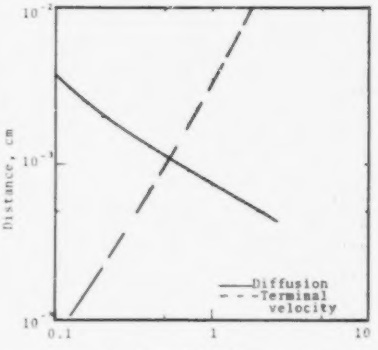

FIGURE 4.3.3-4

COMPARISON BETWEEN BROWNIAN DISPLACEMENT AND SETTLING DISTANCE OF SPHERICAL PARTICLES OF UNIT DENSITY IN AIR, IN ONE SECOND

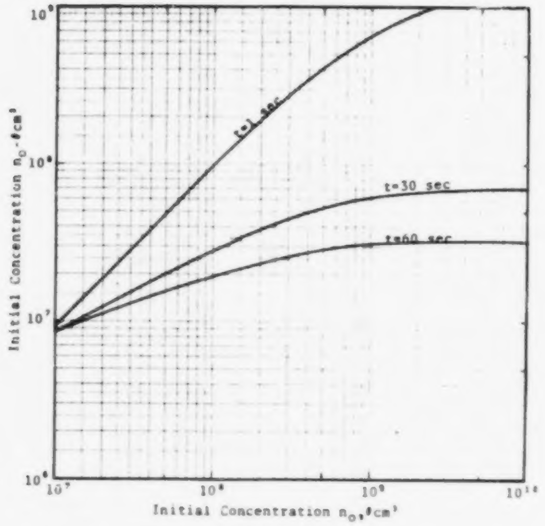

FIGURE 4.3.4-1

CHANGE OF STEARIC ACID PARTICLE CONCENTRATION
WITH TIME FOR VARIOUS INITIAL CONCENTRATIONS
$K = 0.51 \cdot 10^{-9}$ cm^3/sec

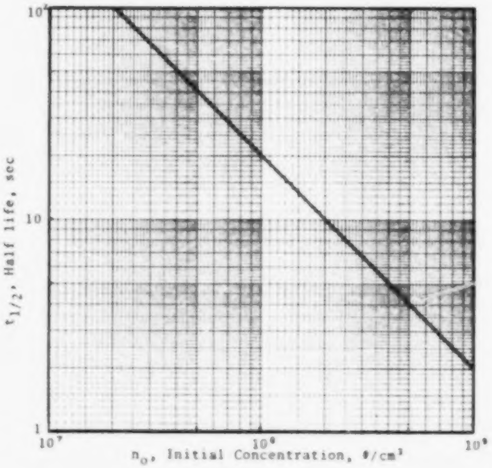

FIGURE 4.3.4-2

COAGULATION HALF LIFE VERSUS INITIAL PARTICLE
CONCENTRATION FOR STEARIC ACID. ($K=0.51 \cdot 10^{-9}$ cm^3/sec)

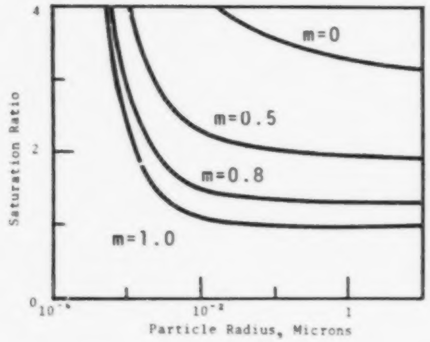

FIGURE 4.3.4-3

SATURATION RATIO FOR CONDENSATION ON SPHERICAL
PARTICLES AT 0°C AS A FUNCTION OF RADIUS, WITH
SURFACE PROPERTIES AS THE PARAMETER.
FLETCHER (1958)

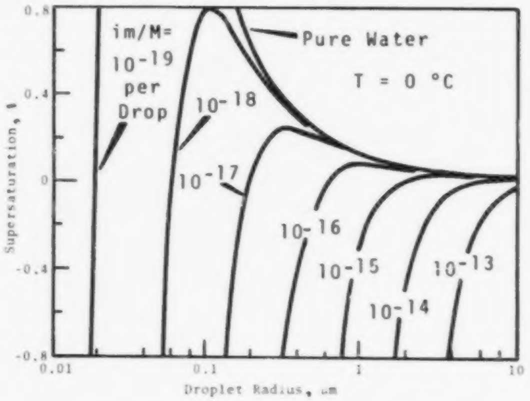

FIGURE 4.3.4-4

EQUILIBRIUM SUPERSATURATION AS A FUNCTION OF DROPLET
RADIUS FOR WATER DROPLETS, EACH CONTAINING MASS "m"
OF SOLUTE OF MOLECULAR WEIGHT "M" AND VAN'T HOFF
FACTOR "i". HOWELL (1949)

SECTION 4.3 NOMENCLATURE

LATIN

c - mass concentration, Kg/m^3 or g/cm^3

C' - Cunningham correction factor

C_D - drag coefficient

d - diameter, m or cm

d_s - Sauter mean drop diameter, m, cm or μm

d_{mm} - mass median drop diameter, m, cm or μm

d_{pln} - mean leght particle diameter, cm or μm

d_{pn} - mean particle diameter, cm or μm

d_{psn} - mean surface particle diameter, cm or μm

d_{pvn} - mean volume particle diameter, cm or μm

D - diffusivity, cm^2/sec

e - electronic charge

E - electric field strength, volt/cm

$f(d_p)$ - size frequency distribution

F - force, dyne or Newton

g - acceleration of gravity, 9.81 m/sec^2 or 981 cm/sec^2

k - thermal conductivity, cal/(sec cm °C)

k $\equiv$ $Rg/N = 1.38 \times 10^{-19}$ mbar $cm^3/°C$, Boltzman constant

m - ionic or molecular mass ($mN=M$)

M - molecular weight, kg/kgmol or g/gmol

n - number concentration, $\#/cm^3$

n - number of particles, Equations 4.3.2-1 to 4.3.2-8

N - Avogadro's number

No - number of ions per unit volume, #/cm

p - partial pressure of solute, mbar or atm

SECTION 4.3 NOMENCLATURE

LATIN

P - total pressure, mbar or atm

q - electric charge, coulombs

q_s - saturation change, coulombs

r - radius

S - saturation ratio

t - time, sec

T - absolute temperature, °K

u - velocity, m/sec or cm/sec

v - root mean square thermal velocity, m/sec or cm/sec, Equation 4.3.3-19

X - distance in X direction

Z - distance in Z direction

DIMENSIONLESS NUMBERS

N_{Sc} $\equiv$ $\mu_G/(\rho_G D_G)$, Schmidt Number

N_{Re} $\equiv$ $\rho du/\mu$, Reynolds Number

GREEK

α - constant

β - ratio of coagulation rate with additional force to Brownian coagulation

$\overline{\Delta}^2$ - mean square displacement of particle in x direction, cm^2

ε - relative dielectric constant

ε_o - $8.86\mathrm{x}10^{-14}$ coulomb cm/(cm^{2}volt)

ε - rate of dissipation of turbulent energy, cm^2/sec^3

θ - angle, radians

η - efficiency due to a unit mechanism

SECTION 4.3 NOMENCLATURE

GREEK

λ - mean free path of gas molecules, cm or μm

ρ - density, kg/m^3 or g/cm^3

σ - standard deviation

σ - liquid surface tension, dyne/cm

μ - viscosity, g/(cm sec)

μ - ion mobility

ϕ - number of particles collected per centimeter of drop movement, #/cm

ϕ - number of particles collected by one particle per sec, #/sec

ϕ - cumulative size frequency distribution

ν - kinematic viscosity cm^2/sec

SUBSCRIPTS

c - charging electric field

E - electrostatic

g - geometric

G - gas phase

M - magnetic

n - mean

p - particle

r - relative

t - terminal velocity

T - thermophoretic

v - vapor

SECTION 4.3 - REFERENCES

Bakanov, S. P., Derjaguin, B. V., Discuss. Faraday Soc. 30, 130 (1960).

Banghali, D. H., Saweris, Z., Trans. Faraday Soc. 34, 554 (1938).

Birks, J., Bradley, R. S., Proc. Roy. Soc. 198A, 226 (1949).

Brandt, O., Hiedemann, E., Trans. Faraday Soc. 32, 1101 (1936).

Brock, J. R., J. Colloid Sci. 17, 768 (1962).

Davies, C. An., "Aerosol Science", Academic Press, Inc. New York (1966).

Derjaguin, B. V., Bakanov, S. P., Doke. Akad. Nauk USSR (Phys. Chem.) 147, 139 (1962).

Epstein, P. S., Z. Phys. 54, 537 (1929).

Fahnoe, F., Lindroos, A. L., Abelson, R. J., Ind. Eng. Chem. 43, 1336 (1951).

Faust, A.S., et al., "Principles of Unit Operations", J. Wiley & Sons, New York (1960).

Glasstone, S., "Textbook of Physical Chemistry", Van Nostrand & Co.(1946).

Fletcher, N. H., J. Chem. Phys. 29, 572 (1958).

Fuchs, N. A., "Evaporation and Droplet Growth in Gaseous Media", Pergamon Press, New York, (1959).

Fuchs, N. A., "The Mechanics of Aerosols", Pergamon Press, New York (1964).

Gillespie, G. R., Johnstone, H. F., Chem. Eng. Prog. 51, 74F (1955).

Goldsmith, P., May, F. G., "Aerosol Science", C. N. Davies, ed., Academic Press, New York (1956).

Green, H. L., Lane, W. R., "Particulate Clouds: Dusts, Smokes, and Mists", Second ed., D. Van Nostrand Co., Princeton, New Jersey, (1964).

Hatch, T. F., J. Franklin Inst., 215, 27, (1933).

Hatch, T. F., Choate, S. P., J. Franklin Inst. 207, 371 (1929).

Hazen, A., Trans. Amer. Soc. Civ. Eng., 77, 1539 (1914).

Hidy, G. M., Brock, J. R., "The Dynamics of Aerocolloidal Systems", Pergamon Press, Oxford, England (1970).

Howell, J. Meteorology, 6, 134 (1949).

Levich, V., Physiochemical Hydrodynamics, Prentice Hall, Englewood Cliffs, New Jersey (1962).

SECTION 4.3
REFERENCES

Oglesby, S. Jr., Nichols, G. B., "A Manual of Electrostatic Precipitator Technology", Part I. Prepared under contract CPA 22-69-73 for O.A.P.-E.P.A. (1970).

Saffman, P., Turner, J., J. Fluid Mech. 1, 16 (1956).

Schumann, T., Quart. J. Roy. Met. Soc. 66, 195 (1940).

Soo, S. L., "Fluid Dynamics of Multiphase Systems" Blaisdell Publishing Co., Waltham, Mass, (1967).

St. Clair, H. W., Spendlove, M. J., Potter, E. V., U. S. Bureau of Mines R. 1. 4218 (1968).

Volmer, M.,"Kinetic der Phasenbildung," Steinkopff, Leipzig (1939).

Von Smoluchowski, M., Phys. Z. 17, 557, 585 (1916).

Von Smoluchowski, M., Z. Phys. Chem. 92, 129 (1917).

Waldmann, L., Z. Naturforsch, 14A, 589 (1959).

Waldmann, L., Schmitt, K., Z. Naturforsch, 15A, 843 (1960).

Whitby, K. T., Liu, B. Y. H., "Aerosol Science", C. N. Davies, ed., pp. 59-86. Academic Press, New York (1966).

4.4 GAS-LIQUID CONTACTING

Intimate gas-liquid contacting, either for mass transfer or particle collection, is generally accomplished by providing an extended gas-liquid interface. One method is to disperse one phase in the other. Gas dispersions in liquid are mostly in the form of bubbles or jets impacting on a plate. The gas jet would normally disintegrate into bubbles as it loses its energy. Liquid dispersions in gas are mostly in the form of liquid drops or liquid jets, with the liquid jets disintegrating into drops. Gas-liquid contacting is also carried out on washed surfaces (packed tower).

It is the purpose of this section to give basic information on drops and bubbles. While it may be best to rely on the experimental mass transfer and particle collection data, the hydrodynamic information given here is useful in predicting performance of the equipment where such data may not be available. We will also look at the effect of various contact methods on mass transfer and particle collection.

4.4.1 BUBBLE HYDRODYNAMICS

There are a number of review on the subject (Calderbank, 1970; Valentin, 1967; Kumar and Kuloor, 1970; Resnick and Gal-Or, 1968) which should be consulted for details.

4.4.1.1 Single Bubbles

Bubble Formation

The simplest mechanism of bubble formation is that in which the bubble is formed very slowly at the open end of a tube immersed vertically in a liquid. The bubble will detach itself when its buoyancy exceeds the surface tension forces. The bubble diameter, at the moment of release, is given by:

$$d_b = \left[\frac{6\ d_h\ \sigma}{(\rho_L - \rho_G)\ g}\right]^{1/3} \qquad (4.4.1\text{-}1)$$

The bubble diameter remains constant whereas the frequency of bubble formation changes in the range of application of this formula, which is up to an orifice Reynolds number of about 200. At higher gas flows the frequency of bubble formation becomes approximately constant while the bubble diameter increases with gas flow rate (orifice Reynolds number of ≈200 to ≈2500). At still higher flows bubbles of a single size are no longer produced; instead there is a considerable spread of bubble sizes with a production of numerous small bubbles. Most industrial applications fall in this range. The average bubble size over the orifice Reynolds number region 2100 - 10,000 is given by:

$$d_b = 0.71\ (N_{Re})^{-0.05} \qquad (4.4.1\text{-}2)$$

where $N_{Re} \equiv \frac{d_h\ u_h}{\nu_G}$ is orifice Reynolds number.

Bubble Shape

Calderbank et al. (1970) summarized their results of various bubble shapes encountered, as a function of bubble velocity in distilled water and two aqueous glycerol solutions as shown in Figure 4.4-1. The results of the study were expressed by smoothed curves through the experimental eccentricity [maximum width/maximum height] vs. "d_e", the diameter of a spherical bubble having the same volume as the bubble in question, data for the four liquids they studied.

Bubble Rise Velocity

The regime of bubble motion varies considerably with the Reynolds number. Bubbles may be termed as small, moderate, or large based upon their Reynolds number being less than 1, or between 1 to 800, or larger than 800, respectively.

Bubbles with diameters less than 0.01 cm have $N_{Re} << 1$ and are considered small bubbles. These bubbles act like solid spherical particles. If the viscosity and density of the gas is negligible compared to the viscosity and density of the liquid medium, respectively, the velocity of rise of a small bubble is of the following form (Levich, 1962).

$$v_b = \frac{1}{3} \frac{g\ d_b^2}{\nu_L} \qquad (4.4.1\text{-}3)$$

Equation 4.4.1-3 is applicable for Reynolds number N_{Re} 1. Therefore, the following inequality holds:

$$\frac{g\ d_b^3}{3\ \nu_L^2} << 1 \qquad (4.4.1\text{-}4)$$

For a bubble moving through water this yields $d_b << 2\times10^{-2}$ cm.

Levich (1962) describes the velocity of rise for moderate size bubbles as in Equation 4.4.1-5. This is in fair agreement with experimental observations when bubble diameter is less than 0.1 cm and interfaces are clean.

$$v_b = \frac{\rho_L\ g\ d_b^2}{9\ \mu_L} \qquad (4.4.1\text{-}5)$$

At Reynolds numbers close to 700, which corresponds to bubble diameters of 0.2 to 0.3 cm, the nature of the motion of the bubbles changes sharply, and they start to be noticeably deformed, acquiring the shape of flattened ellipsoids whose minor axis in in the direction of bubble motion. At the same time, the bubbles begin to vibrate, and they rise by a spiral motion instead of in a straight line. The velocity of motion of bubbles with diameters of 0.2 to 1.5 cm is almost independent of the bubble diameter and amounts to about 25 to 30 cm/sec. The corresponding Reynolds numbers lie within the range of 600 to 4500. Assuming that the distribution of liquid velocities around the bubble remains the same, in principle, as for moderate Reynolds numbers, Levich (1962) estimates that for high Reynolds number and large bubbles:

$$v_b = \left[\frac{2\ \sigma_L^2\ g\ \rho_G}{15\ \rho_L^2\ \mu_L}\right]^{1/5} \qquad (4.4.1\text{-}6)$$

Harmathy (1960) gives for the same situation:

$$v_b = 1.53\left[\frac{g\ (\rho_L - \rho_G)\ \sigma_L}{\rho_L^2}\right]^{1/4} \qquad (4.4.1\text{-}7)$$

Bubbles of larger diameters yet rise at somewhat greater velocities, namely at about 23 to 40 cm/sec, but are not very stable and tend to subdivide into smaller bubbles. Schaftlein (1968) gives for this range:

$$v_b = 0.711\left[\frac{g\ (\rho_L - \rho_G)\ d_b}{\rho_L}\right]^{1/2} \qquad (4.4.1\text{-}8)$$

Figure 4.4.1-2 is a plot of experimental and predicted bubble rise velocities for air and water vs. bubble diameter.

4.4.1.2 Bubble Clouds - Sieve Plates

The physical characteristics and hydrodynamics of bubble clouds in liquids determine mass transfer characteristics and hence, the efficiency and dimensions of the scrubber.

The hydrodynamics of bubble beds are extremely complex to analyze theoretically. It is no longer the case of a single bubble rising through quiescent liquid under the influence of several forces. Bubbles coalesce and divide as they rise in the bubble bed, and circulating currents are formed.

The experimental approach has been to determine interfacial area, bubble bed height, gas hold-up, and average bubble size using very simple systems (mostly air-water) and for a variety of equipment (e.g. bubble-cap plates, sieve plates, agitated bubble-absorbers, bubble columns, etc.). While this type of data is meager, some generalizations have been made for the simple systems considered. These generalizations may be used for preliminary design evaluation. Interfacial area may vary according to the surface properties of the liquid, which are determined by its composition (including the presence of unwetted solid particles) and also, by the system temperature. Such affects have scarcely been investigated.

Calderbank (1959) found that on sieve plates the interfacial area per unit volume of froth, A_{if}, increases nearly in proportion to the superficial velocity of the gas until it reaches 8 cm^{-1} (i.e., cm^2 area/cm^3 volume), whereafter it remains constant. The value of "A_{if}" below 8 cm^{-1} is given by:

$$A_{if} = 0.38\left(\frac{v_s}{v_b}\right)^{0.775}\left(\frac{v_s\ \rho_L}{n\ d_h\ \mu_L}\right)^{0.125}\left(\frac{g\ \ L}{d_h\ \sigma}\right)^{1/3} \qquad (4.4.1\text{-}9)$$

Here, "v_s" is the velocity of gas through the cross-section, "v_b" is the velocity of rise of the bubbles in the froth (taken to be 28 cm/sec under most conditions), "n" is the number of holes per unit area of plate. The formula is based on experiments with a wide range of liquids, gases and sieve plates.

The total interfacial area on the plate of course depends on the volume of froth on the plate, and hence on the depth of froth. The depth of froth, in the case of a plate with downcomer, is approximately equal to the height of the overflow weir; in the case of plates without downcomers the depth will depend on the design of the plate and the gas and liquid flow rates, and must be found by experiment.

In a sieve plate column, the Sauter mean bubble diameter is found to increase with gas flow rate up to an orifice Reynolds number of about 2500 when much smaller bubbles are produced. The mean diameter of the small bubbles is 0.45 cm, which is the practical sieve plate operating range. The mean diameter is substantially unaffected by further increases in gas velocity.

Crozier (1956), in agreement with Calderbank's results (Calderbank et al. 1962) (see Figure 44.1-3) has reported the following equation for the gas hold-up. The formula is based on experiments with a wide range of liquids, gases, and sieve plates.

$$\ln\left(\frac{1}{1 - h_g}\right) = 0.184\ v_s \sqrt{\rho_g} + 0.45 = -\ln F \qquad (4.4.1\text{-}10)$$

where h_g = vol. fraction gas in foam, F = vol. fr. liquid, v_s = superficial gas velocity cm/sec, and ρ_g = gas density g/cm³.

4.4.2 DROP HYDRODYNAMICS

4.4.2.1 Drop Size Distribution by Liquid Atomization

The devices for converting a liquid into droplets may be classed in one of five categories: pressure nozzles, including jet injection, fan swirl, and impact nozzles; two-fluid atomizers in which the liquid stream is disintegrated largely by a high-velocity stream of gas; impinging-type nozzles wherein two streams are made to collide in midair; vibrating nozzles using sonic or mechanical energy; and finally, rapidly rotating cups or disks from the outer rim of which liquid is discharged. Two-fluid pneumatic atomization (venturi scrubber) is most widely used to produce fine sprays and is considered here.

The available drop-size distribution data and correlation of the data for the pneumatic atomization is specific to nozzle designs and applicable only over the ranges of the variables studied. Kim and Marshall (1971) suggest the following general expression for the mean spray size formed with a pneumatic atomizer.

$$d_{bn} = \frac{a}{(v_r^2\ \rho_G)^{\alpha}} + b\left(\frac{G_G}{L_L}\right)^{\beta} \qquad (4.4.2\text{-}1)$$

Here "v_r" is the relative velocity between air and liquid. The exponents "α" and "β" are functions of nozzle design and "a" and "b", are functions of both nozzle design and liquid properties.

A drop-size correlation by Nukiyama and Tanasawa 1938-40) has been the most widely used work in pneumatic atomization. They give Sauter mean diameter as follows:

$$d_s = \frac{58,600}{v_r}\left(\frac{\sigma}{\rho_L}\right)^{1/2} + 597 \quad \frac{\mu_L}{\sqrt{\rho_L \sigma}}^{0.45} \left(1000 \frac{Q_G}{Q_L}\right)^{1.5} \qquad (4.4.2\text{-}2)$$

In this empirical equation, units are as follows:

v_r = cm/sec; σ = dynes/cm; ρ_L = g/cm^3; μ_L = poise; Q = volume/ time); d_d = μm.

Most of the data taken in pneumatic atomization is for liquid injection, either parallel or opposite to the gas flow, and with a small apparatus. Venturi scrubbers are quite large in comparison and, normally, have the liquid injection across the gas flow. While it is questionable that Equation 4.4.2-1 would apply to a venturi scrubber, it has been so applied (Calvert, 1968; Gieseke, 1963; Boll, 1971). Boll (1971) states that the predicted drop size is subject to an uncertainty of about a factor of two. As is shown in Chapter 5.3.5, the drop size may not have a significant effect on inertial collection efficiency.

Hesketh et al. (1970) have experimentally discovered a different type of atomization in a venturi scrubber when liquid injection nozzles larger than 1 mm i.d. are used, and when critical air velocities are above:

$$v_{critical} = \left(\frac{0.795}{d_{nozzle}}\right)^{1/2} \times 10^3 + 466 \qquad (4.4.2\text{-}3)$$

where $v_{critical}$ = cm/sec; d_{nozzle} = cm

The authors have termed it cloud-type atomization. The average drop size produced is roughly less than half the size predicted by Equation 4.4.2-1.

4.4.2.2 Drop Steady State Motion

Most simplified treatments assume drops as rigid spheres, although depending upon the drop size and speed, distortion in shape will occur. The relation between the fluid resistance and drop speed is expressed in the form of a plot of the drag coefficient, C_D, vs. the drop Reynolds number.

The drag coefficient, C_D, is defined as

$$C_D = \frac{F}{(\pi r_d^2)(\frac{1}{2} \rho_L v_r^2)} \qquad (4.4.2\text{-}4)$$

where "F" is the force exerted on the sphere. Newton in 1710 experimentally determined that at high relative velocity v_r, where inertia effects dominate, the following holds:

$$F = 0.22 \pi r_d^2 \rho_L v_r^2 \text{ (i.e. } C_D = 0.44) \qquad (4.4.2\text{-}5)$$

At very low relative velocities, Stokes in 1850 suggested that the inertia effects are so small that they can be neglected from the Navier-Stokes equations (see Equation 4.3.2-4).

Subsequent experiments yielded a so-called standard drag curve (Schlicting 1960) applicable to a single solid sphere moving a constant velocity in a still, isothermal incompressible fluid, which is infinite in extent. Figure 4.4.2-1 is a plot of C_D vs. N_{Re} Reynolds number for a sphere.

The terminal velocity reached by a drop is the velocity it attains when the fluid resistance is equal to the external force applied to the drop. The experimentally determined terminal velocity of a falling drop in air is given in Figure 4.6.2-1 as a function of drop diameter.

4.4.2.3 Drop Acceleration

The effect of acceleration on the drag coefficient has been studied by Hughes et al. (1952), Ingebo (1955), Torobin et al. (1960), Crowe (1961), and others. Hughes et al. state that as a general rule, acceleration drag exists and that it is higher than that for steady motion. Ingebo's results disagree with this statement. He obtained acceleration drag coefficients lower than the standard curve, (See Figure 4.4.2-1.) Boll (1971) concludes that in the case of a venturi, where the Reynolds number range above about five hundred isn't too important, the standard curve of the drag coefficient is the better choice.

4.4.2.4 Drop Behavior in Motion (see also 4.5.1)

Deformation and Oscillation

Drops in either steady state motion or acceleration undergo distortion from the spherical shape. The distortion of drops is of two basic types: those of an equilibrium nature and those of an oscillatory nature resulting from vibrations about the equilibrium position. Observations of drops suspended in an upward air current have shown that deformation is accompanied by oscillation of the drop about its own axes.

Finlay (1957) for unsupported drops and Constan (1963) for supported drops showed that up to about 0.2 cm diameter drop size, the projected cross-sectional area owing to distortion is less than 10%. Finlay (1957) and Garner et al., (1959) measured frequency of oscillation of free drops. Their results correlate well with Lamb's (1932) equation when the oscillation is of the problate oblate ellipsoidal type.

$$f = \left(\frac{8\sigma}{3 \pi V_d \rho_L} \right)^{1/2} \qquad (4.4.2\text{-}6)$$

Here f is the frequency of oscillation and V_d is the drop volume.

Internal Circulation

Falling drops have pronounced internal circulation at the time of drop formation and disengagement, followed by rapid damping during the fall. The oscillating distortion is also a source of internal circulation. Circulation velocities have been measured by Cramer et al. (1959) and Constan (1963). They show the circulation velocity to be linearly related to the relative velocity. The effect of viscosity on circulation is very pronounced. The large drops show greater velocities of circulation. These effects are qualitatively predictable by theory (Hadamard, 1911, 1913) but quantitatively circulation has not been related to oscillation (Constan, 1961).

Drop Breakup

It is well known that when a liquid droplet or jet is subjected to a gas velocity in excess of some critical value, it will disintegrate or shatter. Lane (1951), Goldshmid (1963), Volynskii (1948), and others measured the critical breakup conditions. They all characterized drop shattering by a critical Weber number. The critical condition is

$$7 < N_{We} = \frac{\rho_G \, v_r^2 \, r_d}{\sigma} < 23 \qquad (4.4.2\text{-}7)$$

4.4.3 CONTACTING SCHEME

The net movement of one phase with respect to the other phase is described as being cocurrent, or crosscurrent contact. The amount of mass transfer depends not only on the equilibrium relationship and rate coefficient, but also on the contacting scheme.

If liquid enters the top of a vertical column so that it runs down and gas enters the bottom so that it passes upward through the column, the contacting scheme is said to be countercurrent, and the effluent gas has its last contact with the entering liquid. Were the gas also to enter the top and pass downward through the column, the contact would be cocurrent and the effluent gas would last contact the effluent liquid.

The stream (phase) compositions for these processes may be followed in a graph (Figure 4.4.3-1) in which "y", the gas phase concentration (mole fraction) of the transferring component (i.e., SO_2), is plotted against "x", the liquid phase concentration (mole fraction) of the same component. So as not to complicate the picture, it is assumed that the remaining constituents of the gas phase are insoluble ("inerts") and that those of the liquid phase are nonvolatile. The bulk compositions of the gas and liquid phase at any point in the column are shown by the operating line (x_{if}, y_{if})-(x_o, y_o) for cocurrent contact; and the operating line (x_{if}, y_o)-(x_o, y_{if}) for countercurrent contact. The operating lines (or material balance lines) are defined, for the case of low concentrations and nonvolatile solvent:

$G_M(\hat{y}_i - \hat{y}) = L_M(\hat{x}_o - \hat{x})$ for countercurrent and (4.4.3-1)

$$G_M(\hat{y}_i - \hat{y}) = L_M(\hat{x} - \hat{x}_i) \quad \text{or cocurrent} \tag{4.4.3-2}$$

The slope of the operating line is L_M/G_M in both cases, but it is positive for countercurrent, and negative for cocurrent flow.

When one stream flows in a direction perpendicular to the other stream this is called cross, or crosscurrent, flow. Examples of this are spray chambers in which the gas travels horizontally while spray drops fall vertically; and trays across which liquid flows horizontally while gas flows vertically. These situations are complicated to analyze and are generally treated with the simplifying assumption that one phase is completely and instantaneously mixed along any plane parallel to the flow of the other phase. Thus in a cross-flow spray chamber one might assume that the gas is completely mixed along any vertical plane with the result that the operating line for the liquid-gas contact along a plane (following the liquid) would be a horizontal (constant y) line. The operating line describing the change in gas composition, assuming an average liquid condition as it falls, would be a vertical line.

In a sieve plate column, the overall fluid motion is either cocurrent or countercurrent, but the motion on each plate is essentialy crosscurrent. The situation along a vertical plane across the liquid flow path would be described approximately by a vertical (constant x) operating line. Combinations of these variations may occur in a single piece of equipment and any attempt to its performance requires that the liquid and gas flow paths be known and taken into account. Usually the liquid on the plate is assumed to be completely mixed.

Once the operating conditions are fixed, they, in conjunction with the equilibrium relationship, determine the ultimate performance possible. For a cocurrent scrubber (Figure 4.4.3-1) no matter how long the phases are kept in contact or how efficient the device, the gas composition can never go below the equilibrium limits of "y^∞" or the liquid composition above "x^∞". In a countercurrent scrubber, more efficient contact moves the operating line closer to the equilibrium line (the slope remains L_M/G_M). Best performance would result when the operating line touches the equilbrium line. This is equivalent to stating that the gas can never become leaner (or cleaner) than that in equilibrium with the inlet liquid for countercurrent flow, or with the outlet liquid for cocurrent flow. If L_M/G_M is less than "m", i.e., "y/x" at equilibrium, for countercurrent contacting, the equilbrium limit is reached when the outlet liquid is in equilibrium with the inlet gas. Calvert (1968) presents a graph relating efficiencies for cocurrent and countercurrent contact as dependent on solubility, flow rates, and number of transfer units.

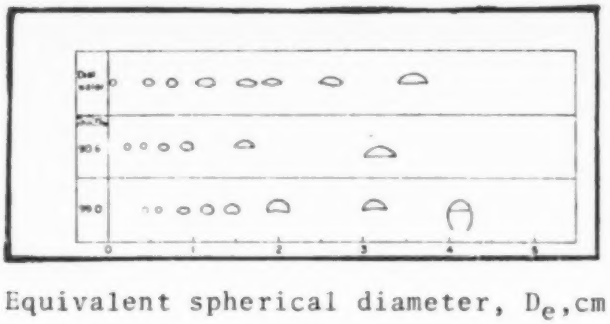

FIGURE 4.4.1-1

BUBBLE SHAPES IN DISTILLED WATER AND AQUEOUS GLYCEROL SOLUTIONS.
(after Calderbank et al. 1970)

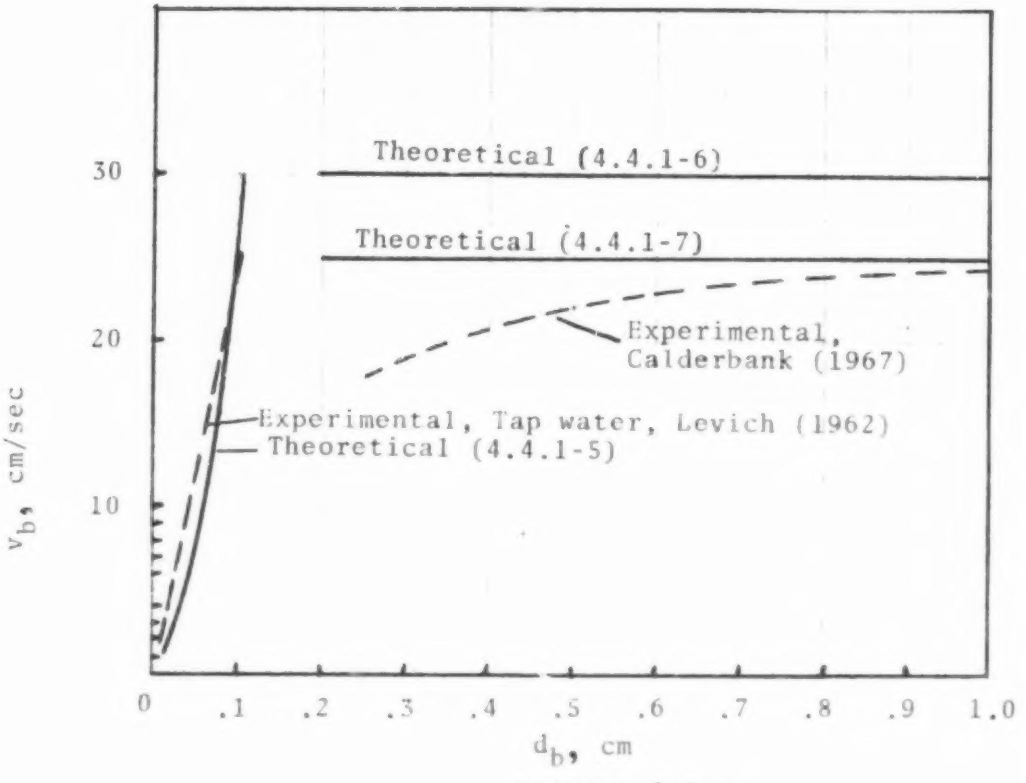

FIGURE 4.4.1-2

AIR BUBBLE RISE VELOCITY IN WATER VS. BUBBLE DIAMETER. PREDICTED AND EXPERIMENTAL VALUES

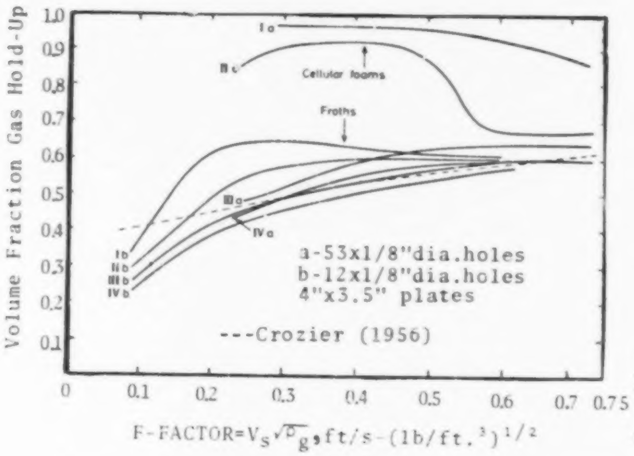

Curve	Liquid rate	Curve	Liquid rate
Ia	0.25, l/min	Ib	1.0, l/min
IIa	2.8	IIb	2.8
IIIa	7.3	IIIb	7.3
IVa	9.5	IVb	9.5

FIGURE 4.4.1-3

GAS HOLD-UP IN VARIOUS SIEVE-PLATE COLUMNS AS A FUNCTION OF F-FACTOR, WITH WATER RATE AS PARAMETER. THE DOTTED LINE IS DUE TO CROZIER (1956). (AFTER CALDERBANK, 1962)

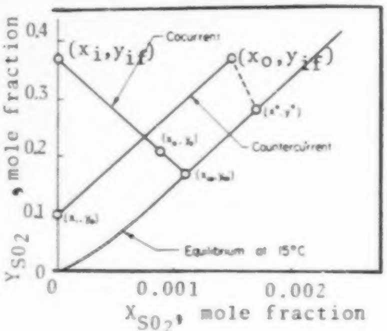

FIGURE 4.4.3-1

PLOT OF PHASE COMPOSITIONS SHOWING OPERATING AND EQUILIBRIUM LINES

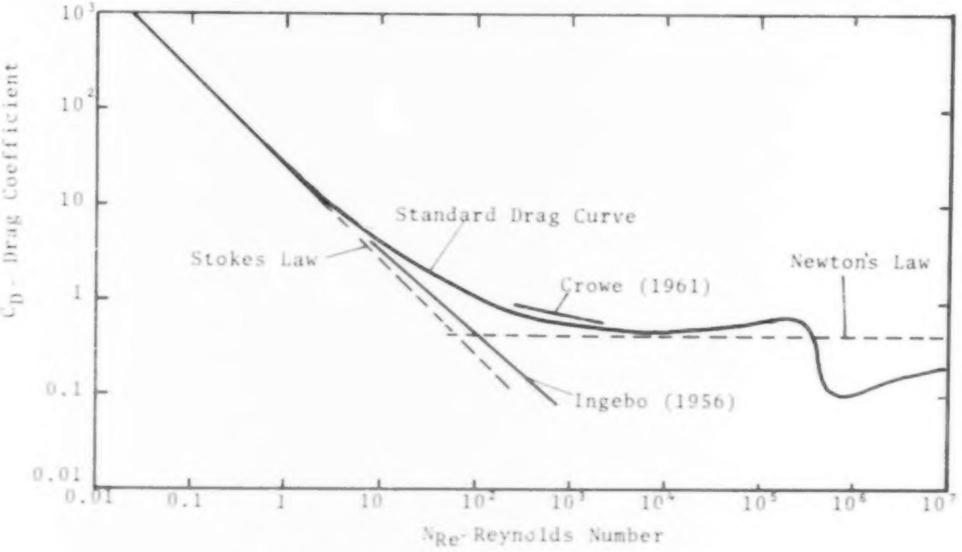

FIGURE 4.4.2-1 DRAG COEFFICIENT OF A SPHERE

SECTION 4.4 NOMENCLATURE

LATIN

a - constant

A - component "A"

C_D - drag coefficient

d - diameter, m or cm

f - frequency of oscillation, sec^{-1}

F - foam density, ratio of clear liquid height to total foam height

g - acceleration of gravity, 9.81 m/sec^2 or 981 cm/sec^2

G_M - gas mass flowrate, kg/sec or g/sec

k_L - liquid film mass transfer coefficient, cm/sec

L_M - liquid mass flowrate, kg/sec or g/sec

Q - volumetric flow rate, m^3/sec, cm^3/sec or lit s/sec

r - radius

u - velocity, m/sec or cm/sec

v - velocity, m/sec or cm/sec

V - volume, m^3 or cm^3

$\hat{x}$ - mole fraction solute in liquid

$\hat{y}$ - mole fraction solute in gas

DIMENSIONLESS NUMBERS

N_{We} $\equiv \rho_L\ d\ u^2/\sigma$, Weber Number

N_{Re} $\equiv \rho du/\mu$, Reynolds Number

GREEK

α - constant

SECTION 4.4 NOMENCLATURE

GREEK

ρ - density, kg/m^3 or g/cm^3

σ - liquid surface tension, dyne/cm

μ - viscosity, g/(cm sec)

ν - kinematic viscosity cm^2/sec

SUBSCRIPTS

b - bubble

G - gas phase

h - perforation in plate

i - interface

L - liquid phase

n - mean

r - relative

s - Sauter (surface to volume)

SUPERSCRIPTS

· - original value, i.e. without reaction

SECTION 4.4 - REFERENCES

Boll, R. H., "Particle Collection and Pressure Drop in Venturi Scrubbers", 69th National AIChE Meeting, Cincinnati, Ohio, May 16-19, (1971).

Calderbank, P. H., Trans. Instn. Chem. Engrs., 34, 79-90, (1956).

Calderbank, P. H.; Rennie, J., Trans. Instn. Chem. Engrs., 40, 3-12, (1962).

Calderbank, P. H., The Chemical Engineer (British), CE 209 - CE 233, October (1967).

Calvert, S., "Air Pollution", Ch. 46, 3, edited by A. C. Stern, Academic Perss (1968).

Constan, G. L., Ph.D. Thesis, Case Institute of Technology, Cleveland, Ohio (1961).

Constan, G. L., Calvert, S., AIChE Journal, 9, 1, 109-115, (1963).

Crowe, C. T., Ph.D. thesis, University of Michigan, Ann Arbor, Michigan, (1961).

Finlay, B. A., Ph.D. thesis, University of Birmingham, Edgbaston, Birmingham, England (1957).

Garner, F. K.; Lane, J. J., Trans. Inst. Chem. Engrs., London 37, 162, (1959).

Gieseke, J. A., Ph.D. Thesis, University of Washington, Seattle, Washington (1963).

Goldshmid, J.; Calvert, S., AIChE Journal 9, 352, (1963).

Hadamard, J., Compt. Rend., 152, 1735 (1911); 154, 107 (1913).

Harmathy, T. Z., AIChE Journal, 6, 281 (1960).

Hesketh, H. E.; Engel, A. J.; Calvert, S, Atmospheric Environ. 4, 639 (1970).

Hughes, R. R., Chem. Eng. Prog. 48, 497 (1952).

Ingebo, R. D., NACA TN 3762, September (1955).

Kim, K. Y.; Marshall, W. R., AIChE Journal, 17, 3, 575-584 (1971).

Kumar, R.; Kuloor, N. R., Section in "Advances in Chemical Engineering", 8, Academic Press, New York (1970).

Lamb, H. L., "Hydrodynamics", 6 ed., Cambridge University Press, London, England (1932).

SECTION 4.4
REFERENCES

Lane, W. R., Ind. Eng. Chem. 43, 1312, (1951).

Levich, V. G., "Physiochemical Hydrodynamics", Prentice-Hall, Inc. (1962).

Nukiyama, S.; Tanasawa, Y., Trans. Soc. Mech. Engrs., Japan, 4, 5, 6, (1938-1940).

Resnick, W.; Gal-Or, B., Section in "Advances in Chemical Engineering," Vol. 7, Academic Press, New York (1968).

Schaftlein, R. W., Ind. Eng. Chem. 60, 12 (1968).

Schlichting, K., "Boundary Layer Theory", McGraw-Hill, New York, (1960).

Torobin, L. B.; Gauvin, W. H., Canad. J. of Chem. Eng. 38, 142,(1960).

Valentin, F. H., "Absorption in Gas-Liquid Dispersions", E. & E. N., Spon. Ltdl, London (1967).

Volynskii, M. S., Doklady Akad. Nauk (USSR) 62, 301, (1948).

4.5 UNIT MECHANISMS FOR MASS TRANSFER

4.5.1 DROPS

The gas-film coefficient for mass transfer to a drop is given over a wide range of conditions by the semi-theoretical equation of Frössling (Sherwood and Pigford, 1952):

$$N_{Sh} = \frac{\hat{k}_G R_g T d}{D_G} = 2 + 0.552\, N_{Re}^{1/2}\, N_{Sc}^{1/3} \qquad (4.5.1\text{-}1)$$

where $N_{Re} \equiv \dfrac{d u \rho_G}{\mu_G}$, Reynolds number (u = relative velocity between drop and gas stream)

$N_{Sc} \equiv \dfrac{\mu_G}{\rho_G D_G}$, Schmidt number

Sherwood and Pigford, and Hobler (1966), cite several investigators whose results agree with Equation 4.5.1-1 for absorption, desorption and evaporation. Penetration theory can be used to estimate coefficients as discussed in 4.2.3.3. Droplet diameters are typically in the range of 10 to 600 microns; for crude estimations 500 microns is a useful average diameter if no other information is available. The relative velocity between the drop and the gas stream can be assumed to be the terminal falling velocity of the drop. Terminal velocities and Reynolds' numbers for water drops falling in air at atmospheric pressure are plotted in Figure 4.6.2-4.

Example: What is the gas-phase mass transfer coefficient for absorption from air by falling water drops with $r_d = 0.025$ cm (250 μm), at 25°C, if the contaminant diffusivity in air is 0.1 cm^2/sec.

From Figure 4.6.2-4, u = 210 cm/sec and $N_{Re} = \dfrac{0.05 \times 210 \times 1.2 \times 10^{-3}}{1.8 \times 10^{-4}} = 70$

$$N_{Sc} = \frac{1.8 \times 10^{-4}}{1.2 \times 10^{-3}(0.1)} = 1.5$$

$$N_{Sh} = 2 + 0.552\,(70)^{1/2}\,(1.5)^{1/3} = 7.3$$

$$\hat{k}_G = \frac{N_{Sh} D_G}{R_g T d} \quad \frac{7.3\,(0.1)}{82.06\,(298)\,0.05} = 6.0 \times 10^{-4} \text{(mol/cm -sec-atm)}$$

Figure 4.5.1-1 shows "k_G" as a function of drop diameter, calculated in the same way as the example, for drops of water falling through air at terminal velocity, with $D_G = 0.1$ (cm /sec) and T = 298°K. The gas-film coefficient per gram of drops, $k_G a'$, is shown in Figure 4.5.1-2 as a function of drop diameter. This is useful in computations for cross-current spray chambers where drops fall at their terminal settling velocity, "u_t", relative to the scrubber. Figure 4.5.1-3 is a plot of water drop area per unit volume of scrubber as a function of upward air velocity and drop diameter for a ratio of water to air flow rates of $Q_W/Q_A = 1$ (ℓ/m^3). This figure is useful for countercurrent spray computations. Interfacial areas, "a", for other water rates can be obtained by multiplying the value for $Q_W/Q_A = 1$ (ℓ/m^3) times the desired (Q_W/Q_A). Since the drop velocity relative to the scrubber, "u_t" depends on the difference between its terminal velocity and the opposing gas velocity, drop holdup changes with "u_G" and so does "a". Mass transfer rate per unit area, and "k_G", depends on the relative velocity, "u_t", so it does not vary with "u_G".

Liquid Film

The liquid-film coefficient for mass transfer to drops can be estimated by Equation 4.2.3-10.

$$k_L = 1.13 \left(\frac{D_L}{\theta}\right)^{1/2} = 2 \left(\frac{D_L}{\pi\theta}\right)^{1/2} \tag{4.2.3-10}$$

(Calvert and Kapo, 1963; Hobler, 1966), where "θ" is the time of exposure of the drop to the gas stream. This penetration theory estimate of "k_L" is in agreement with the results obtained for diffusion into (or out of) a stagnant sphere by Crank (1957), for short exposure times. Figure 4.5.1-7 is a plot of fractional saturation of a sphere as a function of dimensionless diffusion time, ($D\theta/r_d^2$). ("Fractional saturation" means fractional approach to equilibrium and is the equilibrium or "intrinsic" efficiency of transfer to or from a sphere.) The solid line is the computation of Crank for diffusion with a constant surface concentration. One dashed line is computed with "k_L" from Equation 4.2.3-10 and integration of Equation 4.5.1-2, which describes the rate of change of concentration inside a sphere if mass transfer is defined by a constant coefficient and varying driving force. The other dashed line is obtained by substituting "k_L" from Equation 4.5.1-3 and then solving Equation 4.5.1-2.

$$\frac{d\hat{c}}{dt} = \frac{3k_L}{r} (\hat{c}_i - \hat{c}) \tag{4.5.1-2}$$

From Figure 4.5.1-7 it is clear that for short contact times, i.e. where $(D_L\,\theta/r_d)^{1/2} < 0.22$, penetration theory gives a good estimation of "k_L". However, for longer contact time, $(D_L\,\theta/r_d^2)^{1/2} > 0.22$, "$k_L$" is better estimated from Jury's (1967) equation:

$$k_L = \frac{10\,D_L}{d_d}$$

Figure 4.5.1-7 makes it clear that below that value penetration theory gives a better approximation. The exposure time for water drops falling through air at their terminal velocity is shown in Figure 4.5.1-4 for several heights as a function of drop diameter.

Example: What is the liquid phase mass transfer coefficient for absorption from air by 400 μm diameter water drops falling a distance of 2 meters through air if the contaminant diffusivity in water is 2×10^{-5} (cm^2/sec)? From Figure 4.5.1-4, $\theta = 1.2$ sec

$$\left(\frac{D_L\,\theta}{r_d^2}\right)^{1/2} = \left[\frac{2\times10^{-5}(1.2)}{(0.02)^2}\right]^{1/2} = 0.345$$

thus the "long-time" solution (Equation 4.5.1-3) is applicable:

$$k_L = \frac{10\ D_L}{d} \quad \frac{10 \times 2 \times 10^{-5}}{0.04} = 0.005 \text{ cm/sec}$$

For comparison, the "short-time" solution gives

$$k_L = 1.13\left(\frac{D_L}{\theta}\right)^{1/2} = 1.13\left(\frac{2\text{x}10^{-5}}{1.2}\right)^{1/2} = 0.0046 \text{ cm/sec}$$

From Figure 4.5.1-7 we can see that the fractional saturation is about 0.8; or, in other words, the drop would be 80% saturated with the contaminant after 1.2 seconds (if gas phase resistance to transfer were negligible and if there were no circulation inside the drop.)

Figure 4.5.1-5 shows "k_L" as a function of drop diameter, calculated in the same way as the example, for water drops in air falling at terminal velocity, with a representative value of diffusivity, $D_L = 2 \times 10^{-5}$ cm²/sec. In this plot, the "short-time" and "long-time" solutions are blended together. Also, the liquid-film coefficient per gram of water drops, "k_La", is shown in Figure 4.5.1-6 as a function of drop diameter. These two plots are useful in making approximate calculations.

Overall Coefficients

If the operating and equilibrium lines are straight, it is permissible and often more convenient to use the overall coefficients, "K_G" or "K_L", discussed earlier. The effect of transfer resistance both inside andoutside a sphere is shown in Figure 4.5.1-8, based on Workman's extension (1966) of Crank's solution (1957). Figure 4.5.1-8 is a plot of fractional saturation versus dimensionless diffusion time with "Γ" as a parameter for constant concentration outside the sphere. The group "Γ",defined below, is a ratio of resistance inside the sphere to the resistance outside the sphere. When "Γ" is large the outside resistance is less important and the efficiency of transfer approaches that for inside the sphere alone. For transfer to a drop:

$$\Gamma_D = \frac{r_d\ H'\hat{k}_G}{D_L} \tag{4.5.1-4}$$

Example: For SO_2 being absorbed from air by water drops in a cross-current spray chamber where the SO_2 concentration can be considered nearly constant along the path of drop fall, we can illustrate the nature of the relationship in Figure 4.5.1-8. Assume that the drops are 0.04 cm diameter, that "D_L" is 1.7×10^{-5} cm/sec and H = 50.0 atm/mole fraction (as given in Chapter 10), and that "$\hat{k}_G$" is $6.4\text{x}10^{-4}\text{x}\ (D_G/0.1)^{12}$ gmol/sec-cm²-atm) (as given in Figure 4.5.1-1). Gas phase diffusivity is computed as described in Chapter 10, as follows:

$$D_G = \frac{(0.001)\ T^{1.75}\left(\frac{1}{M_1} + \frac{1}{M_2}\right)^{1/2}}{P\ [V_1^{1/3} + V_2^{1/3}]^2} =$$

$$\frac{(10^{-3})\ (300)^{1.75}\left(\frac{1}{64} + \frac{1}{29}\right)^{1/2}}{1\ [(41.1)^{1/3} + (20.1)^{1/3}]^2} = 0.124\ (\text{cm}^2/\text{sec}) \text{ for } SO_2 \text{ in air}$$

"Γ" is computed as

$$\Gamma_D = \frac{(0.02)\ 50\ (6.4 \times 10^{-4})\ (1.24)^{1/2}}{1.7 \times 10^{-5}} = 41.0$$

Thus the efficiency of contact will be close to that for no outside (gas phase) resistance. This is paradoxical in view of the fact that SO_2 solubility is high enough that liquid phase resistance should be a minor factor. It is indicative however, of the peculiar effect of spherical geometry on concentration gradients inside the drop.

Agitation Effects

Coalescence of the drops as they collide with one another increases the average drop size, thus decreasing the total area available for mass transfer. The decrease in total mass transfer rate due to coalescence can be estimated quantitatively from Figures 4.5.1-2 and 4.5.1-6 if the size history of the drops is known. Coalescence, as well as the initial formation of the drops, causes transient oscillation of the drop shape which increases the liquid-film mass transfer coefficient because of internal circulation of the liquid within the drop. (Figures 4.5.1-3 and 4.5.1-6 do not take into account this effect). Wellek and Skelland (1965) suggest that "k_L" is increased roughly 50% when the internal circulation is laminar. This is consistent with the findings of Constan and Calvert (1963), who found increases on that order. For turbulent internal circulation, the approximate theory of Handlos and Baron (1957) gives a "k_L" about twice as large as "k_L" in a stagnant drop, for larger water drops (>400μ) in air. Panno and Calvert (1965) have observed much higher rates than given by Handlos and Baron in drops with forced circulation. Impurities in a liquid drop often accumulate on the surface and act as surfactants, immobilizing surface elements, so that in an industrial situation the liquid mass transfer mechanism may be diffusion through a stagnant liquid film, even under conditions where enhancement by oscillation and internal circulation would be expected.

Chemical Reaction

The effect of the chemical reaction within the drop, in addition to maintaining the full driving force, is to reduce the liquid-film resistance, often so much that an absorption becomes gas-film limited which would be liquid-film limited in the absence of reaction. Section 4.2.6 presents the basis for taking the effects of chemical reaction into account.

4.5.2 BUBBLES (see also 4.4.1)

The gas-film mass transfer coefficient from a bubble in a liquid is influenced by circulation of gas, which depends on how the bubble was formed, its age, and drag exerted on it by the liquid. For short contact times (large bubbles) penetration theory gives an adequate expression (see 4.2):

$$\hat{k}_G R_g T = 1.13 \left(\frac{D_G}{\theta} \right)^{1/2} \qquad (4.5.2\text{-}1)$$

where "θ" is the contact time of the bubble with the liquid (which is assumed to have uniform concentration). "Short" contact time for this case, as discussed in 4.5.1 and illustrated in Figure 4.5.1-7, is roughly $\theta < 0.013\ d_b/D_G$ sec. For gas bubbling through water a "short" time is $\theta \leq 0.35$ sec.

$$\hat{k}_G\ R_g T = 10\ D_G/d_b \qquad (4.5.2\text{-}2)$$

for long contact time Equation 4.5.2-2 applies, as for the case of transfer to drops. Observed "k_G's" are likely to be larger than the estimates provided by Equations 4.5.2-1 and 4.5.2-2, since both equations were derived assuming stagnant gas in the bubble; bubbles typically encountered in wet scrubber applications are large enough sc that appreciable circulation of the gas occurs within the bubble. Calderbank (1967) states that the effective diffusivity for Equation 4.5.2-1 is "many times" the molecular value. The maximum effect would correspond to the gas inside the rising bubble circulating at the same velocity as the rise velocity. Then the contact time for penetration (Equation 4.5.2-1) would be (d_b v_b).

The contact time for a stagnant bubble can be estimated from the rise velocity of the bubble through the liquid and the depth of the liquid as discussed in 4.4.1. Liquid depths, if unknown, can be estimated from information in Chapter 5. Bubble rise velocities are in the range 20 to 30 cm/sec for bubbles 0.1 to 2.0 cm diameter as shown in Figure 4.4.1-2. One can estimate the effect of circulation within the bubble by using the penetration theory relationship that "k_G" is inversely proportional to $\theta^{1/2}$. The ratio of contact time with circulation to that for a stagnant bubble is given by:

$$\frac{\hat{k}_G\ (\text{circulating})}{\hat{k}_G\ (\text{stagnant})} = \left(\frac{\theta_t}{\theta_c}\right)^{1/2} \quad \left(\frac{h/v_b}{d_b/v_b}\right)^{1/2} \quad \left(\frac{h}{d_b}\right)^{1/2} \qquad (4.5.2\text{-}3)$$

where "h" is total foam height above the plate.

If a 0.4 cm diameter bubble is rising through 10 cm of froth height, the maximum effect of circulation on "k_G" would be to increase its value by $(10/0.4)^{1/2} = 5$ times that for a stagnant bubble.

Bubble diameters are usually 0.1 to 0.3 cm when formed from an orifice. An average value for rough estimates is 0.3 cm without coalescence, or 0.4 to 0.45 cm when coalescence is effective. Bubble diameters from a porous plate or diffuser are typically 0.03 to 0.5 cm, with 0.2 cm being a rough average for estimation purposes. 0.2 cm is also a useful average size for bubbles in an agitated gas-liquid or bubbles formed by a plunging liquid jet.

Example: What is the gas-phase mass transfer coefficient for absorption from 0.4 cm diameter air bubbles rising through 10 cm of water? Assume "D_G" is 0.1 cm²/sec and T = 298°K. From Figure 4.4.1-2, bubble rise velocity could range from 20 to 25 (cm/sec).

$\theta = 10/25 = 0.4$ sec at higher velocity.

$$\frac{0.013\ d_b^2}{D_G} \quad \frac{0.013\ (0.4)^2}{0.1} = 0.021 < \theta, \text{ or } \left(\frac{D_G\ \theta}{r_b^2}\right)^{1/2}$$

thus the "long-time" solution, Equation 4.5.2-2, applies and, as Figure 4.5.1-7 shows, the fractional saturation would be nearly 100% for a stagnant bubble.

$$\hat{k}_G = \frac{(10)\ (0.1)}{(82.06)\ (298)\ (0.4)} = 10.2\text{x}10^{-5}\ \text{mol/sec-cm}^2\text{-atm}$$

Figure 4.5.2-1 shows "k_G" as a function of bubble diameter, calculated in the same way as the example, for air bubbles rising through 10 cm of water (typical liquid depth in a plate column) with $D_G = 0.1\ \text{cm}^2/\text{sec}$ and T = 298°K. The gas-film coefficient per cubic meter of gas as bubbles, k_Ga, is shown in Figure 4.5.2-2 as a function of bubble diameter.

The effect of various physical properties on the liquid phase mass transfer coefficient is not definable by a simple relationship. For design estimates the empirical correlations of Calderbank (1967) are recommended; Calderbank suggests:

$$k_L = 0.42 \left[\frac{(\rho_L - \rho_G)\ \mu_L\ g}{\rho_L^{\ 2}}\right]^{1/3} \left(\frac{\mu_L}{\rho_L\ D_L}\right)^{-1/2} \qquad (4.5.2\text{-}5)$$

for large bubbles (d > 0.25 cm) such as are encountered in sieve plate columns and in agitated vessels of pure liquid. For small bubbles (d < 0.25 cm), Calderbank gives:

$$k_L = 0.31 \left[\frac{(\rho_L - \rho_G)\ \mu_L\ g}{\rho_L^{\ 2}}\right]^{1/3} \left(\frac{\mu_L}{\rho_L\ D_L}\right)^{-2/3} \qquad (4.5.2\text{-}6)$$

applicable to bubbles formed by sintered plates, by small perforated plates, and in agitated electrolyte solutions. Calderbank states that the evidence indicates "k_L" is independent of rise velocity and bubble diameter, except for the decrease in "k_L" which occurs "sharply and critically" at the transition from "large" to "small" bubbles (Calderbank, 1959).

Several other correlations of "k_L" are given in the literature based on limited experimental data. Mehta and Calvert (1970), Hobler (1966), Li (1965), and Calderbank (1967) suggest that Higbie's penetration theory,

$$k_L = 1.13 \left(\frac{D_L\ u_t}{d_b}\right)^{1/2} \qquad (4.5.2\text{-}7)$$

does an adequate job. Hughmark (1967) gives empirically,

$$\frac{k_L\ d_b}{D_L} = 2 + a\left[\left(\frac{d_b v_b\ \rho_L}{\mu_L}\right)^{0.484} \left(\frac{\mu_L}{\rho_L\ D_L}\right)^{0.339} \left(\frac{d_b\, g^{1/3}}{D_L^{\ 2/3}}\right)^{0.072}\right]^{1.61} \qquad (4.5.2\text{-}8)$$

where "a" is 0.061 for single spherical bubbles and 0.0187 for swarms of bubbles.

The Frössling equation,

$$\frac{k_L\ d_b}{D_L} = 2 + 0.552 \left(\frac{d_b u \rho_L}{\mu_L}\right)^{1/2} \left(\frac{\mu_L}{\rho_L\ D_L}\right)^{1/3} \qquad (4.5.2\text{-}9)$$

agrees with observed rates of dissolution of small bubbles.

Example: What is the liquid-phase mass transfer coefficient for absorption from 0.4 cm diameter air bubbles? Assume $D_L = 2 \times 10^{-5} cm^2/sec$ and T = 298°K. Equation 4.5.2-5, gives

$$k_L = 0.42 \left[\frac{(1.0)\ (8.94 \times 10^{-3})\ (980.7)}{(1.0)^2}\right]^{1/3} \left[\frac{8.94 \times 10^{-3}}{(1.0)\ (2 \times 10^{-5})}\right]^{-1/2} =$$

$$= 0.42\ (2.06)\ (0.0473) = 0.04092\ (cm/sec)$$

Figure 4.5.2-3 shows a comparison of the "k_L" correlations given above, calculated for air bubbles in water with $D_L = 2 \times 10^{-5}$ (cm^2/sec) and T = 298°K. It can be seen that for the air-water system, Hughmark's single bubble expression and the penetration theory of Higbie are roughly in agreement with Calderbank's large-bubble correlation, and that Hughmarks correlation for swarms and the Frossling equation agree roughly with Calderbank's small-bubble correlation. The liquid-film coefficient per cubic meter of bubbles, k_La, is shown in Figure 4.5.2-4 for air-water as a function of bubble diameter, based on Equations 4.5.2-5 and 4.5.2-6.

Overall Resistance

If the operating and equilibrium lines are straight, it is permissible and often more convenient to use the overall mass transfer coefficients, K_G and K_L, discussed earlier in this chapter. Resistance in both phases with constant liquid concentration can also be accounted for by solving the differential equations for diffusion to or from a stagnant sphere with an outside film resistance. Figure 4.5.1-8 describes fractional saturation (efficiency) as a function of dimensionless diffusion time (based on inside conditions) with Γ as parameter, as discussed in 4.5.1. For the case of a bubble rising through liquid of constant composition;

$$\Gamma_B = \frac{r_b\ R_g T\ k_L}{D_G\ H'} \qquad (4.5.2\text{-}10)$$

If we again look at the example of SO_2 absorption from air by water, as in 4.5.1, assume 0.4 cm diameter bubbles, and take "k_L" from Figure 4.5.2-3 to be 0.04 (cm/sec) (neglecting the effect of D_L being 1.7×10^{-5} instead of 2×10^{-5}) we get;

$$\Gamma_B = \frac{(0.2)\ (82.1)\ (300)\ (0.04)}{(0.124)\ (50)} = 32.$$

This indicates that liquid phase resistance is not important and the efficiency will be nearly the same as for the bubble alone (as in Figure 4.5.1-7).

Other Effects

Coalescence of bubbles generally has a detrimental effect on mass transfer. Except at very high gas flow rates, the effect can be attributed simply to the decrease in surface area associated with larger bubble size. For example, in the studies of Calderbank et al. (1964) on CO_2 bubbles in water, the mean bubble diameter was around 4 mm, but when coalescence was suppressed, the mean diameter was less than 3 mm; thus for the same flow rate the surface area was decreased 25% because of coalescence. Partly due to coalescence, in common situations most of the total mass transfer takes place during and just after creation of the new bubble surface especially for high gas flow rates, when the bubbles begin coalescing almost immediately after formation. In addition, at high gas flow rates, each bubble may spend a sufficient fraction of its life in contact with other bubbles before coalescence; this further decreases "$k_L a$", since a substantial part of the bubble surface area will not be effective for mass transfer.

Distortion of bubbles as they move through the liquid decreases "k_L" slightly by changing the liquid velocity profile. Sy and Lightfoot (1968) have analyzed this change theoretically; their result indicates the decrease in "k_L" could be as much as 3% for large bubbles of air in water. Several authors have noted that surfactants in the liquid, such as carboxylic acids, alcohols, and electrolytes in general, act to increase interfacial area (and thus total mass transfer) by inhibiting coalescence (Sideman et al. review, 1966; Braulick et al., 1965; Zieminsky et al., 1967). In addition, Zieminsky et al. found that at low concentrations, surfactants increase the mass transfer coefficient. On the other hand, high concentrations of surfactants may reduce "k_L" (Sideman et al., 1966). (For possible effects of surfactants on mass transfer, see 4.4.4.2).

Chemical reaction of the diffusing component in the liquid phase enhances mass transfer. This can be accounted for by methods discussed in 4.2.6.

4.5.3 MASS TRANSFER TO LIQUID SHEETS

The concept of mass transfer to liquid sheets is most obviously applied to absorption in a wetted wall column and has also been used to model absorption on wetted packing. Spray nozzles usually emit a conical sheet of liquid which rapidly breaks up into droplets. Other cases of mass transfer into a liquid sheet are when the liquid flows along the side walls of a packed tower, a spray tower, or a venturi scrubber. The usual models of mass transfer to sheets are unsteady-state diffusion using either molecular or turbulent diffusivity or a variant of penetration theory. In any case, a first requirement is that one be able to relate liquid sheet thickness and/or velocity to the total liquid flow rate. One approach (Calvert and Kapo, 1963) is to compute an average liquid velocity from liquid holdup in the apparatus (see Perry, 1963), assuming some velocity distribution such as plug flow or parabolic velocity distribution; in the latter case, the liquid surface velocity is 1.5 times the average. Another approach is to compute the film thickness for laminar flow as follows, and compute velocity from that. The film thickness, x, is,

$$x = \left(\frac{3 \mu_L Lp}{\rho_L^2 g} \right)^{1/3} \qquad (4.5.3\text{-}1)$$

for flow down a vertical surface; "Lp" is the mass flow rate per unit width or perimeter. The liquid surface velocity is given by:

$$v_s = 1.5 \bar{v} = \frac{1.5 Lp}{\rho_L x} = \left(\frac{1.5^3 Lp^2 g}{3 \rho_L \mu_L} \right)^{1/3} = \left(\frac{1.13 Lp^2 g}{\rho_L \mu_L} \right)^{1/3} \qquad (4.5.3\text{-}2)$$

From penetration theory,

$$k_L = 1.13 \left(\frac{D_L v_s}{Z} \right)^{1/2} = 1.15 \left(\frac{D_L}{Z} \right)^{1/2} \left(\frac{Lp^2 g}{\rho_L \mu_L} \right)^{1/6} \qquad (4.5.3\text{-}3)$$

The length of liquid flow, Z, is the distance travelled between formation and re-arrangement of the film. In a wetted wall tower it is the height of the liquid film, although turbulence may cause surface renewal in the film in a shorter distance. In packings it is usually estimated as the height of a packing element.

Observed rates of mass transfer in the liquid film have often been correlated by expressions of the form,

$$N_{Sh} = C N_{Re}^{a} N_{Sc}^{b} r^{d}, \text{ where} \qquad (4.5.3\text{-}4)$$

$$N_{Sh} = \frac{k_L x}{D_L}, \text{ Sherwood number}$$

$$N_{Re} = \frac{4 L_p}{\mu_L}, \text{film Reynolds number}$$

$$N_{Sc} = \frac{\mu_L}{\rho_L D_L}, \text{ Schmidt number}$$

where "L_p" is the distance from the leading edge (cm), and "r" is a ratio characterizing the geometry of the column or packing.

There is no agreement on the values of "a", "b", and (especially) "d"' particular values of "a", "b", "c", and "d" should be used only in situations very similar to the one from which they were obtained.

Gas Phase

Available data for gas phase coefficients in wetted-wall columns are correlated by (Sherwood and Pigford, 1952)

$$N_{Sh} = 0.023 N_{Re}^{0.83} N_{Sc}^{0.44}, \text{ where} \qquad (4.5.3\text{-}5)$$

$$N_{Sh} \equiv \frac{\hat{k}_G d_{col}}{D_G} \frac{P_{BM}}{P}, \text{ gas-phase Sherwood number}$$

$$N_{Re} \equiv \frac{d_{col} G}{\mu_G}, \text{ gas-phase, Reynolds number}$$

$$N_{Sc} \equiv \frac{\mu_G}{\rho_G D_G}, \text{ gas-phase Schmidt number}$$

and "p_{BM}" is the log-mean partial pressure of inert gases through the column, as defined in Equation 4.2.2-3.

Gas phase coefficients may also be predicted from penetration theory when there is some knowledge of penetration (surface renewal) time. In packed columns this may be estimated as the time the gas takes to flow a distance of one packing element.

For air and water flow (counter-current) in typical packed towers, penetration times are on the order of 0.3 sec for liquid and 0.03 sec for gas. If we assume average diffusivities of 0.1 (cm²/sec) for the gas and $2\text{x}10^{-5}$(cm²/sec) for the liquid, penetration theory yields:

$$k_L = 1.13\left(\frac{2\text{x}10^{-5}}{0.3}\right)^{1/2} = 9.2\text{x}10^{-3}(\text{cm/sec}) \simeq 10^{-2}$$

$$k_G = \frac{1.13}{2.46\text{x}10^{4}}\left(\frac{0.1}{0.03}\right)^{1/2} = 8.4\text{x}10^{-5} \simeq 10^{-4}(\text{gmol/cm}^2\text{-sec-atm})$$

Transfer Area

The interfacial area for mass transfer is easy to calculate for a wetted wall column. For a packed column, the interfacial area which is effective is typically from 30% to 70% of the area of the dry packing material, because of uneven liquid distribution, incomplete wetting of each packing piece, and stagnant elements of liquid at contact points in the packing.

Formation of ripples on a flowing liquid sheet considerably increases the rate of mass transfer. Although the ripples increase the surface area by only a few percent, "k_L" is increased 50 to 100% or more (Jepsen et al., 1966; Goren and Mani, 1968). Rippling does not affect the thickness of the flowing film, but the velocity distribution may no longer be parabolic. Rippling sets in at film Reynolds numbers around 4 to 25, although turbulence in the liquid does not appear until "N_{Re}" is about 1,200, to 2,100. The degree of rippling decreases in proportion to the concentration of surfactants in the liquid, and rippling can be eliminated entirely by surfactants.

Gas-side transfer coefficients will be higher than those estimated from Equation 4.5.3-5 if "extra" turbulence is present in the gas stream due to inlet flow conditions or turbulence promoters; the increase can be a factor of 10 in some cases. Observed liquid-film coefficients for inclined flowing sheets are not significantly different from those for vertical falling films. Wetted-wall mass transfer is not much affected by surface tension; however, when the liquid flows over a packing, the effective interfacial area can be greatly decreased if the packing is poorly wet by the liquid. This will be a problem if a high surface tension material like PTFE (e.g. "Teflon") is used because of some other design constraint.

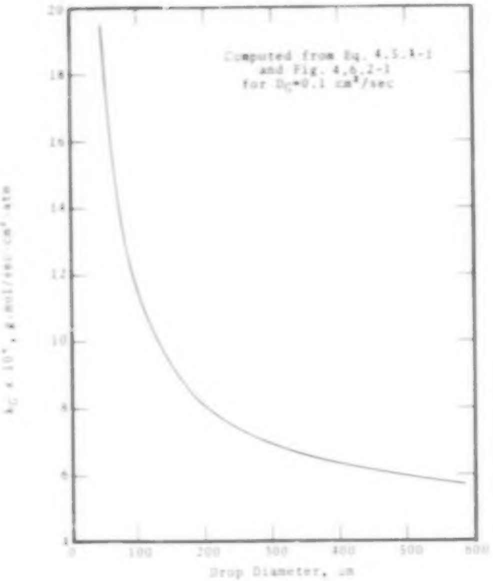

FIGURE 4.5.1-1
GAS-FILM MASS TRANSFER TO FALLING
WATER DROPS IN AIR VS. DROP
DIAMETER

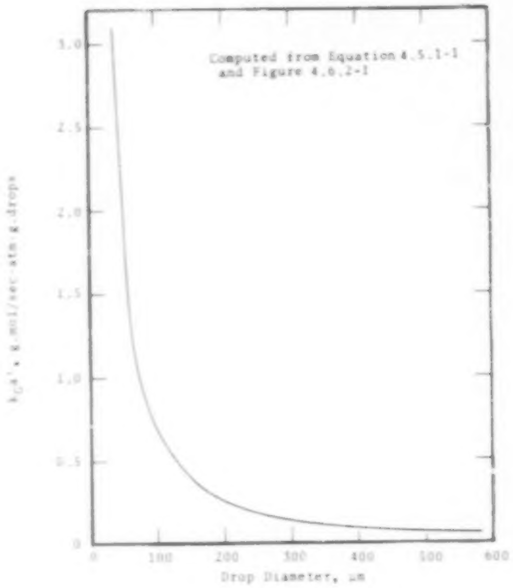

FIGURE 4.5.1-2
GAS-FILM MASS TRANSFER RATE PER
GRAM OF FALLING WATER DROPS
IN AIR VERSUS DROP DIAMETER

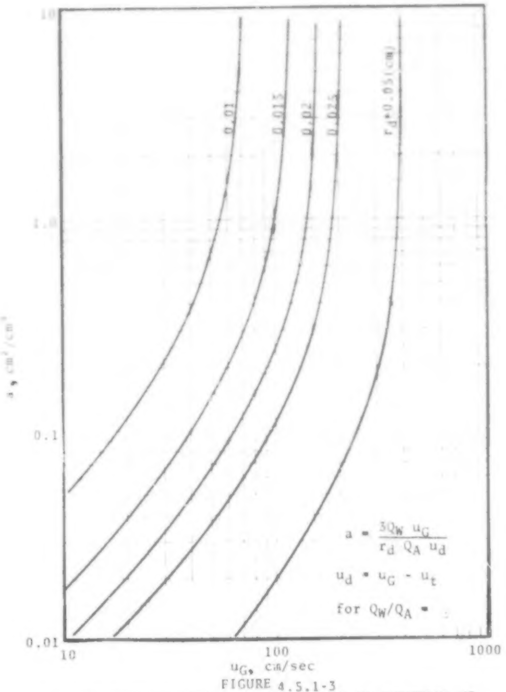

FIGURE 4.5.1-3
SPRAY SURFACE AREA PER UNIT VOLUME OF SCRUBBER VS.
AIR VELOCITY, FOR COUNTER-CURRENT AIR AND WATER WITH
DROP RADIUS AS PARAMETER AND Q_W/Q_A=1

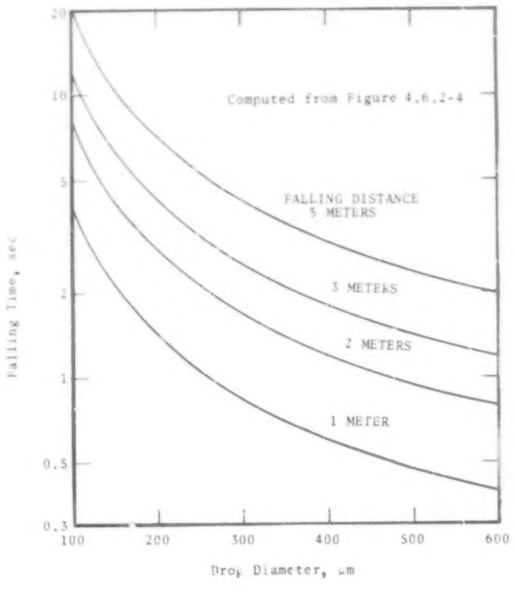

FIGURE 4.5.1-4
EXPOSURE TIME FOR WATER DROPS FALLING IN AIR

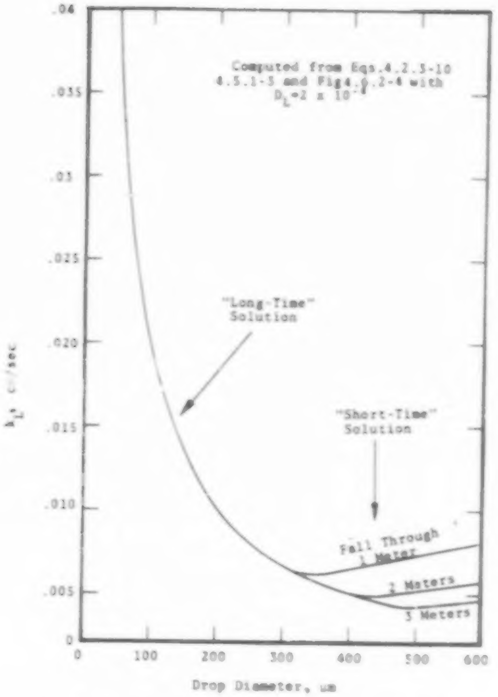

FIGURE 4.5.1-5

LIQUID-FILM MASS TRANSFER TO FALLING WATER DROPS IN AIR VERSUS DROP DIAMETER WITH FALLING DISTANCE AS PARAMETER

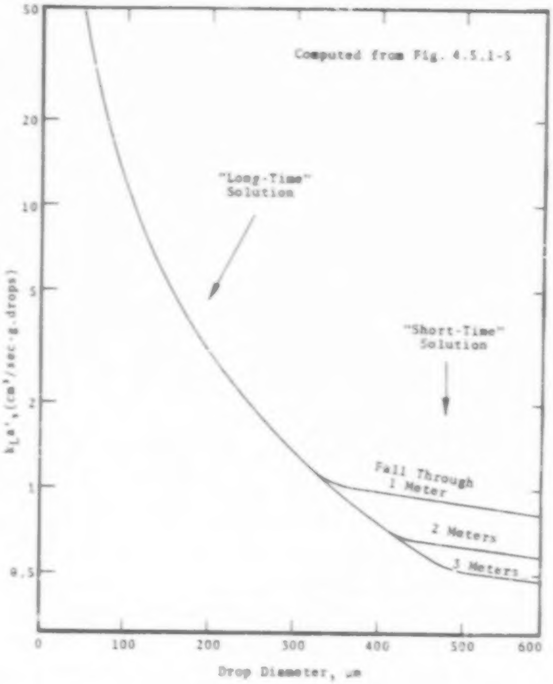

FIGURE 4.5.1-6

LIQUID-FILM MASS TRANSFER PER GRAM OF FALLING WATER DROPS (IN AIR) VS. DROP DIAMETER WITH FALLING DISTANCE AS PARAMETER

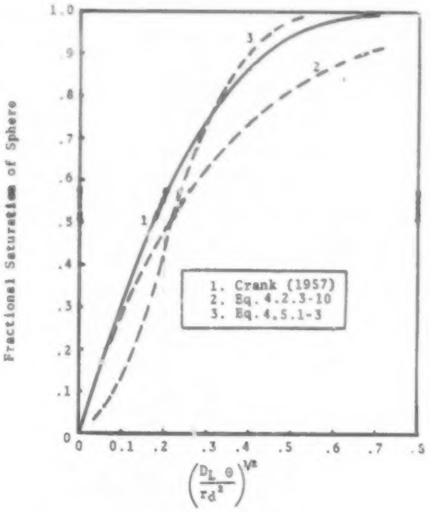

FIGURE 4.5.1-7

FRACTIONAL SATURATION OF SPHERE VS. DIMENSIONLESS DIFFUSION TIME

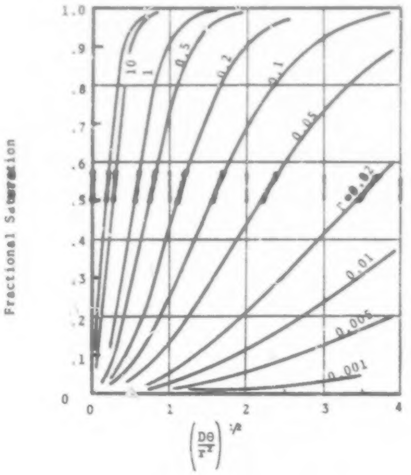

FIGURE 4.5.1-8

FRACTIONAL SATURATION OF A SPHERE VS. DIMENSIONLESS TIME WITH Γ PARAMETER (AFTER WORKMAN AND CALVERT 1966)

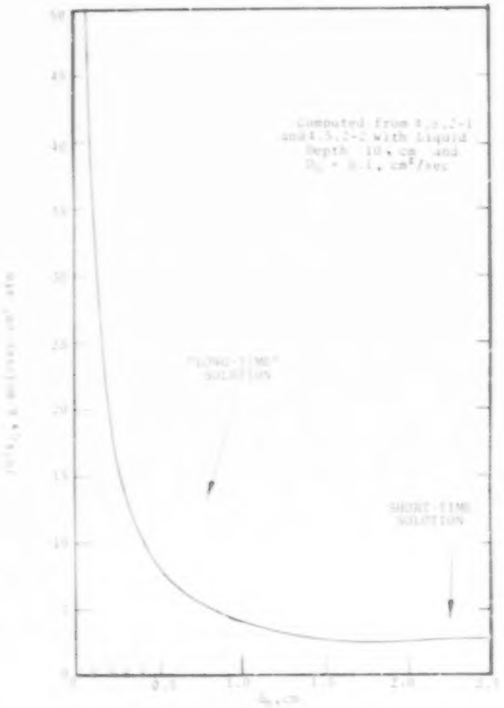

FIGURE 4.5.2-1

GAS-FILM MASS TRANSFER FROM AIR BUBBLES RISING IN WATER

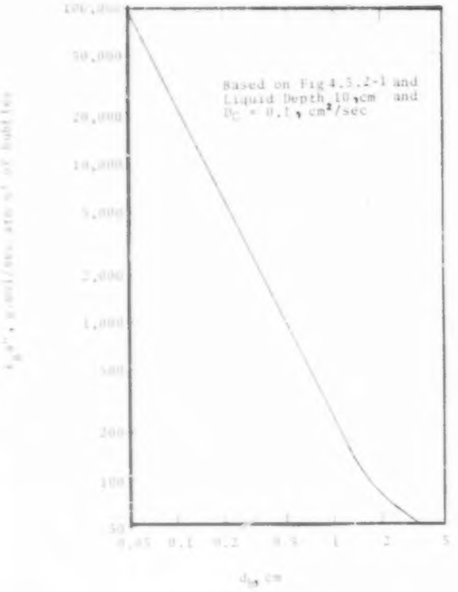

FIGURE 4.5.2-2

GAS-FILM MASS TRANSFER PER CUBIC METER OF RISING AIR BUBBLES

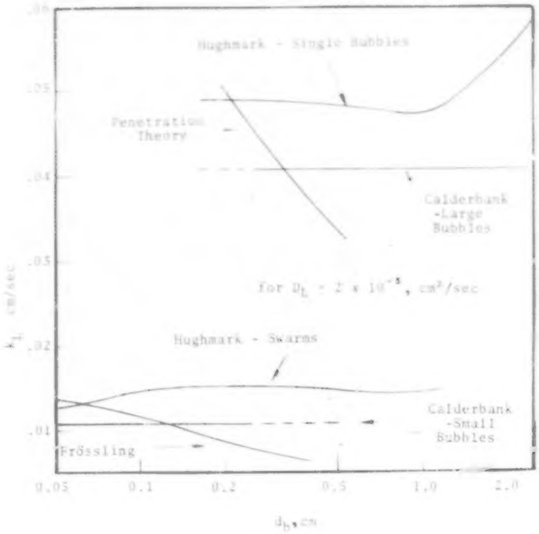

FIGURE 4.5.2-3

LIQUID-FILM MASS TRANSFER COEFFICIENT FROM AIR BUBBLES RISING IN WATER

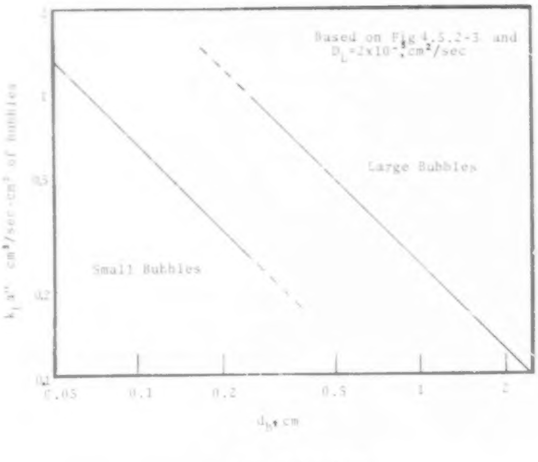

FIGURE 4.5.2-4

LIQUID-FILM MASS TRANSFER PER CUBIC CENTIMETER OF RISING AIR BUBBLES IN WATER

SECTION 4.5 NOMENCLATURE

LATIN

a - constant

c - mass concentration, Kg/m^{3}or g/cm^3

$\hat{c}$ - molar concentration, Kgmol/m^3 or gmol/cm^3

d - diameter, m or cm

d_{col} - column diameter, m or cm

D - diffusivity, cm^2/sec

g - acceleration of gravity, 9.81 m/sec^{2}or 981 cm/sec^2

G - gas mass flux kg/(sec m^2) or g/(sec cm^2)

h - total foam height above plate, m or cm

H' - apparent Henry's law constant, atm/(g/cm^3) or mbar (g/cm^3)

k - first order reaction rate constant, 1/sec

$\hat{k}_G$ - gas film mass transfer coefficient, gmol/(sec cm^{2}atm)

k_L - liquid film mass transfer coefficient, cm/sec

L - thickness of drop surface element, cm

P - total pressure, mbar or atm

P_{BM} - log mean pressure of component B, mbar or atm

r - radius

Rg - ideal gas law constant

t - time, sec

T - absolute temperature, °K

u - velocity, m/sec or cm/sec

v - velocity, m/sec or cm/sec

DIMENSIONLESS NUMBERS

N_{Sc} $\equiv \mu_G/(\rho_G D_G)$, Schmidt Number

N_{Sh} $\equiv k_G R_G Td/D_G$, Sherwood Number

N_{Re} $\equiv \rho du/\mu$, Reynolds Number

SECTION 4.5 NOMENCLATURE

GREEK

Θ - contact time, sec

ρ - density, kg/m^3 or g/cm^3

σ - liquid surface tension, dyne/cm

μ - viscosity, g/(cm sec)

$\Gamma_d \equiv \dfrac{r_d\ H'\ \hat{k}_G}{D_L}$ Equation 4.5.1-4

$\Gamma_b \equiv \dfrac{r_b\ Rg\ T\ k_c}{D_G\ H'}$

SUBSCRIPTS

b - bubble

d - drop

G - gas phase

i - interface

L - liquid phase

t - terminal velocity

1 - bottom

2 - top

SECTION 4.5 - REFERENCES

Braulick, W. J., Fair, J. R., Lerner, B. J., A.I.Ch.E. Journal, 11, 73 (1965).

Calderbank, P. H., Tr.I.Ch.E., 37, 173 (1959).

Calderbank, P. H., The Chem. Engr., 212, 209 (1967).

Calderbank, P. H., Moo-Young, M. B., Biddy, R., Chem. Eng. Sci., 91, Supplement (1964).

Calvert, S., Kapo, G., Chem. Eng., Feb 4 and Mar. 4, (1963).

Constan, G. L., Calvert S., A.I.Ch.E. Journal 9, 109 (1963).

Crank, J., "Mathematics of Diffusion", Oxford Univ. Press, London (1956).

Goren, S. L., Mani, R. V. S., A.I.Ch.E. Journal 14, 57 (1968).

Handlos, A. E., Baron, T., A.I.Ch.E. Journal 3, 127 (1957).

Harmathy, T. Z., A.I.Ch.E. Journal, 6, 281 (1960).

Hobler, T., "Mass Transfer and Absorbers," Pergamon, New York (1966).

Hughmark, G. A., I.E.C. Fundamentals, 6, 408 (1967); I.E.C. Proc. Des. Development, 6, 218 (1967).

Jepsen, J. C., Crosser, O. K., Perry, R. H., A.I.Ch.E. Journal 12, 186, (1966).

Jury, S. H. A.I.Ch.E. Journal, 13, 1124 (1967).

Li, P. S., West, F. B., Vance, W. H., Moulton, R. W., A.I.Ch.E.Journal, 11, 581 (1965).

Mehta, D. S., Calvert, S., Brit. lhem. Eng. 15, 781 (1970).

Panno, A., Calvert, S., "Developments in Mechanics", 2, 776 (1965).

Perry, R. H., editor, "Chemical Engineer's Handbook", McGraw-Hill, San Francisco (1963).

Schaftlein, R. W., Russell, T. W. F., Ind. Eng. Chem., 60(5), 12, (1968).

Sherwood, T. K., Pigford, R. L., "Absorption and Extraction", McGraw-Hill, New York, 1952.

Sideman, S., Hortascu, O., Fulton, J. W., Ind. Eng. Chem., 58(7), 32 (1966).

SECTION 4.5
REFERENCES

Sy, F., Lightfoot, E. N., A.I.Ch.E. Journal, 14, 835 (1968).

Wellek, R. M., Skelland, A. H. P., A.I.Ch.E. Journal 11, 557 (1965).

Workman, W., Calvert S., A.I.Ch.E. Journal 12, 867 (1966).

Yoshida, F., Miura, Y., I.E.C. Proc. Des. Development, 2, 263 (1963).

Zieminsky, S. A., Caron, M. M., Blackmore, R. B., I.E.C. Fundamentals, 6, 233 (1967).

4.6 UNIT MECHANISMS FOR PARTICLE SEPARATION

4.6.1 INTRODUCTION

In this section, equations shall be developed for the different unit mechanisms of particle separation. After the collection efficiency of each unit mechanism has been evaluated, the overall efficiency of the device can be predicted by adding the weighted contribution of each integrated unit mechanism. The overall collection efficiency, E, is:

$$E = 1 - \prod_{i=1}^{n} (1 - w_i E_i) \qquad (4.6.1\text{-}1)$$

where "E_i" is the efficiency calculated for the i'th specific unit mechanism at the given flow conditions, "w_i" is the capability that the i'th mechanism contributes to the device, estimated from the fraction of liquid and/or aerosol participating in this particular mechanism and "n" is the number of unit mechanisms involved.

Different unit mechanisms may come into play at different regions of the same device. For example, a device utilizing a spray and screen might employ different unit mechanisms at the spray from those in use at the screen.

Some phenomena, such as sonic vibration, will cause a change in particle size distribution due to agglomeration, thus improving collection efficiency. In these cases, the change in particle size distribution should be estimated before calculating collection efficiency.

4.6.2 COLLECTION BY DROPS

Particle collection by liquid drops may arise through several mechanisms. However, inertia is the mechanism most commonly effective in scrubbers.

Predicting scrubber performance requires that the interaction between a large population of drops and an aerosol be accounted for over the flight time of each drop. Given drop size, velocity and concentration of drops and particles at each instant, one can apply the factors governing collection by single drops and sum up the contribution of the entire population of drops to get the overall performance of the scrubber.

Liquid drops behave very much the same as rigid spheres when collecting aerosol particles by inertial mechanisms. Goldshmid and Calvert (1963) showed that drop shape and oscillation have a negligible effect on collection efficiency. Interfacial tension as measured by contact angle between the drop and the collected particle, has an influence in the region of the inertia parameter, K, from 0.1 to 0.55. Efficiency is lower for non-wetting combinations of particles and liquids. In the case of submicron particles moving at high velocities, collection on the back of the drop becomes substantial for low values of "K".

4.6.2.1 Inertial Collection

When a moving aerosol stream approaches an obstacle, the fluid streamlines spread around it. At the same time, inertia forces carry particles across the streamlines, so that the particles hit, and in many cases stick to the obstacle. The collection efficiency due to inertia, η_D, is called the target efficiency and is defined as the ratio of the number of particles striking the obstacle to the number which would strike it if the streamlines were not diverted by the obstacle; see Figure 4.6.2-1. The assumption is always made that all the particles adhere on striking. If the particles are uniformly distributed throughout the approaching gas stream, then the collection efficiency equals the ratio of the area swept clean to the cross-sectional area of the obstacle:

$$\eta = \left(\frac{y_o}{r_d}\right)^2 \text{ for spheres and } = \frac{y_o}{r_d} \text{ for cylinders} \qquad (4.6.2\text{-}1)$$

where "y_o" is the distance from the axis of the limiting streamline for impaction and "r_d" is the radius of the collector. When additional fa forces are present that force the particle towards the collection, efficiency can rise above 100%, meaning that the area swept clean by the collector is larger than the crossectional area of the collector.

Three factors determine the inertial collection efficiency. The first is the velocity distribution of the gas flowing by the collector, which varies with the Reynolds number of the gas with respect to the collector. The second factor is the trajectory of the particle. This depends on the mass of the particle, its air resistance, the size and shape of the collector, and the rate of flow of the gas stream. The third factor is the adhesion of the particles to the collector - usually assumed to be 100%.

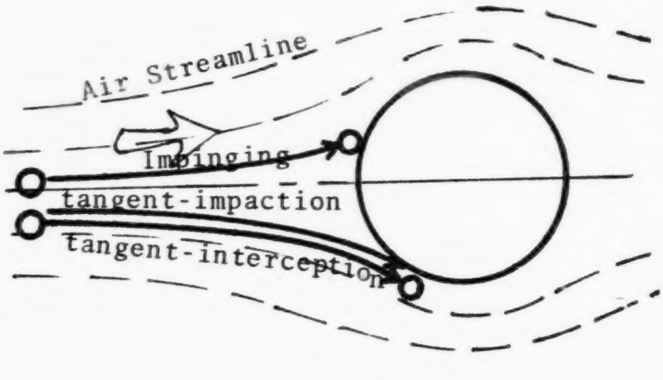

FIGURE 4.6.2-1

AIR STREAMLINES AND PARTICLE TRAJECTORIES AROUND SPHERE

The Reynolds number of the air with respect to the collector is:

$$N_{Red} = \frac{u_o \rho_G d_d}{\mu_G}$$

where "u_o" is the undisturbed upstream air velocity, with respect to the collector, "ρ_G" and "μ_G" are respectively the air density and viscosity, and "d_c" is the collector's diameter. At high values of N_{Red} (potential flow), the parting of the gas streamlines occurs close to the collector. Except near the collector surface, the flow pattern corresponds to that of an ideal gas. When the Reynolds number is low, flow is governed by viscosity (viscous flow) and the effect of disturbance created by the collector is noticed at relatively large distances upstream. The effect of the sudden spreading of the streamlines at high Reynolds numbers is to enhance the influence of particle inertia and therefore cause a higher collection efficiency.

If all field forces are ignored and if it is assumed that the particles obey Stokes' law, then the particles' equations of motion can be derived by equating the particle inertia force to the air drag on the particle. The equations in dimensionless form are:

$$K_p \frac{d\tilde{u}_p}{d\tilde{t}} = (\tilde{u}_G - \tilde{u}_p) \qquad (4.6.2\text{-}3)$$

$$K_p \frac{d\tilde{v}_p}{d\tilde{t}} = (\tilde{v}_G - \tilde{v}_p) \qquad (4.6.2\text{-}4)$$

where:

$$K_p = \frac{C' \rho_p d_p^2 u_o}{9 \mu_G d_c} \qquad (4.6.2\text{-}5)$$

$$\tilde{u}_p = \frac{u_p}{u_o}; \qquad \tilde{v}_p = \frac{v_p}{u_o} \qquad (4.6.2\text{-}6); (4.6.2\text{-}7)$$

$$\tilde{u}_G = \frac{u_G}{u_o}; \qquad \tilde{v}_G = \frac{v_G}{u_o} \qquad (4.6.2\text{-}8); (4.6.2\text{-}9)$$

$$\tilde{t} = \frac{2 u_o t}{d_c} \qquad (4.6.2\text{-}10)$$

$d_c/2$ is a characteristic dimension of the collector. For a sphere it is the radius.

u_p and v_p are particle velocity components in the X and Y directions respectively.

u_G and v_G are air velocity components in the X and Y directions respectively relative to the collector.

C' is the Cunningham correction factor.

The dimensionless inertia parameter, K_p, which characterizes the motion of the particle has a physical meaning too. It is the ratio of the particle "stopping distance" to the radius of the collector. A particle's "stopping distance" is that distance it would travel before coming to rest if injected into a still gas at velocity "u_o", when all forces on the particle except the drag force are zero.

The solutions to the equations of motion will depend upon the velocity field assumed. These equations have been solved for several collectors of different shapes under given boundary conditions, mostly by numerical methods. Figure 4.6.2-2 shows theoretical and experimental collective efficiency for a spherical collector for potential and viscous flow. Figure 4.6.2-3 shows calculated efficiency curves for other shapes of collectors.

For potential flow and for values of "K_p" greater than 0.2 the experimental values of inertial collection efficiency for spheres can be approximated by the correlation:

$$\eta_p = \left(\frac{K_p}{K_p + 0.7}\right)^2 \qquad (4.6.2\text{-}11)$$

Most of the theoretical solutions to Equations 4.6-3 and 4.6-4 yield a critical "K_p" below which no inertial deposition takes place. For cylinders, $K_{crit.} = 0.125$ and for spheres $K_{crit.} = 0.083$. This was shown by many investigators to be a theoretical limit. In reality, in cases of turbulent flow, particles are collected at the back of the collector and collection efficiency for $K_p \leq K_{crit.}$ is not zero.

4.6.2.2 Interception

A particle is collected by interception when its surface (not center) touches the surface of the collector, which can happen without crossing any gas streamlines. This occurs if the streamline the particle rides on passes within a particle radius' distance from the collector surface.

In the model for particle collector by inertial impaction, Section 4.6.2.1, it was assumed that a particle is a massive point, and is captured when that point touches the collector's surface. However, a particle is actually captured when its surface, rather than its center, hits the collector. For this reason there is not a unique curve of collection efficiency versus the inertia parameter, "K". Rather, a family of curves exists, depending upon the ratio of particle diameter to collector diameter.

Ranz and Wong (1952) developed a relation for interception efficiency for the inertia parameter, $K_p = 0$, i.e.: a particle follows a streamline in potential flow. Using this model they showed that for spherical collectors:

$$\eta_I = \left[1 + \frac{d_p}{d_c}\right]^2 - \left[\frac{1}{1 + \frac{d_p}{d_c}}\right] \qquad (4.6.2\text{-}12)$$

4.6.2.3 Gravitational Collection of Particles by Drops

For the collection of particles by free falling drops, collection efficiencies may be calculated for drops of radius "r_d" falling at their terminal velocities. It is assumed that drops will rapidly approach terminal velocity. The particle settling velocities are assumed negligible compared to those of the collecting drops, i.e.: the drops are much larger than the particles. The air is assumed to be saturated so that no drop evaporation or growth takes place: diffusion and interception are neglected. Drop collection efficiencies are read from Figure 4.6.2-2 for potential and viscous flow ($\eta_{pot.}$ and $\eta_{vis.}$). Drop velocities are read from Figure 4.6.2-4. The actual efficiency is then calculated from Langmuir's interpolation (1948) formula:

$$\eta_G = \frac{\eta_{vis.} + \eta_{pot.}\left(\frac{N_{Red}}{60}\right)}{1 + \frac{N_{Red}}{60}} \qquad (4.6.2\text{-}13)$$

Figure 4.6.2-5 shows efficiency as a function of particle diameter with drop diameter as a parameter, and may be used alternatively to Equation 4.6.2-13. It can be seen that the highest collection efficiency per drop is for drops of 0.1 to 0.2 cm in diameter.

The collection of particles per unit volume of water flowing through a spray tower is given by,

$$\frac{\eta_G \, Q_L \, \pi \, r_d^{2}}{Q_L \, \frac{4}{3} \, \pi \, r_d^{3}} = \frac{3 \, \eta_G}{4 \, r_d} \qquad (4.6.2\text{-}14)$$

From Equation 4.6.2-14 we see that the area cleaned per unit volume of water is proportional to η_G/r_d. Figure 4.6.2-6 shows η_G/r_d vs. drop radius with particle radius as a parameter. It can be seen that for each particle radius there is an optimum drop radius for a given quantity of water sprayed. For the smaller particles, which are usually of most concern, the optimum drop radius is 100 - 500 μm.

It should be remembered that saturated air was assumed in the foregoing discussion. When the vapor pressure difference is 5 mm Hg, Frossling (1938) showed that a drop 10 μm in diameter will evaporate after falling 0.014 cm and a 100 μm drop will completely evaporate after traveling 102 cm.

4.6.2.4 Diffusion

Small particles, in the sub-micron size range, are rarely collected by inertial impaction or interception because they follow the gas streamlines surrounding the collecting body, and their ratio of d_p/d_c is small. In a still gas, small particles move freely across gas streamlines due to random bombardment from gas molecules. Some of the particles hit the collector, and are removed from the gas.

If one estimates that the aerosol concentration near the collector surface takes the form, Hidy and Brock (1970)

$$c = c_i \left(1 - \frac{r_c}{\delta}\right) \qquad (4.6.2\text{-}15)$$

where "r_c" is the collector radius, "δ" is the distance from the collector center and "c_i" is the concentration of particles in the main body of the gas stream, then the concentration gradient at the collector surface is:

$$\left.\frac{\partial c}{\partial \delta}\right|_{\delta = r_c} = \frac{c_i}{r_c} \qquad (4.6.2\text{-}16)$$

The rate of deposition, ϕ(g/sec if c_i is g/cm³), on a spherical collector for a gas at rest is equal to:

$$\phi = 4 \, \pi \, Dp \, r_c \, c_i \qquad (4.6.2\text{-}17)$$

Particle diffusivities are several orders of magnitude smaller than diffusivities of gases, and are closer to the values obtained for diffusivities of solutes in liquids. Particle diffusivity may be calculated using the Einstein (1905) equation (see 4.3.3.2). For an aerosol flowing past a spherical collector the rate of diffusion increases and becomes a function of the Reynolds and the Schmidt numbers. The Schmidt number "N_{Sc}" is a dimensionless group indicating the ratio of convective and diffusive transfer rates (at const. N_{Re}). The Schmidt number is defined as

$$N_{Sc} = \frac{\mu_G}{\rho_G D_p} \qquad (4.6.2\text{-}18)$$

For low diffusivities, leading to high Schmidt number ($N_{Sc} \simeq 10^6$), and low Reynolds numbers ($N_{Red} < 3$) Levich (1952) showed that:

$$\phi = 2 \pi D_p r_d c_i N_{Red}{}^{1/3} N_{Sc}{}^{1/3} \qquad (4.6.2\text{-}19)$$

For large Reynolds numbers (600 - 2,600) and the same value of Schmidt number, Akselrud (1953) showed that

$$\phi = 1.6 \pi D_p r_d c_i N_{Red}{}^{1/2} N_{Sc}{}^{1/3} \qquad (4.6.2\text{-}20)$$

For Reynolds number = 100 - 700 and Schmidt number $\simeq 10^3$, according to Garner et al. (1958a and 1958b) showed that

$$\phi = 1.9 \pi D_p r_d c_i N_{Red}{}^{1/2} N_{Sc}{}^{1/3} \qquad (4.6.2\text{-}21)$$

4.6.2.5 Electrostatic Collection

The electrostatic properties of small particles effect their motion and collection in an electric field. Kraemer and Johnstone (1955) solved the equations of motion for particles in an electric field neglecting all other forces. They calculated the collection efficiency of conducting and non-conducting aerosol particles by a conducting sphere due to electrostatic forces, for potential and viscous flows and for several interception parameters. Gas streamline flow and low amplitude Brownian motion relative to the collector diameter were assumed.

There are five aspects of electrical forces acting in a system of particles approaching a collector. For each case a collection parameter, the ratio of the electrostatic force to the Stokes-Cunningham drag force, has been defined by Kraemer and Johnstone.

For the coulombic force between a charged collector and a charged particle:

$$K_{E1} = \frac{C' q_p q_c}{3 \pi \mu_G d_p u_o \varepsilon_o} \qquad (4.6.2\text{-}22)$$

For the induction force between a charged spherical collector and an uncharged particle:

$$K_{E2} = \left(\frac{\varepsilon - 1}{\varepsilon + 2}\right) \frac{2\,C'\,d_p^2\,q_c^2}{3\,\mu_G\,u_o\,d_c\,\varepsilon_o} \qquad (4.6.2\text{-}23)$$

For the induction force between charged particles and uncharged spherical collector:

$$K_{E3} = \frac{C'\,q_p^2}{3\,\pi^2\,\mu_G\,d_p\,u_o\,\varepsilon_o\,d_c^2} \qquad (4.6.2\text{-}24)$$

For the case of the repulsion force exerted by unipolar charged particles on the aerosol particle being deposited:

$$K_{E4} = \frac{C'\,q_p^2\,d_c\,n}{18\,\pi\,\mu_G\,d_p\,u_o\,\varepsilon_o} \qquad (4.6.2\text{-}25)$$

For the attraction between a charged aerosol particle and a grounded collector which has a charge induced by the surrounding unipolar aerosol particles:

$$K_{E5} = \frac{C'\,q_p^2\,n\,b^2}{3\,\pi\,\mu_G\,d_p\,u_o\,d_c\,\varepsilon_o} \qquad (4.6.2\text{-}26)$$

In these equations, "q_p" is the charge on the aerosol particle in coulombs, "q_c" is the charge on the collector per unit area (coulomb/cm^2), ε_o = 8.85x10^{-21} coulomb/dyne-cm^2 is the absolute dielectric constant, "ε" is the dielectric constant of the aerosol particles; "u_o" is the relative velocity between air stream and collector, cm/sec; "n" is the aerosol concentration (# particles/volume), "b" cm is the radius of the spherical aerosol cloud which influences the collector.

Figures 4.6.2-7, 4.6.2-8 and 4.6.2-9 show the calculated collection efficiencies for various collection parameters. It should be noted that when an external force is employed, the collection efficiency may reach values greater than one.

In most cases only one of the five mechanisms is important. When the collector is maintained at a uniform charge and the aerosol particles are oppositely charged, the coulomb attraction forces represented by "K_{E1}" is dominant. On the other hand, when only the aerosol is charged, "K_{E2}" becomes dominant. The force represented by "K_{E3}" is small and in most cases can be neglected. The forces corresponding to "K_{E4}" and "K_{E5}" depend upon aerosol concentration and become important only at high aerosol concentrations ($n \gtrsim 10^7$), as is shown later in the case of bubbles.

Particle Charging

Commonly, aerosol particles are unipolarly charged by passing through a corona discharge section. Particles larger than ≈0.5 μm are charged mainly by field discharge mechanism and can be charged to a maximum charge called the saturation charge. Oglesby and Nichols (1970) calculate the saturation charge from,

$$q_{ps} = 12 \frac{\varepsilon}{\varepsilon + 2} \pi \varepsilon_o r_p^2 E_c \qquad (4.6.2\text{-}27)$$

where E_c is the strength of the charging electric field.

For particles smaller than ≈0.2 μm in diameter diffusion charging predominates. For this case the same authors give the following equation for the charge

$$q = \frac{r_p k T}{e} \ln \left(1 + \frac{\pi r_p \bar{v} N_o e^2 t}{k T} \right) \qquad (4.6.2\text{-}28)$$

where "e" is the electronic charge, "$\bar{v}$" is the rms thermal velocity of the ions and is given by

$$\bar{v} = \left(\frac{8 R_g T}{\pi M} \right)^{1/2} \qquad (4.6.2\text{-}29)$$

"M" is the molecular weight of the ions, "N_o" is the average number of molecules per unit volume, and "t" is time in sec. In this case there is no limiting charge, and the charge increases with exposure time.

In the intermediate range of particle sizes both charging mechanisms contribute significant charges. A third equation can be derived for this case by summing the rate of charging from both mechanisms.

Efficiency Computation

Approximate solutions for the equations of motion and collection efficiency may be obtained if only one term of the electrostatic force is considered and if interception is neglected, as was done by Kraemer and Johnstone (1955). For the collection of a charged aerosol by a charged collector, considering only the coulomb force:

$$\eta_E = -4 K_{E1} \qquad (4.6.2\text{-}30)$$

and for the collection of uncharged aerosol particles by a charged spherical collector considering only the induced charge on the particles:

$$\eta_E = \left(\frac{15}{8} \pi K_{E2}\right)^{0.4} \qquad (4.6.2\text{-}31)$$

Figure 4.6.2-10 shows the agreement between calculated and experimental results obtained by Kraemer and Johnstone (1955).

It should be noted that for maximum collection of aerosol particles by drops, both the particles and the drops should be highly charged. The equations show that collection by the electrostatic mechanism is enhanced with increased retention time in the dust collection equipment and with low relative velocities between the aerosol particles and the collecting drops.

4.6.2.6 Magnetic Collection

Magnetic effects can be included in the equations of particle motion in the same manner electrostatic forces were treated. Magnetic forces result when a magnetic particle is introduced into a magnetic field or close to a ferromagnetic metal, or when a particle is charged and then introduced into a magnetic field. The equation of motion, when solved, will give collection efficiency for different velocity distributions as a function of the magnetic dimensionless number.

4.6.2.7 Diffusiophoresis

Sparks and Pilat (1970) calculated collection efficiencies as a function of inertia parameter, K, for collection of particles on single drops due to inertial impaction and condensation. They made the following assumptions:

a. Interception is neglected [$r_p/r_d<<1$].
b. Every particle which hits the drop sticks to it.
c. Gas flow is potential.
d. Drag force on the particle is given by Stokes' Law.
e. Drop temperature change due to condensing vapor is zero.

The results of their calculations for water condensation, evaporation and equilibrium (no condensation and no evaporation), for dp/dx = $\pm 10^5$ mbar/cm, are presented in Figure 4.6.2-11. It can be seen from the figure that the effect of diffusiophoresis is greater for smaller particles and it decreases as the relative velocity of the droplet with respect to the gas increases.

4.6.3 COLLECTION BY CYLINDERS

Beds of cylindrical fibers are sometimes used for the collection of particles and liquid mists. Collection efficiency of a fiber bed can be predicted from the knowledge of collection efficiency of single fibers. Single fiber efficiency is defined in a manner parallel to sphere efficiency, namely the ratio of the area swept clean to the fiber cros-sectional area. Single fiber efficiency is treated in this section. Section 5.3.3 describes how single fiber efficiencies are used to calculate the overall collection efficiency of a bed of fibers. Fibers may capture particles by several mechanisms. Gravity, Brownian diffusion, electrostatic attraction, impaction and interception all may play a part. The efficiency of a single fiber due to the simultaneous influence of more than one collection mechanism will be covered in Section 5.3.3.

4.6.3.1 Impaction

As in the case of spheres, inertial collection by cylinders is a function of the impaction parameter and the flow regime, defined by the Reynolds number. The inertia parameter, K_p, for a single fiber is defined as:

$$K_p = \frac{C' \, d_p^2 \, \rho_p \, u_o}{9 \, \mu_G \, d_f} \qquad (4.6.3\text{-}1)$$

$$N_{Ref} = \frac{\rho_G \, u_o \, d_f}{\mu_G} \qquad (4.6.3\text{-}2)$$

When $N_{Ref} < 1$ the flow field around the cylinder can be approximated by assuming a viscous flow condition while for $N_{Ref} > 100$ the flow around the cylinder can be approximated by a potential flow (i.e. [illegible] fluid). Values between 1 and 100 represent transition conditions.

A number of theories have been developed to predict the particle collecting efficiency of single fibers due to impaction, including those of Sell (1931), Albrecht (1931), Langmuir and Blodgett (1946) Bosanquet (1950), Davies (1952), Glanert, Pearcey and Hill (1957), Das (1950), Hocking (1959, 1960), Pemberton (1960), Picknett (1960), and Walton and Woolcock (1960). However, no theories produce results completely compatible with experimental results.

Whitby (1965) has analyzed the data of Wong and Johnstone (1953), and developed a plot of single fiber efficiency due to impaction againstinertia parameter, with Reynolds number as parameter, Figure 4.3.6-1. This figure can be used for Reynolds numbers ranging from 150 to 0.2, infringing into both the turbulent and laminar regions. Note that 4.6.3-1 is plotted on log.-probability paper in order to straighten the lines.

4.6.3.2 Interception

Interception is important when particles are large relative to the fiber diameter. The significance of interception is a function of the interception parameter, "K_I".

$$K_I = \frac{d_p}{d_f} \qquad (4.6.3\text{-}3)$$

For particle collection in the laminar region, Torgeson gives:

$$\eta_I = 0.0518 \left(\frac{C_D \, N_{Ref}}{2}\right) K_I^{1.5} \qquad (4.6.3\text{-}4)$$

An alternate approach is given by Ranz (1953) who used a modification of Langmuir's (1942) viscous flow equation. Ranz and Wong (1952) give the collection efficiency due to interception in the turbulent region as:

$$\eta_I = 1 + K_I - \left(\frac{1}{1 + K_I}\right) \qquad (4.6.3\text{-}5)$$

4.6.3.3 Collection of Particles by a Fiber Due to Gravity

The efficiency of a single cylindrical fiber due to the gravitational settling of particles upon it, "η_G" may be significant for large particles and low gas velocities. Ranz and Wong (1952) give the following expression:

$$\eta_G = K_G = \frac{C' d_p^2 \rho_p g}{18 \mu_G u_o} \qquad (4.6.3\text{-}6)$$

Here "K_G" is a gravity parameter, equal to the settling velocity of the particle divided by the velocity of the gas stream flowing past the fiber. This equation applies when the flow past the fiber is laminar.

4.6.3.4 Collection of Particles by a Fiber Due to Brownian Diffusion

Particle collection by Brownian diffusion is of extreme importance for submicron particles, especially when gas velocities are low. Equations for the prediction of single fiber efficiency due to Brownian diffusion are usually a function of the Peclet number, which is a ratio of "bulk" or "gross" transport to "diffusive" transport:

$$N_{Pe} = \frac{u_o d_f}{D_p} = \frac{u_o d_f 3 \pi \mu_G d_p}{C' k T} \qquad (4.6.3\text{-}7)$$

where "d_f" is the diameter of the fiber.

Equations predicting the single fiber efficiency due to diffusion in the laminar region are given by several authors. The Torgeson expression is:

$$\eta_D = 0.75 \left(\frac{C_D N_{Ref}}{2}\right)^{0.4} (N_{Pe})^{-0.6} \qquad (4.6.3\text{-}8)$$

where "C_D" is the drag coefficient of a cylinder - a function of Reynolds number, "N_{Ref}", available in Perry's Handbook (1963) and elsewhere. Alternatively, "C_D" can be calculated using Lamb's equation for cylinders in the laminar region:

$$C_D = \frac{8 \pi}{N_{Ref} [2 - \ln (N_{Ref})]} \qquad (4.6.3\text{-}9)$$

Other equations for calculating the efficiency of single fibers due to particle diffusion in the laminar region are given by Bosanquet (1950), Davies (1952), Landt (1956), Langmuir (1942), Natanson (1957) and Ranz (1953).

4.6.3.5. Electrostatic Attraction

Kraemer and Johnstone (1955) have identified five types of electrostatic forces which may influence particle collection. These are covered in detail in Section 4.6.2.5. Lundgren (1962) and Whitby and Lundgren (1964) have shown that the only mechanism of importance in non-electrified fiber beds is the attractive force between a charged aerosol particle and its image in a collecting fiber. Lundgren has shown experimentally, that the collection efficiency due to this force can be expressed as:

$$\eta_E = 1.5\ (K_E)^{1/2} \qquad (4.6.3\text{-}10)$$

where "K_E" is the cylindrical analog of Equation 4.6.2-23, and is given by:

$$K_E = \frac{\left(\frac{\varepsilon - 1}{\varepsilon + 1}\right) q_p{}^2\ C'}{12\ \pi^2\ \varepsilon_o\ d_f{}^2\ \mu_G\ d_p\ u_o} \qquad (4.6.3\text{-}11)$$

4.6.4 COLLECTION OF PARTICLES BY BUBBLES

When an aerosol stream is bubbled through a liquid layer, collection of particles takes place. Different collectors have been devised to collect aerosol particles through bubbling. The simplest is a sieve plate column.

Particle surface properties have a large effect on particle collection by bubbles. Hydrophilic particles are collected much more easily than hydrophobic particles. The addition of surface active agents to the water decreases collection efficiency [Taheri (1967)]. An increase in water temperature reduces collection efficiency to practically zero at the boiling point, according to Remy, et al. (1926). This is due to repulsion of particles by the evaporating water. On the other hand, collection efficiency can be increased by bubbling hot aerosol saturated with water vapor through a cold liquid layer, as was shown by Rozen and Kostin (1967).

The same collection mechanisms which were previously described in the section on particle collection by drops, 4.6.2, will now be applied to collection by bubbles. Fuchs (1964) shows that collection due to gravitational settling of particles within a circulating bubble is minimal compared to collection by other mechanisms and will be neglected.

4.6.4.1 Inertial Collection

Two modes of inertial collection can be envisioned. One is the collection during bubble formation. The second is deposition during bubble rise due to gas and particle circulation inside the bubble. Taheri and Calvert (1968) showed that in a sieve plate column when both mechanisms are involved, most of the inertial collection is due to the first mode; i.e.: most inertial collection takes place while the bubble is being formed. They described the collection as a jet impacting on a semispherical dome which continuously changes its shape until a bubble is formed. Collection occurs due to the centrifugal deposition of the particles on the bubble's wall.

In deriving the collection equation they made the following assumptions:

1. The particles obey Stokes' Law.

2. The air flow from the jet is divided into eddies confronting the inner face of the bubble.

3. The tangential velocity of the air flowing at the bubble wall remains constant and is equal to the jet velocity.

4. Particle mixing occurs continuously through the flow path.

Based upon these assumptions they derived for the collection efficiency by inertial impaction during bubble formation:

$$\eta_{bp} = 1 - \exp -(a\ K_p) \tag{4.6.4-1}$$

where "a" is an empirical constant and "K_p" is the inertia parameter"

$$K_p = \frac{2\ \rho_p\ r_p^2\ v_h\ C'}{9\ \mu_G\ r_h} \tag{4.6.4-2}$$

"r_h" is the perforation radius and "v_h" is the gas velocity through the perforation.

"F", the foam density, is defined as the ratio of the clear liquid height, 1, to the total foam height, "h". Clear liquid height, 1, is the height of liquid flowing over the plate when no gas is passed through the plate. Total foam height, h, is the height of the bubbling liquid over the plate when gas is passed through it. For sieve plates Taheri and Calvert found "a" to be a function of foam density, "F". Within the limits $0.35 < F < 0.65$:

$$a = 40\ F^2 \tag{4.6.4-3}$$

Equation 4.6.4-1 describes the collection efficiency of hydrophilic aerosols. For hydrophobic aerosols experimental results should be used.

For the case of inertial collection due to gas and particles circulating inside a bubble, which has already been formed and is rising, Fuchs (1964) derived an equation for the collection efficiency making the following assumptions:

1. The bubbles are spherical with $50\mu m < r_b < 10^3 \mu m$ and $1 < N_{Reb} < 700$ and the rate of circulation at the bubble surface is given by:

$$u_{tg} = 1.5\ v_b \sin\Theta \tag{4.6.4-4}$$

2. Inertial deposition is due to centrifugal force. Here, "u_{tg}" is the tangential velocity of the rotating gas within the bubble, evaluated at the bubble surface, "v_b" is the bubble's rise velocity, and "Θ" is the angle between the bubble's vertical axis and the line connecting the bubble center with the point where the velocity measurement is made. This equation applies to bubble diameter from 50 to 1,000 μm.

Fuchs (1964) obtains for the number of particles deposited on the bubble per unit height of bubble rise, ϕ_1:

$$\phi_1 = \frac{\pi\ v_b\ n\ d_p^2\ \rho_p\ r_b\ C'}{3\ \mu_G} \tag{4.6.4-5}$$

In this equation "v_b" and "r_b" are the vertical velocity and the radius of the bubble, respectively, and "n" is the number of aerosol particles per cm^3.

4.6.4.2 Collection by Diffusion

Collection by diffusion takes place inside the bubble during its rise and is enhanced by the air circulation inside the bubble. The inside mass transfer coefficient of the bubble (the gas phase coefficient) can be described in terms of Higbie's Penetration Theory (1935) and might be used to estimate particle transfer by analogy (see Section 4.5.2).

$$\frac{dc}{dt} = \frac{-6}{r_b} \left(\frac{D_p}{\pi \ \tau} \right)^{1/2} c \tag{4.6.4-6}$$

where "r_b" is the bubble radius, "D_p" the particle diffusivity and "τ" the renewal time. "τ" can be calculated:

$$\tau = \frac{\pi^2 \ r_b}{3 \ v_b} \tag{4.6.4-7}$$

Substituting and integrating gives:

$$\ln \frac{c_e}{c_i} = \frac{-6}{r_b} \left(\frac{3 \ D_p \ v_b}{\pi^3 \ r_b} \right)^{1/2} t \tag{4.6.4-8}$$

For a foam column of height "h" the bubble residence time is:

$$t = \frac{h}{v_b} \tag{4.6.4-9}$$

The collection efficiency is therefore:

$$\eta_D = 1 - \exp - \left[\frac{6}{\pi} \ h \left(\frac{3 \ D_p}{\pi \ r_b^3 \ v_b} \right)^{1/2} \right] \tag{4.6.4-10}$$

When collection efficiency of a bubble is plotted vs. particle diameter one gets a minimum at the diameter where particles are too small for collection by inertia but too big for collection by diffusion. It is interesting to study what influences this minimum. To do this one can write the penetration equation for both mechanisms, by combining Equations 4.6.4-1 and 4.6.4-10 to get:

$$\ln \frac{c_e}{c_i} = - \frac{80 \ F^2 \ \rho_p \ v_h}{9 \ \mu_G \ r_h} (r_p^2 + 1.26 \ \lambda \ r_p) - \frac{0.43 \ h}{r_b} \left[\frac{k \ T}{r_b \ \mu_G \ v_b} \left(\frac{r_p + 1.26 \ \lambda}{r_p^2} \right) \right]^{1/2} \tag{4.6.4-11}$$

For $d_p > 0.2$ μm we can neglect the exponential term in the Cunningham correction factor. The highest penetration is when $\ln(c_e/c_i)$ is maximum. Differentiating with respect to "r_p", setting the equation to zero, and rearranging we get

$$\frac{r_p^2\ (2\ r_p + 1.26\ \lambda)\ (r_p + 1.26\ \lambda)^{1/2}}{r_p + 2.52\ \lambda} = \frac{0.0242\ r_h\ h^3}{r_b\ \ell^2\ \rho_p\ v_h}\left(\frac{\mu_G\ k\ T}{r_b\ v_b}\right)^{1/2}$$

(4.6.4-12)

It appears from this equation that changing the column and operating parameters will shift the particle size which is collected least efficiently. Figure 4.6.4-1 shows the effect of changing foam height in an air water system on the maximum penetration diameter, with all other parameters kept constant. (v_h = 1220 cm/sec; d_h = 0.32 cm; d_b = 0.66 cm; $\lambda = 5.9\times10^{-6}$ cm; ρ_p = 1 g/cm^3; T = 0°C; v_b = 24 cm/sec). Increasing foam height from 10 to 30 cm shifts the maximum penetration diameter from 0.2 μm to 0.7 μm. The change in collection efficiency with change in foam height is shown in Figure 4.6.4-3. For lower foam heights collection by the inertia mechanism is more important for particles larger than about 0.1 μm. As a result there is an increase in maximum penetration diameter with increase in foam heights and predominancy of diffusion collection mechanisms at larger particle sizes. Figure 4.6.4-2 shows the effect of increasing perforation diameter on maximum penetration diameter keeping the percent free area of the sieve plate constant (d_b = 0.66 cm; $\lambda = 5.9\times10^{-6}$ cm; ρ_p = 1 g/cm^3; T = 0°C; v_b = 24 cm/sec). Higher perforation diameters give higher maximum penetration diameters.

4.6.4.3 Collection of Particles by Bubbles Due to Combined Effect of Electrostatic and Inertial Forces after Bubble Formation

Consider a system where particles larger than ≈0.3μm in diameter are charged electrically and introduced inside a bubble. During bubble rise the particles will be collected on the bubble's wall due to two forces - the centrifugal force caused by the gas circulating inside the bubble and the electric field force formed by the space charge inside the bubble. To derive an equation predicting the collection efficiency, the derivation of Faith et al. (1967) will be followed.

Consider a system of monodisperse, unipolar, spherical particles in air. Each particle has been charged to a uniform charge "q_p".. The aerosol of original concentration "c_i" is introduced to an already formed, rising bubble of radius "r_b". The bubble rises in a grounded conducting liquor so that zero potential exists at $r = r_b$. Assume redistribution of aerosol particles inside the bubble, so that particle concentration inside the bubble is uniform at all times. Fuchs (1964) has theoretically and experimentally proven this to be the actual case. The charge on the particles is retained throughout the time of bubble rise resulting in a constant particle electrical mobility, "B_E", for each particle. The change in concentration of the particles is given by:

$$\frac{dn}{dt} = -\frac{3\ N_p}{r_b} \qquad (4.6.4\text{-}13)$$

where "N_p" is the particle flux at the bubble wall. If the flux is assumed to be due to centrifugal deposition and electrostatic migration only, then:

$$N_{pC+E} = N_{pC} + N_{pE} \tag{4.6.4-14}$$

where "N_{pC}" is the flux due to the centrifugal force and "N_{pE}" is the flux due to the electric field.

Equation 4.6.4-5 stated that the number of particles removed per unit height of bubble rise would be:

$$\phi_1 = \frac{\pi\, v_b\, n\, d_p^{\,2}\, \rho_p\, r_b\, C'}{3\, \mu_G} \tag{4.6.4-5}$$

To convert to particle flux at the bubble wall "N_{pC}", one should multiply by bubble velocity and divide by bubble surface area:

$$N_{pC} = \frac{\phi_1\, v_b}{4\, \pi\, r_b^{\,2}} = \frac{v_b^{\,2}\, n\, d_p^{\,2}\, \rho_p\, C'}{12\, \mu_G\, r_b} \tag{4.6.4-15}$$

$$\frac{dn}{dt} = -\frac{3}{r_b} N_{pC} = -\frac{v_b^{\,2}\, d_p^{\,2}\, \rho_p\, C'}{4\, \mu_G\, r_b}\, n = -\alpha\, n \tag{4.6.4-16}$$

The flux due to the space charge is calculated from Gauss' law:

$$\nabla \cdot E = -\nabla^2 \phi = \frac{q_p\, n}{\varepsilon_o} \tag{4.6.4-17}$$

The velocity vector of a particle in an electric field of an intensity "E" is:

$$\bar{v} = B_E\, E \tag{4.6.4-18}$$

where "B_E" is the electrical mobility given by

$$B_E = \frac{D'\, q_p}{6\, \pi\, \mu_G\, r_p} \tag{4.6.4-19}$$

Substituting we get: $\nabla \cdot \bar{v} = \dfrac{B_E\, q_p\, n}{\varepsilon_o}$ (4.6.4-20)

The divergence of the particle velocity is defined by

$$\nabla \cdot \bar{v} = -\frac{1}{n}\frac{dn}{dt} \tag{4.6.4-21}$$

Combining Equations 4.6.4-20 and 4.6.4-21 we get

$$\frac{dn}{dt} = \frac{B_E\, q_p}{\varepsilon_o}\, n^2 = -\beta\, n^2 \tag{4.6.4-22}$$

Substituting Equation 4.6.4-22 into 4.6.4-13, one determines that the flux due to the electric field, "N_{pE}" will be:

$$N_{pE} = \frac{rb}{3} \beta n^2 \qquad (4.6.4\text{-}23)$$

Combining Equations 4.6.4-16 and 4.6.4-23 with 4.6.4-14, substituting them all into 4.6.4-13, one finds that:

$$\frac{dn}{dt} = - \alpha n - \beta n^2 \qquad (4.6.4\text{-}24)$$

Boundary conditions are:

$n = n_i$ at $t = 0$ and $n = n_e$ at $t = \frac{h}{v_b}$

$$\int_{n_i}^{n_e} \frac{dn}{\alpha n + \beta n^2} = - \int_{0}^{h/v_b} dt \qquad (4.6.4\text{-}25)$$

The overall collection efficiency of a bubble during its rise due to the combined effect of inertial and electrostatic force will be therefore:

$$\eta_{bp+E} = 1 - \frac{n_e}{n_i} = 1 - \frac{\exp\left(-\frac{\alpha h}{v_b}\right)}{\left(\frac{\alpha + \beta n_i}{\alpha + \beta n_e}\right)} \qquad (4.6.4\text{-}26)$$

The saturation charge a particle can acquire by field discharge mechanism is given by Equation 4.6.2-26:

$$q_{ps} = 3 \frac{\varepsilon}{\varepsilon + 2} \pi \varepsilon_o d_p^2 E_c \qquad (4.6.4\text{-}27)$$

For conducting particles, the dielectric constant "ε" is large. The particle saturation charge becomes:

$$q_{ps} = 3 \pi d_p^2 E_c \varepsilon_o \qquad (4.6.4\text{-}28)$$

After substituting Equation 4.6.4-28 into 4.6.4-26 one obtains the expanded expression:

$$\eta_{bE+P} = 1 - \left\{ \frac{\exp\left[- \frac{v_b d_p^2 \rho_p C' h}{4 \mu_G r_b^2}\right]}{\left(\frac{v_b^2 \rho_p + 12 \pi r_b^2 d_p E_c^2 \varepsilon_o n_i}{v_b^2 \rho_p + 12 \pi r_b^2 d_p E_c^2 \varepsilon_o n_e}\right)} \right\} \qquad (4.6.4\text{-}29)$$

Equation 4.6.4.29 has been solved for 0.2, 0.5 and 2 μm radius particles charged to saturation by an electric field, E_c, of strengths 1, 3, and 6 kV/cm. Figures 4.6.4-4, 4.6.4-5, and 4.6.4-6 depict collection efficiency for the smaller size particles as a function of particle inlet concentration and charging field strength. For the 2 μm particles, penetration $P_t = 1 - E$ is plotted, rather than collection efficiency, because of the extremely high collection. Equation

4.6.4-29 has been solved by a trial and error method. The iteration was stopped when the difference between "η_{pE+p}" assumed and "η_{pE+p}" calculated was smaller than 1%. For the high efficiencies of the 2μm radius the iteration was stopped when the difference in collection efficiencies was smaller than 10^{-5}.

4.6.4.4 Collection of Particles by Rising Bubbles Due to the Combined Effect of Diffusion, Diffusiophoresis and Thermophoresis

Consider a system where an aerosol with particles smaller than ≈0.3μm in diameter is introduced inside a bubble which is already rising. In this case, it will be assumed that the particles are collected on the bubble's wall due to three mechanisms only: diffusion, diffusiophoresis and thermophoresis. Collection by inertia will be neglected, due to the small size of the particles under consideration. Particle collection during bubble formation is also to be neglected. To evaluate collection efficiency, consider a monodisperse spherical aerosol in air saturated with water vapor. Assume also that particle size does not increase during bubble rise.

The aerosol and gas enter the bubble at a temperature "T_i" and saturation vapor pressure "p_{vi}" and leave at temperature "T_e" (which is almost the same as the liquid temperature "T") and saturation pressure "p_{ve}". The air in the bubble is assumed saturated with water vapors all the time. Assume redistribution of aerosol particles inside the bubble so that particle concentration is uniform. The overall aerosol flux is assumed due to the three fluxes associated with the forces mentioned above,

$$N_{(pD + pDP + pT)} = N_{pD} + N_{pDP} + pT \qquad (4.6.4\text{-}30)$$

The rate of particle collection in a bubble by diffusion can be determined by substituting Equation 4.6.4-7 into 4.6.4.6. One finds:

$$\frac{dn}{dt} = -\left[\frac{6}{\pi\, r_b}\left(\frac{3\, D_p\, v_b}{\pi\, r_b}\right)^{1/2}\right] n \qquad (4.6.4\text{-}31)$$

Recalling: $\frac{dn}{dt} = -\frac{3\, N_p}{r_p}$ (4.6.4-13)

The particle flux due to diffusion will be:

$$N_{pD} = \frac{2\, n}{\pi}\left(\frac{3\, D_p\, v_b}{\pi\, r_b}\right)^{1/2} \qquad (4.6.4\text{-}32)$$

To calculate the thermal flux, proceed as follows. The velocity due to temperature gradient between the aerosol and the liquid can be approximated by the Epstein (1929) equation:

$$u_{pT} = \frac{3\, k_G\, \mu_G\, C'}{2\,(2\, k_G + k_p)\, \rho_G\, T}\, \nabla T$$

If a linear temperature gradient inside the bubble is assumed varying only in the radial direction:

$$u_{pT} = \frac{3\ k_G\ \mu_G\ C'}{2\ (2\ k_G + k_p)\ \rho_G\ T} \left(\frac{\Delta\ T}{r_b}\right) \qquad (4.6.4\text{-}33)$$

The effective temperature difference can be calculated from the heat transfer between the gas in the bubble and liquid outside it.

$$h'\ 4 \quad r_b^2\ \Delta\ T = \frac{4}{3}\ \pi\ r_b^3\ \rho_G\ C_p\ (T_i - T_e)\ \frac{v_b}{h} \qquad (4.6.4\text{-}34)$$

where "h'" is the heat transfer coefficient and "C_p" is the gas specific heat.

$$\Delta T = \frac{r_b\ \rho_G\ C_p\ v_b}{3\ h'\ h}\ (T_i - T_e) \qquad (4.6.4\text{-}35)$$

Substituting for "ΔT" into Equation 4.6.4-34 and taking the aerosol temperature, T, as the average between "T_i" and "T_e" one finds that:

$$u_{pT} = \frac{C'\ k_G\ \mu_G\ C_p\ v_b}{(2\ k_G + k_p)\ h'\ h} \left(\frac{T_i - T_e}{T_i + T_e}\right) \qquad (4.6.4\text{-}36)$$

To calculate the flux, assume that because of air circulation patterns inside the bubble, deposition is small at the polar regions since there the streamlines move away from the surface and confine calculations to the region from 45° above to 45° below the equator, i.e. π/4 to 3π/4, as observed by Fuchs (1964). The element of volume cleaned per second due to thermophoresis, V, can be calculated:

$$dV = (\ 2\ \pi\ r_b\ u_{tg}\ \sin\ \Theta\ )\ v_T\ dt \qquad (4.6.4\text{-}37)$$

Note that: $$dt = \frac{r_b\ d\Theta}{u_{tg}} \qquad (4.6.4\text{-}38)$$

where "u_{tg}" is the gas stream (and particle) tangential velocity. Thus

$$\Delta\ V = \int_{\pi/4}^{3\pi/4} 2\ \pi\ r_b^2\ v_T\ \sin\ \Theta\ d\Theta = 2\ \sqrt{2}\ \pi\ r_b^2\ v_T \qquad (4.6.4\text{-}39)$$

The number of particles per volume removed in unit time by the thermophoretic forces is:

$$\frac{dn}{dt} = \frac{\Delta\ V\ n}{\frac{4}{3}\ \pi\ r_b^3} = -\ \frac{3\ \sqrt{2}\ C'\ k_G\ \mu_G\ C_p\ v_b}{2\ (2\ k_G + k_p)\ h\ h'\ r_b} \left[\frac{T_i - T_e}{T_i + T_e}\right] n \qquad (4.6.4\text{-}40)$$

The particle flux due to thermophoresis is:

$$N_{pT} = \frac{\sqrt{2}\ C'\ k_G\ \mu_G\ C_p\ v_b}{2\ (2\ k_G + k_p)\ h\ h'} \left(\frac{T_i - T_e}{T_i + T_e}\right) n \qquad (4.6.4\text{-}41)$$

The diffusiophoresis flux shall be calculated in a similar manner. The diffusiophoretic velocity of particles in a dilute vapor system was shown by Goldsmith and May (1966) to be:

$$u_{pDP} = \frac{-\sqrt{M_V}}{\frac{p_V}{P}\sqrt{M_V} + \left(\frac{P - p_V}{P}\right)\sqrt{M_G}} \left(\frac{D_p}{P - p_V}\right) \nabla \; p_V$$

The vapor pressure gradient can be estimated from the Maxwell condensation flux equation:

$$-\frac{D_p \; M_V}{Rg \; T} \nabla \, p_V = \frac{r_b \; v_b}{3 \; h} (\rho_{Vi} - \rho_{Ve}) \tag{4.6.4-42}$$

or:

$$\nabla \, p_V = -\frac{r_b \; v_b}{3 \; h \; D_p} (p_{Vi} - p_{Ve}) \tag{4.6.4-43}$$

Here, "Rg" is the gas constant. Now, assume that a representative average "p_V" can be obtained from:

$$p_V = \frac{p_{Vi} + p_{Ve}}{2} \tag{4.6.4-44}$$

Substituting Equations 4.6.4-43 and 4.6.4-44 into the Goldsmith and May Equation one obtains:

$$u_{pDP} = \left[\frac{2 \; P \sqrt{M_V}}{(p_{Vi} + p_{Ve}) \sqrt{M_V} + [2 \; P - (p_{Vi} + p_{Ve})] \sqrt{M_G}}\right] \frac{r_b \; v_b}{3 \; h} \left[\frac{p_{Vi} - p_{Ve}}{p - \left(\frac{p_{Vi} + p_{Ve}}{2}\right)}\right] \tag{4.6.4-45}$$

Again applying Equation 4.6.4-39 and 4.6.4-13, remembering that $v = v_{TP}$, one finds:

$$N_{pDP} = \frac{\sqrt{2} \; P \sqrt{M_V}}{(p_{Vi} + p_{Ve}) \sqrt{M_V} + [2 \; P - (p_{Vi} + p_{Ve})] \sqrt{M_V}} \left(\frac{r_b \; v_b}{3 \; h}\right) \left[\frac{p_{Vi} - p_{Ve}}{P - \left(\frac{p_{Vi} + p_{Ve}}{2}\right)}\right] n \tag{4.6.4-46}$$

The total particle flux due to diffusion, thermophoresis and diffusiophoresis is found by substituting Equations 4.6.4-32, 4.6.4-41, and 4.6.4-46 into 4.6.4-30. Applying Equation 4.6.4-13 finds that:

$$- \frac{dn}{dt} = \frac{6}{\pi \, r_b} \left(\frac{3 \, D_p \, v_b}{r_b} \right)^{1/2} n + \left[\frac{3 \sqrt{2}}{2} \, \frac{C' \, k_G \, \mu_G \, C_p \, v_b}{(2 \, k_G + k_p) \, h \, h' \, r_b} \right] \left(\frac{T_i - T_e}{T_i + T_e} \right) n +$$

$$+ \sqrt{2} \left[\frac{P \quad M_V}{(p_{Vi} + p_{Ve}) \sqrt{M_V} + [2 \, P - (p_{Vi} + p_{Ve}) \quad M_V} \right]$$

$$\left(\frac{v_b}{h} \right) \left[\frac{p_{Vi} + p_{Ve}}{P - \left(\frac{p_{Vi} + p_{Ve}}{2} \right)} \right] n \qquad (4.6.4\text{-}47)$$

Boundary conditions are $h = h_i$ at $t = 0$, and $h = h_e$ at $t = h/v_b$. Integrating and simplifying yields, for the overall collection efficiency in a bubble through diffusion, thermophoresis and diffusiophoresis:

$$\eta_{bD,T,DP} = 1 - \frac{n_e}{n_i} = 1 - \exp - \left\{ \frac{6 \, h}{\pi \, r_b} \left(\frac{3 \, D_p}{\pi \, r_b \, v_b} \right)^{1/2} + \right.$$

$$+ \frac{\frac{3}{2} \sqrt{2} \, C' \, k_G \, \mu_G \, C_p}{(2 \, k_G + k_p) \, h' \, r_b} \left(\frac{T_i - T_e}{T_i + T_e} \right) +$$

$$\left. + \left[\frac{\sqrt{2} \, P \sqrt{M_V}}{(p_{Vi} + p_{Ve}) \sqrt{M_V} + [2 \, P - (p_{Vi} + p_{Ve})] \sqrt{M_G}} \right] \left[\frac{p_{Vi} - p_{Ve}}{P - \left(\frac{p_{Vi} + p_{Ve}}{2} \right)} \right] \right\} \qquad (4.6.4\text{-}48)$$

It is interesting to check Equation 4.6.4-48 with experimental results. Rozen and Kostin (1967) ran an experiment in which they introduced an oil mist with an average particle diameter of 0.3μm into a sieve plate column. The column consisted of eight plates. The water on plates number 1, 3, 5, and 7 was kept at a constant predetermined elevated temperature while the water temperature on plates 2, 4, 6, and 8 was kept at 20°C. The aerosol was introduced into plate no. 1 and came out of the column after leaving plate no. 8. The measured collection efficiency on plates 2 and 8 as a function of warm plate temperature and the calculated collection efficiency (Equation 4.6.4-48) are plotted in Figure 4.6.4-7. One can see that the collection efficiency on plate no. 8 in most cases is much higher than the efficiency measured on plate no. 2. It is interesting to note that for plates 2 and 8 Equation 4.6.4-48 describes the collection efficiency adequately up to a temperature difference of 30°C. The agreement of calculated and measured efficiencies is much better on plate no. 2. But when the temperature difference is high, and especially when more than one plate is available for collection, the deviation from the calculated results increases. Two facts are probably responsible for this. The first and most important is particle growth due to steam condensation on the particles. An increase in particle diameter will increase collection by inertial impaction. The second reason is that oil is an hydrophobic aerosol. Slight condensation of water vapors on oil drops will turn it hydrophilic and increase collection efficiency markedly [Taheri and Calvert (1968)].

4.6.4.5 Condensation on Particles

It is impossible to predict exact particle sizes and particle size distribution resulting from vapor condensation, when an aerosol saturated with vapors passes through cold liquid in a sieve plate column, since part of the vapor will condense on the bubble wall and part may condense spontaneously on the particles or form homogeneous drops. Nevertheless, a rough estimate can be obtained from the total quantity of condensed vapors, when inlet and outlet humidities are known. The quantity condensed is:

$$\Delta Y' = \frac{[H_i' - C_{si} (t_i - t_o)] - [H_e' - C_{se} (t_e - t_o)]}{\Delta H_{vo}} \qquad (4.6.4\text{-}49)$$

"Y'" and "H'" are the gas absolute humidity in kg water/kg dry gas and the gas enthalpy in kcal/kg dry gas, "t" is the temperature, "C_s" is the specific heat of the mixture, "ΔH_v" is the vapor's heat of vaporization and the subscripts, "i", "e" and "o" refer to entering, leaving and reference conditions.

Litvinov (1967) has evaluated the three ways in which condensing steam effects the capture of fine particles, namely: diffusiophoresis, particle growth and changes in surface properties. For the conditions which he assumed, very low partial pressure gradient, hydrophobic particles, etc., the changes in surface properties contributed most toward increase in collection efficiency. He found experimentally that for effective removal of hydrophobic particles of apatite dust the optimum water film thickness covering the particle was 0.1μm while in the case of ≈1μm active carbon black the optimum film thickness was 0.5μm. The difference stems from the greater surface roughness of the carbon which led to adsorption of some of the condensed water by the extended surfaces. Knowing the nominal optimum thickness of the water film one can calculate the minimum amount of condensed moisture at which the maximum degree of removal is attained, from:

$$\Delta Y' = \frac{C\ [(\bar{r}_p + \delta)^3 - \bar{r}_p^{\,3}]}{r_p^{\,3}\ \rho_p\ \Psi} \qquad (4.6.4\text{-}50)$$

where "C" is the weight concentration of the dust entering the control device, $r_{av} = 1/2\ \sqrt{\Sigma\ n_i\ d_i^{\,2}/\Sigma n_i}$, "$n_i$" is the number of particles of diameter "d_i" and "Ψ" is a coefficient which takes into account the amount of moisture not condensing on the aerosol particles.

Rozen and Kostin (1967) found experimentally that for oil mist:

$$E = 1 - 12.5\ q^{-0.56} \qquad (4.6.4\text{-}51)$$

where "E" is the collection efficiency for a single plate and "q" is the number of grams of steam condensed on the plate per gram of particles.

Litvinov (1967), Demshin and Ermakov (1967), Rozen and Kostin (1967) and others studied the effect of vapor condensation on the collection of small particles in sieve plate columns. They all concluded that the more vapors condense per plate, the higher the collection efficiency. The increase in collection efficiency is more pronounced in hydrophobic than in hydrophilic particles. Demshin and Ermakov (1965) measured a decrease in pressure drop per plate of 25 - 30% when steam was added to the aerosol. They attribute the decrease in pressure drop to a decrease in foam height and surface tension. Rozen and Kostin (1967) measured an increase in collection efficiency per plate when more than one plate is used and the collection efficiency on the higher plates was better than on the lower plates when the aerosol entered from the bottom. In general the farther the plate from the aerosol entrance, the higher its collection efficiency.

4.6.5 DEPOSITION FROM A MOVING AEROSOL IN PIPES AND DUCTS

Aerosol particles will deposit on surfaces of pipes and ducts for a variety of reasons. Here, deposition from a moving stream of aerosol due to molecular and turbulent diffusion will be discussed. Deposition due to other mechanisms such as sedimentation, impingement, or thermophoresis can be superimposed on the deposition due to molecular and turbulent diffusion.

Many authors [Friedlander and Johnstone (1957); Owen (1960); Schmel and Schwendiman (1963); Davies (1966b) Davies (1965); Davies (1966a) Soo (1967)] have derived equations describing particle deposition under various flow conditions. In this section the derivations presented by Davies (1966c)will be followed, since they are easiest to use and most complete.

4.6.5.1 Diffusive Deposition of Fine Particles in Laminar Flow

For fine particles flowing through a pipe in a laminar flow, deposition takes place by diffusion. An order-of-magnitude value for particle deposition can be obtained if one assumes that particle concentration is maintained at "c_i" at the edge of the diffusion boundary layer, and decreases linearly to zero at the absorbing surface. Under such conditions, the rate of deposition per unit area (particle flux at the surface) is:

$$N_{pD} = D_p \frac{c_i}{\delta_d} \qquad (4.6.5\text{-}1)$$

The thickness of the diffusion boundary layer, δ_d, depends upon the flow regime. For diffusion across the parabolic velocity profile of Poiseuille flow ($N_{ReG} \leq 2000$) to a perfectly absorbing pipe wall, the ratio of the outlet to the inlet concentrations is:

$$\frac{c_e}{c_i} = 0.819 \exp(-14.6272\ \Delta) + 0.0976 \exp(-89.22\ \Delta) + + 0.01896 \exp(-212\ \Delta) \qquad (4.6.5\text{-}2)$$

where:

$$\Delta = \frac{D_p\ \ell\ \rho_G}{\mu_G\ N_{ReG}\ d_p} \qquad (4.6.5\text{-}3)$$

The gas Reynold's number can be found from:

$$N_{ReG} = \frac{u_o \rho_G d_t}{\mu_G} \qquad (4.6.5\text{-}4)$$

where "d_t" is the diameter of the tube through which the gas flows. The particle penetration, c_e/c_i, is a function of the diffusional parameter "Δ" is shown in Figure 4.6.5-1.

4.6.5.2 Diffusion of Small Particles Through a Turbulent Boundary Layer

As a second case, consider deposition of fine particles ($d_p < 0.3\mu m$) in a turbulent flow. The velocity gradient at the surface in a turbulent boundary layer is steeper than in a laminar layer. The rate of diffusion is enhanced because the concentration at the outer part of the much thinner diffusion layer is held near the main stream concentration by eddy diffusion through the center part of the tube.

For turbulent flow through pipes:

$$2 \pi r_t \tau_o = \pi r_t^2 \frac{dP}{d\ell} \qquad (4.6.5\text{-}5)$$

where "r_t" is the pipe's radius, "τ" is the tangential shear stress on the pipe surface, and $dP/d\ell$ is the pressure drop gradient along the pipe. The "friction velocity", u_*, is defined by:

$$u_* = \left(\frac{\tau_o}{\rho_G}\right)^{1/2} = \left(\frac{r_t \; dP}{2 \rho_G \; d\ell}\right)^{1/2} \qquad (4.6.5\text{-}6)$$

and a dimensionless velocity is defined as:

$$\tilde{u} = \frac{u}{u_*} \qquad (4.6.5\text{-}7)$$

The length "y" measured normal to the pipe surface is made dimensionless by defining

$$\tilde{Y} = \frac{Y u_*}{\nu} \qquad (4.6.5\text{-}8)$$

The boundary layer, in a fully developed turbulent flow, is divided into three sub-layers: the laminar sublayer $\tilde{Y} < 5$; the buffer layer $5 < \tilde{Y} < 30$; and the main boundary layer $\tilde{Y} > 30$. The velocity and eddy diffusivity have been shown experimentally to be:

$$\tilde{u} = \tilde{Y} \text{ and } \frac{\varepsilon_p}{\nu} = \left(\frac{\tilde{Y}}{14.5}\right) \text{ for } \tilde{Y} < 5 \qquad (4.6.5\text{-}9)$$

$$\tilde{u} = 5 + 5 \ln \frac{\tilde{Y}}{5} \text{ and } \frac{\varepsilon_p}{\nu} = \frac{\tilde{Y}}{5} - 0.96 \text{ for } 5 < \tilde{Y} < 30 \qquad (4.6.5\text{-}10)$$

$$\tilde{u} = 4 + 6.75 \ln \tilde{Y} \text{ and } \varepsilon_p >> \nu \text{ for } \tilde{Y} > 30 \qquad (4.6.5\text{-}11)$$

where "ε_p" is the particle's eddy diffusivity, assuming an analogy between particle and momentum transfer. The flux of particles through the boundary layer is:

$$N_{pD+\varepsilon} = (D_p + \varepsilon_p)\frac{dc}{dY} \qquad (4.6.5\text{-}12)$$

Now define the velocity of deposition, $v_{pD+\varepsilon}$, as:

$$v_{pD+\varepsilon} = \frac{N_{pD+\varepsilon}}{c_i} \text{ and } \tilde{v} = \frac{v_{pD+\varepsilon}}{u_*} \qquad (4.6.5\text{-}13)$$

In the laminar sublayer,

$$\tilde{v} = \left(\frac{D_p}{\nu} + \frac{\varepsilon_p}{\nu}\right)\frac{d\tilde{c}}{d\tilde{Y}} = \left[\frac{D_p}{\nu} + \left(\frac{\tilde{Y}}{14.5}\right)^3\right]\frac{d\tilde{c}}{d\tilde{Y}} \qquad (4.6.5\text{-}14)$$

Integrating and assuming the concentration at the edge of the boundary layer to be the same as the main stream concentration, i.e.:

$$\tilde{c} = \frac{c}{c_i} = 1 \text{ at } \tilde{Y} = 5 \qquad (4.6.5\text{-}15)$$

one obtains:

$$\tilde{v} = \frac{\left(\frac{D_p}{\nu}\right)^{2/3}}{14.5\left[\frac{1}{6}\ln\frac{(1+\phi_5)^2}{1-\phi_5+\phi_5{}^2} + \frac{1}{\sqrt{3}}\arctan\frac{2\phi_5 - 1}{\sqrt{3}} + \frac{\pi}{6\sqrt{3}}\right]} \qquad (4.6.5\text{-}16)$$

where:

$$\phi_5 = \frac{1}{2.9\left(\frac{D_p}{\nu}\right)^{1/3}} \qquad (4.6.5\text{-}17)$$

In order to find "v" it is necessary to know "u_*" which depends on the degree of turbulence and the roughness of the surface. It is recommended to calculate "u_*" from experimental values of $dp/d\ell$ rather than calculate it from the Fanning friction factor without experimental determination of the actual pipe roughness.

Table 4.6.5-1 compares the velocity of deposition of particles and molecular diffusion of gases, assuming $D_G = 0.15$ (cm²/sec) and $\nu = 0.15$ (cm²/sec). We see the very slow rate of particle deposition, which decreases with increasing particle size.

4.6.5.3 Inertial Deposition from Turbulent Flow

The previous section showed that the rate of deposition of small particles from a turbulent boundary layer due to eddy diffusion followed by molecular diffusion is negligible. This conclusion is only true if the particles are small enough to follow the turbulent fluctuations of fluid motion. It does not hold when the inertia of the particles is sufficient to travel some distance independently. Particles with a stopping distance comparable to the thickness of the laminar sublayer can be projected through the sublayer to the surface. According to the size of the particle and the degree of turbulence, the stopping distance can vary from zero to larger than the radius of the pipe. It is therefore not convenient to break the boundary layer into laminar and transition layers since particles which have appreciable inertia

TABLE 4.6.5-1

Diffusion Through Turbulent Boundary Layer
[C.N. Davis (1966)]

Particle Radius (μ)	$\tilde{v} = \frac{v}{u_*}$
0.001	0.019
0.01	0.0056
0.1	0.000034
1	0.0000052
Gas	
(D_G = 0.15 cm^2/sec)	0.069

are able to short circuit the last and slowest stage of the diffusion transport.

In a turbulent flow with small eddies, as is encountered in pipes, radial diffusion is described by the Fokker-Planck equation which resembles the Fick equation except that the radial eddy diffusion coefficient, ε, decreases rapidly as the surface is approached.

Particles in turbulent flow lag behind the velocity fluctuations of the fluid on account of their inertia. However, the effect of this is counteracted because the random motions which are acquired persist longer. The eddy diffusion coefficient of the fluid is therefore assumed to govern particle diffusion. Owing however, to the rapid decrease in "ε" as the surface is approached, there comes a point at which the projection of the particle towards the surface across the intervening region of diminished turbulence results in deposition. This point is a distance, "ds" (the particle stopping distance), from the surface. Within this distance of the wall, eddy diffusion has no significance. The rate determining factor in particle deposition becomes the concentration at one stop distance from the surface multiplied by the normal component of the velocity fluctuation. The rate of deposition governs the rate of transport resulting from eddy diffusion through the bulk of the flow.

The deposition of smaller particles is associated with the finite radius of the particles and with impingement upon protuberances from the surface of the pipe, i.e.: the roughness of the pipe. For the impingement of particles on protuberances the longitudinal steady velocity is available, but radial diffusion is necessary to feed the particles toward the wall and maintain the concentration near the surface. Davies (1966) derived the following empirical equation to agree with the data obtained by Laufer (1954) and Schlinger and Sage (1953) relating ε/ν to $\tilde{Y}$ over a 10^6 fold range of "$\tilde{Y}$".

$$\frac{\varepsilon}{\nu} = \frac{\tilde{Y}^{(4 - \tilde{Y}^{0.08})}}{1000 \left(\frac{2.5\text{x}10^7}{N_{ReG}}\right)^{\tilde{Y}/(400 + \tilde{Y})}} \qquad (4.6.5\text{-}18)$$

Neglecting molecular diffusion, the dimensionless velocity of deposition of particles due to eddy diffusion is:

$$\tilde{v} = \frac{\varepsilon}{\nu} \frac{d\tilde{c}}{d\tilde{Y}} \qquad (4.6.5\text{-}19)$$

This equation applies to one dimensional diffusion toward a plane surface. In view of the small magnitude of "$\tilde{v}$" and $d\tilde{c}/d\tilde{Y}$ in the center of a cylindrical tube, it is permissible as a first approximation to use a one dimensional equation for calculating the rate of deposition of particles on the wall of a cylinder by eddy impaction. Integrating Equation 4.6.5-20 between the center of the pipe and a distance $(ds + \tilde{r}_p)$ from the wall and substituting Equation 4.6.5-18 for ε/ν one gets:

$$\frac{1}{\tilde{v}} \int_{(\tilde{c})_{\tilde{d}s+\tilde{r}_p}}^{1} d\tilde{c} = \int_{\tilde{d}s+\tilde{r}_p}^{\tilde{r}_t} \frac{1000 \left(\frac{2.5\text{x}10^7}{N_{ReG}}\right)^{\left(\frac{\tilde{Y}}{400+\tilde{Y}}\right)}}{\tilde{Y}^{(4 - \tilde{Y}^{0.08})}} dY = \Big[I \Big]_{\tilde{d}s+\tilde{r}_p}^{\tilde{r}_t}$$

$$\text{where } \tilde{r}_t = \frac{r_t\, u_*}{\nu} \qquad (4.6.5\text{-}20)$$

This equation relates the fall in concentration in going from the center of a smooth tube to a distance $\tilde{Y} = \tilde{d}s + \tilde{r}_p$ from the wall, to the eddy coefficient.

The rate of particle deposition on the wall of the tube is:

$$\tilde{v} = (\tilde{v}')_{ds+r_p}\, (\tilde{c})_{\tilde{d}s+\tilde{r}_p} \qquad (4.6.5\text{-}21)$$

substituting for $[(\tilde{c})_{\tilde{d}s+\tilde{r}_p}]$ one gets from the last two equations for the velocity of deposition:

$$\tilde{v} = \frac{1}{\Big[I \Big]_{\tilde{d}s+\tilde{r}_p}^{\tilde{r}_t} \quad \frac{1}{(\tilde{v}')_{\tilde{d}s+\tilde{r}_p}}} \qquad (4.6.5\text{-}22)$$

In order to calculate "$\tilde{v}$" it is necessary to know the value of the integral and "$\tilde{v}'$" as a function of $Y = \tilde{d}s + \tilde{r}_p$. Davies (1966) has tabulated the values of the integral for various values of "Y" and "$\tilde{v}_t$" at $N_{ReG} = 10^4$; 10^5: and 10^6. These tables are presented here as Tables 4.6.5-2, 4.6.5-3, and 4.6.5-4.

Davies (1966) approximated Laufer's (1954) data by:

$$\frac{\tilde{Y}}{\tilde{v}'} = \tilde{Y} + 10 \qquad (4.6.5\text{-}23)$$

From the definition of the stopping distance:

$$\tilde{d}s = \frac{2\,\rho_p\,r_p^{\,2}}{9\,\mu_G}\,v'\,\frac{u_*}{\nu} = \tau\,\tilde{v}'\,\frac{u_*^{\,2}}{\nu} = \tilde{v}'\,\tilde{\tau} \qquad (4.6.5\text{-}24)$$

where: $\tau = \dfrac{2\,\rho_p\,r_p^{\,2}}{9\,\mu_G}$, and $\tilde{\tau} = \dfrac{\tau\,u_*^{\,2}}{\nu}$

Substituting $(\tilde{v}'\,\tilde{\tau} + \tilde{r}_p)$ for "$\tilde{Y}$" in Equation 4.6.5-23 remembering that $\tilde{d}s = \tilde{v}'\,\tilde{\tau}$ and solving for "v'" one gets:

$$\tilde{v}' = \frac{1}{2}\left(1 - \frac{\tilde{r}_p + 10}{\tilde{\tau}}\right) + \frac{1}{2}\left[\left(1 - \frac{\tilde{r}_p + 10}{\tilde{\tau}}\right)^2 + \frac{\tilde{r}_p}{\tilde{\tau}}\right]^{0.5} \qquad (4.6.5\text{-}25)$$

If one starts with a particle of known radius, and a known degree of turbulence, u_*, it is possible to evaluate "$\tilde{r}_p$", "$\tilde{\tau}$", and calculate "$\tilde{v}'$", then $(\tilde{d}s + \tilde{r}_p)$ is calculated. The value of the integral is read from the table for the known pipe radius, r_t, after "N_{ReG}" has been calculated and the velocity of deposition is found. The collection efficiency of the tube can be calculated from a material balance:

$$-Q_G\,dc = v\,c\,2\,\pi\,r_t\,d\ell \qquad (4.6.5\text{-}26)$$

or,

$$E = 1 - \frac{c_e}{c_i} = 1 - \exp - \left[\frac{2\,\pi\,r_t\,(\ell - \ell')\,v}{Q}\right] = 1 - \exp\left[\frac{A}{Q}\,v\right] \qquad (4.6.5\text{-}27)$$

where "Q_G" is the volumetric gas flow rate, "ℓ" is the length of the tube, and "ℓ'" is the length required to develop turbulent flow in the pipe.

As mentioned earlier, it is preferable to find "u_*" experimentally but it can also be estimated from the Fanning Friction Factor since;

$$\frac{dp}{d\ell} = \frac{2\,f}{r_t}\,\frac{\rho_g\,\bar{u}_G^{\,2}}{2} \qquad (4.6.5\text{-}28)$$

and $$f = 0.039\,N_{ReG}^{-0.17} \qquad (4.6.5\text{-}29)$$

where "$\bar{u}_G$" is the average velocity of the fluid in the pipe.

TABLE 4.6.5-2

DAVIES (1966)

VALUES OF THE INTEGRAL $[I]_{\tilde{y}}^{\tilde{r}}$ /1000

N_{ReG} = 10^4

$\tilde{y} \backslash \tilde{r}_t$	100	500	1000	5000	10,000
0·04	546·9	547·0	547·0	547·2	547·4
0·05	322·8	322·9	322·9	323·1	323·3
0·06	210·8	210·9	210·9	211·1	211·3
0·07	147·5	147·6	147·6	147·8	148·0
0·08	108·5	108·6	108·6	108·8	109·0
0·09	82·96	82·97	82·99	83·18	83·40
0·1	65·34	65·35	65·37	65·56	65·78
0·12	43·38	43·39	43·41	43·60	43·82
0·14	30·80	30·81	30·83	31·02	31·24
0·16	22·95	22·96	22·98	23·17	23·39
0·18	17·75	17·76	17·78	17·97	18·19
0·2	14·12	14·13	14·15	14·34	14·56
0·3	5·965	5·977	5·997	6·188	6·406
0·4	3·290	3·303	3·323	3·514	3·732
0·5	2·096	2·108	2·128	2·319	2·537
0·6	1·460	1·472	1·492	1·683	1·901
0·7	1·081	1·093	1·113	1·304	1·522
0·8	0·8366	0·8487	0·8684	1·059	1·277
0·9	0·6696	0·6817	0·7014	0·8923	1·110
1·0	0·5500	0·5621	0·5818	0·7727	0·9908
1·2	0·3939	0·4060	0·4257	0·6166	0·8347
1·4	0·2989	0·3110	0·3307	0·5216	0·7397
1·6	0·2365	0·2486	0·2683	0·4592	0·6773
1·8	0·1932	0·2053	0·2250	0·4159	0·6340
2·0	0·1617	0·1738	0·1935	0·3844	0·6025
2·2	0·1224	0·1501	0·1698	0·3608	0·5789
2·4	0·1198	0·1319	0·1516	0·3425	0·5606
2·6	0·1053	0·1174	0·1371	0·3280	0·5461
2·8	0·09369	0·1058	0·1255	0·3164	0·5345
3·0	0·08413	0·09621	0·1159	0·3068	0·5249
3·5	0·06652	0·07860	0·09828	0·2892	0·5073
4·0	0·05461	0·06669	0·08637	0·2773	0·4954
4·5	0·04612	0·05820	0·07788	0·2688	0·4869
5·0	0·03980	0·05188	0·07156	0·2625	0·4806
10	0·01650	0·02858	0·04825	0·2393	0·4576
20	0·007689	0·01977	0·03945	0·2304	0·4485
50	0·002580	0·01466	0·03434	0·2253	0·4434
100	—	0·01208	0·03176	0·2227	0·4408
200	—	0·009028	0·02871	0·2197	0·4377
500	—	—	0·01968	0·2107	0·4287
1000	—	—	—	0·1910	0·4090
2000	—	—	—	0·1436	0·3617
5000	—	—	—	—	0·2180

TABLE 4.6.5-3

DAVIES (1966)

VALUES OF THE INTEGRAL $[I]_{\tilde{y}}^{\tilde{r}}$ /1000

$N_{ReG} = 10^5$

$\tilde{y} \backslash \tilde{r}_t$	100	500	1000	5000	10,000
0·04	546·6	546·6	546·6	546·7	546·7
0·05	322·6	322·6	322·6	322·7	322·7
0·06	210·6	210·6	210·6	210·7	210·7
0·07	147·4	147·4	147·4	147·5	147·5
0·08	108·4	108·4	108·4	108·5	108·5
0·09	82·88	82·88	82·89	82·91	82·94
0·1	65·27	65·27	65·28	65·30	65·33
0·12	43·32	43·32	43·33	43·35	43·38
0·14	30·75	30·75	30·76	30·78	30·81
0·16	22·91	22·91	22·92	22·94	22·97
0·18	17·71	17·71	17·72	17·74	17·77
0·2	14·09	14·09	14·10	14·12	14·15
0·3	5·943	5·947	5·952	5·978	6·003
0·4	3·274	3·279	3·283	3·309	3·334
0·5	2·082	2·087	2·091	2·117	2·142
0·6	1·448	1·453	1·457	1·482	1·508
0·7	1·071	1·076	1·080	1·106	1·131
0·8	0·8272	0·8319	0·8364	0·8626	0·8873
0·9	0·6609	0·6656	0·6701	0·6963	0·7210
1·0	0·5421	0·5468	0·5513	0·5775	0·6022
1·2	0·3869	0·3916	0·3961	0·4223	0·4470
1·4	0·2926	0·2973	0·3018	0·3280	0·3527
1·6	0·2307	0·2354	0·2399	0·2661	0·2908
1·8	0·1878	0·1925	0·1970	0·2232	0·2479
2·0	0·1567	0·1614	0·1659	0·1921	0·2168
2·2	0·1333	[illegible]	0·1425	0·1688	0·1934
2·4	0·1153	[illegible]	0·1245	0·1508	0·1754
2·6	0·1010	[illegible]	0·1102	0·1365	0·1611
2·8	0·08954	[illegible]	0·09876	0·1250	0·1496
3·0	0·08014	0·08493	0·08936	0·1156	0·1402
3·5	0·06285	0·06764	0·07207	0·09834	0·1230
4·0	0·05119	0·05598	0·06041	0·08668	0·1113
4·5	0·04290	0·04769	0·05212	0·07839	0·1030
5	0·03675	0·04154	0·04597	0·07224	0·09685
10	0·01432	0·01912	0·02355	0·04985	0·07445
20	0·006160	0·01095	0·01538	0·04165	0·06628
50	0·001823	0·006617	0·01105	0·03731	0·06193
100	—	0·004794	0·009225	0·03549	0·06011
200	—	0·003140	0·007571	0·03383	0·05846
500	—	—	0·004431	0·03069	0·05532
1000	—	—	—	0·02626	0·05088
2000	—	—	—	0·01848	0·04310
5000	—	—	—	—	0·02462

TABLE 4.6.5-4

DAVIES (1966)

VALUES OF THE INTEGRAL $[I]_{\tilde{y}}^{\tilde{r}}/1000$

$N_{ReG} = 10^6$

$\tilde{y} \backslash \tilde{r}_t$	100	500	1000	5000	10,000
0·04	546·4	546·4	546·4	546·4	546·4
0·05	322·4	322·4	322·4	322·4	322·4
0·06	210·5	210·5	210·5	210·5	210·5
0·07	147·2	147·2	147·2	147·2	147·2
0·08	108·3	108·3	108·3	108·3	108·3
0·09	82·79	82·80	82·80	82·80	82·80
0·1	65·19	65·20	65·20	65·20	65·20
0·12	43·26	43·27	43·27	43·27	43·27
0·14	30·69	30·70	30·70	30·70	30·70
0·16	22·86	22·87	22·87	22·97	22·87
0·18	17·67	17·68	17·68	17·68	17·68
0·2	14·05	14·06	14·06	14·06	14·06
0·3	5·921	5·923	5·924	5·928	5·931
0·4	3·257	3·259	3·260	3·264	3·267
0·5	2·068	2·070	2·071	2·075	2·078
0·6	1·436	1·438	1·439	1·443	1·446
0·7	1·060	1·062	1·063	1·067	1·070
0·8	0·8181	0·8202	0·8212	0·8248	0·8276
0·9	0·6527	0·6548	0·6558	0·6594	0·6622
1·0	0·5345	0·5366	0·5376	0·5412	0·5440
1·2	0·3802	0·3823	0·3833	0·3869	0·3897
1·4	0·2866	0·2887	0·2897	0·2933	0·2961
1·6	0·2253	0·2274	0·2284	0·2320	0·2348
1·8	0·1828	0·1849	0·1859	0·1895	0·1923
2·0	0·1520	0·1541	0·1551	0·1587	0·1615
2·2	0·1290	0·1310	0·1320	0·1357	0·1385
2·4	0·1112	0·1132	0·1142	0·1179	0·1207
2·6	0·09714	0·09916	0·1002	0·1038	0·1066
2·8	0·08584	0·08786	0·08887	0·09254	0·09532
3·0	0·07659	0·07861	0·07962	0·08329	0·08607
3·5	0·05962	0·06164	0·06265	0·06632	0·06910
4·0	0·04821	0·05023	0·05124	0·05491	0·05769
4·5	0·04012	0·04214	0·04315	0·04682	0·04960
5	0·03413	0·03615	0·03716	0·04083	0·04361
10	0·01254	0·01456	0·01557	0·01928	0·02202
20	0·004980	0·007000	0·008009	0·01168	0·01447
50	0·001293	0·003314	0·004322	0·007996	0·01078
100	—	0·002020	0·003029	0·006702	0·009484
200	—	0·001116	0·002125	0·005798	0·008580
500	—	—	0·001009	0·004682	0·007464
1000	—	—	—	0·003673	0·006455
2000	—	—	—	0·002386	0·005168
5000	—	—	—	—	0·002782

Extension of the argument to rough surfaces is easily carried out. The effect of roughness on turbulence will be allowed for automatically in the friction velocity if measured experimentally or if the degree of roughness is estimated when calculating "f". Impingement of particles on protuberances of height "δ" will take place because of longitudinal steady velocity as long as the particle center is within a distance $(r_p + \delta)$ of the surface, provided that the protuberances are sufficiently numerous to cover the entire periphery of the pipe. If one assumes this to be the case, the enhanced deposition due to surface roughness will be taken account of if the term "$\tilde{r}$" in the boundary conditions and in the calculation of "$\tilde{v}'$" is replaced by $\tilde{r} + \tilde{\delta}$, where $\tilde{\delta} = \delta u_*/\nu$.

4.6.5.4 Deposition of Aerosol from Turbulent Flow Due to Inertia and Brownian Motion.

When the particles are small so that $\tilde{d}s + \tilde{r}$ is small and close enough to the wall to make molecular diffusion important in maintaining the particle concentration at the distance of $(\tilde{d}s + \tilde{r})$, then Equation 4.6.5-19 has to be modified to include transport due to molecular diffusion. Davies (1966) assumes that when $\varepsilon > 8\ D_p$, Brownian diffusion is inappreciable. He defines a diffusion layer whose thickness is:

$$\tilde{Y}' \simeq 10 \left(\frac{8\ D_p}{\nu}\right)^{1/3} = 20 \left(\frac{D_p}{\nu}\right)^{1/3} \tag{4.6.5-30}$$

when $\tilde{d}s + \tilde{r}$ is smaller than the layer where diffusion transport becomes appreciable relative to eddy transport, meaning that:

$$(\tilde{d}s + \tilde{r}) < 20 \left(\frac{D_p}{\nu}\right)^{1/3} \tag{4.6.5-31}$$

then the velocity of deposition of the particle is given by:

$$\tilde{v} = \left(\frac{D_p}{\nu} + \frac{\varepsilon}{\nu}\right) \frac{d\tilde{c}}{d\tilde{Y}} \tag{4.6.5-32}$$

$$\frac{1}{\tilde{v}} \int_{(\tilde{c})_{\tilde{d}s+\tilde{r}}}^{1} d\tilde{c} = \int_{\tilde{d}s+\tilde{r}}^{Y'} \frac{D d\tilde{Y}}{\frac{D_p}{\nu^{\nu}} + \left(\frac{\tilde{Y}}{10}\right)^3} + \int_{Y'}^{r_t} \frac{d\tilde{Y}}{\frac{D_p}{\nu} + \frac{\varepsilon}{\nu}} \tag{4.6.5-33}$$

and the final equation is:

$$\frac{1}{\tilde{v}} - \frac{1}{(\tilde{v}')_{\tilde{d}s+\tilde{r}}} = 10 \left(\frac{\nu}{D_p}\right)^{2/3} f(\phi) + \Big[I\Big]_{20 \left[\frac{Dp}{\nu}\right]^{1/3}}^{\tilde{r}_t} \tag{4.6.5-34}$$

where:

$$f\ (\phi) = 0.7877 - \frac{1}{6} \ln \frac{(1 + \phi)^2}{1 - \phi + \phi^2} - \frac{1}{\sqrt{3}} \arc\tan \frac{2\ \phi - 1}{\sqrt{3}} \tag{4.6.5-35}$$

and

$$\phi = \frac{\tilde{d}s + \tilde{r}}{10\left(\frac{D_p}{\nu}\right)^{1/3}} \qquad (4.6.5\text{-}36)$$

when $\tilde{d}s + \tilde{r} > 20\,(D_p/\nu)^{1/3} = \tilde{Y}'$, then the particle is projected onto the wall from a distance where the transport by diffusion is negligible compared with the eddy transport, and Equation 4.6.5-22 should be used.

4.6.6 COLLECTION OF PARTICLES BY LIQUID JETS

Collection of particles by liquid jets is small, as long as the jet preserves its stream shape, because of the small area available for collection. Once the jet breaks into a multitude of small drops, collection increases. However, once collection is by liquid drops and the drop size distribution is known, venturi type collection efficiency equations will describe the situation adequately.

The major group of control devices utilizing liquid jets which later break into drops is the ejector venturi group which is discussed in detail in Chapter 5.3.5.4.

4.6.7 COLLECTION OF PARTICLES FROM IMPACTING GAS JETS

4.6.7.1 Introduction

The impaction of aerosol jets on surfaces may lead to the removal of particles from the air stream. The important collection mechanism in this case, which has also been discussed extensively in the literature, is collection due to particle inertia. Collection by diffusion and change in particle size brought about by the various mechanisms discussed in 4.3.4 are usually negligible because of the very short time that the aerosol stays near the impaction plate. This is despite the cooling which takes place due to the adiabatic expension of the gas when leaving the jet. Other forces, such as electrostatic, thermophoretic and diffusiophoretic may influence collection.

The curve describing collection efficiency vs. impaction parameter for inertial impaction is a relatively steep one. That is why jet impaction devices are used for particle size analysis in cascade impactors. Wet impingement devices are also used in industry for gas cleaning. However, Stairmand (1956) doubts if collection in these devices is due only to inertial impaction on the collecting plates and suggests an additional collection mechanism due to the formation of spray droplets and collection by these drops.

4.6.7.2 Inertial Collection

In a jet impactor, an aerosol stream issuing from a rectangular or round jet impinges against a plate and flows around it. Because of inertia, the particles leave the streamlines and are deposited on the plate.

Rectangular Jets

Davies and Aylward (1951) made a theoretical study of the impaction process for rectangular jets and obtained curves of collection efficiency as a function of the particle inertia parameter. They predicted good cut-off characteristics and showed that the efficiency curves could be made steeper and moved to lower values of the inertia parameter by decreasing the distance of separation between the jet orifice and the collection plate. A less rigorous attack on this problem was undertaken by Ranz and Wong (1952), who assumed in their calculation a constant value for the distance between the jet orifice and the collecting plate and a simplified flow field. Mercer and Chow (1968) and Mercer and Stafford (1969) extended the Ranz and Wong solution by including the effect of the collecting plate distance from the jet and assuming a more realistic flow field. Here the Mercer et al. approach in formulating the problem will be followed, since it is simpler than that of Davies and Aylward, and brings out all the important features of the rectangular jet.

Consider a rectangular jet as described in Figure 4.6.6-2. Assume that an aerosol stream emerges from a jet orifice of width "b" and infinite length, and impinges upon a plane surface at a distance "ℓ", from the orifice. The stream will split into two symmetrical branches flowing in opposite directions. By assuming the jet orifice to be very long, the problem is made a two dimensional one. Further assume that the motion of a particle relative to the air is opposed with a purely viscous resistance, the particle diameter is negligible compared to the jet width, the air is an ideal fluid and a particle is captured and retained if the trajectory of its center intersects the collecting plate.

Mercer et al. assumed in formulating the boundary conditions that the air stream begins to diverge immediately upon leaving the jet orifice and that the various volume elements of the air travel equal distances in the Y direction before the X component of theis velocities goes to zero. The first assumption is reasonable when "β" is small, but its validity diminishes rapidly as "β" increases beyond 2. At large values of "ℓ" the air stream actually diverges very little until it is within about one jet width from the plate. They defined "β" as:

$$\beta = \frac{2\,\ell}{b} \qquad (4.6.7\text{-}1)$$

and derived the particle equation of motion from Newton's second law. The gas flow field and the boundary conditions are described by:

$$\left.\begin{aligned} \tilde{u} &= -\frac{\tilde{X}}{\beta} \qquad (4.6.7\text{-}2) \\ \tilde{v} &= \frac{\tilde{Y}}{\beta} \qquad (4.6.7\text{-}3) \end{aligned}\right\}\ \text{for} \begin{cases} -(1+\Delta\tilde{Y}) < \tilde{Y} < (1+\Delta\tilde{Y}) \\ -\beta < \tilde{X} < 0 \end{cases}$$

and

$$\tilde{u} = 0 \quad \text{for} \begin{cases} -(1+\Delta\tilde{Y}) > \tilde{Y}\ ;\ \tilde{Y} > (1+\Delta\tilde{Y}) \\ -\beta < \tilde{X} < 0 \end{cases} \qquad (4.6.7\text{-}4)$$

$$\tilde{u} = \tilde{u}_p = 1 \text{ for } \tilde{X} = -\beta, \text{ and } \tilde{v}_p = 0 \text{ for } \tilde{t} = 0 \qquad (4.6.7\text{-}5)$$

Mercer et al. have set $\Delta\tilde{Y} = |\tilde{Y}_o|$ the ordinate of a given streamline at X = -β, which means that the air stream begins to diverge immediately upon leaving the orifice. This assumption permits the various volume elements of air to travel equal distances in the "y" direction before the "x" components of their velocities goes to zero.

The inertia parameter, K, is defined (with radius rather than diameter as 4.6.2-4) as:

$$K = \frac{2 \rho_p C' u_o r_p^2}{9 \mu_G \frac{b}{2}} \qquad (4.6.7\text{-}6)$$

Figure 4.6.7-1 compares Mercer et al. experimental results with Davies et al. (1951) theoretical computation. The comparison is quite good except at high efficiencies. Mercer attributes this deviation to the end effect, since the slit is not infinitely long as assumed by Davies.

Davies predicted the existence of a critical inertia parameter, K_{cr}, below which there is no deposition of particles on the impaction plate and showed that "K_{cr}" depends upon "β". This was found experimentally to be the case by Mercer et al. and by others. Figure 4.6.7-1 compares Davies prediction with regard to the effect of "β" on $\sqrt{K_{50}}$ (where K_{50} is the impaction parameter corresponding to 50% collection efficiency) with experimental results. It can be seen from Figure 4.6.7-3 that for β > 4, $\sqrt{K_{50}}$ is a constant. The effect of "β" on collection efficiency is only for values of β < 4 where $\sqrt{K_{50}}$ decreases with a decrease in "β".

A parameter which was not considered previously is the flow regime in the slit. Mercer et al. (1968) showed that when a parabolic velocity profile is allowed to develop in the nozzle, collection efficiency will increase at a lower "K". In most jets there is not enough time for the parabolic velocity profile to build up. The dimensionless number used to characterize the flow regime in the slit is the gas Reynolds number, N_{ReG}:

$$N_{ReG} = \frac{b' u_o \rho_G}{\mu_G} \qquad (4.6.7\text{-}7)$$

$$b' = \frac{2 B b}{b + B} \qquad (4.6.7\text{-}8)$$

where "B" is the length of the jet.

Round Jets

Impaction from round jets is similar to impaction from rectangular jets. In a manner analogous to that presented for rectangular jets, a theoretical solution was derived for gas and particle motion by Ranz and Wong (1952). This was later extended by Mercer and Stafford (1969) to include the effect of jet distance from the impaction plate. Mercer et al. experimental results for round jets are given in Figure 4.6.7-4. As can be seen from the figure, the efficiency curves for round jets are steeper than for rectangular jets, and the effect of $\beta = 2\ell/b$ (here "b" represents jet diameter) is much less pronounced. This is also seen in Figure 4.6.7-5, where experimental curve for the variation of $\sqrt{K_{50}}$ with "β" is plotted. From the practical point of designing an impactor, it appears that values of "β" up to at least 10 have little effect on K_{50}, as compared to a ratio of 4 in rectangular jets. The values of $\beta < 2$ are characterized by steeper efficiency curves.

Collection efficiency in round jets is also effected by the development of a parabolic velocity profile in the jet nozzle. Mercer et al. (1969) suggests using Tietjens (1956) correlation which predicts the development of a parabolic velocity profile when:

$$\frac{\ell'}{b\ N_{ReG}} \gtrsim 0.065 \qquad (4.6.7\text{-}9)$$

here "ℓ'" is the transition length and should be made smaller than $0.065\ (b)\ N_{ReG}$.

In the final analysis, round jets are advantageous to rectangular, with respect to collection efficiency at a constant "K"; their efficiency curves are steeper, they are less affected by "β" and are more easily constructed. It should be emphasized that the experimental and the theoretical curves are for the case when there is no overloading of the collecting plate. Once the plate is overloaded, the ratio of "β" decreases, which tends to increase collection efficiency and decrease separation.

Jet Impactor Design Considerations

Let us now review the procedure for designing an impactor. Theoretically and experimentally for a given jet geometry (fixed β), there is only one "K_{50}" regardless of particle size and velocity, if a parabolic velocity profile does not develop. From the definition:

$$\sqrt{K_{50}} = \left(\frac{C'\ \rho_p\ u_o}{9\ \mu_G\ b}\right)^{1/2} d_{p50} \qquad (4.6.7\text{-}10)$$

When $(d_p/\lambda) > 2.7$, namely $d_p > \simeq 0.15$ under room temperature and pressure, the Cunningham correction factor, C', can be approximated by:

$$C' = 1 + 2.46\left(\frac{\lambda}{d_p}\right) \qquad (4.6.7\text{-}11)$$

For air at constant "λ" this equation can be further approximated by:

$$C' = 1 + \frac{1.65}{d_p}\times 10^{-5} \qquad (4.6.7\text{-}12)$$

When $u_o \gtrsim \frac{1}{3}$ Mach, the jet velocity can be estimated by:

$$u_o = \frac{4\ Q_{Gi}}{\pi\ b^2}\ \frac{P_i}{P_e} \qquad (4.6.7\text{-}13)$$

When $u_o \leq \frac{1}{3}$ Mach, "P_e" can be set equal to "P_i", since under these conditions the gas can still be considered as incompressible. Substituting Equations 4.6.7-12 and 4.6.7-13 into Equation 4.6.7-10 and solving for "d_{p50}" we get:

$$d_{p50} = 8.3\text{x}10^{-6} + 68\text{x}10^{-12} + \left(\frac{7.06\ b^3\ \mu_G\ K_{50}\ P_e}{\rho_p\ Q_{Gi}\ P_i}\right)^{1/2} \qquad (4.6.7\text{-}14)$$

For both round and rectangular jets values of "K_{50}" are approximately constant if $\beta < 10$ for round jets and $\beta < 4$ for rectangular ones. For rectangular jets $\sqrt{K_{50}} \simeq 0.8$ while for round ones $\sqrt{K_{50}} \simeq 0.44$. Thus by fixing the jet dimensions and the volumetric flow rate, the cut diameter "d_{p50}" can be calculated. Conversely, if "d_{p50}" is fixed, the jet geometry and flow through are calculated.

The pressure drop of a several stage impactor can be approximated by the pressure drop due to isentropic flow through the smallest jet. Namely:

$$\Delta P = \frac{\rho_G\ u_o^2}{2} \qquad (4.6.7\text{-}15)$$

If one rearranges Equation 4.6.7-10, one obtains:

$$\rho_p\ C'\ d^2_{p50} \equiv d_{pa}^2 = \frac{9\mu_G\ b\ K_{50}}{u_o} \qquad (4.6.7\text{-}16)$$

The group on the right of this equation does not depend upon particle properties, and would not be affected by particle shape. The square root of the left hand side, which consists only of the particle parameters $(\sqrt{\rho_p\ C'})\ d_p$, is defined as the aerodynamic particle diameter, d_{pa} Figure 4.6.7-6 is a plot of the aerodynamic diameter, d_{pa}, vs. particle diameter, d_p, with particle density as a parameter, for spherical particles.

Spherical and any odd shaped particles, which are collected by the same stage of a jet impactor, have the same aerodynamic diameter. Once the various values of "K_{50}" are determined experimentally for the different stages using monodisperse spherical aerosols of known density, the impactor can be used to determine the aerodynamic diameter of any aerosol.

Mercer et al. (1969) investigated the adhesion of particles emerging from a round jet on a collection plate. They found that loss of particles occurred due to the rebound of impacting particles rather than to re-entrainment of particles already deposited. They found that when the collecting plate is covered with an oily coat, the coat serves as a cushion rather than an adhesive. Lundgren (1967) reached a similar conclusion. He found that the exact thickness of the coating does not appear critical if it is at least as thick as the size of the particles to be collected. Fuchs (1964 says that the collection efficiency for coarse aerosol particles may be reduced considerably, since after deposition the large particles may be swept off the plate. Fuchs says this results in an upper limit to the size of the particles collected.

4.6.7.3 Combined Inertial and Diffusiophoretic Collection

When the collecting plate is maintained under conditions which promotes condensation of vapors from the impinging gas stream, a diffusiophoretic force will develop in addition to the particle inertia. No experimental or theoretical description of this combination of forces was found in the literature.

The formulation of the differential equations is straight-forward if one makes the same assumptions made in deriving the inertial equations. Start from Newton's second law, ma = Σ F(t) where Σ F(t) is the vector sum of all external forces acting on the particle, which may be a function of time. Assume that the only forces acting on the particle are the drag force, which is given by Stokes' law, and the diffusiophoretic force. For $r_p > \lambda$ the diffusiophoretic force in the "X" direction is given by:

$$F_{DPX} = \frac{6 \pi \mu_G r_p \sqrt{M_V} D_p}{(y_V \sqrt{M_V} + y_G \sqrt{M_G}) y_G} \frac{d\hat{y}_v}{dX} \qquad (4.6.7\text{-}17)$$

substituting and making the equation dimensionless, we get the equations of motion in the "x" and "y" directions

$$\frac{d^2\tilde{X}}{d\tilde{t}^2} = \frac{1}{K} (\tilde{u}_G - \tilde{u}_p) + \frac{9 \mu_G D_p \sqrt{M_V}}{2 \rho_p r_p^2 u_o^2 y_G (y_V \sqrt{M_V} + y_G \sqrt{M_G})} \frac{d\hat{y}_V}{d\tilde{X}} \qquad (4.6.7\text{-}18)$$

$$\frac{d^2\tilde{Y}}{d\tilde{t}^2} \quad \frac{1}{K} (\tilde{v}_G - \tilde{v}_p) + \frac{9 \mu_G D_p \sqrt{M_V}}{2 \rho_p r_p^2 u_o^2 y_G (y_V \sqrt{M_V} + y_G \sqrt{M_G})} \frac{d\hat{y}_V}{dY} \qquad (4.6.7\text{-}19)$$

where "y_V" is the mole fraction of the vapor in the gas.

We have solved these equations for the case where $dy_V/d\tilde{X}$ is constant and $dy_V/dY = 0$ in the range $-(1 + Y_o) < \tilde{Y} < (1 + \tilde{Y}_o)$ and $-\beta < \tilde{X} < 0$, and $dy_V/d\tilde{X} = dy_V/d\tilde{Y} = 0$ outside of this range, using Mercer et al. boundary conditions and flow field description. The solution showed that under regular operating conditions the diffusiophoretic effect will be negligible. It takes a relatively high vapor pressure gradient, in the order of magnitude of 300 mm Hg, when b $\approx$ 0.1 cm, for the effect to be noticeable.

4.6.7.4 Combined Inertial and Thermophoretic Collection

If the collecting plate is maintained at a lower temperature than the gas stream, thermophoretic forces will act on the particles, forcing them toward the plate, and as a result increase collection efficiency.

The differential equations of motion for particles larger than the mean free path of the gas ($r_p > \lambda$) can be formulated in the same manner as for diffusiophoresis giving:

$$\frac{d^2\tilde{X}}{d\tilde{t}} = \frac{1}{K}(\tilde{u}_G - \tilde{u}_p) + \frac{27\,\mu_G^2\,T_o}{4\,\rho_p\,r_p^2\,u_o^2\,\rho_G\,T}\left(\frac{k_G}{2\,k_p + k_G}\right)\frac{d\tilde{T}}{d\tilde{X}} \qquad (4.6.7\text{-}20)$$

$$\frac{d^2\tilde{Y}}{d\tilde{t}} = \frac{1}{K}(\tilde{v}_G - \tilde{v}_p) + \frac{27\,\mu_G^2\,T_o}{4\,\rho_p\,r_p^2\,u_o^2\,\rho_G\,T}\left(\frac{k_G}{2\,k_p + k_G}\right)\frac{d\tilde{T}}{d\tilde{Y}} \qquad (4.6.7\text{-}21)$$

where "T_o" is the plate temperature assumed to be constant. Fixing boundary conditions, flow field and temperature gradient, in the same manner as in the diffusiophoresis case and solving the equation will yield the same results as in the preceeding case, namely; it takes a high temperature gradient for the force to be effective. This is due to the high velocity and short residence time of the particle in the thermal field.

4.6.7.5 Combined Inertial and Electrostatic Collection

Increased collection by the impaction plate can be achieved by applying a voltage difference between the collecting plate and the nozzle plate. One can approximate the situation by assuming the collecting plate and the nozzle body to resemble a charged plate condensor with a tiny hole. (This geometric configuration reminds one of the Millikan apparatus). The aerosol particles may be charged opposite to the collection plate charge, or may assume an induced charge when entering the condensor field. Let us analyze the first case, when a charged aerosol is collected by an oppositely charged plate maintained at a constant voltage with respect to the nozzle plate. The electric field between the plates is constant and acts only in the "X" direction. Thus an additional constant force equal to "q_p E", where "q_p" is the charge on the particle and "E" the electric field strength, acts on the particle and should be added to the "X" component in the equation of motion, yielding:

$$\frac{d^2\tilde{X}}{d\tilde{t}} = \frac{1}{K}(\tilde{u}_G - \tilde{u}_p) + \frac{3\times10^7\,q_p\,V\,\beta}{2\,\pi\,r_p^3\,\rho_p\,u_o^2} \qquad (4.6.7\text{-}22)$$

$$\frac{d^2\tilde{Y}}{d\tilde{t}} = \frac{1}{K}(\tilde{v}_G - \tilde{v}_p) \qquad (4.6.7\text{-}23)$$

OPERANT UNIT MECHANISMS FOR SCRUBBERS

Scrubber	Drops	Cylinders	Bubbles	Surfaces	Gas Jets
	UNIT MECHANISM				
Plate			X		X
Massive Packing				X	
Fibrous Packing		X			
Pre-formed Spray	X				
Gas Atomized Spray	X				
Centrifugal	X			X	
Baffle and Secondary Flow				X	
Impingement & Entrainment	X				
Mechanically Aided	X				
Moving Bed	X		X	X	

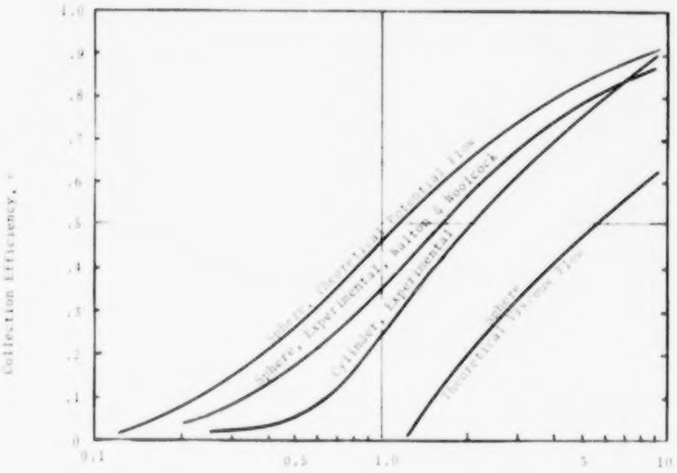

$$k = \frac{C' \rho_p d_p^2 U_o}{9 \mu_G d_c}$$

FIGURE 4.6.2-2

EXPERIMENTAL AND CALCULATED COLLECTION EFFICIENCIES
FOR SPHERE AND CYLINDER

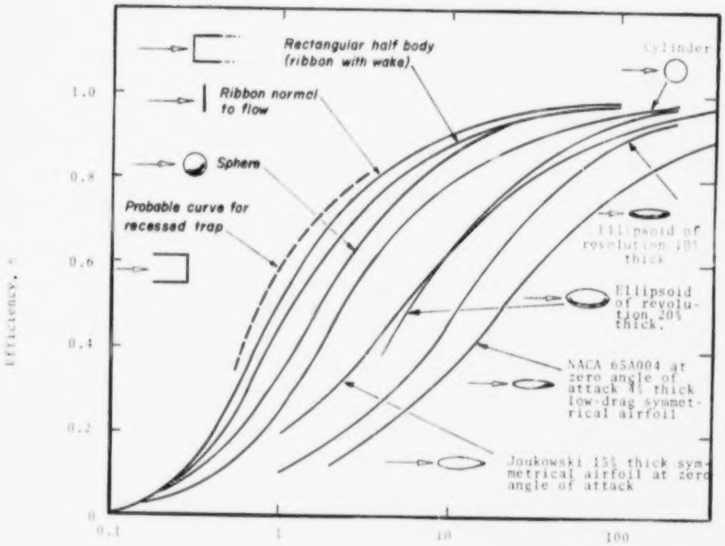

Inertial Parameter, $k = \frac{C' \rho_p d_p^2 U_o}{9 \mu_G d_c}$

FIGURE 4.6.2-3

THEORETICAL IMPACTION EFFICIENCY AS A FUNCTION
OF INERTIAL PARAMETER FOR DIFFERENT TARGETS
[GOLOVIN AND PUTNAM (1962)]

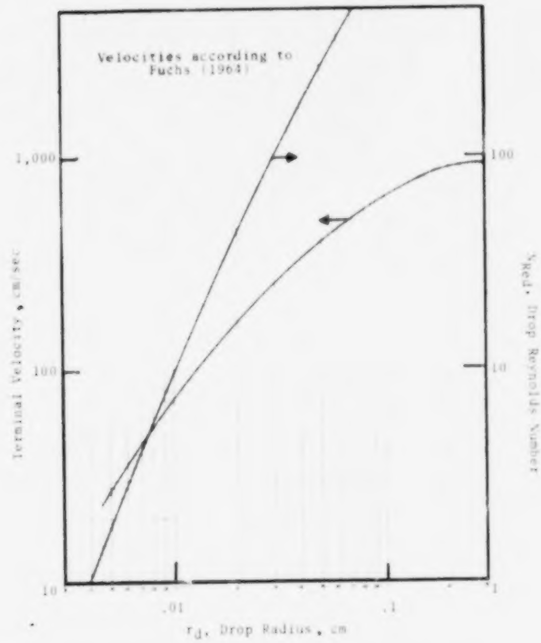

FIGURE 4.6.2-4

TERMINAL SETTLING VELOCITY AND REYNOLDS NUMBER FOR WATER DROPS IN AIR AT 20°C and 760 mmHg.

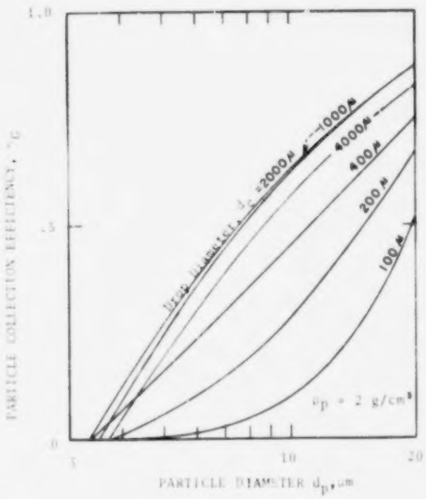

FIGURE 4.6.2-5

COLLECTION OF PARTICLES BY FREE FALLING WATER DROPS

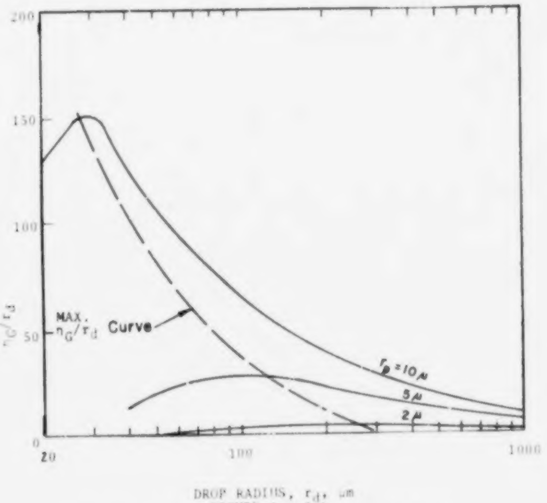

FIGURE 4.6.2-6

EFFECTIVE CAPTURE CROSS-SECTION VS. WATER DROP DIAMETER WITH PARTICLE RADIUS AS PARAMETER

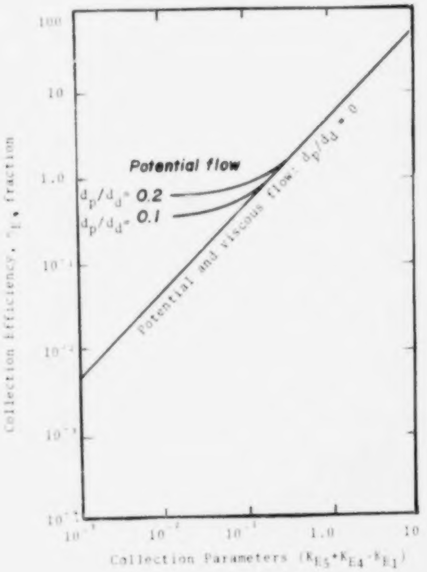

FIGURE 4.6.2-7

COLLECTION EFFICIENCY FOR A UNIPOLAR CHARGED AEROSOL ON A SPHERICAL COLLECTOR WITH THE OPPOSITE CHARGE [KRAEMER AND JOHNSTONE] (1955)

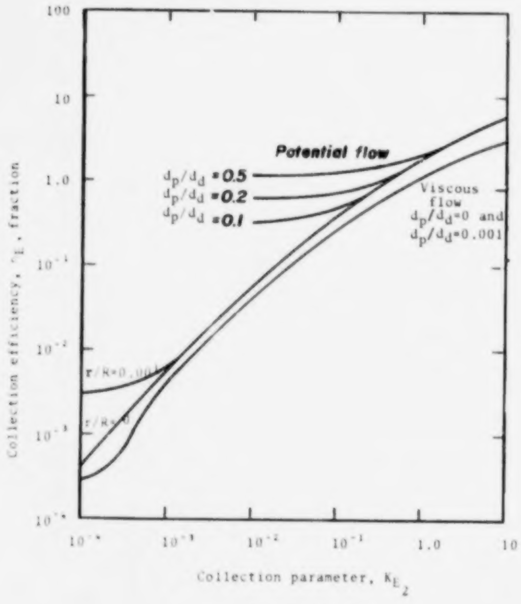

FIGURE 4.6.2-8

COLLECTION EFFICIENCY OF AN UNCHARGED AEROSOL ON A CHARGED SPHERICAL COLLECTOR. [KRAEMER AND JOHNSTONE (1955)]

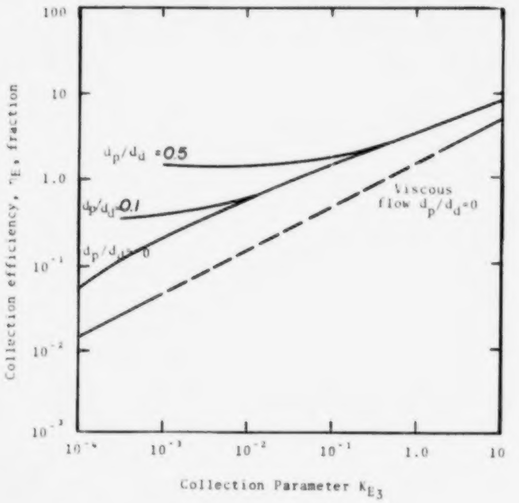

FIGURE 4.6.2-9

COLLECTION EFFICIENCY OF A CHARGED AEROSOL ON AN UNCHARGED SPHERICAL COLLECTOR [KRAEMER AND JOHNSTONE 19 5]

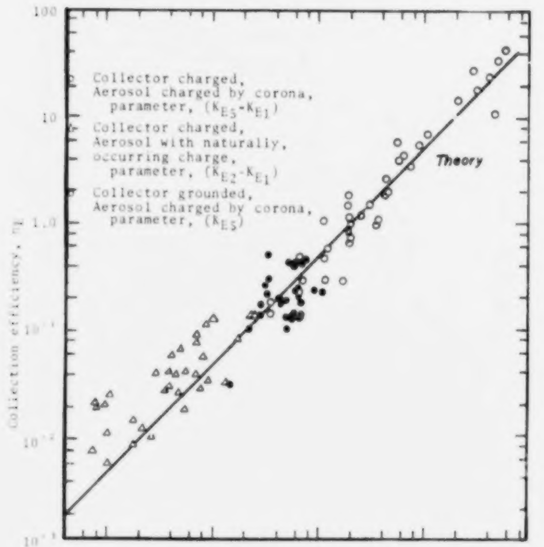

FIGURE 4.6.2-10

COLLECTION OF CHARGED DIOCTYLPHTHALATE MIST ON SPHERE. THEORY AND EXPERIMENT. [KRAEMER AND JOHNSTONE (1955)]

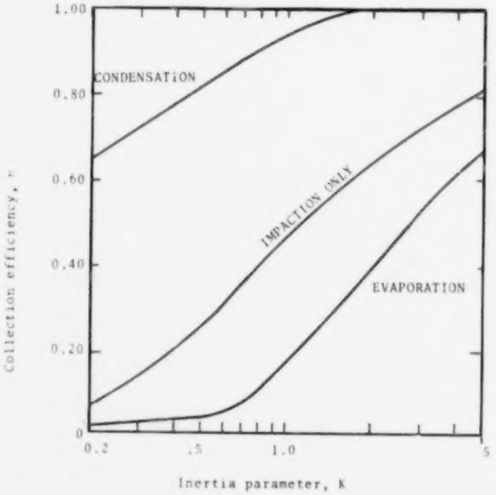

FIGURE 4.6.2-11

EFFECT OF DIFFUSIOPHORESIS ON COLLECTION BY A SINGLE DROP. SPARKS AND PILAT (1970)

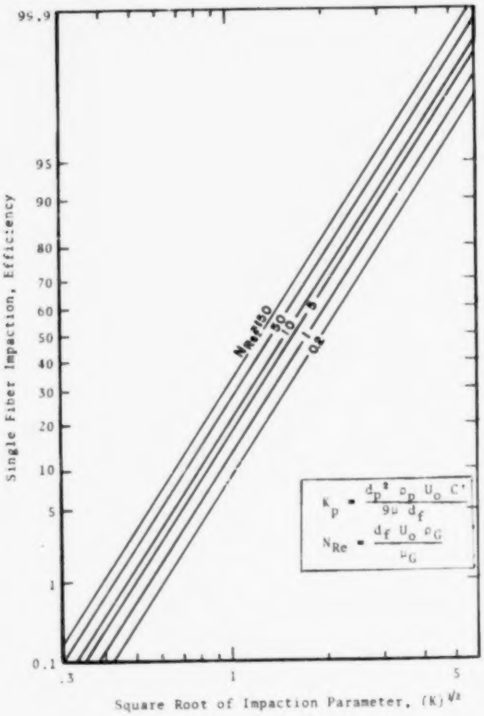

FIGURE 4.6.3-1

SINGLE FIBER IMPACTION EFFICIENCY, AS FUNCTION OF IMPACTION PARAMETER AND REYNOLDS NUMBER.

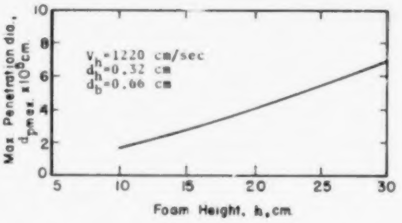

FIGURE 4.6.4-1

EFFECT OF FOAM HEIGHT IN A SIEVE PLATE COLUMN ON MAXIMUM PENETRATION DIAMETER

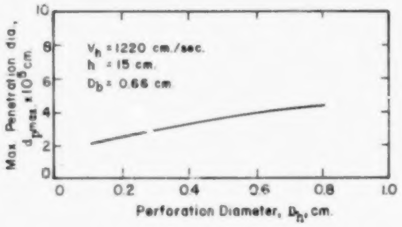

FIGURE 4.6.4-2

EFFECT OF PERFORATION DIAMETER IN A SIEVE PLATE COLUMN ON MAXIMUM PENETRATION DIAMETER

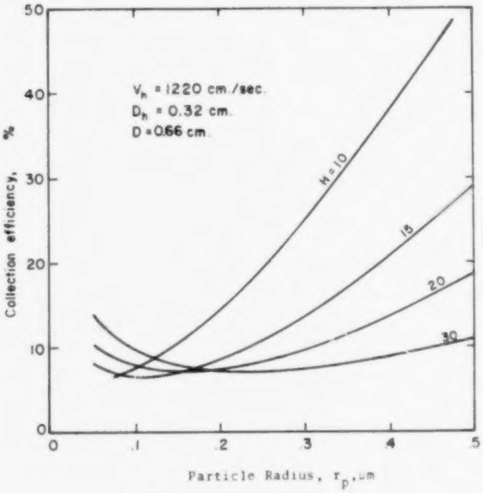

FIGURE 4.6.4-3

COLLECTION EFFICIENCY IN A SIEVE PLATE VS. PARTICLE RADIUS WITH FOAM HEIGHT AS PARAMETER

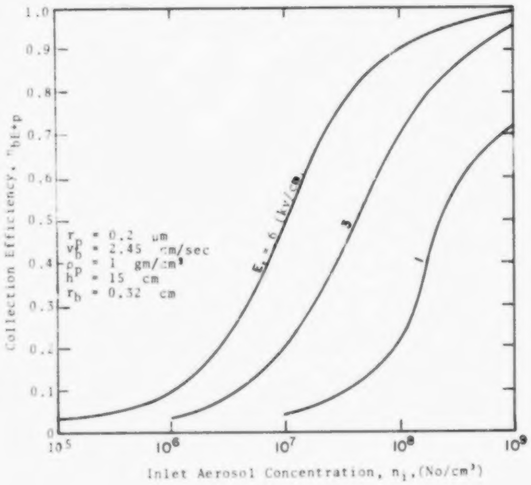

FIGURE 4.6.4-4

COLLECTION OF 0.4 µm DIAMETER PARTICLES BY BUBBLES AS A FUNCTION OF AEROSOL INLET CONCENTRATION AND CHARGING FIELD STRENGTH

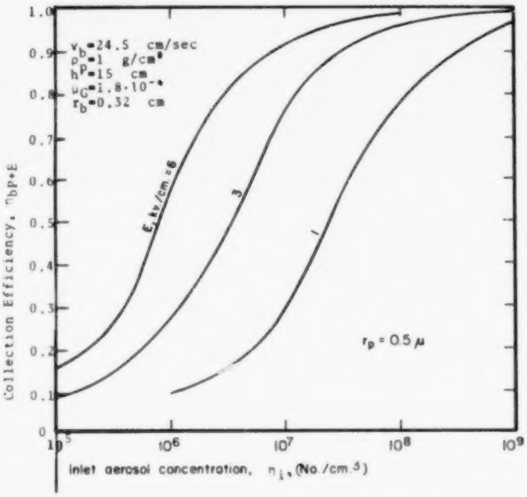

FIGURE 4.6.4-5

COLLECTION OF $1\mu m$ DIAMETER PARTICLES BY BUBBLES AS A FUNCTION OF AEROSOL INLET CONCENTRATION AND CHARGING FIELD STRENGTH

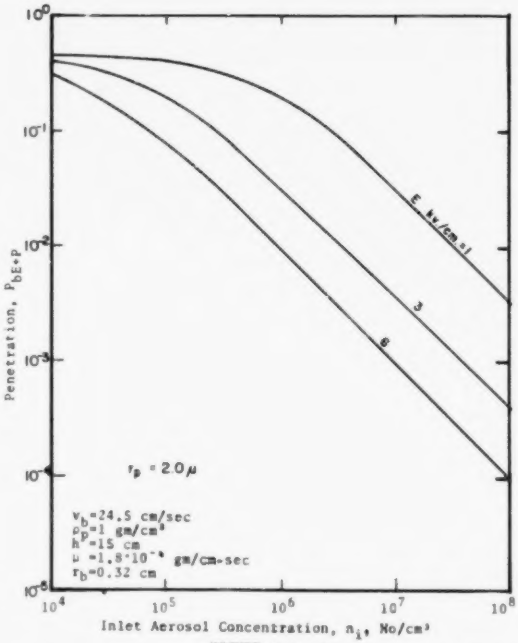

FIGURE 4.6.4-6
PENETRATION OF $4\mu m$ DIAMETER PARTICLES BY BUBBLES AS A FUNCTION OF INLET CONCENTRATION AND CHARGING FIELD STRENGTH

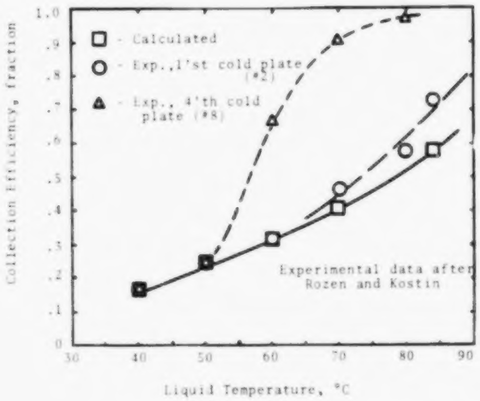

FIGURE 4.6.4-7

EFFECT OF HEAT AND MASS TRANSFER ON COLLECTION EFFICIENCY IN A SIEVE PLATE. THEORY AND EXPERIMENT.

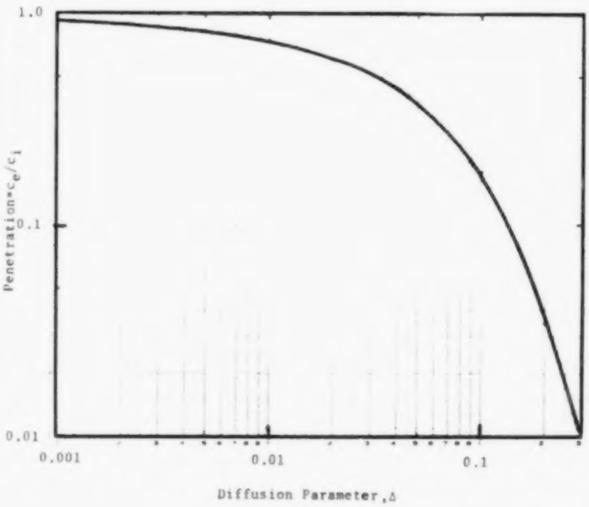

FIGURE 4.6.5-1

PARTICLE PENETRATION VS. DIFFUSION PARAMETER FOR VISCOUS FLOW IN LONG TUBE (After Davies, 1966)

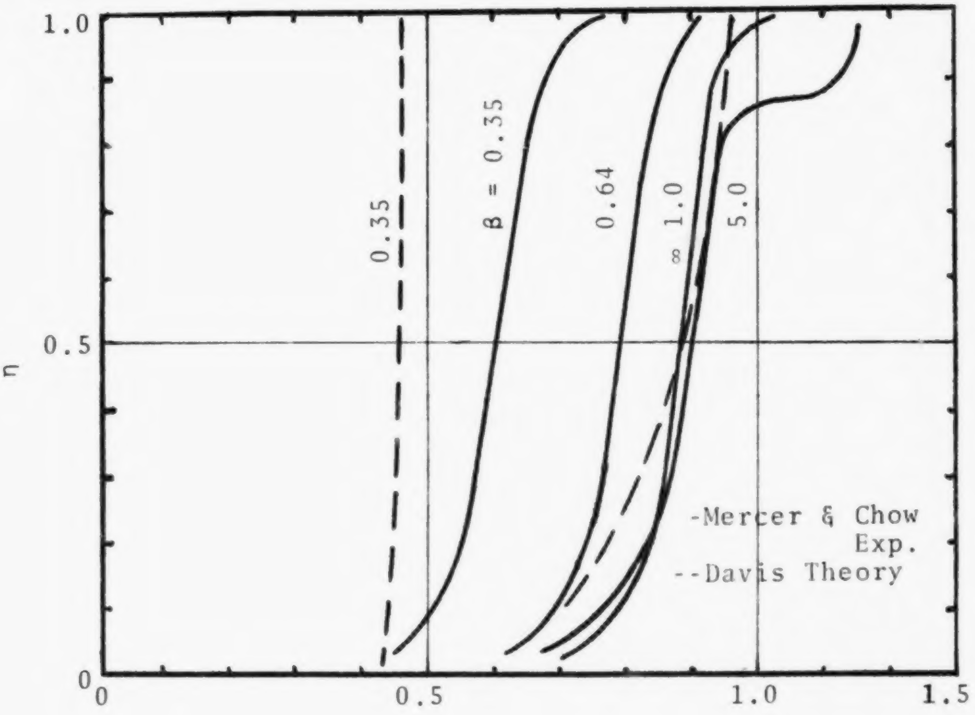

$$\sqrt{K} = \left(\frac{2\rho_p \; C' \; u_o}{9 \; \mu_G \; \frac{b}{2}}\right)^{1/2} r_p$$

FIGURE 4.6.7-1

THEORETICAL AND EXPERIMENTAL COLLECTION EFFICIENCIES OF RECTANGULAR AEROSOL JETS

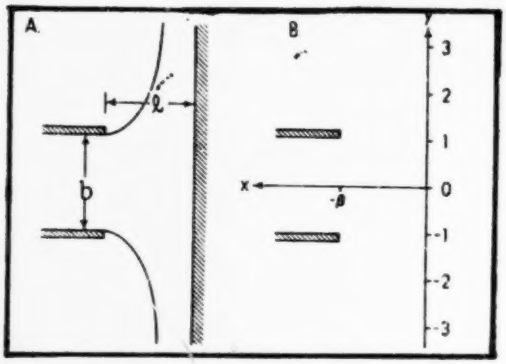

FIGURE 4.6.7-2

TWO-DIMENSIONAL REPRESENTATION OF IMPACTION STAGE. A-SCHEMATIC B-COORDINATE SYSTEM.

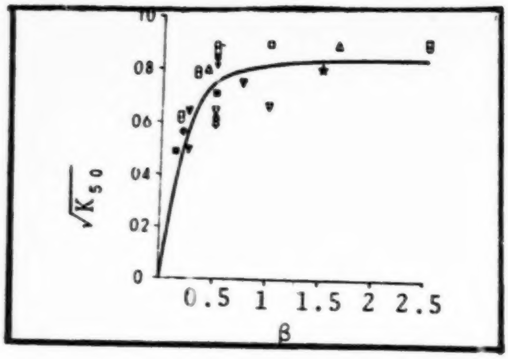

FIGURE 4.6.7-3

CURVES OF $\sqrt{K}$ AT AN EFFICIENCY OF 0.5 AS A FUNCTION OF β. ▼-LASKIN (1949), ●-LUNDGREN (1967), ■-MAY (1945), ◆-STERN ET AL. (1962) *-RANZ AND WONG (1952). AFTER MERCER AND CHOW (1968).

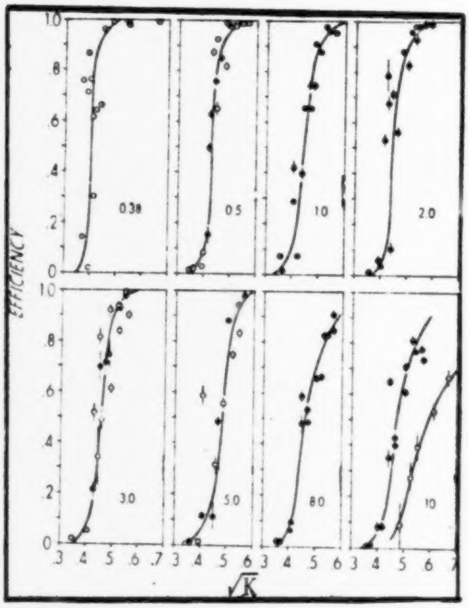

FIGURE 4.6.7-4

EXPERIMENTAL EFFICIENCY CURVES FOR VARIOUS VALUES OF ℓ/b FOR ROUND JETS. MERCER AND STAFFORD (1969)

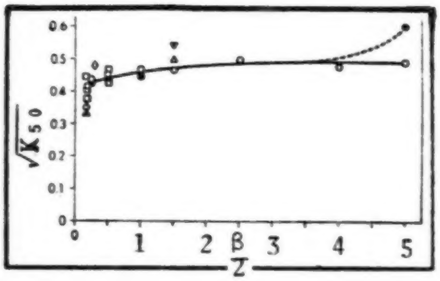

FIGURE 4.6.7-5

EXPERIMENTAL CURVE OF VARIATION OF K_{50} WITH β. AFTER MERCER AND STAFFORD (1969).

o MERCER AND STAFFORD (1969)
Δ STERN ET AL. (1962)
□ MITCHELL AND PILCHER (1958)
◊ ZELLER (1960)
∇ RANZ AND WONG (1952)

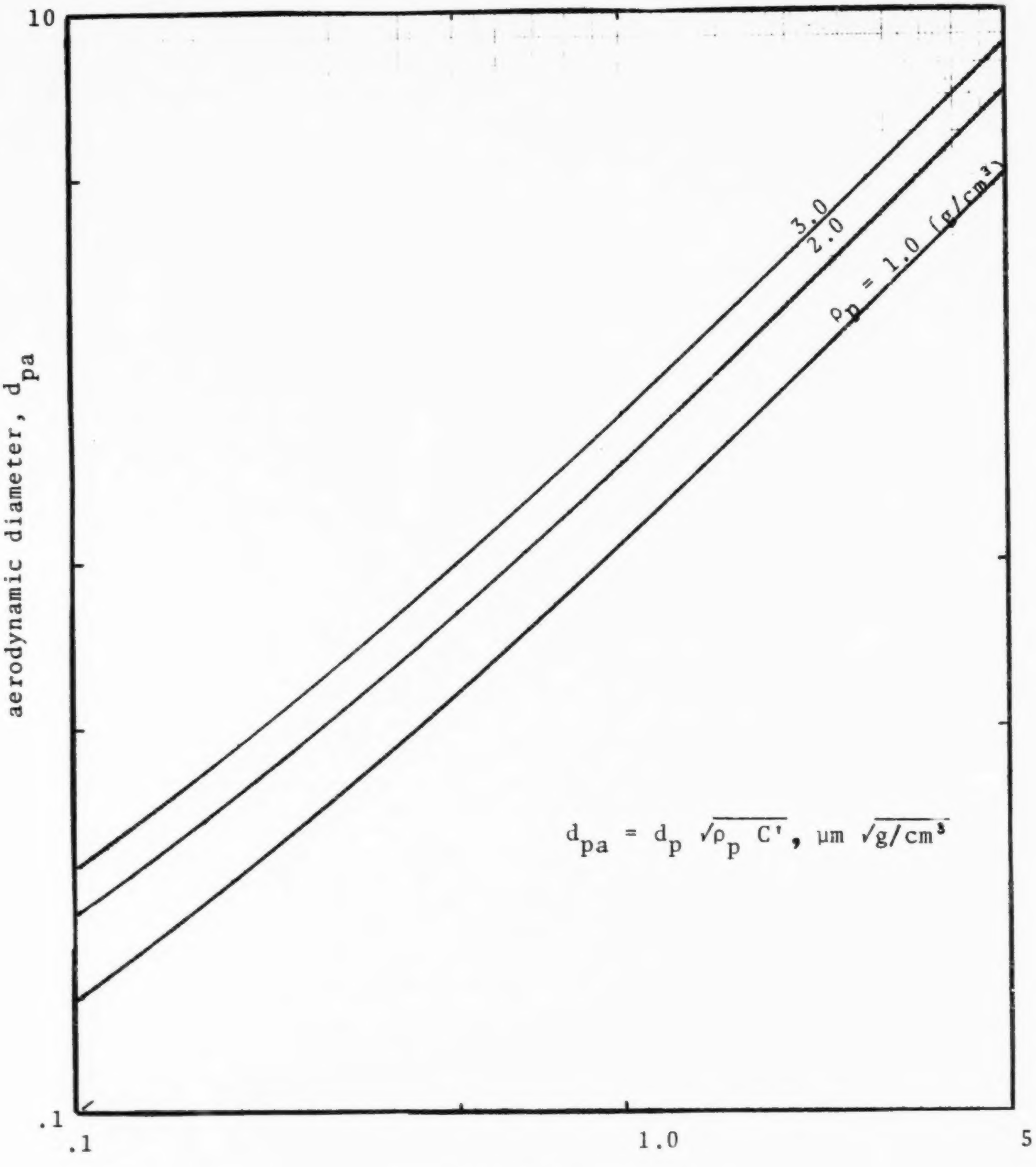

FIGURE 4.6.7-6

AERODYNAMIC DIAMETER VS. PARTICLE DIAMETER WITH PARTICLE DENSITY AS PARAMETER. (Includes C')

SECTION 4.6 NOMENCLATURE

LATIN

a - constant

b - diameter of spherical aerosol cloud influencing collector, m or cm

b - one half width of gas jet, m or cm

B - length of gas jet, m or cm

B_E - particle electrical mobility, $cm^2/(volt\ sec)$

c - mass concentration, Kg/m^3 or g/cm^3

C' - Cunningham correction factor

C_D - drag coefficient

C_p - specific heat, kcal/(kg°C) or cal/(g°C)

d - diameter, m or cm

ds - particle stopping distance, m or cm

d_{p50} - particle diameter collected with 50% efficiency, cm or μm

D - diffusivity, cm^2/sec

e - electronic charge

E - electric field strength, volt/cm

E - device particle collection efficiency

f - friction factor

F - foam density, ratio of clear liquid height to total foam height

F - force, dyne or Newton

g - acceleration of gravity, $9.81\ m/sec^2$ or $981\ cm/sec^2$

h - total foam height above plate, m or cm

h' - heat transfer coefficient, $cal/(sec\ cm^2\ °C)$

k - thermal conductivity, cal/(sec cm °C)

$k \equiv Rg/N = 1.38 \times 10^{-19}\ mbar\ cm^3/°C$, Boltzman constant

SECTION 4.6 NOMENCLATURE

LATIN

K_p - inertial parameter

K_E - electrostatic parameter

K_p - inertia parameter for particle collected with 50% efficiency

ℓ - length, m or cm

ℓ - distance between gas jet and collecting plate, m or cm

ℓ - clear liquid height above plate, m or cm

M - molecular weight, kg/kgmol or g/gmol

n - number concentration, #/cm^3

N - mass flux, kg/(m^{2}sec) or g/(cm^{2}sec)

No - number of ions per unit volume, #/cm

p - partial pressure of solute, m bar or atm

P - total pressure, mbar or atm

q - electric charge, coulombs

q_s - saturation change, coulombs

Q - volumetric flow rate, m^3/sec, cm^3/sec or lit s/sec

r - radius

r - radial distance, m or cm

R - interception parameter

Rg - ideal gas law constant

t - time, sec

T - absolute temperature, °K

u - velocity, m/sec or cm/sec

u_* - friction velocity, m/sec or cm/sec

v - velocity in y direction, m/sec or cm/sec

v - root mean square thermal velocity, m/sec or cm/sec, Equation 4.3.3-19

V - volume, m^3 or cm^3

SECTION 4.6 NOMENCLATURE

LATIN

X - distance in X direction

Y - distance in "Y" direction

y - coordinate

Z - diffusion parameter

DIMENSIONLESS NUMBERS

N_{Sc} $\equiv \mu_G/(\rho_G D_G)$, Schmidt Number

N_{Pe} $\equiv du/D$, Peclet Number

N_{Re} $\equiv \rho du/\mu$, Reynolds Number

GREEK

α - constant

ε - eddy diffusivity, cm^2/sec

ε - relative dielectric constant

ε_o - 8.86×10^{-14} coulomb cm/(cm^{2}volt)

θ - angle, radians

η - efficiency due to a unit mechanism

λ - mean free path of gas molecules, cm or μm

ρ - density, kg/m^3 or g/cm^3

τ - renewal time, sec

τ_o - tangential shear stress, dyne/cm^2

μ - viscosity, g/(cm sec)

ϕ - number of particles collected per centimeter of drop movement, #/cm

ϕ - rate of deposition of a spherical collector, g/cm

ν - kinematic viscosity cm^2/sec

SECTION 4.6 NOMENCLATURE

SUBSCRIPTS

b - bubble

C - centrifugal

c - collector

c - charging electric field

d - drop

D - diffusion

DP - diffusiophoretic

e - exit

E - electrostatic

f - fiber

G - gas phase

G - gravity

h - perforation in plate

i - in

I - Interception

L - liquid phase

o - undisturbed or upstream or bulk

p - particle

P - inertial impaction

s - saturation

t - pipe

tg - tangential

T - thermophoretic

v - vapor

SUPERSCRIPTS

~ - dimensionless quantity

SECTION 4.6 - REFERENCES

Akselrud, G., Zh. Fiz. Khim. 27, 1445, (1953).

Albrecht, F., Physik, Z., 32, 48 (1931).

Best, A., Quart. J. Roy. Met. Soc. 76, 302, (1950).

Bosanquet, C. H., Trans. Inst. Chem. Engrg. (London) 28, 130. Appendix to paper by C. J. Stairmand. (1950)

Chen, C. Y., Eng. Exptl. Sta., University of Illinois, March (1955).

Das, P. K., Indian J. Met. Geophys. 1, 137, (1950).

Davies, C. N., Aylward, M., Proc. Phys. Soc. B64, 889 (1951).

Davies, C. N., Proc. Inst. Mech. Engrg. 1B, 185 (1952).

Davies, C. N., Ann. Occup. Hyg. 8, 239, (1965).

Davies, C. N., Aerosol Science, C. N. Davies editor, 393-446 (1966a)

Davies, C. N., Proc. Royal Soc. A, 289, 235 (1966b)

Demshin, V. Y., Ermakov, G. V., Zhu. Prik. Khim. 38, 691 (1965).

Einstein, A., Ann. Physik. 17, 549 (1905).

Epstein, P., Z. Physik. 54, 537 (1929).

Faith, L. E., Bustany, S. N., Hanson, D. N., and Wilke, C. R., Ind. Eng. Chem. Fund. 6, 519 (1967).

Friedlander, S. K., Johnstone, H. F., Ind. Eng. Chem. 49, 1151 (1957).

Frössling, N., Beitr. Geophys. 52, 170 (1938).

Fuchs, N. A., "The Mechanics of Aerosols", Pergamon Press, New York (1964).

Garner, F., Suckling, R., A.I.Ch.E. Journal 4, 114 (1958).

Garner, F., Keey, R., Chem. Eng. Sci. 9, 119 (1958).

Glauert, M., Aeronautical Research Comm. Report No. 2025 (London), H.M.S.O.

Goldshmid, Y., and Calvert, S., A.I.Ch.E. Journal 9, 352 (1963).

Goldsmith, P. and May, F. G., Aerosol Science, C. N. Davies editor, Academic Press, 163-194 (1966).

SECTION 4.6
REFERENCES

Golovin, M. N., Putnam, A. A., Ind. Eng. Chem. Fund.1, 264 (1962).

Gunn, R., J. Met. 6, 243 (1949).

Hidy, G. M. and Brock J. R., "The Dynamics of Aerocolloidal Systems", Pergamon Press, New York (1970).

Higbie, R. W., Trans. A.I.Ch.E. 31, 365, (1935).

Hocking, L. M., Quart. J. Royal Met. Soc. 85, 44 (1959).

Johnstone, H. F., Roberts, M. H., Ind. Eng. Chem. 41, 2417 (1949).

Kraemer, H. F., Johnstone, H. F., Ind. Eng. Chem. 47, 2426 (1955).

Landt, E., Gasundheits Ing. 77, 139 (1956).

Langmuir, I., O.S.R.P. Report No. 865 (1942).

Langmuir, I., Blodgett, K., Amer. A. F. Tech. Report 5418 (1946).

Langmuir, I., J. Met 5, 175 (1948).

Laufer, J., N.A.C.A. Report 1174, (1954).

Levich, V., Physico-Chem. Hydrodyn. Acad. Sci. USSR, Moscow (1952).

Litvinov, A. T., Zhu. Prik. Khim. 40, 353, (1967).

Lundgren, D. A., J. Air Poll. Cont. Assoc. 17, 225-229 (1967).

Lundgren, D. A., Masters Thesis, University of Minnesota, Minn., (March 1962).

Mercer, T. T., Chow, H. Y., J. of Coll. and Interface Sci. 27, 75-83, (1968).

Mercer, T. T., Stafford, R. G., Am. Occup. Hyg. 12, 41-48 (1969).

Natanson, G. L., Dok. Akad. Nauk. USSR Physical Chem. Sect. 112, 100, English edition, 112, 21 (1957).

Oglesby, Jr., S., and Nichols, G. B., "A Manual of Electrostatic Precipitator Technology", Part 1. Southern Research Institute, p. 75 (1970).

Owen, P. R., Int. J. of Air Pollution 3, 8 (1960).

Pearcy, T., Hill, G. W., Quart. J. Royal Met. Soc. 83, 77 (1957).

Pemberton, C. S., Int. J. Air Pollution 3, 168 (1960).

Perry, R. H., Editor, "Chemical Engineer's Handbook", 4th Edition, McGraw-Hill, N. Y. (1963).

SECTION 4.6
REFERENCES

Picknett, R. G., Int. J. of Air Pollution 3, 160 (1960).

Ranz, W. E., Technical Report No. 8, January 1, University of Illinois, Eng. Exptl. Sta. (1953).

Ranz, W. E., Wong, J. B., Ind. Eng. Chem. 44, 1371-1381 (1952).

Remy, H. and Finnern, H., Z. Inorg. Chem. 159, 241 (1926).

Rober, R., Staub 48, 41 (1957).

Rozen, A. M., Kostin, V. M., Intern. Chem. Eng. 7, 464 (1967).

Schlinger, W. G., Sage, B. H., Ind. Eng. Chem. 45, 657 (1953).

Sehmel, G. A., Schwendiman, L. C., HW-SA-3183, Sept. 18, Hanford Atomic Products Operations, Richland, Washington (1963).

Sell, W., Ver. Deut. Ing. Forschungsheft 347, (1931).

Soo, S. L., "Fluid Dynamics of Multiphase Systems", Blaisdell Publishing Company (1967).

Sparks, L. E., Pilat, M. J., Atmos. Environ. 4, 1 (1970).

Sparrow, E. M., Hixion, C. W., Shavit, G., J. Basic. Eng. 89, 116 (1967).

Stairmand, C. J., J. Inst. Fuel 29, 58 (1956).

Taheri, M., Ph.D. Thesis, Pennsylvania State University (1967).

Taheri, M., Calvert S., J. Air Poll. Contr. Assoc. 18, 240 (1968).

Tietjens, O. G., Applied Hydro- and Aeromechanics, p. 22, Dover Publications, New York (1957).

Torgeson, W. L., Paper J-1057, Applied Science Division, Litton Systems, Inc., St. Paul, Minnesota

Walton, H. W., Woolcock, A., Int. J. Air Pollution 3, 129 (1960).

Whitby, K. T., ASHRAE Journal, September (1965).

Whitby, K. T., Lundgren, D. A., Presented 1964 Ann. Meeting Amer. Soc. of Agric. Engrs., Ft. Collins, Colo. (June 21-24, 1964).

Wong, J. B., Johnstone, J. F., Eng. Exptl. Sta., University of Illinois Tech. Report No. 11, (October 1953).

4.7 EFFECT OF PRESSURE AND TEMPERATURE ON THE COLLECTION OF PARTICLES IN WET SCRUBBERS

The regular operating conditions of wet scrubbers would not lead to high pressures and temperatures. However, operating pressures and temperatures may vary. We shall limit our discussion to pressure variation of 1 to 10 atm. and temperatures of 0 to 100°C.

Changes in temperature and pressure will change the physical properties of the carrier gas, the dust particles and the collecting drops. The vapor pressure of a particle collecting drops will also depend on temperature. Data and equations which predict the changes of these properties with pressure and temperature are discussed in Chapter 10. Here we shall consider the effect these changes have on the different collection mechanisms. Table 4.7-1 presents a summary of the main relationships developed.

In the removal of particles from gas streams, either an external force acting on the particle withdraws it against the resistance of the fluid or the particle is captured by a combination of aerodynamic mechanisms, namely: inertia, interception and diffusion. It is usually assumed that the fluid is in streamline flow as it passes through the gas cleaning equipment. A change in temperature and pressure will change the kinematic viscosity of the gas and thus the Reynolds number. However, as Strauss and Lancaster (1968) pointed out, the assumption of streamline flow can usually be made in the absence of accurate flow behavior data. Thus, for a sphere in steady state motion in the laminar flow region, the fluid resistance "F" is in accordance with Stokes' law:

$$F = \frac{3 \pi \mu_G d_p u}{C'} \tag{4.3.3-1}$$

Both "μ_G" and "C", the gas viscosity and the Cunningham correction factor, are changed when pressure and temperature are changed. This changes the inertial parameter

$$K_p = f\left(\frac{C'}{\mu_G}\right) \tag{4.7-1}$$

Let us now examine the effect of changing air temperature from 0°C to 100°C. An increase in temperature from 0°C to 100°C will increase viscosity from 1.7×10^{-4} to 2.1×10^{-4} poise and C' from 1.148 to 1.215 for 1 μm particles and from 2.67 to 3.5 for 0.1 μm particles. The net effect will be a decrease in "K_p" for particles larger than about 0.1 μm, which are collected by inertial impaction. For particles smaller than 0.1 μm collection by inertia is insignificant. Since the collection efficiency curve is steepest at about $K_p = 1$, the largest decrease in efficiency due to gas temperature increase, will occur there. For higher or lower values of "K_p" where the curve flattens the decrease in efficiency is much smaller. The collection efficiency at higher air temperatures will further decrease, because for air, (N_{Re} at 0°C)/(N_{Re} at 100°C) = 1.83, which means that the flow will tend to be more viscous.

Increasing air pressure from 1 to 10 atm will effect both "K_p" and "N_{Re}". The change in viscosity is negligible ($\approx 2\%$) but the change in gas density will increase "N_{Re}", thus increasing collection efficiency. For particles larger than 0.3 µm in diameter, the exponential part of the Cunningham correction factor can be neglected. Thus increasing pressure ten times has the same effect on the Cunningham correction factor as increasing particle diameter ten times, and particles of 0.1 µm have the same correction factor at 10 atm as particles of 1 µm at 1 atm pressure. The decrease of the Cunningham correction factor with pressure, about 14% for a 1 µm particle, decreases "K_p", and collection efficiency. The net effect of the increase in pressure should be evaluated each time, to find which weighs more heavily, the increase in the Reynolds number or the decrease in "K_p".

Some examples of the effects of temperature and pressure on "K_p" for several particle diameters are as follows:

d_p (µm)	0.5	1.0	5.0
K_p @100°C, 1 atm/K_p @0°C, 1 atm	1.02	0.94	0.81
K_p @0°C, 10 atm/K_p @0°C, 1 atm	0.79	0.91	1.0

Since target efficiency is a function of "K_p" and "N_{Re}", one can estimate the effect of changes in pressure and temperature on collection efficiency through these ratios of "K_p" and Figure 4.6.2-2.

Interception is a function of the relative diameters of the particle to the drop and of the flow field, which in turn, is a function of Reynolds number. The relative diameters are not influenced by changes in pressure and temperature but the flow field is. The effect of increased pressure and temperature on "N_{Re}" was already discussed, and the effect on collection efficiency depends on the particular flow regime.

For collection by diffusion, the effect of temperature increase from 0°C to 100°C, is only on the diffusivity. From the Einstein equation:

$$D_p = \frac{C' \, k \, T}{3 \, \pi \, \mu_G \, d_p} \qquad (4.3.3\text{-}13)$$

for a $d_p = 0.01$ µm particle in air, $D_{p0°C} = 0.69 \, D_{p100°C}$ and for $d_p = 0.1$ µm in air $D_{p0°C} = 0.69 \, D_{p100°C}$.

As we have seen before, the effect of change in temperature on the Reynolds number is small. Thus the total effect of temperature increase on diffusivity, is to increase collection efficiency in the particle size range where collection by diffusion is the major collection mechanism.

The effect of pressure increase on collection by diffusion comes through its effect on "D_p" and Reynolds number. The diffusion coefficient

$$D_p = f\left(\frac{C'}{\mu_G}\right) \qquad (4.7\text{-}2)$$

which is the same dependence found for "K_p". An increase in pressure will decrease the diffusivity leading to a decrease in collection efficiency.

Figure 4.7-1 shows the change in the rate of particle collection by diffusion due to changes in pressure, temperature, and particle size. The curve was calculated for the collection by a 200 μm diameter water drop falling through an aerosol cloud at its final settling velocity. The number collected was calculated from Equation 4.6.2-20 and diffusivity from the Einstein equation. The figure shows clearly the effect of operating conditions on collection efficiency for different size aerosols.

In those cases when the collection of particles is due to additional forces like electrostatic, thermophoretic etc., a material balance leads to the equation:

$$E = 1 - \exp\left[-\frac{A}{Q_G} u_T\right] \qquad (5.3.5\text{-}23)$$

This equation is derived by assuming that the distance a particle travels in one second due to the additional force, which is numerically equal to "u_T" is smaller than the drop radius. Here "A" is the total collection area and "Q_G" the volumetric flow rate of the gas stream. For $d_p/2 > \lambda$, Epstein's (1929) theory shows for thermophoretic velocity an expression given in Equation 4.3.3-27. The modification of the group $(k_G)/(2k_G + k_p)$, by Brock (1962), which gives better agreement for high thermal conductivity particles, makes little difference to the change with pressure. The thermal velocity dependence on temperature is:

$$u_T = f\left[\frac{C' \mu_G}{\rho_G T}\left(\frac{1}{2 + \frac{k_p}{k_G}}\right)\right] \qquad (4.7\text{-}3)$$

The value of (k_p/k_G) varies with particle material and the composition of the carrier gas. In most cases, the effect of a change in temperature or pressure on the ratio (k_G/k_p) is small and we will not consider it. If we assume the gas obeys the ideal gas law over the range discussed, then at a constant pressure $\rho_G T$ = constant. Thus to a first approximation, the thermophoretic velocity changes with temperature proportionally with $C' \mu_G$. For particles 1 μm in diameter and larger ($u_{T0°C} \simeq 0.765\, u_{T100°C}$), for $d_p = 0.1$ μm, $u_{T0°C} \simeq 0.62\, u_{T100°C}$ and for $d_p = 0.01$ μm, $u_{T0°C} \simeq u_{T100°C}$. A decrease in operating temperature will usually decrease collection efficiency due to thermal forces. As always, one should also consider the changes in the Reynolds number.

The effect of pressure increase will be to change the gas density, and the Cunningham correction factor. The smaller the particle, the larger will be the effect. For $d_p = 0.1$ μm, $u_{T(1\,atm)} = 23\, u_{T(10\,atm)}$ and for $d_p = 0.01$ μm, $u_{T(1\,atm)} = 75\, u_{T(10\,atm)}$, $N_{Re(1\,atm)} = 0.1\, N_{Re(10\,atm)}$. One should expect a decrease in collection efficiency with an increase in operating pressure.

Equation 4.3.3-27 above was used to calculate the thermophoretic velocity for various temperature gradients. Results are shown in Figure 4.7-2, a plot of thermophoretic velocity vs. temperature gradient. The temperature gradient, between the air and the collecting water drop, was estimated from the heat transfer equations:

$$q = h'A \, \Delta T = A \, k \frac{dT}{dX} \quad (4.7\text{-}4)$$

and

$$\frac{dT}{dX} = \frac{h' \Delta T}{k} \quad (4.7\text{-}5)$$

for evaporating drops when $N_{Red} < 20$, $h = 2 \, k/d_d$ (for $N_{Red} > 20$ the coefficient "2" will become higher, so that higher temperature gradient for the same temperature difference, would be realized.)

$$\frac{dT}{dX} = \frac{2 \, k \, \Delta T}{d_d \, k} = \frac{2\Delta T}{d_d} \quad (4.7\text{-}6)$$

Assuming the same drop diameter as before, $d_d = 200$ µm, we get:

$$\frac{dT}{dX} = \frac{\Delta T}{10^{-2}} \quad (°C/cm) \quad (4.7\text{-}7)$$

Calculations were carried out for water temperatures of 0°C and 50°C. "k_p/k_G" was assumed equal to 10, which is a representative figure for most non-conductive liquid and solid particles, when the gas is air. To calculate "C'" the Cunningham correction factor, particle diameters of 1 µm and 0.1 µm were assumed.

After the thermophoretic velocity has been calculated, the collection efficiency by a spray, or for that purpose by a shower of rigid spheres, could be estimated, if the ratio of A/Q_G sec/cm, - the ratio of total collection area to the gas volumetric flow rate, is known. Figures 4.7-3 and 4.7-4 are such curves for 1 µm and 0.1 µm diameter particles at 0°C and 1 atm. It is interesting to note that for a constant 1°C temperature difference a collection efficiency of about 50% for 0.1 µm particles and $A/Q_G = 12$ sec/cm is realized. The collection efficiency on 1 µm particles under the same conditions is about to 10%.

In an electric field, one or several of the forces discussed in Chapter 4 may be involved, depending on the operating conditions. In all cases, an increase in temperature will effect the electrical migration velocity through:

$$u_E = f\left(\frac{C'}{\varepsilon \, \mu_G}\right) \quad (4.7\text{-}8)$$

The effect of temperature on the dielectric constant of the gas "ε" is small and can be neglected. Then the effect is the same as for inertial collection. For $d_p > 0.1$ µm an increase in temperature will decrease collection efficiency, and for $d_p \leq 0.1$ µm an increase in temperature will increase collection efficiency.

The effect of pressure on the electrostatic forces is through:

$$u_E = f\left(\frac{C'}{\varepsilon\ \mu_G}\right) \qquad (4.7\text{-}9)$$

The dielectric constant does not change much as pressure increases from 1 to 10 atm. The major effect remains the decrease in the Cunningham correction factor and the increase in the Reynolds number. An increase in pressure will decrease electrostatic collection efficiency.

Figure 4.7-5 predicts the velocity of a charged particle in an electric field of a given strength. The charge on the particles was assumed to be the saturation charge in a field of the same strength as the collecting field, and was calculated from the equation for conducting particles.

$$q_s = \frac{7.54}{4} \times 10^{19}\ \pi\ d_p^{\,2}\ \varepsilon_0\ E_c \qquad (4.3.3\text{-}15)$$

where "d_p" is in cm, "E_c" is the strength of the charging field in volt/cm, "q_s" is in coulombs, the particle velocity was calculated from:

$$u_E = \frac{q_s\ E\ C'\ 10^7}{3\ \pi\ \mu_G\ d_p} \quad (\text{cm/sec}) \qquad (4.3.3\text{-}21)$$

where "E" is the value of the ambient electric field in the collection zone in volts/cm. To estimate the Cunningham correction factor a particle diameter of 1 μm was assumed.

The centrifugal force is also influenced by changes in operating pressure and temperature. Since cyclones usually operate at high Reynolds numbers, the effect of the change in the Reynolds number can be neglected. Sproull (1970) suggested that Equation 5.3.5-23 where "w" is the particle radial velocity, can be used to predict collection efficiency. In cyclones, Sproull says:

$$E = 1 - \exp\left[\frac{A}{Q_G}\ w\right] \qquad (5.3.5\text{-}23)$$

$$w = \frac{\rho_p\ d_p^{\,2}\ u_{ptg}^{2}}{9\ \mu_G\ d_c} \qquad (4.7\text{-}10)$$

where "u_{ptg} is the particle tangential velocity.
Since cyclones are used for particles larger than a few microns the Cunningham correction factor can be neglected and:

$$w = f\left(\frac{1}{\mu_G}\right) \qquad (4.7\text{-}11)$$

An increase in operating temperature decrease collection efficiency and an increase in operating pressure will have a negligible effect on collection efficiency.

Figure 4.7-6 shows the effect of operating conditions on the radial velocity in a cyclone type device. The radial velocity was calculated from Equation 4.7-10 for 1 μm diameter particles and a 100 cm diameter cyclone.

The total effect of diffusiophoresis for ($d_p > \lambda$) is given by:

$$u_{DP} = \frac{\sqrt{m_V}}{\frac{p_V}{P}\sqrt{m_V} + \frac{p_G}{P}\sqrt{m_G}} \frac{D_{VG}}{p_G} \frac{dp_V}{dX} \qquad (4.3.3\text{-}32)$$

This equation holds within 10% for particles up to about 1 μm in diameter. The effect of temperature comes mainly through "Δp_V" the difference between vapor pressure of the condensing liquid in the gas and the equilibrium vapor pressure on the collecting drop surface. Because of the way the vapor pressure curve changes with temperature, "Δp_V" will be larger for higher temperature and the same "ΔT" and an increase in operating temperature will lead to an increase in collection efficiency.

The effect of pressure is mainly through the total pressure, "P", and an increase in pressure will lead to a decrease in collection efficiency.

Figures 4.7-7 and 4.7-8 show the diffusiophoretic velocity for an assumed vapor pressure gradient, and the corresponding temperature gradient between water drops and aerosol. The difference between the two curves stems from the characteristics of the water vapor pressure temperature curve. The gradients were calculated by assuming $\Delta x = R$, Perry (1950). Based on diffusiophoretic velocities, collection efficiencies were calculated using "A/Q_G" as a parameter and are shown in Figures 4.7-9, 4.7-10, 4.7-11, and 4.7-12 as a function of vapor pressure gradient and temperature gradient, respectively. These curves were also plotted twice for each water temperature, once as a function of vapor pressure gradient and once as a function of temperature gradient. It is interesting to note that by raising water temperature from 0°C to 25°C the collection efficiency for A/Q_G = 12 sec/cm rose from ≈52% to ≈64% and the effect will be much larger when we compare efficiencies at water temperatures of 50°C and 25°C. However, it should not be forgotten that the higher the temperature the larger will be the volume of the gas processed and the larger will be the fraction of the water vapor in the gas.

TABLE 4.7-1

EFFECT OF INCREASE IN TEMPERATURE FROM 0°C to 100°C AND PRESSURE FROM 1 TO 10 atm ON COLLECTION EFFICIENCY.

Collection Mechanism	f (T)	Effect of an increase in Temperature on Collection Eff.	f (P)	Effect of increase in Pressure on Collection Eff.
Inertial	$K_p = f\left(\frac{C'}{\mu_G}\right)$	decrease collection eff. for $d_p > 0.1$ μm; max. effect when $K \simeq 1.0$	$K_p = f\left(\frac{C'}{\mu_G}\right)$	decrease collection eff. when N_{Re} effect is small
Interception	$N_{Re0} \simeq 1.8 N_{Re100}$	depends upon N_{Re} regime	$N_{Re1} \simeq 0.1 N_{Re10}$	depends upon N_{Re} regime
Diffusion	$D_p = f\left(\frac{C'T}{\mu_G}\right)$	increase in diffusivity of over 30% when $d_p < 0.1$ μm	$D_p = f\left(\frac{C'}{\mu_G}\right)$	decrease collection eff. when N_{Re} effect is small
Thermal	$u_T = f\left[\frac{C'\mu_G}{\rho_G T}\left(\frac{1}{2+\frac{k_p}{k_G}}\right)\right]$	increase collection eff.: for $d_p > 1\mu m: v_o \simeq 0.77 v_{100}$ for $d_p = 0.1\mu m: v_o \simeq 0.62 v_{100}$ for $d_p = 00.1\mu m: v_o \simeq 0.56 v_{100}$	$u_T = f\left[\frac{C'\mu_G}{P_G}\left(\frac{1}{2+\frac{k_p}{k_G}}\right)\right]$	decrease collection eff. for $d_p = 0.1\mu m: v_1 \simeq 23 v_{10}$ for $d_p = 00.1\mu m: v_1 = 75 v_{10}$
Electrostatic	$u_E = f\left(\frac{C'}{\varepsilon\,\mu_G}\right)$	decrease collection eff. for $d_p > 0.1\mu m$; increase eff. for $d_p \leq 0.1\mu m$	$u_E = f\left(\frac{C'}{\varepsilon\,\mu_G}\right)$	decrease collection eff.
Centrifugal	$w = f\left(\frac{1}{\mu_G}\right)$	decrease collection eff.		negligible effect
Diffusiophoresis	$u_{DP} = f\left(\frac{D_{vG}}{P_G}\frac{dp}{dx}\right)$	increased collection eff.	$u_{DP} = f\left(\frac{D_{vG}}{P_{vG}}\right)$	decrease collection eff.

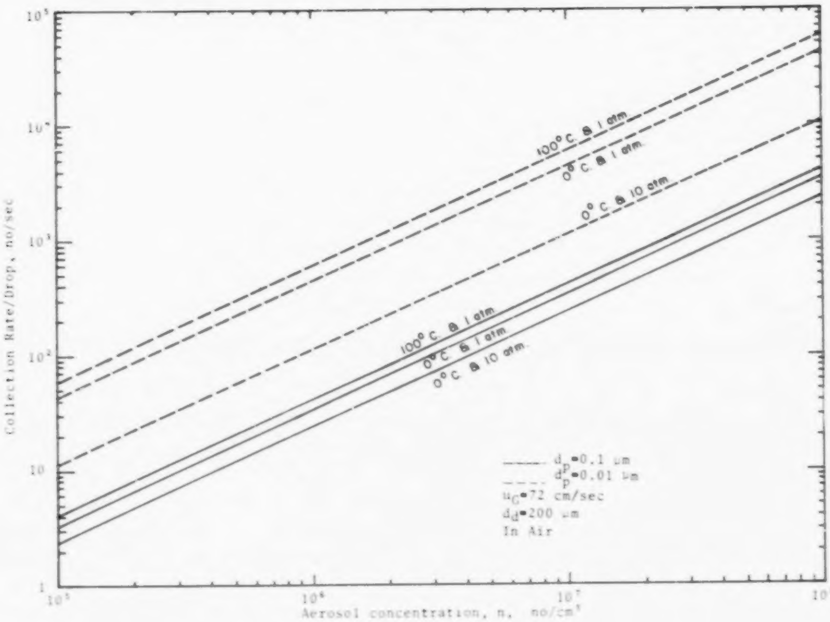

FIGURE 4.7-1

RATE OF COLLECTION OF AEROSOL PARTICLES BY DIFFUSION AT DIFFERENT OPERATING CONDITIONS

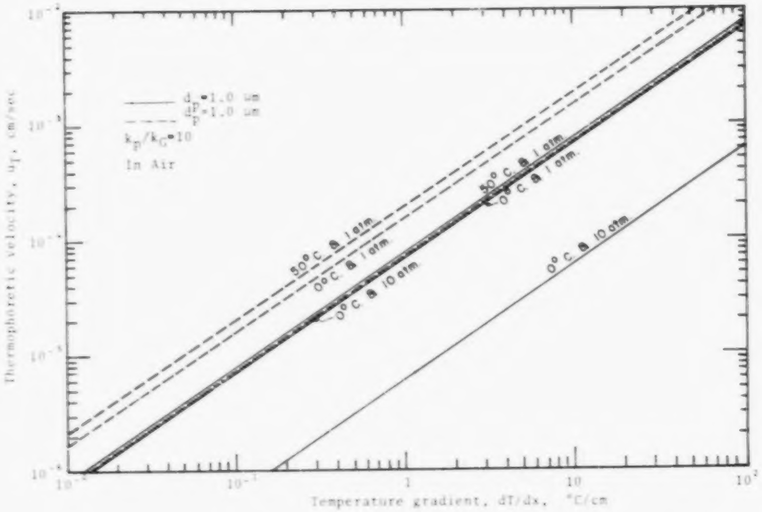

FIGURE 4.7-2

THERMOPHORETIC VELOCITY AS A FRACTION OF TEMPERATURE GRADIENT FOR DIFFERENT OPERATING CONDITIONS

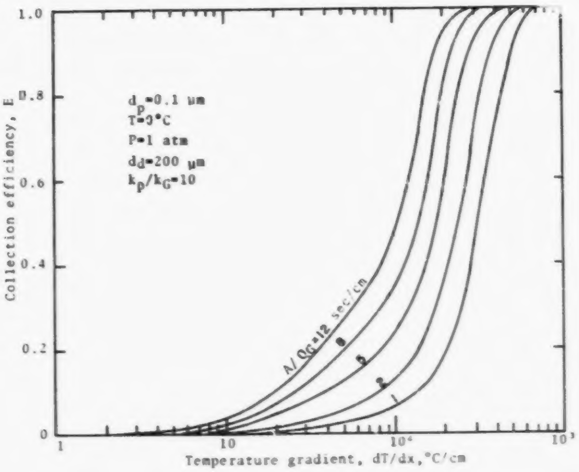

FIGURE 4.7-3

COLLECTION EFFICIENCY OF AEROSOL PARTICLES BY SPHERES DUE TO THERMOPHORESIS AT DIFFERENT A/Q_G RATIOS

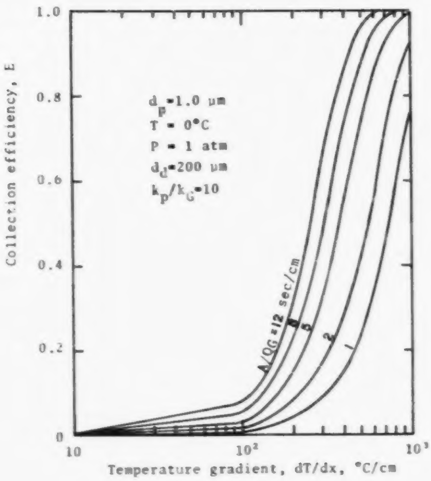

FIGURE 4.7-4

COLLECTION EFFICIENCY OF AEROSOL PARTICLES BY SPHERES DUE TO THERMOPHORESIS AT DIFFERENT A/Q_G RATIOS

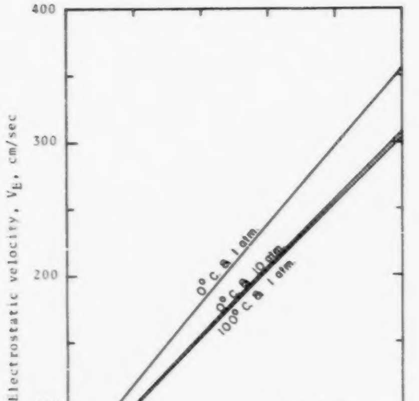

FIGURE 4.7-5

ELECTROSTATIC VELOCITY AT DIFFERENT ELECTRIC FIELD STRENGTHS AND DIFFERENT OPERATING CONDITIONS

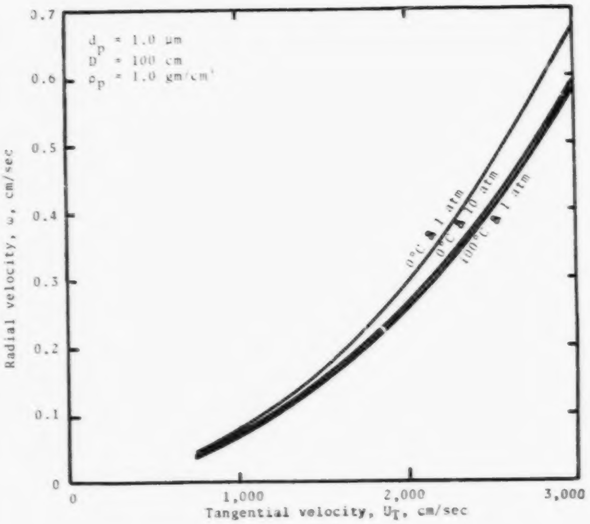

FIGURE 4.7-6

RADIAL VELOCITY IN A CENTRIFUGAL COLLECTOR OF DIAMETER "D" AT DIFFERENT TANGENTIAL VELOCITIES AND OPERATING CONDITIONS

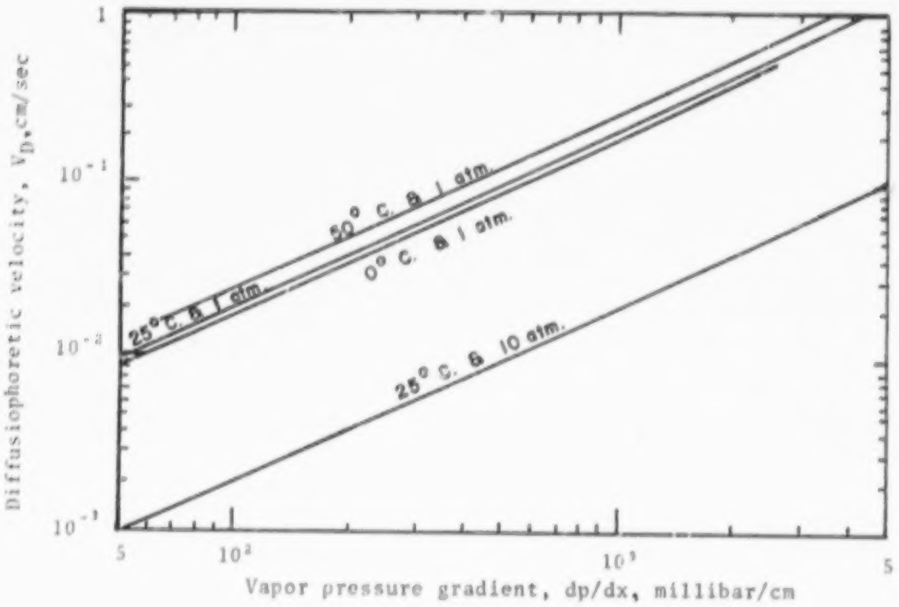

FIGURE 4.7-7

DIFFUSIOPHORETIC VELOCITY OF AEROSOL PARTICLES IN AIR SATURATED WITH WATER VAPORS AT DIFFERENT OPERATING CONDITIONS

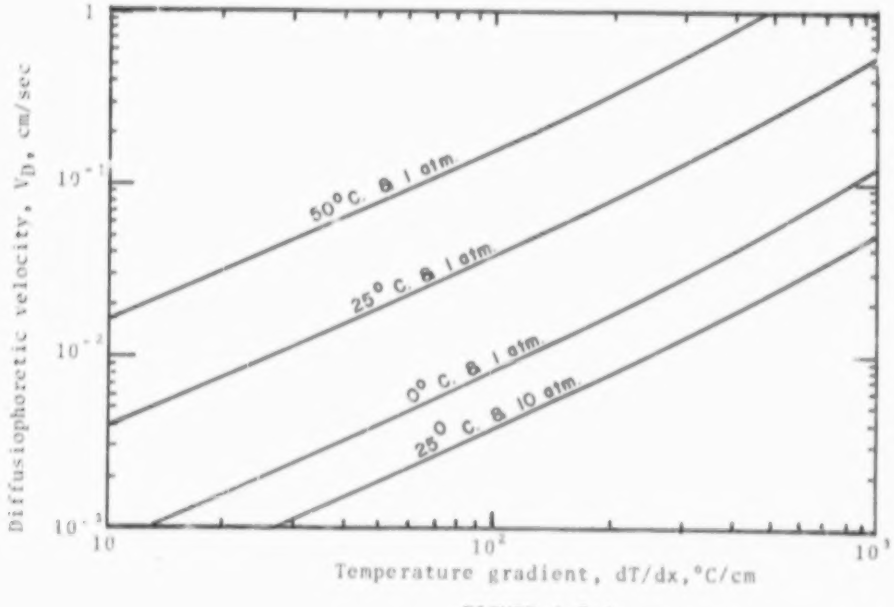

FIGURE 4.7-8

DIFFUSIOPHORETIC VELOCITY OF AEROSOL PARTICLES IN AIR SATURATED WITH WATER VAPORS AT DIFFERENT OPERATING CONDITIONS

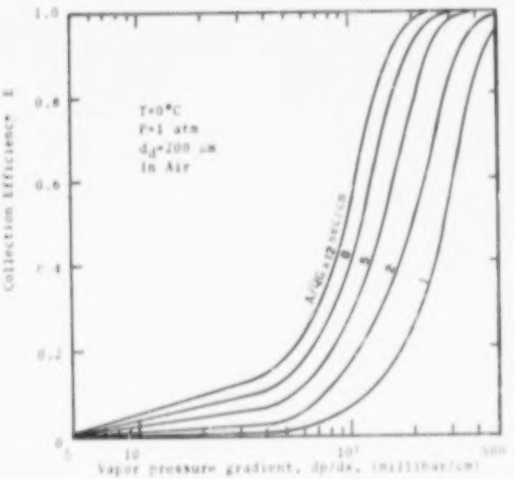

FIGURE 4.7-9

COLLECTION EFFICIENCY OF AEROSOL PARTICLES BY LIQUID DROPS DUE TO DIFFUSIOPHORESIS AT DIFFERENT A/Q_G RATIOS

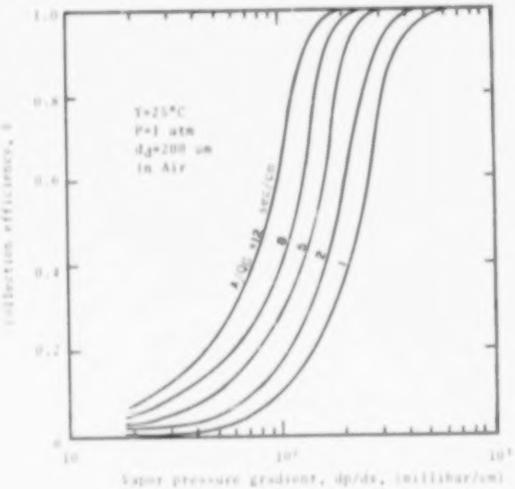

FIGURE 4.7-10

COLLECTION EFFICIENCY OF AEROSOL PARTICLES BY LIQUID DROPS DUE TO DIFFUSIOPHORESIS AT DIFFERENT A/Q_G RATIOS

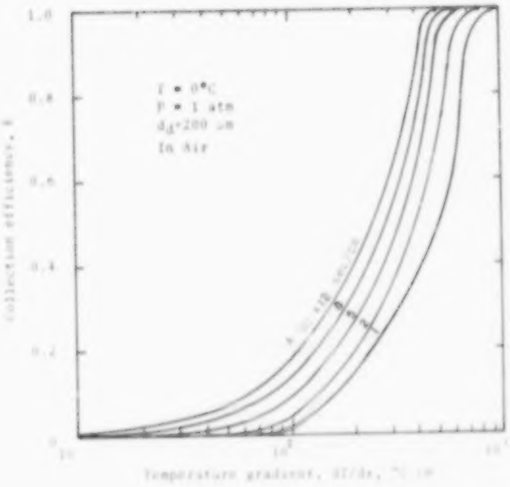

FIGURE 4.7-11

COLLECTION EFFICIENCY OF AEROSOL PARTICLES BY LIQUID DROPS DUE TO DIFFUSIOPHORESIS AT DIFFERENT A/Q_G RATIOS

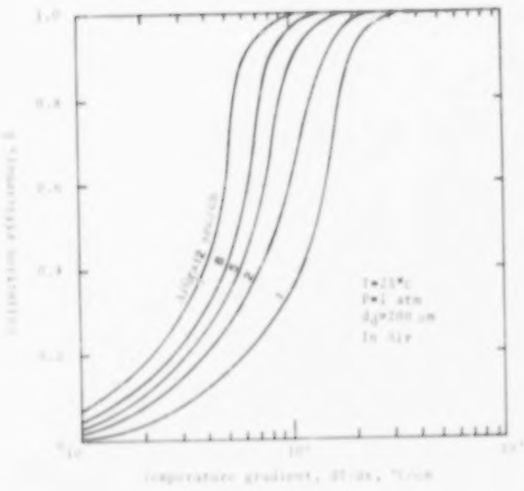

FIGURE 4.7-12

COLLECTION EFFICIENCY OF AEROSOL PARTICLES BY LIQUID DROPS DUE TO DIFFUSIOPHORESIS AT DIFFERENT A/Q_G RATIOS

SECTION 4.7 NOMENCLATURE

LATIN

A - area cm^2

C' - Cunningham correction factor

d - diameter, m or cm

D - diffusivity, cm^2/sec

E - electric field strength, volt/cm

E - overall plate efficiency

F - force, dyne or Newton

h' - heat transfer coefficient, cal/(sec cm^2 °C)

k - thermal conductivity, cal/(sec cm °C)

k $\equiv$ $Rg/N = 1.38 \times 10^{-19}$ mbar cm^3/°C, Boltzman constant

K_p - inertia parameter

m - ionic or molecular mass ($mN = M$)

p - partial pressure of solute, mbar or atm

P - total pressure, mbar or atm

q - electric charge, coulombs

q - heat flux, cal/(sec cm^2)

q_s - saturation change, coulombs

Q - volumetric flow rate, m^3/sec, cm^3/sec or lits/sec

T - absolute temperature, °K

u - velocity, m/sec or cm/sec

X - distance in X direction

GREEK

ε - relative dielectric constant

ε_o - 8.86×10^{-14} coulomb cm/(cm^{2}volt)

λ - mean free path of gas molecules, cm or µm

SECTION 4.7 NOMENCLATURE

GREEK

ρ - density, kg/m^3 or g/cm^3

μ - viscosity, g/(cm sec)

SUBSCRIPTS

c - collector

c - charging electric field

d - drop

DP - diffusiophoretic

E - electrostatic

G - gas phase

G - gravity

p - particle

s - saturation

tg - tangential

T - thermophoretic

v - vapor

CHAPTER 5

DESIGN METHODS

TABLE OF CONTENTS

5.1 Introduction 5-4
  5.1.1 General Approach. 5-4
  5.1.2 New Developments. 5-4
  5.1.3 Empirical Approach. 5-5
  References. 5-7

5.2 Mass Transfer. 5-8
  5.2.1 Computation Methods 5-8
    5.2.1.1 Stage Processes. 5-8
    5.2.1.2 Continuous Contacting. 5-10
  5.2.2 Plate Column Scrubbers. 5-15
    5.2.2.1 Unit Mechanisms. 5-16
    5.2.2.2 Column Diameter. 5-16
    5.2.2.3 Pressure Drop. 5-19
    5.2.2.4 Column Height. 5-25
  5.2.3 Packed Column Scrubbers 5-28
    5.2.3.1 Unit Mechanisms. 5-28
    5.2.3.2 Column Diameter. 5-29
    5.2.3.3 Pressure Drop. 5-33
    5.2.3.4 Column Height. 5-33
    5.2.3.5 Other Design Considerations. 5-36
  5.2.4 Fibrous-Packed Scrubbers. 5-38
    5.2.4.1 Unit Mechanisms. 5-38
    5.2.4.2 Column Diameter. 5-39
    5.2.4.3 Pressure Drop. 5-39
    5.2.4.4 Height of Column (Mass Transfer) 5-40
    5.2.4.5 Other Operating Characteristics. 5-40
  5.2.5 Pre-Formed Sprays 5-42
    5.2.5.1 Unit Mechanisms. 5-42
    5.2.5.2 Sizing 5-43
    5.3.5.3 Pressure Drop. 5-44
    5.2.5.4 Mass Transfer. 5-44
    5.2.5.5 Other Design Considerations. 5-46
  5.2.6 Gas-Atomized Sprays 5-46
    5.2.6.1 Unit Mechanisms. 5-48
    5.2.6.2 Mass Transfer. 5-48
  5.2.7 Centrifugal Devices 5-52
    5.2.7.1 Unit Mechanisms. 5-54
    5.2.7.2 Mass Transfer. 5-54
  5.2.8 Moving Bed Scrubbers. 5-54
  Nomenclature. 5-70
  References. 5-75

5.3 Particle Separation. 5-81
  5.3.1 General Computational Method. 5-81
    5.3.1.1 Difficulty of Separation.. 5-81
    5.3.1.2 Scrubber Capability. 5-82
    5.3.1.3 Size-Penetration Integration 5-83

CHAPTER 5
TABLE OF CONTENTS

5.3.1.4 Analytical Solutions 5-83
5.3.2 Particle Collection in Plate Type Scrubbers 5-83
5.3.2.1 Introduction 5-83
5.3.2.2 Wet Impingement. 5-84
5.3.2.3 Sieve Plate Columns. 5-87
5.3.3 Particle Collection in Massive Packing Scrubbers. 5-89
5.3.3.1 Principle of Operation 5-89
5.3.3.2 Particle Collection Efficiency 5-89
5.3.3.3 Pressure Drop 5-92
5.3.4 Particle Collection in Fiber Beds. 5-93
5.3.4.1 Principle of Operation 5-93
5.3.4.2 Particle Collection Efficiency in Beds of Fibers 5-94
5.3.4.3 Determination of the Solidarity Factor, S. 5-94
5.3.4.4 Determination of Single Fiber Efficiency . 5-94
5.3.4.5 Overall Efficiency of a Bed of Fibrous Packing. 5-97
5.3.4.6 Pressure drop 5-97
5.3.5 Collection of Particles by Devices Employing Preformed sprays. 5-101
5.3.5.1 Introduction. 5-101
5.3.5.2 Spray Nozzles 5-102
5.3.5.3 Spray Chambers. 5-108
5.3.5.4 Ejector Venturi 5-113
5.3.6 Particle Collection in Gas Atomized Spray Scrubbers 5-117
5.3.6.1 Principle of Operation. 5-117
5.3.6.2 Particle Collection Efficiency 5-117
5.3.6.3 Pressure Drop 5-122
5.3.7 Particle Collection in Centrifugal Scrubbers 5-123
5.3.7.1 Principle of Operation. 5-123
5.3.7.2 Particle Collection by Centrifugal Force. .5-123
5.3.7.3 Particle Collection by Sprays 5-126
5.3.7.4 Particle Collection by Both Centrifugal Force and Sprays 5-127
5.3.7.5 Pressure Drop in a Centrifugal Scrubber . .5-128
5.3.7.6 Other Factors Influencing the Performance of Centrifugal Scrubbers 5-128
5.3.8 Baffled and Secondary Flow Scrubbers 5-131
5.3.8.1 Baffle Type Collectors. 5-131
5.3.8.2 Secondary Flow Collectors 5-133
5.3.9 Impingement and Entrainment. 5-136
5.3.10 Mechanically Aided Particle Separations. 5-142
5.3.11 Moving Bed Scrubbers 5-154
5.3.11.1 Mobile Bed Scrubbers. 5-154
5.3.11.2 Fluidized Bed Scrubbers 5-155
Nomenclature 5-198
References 5-203

CHAPTER 5
TABLE OF CONTENTS

5.4 Scrubbed Liquid Entrainment Separators 5-209
  5.4.1 Introduction. 5-209
  5.4.2 General 5-209
  5.4.3 Gravity Settlers. 5-209
  5.4.4 Knitted Wire Mesh Entrainment Separators. 5-210
  5.4.5 Other Impingement Type Entrainment Separators 5-211
  5.4.6 Centrifugal Separators. 5-212
  Nomenclature 5-214
  References. 5-216

CHAPTER 5

DESIGN METHODS

5.1 INTRODUCTION

5.1.1 GENERAL APPROACH

Most of what needs to be said about the general approach to scrubber design has been given in previous chapters and will not be repeated at length here. Chapter 5 addresses itself to design methods but it applies as well to the selection of scrubbers for purchase, the improvement of existing systems, and the organization of research concepts. All of these activities are best served by an understanding of basic principles and the application of them to the problem.

If, for example, it is necessary to check out a manufacturer's claims for a scrubber of unusual design and for which no published data exist, you can develop an estimate of what could reasonably be expected. Knowing how and why things happen at the microscopic level (Chapter 4), you can build your own performance equation(s) and chart(s) from scratch. By studying the available information on the scrubber, you can decide what unit mechanism(s) are involved, or might be. Then you can predict the probable performance due to these mechanisms and see whether the predictions agree in magnitude and functionality (i.e., dependence on flow rate, particle properties, solubility, etc.) with the manufacturer's claims.

5.1.2 NEW DEVELOPMENTS

Chapter 5 gives numerous examples of "designing from scratch", based on the unit mechanisms approach. Many of the equations and charts are the result of new developments made in the present study and many others represent improvements upon existing methods. Table 5.1.2-1 indicates which sections contain methods which are new, improved, or about as-found in the literature.

TABLE 5.1.2-1

GENERAL ORIGINS OF DESIGN METHODS IN CHAPTER 5

As Found in Literature	Improved in This Study	New in This Study
5.2.1	5.3.2.3	5.2.5
5.2.2	5.3.3	5.2.6
5.2.3	5.3.4	5.3.1
5.2.4	5.3.5 some	5.3.2.2
5.2.7	5.3.6	5.3.5 some
5.2.8	5.3.7	5.3.9
5.3.8	5.4.4	5.3.10
5.3.11		
5.4 most		

5.1.3 EMPIRICAL APPROACH

In the scrubber field, frequent mention is made of the "power law" and many of the people contacted in the surveys of users and manufacturers have asked questions about its utility. The power law is the outgrowth of the observation by Lapple and Kamack (1955) that particle collection efficiency in spray-type scrubbers was mainly determined by pressure drop for the gas plus any power expended in atomizing the liquid.

Further embellishment by Semerau et al. (1958) and Semerau (1960) set forth a relationship between number of dust transfer units and the power input to the scrubber. Dust transfer units are defined by analogy to mass transfer with chemical reaction, where there is no equilibrium vapor pressure above the liquid, and is the same as the negative logarithm of penetration. The relationship is by no means unique, however, and the number of transfer units for a given value of contacting power (usually H.P./M.C.F.M.) or visa-versa, varies over nearly an order of magnitude. For example, at 2.5 transfer units ($Pt = 0.082$), the contacting power ranges from about 0.8 to 10.0 H.P./M.C.F.M., depending on the scrubber and the particulate.

For given scrubber and particulate properties there will usually be a very distinct relationship between dust transfer units and contacting power. Thus the power law is a very convenient way of correlating experimental data for a particular situation. It can be shown (Calvert and Taheri, 1966, and Calvert, 1968) that there is a theoretical basis for such a relationship for any type of scrubber (not just sprays) when the major collection mechanism is inertial impaction. In Section 5.3.6 it is further shown why the power law fits venturi scrubbers even though drop size is variable with flow rates.

While the power function relationship indicated by a straight line when $\ln(Pt)$ is plotted against H.P./M.C.F.M. or against "ΔP" on log-log paper can represent what has been observed, it can not be used to predict what will happen except for the identical conditions. In order to predict collection efficiency for any particle size and various scrubber configurations and operating conditions, it is necessary to use a more accurate representation of the collection mechanism.

Section 5.3.1 presents a general approach to estimating particle collection performance which is based on more proper parameters to define the difficulty of separation of a given size dust and the capability of the scrubber. If one wishes to make the proper analogy to mass transfer units, he should use a parameter which involves both the change in composition and the driving force. For particle separation, the driving force, or measure of the tendency for transfer, depends on particle properties and the change in composition is analogous to the fraction of particles removed.

For example, it is more difficult to separate 0.5 μm particles at 90% efficiency than 5.0 μm particles at the same efficiency, just as it would be more difficult to scrub out 90% of the SO_2 in a gas stream by means of a limited amount of water than by means of a lot of NaOH solution.

As will be shown, the difficulty of separation is better described by the "separation cut diameter" than by overall penetration required (i.e., dust transfer units).

So far as applying the power law to mass transfer is concerned, there is little hope that this could have more than limited correlative use (see Section 5.2.6). The essential problem is that while inertial separation depends on an abrupt change in gas flow direction and this implies an energy loss, diffusional transfer does not require a significant momentum loss. In other words, a high mass transfer rate can be obtained if enough transfer surface is provided, even though the flow rate and mass transfer coefficient were very low. Equipment size can be traded off against power cost.

SECTION 5.1 - REFERENCES

Calvert, S. C., Taheri, M., Brit. Chem. Eng. 43, 254 (1966).

Lapple, C. E., Kamack, H. J., Chem. Engr. Progr. 51, 110 (1955).

Semrau, K. T., Marynowski, C. W., Lunde, K. E., Lapple, C. E., Ind. Eng. Chem. 50, 1615 (1958).

Semrau, K. T., J. Air Pollution Control Assoc. 10, 200 (1960).

Stern, A. C., Ed., Air Pollution, Vol. III, Chapt. 46 (1968).

5.2 MASS TRANSFER

5.2.1 COMPUTATION METHODS

A large proportion of industrial mass transfer separations are performed in two major categories of equipment. One type involves continuous contact between two fluid phases in a countercurrent or cocurrent manner, such as in a packed tower. The other type involves countercurrent contact in stages, such as in a plate column. The contact between the phases as they move through the device is intermittent rather than continuous.

The plate and packed tower type equipment is most common in gas-liquid mass transfer operations. Though the computation methods for design are primarily in terms of these, they can be used for other equipment with modification. If they do not fall in either of these categories, continuous contact or contact in stages, then design equations have to be developed with the use of mass transfer coefficients. For convenience, we will refer to plate columns in describing stage processes and to packed columns in continuous contact processes.

5.2.1.1 Stage Processes

Ideal (Equilibrium) Stage

A plate column with "n" stages is illustrated in Figure 5.2.1-1. In an ideal, or equilibrium stage, the phases are mixed long enough so that the streams leaving the stage are in equilibrium. In a real stage there may not be sufficient contact between the phases to bring the streams into equilibrium, so it accomplishes less interphase transfer than an ideal stage. The difference in performance is described by stage or plate efficiency.

Graphical Calculation of Ideal Stages Required

Given the gas and liquid flow rates, the number of theoretical plates required to reduce the gas composition to a given level can be determined by a graphical procedure. Since in a theoretical plate the gas and liquid streams leaving it are in equilibrium, for any plate, m, (Figure 5.2.1-1) the compositions "x_m-1" and "y_m" leaving that plate are related by the equilibrium line of Figure 5.2.1-2. (Equilibrium data for many systems of interest are given in Chapter 10).

The gas and liquid compositions between plates are related by a material balance:

$$\hat{G}_m \hat{y}_m + \hat{L}_n \hat{x}_n = \hat{G}_n \hat{y}_n + \hat{L}_m \hat{x}_m \qquad (5.2.1\text{-}1)$$

where "$\hat{L}$" and "$\hat{G}$" are flow rates in kgmol/(sec m^2), "n" denotes the top of the scrubber and "m" denotes the stream between the plates above plate "m". In many practical scrubbing situations the gas and liquid flow rates are essentially constant, and the material balance is:

$$\hat{G}(\hat{y}_m - \hat{y}_n) = \hat{L}\,(\hat{x}_m - \hat{x}_n) \qquad (5.2.1\text{-}2)$$

Thus the stream compositions between any two plates "n" and "m" are related by Equation 5.2.1-2 which is plotted as the operating line of Figure 5.2.1-2. The graphical construction involves stepping off the plates as indicated in Figure 5.2.1-2 starting with the point $(\hat{x}_n, \hat{y}_n)$, until the exist composition "$\hat{x}_o$" is crossed (or approximately so). Each horizontal segment represents one theoretical plate. Points on the equilibrium line represent the gas and liquid compositions leaving a plate. Points on the operating line represent the compositions of gas and liquid streams passing one another at any plane perpendicular to the flow.

If the solute gas constitutes a high percentage (more than 5% to 10%) of the gas entering the tower it is necessary to take account of the reduction in quantity of the gas as absorption proceeds, which affects the materials balance. When the inert component, B, of the gas is completely insoluble in the liquid, the material balance can be calculated by assuming that its flow rate, $\hat{G}_B$, is constant at all levels in the tower. Also if none of the solvent is vaporized its flow rate, L_S, is constant. A material balance over the whole tower equating the amount of "A" absorbed is:

$$\hat{G}_B \left(\frac{\hat{y}_o}{1 - \hat{y}_o} - \frac{\hat{y}_m}{1 - \hat{y}_m} \right) = \hat{L}_S \left(\frac{\hat{x}_o}{1 - \hat{x}_o} - \frac{\hat{x}_m}{1 - \hat{x}_m} \right) \qquad (5.2.1\text{-}3)$$

As before, this equation can be plotted on a $\hat{y} - \hat{x}$ diagram between the points $(\hat{x}_o, \hat{y}_o)$ and $(\hat{x}_n, \hat{y}_n)$ as an operating line. The graphical method for calculating the number of ideal stages can be applied as explained for a straight operating line.

Analytical Calculation of Ideal Stages Required

The number of theoretical plates can be calculated directly (without the graphical construction) if both the operating line and the equilibrium line are straight. The operating line is straight if the ratio of the liquid and gas flow rates is substantially constant throughout the tower, since the slope of the operating line is then a constant, $\hat{L}/\hat{G}$. This is the case in many scrubbers, where the component to be scrubbed is present at low concentrations in both phases and $\hat{L}/\hat{G}$ is approximately constant.

The equilibrium line is straight if:

$$\hat{y}_m{}^* = m\,\hat{x}_m + B \qquad (5.2.1\text{-}4)$$

where "B" is the intercept of the equilibrium line on the "y" axis.

Henry's law is a special case of Equation 5.2.1-4 with B = 0 and m = H/P, where: "P" is the total pressure at the m'th plate and "H" is Henry's constant. ("P" would have to be unchanged throughout the column in order for "m" to be constant).

If the operating and equilibrium lines are straight, the number of theoretical plates, N_p, is:

$$N_p = \frac{\ln\left[\left(1 - \frac{m\hat{G}}{\hat{L}}\right)\left(\frac{\hat{y}_o - m\hat{x}_n}{\hat{y}_n - m\hat{x}_n}\right) + \frac{m\hat{G}}{\hat{L}}\right]}{\left(\ln \frac{\hat{L}}{m\hat{G}}\right)} \qquad (5.2.1\text{-}5)$$

where "$\hat{y}_o$" is the inlet gas composition at the bottom of the column.

Curved operating and equilibrium lines can sometimes be made straight by changing the basis of the compositions and flow rates in a consistent manner. For example, if equilibrium and operating lines are not straight when expressing compositions as mole fraction, expressing compositions as mass fraction may make them straight.

The groups in Equation 5.2.1-5 have the following significance:

$\frac{m\hat{G}}{\hat{L}}$ = = ratio of the slope of the equilibrium line to the slope of the operating line

$(\hat{y}_n - m\hat{x}_n)$ = gas-phase driving force at the top of the column

$(\hat{y}_o - m\hat{x}_n)$ = theoretical maximum possible driving force between the inlet gas stream and the inlet liquid stream.

For a more complete discussion of how to calculate the ideal number of stages required, see any unit operations textbook, or Perry (1963).

Calculation of the Number of Real Stages

Earlier we defined the Murphree stage efficiency (Equation 4.2.5-1) based on vapor phase composition. In the graphical calculation of stages it is applied by modifying the graphical construction of Figure 5.2.1-2. For each plate the vertical step on the plot extends from the operating line down a fraction, E_{MV}, of the way to the equilibrium line, rather than all the way to the equilibrium line. From the end of the vertical line, the horizontal part of the step is drawn back to the operating line.

Another approach is to use an overall efficiency, E_O; the ratio of the total number of ideal stages to the number of real stages. If this ratio is known, it is a simple matter to obtain the number of real stages after calculating the number of ideal stages. However, the value of "E_{MV}" may vary with position in a contactor, and even if "E_{MV}" is constant, "E_O" does not equal "E_{MV}" unless the operating and equilibrium lines are straight and parallel.

5.2.1.2 Continuous Contacting

Mass Transfer Coefficients

Mass transfer coefficients have been defined in 4.2.3.1. We have shown how to predict mass transfer coefficients based on mass transfer theories in 4.5 for drops, bubbles, and liquid films. Also, empirical and semi-empirical correlations have been given for the shapes mentioned.

Here, we give methods for sizing equipment based on mass transfer coefficients. While we will refer to packed columns in developing the equations, these equations are general for countercurrent contact.

Equation 4.2.3-6 can be rewritten as:

$$\hat{N}_A = \hat{K}_G (p_A - p_A^*) = \hat{K}_G P (\hat{y}_A - \hat{y}_A^*) \qquad (5.2.1\text{-}6)$$

Figure 5.2.1-3 is a schematic diagram of a packed column. Let the surface area of packing per tower volume be "a". The available surface area in a tower element of cross sectional area, A, and height "dZ" will be "a A dZ". Then the rate of absorption in this element is given by the equation:

$$\hat{N}_A a\ A\ dZ = \hat{K}_G a\ P\ (\hat{y}_A - \hat{y}_A^*)\ A\ dZ = -\hat{G}\ A\ d\hat{y} = \hat{L}\ A\ d\hat{x} \qquad (5.2.1\text{-}7)$$

Various ways to express the height, Z, are summarized in Table 5.2.1-1 under both equimolar counter diffusion and diffusion through a stationary layer. The phenomenon of the rates of diffusion of "A" and "B" being equal but in opposite direction is known as equimolar counter diffusion. While this is generally not the case for gas absorption, the equations are the same as would result from the simplification of the strictly correct equations, when "$\hat{x}$" or "$\hat{y}$" are small, as will be seen later. It is necessary to know the driving force over the height of the tower to integrate the above equation. In many cases involving dilute solutions this problem is simplified by assuming that the solubility obeys Henry's law. The Equation 5.2.1-7 can now be integrated between the terminal compositions, using material balance relationship equation, $y_1 - \hat{y} = \hat{L}/\hat{G}\ (x_1 - \hat{x})$,

$$Z = \left(\frac{\hat{y}_1 - \hat{y}_2}{\hat{y}_{LM}}\right)\left(\frac{\hat{G}}{\hat{K}_G\ a\ P}\right) \qquad (5.2.1\text{-}8)$$

where,

$$\hat{y}_{LM} = \frac{(\hat{y}_1 - \hat{y}_1^*) - (\hat{y}_2 - \hat{y}_2^*)}{\ln\left(\dfrac{\hat{y}_1 - \hat{y}_1^*}{\hat{y}_2 - \hat{y}_2^*}\right)} = \text{logarithmic mean driving force at the ends of the tower.} \qquad (5.2.1\text{-}9)$$

The corresponding equation in terms of partial pressure is:

$$Z = \left(\frac{(p_{Ai} - p_{Ae})}{p_{LM}}\right)\left(\frac{\hat{G}}{\hat{K}_G\ a\ P}\right) \qquad (5.2.1\text{-}10)$$

where "p_{Ai}" is the partial pressure of "A" corresponding to "y_1", and "p_{Ae}" is that corresponding to "y".

This method is applicable to diffusion through a stagnant gas when only a small proportion of the total gas is absorbed, which means that the operating line is straight. If the solute gas constitutes more than 5% to 10% of the gas entering the tower it is necessary to take account of the reduction in quantity of the gas as absorption proceeds. The resulting material balance equation is the same as Equation 5.2.1-3. The rate of transfer in any element of a column of unit cross-section and height "dZ" is given by the equation:

Table 5.2.1-1

Equations Determining Height of a Packed Column, NTUs and HTUs.

MECHANISM	HEIGHT OF A PACKED COLUMN	NTU NUMBER OF TRANSFER UNITS	HTU HEIGHT OF A TRANSFER UNITS
Equimolar Counter Diffusion	$Z = \frac{\hat{G}}{\hat{k}_G \ a \ P} \int_{\hat{y}_2}^{\hat{y}_1} \frac{d\hat{y}}{\hat{y} - \hat{y}_i}$	$N_G = \int_{\hat{y}_2}^{\hat{y}_1} \frac{d\hat{y}}{\hat{y} - \hat{y}_i}$	$H_G = \frac{\hat{G}}{\hat{k}_G \ a \ P}$
	$Z = \frac{\hat{G}}{\hat{K}_G \ a \ P} \int_{\hat{y}_2}^{\hat{y}_1} \frac{d\hat{y}}{\hat{y} - \hat{y}^*}$	$N_{OG} = \int_{\hat{y}_2}^{\hat{y}_1} \frac{d\hat{y}}{\hat{y} - \hat{y}^*}$	$H_{OG} = \frac{\hat{G}}{\hat{K}_G \ a \ P}$
	$Z = \frac{\hat{L}}{\hat{k}_L \ a \ \hat{\rho}} \int_{\hat{x}_2}^{\hat{x}_1} \frac{d\hat{x}}{\hat{x}_i - \hat{x}}$	$N_L = \int_{\hat{x}_2}^{\hat{x}_1} \frac{d\hat{x}}{\hat{x}_i - \hat{x}}$	$H_L = \frac{\hat{L}}{\hat{k}_L \ a \ \hat{\rho}}$
	$Z = \frac{\hat{L}}{\hat{K}_L \ a \ \hat{\rho}} \int_{\hat{x}_2}^{\hat{x}_1} \frac{d\hat{x}}{\hat{x}^* - \hat{x}}$	$N_{OL} = \int_{\hat{x}_2}^{\hat{x}_1} \frac{d\hat{x}}{\hat{x}^* - \hat{x}}$	$H_{OL} = \frac{\hat{L}}{\hat{K}_L \ a \ \hat{\rho}}$
Diffusion through a Stationary Component	$Z = \left[\frac{\hat{G}}{\hat{k}_G \ a \ P \ (1 - \hat{y})_{LM}}\right]_{av} \int_{\hat{y}_2}^{\hat{y}_1} \frac{(1 - \hat{y})_{LM}}{(1 - \hat{y}) \ (\hat{y} - \hat{y}_i)} \ d\hat{y}$	$N_G = \int_{\hat{y}_2}^{\hat{y}_1} \frac{(1 - \hat{y})_{LM}}{(1 - \hat{y}) \ (\hat{y} - \hat{y}_i)} \ d\hat{y}$	$H_G = \left[\frac{\hat{G}}{\hat{k}_G \ a \ P \ (1 - \hat{y})_{LM}}\right]_{av}$
	$Z = \left[\frac{\hat{G}}{\hat{K}_G \ a \ P \ (1 - \hat{y})_{LM}}\right]_{av} \int_{\hat{y}_2}^{\hat{y}_1} \frac{(1 - \hat{y})_{LM}}{(1 - \hat{y}) \ (\hat{y} - \hat{y}^*)} \ d\hat{y}$	$N_{OG} = \int_{\hat{y}_2}^{\hat{y}_1} \frac{(1 - \hat{y})_{LM}}{(1 - \hat{y}) \ (\hat{y} - \hat{y}^*)} \ d\hat{y}$	$H_{OG} = \left[\frac{\hat{G}}{\hat{K}_G \ a \ P \ (1 - \hat{y})_{LM}}\right]_{av}$
	$Z = \left[\frac{\hat{L}}{\hat{k}_L \ a \ \hat{\rho} \ (1 - \hat{x})_{LM}}\right]_{av} \int_{\hat{x}_2}^{\hat{x}_1} \frac{(1 - \hat{x})_{LM}}{(1 - \hat{x}) \ (\hat{x}_i - \hat{x})} \ d\hat{x}$	$N_L = \int_{\hat{x}_2}^{\hat{x}_1} \frac{(1 - \hat{x})_{LM}}{(1 - \hat{x}) \ (\hat{x}_i - \hat{x})} \ d\hat{x}$	$H_L = \left[\frac{\hat{L}}{\hat{k}_L \ a \ \hat{\rho} \ (1 - \hat{x})_{LM}}\right]_{av}$
	$Z = \left[\frac{\hat{L}}{\hat{K}_L \ a \ \hat{\rho} \ (1 - \hat{x})_{LM}}\right]_{av} \int_{\hat{x}_2}^{\hat{x}_1} \frac{(1 - \hat{x})_{LM}}{(1 - \hat{x}) \ (\hat{x}^* - \hat{x})} \ d\hat{x}$.	$N_{OL} = \int_{\hat{x}_2}^{\hat{x}_1} \frac{(1 - \hat{x})_{LM}}{(1 - \hat{x}) \ (\hat{x}^* - \hat{x})} \ d\hat{x}$	$H_{OL} = \left[\frac{\hat{L}}{\hat{K}_L \ a \ \hat{\rho} \ (1 - \hat{x})_{LM}}\right]_{av}$

$(1 - \hat{y})_{LM}$ = log mean of $(1 - \hat{y})$ and $(1 - \hat{y}^*)$

$(1 - \hat{x})_{LM}$ = log mean of $(1 - \hat{x})$ and $(1 - \hat{x}^*)$

$$N_A\, a\, A\, dZ = \hat{K}_G\, a\, P\, (\hat{y}_A - \hat{y}_A^*)\, A\, dZ = -A\, d(\hat{G}\, \hat{y}) =$$

$$= -A\, \hat{G}_B\, d\left(\frac{\hat{y}}{1 - \hat{y}}\right) = -A\, \hat{G}_B\, \frac{d\hat{y}}{(1 - \hat{y})^2} \qquad (5.2.1\text{-}11)$$

The height of the packing, Z, is obtained by integrating the above equation:

$$Z = \int_{\hat{y}_2}^{\hat{y}_1} \frac{\hat{G}_B\, d\hat{y}}{\hat{K}_G\, a\, P\, (1 - \hat{y})^2\, (\hat{y} - \hat{y}^*)} \qquad (5.2.1\text{-}12)$$

If Equation 5.2.1-12 is used as written, "Z" can be determined by plotting $\hat{G}_B/\hat{K}_G\, a\, P\, (1 - \hat{y})^2\, (\hat{y} - \hat{y}^*)$ vs. "$\hat{y}$" and integrating graphically from the outlet gas concentration "$\hat{y}_2$" to the inlet concentration, "$\hat{y}_1$".

Equation 5.2.1-12 is based on gas-side mass transfer. If the scrubbed component is very soluble (including situations where the scrubbed component reacts rapidly in the solvent or dissociates in the liquid) the overall gas phase transfer coefficient, "$\hat{K}_G\, a$" is approximately equal to "$k_G\, a$", the individual gas-film coefficient. If the liquid phase resistance to mass transfer is not negligible, the overall gas phase mass transfer coefficient, $\hat{K}_G$, is given by:

$$\frac{1}{\hat{K}_G\, a} = \frac{1}{k_G\, a} + \frac{\hat{H}}{k_L\, a} \qquad (5.2.1\text{-}13)$$

where "$\hat{H}$" is the Henry's law constant.

The liquid phase mass transfer analog of Equation 5.2.1-12 for the packed height is:

$$Z = \int_{\hat{x}_2}^{\hat{x}_1} \frac{\hat{L}_S\, d\hat{x}}{K_L\, a\, \hat{\rho}\, (1 - \hat{x})^2\, (\hat{x}^* - \hat{x})} \qquad (5.2.1\text{-}14)$$

where "$\hat{\rho}$" is the molar density of the liquid stream, including inerts. If liquid phase mass transfer controls, $K_L\, a \approx k_L\, a$; otherwise;

$$\frac{1}{K_L\, a} = \frac{1}{k_L\, a} + \frac{1}{\hat{H}\, \hat{K}_G\, a} \qquad (5.2.1\text{-}15)$$

Table 5.2.1-1 summaries these equations under diffusion through a stationary component.

The Transfer Unit Method

Equation 5.2.1-7 can be rewritten:

$$Z = \frac{\hat{G}}{\hat{K}_G \; a \; P} \int \frac{d\hat{y}}{(\hat{y} - \hat{y}^*)} \qquad (5.2.1\text{-}16)$$

The group $\int d\hat{y}/(\hat{y} - \hat{y}^*)$ has been defined as the number of overall gas transfer units "N_{OG}". It represents an integrated value of the number of times the driving force must be divided into the change in gas concentration, and therefore the difficulty of the separation. The height of transfer is defined as:

$$H_{OG} = \frac{\hat{G}}{\hat{K}_G \; a \; P} \qquad (5.2.1\text{-}17)$$

According to this concept, the packed height can be expressed as the product of the "height of a transfer unit" (HTU) times the "number of transfer units" (NTU) required to accomplish the separation. The various ways of expressing HTUs and NTUs are summarized in Table 5.2.1-1.

It is possible to compute the number of transfer units mathematically when the operating and equilibrium lines are straight and Henry's law applies. The following equation gives "N_{OG}" in terms of the gas composition at the inlet and outlet of the tower, "$\hat{y}_1$" and "$\hat{y}_2$", and the liquid composition at the inlet, "$\hat{x}_2$":

$$N_{OG} = \frac{\ln\left[\left(1 - \frac{m\,\hat{G}}{\hat{L}}\right)\left(\frac{\hat{y}_1 - m\,\hat{x}_2}{\hat{y}_2 - m\,\hat{x}_2}\right) + \frac{m\,\hat{G}}{\hat{L}}\right]}{1 - \left(\frac{m\,\hat{G}}{\hat{L}}\right)} \qquad (5.2.1\text{-}18)$$

The ratio $(m\,\hat{G}/\hat{L})$ may be greater or less than unity, but for substantially complete absorption of solute from a gas this ratio must be less than unity. Commercial absorbers are generally operated at a ratio between 0.4 and 0.8.

Drew (1940) has shown that for the special case of $\hat{y}^* = 0$ (for example when the absorption is followed by a fast chemical reaction in the liquid), the equation for "N_{OG}" given in Table 5.2.1-1 reduces to:

$$N_{OG} = -\int_{\hat{y}_2}^{\hat{y}_1} \frac{d\hat{y}}{(1 - \hat{y})\ln(1 - \hat{y})} = \ln\left[\frac{\ln(1 - \hat{y}_1)}{\ln(1 - \hat{y}_2)}\right] \qquad (5.2.1\text{-}19)$$

This expression is accurate for gas compositions varying over a wide range, and for low concentrations it reduces to the simple equation:

$$N_{OG} = \ln\frac{\hat{y}_1}{\hat{y}_2} \qquad (5.2.1\text{-}20)$$

It should be noted that when large concentration changes occur or the equilibrium phase has a marked curvature the value of $(m\,\hat{G}/L)$

changes as absorption proceeds and this affects the values of "H_{OG}". Under these circumstances it will be necessary to consider the absorption in several increments calculating average values of "H_{OG}" for each.

Performance data for packed columns are sometimes expressed as HETP, the height equivalent to a theoretical plate. Then the height of the column is N_p x HETP; "N_p" can be determined according to the methods given previously (5.2.1.1), if the equilibrium and operating lines are straight.

$$Z = (N_{OG})\ (H_{OG}) = (N_p)\ (\text{HETP}) \qquad (5.2.1\text{-}21)$$

combined with Equation 5.2.1-5 and 5.2.1-18 gives:

$$H_{OG} = \frac{1 - \left(\frac{m\ \hat{G}}{\hat{L}}\right)}{\ln\left(\frac{\hat{L}}{m\ \hat{G}}\right)}\ (\text{HETP}) \qquad (5.2.1\text{-}22)$$

as the relationship between "H_{OG}" and "HETP". This equation shows that $H_{OG} \rightarrow$ HETP as $(m\ \hat{G}/\hat{L}) \rightarrow 1$. If the equilibrium and operating lines are parallel, H_{OG} and HETP are equal.

5.2.2 PLATE COLUMN SCRUBBERS

For many of the presently available plate type scrubbers, the standard chemical engineering texts give detailed design methods. The purpose of this section is:

1. to provide simplified methods adequate for rapid approximate design calculations, thus giving the designer the basis for cost estimation and consultation with equipment suppliers,

2. to gather the information required for such a design in one location for easy reference by the designer, and,

3. to summarize methods for predicting the performance characteristics of new or existing scrubbers.

In a plate column, the scrubbing liquid is fed at the top and flows down by gravity from plate to plate. The gas to be scrubbed enters at the bottom and flows up through the liquid on each plate. The two common liquid flow patterns are cross-flow and counter-flow. The cross-flow situation is the most common and it involves a lateral movement of the liquid from a "downcomer" from the plate above to another downcomer inlet going to the plate below. Counter-flow is achieved in some perforated plates which operate without downcomers as the liquid drains through the holes.

The classic type of plate is the bubble-cap tray (see Figure 3.1.1 for illustration); the liquid flows across the tray, down a downcomer, and across the next tray in the reverse direction, while the gas flows up and through the holes in the tray and bubbles out from slots or notches in the cap. The purpose of the cap is to disperse the gas effectively and to keep liquid from falling through the holes if the gas flow decreases momentarily.

The simplest plate is the sieve (or perforated) tray, a plate with circles or rectangles punched in a regular pattern. In the cross-flow configuration, the liquid flows across the tray, and the gas bubbles up through the perforations fast enough to keep the liquid from "weeping through the holes. Sieve trays are occasionally designed in a counter-flow configuration and downcomers are omitted.

Valve trays (ballast trays, floating cap plates) were introduced around 1952 (Nutter float-valve tray, Koch "Flexitray"). The movable caps act as check valves, allowing a wide range of operating conditions. Another example of this type of tray is the Glitsch ballast tray. The valve tray is a very common choice for plate columns because of its low cost and favorable operating characteristics.

Grid trays, such as the original Shell Development Co. "Turbogrid", are composed of a coarse grid or parallel slots; they use no downcomers and thus have the counter-flow configuration; in general, flow capacities are larger and the pressure drop is less than that of the sieve tray.

5.2.2.1 Unit Mechanisms

A first-principles analysis of mass transfer in a plate column scrubber could be made by considering several of the unit mechanisms operating in parallel. Most of the absorption is accomplished by mass transfer from the gas bubbles emerging from the bubble-cap slots or sieve-tray perforations, to the liquid flowing across or through the tray. Additional absorption takes place by transfer from the vapor phase above the tray to liquid droplets formed by the violent frothing action of the bubbles at the surface of the liquid. Finally, a small part of the absorption is due to mass transfer from the vapor phase above the tray to the liquid surface and wetted walls (mass transfer to sheets); the liquid has a high rate of surface renewal due to agitation by the bubbles breaking through the surface.

5.2.2.2 Column Diameter

The diameter of a plate column can be determined from the allowable superficial gas velocity, the velocity through the entire cross-section of the column. Excessive superficial velocities cause "priming" (foam level rises to the tray above) or entrainment of liquid in the vapor. Since priming and entrainment are closely related, the empirical correlations given below do not distinguish between them.

The Souders-Brown equation gives the maximum superficial gas velocity by:

$$u_{s,max} = a \left(\frac{\rho_L - \rho_G}{\rho_G} \right)^{1/2} \qquad (5.4.4\text{-}1)$$

where "a" is an empirical constant with dimensions of velocity. The smallest allowable column diameter is then:

$$d_c = \left(\frac{4\ Q_G}{\pi\ u_{s,max}} \right)^{1/2} \qquad (5.2.2\text{-}1)$$

where "Q_G" is the volumetric gas flowrate. Substitution of Equation 5.4.4-1 in Equation 5.2.2-1 gives:

$$d_c = \left[\frac{4}{\pi}\frac{Q_G}{a}\left(\frac{\rho_G}{\rho_L - \rho_G}\right)^{1/2}\right]^{1/2} \qquad (5.2.2\text{-}2)$$

In individual cases there are more sophisticated methods for sizing plate columns; however, Equation 5.2.2-2 provides a single method applicable to most types of plates, and this approach has been used successfully by column designers for many years.

For purposes of scrubber design, Equation 5.2.2-2 can be written:

$$d_c = \psi\left(Q_G\sqrt{\rho_G}\right)^{1/2} \qquad (5.2.2\text{-}3)$$

where: $\psi \equiv \left(\frac{4}{\pi a\sqrt{\rho_L - \rho_G}}\right)^{1/2}$

The Souders-Brown constant "a" (and hence "ψ") depends on several operating parameters, but to a good approximation "ψ" is constant for a given tray geometry and tray spacing. Values of "ψ" for use in Equation 5.2.2-3are given in Table 5.2.2-1. These values were derived from a wide variety of empirical data on absorber design; they are based on a liquid specific gravity of 1.05 and 61 cm (24") tray spacing, and they result in moderately conservative designs. A plot of "d_c" vs. "Q_G" with "ρ_G" as a parameter is given in Figure 5.2.2-1 for a bubble cap column. This plot can also be used to determine column diameters for a sieve tray or a valve tray by correcting the diameter obtained. The correct diameter is obtained by multiplying the diameter obtained from Figure 5.2.2-1with the appropriate "ψ" from Table 5.2.2-1 for the tray under consideration and dividing it by the "ψ" for the bubble cap. For tray spacings other than 61 cm, the column diameter is to be multiplied by the correction factor given by Figure 5.2.2-2. (A smaller column diameter can be used if tray spacing is increased, but this is rarely desirable economically.)

In applications requiring very high liquid rates (a quench tower, for instance) it may be necessary to use multiple-pass trays in order to handle the liquid load. Relatively less area is available for caps or holes on a multiple-pass tray, so that a bigger column diameter will be required for the same gas flow rate; approximate correction factors are given as 1.046 for a double-pass tray and 1.07 for a triple-pass tray.

The operable ranges of a single-pass tray are indicated very roughly in Figure 5.2.2-3, adapted from Huang and Hodson's (1958) sieve-tray study.

Example

Determine the minimum allowable diameter for a sieve tray scrubber for the following conditions:

Vapor density	3 kg/m^3	(0.19 lb/ft^3)
Vapor rate	6000 m^3/hr	(3500 cfm)

TABLE 5.2.2-1

EMPIRICAL CONSTANTS FOR EQUATION 5.2.2-3

Type of Tray	Metric ψ [a]	Engineering ψ [b]
Bubble cap	0.0162	0.1386
Sieve tray	0.0140	0.1198
Valve tray	0.0125	0.1069

[a] Metric ψ is in $m^{1/4}\ hr^{1/2}/kg^{1/4}$, for use with Q_G in m^3/hr and ρ_G in kg/m^3.

[b] Engineering ψ is in $ft^{1/4}\ min^{1/2}/lb^{1/4}$, for use with Q_G in cfm and ρ_G in lb/ft^3.

Liquid rate	40 m^3/hr	(175 gpm)
Tray spacing	0.5 m	(18 inches)

From Figure 5.2.2-1 the column diameter is 1.6 m for 61 cm tray spacing. From Table 5.2.2-1correcting 1.6 m for the sieve tray, as mentioned before, the column diameter becomes 1.38 m (1.6x0.014/0.0162 = 1.38). From Figure 5.2.2-2 the correction factor for 0.5 m tray spacing is 1.085; thus d_c = 1.085 x 1.38 = 1.5 m (5 ft). The column would probably be specified at 1.6 meters or 5 1/2 feet, to allow for a safety factor.

For counter-flow trays the minimum column diameter is probably limited by weeping (see stability discussion below) rather than entrainment. An empirical correlation of Majeweski (1959) for the superficial gas velocity where weeping occurs is:

$$\frac{u_{s,flood}^2}{g\ d_h\ f_h^2}\ \frac{\rho_G}{\rho_L}\left(\frac{\mu_L}{\mu_W}\right)^{0.16} = 10\ \exp\left[-4\left(\frac{L}{G}\right)^{0.25}\left(\frac{\rho_G}{\rho_L}\right)^{0.125}\right] \qquad (5.2.2\text{-}4)$$

where: g = acceleration of gravity
d_h = equivalent diameter of tray holes or slots
f_h = holes fraction of total tray area
μ_L = liquid viscosity
μ_W = viscosity of water at the same conditions

The constant 10 is dimensionless. Combining this equation with Equation 5.2.2-1 the minimum column diameter is:

$$d_c = 0.635 \left\{ \frac{Q_G^2}{g \; d_h \; f_h^2} \frac{\rho_G}{\rho_L} \left(\frac{\mu_L}{\mu_W} \right)^{0.16} \exp \left[4 \left(\frac{L}{G} \right)^{0.25} \left(\frac{\rho_G}{\rho_L} \right)^{0.125} \right] \right\}^{1/4} \qquad (5.2.2\text{-}5)$$

The constant 0.635 is dimensionless.

5.2.2.3 Pressure Drop

Pressure drop in a plate column scrubber is important because the total column pressure drop partially determines the capital cost of the scrubber auxiliaries and the operating cost of the entire scrubber system. There are differing views on the importance of the tray pressure drop to operating stability, but it is generally agreed that this effect is more significant for sieve trays and counter-flow trays than for bubble-cap trays.

Numerous methods for estimating pressure drop through bubble-cap, sieve, and valve trays are available. They differ primarily in the manner in which the tray pressure drop is divided into contributions of liquid seal, change in gas velocity, etc. The methods given below were chosen both because the results agree with observed data and because they are easy to apply.

For bubble-cap trays, the approach given by Treybal (1955) is typical of the various methods available, and is widely and successfully used in industry. The pressure head through a tray is expressed as:

$$h = h_{ow} + h_d + h_c + \frac{h_g}{2} \qquad (5.2.2\text{-}6)$$

The separate terms in this equation are defined below and illustrated in Figure 5.2.2-4.

The head over the weir, h_{ow} (m), can be estimated by the Francis weir formula for a segmental weir:

$$h_{ow} = 0.00282 \; F_w \left(\frac{Q_L}{W} \right)^{2/3} \qquad (5.2.2\text{-}7)$$

where "Q_L" is the liquid flow (m^3/hr), and "W" is the weir length (m). "F_w" is a correction for the column wall curvature and can be as high as 1.2 for high liquid loads and short weirs. A typical value for design purposes is 1.1 Equation 5.2.2-7 is given by Teller (1963) in engineering units as:

$$h_{ow} \text{ (in.)} = 0.48 \; F_w \left(\frac{Q_L}{W} \right)^{2/3} \qquad (5.2.2\text{-}8)$$

where "Q_L" is in gpm, and "W" is in inches).

The depth of the bubble-cap slots, h_d, is the depth from the edge of the weir to the top of the slots, and is a design parameter. A typical "h_d" is 1.3 cm (0.5 in).

"h_c" is the head loss due to gas flow through the caps and slots, and can be further divided into

$$h_c = h_r + h_s \tag{5.2.2-9}$$

"h_r", the loss due to flow reversal, is adequately approximated by six gas velocity heads:

$$h_r = \frac{6\,u^2_{c,max}}{2g}\,\frac{\rho_G}{\rho_L} = 2.36\text{x}10^{-8}\ \frac{u^2_{c,max}\,\rho_G}{\rho_L} \tag{5.2.2-10}$$

where "h_r", is in meters, and "$u_{c\ max}$", the highest velocity attained by the gas in traveling through the riser and the inside of the cap, is in m/hr.

"h_s", the head loss through the cap slots, is given by the following equations for rectangular slots of width "b":

$$h_s = \alpha \text{ for } Q_s < \left(\frac{\alpha}{\beta}\right)^{3/2} \tag{5.2.2-11}$$

$$= \beta Q_s^{2/3} \text{ for } Q_s > \left(\frac{\alpha}{\beta}\right)^{3/2} \tag{5.2.2-12}$$

where

$$\alpha \equiv 0.01019\ \frac{\sigma}{100\ b\ \rho_L} + \left[0.000104\ \left(\frac{\sigma}{100\ b\ \rho_L}\right)^2 + 0.02037\ \left(\frac{\sigma}{100\ \rho_L}\right)\right]^{1/2} \tag{5.2.2-13}$$

$$\beta \equiv 0.00299\ \left(\frac{1}{b}\sqrt{\frac{\rho_G}{\rho_L - \rho_G}}\right)^{2/3} \tag{5.2.2-14}$$

In these equations "Q_s" is the gas flow through each slot in m³/hr, "σ" is the liquid surface tension in dyne/cm, "b" is in meters and "ρ" is in kg/m³. The criterion for using Equation 5.2.2-11 or 5.2.2-12 is whether the slot is fully open, expressed by the ratio $(\alpha/\beta)^{3/2}$.

The term "$h_g/2$" in Equation 5.2.2-6 is an average of the hydraulic gradient across the tray. Although Treybal gives a method for calculating "hg", it is usually the smallest term in the tray pressure drop and for a reasonable tray design "h_g" will be 1.3 to 2.5 cm (0.5-1 in). Use 1.3 cm as an estimate.

The pressure drop expressed in liquid head is converted to pressure units as follow:

$$\Delta P = \rho_L h \tag{5.2.2-15}$$

If "ρ_L" is in kg/m³ and "h" is in "m", "ΔP" will be in kg/m².

Example - Estimate the pressure drop through a 5-plate bubble-cap scrubber at the following conditions:

Vapor rate	6000 m^3/hr	(3530 cfm)
Liquid rate	40 m^3/hr	(175 gpm)
Vapor density	3 kg/m^3	(0.19 lb/ft^3)
Liquid density	1050 kg/m^3	(65.6 lb/ft^3)
Surface tension	50 dyne/cm	
Weir length	1.1 m	(43 inches)
Caps	60	
Cap diameter (outside)	10 cm	(4 inches)
Slots per cap	24	
Slot dimensions	0.6 x 3.8 cm	(1/4 x 1-1/2 in)

Head over weir: Use F_w = 1.1 as an estimate, since the liquid rate is relatively high but the weir is not very short. From Equation 5.2.2-7,

$$h_{ow} = 0.00282\ (1.1) \left(\frac{40}{1.1}\right)^{2/3} = \underline{0.034\ m}$$

Slot depth: use typical $h_d = \underline{0.013\ m}$

Flow reversal: The gas flow through each cap is $Q_c = \frac{6000}{60} = 100\ m^3/hr$

Cross-sectional area of a cap (assuming 3 mm wall which is typical) is

$$\frac{\pi d_{cap}^2}{4} = \frac{3.142\ (.1 - .006)^2}{4} = 0.00694\ m^2$$

Assume equal cross-sectional areas for the riser and for the annulus between the riser and the cap, i.e.

$$\frac{0.00694}{2} = 0.00347\ m^2$$

Riser diameter is then $\left(\frac{4 \times 0.00347}{\pi}\right)^{1/2} = 0.0665$ m

and the riser wall (assume 5 mm thickness as typical) takes

$$\frac{\pi d_r t}{2} = \frac{3.142\ (0.0665)\ (0.005)}{2} = 0.00052\ m^2$$

from the areas of the riser and the annulus. The area for gas flow is then $a_c = 0.00347 - 0.00052 \approx 0.0030\ m^2$

Thus, $u_c = \frac{Q_c}{a_c} = \frac{100}{0.0030} = 33{,}300$ m/hr

From Equation 5.2.2-10,

$$h_r = \frac{2.36 \times 10^{-8}\ (33{,}300)^2\ (3)}{(1050)} = \underline{0.075\ m}$$

Loss through slots: the flow rate through each slot is

$$Q_s = \frac{Q_c}{24} = \frac{100}{24} = 4.17\ m^3/hr$$

From Equation 5.2.2-13,

$$\alpha = \frac{0.01019\ (50)}{100\ (0.006)\ (1050)} + \left\{0.000104 \left[\frac{50}{100 (0.006) (1050)}\right]^2 + 0.02037 \left[\frac{50}{100\ (1050)}\right]\right\}^{1/2} = 0.000809 + 0.003218 = 0.004027$$

From Equation 5.2.2-14, $\beta = 0.00299 \left(\frac{1}{0.006} \sqrt{\frac{3}{1047}} \right)^{2/3} = 0.01286$

Then $(\alpha/\beta)^{3/2} = \left(\frac{0.004027}{0.01286} \right)^{3/2} = 0.175$

$Q_s = 4.17 > 0.175$, so the slots are fully open, and Equation 5.2.2-12 applies:

$$h_s = 0.01286\,(4.17)^{2/3} = \underline{0.033\ \text{m}}$$

Hydraulic gradient: assume 0.013 m (1/2 inch), $h_g/2 = 0.013/2 = \underline{0.006\ \text{m}}$

Total for tray: $0.034 + 0.013 + 0.075 + 0.033 + 0.006 = \underline{0.161\ \text{m}}$ (6.3 inches)

for the 5-tray scrubber, $h_{total} = (5)(0.161) = 0.805$ m (31.7 in)

The pressure drop through the scrubber is then

$$\Delta P = \rho_L h_{total} = 1050\,(0.805) = \underline{845\ \text{kg/m}^2\ (= 85\ \text{cm W.C.} = 1.20\ \text{psi})}$$

For sieve trays, Huang and Hodson (1958) give a straightforward scheme for estimating pressure drop. The pressure head through the tray is expressed as $h = h_w + h_{ow} + h_{dp} + h_r$ (5.2.2-16)

The terms in this equation are defined below and illustrated in Figure 5.2.2-5.

The head over the weir, h_{ow}, is given by the Francis weir equation, Equation 5.2.2-7. The weir height, h_w, is a design parameter, usually 4 to 9 centimeters. If the weir height of the device is not known, 5 cm (2 inches) is a good estimate.

The dry plate pressure drop, h_{dp}, is calculated from an orifice equation:

$$h_{dp} = \frac{1}{C^2} \frac{\rho_G}{\rho_L} \frac{u_h^2}{2g} \qquad (5.2.2\text{-}17)$$

where "C" is the orifice coefficient. For plates where the thickness is equal to the hole diameter, Hunt et al. (1955) correlated "C" by

$$\frac{1}{C^2} = 1.14\,[0.4(1.25 - f_h) + (1 - f_h)^2] \qquad (5.2.2\text{-}18)$$

where "f_h" is the fraction of the perforated open area in the plate.

Hughmark and O'Connell (1957) give orifice coefficients as follows:

Hole diameter/plate thickness	1	2	4	7	10
Orifice coefficient, C	0.9	0.77	0.72	0.65	0.61

Recommended values for $1/C^2$ are shown in Figure 5.2.2-6 using Equation 5.2.2-18 with the correction factors implied above for the effect of hole diameter and plate thickness.

Operating sieve plates show pressure drops slightly greater than the sum of the liquid seal and the dry-plate loss. The discrepancy, called the residual pressure drop, h_r, is approximately

$$h_r = 0.013 \frac{\rho_{water}}{\rho_L} \qquad (5.2.2\text{-}19)$$

according to Hunt et al. (1955), where "h_r" is in meters.

After determining the tray head losses from Equations 5.2.2-16 through 5.2.2-19 the pressure drop is calculated from Equation 5.2.2-15.

Example - Estimate the pressure drop through a 5-tray sieve tray scrubber at the following conditions:

Vapor rate	6000 m^3/hr	(3530 cfm)
Liquid rate	40 m^3/hr	(175 gpm)
Vapor density	3 kg/m^3	(0.19 lb/ft^3)
Liquid density	1050 kg/m^3	(65.6 lb/ft^3)
Weir length	1.1 m	(43 inches)
Available tray area	1.25 m^2	(13.4 ft^2)
% hole area	15%	
Hole diameter	0.006 m	(1/4 inch)
Plate thickness	0.003 m	(1/8 inch)
Weir height	0.05 m	(2 inches)

Head due to weir: $h_w = \underline{0.050 \text{ m}}$

Assume $F_w = 1.1$

From Equation 5.2.2-7, $h_{ow} = 0.00282 \, (1.1) \left(\frac{40}{1.1}\right)^{2/3} = \underline{0.034 \text{ m}}$

Dry-plate head loss: The total hole area is $A_o = 1.25 \times 0.15 = 0.1875 \text{ m}^2$

Velocity through holes is then $u_{hole} = \frac{Q_G}{A_o} = \frac{6000}{0.1875} = 32000$ m/hr

$d_{hole}/t_{plate} = 0.006/0.003 = 2$, and $f_h = 0.15$, so from Figure 5.2.2-6 $1/C^2 = 1.80$. Thus,

$$h_{dp} = \frac{1.80 \, (3) \, (32000)^2}{1050 \, (2)(1.271 \times 10^8)} = \underline{0.021 \text{ m}}$$

Residual pressure drop: From Equation 5.2.2-19,

$$h_r = 0.013 \left(\frac{1000}{1050}\right) = \underline{0.012 \text{ m}}$$

The total head loss through one plate is then

$h = 0.050 + 0.034 + 0.021 + 0.012 = \underline{0.117 \text{ m}}$ (4.6 inches)

for the 5-plate scrubber, $h_{total} = (5) \, (0.117) \quad 0.585$ m (23 inches)

The pressure drop through the scrubber is then

$\Delta P = \rho_L h_{total} = 1050 \, (0.585) = \underline{614 \text{ kg/m}^2 \text{ (=24.2" } H_2O = 0.9 \text{ psi)}}$

For valve trays, the total tray pressure drop can be estimated by adding a dry plate pressure drop and an effective liquid head. The hydraulic gradient is negligible, as in the case of sieve trays. Thus, $h = h_e + h_{dp}$ (5.2.2-20)

Empirical pressure drop correlations are available in the design manuals of several manufacturers of valve trays. The methods given below are from Koch Engineering Co., and should provide a reasonable approximation for other types of valve-cap trays.

The equivalent depth of clear liquid, h_e, is obtained from Figure 5.2.2-7. The equivalent flow of air through each valve cap $Q_{c,air}$ is given

$$Q_{c,air} = Q_c \left(\frac{\rho_G}{1.177}\right)^{1/2} \qquad (5.2.2\text{-}21)$$

where "ρ_G" is in kg/m^3, where $Q_{c,air}$ and Q_c are given in the same units. The liquid flow in Figure 5.2.2-7 is the flow divided by the weir length, Q_L/W. Figure 5.2.2-7 is based on a 0.050 m (2-inch) weir height; a 0.013 m increase in weir height gives roughly a 10% increase in h_e.

The dry plate head loss, h_{dp}, is:

$$h_{dp} = h_{dp}' \times \frac{\rho_{water}}{\rho_L} \qquad (5.2.2\text{-}22)$$

h_{dp}' is obtained from Figure 5.2.2-8. The horizontal coordinate, "$Q_{c,air}$" is again calculated by Equation 5.2.2-21.

After determining the tray head losses, "h_e" and "h_{dp}'" the tray pressure drop is calculated from Equation 5.2.2-15.

Example - Estimate the pressure drop through a 5-plate valve tray scrubber at the following conditions:

Vapor rate	6000 m^3/hr	(3530 cfm)
Liquid rate	40 m^3/hr	(175 gpm)
Vapor density	3 kg/m^3	(0.19 lb/ft^3)
Liquid density	1050 (kg/m^3)	(65.6 lb/ft^3)
Weir length	1.1 (m)	(43 inches)
Valve caps	160	

Equivalent liquid head: From Equation 5.2.2-21.

$$Q_{c,air} = \frac{6000}{160}\left(\frac{3}{1.177}\right)^{1/2} = 60\,(\text{m}^3/\text{hr}) \text{ and } \frac{Q_L}{W} = \frac{40}{1.1} = 36.4\,(\text{m}^3/\text{hr})$$

From Figure 5.2.2-7, $h_e = \underline{0.050 (m)}$

Dry plate head loss: From Figure 5.2.2-8 and Equation 5.2.2-22.

$$h_{dp} = 0.023\ \frac{1000}{1050} = \underline{0.022(m)}$$

From Equation 5.2.2-20, $h = 0.050 + 0.022 = \underline{0.072(m)}$ (2.8 inches)

For the 5-plate scrubber, the head loss is

$h_{total} = 5 \times 0.072 = 0.360$ (m) (14.2 inches)

From Equation 5.2.2-1 $\Delta P = 1050\ (0.360) =$

$378\ (kg/m^2)(=14.9''\ H_2O = 0.5\ psi)$

Summary

The tabulation below shows the terms which contribute to pressure drops through bubble-cap trays, sieve trays and valve trays. The numbers are the meters of liquid head loss per tray obtained in the example calculations, and they give a rough picture of the relative pressure drops through the three types of tray.

TABLE 5.2.2-2
PRESSURE DROP COMPONENTS FOR PLATE COLUMN SCRUBBERS

Tray type	h_{ow}(m)	h_w(m)	h_d(m)	h_c(m)	h_{dp}(m)	$h_g/2$(m)	h(m)
B.C.	0.034		0.013	0.108		0.006	0.161
Sieve	0.034	0.050			0.033*		0.117
Valve	0.050				0.022		0.072

*Includes residual loss h_r.

For similar operating conditions, the liquid head on a valve tray, h_e, should be the same as $h_{ow} + h_w$ on a sieve tray. The sum of $h_{ow} + h_w$ in the sieve tray example is larger because the estimation method assumes (conservatively) clear liquid on the plate; in contrast, the empirical correlation for "h_e" on valve trays includes the effect of frothing, which lowers the liquid-phase density and thus decreases the liquid head.

5.2.2.4 Column Height

The height of a plate column scrubber can be expressed as

$$\frac{\text{Tray spacing x No. of theoretical plates}}{\text{Overall plate efficiency}} + \text{height of ends}$$

Tray spacing

Physical considerations usually dictate the choice of the distance between trays; 45 cm (18 inches) is the practical minimum if maintenance and repair are to be done by workmen inside the column, and 70 cm is preferable. If the column is designed so that the internals can be lifted out as a unit, smaller spacings are practical, subject to entrainment and flooding limitations. Most plate columns are designed with 50 to 70 cm tray spacing (20 to 28 inches). Indoor scrubbers often have smaller spacings, from 20 to 50 cm (8 to 20 inches), because of building height constraints.

Number of Theoretical Plates

Given the gas and liquid flow rates, and the equilibrium relationship, the number of theoretical plates can be determined by a graphical procedure described in Section 5.2.1.1. An example of the use of the method is given below.

Example - Determine the number of theoretical plates required to water-scrub 98 mole percent of the NH_3 from an air stream containing 2 mole percent NH_3, at the following conditions:

Inlet air pressure	1 atm	
Gas flow rate	1200 kg/m^2-hr	(246 lb/ft^2-hr)
Liquid flow rate	1200 kg/m^2-hr	(246 lb/ft^2-hr)
Temperature	20°C	(68°F)

Equilibrium data for partial pressure of NH_3 over aqueous NH_3 solutions (Sherwood and Pigford, 1952):

p, mm Hg	12.0	18.2	31.7
x', kg NH_3/kg H_2O	0.02	0.03	0.05

To insure a straight operating line, use flow rates of NH_3- free water and air:

$$\hat{L} = \frac{1200}{18} = 66.7 \text{ (kgmol/m}^2\text{-hr)}$$

$$\hat{G} = (0.98)\frac{1200}{0.02(17) + 0.98(29)} = 40.9 \text{ (kgmol/m}^2\text{-hr)}$$

The appropriate composition variables are $\hat{x}$ (kgmol NH_3/kgmol H_2O) and $\hat{y}$ (kgmol NH_3/kgmol air). Refer to Figure 5.2.1-1 for the subscript notation. The NH_3 in the inlet air is

$$\hat{y}_0 = \frac{0.02}{0.98} = 0.02041$$

The inlet water is $\hat{x}_n = 0$. The NH_3 in the outlet air is

$$\hat{y}_n = \hat{y}_o\,(1-0.98) = 0.02040(0.02) = 0.00041$$

The NH_3 in the outlet water is then

$$\hat{x}_0 = \frac{(\hat{y}_o - \hat{y}_n)\,\hat{G} + \hat{x}_n\,\hat{L}}{\hat{L}} = \frac{(0.02000)(40.9) + 0}{66.7} = 0.01226$$

The operating line is a straight line between (0, 0.00041) and (0.01226, 0.02041), with slope $\hat{L}/\hat{G} = 1.63$. (See Figure 5.2.2-9).

The equilibrium line is calculated from the given data by

$$\hat{y} = \frac{p}{760-p} \quad \text{and} \quad \hat{x} = \frac{18}{17}\,x'$$

In the range of interest, the equilibrium line is almost straight.

Stepping off plates as shown in Figure 5.2.2-9, the number of theoretical plates required is 4.1.

Since the equilibrium line is almost straight, Equation 5.2.1-5 should give approximately the same result. The slope of the equilibrium line is about 0.74. Then,

$$N_p = \frac{\ln\left[\left(1 - \frac{0.74}{1.63}\right)\left(\frac{.02041 - (.74)\ (0)}{.00041 - (.74)\ (0)}\right) + \frac{0.74}{1.63}\right]}{\ln \frac{1.63}{0.74}} = \underline{4.2 \text{ plates}}$$

This is well within the accuracy of the graphical techniques.

Plate efficiency

Various plate efficiencies have been defined in Section 4.2.5. Overall plate efficiencies are less than 100% (usually), because the theoretical plate concept assumes that the liquid on the plate is perfectly mixed and that the vapor reaches complete equilibrium with the liquid, and these conditions are not normally attained in actual plate columns.

Other definitions of efficiency are more fundamentally related to the interphase resistance to mass transfer on the plates. The Murphree vapor efficiency for a plate compares the change in vapor composition entering and leaving the plate with the theoretically attainable change in vapor composition assuming the vapor leaving to be at equilibirum with the liquid leaving the same plate. The point efficiency relates similarly the vapor compositions below and above a single point on a plate.

An empirical correlation for "E_{MV}", Murphree vapor efficiency, applicable to a large variety of bubble-cap absorbers, is:

$$E_{MV} = 1 - \exp(-K) \qquad (5.2.2\text{-}23)$$

where $K \equiv \dfrac{h_d'}{\left(0.21 + 0.51 \dfrac{m\ M_L}{\rho_L}\right) \mu_L^{0.68}\ b^{0.33}}$

proposed by Walter and Sherwood (1941). In this equation "h_d'" is the height of the outlet weir above the vertical midpoint of the cap slots (range 0.025m to 0.045m) and "b" is the slot width, both in m; "μ_L" is the liquid viscosity (cp); "m" is the slope of the y-x equilibrium line; "ρ_L" is the liquid density (kg/m^3); and "M_L" is the molecular weight of the liquid. Equation 5.2.2-23 is valid over a wide range of variables but should be regarded as approximate. Experimental values of "E_{MV}" are much to be preferred, if they are available for the conditions of interest.

Murphree vapor efficiencies are applied by modifying the graphical construction of Figure 5.2.2-9 in a manner described in Section 5.2.1.1.

Unless reliable experimental values of the Murphree vapor efficiency are available, it is usually easier and as accurate to use an overall plate efficiency obtained from an empirical correlation. The correlation of Chu et al. (1951) is recommended.

$$E\ (\%) = 13.84\text{x}10^{0.302h'} \left(\frac{\hat{L}}{\hat{G}}\right)^{0.245} \left(\frac{\rho_L}{m\ M_L\ \mu_L}\right)^{0.38} \qquad (5.2.2\text{-}24)$$

where "h'" is the liquid depth to the vertical midpoint of the cap slots in m; "ρ_L" is in kg/m^3, and "μ_L" is in cp. For liquid depth h' = 0.03 m, is a typical value, Equation 5.2.2-24 is plotted in Figure 5.2.2-10 against group m M_L μ_L/ρ_L.

Height of ends

The height of a plate column above the top tray consists of a space for liquid disengagement, plus the height of the domed end if the scrubber is a pressure vessel. The disengagement height is typically 0.6 to 0.75 meter, and the dome height is one-fourth of the column diameter. The column height below the bottom tray should be 0.6 to 1.0 meter in addition to the tray spacing, to allow space for the gas stream inlet and some depth of liquid to provide a seal on the liquid outlet.

5.2.3 PACKED COLUMN SCRUBBERS

The packed column is a commonly used device for scrubbing operations involving absorption of a gas but less common for particle separation. A typical column is shown in Figure 5.2.3-1, containing inert packing material, a support plate, liquid redistribution plates, and a liquid inlet. The liquid and gas flows are usually countercurrent, with the solvent flowing down over the packing and the gas flowing up through the spaces between the packing. Sometimes the process layout makes it more convenient to use two shorter columns in series, in which case it is possible to run the first one cocurrently, and the second countercurrently.

A great number of packing materials are available commercially, with a wide range of cost, specific surface area, pressure drop, weight, and corrosion resistance. Packings can be divided broadly into two categories; dumped pieces (random packing), and regular packings. Random packings are designed with high surface area for good gas-liquid contacting. Regular packings, including stacked pieces and grids, have the advantage of lower pressure drop, better liquid distribution and higher gas capacity because of their greater open area, but they are more expensive to install. Examples of random and regular packings are given in Chapter 3.

5.2.3.1 Unit Mechanisms

Higbie (1935) suggested that mass transfer in a packed tower could be analyzed by supposing that the liquid passes over each packing piece in laminar flow and is then completely mixed with other liquid at the point of contact with the next piece of packing. Danckwerts (1955) reviews his own and other modifications of Higbie's model. The major mechanism is transfer to liquid sheets. For design purposes, however, empirical correlations are recommended because of the uncertainties of liquid flow patterns, wetted area, and gas mixing. Some of these correlations, as well as available data, are discussed or referenced below. One would, however, have to fall back on unit mechanisms when considering a new packing or where empirical correlation or data is not available. Further, models based on unit mechanisms provide valuable insight into performance characteristics as they depend upon geometric and flow parameters.

5.2.3.2 Column Diameter

The diameter of a packed column is set by the allowable gas velocity through the open spaces in the packing. The effect of gas velocity on packed column operation is due to its influence on the pressure drop, liquid entrainment, and the operating stability of the column.

As shown schematically in Figure 5.2.3-2, at low gas rates the slope of the pressure drop curve is the same for irrigated packing as for dry packing. At the "loading" point, the slope of the curve changes, and the slope increases again at the "flooding" points. At flooding, liquid builds up in the packing, so the dispersed phase becomes gas, rather than liquid.

The column diameter should be selected to give a gas velocity below the load point, but since the flooding condition is easier to define experimentally, the usual design criterion is operation at 50 to 75% of the flooding velocity; this usually insures a gas rate below loading. In industrial practice the percent of flooding used for various packings is: Raschig rings from 60 to 80%; Berl saddles from 65 to 80%, and intalox saddles from 65 to 85%.

Eckert (1961) has improved generalized flooding correlation presented by Sherwood et al. (1938) and later modified by Lobo et al. (1945), and Leva (1954). The gas mass velocity "G" as the group $(G^2 F \psi \mu_L^{0.2})/(\rho_G \rho_L g)$ [units in centipoise to the 0.2 power] is plotted against $(L/G)(\rho_G/\rho_L)^{0.5}$ [dimensionless] as given by Eckert in Figure 5.2.3.3.

To determine the required column diameter, first calculate the group $X \equiv (L/G)(\rho_G/\rho_L)^{0.5}$, where "L" and "G" are the mass flowrates. Any consistent set of units can be used so that "X" is dimensionless. Next select a pressure drop; most scrubbing processes are designed for a low pressure drop, 5 to 10 cm H_2O per meter of packing, (about 0.5" to 1" H_2O/ft.). From the value of "X" and the desired pressure drop, read the ordinate "Y" (which has units of centipoises to the 0.2 power) from the chart, where

$$Y \equiv \frac{G^2 F \psi \mu_L^{0.2}}{\rho_G \rho_L g}, \ (\mu_L \text{ in } \underline{\text{cp}}), \text{ units are } (\text{cp})^{0.2} \qquad (5.2.3\text{-}1)$$

Then "G", the mass flowrate of the gas per unit cross-sectional area of column, is

$$G = \left(\frac{Y \rho_G \rho_L g}{F \psi \mu_L^{0.2}}\right)^{1/2} \qquad (5.2.3\text{-}2)$$

Here, "F" is a packing factor, and can be found from Table 5.2.3-1.

The column diameter is then

$$d_{col} = 1.13\left(\frac{G_M}{G}\right)^{1/2} \qquad (5.2.3\text{-}3)$$

where G_M is the total mass flowrate of gas. In Equations 5.2.3-1 and 5.2.3-2, the liquid viscosity must be in centipoise; all other

TABLE 5.2.3-1

PACKING FACTORS, F, FOR DUMPED PIECES[1]

	Nominal size of packing, inches [cm]										
	1/4" [0.64]	3/8" [0.95]	1/2" [1.27]	5/8" [1.59]	3/4" [1.9]	1" [2.5]	1-1/4" [3.2]	1-1/2" [3.8]	2" [5]	3" [8]	4" [10]
Raschig rings, ceramic											
1/16" wall	5250	3280									
1/18" wall						510					
1/4" wall								430	210		
3/8" wall										121	98
Raschig rings, carbon											
1/16" wall	5250		1340								
1/8" wall					920	525					
1/4" wall								430	210		
5/16" wall										118	
Raschig rings, metal											
1/32" wall	2300	1280	980	560	510	380					
1/16" wall			1340	950	720	450	360	272	187	105	
Lessing rings, porcelain											
1/8" wall						(800)[2]					
1/4" wall									(360)		
Lessing rings, metal											
1/32" wall			(1060)		(630)						
1/16" wall						(472)	(387)	(295)	(200)		
Partition rings										262	190
Pall rings, plastic				318		171		105	82		
Pall rings, metal				230		158		92	66		
Berl saddles	2950		790		560	360		213	148		
Intalox saddles, ceramic	2380	1080	660		475	322		171	131	72	
Intalox saddles, plastic						108			69	52	
Super-Intalox, ceramic						200			100		
Tellerettes									150		

---

[1] Packing factor F is given in m^2/m^3. To convert to ft^2/ft^3, multiply by 0.3048.

[2] Parentheses denote a value of a/ε^3, rather than empirical F.

TABLE 5.2.3-2

PACKING FACTORS, F, FOR GRIDS AND STACKED PIECES[1]

	Nominal size of packing, inches [cm]							
	1 [2.5]	1-1/2 [3.8]	2 [5]	3 [8]	4 [10]	5 [13]	5-1/2 [14]	6 [15]
Wood grid	20	11	8.2	5.9	4.9			
Metal grid	8.2							
Grid tiles						118		
Checker brick, $\varepsilon=0.55$							135	
Raschig rings, ceramic								
1/4" wall			95	16				
3/8" wall				36	12.8			
Raschig rings, metal				21				
Partition rings, diameter								
3" length				(1200)[2]	(725)			
4" length					(705)			(410)
6" length								(375)
Partition rings, square-set								
3" length				(690)	(460)			
4" length					(450)			(275)
6" length								(260)

---

[1] Packing factor F is given in m^2/m^3. To convert to ft^2/ft^3, multiply by 0.3048.

[2] Parentheses denote a value of a/ε^3, rather than empirical F.

quantities can be in any consistent units that make "Y" dimensionless (except for the $\mu_L^{0.2}$ dependence). Values of "F" are given for commercial packings in Tables 5.2.3-1 and 5.2.3-2 obtained from sources listed at the end of the chapter and from manufacturers' literature. Where an empirical "F" is not available, the manufacturer's value of a/ε^3 can often be used without gross error, especially in view of the 1/4 power dependence of d_{col} on "F". Such values of a/ε^3 are identified by parentheses in the two tables. Theoretically, $F = a/\varepsilon^3$.

Example

Determine the packed column diameter required to water-scrub essentially all the SO_2 from a gas at 20°C and 1 atm containing 15% SO_2, 6% O_2, and 79% N_2, using the following additional design information:

Gas rate:	500 m^3/hr	(294 cfm)
Water rate:	10,000 kg/hr	(22,050 lb/hr)
Packing:	1-inch ceramic Raschig rings	
Pressure Drop:	3.5 cm H_2O/meter (≈0.4"/ft) of packed height	

The column should be designed for the largest gas and liquid streams, which will be at the bottom of the column, assuming countercurrent operation. The gas rate entering in moles is:

$$\frac{(500)\ (273)}{(22.414)\ (293)} = 20.78 \text{ kgmol/hr, and its molecular weight is}$$

$$0.15\ (64) + 0.06\ (32) + 0.79\ (28) = 33.64 \text{ kg/kgmol.}$$

Then G_M = 20.78 x 33.64 = 699.0 kg/hr.
Weight SO_2 absorbed: 0.15 x 20.78 x 64 = 199.5 kg/hr.
Thus L_M = 10,000 + 199.5 = 10,200 kg/hr. The solution leaving is dilute enough so that its properties are essentially the same as water, i.e.: ρ_L = 1,000 kg/m and μ_L = 1 cp.
Gas density: ρ_G = 699.0/500 = 1.398 kg/m^3

$$X = \frac{10{,}200}{699}\left(\frac{1.398}{1000}\right)^{1/2} = 0.546$$

From Figure 5.2.3-3, at 0.4 inches W.C./ft column height (0.033 m W.C./m column height) pressure drop, Y = 0.017. From Table 5.2.3-1 for 1-inch ceramic Raschig rings, F = 510 m^{-1}. By Equation 5.2.3-2, with $g = 1.27\text{x}10^8 (m/hr^2)$;

$$G = \left(\frac{(0.017)(1.398)(1000)(1.27(10^8)}{(510)\ (1)\ (1)}\right)^{1/2} = 2{,}430 \text{ kg/hr-m}^2 \ (498 \text{ lb/hr-ft}^2)$$

Then by Equation 5.2.3-3,

$$d_{col} = 1.13\left(\frac{699}{2430}\right)^{1/2} = \underline{0.61 \text{ m}} \quad (2.0 \text{ ft})$$

The percent of flooding is determined by the value of "Y" at the flooding line. From Figure 5.2.3-3, at X = 0.546, Y_{flood} = 0.040. Then,

$$\%\ \text{flood} \equiv \frac{G}{G_{flood}} = \left(\frac{Y}{Y_{flood}}\right)^{1/2} = \left(\frac{0.017}{0.04}\right)^{1/2} = \underline{65\%\ \text{flooding}}$$

5.2.3.3 Pressure Drop

The pressure drop in a packed column as usually operated is small; in fact this is one of the major advantages of a packed column over a plate column when a choice is possible. The pressure drop at flooding is in the range 12 to 35 cm H_2O/m of packing height (1.5 to 4"/ft) for most packings, with 15 cm H_2O/m (2"/ft) being an average value for crude estimation purposes. Pressure drops in an operating absorber are usually 0.04-0.08 m/m (0.05 to 1.0 inches H_2O per ft of height) as mentioned in the previous section.

By using Figure 5.2.3-3 for column design, one can simply estimate pressure drop. In the example of the previous section, the pressure drop was specified as a design parameter; the column diameter was then determined, and the percent-of-flooding was checked and found reasonable. Alternatively, the flooding percent can be specified as a design variable. In that case, G_{flood} is determined from the flooding line on Figure 5.2.3-3, and G is calculated as the desired percent of G_{flood}; the pressure drop is determined in turn from the pressure drop lines.

Many other methods for estimating pressure drop are available. Some of the more comprehensive discussions are those of Sherwood and Pigford (1952), Treybal (1955), Norman (1961), and Morton et al. (1964). However, all the widely applicable methods are quite approximate, because the pressure drop is so small and is sensitive to so many operating variables; consequently, there is no particular reason to prefer any of them over Eckert's (1961) generalized correlation in Figure 5.2.3-3.

A substantial amount of pressure drop data is available in packing manufacturers' literature and in the references given for this section. These data can be useful if the operating conditions of the scrubber being designed are exactly identical to a situation for which there are data; otherwise Eckert's (1961) generalized correlation is easier to use and just as reliable.

5.2.3.4 Column Height

The methods for the calculation of column height in terms of HTU and NTU have been presented in Section 5.2.1.2. While the number of transfer units can be calculated according to the methods outlined, the height of transfer unit is calculated from mass transfer coefficients. Either theoretically or experimentally determined mass transfer coefficients may be used for this calculation.

A great deal of reliable experimental data is available in the literature, covering HTU's and related measures of packed column performance. In addition, several generalized HTU correlations have been presented which, however, are usually relatively restricted in applicability. As a way to make the best use of the available information, the following procedures are recommended, listed in order of decreasing preference.

1. Find HTU data for the scrubbing process of interest at the desired flow conditions, packing, etc. References are given in Table 5.2.3-3.

2. Alternatively, locate data for a similar system, and use the methods suggested in this section to adjust the literature values for the effects of temperature, diffusivities, viscosities, and flowrates.

3. Use the very rough rule that an HTU is about 0.5 to 1.0 m.

Experimental mass transfer studies are listed in Table 5.2.3-3. The most convenient form of HTU for scrubber design is usually H_{OG}; if the literature data are not given as H_{OG}, they can be converted by equations in Section 5.2.1.2.

Limited experimental data can often be extended to other conditions of interest with considerable confidence by using one or more of the semi-theoretical and empirical correlations which have been developed in the last twenty years. For example, given that

$N_{Sh} = \dfrac{\hat{k}_G \, Rg \; T \, d}{D_G} \sim N_{Re}{}^{1/2} \; N_{Sc}{}^{1/3}$, and $p_B \, M_B \approx \rho_G Rg \; T$, it is easy to obtain

$$H_G = \frac{\hat{G}}{\hat{k}_G \; a \; p_B \; M_B} \sim \left(\frac{G}{\mu_G}\right)^{1/2} \left(\frac{\mu_G}{\rho_G \; D_G}\right)^{2/3} \qquad (5.2.3\text{-}4)$$

where "p_B" is the partial pressure of B, and "M_B" is the molecular weight of "B".

If a liquid flowrate dependence is added, much of the experimental packed column work in the literature can be fitted by expressions similar to Equation 5.2.3-4.[For further discussion of literature correlations, see Sherwood and Pigford (1952), Norman (1961), and Perry's Handbook (1963).] For general use in adjusting literature values of "H_G" for slightly different conditions, the following dependence is recommended:

$$H_G \sim \left(\frac{G}{\mu_G}\right)^{1/4} L^{-1/4} \left(\frac{\mu_G}{\rho_G \; D_G}\right)^{1/2} \qquad (5.2.3\text{-}5)$$

In any given system, the effect of temperature on "H_G" is minor; Sherwood and Pigford suggest an increase of 0.4 to 1.3 percent in "H_G" for every degree Centigrade of temperature rise.

For the height of a liquid phase transfer unit,

$$H_L \sim \left(\frac{L}{\mu_L}\right)^{1/4} \left(\frac{\mu_L}{\rho_L \; D_L}\right)^{1/2} \qquad (5.2.3\text{-}6)$$

is recommended, based on the work of Sherwood and Holloway (1940) and the comments of Norman (1961). The effect of temperature on "H_L" is appreciable, and can be allowed for by multiplying "H" at the reference temperature by exp $(-0.023 \, \Delta t)$, where "Δt" is the change in °C in going from the reference temperature to the temperature of interest; "H_L" decreases with increasing temperature.

The adjustments suggested in Equations 5.2.3-5 and 5.2.3-6 cannot be applied blindly if the nature of the design system is very different from the measured system. Table 5.2.3-4 shows the major resistance to mass transfer for many common scrubber systems; the adjustment procedures described above can usually be applied safely if the design

TABLE 5.2.3-3 SOURCES OF MASS TRANSFER DATA

Solute	Solvent[a]	Packing[b]	References[c]
Acetaldehyde	Water	Rings	Sitaraman (1968)
	Alcohol	Rings	Sitaraman (1968)
	Glycerol	Rings	Sitaraman (1968)
Acetone	Water	Rings	Zabban and Dodge (1954)
		Rings	Houston and Walker (1950)
		Rings	Hutchings et al. (1949)
		Rings	Schiebel and Othmer (1944)
		Rings	Othmer and Schiebel (1941)
		Berl saddles	Zabban and Dodge (1954)
		Intalox saddles	Eckert (1963)
		Stedman	White and Othmer (1942)
Acetylenes	Copper ammonium acetate	Rings	Molstad and Parsly (1950)
Ammonia	Water	WWC	Hollings and Silver (1934)
		WWC	Cogan and Cogan (1932); SP
		Spheres	Sherwood and Holloway (1940)
		Rings	Houston and Walker (1950)
		Rings	Cryder and Maloney (1941)
		Rings	Fellinger (1941); SP; KR
		Rings	Dwyer and Dodge (1941)
		Rings	Sherwood and Holloway (1940)
		Berl saddles	Molstad et al. (1943)
		Berl saddles	Fellinger (1941); SP
		Intalox saddles	Eckert (1967)
		Partition rings	Molstad et al. (1943)
		Spiral rings	Molstad et al. (1943)
		Spiral rings	Fellinger (1941); KR
		Spiral rings	Kowalke et al. (1925b)
		Grid titles	Parsly et al. (1950); KR
		Grid titles	Molstad et al. (1943)
		Grids	Molstad et al. (1943)
		Grids	Kowalke et al. (1925a); KR
Ammonia	Acetic acid	Grids	Johnstone and Singh (1937)
Carbon dioxide	Water	Plane	Grimley (1945); SP
		Plane	Vyazovov (1940); SP
		Plane	Hatta and Katori (1934); SP
		Spheres	Yoshida and Koyanagi (1958)
		Rings	Yoshida and Koyanagi (1958)
		Rings	Fujita and Hayakawa (1956)
		Rings	Shulman and DeGouff (1952)
		Rings	Koch et al. (1949)
		Rings	Rixon (1948); KR
		Rings	Deed et al. (1947)
		Rings	Cooper et al. (1941); SP; KR
		Rings	Sherwood and Holloway (1940)

Table 5.2.3-3

Solute	Solvent[a]	Packing[b]	References[c]
Carbon dioxide		Berl saddles	Yoshida and Koyanagi (1958)
		Berl saddles	Fujita and Hayakawa (1956)
		Berl saddles	Sherwood and Holloway (1940)
		Intalox saddles	Eckert (1967)
		Spiral rings	Sherwood and Holloway (1940)
	Sodium hydroxide	Rings	Leva (1955) Greenwood and Pearce (1953) Blum et al. (1952) Tepe and Dodge (1943); KR
		Lessing rings	Greenwood and Pearce (1953)
Carbon dioxide	Sodium hydroxide	Pall rings	Eckert et al. (1958)
		Berl saddles	Leva (1955)
		Intalox saddles	Eckert (1967) Leva (1955)
	Potassium hydroxide	Rings	Blum et al. (1952)
		?	Spector and Dodge (1946)
		Intalox saddles	Eckert (1967)
	Mono-ethanol amine	Rings	KR Teller and Ford (1958) Kohl (1956); KR Gregory and Scharmann (1937)
		Berl saddles	KR Teller and Ford (1958)
		Intalox saddles	Eckert (1967)
		Tellerettes	Teller and Ford (1968); KR
	Di-ethanol amine	Rings	Cryder and Maloney (1941); KR
Carbon dioxide	Sodium carbonate	Rings	Blum et al. (1952)
		Rings	Furnas and Bellinger (1938);KR
		Rings	Comstock and Dodge (1937)
		Berl saddles	Furnas and Bellinger (1938);KR
	Potassium carbonate	Rings	Benson et al. (1956)
		Rings	Benson et al. (1954); KR
		Rings	Comstock and Dodge (1937)
	diAmino isopropanol	Rings	Gregory and Scharmann (1937)
Carbon monoxide	Copper ammonium formate	Rings	KR
		Rings	Van Krevelen and Baans(1950);KR
Chlorine	Water	WWC	Krebs (1938)
		Rings	Vivian and Whitney (1947);KR
		Intalox saddles	Eckert (1967)
	Sodium hydroxide	?	Vivian (1945)
		Intalox saddles	Eckert (1967)
Chlorine	Ferrous sulfate	Rings	Riggle and Tepe (1950)

Table 5.2.3-3

Solute	Solvent[a]	Packing[b]	References[c]
Diolefins	Copper ammonium acetate	Rings	Morrell et al. (1946)
Ethanol	Water	Rings Rings	Houston and Walker (1950) Molstad and Parsly (1950)
		Berl saddles	Molstad and Parsly (1950)
		Grid titles	Molstad and Parsly (1950)
Ethylene	Cuprous chloride (acidic)	Rings	Seebold and Gilliland (1941)
Hydrogen chloride	Water	Rings	Oldershaw et al. (1947) Sherwood and Holloway (1940)
		Berl saddles	Sherwood and Holloway (1940)
		Intalox saddles	Eckert (1967)
		Spiral rings	Sherwood and Holloway (1940)
Hydrogen sulfide	Water	WWC.	Krebs (1938)
		Intalox saddles	Eckert (1967)
	MEA	Rings	Leibush and Shneerson(1950);KR
		Intalox saddles	Eckert (1967)
	DEA	Rings	Leibush and Shneerson(1950);KR
		Intalox saddles	Eckert (1967)
	Sodium carbonate	WWC	Litvinenko (1952)
		Rings	Litvinenko (1952)
	Potassium carbonate	WWC	Litvinenko (1952)
		Rings	Litvinenko (1952)
Methanol	Water	Rings Rings	Zabban and Dodge (1954) Houston and Walker (1950)
		Berl saddles	Zabban and Dodge (1954)
Methyl ethyl ketone	Water	Rings	Scheibel and Othmer (1944)
Methyl i-butyl ketone	Water	Rings	Schiebel and Othmer (1944)
Methyl n-amyl ketone	Water	Rings	Scheibel and Othmer (1944)
Olefins	Copper ammonium acetate	Rings	Morrell et al. (1946)
Oxygen	Water	WWC	Miller (1948); SP
		Rings Rings Rings Rings Rings	Whitney and Vivian (1949) Deed et al. (1947) Vivian and Whitney (1947) Molstad et al. (1942) Sherwood and Holloway (1940)
		Berl saddles Berl saddles	Molstad et al. (1942) Sherwood and Holloway (1940)

Table 5.2.3-3

Solute	Solvent[a]	Packing[b]	References[c]
Oxygen		Intalox saddles	Eckert (1967)
		Partition rings	Molstad et al. (1943); SP
		Partition rings	Molstad et al. (1942)
		Spiral rings	Molstad et al. (1943); SP
		Spiral rings	Molstad et al. (1942)
		Spiral rings	Sherwood and Holloway (1940)
Oxygen	Water	Grid titles	Molstad et al. (1943); SP
		Grids	Molstad et al. (1943); SP
		Stedman	Knoedler and Bonilla (1954)
Sulfur dioxide	Water	WWC	Krebs (1938)
		WWC	Hollings and Silver (1934)
		WWC	Haslam et al. (1924)
		WWC	Haslam et al. (1923)
		Rings	Pearson et al. (1951)
		Rings	Whitney and Vivian (1949);SP
		Rings	Jenness and Caulfield (1939)
		Rings	Cantelo et al. (1927)
		Intalox saddles	Eckert (1967)
		Spiral rings	Adams (1933)
		Spiral rings	Haslam et al. (1923)
	Sodium Hydroxide	Rings	Johnstone and Singh (1937)
		Intalox saddles	Eckert (1967)
		Wire helices	Johnstone and Singh (1937)
		Spiral rings	Johnstone and Singh (1937)
		Grids	Johnstone and Singh (1937)
Sulfur dioxide	Sodium carbonate	Rings	Whitney et al. (1953)
Water	Brine	Grids	Norman et al. (1954)
Water (air humidification)	Water	WWC	Greenewalt (1926); SP
		Rings	Yoshida (1955)
		Rings	Yoshida and Tanaka (1951)
		Rings	McAdams et al. (1949)
		Rings	Sherwood and Holloway (1940)
		Berl saddles	Hensel and Treybal (1952)
		Grids	Norman (1951)
Water (Helium humidification)	Water	Rings	Yoshida (1955)
Water(CO_2 humidification)	Water	Rings	Yoshida (1955)

---

[a] All solvents are aqueous solutions unless otherwise noted.

[b] WWC = wetted wall column.

[c] SP = Sherwood and Pigford (1952); KR = Kohl and Riesenfeld (1960).

system is in the same column as the system for which HTU data are available.

TABLE 5.2.3-4
MAJOR RESISTANCE TO MASS TRANSFER[a]

Liquid Phase	Both Phases	Gas Phase
O_2 - H_2O	SO_2 - H_2O	NH_3 - H_2O
H_2 - H_2O	NO_2 - H_2SO_4	amine - acid
CO_2 - H_2O	Acetone - H_2O	SO_2 - alkali
Cl_2 - H_2O	H_2S - alkali	HCl - H_2O
CO_2 - NaOH		H_2O - acid
CO_2 - amines		H_2O - brine

---

[a] From Emmert and Pigford (1963).

5.2.3.5 Other Design Considerations

The performance of a packed column depends heavily on the specific interfacial area, a, effective for mass transfer. Quantitative information about effective interfacial area is only fragmentary, and this is a primary reason for the empirical nature of packed tower design techniques. Interfacial area is not equal (or even proportional) to the actual surface area of the packing pieces. The effective area is diminished by (1) uneven distribution of liquid through the packing, which is discussed below; (2) incomplete wetting of the individual pieces; and (3) stagnant, ineffective regions of liquid at the points of contact between pieces.

The effective interfacial area can be as low as 30% of the dry packing surface area, and Treybal (1955) suggests that it is not 100% until near flooding conditions. The percent of the packing surface wetted depends on the liquid flowrate but not the gas flowrate; the dependence on liquid flow is shown qualitatively in Figure 5.2.3-4 adapted from Sherwood and Pigford (1952). Another way to allow for the effect of wetted area on performance is through the minimum wetting rate (MWR) required to completely wet the packing. The MWR is expressed in several ways, and the available information for various packings is sketchy and largely empirical.

Ponter (1954) gives a correlation for "Γ", the MWR expressed as mass of liquid per time per length of packing periphery, and cites experimental values from 0 to 450 (kg/hr-m) (0 to 300 lb hr/ft), for wetted wall columns and a variety of packings. Treybal (1955) suggests a MWR of L = 1,200 (kg/hr-m²), and Norman (1961) quotes work recommending L = 1,500 (kg/hr-m²); these two authors regard the MWR as the liquid rate below which the overall transfer coefficient "K_Ga" or "K_La" decreases rapidly with decreasing liquid rate. (The two definitions are roughly equivalent.) The MWR is not a lower limit for liquid rate; it is simply a measure of how easily the packing is wetted. Scrubbers can be (and often are) operated at far less than the MWR if maximum performance is not required.

The methods presented in Section 5.2.1.2 for determining NTU ignored heat effects. In some industrially important scrubbing operations, the effects of solute absorption, solvent evaporation and sensible heat transfer between the gas and the liquid, change the effective equilibrium curve, and sometimes the operating line. The common examples are the scrubbing of HCl, HF or NH_3 with water, and condensation of steam by cooling water. The design is accomplished by including a heat balance and solving the heat and mass balances simultaneously. Examples of calculations including heat effects are given in Chapter 4.

Maldistribution, or uneven flow of the liquid through the column, is detrimental to performance primarily because some of the packing will be incompletely wet and some will stay dry. In addition, even on wetted packing pieces, the gas-liquid contact times will vary over such a wide range that some liquid streams will not have enough time for the intended amount of mass transfer, while other streams become saturated prematurely and are then ineffective for further absorption. Near the top of the packing, maldistribution is avoided by a well-designed liquid distributor.

Small-diameter towers require relatively more distribution points (nozzles, orifices, weir notches, etc.) than large columns. The recommendations in Table 5.2.3-5 are based on Eckert's design techniques (1961). Below the top meter or so of packing, good distribution

TABLE 5.2.3-5
LIQUID DISTRIBUTION POINTS PER BED CROSS-SECTIONAL AREA

Column diameter		Recommended No. of points	
m	ft	per m^2	per ft^2
≥ 1.5		≥ 43	
	≥ 4		≥ 4
1.0		95	
	2.5		16
0.5		280	
	1.25		32

depends on the packing. In general, better distribution is achieved with smaller packing pieces, larger column diameters, and "irregular" shapes such as Intalox saddles. Even the "best" packing shapes (from a liquid distribution standpoint) will require re-distribution of the liquid if the packing is more than a certain depth. Stacked packings maintain liquid distribution better than dumped packings. Recommendations are summarized in Table 5.2.3-6, based on suggestions of Eckert (1961).

TABLE 5.2.3-6
SIZING FOR GOOD DISTRIBUTION IN PACKING

Packing	Ratio of column diameter to packing size	Maximum packing depth without redistribution *
Raschig rings	>30	2-1/2 to 3 column diameters
Saddles (Berl, Intalox)	>15	5 to 8 column diameters
Pall rings	>10	5 to 10 column diameters

---

* But should not exceed 6 m (20 ft).

5.2.4 FIBROUS-PACKED SCRUBBERS

As viewed in this section, fibrous packings include a variety of materials ranging from fibers to vertical springs, with less than 1 mm diameter of the fiber and less than 10 per cent volume solids. As opposed to dumped or stacked packings, fibrous packings are usually installed in sections or even complete column-size units.

Fibrous packings are made up of inert fibers matted together and usually installed in column-diameter pads or horizontal strips. Fiberglas, Dynel, Saran, and K-115 are among the materials used. Knitted mesh packings are typified by Goodloe packing, Hyperfil packing, and York Demisters; they consist of pads made by crimping a knitted wire mesh in strips, and then folding or coiling the strips into a pad configuration. Woven fabric packings are made of fine wire screen in various shapes; examples are Koch-Sulzer packing and Neo-Kloss packing. A sort of cross-breed is the McMahon packing, which consists of small saddle shaped pieces of woven wire mesh. Spring packings, such as Kloss packing, consist of many long vertical springs each made up of a pair of helical wires.

5.2.4.1 Unit Mechanisms

In a wettable fibrous packing, drops of liquid have some tendency to cover the fiber in a film, but usually it takes the form of spread out drops along the fiber. These drops may grow big enough to fall off the fiber. Thus, some of the liquid flows down the fiber to the next fiber as a film or as drops, while some of the liquid actually drops to the next fiber. The unit mechanisms involved are then mass transfer to liquid films, mass transfer to drops on the fibers, and mass transfer to falling drops. The amount of mass transfer by each of these mechanisms will vary considerably for the different types of fibrous packing; for example, mass transfer to drops is much more important in the true fiber type of packing than in the packing made of wire mesh. Also, the degree of wettability of the packing material will effect the degree to which a liquid film coalesces into drops on the packing surface.

The mechanisms of mass transfer in fibrous packings are quite different from the mechanisms of particulate collection, and in contrast to particulate collection, theoretical treatments of mass transfer on fibrous packings are almost nonexistent in the literature.

5.2.4.2 Column Diameter

The diameter of a fibrous-packed column is determined from the allowable gas velocity through the packing, which is affected by the gas and liquid densities, the liquid flow rate, the liquid surface tension and viscosity, and the specific surface area of the packing.

The allowable velocity is limited by entrainment; as in the case of plate columns (Section 5.2.2), the minimum column diameter can be estimated from Equation 5.2.4-1

$$d_c = \psi \left(Q_G \sqrt{\rho_G}\right)^{1/2} \qquad (5.2.4\text{-}1)$$

Little useful information is available on which to base a value of ψ, because fibrous packings have not found wide use in scrubbing applications. For rough design purposes, the values given in Table 5.2.4-1 are suggested, based on design methods of York and Poppele (1963) for wire mesh mist eliminators, and assuming a liquid specific gravity of 1.05.

TABLE 5.2.4-1

VALUES OF "ψ" FOR WIRE MESH MIST ELIMINATORS

Units	Q_G	ρ_G	ψ	d_c
Metric	m^3/hr	kg/m^3	0.0101	m
English	cfm	lb/ft^3	0.0865	ft

5.2.4.3 Pressure Drop

The pressure drop in fibrous packings is even less than in dumped packings, partly because of the high percentage of void space (from 90 to 97% in the packings considered here); consequently the pressure drop is unlikely to be the limiting design factor in this type of scrubber. The plot of Figure 5.2.4-1 shows observed pressure drop per height of packing for several fibrous packings. The data were obtained from manufacturer's literature and, for Fiberglas fibers, from Williams et al. (1947).

The data used for Figure 5.2.4-1 are limited, but they suggest that the pressure drop can be represented crudely by

$$\frac{\Delta P}{Z} = c \left(\frac{G}{1000}\right)^{1.6} \qquad (5.2.4\text{-}2)$$

where $\Delta P/Z$ is the pressure drop per height of packing in kg/m^2-(m of packing); and "G" is the mass flow rate of gas, in $kg/hr - m^2$. Values of the empirical constant "c", and the accuracy of Equation 5.2.4-2, are shown in Table 5.2.4-2 based on the "wet" packing (zero liquid rate) data of Figure 5.2.4-1. To convert from metric to English units, divide G in kg/(hr. m^2) by 4.88 to get G in lb/(hr ft^2), $\Delta P/Z$ in kg_f/m^2 - (m of packing) by 83.33 to get $\Delta P/Z$ in inches H_2O/(ft of packing).

Fully turbulent gas flow is characterized by an exponent of 1.8 to 2.0 in pressure drop equations like Equation 5.2.4-2 (Norman, 1961). The exponent of 1.6 may indicate that the flow is in the transition region between turbulent and laminar (exponent 1.0); the gas Reynolds number could be expected to be significantly less in fibrous packings than in dumped packing, both because the high percentage of void space decreases the true gas velocity, and because (in true fibers) the size of the gas flow passages is small. In work with glass fibers, Berly et al. (1954) concluded that the gas flow was transitional. However, York (1963) states that the flow of gas through a Dimester is "predominately turbulent."

TABLE 5.2.4-2
CONSTANTS FOR EQUATION 5.2.4-2

Packing	c	$\Delta P/Z$ accuracy	Range of G (kg/hr-m^2)
Fiberglas and Demister	1.5	±20%	500 - 20,000
Goodloe	4.7	±30%	800 - 2,500
Koch-Sulzer	0.64	±25%	2,000 - 10,000

5.2.4.4 Height of Column (Mass Transfer)

Other conditions being equal, HTU's are usually lower (i.e., mass transfer efficiency is higher) in fibrous packings than in dumped or stacked packings, because of their very large specific area. In the absence of any extensive body of experimental data covering mass transfer in fibrous packings, it can be assumed that the effects of physical properties and flow rates on the height of a transfer unit are similar to the dependences suggested for dumped packing HTU's in the previous section. The work of Williams et al. (1947) on a column packed with Fiberglas, for instance, shows almost no dependence on gas flow rate, and a liquid rate dependence approximately proportional to $L^{0.4}$.

For design purposes, a very rough idea of the H_{OG}'s to be expected is given by Figure 5.2.4-2. The data for this figure were obtained from manufacturers' literature and from Williams et al. Some of the values are for unspecified chemical systems and others are for distillation processes, thus they must be regarded as extremely rough and are given only to suggest order of magnitude.

Berly et al. (1954) carried out absorption of hydrogen fluoride by water using wetted saran fiber pads. Their data indicated better than 99% efficiencies with 2 to 3 wetted cells in series. Air velocities ranged from 50 to 100 cm/sec. Each stage was 5 cm (2 in.) deep. Their observation of differences in surface area available in various packings is interesting and reported in Table 5.2.4-3.

TABLE 5.2.4-3
PHYSICAL CHARACTERISTICS OF GAS ABSORPTION PACKINGS

Material	Size	Weight g/cc	Surface area cm^2/cc	Porosity, Fraction Voids
Porcelain Berl Saddles	1/2 in.	0.72	4.62	0.68
Porcelain Berl Saddles	1 in.	0.67	2.6	0.69
Porcelain Raschig Rings	1/2 in.	1.04	3.75	0.53
Porcelain Raschig Rings	1 in.	0.72	1.9	0.68
Coke	3 in.	0.465	.43	0.58
Crushed Stone	3/4 in.	1.31	2.9	0.5
Ceramic Balls	3/4 in.	1.36	1.6	0.49
Saran Fibers, diam.	178 μm	.109	14.4	0.94
Saran Fibers, diam.	78 μm	.058	17.4	0.97
Saran Fibers, diam.	51 μm	.0512	31	0.96

They found fiber beds to be five to ten times more efficient than Raschig Rings on a volume basis. When compared on the basis of weight of packing, one pound of 78-micron diameter saran fibers was 75 times more effective for the absorption of hydrogen fluoride gas than one pound of 1/2 inch Berl saddles.

5.2.4.5 Other Operating Characteristics

Flooding and Loading

The most widely applicable definitions of flooding and loading are in terms of the points where the log ΔP vs. log "G" curves show abrupt changes in slope (see Figure 5.2.3-2.) The experimental results of Williams et al. (1947) and York and Poppele (1963) suggest that pressure drop curves for fibrous packings do show these breakpoints. Williams et al. observed, however, that even when the flooding velocity (as defined by the second breakpoint of the curve) was exceeded, there was no liquid buildup on the top of the packing (Fiberglas) and that the column was operable well beyond the flooding velocity.

Distribution and Channeling

In general, a good distribution of liquid across the column is said to be easier to maintain in fibrous packings than in dumped packings because the characteristic dimension of each "piece" - each fiber, or each wire in a mesh - is small in relation to the column diameter. Williams et al. (1947) observed that the liquid in their Fiberglas column fell in small continuous streams, with slight channeling at the column walls amounting to "a small percentage" of the total flow. Koch-Sulzer literature states that the special geometry of the crimped wire mesh encourages good liquid distribution and, in fact, can alleviate initial maldistribution of the liquid. Nygren and Connolly (1970) indicate that Goodloe and Hyperfil packings are sensitive to initial maldistribution.

Wetting

The mesh of Koch-Sulzer packing is designed to be "self-wetting", i.e. liquid tends to spread on the mesh because of capillary forces and thus provide maximum interfacial area for mass transfer to a liquid film. With separated fibers, on the other hand, a greater part of the absorption occurs by mass transfer to falling liquid streams and to drops. The wettability of the fiber has an effect on the shape of drops suspended on them. Nonhebel (1964) gives photographs of drops on wettable glass, silicone treated glass, and hydrophobic terylene polyester fibers, showing, that the drops on hydrophobic fibers are nearly spherical.

Mixing

The knit-mesh packing manufacturers (Koch, Goodloe, and Hyperfil) state that both the liquid and the gas phases are well-mixed across the column because of the multiple channels of the crimped wire mesh. This aids the mass transfer efficiency of the packing.

5.2.5 PRE-FORMED SPRAYS

The devices discussed in this section are the ordinary spray devices, including countercurrent, cocurrent, and cross-flow configurations, and the ejector venturi. These devices all have in common the introduction of power to the liquid phase. In spray scrubbers, however, the liquid power input only creates the spray, and the gas phase is moved separately by a fan or blower; while in the ejector venturi, the liquid power input not only creates the liquid dispersion but also propels the gas by momentum transfer from the liquid.

Cyclonic spray devices for mass transfer are discussed in Section 5.2.7.

5.2.5.1 Unit Mechanisms

Obviously the predominant mechanism in spray devices is mass transfer to liquid drops, for which equations and correlations are discussed in Section 4.5.1. Transfer to a liquid film on the walls of the scrubber might also be expected to account for part of the scrubbing action; however, Mehta and Sharma (1970) analysed their and earlier workers' data and concluded that most of the wall liquid has already absorbed a substantial fraction of its capacity while in droplet form before hitting the wall, so that the wall-effect amounts to a negligible part of the total mass transfer.

Drop sizes must be estimated in order to use the equations of Section 4.5.1. For rapid approximations in spray towers, Hobler (1966) suggests a 600 µm drop size, which is conservative.

(See Section 5.3.5.2 for a discussion of spray nozzles). Johnstone and Williams (1939) give the drop size distribution obtained in their laboratory spray column, and state that the important size range for mass transfer in their experiments was 200-600 μm. Hobler gives some size distributions as a function of nozzle orifice size and water pressure, as does Perry (1963). Pigford and Pyle (1951) give size distributions and the cut-point diameters (the median size) of drops from commercial spray nozzles at 25 and 50 psi. Harris and Haun (1964) show drop size distributions for ejector venturi scrubbers.

The unit mechanism equations of Section 4.5.1 provide a rational basis for correlation and extension of the meager data available for spray scrubbers. Although the basic equations may be helpful in obtaining an order-of-magnitude estimate when no commercial scale data are available, they should not be expected to describe accurately conditions in a commercial spray scrubber. Effects of drop agglomeration, droplet entrainment, spray pattern over-lapping, wall losses, secondary gas flow patterns, and other factors introduce great variation from the behavior of simplified models.

5.2.5.2. Sizing

The diameter of a countercurrent spray tower is determined by the allowable gas velocity. Perry's Handbook (1963) and Norman (1961) suggest a maximum gas rate of $G_{max}=3,900$ kg/hr-m^2 (800 lb/hr-ft^2), above which there is excessive entrainment. The tower diameter can be calculated from

$$d_c = \psi \left(Q_G \sqrt{\rho_G} \right)^{1/2} \qquad (5.2.5\text{-}1)$$

The value of "ψ" calculated from the G_{max} given above is 0.01885 for use with metric units (d_c in m, Q_G in m^3/hr, ρ_G in kg/m^3), and 0.1613 for use with engineering units (d_c in ft, Q_G in cfm, ρ_G in lb/ft).

Cross-flow spray scrubbers are usually sized by setting the gas velocity. If no other mechanism is involved besides transfer to the sprayed droplets, typical velocities are 2,000-5,000 m/hr (2-5 ft/sec); in such cases Equation 5.2.5-1 can be used as a rough guide, the area normal to gas flow being given by $A = \pi d_c^2/4$. Spray scrubbers which combine other mechanisms, such as impingement baffles or orifice plates, use gas velocities up to 30,000 m/hr (30 ft/sec). Entrainment separators are required regardless of the gas velocity (Treybal, 1955).

Ejector venturis are sized according to the gas volume flow rate, the draft to be produced by the spray, and the liquid pressure available at the nozzle. Generally, the lower the gas flow rate, the greater the draft which will be created to pull the gas. Generalized size correlations have not appeared in the literature, but sizing information adequate for a first design is available in most manufacturers' brochures. For example, to move 8,000 m^3/hr of gas (4,700 cfm) at a draft of 5 cm W.G. (2" W.G.) with water pressure available at 70,000 kg/m² (100 psig) calls for an ejector with a 46 cm (18") diameter gas inlet, operating with 40 m³/hr of water (180 gpm) according to Harris (1963). Also see Section 5.3.5.

5.2.5.3 Pressure Drop

The pressure drop through a spray scrubber is very low. Mehta and Sharma (1970), for instance, found pressure drops of 1 to 2 mbar/m of column - - (0.4 to 0.8 inches water per ft of column height) - - for gas velocities of 500 to 1,600 m/hr (0.5 to 1.5 ft/sec), with the liquid flow rate having negligible effect for L = 20,000 to 80,000 kg/hr-m² (4,100 to 16,000 lb/hr-ft²).

For vertical countercurrent flow the gas pressure drop has to be sufficient to support the weight of liquid holdup, overcome frictional loss against the walls, and absorb any excess momentum imparted to the drops by spray nozzles. If the latter two components are neglected, the pressure drop for countercurrent scrubbing is given by:

$$\Delta P\ (\text{mbar}) = Hd\ \rho_L\ Z = \frac{Q_L\ \rho_L\ Z}{(u_t - u_G)\ A} \qquad (5.2.5\text{-}2)$$

where "u_t" is drop terminal velocity, "u_G" is upward gas velocity and "A" is tower cross-sectional area.

For crosscurrent and cocurrent flow, Calvert (1968) estimated the pressure drop on the basis of the change in momentum of the liquid when accelerated from zero velocity to the gas velocity, u_G.

$$\Delta P\ (\text{mbar}) = 1.03\text{x}10^{-3} \left[u_G\left(\frac{\text{cm}}{\text{sec}}\right)\right]^2 \frac{Q_L}{Q_G} \quad \text{(also see 5.3.6-10)} \quad (5.2.5\text{-}3)$$

5.2.5.4 Mass Transfer

The number of transfer units required in a given scrubbing application can be determined by methods discussed earlier (Section 5.2.1). This section is concerned with estimation of the number of transfer units attainable in pre-formed spray devices.

Spray scrubbing devices are inexpensive and have low pressure drop but for mass transfer applications they are limited to usually between 2 and 4 transfer units. The accepted (Sherwood and Pigford, 1952; Norman, 1961; Perry, 1963) explanation for the observed limitation is that even in a "countercurrent" spray, gas-liquid contact is not truly countercurrent because of mixing and recirculation of the gas by the droplets and entrainment of the droplets.

Fundamental experimental studies have been carried out to measure mass transfer coefficients in spray devices. Typical of these are the older work of Johnstone and Williams (1939) on 5 different solute gases, and the recent investigations of Mehta and Sharma (1970) on SO_2 absorption in caustic solution. The complexities of absorption in a spray column are exemplified by Mehta and Sharma conclusion that "k_G" is independent of the column height, and that "a", the interfacial area, decreases as distance from the nozzle increases; while Johnstone and Williams found "k_G" to decrease with height and "a" to be independent of position.

The number of overall gas-phase transfer units, N_{OG}, is a useful basis on which to compare mass transfer performance of various spray scrubbers. The literature data are often expressed as "K_Ga", or as "H_{OG}", the height of a gas-phase transfer unit, by analogy with packed columns. Attempts have been made to correlate the number of transfer units with operating variables. Lunde (1958) related "N_{OG}" for a spray tower to the power supplied to the liquid and to the gas:

$$N_{OG} \propto P_L^{1} P_G^{-0.1} \qquad (5.2.5\text{-}4)$$

Since "P_L" is proportional to liquid flowrate and therefore to "a" and "N_{OG}", Lunde's approach is consistent with other authors who suggest that "N_{OG}" is proportional to the liquid rate (Norman, 1961; Treybal, 1955). For illustration, Lunde's data for "HF" scrubbing in water and in lime solution are shown in Figure 5.2.5-1, as "N_{OG}" vs. watts per m^3/hr of gas flow.

For ejector venturis, Harris and Haun's data (1964), plotted on Figure 5.2.5-1, suggest that

$$N_{OG} \propto P_L^{0.3} \qquad (5.2.5\text{-}5)$$

An obstacle to the designer in applying Equation 5.2.5-4 or 5.2.5-5 is that the proportionality constants can not be predicted in advance. The equations are useful only for correlating performance data for a specific case. If spray tower performance is expressed as "$\hat{K}_Ga$", it is possible to use

$$N_{OG} = \hat{K}_Ga\ P\ Z/\hat{G} \qquad (5.2.5\text{-}6)$$

in this equation "K_Ga" is given as an average over the tower height and the tower height is specified. Likewise, if the measure of performance is "H_{OG}", it may be valid to use $N_{OG} = Z/H_{OG}$. If the performance is given as the overall gas-phase efficiency, E, and the equilibrium gas-phase concentration over the bulk liquid, $\hat{y}^*$, is negligible, as in the case of a dissociation or a rapid chemical reaction occurring in the liquid, then $N_{OG} = -\ln(1-E)$.

Pigford and Pyle (1951) present detailed data on mass transfer in two countercurrent spray chambers; 30 cm square (12") and 96 cm diameter (31.5"). Several types of spray nozzles were used and transfer rates were determined for oxygen, ammonia, and water vapor. Comparison of their results with predictions of mass transfer rate along the lines of Section 4.5.1 shows two features.

1. The spray drop size must vary with liquid mass flow rate "L", in order to fit the experimentally determined relationship between number of transfer units and gas flow rate. Because drop holdup depends so strongly on the terminal settling velocity, the shape of a plot of "N_{OG}" versus gas velocity is very dependent on drop size. For the large column the data indicate that for L = 80, 60, and 30 [kg/(cm^2-sec)] the effective drop diameters were 500, 450, and 400 (μm), respectively. These are larger than measured and show a variation with liquid flow rate (or nozzle pressure) greater than observed for the nozzles operated outside the column. It suggests that drop agglomeration takes place which increases with liquid flow rate, and is dependent on "H_d".

2. The number of gas phase transfer units predicted is approximately 5 times higher than the experimental determined value. This suggests that only about 20% of the spray is effective and the remainder runs down the walls with less exposed surface. The measured ratio of water running down the wall to total spray input was roughly 3/4, depending on "L" and "G"; which is consistent with the mass transfer data.

Computation of overall performance is carried out in the same general way as for packed columns. The mass transfer area and coefficient depend on the drop size and flow configuration as well as on gas and liquid flow rates. Methods of computing transfer coefficients are discussed in Section 4.5, general relationships in Section 4.2, and drop holdup and interfacial area in Sections 4.4 and 5.3.5. The general approach depends on the flow configuration as follows:

1. Countercurrent flow - Use same material balance and rate equations as for packed columns (Section 5.2.1.2) with coefficients for transfer to drops (Section 4.5.1) and area from drop holdup.

2. Cocurrent flow - Use method given in Section 5.2.6.

3. Crossflow - Exact material balance is difficult, assume liquid composition on any plane perpendicular to gas flow is the average between inlet and outlet liquid at that position (gas composition) and perform an incremental stage calculation. Mass transfer coefficients and drop holdup are evaluated for drops falling at terminal velocity, [Cabibbo and Teller (1969)].

Some of the available sources of spray device performance data are given in Table 5.2.5-1. This list is not exhaustive of the literature, and some of the data are not in a form convenient for design.

5.2.5.5 Other Design Configurations

Tower Height - An increase in spray tower height (or length, in the case of a horizontal cross-flow configuration) may result in a slightly increased "N_{OG}", due to the increased contact time between each drop and the gas. However, the increase in "N_{OG}" is not proportional to the height increase, because of wall losses, agglomeration, damping of drop circulation, and other effects as the drops fall.

Heat Transfer - Simultaneous heat and mass transfer are significant in spray scrubbers. Spray chambers are commonly used to quench and scrub hot gases. The sensible heat of the gas and the heat of absorption of the solute in the liquid are removed by evaporation (or condensation) of some of the liquid (usually water). These heat effects must be taken into account in determining the number of transfer units required for the desired degree of absorption. A detailed example is given in Section 4.2.8.

5.2.6 GAS-ATOMIZED SPRAYS

This section discusses design techniques for scrubbers in which a spray of fine droplets is created by transfer of momentum from the

TABLE 5.2.5-1

MASS TRANSFER DATA FOR SPRAY DEVICES

System	Configuration	Data	Reference[a]
CO_2 - aq. NH_3	Cocurrent	k_Ga	Rumford et al. (1954)
CO_2 - aq. NaOH	Countercurrent	k_G, k_Ga	Johnstone and Williams (1939)
HCl - water	Ejector	N_{OG}	Harris and Haun (1964)
HCl - water	Ejector	E	Harris (1966)
HCl - aq. NaOH	Countercurrent	k_G, K_Ga	Johnstone and Williams (1939)
HF - water	Countercurrent	N_{OG}	Lunde (1958); KR
HF - water	Cross-flow	N_{OG}	Lunde (1958); KR
HF - lime water	Cross-flow	N_{OG}	Lunde (1958); KR
HF - lime water	Cocurrent	N_{OG}	Lunde ([illegible]); KR
H_2S - aq. NH_3	Countercurrent	E	Bayerlein (1954); KR
H_2S - aq. NH_3	Countercurrent	E	Williams (1954); KR
H_2S - aq. NaOH/H_2O_2	Countercurrent	k_G, k_Ga	Johnstone and Williams (1939)
NH_3 - water	Countercurrent	N_{OG}	Pigford and Pyle (1951)
NH_3 - water	Countercurrent	k_Ga	Kowalke et al. (1925)
NH_3 - aq. H_2SO_4	Countercurrent	k_G, k_Ga	Johnstone and Williams (1939)
SiF_4 - water	Countercurrent and cocurrent	N_{OG}, E	Sherwin (1954); KR
SiF_4 - water	Countercurrent and cocurrent	E	Pettit (1951); KR
SiF_4 - water	Cross-flow	E	Pettit (1951)
SiF_4 - water	Ejector	E	Sherwin (1954); KR
SiF_4 - water	Ejector	E	Pettit (1951)
SO_2 - water	Countercurrent	k_Ga	Haslam et al. (1923)
SO_2 - aq. NaOH	Countercurrent	k_G, k_Ga	Johnstone and Williams (1939)
Air - water (humidification)	Countercurrent	k_Ga	Bonilla et al. (1950)

---

[a] KR = Kohl and Riesenfeld (1960).

gas phase. All (or most) of the power consumed by such scrubbers is introduced into the gas phase in contrast to the "pre-formed" sprays of the preceding section. For the purposes of this section, gas atomized spray devices include venturis, orifice scrubbers, and flooded disc scrubbers. All of them require entrainment separation to remove the droplets after the absorption has taken place; see the section on particulate scrubbing.

5.2.6.1 Unit Mechanisms

The predominant mechanism for mass transfer in gas-atomized spray devices is absorption by droplets. Almost all the mass transfer takes place where the gas velocity is highest (orifice, venturi throat, etc.) and immediately downstream. Here, at the point of droplet formation, both the liquid and gas phases are highly turbulent. They become much less turbulent very rapidly, and because the droplets agglomerate during their passage through the scrubber, the total surface area decreases. Fragmentary knowledge of the exact drop size, size distribution, agglomeration of drops, relative velocity at the point of atomization, liquid losses along the venturi length, etc. make it difficult to estimate performance in a commercial device using the basic equations alone. It is, however, possible to establish upper limits of efficiency based on an idealized situation while the real situation will tend to give lower efficiencies for reasons mentioned above.

5.2.6.2 Mass Transfer

In a gas atomized device, both the gas and the liquid phase are usually highly turbulent and the individual film transfer coefficient "k_G" and "k_L" are both relatively high during the brief period of drop formation and acceleration. However, the transfer is limited to equilibrium between the two phases by the cocurrent flow. For physical absorption this means:

$$\hat{G}\,(\hat{y}_1 - \hat{y}_2) = \hat{L}\,(\hat{x}_2 - \hat{x}_1) \qquad (5.2.6\text{-}1)$$

if $\hat{x}_1 = 0$, as normally would be the case,

$$\hat{G}\,(\hat{y}_1 - \hat{y}_2) = \hat{L}\,\frac{P\,\hat{y}_2}{\hat{H}\,\hat{\rho}}\ ;\ \hat{x}_2 = \frac{P\,\hat{y}_2}{\hat{H}\,\hat{\rho}} \qquad (5.2.6\text{-}2)$$

$$\frac{\hat{y}_2}{\hat{y}_1} = \frac{1}{\dfrac{P\,\hat{L}}{\hat{H}\,\hat{\rho}\,\hat{G}} + 1} \qquad (5.2.6\text{-}3)$$

where, P = total gas pressure, (atm)

$\hat{x}_1$, $\hat{x}_2$ = inlet and exit mole fraction of the soluble component in the liquid phase.

$\hat{y}_1$, $\hat{y}_2$ = inlet and exit mole fraction of the soluble component in the gas phase.

$\hat{H}$ = Henry's law constant, [atm/(gmol/cm³)]

$\hat{\rho}$ = Liquid molar density, gmol/cm³)

Figure 5.2.6-1 is a plot of the equilibrium penetration limits vs. Henry's law constant in a venturi type cocurrent device. This plot represents Equation 5.2.6-3 with $\hat{\rho} = 1/18$ gmol/cm³.

As mentioned before, the predominant mechanism for mass transfer is absorption by drops. Gas-film and liquid-film transfer coefficients, "k_G" and "k_L" may be predicted from penetration theory (see 4.2.3). Hence,

$$k_G = \frac{2}{Rg\ T}\left(\frac{D_G}{\pi\ \Theta}\right)^{1/2} \text{ and } k_L = 2\left(\frac{D_L}{\pi\ \Theta}\right)^{1/2} \qquad (5.2.6\text{-}4)$$

The ratio of the drop diameter to the relative velocity between the gas and the drop approximates the exposure time for the gas-film, and "k_G" becomes

$$k_G = \frac{2}{Rg\ T}\left(\frac{D_G\ f\ u_G}{\pi\ d_d}\right)^{1/2} ;\ f = \frac{u_r}{u_G} \qquad (5.2.6\text{-}5)$$

Estimating "Θ" for the liquid phase is more difficult. Drops have pronounced internal circulation at the time of formation, but what this velocity is and how it changes as the drop accelerates are not known. In further discussion we will assume liquid-film exposure time to be constant, i.e. "k_L" is constant. On the conservative side, the exposure time will be taken as the time the liquid drop is exposed in its travel through the venturi. In other words, the liquid drop is considered to have no internal circulation velocity. Values of "k_G" and "k_L" will yield "K_G", the overall gas phase transfer coefficient, from Equation 4.2.3-8. Then the transfer from the gas to the liquid phase can be written as follows:

$$-\hat{G}\ d\hat{y} = \hat{K}_G\ A_d\ P\ (\hat{y}-\hat{y}^*) \qquad (5.2.6\text{-}6)$$

where $\hat{G}$ = molar flow rate of gas, gmol/sec
A_d = surface area of liquid drops in the volume (A_T dZ), (cm²)
A_T = cross sectional area of throat at "Z", (cm²)
$\hat{y}, \hat{y}^*$ = gas soluble component mole fraction, and gas phase soluble component fraction that would be in equilibrium with the bulk liquid concentration of the soluble component.
dZ = Differential element of venturi length in which gas phase concentration of soluble component changes by "dy", (cm)

The average liquid drop diameter is approximated by Nukiyama and Tanasawa equation (see Section 4.4.2.1 and Figure 5.3.6-2). Liquid drop area "A_d" is variable with "Z", the distance from the point of atomization. Variable liquid holdup has been defined by Calvert (1970) as $Hd = Q_L/u_d\ A_T$. Then,

$$Hd = \frac{Q_L}{Q_G\,(1-f)} \qquad (5.2.6\text{-}7)$$

$$A_d = Hd\ A_T\ dZ\ \frac{6}{d_d} = \frac{Q_L}{Q_G\,(1-f)}\ A_T\ \frac{6}{d_d}\ dz \qquad (5.2.6\text{-}8)$$

$$A_d' = \frac{Q_L}{Q_G\,(1-f)}\ \frac{6}{d_d} = \text{drop area per unit volume, } (cm^2/cm^3) \qquad (5.2.6\text{-}9)$$

It is well to remember at this point that the maximum value of "Hd" is 1.0. Therefore, "f" will have a limiting initial value "f_2" which is always less than 1.0, and can be found from Equation 5.2.6-7 with Hd = 1.

Towards the exit from the venturi the drop velocity reaches a velocity equal to the gas velocity and f=0. The liquid holdup "Hd", the relative velocity "u_r", the velocity ratio "f" and the drop area per volume "A_d" and "A_d'", all change inside the venturi. At the limit "Hd", for example, changes from a maximum value of 1 to a minimum value of Q_L/Q_G when f=0.

The major part of the mass transfer takes place in that part of the venturi where "Hd" varies continuously with length. Constant values of "Hd" are reached at considerable distance downstream from the point of atomization. Figure 5.2.6-2 is a plot of "$\hat{k}_G\ A_d'$" with distance "Z". Equation 5.2.6-5 was used to compute "$\hat{k}_G$"., "k_L" as mentioned before is assumed constant. The product "$k_L\ A_d'$" will vary according to the variation in "A_d'". Small drop sizes (≈.01 cm) and high gas velocities (10,000 cm/sec) result in high transfer coefficients. Johnstone et al. (1954) observed this experimentally. They found that when liquid-phase diffusion controls, equilibrium was almost reached at a distance of 10 cm from the point of injection of the liquid.

Equation 5.2.6-6 can now be integrated after the following assumptions are made:

1. Equation 5.3.5-33 describes the acceleration of drops with position inside the venturi.
2. The venturi cross-sectional area is constant throughout.
3. Corresponding with the approach taken in particle collection $f=f_1$ at Z=0 and f=0 at Z=Z.

Several solutions of Equation 5.2.6-6 for different cases are presented in Table 5.2.6-1. In a given situation any one of these equations may be applied, depending upon how well the assumptions reflect the real situation.

Johnstone et al. (1954) have carried out absorption and desorption of SO_2, CO_2, and O_2 in a venturi scrubber. Their data of CO_2 desorption are plotted in Figure 5.2.6-3. Equation 5.2.6-11 would apply to this situation, with the modification that $f_2 \neq 0$. Since their data give the fractional equilibrium desorption as a function of "Z", Equation 5.2.6-11 is rewritten below in terms of "f_1" and "f_2"

$$\frac{\hat{y}_2}{\hat{y}_1} = \frac{\frac{m}{p} + \left\{ \frac{k_L + \frac{2\,\hat{H}}{R_g\,T}\left(\frac{D_G\,u_G\,f_2}{\pi\,d_d}\right)^{1/2}}{k_L + \frac{2\,\hat{H}}{R_g\,T}\left(\frac{D_G\,u_G\,f_1}{\pi\,d_d}\right)^{1/2}} \right\}^{k}}{1 + \frac{m}{p}} \qquad (5.2.6\text{-}10)$$

The only unknown in the Equation above is the exposure time for the liquid film. It is known that the drop circulation velocity can be as high as 3 to 4 percent of the relative velocity. The theoretical desorption curves for liquid drop internal circulation velocity equal to one and zero percents of the gas velocity are shown in Figure 5.2.6-3. "f_1" was taken to be 1. Comparison of the theoretical curves with the experimental curve indicates a finite internal circulation velocity.

While there is much mass transfer research being carried out in venturis, the literature contains only a few experimental data useful for analysis. Of particular interest is data on SO_2 removal by limestone slurries. SO_2 reactions in the liquid phase in a limestone slurry are quite complex. In any event, the reaction enhances the liquid phase mass transfer. At best, the liquid phase mass transfer resistance may become small enough to be neglected in comparison to the gas phase transfer resistance. And the SO_2 bulk concentration may be negligible. Under these circumstances, Equation 5.2.6-17 would apply and provide an upper limit on the maximum possible transfer that may be accomplished.

Figure 5.2.6-4 is a plot of Equation 5.2.6-17 for the system air water giving penetration vs. "f" with $(\hat{L}/\hat{G})$ as parameter at 15,000 (cm/sec) gas velocity and drop diameter calculated from Nukiyama and Tanasawa equation. It is important to know the value of "f", which relates to the length of the venturi and the point of atomization, to predit the mass transfer. For a constant length of the venturi, "f" will vary depending upon the gas velocity and the liquid to gas flow rate. With all the simplicity of this model, which does not take into account the liquid losses to the wall or the variation in the venturi cross-section area, etc., it shows upper limits of SO_2 removal in line with experimental data of many researchers reported in "Lime/Limestone Wet Scrubbing Symposium", (NAPCA, 1970).

Johnstone and Roberts (1949) carried out absorption of SO_2 by alkaline solution. Their results are shown in Figure 5.2.6-5 as number of transfer units, N_{OG}, vs. $\hat{L}/\hat{G}$. Gas velocities ranged from 4,000 cm/sec to 7,600 cm/sec. Equation 5.2.6-17 was used, with f=1, to predict the experimental data. Theoretical "N_{OG}" was high dependence on $(\hat{L}/\hat{G})$ but it depends very little on the gas velocity and the curve in Figure 5.2.6-5 pretty much represents the velocity range mentioned. Agreement between data and theory is good. It would be expected that since Equation 5.2.6-17 predicts the upper limit of transfer, all the experimental data would lie below the curve. The reason some of the data falls above the line may be due to additional transfer accomplished on the walls and in the entrainment separator. Venturi walls contribute (4/diameter of venturi) cm^2/cm^3 area for mass transfer. Depending upon the size of the venturi, this may become a significant percent of the area due to liquid drops.

To use Equation 5.2.6-17 to predict the efficiency of a venturi, it is necessary to have a value for the coefficient "f". To evaluate this constant, experimental data have been analyzed. SO_2 absorption data of Johnstone et al. (1949) in a venturi and Walker (1970) in a flooded disc scrubber, were used to evaluate "f". The results are shown in Figure 5.2.6-6. In a flooded disc, the drop diameter was calculated at the throat velocity and during the mass transfer part the gas velocity was based on the total open throat area following the disc. "f" values for mass transfer are higher than for the particle collection. This may be due to the transfer accomplished on the wetted walls and in the entrainment separator.

In summary, the equations presented in this section provide means to calculate an upper limit of mass transfer for various situations as follows:

1. Equation 5.2.6-3 gives the equilibrium limit of mass transfer for physical absorption.

2. Equation 5.2.6-11 indicates how closely the equilibrium limit may be approached in the case of both phases governing the transfer.

3. Equation 5.2.6-14 indicates the approach to equilibrium in the case of a highly soluble gas.

4. Equation 5.2.6-15 may be used when nearly zero solute concentration can be maintained in the liquid phase, (such as when a reactive and soluble slurry is used).

Liquid phase reaction can enhance mass transfer rate on the liquid side. It may also maintain zero bulk concentration of the solute. In this situation, Equation 5.2.6-17 can be used to establish the upper limit on mass transfer. As shown in Figure 5.2.6-4, this limit is lower than complete removal of the solute gas and provides a useful guide.

5.2.7 CENTRIFUGAL DEVICES

The cyclonic spray scrubber, which is illustrated in Section 5.3.7, is considered in this section for mass transfer characteristics. A cyclonic scrubber uses preformed spray from a manifold located either along the lengthwise center axis of the cyclone or along the wall, directed inward. If the spray droplets are sufficiently large and have high enough initial velocity, they are thrown to the wall. When this is the case the gas-liquid contact is of the cross-flow type. On the other hand, when liquid drops are small, they may get carried by the gas flow part of the way before being thrown out to the wall by centrifugal force. Then, the gas-liquid contact is a combination of cross-flow and cocurrent-flow.

TABLE 5.2.6-1

EQUATIONS FOR MASS TRANSFER IN A VENTURI

1. Physical absorption with gas and liquid resistance, zero concentration of solute in the inlet liquid.

$$\frac{\hat{y}_2}{\hat{y}_1} = \frac{\frac{m}{P} + \left[\frac{k_L}{k_L + \frac{2\,\hat{H}}{R_g\,T}\left(\frac{D_G\,u_G\,f}{\pi\,d_d}\right)^{1/2}}\right]^k}{1 + \frac{m}{P}} \qquad (5.2.6\text{-}11)$$

where, $k = 0.291\,\frac{\rho_L\,k_L\,d_d}{\mu_G}\left(1 + \frac{P}{m}\right)$ (5.2.6-12)

$$m = \frac{\hat{H}\,\hat{\rho}\,\hat{G}}{\hat{L}} \qquad (5.2.6\text{-}13)$$

2. Physical absorption with gas phase resistance alone, zero concentration of solute in the inlet liquid.

$$\frac{\hat{y}_2}{\hat{y}_1} = \frac{\frac{m}{P} + \exp\left[-0.291\,\frac{\rho_L\,d_d}{\mu_G}\left(\frac{P}{m} + 1\right)\frac{2\,\hat{H}}{R_g\,T}\left(\frac{D_G\,u_G\,f}{\pi\,d_d}\right)^{1/2}\right]}{1 + \frac{m}{P}} \qquad (5.2.6\text{-}14)$$

"m" is defined by Equation 5.2.6-13.

3. Physical abosrption with gas and liquid resistance, bulk liquid concentration of solute zero throughout, i.e. zero back pressure.

$$\frac{\hat{y}_2}{\hat{y}_1} = \left\{\frac{k_L}{k_L + \frac{2\,\hat{H}}{R_g\,T}\left(\frac{D_G\,u_G\,f}{\pi\,d_d}\right)^{1/2}}\right\}^{k_1} \qquad (5.2.6\text{-}15)$$

where, $k_1 = 0.291\,\frac{\rho_L\,k_L\,d_d}{\mu_G}\left(\frac{P}{m}\right)$ (5.2.6-16)

"m" is defined by Equation 5.2.6-13.

4. Absorption with gas phase resistance alone, zero back pressure.

$$\frac{\hat{y}_2}{\hat{y}_1} = \exp\left[-0.291\,\frac{\rho_L\,d_d}{\mu_G}\,\frac{P\,\hat{L}}{\hat{\rho}\,\hat{G}}\,\frac{2}{R_g\,T}\left(\frac{D_G\,u_G\,f}{\pi\,d_d}\right)^{1/2}\right] \qquad (5.2.6\text{-}17)$$

5.2.7.1 Unit Mechanisms

The mechanisms for mass transfer in a cyclonic spray scrubber are primarily absorption by liquid droplets and absorption by the falling liquid film at the wall of the scrubber. An advantage of the cyclonic spray over a pre-formed spray is that due to the outward force on the drops, their velocity relative to the gas is much higher than it would be in free fall; consequently the gas film coefficient is higher than in an ordinary spray chamber.

5.2.7.2 Mass Transfer

It has been observed by Johnstone and his co-workers (1938, 1947) that if the gas is highly soluble or reacts with the liquid, several overall gas-phase transfer units may be achieved in a cyclonic scrubber. They observed "N_{OG}'s" from 0.6 to 3.4 for pilot scale and large industrial cyclonic scrubbers absorbing SO_2 in sodium carbonate solutions. Here the partial pressure of the scrubbed component in the liquid phase was negligible.

Johnstone and Silcox (1947) have correlated the results of their experiments and presented the following semi-empirical equation

$$N_{OG} = \frac{8{,}140\ Q_L\ d_c\ P}{\hat{G}^{0.8}\ A_i\ d_d\ N_{Sc}^{2/3}} + \frac{0.0581\ A_W\ P}{\hat{G}^{0.37}\ A_i\ N_{Sc}^{2/3}} \qquad (5.2.7\text{-}1)$$

where "Q_L" is the liquid flow, in m³/hr; "d_c" is the cyclone diameter, in "m"; "P" is the total pressure, in atmospheres; "$\hat{G}$" is the gas flow, in kgmol/hr-m² of inlet duct cross section; "A_i" is the inlet duct cross-sectional area, in m²; "d_{dmm}" is the mass-mean diameter of the liquid droplets, in microns; "N_{Sc}" is the Schmidt number; and "A_W" is the wall area wetted by the spray. The original correlation, in engineering units, is given in Perry (1963).

Johnstone and Silcox's correlation should be applicable to scrubbing systems where the equilibrium partial pressure of the scrubbed component over the liquid phase is negligible, i.e. if there is no back pressure. There is little information available in the literature on mass transfer situation other than that mentioned above.

The mass-median diameter of the spray droplets can be estimated from nozzle manufacturers' catalogs. Sherwood and Pigford give values of 175 and 595 microns for nozzles with 0.117 cm (0.046 inch) and 0.48 cm (0.187 inch) orifices respectively, at 4.5 atm (67 psi) nozzle pressure. Other sources of drop size information are discussed in Section 5.3.5

5.2.8 MOVING BED SCRUBBERS

Moving bed scrubbers were introduced to solve the problem of collection of sticky particles in scrubbers. Moving bed scrubbers can be classified into two group: 1) Mobile bed scrubbers such as "Hydro-Filter"; and 2) Fluidized bed scrubbers, such as "TCA". General description, pictures, and operating characteristics of these two types of scrubbers can be found in Section 5.3.11.

Design Equation:

Design equations for mobile bed scrubbers are not readily available. These are relatively new devices, and mass transfer studies with them have been mostly for SO_2 scrubbing. Douglas (1964) presents results of ammonia absorption, humidification and dehumidification studies in a turbulent bed contactor. The packing used consisted of hollow polyethylene spheres, 3.82 cm (1 1/2 inch) in diameter and weighing 4.5 grams. His results for ammonia absorption are given in Figures 5.2.8-1 through 5.2.8-3. The results are based on static bed height which has the advantage of being accurately known, as opposed to the expanded bed height.

Douglas'study indicates increasing efficiency of absorption is obtained by decreasing the bed height, (see Figure 5.2.8-3). This may be explained by the fact that beds were in much more uniform motion when thin beds were used. Figure 5.2.8-1 shows that the over-all height of transfer unit, H_{OG}, in general decreases with increasing liquid mass velocity. Similarly, from Figure 5.2.8-2 it can be observed that the general trend is for "H_{OG}" to increase with increasing mass velocity. These results can be used to design a turbulent bed contactor, taking into account the solubility and diffusivity differences between the gas under consideration and ammonia.

Bechtel (1970) derived a model for gas-phase-controlled SO_2 absorption in a Hydro-Filter. The major assumptions in the model are as follows:

1. Completely back-mixed liquid phase.

2. Plug flow of gas phase.

3. Gas-phase controlled mass transfer within glass-sphere section and turbulent layer.

4. Rate of dissolution of solid calcium and/or magnesium hydroxide fast with respect to liquid phase holdup.

Then, the equation describing the mass transfer of SO_2 within the Hydro-Filter is:

$$\hat{y}_2 = (\hat{y}_1 - \hat{y}^*) \exp \frac{(\hat{K}_G\ a)_S\ h_S\ A_f}{\hat{G}} + \frac{(\hat{K}_G\ a)_T\ h_T\ A_f}{\hat{G}} + \hat{y}^* \qquad (5.2.8\text{-}1)$$

where, A_f = filter cross section, cm²

A = mass transfer surface area per unit volume

$\hat{K}_G$ = overall gas-phase mass transfer coefficient

$\hat{y}_1$ = mole fraction of SO_2 in inlet gas

$\hat{y}_2$ = mole fraction of SO_2 in outlet gas

$\hat{y}^*$ = equilibrium mole fraction of SO_2, mole fraction of SO_2 at gas-liquid interface subscript s = glass sphere section

subscript T = turbulent layer

The overall $(K_G\ a)_s$ and $(K_G\ a)_T$ are given as follows

$$(K_G\ a)_s = 0.61\ N_{Re}^{\ 0.41}\ N_{Sc}^{\ -2/3}\ GM/A_c \cdot 4/d_s \qquad (5.2.8\text{-}2)$$

$$(K_G\ a)_T = \frac{6}{A_f} \left(\frac{D_G\ \rho_G\ \hat{G}}{h_T} \right)^{1/2} \qquad (5.2.8\text{-}3)$$

where $$N_{Re} = \frac{\hat{G}\ d_s}{A_f\ \mu_G\ 4} \qquad (5.2.8\text{-}4)$$

$$N_{Sc} = \frac{\mu_G}{\rho_G\ D_G} \qquad (5.2.8\text{-}5)$$

d_s = diameter of glass sphere

Note that the above equations will describe the mass transfer for any system where the assumptions made hold. The maximum fractional removal of SO_2 will result when $\hat{y}^* \to 0$. In Figure 5.2.8-4, Bechtel (1970) shows the limiting fractional removal of SO_2 in the Hydro-Filter plotted as a function of gas flow rate and glass-sphere diameter.

Pollock et al. (1967) presents results of SO_2 removal with sodium carbonate and with calcium carbonate. The scrubber was a Turbulent Contact Absorber (TCA) as designed and manufactured by UOP Air Correction Division. It was operated at the Oak Creek plant of the Wisconsin Electric Power Company during 1964. Figure 5.2.8-5 gives results of the SO_2 absorption efficiencies with sodium carbonate and calcium carbonate. The absorption efficiency increases with liquid rate and decreases with increasing gas flow. Figure 5.2.8-5 also illustrates the superiority of sodium carbonate as the absorbent which is probably due to the higher solubility of sodium carbonate and monosulfite compared to the corresponding calcium compounds.

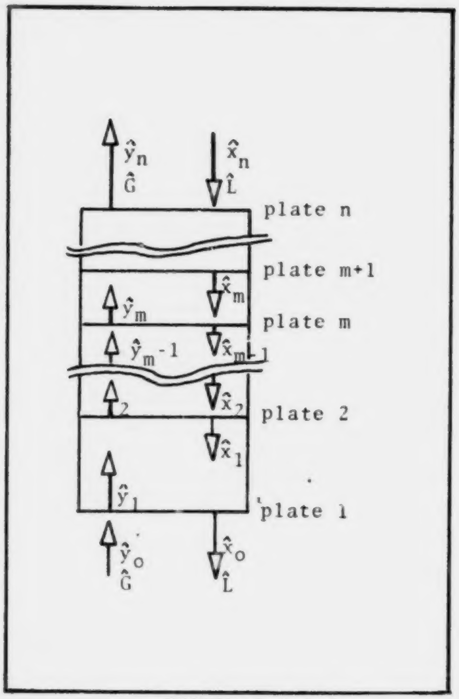

FIGURE 5.2.1-1

PLATE COLUMN MATERIAL BALANCE

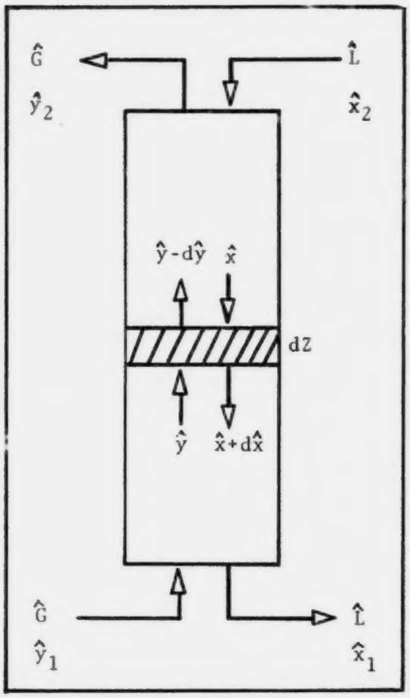

FIGURE 5.2.1-3

SCHEMATIC DIAGRAM OF PACKED COLUMN

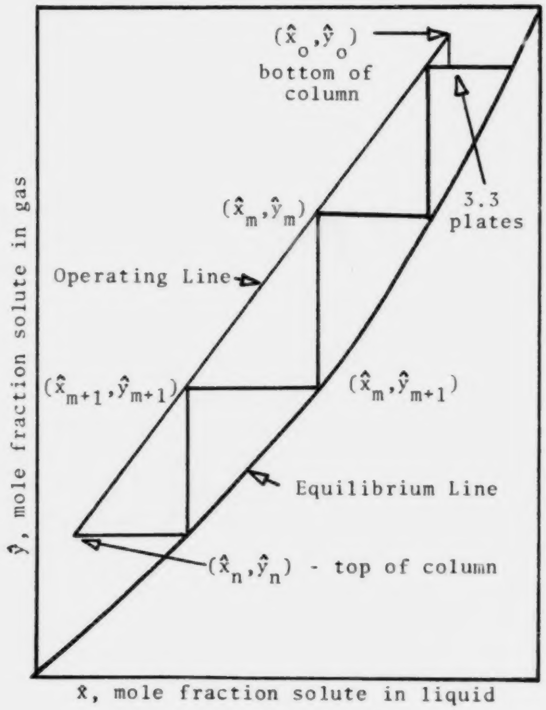

FIGURE 5.2.1-2

GRAPHICAL DETERMINATION OF THEORETICAL PLATES

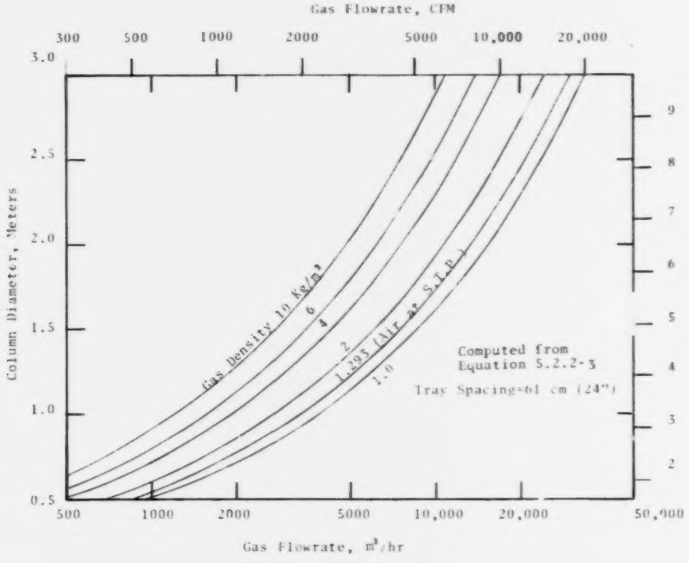

FIGURE 5.2.2-1
BUBBLE-CAP COLUMN DIAMETER

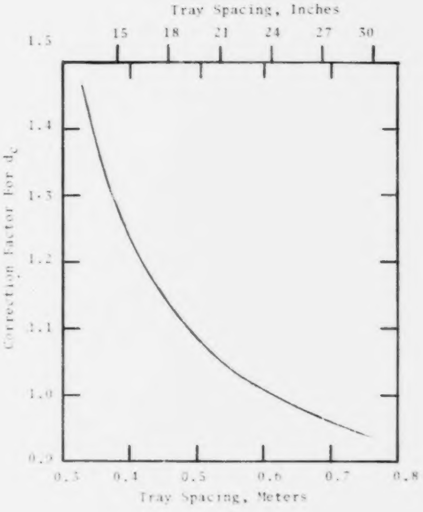

FIGURE 5.2.2-2
TRAY SPACING CORRECTION

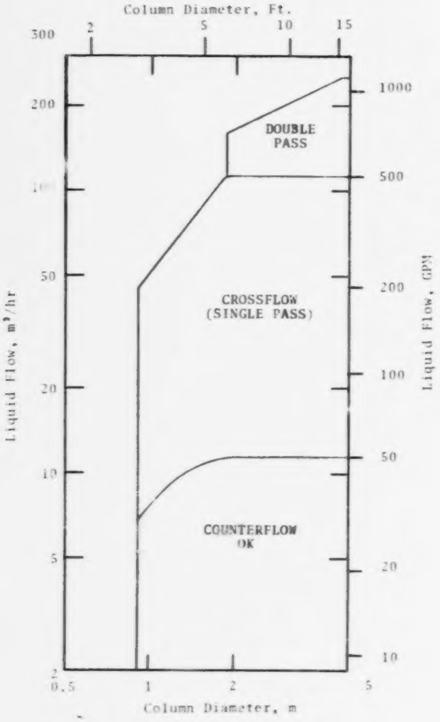

FIGURE 5.2.2-3
RANGE OF LIQUID RATES FOR TRAYS

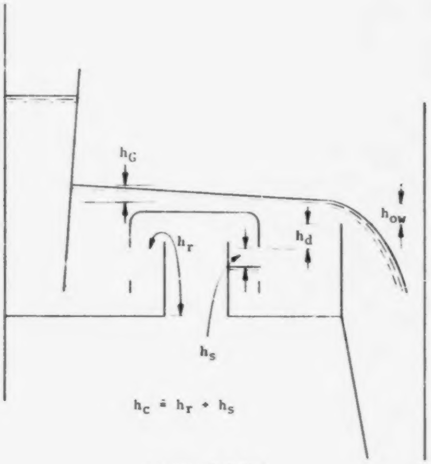

FIGURE 5.2.2-4

BUBBLE-CAP PRESSURE DROPS

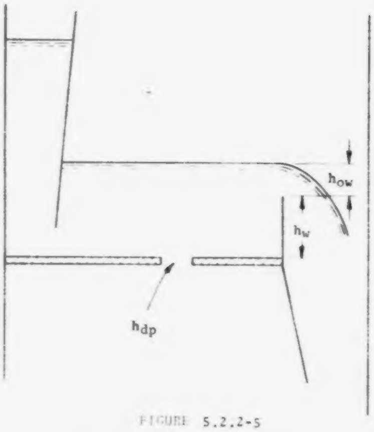

FIGURE 5.2.2-5

SIEVE TRAY PRESSURE DROPS

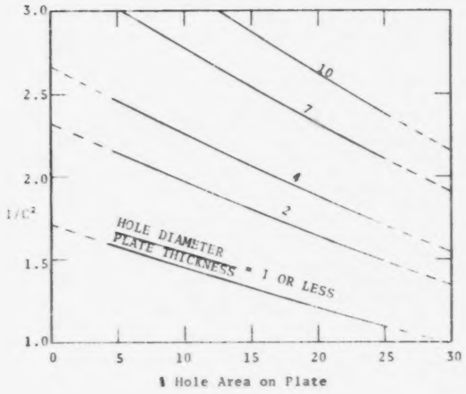

FIGURE 5.2.2-6

SIEVE PLATE ORIFICE COEFFICIENT,C
(Equation 5.2.2-19

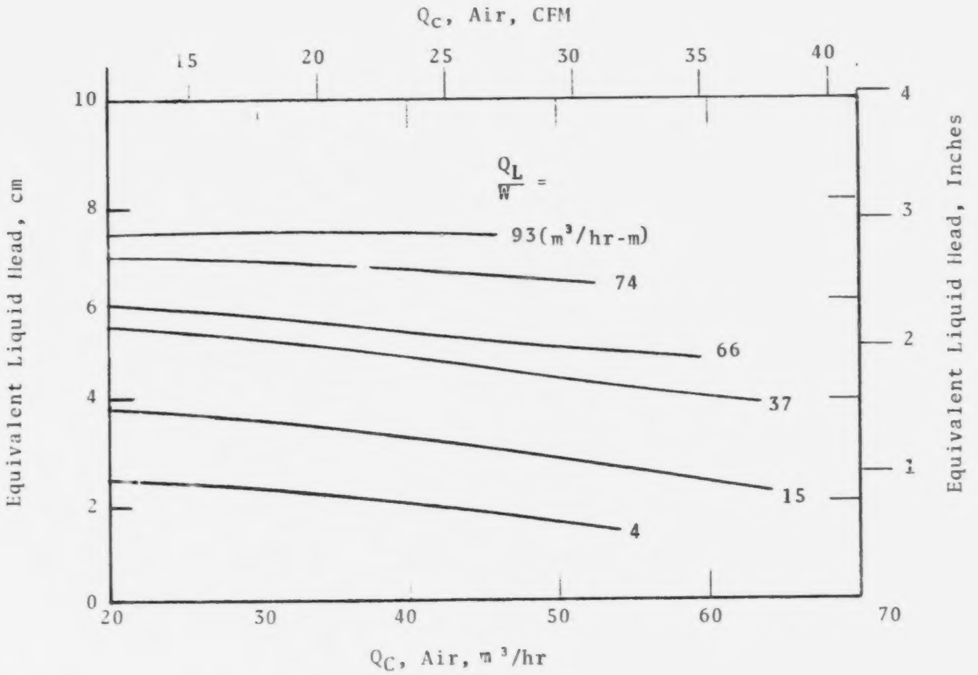

FIGURE 5.2.2-7

VALVE TRAY LIQUID HEAD

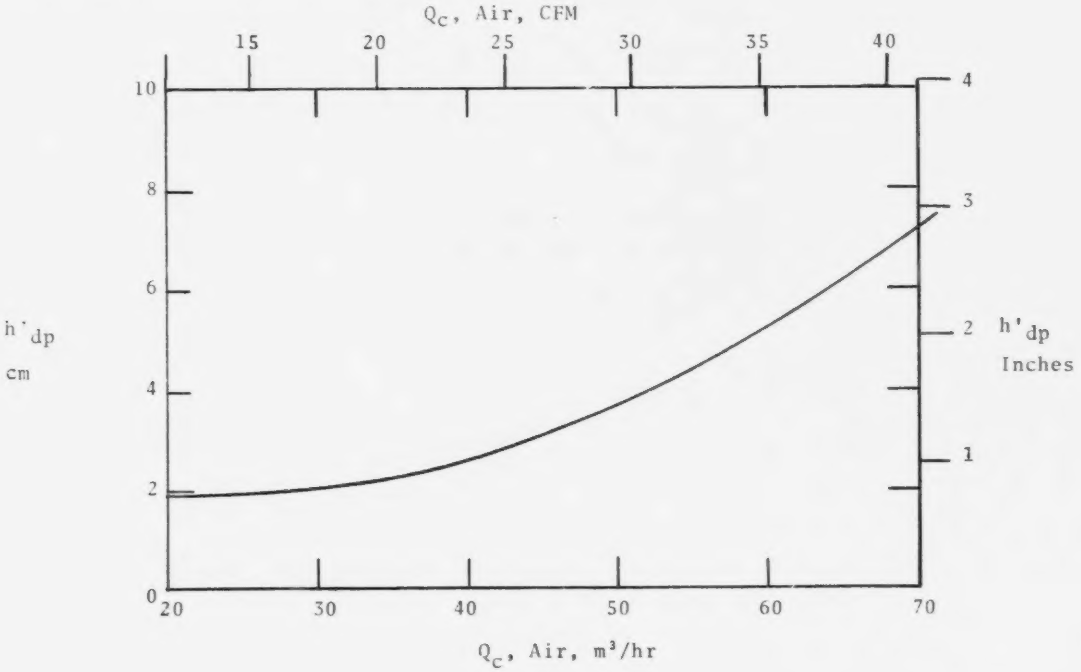

FIGURE 5.2.2-8

VALVE TRAY DRY PLATE HEAD LOSS

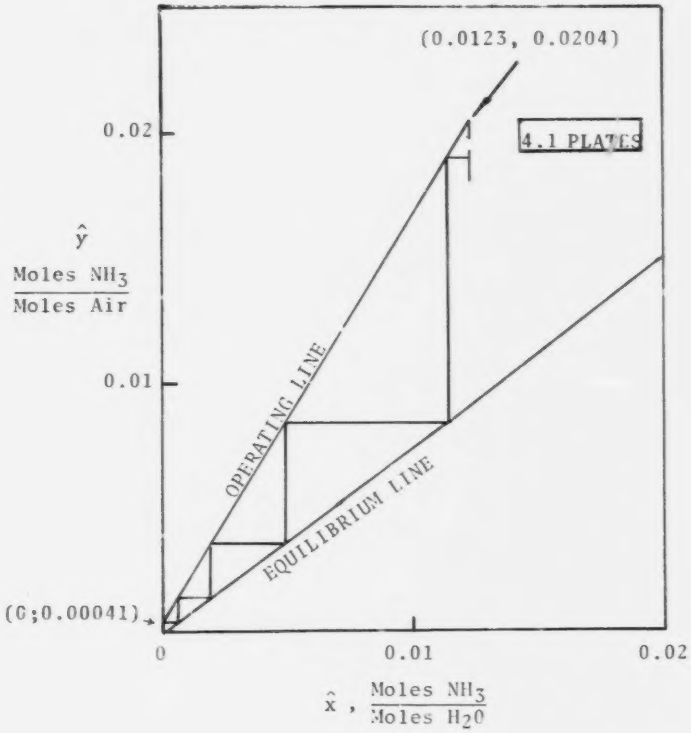

FIGURE 5.2.2-9

NUMBER OF THEORETICAL PLATES REQUIRED FOR NH_3 ABSORPTION EXAMPLE

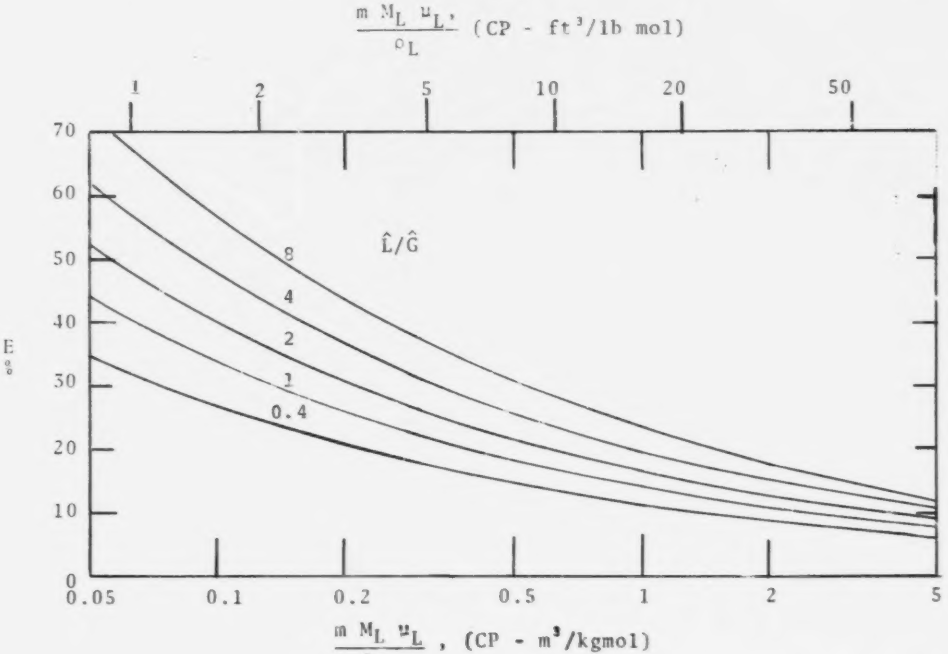

FIGURE 5.2.2-10
OVERALL PLATE EFFICIENCY

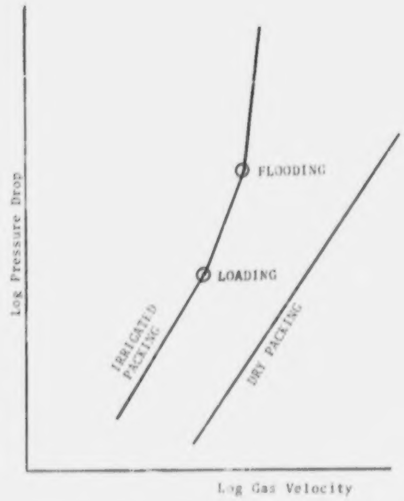

FIGURE 5.2.3-2

TYPICAL PRESSURE DROP VS. VELOCITY PLOT SHOWING LOADING AND FLOODING POINTS

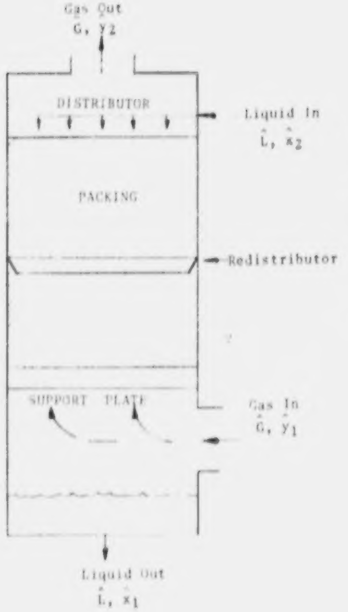

FIGURE 5.2.3-1

SCHEMATIC OF A TYPICAL PACKED COLUMN

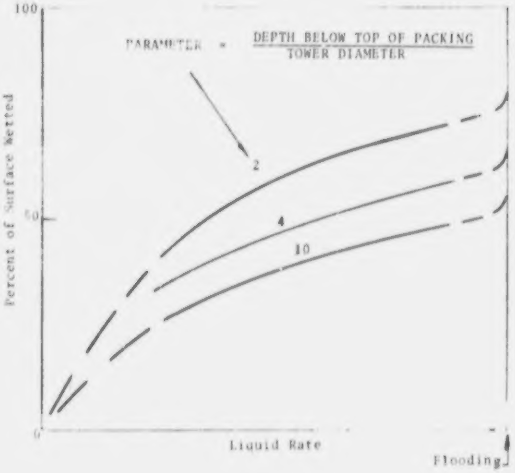

FIGURE 5.2.3-4

EFFECT OF LIQUID RATE ON WETTED SURFACE (After Sherwood and Pigford, 1952)

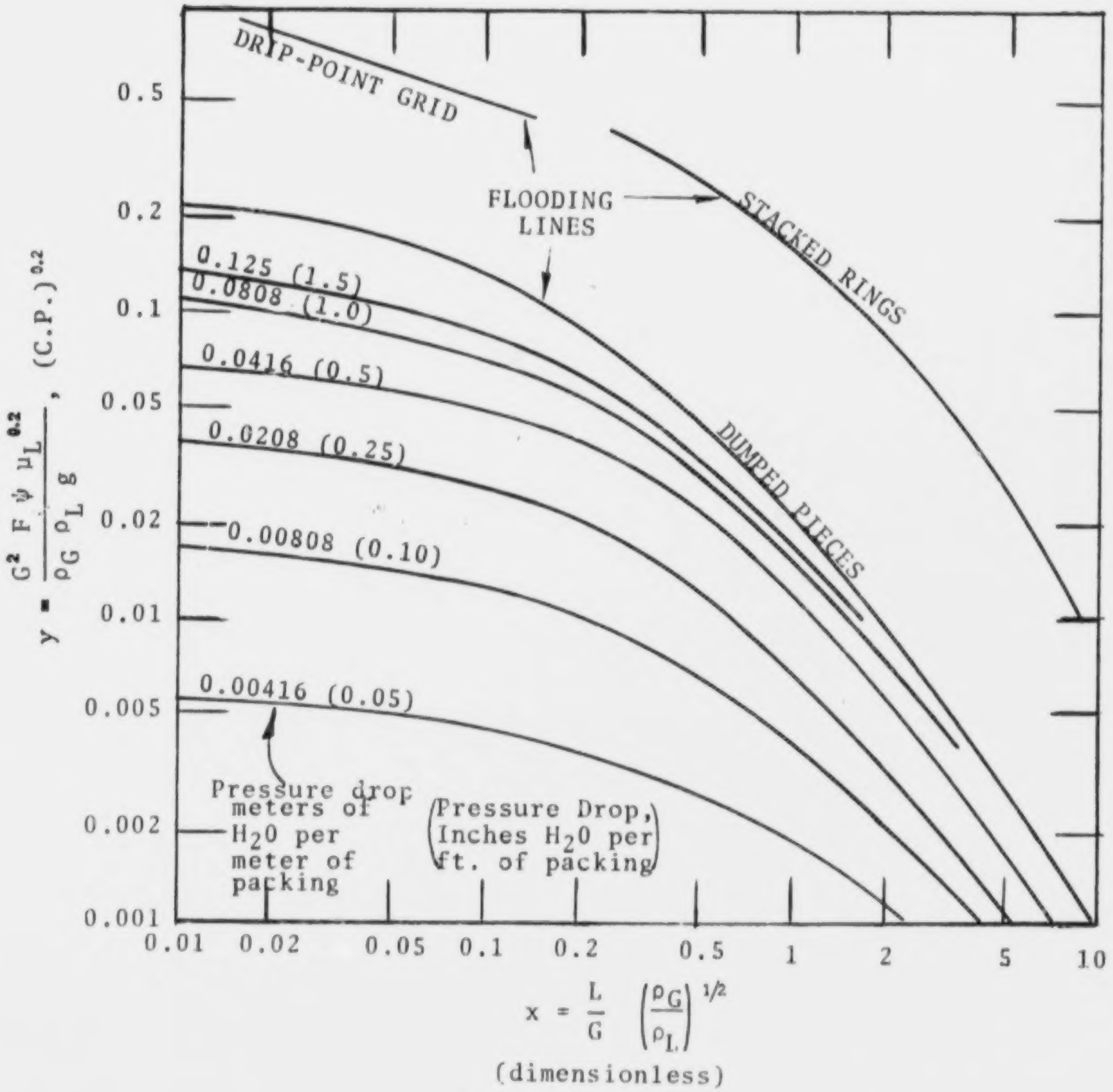

FIGURE 5.2.3-3

GENERALIZED FLOODING AND PRESSURE DROP CORRELATION

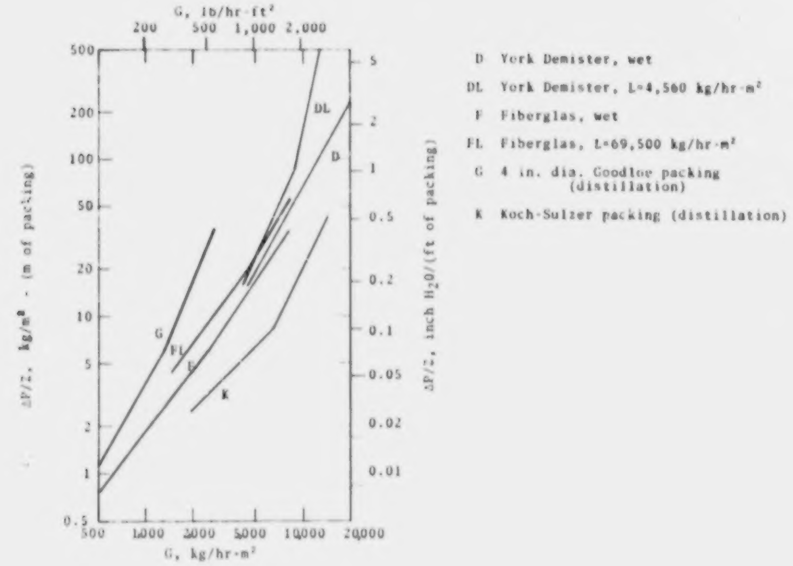

FIGURE 5.2.4-1

PRESSURE DROP THROUGH FIBROUS PACKINGS

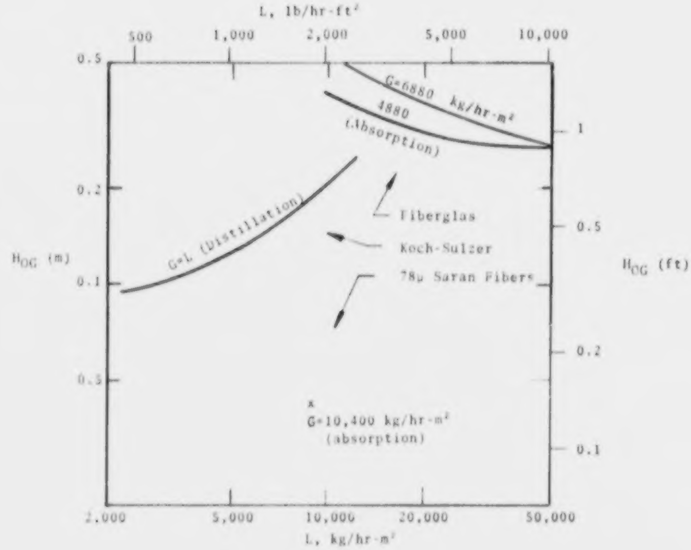

FIGURE 5.2.4-2

HEIGHT OF TRANSFER UNIT FOR TYPICAL FIBROUS PACKINGS

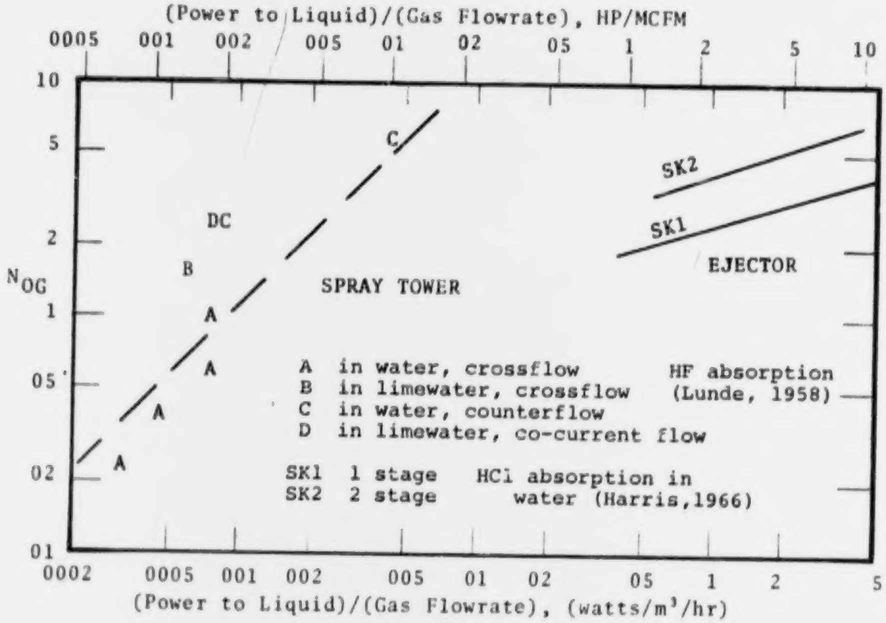

FIGURE 5.2.5-1

NUMBER OF TRANSFER UNITS FOR TWO SPRAY DEVICES

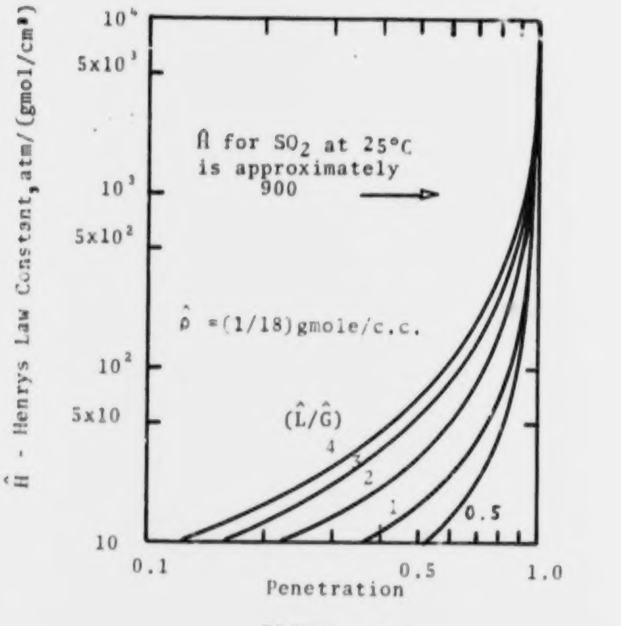

FIGURE 5.2.6-1

EQUILIBRIUM (MINIMUM) PENETRATION FOR PHYSICAL ABSORPTION IN A COCURRENT GAS-LIQUID FLOW

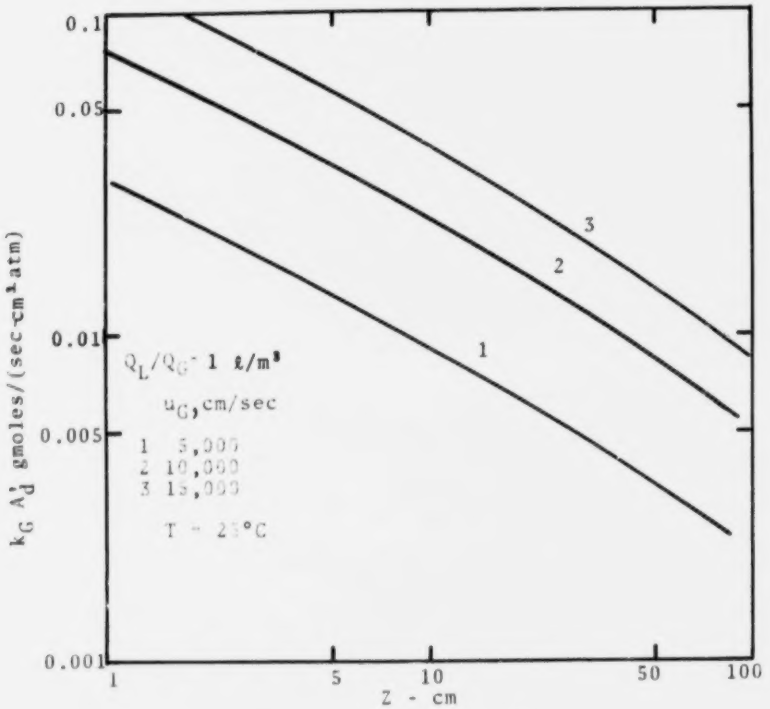

FIGURE 5.2.6-2

GAS AND LIQUID PHASE ABSORPTION COEFFICIENT WITH DISTANCE FROM THE POINT OF ATOMIZATION

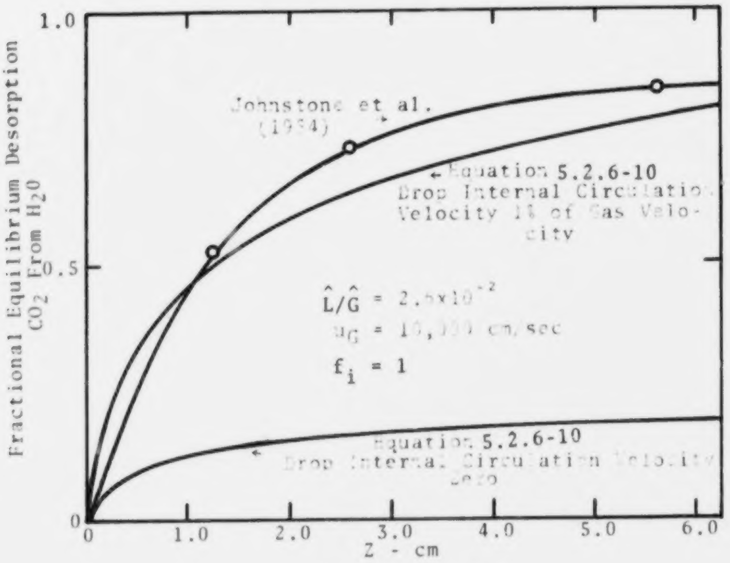

FIGURE 5.2.6-3

CO_2 DESORPTION WITH RESPECT TO LENGTH OF VENTURI FROM THE POINT OF LIQUID ATOMIZATION

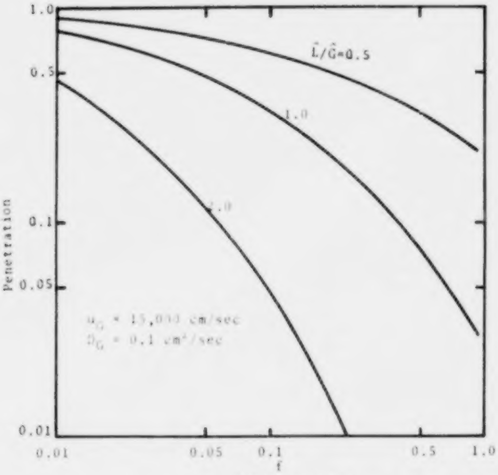

FIGURE 5.2.6-4

PENETRATION OF A SOLUBLE GAS VS. "f" IN A VENTURI WITH GAS PHASE RESISTANCE CONTROLLING AND ZERO BACK PRESSURE IN THE FLUID

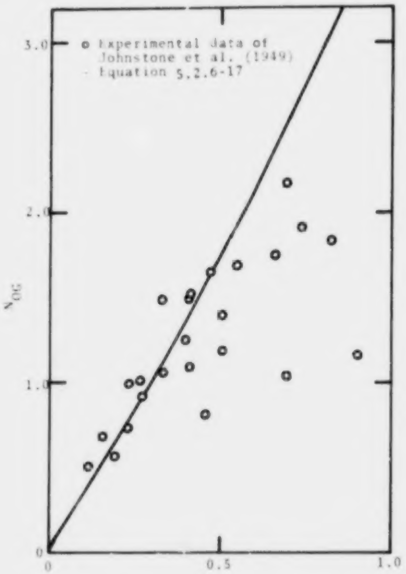

FIGURE 5.2.6-5

NUMBER OF OVERALL TRANSFER UNITS VS. ($\hat{L}/\hat{G}$) EXPERIMENTAL DATA OF JOHNSTONE ET AL. (1949) AND PREDICTION BY EQUATION 5.2.6-18 WITH u_G=200 ft/sec

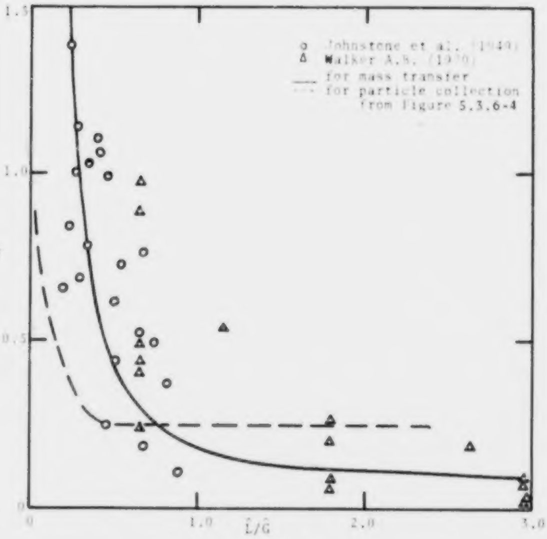

FIGURE 5.2.6-6

VALUES OF "f" VS. (L_M/G_M) FOR SO_2 ABSORPTION BY SODIUM HYDROXIDE SOLUTION

Curve No.	A	B	C	D	E	F
Z	33"	18"	18"	18"	14"	14"
G	1,525	1,040	1,300	1,610	1,320	1,985

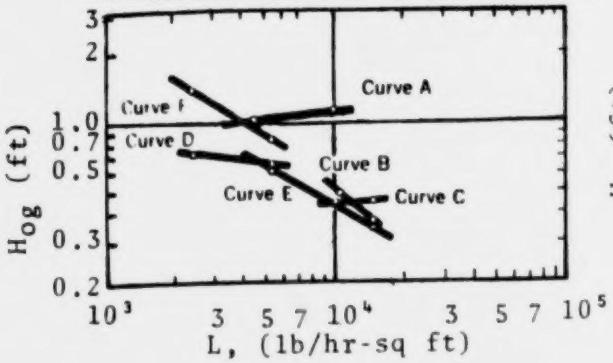

FIGURE 5.2.8-1

HEIGHT OF TRANSFER UNIT VS.
LIQUID VELOCITY
(after Douglas 1964)

Curve No.	A	B	C	D
Z	18"	18"	18&14"	14"
L	2,460	10,330	14,950	5,315

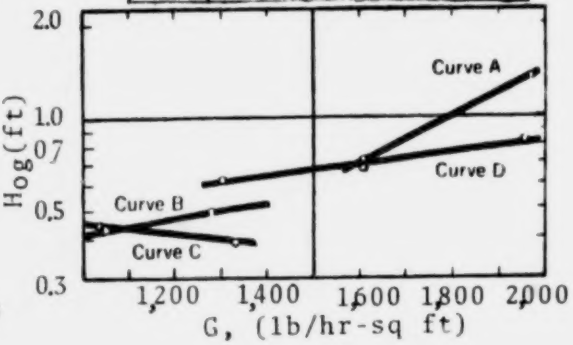

FIGURE 5.2.8-2

HEIGHT OF TRANSFER UNIT VS.
GAS VELOCITY (after Douglas
1964)

Curve No.	A	B	C	D
L = Liquid mass velocity lb/hr-sq ft	2,460	4,560	10,330	14,950
G = Gas mass velocity lb/hr-sq ft	1,990	1,525	1,278	1,320

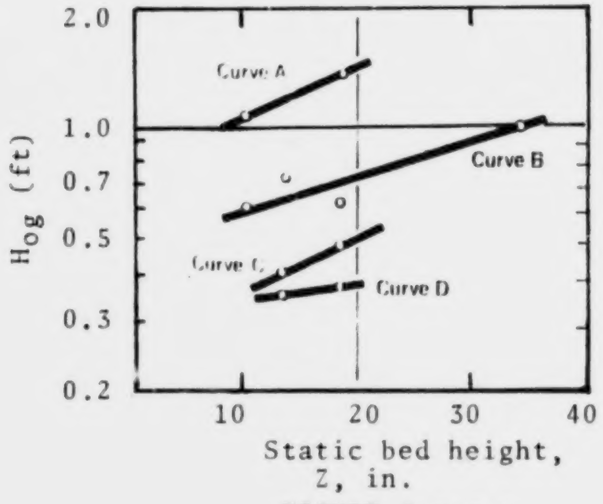

FIGURE 5.2.8-3

HEIGHT OF TRANSFER UNIT VS.
STATIC BED HEIGHT
(after Douglas 1964)

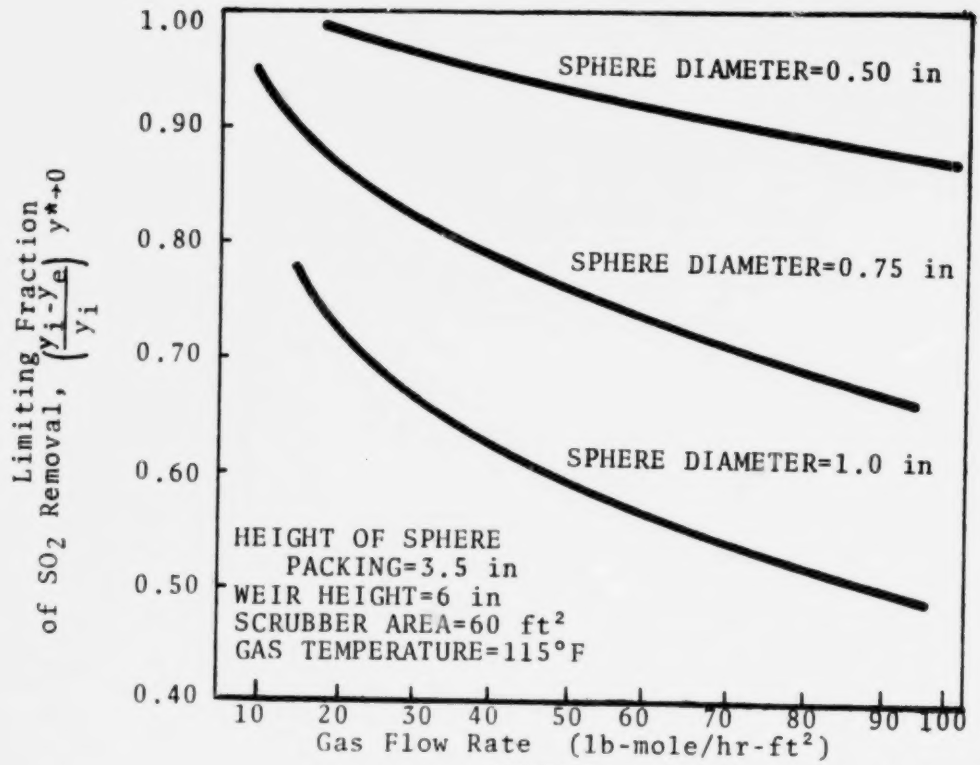

FIGURE 5.2.8-4

MAXIMUM (LIMITING) FRACTION OF SO_2 REMOVAL IN HYDRO-FILTER (after Bechtel 1970)

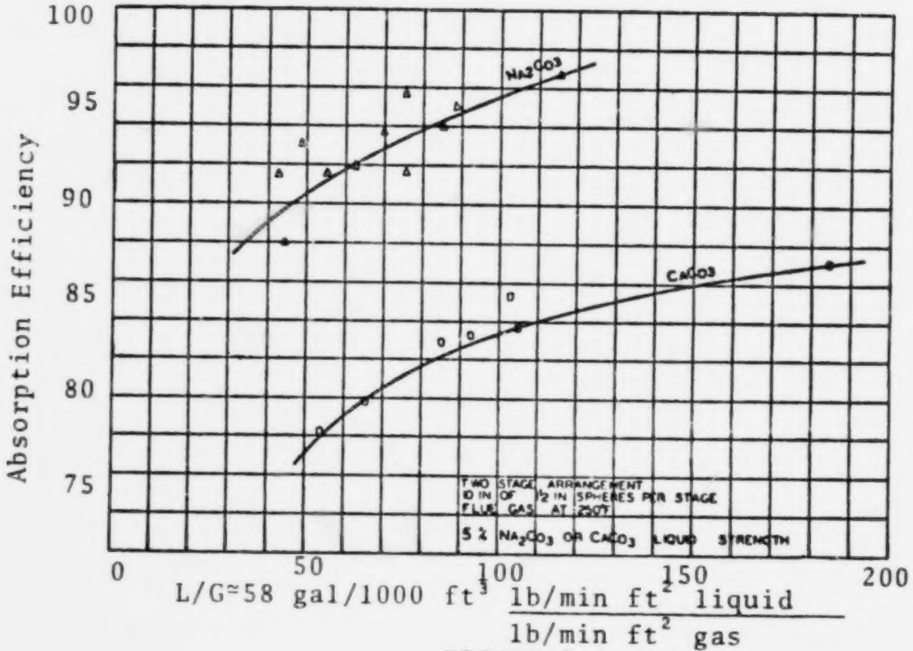

FIGURE 5.2.8-5

TURBULENT CONTACT ABSORBER-SO_2 ABSORPTION EFFICIENCIES (After Pollock et al. 1967)

SECTION 5.2 NOMENCLATURE

LATIN

a - constant

a - specific surface area m^2/m^3 or cm^2/cm^3

ac - area for gas flow through bubble cap, m^2 or cm^2

A - component "A"

A - cross sectional area, m^2 or cm^2

Ao - total hole area of plate, m^2 or cm^2

At - throat area, m^2 or cm^2

Aw - wetted wall area, m^2

b - bubble cap slot width, m or cm

b - width of channels in packed tower, m or cm

C - orifice coefficient

d - diameter, m or cm

d_c - cyclone diameter, m or cm

d_c - minimum allowable column diameter, m or cm

d_{col} - column diameter, m or cm

d_r - diameter of bubble cap riser, m or cm

d_{mm} - mass median drop diameter, m, cm or μm

D - diffusivity, cm^2/sec

E - overall plate efficiency

E_{MV} - Murphree vapor efficiency

f - ratio of drop velocity relative to gas, to gas velocity

f_h - holes area as fraction of total counterflow tray area

F - empirical packing factor, 1/m

F_w - wall curvature correction factor, Equation 5.2.2-7.

g - acceleration of gravity, 9.81 m/sec^2 or 981 cm/sec^2

SECTION 5.2 NOMENCLATURE

LATIN

G - gas mass flux kg/(sec m^2) or g/(sec cm^2)

$\hat{G}$ - gas molar flux, kgmol/(sec m^2) or gmol/(sec cm^2)

$\hat{G}'$ - inert gas molar flux, kgmol/(sec m^2) or gmol/(sec cm^2)

G_M - gas mass flowrate, kg/sec or g/sec

h - tray head loss, m or cm of W.C.

h' - liquid depth to midpoint of slots, m or cm of W.C.

h_c - head loss through caps and cap slots, m or cm of W.C.

h_d - depth of cap slots, m or cm

h'_d - height of weir above slot midpoint, m or cm

h_{dp} - dry-plate head loss (sieve tray) m or cm of W.C.

h'_{dp} - valve tray dry plate head loss, m or cm of W.C.

h_e - valve tray equivalent clear liquid depth, m or cm of W.C.

h_g - hydraulic gradient, m or cm of W.C.

h_{ow} - height over weir, m or cm

h_r - head loss through bubble caps due to flow reversal, m or cm of W.C.

h_r - residual head loss for sieve plate, m or cm of W.C.

h_s - head loss through slots, m or cm of W.C.

h_{total} - head loss through scrubber, m or cm of W.C.

h_w - height of weir, m or cm

Hd - liquid holdup

$\hat{H}$ - Henry's law constant, atm/(kgmol/m^3), or mbar/gmol/cm^3).

H_G - height of gas film transfer unit, m or cm

H_L - height of liquid film transfer unit, m or cm

H_{OG} - height of overall gas phase transfer unit, m or cm

H_{OL} - height of overall liquid phase transfer unit, m or cm

SECTION 5.2 NOMENCLATURE

LATIN

HTU - height of a transfer unit, m or cm

HETP - height equivalent to a theoretical plate, m

$\hat{k}_G$ - gas film mass transfer coefficient, gmol/(sec cm^2 atm)

k_L - liquid film mass transfer coefficient, cm/sec

K_L - overall liquid phase transfer coefficient, cm/sec

$\hat{K}_G$ - overall gas phase transfer coefficient, gmol/(sec atm cm^2)

L - liquid mass flux, kg/(sec m^2) or g/(sec cm^2)

L_M - liquid mass flowrate, kg/sec or g/sec

$\hat{L}$ - liquid molar flux, kgmol/(sec m^2) or gmol/(sec cm^2)

m - slope of x-y equilibrium line

M - molecular weight, kg/kgmol or g/gmol

MWR - minimum wetting rate

$\hat{N}$ - molar flux, kgmol/(m^{2}sec) or gmol/(cm^{2}sec)

N_G - number of gas phase transfer units

N_L - number of liquid phase transfer units

N_{OG} - number of overall gas phase transfer units

N_{OL} - number of overall liquid phase transfer units

N_p - number of theoretical plates

NTU - number of transfer units

p - partial pressure of solute, mbar or atm

P - total pressure, mbar or atm

P_{BM} - log mean pressure of component B, mbar or atm

Q - volumetric flow rate, m^3/sec, cm^3/sec or lit s/sec

Q_S - gas flow through each slot, m^3/hr

Rg - ideal gas law constant

SECTION 5.2 NOMENCLATURE

LATIN

T - absolute temperature, °K

t_{plate} - sieve plate thickness, m or cm

u - velocity, m/sec or cm/sec

u_c - gas velocity through bubble caps, m/sec or cm/sec

u_r - relative velocity between gas and liquid, m/sec or cm/sec

u_s - superficial gas velocity, m/sec or cm/sec

W - weir length, m or cm

$\hat{x}$ - mole fraction solute in liquid

$\hat{y}$ - mole fraction solute in gas

Z - diffusion parameter

DIMENSIONLESS NUMBERS

$N_{Sc} \equiv \mu_G/(\rho_G D_G)$, Schmidt Number

$N_{Sh} \equiv k_G R_G Td/D_G$, Sherwood Number

$N_{Re} \equiv \rho du/\mu$, Reynolds Number

GREEK

ε - porosity, fractional volume void space

Θ - contact time, sec

ρ - density, kg/m^3 or g/cm^3

$\hat{\rho}$ - molar density, kgmol/m^3 or gmol/cm^3

σ - liquid surface tension, dyne/cm

μ - viscosity, g/(cm sec)

ψ - column sizing constant

SECTION 5.2 NOMENCLATURE

SUBSCRIPTS

A - component "A"

B - component "B"

d - drop

G - gas phase

h - perforation in plate

i - interface

L - liquid phase

r - relative

s - sphere section

t - terminal velocity

T - turbulent layer

W - water

SECTION 5.2 - REFERENCES

Adams, F. W., Ind. Eng. Chem. 25, 424 (1933).

Baker, T. C., Ind. Eng. Chem. 27, 977 (1935).

Bayerlein, K., Gas, Wasser, Wärme 8(2), 25 (1954).

Bechtel, "The Limestone Test Facility at TVA's Paducah Power Plant", Presented at NAPCA Symposium on Wet Limestone Scrubbing, Pensacola, Florida, March 16-20, 1970.

Benson, H. E., Field, J. H., Haynes, W. P., Chem. Eng. Progress 52, 433 (1956).

Benson, H. E., Field, J. H., Jimeson, R. M., Chem. Eng. Progress 50, 356 (1954).

Blum, H. A., Stutzman, L. F., Dodds, W. S., Ind. Eng. Chem. 44, 2969 (1952).

Bonilla, C. F., Mottes, J. R., Wolf, M., Ind. Eng. Chem. 42, 2521 (1950).

Cabibbo, S.V., Teller, A.J., "The Cross Flow Scrubber, A Digital Model for Absorption", Paper No. 69-186, Presented 62nd APCA Annual Meeting, New York, June 22-26 (1969).

Calvert, S., "Air Pollution", Stern, A.C., Ed., 3, Academic Press, New York (1968).

Calvert, S., A.I.Ch.E.J. 16, (3), 392-6. (1970).

Cantelo, R. C., Simmons, C. W., Giles, E. M., Brill, F. A., Ind. Eng. Chem. 19, 989 (1927).

Carey, W. F., Williamson, G. J., Proc. Inst. Mech. Eng. 1963, 41 (1950).

Chilton, T. H., Colburn, A. P., Ind. Eng. Chem. 27, 255 (1935).

Chu, J. C., et al., J. Appl. Chem. 1, 529 (1951).

Cogan, J. D., Cogan, J. P., thesis in chemical engineering, MIT, (1932).

Comstock, C. S., Dodge, B. F., Ind. Eng. Chem. 29, 520 (1937).

Cooper, C. M., Christl, R., Peery, L. C., Trans.A.I.Ch.E. 37, 979 (1941).

Cryder, D. S., Malone, J. O., Trans.A.I.Ch.E. 37, 827 (1941).

Danckwerts, P. V., A.I.Ch.E.J. 1, 456 (1955).

Deed, D. W., Schutz, P. W., Drew, T. B., Ind. Eng. Chem. 39, 766 (1947).

Dwyer, O. E., Dodge, B. F., Ind. Eng. Chem. 33, 485 (1941).

Eckert, J. S., Chem. Eng. Progress, 59(5), 76 (1963).

5.2 - REFERENCES (cont'd)

Eckert, J. S., Chem. Engrg. Progress 57, (9), 54 (1961).

Eckert, J. S., et al., Ind. Eng. Chem. 59 (2), 42 (1967).

Eckert, J. S., Foote, E. M., Huntington, R. L., Chem. Eng. Progress 54(1), 70 (1958).

Emmert, R. E., Pigford, R. L., "Gas Absorption", in Chemical Engineer's Handbook, 4th ed., McGraw-Hill, San Francisco, (1963).

Fellinger, L., Sc.D. thesis in chemical engineering, MIT, (1941).

Fujita, S., Hayakawa, T., Chem. Eng. (Japan) 20, 113 (1956).

Furnas, C. C., Bellinger, F., Trans.A.I.Ch.E. 34, 251 (1938).

Greenewalt, C. H., Ind. Eng. Chem. 18, 1291 (1926).

Greenwood, K., Pearce, M., Trans.A.I.Ch.E. 31, 201 (1953).

Gregory, L. B., Scharmann, W. G., Ind. Eng. Chem. 29, 514 (1937).

Grimley, S. S., Trans. I.Ch.E. 23, 228 (1945).

Harris, L. S., Chem. Eng. Progress 62(4), 55 (1966).

Harris, L. S., Haun, G. R. Chem. Eng. Progress 60(5), 100 (1964).

Haslam, R. T., Hershey, R., Kean, R. H., Ind. Eng. Chem. 16, 1224 (1924).

Haslam, R. T., Ryan, W. P., Weber, H. C., Trans.A.I.Ch.E. 15, 177 (1923; Ind. Eng. Chem. 15, 1105 (1923).

Hatta, S., Katori, M., J. Soc. Chem. Ind. Japan 37, 280B (1934).

Hensel, S. L., Treybal, R. E., Chem. Eng. Progress 48, 362 (1952).

Higbie, R., Trans.A.I.Ch.E. 31, 365 (1935).

Hobler, T., "Mass Transfer and Absorbers," Pergamon, New York, (1966).

Hollings, H., Silver, L., Trans. I.Ch.E. 12, 49 (1934).

Houston, R. W., Walker, C. A., Ind. Eng. Chem. 42, 1105 (1950).

Huang, C. J., Hodson, J. R., Petrol. Ref. 37, 103 (1958).

Hughmark, G. A., O'Connell, H. E., Chem. Eng. Progr. 53, 127M (1957).

5.2 - REFERENCES (cont'd)

Hunt, C. A., Hanson, D. N., and Wilke, C. R., A.I.Ch.E.J. 1, 441 (1955).

Hutchings, L. E., Stutzman, L. F., Koch, H. A., Chem. Eng. Progress 45, 253 (1949).

Jenness, L. C., Caulfield, J. G. L., Paper Trade J. 109 (26), 37 (1939).

Johnstone, H. F., Field, R. B. and Tassler, M. C., Ind. Eng. Chem. 46, 1601, (1954).

Johnstone, H. F. and Kleinschmidt, Trans. Am. Inst. Chem. Engrs. 34, 181 (1938).

Johnstone, H. F., Singh, A. D., Ind. Eng. Chem. 29, 286 (1937).

Johnstone, H. F. and Silox, H. E., Ind. Eng. Chem. 39, 808 (1947).

Johnstone, H. F., Williams, G. C., Ind. Eng. Chem. 31, 993 (1939).

Johnstone, H. F., Roberts, M. H., Ind. Eng. Chem. 41, 2417 (1949).

Knoedler, E. L., Bonilla, C. F., Chem. Eng. Progress 50, 125 (1954).

Koch, H. A., Stutzman, L. F., Blum, H. A., Hutchings, L. E., Chem. Eng. Progress 45, 677 (1949).

Kohl, A. L., A.I.Ch.E.J. 2, 264 (1956).

Kohl, A. L., Riesenfeld, F. C., "Gas Purification", McGraw-Hill, New York, (1960).

Kowalke, O. L., Hougen, O. A., Watson, K. M., Chem. Met. Eng. 32, 443, 506 (1925)a.

Kowalke, O. L., Hougen, O. A., Watson, K. M., Univ. Wis. Eng. Expt. Sta. Bulletin 68, June (1925)b.

Krebs, R. W., thesis, Univ. of Illinois, (1938).

Leibush, A. G., Shneerson, A. L., J. Appl. Chem. SSSR 23, 1253 (1950).

Leva, M., Chem. Engrg. Progr. Symp. Series No. 10, 50, 51 (1954).

Leva, M., A.I.Ch.E.J. 1, 224 (1955).

Litvinenko, M. S., J. Appl. Chem. USSR 25, 775 (1952).

Lobo, W. E., Friend, L., Hashmall, F., Zenz, F. A., Trans.A.I.Ch.E. 41, 693 (1945).

5.2 - REFERENCES (cont'd)

Lunde, K. E., Ind. Eng. Chem. 50, 293 (1958).

McAdams, W. H., Poblenz, J. B., St. John, R. C., Chem. Eng. Progress 45, 241 (1949).

Mehta, K. C., Sharma, M. M., Brit. Chem. Eng. 15, 1440, 1556 (1970).

Miller, E. G., S. B. thesis in chemical engineering, Univ. Delaware (1948).

Molstad, M. C., Abbey, R. G., Thompson, A. R., McKinney, J. F., Trans. A.I.Ch.E. 38, 410 (1942).

Molstad, M. C., McKinney, J. F., Abbey, R. G., Trans. A.I.Ch.E. 39, 605 (1943).

Molstad, M. C., Parsly, L. F., Jr., Chem. Eng. Progress 46, 20 (1950).

Morrell, C. E., Paltz, N. J., Packie, J. W., Asbury, W. C., Brown, C. L., Trans. A.I.Ch.E. 42, 473 (1946).

Morton, F., King, P. J., Atkinson, B., Trans. I.Ch.E. 42, 35, 45, 49 (1964).

NAPCA, Private communication, (1970).

Norman, W. S., Algawi, M. O., Garner, F. H., Trans. I.Ch.E. 32, S.14 (1954).

Norman, W. S., Trans. I.Ch.E. 29, 226 (1951).

Norman, W. S., "Absorption, Distillation, and Cooling Towers," Wiley, New York, 1961.

Oldershaw, C. F., Simenson, L., Brown, T., Radcliffe, F., Chem. Eng. Progress 43, 371 (1947).

Othmer, D. F., Scheibel, E. G., Trans. A.I.Ch.E. 37, 211 (1941).

Parsly, L. F., Jr., Molstad, M. C., Cress, H., Bauer, L. G., Chem. Eng. Progress 46, 17 (1950).

Pearson, D. A., Lundberg, L. A., West, F. B., McCarthy, J. L., Chem. Eng. Progress 47, 257 (1951).

Perry, J. H., "Chemical Engineers' Handbook", 4th ed., McGraw-Hill, New York (1963).

Pettit, A. B., Chem. Eng. 58 (8), 250 (1951).

Pigford, R. L., Pyle, C., Ind. Eng. Chem. 43, 1649 (1951).

5.2 - REFERENCES (cont'd)

Pollock, W. A., Tomany, J. P., Frieling, G., "Sulfur Dioxide and Fly Ash Removal From Coal Burning Power Plant", Air Eng. (September, 1967).

Ponter, A. B., Thornley, P. G., Chem. and Proc. Engrg. 402 (August, 1964).

Riggle, J. W., Tepe, J. B., Ind. Eng. Chem. 42, 1036 (1950).

Rixon, F. F., Trans.A.I.Ch.E. 26, 119 (1948).

Rumford, F., Edwards, G., Robertson, R., Thomson, I., Trans.A.I.Ch.E. 32, 181 (1954).

Scheibel, E. G., Othmer, D. F., Trans.A.I.Ch.E. 40, 611 (1944).

Seebold, J. E., Gilliland, E. R., Ind. Eng. Chem. 33, 1143 (1941).

Sherwin, K. A., Trans. I.Ch.E. 32(Suppl.), 129 (1954).

Sherwood, T. K., Holloway, F. A. L., Trans.A.I.Ch.E. 36, 21 (1940).

Sherwood, T. K., Shipley, G. H., Holloway, F. A. L., Ind. Eng. Chem. 30, 765 (1938).

Sherwood, T. K., Pigford, R. L., "Absorption and Extraction", McGraw-Hill, New York, (1952).

Shulman, H. L., DeGouff, J. J., Jr., Ind. Eng. Chem. 44, 1915 (1952).

Sitaraman, R., Ibrahim, S. H., Kuloor, N. R., Chem. Proc. Engrg., 115 (October, 1968).

Skelland, A. H. P., "Mass Transfer", in Kirk-Othmer Encyclopedia of Chemical Technology, 2nd ed., Wiley, New York, (1967).

Spector, N. A., Dodge, B. F., Trans.A.I.Ch.E. 42, 827 (1946).

Teller, A. J., "Liquid-Gas Systems," in Chemical Engineer's Handbook, 4th ed., McGraw-Hill, San Francisco, (1963).

Teller, A. J., Ford, H. E., Ind. Eng. Chem.50, 1201 (1958).

Tepe, J. B., Dodge, B. F., Trans.A.I.Ch.E. 39, 255 (1943).

Treybal, R. E.,"Mass Transfer Operations", McGraw-Hill, New York, (1955).

Van Krevelen, D. W., Baans, C. M. E., J. Phys. Coll. Chem. 54, 370 (1950).

Vivian, J. E., Sc.D. thesis in chemical engineering, MIT, (1945).

5.2 - REFERENCES (cont'd)

Vyazovov, V.V., J. Tech. Phys. USSR 10, 1519 (1940).

Walker, A. B., "Mass Transfer Characteristics of Variable Annular Throat Venturi Scrubbers", Presented at NAPCA symposium on Wet Limestone Scrubbing, Pensacola Florida, March 16-20, 1970.

White,R.E., Othmer, D.F., Trans.A.I.Ch.E., 38, 1067 (1942).

Whitney, R. P., Han, S.T., David, J.L., TAPPI 36, 172 (1953).

Whitney, R.P., Vivian, J.E., Chem. Eng. Progress 45, 323 (1949).

Yoshida, F., Chem. Eng. Progress Symp. Series No. 16, 51, 59 (1955).

Yoshida, F., Koyanagi, T., Ind. Eng. Chem. 50, 365 (1958).

Yoshida, F., Tanaka, T., Ind. Eng. Chem. 43, 1467 (1951).

Zabban, W., Dodge, B.F., Chem. Eng. Progress Symp. Series No. 10, 50, 61 (1954).

5.3 PARTICLE SEPARATION

5.3.1 GENERAL COMPUTATIONAL METHOD

Particle separation computations usually have the object of predicting collection efficiency for a distribution of particle sizes under a given set of operating conditions for a scrubber. Whether for the purpose of designing a scrubber to meet certain performance specifications or determining the probable capability of a particular scrubber, the basic computational process is the same. One must provide a relationship between performance and particle size and then determine the integrated effect of this over the particle size distribution of the aerosol in question. This computation is repeated as may be necessary to explore the effects of operating conditions or configuration changes. The method, while straightforward, is somewhat cumbersome if one wants to remember only a few key principles and facts.

A concise description of both scrubber capability and the difficulty of a given particle separation is very useful for conceptual and quick-estimation purposes. In this program we have developed a general approach for this purpose and, as will be seen, it not only meets the requirements of simplicity and clear significance, but also proves to be quite accurate for a large percentage of scrubber applications.

5.3.1.1 Difficulty of Separation

Difficulty of separation depends on particle size, those other properties which are significant in the unit mechanism(s) involved, and the desired collection efficiency. As discussed in Section 5.1, collection efficiency (or penetration, or transfer units) alone does not define it. By analogy to mass transfer we see that the number of transfer units includes both the change in composition and the "equilibrium driving force". The driving force is a measure of the gas molecule's tendency to transfer from say the gas phase to the liquid. The tendency of a particle to transfer relates to its properties and the mechanism involved, and may have nothing to do with concentration of particles.

For inertial impaction, the most common particle separation process, aerodynamic diameter, $d_{pa} \equiv d_p (\rho_p C')^{1/2}$, defines the particle properties of importance. When other separation mechanisms such as diffusion are important, other particle properties such as particle diffusivity are more significant.

Difficulty of separation can be characterized by the particle aerodynamic diameter for which collection efficiency (or penetration) should be 50%, "d_{p50}", if the required overall penetration $\overline{Pt}$ for the entire particle size distribution is to be attained. A log normal particle size distribution is characterized by the mass median diameter, d_{pg}, and the geometric standard deviation, σ_g. When the examined scrubber penetration is proportional to the exponential of particle diameter squared, i.e. $Pt \; \alpha \; \exp[-d_p^2]$, then Figure 5.3.1-4 is a convenient tool for finding the particle diameter which must be collected with 50% efficiency, d_{p50}, in order to achieve the desired overall penetration, $\overline{Pt}$, given d_{pg} and σ_g. For example, if 2% overall penetration is required for a log normally distributed dust with d_{pg} = 10 μm and σg = 3, then Figure 5.3.1-4 shows that the particle size which must be collected with at least 50% efficiency, d_{p50}, will be 0.9 μm. If the scrubber in question collects 0.9 μm particles with better than 50% efficiency, overall penetration will be even less than 2%.

A useful rule of thumb is that the cut diameter required, d_{p50}, will be about the same as the diameter at the cumulative fraction corresponding to the desired penetration. Figure 5.3-1 shows a log-probability plot of an aerosol with d_{pg}=10(μm) and σg=3.0. Note that the ratio of diameter at about 84% undersize to mean diameter equals $30/10=\sigma_g$, the geometric standard deviation. At the point where the cumulative fraction (could be weight or number fraction) is 0.02 (2%), the particle diameter is about 1.0(μm). This is close to the 0.9(μm) which was obtained through the use of Figure 5.3.1-4. The reason that this approximation works is that the effects of lower penetration for particles larger than "d_{p50}" and the higher penetrations for smaller particles nearly cancel each other.

To get d_{pa50} from d_{p50}, use Figure 4.6.7-6. For $\rho_p = 3(g/cm^3)$, d_{p50}= 1.0(μm), and moderate temperature, $d_{pa50} \simeq 1.9$. To check this, note that $C' \simeq 1.16$ @ d_p=1.0 and therefore, $d_p (\rho_p C')^{1/2} = 1.0 (3x1.16)^{1/2}$ = 1.87.

5.3.1.2 Scrubber Capability

Actual performance data which has been measured and interpreted correctly is the most reliable way to define scrubber capability. Unfortunately, it is rare that reliable data are available for the complete range of operating conditions and design modifications. It is necessary to use performance relationships which are derived from basic principles and make use of the good data which are available. The only sound way to extrapolate performance data is by means of a mathematical model derived from knowledge of the unit mechanism of collection.

In this program we have, to the extent possible within the time and manpower limits, presented design methods based upon that concept. The particle collection efficiency is related to system parameters in a way which is dictated by an understanding of what is going on at the microscopic level. In most of the important cases we have been able to describe the available method where it was adequate, improve it, or develop an entirely new method where necessary. In other cases there was not sufficient time to do more than present the available technology, even though it is questionable.

The cut diameter approach which has previously been used for cyclone separators and cascade impactors, proved to be a good way to characterize scrubber performance. We have applied it to a number of the important types of scrubbers and developed performance graphs for them. This approach has the great virtue of being a single-number criterion with a wide range of quantitative validity.

5.3.1.3 Size-Penetration Integration

Integration of the penetration-particle diameter relationship over the entire particle size distribtuion will yield overall penetration as shown below (see also 8.2.1 and 9.3.1):

$$\overline{Pt} = \int_{0=}^{\infty} Pt \; f\,(d_p)\; d\,(d_p) \qquad (5.3.1\text{-}1)$$

Where: $\overline{Pt}$ = Overall penetration for the mass size distribution (fractional)

Pt = Penetration at a given particle diameter (fractional)

$f(d_p)$= Size frequency (fraction of weight/μm)

The integration of Equation 5.3.1-1 can be done graphically as shown in Figures 5.3.1-2 and 5.3.1-3. The size distribution of Figure 5.3.1-1 provides the frequency distribution data and Figure 5.3.1-2 is an arbitrarily drawn plot of penetration versus particle diameter for some kind of scrubber. By plotting the penetration versus the weight fraction undersize for several diameters, the curve shown in Figure 5.3.1-3 can be drawn. One point, for the cut diameter, d_{p50}, is shown on all 3 plots for illustration.

The area under the curve (cross-hatched) is the value of the integration of 5.3.1-1 for the given size distribution and penetration functions. It is about 0.09 (9%) for this illustration. The rule of thumb indicates an overall penetration of 0.075 at d_p=2(μm). Note that this can be done for either "d_p" or "d_{pa}". If aerodynamic diameter is used, the size distribution and efficiency functions must be put in this form.

5.3.1.4 Analytical Solutions

The integration to determine overall penetration can also be done analytically if the required mathematical expressions are available A number of cases can be handled by treating "$\overline{Pt}$" as a function of $(d_p)^2$ for a given scrubber and set of operating conditions. This and other solutions are discussed in Chapter 8 and graphs suitable for use in making computations are given there.

5.3.2 PARTICLE COLLECTION IN PLATE TYPE SCRUBBERS

5.3.2.1 Introduction

Collection devices in which the dust-laden gas is cleaned by passing through one or more plates as described in Section 3.1 are classified as plate type scrubbers. The two major groups of plate scrubbers are the sieve plate and the wet impingement plate columns. Collection in these devices is mainly due to inertia and diffusion, however other forces can be added to increase collection efficiency as was shown in Section 4.6.4. Although plate type scrubbers are versatile, collection may only be increased by a few percent by adding additional plates or increasing pressure drop, when in the inertial regime. This is illustrated in Section 9.3.1.1.

5.3.2.2 Wet Impingement

Collection devices in which the gas passes through one or more jets and impinges on an impactor plate located a short distance away are classified as impingers. When the impaction plates are covered with water, the devices belongs to the "wet impingement" family. Collection of the particles is due to impaction of the jets on the collecting plate. At the same time, collection is also obtained from the impaction of the particles on droplets sprayed and accelerated by the emerging gas stream. Since jet impactors exhibit steep target efficiency curves, it is possible that particle collection will be primarily due to one of the two mechanisms described as is also suggested by Stairmand (1956). Because of possible variability of air velocity across the plate, collection may be due to jet impaction in part of the plate, and due to collection by accelerating drops in the other part of the plate.

Principle of Operation

A wet impingement scrubber consists essentially of a vertical tower containing one or more impingement baffle stages. In one design, perforated sheets having from 6,000 to 30,000 holes per square meter are used (perforation diameter 3-5 mm) Figure 5.3.2-1. The impingement plates are so arranged over the perforated sheet that each hole is directly baffled as shown in Figure 5.3.2-2. The impingement baffle is usually placed at the vena contracta of the gas jets formed by the perforation, several millimeters above the plate. In most designs, the gas stream enters a lower section of the scrubber and rises through a water spray zone where it is cooled and humidified. These lower sprays are pointed towards the bottom of the perforated plate, helping to prevent clogging. The flow of the gas past the edge of the orifice gives rise to the formation of spray droplets. Such droplets are initially at rest and there is a large relative velocity between the dust particles and the droplets.

The gas velocity through the jets is higher than about 15 m/sec (50 ft/sec) and increases with increased pressure drop. The standard operating pressure drop is about 4 mbar, (≈1.5") and can be increased to higher values to increase collection efficiency. The average water flow is 0.13-0.27 ℓ/m^3 (1 - 2 gpm/1,000 cfm) per plate. The overall efficiency of a single stage impingement baffle scrubber for particle density of 2.7 g/cm^3 , is shown in Figure 5.3.2-3, Stairmand (1956). Figure 5.3.2-4 shows the effect of additional stages on collection efficiency of one device and Figure 5.3.2-5 shows the effect of increased pressure drop from the standard of 4 mbars (1.5"), on collection efficiency of the same device.

Design Equations

Let us consider collection by impaction first. Collection from a round jet was discussed in Section 4.6.6 and it was shown there that when $N_{Ref} \geq 100$ and parabolic flow profile does not develop, the collection efficiency curve is steep and characterized by $(K_{p50})^{1/2}$ When the ratio of the distance of the impaction plate from the jet to the jet diameter is in the range of $0.5<\ell/d_h<8$, then $0.4<(K_{p50})^{1/2}<0.48$ with an average of 0.44. This is also the "K_p" value for most customary designs where $1<\ell/d_h<2$. From the definition of "K_p" in Equation 4.6.7-10:

$$(K_{p50})^{1/2} = \left[\frac{\rho_p\ u_o\ C'}{9\ \mu_G\ d_h}\right]^{1/2} d_{p50} = 0.44 \qquad (5.3.2\text{-}1)$$

For air at room temperature and pressure, the Cunningham correction factor can be approximated by

$$C' = 1 + 1.65\text{x}10^{-5}/d_p \qquad (5.3.2\text{-}2)$$

where "d_p" is particle diameter in centimeters.

"d_{p50}" is the diameter of the particles which are collected with an efficiency of 50%. It can be approximated by the cut-off particle diameter, d_{pc}, which is defined as

$$\int_{d_{pc}}^{\infty} f(d_p)\ d(d_p) = \int_{o}^{\infty} E(d_p)\ f(d_p)\ d(d_p) \qquad (5.3.2\text{-}3)$$

where "$f(d_p)$" describes the mass size frequency distribution and "$E(d_p)$" describes the collection efficiency, both as functions of particle diameter. When $u_o<1/3$ Mach, no pressure correction is needed and

$$u_o = \frac{4\ Q_G}{n\ \pi\ d_h^{\,2}} \qquad (5.3.2\text{-}4)$$

where "n" is the number of holes in a plate. Substituting and solving for "d_{p50}" we get

$$d_{p50} = -0.0825 + \left[0.0068 + \frac{1.382\cdot10^{8}\ n\ \mu_G\ d_h}{\rho_p\ Q_G}\right]^{1/2} \qquad (5.3.2\text{-}5)$$

Here "d_{p50}" is in "μm" while all the other parameters are in c.g.s. units.

When "Q_G" is known, the perforation diameter and the number of holes per square foot required to give a cut-off diameter "d_{p50}" are calculated.

For particles which are not spherical in shape or when the particle density is not known, it is better to use the aerodynamic diameter. From the definition of aerodynamic diameter and substituting for the jet velocity, we get

$$d_{pa50} = \left(\frac{1.37\ \mu_G\ n\ d_h^{\,3}}{Q_G}\right)^{1/2} \qquad (5.3.2\text{-}6)$$

Before designing a wet impingement collection device, one should test the aerosol with a cascade impactor and determine the aerodynamic diameter frequency distribution.

The second collection mechanism in a wet impingement type collector, is the collection of particles by the torn-up drop. In this case it can be assumed that all of the collection takes place within a very short distance after drop formation, and the relative velocity can be approximated by the jet velocity. This is in analogy to Tillman (1971) who calculated collection efficiency in a venturi. He showed that almost all of the collection takes place within the venturi throat, even when the water is introduced into the throat. Thus collection efficiency can be calculated after assuming a drop diameter.

The total pressure drop per plate can be divided into three main components: ΔP_j = dry plate pressure drop; ΔP_d = wet plate pressure drop and ΔP_f = pressure drop due to friction losses in the scrubber unit. ΔP_d can be estimated from liquid depth above the plate. ΔP_f must be evaluated from experimental work.

The dry plate pressure drop which is mainly due to jet exit, for $\ell/d_h>1$, can be approximated by Equation 5.3.2-7, where "ℓ" is the distance between the baffle and the plate.

$$\Delta P_j = \frac{\rho_G u_o^2}{2g} = \frac{0.81\ \rho_G Q_G^2}{n^2\ g\ d_h^4} \qquad (5.3.2\text{-}7)$$

where "ΔP_j" is in g/cm².

Substituting for "Q_G" from Equation 5.3.2-6, we get, for air at room temperature and pressure

$$\Delta P_j = 588 \left[\frac{d_h}{d_{pa50}^{\ 2}}\right]^2 \qquad (5.3.2\text{-}8)$$

When "ΔP_j", the dry plate pressure drop, is measured in mbars, and d_{pa} in $(g/cm^3)^{1/2}\mu m$.

This equation is plotted in Figure 5.3.2-6 as cut-off aerodynamic particle diameter in $(g/cm)^{0.5}\cdot 10^4$ vs. pressure drop in mbar with perforation diameter in cm as a parameter.

Example

To illustrate the calculations involved let us follow the example discussed by Stairmand (1956). Consider a wet impingement type scrubber with a perforation diameter of 0.47 cm (3/16"). Each hole takes about 1 m³/hr of gas. What will be the collection efficiency of 1μ diameter particles with density 2.7 gm/cm.

The velocity at the vena contracta is ≈2,300 cm/sec if we assume a ratio of 0.7 between orifice cross-section and vena contracta cross-section. Assuming a zero drop velocity at the vena contracta we get for the relative velocity u_r = 2,300 cm/sec. Assuming an average drop diameter of 100 μm as typical we get for "K_p":

$$K_{pd} = \frac{(2)(1.16)(2.7)(0.5^2)(10^{-8})(2,300)}{(9)(1.8\text{x}10^{-4})(5\text{x}10^{-3})} = 4.45 \qquad (5.3.2\text{-}9)$$

From Figure 4.6.2-2 for collection by spheres the efficiency is close to 80%. The collection by impaction on the plate would now be calculated.

$$K_{pj} = \frac{(2)(1.16)(2.7)(0.25)(10^{-8})(2,300)}{(9)(1.8\times10^{-4})(0.24)} = 9\times10^{-2} \qquad (5.3.2\text{-}10)$$

From Figure 4.6.7-4 the collection efficiency for impaction from a round jet for $\sqrt{K_p} = 0.3$ and $\ell/d_h = 1.0$ is practically zero.

Experimental results for this case as shown in Figure 5.3.2-3 are about 90% which means that most of the collection is by drops. Figure 5.3.2-7 is a plot of aerodynamic cut diameter against hole velocity, with hole diameter as parameter for an impingement plate column.

5.3.2.3 Sieve Plate Columns

Principle of Operation

Sieve plate columns (see Section 5.2.2 also) consist of a vertical tower containing one or more perforated trays. On a sieve tray the liquid is maintained above the tray surface by the kinetic energy of the gas. The two basic designs of sieve trays are cross-flow and countercurrent. In the first case the liquid enters the tray through a downcomer, flows across the tray, and leaves through a second downcomer. In the countercurrent tray, both the gas and liquid flow through the perforations. The cross-flow tray is more generally used due to its larger range of stable operation.

In the cross-flow tray the perforation diameter is usually 3-10 mm. The gas velocity has to be large enough to maintain the liquid on the tray (prevent weeping), and smaller than the flooding or priming velocities. Usually a perforation gas velocity of 1,800-3,000 cm/sec is used. Most sieve plate columns are operated in the range of orifice Reynolds number between 3,100 and 10,000. In this range the bubble diameter is almost constant (≈0.45 cm) as can be seen from Equation 4.4.2-1.

Design Equations

Unit mechanisms for collection of particles in a sieve plate column has been discussed extensively in Section 4.6.3. When collection is by inertial impaction Taheri and Calvert (1968) have shown that for hydrophilic particles in water

$$E_p = 1 - \exp\left[-40\ F^2\ K_p\right] \qquad (4.6.4\text{-}1 \text{ and } 4.6.4\text{-}3)$$

where foam density is in the range of $0.38 < F < 0.65$ and "K_p" is the inertial parameter given by:

$$K_p = \frac{\rho_p\ d_p^2\ u_h}{9\ \mu_G\ d_h} \qquad (4.6.2\text{-}4)$$

Figure 5.3.2-8 is a plot of collection efficiency vs. "$F^2\ K_p$" in a sieve column. Foam density can be estimated from the relationships discussed in Section 4.4.1.2. Figure 5.3.2-9 is a performance cut diameter plot.

For collection of particles smaller than 0.1 (μm) in diameter when diffusion predominates, particle collection efficiency is given by

$$E_D = 1 - \exp - \left[1.87\ h \left(\frac{D_p}{r_b^{\,3}\ v_b} \right)^{0.5} \right] \qquad (4.6.4\text{-}10)$$

where "h" is foam height, "r_b" and "v_b" are the radius and rise velocity of the bubbles, and D_p is particle diffusivity.

When both collection mechanisms are important,

$$E_{DP} = 1 - \exp - \left[40\ F^2\ K_p + 1.87\ h \left(\frac{D_p}{r_b^{\,3}\ v_b} \right)^{0.5} \right] \qquad (5.3.2\text{-}11)$$

Collection efficiency in a sieve plate column can be increased by employing additional mechanisms as discussed in Section 4.6.3. When diffusiophoresis, thermophoresis, electrostatic or combinations of these forces become important, then the equations derived in Section 4.6.3 should be used to predict collection efficiency. Figure 5.3.2-10 is a comparison of the collection efficiency of oil mist in a sieve plate column with and without diffusio and thermophoresis. The results are plotted as collection efficiency vs. particle diameter with "N", the number of plates, as a parameter. For small particles a difference of 50% (from 6% to 54% for 0.2μ particles) in collection efficiency is common. As the particle size increases, collection by inertia becomes more important and the difference in collection efficiency decreases.

For hydrophobic aerosols the assumption that every particle which hits the bubble wall sticks to it, does not hold, and collection efficiency will be a function of the interfacial tension, which can be approximated by the wetting angle, as well as the inertia parameter. Collection efficiency for hydrophobic particles cannot be predicted with confidence, based on present knowledge.

Taheri and Calvert (1968) also showed that for hydrophilic particles, changes in perforation diameter and air flow rate have only a slight effect on collection efficiency. Water flow rate and percent plate free area affect collection efficiency only slightly. Addition of surface active agent to demineralized water reduced collection efficiency by reducing form density. Fuchs (1964) reports an increase in collection efficiency of hydrophobic particles when surface active agents were added to water. Goldshmid (1963) also showed the influence of interfacial tension, as discussed in Section 4.6.2 .

Increasing the number of plates of any type to more than one will decrease penetration in accordance with the penetration for one stage Pt_1 raised to the power "n". That is, $Pt=(Pt_1)^n$, where "n" is the number of stages.

Pressure Drop

Pressure drop in a sieve plate column under usual operating conditions runs about 2.5-10 mbars per plate. Section 5.2.2, Perry's Handbook (1963) and Chase (1967) give the necessary equations and correlations to calculate the pressure drop in a sieve plate column. Also see Section 5.2.2.3.

5.3.3 PARTICLE COLLECTION IN MASSIVE PACKING SCRUBBERS

Packed beds are commonly used for mass transfer operations. They can also be used to collect particles, most commonly liquid mists. Packed beds can be made more efficient by increasing the height of the packing material they contain.

A countercurrent packed bed consists of a vertical shell, usually cylindrical, which contains packing material. Gas passes up through the bottom of the bed, and out the top. Liquid is fed to the top of the packing, to trickle down through the bed and keep the packing elements clean of collected particles. Cocurrent and cross-flow cofigurations are also used.

5.3.3.1 Principle of Operation

The particle laden gas stream passing through a packed bed follows a tortuous path. The packing elements can be thought of as a series of impediments around which the gas stream must flow.

The theoretical models of collection efficiency by Calvert (1968) consider impaction the only significant means of particle collection, and are verified with experimental data for particles larger than one micron in diameter collected in dry beds. The ratio of particle to packing diameter is usually small enough that collection by interception can be neglected. Electrostatic effects, collection by Brownian or turbulent diffusion, and by gravity are also neglected. The growth of particles due to vapor condensation upon them may be significant, although this effect also is neglected.

5.3.3.2 Particle Collection Efficiency

Jackson and Calvert (1966) and Calvert (1968) have developed a theoretical relationship between particle collection efficiency and packed bed operating parameters. The following assumptions were made.

1. Gas (and particle) flow through the bed may be described as flow through a series of "n" semicircular channels of width "b".

2. The number of semicircular bends, n, is related to the overall height of the packed section of the bed, Z, the packing diameter, d_c, and the channel width, b, where any consistent units may be used:

$$n = \frac{Z}{d_c + b} \qquad (5.3.3\text{-}1)$$

3. The gas (and particle) velocity through the channels, v_{Gb} is inversely proportional to the free volume of the bed available for gas flow, where any consistent units may be used:

$$v_{Gb} = v_G \left(\frac{1}{\varepsilon - Hd}\right) \qquad (5.3.3\text{-}2)$$

where v_G is the superficial gas velocity of the bed (volumetric flow rate divided by total cross sectional area of the shell), "ε" is the bed void fraction (porosity), and "Hd" is the liquid holdup within the bed, i.e. the fraction of the total bed volume taken up with liquid. Table 5.3.3-1 lists values of bed porosity, ε, for beds using various packing materials.

4. Particles are collected by centrifugal force on the outside channel walls as gas and particles pass through the channels.

5. Uncollected particle concentration is constant through any plane perpendicular to the direction of gas (and particle) flow due to turbulence of the gas.

6. The width of the semicircular channels, b, can be described as a fraction, j, of the diameter of a single packing element:

$$b = j\, d_c \qquad (5.3.3\text{-}3)$$

These assumptions lead to the following equation for predicting the particle penetration for a packed bed:

$$Pt = \exp -\left[\frac{\pi}{2\,(j + j^2)\,(\varepsilon - Hd)}\;\frac{Z}{d_c}\;K_p\right] \qquad (5.3.3\text{-}4)$$

where "K_p" is the inertia parameter for the packed bed:

$$K_p = \frac{v_G\, d_{pa}^{2}}{9\, \mu_G\, d_c} \qquad (5.3.3\text{-}5)$$

The experimental data of Jackson (1964) were analyzed to determine appropriate values of "j" to use in Equation 5.3.3-4 with all quantities in the equation known except "j", which was calculated. The results are given in Table 5.3.3-2 which lists "j" values for various types and sizes of packing material. For the manufactured packing materials, "j" is fairly constant at about 0.16 - 0.19. The very low value of 0.03 for coke may be due to the small passages within the coke itself, which make each large piece of coke function effectively as a number of smaller pieces.

Figure 5.3.3-1 is a plot of particle penetration versus aerodynamic particle diameter, with bed height "Z" as parameter, assuming 3.8 (cm) Raschig ring packing, no liquid holdup, superficial gas velocity of 300 (cm/sec), air at 25°C and "j" value of 0.165. Figure 5.3.3-2 shows two plots of performance cut diameter as a function of bed height and other factors.

Baskerville (1941) developed a set of empirical equations for predicting the collection efficiency of phosphorus pentoxide mist in a bed of 2.54 (cm) Raschig rings. His relationships neglect the influence of variables such as particle size, and probably should not be used for situations dissimilar to his experiments.

Strauss and Thring (1959, 1960) used regression analysis to correlate efficiency with mass air flow rate, temperature, and particle inlet concentration. High temperature insulating brick and fireclay refractories were used to collect the fume from open hearth furnaces.

TABLE 5.3.3-1

BED POROSITY, ε, FOR VARIOUS PACKING MATERIALS

Name	Stoneware Raschig Rings	Carbon Raschig Rings	Steel Raschig Rings (1/16" thick)	Stoneware Berl Saddles	Stoneware Intalox Saddles	Steel Pall Rings
Size (cm)						
1.27	0.57 *	0.71 *	--	--	--	--
1.9	0.67	--	--	0.65	--	--
2.54	0.68	0.75	0.92	0.69	0.70	0.93
3.8	0.68	0.67	0.92	0.70	0.81	0.94
5.1	0.75	--	--	--	--	--

*Treybal (1955) All other data from Perry (1963)

TABLE 5.3.3-2

EXPERIMENTAL VALUES OF j, CHANNEL WIDTH AS FRACTION OF PACKING DIAMETER

Size (cm)	Type of Packing	j
1.27	Berl Saddles, marbles, Rachig Rings, Intalox Saddles	0.192
2.54	Berl Saddles, Raschig Rings, Pall Rings	0.190
3.8	Berl Saddles, Raschig Rings, Pall Rings	0.165
7.6 - 12.7	Coke	0.03

Adapted from Jackson (1964) and Calvert (1968)

Efficiencies of 80 to 90 per cent for the brick and 50% for the fireclay were reported for gas containing 0.8 to 6 micron diameter particles.

In his experiments on collecting oil mists in packed beds of varying dimensions, using a wide range of packing materials, Jackson (1964) found that in all cases the bed efficiency was lowered from 1 to 3 per cent due to oil mist reintrainment. Jackson's beds had gas inlet velocities of from 150 - 900 cm/sec (5-30 ft/sec). Vincent (1967) recommends velocities be kept below 200 cm/sec (67 ft/sec) for "general purpose beds," and below 25 cm/sec (0.83 ft/sec) for "finely packed beds". Decreasing velocity through the bed will decrease reintrainment, but will also decrease efficiency.

5.3.3.3 Pressure Drop

For methods of predicting pressure drop in packed beds, see Section 5.2.3.

Example Calculation

Problem

It is desired to collect 3 micron diameter oil droplets of density 1(g/cm³) in a bed of 3.8 (cm) stoneware Raschig Rings. 10,000 (m³/hr) of gas at 25°C are to be processed (5,860 cfm). What diameter and how tall should a suitable packed tower be? It is necessary to achieve 90% efficiency on the mist.

Solution

Choose a typical superficial gas velocity through the tower of 300 (cm/sec). At this velocity, some mist re-entrainment should be expected, and should be allowed for in the design.

The area of the tower should be:

$$A = \frac{Q_G}{v_G} \quad \frac{10^4 \left(\frac{m^3}{hr}\right) \quad 10^6 \left(\frac{cm^3}{m^3}\right)}{3x10^2 \left(\frac{cm}{sec}\right) \quad 3.6x10^3 \left(\frac{sec}{hr}\right)} = 9.26x10^3 \ (cm^2)$$

The tower diameter should be about:

$$D = \left(\frac{4}{\pi} A\right)^{1/2} = \left[\frac{4}{\pi} \ (9.26)x10^3\right]^{1/2} = 108.5(cm) \text{ or } (43")$$

If 5% of the mist re-entrains, the penetration of the tower will have to be:

$$Pt = 1 - \eta = 1 - (.90 + .05) = 0.05$$

Some re-entrainment should be expected. The 5% figure is arbitrary.

The tower height can now be calculated using Equation 5.3.3-4:

$$Pt = \exp\left[\frac{-\pi}{2\,(j + j^2)\,(\varepsilon - Hd)}\left(\frac{Z}{d_c}\right)\,Kp\right] \qquad (5.3.3\text{-}4)$$

$$0.05 = \exp\left[\frac{-\pi\ \ Z}{2\,(0.165 + 0.165^2)\,(0.68 - 0)\,(3.8)}\left(\frac{3x10^{2}\ \ 9x10^{-8}}{9\ 1.8x10^{-4}\ (3.8)}\right)\right]$$

A liquid holdup, Hd, of zero was assumed, i.e., the bed drains collected mist rapidly.

$0.05 = \exp\,[1.38x10^{-2}\ Z]\ ; \quad Z = 216$ cm

The tower must be 216 cm tall (about 7 feet)

The conditions of the problem enable checking the calculated result with Figure 5.3.3-1 a plot of penetration versus aerodynamic particle diameter with bed height as parameter. This figure shows that a proper bed should be slightly over 200 cm tall, in agreement with the above calculation.

5.3.4 PARTICLE COLLECTION IN FIBER BEDS

Beds of fibers are used for both mass transfer operations and for particle collection. Fiber beds are frequently used to capture fine liquid mists. A variety of materials are used and the bed or mat, can be formed in several ways, such as random laying, weaving, knitting.

5.3.4.1 Principle of Operation

The porosity, ε, (volume fraction void) of fibrous bed filters is high - typically 97 to 99 per cent. As a result, the distances between the fibers within the bed is large compared to the diameter of the fibers. Particle collection, then, is not primarily by the seiving of particles attempting to pass between two adjacent fibers.

Single fibers can capture particles moving past them by mechanisms such as gravity, Brownian diffusion, electrostatic attraction, impaction and interception. The efficiency of a single fiber due to each of these unit mechanisms is described in Section 4.6.3. The efficiency of a bed of such fibers is then dependent upon the efficiency with which each fiber within the bed can capture particles and upon the quantity and arrangement of these fibers within the bed.

As a fiber bed is used, collected particles will build up within it. If no action is taken, eventually the buildup will become so great as to cause excessive pressure drop through the bed. This necessitates replacing the old, clogged bed with a new, clean one. A viable alternative to periodic replacement is continuous washing of the fibers with liquid. This serves the dual purpose of keeping the particle collecting elements clean, and spreading the liquid out to give it high surface area. This is conducive to intimate gas liquid contacting for the removal of gaseous pollutants by mass transfer.

In the following treatment of the problem, we will assume that collection efficiency for the dry fibers is not affected by the presence of scrubbing liquid. Little work has been done on wetted fibers.

5.3.4.2 Particle Collection Efficiency in Beds of Fibers

The efficiency of a bed of clean fibrous packing, E, on particles of a specified size can be given by the following equation, (Whitby, 1965):

$$E = 1 - \exp(-\eta_s S) \qquad (5.3.4\text{-}1)$$

where "η_s" is the effective collection efficiency of a single fiber by all collection mechanisms, and "S" is the bed "solidarity factor." According to Whitby and Lundgren (1964), "physically, 'S' represents the ratio of the total projected area of the fibers to the face area of the filter mat in the direction of the gas flow."

5.3.4.3 Determination of the Solidarity Factor, S

The solidarity factor is related to the characteristics of the fiber bed in the following way:

$$S = \frac{4\, \ell}{\pi\, d_f}\, \alpha = \frac{4\, W'}{\pi\, \rho_f\, d_f} \qquad (5.3.4\text{-}2)$$

Here, "ℓ" is the length of the bed measured in direction of gas flow, "d_f" is the average fiber diameter, "α" is the volume fraction of the fibrous bed which is solid ($\alpha = 1 - \varepsilon$), W' is the weight per face area of the fiber mat, and "ρ_f" is the density of the fibers.

5.3.4.4 Determination of Single Fiber Efficiency

The efficiency of a single cylindrical fiber due to gravity, or Brownian diffusion, or electrostatic effects, or impaction, or interception is described in Section 4.6-3.

In a realistic situation, several or all of the unit mechanisms could operate simultaneously. There is, then, an interplay of mechanisms which leads to a net efficiency for a fiber which is greater than that of any one participating mechanism. For example, a particle may settle by gravity into the zone where it can be collected by impaction. The net effect would be to increase the collection of the fiber to an amount greater than that described by impaction alone.

In another sense, the overall collection efficiency of the single fiber should be less than the sum of the efficiencies of the participating unit mechanisms. For example, a large particle, captured by impaction, might in the absence of impaction have been captured by gravity. The efficiency of collection by gravity must be diminished by an amount corresponding to the removal of particles by impaction which otherwise would have been collected by gravity. In summary, the collection efficiency of a single fiber will probably be greater than the efficiency of any single collection mechanism, but less than the sum of the efficiencies of all participating mechanisms.

To calculate the efficiency of a single fiber which may be collecting particles due to several unit mechanisms, it is first necessary to determine which unit mechanisms are causing particle collection. To do this, first calculate the fiber's efficiency due to each unit mechanism alone, using the equations given in Section 4.6.3. Based on these calculations, decide which unit mechanisms are significant. If only one unit mechanism is significant, the single fiber efficiency will be equal to its efficiency as calculated for that unit mechanism alone; however if more than one unit mechanism is significant, the appropriate equations presented in the following paragraphs must be used, to allow for interactions between the mechanisms as described above.

Alternatively, it can be assumed that all unit mechanisms are operant. The equations for particle collection when all unit mechanisms are significant can then be used immediately. If it turns out that one or more unit mechanisms actually do not contribute, they will be automatically discounted.

A variety of equations have been proposed for predicting the efficiency of a single fiber under the influence of several collection mechanisms, and will be presented in the following sections.

Impaction and Interception

Torgeson predicts the single fiber efficiency due to impaction and interception as:

$$\eta_{PI} = 0.0518 \left(\frac{C_D\ N_{Ref}}{2}\right) \left(K_I\right)^{3/2} + 0.16 \left[\left(0.5 + 0.8K_I\right)\left(\frac{K_P}{2}\right) - 0.1052\ K_I \left(\frac{K_P}{2}\right)^2\right] \qquad (5.3.4\text{-}3)$$

This equation is a modification of Davies' (1952) equation for predicting collection due to impaction and interception where Reynolds number is 0.2. The Torgeson equation applies in the viscous region. It will be recalled from Section 4.6.3 that "C_D" is fiber drag coefficient, Equation 4.6.3-9 ; N_{Ref} is fiber Reynolds number, Equation 4.6.3-2; K_I is interception parameter, Equation 4.6.3-3; and K_p is inertial parameter, Equation 4.6.3-1.

Diffusion and Interception

Friedlander (1957) has shown that a fiber's collection efficiency when impaction is not significant: ($K_p<1$; $N_{Re}<1$)

$$\eta_{DI} = 6\ N_{Sc}^{-2/3}\ N_{Ref}^{-1/2} + 3\ K_I^2\ N_{Ref}^{1/2} \qquad (5.3.4\text{-}4)$$

where "N_{Sc}" is the Schmidt number, defined by:

$$\frac{N_{Pe}}{N_{Ref}} = N_{Sc} = \frac{3 \pi \mu_G^2 d_p}{\rho_G C' k T} \qquad (5.3.4\text{-}5)$$

where "k" is Boltzmann's constant.

An alternate approach has been suggested by Langmuir (1942). Both Friedlander's and Langmuir's relationships are valid in the viscous region.

Diffusion, Interception and Impaction

Torgeson has developed a complicated relationship to determine single fiber efficiency due to diffusion, interception and impaction, involving the Torgeson impaction and interception equation, 5.3.4-3, and the Torgeson diffusion equation, 4.6.3-8. His expression is:

$$\eta_{DIP} = 0.75 \quad \eta_P + F\, G(M)\, \eta_D \qquad \text{where} \qquad (5.3.4\text{-}6)$$

$$F = 1 + 0.025 \left(\frac{C_D N_{Ref}}{2}\right)^{0.6} N_{Pe}^{\;0.6} \left(\frac{K_P}{2}\right) \left[0.5 + 9.48\left(\frac{C_D N_{Ref}}{2}\right)^{-0.4} N_{Pe}^{\;-0.4}\right] \qquad (5.3.4\text{-}7)$$

and G (M) is found from Figure 5.3.4-1 a plot of "G(M)" vs. "M." Torgeson's approach applies in the viscous region, $N_{Re} \lesssim 0.5$.

Alternate equations have been presented by Friedlander and Pascari (1960, 1962) and by Davies (1952) in the case where Reynolds number is 0.2.

Evaluation of Equations

Whitby (1965) has compared the theoretical overall single fiber efficiencies calculated according to Langmuir (1942), Davies (1952), Friedlander (1957), Torgeson, and Whitby (1965), with a range of experimental data. He concluded that the single fiber efficiency calculated according to Torgeson, Equation 5.3.4-6 works best most of the time. Single fiber efficiencies calculated by the Torgeson method are plotted in Figures 5.3.4-2, -3, -4, and -5, against particle diameter, and with gas velocity as parameter.

It will be noted that all equations for particle collection due to more than one mechanism which have been presented thus far are valid only in the viscous region. No equations have been developed for simultaneous collection due to multiple mechanisms in the transition or potential regions. For this situation, Strauss's relationship can be used. He says that the single fiber efficiency due to a number of mechanisms, $\eta_{DIP\ldots}$ will be:

$$\eta_{DIP\ldots} = 1 - (1 - \eta_D)\,(1 - \eta_I)\,(1 - \eta_P)\ldots \qquad (5.3.4\text{-}8)$$

where values of "η" are less than 1.

or; $Pt_{DIP} = Pt_D\ Pt_I\ Pt_p$

where η_D, η_I, η_P etc. are the single fiber efficiences and the Pt's are penetrations due to the individual mechanisms alone, as calculated in Section 4.6.3. Strauss' relationship can also be used to determine the efficiency of a single fiber in the viscous region which is collecting by electrostatic attraction and/or gravity, as well as by other unit mechanisms.

Influence of Neighboring Fibers on Single Fiber Efficiency

Although it was stated earlier that fibers have little interaction with one another in collecting particles, this is not strictly true. The bulk of neighboring fibers will increase the velocity of the gas flowing past each fiber individually. The presence of nearby fibers will twist and turn the gas stream so that it does not approach each fiber in the uniform way which has been postulated.

Kimura and Iinoya (1965) have shown that the efficiency of a single fiber within a bed, η_S, is related to the efficiency of a single fiber far away from a neighboring fiber, $\eta_{DIP...}$:

$$\eta_S = \eta_{DIP...} \left[1 + 10 \left(N_{Ref}\right)^{1/3} \alpha \right] \qquad (5.3.4\text{-}9)$$

Other equations for the same purpose have been given by Chen (1955) and Davies (1952).

5.3.4.5 Overall Efficiency of a Bed of Fibrous Packing

Once the filter solidarity factor, S, has been calculated from Equation 5.3.4-2 and the single fiber efficiency of a fiber within the packing, η_S, has been determined from Equation 5.3.4-9, the particle collection efficiency of the device, E, can be calculated from Equation 5.3.4-1.

However, the collection efficiency (and pressure drop) of a fiber bed, which is not washed, or which is not completely washed, will gradually increase as the bed is used. One explanation for the increase in efficiency may be that as particles collect on the fibers, the distances between the fibers decreases, allowing sieving action to take place.

The increase in particle collection efficiency with time for a dry bed can be calculated from an equation given by Kimura and Iinoya (1964):

$$Ef(t) = 1 - (1 - E) \exp \left[-50 \left(\frac{\alpha}{\pi}\right)^{1/2} \left(\frac{\nu_G \; c_i \; \eta_S}{\rho_G \; \rho_p \; d_p \; d_f} \, t \right) \right] \qquad (5.3.4\text{-}10)$$

where "c_i" is the inlet dust loading, and "t" is time.

5.3.4.6 Pressure Drop

Many equations for predicting the pressure drop through fiber beds have been developed. The equation of Chen (1955) is given below:

$$\Delta P = \frac{4}{\pi} \frac{k_4}{\ln (k_5 \alpha^{-.5})} \left(\frac{\alpha}{1-\alpha}\right) \frac{\mu_G u_o \ell}{d_f^2} \qquad (5.3.4\text{-}11)$$

where k_4 and k_5 are constants which must be evaulated experimentally. Chen gives values of $k_4 = 6.1$; $k_5 = 0.64$.

Figure 5.3.4-6,"Pressure Drop per Unit Thickness for Fiber Filter" is a plot of $\Delta P/\ell$ as a function of u_o/d_f^2 and "α" for air at 300°K.

Example Calculation

A fiber bed is to be used to capture an oil mist. With what efficiency will it perform? What will be its pressure drop? Properties of the bed, mist and gas stream are listed below:

Fiber Bed

1 m x 1 m x 10 cm, fiber diameter = 16 microns (0.0016 cm), weight = 4 Kg, density of fiber material = 2.3 g/cm³

Oil Mist

density = 1 g/cm³, d_p = 2 microns (0.0002 cm), inlet concentration: = 1 g/m³

Gas Stream

500 m³/hr of air, T = 300°K.

Find whether the bed is operating in the viscous or in the potential region by calculating the Reynolds number using Equation 4.6-3-2.

$$N_{Ref} = \frac{u_o \rho_G d_f}{\mu_G} \qquad (4.6.3\text{-}2)$$

To do this, first calculate the superficial bed velocity, u_o:

$$u_o = \frac{\left(500 \frac{m^3}{hr}\right)\left(\frac{1\ hr}{3600\ sec}\right)}{1\ m^2} \left(\frac{100\ cm}{m}\right) = 13.9\ cm/sec$$

$$N_{Ref} = \frac{\left(13.9 \frac{cm}{sec}\right)\left(1.2x10^{-3} \frac{g}{cm^3}\right)(1.6x10^{-3}\ cm)}{\left(1.8x10^{-4} \frac{g}{cm\ sec}\right)} = 0.148$$

The situation is close to the viscous region, but slightly into the transition region. The assumption will be made that the situation is close enough to the viscous region to apply the Torgeson relationships.

First determine the single fiber efficiency. Assume gravity and electrostatic effects are negligible.

1. Determine the contribution of diffusion, η_D. Calculate Peclet number.

From Equation 4.6.3-7,

$$N_{Pe} = \frac{u_o \; d_f \; 3 \; \pi \; \mu_G \; d_p}{C' \; k \; T} =$$

$$\frac{(13.9 \; \frac{cm}{sec}(1.6x10^{-3} \; cm)(9.42)(1.8x10^{-4} \; \frac{g}{cm \; sec})(2x10^{-4} \; cm)}{(1.07)\left(1.38x10^{-16} \; \frac{g \; cm^2}{°K \; sec^2}\right) \; (300°K)} = 1.7x10^5$$

From Perry's Handbook, when N_{Ref} = 0.148, C_D = 50. Therefore, applying Equation 4.6.3-8

$$\eta_D = 0.75 \left(\frac{C_D \; N_{Ref}}{2}\right)^{0.4} (N_{Pe})^{-0.6} = 0.75 \left(\frac{0.148x50}{2}\right)^{0.4} (1.7x10 \;)^{-0.6}$$

$$= 9.45x10^{-4}$$

2. Determine the contribution of impaction and interception:

From Equation 4.6.3-3

$$K_I = \frac{d_p}{d_f} = \frac{0.0002 \; cm}{0.0016 \; cm} = 0.125$$

From Equation 4.6.3-1

$$K_P = \frac{d_p{}^2 \; \rho_p \; u_o \; C'}{9 \; \mu_G \; d_f} = \frac{(2x10^{-4} \; cm)^2 \; (1.0 \; \frac{g}{cm^3})(13.9\frac{cm}{sec})(1.07)}{(9) \; (1.8x10^{-4} \; \frac{g}{cm \; sec})(1.6x10^{-3} \; cm)} = 0.23$$

Now applying Equation5.3.4-3

$$\eta_{PI} = 0.0518 \left(\frac{C_D \; N_{Ref}}{2}\right) K_I{}^{3/2} + 0.16 \left[(0.5+0.8 \; K_I)\left(\frac{K_P}{2}\right) -0.1052K_I \left(\frac{K_P}{2}\right)^2\right]$$

$$= (0.0518) \; \frac{50x0.148}{2} \; (0.125)^{3/2} + 0.16 \left[(0.5+0.8x0.125)\right.$$

$$\left.\left(\frac{0.23}{2}\right) - 0.1052 \; (0.125) \; \left(\frac{0.23}{2}\right)^2\right] = 0.0194$$

3. Finally determine the single fiber efficiency. First Equation 5.3.4-7

$$F = 1.0+0.025 \left(\frac{C_D\ N_{Re}}{2}\right)^{0.6} N_{Pe}^{0.6} \left(\frac{Kp}{2}\right)\left[0.5+9.48 \left(\frac{C_D\ N_{Re}}{2}\right)^{0.4} N_{Pe}^{-0.4}\right]$$

$$= 1.0+0.025 \left(\frac{50x0.148}{2}\right)^{0.6} (1.7x10^5)^{0.6} \left(\frac{0.23}{2}\right)\left[0.5+9.48\right.$$

$$\left.\left(\frac{50x0.148}{2}\right)^{-0.4} (1.7x10^5)^{-0.4}\right] = 5.75$$

Now from Figure 5.3 .4-1

$$M = \left(\frac{C_D\ N_{Ref}}{2}\right) K_I^{5/2}\ N_{Pe} = \left(\frac{50x0.148}{2}\right) (0.125)^{5/2} \quad (1.7x10^5) = \underline{3,460}$$

extrapolating Figure 5.3.4-1, $G(M) \cong 1.85$. Finally applying Equation 5.3.4-6

$$\eta_{DIP} = 0.75\ E_{IP} + F\ G(M)\ \eta_D = (0.75)(0.0194) + (5.75)(1.85)$$

$$(9.45x10^{-4}) = 0.0145 + 0.0100 = \underline{0.0245}$$

Alternatively, η_{DIP} could be found on Figure 5.3.4-3 as: $\eta_{DIP} = 0.024$

4. Calculate the solidarity factor, S, using Equation 5.3.4-2:

$$S = \frac{4\ W'}{\pi\ \rho_f\ d_f} = \frac{(4)\left(\frac{4000\ g}{10,000\ cm^2}\right)}{\pi(2.3\ \frac{g}{cm^3})(1.6x10^{-3} cm)} = 138$$

5. Calculate the overall efficiency of the clean bed. First calculate "α", from Equation 5.3.4-2.

$$\alpha = \frac{W'}{\ell\ \rho_f} = \frac{\left(\frac{4000\ g}{10,000\ cm^2}\right)}{(10\ cm)(2.3\ \frac{g}{cm^3})} = \underline{0.0174}$$

Then calculate the effective efficiency of a single fiber via Equation 5.3.4-9

$$\eta_S = \eta_{DIPEG}\ [1+10(N_{Re})^{1/3}\ \alpha] = (0.0245)[1+10(0.148)^{1/3}\ 0.0174] = \underline{0.0268}$$

Note that $\eta_{DIPEG} = \eta_{DIP}$ since the contributions of gravity and electrostatic attraction were assumed negligible. Then calculate the efficiency of the clean fiber bed using Equation 5.3.4-1.

$$E = 1-\exp[-\eta_S\ S] = 1-\exp[-(0.0268)(138)] = \underline{0.974 = 97.4\%}$$

As time passes, the oil droplets caught will coalesce and drip out through the bottom of the bed. The presence of the droplets within the bed will have an influence on the bed efficiency. Equation 5.3.4-10 was developed to show the effect of a constantly increasing number of captured solid particles on the efficiency of a fiber bed. It cannot be used in the present example, as the amount of captured maeterial is not continuously increasing. Rather, the amount of oil within the filter will eventually reach a steady-state when the rate of oil mist capture equals the rate of oil dripping from the bottom of the bed. The bed efficiency at this steady-state cannot be calculated with the equations at hand. If the trend shown by Equation 5.3.4-10 holds the bed's steady-state efficiency should be greater than its initial efficiency.

Next calculate the pressure drop. Use Figure 5.3.4-6, "Pressure Drop Per Unit Thickness for Fiber Filters."

$$\frac{u_o \ \left(\frac{cm}{sec}\right)}{(d_{f_{\mu m}})^2 \ (\mu m^2)} = \frac{13.9}{(16)^2} = 0.0542$$

Remembering that $\alpha = 0.0174$, one finds from the figure that

$$\frac{\Delta P(\text{cm } H_2O)}{\ell \ (\text{cm})} \cong 0.082$$

Since $\ell = 10$ cm, $\underline{\Delta P = 0.82 \text{ cm } H_2O}$

5.3.5 COLLECTION OF PARTICLES BY DEVICES EMPLOYING PREFORMED SPRAYS

5.3.5.1 Introduction

Spray scrubbers in which the liquid is atomized by some means other than energy transferred from the gas being cleaned are classified as "Preformed Sprays". The spray can be formed by a single or two-fluid atomizer. The main two groups in this section are spray chambers and ejector venturis. These may stand by themselves or serve as one part (usually the first stage) of a more complex unit. There are many variations in design of preformed spray devices, especially in the spray chamber group. The gas stream may make a simple direct pass through the chamber, or may follow a path controlled by a series of baffles. In the first case, the gas to be cleaned and the liquid droplets may flow in a cocurrent, countercurrent, or crosscurrent fashion. In the latter case, there is the opportunity for repeated contact of the particulates with the scrubbing liquid. Cyclone spray scrubbers are discussed in Section 5.3.7, although they are also in the category of preformed sprays.

The unit mechanisms which predominate in this type of devices are described in Section 4.6.2 under collection by drops, and the most common one is collection due to inertial impaction. To calculate the overall efficiency of the device, several assumptions are usually made:

1. There is no interaction between the individual drops and the collection efficiency of the device is computed by integrating over all of the individual drops.

2. Drops are spherical. Changes in drop shape and drop oscillation are neglected. This is in line with Goldshmid and Calvert (1963) findings.

3. Changes in drop and particulate properties when flowing through the device, are neglected. When this assumption is not justified, the device should be divided into several sections, each with different particulate and drop properties.

4. Each particle which hits a drop sticks to it. The validity of this assumption depends upon the wettability of the particles by the drop liquid.

To calculate overall efficiency in a spray chamber, a material balance is made over a small section "dZ" which is later integrated over the entire spray chamber. For ejector venturi type devices, an equation resembling the venturi equation is used. See Calvert (1968).

5.3.5.2 Spray Nozzles

Nozzle Types

Spray scrubbers require droplets which are fairly closely sized, in order to avoid entrainment and act most effectively. As the scrubbing liquid is often re-circulated to reduce liquid consumption, the nozzles must be capable of handling liquids with a fairly high solid concentration. Most spray nozzles may be classified under one of the following types:

1. Pressure nozzles
2. Rotating nozzles
3. Gas atomizing nozzles
4. Sonic nozzles

Pressure nozzles

Pressure nozzles as a class are relatively simple, small and inexpensive, and usually consume less power than other types. They may be used with all fluids that have a kinematic viscosity less than about 1 cm/sec, and that do not contain solid particles larger than the passage in that nozzle. The capacity of pressure nozzles is nearly proportional to the square root of the pressure, except at extremely high pressures where friction limits the discharge.

The simplest pressure nozzle is the Hollow-cone nozzle. Here, the fluid is fed into a whirl chamber through tangential passage, or through a fixed spiral so that it acquires a rapid rotation. Hollow cone nozzles are made with orifices from 0.5 to 50 mm in diameter, with corresponding discharge rates of from less than 0.04 ℓ/min to more than 750 ℓ/min. Their spray angle usually varies from 15 to 135 degrees. Operating pressure does not usually exceed 20 atm. For a given design of nozzle, the discharge at constant pressure is approximately proportional to the area of the orifice, although the orifice does not run full.

Another type of the pressure nozzles is the solid cone nozzle which gives a full coverage of the area sprayed. It's spray angle usually varies between 30 and 100 degrees and the discharge rates from 4 to ≈1000 ℓ/min.

The third form of pressure nozzle is the fan nozzle, which sprays the liquid in a flat fan shaped sheet which later breaks into drops. Owing to surface tension, the edges of the sheet are usually bounded by solid streams or "horns", which may comprise from one fourth to one half of the total amount of liquid sprayed. These streams break up into larger drops than the central sheet. The included angle of the fan is from 10 to 130 degrees and capacities range from ≃0.5 to 100 ℓ/min.

The fourth type is the impact nozzle where a solid stream of liquid under pressure is caused to strike a fixed surface or another similar stream. An impact nozzle may yield a hollow cone, fan, or disk shaped fluid sheet. It has been found possible to produce drops of more uniform size with an impact nozzle than with other types of pressure nozzles if laminar flow is maintained.

Rotating Nozzles

In a rotating nozzle, the liquid to be sprayed attains its velocity with little or no pressure increase. The feed is brought at low pressure to the center of the disk, or near it. The atomizer may be a smooth disk, it may have peripheral vanes, or it may be hollow with radial vanes, or channels in its interior. The disk may be from 5 to 75 cm in diameter, it is driven at high speed of several hundred up to 50,000 rpm and the feed rate is controlled independently of the atomizer operating conditions. The spray pattern is complicated by the large number of simultaneous effects and is impossible to calucate. A desired pattern can be achieved through experiments. Marshall (1954) gives the following table which correlates nozzle pressure and disk speed resulting in the same liquid discharge velocity.

TABLE 5.3.5-1

NOZZLE PRESSURES AND DISK SPEEDS RESULTING IN THE SAME LIQUID DISCHARGE VELOCITY

atm	Pressure lb/sq.in)	Speed, r.p.m. of disk of diameter indicated		
		10cm (4 in)	15 cm (6 in)	30 cm (12 in)
0.68	10	1,260	840	420
6.8	100	4,160	2,770	1,385
27	400	9,300	6,200	3,100
68	1,000	13,100	8,750	4,375
340	5,000	29,200	19,580	9,790

Gas Atomizing Nozzles

Gas atomizing nozzles, also called pneumatic nozzles or two fluid atomizers, break up a stream of liquid by contact with a high velocity gas stream, usually air or steam. The contact between the liquid and the gas usually takes place at the point of discharge, but it may take place within or without the chamber. Gas atomizing nozzles are used when very small drops are desired or when a viscous fluid is to be sprayed. They require several-fold the power of a pressure nozzle.

Liquid pressure feed of 3 to 4 atm is the common way of liquid introduction. In most cases the discharge rate is small, less than 1 ℓ/min.

Sonic Spray Nozzles

Sonic spray nozzles produce smaller and more uniform drops. The liquid flows out of an annular chamber through holes under low pressure of less than 1 atm. The liquid filaments are shattered by the sound waves, produced by the impingement of a jet of compressed air or steam of 1 to 4 atm, impinging on a resonator placed centrally between the holes. The liquid throughput of the nozzle is about 3 ℓ/min.

Power Requirements

The power required to pump liquid through a pressure nozzle is calculated from

$$E = 2.3\times10^{-3}\ Q_L \cdot \Delta P \tag{5.3.5-1}$$

where E = power consumed at the nozzle, HP, ΔP = pressure drop across the nozzle in atm, and "Q_L" the volumetric flow rate in ℓ/min. To convert horse power to kilowatts, multiply by 0.745.

The liquid pumping power for a rotating nozzle, can be calculated for its maximum condition (assuming no slip and neglecting interaction between disk and its gaseous environment) from:

$$E = 4.64\times10^{-13}\ Q_L \cdot \rho_L \cdot n^2\left(\frac{d^2 - d_o{}^2}{2}\right) \tag{5.3.5-2}$$

where E = power (KW). Q_L = liquid flow rate (ℓ/min), ρ_L = liquid density (g/cm³), n = rpm, d = disk diameter (cm), d_o = diameter at which feed is applied to disk (cm). Adler and Marshall (1951) found that Equation 5.3.5-2 was ≈6% higher than their experimental data for a vaned disk atomizer.

For pneumatic atomizers, the power can be calculated from the gas isothermal expansion:

$$E = n\ R_g\ T\ \ln\left(\frac{P_1}{P_2}\right) \tag{5.3.5-3}$$

where "n" is the number of moles of air used to atomize 1 liter of liquid, the air expands from pressure "P_1" to "P_2" and "T" is the absolute temperature of the expansion.

Drop Size

Pressure Nozzles

Pressure nozzles of like capacity give a similar distribution of drop sizes when operated at a given pressure. The hollow cone nozzles usually yield a somewhat smaller range of drop sizes than the solid cone nozzles. The central sheet of small fan nozzles is also good, but the "horns" at the edges break up into much larger drops. The smallest range of drop size at a given pressure and capacity will be formed by an impact nozzle producing a laminar fluid sheet. For applications which require the smallest possible range of drop size, a large number of small nozzles should be used. If a maximum number of small drops is required nozzles of the smallest size practicable should be used at the highest possible pressure.

Most pressure nozzles give drop size distribution which follow the Rosin-Rammler (1933) distribution.

$$\phi_d = e^{-bd^a} \qquad (5.3.5\text{-}4)$$

where "ϕd" is the fraction of the mass of the sample contained in drops of diameter greater than "d" and "a" and "b" are constants. This distribution yields a straight line when log log ($1/\phi d$) is plotted against log (d). The slope of the line is a measure of the breadth of the distribution.

For a hollow cone nozzle spraying water Orr (1966) suggests that

$$\log \left(\frac{d_v}{d_o}\right) = 0.144\ Z^2 + 0.702\ Z + 1.26 \qquad (5.3.5\text{-}5)$$

where

$$Z = \log \left\{ N_{Re} \left(\frac{N_{We}}{N_{Re}}\right)^{0.2} \left(\frac{u_t}{u_a}\right)^{1.2} \right\} \qquad (5.3.5\text{-}6)$$

$$N_{Re} = \left(\frac{d_o\ u_a\ \rho_L}{\mu_L}\right) \quad \text{and} \quad N_{We} = \left(\frac{u_a^2\ d_o\ \rho_G}{\sigma}\right).$$

$u_t = u_a \tan(\Theta/2)$ is the mass average tangential velocity through the orifice, $u_a = Q_L/A$ is the mass average axial velocity through the nozzle, "d_v" is the volume mean drop diameter, "d_o" is the orifice diameter, "A" is the area of flow and "Θ" is the maximum cone angle.

Quite often hollow cone nozzles give straight line on a probability grid when the square root of droplet diameter is plotted against cumulative percent less than that diameter. For a full cone nozzle injecting into a fast moving gas stream, Orr (1966) recommends:

$$\frac{d_{mm}\ \rho_G\ u_r^2}{\sigma} = 0.61 \left(\frac{u_r\ \mu_L}{\sigma}\right)^{2/3} \left(1 + \frac{10^3\ \rho_G}{\rho_L}\right)\left(\frac{d_o\ \rho_L \sqrt{u_L}\ \mu_G}{\mu_L^2}\right) \qquad (5.3.5\text{-}7)$$

where "d_{mm}" is the mass median droplet diameter in microns, "u_r" is the relative velocity between gas and liquid streams and "u_L" is the liquid injection velocity, and "σ" is liquid surface tension. The approximate ranges of the variables covered by correlation is

$60\ \text{m/sec} < u_r < 300\ \text{m/sec};$
$0.74\text{x}10^{-3}\text{g/cm}^3 < \rho_G < 4.2\text{x}10^{-3}\ \text{g/cm}^3;$
$1.2\ \text{m/sec} < u_L < 30\ \text{m/sec}$
$3.3\ \text{c.p.} < \mu_L < 11.3\ \text{c.p.}$
$19\ \mu\text{m} < d_{mm} < 118\ \mu\text{m} =$
$0.12 < d_o < 0.5\ \text{cm}$

For fan nozzles spraying water, Fraser et al. (1959) found for the surface mean droplet diameter:

$$\ln \bar{d}_s = 1.823 + \frac{0.3}{\Delta P} + 0.695 \frac{Q_L}{\sqrt{\Delta P}} \qquad (5.3.5\text{-}8)$$

where "ΔP" is the pressure drop through the nozzle (atm), and "Q_L" is the liquid flow rate (ℓ/min), and $\bar{d}_s$ is in microns. Fan nozzle droplet size often follows the log-normal distribution as was shown by Dorman (1952).

Fraser et al. (1957) reported that for an impact nozzle with water striking a flat plate tilted 30° to the nozzle axis, the mass median drop diameter measured in microns is:

$$d_{mm} = 13,400\ Q_L^{1/3}\ \Delta P^{1/2} \qquad (5.3.5\text{-}9)$$

where "Q_L" is measured in (ℓ/min) and "ΔP" in (atm).

Rotating Nozzles

From the standpoint of drop size, the only difference between a rotating nozzle and a pressure nozzle is that in the former the liquid is formed into a thin sheet by centrifugal force instead of by direct fluid pressure. As a result, the drop size distribution of a rotating nozzle is quite similar to that of a pressure nozzle. Based on studies of a variety of vaned, cupped and shrouded disks, Friedman et al. (1952) found the following correlation for the Sauter mean drop diameter:

$$\frac{\bar{d}_d}{r_o} = 0.4 \left(\frac{M_L}{\rho_L\ \ell \cdot n \cdot r_o}\right)^{0.6} \left(\frac{\mu_L}{M_L}\right)^{0.2} \left(\frac{\sigma\ \rho_L\ \ell}{M_L^2}\right)^{0.1} \qquad (5.3.5\text{-}10)$$

where "r_o" is the disk radius, "M_L" is the liquid feed rate based on wetted perimeter (g/cm sec), "ℓ" is the wetted perimeter of the disk and "n" is the number of revolutions per second. The correlation covers the following range of parameters: $60 < n < 220$,
$1\ \text{c.p.} < \mu_L\ 90\ \text{poise}\ 1 < \rho_L < 1.4\ \text{gm/cm}^3$,
$73 < \sigma < 99$ dyne/cm

The distribution of the diameters follows the log normal distribution with the log-standard geometric deviation $\sigma_g \simeq 3.3(\bar{d}_d)^{0.1}$ where $\bar{d}_d$ is in microns.

Gas Atomizing Nozzles

As ordinarily operated, the gas atomizing nozzles produce much smaller drops than pressure or rotating nozzles. Although the smaller atomizing nozzles tend to give a somewhat narrower range of drop sizes than the larger nozzles, the size factor is not important as in the case of the pressure nozzles. The determining factor is the relation between the quantities of gas and liquid. When insufficient gas is used, large drops are formed. When proper operation is maintained, the drop size can be controlled by varying the gas pressure, higher pressures yielding smaller drops.

The liquid pressure has little effect on drop size and for the most part only determines the quantity of liquid delivered, which is also a function of the gas pressure. As mentioned in Section 4.4.2.1, the Nukiyama and Tanasawa (1938) empirical correlation, given as

Equation 4.4-10 in this text, describes the Sauter mean diameter of gas atomized sprays. The distribution of droplet sizes within the gas atomized sprays was shown by Nukiyama and Tanasawa (1939) to follow an expression of the same form as the Maxwell equation for the distribution of molecular velocities in a perfect gas

$$\log\left(\frac{1}{d_d^2}\,\frac{N}{\Delta d_d}\right) = \log a - \frac{(bd_d)^{\alpha}}{2.303} \qquad (5.3.5\text{-}11)$$

where "d_d" is the droplet diameter in microns, "N" is the number of droplets in the diameter range "Δd_d", and "a", "b", and "α" are constants. A plot of the data with $\log[(1/d_d^2)(N/\Delta d_a)]$ vs. "$d_d\alpha$" should yield a straight line upon selection of the proper value for "α". "b" can then be found from the slope of the line and "a" from the equation. The constant "α" is truly a constant for a given nozzle over a wide range of operating conditions. Its value is very sensitive to nozzle size and nozzle type, and must be determined experimentally for each nozzle type.

5.3.5.3 Spray Chambers

A spray chamber consists essentially of a chamber into which water is introduced through one or more sprays. Drop size depends upon liquid pressure drop and the type of nozzle used. Water pressure drop varies from 1.4 to 7.3 atm (20 to 100 psi) and water consumption is usually in the range of 0.066 to 0.266 (ℓ water/m^3 gas) = (0.5 - 2 gal/MCF). When the spray cools and humidifies the gas, water consumption is higher. In order not to be entrained by the gas stream in countercurrent and crosscurrent flows, the droplets must be sufficiently large to have a settling velocity greater than the gas velocity, or have large enough initial velocity to prevent them from being carried away. In practice, a gas velocity of 61 to 122 (cm/sec) (2 to 4 ft/sec) is used and the gas pressure drop is about 2 cm of water.

The spray chamber is a low pressure drop device performing at acceptable efficiencies for large particulate material, 5 micron or larger. Water sprays at 24 to 30 atm produce fine liquid droplets and have high collection efficiencies for particles in the 1 to 2 micron size range. However, one should always remember that the lifetime of small drops is short due to evaporation. For instance, a 10μ drop has a lifetime of about 1 sec in a 90% relative humidity atmosphere. Optimum drop size for the collection of various sized particles is given in Figure 4.6.2-6. It should be noted, however, that the effects of spray agglomeration and impingement on the chamber walls make it very difficult to predict the size and quantity of spray which contacts the gas.

Equipment Design

Spray chambers are operated in three different manners: countercurrent, cocurrent, and crosscurrent flows. Each has its advantages.

High relative velocity between drops and particles can be realized only in a cocurrent device which resembles a venturi type device.

Vertical Countercurrent Flow - Inertial Impaction

A material balance over a short segment of the spray chamber yields:

$$-Q_G \, dc = \frac{3 \, Q_L \, (u_G + u_d) \, \eta_p \, c}{4 \, u_d \, r_d} \, dZ \qquad (5.3.5\text{-}12)$$

In most cases, the drops reach terminal velocity in a short distance and $(u_C + u_d) \approx u_t$. Integrate this equation assuming a constant drop velocity and a constant target efficiency throughout the column, and only one drop size:

$$Pt = \exp\left[-\frac{3 \, Q_L \, u_t \, \eta_p \, Z}{4 \, Q_G \, r_d \, (u_t - u_G)}\right] = \exp\left[-0.25 \left(\frac{A_d \, u_t \, \eta_p}{Q_G}\right)\right] \qquad (5.3.5\text{-}13)$$

where "A_d" is total drop surface area in the scrubber given by:

$$A_d = \frac{3 \, Q_L \, Z}{r_d \, (u_t - u_G)} \qquad (5.3.5\text{-}14)$$

Target efficiency is greatly influenced by the drop "N_{Re}" and is calculated from Equation 4.6.2-12. "η_{vis}" and "η_{pot}" are most conveniently found from Figure 4.6.2-2. The potential flow solution gives $\eta_{pot}=0$ for $K_p \leq 0.0835$ leading to zero collection efficiency in the tower. When operating at these low "K_p" values, interception may become important and one should correct for interception. Figure 5.3.5-1 presents four plots of performance cut diameter as a function of spray drop size, air velocity, water/air ratio, and height, as predicted by Equation 5.3.5-13.

Use of the Langmuir interpolation formula (Equation 4.6.2-12) will lead to a shift in the collection efficiency at $K_p > 1.245$ when $\eta_{vis} > 0$. It is recommended that the curve of collection efficiency vs. "K_p" be smoothed in this region.

Equation 5.3.5-13 gives a steep curve for "E" vs. "K_p" reaching 100% for $d_{pa} \approx 8 \mu m \, (g/cm^3)^{0.5}$ when $Q_L/Q_G \gtrsim 1 \, \ell/m^3$ (8 gal/MCF), which differ from experimental results. Thus the equation should be used with caution for efficiencies higher than ≈95%. The use of drop area in the scrubber, A_d, reveals a pattern of similarity among the several equations for scrubber performance.

Diffusion

For particles smaller than ≈0.1 μm in diameter, collection by diffusion predominates. The number of particles collected by one drop in a unit time depends upon the flow conditions and the relative thickness of the diffusion layer to the hydrodynamic boundary layer, which are described by "N_{Re}" and "N_{Sc}". For various conditions, different expressions for "ϕ", as given in Section 4.6.2-4, are integrated over the whole chamber assuming as before that relative velocity between drops and gas is the drop terminal settling velocity.

For $N_{Sc} \approx 10^6$ and $N_{Red} < 3$ ($d_d < 0.016$ cm) the weight of aerosol collected by one drop per second is given by Equation 4.6.2-18. A material balance over a height "dZ" of the chamber gives:

$$-Q_G \, dc = \frac{3 \, Q_L \, \phi \, c}{4 \, u_d \, \pi \, r_d^3} \, dZ \qquad (5.3.5\text{-}15)$$

Substituting Equation 4.6.2-18 for "ϕ" and integrating yields for the overall penetration

$$Pt = \exp\left[- \frac{3 \, Q_L \, D_p \, Z}{2 \, Q_G \, (u_t - u_G) \, r_d^2} \, N_{Pe}^{1/3}\right] = \exp\left[- \, 0.5 \left(\frac{A_d \, D_p}{Q_G \, r_d}\right) N_{Pe}^{1/3}\right]$$

or,

$$\ln Pt = - \left[0.5 \left(\frac{A_d \, D_p}{Q_G \, r_d}\right) N_{Red}^{1/3} \, N_{Sc}^{1/3}\right] \qquad (5.3.5\text{-}16)$$

For large N_{Red} (600-2,600 and $0.16 < d_p \leq 0.32$ cm) and the same values for N_{Sc}, substituting Equation 4.6.2-19 for "ϕ" in Equation 5.3.5-15 and integrating yields for the penetration:

$$\ln Pt = - \left[0.4 \left(\frac{A_d \, D_p}{Q_G \, r_d}\right) N_{Re}^{1/2} \, N_{Sc}^{1/3}\right] \qquad (5.3.5\text{-}17)$$

For N_{Red} = 100-700 ($.06 < dp < 0.18$ cm) and $N_{Sc} \approx 10^3$ substitution of Equation 4.6.2-20 for "ϕ " and integration yields:

$$\ln Pt = - \left[0.473 \left(\frac{A_d \, D_p}{Q_G \, r_d}\right) N_{Red}^{1/2} \, N_{Sc}^{1/3}\right] \qquad (5.3.5\text{-}18)$$

To calculate collection efficiency from these equations particle diffusivity is calculated from Equation 4.3.3-13 or from Figure4.3.3-3. Drop diameter, or drop size distribution is obtained from the spray nozzle characteristics and drop settling velocity and "N_{Re}" are found in Figure4.6.2-1. When evaluating the collection by drops of various sizes, the contribution of each size group is calculated, and the collection of all the groups when added gives the overall collection efficiency. Once "Z", the chamber height is assumed,penetration as a function of (Q_L/Q_G) can be calculated. It can be seen that the differences between the three equations for different "N_{Red}" and "N_{Sc}" are not great; depending on $(N_{Red})^{1/6}$.

Thermophoresis, Diffusiophoresis and Electrostatic Attraction

When each of these forces by itself contributes to particle collection, the overall efficiency can be calculated from a material balance over a chamber segment "dZ" in a unit time. The differential equation is:

$$-Q_G \, dc = \frac{Q_L}{r_d^3} \left[(r_d + \frac{u_p}{u_d} \, dZ)^3 - r_d^3\right] C \qquad (5.3.5\text{-}19)$$

where "u_p"is the velocity due to the particular force encountered, and is given in 4.3.3-5.

When more than one force acts on the particles, the sum of the velocities is used to calculate "u_p". Integration of Equation 5.3.9-19 gives for the overall penetration, neglecting the terms with "dZ" squared and "dZ" cubed:

$$Pt = \exp\left[\frac{-3\ Q_L\ u_p\ Z}{Q_G\ u_d\ r_d}\right] \qquad (5.3.5\text{-}20)$$

The total drop surface area in the chamber, which is the total collecting area

$$A_d = \frac{3\ Q_L\ Z}{u_d\ r_d} \qquad (5.3.5\text{-}21)$$

Substituting into Equation 5.3.5-20

$$Pt = \exp\left(-\frac{A_d\ u_p}{Q_G}\right) \qquad (5.3.5\text{-}22)$$

The assumption was made throughout the derivation that the velocity due to the external force "u_p", is a constant. This assumption will yield optimistic values for the collection efficiency, because of the change in driving force with time as the drop passes through the chamber. To get an accurate solution, the rate of change of the driving force with chamber height should be known and the equation integrated accordingly. When the driving force is known only at the two ends of the chamber, an average value could be used in calculating "u_p".

The equations for collection by impaction and diffusion can also be put in terms of a collector surface area, A_d, and a deposition velocity, "u_p". As discussed in Chapter 4, this provides a means for adding the contributions of various deposition mechanisms, by adding their velocities. Where the deposition velocities do not vary with distance of gas travel through the scrubber, the velocities may simply be added and the total used in the integrated equation for collection efficiency. It is also helpful in understanding the influence of various mechanisms to compare the deposition velocities due to each.

Cross Flow - Inertial Impaction

In the cross-flow case, the water is sprayed at the top of the spray chamber, while the gas flows horizontally. For collection by inertial impaction in a spray chamber Calvert (1968) after making the following assumptions, derived an equation predicting the collection efficiency.

1. Droplets attain terminal velocity instantaneously and are evenly distributed over the entire chamber volume.

2. All the water sprayed into the chamber maintains its uniform drop shape and size throughout the chamber.

3. The drops attain the gas velocity in the horizontal direction instantaneously. Thus, collection takes place only due to the drops relative vertical velocity.

4. The spray is slanted at the same angle at both ends of the chamber, where the gas enters and leaves.

5. The dust concentration is uniform across any plane perpendicular to the gas flow.

After making these assumptions, Calvert (1968) gets:

$$E = 1 - \exp\left(\frac{3\ Q_L\ h\ \eta_p}{4\ Q_G\ r_d}\right) = 1 - \exp\left\{-\ 0.25\left(\frac{A_d\ u_t\ \eta_p}{Q_G}\right)\right\} \quad (5.3.5\text{-}23)$$

where "h" is the height of drop fall.

Efficiency increases with the height of drop fall while the length of the gas flow path does not enter into Equation 5.3.5-23.

In several cases an empirical correlation factor should be introduced into the last equation to account for divergence from the assumptions made. For drops larger than ≈300 μm in diameter, assumptions 1 and 3 are not exactly correct. However, decreased collection due to lower vertical velocity in the first part of the drop trajectory, is somewhat compensated for by increased collection in the horizontal direction due to relative velocity between the gas and the drop. The size of the correction factor should be determined from experimental data. Such data is not available at present.

Assumption 2, namely the uniformity of drop distribution, may vary from one spray chamber to another, and will introduce an empirical correction factor into the equation. Figure 5.3.5-2 presents two plots of performance cut diameter for air and water, using Equation 5.3.5-23 for several sets of parameters.

Diffusion

Making the same assumptions that Calvert made for collection by inertial impaction in a cross flow spray chamber and describing collection by a single drop due to diffusion by Equation 4.6.2-18 gives for the penetration, when "N_{Red}" is small (<3) and "N_{Sc}" is large (≈106);

$$Pt = \exp\left[-\left(\frac{3\ Q_L\ h}{Q_G\ r_d}\right)(N_{Pe})^{-2/3}\right] = \exp\left[-\left(\frac{A_d\ u_d}{Q_G}\right)(N_{Pe})^{-2/3}\right] \quad (5.3.5\text{-}24)$$

Comparing this equation with the comparable one for collection by inertial impaction 5.3.5-23, one sees that it is the same equation with $(N_{Pe})^{-2/3}$ replacing $\eta_p/4$.

For large N_{Red} (600-2,600) and the same values of N_{Sc}, one gets for the penetration after substituting Equation 4.6.2-19 into the material balance equation and integrating:

$$Pt = \exp\left[-\left(\frac{2.4\ Q_L\ h}{Q_G\ r_d}\right)(N_{Red})^{-1/2}\ (N_{Sc})^{-2/3}\right] =$$

$$= \exp\left[-0.8\left(\frac{A_d\ u_d}{Q_G}\right)(N_{Re})^{-1/2}\ (N_{Sc})^{-2/3}\right] \quad (5.3.5\text{-}25)$$

For N_{Red} = 100-700 and $N_{Sc} \approx 10^3$ substituting Equation 4.6.2-20 and ingrating leads to

$$Pt = \exp\left[-\left(\frac{2.92\ Q_L\ h}{Q_G\ r_d}\right) (N_{Red})^{-1/2} (N_{Sc})^{-2/3}\right] \simeq \exp\left[-\left(\frac{A_d\ u_d}{Q_G}\right) (N_{Red})^{-1/2} (N_{Sc})^{-2/3}\right] \qquad (5.3.5\text{-}26)$$

Thermophoresis, Diffusiophoresis and Electrostatic Attraction

Following the procedure used for counter-current spray one gets the same equation for cross-current spray chambers, namely:

$$Pt = \exp\left\{-\left(\frac{Q_L\ h}{Q_G\ v_t\ r_d^3}\right)\left[\left(r_d + \frac{u_p}{u_d}\, dZ\right)^3 - r_d^3\right]\right\} \qquad (5.3.5\text{-}27)$$

Neglecting terms with second and third powers of "dZ" yields:

$$Pt = \exp\ - \frac{A_d\ u_p}{Q_G} \qquad (5.3.5\text{-}28)$$

where "A_d" is drop area as defined in Equation 5.3.5-21.

Co-Current Spray Chamber - Inertial Impaction

Cocurrent flow occurs in high velocity scrubbers such as venturi, flooded disc, orifice and other variations. Due to the high velocities involved, the dominant collection mechanism is inertial impaction. This case is discussed in detail in the next Section 5.3.6.

Diffusion

With particles smaller than about 0.1 μm in diameter and at relatively low velocities a cocurrent spray chamber will collect particles by diffusion. However, one expects that, as with other devices, collection by diffusion will depend strongly upon the contact time allowed. Or in other words, collection will be inversely proportional to the gas velocity.

Collection efficiency in a cocurrent type device can be calculated from a material balance over a small section followed by integration.

$$-Q_G\ dc = \frac{Q_L\ dx\ \phi\ c}{u_d\ \frac{4}{3}\ \pi r_d^3} \qquad (5.3.5\text{-}29)$$

Substituting "ϕ" from Equation 4.6.2-19 for low "N_{Red}" and high "N_{Sc}" and defining

$$u_r = f\ u_G \qquad (5.3.5\text{-}30)$$

one gets after rearranging:

$$\frac{-dc}{c} = \frac{1.2(2)^{1/3}\ Q_L (D_p)^{2/3}}{Q_G (u_G)^{2/3}\ (r_d)^{5/3}} \left(\frac{f}{1-f}\right)^{1/3} dx \qquad (5.3.5\text{-}31)$$

Using Calvert's (1968) approximation to Ingebo (1956) data one gets for accelerating drops

$$- dx = \frac{2(r_d)^2 \; 8 \; \rho_d \; u_G}{3(55) \; \mu_G} \left(\frac{1 - f}{f}\right) df \qquad (5.3.5\text{-}32)$$

Substituting and integrating from $c = c_i$ and $f = f$ to $c = c_e$ and $f = 0$, one gets the equation for collection efficiency by diffusion in a co-current spray chamber:

$$E = 1 - \exp - \left[\frac{0.35 \; Q_L \; \rho_d}{Q_G \; \rho_G} \; \frac{(N_{Red})^{1/3}}{(N_{Sc})^{2/3}} \; (f^{1/3})\right] \qquad (5.3.5\text{-}33)$$

The value of "f" in Equation 5.3.5-33 is unknown, and must be evaluated from experimental data. For collection by impaction, "f" has been evaluated as about 0.25, as discussed in Section 5.3.6.

Thermophoresis, Diffusiophoresis and Electrostatic Attraction

Here again collection efficiency will depend upon contact time and the magnitude of the gradient responsible for the particle collection. Collection efficiency can be calculated as before, assuming a constant gradient throughout. When this is not the case, an average gradient will approximate the collection efficiency. If the change in gradient with "x" is known, an integration can be attempted.

Material balance leads to:

$$-Q_G \; dc = \frac{Q_L}{r_d{}^3} \; [(r_d + \frac{u_p}{u_d} dx)^3 - r_d{}^3]c \qquad (5.3.5\text{-}34)$$

Assuming "u_p" is independent of "x", and using Calvert's approximation to Ingebo's data, one gets an expression similar to 5.3.5-32 for "u_d" as a function of "dx". Due to our assumption of a constant "u_G" we could not integrate the equation to $u_d = u_G$, since this will happen at $t = \infty$. So let us assume $u_{d_2} = 0.99 \; u_G$. This assumption will be a function of venturi operating parameters and geometry, and is expected to vary from one device to the other. Substituting for "dx" and integrating gives:

$$Pt = \exp \left[\frac{-16 \; Q_L \; \rho_d}{55 \; Q_G \; \mu_G} \; u_p \; r_d \; \ln\left(\frac{f}{0.01}\right)\right] \qquad (5.3.5\text{-}35)$$

Substituting f = 0.25

$$Pt \simeq \exp \left[\frac{-16}{55} \frac{Q_L}{Q_G} \frac{\rho_d \; u_p \; r_d}{\mu_G} \; \ln \left(\frac{0.25}{0.01}\right)\right] \qquad (5.3.5\text{-}36)$$

and therefore:

$$Pt \simeq \exp - \left[\frac{0.935 \; Q_L \; \rho_d \; u_p \; r_d}{Q_G \; \mu_G}\right] \qquad (5.3.5\text{-}37)$$

5.3.5.4 Ejector Venturi

The ejector venturi scrubber is a gas-liquid contactor which utilizes the velocity of the contacting liquid to both pump and scrub the entrained gas. The unit is basically comprised of a 90° angle inlet and turn section, a spiral type spray nozzle, and a conventional venturi section. The spiral spray nozzle imparts a combination of axial and tangential velocities to the liquid jet stream. The contacting liquid, after leaving the scrubber, is removed from the air or gas streams by gravity or centrifugal force.

The ejector venturi finds use when the gas to be cleaned is corrosive or erosive. It combines the functions of primary gas mover, steam and vapor condenser and gas cleaner. The ejector has no moving mechanical parts in contact with the gas stream and it eliminates the need for a corrosion or erosion resistant blower. When compared to a venturi scrubber it usually requires more liquid and more power to accomplish the same degree of particle collection.

Drop size distribution in the ejector venturi depends upon two parameters, the nozzle proportions and the motive pressure. Figures 5.3.5-3 and 5.3.5-4, from Harris (1963) are experimental determinations of drop size distribution in a 10 cm (4 inch) and 30 cm (12 inch) throat diameter ejector, each under two motive pressures. It is evident from these figures that the number mean drop size decreases with increases in motive pressure and that larger nozzles produced smaller drops. The number mean drop size for all of the nozzles tested in the 7.6 cm (3 inch) to 117 cm (42 inch) scrubber diameter range were found by Harris (1963) to be from 1,000 μm for the smaller nozzles at low pressure to 400 μm for the very large nozzles at higher pressures.

The literature contains only a few experimental data describing collection efficiency of ejector venturis, including that of Takashima et al. (1961) and of Harris (1963). Assuming collection to be due to inertial impaction only, a constant relative velocity "u_r" between drops and particles, one drop size "r_d" and one particle size "r_p", then a material balance leads to the following equation for the collection efficiency:

$$E = 1 - \exp\left(-\frac{3}{2}\,\frac{Q_L\, u_r\, t\, \eta_p}{Q_G\, d_d}\right) \qquad (5.3.5\text{-}38)$$

where "t" is the retention time of the gas in the spray zone, "Q_L" and "Q_G" are the volumetric flow rates of water and gas introduced, and "η_p" is the droplet target efficiency due to impaction, given by Equation 4.6.2-10.

K_p is the inertia parameter given by:

$$K_p = \frac{2\,\rho_p\, r_p^{\,2}\, u_r\, C'}{9\,\mu_G\, r_d} \qquad (5.3.5\text{-}39)$$

It has been suggested by Harris (1963) that in Equation 5.3.5-38, "u_r t" can be approximated by the effective length of the contact section in the scrubber, "Z". Analysis of test results in terms of expected performance showed only qualitative agreement with theory. Perhaps a more adequate equation could be derived by using the same approach used in deriving the venturi equation with a different equation for predicting drop size than the Nukiyama Tanasawa equation.

Analysis of Equation 5.3.5-38 yields some interesting trends. It has been found experimentally that when $\eta_p < 0.30$ (30%) it is very probable that the collection efficiency of the ejector venturi will be unsatisfactory. Thus for the collection of submicron particles a special ejector is used in which a secondary stream of high pressure air or steam is added to get smaller drops, followed by a second regular ejector venturi. However, experimental collection efficiencies for this system are available only for ammonium chloride particles $0.01 < d_p < 1$ μm which are hygroscopic and will grow in size and change properties when passing through the first ejector. From the available data it is difficult to predict what the collection efficiency will be for submicron hydrophobic particles.

Equation 5.3.5-38 also says that collection efficiency increases with the increase of the liquid to gas ratio, Q_L/Q_G, and with a decrease in drop size, d_d. As already seen, average drop size decreases with increase in motive pressure.

As noted above, Equation 5.3.5-38 assumes a constant relative velocity between drops and particles (gas). Actually, the relative velocity between a particular drop and the gas through which it passes will decrease with time from an initial value when the drop is formed to zero when the drop and gas are travelling at the same speed. The relationship between "u_r" and "t" depends upon the properties of the gas and drop, and not upon the length of the diffuser cone, Z. Therefore, altering the length of the cone will have little effect on efficiency.

It was found experimentally by Harris (1964) that a decrease in dust loading increases collection efficiency as is shown in Figure 5.3.5-5.

Figure 5.3.5-6 describes weight collection efficiency as a function of observed energy for ejector venturi scrubber using iron oxide and fly ash dusts. The iron oxide had a mass mean particle diameter of 17 μm and was collected with a 12" ejector. The fly ash had a mass mean diameter of 5.5 μm, a density of 2 g/cm³, and was collected by a 3" ejector. The liquid to gas ratio in the iron oxide case was approximately 5 ℓ/m³ and particle density was 5.2 g/cm³. The variation in performance was obtained with approximately constant liquid to gas ratio by varying both nozzle size and nozzle pressure from 1.36 to 6.8 atm, (20-100 psig). The fly ash nozzle was operating with 3.4 atm (50 psig) nozzle pressure and the variation in performance was obtained by varying the liquid to gas ratio from 9.3 to 19.3 ℓ/m³ (70-145 GPM/1000 CFM).

Figures 5.3.5-7 and 5.3.5-8 are comparisons between experimental and theoretical efficiency curves for the same iron oxide and fly ash particles. Figure 5.3.5-9 compares the theoretical energy requirements for the same fly ash and 0.01 μm to 1 μm ammonium chloride aerosol using the two stage submicron ejector depicted in Figure 5.3.5-10. Figure 5.3.5-11 shows the theoretical collection efficiency curves for a constant liquid to gas ratio of 5.3 ℓ/m³ (40 GPM/1000 CFM) varying the motive pressure. While in Figure 5.3.5-12, the motive pressure was kept constant at 8.16 atm (120 psig) and the collection efficiency is given with Q_L/Q_G as a parameter.

As mentioned already, the liquid drops leaving the ejector are separated from the gas stream by either a gravity separator or an impaction separator. Figure 5.3.5-13 compiled by Harris and Hartenbaum (1961) shows the amount of liquid carryover for two such separators.

5.3.6 PARTICLE COLLECTION IN GAS ATOMIZED SPRAY SCRUBBERS

The growing importance of venturi, and other gas atomized spray scrubbers, hinges on their flexibility and simplicity. Collection efficiency is variable, and can be increased by increasing pressure drop in the scrubber. Simplicity of design makes these devices relatively inexpensive to build or buy.

Venturi scrubbers employ gradually converging, then diverging sections, such as is shown in Figure 5.3.6-1. The venturi throat is the section between the converging and diverging sections. Usually liquid enters the venturi upstream of the throat through nozzles. Alternately, the liquid may flow along the converging section walls until reaching the throat. At the throat, the liquid is shattered into droplets by the high velocity gas. Sometimes the liquid is introduced as preatomized drops at or before the throat through a pressure nozzle. The venturi may have a round, square or rectangular cross section.

5.3.6.1 Principle of Operation

In a venturi scrubber, small, polluting particles are collected on larger liquid drops, then the drops are separated from the gas in an entrainment separator. As the entrainment separator can capture the larger droplets with virtually 100 per cent efficiency, the efficiency of the venturi depends upon what fraction of the particles are collected on the drops. The most important mechanism by which droplets collect particles in a venturi is impaction.

Gas moves rapidly past the liquid droplets which have just been introduced or atomized at the venturi throat. The high relative velocity between gas and droplets leads to a drag force on the droplets, which accelerates them to the gas velocity. While accelerating the droplets, the particle laden gas sweeps past the drops. Some of the particles in the gas impact upon the droplets and are collected.

5.3.6.2 Particle Collection Efficiency

Venturi scrubbers have been used in a variety of applications for a long time. Experience has been vast, and yet a condensation of this experience in terms of a reliable design equation has been lacking. Calvert (1970) and Calvert et al. (1970) have developed an equation for predicting particle penetration based upon an analysis of particle and droplet motion in a venturi throat. Their approach appears to be the best available for the rational explanation of various factors influencing performance, and for the correlation of available data. The following assumptions were made:

1. Particles move with the gas stream at all times (no slip) and are collected only by liquid drops.

2. Average liquid drop diameter is as given by the empirical correlation of Nukiyama and Tanasawa (1938):

$$d_d(\text{cm}) = \frac{50}{u_G \frac{\text{cm}}{\text{sec}}} + 91.8 \left(\frac{Q_L}{Q_G}\right)^{1.5} \qquad (5.3.6\text{-}1)$$

This equation, for air and water at standard conditions, gives drop diameter in centimeters, where gas velocity, u_G, is in cm/sec, and Q_L/Q_G is the volumetric ratio of liquid to gas throughout (units cancel). Figure 5.3.6-2 contains a plot of atomized drop diameter against gas velocity with liquid to gas ratio as parameter.

There was some concern expressed by (Calvert, 1970) about using this equation for gas velocities below 7,500 cm/sec, the lower limit of the experimental range upon which the correlation is based.

3. The acceleration of liquid drops may be calculated using an approximation of Ingebo's (1956) data on drag coefficient, C_D, for accelerating atomized drops, whose Reynolds numbers are between 6 and 400. The approximation is:

$$C_D \approx \frac{55}{N_{Red}} \qquad (5.3.6\text{-}2)$$

4. The collection of particles by single drops is due to inertial impaction only, and is therefore based on Equation 4.6.2-10 for particle collection by drops due to inertia.

Therefore collection is a function of the inertial parameter, K_p,

$$K_p = \frac{u_r \rho_p C' d_p^2}{9 \mu_G d_d} = \frac{u_r d_{pa}^2}{9 \mu_G d_d} \qquad (5.3.6\text{-}3)$$

where "d_{pa}" is the aerodynamic particle diameter defined in Equation 4.6.7-16, and "u_r" is the relative velocity between the particle (traveling at the gas velocity) and the droplet.

5. There is a uniform concentration of particles in any plane perpendicular to the direction of gas flow.

6. Liquid is not atomized and distributed over the cross-section until the relative velocity between the liquid and gas is:

$$u_r|_{\text{atomization}} = f\, u_G \qquad (5.3.6\text{-}4)$$

In the practical utilization of the resulting equations, non uniformity with the above assumptions is taken up in the evaluation of the unknown factor, f.

Taking into account the continuous change in relative velocity, u_r, as the droplets accelerate from the point of their atomization to the gas velocity yielded the following equation:

$$Pt = \exp\left[\frac{2\, Q_L\, u_G\, \rho_L\, d_d}{55\, Q_G\, \mu_G} F\,(K_{pt}, f)\right] \qquad (5.3.6\text{-}5)$$

where "K_{pt}" is the inertial parameter evaluated at the velocity of the gas in the throat, u_G, and:

$$F(K_{Pt},f) = \left[-0.7 - K_{Pt}f + 1.4 \ln \left(\frac{K_{Pt}\, f + 0.7}{0.7} \right) + \frac{0.49}{0.7 + K_{Pt}\, f} \right] \frac{1}{K_{Pt}} \qquad (5.3.6\text{-}6)$$

$F(K_{Pt},f)$ is plotted on Figure 5.3.6-3 against "K_{Pt}" with "f" as parameter.

To use Equation 5.3.6-5 to predict the efficiency of a venturi, it is necessary to have a value for the coefficient "f". Therefore "f", defined in terms of theory in Equation 5.3.6-4, becomes in fact a constant which must be determined from experiments. To evaluate this constant, experimental data have been analysed.

Ekman and Johnstone (1951) present data for the collection of 0.8, 1-0 and 5.5 micron diameter particles in a venturi. With all quantities in Equation 5.3.6-5 known, except "f", values of "f" were calculated and plotted in Figure 5.3.6-4 against the ratio of liquid to gas throughput. Dioctyl phthalate particles were used. A similar analysis was made for the data of Calvert et al. (1970), who used methylene blue particles. Their results are shown in Figure 5.3.6-5, again a plot of "f" versus liquid to gas ratio. NAPCA (1970) has carried out an experimental investigation of fly ash collection in a venturi. They varied throat diameter from 7.5 cm (3 inches) to 13 cm (5 inches) and gas temperature from 68°C to 163°C. APT has analyzed the NAPCA data and a plot of "f" versus liquid to gas ratio is given in Figure 5.3.6-6.

The value of "f" was defined in Equation 5.3.6-4 as the ratio of relative velocity between droplet and gas when distributed atomization occurs, to the velocity of the gas in the throat. In practice, "f" becomes a factor which absorbs the influence of various parameters not included explicitly in Equation 5.3.6-5. These parameters include collection by means other than impaction, particle growth due to condensation or other effects, drop sizes other than those predicted in Equation 5.3.6-1 loss of liquid to the venturi walls, and other effects. From Figures 5.3.6-4, 5.3.6-5, and 5.3.6-6, it appears that the range of "f" values levels off, if the ratio of liquid to gas throughput is high. At low values of (Q_L/Q_G), "f" is high, indicating better utilization of the liquid than at high ratios.

For design purposes, the choice of a proper value of "f" is not clearly indicated by the data. For the hydrophobic aerosols dioctyl phthalate and fly ash, values of "f" range from under 0.1 to over 0.3, even for high liquid to gas ratios. For particles with aerodynamic diameter of $1 \mu m \sqrt{g/cm^3}$, gas velocity of 10,000 cm/sec, and liquid to gas ratio of 10^{-3}, changing "f" from 0.1 to 0.3 will alter the penetration predicted by Equation 5.3-56 from 0.815 to 0.182. The design graphs which follow were developed by assuming an "f" value of 0.25; a value of 0.25 is about average for the available data. The uncertainty in "f" and the resulting uncertainty in predicted penetration, must be borne in mind when using these graphs. For hydrophilic aerosols, exemplified by methylene blue, values of "f" will be significantly higher.

Drop diameter, d_d, enters the venturi penetration equation, 5.3.6-5, both explicitly, and implicitly within $F(K_{Pt},f)$. For each combination of aerodynamic particle diameter, gas velocity and temperature, an optimum drop diameter exists. The optimum drop diameter combines the slow acceleration of a large drop (which results in a longer period for particle collection), with the high target efficiency of a small drop. Optimum drop diameters are plotted in Figure 5.3.6-2 versus gas velocity, with aerodynamic particle diameter as parameter. Also plotted is atomized drop diameter according to Equation 5.3.6-1 with liquid to gas ratio as parameter.

The optimum drop diameter and the actual drop diameter may differ substantially. However, for particles with aerodynamic diameter of about 1 $\mu m\sqrt{g/cm^3}$, it is possible to adjust liquid to gas ratio and gas velocity until the actual and optimum drop sizes are the same. For small particles, of aerodynamic diameter about $0.5\mu m\sqrt{g/cm^3}$ or smaller, it appears that the very high gas velocity and very low liquid to gas ratio necessary to atomize optimum sized drops are out of the range where venturis are usually operated. Similarly, for large particles, of aerodynamic diameter $2\mu m\sqrt{g/cm^3}$ or larger, the low gas velocities and high liquid to gas ratios necessary to atomize optimum drops may also be out of the usual range.

Note that the trend for optimum drop diameter (and collection) for small particles is to operate at high gas velocities and low liquid to gas ratios, while the trend for optimum collection of large particles is the opposite, requiring low gas velocities and high liquid to gas ratios. As will be seen, proper venturi operation on a range of particle sizes will be a compromise between these two trends. Figures 5.3.6-7, 5.3.6-8 and 5.3.6-9 are plots of penetration against aerodynamic particle size, with gas velocity as parameter, for a given ratio of liquid to gas throughput. These figures were calculated from Equation 5.3.6-5, for an "f" value of 0.25.

Several inferences can be drawn from these figures. For all velocities and liquid to gas ratios, the penetration of particles with an aerodynamic diameter less than about $0.5\mu m\sqrt{g/cm^3}$ is high. No matter what velocity and liquid to gas ratio are chosen, these particles will be difficult to separate in a venturi. As aerodynamic diameter increases from 1 to 10, penetration decreases sharply. In this region, increasing aerodynamic diameter leads to increasing the efficiency with which each droplet collects particles. However, when aerodynamic diameter becomes greater than about 10, penetration levels off. Further increase in particle size brings little change in penetration. At this point, each drop is functioning with nearly 100 percent efficiency. The only way to decrease penetration further is to provide more drops, i.e.: increase the ratio of liquid to gas throughput. The effect of such an increase can be seen in comparing Figures 5.3.6-7, 5.3.6-8, and 5.3.6-9, plots of penetration versus aerodynamic diameter, for different values of liquid to gas ratio.

To further illustrate the influence of gas velocity and liquid to gas ratio on particle penetration, Figures 5.3.6-10, 5.3.6-11 and 5.3.6-12 were prepared. These are plots of penetration versus gas velocity with liquid to gas ratio as parameter, for a constant aerodynamic particle size. Constant pressure drop lines are also plotted, using Equation 5.3.6-10. Comparing the constant pressure drop lines on the three figures yields an interesting result. For small particles (aerodynamic diameter, d_{pa}=0.5 $\mu m\sqrt{g/cm^3}$, Figure 5.3.6-10) it appears that for a given pressure drop, lowest penetration is achieved by operating at high velocities and low liquid to gas ratios. As was seen previously, operating with high velocity and low liquid to gas ratio produces optimum sized drops for the collection of small particles. For this reason, adjusting operating conditions at constant pressure drop to achieve these conditions gives lowest penetration on small particles.

For intermediate sized particles (d_{pa}=1.0$\mu m\sqrt{g/cm^3}$, Figure 5.3.6-11) minima appear in the pressure drop lines. The minima correspond to operation with the optimum drop diameter. Conditions to the left or right of the minima correspond to operating with drop diameters which are larger or smaller, respectively, than the optimum. For larger particles, however, (d_{pa}=2.0$\mu m\sqrt{g/cm^3}$, Figure 5.3.6-12), it appears that the higher the liquid to gas ratio, and the lower the gas velocity, the better. For large particles, the optimum droplet diameter is approached as gas velocity falls and liquid to gas ratio increases. For a realistic dust collection problem where small, intermediate and large particles must all be collected simultaneously, a balance must be reached between the best efficiencies achievable on both small and large particles, for a given pressure drop.

As discussed in 5.3.1 and in Chapters 8 & 9, it is frequently convenient to express the efficiency of a venturi in terms of its performance cut particle diameter, d_{pa50}. This is the aerodynamic diameter which will be collected with 50 percent efficiency. A plot of aerodynamic cut size against liquid to gas ratio, with gas velocity as parameter, and with constant pressure drop lines indicated, is given in Figure 5.3.6-13. For example, if it is desired to collect particles of a certain aerodynamic diameter with 50 percent efficiency (aerodynamic cut size specified), appropriate combinations of gas velocity and liquid to gas ratio can be chosen with the aid of this figure.

In accordance with 5.3.1 and 8.2, a smaller aerodynamic cut diameter leads to a lower overall penetration for a venturi collecting dust with a distribution of particle sizes. Note that the constant pressure drop lines in Figure 5.3.6-13, the plot of aerodynamic cut diameter against liquid to gas ratio, with gas velocity as parameter, have minima. For any specified pressure drop, the region to the left of the minimum has the higher gas velocities and lower liquid to gas ratios which correspond to higher efficiencies on small particles, but lower efficiencies on large particles. Conversely, the region to the right of the minimum has lower gas velocities, higher liquid to gas ratios, and reflects a trend toward higher efficiencies on large particles, but lower efficiencies on small particles. The minimum in the pressure drop line represents an optimum compromise for collecting both small and large particles, from the standpoint of achieving the best total efficiency on the whole range of both small and large particles.

Other equations for predicting the efficiency of a venturi have been presented. During the early period of venturi development, Eckman and Johnstone (1951) correlated particle penetration by:

$$Pt = \exp\left[-A' \ell S \eta_p\right] \qquad (5.3.6\text{-}7)$$

Here, "A'" is an empirical constant, "ℓ" is an effective path length of a water drop, and "S" is effective drop surface per unit scrubber volume. However, their approach does not account for all pertinent values.

Johnstone (1954) took into account the ratio of liquid to gas, and the inertial parameter, plus an empirical constant, "A":

$$Pt = \exp\left[-A'' \frac{Q_L}{Q_G} \sqrt{Kp}\right] \qquad (5.3.6\text{-}8)$$

Gieseke (1964) arrived at the following equation, based on constant liquid holdup in a gas volume. His result is questionable due to the fact that the liquid holdup is variable in a venturi.

$$Pt = \exp\left[-\frac{\pi}{4} d_d^2 n_d \ell_r \eta_p\right] \qquad (5.3.6\text{-}9)$$

Here "n_d" is the concentration of drops and "ℓ_r" is the distance traveled by the droplets relative to the gas.

Stairmand's (1965) approach has the same objection of constant liquid holdup.

5.3.6.3 Pressure Drop

Calvert (1968) has developed a method for estimating the pressure drop through a venturi scrubber by assuming all energy is used to accelerate the liquid droplets to the throat velocity of the gas:

$$\Delta P_{(cm\ H_2O)} = 1.03 \times 10^{-3} \left[u_G \left(\frac{cm}{sec}\right)\right]^2 \frac{Q_L}{Q_G} \qquad (5.3.6\text{-}10)$$

Figure 5.3.6-14 is a plot of pressure drop against gas velocity, with liquid to gas ratio as parameter. Pressure drop utilizing this equation has also been plotted in previous figures, as has been noted.

Note that in Figure 5.3.6-3, the plot of $F(Kp_t,f)$ versus "Kp_t" with "f" as parameter, for values of "Kp_t" between about 2 and 8, $F(Kp_t,f)$ can be approximated by:

$$F(Kp_t, f) \simeq -0.156\ Kp_t\ f^2 \qquad (5.3.6\text{-}11)$$

Substituting both the $F(Kp_t,f)$ approximation and the pressure drop equation into Equation 5.3.6-5, yields:

$$Pt \simeq \exp\left[6.1\text{x}10^{-9} \frac{\rho_L (d_{pa})^2\ \Delta P\ f^2}{\mu_G^{\ 2}}\right] \qquad (5.3.6\text{-}12)$$

where "d_{pa}" is the aerodynamic particle diameter in $\mu m\sqrt{g/cm^3}$, "ΔP" is in cm water, "ρ_L" is in (g/cm^3) and "μ_G" is in poise. After assuming standard properties for air and water, and a value of $f = 0.25$, penetration becomes a function of only pressure drop and aerodynamic particle diameter. This relationship is plotted in Figure 5.3.6-15.

Also plotted are the relationships between penetration and pressure drop cited in several references. It can be seen that the penetration - pressure drop relationships given in the references correspond to aerodynamic particle diameters from 1 to 4 $\mu m\sqrt{g/cm^3}$, the range of particle sizes for which a venturi is frequently used.

5.3.7 PARTICLE COLLECTION IN CENTRIFUGAL SCRUBBERS

Centrifugal devices may be used at several points in a gas scrubbing system. Dry cyclones are commonly used as precleaners to reduce the dust load to a more efficient cleaning device which follows. Centrifugal entrainment separators are frequently used to separate liquid droplets from the gas coming from a scrubber upstream.

Figure 5.3.7-1 shows a typical cyclone, such as might be used as a gas precleaner, or as a droplet entrainment separator. Another configuration, more commonly used for entrainment separation, is shown in Figure 5.3.7-2. These devices collect particles or droplets by centrifugal force.

Sprays are often used in centrifugal collectors to increase their efficiency. Figure 5.3.7-3 shows a dry cyclone which has been converted to a scrubber by wetting its walls. Sprays are sometimes introduced through a vertical spray pipe, as shown in Figure 5.3.7-4. This type of device combines particle collection by liquid droplets with collection by centrifugal force. The top region of this collector contains no sprays, and acts as a self contained entrainment separator.

5.3.7.1 Principle of Operation

Conventional cyclones separate particles from a gas stream by subjecting the particles to centrifugal force. The dirty gas enters through a tangential inlet and forms a rapidly rotating spiral, which throws the particles or droplets present to the collector wall. Reentrainment of collected dry particles, and dry particles bouncing from the collector wall will reduce collector efficiency for devices collecting dry dusts. This problem can be overcome by wetting the collector walls. Reentrainment of collected liquid mists is not normally a problem.

The more efficient centrifugal scrubber shown in Figure 5.3.7-4 sprays water droplets across a rotating gas stream. Gas enters tangentially at the bottom of the vertical cylinder, spins past water spray nozzles, and leaves through the top. Liquid drops sweep across the gas stream collecting particles by impaction before being collected themselves on the collector wall.

5.3.7.2 Particle Collection by Centrifugal Force

The following deals with particle collection in cyclones and in cyclones converted to scrubbers by wetting their walls. The function of the wetted wall is to prevent reintrainment of collected particles and particles bouncing from the collector wall. As the equations developed to predict efficiency in dry devices assume that all particles reaching the collector wall are collected, they are appropriate for predicting efficiency of devices with wetted walls. However, due to their ability to suppress particle reintrainment, wetted wall devices should perform more efficiently, and in closer approximation with theoretical predictions, than their dry counterparts.

Many workers have calculated the size of particles which a cyclone should theoretically collect with 100 per cent efficiency. This is called the cyclone's "critical particle size". Several equations for predicting critical size are given in Table 5.3.7-1. Virtually all experimental evidence points out the fact that a cyclone does not collect any size particle with 100 per cent efficiency. Rather, efficiency approaches 100 per cent asymtotically, as particle size becomes larger and larger.

Leith and Licht (1971) have developed a theoretical method for determining cyclone efficiency based on the following assumptions:

1. particles are spherical in shape
2. particle motion is not influenced by the presence of neighboring particles
3. the drag force on the particle is given by Stokes' Law
4. the radial velocity of the gas is zero
5. the tangential velocity component of the particle is the same as that of the gas stream
6. the tangential velocity component is related to the radial position by a modified form of the equation for a free vortex in an ideal fluid:

$$u_{tg}\, r^{n} = \text{constant} \qquad (5.3.7\text{-}1)$$

7. uncollected particles are continuously remixed through the horizontal plane.

The Leith - Licht efficiency equation is:

$$E = 1 - \exp\left[-2\,(C\,\Psi)^{1/(2n+2)}\right] \qquad (5.3.7\text{-}2)$$

where:

$$C = \frac{\pi\, d_c}{a\, b}\left[\, 2\left(1 - \frac{d_e^{2}}{d_c^{2}}\right)\left(S - \frac{a}{2}\right) + \frac{1}{3}\,(\ell + S - h_s)\left(1 + \frac{d_\ell}{d_c} \quad \frac{d_\ell^{2}}{d_c^{2}}\right) + h_s - \frac{d_e^{2}}{d_c^{2}}\,\ell - S\right] \qquad (5.3.7\text{-}3)$$

$$d_\ell = d_c - (d_c - b_e)\left(\frac{S + \ell - h_s}{h - h_s}\right) \qquad (5.3.7\text{-}4)$$

Terms are defined in Figure 5.3.7-1.

TABLE 5.3.7-1

EQUATIONS FOR PREDICTING THE CRITICAL (100%) PARTICLE SIZE OF A CYCLONE

NAME	EQUATION
Rosin, Rammler & Intelmann (1932)	$d_{cp} = 3 \left[\frac{\mu_G b}{\pi N u_{tg} \rho_p} \right]^{1/2}$
Lapple & Shepherd (1940)	$d_{cp} = 3 \left[\frac{\mu_G d_e}{2 \pi N u_{tg} \rho_p} \right]^{1/2}$
Gardiner	$d_{cp} = 3 \left[\frac{\mu_G \frac{d_c - d_e}{2}}{\pi N u_{tg} \rho_p} \right]^{1/2}$
Davies (1952)	$d_{cp} = 3 \left\{ \frac{\mu_G r_c^2}{2 h \rho_p u_{tg}} \left[1 - \left(\frac{d_e}{d_c} \right)^4 \right] \right\}^{1/2}$
Strauss (1966)	$d_{cp} = 3 \left\{ \frac{\mu_G Q_G r_c^2}{2 V_c \rho_p u_{tg}^2} \left[1 - \left(\frac{2 d_e}{3 d_c} \right)^4 \right] \right\}^{1/2}$

N is the number of turns the gas stream makes in the cyclone

V_c is the volume of the cyclone

$$\ell = 2.3\ d_e \left(\frac{d_c^{\,2}}{a\ b}\right)^{1/3} \qquad (5.3.7\text{-}5)$$

$$\psi = K_p \left(\frac{n+1}{2}\right) = \left(\frac{\rho_p\ d_p^{\,2}\ u_{tg}}{18\ \mu_G\ d_c}\right)(n+1) \qquad (5.3.7\text{-}6)$$

$$u_{tg} = \frac{Q_G}{a\ b} \qquad (5.3.7\text{-}7)$$

$$n = 1 - \left(\frac{T}{283}\right)^{0.3}\left[1 - \left(\frac{0.393 d_c}{2.5}\right)^{0.14}\right] \qquad (5.3.7\text{-}8)$$

Note:
d_c is cyclone diameter in centimeters

Here, "C" is a parameter reflecting the shape of the cyclone, but independent of the size or operating characteristics which are expressed in "Ψ". Temperature "T" in Equation 5.3.7-8 is in degrees Kelvin.

Equation 5.3.7-2 is plotted in Figure 5.3.7-5, and can be used to determine efficiency directly, after "C", "ψ" and "n" are calculated. Figure 5.3.7-7 gives four plots of performance cut diameter based on Equation 5.3.7-2 for several sets of parameters.

For rough approximations of the particle size which should be mostly collected in a centrifugal device, one of the "critical diameter" equations can be used. If a grade efficiency curve (efficiency vs. particle size) is desired, Equation 5.3.7-2 should be used.

5.3.7.3 Particle Collection by Sprays

Commonly, sprays are used in a centrifugal scrubber to combine collection by drops with centrifugal force. A typical spray arrangement is shown in Figure 5.3.7-4.

Picture a differential volume of such a scrubber, as described in Figure 5.3.7-6. The rates with which particles pass through surfaces (1) and (2) of the segment are, respectively:

$$\text{rate particles pass through (1)} = c\ Z \int_0^{r_2} u_{tg}\, dr = \frac{c\ Z\ u_{tg2}\ r_2}{1-n} \qquad (5.3.7\text{-}9)$$

$$\text{rate particles pass through (2)} = (c + dc)\ Z \int_0^{r_2} u_{tg}\, dr = \frac{(c + dc)\ Z\ u_{tg2}\ r_2}{1-n} \qquad (5.3.7\text{-}10)$$

if the tangential gas velocity at any point in the collector can be described by Equation 5.3.7-1, i.e.:

$$u_{tg} = u_{tg2} \left(\frac{r_2}{r}\right)^{n} \qquad (5.3.7\text{-}11)$$

where subscript 2 refers to conditions at the scrubber wall and "n" is found from Equation 5.3.7-8. The particles passing through surface 3 will be those which have been collected by the drops passing through that surface:

rate particles pass through (3) $\int_{r_s}^{r_2} r \; Z \; Hd \; \frac{3}{4 \; r_d} \eta p \; c \; v_d \; d\Theta \; dr$

$$= \frac{3 \; Q_L \; \eta_p \; c \; (r_2 - r_s) \; d\Theta}{8 \; \pi \; r_d} \qquad (5.3.7\text{-}12)$$

where liquid holdup is given by:

$$Hd = \frac{Q_L}{2 \; \pi \; r \; Z \; v_d} \qquad (5.3.7\text{-}13)$$

All particles entering through surface (1) must leave through either surface (2) or (3). Combining Equations 5.3.7-9, 5.3.7-10 , and 5.3.7-12, integrating yields:

$$E = \frac{c_i - c_e}{c_i} = 1 - \exp\left[-\frac{3 \; Q_L \; (r_2 - r_s)(1 - n) \; \eta_p}{4 \; u_{tg2} \; r_2 \; Z \; r_d} \; \frac{\Theta}{2\pi}\right] \qquad (5.3.7\text{-}14)$$

In this expression, "Θ" is the angle the gas sweeps through in passing through the collector. Therefore, $(\Theta/2\pi)$ is the number of "turns" the gas makes while within the collector. The number of turns is equal to the rate at which the gas sweeps through the collector, divided by the volumetric flow rate going to the collector, Q_G.

$$\frac{\Theta}{2\pi} = \frac{\int_0^{r_c} Z \; u_{tg} \; dr}{Q_G} = \frac{Z \; r_2 \; u_{tg2}}{Q_G \; (1 - n)} \qquad (5.3.7\text{-}15)$$

Substituting this into Equation 5.3.7-14 yields:

$$E = 1 - \exp\left[-\frac{3 \; Q_L \; (r_2 - r_s)}{4 \; Q_G \; r_d} \; \eta_p\right] \qquad (5.3.7\text{-}16)$$

The efficiency with which a single drop will collect particles due to impaction, η_p, is given by Equation 4.6.2-10.

For a device spraying radially outward from a central manifold, "r_s" is zero and:

$$E = 1 - \exp - \left(\frac{3 \; Q_L \; r_2}{4 \; Q_G \; r_d} \; \eta_p\right) \qquad (5.3.7\text{-}17)$$

5.3.7.4 Particle Collection by Both Centrifugal Force and Sprays

A device such as shown in Figure 5.3.7-4 collects particles by both droplets and centrifugal force. Strauss (1966) has proposed that the efficiency of a single device collecting particles by more than one mechanism be given by:

$$E_{overall} = 1 - (1 - E_a) \; (1 - E_b) \qquad (5.3.7\text{-}18)$$

The collection efficiency of a device using both centrifugal force and sprays becomes:

$$E = 1 - \exp\left[-2\,(C\,\Psi)^{\frac{1}{2n+2}} - \frac{3\,Q_L\,(r_2 - r_s)}{4\,Q_G\,r_d}\,\eta_p\right] \qquad (5.3.7\text{-}19)$$

5.3.7.5 Pressure Drop in a Centrifugal Scrubber

Strauss (1966) lists the following sources of pressure losses in a dry cyclone. The same sources should apply to a wetted wall centrifugal scrubber.

1. Friction loss in the entrance pipe.
2. Losses due to gas compression or expansion at the entry.
3. Losses due to wall friction in the collector.
4. Kinetic energy losses in the collector.
5. Losses at the entrance to the exit pipe.
6. Static load losses between inlet and exit pipe.
7. Recovery of energy in the exit pipe.

If sprays are employed, an additional source of pressure loss is the energy necessary to accelerate the water droplets.

Many expressions have been developed to determine the pressure loss through conventional dry cyclones. Several are listed in Table 5.3.7-2. No equations have been developed to determine pressure losses through centrifugal scrubbers. To get an approximation of expected pressure loss in a centrifugal scrubber, one might use one of the equations in Table 5.3.7-2.If the scrubber employs sprays, the energy used to accelerate the spray droplets will not be accounted for, and calculated pressure drops will be low.

Stern, Caplan and Bush (1955) compared pressure drop equations with experimental data. They found that no equation performed well. The equation of Shepherd and Lapple (1940) which appeared to work best most of the time, was off by an average of about 100 per cent from their experimental data. Direct measurement of the pressure drop through a similar centrifugal scrubber is much safer than relying on calculated values.

5.3.7.6 Other Factors Influencing the Performance of Centrifugal Scrubbers

Experimental evidence of Briggs (1946), Johnson et al. (1955), van Ebbenhorst Tengbergen (1965) and others shows that collection efficiency increases and pressure drop decreases with increased dust

TABLE 5.3.7-2

EQUATIONS FOR PREDICTING CYCLONE PRESSURE DROP

Name	Equation for ΔP, cm of H_2O (cgs units throughout)	Comment
Shepherd & Lapple (1939)	$0.000513\ \rho_G \left(\frac{Q_G}{a\ b}\right)^2 \left(16\ \frac{a\ b}{d_e^{2}}\right)$	direct tangential entry
Shepherd & Lapple (1940)	$0.000513\ \rho_G \left(\frac{Q_G}{a\ b}\right)^2 \ 7.5\ \frac{a\ b}{d_e^{2}}$	with inlet vane
Alexander (1949)	$0.000513\ \rho_G \left(\frac{Q_G}{a\ b}\right)^2 \left[\frac{4.62\ a\ b}{d_c\ d_e}\right] \left\{\left[\left(\frac{d_c}{d_e}\right)^{2n} - 1\right] \left[\frac{1 - n}{n}\right] + f \left[\frac{d_c}{d_e}\right]^{2n}\right\}$ n: See Equation 5.3.7-7 $f = 0.8 \left[\frac{1}{n(1 - n)} \left(\frac{4 - 2^{2n}}{3}\right) - \left(\frac{1 - n}{n}\right)\right] + 0.2 \left[\left(2^{2n} - 1\right)\left(\frac{1 - n}{n}\right) + 1.5\left(2^{2n}\right)\right]$	
Stairmand (1949)	$0.000513\ \rho_G \left(\frac{Q_G}{a\ b}\right)^2 \left[1 + 2\ \phi^2 \left(\frac{2\ (dc - b)}{d_e} - 1\right) + 2\ {\frac{4\ a\ b}{\pi\ d_e^{2}}}^{2}\right]$ $\phi = \frac{-\left(\frac{de}{2\ (dc - b)}\right)^{1/2} + \left(\frac{de}{2\ (dc - b)} + \frac{0.02\ A}{a\ b}\right)^{1/2}}{\left(\frac{0.01\ A}{a\ b}\right)}$; A = interior area of device exposed to gas flow	
Barth (1956)	$0.000513\ \rho_G\ u_i^{2}\ \varepsilon$ $\varepsilon = \varepsilon_e + \varepsilon_i$ $u_i = \left(\frac{u_i}{v_i}\right) \left(\frac{4\ ab}{\pi\ de^{2}}\right) Q_G$ $\frac{u_i}{v_i} = \frac{\frac{de}{2}\ \ \frac{dc - b}{2}\ \ \pi}{a\ b\ \alpha + (h_s - S)\ \left(\frac{dc - b}{2}\right)\ \pi\ \lambda}$ $\alpha \cong 1 - 1.2\left(\frac{b}{dc}\right)$; $\lambda \cong 0.02$; $\varepsilon = \varepsilon_e + \varepsilon_i$ $\varepsilon_e = \frac{de}{dc}\left[\frac{1}{\left[1 - \frac{u_i}{v_i}\ (h_s - S)\ \frac{2}{de}\ (\lambda)\right]^2} - 1\right]$; $\varepsilon_i = \frac{K}{\left(\frac{u_i}{v_i}\right)^{2/3}} + 1$ K = 4.4 for "standard round" exit ducts	

loading to a dry cyclone. A suitable explanation for this enigma has not been forthcoming.

Briggs (1946) has presented an empirical relationship between pressure drop and inlet dust loading:

$$\frac{\Delta P_d}{\Delta P_c} = \frac{1}{0.013\sqrt{c_i} + 1} \qquad (5.3.7\text{-}20)$$

Here, "ΔP_d" and "ΔP_c" are pressure drops with and without an inlet dust load, and "c_i" is the inlet dust loading in grains per cubic foot.

Sproull (1966) has hypothesized that the apparent viscosity of dusty air decreases with increased dust loading. His experiments confirm the hypothesis, but he offers no explanation for why this phenomenon should take place.

Many manufacturers and some experimenters have added devices to the internals of cyclonic collectors to aid in boosting efficiency or reducing pressure drop. Such devices include vanes extending the gas inlet into the collector body, baffles, radial vanes in the region of the collector's central core, helical gas inlet ducts, scroll type inlet ducts, and many more. Referring to a dry cyclone, Alexander (1949) states that, "many commercial adaptations are made solely on the basis of pressure drop improvement, without taking into account the effect of separation efficiency, probably because the latter is so difficult to assess correctly. It appears unfortunate but true that the majority of such adaptations and patent gadgets fitted to cyclones which decrease pressure drop, do have an adverse effect on separation efficiency. Without a knowledge of what actually goes on inside a cyclone, it is impossible to fully appreciate the real effect of a modification."

Caplan (1968) gives a description of some practical problems which may be encountered when using a centrifugal scrubber. Sprays should be carefully arranged so that the scrubber wall is thoroughly wetted. If any portion is merely moist, caking and plugging may result. Difficult regions may include the inlet duct, the gas outlet, and in a converted dry cyclone, the dust outlet. To prevent liquid creeping along the scrubber walls to the gas outlet, a skirt around the gas outlet duct from the collector may be provided. Liquid should be continuously and completely drained from the bottom of a centrifugal scrubber, to prevent atomization of the effluent by the high velocity air moving past. Atomization leads to excessive pressure drop, as well as reintrainment of collected liquid. Caplan recommends a maximum tangential air velocity of 3,850 cm/sec (150 ft/sec) at the scrubber wall-airstream interface. However, typical interfacial velocities are lower than this and are usually on the order of 1,500 cm/sec (50 ft/sec).

5.3.8 BAFFLED AND SECONDARY FLOW SCRUBBERS

Both baffled and secondary flow devices use baffles to cause particle collection. In the first case, the baffles change the gas flow direction and velocity. In the second case, the particles are collected due to secondary flow patterns created by the baffles. In both cases, particle deposition on the targets occurs primarily due to impaction and interception, and, in some cases, diffusion. Both types of collectors may be run either dry or wet. When running wet the liquid's main purpose is to wash off the collecting surfaces and remove the particles. Baffles and secondary flow devices can also be used for mass transfer. Little experimental data is available in the literature concerning this kind of collector.

5.3.8.1 Baffle Type Collectors

Baffled separators, also called impingement, inertia, or momentum separators, depend on the inertial deposition of particulates in a discontinuous fashion, as the gas passes around or through specially shaped obstacles or openings. The baffles and openings are made with dimensions in the order of several centimeters and take on different shapes, such as baffles, perforated plates, or shaped orifices. When running wet, efficiency usually improves at the expense of increased pressure loss. Baffled separators find much use in entrainment separation and as such are discussed in Chapter 5.5. They are also used to remove relatively large dust particles or as precleaners.

Principle of Operation

All baffle plates use a sudden change in the flow direction of the main gas stream to remove particles. The larger particles continue to move straight ahead when the air stream is deflected and are collected by the baffle or bounce off it. Several commercially available devices are described in Figures 5.3.8-1, 5.3.8-2, 5.3.8-3, 5.3.8-4, 5.3.8-5. The shutter type collector, Figure 5.3.8-1, which is sometimes used as a low resistance precleaner, cleans about 80% of the gas stream, while the rest of the dusty gas is diverted to a more efficient collector.

The separator depicted in Figure 5.3.8-2 is used mainly as an entrainment separator. Here again the rising gas makes abrupt turns as it passes through the horizontally mounted baffles. The wet scrubber depicted in Figure 5.3.8-3 adds the centrifugal effect to the inertial impaction. This scrubber consists of a series of elements which have a crescent shape. The concave surfaces of these elements face into the gas stream. Water flows down the crescent shaped elements washing down collected particles.

A different form of baffle separator is the louver type, illustrated in Figure 5.3.8-4 and 5.3.8-5. Here the hard large particles impinge on and either bounce off, or are washed off the louver elements by the air back into the louver core. Smaller particles, those particles which approach the louver elements at a large angle, and soft particles which do not bounce well, are carried out of the cone into the exhaust air stream. Approximately 5-10% of the entering gas travels the length of the cone and become concentrated with the dust particles. The concentrated "blow down" gas enters a secondary collector, usually a cyclone, where it is cleaned.

Baffle type collectors operate most often at low overall efficiency (50-80%). They are designed to collect relatively large particles. Louver collectors yield good efficiencies down to about 20 μm particles while other designs, used mainly as entrainment separators, show high efficiencies down to ≈5 μm diameter.

Most baffle type collectors are operated at a gas stream velocity of around 500-2500 cm/sec (17-85 ft/sec) with pressure losses ranging from a fraction of a mbar to ≈7.5 mbar (≈3 inches W.C.).

Design Equations

Baffled collectors are mostly inertial separators and depend for collection upon a sudden change in gas velocity and direction. Their collection efficiency is a function of the inertia parameter, K_p, as defined in Equation 4.6.2-4, where collector diameter, d_c, in the denominator of K_p is replaced by some fraction of the baffle spacing. The function between "K_p" and the collector's efficiency differs from one device to another. In most cases there is not enough experimental data in the literature to allow exact definition of the dependence of collection efficiency on "K_p". In several cases efficiency information is available in the literature, such as given in Figure 5.3.8-6, for a louver cone. In these cases, use can be made of this information.

Despite the lack of exact design equations, the dependence of collection efficiency on the inertial parameter leads to some general conclusions: 1) Penetration will decrease with increase in air velocity, and 2) Penetration will decrease with decrease of the device characteristics length. These can not be changed indefinitely since there is usually a minimum of penetration with velocity, due to increased reentrainment and the characteristic length cannot be made too small, to prevent clogging.

When the dust is collected by concave circular or segmental baffles, see Figure 5.3.8-3, a material balance leads to the following expression for the collection efficiency:

$$\eta_{cp} = 1 - \exp\left[-\left(\frac{A}{Q_G}\right) u_r\right] \qquad (5.3.8\text{-}1)$$

where "A" is the collection area defined as the total surface area of the collecting elements, perpendicular to the direction of gas flow, and "u_r" is the radial velocity of a particle given by

$$u_r = \frac{p\, d_p^2\, u_o^2}{18\, \mu_G\, r_c} = K_p\, u_o \qquad (5.3.8\text{-}2)$$

where "u_o" is the superficial gas velocity and "r_c" is the radius of the curvature of the collector. Substituting Equation 5.3.8-2 into Equation 5.3.8-1 we get

$$\eta_{cp} = 1 - \exp\left[\left(\frac{A}{A'}\right) K_p\right] \qquad (5.3.8\text{-}3)$$

where "A'" is the overall cross-sectional area of the device.

Ariman et al. (1972) derived a similar equation for the collection of large particles. Since constant mixing was not assumed in their derivation, their equation does not take the exponential form. They have shown experimentally that collection of small particles is due mainly to impaction on water drops, which are torn away from the curved surfaces. Collection efficiency of small particles in a single row can be calculated from the venturi Equation 5.3.6-5. Larger particles are collected by both mechanisms. For a single row the total collection efficiency

$$\eta_T = \eta_{cp} + \eta_{vp} - \eta_{cp}\eta_{vp} \qquad (5.3.8\text{-}4)$$

where "η_{cp}" is collection efficiency due to the centrifugal force and "η_{vp}" is collection by drops. For "n" rows the overall collection efficiency is:

$$E = 1 - [1 - \eta_T]^{\eta} \qquad (5.3.8\text{-}5)$$

5.3.8.2 Secondary Flow Collectors

Flow patterns which are neither random nor in the main direction of flow are called secondary flow patterns. Numerous examples of systems producing secondary flow patterns can be given, for any sort of obstruction in a flowing fluid stream will set up secondary flow patterns. Thus baffle collectors form secondary flow systems. Baffle devices where most of the collection takes place due to secondary flow and not due to direct collection on the baffles surface will be discussed in this section.

Principle of Operation

Calvert and Hodous (1962) described an experimental unit designed to study collection of particles by secondary flow. The collector shown in Figure 5.3.8-7 is a rectangular conduit with baffles cemented to the floor plate. The aerosol enters one side of the conduit, the particles are collected by the vortices formed in the spaces between the two adjacent baffles, and the cleaned gas stream leaves through an exit on the other side of the conduit.

Calvert and Taheri (1966) describe a different kind of secondary flow collector which was used in their experimental studies. They used a rectangular conduit, shown in Figure 5.3.8-8, with baffles inside. The baffles were made from metal sheets with 3 to 6 slots cutting across the plate. The distance between two adjacent slots on the same plate was 6 to 12 times the slot width. The aerosol stream entered the bottom of the column and exited through the top.

In both cases the main air stream formed secondary rotating flow patterns between the baffles. In the turbulent regime the formation and form of these vortex patterns depend only on the ratio of baffle spacing to baffle height. Visual studies conducted by Sweeney and Calvert (1965) indicate a rapid exchange of material between the main stream and the vortices. The rotational velocity of the vortex increases with increasing main stream velocity. When the cut out between the baffles is square and the height above the baffle is small relative to the baffle height, there is one vortex and the ratio of the vortex tangential velocity at the collecting surface to the main stream velocity is ≃1/3. When the cut out is rectangular with the ratio of height to width of less than 1, several vortices are formed and the tangential velocity at the collecting surface may fall to a few percent of the main stream velocity. A decrease in tangential to main stream velocity ratio was also observed when the rectangle height to width ratio was more than 1.

Design Equations

Calvert and Hodous (1962) assumed that when secondary flow takes place in a baffled conduit collection is due to impaction of the particle on the baffles, caused by centrifugal force. They made the following assumptions in deriving an equation to predict the collection efficiency:

1. There is instantaneous and complete mixing of particles within the main fluid stream and between the main stream and adjacent eddy.

2. The eddy is circular and its diameter is equal to the spacing between baffles.

3. The particles reach their terminal velocities in the centrifugal force field instantaneously.

4. All particles which strike the wall stick to it.

5. Terminal velocities may be approximated by Stokes law.

Making these assumptions they derived for the overall collection efficiency:

$$E = 1 - (1 - \eta)^n \qquad (5.3.8\text{-}6)$$

where "n" is the number of baffles in series and "η" is the collection efficiency for the eddy following each baffle,

$$\eta = \frac{\pi \, d_p^2 \, \rho_p \, \bar{u}}{12 \, \mu_G \, h \, \alpha^2} \qquad (5.3.8\text{-}7)$$

Here "ū" is the average linear velocity based on the unobstructed flow area, "h" is the free height for flow above the baffles and "α" is the ratio of the main stream velocity to the tangential velocity of the eddy at the collector surface. Calvert and Hodous determined the following values for "α" for different geometries:

TABLE 5.3.8-1

PERFORMANCE PARAMETER FOR BAFFLES, Calvert and Houdous (1962)

w/s	h/w	α
1	0.11 - 0.18	3.3
1	0.5 - 1	6.35
2.3	0.19	5.75
0.86	0.14	5.75
0.86	0.36	4.5

Here "w" is the baffle height and "s" the baffle spacing.

Figure 5.3.8-9 shows four plots of performance cut diameter and pressure drop as predicted by Equation 5.3.8-6 for several sets of parameters.

When calculating pressure drop different considerations apply to the device shown in Figure 5.3.8-7 and the one shown in Figure 5.3.8-8 If "h" is large relative to "w", drag friction is the dominant factor, while if "h" is small relative to "w", flow friction loss through an orifice-like device dominates.

For the case where the flow area is relatively large Sweeney and Calvert (1965) employing the pressure drop equation for flow in circular pipes found:

$$\frac{\Delta P}{X} = \frac{2\,\rho_G\,f\,u^2}{d_{eq.}} \qquad (5.3.8\text{-}8)$$

Neglecting the drag on the smooth walls they found the equivalent diameter for a rectangular conduit, formed by two fin walls and two smooth walls, or by one fin wall and three smooth walls, to be:

$$d_{eq.} = 4\,h \qquad (5.3.8\text{-}9)$$

Figure 5.3.8-10 is a plot of Calvert and Hodous (1962) and Sweeney and Calvert (1965) experimental data of pressure drop vs. gas flow rate in single and double fin rectangular conduits. Sweeney (1962) correlated the data of Boelter et al. (1951), Calvert and Hodous (1962) and Sweeney (1962) and found that the friction factor, "f", lies in the range 0.05 to 0.10 for $1{,}500 < N_{Re} < 700{,}000$.

The effect of liquid rate on pressure drop in a fin column is shown in Figure 5.3.8-11. The data are given as the ratio of the pressure drop of an irrigated column to the pressure drop of a dry cyclone, both at the same gas rate. As the gas flow rate is increased, at a constant liquid rate, the column becomes loaded. Sweeney and Calvert (1965) determined the gas and liquid rates at loading from the pressure drop curve. Their data are well represented by:

$$G = 6.35\left(\frac{L}{G}\right)^{-0.3} \qquad (5.3.8\text{-}10)$$

where "G" is in $kg/(m^2\text{-sec})$

When friction loss through a narrow slot in an orifice-like device is dominant, Calvert and Taheri (1966) have shown that the friction factor, f, is given by:

$$f = \frac{C}{2}\left(\frac{2h}{w}\right) + \frac{2.5\sqrt{2}}{\alpha\sqrt{\alpha}}\left(\frac{2h}{w}\right)^{0.5}\left(N_{Re}\right)^{-0.5} \qquad (5.3.8\text{-}11)$$

Correlation of the pressure drop data, after correction by deducting the pressure drop because of contraction at the entrance and expansion at the exit, is given in Figure 5.3.8-12. This correlation leads to two conclusions.

1. The value of "C" is almost constant between 0.4 and 0.43.

2. The pressure drop caused by establishing the boundary layer on the surface of the baffles at $N_{Re} < 2{,}000$ is not more than 10% of the total pressure drop, and at $N_{Re} > 3{,}000$ it is negligible. Consequently, the friction factor can be assumed a function of only (2h/w).

The friction factors for wet operation in Calvert and Taheri's work can be approximated from Figure 5.3.8-12.

5.3.9 IMPINGEMENT AND ENTRAINMENT

Impingement and entrainment separators have variously been named as "scrubbers with self-induced sprays", "self-induced spray scrubbers", "orifice type collectors", "swirl orifice collectors", and many other names. They are usually classified in the medium energy class of dust collectors, and rely mainly on inertial impaction and interception for collection of particles. Several designs are manufactured under various trade names and most of them have proven themselves in years of service. Though this class of collectors has been studied quite extensively by various manufacturers, no mathematical analysis of their collection ability could be found in the literature.

Principle of Operation

This group of scrubbers is characterized by the gas flowing through or past the liquid, atomizing it into a multitude of drops which collect the particles. The droplets are then separated from the gas stream and return to the liquid reservoir. There are many ways to achieve this aim. In Figure 5.3.9-1, a device is depicted which consists of an S-shaped impeller whose lower opening is partly submerged in water. The gas is passed at a relatively high velocity through the impeller and raises a turbulent sheet of water, which later breaks into drops. The dust and droplet mixture is deflected by the lower blade through an angle of ≈150° and is then projected downward by the upper blade (see Figure 5.3.9-2). The entrained dust particles are thereby forced below the water surface in the liquid holding tank, from which they are removed as sludge, while the cleaned gas passes through a mist eliminator before being discharged.

In Figure 5.3.9-3 the inlet air is accelerated by reducing the cross-sectional area available for flow. At its highest velocity the air hits the water surface, creates water droplets that clean the gas. Air velocity is limited by air channeling under the submerged pipe. Two more designs employing the same principles are shown in Figure 5.3.9-4 and Figure 5.3.9-5.

In most designs, the gas velocity at the dedusting zone is ≈1,500 cm/sec (50 ft/sec) except for the Doyle Scrubber shown in Figure 5.3.9-3 where the air velocity at the exit from the annular opening, ranges from 2,700 to 7,200 cm/sec (90 - 240 ft/sec) with the average being 4,500 cm/sec (150 ft/sec).

Impingement and entrainment scrubbers usually are not sensitive to changes in gas flow rates of ±25%. The pressure drop is about 10 to 20 cm (4" to 8") W.G. with the exception of the Doyle Scrubber, which is higher; 12 - 30 cm (4" - 12") W.G. Water consumption is usually low, 0.03 - 0.67 ℓ/m^3(0.2 to 5 gal/1,000 C.F.), depending upon gas temperature and desired concentration of solids in the slurry (which is usually kept at 5 - 10%, to permit slurry flow). The higher the temperature of the entering gas, the more water will evaporate to saturate the gas stream leaving the collector and the higher the water consumption will be.

Important advantages of this class of wet scrubber are:

1. The construction does not involve any close clearances which might become choked under heavy dust loading. The whole apparatus is well irrigated and periodic hosing-down of the interior can easily be carried out.

2. The spray is generated without employing mechanical devices or small orifices. Circulating water is used without clarification, excessive build-up of solids being avoided by a purge of settled solids and addition of clean water. The collected material can be removed from the unit with a hopper in which a drag type sludge ejector is placed, or alternatively by sluicing the sludge to a central disposal unit. The capacity of commercially available equipment ranges from 500 to 50,000 cfm (850 to 85,000 m^3/hr).

Design Equations

As in the case of other wet scrubbers, many operating factors should be considered during the design of impingement and entrainment wet scrubbers. They include:

1. Dust particle size distribution and density.

2. Efficiency and power requirements.

3. Wettability and solubility of particulates in water.

4. Inlet and outlet dust loading. (Collection efficiency usually increases slightly with increase in dust loading).

5. Temperatures and cooling effect. Increased gas temperature will increase water evaporative losses and slightly decrease collection efficiency.

The major particle collection mechanism is by inertial impaction on accelerating water drops. The drops are formed and accelerated by the gas stream, similar to the situation in a venturi scrubber. An equation predicting collection efficiency can be derived in a similar manner after making the following assumptions:

1. The collection of particles is due only to inertial impaction upon single drops, and follows from the relative velocity between the drops and the gas. The collection by a single drop is a function of the inertia parameter, K_p, given in Equation 4.6.2-4, where:

$$K_p = \frac{C' \rho_p d_p^2 u_r}{9 \mu_G d_c}$$

2. Hesketh et al. (1970) report for comparable conditions (air velocity of 1,800 cm/sec and cloud atomization)that drop diameters are 2 - 4 times smaller than the mean drop diameter predicted from Nukiyama-Tanasawa (1938) equation. A value 1/3 of that predicted from Nukiyama-Tanasawa equation will be used. Maximum stable drop diameter can be estimated from the critical Weber number, $N_{We} = 7.1$, as measured by Goldshmid and Calvert (1963). However, smaller drops are also formed during the process of atomization.

3. The drag coefficient for accelerating liquid drops is calculated from Calvert's (1968) approximation to Ingebo's (1956) data:

$$C_D = \frac{55}{N_{Red}} \tag{5.3.9-1}$$

4. The gas velocity is constant throughout the collection segment of the equipment. A momentum balance around a volume of differential length, neglecting mass exchange between gas and liquid yields:

$$A\ dP = \rho_G Q_G du_G + \rho_L Q_L du_d \tag{5.3.9-2}$$

Assuming the gas velocity to be constant, we get after integration:

$$\Delta P_d = \frac{\rho_L Q_L u_{de}}{A} \cong \frac{\rho_L Q_L u_G}{A} \tag{5.3.9-3}$$

where "u_{de}" is the drop velocity at the outlet from the collection section, and "ΔP_d" is the pressure drop due only to liquid acceleration. An approximation to "ΔP_d" can be made by assuming the drops are fully accelerated to the gas velocity by the time they leave the collecting segment ($u_{de} = u_G$).

The drop hold-up, Hd, defined as the volume fraction liquid in a differential volume is:

$$Hd = \frac{Q_L}{u_d\ A} = \frac{\Delta P_d}{\rho_L\ u_d\ u_G} \qquad (5.3.9\text{-}4)$$

A material balance for dust over a differential volume gives:

$$-Q_G\ dc = \frac{Hd\ A\ dX\ \pi\ r_d{}^2\ \eta_p\ u_r\ c}{\frac{4}{3}\ \pi\ r_d{}^3}$$

Substituting for "Hd" and rearranging gives:

$$-\frac{dc}{c} = \frac{3\ \Delta P_d\ u_r\ \eta_p}{4\ \rho_L\ r_d\ u_G{}^2\ u_d}\ dX \qquad (5.3.9\text{-}5)$$

If we define the magnitude of drop velocity relative to the gas as a function of the gas velocity relative to the wall, we get:

$$|u_r| = f\ u_G \quad \text{and } u_d = (1 - f)\cdot u_G \qquad (5.3.9\text{-}6)$$

Substituting these definitions in Equation 5.3.9-5 gives:

$$-\frac{dc}{c} = \frac{3\ \Delta P_d\ f\ \eta_p}{4\ \rho_L\ r_d\ u_G{}^2\ (1 - f)}\ dX \qquad (5.3.9\text{-}7)$$

We still need to know drop velocity and collection efficiency as a function of distance the drop travels relative to the wall "X". For this purpose, we shall use Calvert's (1968) approximation to Ingebo's (1956) findings on the acceleration of liquid drops by air drag. Within the range of Reynolds numbers of 100 to 400, this approximation is: $C_D = 55/N_{Re}$.

Fuchs (1964) describes unsteady drop motion relative to the gas, due only to drag and inertial forces:

$$\frac{2\ r_d}{C_D\ N_{Re}}\frac{\rho_G}{\mu_G}\ du_r = -\frac{3\ \rho_G}{8\ r_d\ \rho_L}\ dw \qquad (5.3.9\text{-}8)$$

where "w" is the distance the drop travels relative to the gas, $dw = u_r dt$. From the definition of "u_r" and "u_d", Equation 5.3.9-6, it follows that:

$$dX = \left(\frac{1 - f}{f}\right)\cdot dw \qquad (5.3.9\text{-}9)$$

Substituting for $du_r = u_G\, df$, for $C_D\, N_{Re} = 55$, and for "dw" in Equation 5.3.9-8 we get:

$$dX = -\frac{16\, r_d^2\, u_G\, \rho_L\, (1 - f)}{(3)\,(55)\, \mu_G\, f}\, df \qquad (5.3.9\text{-}10)$$

Substituting Equation 5.3.9-10 into Equation 5.3.9-7, we get:

$$\frac{dc}{c} = \frac{4\, \Delta P_d\, r_d}{55\, u_G\, \mu_G}\, \eta_p\, df \qquad (5.3.9\text{-}11)$$

Using the approximation for η_p from Equation 4.6.2-10 and substituting from Equation 5.3.9-6 for "u_r" in Equation 4.6.2-4, we get:

$$\eta_p = \frac{K_{Pt}^2\, f^2}{(K_{Pt}\, f + 0.7)^2} \qquad (5.3.9\text{-}12)$$

where "K_{Pt}" is a constant defined by:

$$K_{Pt} = \frac{C'\, \rho_p\, d_p^2\, u_G}{9\, \mu_G\, d_c} \qquad (5.3.9\text{-}13)$$

Substituting Equation 5.3.9-12 into Equation 5.3.9-11 and integrating from $f = f$ at $c = c_i$ to $f = 0$ at $c = c_e$, we get:

$$\int_{c_i}^{c_e} \frac{dc}{c} = \frac{4\, \Delta P_d\, r_d\, K_{Pt}^2}{55\, u_G\, \mu_G} \int_{f}^{0} \frac{f^2}{(K_{Pt}\, f + 0.7)^2}\, df \qquad (5.3.9\text{-}14)$$

the integral on the right-hand side is the same as the one already solved in the venturi equation, thus:

$$\ln \frac{c_e}{c_i} = \frac{4\, \Delta P_d\, r_d}{55\, u_G\, \mu_G}\, F\,(K_{Pt}, f) \qquad (5.3.9\text{-}15)$$

and $F\,(K_{Pt}, f)$ is defined in Equation 5.3.6-6 and plotted in Figure 5.3.6-3 vs. "K_{Pt}" for $f = 0.25$. The device efficiency is:

$$E = 1 - \exp\left[\frac{4\, \Delta P_d\, r_d}{55\, u_G\, \mu_G}\, F\,(K_{Pt}, f)\right] \qquad (5.3.9\text{-}16)$$

Example Calculation

To illustrate the use of this equation, calculate the following example. Predict the collection efficiency of 1 μm diameter particles of density $\rho_p = 2.7$ g/cm³ in an impingement and entrainment type collector. The gas enters the collection section at a velocity $u_G = 1{,}500$ cm/sec, the total pressure drop is 14 cm (5.5") W.C. and the dry pressure drop is 6.5 cm (2.5") W.C.

From the above data $\Delta P_d \approx 7.5$ cm (3") W.C. Equation 5.3.6-10 can be used to calculate the liquid to gas ratio, Q_L/Q_G, as pressure drop and gas velocity are known. From Nukiyama-Tanasawa equation, 5.3.6-1; $d_d \approx$ 335 µm; thus according to Hesketh et al., 1/3 d_d = 111 µm.

$$K_{Pt} = \frac{(2)\ (2.7)\ (0.25\times10^{-8})\ (1.16)\ (1{,}500)}{(9)\ (1.8\times10^{-4})\ \ (5.6\times10^{-3})} = 127$$

For f = 0.25 (the same "f" as in a venturi) F (K_{Pt}, f) = -0.19.
The collection efficiency is:

$$E = 1 - \exp\left[\frac{(4)\ (7.5)\ (9.8\times10^{2})\ (5.6\times10^{-3})\ (-0.19)}{(55)\ (1.8\times10^{-4})\ (1{,}500)}\right] = 0.878 \text{ or } 87.8\%$$

Note that the factor 980 is necessary to convert pressure drop in cm H_2O to units consistent with the rest of the terms used. Stairmand (1956) found experimentally for the same device a collection efficiency of 93%

Possibly more accurate estimates could be calculated if one used the exact relations for "c_D" and "η_D", rather than the approximation. R.H. Boll (1971) gives the design equations for a venturi scrubber and his method can be followed to obtain a closer estimate of this class of collection equipment. However, there is so much uncertainty about the applicability of the atomization relationship at such low velocities, the efficiency of water utilization, and other factors that these refinements seem premature and not worth the mathematical complexity they bring.

5.3.10 MECHANICALLY AIDED PARTICLE SEPARATORS

Mechanically aided particle separators, also known as Dynamic Separators, mechanical scrubbers and a variety of other names, are a combination of a moving impeller or fan and a dust collecting device. All designs rely on impaction and interception caused by centrifugal forces for particle collection and some use water spray to increase collection efficiency. In the following only the more common devices are discussed and analyzed in detail, while others are mentioned in short.

Principle of Operation

Figure 5.3.10-1 depicts one kind of mechanically aided dust precipitator. Here, in addition to the usual centrifugal force away from the axis, there is also a centrifugal force parallel to the axis caused by the reversal of the gas direction at the curved back plate. When the impeller, which consists of an inverted streamlined disc to which is fixed a large number of hyperbolically shaped blades, is rotated, a vacuum is created drawing in dust laden air axially at the center inlet. The impeller blades have 3 to 6 times the total blade area of a comparable size centrifugal exhauster to reduce the rate of impeller wear. The number and length of the blades is increased with equipment size, the blade spacing however remains fixed and the longer length compensates for the lower centrifugal acceleration caused by reduced impeller speed. This way, collection efficiency remains relatively constant regardless of equipment size.

The larger and heavier dust particles move in a slightly curved path until intercepted by the back disc and then follow the curvature of its surface. Lighter particles are intercepted by the blades, which due to their shape and rotation, cause the particles to collect on their advancing surface. The hyperbolic contour of the blade and the centrifugal force focus the various size particles to the tip of the blade. At this point, where the heavier and lighter dust particles converge, there is a narrow annular opening through which the dust escapes into a surrounding annular chamber. The clean air is discharged into the scroll shaped discharge. From the annular collecting chamber, the dust is conveyed by means of a secondary air stream into the hopper below. The secondary air stream is maintained by the tip of the impeller blades. The secondary air entering the hopper is permitted to return to the annular collecting chamber and thus maintains a continuous circuit. There is no return of partly dusty air to the main gas flow.

This mechanically aided collector operates in the range of a medium pressure exhauster and shows performance characteristics of a forward curved fan. Performing as a fan, the collector has no pressure loss as such; the energy needed for particle collection appears as a decrease in mechanical efficiency. Under normal operating conditions the collector has a mechanical efficiency of 40% - 50% as compared to 60% - 65% for an ordinary fan performing the same duty. This difference may be regarded as power cost for dust collection. This type of collector keeps a constant air volume for a constant operating pressure in keeping with its forward curved fan characteristics.

The collector shown in Figure 5.3.10-1 ranges in size from 170 - 42,500 m³/hr (100 - 25,000 CFM), can operate at temperatures up to 370°C (700°F) and its inlet gas velocity is in the range of 17.5 - 22.5 m/sec (3,500 - 4,500 ft/min). Its collection efficiency when running dry falls midway between conventional cyclone and high efficiency multiple cyclone. Efficiency for fine dust can be increased by spraying water into the fan inlet. Figure 5.3.10-2 shows collection efficiency of such a device. Water consumption is low, 0.07 - 0.14 ℓ/m³ (0.5 - 1 gal/MCF).

Different types of mechanically aided dust collectors are shown in Figures 5.3.10-3 and 5.3.10-4. Here the dust laden air and the water enters an impeller whose main purpose is to accelerate the drops in the radial direction and thus create a high relative velocity in the scroll. Water consumption is low, 0.07 ℓ/m³ (0.5 gal/MCF) and the pressure drop is ≈17 cm (7") W.G.

Another variation is depicted in Figure 5.3.10-5. This one consists of a housing, a rotor, a blower and a driving motor. The rotor is provided with radial blades (1) designed in such a way that the cleaned gas can be led off between the blade roots into the core of the rotor along the length "L_2". The separator housing (4) is cylindrical with an annular opening (5) where the gas enters. The clean gas leaves through the other opening (6). The cylinder is provided with a rectangular expulsion slot (7) on its circumference through which the dust with a small portion of the gas is led off. This device is discussed extensively by K. Budinsky (1970). Figure 5.3.10-6 shows calculated collection efficiency for this device.

A different device called a "Rotary Filamentary Filter" is built as a disc to which many filaments are attached at the periphery. The dust particles impact on the rotating filaments and are collected. This device is discussed extensively, analyzed and optimized in a series of articles by H. W. Pyne, R. B. Wilson and B. W. Soole (1967); by B. W. Soole (1968) and again by B. W. Soole (1970).

Another device called "Disintegrator Gas Washer" (depicted in Figure 5.3.10-7) is described and discussed by Stairmand (1956). This scrubber consists of an outer casing containing alternate rows of stator and rotor bars. The average relative velocity between adjacent bars is of the order of 60 m/sec (200 ft/sec). Water is injected axially and is broken up into fine particles which bombard and collect the dust. The disintegrator is efficient in collecting particles (Figure 5.3.10-8), however its total power consumption is high, ≈0.57 - 0.7 HP/m³/min. (16 - 20 HP/MCFM).

Design Equations

In the following we will develop design equations for two cases: one is the collector shown in Figure 5.3.10-3 where the centrifugal force acts only away from the axis as shown diagrammatically in Figure 5.3.10-9. The second case is the apparatus depicted in Figure 5.3.10-1 where centrifugal force acts parallel to the axis, shown diagrammatically in Figure 5.3.10-10.

As a first step the radial and angular velocities of both the particles and the drops as a function of time should be calculated. After these values are substituted in the efficiency equation the collection efficiency can be estimated. Where centrifugal forces act only perpendicular to the axis, if we neglect all forces except for the centrifugal force and the gas resistance, assume that the flow is laminar and that the gas resistance can be described by Stokes' law, then force balances lead to the following equations in cylindrical coordinates:

$$m\left[\frac{d^2r}{dt^2} - r\left(\frac{d\psi}{dt}\right)^2\right] = 3\,\pi\,\mu_G\,d_p\,(u_G - u_p)_r \qquad (5.3.10\text{-}1)$$

$$m\left(r\,\frac{d^2\psi}{dt^2} + 2\,\frac{dr}{dt}\,\frac{d\psi}{dt}\right) = 3\,\pi\,\mu_G\,d_p\,(u_G - u_p)_{tg} \qquad (5.3.10\text{-}2)$$

The boundary conditions are:

$$\text{for } t = 0,\ r = r_1 \text{ where } 0 \le r_1 \le r_0,\ u_{pr} = \frac{dr}{dt} = 0 \qquad (5.3.10\text{-}3)$$

$$\psi = \psi_1 \text{ where } 0 \le \psi_1 \le \frac{2\,\pi}{N} \text{ and } \omega_p = \frac{d\psi}{dt} = 0 \qquad (5.3.10\text{-}4)$$

The terms are defined in Figure 5.3.10-9.

To simplify the equations the following assumptions are made:

In Equation 5.3.10-1 the average angular velocity of the particle is substituted for the instantaneous angular velocity $\bar{\omega}_p{}^2 \approx (d\psi/dt)^2$.

1) In Equation 5.3.10-2 an average particle radial velocity over "r" is substituted for the instantaneous one: $\bar{\varepsilon} = (\bar{u}_{pr}/r) \approx 1/r\ (dr/dt)$.

2) The first boundary condition is simplified and at t = 0, all the particles are assumed to be at $r_0/2$ rather than distributed throughout the inlet pipe.

3) The average radial gas velocity "$\bar{u}_{Gr}$" is substituted for the instantaneous one.

4) Making these assumptions and rearranging Equations 5.3.10-1 and 5.3.10-2 one gets, where "τ_p" is particle relaxation time,

$$\frac{d^2r}{dt^2} + \frac{1}{\tau_p}\frac{dr}{dt} - \frac{\bar{u}_{Gr}}{\tau_p} - r\,\bar{\omega}_p{}^2 = 0 \qquad (5.3.10\text{-}5)$$

$$\frac{d^2\psi}{dt^2} + 2\left(\bar{\varepsilon} + \frac{1}{\tau_p}\right)\frac{d\psi}{dt} - \frac{\omega}{\tau_p} = 0 \qquad (5.3.10\text{-}6)$$

The solution to these two equations is:

$$r = \frac{\bar{\omega}_p{}^2\,\tau_p\,r_0 + 2\,\bar{u}_{Gr}}{4\,\bar{\omega}_p{}^2\,\tau_p\,\beta}\left\{(\beta - 1)\exp\left[-\frac{(1 + \beta)\,t}{2\,\tau_p}\right] + (1 + \beta)\exp\left[\frac{(\beta - 1)\,t}{2\,\tau_p}\right]\right\} + \frac{\bar{u}_{Gr}}{\bar{\omega}_p{}^2\,\tau_p} \qquad (5.3.10\text{-}7)$$

$$u_{pr} = \frac{dr}{dt} = \frac{\bar{\omega}_p^2 \tau_p r_0 + 2 \bar{u}_{Gr}}{2 \beta} \left\{ \exp \left[\frac{(\beta - 1) t}{2 \tau_p} \right] - \exp \left[- \frac{(1 + \beta) t}{2 \tau_p} \right] \right\} \quad (5.3.10\text{-}8)$$

$$\text{where } \beta = (1 + 4 \bar{\omega}_p^2 \tau_p^2)^{0.5} \quad (5.3.10\text{-}9)$$

$$\psi = \psi_1 + \frac{\omega \tau_p}{(2 \bar{\epsilon} \tau_p + 1)^2} \left[\exp \left(- \frac{(2 \bar{\epsilon} \tau_p + 1) t}{\tau_p} \right) - 1 \right] + \frac{\omega t}{2 \bar{\epsilon} \tau_p + 1} \quad (5.3.10\text{-}10)$$

$$\omega_p = \frac{d\psi}{dt} = \frac{\omega}{2 \bar{\epsilon} \tau_p + 1} \left\{ 1 - \exp \left[- \frac{(2 \bar{\epsilon} \tau_p + 1) t}{\tau_p} \right] \right\} \quad (5.3.10\text{-}11)$$

These equations apply only in the Stokes' region $N_{Rep} \leq 1$. For larger Reynolds numbers $40 < N_{Rep} < 400$, and for accelerating drops Calvert's (1968) approximation to Ingebo's data gives a relatively simple approximate solution. The drag force is approximated by:

$$F = \frac{55}{24} 3 \pi \mu_G d_p (u_G - u_p) \quad (5.3.10\text{-}12)$$

To illustrate the use of this assumption let us substitute Equation 5.3.10-12 in the force equations of 5.3.10-1 and 5.3.10-2. This gives:

$$m \left[\frac{d^2 r}{dt^2} - r \left(\frac{d\psi}{dt} \right)^2 \right] = \frac{55}{24} 3 \pi \mu_G d_p (u_G - u_p)_r \quad (5.3.10\text{-}13)$$

$$m \left[r \frac{d^2 \psi}{dt^2} + 2 \frac{dr}{dt} \frac{d\psi}{dt} \right] = \frac{55}{24} 3 \pi \mu_G d_p (u_G - u_p)_{tg} \quad (5.3.10\text{-}14)$$

The solutions to these equations using the boundary conditions in Equation 5.3.10-3 (as later modified) and 5.3.10-4 are:

$$r = \left\{ \frac{12 \tau_d \bar{\omega}_d^2 r_0 + 55 \bar{u}_{Gr}}{48 \tau_d \bar{\omega}_d^2 \sigma} \right\} \quad (5.3.10\text{-}15)$$

$$\left\{ (\sigma - 1) \exp \left[- \frac{55 (1 + \sigma) t}{48 \tau_d} \right] + (1 + \sigma) \exp \left[\frac{55 (\sigma - 1) t}{48 \tau_d} \right] \right\} - \frac{55 \bar{u}_{Gr}}{24 \tau_d \bar{\omega}_d^2}$$

$$u_{dr} = \frac{dr}{dt} = \frac{12 \tau_d \bar{\omega}_d^2 r_0 + 55 \bar{u}_{Gr}}{55 \sigma} \left\{ \exp \left[\frac{55 (\sigma - 1) t}{48 \tau_d} \right] - \exp \left[- \frac{55 (1 + \sigma) t}{48 \tau_d} \right] \right\} \quad (5.3.10\text{-}16)$$

$$\text{where } \sigma = \left(1 + \frac{2{,}304 \bar{\omega}_d^2 \tau_d^2}{3{,}025} \right)^{0.5} \quad (5.3.10\text{-}17)$$

$$\psi = \psi_1 + \frac{1{,}320 \omega \tau_d}{(48 \bar{\epsilon} \tau_d + 55)^2} \left\{ \exp \left[- \frac{48 \bar{\epsilon} \tau_d + 55) t}{24 \tau_d} \right] - 1 \right\} + \frac{55 \omega t}{48 \bar{\epsilon} \tau_d + 55} \quad (5.3.10\text{-}18)$$

$$\omega_d = \frac{d\psi}{dt} = \frac{55\ \omega}{48\ \bar{\varepsilon}\ \tau_d + 55} \left\{1 - \exp\left[- \frac{(48\ \bar{\varepsilon}\ \tau_d + 55)\ t}{24\ \tau_d}\right]\right\} \quad (5.3.10\text{-}19)$$

In a mechanically aided scrubber it is usually the drops that move at a high "N_{Re}" and not the particles. That is why Equations 5.3.10-15 to 5.3.10-19 are marked with the subscript "d". However, these equations apply equally to accelerating particles moving at high "N_{Re}".

Centrifugal Force Acting Parallel to the Axis

For the case where collection takes place mainly due to the centrifugal force acting parallel to the axis, a similar derivation can be made. Assuming that the gas radial velocity, $u_{Gr} = 0$, gives the same differential equations although the boundary conditions are different.

For $t = 0$, $r = r_1$ where $r_0 \leq r_1 \leq r_0 + 2\ B$, $u_{pr} = 0$ (5.3.10-20)

and $\psi = 0$, $\frac{d\psi}{dt} = \frac{u_G}{r_1}$ (5.3.10-21)

The terms are defined in Figure 5.3.10-10.
where "u_G" is the gas velocity at the inlet to the collector.

The solutions to these equations are:

$$r = \frac{r_1}{2\ \beta} \left\{(\beta - 1) \exp\left[- \frac{(1 + \beta)\ t}{2\ \tau_p}\right] + (1 + \beta) \exp\left[\frac{(\beta - 1)\ t}{2\ \tau_p}\right]\right\} \quad (5.3.10\text{-}22)$$

$$u_{pr} = \frac{dr}{dt} = \frac{\bar{\omega}_p^2\ \tau_p\ r_1}{\beta} \left\{\exp\left[\frac{(\beta - 1)\ t}{2\ \tau_p}\right] - \exp\left[- \frac{(1 + \beta)\ t}{2\ \tau_p}\right]\right\} \quad (5.3.10\text{-}23)$$

$$\psi = \left[\frac{\bar{\omega}_G\ \tau_p}{(2\ \bar{\varepsilon}\ \tau_p + 1)^2} - \frac{\tau_p}{(2\ \varepsilon\ \tau_p + 1)} \left(\frac{u_G}{r}\right)_1\right] \left\{\exp\left[-\left(\frac{2\ \bar{\varepsilon}\ \tau_p + 1}{\tau_p}\right) t\right] - 1\right\} + $$

$$+ \frac{\bar{\omega}_G\ t}{2\ \bar{\varepsilon}\ \tau_p + 1} \quad (5.3.10\text{-}24)$$

$$\omega_p = \frac{d\psi}{dt} = \left[\left(\frac{u_G}{r}\right)_1 - \frac{\bar{\omega}_G}{2\ \bar{\varepsilon}\ \tau_p + 1}\right] \exp\left(- \frac{2\ \bar{\varepsilon}\ \tau_p + 1}{\tau_p}\right) t + \frac{\omega_G}{2\ \bar{\varepsilon}\ \tau_p + 1} \quad (5.3.10\text{-}25)$$

$$\text{where } \bar{\omega}_G = \frac{u_G}{2\ (r_0 + B)} + \frac{u_G}{2\ r_0 + B} = \frac{u_G}{2} \left[\frac{4\ r_0 + 3\ B}{(r_0 + B)(2\ r_0 + B)}\right] \quad (5.3.10\text{-}26)$$

Collection Efficiency

Now we can proceed to the second step and calculate collection efficiency. As a first case consider the collector where the centrifugal force acts perpendicular to the axis and water is sprayed to help collection. In deriving the equations the following assumptions are made:

1. Collection of particles is only due to impaction between the water drops and the particles. Target efficiency is described by Figure 4.6.2-3 and approximated by Equation 4.6.2-10.

2. The gas stream in the impeller and leaving the impeller is fully mixed and there is no particle concentration gradient with "ψ".

3. The water drops leaving the impeller continue their flight without changing speed and direction until they hit the scroll wall. Gas velocity in the radial direction in the scroll is negligible and gas velocity in the tangential velocity in the scroll is constant and equal to (Q_G/A_e) where "A_e" is the scroll cross-sectional area at the exit. Thus in the scroll $u_{dr_2} >> u_{Gr}$ and $u_{Gtg} >> u_{dtg}$.

4. Collection efficiency in the scroll is estimated by first assuming that only the drop moves in the radial direction and then adding to it the collection resulting from a still drop and a gas moving past it in the tangential direction.

The liquid hold up is:

$$Hd = \frac{Q_L}{u_{dr}\ 2\ \pi\ r\ h} \qquad (5.3.10\text{-}27)$$

where "h" is the impeller thickness, and "r" is the radial distance.

Collection takes place inside the impeller and in the scroll. A material balance inside the impeller gives:

$$-Q_G\ dc = \frac{Hd\ 2\ \pi\ r\ h\ d_r\ \eta\ |u_p - u_d|_r\ c}{\frac{4}{3}\ r_d} \qquad (5.3.10\text{-}28)$$

Substituting for "Hd" and assuming that the small particles move at the gas velocity, one gets:

$$-\frac{dc}{c} = \frac{3\ Q_L\ |u_G - u_d|_r\ \eta}{4\ Q_G\ r_d\ u_{dr}}\ dr \qquad (5.3.10\text{-}29)$$

from the definitions:

$$\eta = \left[\frac{\frac{\tau_p}{r_d}\ |u_G - u_d|_r}{\frac{\tau_p}{r_d}\ |u_G - u_d|_r + 0.7}\right]^2 = \left[\frac{\tau_p\ |u_G - u_d|_r}{\tau_p\ |u_G - u_d|_r + 0.7\ r_d}\right]^2 \qquad (5.3.10\text{-}30)$$

$$\int_{c_i}^{c_{e_1}} \frac{dc}{c} = \frac{3\ Q_L\ \tau_p^{\ 2}}{4\ Q_G\ r_d} \int_{r_0}^{r_2} \frac{|u_G - u_d|_r^3\ dr}{(\tau_p\ |u_G - u_d|_r + 0.7\ r_d)^2\ u_{dr}} \qquad (5.3.10\text{-}31)$$

In the scroll a material balance yields:

$$-u_{Gtg}\ h\ b\ dc = \frac{Hd\ h\ b\ (r_2 + \frac{b}{2})\ d\psi\ c\ (\eta_1\ u_{dr_2} + \eta_2\ u_{Gtg})}{\frac{4}{3}\ r_d} \qquad (5.3.10\text{-}32)$$

where "b" is the width of the scroll at "ψ". Approximate the change in "b" with "ψ" by:

$$b = b_e \frac{\psi}{2\ \pi} \qquad (5.3.10\text{-}33)$$

where "b_e" is the maximum thickness of the scroll at the exit. Rearrangement and substitution gives:

$$\frac{-dc}{c} = \frac{3\ Q_L}{8\ \pi\ r_2\ h\ r_d}\left[\frac{\eta_1}{u_{Gtg}} + \frac{\eta_2}{u_{dr_2}}\right]\left(r_2 + \frac{b_e\ \psi}{4\ \pi}\right) d\psi \qquad (5.3.10\text{-}34)$$

Assuming that the drop radial velocity, "η" and "u_{Gtg}" are constant in the scroll and that "η_1" and "η_2" can be approximated by the collection efficiency of a sphere, then combining Equation 5.3.10-31 with Equation 5.3.10-34 and integrating gives:

$$-\int_{c_i}^{c_e} \frac{dc}{c} = \frac{3\ Q_L}{4\ r_d}\left\{\frac{\tau_p{}^2}{Q_G}\int_{r_0}^{r_2} \frac{|u_G - u_d|_r^3\ dr}{u_{dr}\ (\tau_p\ |u_G - u_d|_r + 0.7\ r_d)^2} + \frac{1}{2\ \pi\ r_2\ h}\right\}$$

$$\left[\frac{\eta_1}{u_{Gtg}} + \frac{\eta_2}{u_{dr_2}}\right]\int_0^{2\pi}\left(r_2 + \frac{b_e\ \psi}{4\ \pi}\right) d\psi \qquad (5.3.10\text{-}35)$$

$$\ln \frac{c_e}{c_i} = -\frac{3\ Q_L}{4\ Q_G\ r_d}\left\{\left[\eta_1\ \frac{u_{Gr_2}}{u_{Gtg}} + \eta_2\ \frac{u_{Gr_2}}{u_{dr_2}}\right]\left(2\ \pi\ r_2 + \frac{b_e\ \pi}{2}\right) + \right.$$

$$\left. + \tau_p + \tau_p{}^2 \int_{r_0}^{r_2} \frac{|u_G - u_d|_r^3\ dr}{(\tau_p\ |u_G - u_d|_r + 0.7\ r_d)^2\ u_{dr}}\right\} \qquad (5.3.10\text{-}36)$$

The integral in the last equation can be integrated graphically if one uses Equation 5.3.10-16 to calculate the variation in drop velocity with "r". "η_1" is the approximate target efficiency where "K_p" is calculated from "u_{dr_2}" and "η_2" is the approximate target efficiency for the velocity "u_{Gtg}".

In the case of a mechanically aided collector where centrifugal acceleration parallel to the axis is also developed, collection efficiency of relatively large particles in a dry collector can be calculated after making the following assumptions:

1. The cross-sectional area available for flow between two adjacent blades is constant along the blade. Thus the tangential velocity of the gas stream is constant inside the impeller.

2. Neglect the curvature of the blades in the direction perpendicular to the axis.

3. Assume continuous mixing inside the impeller.

4. The radius "r_2", see Figure 5.3.10-10, can be approximated by:

$$r_2 = r_0 + 2\ B \left(1 - \frac{\psi}{2\ \pi}\right) \qquad (5.3.10\text{-}37)$$

A material balance over a segment "$d\psi$" gives:

$$-u_{Gtg}\ A\ dc = u_{pr_2} \frac{A}{r_2 - r_0}\ r_2\ d\psi\ c \qquad (5.3.10\text{-}38)$$

Rearranging gives:

$$-\frac{dc}{c} = \frac{1}{u_{Gtg}} \left(\frac{r_2}{r_2 - r_0}\right) u_{pr_2}\ d\psi \qquad (5.3.10\text{-}39)$$

Substitution for "r_2" from Equation 5.3.10-37 and for "u_{pr}" from Equation 5.3.10-23 and approximating $r_1 \approx r_2$ in Equation 5.3.10-23 yields:

$$- \int_{c_i}^{c_e} \frac{dc}{c} = \qquad (5.3.10\text{-}40)$$

$$= \frac{\bar{\omega}_p^{2}\ \tau_p}{u_{Gtg}\ \beta\ B} \int_0^{\pi} \left\{ \frac{r_0 + 2\ B - \frac{B\ \psi}{\pi}}{2 - \frac{\psi}{\pi}} \right\}^2 \left\{ \exp\left[\frac{(\beta - 1)\ t}{2\ \tau_p}\right] - \exp\left[-\ \frac{(1 + \beta)\ t}{2\ \tau_p}\right] \right\} d\psi$$

Numerical or graphical integration of this equation is recommended. This can be done by assuming values of "ψ" and calculating the corresponding "t" values from Equation 5.3.10-24.

Approximate collection efficiency can be calculated if we assume that the motion of the particle is quasi-stationary then:

$$u_{pr} = \frac{u_G^{2}\ \tau_p}{r} \qquad (5.3.10\text{-}41)$$

Substitution into Equation 5.3.10-39 and rearrangement gives:

$$- \int_{c_i}^{c_e} \frac{dc}{c} = \frac{u_G\ \tau_p\ \pi}{B} \int_0^{\pi} \frac{d\psi}{2\ \pi - \psi} \qquad (5.3.10\text{-}42)$$

The final expression after integration is:

$$E = 1 - \exp\left(-\ \frac{0.69\ \pi\ u_G\ \tau_p}{B}\right) \qquad (5.3.10\text{-}43)$$

The collection efficiency of smaller particles on the blades can be calculated in a fashion similar to the first example.

Water Spray

As a last case consider the last device only with water sprayed into the inlet pipe ahead of the impeller. Again make assumptions 1 - 4 as made in the previous case and also assume that the particles follow the gas streamlines and collection takes place as a result of inertial impaction of the particles on the drops in the radial direction. Neglect collection of the particles due to the particle centrifugal acceleration.

A material balance over the part of section "dψ" from "r" to "r + dr" gives:

$$u_{Gtg} \frac{A}{(r_2 - r_0)} dr\ dc = \frac{Hd\ A\ dr\ r\ d\psi\ u_{dr}\ \eta_p c}{(r_2 - r_0)\ \frac{4}{3}\ r_d} \qquad (5.3.10\text{-}44)$$

Assuming that Hd = $(Q_L)/(u_{dtg}\ A)$ is constant throughout the collector where drops are present and collection takes place, then:

$$-\int_{c_i}^{c_e} \frac{dc}{c} = \frac{3\ Q_L}{4\ Q_G\ r_d} \int_0^{\psi_1} \frac{1}{\omega_d} \frac{\int_{u_{dr}t}^{r} u_{dr}\ \eta_p\ dr}{\int_{u_{dr}t}^{r} dr}\ d\psi \qquad (5.3.10\text{-}45)$$

The double integral can be solved graphically or numerically after substituting for "η" from Equation 4.6.2-10, and for "u_{dr}" from Equation 5.3.10-16.

To get an estimate of the collection efficiency, an average value of "u_{dr}" and "η" for each "ψ" can be substituted in the last equation. Then:

$$-\int_{c_i}^{c_e} \frac{dc}{c} = \frac{3\ Q_L}{4\ Q_G\ r_d} \int_0^{\psi_1} \frac{u_{dr} \cdot \eta}{\omega_d}\ d\psi \qquad (5.3.10\text{-}46)$$

The right hand integral can be solved graphically by assuming a value for "ψ" finding the corresponding "t" from which values for "u_{dr}" and "ω_d" can be calculated. (The differential equations for this case were not solved here but can be derived and solved in the same manner as Equations 5.3.10-22 to 5.3.10-25, were solved using Equation 5.3.10-12 for the Stokes resistance.)

The integral on the right hand side of Equation 5.3.10-46 can be solved if we make the following assumptions:

1. Drop acceleration in the radial direction is neglected, then:

$$u_{dr} = u_{dtg}\ \omega_d\ \tau_d \qquad (5.3.10\text{-}47)$$

2. The drop tangential velocity can be approximated by the gas entering velocity $u_{dtg} \approx u_G$ which is a constant.

3. Drop target efficiency is given by Equation 4.6.2-10.

4. The particle impaction parameter "K_p" is given by:

$$K_p = \frac{2\ \tau_p\ u_{dr}}{d_c} = \frac{2\ \tau_p\ \tau_d\ u^2_{dtg}}{d_c\ r} = \frac{\alpha}{r} \qquad (5.3.10\text{-}48)$$

where "τ_p" is particle relaxation time

Thus $$\eta_p = \left(\frac{\alpha}{\alpha + 0.7\ r}\right)^2 \qquad (5.3.10\text{-}49)$$

5. Assume $r = r_2$. This will give a somewhat lower target efficiency but permit integration to "ψ_1". The radius "r_2" will be approximated by Equation 5.3.10-37.

After all these assumptions we get:

$$\int_{c_i}^{c_e} \frac{dc}{c} = \frac{3\ Q_L\ \tau_d\ u_{dtg}\ \alpha^2}{4\ Q_G\ r_d} \int_0^{\psi_1} \frac{d\psi}{\left[\alpha + \left(r_0 + 2\ B - \frac{B\ \psi}{\pi}\right) 0.7\right]^2} \qquad (5.3.10\text{-}50)$$

The final answer is:

$$E = 1 - \exp\left[- \frac{6\ Q_L\ \tau_d^3\ \tau_p^2\ u_G^5\ \psi_1}{Q_G\ d_d^3} f\ (\psi_1)\right] \qquad (5.3.10\text{-}51)$$

where:

$$f(\psi_1) = \left[\left(\alpha + 0.7\ r_0 + 1.4\ B - \frac{0.7\ B\ \psi_1}{\pi}\right) \left(\alpha + 0.7\ r_0 + 1.4\ B\right)\right]^{-1} \qquad (5.3.10\text{-}52)$$

Further approximation can be made by assuming a constant average value for "$\bar{\eta}$". Collection efficiency is then given by:

$$E = 1 - \exp\left[- \frac{3\ Q_L\ \bar{\eta}\ u_G\ \tau_d\ \psi_1}{4\ Q_G\ r_d}\right] \qquad (5.3.10\text{-}53)$$

where "ψ_1" is the angle when all the water drops have already been collected by the blade or the back plate. "$\bar{\eta}$" is the average target efficiency for spheres estimated from $|\bar{u}_{dr} - \bar{u}_{pr}|$. For small particles "$\bar{u}_{pr}$" is very small and can be neglected.

Examples

To illustrate the use of these equations and demonstrate the relative accurary of the approximations, let us consider several examples. We shall start with the device shown in Figure 5.3.10-3. Given the following data estimate collection efficiency for $d_p = 10$ μm particles of density $\rho_p = 2.7$ g/cm³. $n = 3{,}600$ RPM; $Q_G = 2.36 \times 10^5$ cm³/sec (500 CFM); $r_0 = 7.5$ cm; $r_2 = 15$ cm; $h = 3$ cm; $b_e = 13$ cm; $Q_L = 32$ cm³/sec (1 gal/1,000 C.F.); $h_e = 5.5$ cm; $d_d = 300$ μm.

$$\omega = \frac{2\ \pi\ n}{60} = 377 \text{ rad/sec}$$

$$u_{Gtg} = \frac{2.36\text{x}10^{5}}{(5.5)\ (13)} = 3{,}300 \text{ cm/sec}$$

$$\bar{u}_{Gr} = \frac{u_{Gr_0} + u_{Gr_2}}{2} = \frac{Q_G}{4\ \pi\ h}\left(\frac{r_0 + r_2}{r_0\ r_2}\right) = 1{,}250 \text{ cm/sec}$$

$$\tau_d = \frac{(2)\ (1.5^2\text{x}10^{-4})}{(9)\ (1.8\text{x}10^{-4})} = 0.278 \text{ sec}$$

$$\tau_p = \frac{(2)\ (2.7)\ (5^2\text{x}10^{-8})}{(9)\ (1.8\text{x}10^{-4})} = 8.3\text{x}10^{-4} \text{ sec}$$

Collection efficiency for this case is estimated from Equation 5.3.10-36. To calculate the value of the integral "u_{dr}" and "$\bar{u}_{Gr}$" at various "r" are calculated. To calculate "u_{dr}" a value for "$\bar{\omega}_d$" is assumed and checked through a trial and error method. Once the values for "u_{dr}" are found for various "r", the integral is evaluated graphically in Figure 5.3.10-11, where the group under the integral is called "Group A". It gave a value of $1.74\text{x}10^7$ cm/sec^2 and when multiplied by "$\tau_p{}^2$" we get 12 cm. The collection in the scroll is evaluated from the second part of Equation 5.3.10-36. Approximate values for "η_1" and "η_2" are estimated from the collection efficiency for spheres (Equation 4.6.2-10). The final equation is:

$$-\ln \frac{c_e}{c_i} = \frac{(3)\ (32)}{(2)\ (2.36\text{x}10^5)\ (3\text{x}10^{-2})}\left\{12 + 114.7\ (0.25 + 0.8)\right\}$$

$$E = 1 - \exp\ (-0.895) = 59\%$$

Before discussing these results let us examine the angular position of the water drops with respect to the impeller blade at the exit from the impeller. Assuming that the drops are equally dispersed when entering the channels between the blades then Equation 5.3.10-18 gives the angle "ψ_d" that the drop has traveled at the time $t = t_2 - t_0$ calculated earlier. The angle "ψ" that the blade has traveled at the same time is calculated from "ωt". The difference between these two angles which comes out to be 15.95° is the angle that the drop is lagging behind the blade. This decreases the calculated efficiency which was based on the assumption that the water drops were evenly distributed in the scroll. How much the efficiency will decrease depends upon the degree of agglomeration of the drops and will have to be determined experimentally.

If one examines the numbers in the example closely, it appears that under constant drop holdup conditions, the drops in the scroll collect about 91% of the particles. In the scroll ≈76% of the collection is attributed to the high velocity gas flowing past the drop as compared to ≈24% due to the drop velocity perpendicular to the gas. Thus the major part of the collection is independent of the drops impinging on the blades, provided of course that drop size and velocity does not change when being thrown off the blade. Another conclusion is that it would be advantageous to have many blades and a small angle between them. This way the collection due to drop radial velocity increases since the drops cover more of the scroll area.

Another interesting characteristic can be observed from Figure 5.3.10-11. Since the parameters chosen for this example do not represent an actual device but where chosen arbitrarily to illustrate the calculation method, it seems that these are not the best design parameters. Figure 5.3.10-11 shows that the relative velocity between the drops and the particles and thus the collection efficiency in the impeller, is decreasing rapidly with "r". Using the design equations, the device can be optimized by varying the parameters and studying the effect of these variations on overall collection efficiency.

Some of these conclusions are quite general, like the fact that only a small fraction of the collection takes place in the impeller, others depend on the special design and operating conditions. One thing should be emphasized, if the quasi-stationary radial drop velocity calculated from $u_{dr} = \omega^2 \, r \, \tau_d$ is used rather than Equation 5.3.10-16 collection efficiency would be over estimated by more than 10%.

Example of Dry Collection Component

As a second example the collection efficiency of the device depicted in Figure 5.3.10-1 and operating dry will be calculated. The following dimensions and data are assumed: r_p = 10 μm; ρ_p = 2.7 g/cm³ ; r_0 = 1 cm; B = 1.13 cm; $u_G = u_{Gtg}$ = 1,500 cm/sec (50 ft/sec).

$$\tau_p = \frac{(2)\ (2.7)\ (25\text{x}10^{-8})}{(9)\ (1.8\text{x}10^{-4})} = 8.3\text{x}10^{-4} \text{ sec}$$

A first estimate for "$\bar{\omega}_p$" is calculated by assuming that the particle moves with the gas velocity.

$$\bar{\omega}_p = \frac{u_G}{2\ (r_0 + B)} + \frac{u_G}{2\ r_0 + B} = 795 \text{ sec}^{-1}$$

Thus "β" can be estimated from Equation 5.3.10-9. The time at the exit "t_e" is estimated from:

$$t_e = \frac{\pi}{\bar{\omega}} = 3.95\text{x}10^{-3} \text{ seconds}$$

The next step is to estimate "$\bar{\varepsilon}$"; at $t_i = 0$, $u_{pr} = 0$ from Equation 5.3.10-23; at "t_e", "u_{pre}" is calculated from Equation 5.3.10-23 and $\bar{\varepsilon} = 905$ is the sum of $(u_{pr}/2\ r)_i + (u_{pr}/2\ r)_e$. Once "$\bar{\varepsilon}$" is known, "$\omega_p$" is calculated again and compared with the original assumption. This way, employing a trial and error method the calculation contines until one gets a close enough approximation of "$\bar{\omega}_p$". Our final figures for this case were:

$$\bar{\varepsilon} = 485 \text{ seconds}^{-1}, \quad t_e = 6.75\text{x}10^{-3} \text{ seconds}, \quad \bar{\omega}_p = 578 \text{ seconds}^{-1}$$

The values of the function (Group "B") in the integral on the right hand side of Equation 5.3.10-40 were then calculated for ψ = 0, π/4, π/2, 3 π/4, π and plotted in Figure 5.3.10-12. Graphical integration gave for the integral the value of 31.2. Substituting this value in Equation 5.3.10-40, the collection efficiency is:

$$E = 1 - \exp\left[- \frac{(3.34\text{x}10^{5})\ (8.3\text{x}10^{-4})\ (31.2)}{(1{,}500)\ (1.385)\ (1.13)} \right] = 97\%$$

Using the approximate Equation 5.3.10-43:

$$E = 1 - \exp\left[- \frac{(0.69)\ \pi\ (1{,}500)\ (8.3 \times 10^{-4})}{1.13}\right] = 91\%$$

For smaller particles, collection on the blades is important and should be added.

5.3.11 MOVING BED SCRUBBERS

Moving bed scrubbers were first designed to overcome scrubber fouling by tar-like sticky particles collected in the scrubber. The movement of the packing material cleans the surfaces and prevents fouling. Later it was found that this group has further advantages on top of keeping the scrubber clean. In the following discussion the group will be divided into two: 1) Mobile bed scrubbers, like the "HydroFilter", where the packing is relatively heavy and expands only a little during operation. 2) Fluidized Bed Scrubbers, like the T.C.A., where low density packing is placed between retaining grids sufficiently far apart, to permit turbulent and random motion of the packing.

5.3.11.1 Mobile Bed Scrubbers

Principal of Operation

A picture of one of the commercially available mobile bed scrubbers is shown in Figure 5.3.11-1. The main liquor stream is sprayed through nozzles onto the bottom side of a bed packed with glass marbles. Simultaneously, a secondary flow of liquor is sprayed onto the top side of a "turbulent layer" formed above the spheres. Dust enters the scrubber at the bottom, concurrently contacts the main liquor stream, bubbles upward through the turbulent layer, and leaves at the top. Most of the solid particles in the entering gas stream are drained out the bottom of the scrubber. The main effluent liquor stream is collected in downcomers within the turbulent layer and is directed out of the bottom of the scrubber.

Superficial gas velocity is usually 2.4 - 3 m/sec (8 - 10 ft/sec) and scrubbing liquid flow rate is 0.27 - 0.54 ℓ/m^3 (2 - 5 gal/MCF). Water comsumption varies with the gas temperature and humidity and with solid concentration in blow-off liquor. (Recirculating slurry of 35% by weight solids can be used.) Static pressure loss is usually 10 - 12.5 mbar (4 - 5" W.C.) per stage.

Design Equations

One can look on the mobile bed as a packed bed, and use the equations given in Section 5.3.3 to predict collection efficiency. Bechtel(1970) in their report, estimated the constant for glass marbles bed from data given by National Dust Collector Corp. (1968). Bechtel gives the following equation, based on Calvert (1968), for a mobile bed scrubber packed with glass spheres.

$$E = 1 - \exp\left[-19\ \frac{Z}{d_c}\ K_p\right] \qquad (5.3.11\text{-}1)$$

where "K_p", the inertia parameter, is calculated based on the interstitial gas velocity in the packed section.

In the same report (Bechtel, 1970) the pressure drop is calculated as follows. The total gas phase pressure drop, ΔP, is assumed to be the sum of the pressure drop through the packed section and the turbulent-layer region. The pressure drop in the packed section is estimated from a correlation given in Perry (1950) for pressure drop of gases flowing through beds packed with spheres of diameter "d_c":

$$P_1 = 0.0010 \frac{4 \; f \; Z \; G^2 \; A_f}{2 \; \rho_G \; d_c} \text{ mbar} \qquad (5.3.11\text{-}2)$$

and $N_{Re} = \dfrac{d_c \; G'}{\mu_G}$

where "A_f" is a wall effect factor. For most mobile bed scrubbers, $N_{Re} > 1{,}000$ thus $A_f = 1.0$ and:

$$f = \frac{38}{N_{Re}^{0.15}} \qquad (5.3.11\text{-}3)$$

The pressure drop through the turbulent layer is estimated from a correlation given in Ludwig's (1960) book:

$$\Delta P_2 = 1.9 + 0.93 \; Z \text{ mbar} \qquad (5.3.11\text{-}4)$$

The height of liquid in the turbulent layer is estimated from a correlation presented by Lowry and Van Winkle (1969):

$$Z(\text{cm}) = 2.77 + 0.0264 \; u_b^2 \left(\frac{\rho_G}{\rho_L - \rho_G}\right) \qquad (5.3.11\text{-}5)$$

where "u_b" is the velocity of gas bubbles in the turbulent layer, in cm/sec. "Z" can not be less than the scrubber weir height.

5.3.11.2 Fluidized Bed Scrubbers

This type of scrubber, an example of which is depicted in Figure 5.3.11-2, is characterized by the use of essentially non-flooding grids sufficiently far apart to permit turbulent and random motion of the spheres. Thus both high gas and liquid velocities at modest pressure drops are allowed. The packing commonly used is 2.5 or 3.75 cm (1 or 1.5 in) diameter hollow plastic spheres. The static packing depth is 15 - 60 cm (0.5 - 2 ft) while the distance between grids is large ≈150 cm (5 ft). The increase in the zone area height, in which the spheres operate, to more than twice the packing static height, permits the use of high gas and liquid flow rates through the unit before flooding occurs.

When the static volume of packing exceeds 50% of the volume enclosed between the grids, the spheres tend to move as a bed, and there is a marked decrease in gas flow and a sharp increase in pressure drop. At gas velocities of 3 - 5 m/sec (10-17 ft/sec) in combination with moderate liquid velocities of 1.35 - 2 cm/sec the spheres are in turbulent motion. At very low gas and high liquid velocities sphere motion is slow, while at high gas velocity and low liquid velocity, the bed tends toward plug flow, eventually ending in flooding of the scrubber. The normal design range is 2.5-5.5 m/sec (10-17 ft/sec) gas velocity for one stage and less for two stages, and 1 - 4 cm/sec liquor rate. The liquid volume circulating is 4.1 - 13.7 ℓ/m^3. The water makeup flow rate depends upon gas temperature and humidity and desired slurry concentration.

Since the packing is usually made of plastic materials, maximum operating temperature is limited to that temperature which would not deform the packing. Hotter gases have to be quenched by water sprays.

Design Equations

The flooded bed scrubber can be looked upon as a special case of packed bed, a sieve column, or a combination of the two. It differs from a packed bed since the packing is fluidized and a large quantity of water is retained on the plate. It differs from the sieve plate in the large perforation diameter and sieve free area, high gas and liquid flow velocities and foam height. Figure 5.3.11-4 from the work of Pollock, Tomany and Frieling (1967) show experimental results for the collection of fly ash in one and two stage fluidized bed scrubbers. Bechtel (1971) used a modified packed bed equation to correlate these data.

$$E = 1 - \exp\left[-2.45\text{x}10^6 \, (u_L)^{3.3} \, (u_G)^{0.36} \, K_p \frac{Z}{d_c}\right] \qquad (5.3.11\text{-}6)$$

where "u_L" and "u_G" are the superficial liquid and gas flow velocities inside the tower, in cm/sec respectively, "Z" is the stage height in cm, and "d_c" is the packing diameter in cm. "K_p", the inertial parameter, is calculated from Equation 5.3.3-5 based on interstitial gas velocity, V_{Gb}, rather than superficial gas velocity, V_G. Equation 5.3.2-2 relates V_{Gb} to V_G.

It should be remembered that the coefficient in Equation 5.3.11-6, namely, $2.45\text{x}10^6 \, (u_L)^{3.3} \, (u_G)^{0.36}$, was derived by curve fitting technique and may not describe the collection efficiency adequately in other cases. Due to lack of data it was not possible to check the collection efficiency using the sieve plate equation, which may be more adequate in this case.

Figure 5.3.11-5 also taken from the work of Pollock, Tomany and Frieling (1967) gives experimental pressure drop in the fluidized bed scrubber. Their data is in good agreement with the experimental data reported by Douglas, Snider, and Tomlinson (1963) and the pressure drop curve given in U.O.P. Bulletin No. 608 (1967). Bechtel (1971) analyzed the data given by U.O.P. (1970) using a multiple regression technique and found for pressure drop in mbar:

$$\Delta P_{\text{packing}} = Z\left\{0.119 \, u_L^{0.33} + 3.53\left[285 \, u_L^{-0.25} - 1.97 \, u_G\right]^{-1.02}\right\} \qquad (5.3.11\text{-}7)$$

$$\Delta P_{demister} = 1.7\text{x}10^{-6}\ u_G^2 \exp\left[0.77\ u_L\right] \text{ mbar} \qquad (5.3.11\text{-}8)$$

In Equations 5.311-7 and 8, "u_G" and "u_L" are in cm/sec.

$$\Delta P_{total} = \Delta P_{packing} + \Delta P_{demister}$$

These equations and Figure 5.311-5 give a good estimate of the fluidized bed scrubber pressure drop.

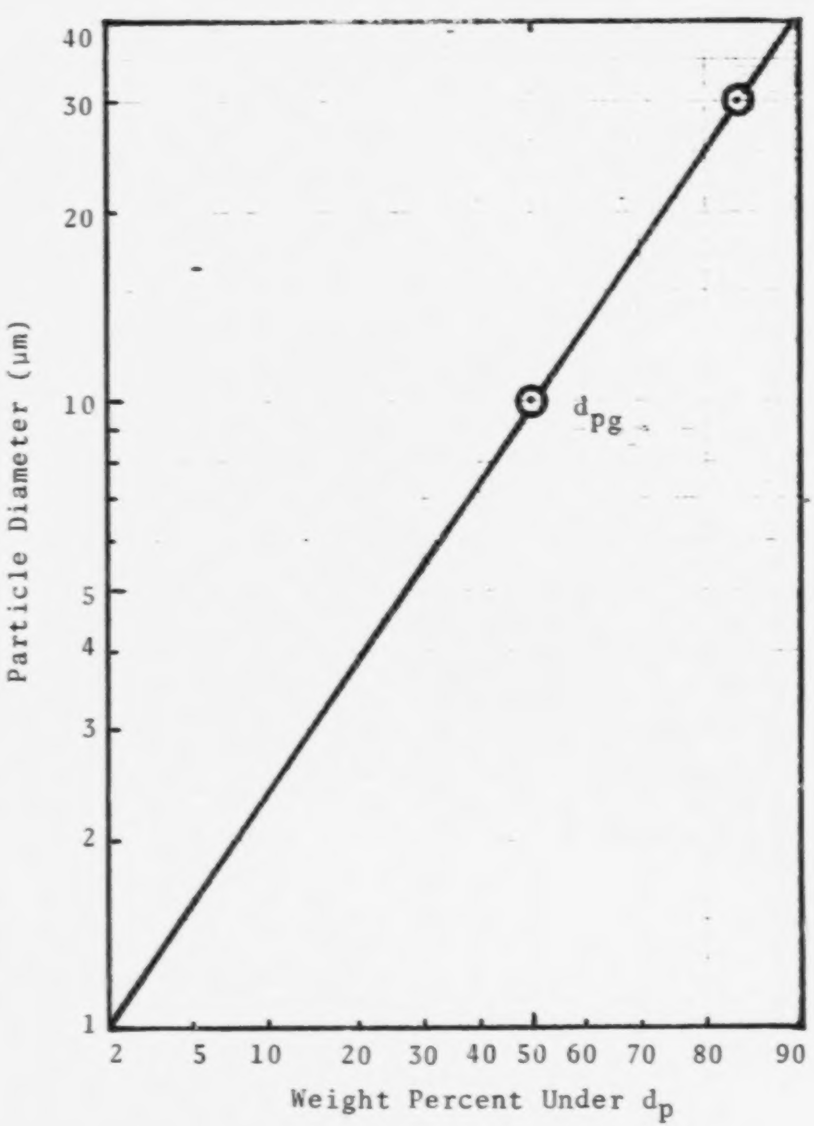

FIGURE 5.3.1-1
ILLUSTRATIVE PARTICLE SIZE DISTRIBUTION

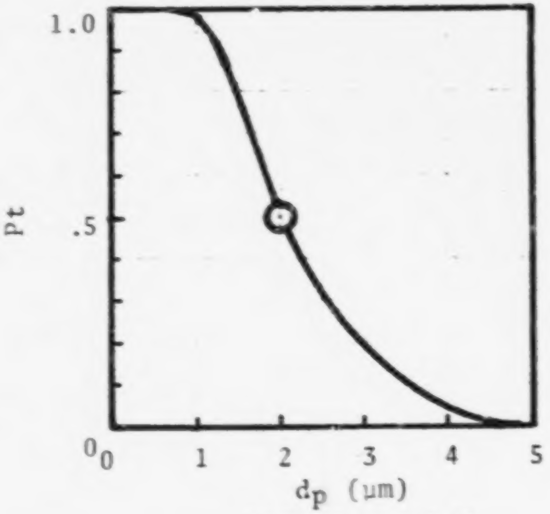

FIGURE 5.3.1-2
ILLUSTRATIVE PENETRATION-DIAMETER RELATIONSHIP

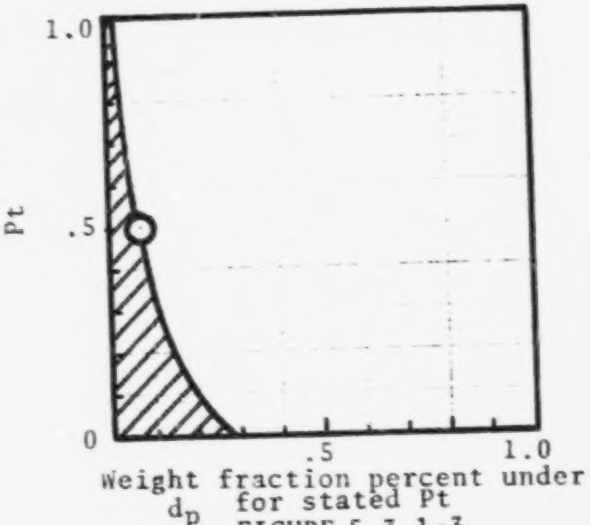

FIGURE 5.3.1-3
GRAPHICAL INTEGRATION FOR OVERALL PENETRATION

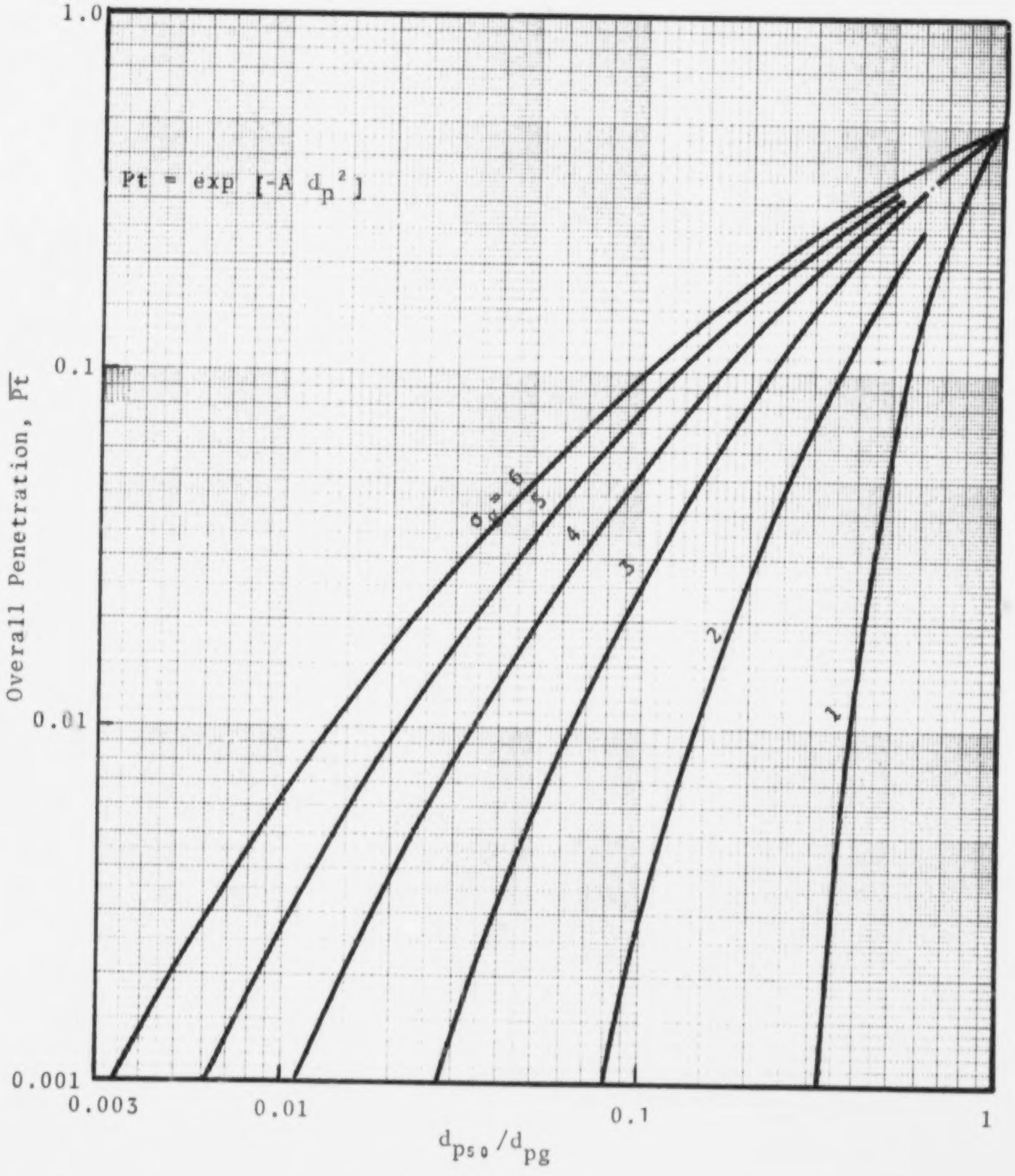

FIGURE 5.3.1-4

OVERALL PENETRATION VERSUS CUT TO MEAN PARTICLE DIAMETER RATIO, FOR LOG NORMAL DUSTS, WITH DUST STANDARD DEVIATION AS PARAMETER

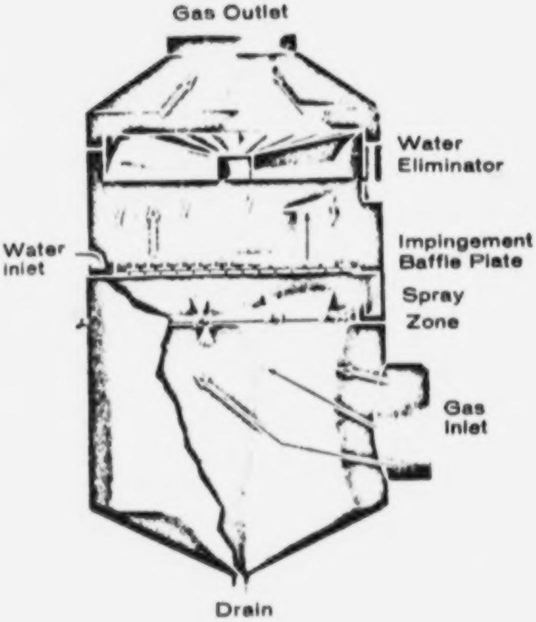

FIGURE 5.3.2-1

IMPINGEMENT BAFFLE WET COLLECTOR. COURTESY PEABODY ENGINEERING CORP.

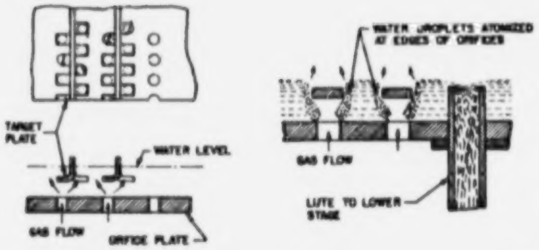

Detail of an impingement baffle stage

Liquor spray formation in an Impingement baffle stage

FIGURE 5.3.2-2

IMPINGEMENT GAS SCRUBBER.(AIHA 1968)

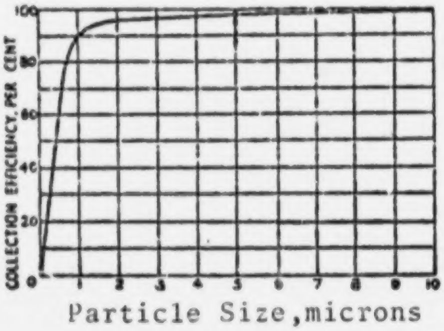

FIGURE 5.3.2-3

GRADE-EFFICIENCY CURVE FOR WET-IMPINGEMENT SCRUBBER. EFFICIENCY AT 5μ= 97 per cent(Stairmand, 1956)

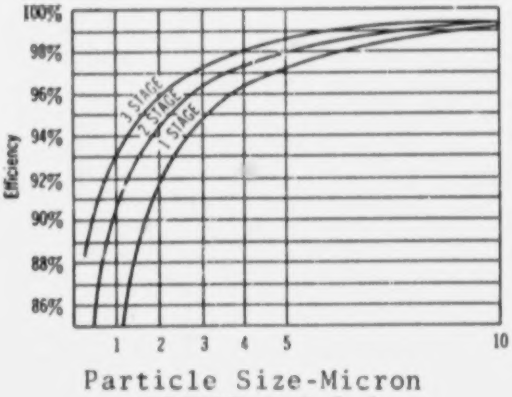

FIGURE 5.3.2-4

STANDARD IMPINJET EFFICIENCY @ PRESSURE DROP OF 4 mbar PER STAGE (SLY CATALOG, 1969)

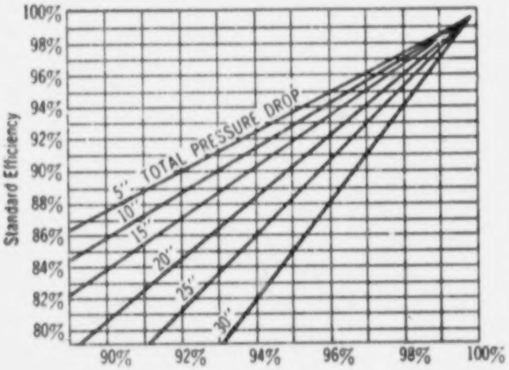

FIGURE 5.3.2-5

HIGH PRESSURE DROP EFFICIENCY SLY CATALOG (1969)

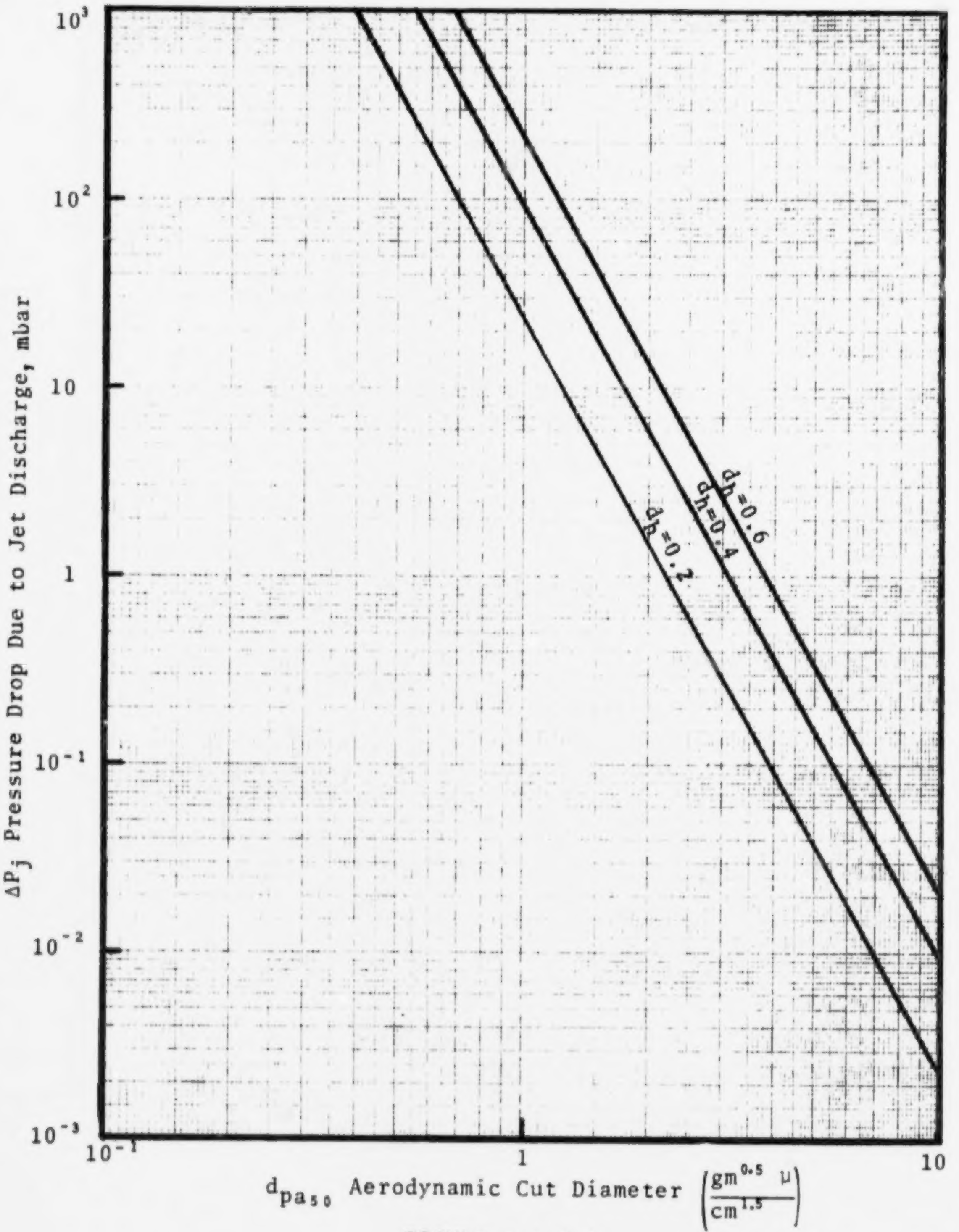

FIGURE 5.3.2-6
PRESSURE DROP IN A WET IMPINGEMENT SCRUBBER VS. PARTICLE CUT DIAMETER WITH PERFORATION DIAMETER AS A PARAMETER. FROM EQUATION 5.3.2-8

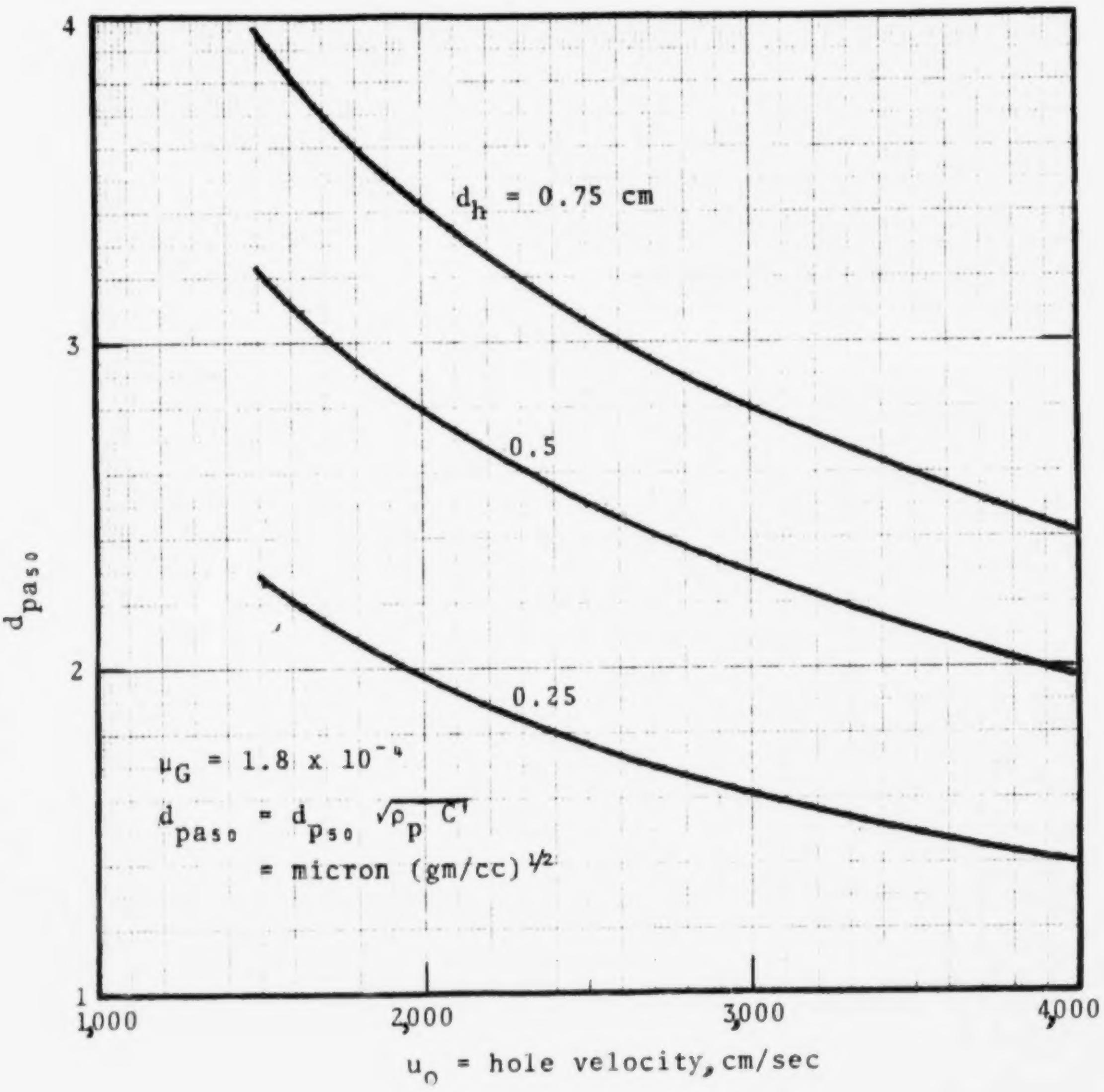

FIGURE 5.3.2-7

PREDICTED IMPINGEMENT PLATE PERFORMANCE, d_{pa50} VS. u_o WITH d_h AS PARAMETER

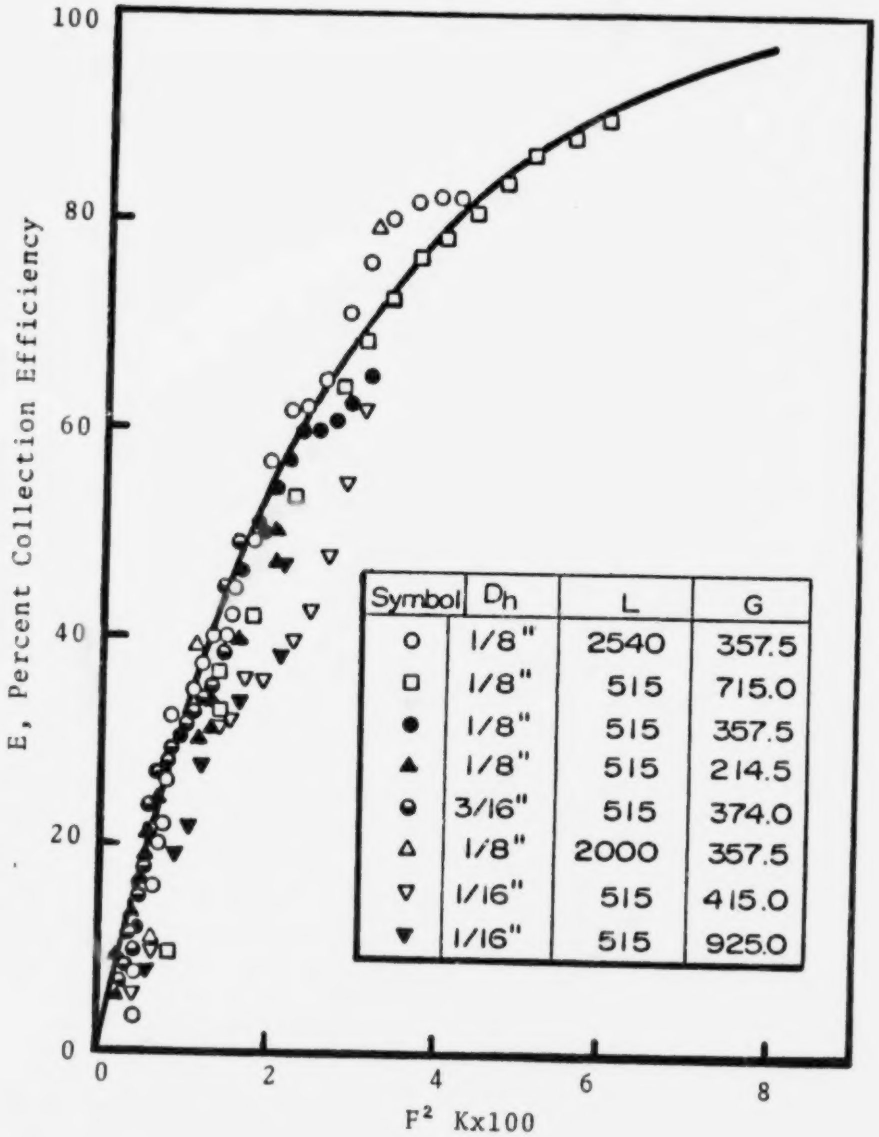

Symbol	D_h	L	G
○	1/8"	2540	357.5
□	1/8"	515	715.0
●	1/8"	515	357.5
▲	1/8"	515	214.5
◒	3/16"	515	374.0
△	1/8"	2000	357.5
▽	1/16"	515	415.0
▼	1/16"	515	925.0

FIGURE 5.3.2-8

COLLECTION EFFICIENCY VS. GENERALIZED PARAMETER IN A SIEVE PLATE COLUMN. AFTER TAHERI AND CALVERT (1968)

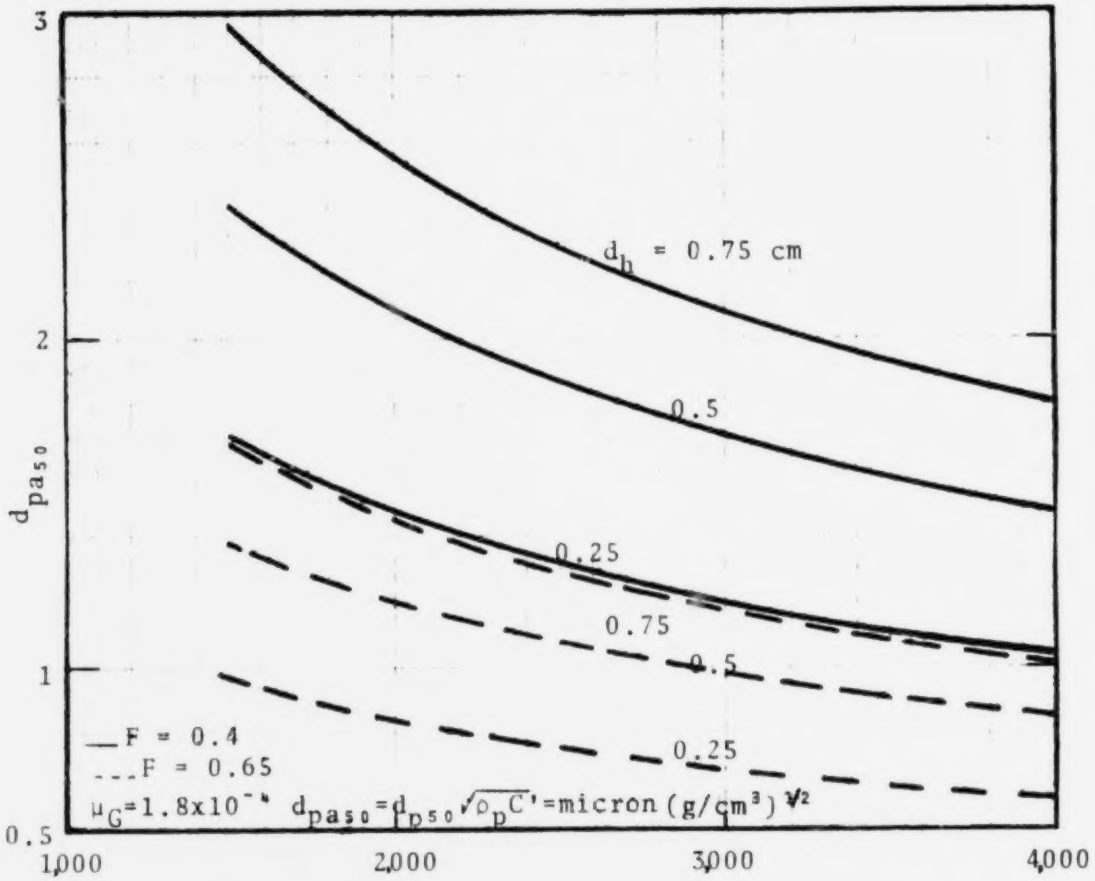

FIGURE 5.3.2-9

PREDICTED SIEVE PLATE PERFORMANCE, d_{pa50} VS. u_o WITH F and d_h AS PARAMETERS, FOR IMPACTION ONLY

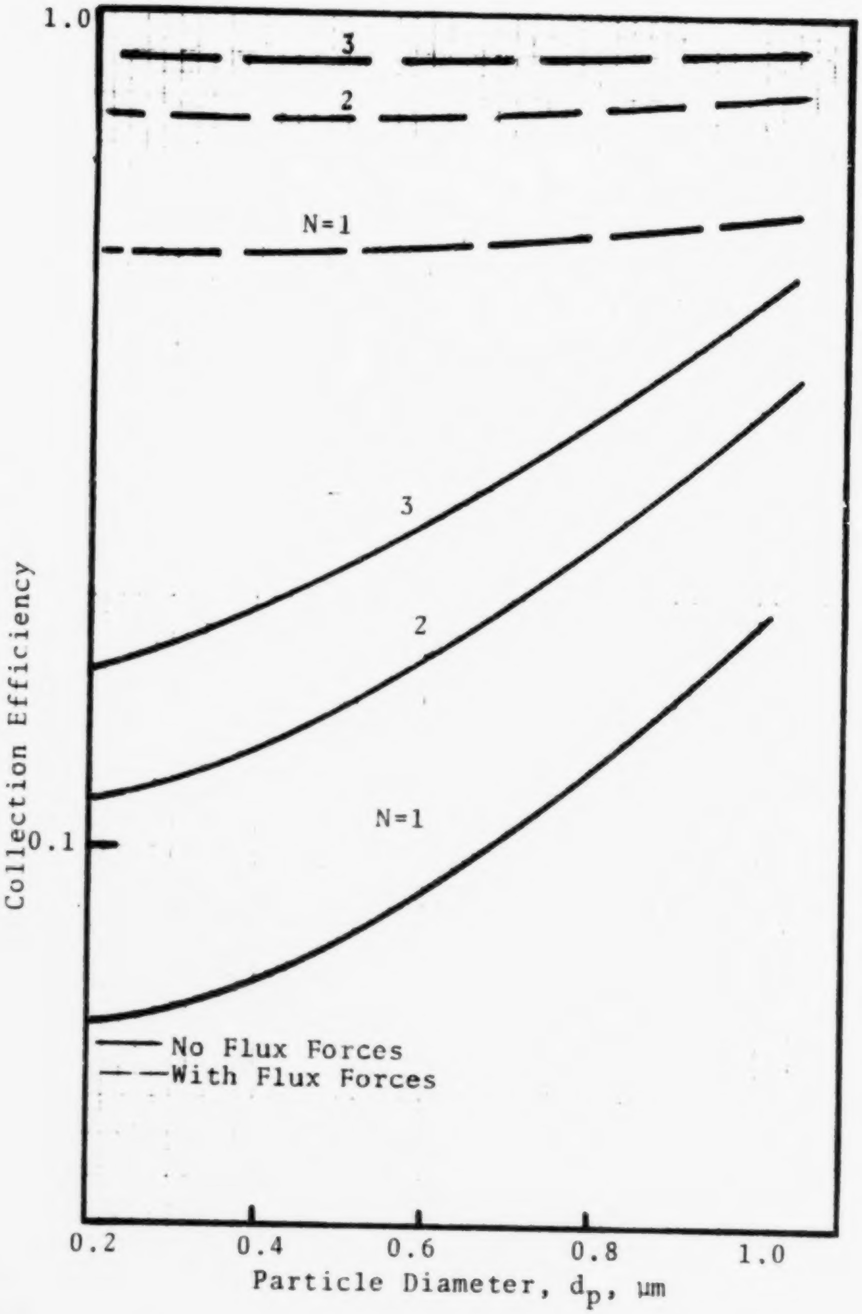

FIGURE 5.3.2-10

COMPARISON OF EFFICIENCY FOR OIL MIST IN SIEVE PLATE COLUMN WITH AND WITHOUT DIFFUSION AND THERMOPHORESIS. PLOT OF "E" VS. "d_p" WITH # OF PLATES,"N",AS PARAMETER

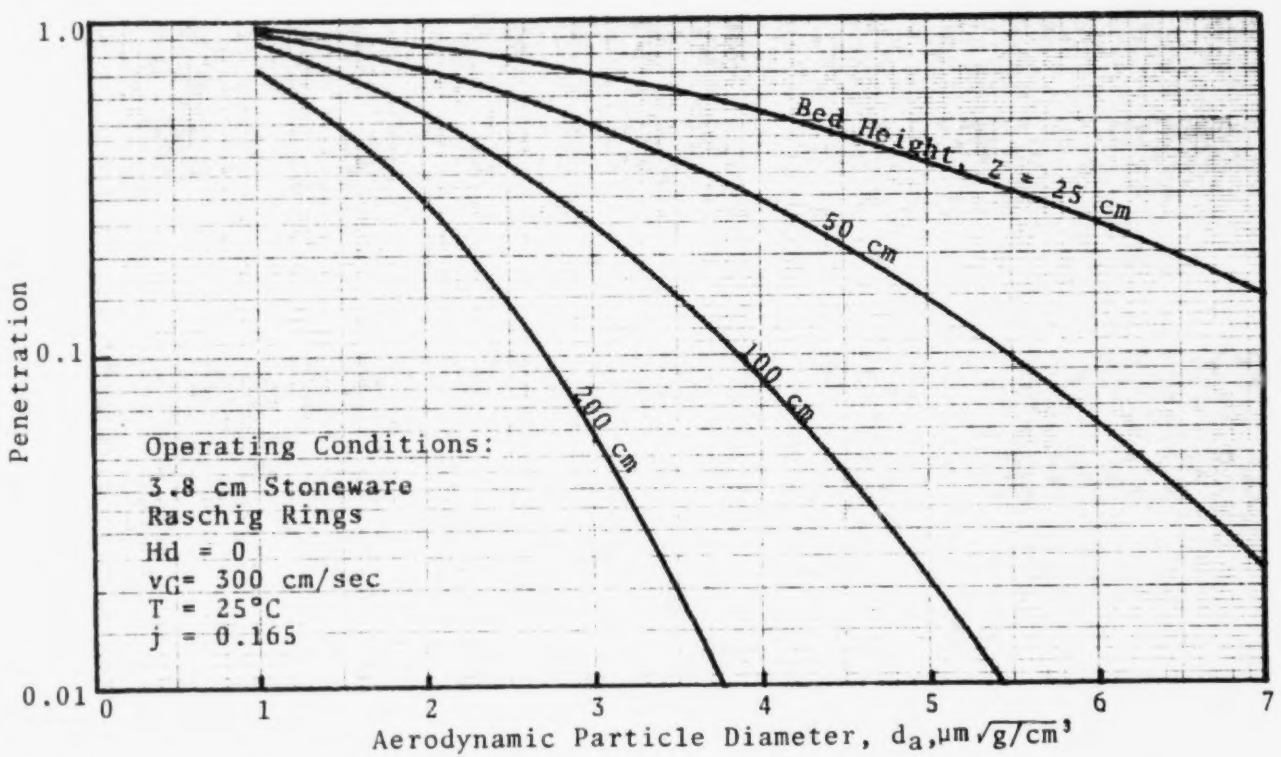

FIGURE 5.3.3-1

PENETRATION VS. AERODYNAMIC PARTICLE DIAMETER WITH BED HEIGHT AS PARAMETER FOR PACKED BED

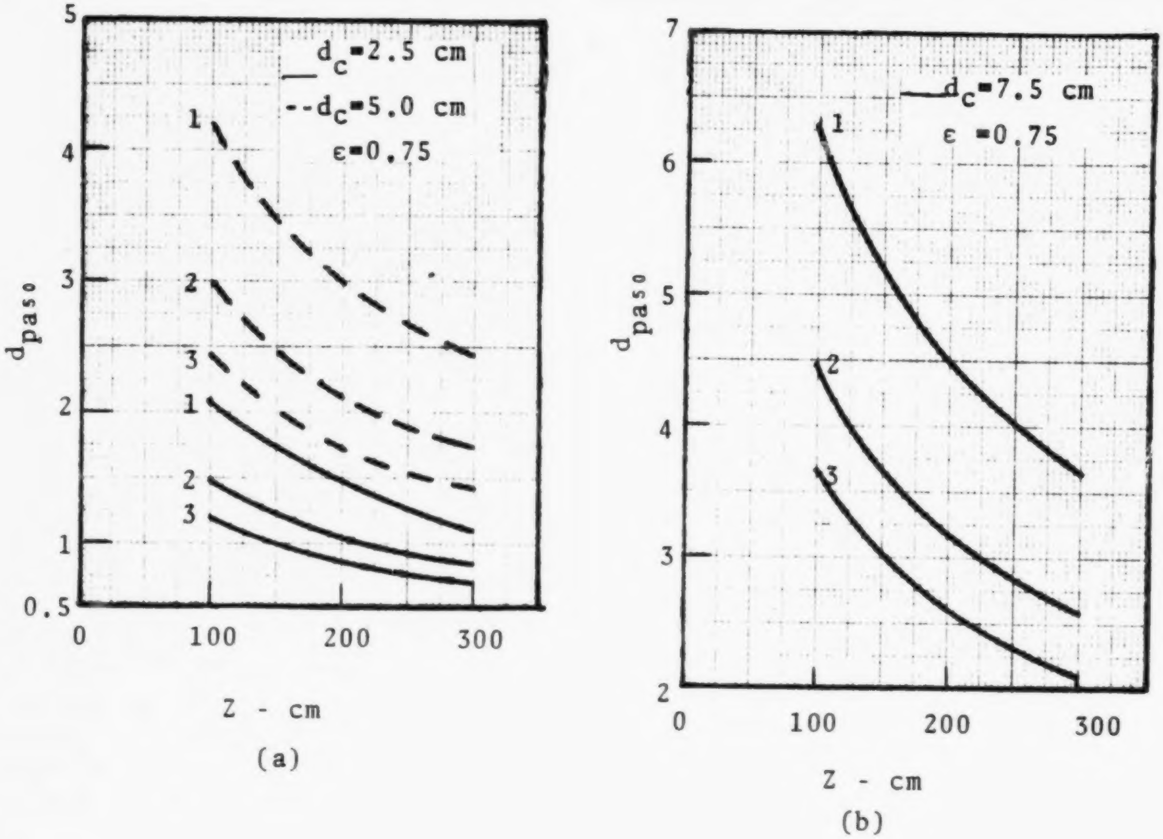

Curve No. 1. u = 150 cm/sec; 2. u = 300 cm/sec; 3. u = 450 cm/sec

d_{pa50} = μm $(g/cm^3)^{1/2}$

FIGURE 5.3.3-2

PREDICTED PACKED BED PERFORMANCE CUT DIAMETER AS A FUNCTION OF GAS VELOCITY, PACKING SIZE, POROSITY, AND DEPTH

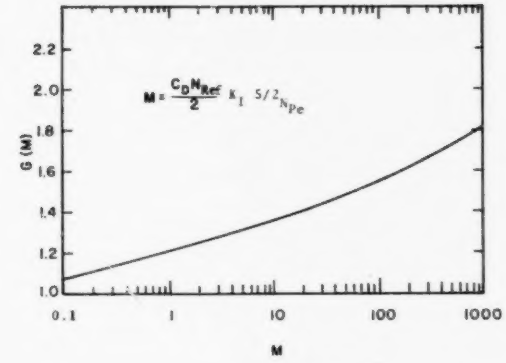

FIGURE 5.3.4-1

G(M) VERSUS "M" FOR TORGESON THEORY

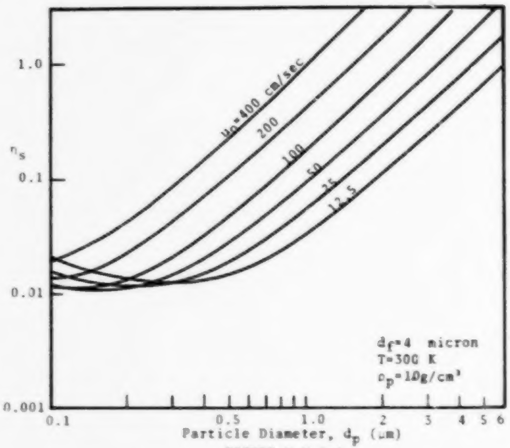

FIGURE 5.3.4-2

SINGLE FIBER EFFICIENCY DUE TO INERTIA, INTERCEPTION AND DIFFUSION, ACCORDING TO TORGESON. FIBER DIAMETER IS 4 MICRONS.

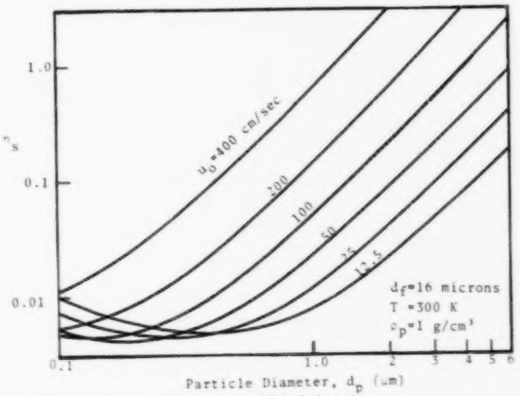

FIGURE 5.3.4-3

SINGLE FIBER EFFICIENCY DUE TO INERTIA, INTERCEPTION AND DIFFUSION, ACCORDING TO TORGESON. FIBER DIAMETER IS 16 MICRONS

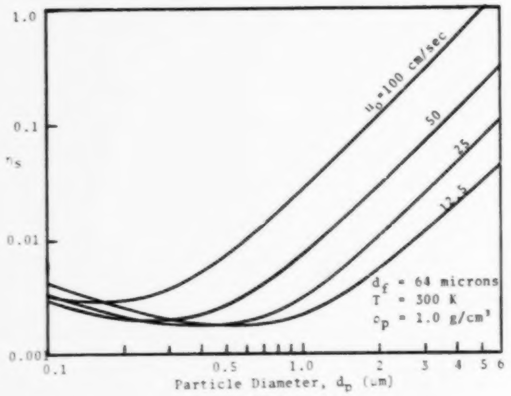

FIGURE 5.3.4-4

SINGLE FIBER EFFICIENCY DUE TO INERTIA, INTERCEPTION AND DIFFUSION, ACCORDING TO TORGESON. FIBER DIAMETER IS 64 MICRONS.

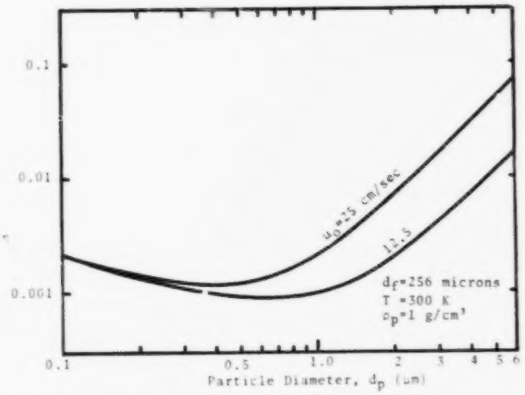

FIGURE 5.3.4-5

SINGLE FIBER EFFICIENCY DUE TO INERTIA INTERCEPTION AND DIFFUSION, ACCORDING TO TORGESON. FIBER DIAMETER IS 256 MICRONS.

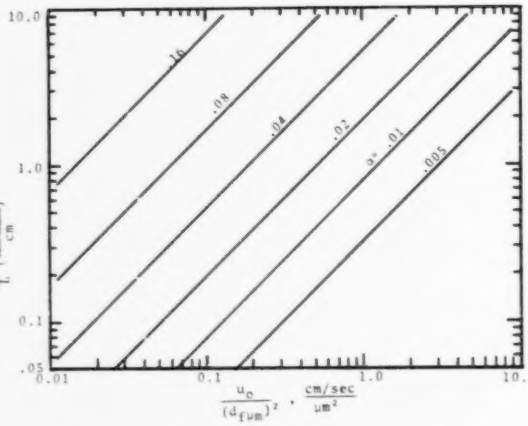

FIGURE 5.3.4-6

PRESSURE DROP PER UNIT THICKNESS, FOR FIBER FILTER AS FUNCTION OF GAS VELOCITY, FIBER DIAMETER, AND BED POROSITY, ACCORDING TO CHEN (1955)

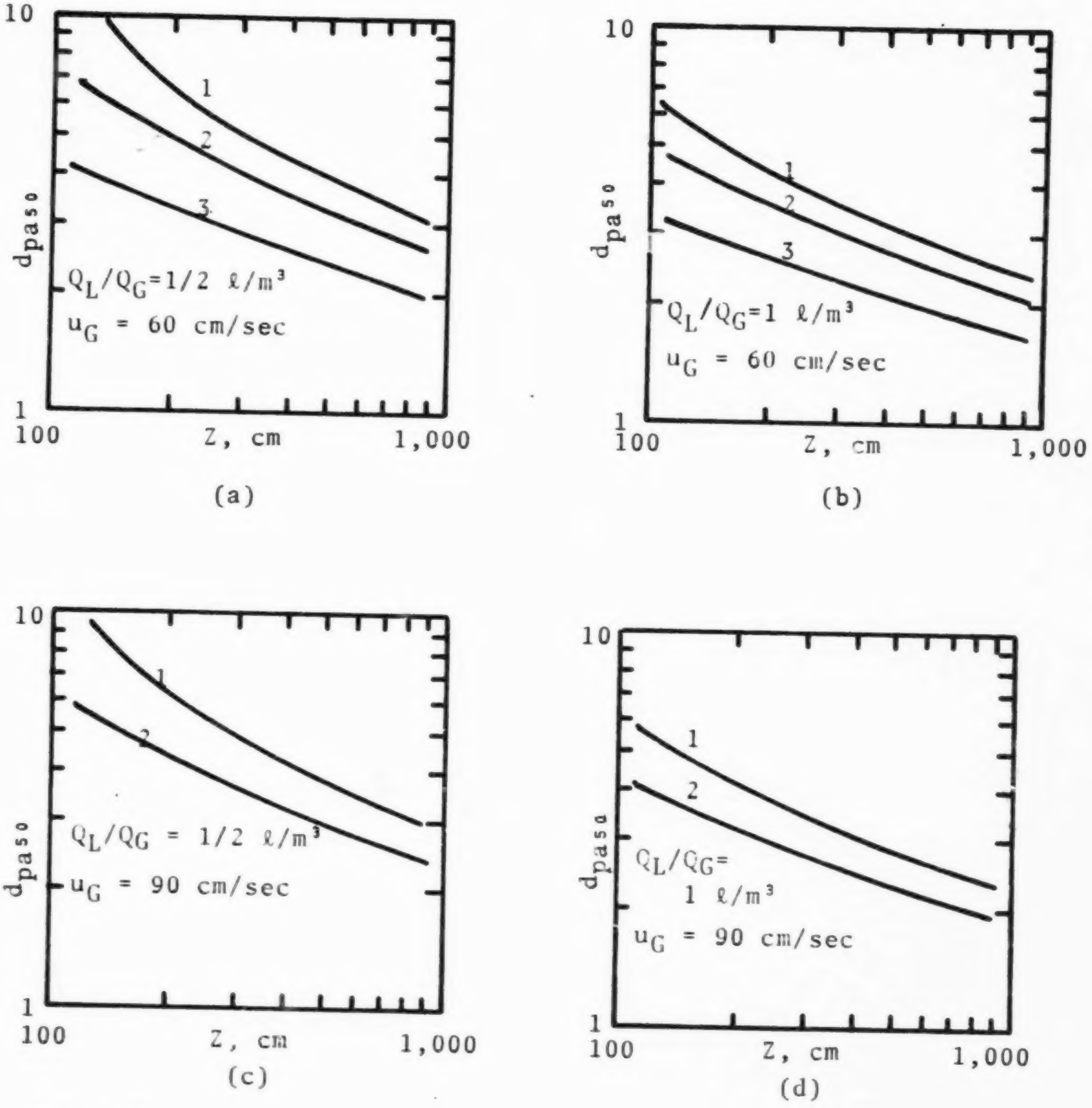

(a) (b) (c) (d)

Curve No:

1. d_d = 1,000 μm; 2. d_d = 500 μm; 3. d_d = 200 μm

FIGURE 5.3.5-1

PREDICTED COUNTER FLOW-SPRAY CHAMBER PERFORMANCE CUT DIAMETER FOR AIR AND WATER FOR SEVERAL CASES, IMPACTION ONLY

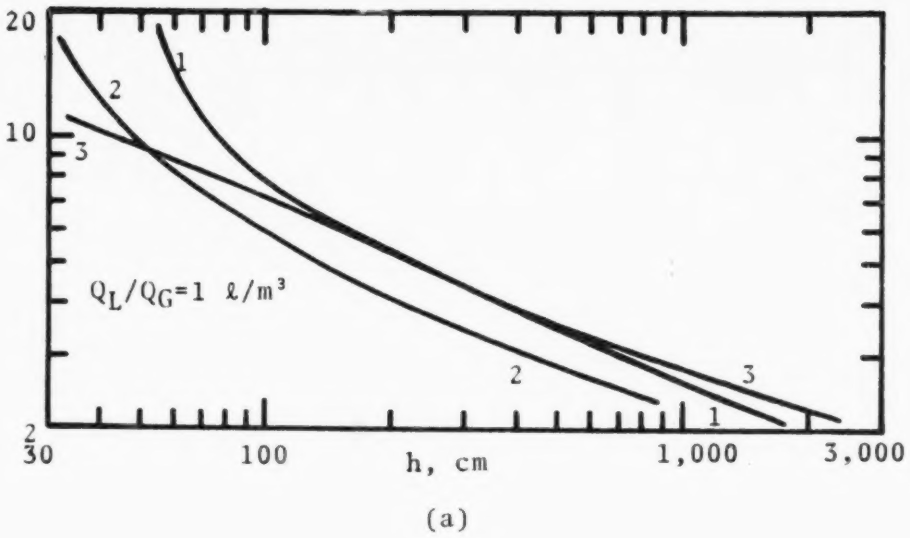

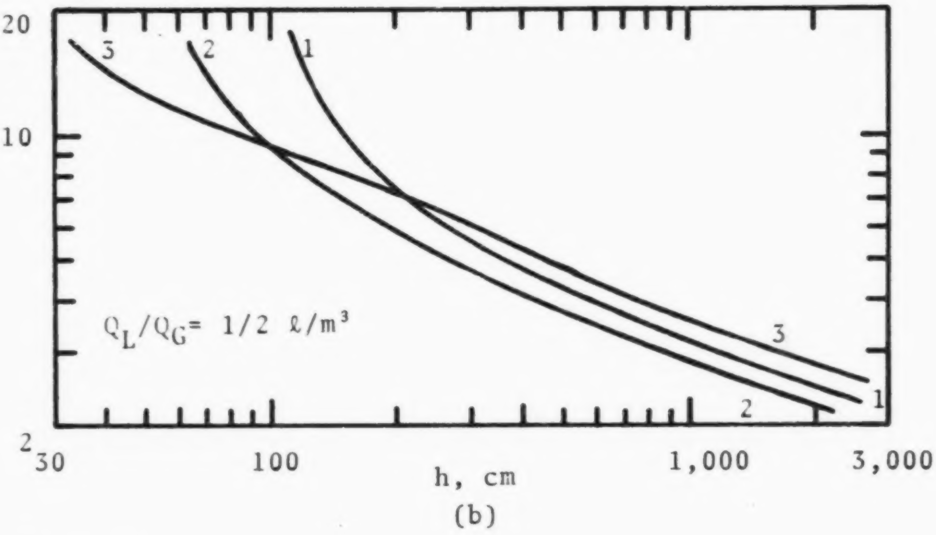

Curve No.
1. d_d=1,000 μm; 2. d_d=500 μm; 3. d_d = 200 μm

FIGURE 5.3.5-2
PREDICTED CROSS-FLOW SPRAY CHAMBER PERFORMANCE CUT DIAMETER FOR AIR AND WATER FOR SEVERAL CASES, IMPACTION ONLY

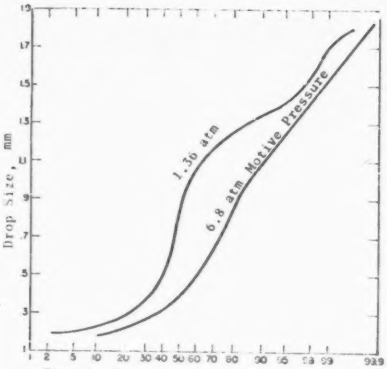

FIGURE 5.3.5-3

DROP SIZE DISTRIBUTION CURVE FOR 12 INCH EJECTOR VENTURI SCRUBBER

Harris (1963)

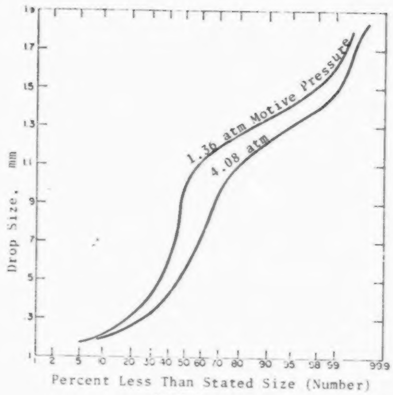

FIGURE 5.3.5-4

DROP SIZE DISTRIBUTION CURVE FOR FOUR INCH EJECTOR VENTURI SCRUBBER

Harris (1963)

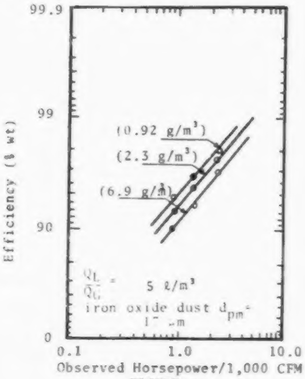

FIGURE 5.3.5-5

OBSERVED ENERGY AND WEIGHT COLLECTION EFFICIENCY CHARACTERISTICS FOR 12" EJECTOR VENTURI SCRUBBER WITH VARYING INLET FUME LOADING. HARRIS (1964)

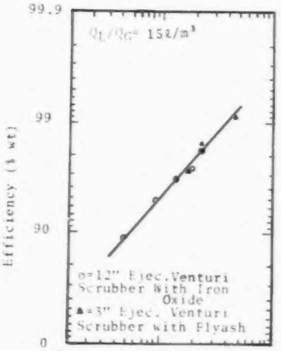

FIGURE 5.3.5-6

OBSERVED ENERGY AND WEIGHT COLLECTION EFFICIENCY CHARACTERISTICS FOR EJECTOR VENTURI SCRUBBERS. HARRIS (1964)

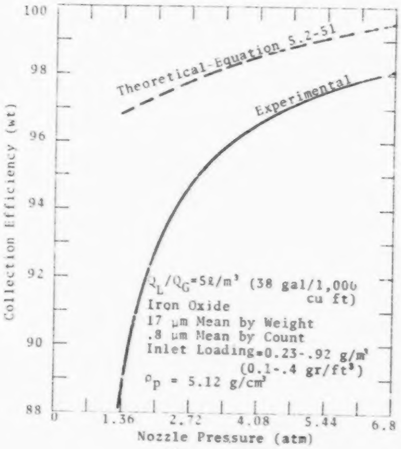

FIGURE 5.3.5-7

SCRUBBING PERFORMANCE FOR 12 IN. EJECTOR VENTURI SCRUBBER.

Harris (1963)

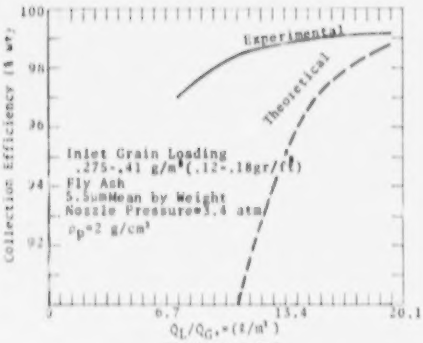

FIGURE 5.3.5-8

SCRUBBING PERFORMANCE OF THREE INCH EJECTOR VENTURI Harris (1963)

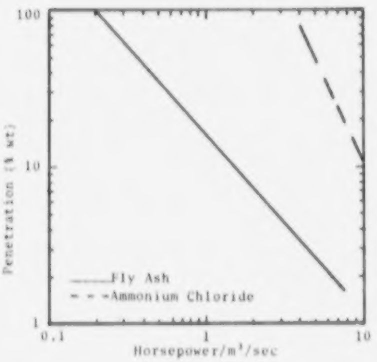

FIGURE 5.3.5-9

OBSERVED ENERGY REQUIREMENT FOR EJECTOR VENTURI SCRUBBER SYSTEM, HARRIS (1966)

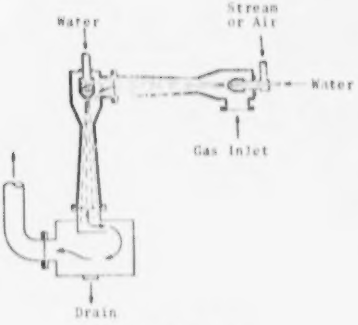

FIGURE 5.3.5-10

SCHUTTE AND KOERTING COMPANY SUB-MICRON SCRUBBER SYSTEM, HARRIS (1966)

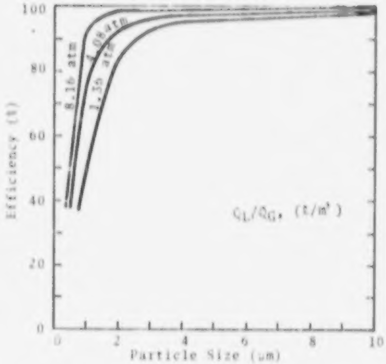

FIGURE 5.3.5-11

FAMILY OF THEORETICAL COLLECTION EFFICIENCY CURVES AT CONSTANT L/G AND VARIOUS MOTIVE PRESSURES HARRIS (1966)

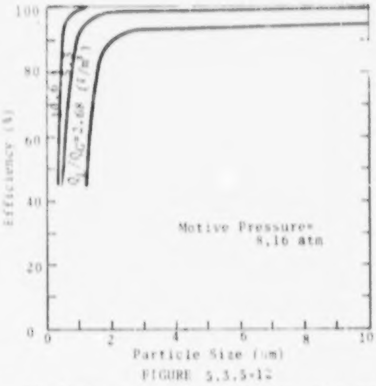

FIGURE 5.3.5-12

FAMILY OF THEORETICAL COLLECTION EFFICIENCY CURVES AT CONSTANT MOTIVE PRESSURE AND VARIOUS Q_L/Q_G RATES. HARRIS (1966)

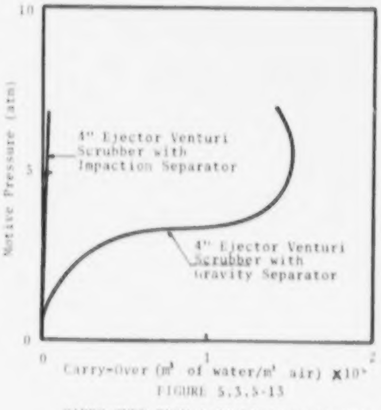

FIGURE 5.3.5-13

CARRY-OVER FROM A 4" EJECTOR VENTURI HARRIS ET AL. (1961)

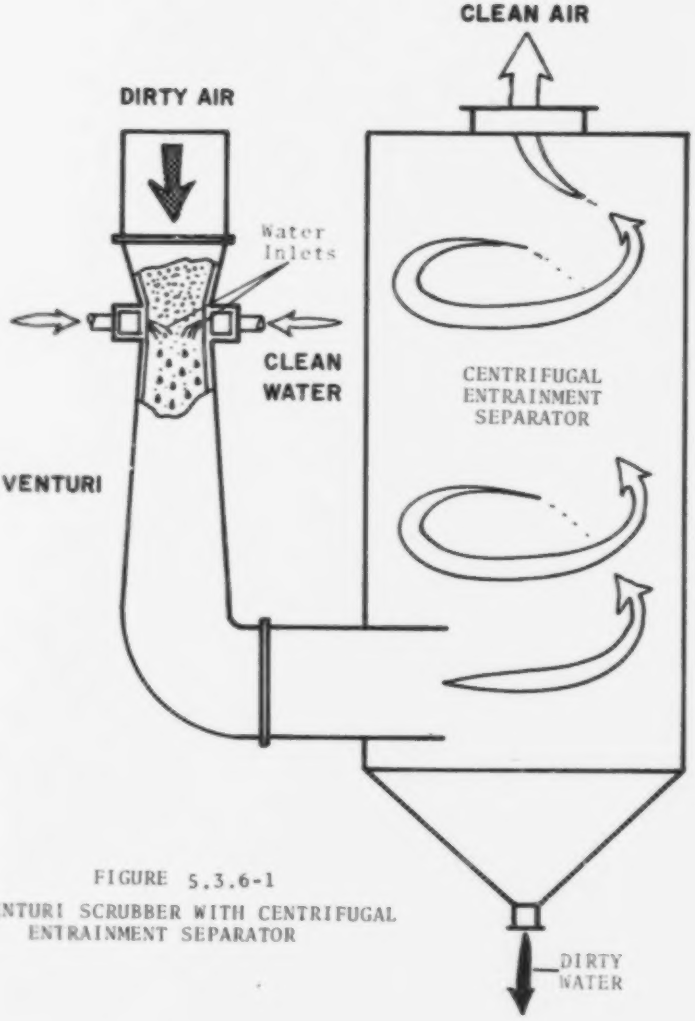

FIGURE 5.3.6-1

VENTURI SCRUBBER WITH CENTRIFUGAL ENTRAINMENT SEPARATOR

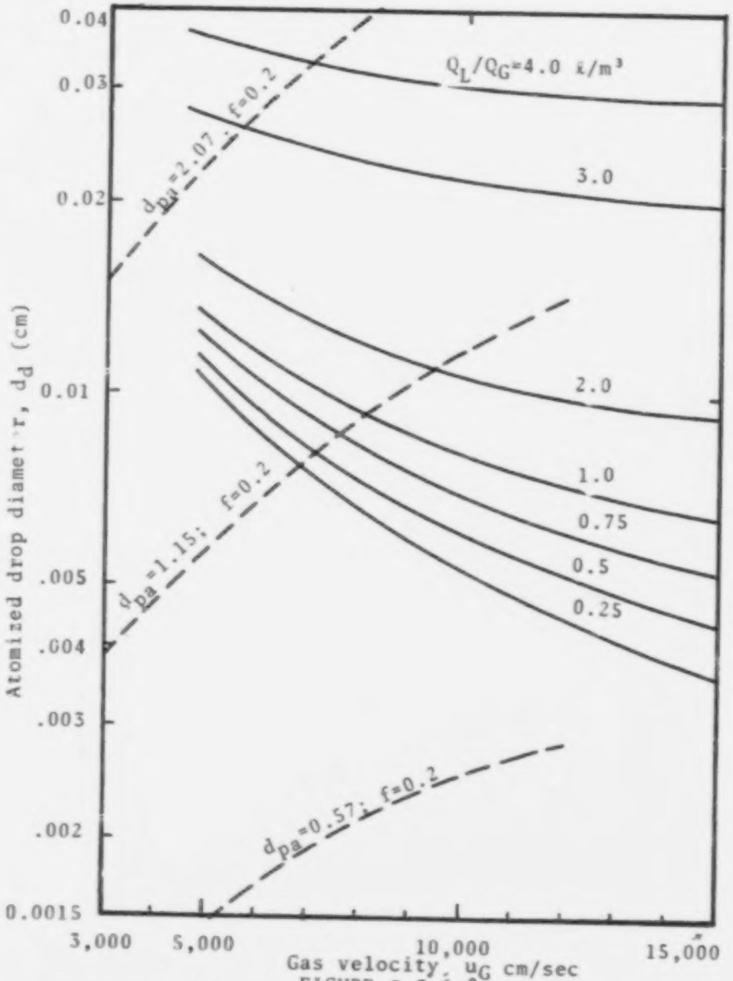

FIGURE 5.3.6-2

OPTIMUM AND ACTUAL DROP DIAMETER VS. GAS VELOCITY

—Calculated from Equation 5.3.6-1

---Optimum Drop Diameter

——— $F(K_{Pt},f)=[-0.7-K_{Pt}f+1.4\ln(\frac{K_{Pt}f+0.7}{0.7})+(\frac{0.49}{0.7+K_{Pt}f})]\ \frac{1}{K_{Pt}}$

– – – – $F(K_{Pt},f) = -0.156\ K_{Pt}f^2$

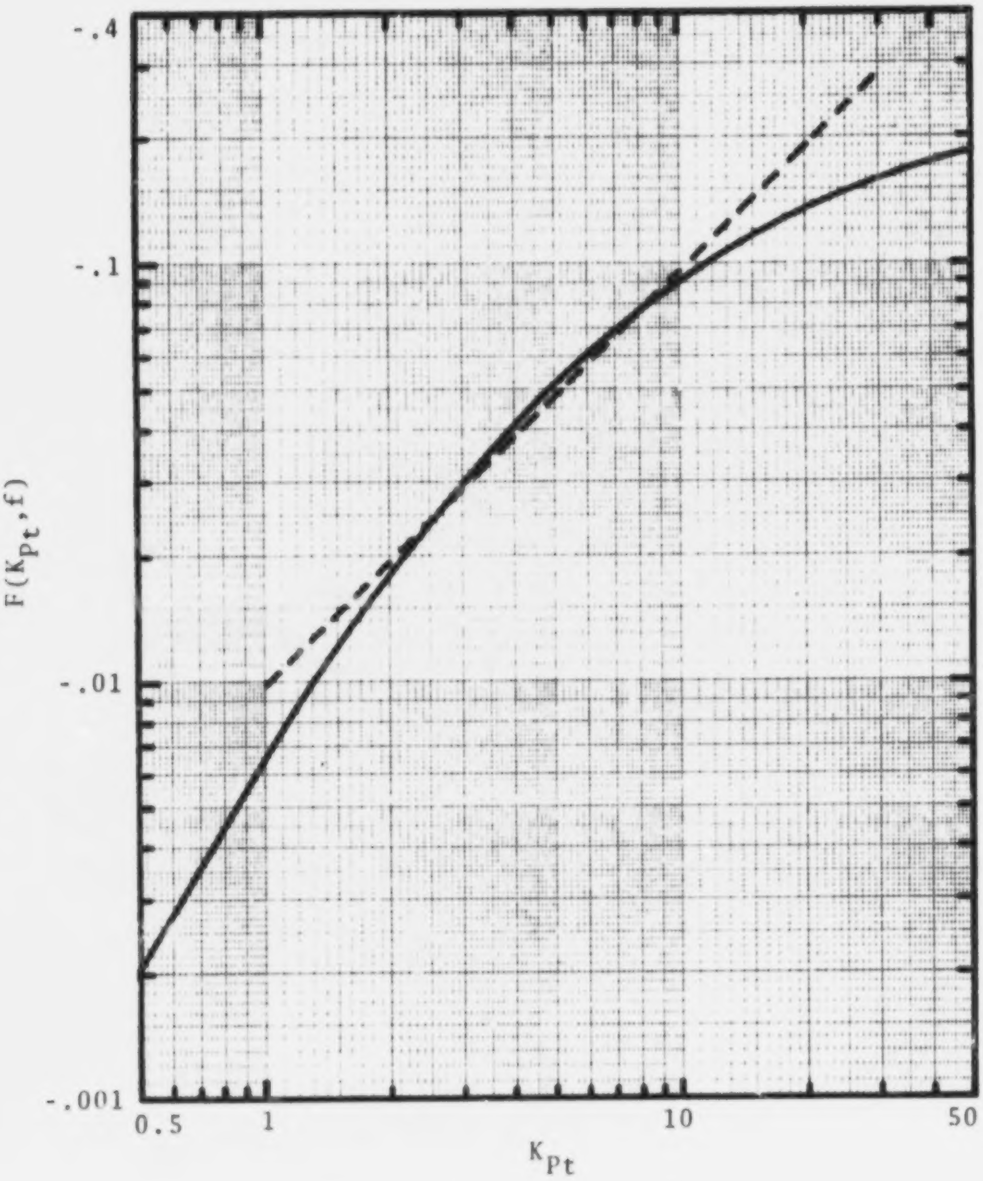

FIGURE 5.3.6-3

$F(K_{Pt},f)$ VERSUS K_{Pt} FOR $f = 0.25$

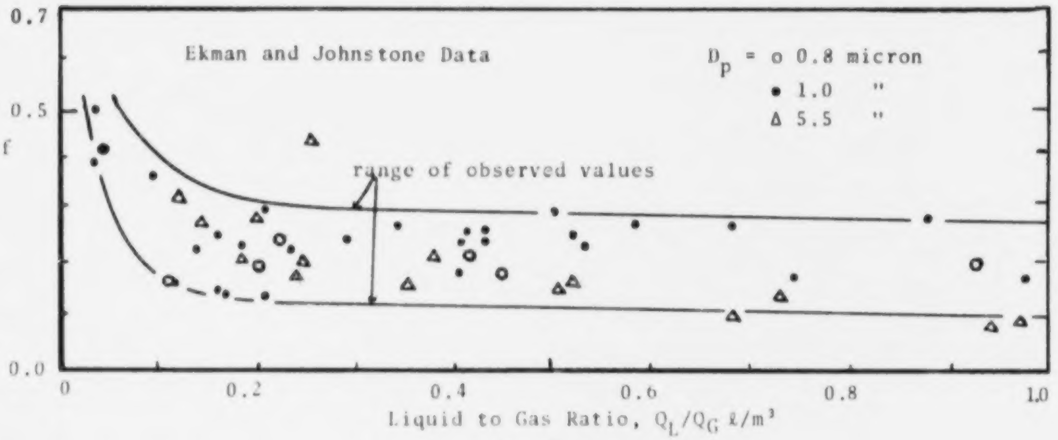

FIGURE 5.3.6-4

VALUES OF "f" VERSUS
LIQUID TO GAS RATIO FOR DIOCTYL PHTHALATE PARTICLES

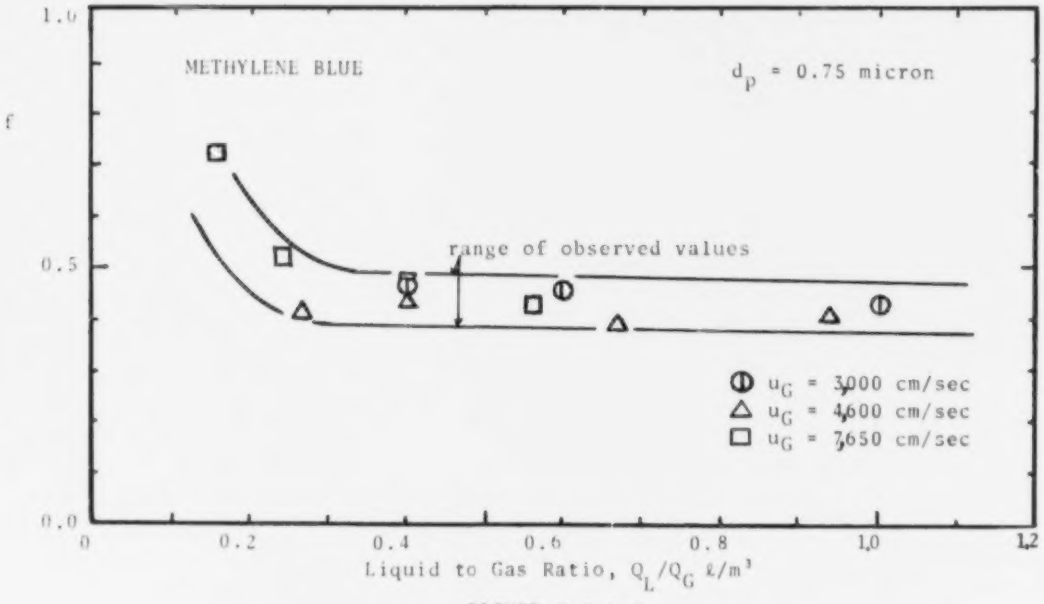

FIGURE 5.3.6-5
VALUES OF "f" VERSUS
LIQUID TO GAS RATIO FOR METHYLENE BLUE PARTICLES

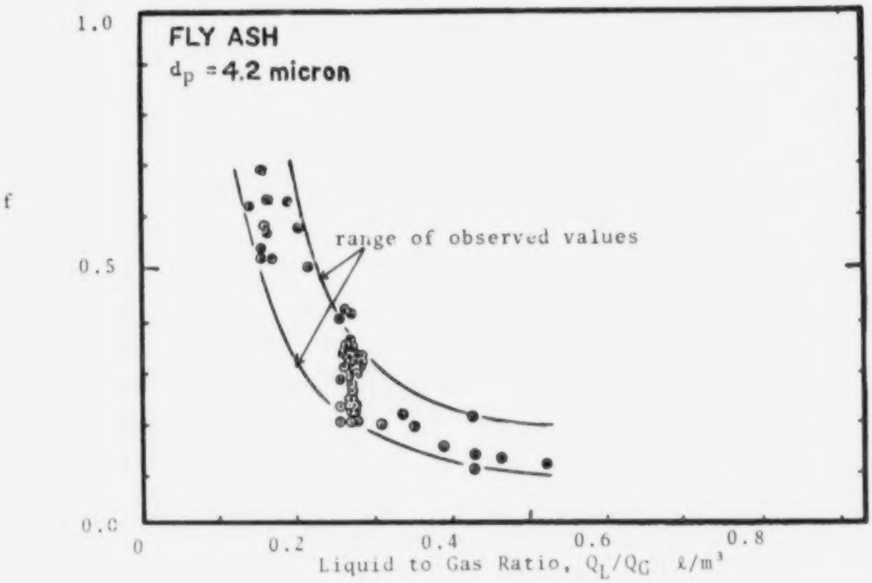

FIGURE 5.3.6-6

VALUES OF "f" VERSUS
LIQUID TO GAS RATIO FOR FLY ASH

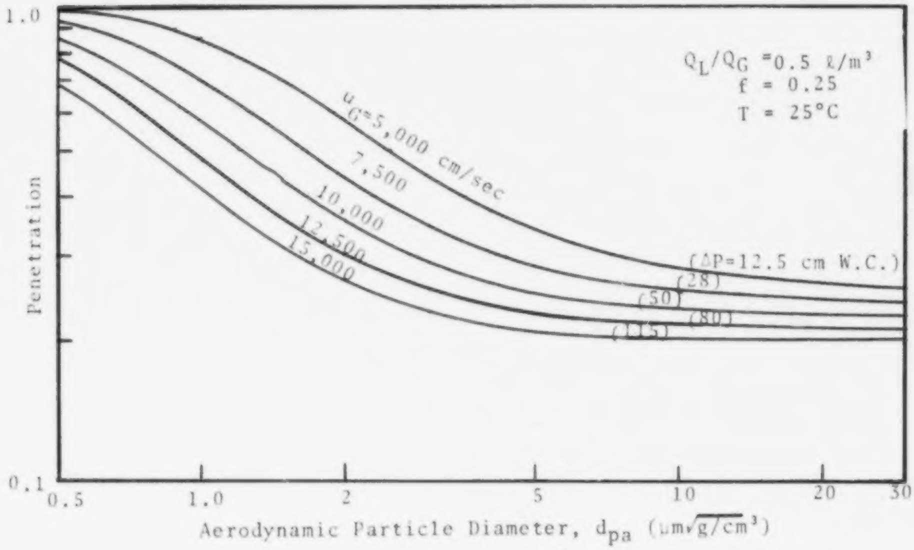

FIGURE 5.3.6-7

VENTURI SCRUBBER PENETRATION VS.
AERODYNAMIC PARTICLE DIAMETER WITH GAS VELOCITY AS PARAMETER

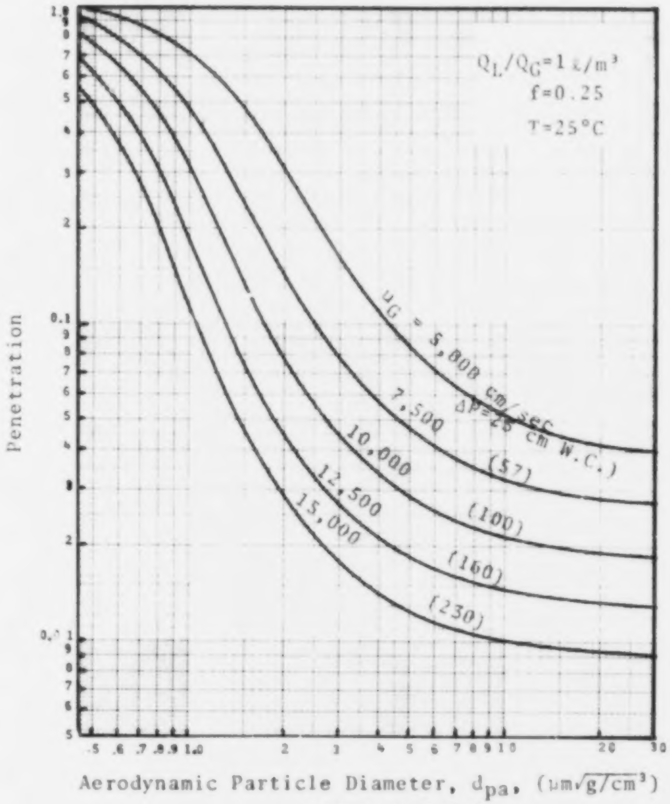

FIGURE 5.3.6-8

VENTURI SCRUBBER PENETRATION VS.
AERODYNAMIC PARTICLE DIAMETER WITH GAS
VELOCITY AS PARAMETER

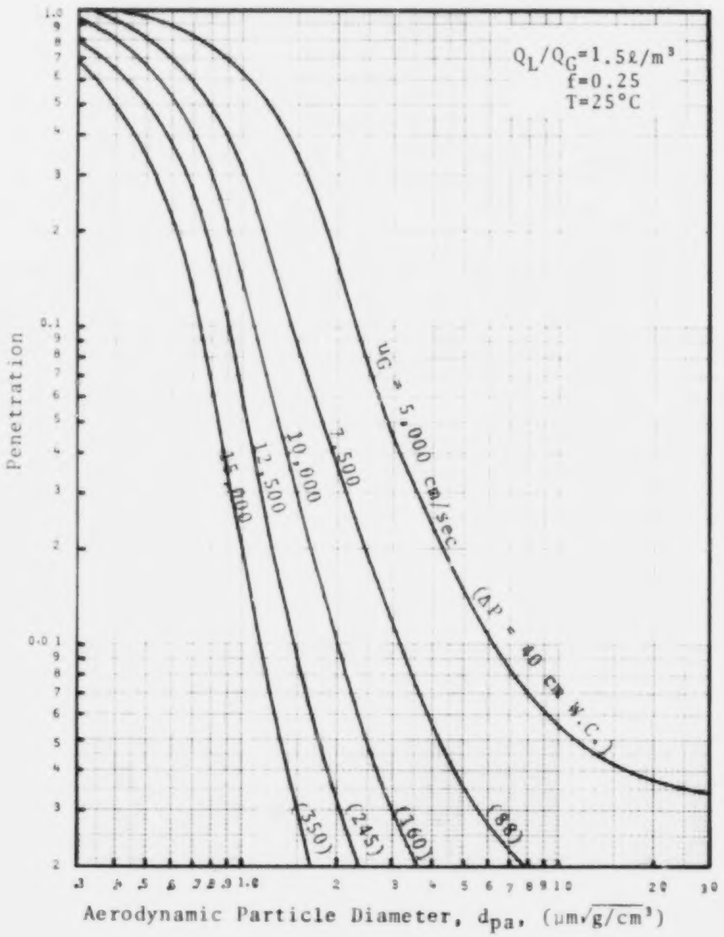

FIGURE 5.3.6-9

VENTURI SCRUBBER PENETRATION VS.
AERODYNAMIC PARTICLE DIAMETER WITH GAS
VELOCITY AS PARAMETER

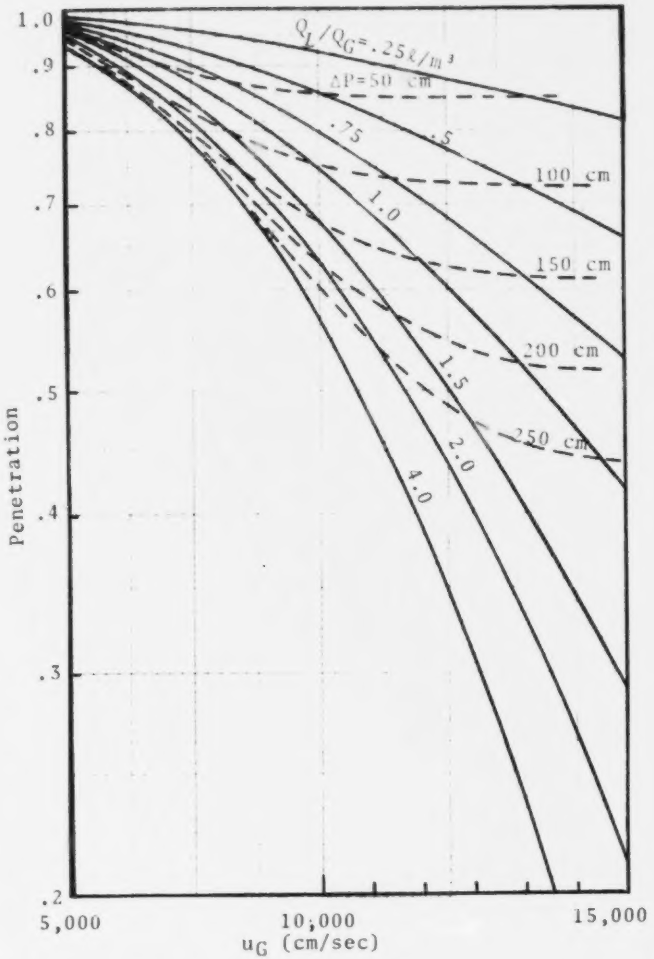

FIGURE 5.3.6-10
VENTURI SCRUBBER PENETRATION VS. GAS THROAT VELOCITY WITH LIQUID TO GAS RATIO AND PRESSURE DROP AS PARAMETERS

$d_{pa} = d_p\sqrt{C' \rho_p} = 0.5\mu\sqrt{g/cm^3}$

f = 0.25

Calculated from
Equations 5.3.6-5 and 5.3.6-6

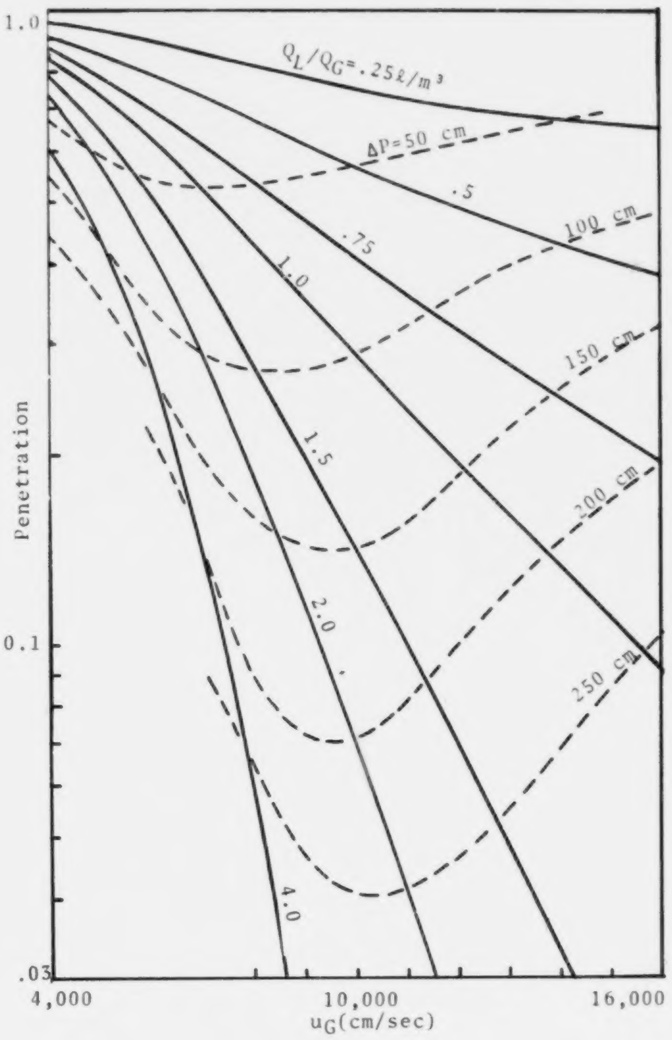

FIGURE 5.3.6-11

VENTURI SCRUBBER PENETRATION VS. GAS THROAT VELOCITY WITH LIQUID TO GAS RATIO AND PRESSURE DROP AS PARAMETERS

$d_{pa} = d_p\sqrt{C' \rho_p} = 1\mu m\sqrt{g/cm^3}$; f = 0.25
Calculated from Equations 5.3.6-5 and 5.3.6-6

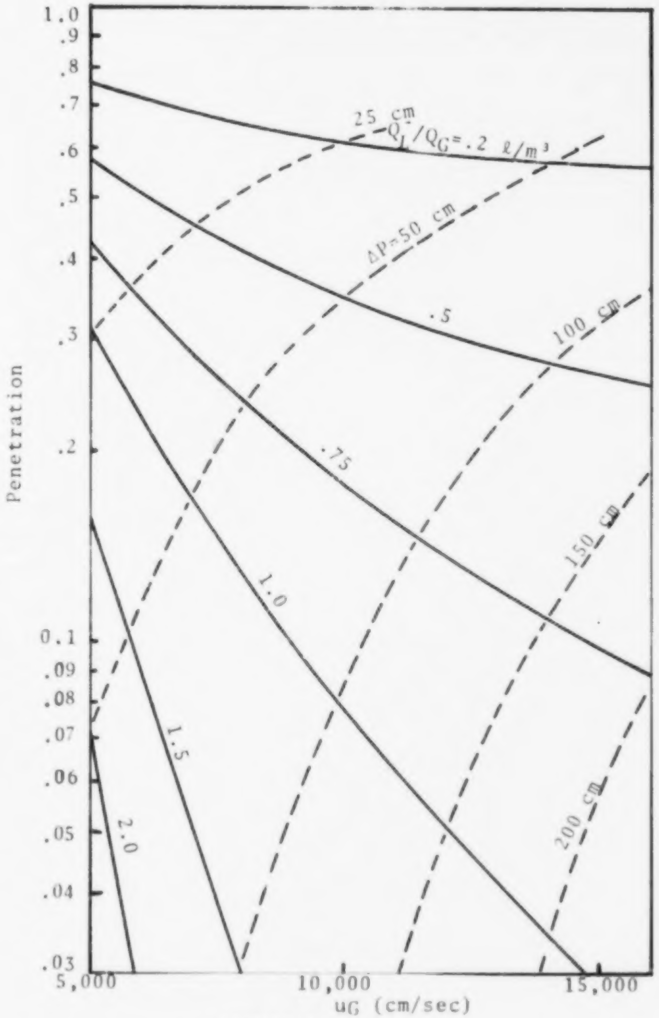

FIGURE 5.3.6-12

VENTURI SCRUBBER PENETRATION VS. GAS THROAT VELOCITY WITH LIQUID TO GAS RATIO AND PRESSURE DROP AS PARAMETERS

$d_{pa} = d_p\sqrt{C'\ \rho_p} = 2\ \mu m\sqrt{g/cm^3}$; f = 0.25

Calculated from Equations 5.3.6-5 and 5.3.6-6

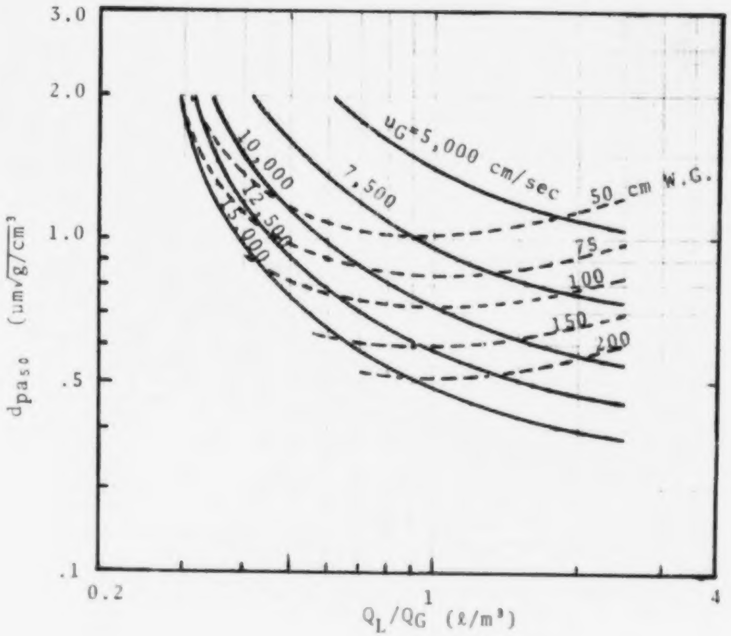

FIGURE 5.3.6-13

PREDICTED VENTURI PERFORMANCE,
d_{pa50} VS. Q_L/Q_G WITH "u_G" PARAMETER
AND ΔP PARAMETER

COMPUTED FROM EQUATION 5.3.6-5 and 5.3.6-6
WITH f = 0.25
ρ_L=1.0
μ_G= 1.8x10⁻⁴

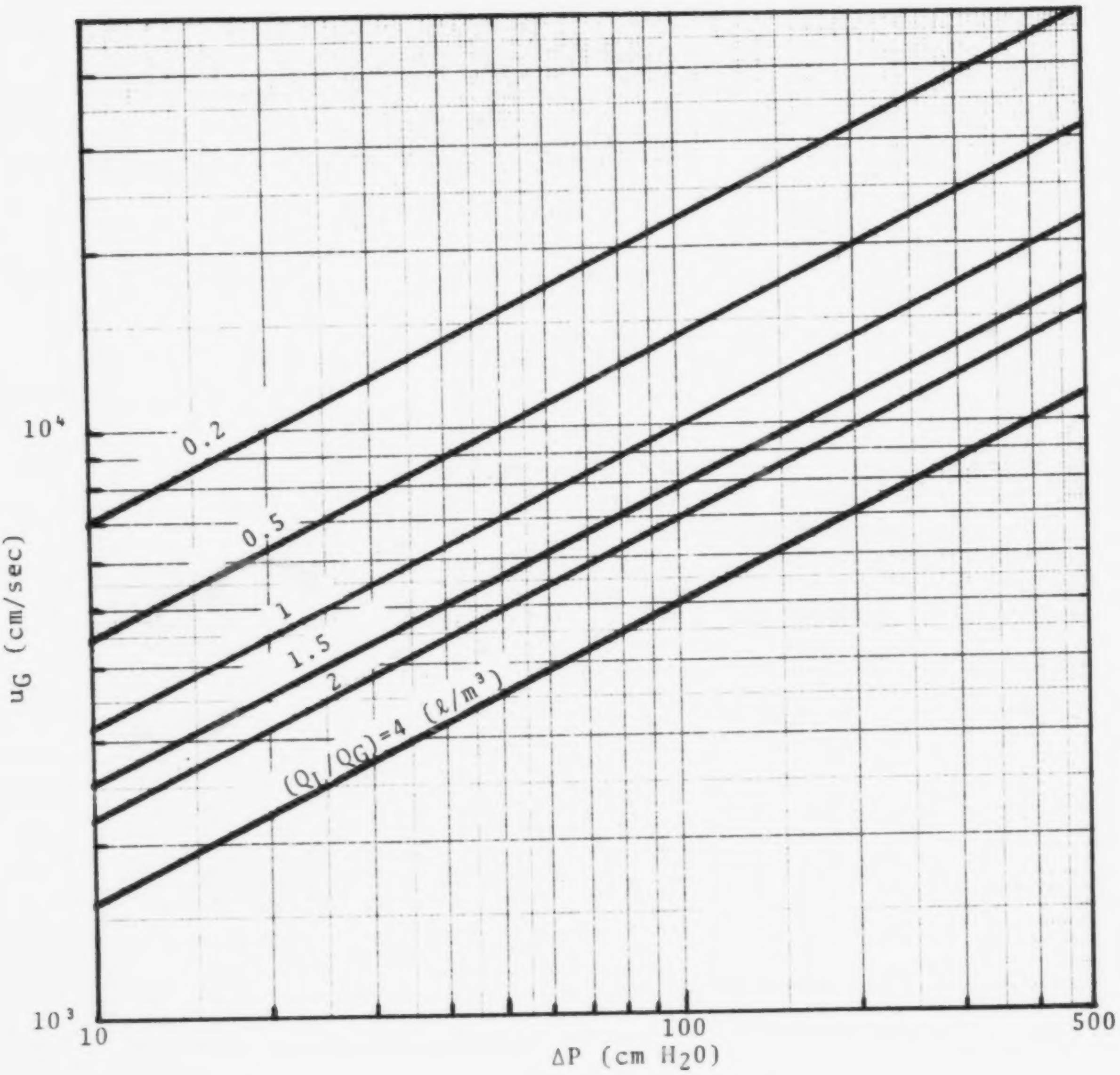

FIGURE 5.3.6-14

PREDICTED PRESSURE DROP FOR VENTURI WITH STANDARD AIR AND WATER

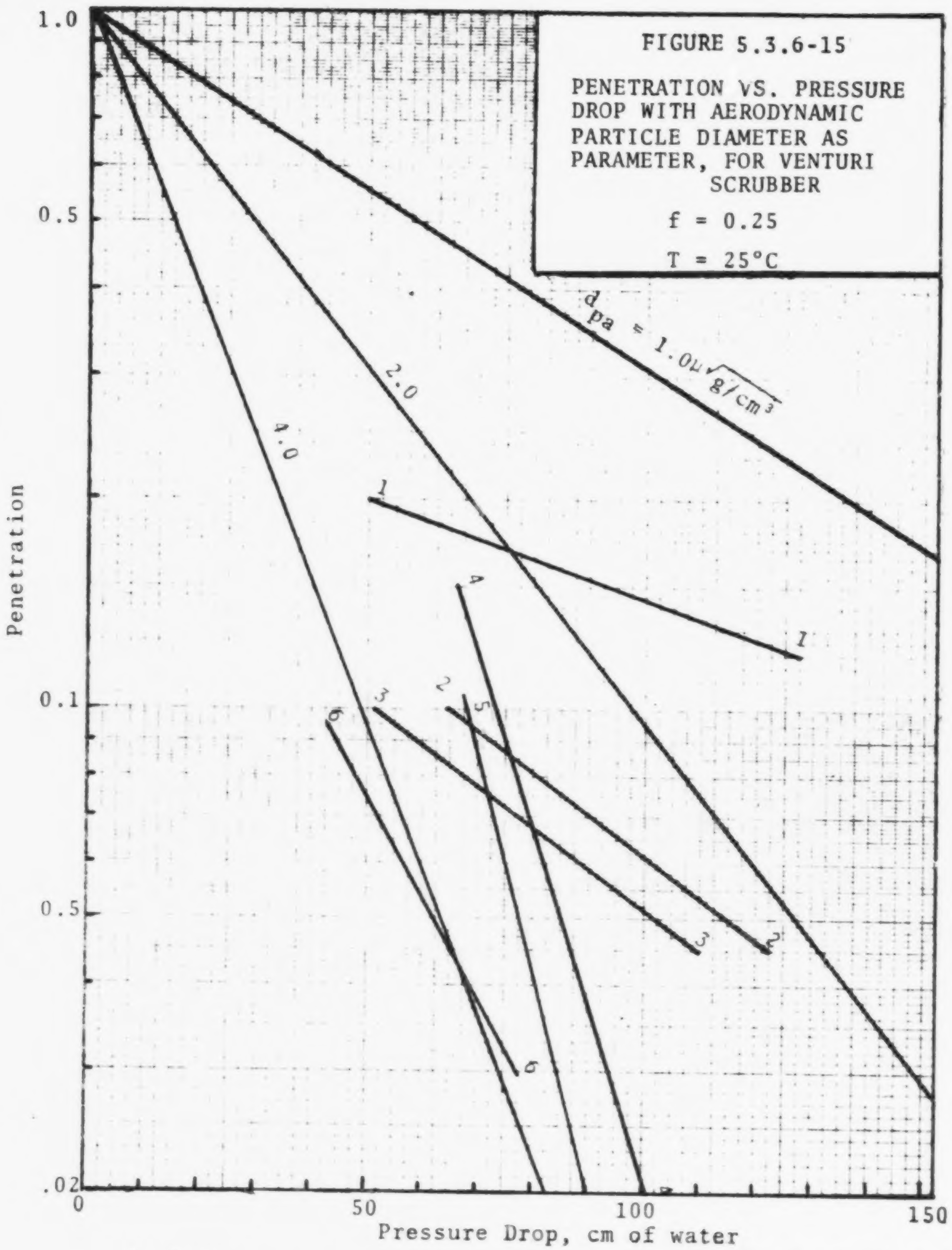

FIGURE 5.3.6-15

PENETRATION VS. PRESSURE DROP WITH AERODYNAMIC PARTICLE DIAMETER AS PARAMETER, FOR VENTURI SCRUBBER

f = 0.25

T = 25°C

1 Basse
2 Taheri & Haines (1968)
3 Taheri & Haines (1968)
4 MRI Handbook (1970)
5 MRI Handbook (1970)
6 Basse

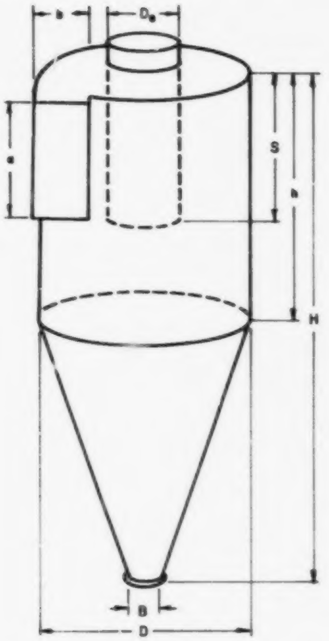

FIGURE 5.3.7-1
TYPICAL CYCLONE COLLECTOR

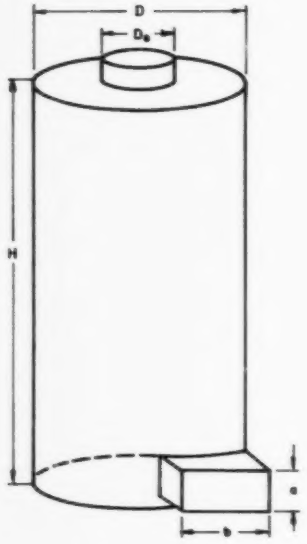

FIGURE 5.3.7-2
TYPICAL CYLINDRICAL CENTRIFUGAL SCRUBBER

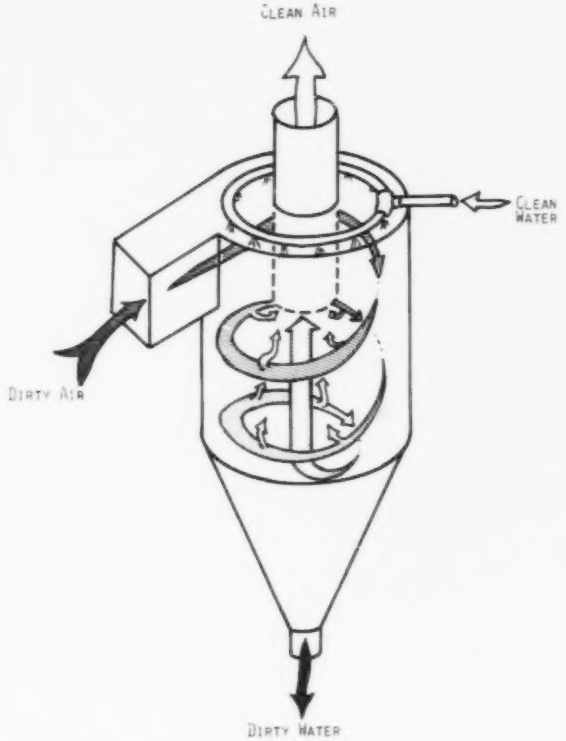

FIGURE 5.3.7-3
CONVERTED CYCLONE

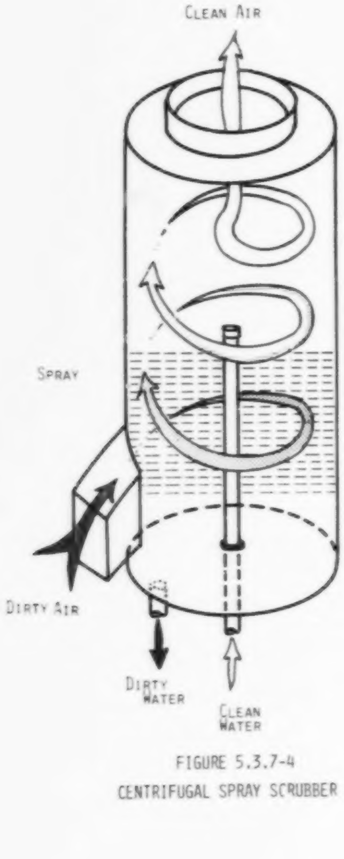

FIGURE 5.3.7-4
CENTRIFUGAL SPRAY SCRUBBER

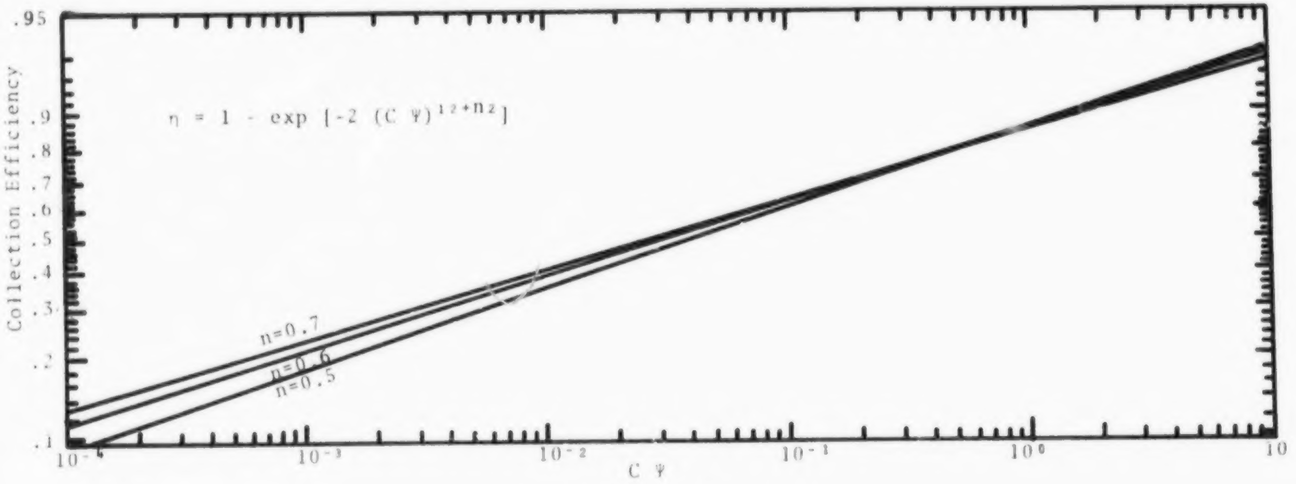

FIGURE 5.3.7-5
GENERALIZED CYCLONE EFFICIENCY CURVE

FIGURE 5.3.7-6
DIFFERENTIAL VOLUME OF A SPRAY
CENTRIFUGAL

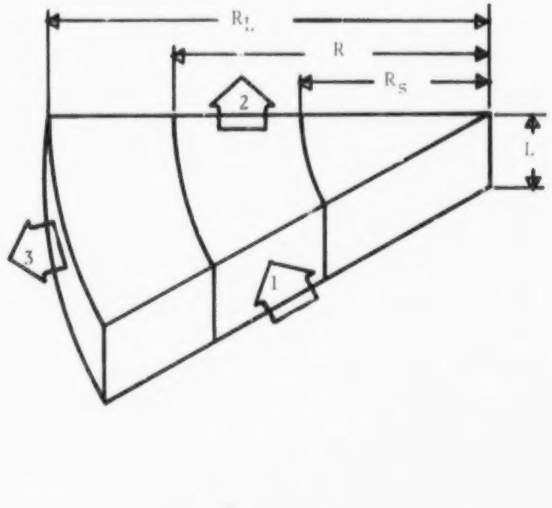

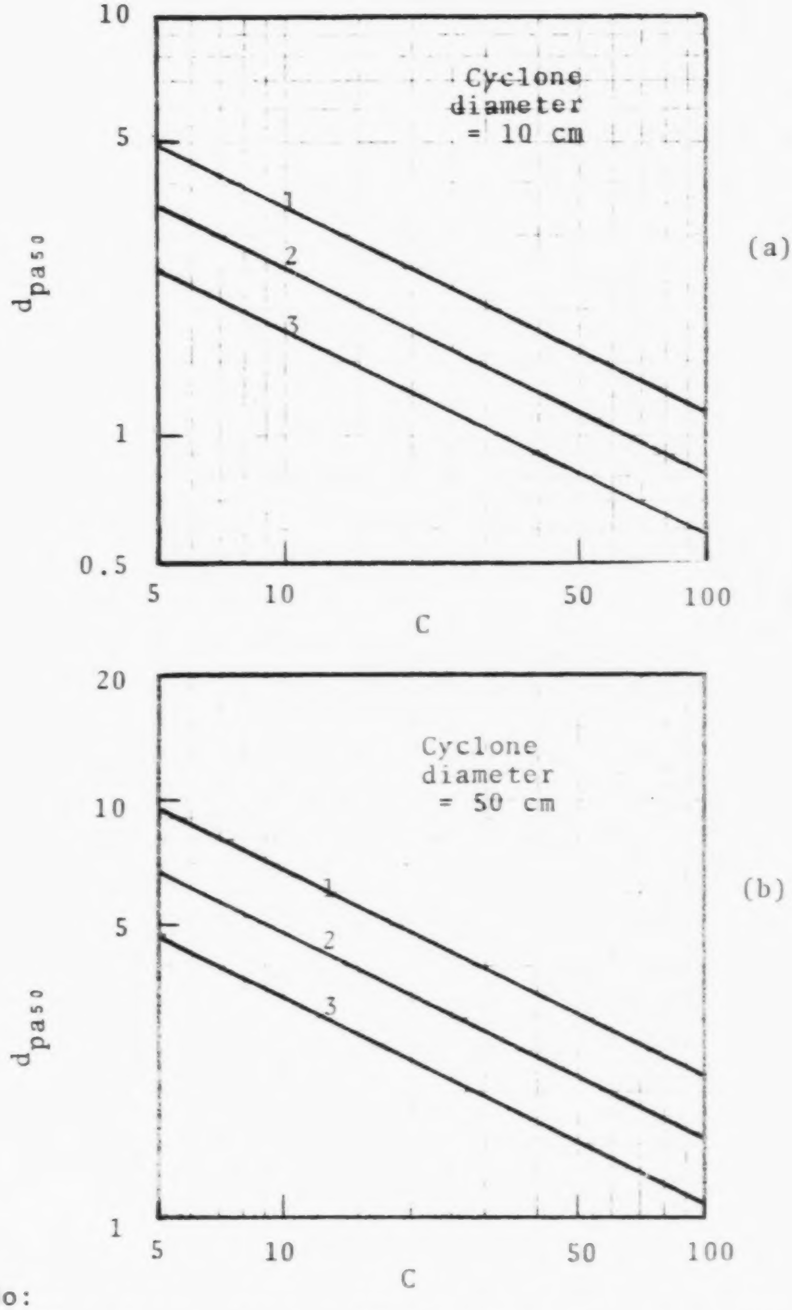

Curve No:
1. u = 750 cm/sec; 2. u = 1,500 cm/sec; 3. u = 3,000 cm/sec

$$d_{pa50} = d_{p50} \sqrt{\rho_p}\, C' = \mu m\ (g/cm^3)^{1/2}$$

FIGURE 5.3.7-7 (a & b)

PREDICTED CYCLONE PERFORMANCE, d_{pa50} VS. "C", WITH INLET VELOCITY AS PARAMETER, FOR SEVERAL CYCLONE DIAMETERS

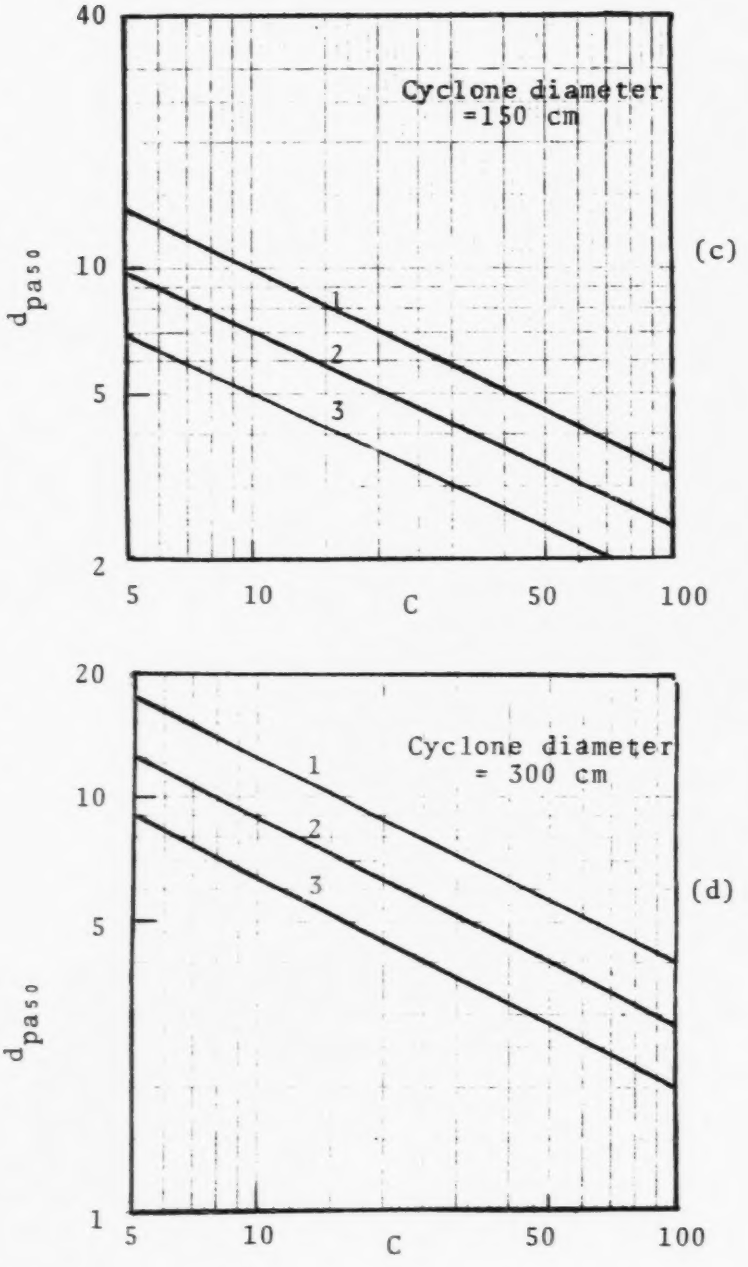

Curve No.:
1. u = 750 cm/sec; 2. u = 1,500 cm/sec; 3. u = 3,000 cm/sec

$$d_{pa50} = d_{p50}\sqrt{\rho_p C'} = \mu m\ (g/cm^3)^{1/2}$$

FIGURE 5.3.7-7 (c & d)
PREDICTED CYCLONE PERFORMANCE, d_{pa50} VS. "C", WITH INLET VELOCITY AS PARAMETER, FOR SEVERAL CYCLONE DIAMETERS

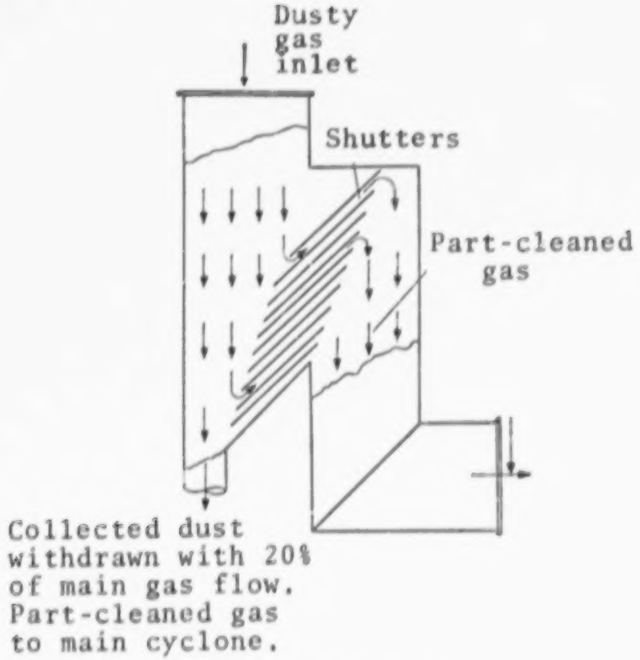
Dusty gas inlet
Shutters
Part-cleaned gas
Collected dust withdrawn with 20% of main gas flow. Part-cleaned gas to main cyclone.

FIGURE 5.3.8-1

SHUTTER-TYPE COLLECTOR
STAIRMAND (1951)

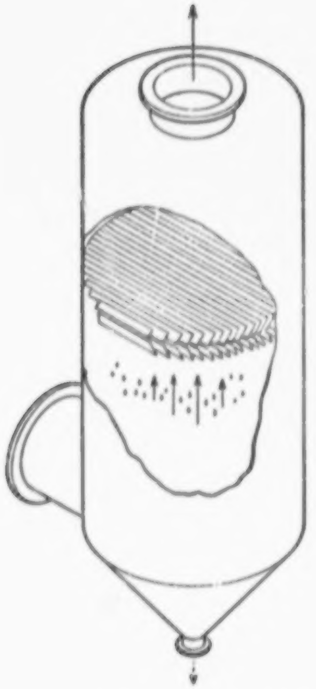

FIGURE 5.3.8-2

BAFFLE TYPE SEPARATOR
KOCH ENGINEERING

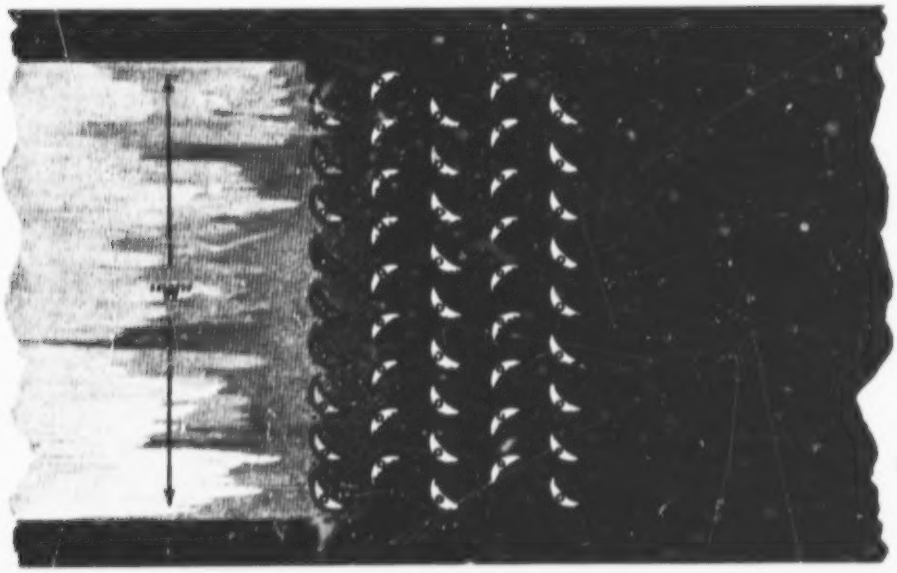

FIGURE 5.3.8-3

CRESCENT SHAPE BAFFLE COLLECTOR. DETRICK CO. (1971)

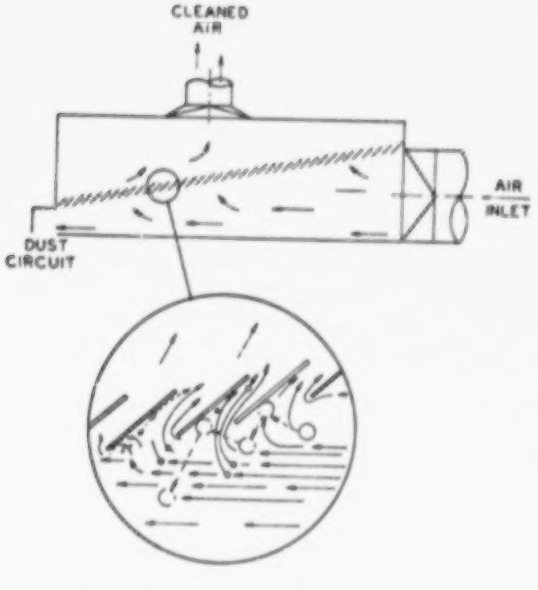

FIGURE 5.3.8-4

FLAT LOUVER IMPINGEMENT SEPARATOR
A.I.H.A. (1968)

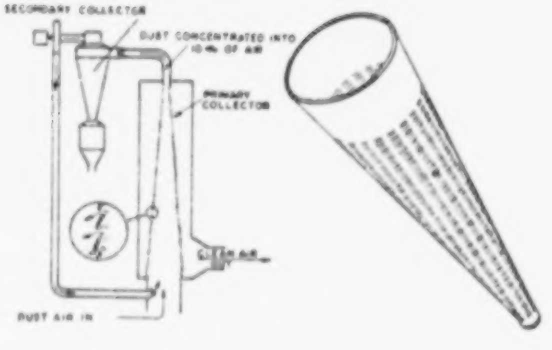

FIGURE 5.3.8-5

CONICAL LOUVER IMPINGEMENT SEPARATOR. A.I.H.A. (1968)

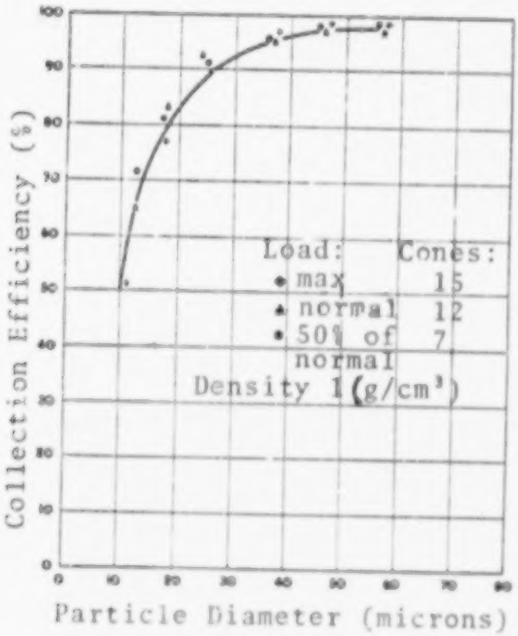

FIGURE 5.3.8-6
EFFICIENCY OF LOUVRED CONE COLLECTOR (NUMBER OF CONES ADJUSTED TO BE PROPORTIONAL TO GAS FLOW RATE).
HANSEN (1956)

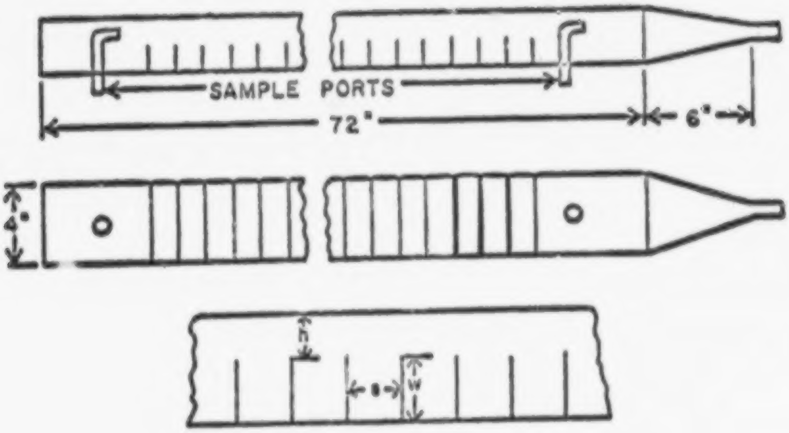

FIGURE 5.3.8-7

COLLECTOR WITH ONE BAFFLED WALL

CALVERT AND HODOUS (1962)

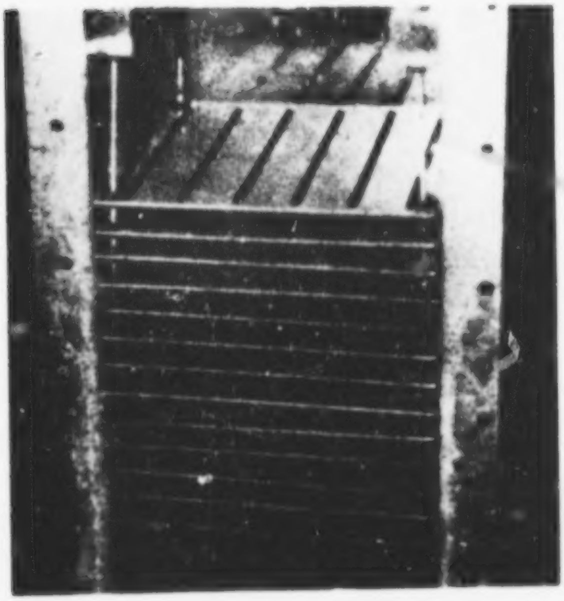

FIGURE 5.3.8-8

BAFFLED CONDUIT

CALVERT AND TAHERI (1966)

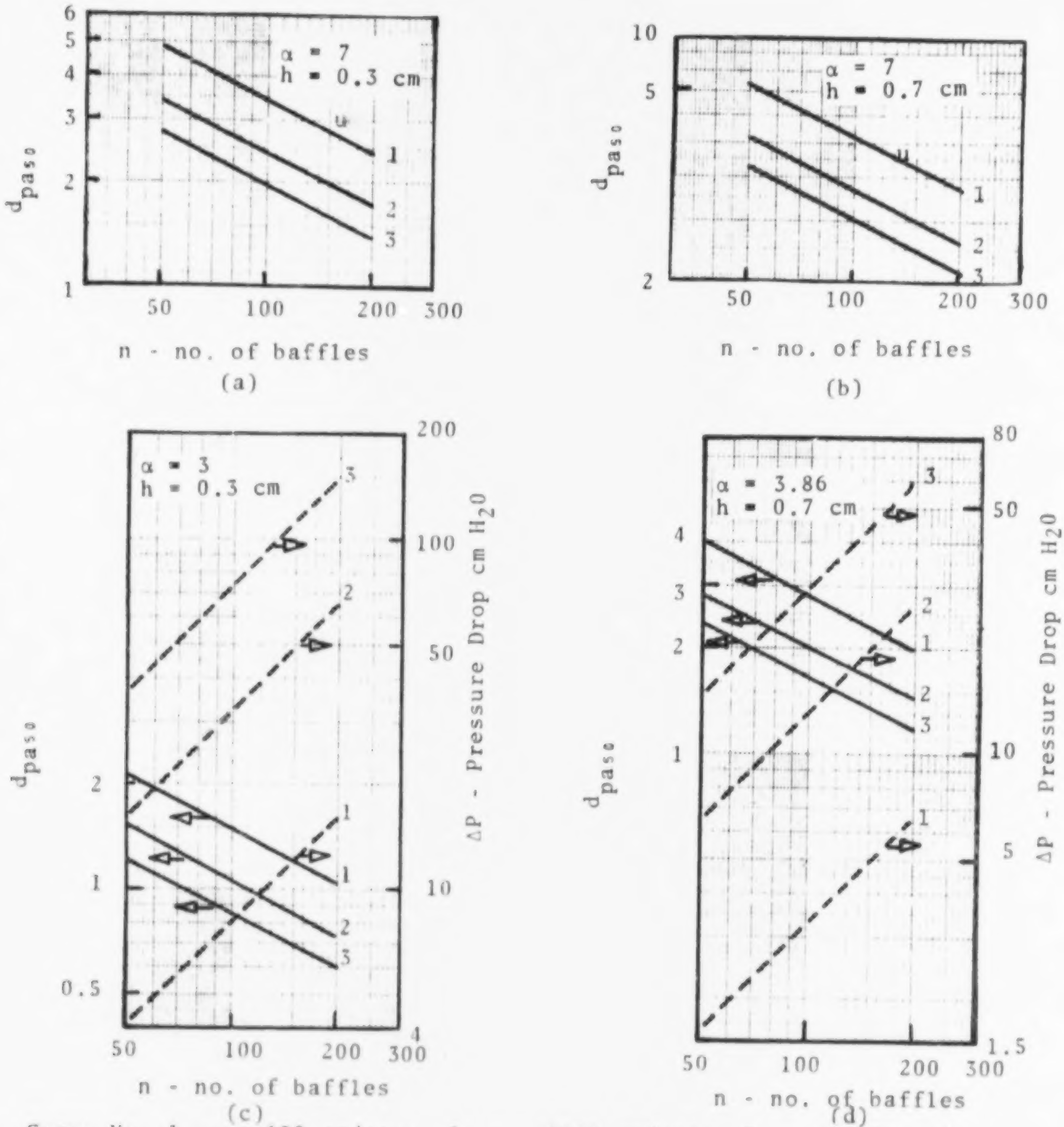

Curve No. 1. u = 600 cm/sec; 2. u - 1200 cm/sec; 3. u = 1800 cm/sec

$d_{pa_{50}} = d_{p_{50}} \sqrt{\rho_p C'}$ = micron (g/cc)$^{1/2}$

FIGURE 5.3.8-9
PREDICTED SECONDARY FLOW BAFFLES DEVICE PERFORMANCE, $d_{pa_{50}}$ VS. "n" WITH "u" AS PARAMETER AT VARIOUS "α" and "h".

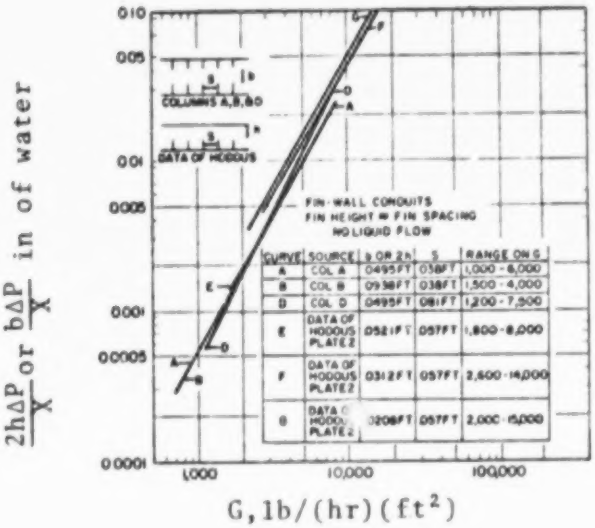

FIGURE 5.3.8-10

PRESSURE DROP VS. GAS FLOW RATE IN A SINGLE AND DOUBLE FIN RECTANGULAR CONDUIT SWEENEY AND CALVERT (1965)

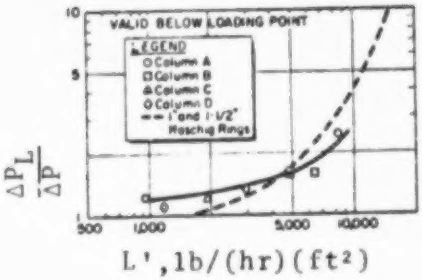

FIGURE 5.3.8-11

EFFECT OF LIQUID RATE ON PRESSURE DROP IN A FIN COLUMN. SWEENEY AND CALVERT (1965)

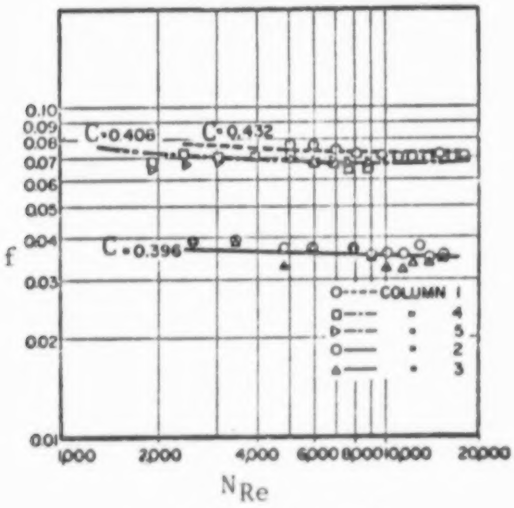

FIGURE 5.3.8-12

FRICTION FACTOR VERSUS REYNOLDS NUMBER FOR VARIOUS GEOMETRIES.

CALVERT AND TAHERI(1966)

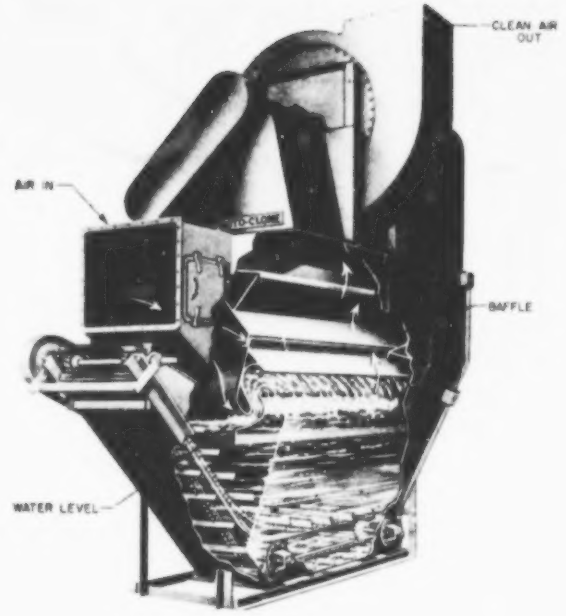

FIGURE 5.3.9-1

SELF-INDUCED SPRAY WET COLLECTO .
COURTESY AMERICAN AIR FILTER ([illegible]).

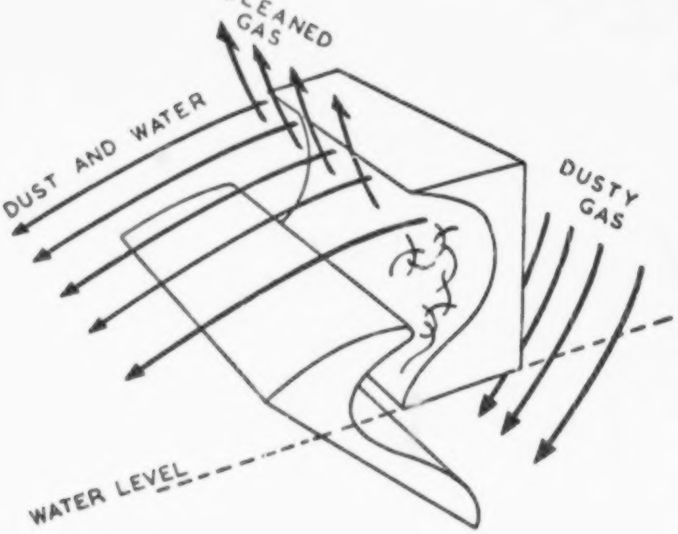

FIGURE 5.3.9-2

'ROTOCLONE' TYPE N PRECIPITATOR

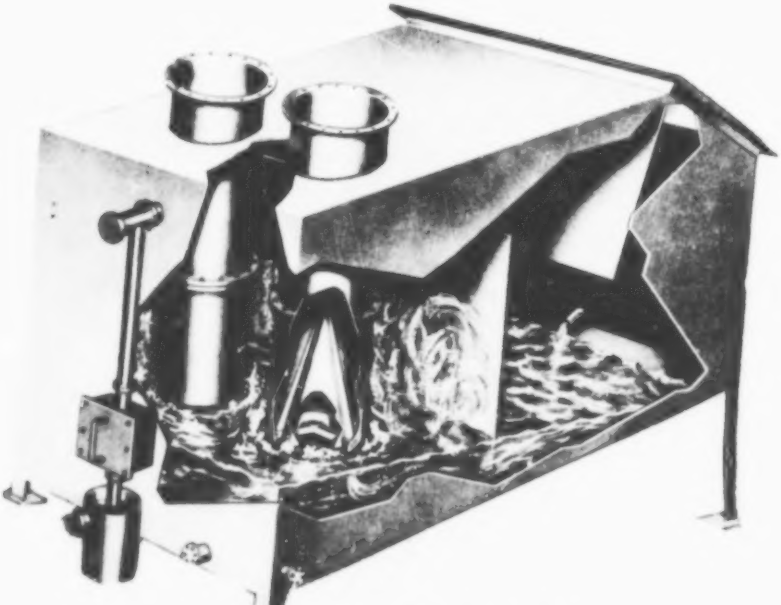

FIGURE 5.3.9-3

SELF-INDUCED SPRAY TYPE SCRUBBER (DOYLE).

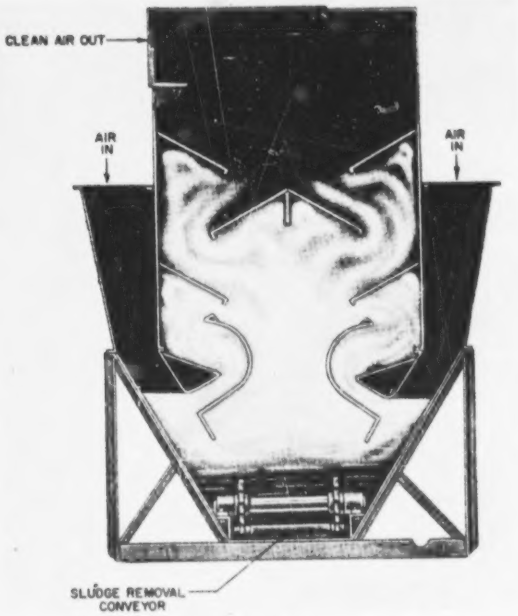

FIGURE 5.3.9-5

SELF-INDUCED SPRAY WET COLLECTOR
COURTESY SCHMEIG INDUSTRIES, INC.

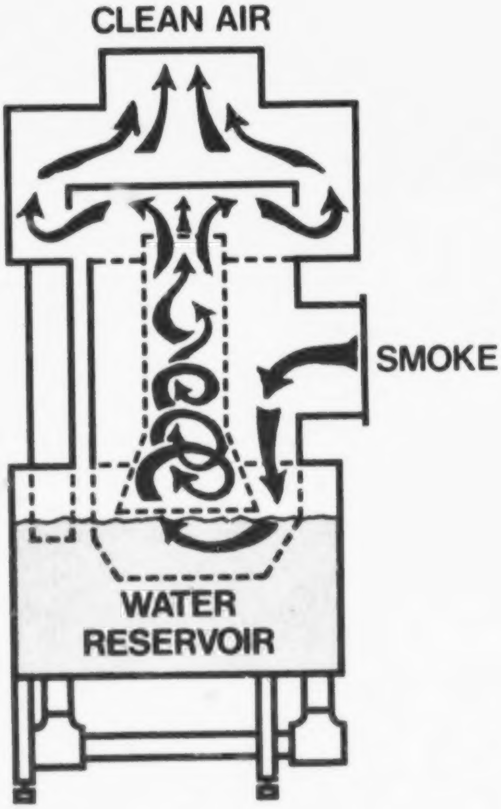

FIGURE 5.3.9-4

SELF-INDUCED SPRAY WET COLLECTOR
COURTESY LECKENBY COMPANY.

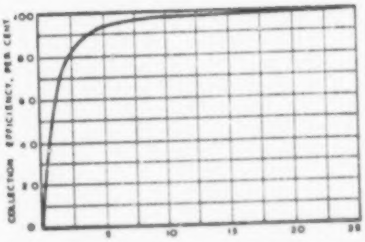

Particle Diameter,Microns

FIGURE 5.3.9-6

SELF-INDUCED SPRAY COLLECTOR
EFFICIENCY AT 5 MICRONS-93%

Stairmand (1956)

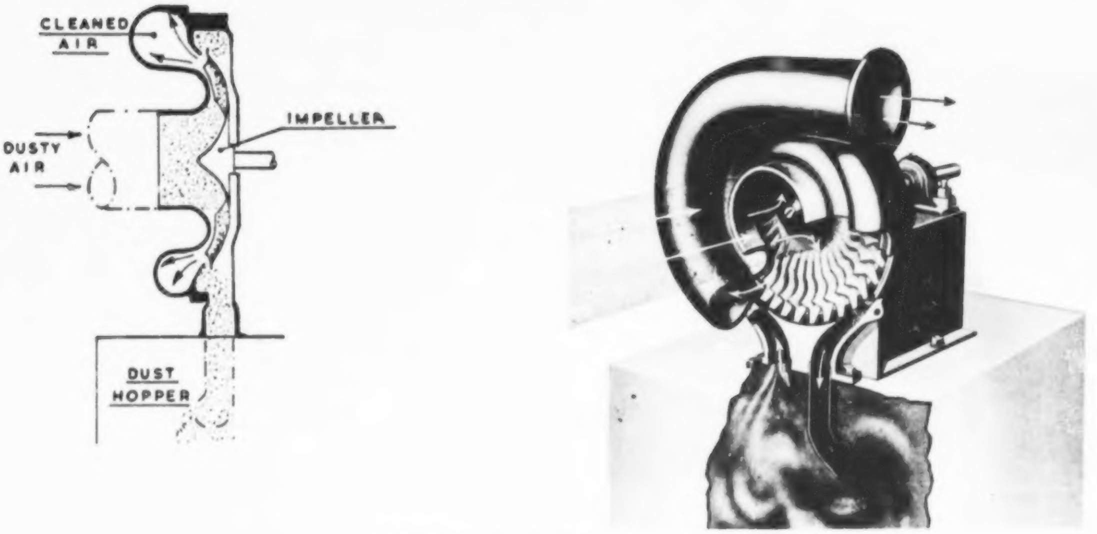

FIGURE 5.3.10-1
MECHANICALLY AIDED DUST PRECIPITATOR, AMERICAN AIR FILTER (1969)

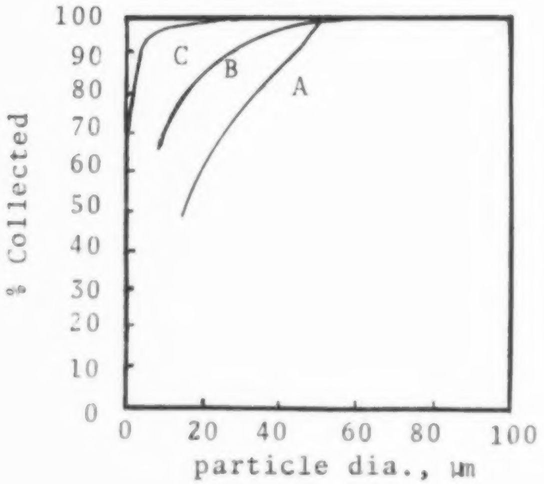

FIGURE 5.3.10-2
EFFICIENCIES OF MECHANICALLY AIDED COLLECTORS

A. Rotoclone (dry)(Wilson 1956)
B. Rotoclone (dry)(Wright 1958)
C. Rotoclone (wet)(Wright 1958)

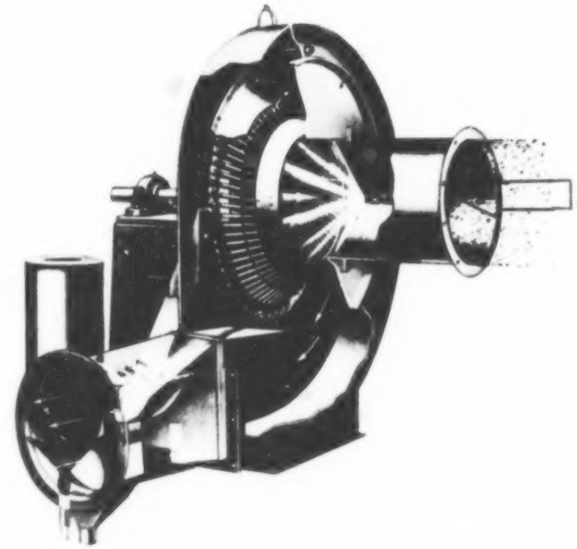

FIGURE 5.3.10-3

MECHANICALLY AIDED SCRUBBER. AMERICAN AIR FILTER (1967)

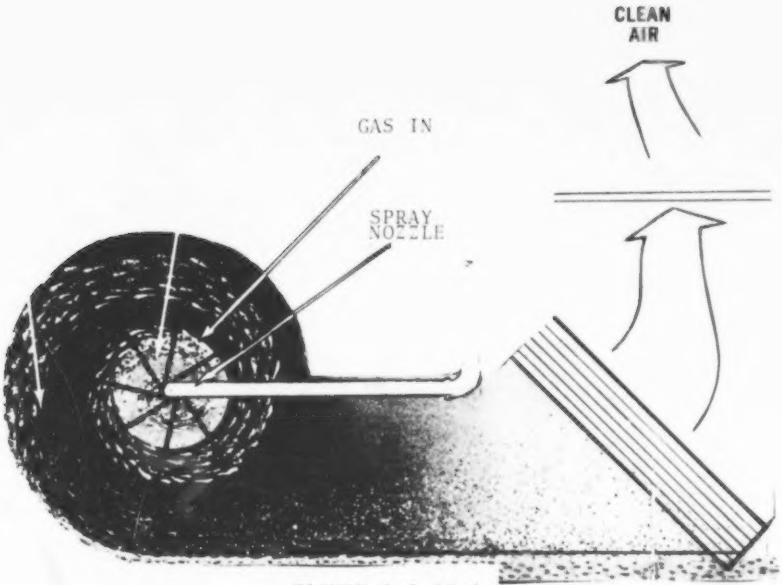

FIGURE 5.3.10-4

MECHANICALLY AIDED COLLECTOR
(TRI-MER 1968)

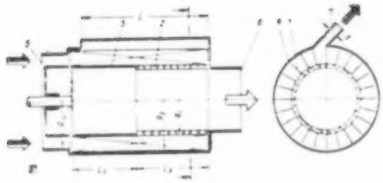

FIGURE 5.3.10-5
SCHEMATIC REPRESENTATION OF THE ROTATING CENTRIFUGAL OPERATOR WITH CONTINUOUS DUST REMOVAL (EXPLANATIONS IN TEXT) BUDINSKY (1970)

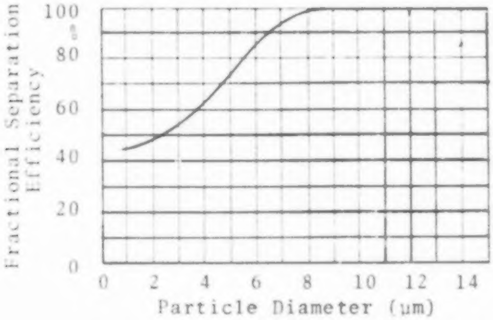

FIGURE 5.3.10-6
THEORETICAL CURVE OF THE FRACTIONAL SEPARATION EFFICIENCY OF THE CENTRIFUGAL SEPARATOR. BUDINSKY (1970)

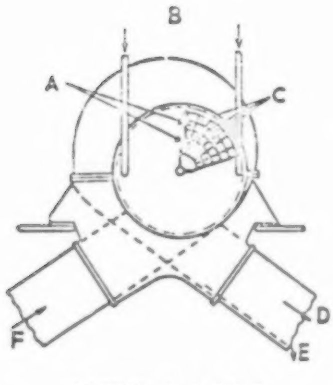

A. Stators
B. Water In
C. Rotors
D. Gas Out
E. Water Out
F. Gas In

FIGURE 5.3.10-7

DIAGRAM OF DISENTREGRATOR GAS WASHER
Stairmand (1956)

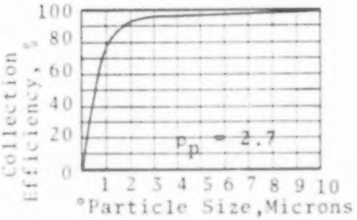

FIGURE 5.3.10-8

DISINTEGRATOR GAS WASHER
(EFFICIENCY AT 5 MICRONS-98%)
Stairmand (1956)

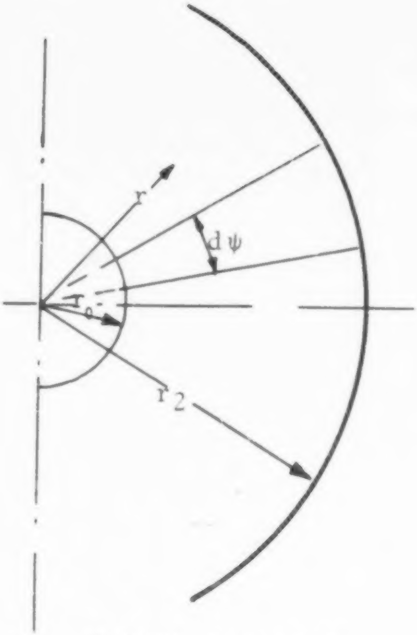

FIGURE 5.3.10-9

DIAGRAM OF CENTRIFUGAL COLLECTOR WITH CENTRIFUGAL FORCE ACTING PERPENDICULAR TO AXIS

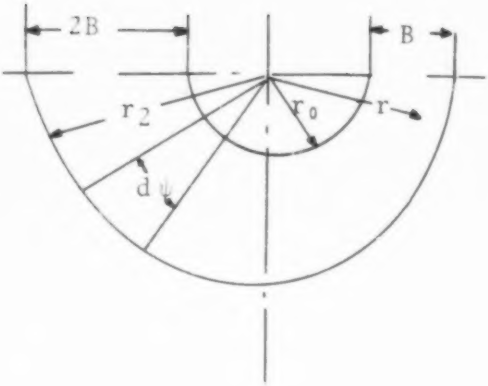

FIGURE 5.3.10-10

DIAGRAM OF CENTRIFUGAL COLLECTOR WITH CENTRIFUGAL FORCE ACTING PARALLEL TO AXIS

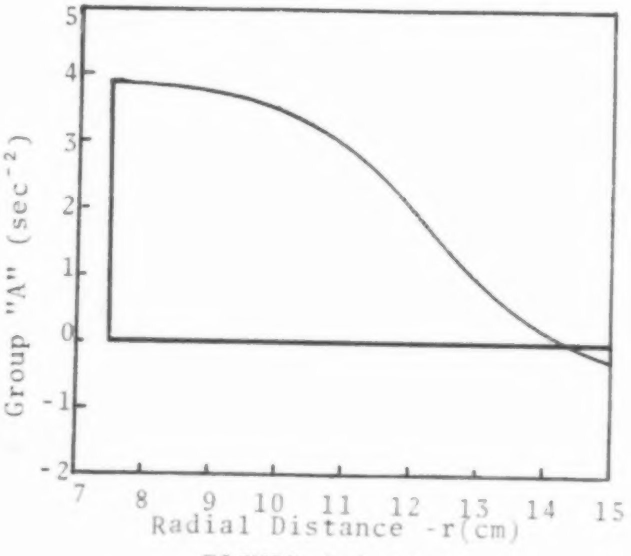

FIGURE 5.3.10-11

GRAPHICAL INTEGRATION OF THE INTEGRAL PART IN EQUATION 5.3.10-36

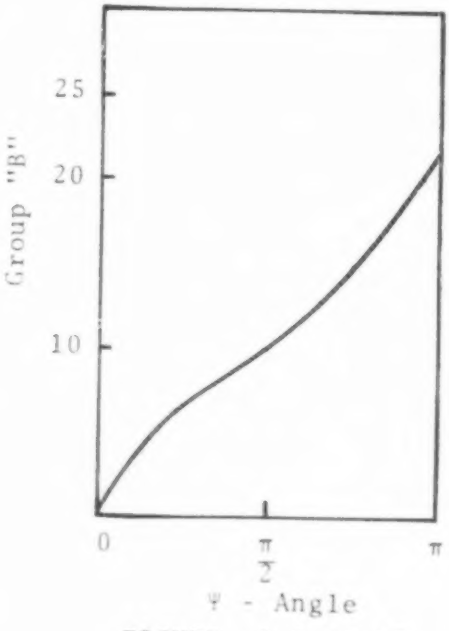

FIGURE 5.3.10-12

GRAPHICAL INTEGRATION OF EQUATION 5.3.10-40

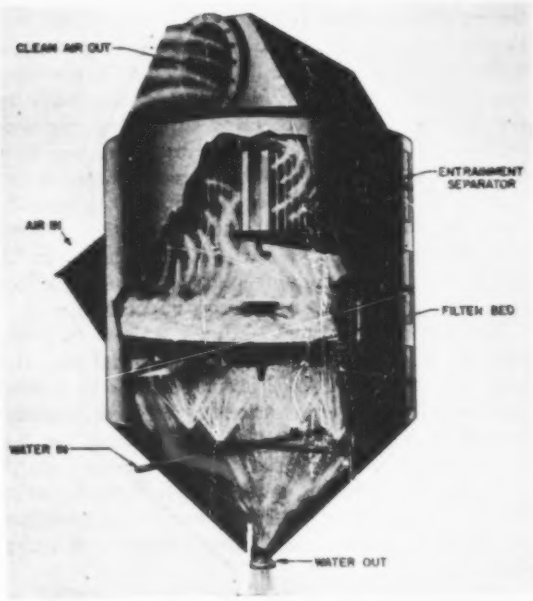

FIGURE 5.3.11-1

MOBILE BED TYPE SCRUBBER HYDRO-FILTER COURTESY OF NATIONAL DUST COLLECTOR COMPANY (1965)

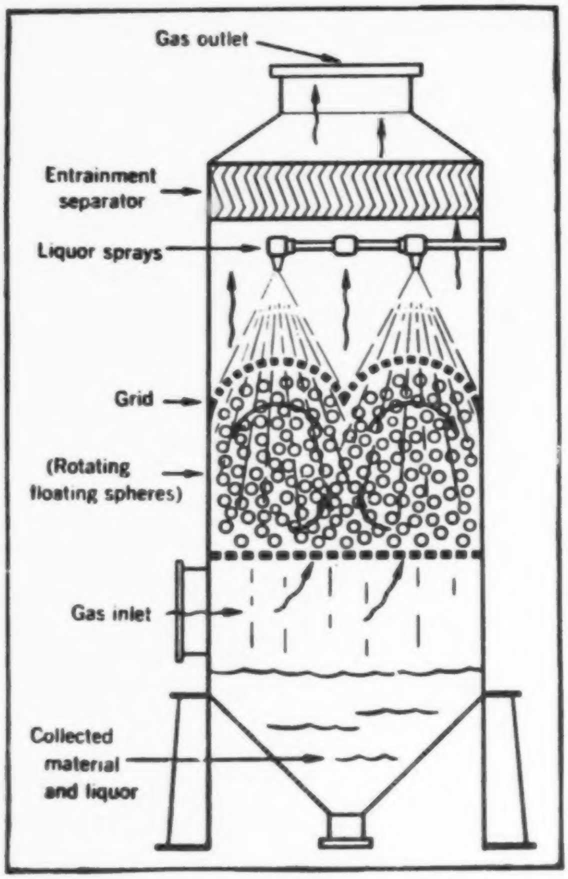

FIGURE 5.3.11-2
FLUIDIZED BED SCRUBBER
DOUGLAS ET AL. (1963)

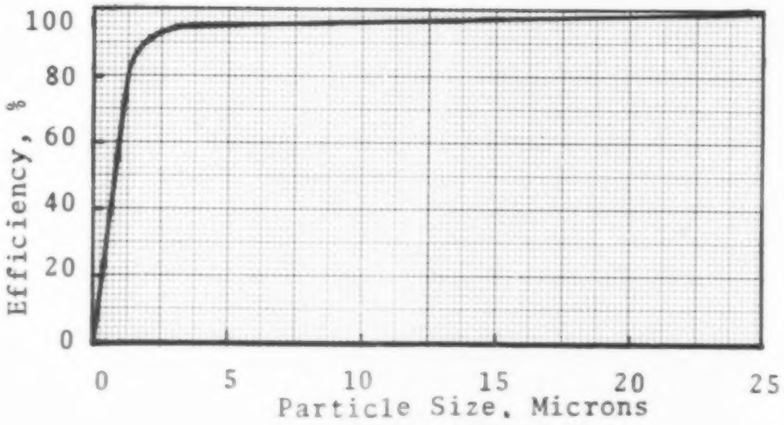

FIGURE 5.3.11-3
COLLECTION EFFICIENCY OF MOBILE BED SCRUBBER. NATIONAL DUST COLLECTOR CORPORATION. (1966)

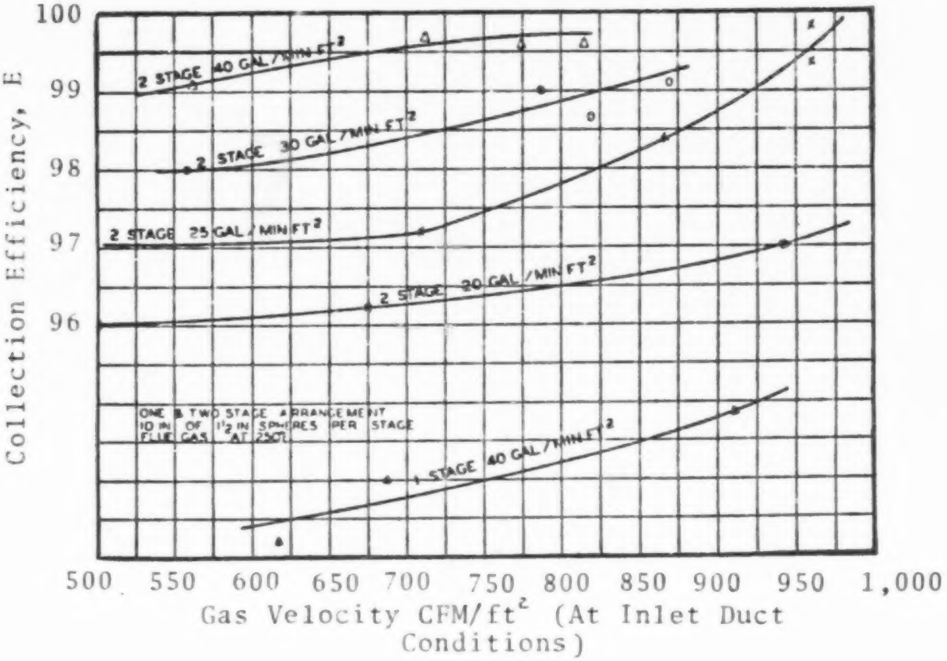

FIGURE 5.3.11-4

COLLECTION EFFICIENCY IN A FLUIDIZED BED SCRUBBER. POLLOCK ET AL (1967)

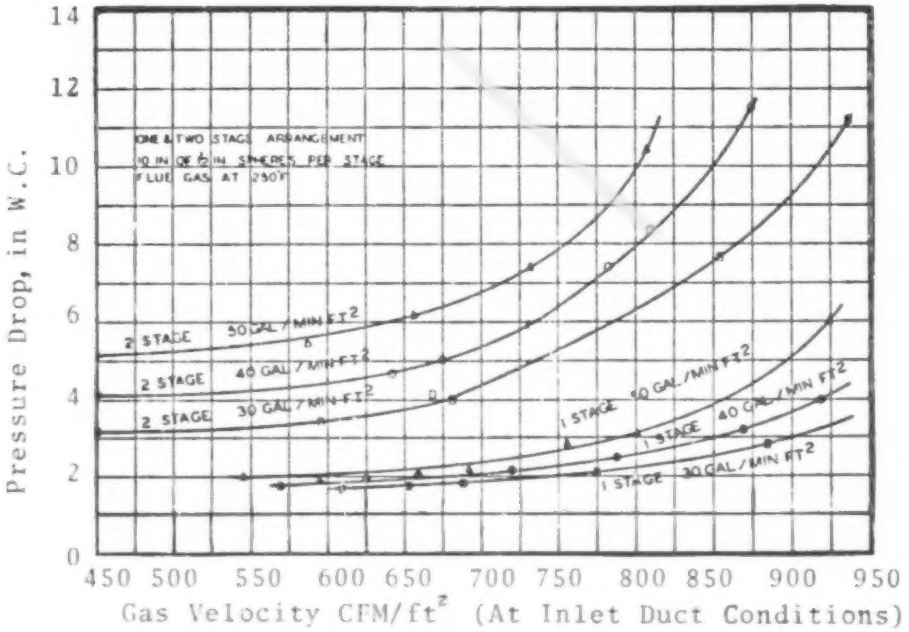

FIGURE 5.3.11-5

PRESSURE DROP IN A FLUIDIZED BED SCRUBBER. POLLOCK ET AL. (1967)

SECTION 5.3 NOMENCLATURE

LATIN

a - constant

a - cyclone inlet height, m or cm

A - cross sectional area, m^2 or cm^2

Ao - total hole area of plate, m^2 or cm^2

Af - wall effect factor, Equation 5.3.11-2

b - constant

b - width of channels in packed tower, m or cm

b - cyclone inlet width, m or cm

b - scroll width in radial direction, m or cm

b - one half width of gas jet, m or cm

be - dust exit diameter, m or cm

be - maximum scroll width, m or cm

c - mass concentration, Kg/m^3 or g/cm^3

C - cyclone geometry coefficient

C' - Cunningham correction factor

C_D - drag coefficient

d - diameter, m or cm

d_s - Sauter mean drop diameter, m, cm or μm

d_c - cyclone diameter, m or cm

d_e - cyclone exit pipe diameter, m or cm

d_{eq} - equivalent diameter, m or cm

d_{mm} - mass median drop diameter, m, cm or μm

d_{psn} - mean surface particle diameter, cm or μm

d_{pg} - geometric mean particle diameter, cm or μm

d_{pa} - aerodynamic particle diameter, μm (g/cm^3)$^{1/2}$

SECTION 5.2 NOMENCLATURE

LATIN

d_{pa50} - aerodynamic particle diameter collected with 50% efficiency, μm $(g/cm^3)^{1/2}$

d_{p50} - particle diameter collected with 50% efficiency, cm or μm

d_{pcr} - critical particle diameter; collected with 100% efficiency, cm or μm

D - diffusivity, cm^2/sec

E - device particle collection efficiency

E - power, kw or HP

f - friction factor

f - ratio of drop velocity relative to gas, to gas velocity

$f(d_p)$ - size frequency distribution

F - foam density, ratio of clear liquid height to total foam

F - force, dyne or Newton

g - acceleration of gravity, 9.81 m/sec^2 or 981 cm/sec^2

G - gas mass flux $kg/(sec\ m^2)$ or $g/(sec\ cm^2)$

h - distance between baffle plates, m or cm

h - impeller thickness, m or cm

h - total foam height above plate, m or cm

h - overall cyclone height, m or cm

h_s - cyclone cylinder height, m or cm

h' - heat transfer coefficient, $cal/(sec\ cm^2\ °C)$

Hd - liquid holdup

j - fraction of packing diameter

k $\equiv$ $Rg/N = 1.38 \times 10^{-19}$ mbar $cm^3/°C$, Boltzman constant

K_I - interception parameter

K_p - inertia parameter

K_{p50} - inertia parameter for particle collected with 50% efficiency

SECTION 5.3 NOMENCLATURE

LATIN

K_{pt} - inertial parameter evaluated at throat conditions
ℓ - length, m or cm
ℓ - distance between gas jet and collecting plate, m or cm
ℓ - clear liquid height above plate, m or cm
ℓ - perimeter of wetted disk, m
ℓ - length of bed measured in direction of gas flow, m or cm
L - liquid mass flux, kg/(sec m^2) or g/(sec cm^2)
m - mass, kg or g
m - ionic or molecular mass ($mN=M$)
n - number of semicircular bends in packed tower
n - revolutions per minute
n - vortex exponent
n - number of eddies in series
n - number of concentration, #/cm^3
n - number of actual plates
n - number of blades in an impeller
P - total pressure, mbar or atm
P - power, kw or HP
Pt - penetration (one minus efficiency)
$\overline{Pt}$ - average (integrated) penetration
Q - volumetric flow rate, m^3/sec, cm^3/sec or lit s/sec
r - radius
r - radial distance, m or cm
r_o - disk radius, m or cm
r_o - see Figures 5.3.10-9 and 5.3.10-10

SECTION 5.3 NOMENCLATURE

LATIN

r_s - radial distance to where drops are sprayed, m or cm

Rg - ideal gas law constant

S - solidarity factor

S - distance from plate to impingement surface, m or cm

S - cyclone exit pipe length, m or cm

t - time, sec

T - absolute temperature, °K

u - velocity, m/sec or cm/sec

u_a - mass average axial drop velocity through orifice, m/sec or cm/sec

u_c - gas velocity through bubble caps, m/sec or cm/sec

u_{Gb} - gas velocity through channel between packings, m/sec or cm/sec

u_r - relative velocity between gas and liquid, m/sec or cm/sec

u_{tg} - mass average tangential drop velocity through orifice, m/sec or cm/sec

v - velocity, m/sec or cm/sec

V - volume, m^3 or cm^3

W' - weight of [illegible] per unit area, kg/m^2 or g/cm^2

X - distance in X direction

Y - distance in "Y" direction

Z - distance in Z direction

Dimensionless Numbers

$N_{Sc} \equiv \mu_G/(\rho_G D_G)$, Schmidt Number

$N_{Pr} \equiv C_p \mu/k$, Prandtl Number

$N_{Pe} \equiv du/D$, Peclet Number

SECTION 5.3 NOMENCLATURE

Subscripts

d - drop

D - diffusion

DP - diffusiophoretic

e - exit

f - fiber

G - gas phase

h - perforation in plate

i - in

I - interception

L - liquid phase

o - undisturbed or upstream or bulk

p - particle

P - inertial impaction

r - relative

r - radial

s - Sauter (surface to volume)

t - terminal velocity

t - pipe

tg - tangential

T - thermophoretic

v - vapor

w - wire

Superscripts

~ - dimensionless quantity

SECTION 5.3 - REFERENCES

Alder, C. R., Marshall, W. R., Jr., Chem. Eng. Progr. 47, 515 (1951).

Albrecht, F., Physik, Z. 32, 48 (1931).

American Industrial Hygiene Association, "Air Pollution Manual", Part 2 (1968).

Alexander, R. McK., Austrailian Institute Mining & Met. Proc. [N.S.] 152-3, 202 (1949).

American Air Filter Company, Dust Control Bulletin No. 320, 3 (1969).

American Air Filter Company, Dust Control Bulletin No. 304, 3 (1969-B).

Ariman, T., Young, R. J., Yang, K. T. and Hasbein, R. L., "On Particle Collection by Liquid Scrubbing", Presented at the 2nd Annual Environmental Engineering and Science Conference, Louisville, April 21 (1972).

Barth, Walter, Brennstoff-Warme-Kraft. 8, 1 (January, 1956).

Baskerville, W. H., Trans. A.I.Ch.E. 37, 79 (1941).

Bechtel Corporation, Report to NAPCA Contract No. PH 22-68-67, (1970).

Bechtel Corporation, Report to O.P.A. - EPA Contract No. PH 22-68-67 (1971)

Boetter, L. M. K., Young, G., Greenfield, M. L., Sanders, V. D., and Morgan, M., National Advisory Committee Aeronaut. Tech. Note 2517, (1951).

Bosanquet, C. H., Trans. A.I.Ch.E. London, 28, 130, Appendix to paper by C. J. Stairmand (1950).

Briggs, Leo W., Trans. A.I.Ch.E. 42, 511 (March, 1946).

Budinsky, K., Staub, 30, No. 9, p. 7 (English trans), (1970).

Calvert S., "Air Pollution", Stern A.C., Ed., 3, Academic Press, New York (1968).

Calvert, S., and Taheri, M., British Chem. Eng. 11, 254, (1966).

Calvert S., Hodous, R., A.P.C.A.J. 12, 326, (1962).

Calvert, S., AIChE Journal 16, 392-396 (1970).

Calvert, S., Lundgren, D., Mehta, D., presented at 63rd APCA Annual Meeting, St. Louis, (1970).

5.3 - REFERENCES (cont'd)

Caplan, K. J., "Air Pollution", 3, Stern, A. C., Ed., Academic Press, 359-366 (1968).

Chase, J. D., Chemical Engineering 74, 105-116 and 139-146 (1967).

Chen, C. Y., "Filtration of Aerosols by Fibrous Media," Eng. Expt. Sta., University of Illinois, March (1955).

Das, P. K., Indian J. Met. Geophys. 1, 137 (1950).

Davies, C. N., Proc. Inst. Mech. Engrg. 18, 185 (1952).

Davies, C. N. Proc. Inst. Mech. Engrg. 18, 85 (May.)

Detrick, M. H. Company, Bulletin D-67, (1971).

Douglas, H. R., Snider, I. W. A., Tomlinson, G. H. II, Chem. Eng. Prog. 59, 85-89 (1963).

Ekman, F. O., Johnstone, H. F., Ind. Eng. Chem. 43, 1358 (1961).

Fraser, R. P., Eisenklam P., Dombrowski, N., Brit. Chem. Eng. 2, 417 (1957).

Friedman, S. J., Gluckert, F. A., Marshall, W. R. Jr., Chem. Eng. Prog. 48, 181 (1952).

Friedlander, S. K., "The Theory of Aerosol Filtration", A.I.Ch.E.J. 3, 43 (1957).

Friedlander, S. K. and Pasceri, R. E., "Aerosol Filtration by Fibrous Filters", Report Dept. Chem. Eng., Johns Hopkins Univ., Baltimore, Md. April (1962).

Friedlander, S. K., Pasceri, R. E., Canad. J. Chem. Engrg. 38, 212 (1960).

Fuchs, N. A., "The Mechanics of Aerosols", Pergamon Press, New York (1964).

Gardiner, J. E., Tech. Report N.1-CT/19, The Shell Petroleum Co., Ltd. Shell Court, London.

Gieseke, J., Ph.D., thesis University of Washington (1964).

Glanert, M., Aeronautical Research Comm. Rept. No. 2025 (London). H.M.S.O.

Goldshmid, Y., Calvert, S., A.I.Ch.E.J. 9, 352 (1963).

Hansen, K.,Fifth World Power Conf. Vienna, Paper 101 M/4, (1956).

5.3 - REFERENCES (cont'd)

Harris, L. S., Hartenbaum, R., "Performance Test Techniques for Ejector Venturi Scrubber", 54th Annual Meeting APCA, (1961).

Harris, L. S., "Scrubbing Characteristics of the Ejector Venturi Scrubber, 56th Annual Meeting of APCA, (1963).

Harris, L. A., "Energy and Efficiency Characteristics of the Ejector Venturi Scrubber", 57th Annual Meeting of APCA (1964).

Harris, L. S., "Fume Scrubbing with the Ejector Venturi System", C.E.P. 62, 55-59 (1966).

Hesketh, H. E., Engel, A. J., Calvert, S., Atmospheric Environ. 4, 639 (1970).

Hocking, L. M., Quart. J. Roy. Met. Soc., 85, 44 (1959).

Ingebo, R., NASA Tech. Note 3762 (1956).

Jackson, S., Calvert, S., A.I.Ch.E.J., 12, 1075 (1966).

Jackson, S., M.S. Thesis, Pennsylvania State University (1964).

Johnstone, H. F., Field, R. B., Tassler, M. C., Ind. Eng. Chem. 46, 1601 (1954).

Johnstone, H. F., Roberts, M. H., Ind. Eng. Chem. 41, 2417 (1949).

Kimura, N., Iinoya, K., Chem. Eng. (Tokyo) 28, 39 (1964), abridged ed. in English 2, 136 (1964).

Kimura, N., Iinoya, K., Chem. Eng. (Tokyo) 29, 538 (1965).

Kraemer, H. F., and Johnstone, H. F., Ind. Engrg. Chem. 47, 2426 (1955).

Koch Engineering Company, Pollution Control Division, Bulletin KPC-1.

Landt, E., Gesundheits Ing., 77, 139 (1956).

Langmuir, I., O.S.R.P. Report No. 865 (1942).

Langmuir, I., Blodgett, K., Amer. A. F. Tech. Report 5418 (1946).

Lapple, C. E., Ind. Hyg. Quarterly 11, 40 (March, 1950).

Lapple, C. E., Shepherd, C. B., Ind. & Eng. Chem. 32, 5, 605 (1940).

Leith, David, Licht, William, "The Collection Efficiency of Cyclone Type Particle Collectors - A New Theoretical Approach". Paper presented at San Francisco meeting of A.I.Ch.E., December (1971).

5.3 - REFERENCES (cont'd)

Lowry, R. P., Van Winkle, M., A.I.Ch.E.J. 15, 665 (1969).

Ludwig, F. E.,"Applied Process Design for Chemical And Petrochemical Plants", Vol. 2, 98, Gulf Publishing Company, Houston, Texas, (1960).

Lundgren, D. A., M.S. Thesis, University of Minnesota, Minneapolis, (March, 1962).

Marshall, W. R., Jr., Chem. Eng. Prog. Monogr. Ser. No. 2 (1954).

Marshall, W. R. Jr., Seltzer, E., Chem. Eng. Prog. 46, 501 (1950).

NAPCA, private communication (1970).

Natanson, G. L., Dok. Akad. Nank. S.S.R. Physical Chemistry Section, 112, 100 (1957), English ed. 112, 21 (1957).

National Dust Collector Corporation, private communication, (1966).

National Dust Collector Corporation, General Catalog (1968).

Nukiyama, S., Tanasawa, Y., Trans. Soc. Mech. Engrs. (Japan) 4, 86 (1938).

Orr, C., Jr., "Particulate Technology", MacMillan Company, New York (1966).

Pearcy, T., Hill, G. W., Quart. J. Royal Met. Soc. 83, 77 (1957).

Pemberton, C. S., Int. J. Air Pollution 3, 168 (1960).

Perry, R. H., ed. "Chemical Engineers' Handbook", 4th ed., McGraw Hill, N.Y. (1963).

Perry, J. H., Chemical Engineering Handbook, 3rd ed. 393, McGraw-Hill, New York (1950).

Picknett, R. G., Int. J. Air Pollution, 3, 160 (1960).

Pollock,W. A., Tomany, J. P., Frieling, G., ASME Publication 66 - WA/CD-4 (1966).

Pyne, H. W., Wilson, R. B., Soole, B. W., Brit. J. Appl. Phys. 18, 1177-1191 (1967).

Ranz, W. E., Techn. Report No. 8, Univ. Illinois Engrg. Exptl. Sta., (Jan. 1, 1953).

Ranz, W. E., Wong, J. B., Ind. Eng. Chem. 44, 1371 (1952).

Rosin, P., Rammler, J., J. Inst. Fuel 7, 29, (1933).

5.3 - REFERENCES (cont'd)

Rosin, P., Rammler, W., Intelmann, W., Zeit. Ver. Deut. Ing. 76, 433 (1932).

Sell, W., Ver. Deut. Ing. Forschungsheft, 347, (1931).

Shepherd, C. B., Lapple, C. E., Ind. & Eng. Chem. 31, 972 (Aug. 1939).

Shepherd, C. B., Lapple, C. E., Ind. & Eng. Chem. 31, 1246 (Sept. 1939).

Silverman, L., in "Proceedings of the U.S. Technical Conference on Air Pollution", ed. L. McCabe, McGraw-Hill, New York (1952).

Soole, B. W., Staub 28, 7, 14 (English Trans.) (1968).

Soole, B. W., Staub 30, 3, 18 (English Trans.) (1970).

Sproull, Wayne T., APCA Journal 16, 439 (August 1966).

Stairmand, C. J., Chem. Engrg., 409 (October, 1949).

Stairmand, C. J., Journal of the Inst. of Fuel, 29, 58 (1956).

Stairmand, C. J., Trans. Inst. Chem. Engrs. 29, 356 (1951).

Stern, A. C., Caplan, K. J., Bush, P. B., "Cyclone Dust Collectors", Am. Petrol. Inst., New York (1955).

Strauss, W., "Industrial Gas Cleaning", Pergamon Press, New York. (1966).

Strauss, W., Thring, M. W., Iron & Steel Journ. 196, 62 (1960).

Striplin, M. M., "Tennessee Valley Authority Chem. Eng. Rept. No. 2, 1st ed., U. S. Government Printing Office, Washington D.C. (1948).

Sweeney, T. L., Ph.D. Thesis, Case Inst. of Tech., Cleveland, Ohio, (1962).

Sweeney, T. L., Calvert, S., A.I.Ch.E. Journal 11, 785 (1965).

Taheri, M., Calvert, S., Journal of APCA 18, 240-245 (1968).

Takashima, Y., Kyritsis, W. T., Dennis, R., Silverman, L., "Waste Processing Off-Gas Scrubber Studies," 557-579, Proceedings of 7th AEC Air Cleaning Conference, Brookhaven Nat. Lab, (1961).

Torgeson, W. L., "The Theoretical Collection Efficiency of Fibrous Filters Due to the Combined Effects of Inertia, Diffusion and Interception." Paper No. J-1057. Applied Science Division, Litton Systems, Inc., St. Paul, Minn.

5.3 - REFERENCES (cont'd)

Treybal, R. E., "Mass Transfer Operations," McGraw-Hill, New York (1955).

Tri-Mer Fan/Separator, (1968).

U.O.P. Air Correction Division, Bulletin No. 608 (1967).

Vincent, E. J., "Air Pollution Engineering Manual," U.S. Dept. of Health, Education and Welfare, Public Health Service No. 999-AP-40, Cincinnati (1967).

Walton, H. W., Woolcock, A., Int. J. Air Pollution, 3, 129 (1960).

Whitby, K. T., "Calculation of the Clean Fractional Efficiency of Low Media Density Filters", ASHRAE Journal, (Sept. 1965).

Whitby, K. T., Lundgren, D. A., "The Mechanics of Air Cleaning", Presented at 1964 Annual Meeting of American Society of Agricultural Engineers, Ft. Collins, Colo. (June 21-24, 1964).

Wilson, A., British Dust Collection Equipment, Paper to Combustion Engineering Association (1956).

Wong, J. B., Johnstone, J. F., "Collection of Aerosols by Fiber Mats," Eng. Exp. Sta., University of Illinois Tech. Report No. 11, (October 1953).

Wright, F., Iron & Steel Inst., Spec. Rept. No. 61, 103 (1958).

5.4 ENTRAINMENT SEPARATORS

5.4.1 INTRODUCTION

In many operations where a gas or vapor is generated from a liquid, or where a gas passes through a liquid, complete separation of the two phases is difficult. The gas will entrain and carry with it varying quantities and sizes of liquid droplets. The size of the droplets, which determines the difficulty in separating them, depends upon the way the drops were formed. Drops which are torn from the bulk of the liquid are usually large, in the order of magnitude of tens to hundreds of microns. Drops which form as a result of condensation or chemical reaction are small, several microns and less in diameter.

5.4.2 GENERAL

In separation of liquid entrainment we are concerned with particles of density of ≈ 1 g/cm^3 in a wide size range. These particles can be removed from the gas stream by a large variety of devices, most of them already described in the previous sections. All of the mechanisms for particle separation discussed in Section 4.6 are also used for entrainment separation. These include: settling, centrifugation, impingement, electrostatic attraction and diffusion. Montross (1953) reviewed and compared the various types of entrainment separators and gave some appropriate design equations.

The most important single factor in choosing and designing an entrainment separator is drop size. Drops larger than 50 μm dia. are settled easily due to gravitational forces. Thus in many cases reduction of gas velocity by expanding flow area, will be enough to separate the entrained drops from the gas stream. Drops larger than about 5 μm dia. are collected by centrifugal and impingement type collectors. Smaller drops are either agglomerated first to larger ones, or collected by the more efficient collecting devices, like high efficiency cyclone, electrostatic precipitators and the like.

Three factors affect the design and operation of most entrainment separators: pressure drop, reentrainment velocity and collection efficiency. Once design equations predicting these three parameters are available, operating characteristics of the entrainment separator can be established.

5.4.3 GRAVITY SETTLERS

The function of a gravity separator is to reduce the stream velocity, from one which permits entrainment, down to a velocity that will permit gravity to remove the entrained droplets. There are two basic types, tranquil and stirred. The only effect of stirring is to maintain an even concentration throughout the separator. In most cases it neither helps nor hinders the settling.

For complete removal to take place the drop terminal velocity multiplied by the residence time, must equal the maximum settling height:

$$u_t = \frac{Q_G}{b\ \ell} \tag{5.4.3-1}$$

and the efficiency is given by:

$$E = \frac{u_t\ b\ \ell}{Q_G} \tag{5.4.3-2}$$

For droplets greater than ≈0.15 cm ($500 < N_{Re}$) Newton's law applies and:

$$u_t = 1.74 \left(\frac{g\ d_p\ \rho_p}{\rho_G}\right)^{1/2} \tag{5.4.3-3}$$

When $d_p < 100$ µm, Stokes law applies:

$$u_t = \frac{2\ r_p^2\ g\ \rho_p}{9\ \mu_G} \tag{5.4.3-4}$$

For drops larger than 100 µm in diameter and smaller than 0.15 cm, drop settling velocity can be taken from Figure 4.6.2-4.

5.4.4 KNITTED WIRE MESH ENTRAINMENT SEPARATORS

Knitted wire mesh entrainment separators are used extensively due to their low pressure drop and high collection efficiency. Usually the bed is 10 - 15 cm (4 - 6") deep, consists of 97-99% free volume, and is knitted of thin metal wires, though other materials are also used. In most cases the pressure drop is less than 2.5 mbar [1" W.C.] and the curve of pressure drop vs. air flow velocity behaves like that of a packed bed, and shows a break at the loading and flooding points.

The allowable air velocity, which is the highest velocity that does not cause re-entrainment, is calculated from Souders Brown (1934) equation:

$$u = 30.5\ a\left(\frac{\rho_L - \rho_G}{\rho_G}\right)^{1/2} \tag{5.4.4-1}$$

The constant "a" varies with the operating conditions. The A.C.S. "Entrainment Separators Design Manual" gives the following values of "a": for most cases "a" = 0.35, for steam at 1 atm and higher pressures "a" = 0.25, for most vapors under vacuum where the absolute pressure is 250 to 700 mm Hg "a" = 0.2, and for vacuum evaporators of salt, caustic, and acids, "a" = 0.15 - 0.2. All values of "a" and "u" are in cm/sec.

The wires of the separator furnish targets with which the particles must collide in order to be captured. Carpenter and Othmer (1955) showed that the efficiency of the knitted mesh separator can be estimated from:

$$E = 1 - \left(1 - \frac{\eta\, b\, \ell\, d_w}{N\, A}\right)^N \qquad (5.4.4\text{-}2)$$

where "η" is the target efficiency for cylinders for the specific "K_p", "N" is the total number of "layers" of wire, "A_w" $= \ell\, d_w$ is the total wire cross-sectional area, which can easily be calculated from the weight of the separator and the density and diameter of the wire, "A" is the cross-sectional area of the bed, "ℓ" is the total length of the wire strands, "d_w" is the wire diameter, and "b" is the fraction of the total wire in an effective position (for a knitted mesh, Carpenter and Othmer found b=0.67).

Figure 5.4.4-1 shows the calculated change in collection efficiency of water droplets of various diameters with air velocity, in a 48 layer 0.02 cm diameter wire. We see what has also been found experimentally that knitted wire mesh separators are efficient for drops larger than ≈8 μm in diameter. For the separation of smaller size droplets, composite meshes are used. These incorporate multicomponent yarn such as glass, dacron, orlon or cotton into the basic wire mesh. The allowable velocity of these separators is usually about half of the wire mesh style, and the pressure drop ranges between 7.5 - 10 mbar [≈3 - 10" W.C.]. The composite meshes can be used as entrainment separators or as agglomerators when operated at air velocities above the reentrainment velocity. In the second case, the composite mesh is followed by an all metal separator.

When solid particles or high viscosity liquids are present in the gas stream, provisions have to be made to trap the solid material in an open density mesh so that the captured material can be easily removed from the mesh.

5.4.5 OTHER IMPINGEMENT TYPE ENTRAINMENT SEPARATORS

To illustrate the method of analysis of performance of impingement type separators with large elements, we shall consider the Union Carbide and Carbon "M.V." separators, Ullock (1956). All other devices, and many are available, required the same three basic equations describing pressure drop, reentrainment velocity and collection efficiency as a function of the specific geometry and operating conditions.

Streamlined teardrop shaped rods, arranged in staggered rows were chosen for impingement targets. The pressure drop through the device can be calculated from the known value of "C_D", the drag coefficient if the elements are far enough apart. If the rods are closely packed, the pressure drop may be more closely related to that for flow through a rectangular slot.

They found experimentally that "C_D" was usually less than the 0.05 value reported in the literature for $N_{Re} > 25$. However, the pressure drop across the streamline tubes is usually a minor fraction of the total pressure loss across the separator and its housing.

For the re-entrainment velocity it was found experimentally that:

$$u = 2,220 \frac{\sigma^{0.127} \rho_L^{1.27}}{\rho_G^{0.5}} \qquad (5.4.5\text{-}1)$$

where the velocity is in cm/sec, "σ" the surface tension in dyne/cm and "ρ_L" and "ρ_G" are the liquid and gas densities in g/cm³. It is interesting to compare this equation to Goldshmid and Calvert (1963) findings, that shattering of liquid drops takes place at a constant "N_{We}" regardless of drops volume, and different liquids had different shattering "N_{We}", but the numbers were all close to one another.

For widely spaced rods, the target efficiency, η, can be calculated from the impaction parameter for streamlined teardrop shape rods given in Figure 4.6.2-3, the cross-sectional area and the number of rows. The collection efficiency for "N" rows is:

$$E_n = 1 - \left(1 - \eta \frac{a}{A}\right)^N \qquad (5.4.5\text{-}2)$$

where "a" is the cross-sectional area of all the rods in one row and "A" is the total flow area.

For closely packed rods (as in the "M.V.") Calvert and Lundgren (1970) found that the collection efficiency is that for rectangular jet impaction (see Section 4.6.7). The efficiency of each stage of impaction can be found in Figure 4.6.2-20. Total penetration for the bank or rods is given by:

$$Pt = (1-\eta_J)^N \qquad (5.4.5\text{-}3)$$

where "η_J" is the collection efficiency for a given particle diameter in one stage of rectangular jet impingement.

5.4.6 CENTRIFUGAL SEPARATORS

Many devices utilize centrifugal forces in one way or another in addition to impaction, by making the gas take a turn, or several turns. Cyclones are an example of devices relying only on centrifugal forces for entrainment separation (see Section 5.3.7). They are widely used for the removal of drops larger than ≈5 µm. However, there is always the danger that wall creep of the liquid film will reduce efficiency. This can be prevented by adding a concentric cylindrical shield around the gas outlet or by fastening a conical skirt to the outside of the gas outlet duct.

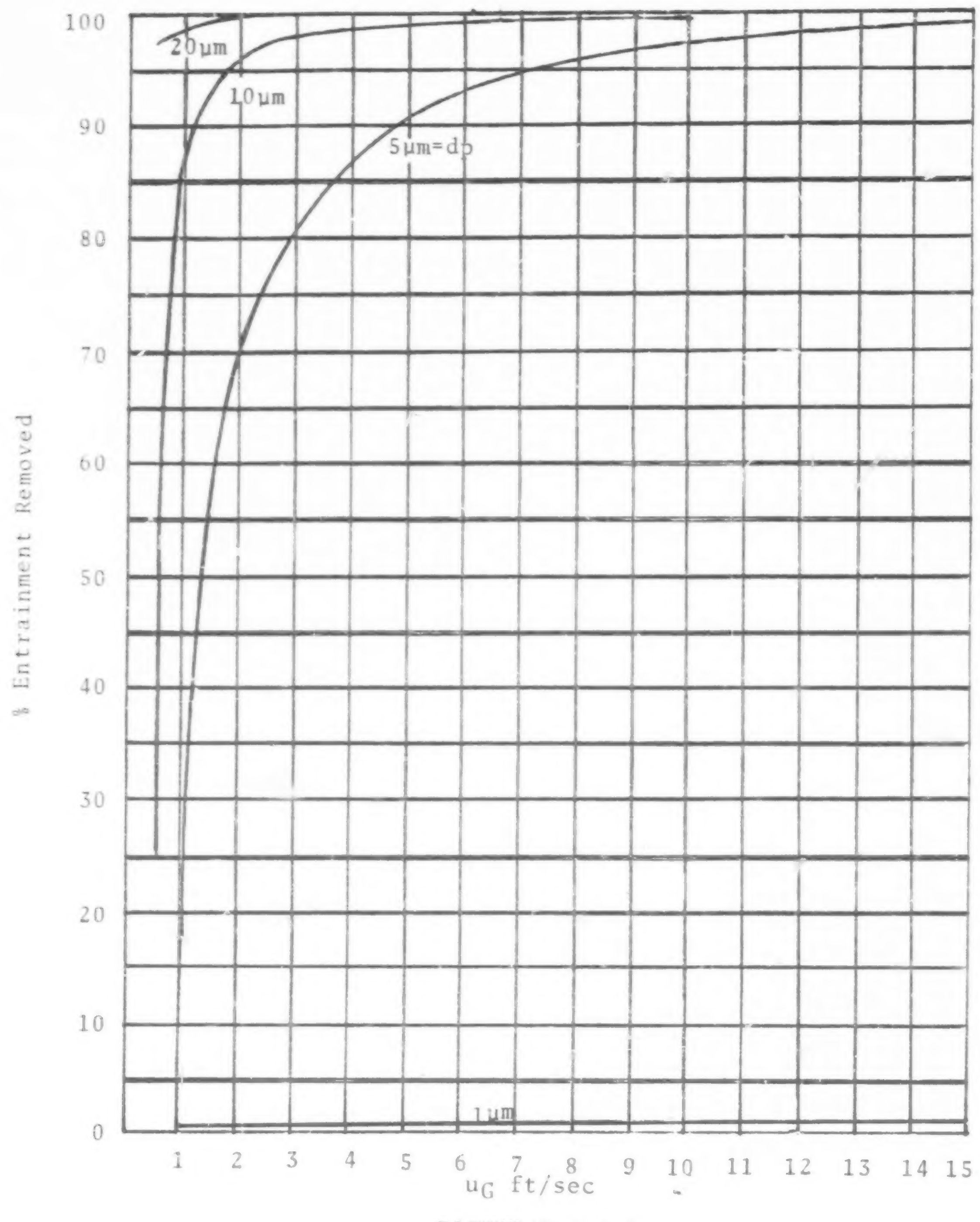

FIGURE 5.4.4-1

SEPARATION EFFICIENCY WATER
DROPLETS IN AIR 48 LAYERS .01" DIA. WIRE
DROPLET SIZES 1 TO 20 MICRONS

From ^ C.S. Industries

SECTION 5.4 NOMENCLATURE

LATIN

a - constant

A - cross sectional area, m^2 or cm^2

b - fraction of wire in "effective" position

c - mass concentration, Kg/m^3 or g/cm^3

d - diameter, m or cm

E - device particle collection efficiency

g - acceleration of gravity, 9.81 m/sec^2 or 981 cm/sec^2

K_p - inertia parameter

ℓ - length, m or cm

ℓ - length of bed measured in direction of gas flow, m or cm

m - mass, kg or g

n - number of rows of rods

n - number of layers of wire

Pt - penetration (one minus efficiency)

Q - volumetric flow rate, m^3/sec, cm^3/sec or lit s/sec

r - radius

u - velocity, m/sec or cm/sec

u - entrainment velocity, m/sec or cm/sec

V - volume, m^3or cm^3

W' - weight of bed per unit area, kg/m^2 or g/cm^2

Greek

η - efficiency due to a unit mechanism

ρ - density, kg/m^3 or g/cm^3

σ - liquid surface tension, dyne/cm

μ - viscosity, g/(cm sec)

SECTION 5.4 NOMENCLATURE

Greek

Subscripts

d - drop

G - gas phase

L - liquid phase

n - number of rows

p - particle

P - inertial impaction

t - terminal velocity

w - wire

SECTION 5.4 - REFERENCES

ACS Industries, "Mistermesh Entrainment Separator Design Manual".

Calvert, S., Lundgren, D., "Particle Collection in Close Packed Arrays", presented at A.I.H.A. Meeting, May (1970).

Carpenter, C. L., Othmer, C. F., A. I. Ch.E. Journal 1, 549-557. (1955).

Goldshmid, Y., Calvert, S., A.I.Ch.E. Journal, 9, 352 (1963).

Matthews, W. D., York, O., Presented at Gas Conditioning Conference, Univ. of Okla., (April 1963).

Montross, C. F., "Entrainment Separation", Chem. Eng. 60, 213-236, (1953).

Souders, M., Brown, G. G., Ind. Eng. Chem. 26, 98, (1934).

Ullock, D.S., "Summary of Experimental Measurements, Performance and Design of Streamline Tube or Rod Entrainment Separators", Memorandum Union, Carbide and Carbon Corporation, January 20, 1956.

CHAPTER 6

AUXILIARIES

TABLE OF CONTENTS

6.1 Introduction 6-3

6.1.1 Auxiliaries Needed 6-3

6.1.2 Chapter Outline 6-3

6.2 Gas Moving 6-4

6.2.1 Hoods, Ducts and Stacks 6-4

6.2.1.1 Hoods 6-4

6.2.1.2 Ducts 6-5

6.2.1.3 Stacks 6-6

6.2.2 Fans and Blowers 6-7

6.2.2.1 General 6-7

6.2.3 Motors 6-9

6.2.3.1 Totally Enclosed Motors 6-9

6.3 Liquid Moving 6-12

6.3.1 Pipework 6-12

6.3.1.1 Metal Pipework 6-12

6.3.1.2 Lined Metal Pipe 6-12

6.3.1.3 Non-Metallic Piping 6-13

6.3.1.4 Pipework Design 6-13

6.3.2 Pumps 6-13

6.3.2.1 Pump Operational Requirements 6-14

6.3.2.2 Standardization 6-14

6.3.2.3 Comparison of Pumps 6-14

6.3.2.4 Suction Head Requirements 6-14

CHAPTER 6
TABLE OF CONTENTS

6.4 Entrainment Separation 6-16
    6.4.1 Knock Out Pots. 6-16
    6.4.2 Gravity Settlers. .6-16
    6.4.3 Cyclones. 6-16
    6.4.4 Wire Mesh De-Entrainers or Demisters. 6-16
6.5 Solvent Recycle. 6-17
    6.5.1 Acidic Water. 6-17
    6.5.2 Alkaline Scrubbing Effluent 6-17
    6.5.3 Water Recirculation from Solid Contaminated Water . . .6-18
6.6 Sampling and Analysis. 6-19
6.7 Controls 6-20
    6.7.1 Gas Flow. 6-20
    6.7.2 Pressure Readings 6-21
    6.7.3 Control of Absorbers. 6-21
6.8 Health and Safety. .6-22
    6.8.1 Harmful Pollution Concentrations. 6-22
    6.8.2 Operational Safety Measures 6-22
    References. 6-25

CHAPTER 6

AUXILIARIES

6.1 INTRODUCTION

6.1.1 AUXILIARIES NEEDED

The engineering design of the scrubber itself is only a relatively small part of the engineering of the whole system. The rest of the system includes fan, pumps, gas ducts, liquid pipework, structures, the disposal of liquids and the dispersal of exhaust gases. All these different aspects must be considered in order to make a coherent system.

6.1.2 CHAPTER OUTLINE

The purpose of this chapter is to draw the reader's attention to the many facets of a pollution abatement system design which should be considered, apart from the scrubber itself. It is not the intent to give detailed theory of, say, centrifugal pump or fan design, but rather to guide the reader to the most convenient methods for pressure drop estimating, choosing pumps and fans, and the points to be considered in designing a complete installation.

Where appropriate, the sub-sections contain the following:

(a) Classification of equipment generally available, giving equipment characteristics.

(b) Typical pump and fan curves or appropriate design equations.

(c) The major design steps.

(d) Evaluation and choice of equipment.

6.2 GAS MOVING

6.2.1 HOODS, DUCTS AND STACKS

6.2.1.1 Hoods

In many cases involving chemical process scrubbers, the gases to be scrubbed emanate from substantially closed vessels. In these cases the scrubber will be connected by pipe or duct work and no hood will be used.

For such processes as wire pickling, steel strip pickling, metal plating, shot blasting and paint spraying, suction hoods are used. Even such enormous plants as blast furnaces have extraction hoods for removal of grit, fume and noxious exhaust gases. In this case the vessel tips away from the hood for pouring the charge of molten metal.

Suction hoods can be classified into three broad types: enclosures, receiving hoods and exterior hoods. Enclosures surround the point of emission, receiving hoods have the contaminant injected into them and exterior hoods capture contaminants from a source some distance away. An important function of hoods is the isolation of the pollutant source so that the minimum amount of ambient air is drawn in along with the process gas. This has the effect of reducing the control equipment size and often improving efficiency of operation by maintaining a high concentration of pollutant. Details of hood design can be found in Danielson (1967) and Hemeon (1963).

Of the three types of hoods outlined, consideration to the design of exterior hoods is of value. Baffling may be needed to prevent drafts from disturbing the air pattern and thus rendering an exterior hood ineffective.

A duct pulling air in one direction modifies the air flow in the room. The velocity of air along the axis of a suction duct falls off as the square of the distance from the opening. The percentage of the original velocity at distance x is given by Danielson (1967) as approximately:

$$\frac{Y}{100 - Y} = \frac{0.1\ A}{x^2} \qquad (6.2\text{-}1)$$

where Y = percent of the velocity at the opening which is found at point x on the axis.

x = the distance along the axis of the duct from the opening, m. or ft.

A = the area of the opening, m^2 or ft^2.

The velocity at the opening is given by:

$$u = \frac{Q}{A} \qquad (6.2\text{-}2)$$

If u_x = velocity at point x

u = velocity in the hood mouth

from Equation 6.2-1 and 6.2-2,

$$Q = u_x \, (10\ x^2 + A) \tag{6.2-3}$$

where Q = air volume required in any consistent units.

Equation 6.2-3 is for the air flow into a freestanding or unobstructed hood but it can be applied to a rectangular hood bounded on one side by a plane surface. In this case the hood is considered to be twice its actual size, the additional portion being the mirror image of the actual hood, with the bounding plane being the bisector, Danielson (1967). Equation 6.2-3 then becomes:

$$Q = u_x \, \left(\frac{10\ x^2 + 2\ A}{2}\right) \tag{6.2-4}$$

The point at which contaminants ejected into the air lose their velocity, due to air resistance is called the "null point". Imposed air velocities at the "null point" should never be less than 0.51 m/sec (100 ft/min). Draft velocities in industrial situations are normally 1 - 1.5 m/sec (200 - 300 ft/min).

For open tanks, slot extraction is used, with the slots situated along each side of the tank, or sometimes one side with blowing jets on the opposite side to give push-pull hooding. The slot velocity is normally 10 m/sec (2000 fpm). Tables of the volume of air per ft^2 of tank area for tanks of differing width to length ratio are given in Danielson (1967) and Hemeon (1963).

Tables are also given in the same references for exhaust requirements for various operations, such as bagging machines, screens, elevators and conveyors.

To design a hood first determine from tables the required air velocity in the room or at a point a known distance in front of the hood. Then proceed as follows:

(a) For a hood with one open face where work is done at x feet in front of the hood face, apply Equation 6.2-4. This will give the air volume required for a known hood area.

(b) For slots or tanks,

  (i) Find the surface area of the tank

  (ii) Determine the ratio of width to length

  (iii) From tables like those given in Danielson (1967) find the volume of air per ft^2 of tank area for the particular operation involved.

  (iv) From the recommended slot air velocity of 10 m/sec (2000 ft/min) the volume needed, and the length of the tank, calculate the width of the slot.

6.2.1.2 Ducts

In the design of a scrubbing system the pressure loss in the gas ducting should be a small fraction of the total pressure loss.

However, there is an economic balance between the cost of the duct and the pressure loss through the duct, or in other words, the fan power. Perry's Handbook (1963) gives economic pipe sizes. Approximate velocities of 9 - 15 m/sec (30 - 50 ft/sec) can be used for gases, in rough design calculations.

The pressure drop in a straight pipe can be estimated by means of the "velocity heads lost" method. This is a simplified approach based upon the fact that friction factor varies over only a small range for turbulent flow in moderately rough conduits.

On the average for turbulent air flow in large ducts, the frictional pressure drop is equal to one velocity head in a duct length of 60 duct diameters. The head loss (cm of air) is:

$$\frac{\Delta P}{\rho_G} = \left(\frac{\ell}{60\ d_t}\right) \frac{u^2}{2\ g} \simeq \left(\frac{\ell}{60\ d_t}\right) h_v \qquad (6.2\text{-}5)$$

where ℓ = pipe length, cm

d_t = pipe diameter, cm

ρ_G = gas density, g/cm³

u = gas velocity, cm/sec

g = gravitational constant, 980 cm/sec²

h_v = velocity head, cm of fluid flowing

For low pressure drop systems, such as those normally found in gas ducting, the additional losses due to bends in the duct, orifices, valves and fittings can be expressed as the number of velocity heads lost for each fitting. Tables of the velocity head loss can be found in Perry's Handbook (1963).

For multiple suction points of fume extraction equipment, the duct diameters can be calculated and installed using the "balance duct" method described in Danielson (1967) or by the blast gate method. In the balanced duct method start at the branch of maximum resistance, choose a velocity necessary to keep dust suspended, in a dust extraction system, and calculate the diameter and pressure drop. The next parallel duct must then be calculated to give the same pressure drop up to the point where they meet.

Flow straighteners or splitters mitred ducts can sometimes be used, in order to reduce the pressure drop, Perry (1963), but these must be used with caution on dusty or hot and corrosive duties.

6.2.1.3 Stacks

Large boiler plant stacks have a wind shield of reinforced concrete or of steel, with a separate inner flue or numerous flues of steel, moler brick, or occasionally stainless steel. The space between the inner flue and the outer wind shield, may be insulated with Perlite, or sometimes the inner metal flue is insulated with a mineral wool wrapping. This is to prevent the formation of acid dew on the inside of the metal chimney, which occurs below a temperature of ~130°C

(270°F) and also to prevent acid "smut" from being blown out of the chimney, Beaumont (1971) and "Symposium on Stack Design" (1966).

For wet scrubbing practice, chimneys for vapor saturated gases containing corrosive substances have to be made of rubber-lined steel, or of fiberglass reinforced resin. Occasionally very large central chimneys, with multiple flues as described above, are used for the dispersal of noxious exhaust gases from a number of separate processes in a chemical complex. In this case, the inner flues can be of acid resisting constructional materials and they are protected from the wind by an outer shell of reinforced concrete. With positive pressure chimneys, acid brick internal construction is best avoided because leaks can become progressively worse.

Fiberglass or plastic stacks can be supported in an open steel structure. In the case of plastic or rubber lined steel stacks, it is usual to take the lining over the end and down the outside for one diameter. Stacks are normally equipped with a sloping, lined false bottom below the side gas inlet, from which liquid can be drained through a seal leg.

Chimney or stack velocities are usually of the order of 9 - 15 m/sec (30 - 50 ft/sec), and sometimes cones are fitted at the top to give efflux velocities as high as 23 m/sec (75 ft/sec). The chief reason for high velocities is to eject the gases well away from the top of the stack and thus to increase the effective height and to avoid down-wash. Down-wash can damage the metal structure supporting the stack or the stack itself, or with a lined metal stack the steel on the outside can be damaged.

6.2.2 FANS AND BLOWERS

6.2.2.1 General

The range of pressure and flow in which various types of fans operate is given in Table 6.2-1.

TABLE 6.2-1

OPERATING RANGES OF FANS

Fan Type	Flow Range	Pressure Range atm
Axial (Propeller type)	Flows > 3 m^3/min (100 cfm)	up to 0.034 atm (14 inches water gauge) (0.5 psig)
Centrifugal (Closed impellers)	0.3 - 425 m^3/min (10 - 15,000 cfm)	Suction 0.395 atm (12" Hg) up to 0.68 atm (10.0 psig)
	Series connection to	0.53 atm
Centrifugal	to 1275 m^3/min (45,000 cfm)	to 0.175 atm (6.5 psig)

For fans, the basic laws governing volume, pressure and brake horsepower are as follows:

Volume $\propto$ rotor speed

Pressure $\propto$ (rotor speed)^2

Brake Horsepower $\propto$ (rotor speed)^3

Thus to attempt an increase in the output of a fan above its rated output is not recommended because the power required will increase as the cube of the speed of the rotor.

Noise generated by a fan is a function of the speed of the blade tip, or of the lobes of a positive displacement rotary type blower. The manufacturer should be consulted to ensure that too high a speed is not employed because the noise can be extremely irritating and can be transmitted through the pipework.

Typical characteristic curves of radial, backward and forward curved blades are presented in Figure 6.2-1. Care should be taken to design the fan and system to keep away from the region of instability or pulsing, which can occur below 30 - 50% of the optimum flow for the fan or blower. Backward curved bladed fans have the best characteristics from the point of view of stability and efficiency, because the horsepower curve and the efficiency curve peak at about the same zone on the volume/pressure curve.

Radial bladed fans lend themselves best to chemical process work because of their simplicity of construction and ease of rubber covering. They can be operated in series or parallel. Corrosion resistant fans can be obtained in fiberglass reinforced plastic, rubber-lined and sheet plastic lined or covered. Metal plated fans, vapor deposited metal coated fans and plastic dipped coated fans should be avoided on severely corrosive duties due to pinholes in the coatings. For chloride, chlorine, or hydrochloric acid under oxidizing conditions, titanium is a good material, especially so for fans, due to its high strength to density ratio. Sometimes a rubber-lined casing is used with a metal rotor of an exotic alloy. With rubber covered rotors the speeds have to be limited to prevent the adhesion between blade and the rubber covering from breaking down.

Compressors cannot normally be employed on scrubbing duties due to the corrosive nature of wet exit gases. They are, however, used for compressing vapors produced from the storage of volatile materials and transporting the vapors to scrubbing units or condensors.

Liquid ring pumps are used for vacuum systems and can be operated with sealing liquids, which will neutralize acid vapors or droplets, carried into the pump.

Ejectors are used to pump exhaust gases and scrub them at the same time. This is the case for HF guard scrubbers on HF storage systems, for soluble gas systems, or for guard scrubbers on chlorine where caustic soda solution, or Na_2CO_3 solution can be used as the absorbing medium. At the same time the ejector can be used to keep a slight negative pressure on the pipe work system.

Steam or air operated ejectors can also be used for the removal of inert gases from corrosive systems. Steam ejectors can be obtained having carbon linings which will withstand very corrosive conditions.

6.2.3 MOTORS

6.2.3.1 Totally Enclosed Motors

In the most corrosive chemical atmospheres, it is necessary to use totally enclosed fan cooled (TEFC) motors. Three phase motors are almost always used except for ratings below 1 or 2 hp, where single phase is often used due to the simpler wiring. The alternating current squirrel cage 3-phase induction motor is the most common motor used in industry.

Fans and compressors are often designed for certain specific speeds which are multiples of the cycles of the alternating current. With other speeds, it is usual to use "V" belt drives and pulleys, between the motor and the fan. Gear box drives are extremely expensive.

Alternating current motors may be either synchronous or induction motors. Synchronous motors operate at constant speed and induction motors operate at speeds slightly less than synchronous speed. Motor efficiencies average 97-98%. Synchronous motors can operate at very low speed (below 500 rpm) and are cheaper for high horsepower low speed duties. Induction motors do not usually operate below 720 rpm.

Motors and motor control equipment are manufactured for various classes of hazardous locations. These locations are defined by the National Electric Code Handbook.

Motors are also classified in accordance with a system laid down by the National Electrical Manufacturers Association (known as NEMA standards), where methods of cooling and mechanical protection are defined (NEMA Standards Publication). Any manufacturer's electric motor catalog will give details of the standard. There are nineteen standards for motor enclosures, that is, for the different types of protection for internal working parts. For chemical motors the most important enclosure types are:

(a) Splash proof

(b) Weather protected Type I

(c) Weather protected Type II, for driven snow, rain or dust

(d) Totally enclosed fan cooled (TEFC) for moisture, corrosive vapors, dust, and dirt

(e) Below 3 hp, totally enclosed, but no forced cooling

(f) Separately ventilated machines, with forced clean air cooling

(g) Motors for hazardous locations. Class I, vapors; Class II, dust; Class III, fibers and according to the degree of hazard:

Division 1, severe; Division 2, semi-hazardous. Division 1 motors are normally "explosion proof" motors.

Motors labelled "explosion proof" must be inspected by an approved representative of the Underwriters' Laboratories (1950). They are available up to 3000 hp at 3600 rpm. Further details on motors and starters can be obtained from Mead (1964), where types of motors and motor codes are concisely described.

Approximate relative prices of motors is as follows:

Drip Proof	100%
TEFC	190%
Explosion proof TEFC	210%

To give an idea of 1970 prices see Table 6.2-2 by Godfrey which is reproduced from "Building Construction Cost Data" (1970).

TABLE 6.2-2

ELECTRIC MOTORS PRICES (1970) FROM GODFREY (1970)

230/460 V A.C., 3ϕ, 60 cycle ball bearing squirrel cage induction motors, NEMA design A or B Standard Line, no installation included.

Horse-power	Synchronous Speed in RPM	Drip proof Class B ins. 1.15 Serv. fact.	Tot. enclosed Class B ins. 1.0 Serv. fact	Drip proof Epoxy Seal F ins. 1.0 Serv. fact.	Explosion proof Class B ins. 1.0 Serv. fact.
1	1800	$ 40	$ 55	$ 60	$ 77
	1200	49	63	70	84
5	1800	69	105	115	136
	1200	113	160	170	190
10	1800	110	195	210	225
	1200	180	250	245	290
15	1800	145	260	255	290
	1200	230	340	345	400
25	1800	215	390	380	450
	1200	340	510	505	580
50	1800	375	725	700	810
	1200	575	930	960	1050
75	1800	530	1140	1110	1300
	1200	790	1300	1250	1460
100	1800	690	1430	1350	1600
	1200	1225	1830	1750	2050
125	1800	830	1850	1700	2060
	1200	1480	2225	2225	2450
150	1800	1200	2100	1950	2300
200	1800	1550	2750	2350	3000

6.3 LIQUID MOVING

6.3.1 PIPEWORK

For most scrubbing duties the liquid to be conveyed will be corrosive and normally at 70 - 80°C (160 - 180°F). There is a wide variety of acid resisting pipework to choose from, but generally speaking rubber-lined pipe has the most versatility. It is easy to support, has the strength of steel and will withstand increase in temperature for a short time, will not disintegrate from vibration or liquid hammer. Fiberglass filament wound plastic pipe is also suitable for a very wide range of conditions of temperature, pressure and chemicals. The chief disadvantage of rubber-lined pipe is that it cannot be cut to size and has to be precisely manufactured with correct bands, flange drilling, etc. Site fabrication is not possible.

Most piping is manufactured to USA Standards Institute (1955) code for Pressure Piping.

6.3.1.1 Metal Pipework

Nominal pipe sizes are based on the approximate bore or internal diameter in inches. The sizes range from 1/8" to 12 inch. For sizes above 12", that is 14" or larger, the nominal size is based on the outside diameter. Small size pipe is available in two wall thicknesses, known as Schedule 40 and Schedule 80. For sizes of 14 inch and above the wall thickness varies from schedule number 10 to 160.

Tubing sizes are specified on the exact outside diameter and wall thickness and can be obtained in steel, bronze, brass, copper alloys and stainless steel. Tubing is thin walled and cannot be threaded.

Metal pipework can be flanged, threaded or welded. Generally speaking, for even slightly corrosive service, threaded pipe is not used. The thinner wall, stagnant zones, and stresses at the thread, can all lead to rapid localized destruction of the pipe.

With flanged metal pipe, or rubber lined flanged metal pipe, gaskets are used to seal the flanges. The gaskets must be suitable for the material being handled since the inner edge of the gasket is exposed to the process fluid.

6.3.1.2 Lined Metal Pipe

Rubber Linings

Hard rubber linings have good resistance to many strong acids and alkalis. To resist abrasion soft rubber linings are used. It is usual to use gaskets with rubber-lined flanged pipe since it protects the lining of the pipe, which is carried over the flange face, from damage.

Lead Lined Steel Pipe

This can be sheet lead or homogeneous lead. The homogeneous lead is bonded to the pipe by tinning and is good for temperature fluctuations and for temperatures to about 175°C. Sheet lead lined pipe is not recommended, but if used, breather holes should be put in the outer steel pipe to prevent trapped gases from buckling the inner lead lining. Lead linings are not commonly encountered due to the advent of plastic materials which have better properties.

Glass Lined Pipe

Useful for a wide variety of conditions but must be handled carefully.

Thermoplastic Lined Pipe

This can be obtained in PVC, Saran, polyethylene, polypropylene, fluorocarbons, and has better resistance to temperature than solid plastic pipe, due to the metal support. It is very useful for site fabrication, where with some varieties, the plastic can be cut to length, slid into a metal pipe and then swaged out at the flanged joints.

6.3.1.3 Non-Metallic Piping

Non-metallic pipe includes a wide variety of materials such as clay, concrete, stoneware, etc. and some specialized materials like glass and carbon. The solid plastic materials most commonly encountered for use with corrosive aqueous solutions are polypropylene, PVC and ABS (Acrylonitrile-Butadiene-Styrene) copolymer solid wall pipe with socket solvent welded connections. It is very easy to use, it can be cut with a hack saw and it doesn't take much skill to make a leak-proof joint. All types of fittings are available. Pipe supports should be at 1/3 of the distance used for steel pipe.

Fiberglass Reinforced Pipe

This is also useful for a wide variety of chemicals. It can be fabricated and assembled on site. Reinforced wound continuous filament pipe is inherently strong and can operate at higher temperatures and pressures than plain plastic pipe.

6.3.1.4 Pipework Design

The design of pipework for liquids is based on the same principles as described in the discussion of the flow of gases through ducts (Section 6.2.1.2) and is based on the same equations. For a detailed review of pipework the reader is referred to a Chemical Engineering Deskbook Issue (1969), to Perry's Handbook (1963), and to Rase and Barrow (1957).

6.3.2 PUMPS

Electric motor driven rotating pumps, especially centrifugal, are the most frequent pumps found in scrubbing equipment. Occasionally it is necessary to use reciprocating diaphragm sludge pumps, either air driven or mechanically driven, for thick slurries, though centrifugal pumps are also good for handling slurries of up to 30% solids (settled volume).

The selection of the correct pump is very important because good operation of the whole scrubbing system will probably depend on the pump. Breakdowns, or off-specification performance, can lead to loss of production or shut down of the main process for which the scrubber is only a minor part. A reliable trouble-free pump is therefore extremely important.

6.3.2.1 Pump Operational Requirements

There is such a wide selection of pumps to choose from that the best start is to define the duty required of the pump. To do this it is helpful to use a pump specification sheet which should be completed in as much detail as possible and sent to various vendors with the request for pump quotations. Centrifugal pumps have close ranges of flow and head in which they are operating at their best efficiency and the best choice of impeller size and speed can be made by the vendor. The specification should give enough information to define the head/flow characteristics required of the pump under different conditions which might be encountered during operation, so that the pump can be designed to be operated over a range of pressures and flows demanded by the external circuit.

6.3.2.2 Standardization

For refinery service the most widely used standard employed is the American Petroleum Institute (API) Spec. No. 610 (1965). Use of this engineering specification ensures a high quality pump to the best engineering standards.

Also the Chemical Standard Pump, or as sometimes called, the American Voluntary Standards (AVS) Pump specification ensures the purchase of a horizontal overhung impeller pump having certain standard dimensions, such as base mountings, pipe flange drillings and pipe connection locations.

6.3.2.3 Comparison of Pumps

Once the system pressure drop flow characteristics have been matched to the pump flow head curve, and the specifications sent to a number of vendors, it will probably be found from the quotations received that the choice of pump will become obvious by reasons of price and delivery and possibly power consumption. Sometimes with chemical pumps, such as rubber-lined pumps, the speeds of the pump will be limited by reason of adhesion or abrasion of the rubber. Under these conditions it will be necessary to select a speed which is not a normal multiple of the synchronous speed of a multipole induction motor. For this type of pump belt drives will be needed instead of the normal direct coupled motor.

6.3.2.4 Suction Head Requirements

Suction conditions cause more trouble than anything else. Too high a negative pressure at the eye of the impeller can cause boiling of the liquid, cavitation, and severe vibration with erosion of the impeller and noise and shaking of the pipework. This is especially true with hot or volatile liquids.

The net positive suction head (NPSH) available for the system should be calculated, including the velocity head of the liquid, and the subtraction of the liquid vapor pressure. This will give the absolute pressure available at the inlet to the pump. Under the conditions of maximum flow likely to occur the system must have a net positive suction head greater than the NPSH required by the pump. If insufficient NPSH is available from the system, cavitation will occur.

6.4 ENTRAINMENT SEPARATION

Removal of entrainment spray is possible by numerous methods. These include:

1. Gravity settling chambers.
2. Knock out pots. These are vessels in which the gas goes through a 180° reversal.
3. Cyclones.
4. A packed section of column.
5. Knitted wire mesh or plastic mesh demisters.
6. Swirl vanes, or zigzag vanes.
7. Specialized designs which depend on impingement due to directional changes in the gas stream, for example jets of gas impinging on a target plate.

Entrainment separator are discussed in more detail in Chapter 5.4.

6.4.1 KNOCK OUT POTS

These are usually designed with a side inlet pipe which is turned down pointing towards the base of the vessel. The gases enter at 6 - 9 m/sec (20-30 ft/sec) in the pipe and rise in the vessel at 1.5 - 3.0 m/sec (5 -10 ft/sec). The droplets impinge on a pool of liquid in the vessel. Droplets may also fall out due to gravity effects.

6.4.2 GRAVITY SETTLERS

The gas enters at one side and travels slowly through the vessel. The size of droplet removed can be estimated from the terminal settling velocity of the droplet and the residence time of the gas in the vessel.

6.4.3 CYCLONES

The principles and design methods for cyclone separator have been described in Chapter 5. When used solely for the purpose of separating entrained scrubber liquid, which has fairly large drop size, the cyclone duty is simpler than for the usual particulate pollution control.

6.4.4 WIRE MESH DE-ENTRAINERS OR DEMISTERS

These are very effective with clean liquid sprays but can become completely blocked with scaling liquids or dusty gases.

Wire mesh demisters operate with high efficiency on entrainment sprays. (Packing densities range from 112 - 166 kg/m^3 (7 - 10 lb/ft^3).) If dirty conditions are suspected, lower wire packing densities are used 112 kg/m^3 (7 lb/ft^3) for steel.

6.5 SOLVENT RECYCLE

The most general solvent used in wet gas scrubbers is water. When designing a complete gaseous effluent scrubbing system the treatment and disposal, or re-use, of the water must be considered, otherwise a gaseous pollutant will have been changed to a liquid pollutant. Details on liquid waste disposal are given in Chapter 12.

6.5.1 ACIDIC WATER

The normal system of acid scrubber water treatment is to neutralize the acid with a lime or limestone slurry to a pH which conforms to the local regulations,normally pH 6.5 to 7.0 In this way sulfates, fluorides and phosphates can be substantially removed from the water due to the low solubility of their calcium salts. It is normally necessary to pre-wet or pre-slurry the limestone, then to react this with the acid effluent in two stages. The second stage will have to operate with lime in order to complete the reaction, since it is not possible to raise the pH above about 4 using limestone alone.

The neutralized slurry then has to pass a thickener and the sludge settled out. It may be necessary to further dewater the underflow from the thickener with a rotary vacuum filter. The clear overflow can be returned to the process for re-use.

This treatment will also precipitate many metal in the form of hydroxides. The use of flocculant may be called for to achieve sufficient clarification of the overflow.

In the case of chloride effluents, neutralizing with limestone or lime will remove the metals but produce an effluent of calcium chloride. A portion of this could be recycled, depending on its concentration, but calcium chloride is becoming difficult to dispose of.

Scrubbing water recycle systems are frequently used where the contaminated water is isolated in a ponding system and is recycled to various scrubbers. The overflow from the pond has to be treated, as described above, before discharge to a receiving water.

With HCl processes, the HCl can often be recovered from a scrubber at a high enough strength to be recycled to a process or to be sold, if pure enough, or it can be purified before sale. Oxides of nitrogen frequently arise in processes and they will appear as nitrates in scrubber effluents. Reduction to nitrogen is one method of disposal; removal by ion exchange resins is also a possibility.

6.5.2 ALKALINE SCRUBBING EFFLUENT

Although not so commonly encountered,the pH adjustment of alkaline waste from industrial processes is usually accomplished by treatment with sulfuric acid, since this is the cheapest acid available. Hydrochloric acid could also be used if for some reason the sulfate were objectionable. In some cases it may be possible to use CO_2 from waste process gases or from submerged combustion of natural gas. This is used to remove soluble calcium ion from solution in alkaline wastes where the pH is maintained at 10 or higher.

6.5.3 WATER RECIRCULATION FROM SOLID CONTAMINATED WATER

Many wet scrubbing treatments produce fine solid suspensions such as from steel works, from coal drying operations and from grinding and screening.

Sedimentation is the most common way to clean up the water. Sometimes the solids are so fine that chemical coagulation has to be used. Salts of polyvalent metals can be used to neutralize the charge on a suspended colloid. Also synthetic and natural organic polymers are gaining acceptance for coagulation. Often an economic case can be made for their use, due to the reduction in settling area and equipment, needed to clarify water.

The final solid waste produced has to be buried, used as land fill, dumped in a mined out area, or disposed of by incineration; in some cases it can be used for constructing roads.

The continuous recirculation of scrubber water can result in a build up of dissolved solids due to evaporation of the water. Solids can become concentrated to such an extent as to render the discharge unacceptable to the local authorities. This can be overcome best by increasing the make up of fresh water to the system. Most methods of purification, other than those producing a precipitate, will result in a more concentrated effluent. Reverse osmosis, electrodialysis, or ion exchange inevitably produces a clean stream and a more concentrated waste stream.

6.6 SAMPLING AND ANALYSIS

Sampling and analysis are important at all stages of scrubber design and operation. First it is necessary to determine the concentrations and properties of contaminants coming from the uncontrolled source. Then it is necessary to test the equipment after installation to ensure that it meets specifications. When problems occur and modifications must be made to improve performance, measurements must also be made. Finally, the scrubber effluent must be monitored to detect any deviation from satisfactory operation.

Both sampling and analysis methods are continually being developed and in an increasing number of cases, legally approved (or required) methods are being set by EPA, and are published in the Federal Registrar. Other air pollution control agencies also set up approved sampling and analysis methods. Before departing on an independently chosen course, it is essential to check the appropriate local, state, and federal requirements.

Sampling is generally the most difficult operation. Variations in pollutant concentration with time, location along the duct axis and across the duct, proximity to mixing streams and location following turns are generally to be expected. Consideration of sources of sample bias and adequate means for counteracting them are mandatory.

For the designer the most important thing to do is provide good sampling locations and facilities. This means 5 to 10 diameters of straight duct following any flow disturbance, several diameters of straight duct preceding a disturbance, and flow straighteners where possible. Sampling facilities should give a good safe platform, easy access, utilities for operating sampling equipment, hoisting equipment, and shelter for personnel. Details can be found in Stern (1968), Danielson (1967) and other texts.

Analytical methods for gases are so numerous and specific that it is impossible to even represent them here. Approved analytical methods can be obtained from EPA. Good background information is given in Stern (1968), Danielson (1967), and Ruch (1967). Specific methods are given in some instances by control agencies.

Particle size analysis is extremely important for scrubber design and no simple, general purpose method or apparatus is available. It is essential that this type of analysis be done by a competent specialist. For particles of about 1/2 micron diameter and larger, the cascade impactor is a good instrument, especially if backed up with some microscopic examination. Particles smaller than about 1/2 micron are most reliably measured with an electron microscope. Several instruments are available and, in general, they have regions of greater and lesser reliability.

Particle size measurements made on collected and then re-dispersed dust are questionable. It is always necessary to know whether the dust was agglomerated when analyzed, or vice versa. For particles larger than one or a few microns, this becomes less sensitive and careful techniques can yield good data. References such as Cadle's "Particle Size" (1965), Stern (1968), and Strauss (1966) give good background.

6.7 CONTROLS

Some of the equipment available for the control of absorption systems and the more likely systems to be encountered are listed here. A control loop consists of the measuring element and the control instrument, which compares the variable measured with some standard and sends out a pneumatic or electrical signal to a control valve.

Normally control valves are pneumatically actuated rather than electrically, due to the more rapid response and freedom from wear. The different types of control valve are illustrated in Perry's Handbook (1963).

Measuring devices

(1) Flow - Venturi meters or orifice plates can be used, in which the pressure drop is measured or recorded. If desired the flow recorder controller can be used to send a signal to a valve to control the flow at some desired rate. The differential head is measured by means of force balance diaphragms or U tube manometers (Byrne (1969)). Because of the square root relationship between flow rate and head, the range of such meters is usually about 3 to 1.

Electromagnetic meters are useful for flow measurement of corrosive media or for slurries. They have the advantage that they do not obstruct the pipe bore.

(2) Level - Simple level controllers of the direct acting pneumatic type, that is those that send a signal directly to a valve without going through a controller, are very useful. These can be used to keep the level constant on a recycle tank by means of water addition, or to sound a low or high level alarm if connected to a pressure switch. Bubbling level devices connected to differential pressure transmitters are also useful.

(3) Temperature - Gas filled, liquid filled or bi-metallic elements can be used in conjunction with a pneumatic transmitter to record, control or give temperature alarm. With quenching systems for high temperature gases, a high temperature alarm can be used to trigger an emergency water supply, either from an emergency head tank or from an emergency water main connected to a well.

(4) Density - This can be controlled by bubblers, floats or by systems whereby a loop containing the fluid is continuously weighed. All these devices normally give pneumatic signals ranging from 0.2 to 1 atm (3 psig to 15 psig) over the full range of the variable measured and normally a 1.7 atm (25 psig) air supply is required to supply the instrument and any control valve or pneumatic actuator.

6.7.1 GAS FLOW

The quantity of gas passing through the system is usually controlled by the suction fan characteristic and the design pressure drop of the system. If necessary, the fan discharge can be controlled by a damper or butterfly valve. In the blast gate system the flows in the lines are controlled by dampers.

6.7.2 PRESSURE READINGS

(a) Gases. It is advisable to have pressure tappings and pressure drop readings at regular intervals through the scrubbing system. In this way changes in flow due to a change in fan performance or due to blockages and flooding can be detected.

(b) Liquids. Pumps should be equipped with pressure gauges. By measuring the motor amperes on the pump and the discharge pressure, the pump characteristic curve can be checked to ensure that the pump is operating correctly.

Orifice plates can also be installed in crucial liquid lines to ensure that the correct flow is passing. Pressure gauges should be installed upstream of the spray nozzles.

6.7.3 CONTROL OF ABSORBERS

With a packed column absorber, liquid flow should be controlled with a valve and rotameter or orifice plate, to ensure the correct liquid loading in the packing.

Sometimes a definite concentration of solute is desired in the column effluent. In such cases the make up water can be automatically controlled by measuring and controlling some property of the solution, such as the specific gravity, electrical conductivity or even boiling point. With some HCl absorbers a small side stream is taken to an electrically operated boiling tube and the boiling point of the acid measured. This varies from 100° to 108°C with a change in concentration from zero to 21% HCl. It is sensitive in the range of 5 to 15% HCl.

With spray absorbers and other scrubbers where the liquid is dispersed through nozzles, blockage can be detected by changes in pressure at the supply pumps.

6.8 HEALTH AND SAFETY

One of the main objectives of any scrubbing system is the protection of the health of the people living and working in the vicinity of the plant. Although community air pollution requirements are well known, because they are the basis for requiring scrubbers, in-plant occupational health considerations are sometimes neglected. A scrubber which produces a satisfactory effuent in terms of the community air mass may cause very high concentrations in its immediate vicinity due to leaks, maintenance operations, etc.

Apart from gaseous pollutants, small particles and mist droplets are a major problem in air pollution control. Fumes, from low melting point metals, such as lead, arsenic, beryllium and zinc are extremely toxic and a high collection efficiency is necessary.

6.8.1 HARMFUL POLLUTION CONCENTRATIONS

Tables of T.L.V. (threshold limit values) are issued by the American Conference of Governmental Industrial Hygienists (A.C.G.I.H.) (1957). These are the limits for healthy people, working 40 hours/ week. More recent T.L.V. may be found in the appendix to Industrial Ventilation (1970).

Another useful source of information on toxic limits of various chemicals and on the safety aspects of handling chemicals is that of the Manufacturing Chemists Association, who issue safety data sheets covering a large spectrum of chemicals, and also pamphlets of "Recommended Safe Practices and Procedures - Training of Process Operators" (Safety Guide SG 15).

6.8.2 OPERATIONAL SAFETY MEASURES

Certain safety requirements are common to all industrial plants. Many are set by local building codes or by insurance requirements.

Elevated equipment on structures should have alternative means of escape, should a fire or escape of noxious gases occur. Operators should not have to work more than 40 feet from an escape door or from a ladder.

Process equipment which has access manholes, often used valves, or equipment which may need regular maintenance, should have platforms for ease of access when the location is more than eight feet from the ground. Hand-rails should be provided around all platforms, and ladders more than 12 feet above ground should have cages extending to eight feet above ground. Pits and pumps should be protected by handrails.

Handling equipment is needed for lifting items which must be lifted during maintenance. Either access should be provided for mobile cranes, or davits are needed for manway covers, for heat exchanger headers and heavy equipment. All moving equipment, drive couplings, belt drivers and especially conveyors should be enclosed.

Stringent rules must be observed for the isolation of equipment that is to be entered by personnel for maintenance; especially double valving and bleeding of lines, rules to do with opening manways, supervision of people entering vessels and the testing of atmospheres for explosive or toxic materials, as well as the isolation of electrical equipment. These are discussed in detail in Perry (1963).

For testing of the environment for toxic gases, testing units are available which operate by sucking a gas sample through a tube filled with chemicals by means of a small hand-operated bellows. The tube is calibrated and a color change will take place in the material packed in the glass tube to a certain height up the tube. The concentration can then be read off. It is possible to obtain these samplers or testers to cover a wide range of gases, tubes being specific for certain gases.

Further information on safety may be found in Kirk-Othmer (1965).

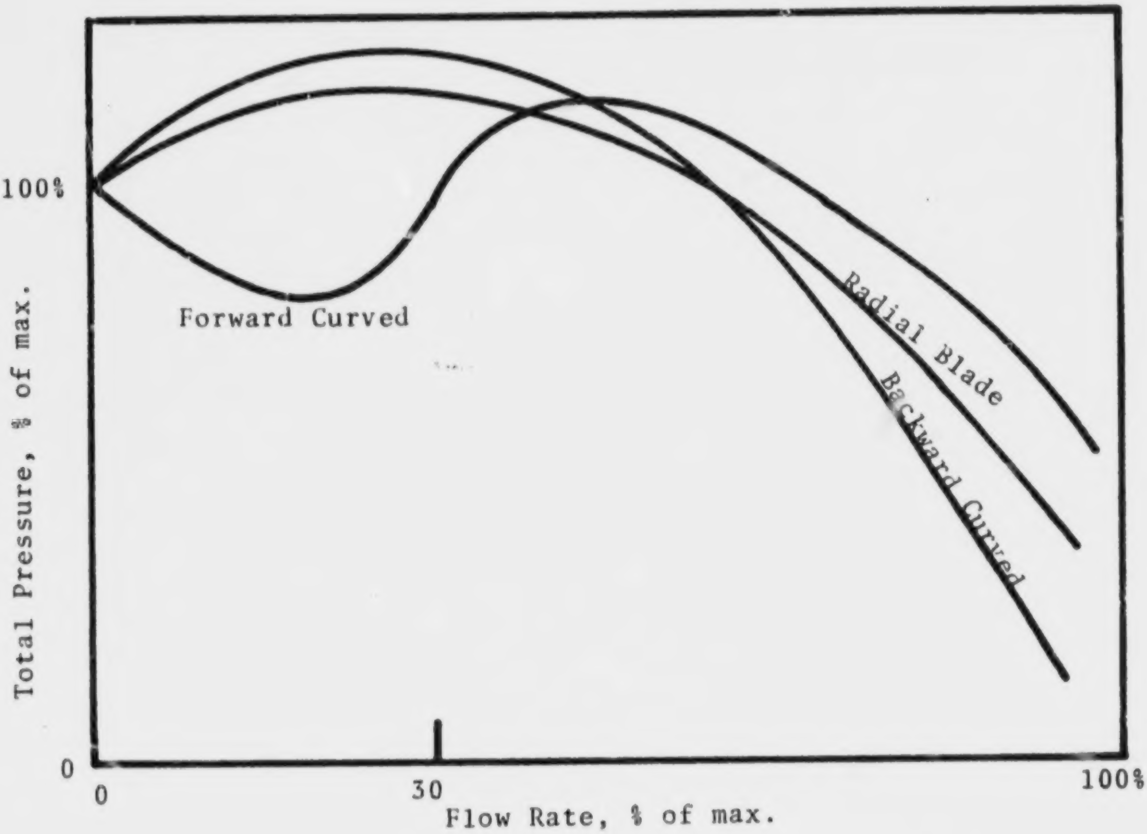

FIGURE 6.2-1

TYPICAL CHARACTERISTIC CURVES OF FANS

CHAPTER 6 - REFERENCES

American Petroleum Institute, "Centrifugal Pumps for Refinery Service", Spec. No. 610, 4th ed., API, 1271 Ave. of the Americas, New York, 10020 (1965).

American Voluntary Standards (AVS), "Pump Specifications", The Hydraulic Institute, 122 E. 42 St., New York, N.Y., 10017.

Beaumont, M., Journal of the Inst. of Fuel, 44, p. 92 (1971).

Byrne, E. J., Chemical Eng. Deskbook Issue, p. 189 (1969).

Cadle, R. D., "Particle Size", Reinhold Pub. Corp., New York(1965).

Chemical Engineering - Deskbook Issue, McGraw-Hill, April 14 (1969).

Danielson, J. A., Ed., "Air Pollution Engineering Manual", L. A. Air Pollution Control District and Department of HEW, Cincinnati (1967).

Godfrey, R. S., "Building Construction Cost Data, 1970", Robert Snow Means Company, Inc., Duxbury, Mass. (1970).

Hemeon, W. C. L., "Plant and Process Ventilation", 2nd ed., The Industrial Press, New York (1963).

Industrial Ventilation, "A Manual of Recommended Practice", 11th ed. by A.C.G.I.H. (1970).

Kirk-Othmer, "Encyclopedia of Chemical Technology", 2nd ed., Vol. 7, John Wiley & Sons, New York (1965).

Mead, W. J., Ed., "The Encyclopedia of Chemical Process Equipment", Reinhold Publishing Corp., New York (1964).

NEMA Standards Publication - Motors and Generators, National Electrical Manufacturers Association, New York.

Perry, R. H., Ed., "Chemical Engineers Handbook", 4th ed., Chapter 5, McGraw-Hill Book Co., New York (1963).

Rase, H. F., Barrow, M. H.,, "Project Engineering of Process Plant", Chapter 18, John Wiley & Sons, Inc., New York (1957).

"Recommended Safe Practices and Procedures - Training of Process Operators" (Safety Guide SG 15), Published by the Manufacturing Chemists Assoc., 1825 Connecticut Avenue, N.W., Washington D.C., 20009.

Ruch, W. E., Ed., "Chemical Detection of Gaseous Pollutants", Ann Arbor Science Publishers, Ann Arbor, Michigan (1967).

"Standards for Electric Motors and Generators for Use in Hazardous Locations", Underwriters Laboratories, Inc., Chicago, Ill. (1950).

CHAPTER 6
REFERENCES

Stern, A. E., "Air Pollution", 2nd Ed., Vol. 2, Chap. 28, Academic Press, New York (1968).

Strauss, W., "Industrial Gas Cleaning", Pergamon Press, Oxford (1966).

"Symposium on Stack Design", Journal of the Inst. of Fuel 39, pp. 21-29 (1966).

T.L.V. Tables by Amer. Conf. of Gov. Indust. Hyg. (A.C.G.I.H.) (1957).

USA Standard Institute - Code for Pressure Piping, B.31.1, Published by A.S.M.E., United Engineering Center, New York (1955).

CHAPTER 7

SCRUBBER PERFORMANCE ON INDUSTRIAL EMISSIONS

TABLE OF CONTENTS

7.1 Introduction 7-2

7.2 Processes Utilizing Scrubbers. 7-6
  7.2.1 Mineral Industries. 7-6
    7.2.1.1 Coal Drying. 7-6
    7.2.1.2 Stone Crushing 7-11
    7.2.1.3 Clay Products. 7-14
    7.2.1.4 Lime Preparation 7-17
    7.2.1.5 Miscellaneous Mineral Industries 7-20
  7.2.2 Fuel Combustion 7-22
  7.2.3 Metallurgical Processes 7-36
    7.2.3.1 Blast Furnaces 7-36
    7.2.3.2 Steel Manufacture. 7-39
    7.2.3.3 Iron Foundries 7-44
    7.2.3.4 Ferroalloys 7-49
    7.2.3.5 Copper Smelting and Refining 7-52
    7.2.3.6 Aluminum Processing. 7-56
    7.2.3.7 Electroplating 7-61
    7.2.3.8 Nonferrous Salvage Operations. 7-64
    7.2.3.9 Chemical Cleaning, Etching and Milling of Metals 7-68
    7.2.3.10 Miscellaneous Metallurgical Industries . . . 7-70
  7.2.4 Chemical Processes. 7-73
    7.2.4.1 Petroleum Refining 7-73
    7.2.4.2 Pulp Manufacture 7-77
    7.2.4.3 Acid Manufacture 7-83
    7.2.4.4 Fertilizer Manufacture 7-91
    7.2.4.5 Asphaltic Pavement Manufacture 7-97
    7.2.4.6 Chlorine Gas Manufacture 7-103
    7.2.4.7 Miscellaneous Chemical Industries. 7-106
  7.2.5 Food and Feed Industry 7-112
  7.2.6 Waste Disposal. 7-116
  7.2.7 Miscellaneous Processes 7-121

7.3 Generalizations Regarding Scrubber Use 7-123

  7.3.1 Unit Processes to Which Scrubbers are Applied 7-123
    7.3.1.1 Calcining Processes. 7-123
    7.3.1.2 Combustion Processes 7-123
    7.3.1.3 Crushers and Mills 7-126
    7.3.1.4 Driers 7-126
    7.3.1.5 Gases 7-129
    7.3.1.6 Liquid Mists 7-129
    7.3.1.7 Smelting 7-129
  7.3.2 Processes to Which Each Type of Scrubber is Applied . 7-133
  7.3.3 Sales of Scrubbers Compared with Other Equipment . . 7-135

CHAPTER 7

7.1 INTRODUCTION

Purpose

The same general types of scrubbers control the emissions from many potentially polluting processes. However, scrubber performance gauged in terms of efficiency, reliability, and cost, is widely variable. Before designing a new scrubbing system or upgrading an old one, it is often helpful to evaluate those systems devised by others with a similar problem. In this way, past mistakes due to unforeseen peculiarities of the individual situation can sometimes be avoided. A survey of industrial scrubber users was performed in conjunction with the present scrubber study. The questionnaire form used presented in the appendix, indicates the differences between information requested and that available or provided. The information gathered from the survey is presented in the following sections.

Method of Presenting Data

Section 7.2 supplies information on the scrubbers which have been applied to certain industrial processes. The processes covered are those to which scrubbers have been frequently applied, and are listed in Table 7.1-1. The suitability of a particular scrubber to a certain process depends upon the type of emissions which come from the process, the type of scrubber used, process conditions such as temperature, and the way in which the scrubber is operated. Information on each of these factors is presented.

A general description of each process is given. Then follows a description of the emissions from that process, and the types of scrubbers used to control the emissions. The tables present data on the type, quantity and properties of the particulate and gaseous emissions coming from the process. Emission data are included for comparative purposes, and for qualitative problem analysis. They should not be used to design a pollution control device; tests should be run. Particle size distribution data have been taken from the Midwest Research Institute report (1970). Their size vs. frequency data were converted to a log vs. probability plot, a straight line forced through the data, and the characteristic particle sizes picked off for inclusion here.

The data obtained from the scrubber user survey is presented in a rationalized format. An explanation of the format is given in Table 7.1-2. For those readers preferring English units to the metric ones used, Table 7.1-3 supplies some commonly used conversion factors.

Most of the data were obtained by the source operator for air pollution control agency acceptance tests. Some were developed for internal company information and evaluation purposes. In many cases, the data are incomplete. This is because the complete information desired for the present study was unnecessary to achieve the purpose for which the tests were run. For example, most regulations specify an outlet loading and are not concerned with scrubber inlet loading or efficiency.

TABLE 7.1-1

PROCESSES TO WHICH SCRUBBERS ARE FREQUENTLY APPLIED

Section	Process
7.2.1	Mineral Processing
7.2.1.1	Coal Drying
7.2.1.2	Stone Crushers
7.2.1.3	Clay Processing
7.2.1.4	Lime Processing
7.2.1.5	Miscellaneous Mineral Processes
7.2.2	Fuel Combustion
7.2.3	Metallurgical Processes
7.2.3.1	Blast Furnaces
7.2.3.2	Steel Manufacture
7.2.3.3	Iron Foundries
7.2.3.4	Ferroalloys
7.2.3.5	Copper Smelting & Refining
7.2.3.6	Aluminum Smelting & Refining
7.2.3.7	Electroplating
7.2.3.8	Nonferrous Reclamation Processes
7.2.3.9	Chemical Milling
7.2.3.10	Miscellaneous Metallurgical Processes
7.3.4	Chemical Processes
7.2.4.1	Petroleum Refining
7.2.4.2	Wood Pulping Industry
7.2.4.3	Acid Manufacture
7.2.4.4	Fertilizer Manufacture
7.2.4.5	Asphaltic Pavement Manufacture
7.2.4.6	Chlorine Gas Manufacture
7.2.4.7	Miscellaneous Chemical Processes
7.2.5	Food and Feed Processes
7.2.6	Waste Disposal
7.2.7	Miscellaneous Processes

TABLE 7.1-2

DATA PRESENTATION FORMAT - EXPLANATION

General

1) # - for reference purposes

2) Process - process to which scrubber is applied

Carrier Gas

1) m^3/hr - cubic meters per hour of gas going to scrubber, at inlet conditions

2) T_i - temperature of inlet gas, centigrade

3) T_e - temperature of outlet gas, centigrade

Particles

1) name - name of contaminant dust

2) $(g/m^3)_e$ - grams of dust per cubic meter of gas - coming from scrubber, at outlet conditions

3) % E - percent efficiency of dust removal in scrubber

Gas

1) name - name of contaminant gas

2) $(ppm)_e$ - volumes contaminant gas per million volumes gas coming from scrubber

3) % E - percent efficiency of gas removal in scrubber

Solution

1) composition - composition of scrubbing liquid

2) m^3/hr - cubic meters per hour of solution passing through scrubber

Cost

1) ΔP cm - pressure through scrubber, in centimeters of water

2) installed $ - total installed cost of scrubber system

3) OP $/mo - scrubber system operating cost in dollars per month

TABLE 7.1-3

CONVERSION FACTORS - METRIC AND ENGLISH UNITS

To Convert From	To	Multiply By
centimeters of water	inches of water	0.394
cubic feet per min	cubic meters per hour	1.70
cubic feet	cubic meters	0.0283
cubic meters	cubic feet	35.3
cubic meters per hour	cubic ft per minute	0.589
cubic meters per hour	gallons per minute	4.4
feet	meters	0.3048
gallons per minute	cubic meters per hour	0.227
grains per cubic ft	grams per cubic meter	2.29
grams per cubic meter	grains per cubic foot	0.437
inches of water	centimeters of water	2.54
meters	feet	3.28

7.2 PROCESSES UTILIZING SCRUBBERS

7.2.1 MINERAL INDUSTRIES

7.2.1.1 Coal Drying

Process Description

Markets have expanded for high quality coal. The sizing and beneficiation procedures followed to achieve the desired quality are primarily wet methods. To prevent freezing or to meet customer specifications, the wet product is usually passed through a drier which contacts the wet coal with hot gas produced by fuel combustion.

The hot gas dries the coal, but also sweeps up small coal particles which are then exhausted with the gas to whatever air pollution control equipment may be fitted. Particle loading to the equipment is about 450 grams per cubic meter, but this value is widely variable, depending on the way the drier is operated, and the properties of the coal dried.

Scrubbers Used

Control equipment almost always utilizes a cyclone, which decreases the particle loading to about 7 - 12 grams per cubic meter. The cyclone system may be followed by a scrubber, usually of the moving bed, plate, or venturi type. Scrubbers further lower particle loadings to from 0.7 to 0.07 grams per cubic meter.

The hot gases used to dry coal include the combustion products of sulfur-bearing fuels. To prevent corrosion from the sulphuruous gases, those parts of scrubbers which come into contact with the gases are usually made of stainless steel. Data for thermal coal driers is in Table 7.2-1. Information on typical uncontrolled emissions from thermal coal driers is presented in Table 7.2-2.

TABLE 7.2-1 SCRUBBER PERFORMANCE DATA - Coal Drying.

GENERAL		SCRUBBER		CARRIER GAS			PARTICLES			POLLUTANT GAS			SOLUTION		COST		
#	Process	Name	Description	m^3/hr	T_i °C	T_e °C	Name	$(g/m^3)_e$	%E	Name	$(ppm)_e$	%E	Composition	m^3/hr	ΔP cm.	Installed $	OP. $/mo.
1	Coal Thermal Drier	Moving Bed		51,000		66	Coal Dust	0.069					Water	57	53.5	74,000	
2	Coal Thermal Drier	Moving Bed		71,500		58	Coal Dust	0.323					Water	34	23.9	75,700	
3	Coal Thermal Drier	Impnge. Plate		71,500		66	Coal Dust	0.218					Water	79.5	15.2	65,000	
4	Coal Thermal Drier	Impnge. Plate		127,000		54	Coal Dust	0.103					Water	79.5	15.4	125,000	
5	Coal Thermal Drier	Impnge. Plate	6m x 6m	196,000		51	Coal Dust	0.17					Water	79.5	12.7	150,000	
6	Coal Thermal Drier	Impnge. Plate	316 S.S.	340,000		66	Coal Dust	<0.23					Water	145	20.3		
7	Coal Drier	Venturi		161,000			Coal Dust	0.115					Water		50.9	143,000	
8	Coal Drier	Venturi		170,000			Coal Dust	0.083	99.8				Water	18.1	101		
9	Coal Drier	Venturi					Coal Dust	0.149					Water		25.4		
10	Coal Drier	Venturi					Coal Dust	0.137					Water		38.2		
11	Coal Drier	Venturi					Coal Dust	0.110					Water		52		
12	Coal Drier	Venturi					Coal Dust	0.027					Water		66		
13	Coal Drier	Venturi		180,000			Coal Dust						Water			120,000	
14	Coal Drier	Venturi		170,000			Coal Dust						Water			200,000	
15	Coal Drier	Venturi		170,000		52	Coal Dust	<0.114					Water		≈100	200,000	
16	Coal Drying	Venturi		340,000			Coal Dust						Water			180,000	

TABLE 7.2-1 cont'd. SCRUBBER PERFORMANCE DATA - Coal Drying.

GENERAL		SCRUBBER		CARRIER GAS			PARTICLES			POLLUTANT GAS			SOLUTION		COST		
#	Process	Name	Description	m³/hr	T_i °C	T_e °C	Name	$(g/m^3)_e$	%E	Name	$(ppm)_e$	%E	Composition	m³/hr	ΔP cm.	Installed $	OP. $/mo.
17	Coal Drying	Flooded Disk		344,000			Coal Dust						Water	229	89		
18	Coal Drying	Impnge. Plate	6.1 m tall	170,000	53		Coal Dust	0.115	99				Water	166		200,000	
19	Coal Thermal Drier	Impnge. Plate		330,000	66		Coal Dust						Water		20		
20	Coal Thermal Drier	Impnge. Plate		178,000	66		Coal Dust						Water		10		
21	Coal Thermal Drier	Venturi		151,000	82		Coal Dust		99				Water				
22	Coal Thermal Drier	Venturi					Coal Dust						Water			75,000 (FOB)	
23	Coal Thermal Drier	Venturi		37,400			Coal Dust	0.103	99.5				Water				

TABLE 7.2-2

TYPICAL COAL DUST EMISSIONS FROM THERMAL COAL DRIERS

Type of Drier	°C out	g dust / Kg coal dried	loading, typical g/m³	particle density g/m³	Particle Size microns 16% under	Particle Size microns 50% under
Fluidized Bed Driers	32-200	6.5	460	1.35	45	200
Multilouver Driers			460	1.35	6.6	28
Flash Driers		6 See note 3	46 see note 3	1.35	0.68	3
Cascade Driers			460	1.35	6.6	28

Notes:

(1) Apparent density of particles is variable due to porosity and water content of coal

(2) Quantities of dust produced given above are very approximate, and depend upon factors such as moisture content of the product, coal friability, etc.

(3) After cyclone precleaner

All data adapted from Midwest Research Institute (1970)

SECTION 7.2.1.1 - REFERENCES

Eckman, Frank (1969)
"Scrubbing Coal Drier Exhaust Gases, " APCA Meeting, June 1969, paper 69-85.

Jackson, Daniel, Jr. (1966)
"Dust Control and Sound Abatement," Coal Age, November 1966.

Jones, Donald W. (1969)
"Dust Collection at Moss No. 3," Mining Congress Journal, July 1969.

King, D. T. (1967)
"Dust Collection in Coal Preparation Plants," Mining Engineering, August 1967.

Midwest Research Institute (1970)
"Handbook of Emissions, Effluents, and Control Practices for Stationary Particulate Pollution Sources," NAPCA Contract No. CPA 22-69-104, November 1, 1970.

Northcott, Elliot (1967)
"Dust Abatement at Bird Coal," Mining Congress Journal, 53, November 1967.

Walling, J. C. (1969)
"Air Pollution Control System for Thermal Dryers," Coal Age, September 1969.

7.2.1.2 Stone Crushing

Process Description

Dust is discharged due to air motion from stone crushing and processing machines. Factors influencing the dust properties include moisture content of the stone, type and amount of stone processed, and the design of the crushing and processing equipment.

If raw material drying is necessary prior to processing, the drier can be a significant source of dust. Direct fired rotary driers, either parallel or counter flow, are generally used. Emissions depend upon the degree of drying achieved, the type and amount of material dried, and the design of the drier.

Scrubbers Used

Dust can be suppressed by keeping the stone moist throughout the crushing and screening process. As crushing produces new dry stone surface area, spray nozzles are often located at the crusher inlet and outlet ports.

As stone dust is salable, some plants prefer to let the dust form, and then collect as much as possible in the dry state. If centrifugal dry collectors are used, venturi or other high energy type collectors are utilized for secondary air cleaning, if air pollution codes are strict.

Data from a scrubber used on a drying kiln are given in Table 7.2-3. Emission characteristics are given in Table 7.2-4.

TABLE 7.2-3 SCRUBBER PERFORMANCE DATA-Stone Crushing.

GENERAL		SCRUBBER		CARRIER GAS			PARTICLES			POLLUTANT GAS			SOLUTION		COST		
#	Process	Name	Description	m³/hr	T_i °C	T_e °C	Name	$(g/m^3)_e$	%E	Name	$(ppm)_e$	%E	Composition	m³/hr	ΔP cm.	Installed $	OP. $/mo.
1	Crushed Stone Drying Kiln	Moving Bed		4,250	316		Stone Dust	0.115	98.7				Water	1.6	15		

TABLE 7.2-4

CHARACTERISTICS OF EMISSIONS FROM STONE CRUSHING OPERATIONS

Process	Gas Temp °C	Dew Point °C	Typical loading g/m^3	Particle density g/cm^3	Particle Size Dist 50% under (microns)	16% under (microns)	g emitted/Kg crushed
Jaw crushing (primary)	ambient				200	20	0.25
Conveying	ambient				10	3	0.85
Secondary Crushing & Screening	ambient						0.75
Tertiary Crushing & Screening	ambient						3.0
Fines Milling	ambient						3.0
Recrushing & Screening							2.5

All data adapted from Midwest Research Institute (1970)

7.2.1.2 Stone Crushing - REFERENCES

Danielson, John A. (1967)
"Air Pollution Engineering Manual," U.S. Dept. of HEW, Public Health Service Publication No. 999-AP-40.

Duprey, R.L. (1968)
"Compliation of Air Pollutant Emission Factors," U.S. Dept. of HEW, Public Health Service Publication No. 999-AP-42.

Midwest Research Institute (1970)
"Handbook of Emissions, Effluents, and Control Practices for Stationary Particulate Pollution Sources," NAPCA Contract No. CPA 22-69-104, November, 1970.

Sussman, Victor H. (1968)
"Nonmetallic Mineral Products Industries," in Air Pollution III, 2nd edition, edited A.C. Stern, Academic Press, New York.

7.2.1.3 Clay Products

Process Description

The manufacture of clay products involves processing raw materials such as kaolinite and montmorillonite clays into finished products such as clay pipe, pottery and refractory brick. Processing procedures vary widely from plant to plant and depend also on the properties of the finished product. However, the basic operations involved in most clay processing are somewhat similar.

Ceramic clay is screened, beneficiated by selective settling in water, filtered, dried in a rotary kiln or spray drier, and then sometime bleached by contacting with bleaching agents such as chlorine or carbon tetrachloride. The product is suitable for further processing into brick, stoneware, or ceramics manufacture.

Bricks and pottery are made by grinding and screening of raw material, blending, forming, drying and firing at high temperature. If refractory products are to be made, the material may be calcined prior to blending.

Particles may be released from the raw materials handling, grinding, drying, or firing kilns. Fluorides and acid gases may come from the drying kilns, and depend upon the fluorine content in the raw material.

Scrubbers Used

Scrubbers can be effectively used to control the fluoride emissions from clay processing plants. Cyclones are sometimes used as precleaners. Data from scrubbers used on clay processing plants is given in Table 7.2.5. Typical emissions from these plants are given in Table 7.2.6.

TABLE 7.2-5 SCRUBBER PERFORMANCE DATA - Clay Products.

GENERAL		SCRUBBER		CARRIER GAS			PARTICLES			POLLUTANT GAS			SOLUTION		COST		
#	Process	Name	Description	m³/hr	Ti °C	Te °C	Name	(g/m³)e	%E	Name	(ppm)e	%E	Composition	m³/hr	ΔP cm.	Installed $	OP. $/mo.
1	Clay Processing	Moving Bed		4,250	116	60	Clay Dust	0.83	98.3				Water	8	15.2		
2	Clay Processing	Moving Bed		4,250	99	57	Clay Dust	0.175	97.8				Water	8	13.7		
3	Clay Processing	Ventur	Hastalloy	12,000	232+	43	Frit Dust	0.056 to 0.095	90				Water		90	70,000	1,200
4	Clay Processing		C.S.; carbon steel	22,100	95		Clay Dust						Water	8.3		10,655	
5	Clay Handling	Venturi & Centrif	carbon steel	8,500	22	12	Clay Dust		>99				Water	19	20	4,000	68
6	Refractory Kiln	Venturi & Centrif	carbon steel	20,400	87.8	41.7	Refractory Dust		93.0				Water	5.4	28	15,000	280
	+Radiational Cooling 650-732°C																

TABLE 7.2-6

EMISSIONS FROM CLAY PROCESSING PLANTS

Process	Gas Temp °C	Dew Point °C	Typical loading g/m³	Particle density g/cm³	Particle Size Dist 50% under (microns)	16% under (microns)	g emitted / Kg product
Ceramic Clay							
rotary drier	19						35
kiln and cooler	71						30+
spray drier	119						
Refractory Clay							
bauxite calcine kiln					25-40%	< 10μ	
inaguesite calcine kiln					50%	< 10μ	
electric arc furnace					100%	< 2μ	

+ following cyclone precleaner

All data adapted from Midwest Research Institute (1970)

7.2.1.3 Clay Processing - REFERENCES

Danielson, John A. (1967)
"Air Pollution Engineering Manual", U.S. Dept. of HEW, Public Health Service Publication No. 99-AP-40.

Duprey, R.L. (1968)
"Compliation of Air Pollutant Emission Factors", U.S. Dept. of HEW, Public Health Service Publication No. 999-AP-42.

Midwest Research Institute (1970)
"Handbook of Emissions, Effluents and Control Practices for Stationary Particulate Pollution Sources", NAPCA Contract No. CPA 22-69-104, November, 1970.

7.2.1.4 Lime Preparation

Process Description

Lime preparation involves processing of limestone ($CaCO_3$ plus impurities) into quicklime (CaO) or hydrated lime [$Ca(OH)_2$]. Limestone is quarried and crushed, then passed to a calcining kiln. Vertical and rotary kilns are used, but the rotary type is more popular. The heat in the kiln drives carbon dioxide from the stone, leaving quicklime (CaO) to be sold as is, or to be hydrated to give hydrated lime, $Ca(OH)_2$.

The primary pollution source in lime processing is the rotary calcining kiln. Dust from calcining kilns is composed of both relatively large particles of lime entrained in the gas stream, and a fume of sodium salts, primarily carbonate and sulfate, volatilized from impurities in the limestone at the high kiln temperatures. The sodium compounds are difficult to remove from the gas stream due to their small size, but may be eliminated by processing of the material to be calcined. Limestone crushing may release particles. (See section 7.2.1.2). Calcium carbonate waste sludge is sometimes calcined to make lime for reuse, and to eliminate sludge disposal problems.

Scrubbers Used

Scrubbers are used to control the effluent from limestone calcining kilns. Venturi scrubbers appear to work well; centrifugal and impingement plate scrubbers are used also. Scrubbers may also be used to control the effluent from a lime hydrator, as hydrated lime is soluble and easily wetted. Data on scrubbers used to control the emissions from a calcining kilns are given in Table 7.2-7. The information on the emissions from lime processing operations is given in Table 7.2-8.

TABLE 7.2-7 SCRUBBER PERFORMANCE DATA - Lime Preparation

GENERAL		SCRUBBER		CARRIER GAS			PARTICLES			POLLUTANT GAS			SOLUTION		COST		
#	Process	Name	Description	m³/hr	T_i °C	T_e °C	Name	$(g/m^3)_e$	%E	Name	$(ppm)_e$	%E	Composition	m³/hr	ΔP cm.	Installed $	OP. $/mo.
1	Lime Mfg.	Venturi	0.895 m dia.	106,000	180	72	Lime Dust	0.388	92.6				Water	170 avg.	23 avg.		
2	Lime Mfg.	Venturi	0.895 m dia.	104,000	163	70	Lime Dust	0.576	96.5				Water	170 avg.	23 avg.		
3	Lime Mfg.	Venturi	0.895 m dia.	101,000	177	74	Lime Dust	0.154	98.7				Water	170 avg.	23 avg.		
4	Lime Mfg.	Venturi	0.895 m dia.	97,500	154	73	Lime Dust	0.275	96.3				Water	170 avg.	23 avg.		
5	Lime Mfg.	Venturi	0.895 m dia.	103,5000	164	73	Lime Dust	0.595	94.0				Water	170 avg.	23 avg.		
6	Lime Mfg.	Venturi		57,600	164	72	Lime Dust	1.03	85				Water	116	28.6		
7	Lime Mfg.	Venturi		57,600	130	72	Lime Dust	0.48	97				Water	66	17.2		
8	Lime Mfg.	Venturi		57,600	38	72	Lime Dust	0.688	97.3				Water	93	27.3		
9	Lime Mfg.	Venturi		60,000	138	66	Lime Dust	0.09	99.5				Water	138		42,100	
10	Lime Mfg.	Impnge.	10 ga. M.S.	16,100	38	32	Lime Dust	0.87	95				Water	6.8	17.5	21,000	350
11	Lime Mfg.	Venturi		30,600			Lime Dust						Water			25,700 (FOB)	
12	Lime Mfg.	Spray Tower		84,000			Lime Dust	0.32					Water	30			
13	Lime Mfg.	Venturi		94,500			Lime Dust	0.32					Water				
14	Lime Mfg.	Spray Tower		65,000			Lime Dust	0.325					Water				

TABLE 7.2-8

CHARACTERISTICS OF EMISSIONS FROM LIME PROCESSING INDUSTRY

Process	Gas Temp °C	Dew Point °C	Typical loading g/m³	Particle density g/cm³	Particle Size Dist 50% under (microns)	16% under (microns)	g emitted/Kg lime
Calcining							
Rotary Kiln	300-650°		34	2.6-3.0	40	3.5	90
Vertical Kiln			1.4		30	13	3.5

All data adapted from Midwest Research Institute (1970).

7.2.1.4 Lime Preparation - REFERENCES

Blackmore, S. S. (1964)
"Dust Emission Control Program", Union Carbide Crop., Metals Division. Presented at 57th annual meeting of APCA, Houston, June 1964.

Collins, T. T., Jr. (1959)
"The Venturi Scrubber on Lime Kiln Stack Gases", TAPPI, 42, 1, Jan. 1959.

Kirk-Othmer (1967)
"Encyclopedia of Chemical Technology", 2nd ed., Interscience Publishers.

Lewis, C. J. and B. B. Crocker (1964)
"The Lime Industry's Problem of Airborne Dust", Journ. of APCA 19, p. 31.

Lewis, C. J. (1966)
"The Lime Industry's Problem of Airborne Dust", Presented at 64th annual convention of the Nat'l Lime Ass'n., Phoenix, April 1966.

Loquenz, Heinz (1967)
"Experience and Results with an Instrument for Determination of Electrical Dust Resistance", Staub, 27, 5, p. 41.

Midwest Research Institute (1970)
"Handbook of Emissions, Effluents and Control Practices for Stationary Particulate Pollution Sources", NAPCA Contract CPA 22-69-104, November 1970.

Minnick, J. L. (1970)
"Control of Particulate Emissions from Lime Plants", Presented at 63rd annual meeting, APCA, St. Louis.

Shreve, R. N. (1956)
"The Chemical Process Industries", 2nd Ed., McGraw-Hill, New York.

Stuart H. H. and R. E. Bailey (1965)
"Performance Study of a Lime Kiln and Scrubber Installation", TAPPI 48, 5, p. 104A.

7.2.1.5 Miscellaneous Mineral Industries

In this section, data is presented on mineral industries not fitting into the preceeding four sections. A table of contents is below.

TABLE 7.2-9

DATA ON MISCELLANEOUS MINERAL PROCESSES

Process	Number
Borax Fusion Furnace	1
" " "	2
" " "	3
" " "	4
Cement Kiln	5
Fullers Earth	6
Mineral Wool	7
Mineral Wool	8

Table 7.2-10 lists data on emissions from miscellaneous mineral industries.

TABLE 7.2-10 SCRUBBER PERFORMANCE DATA - Miscellaneous Mineral Processes.

GENERAL		SCRUBBER		CARRIER GAS			PARTICLES			POLLUTANT GAS			SOLUTION		COST		
#	Process	Name	Description	m³/hr	T_i °C	T_e °C	Name	$(g/m^3)_e$	%E	Name	$(ppm)_e$	%E	Composition	m³/hr	ΔP cm.	Installed $	OP. $/mo.
1	Borax Fusion Furnace	Impnge. & Entrn.		97,000 to 133,000	260	66	Borates	0.39	96				Borate Liquor	9.1-13.6+	19	170,000	
2	Borax Fusion Furnace	Impnge. & Entrn.		97,000 to 133,000	260	66	Borates	0.39	96				Borate Liquor	9.1-13.6+	25.4	100,000	
3	Borax Fusion Furnace	Impnge. & Entrn.		220,000	1100	82	Borates	1.24	95				Borate Liquor	68-112	89	500,000	
4	Borax Fusion Furnace	Venturi	316 SS	212,000	980	27	Borates	0.0275	98				Borate Liquor	32	102	500,000	
5	Cement Kiln	Venturi		159,000					98+							550,000	2,500
6	Fullers Earth	Mech. Aided		4,050	ambient		Fullers Earth	0.42					Water	0.34	19		
7	Mineral Wool Cupola	Venturi		16,600			Cupola Dust	0.45		SO_x HC NO_2	560 88 23		Water		155		
8	Min. Wool Blow Chamber	Venturi		36,000			Oil Mist, Fibers	0.046		SO_x NO_2 CO	11 17 20		Water				

+ Reclaimed

7.2.2 FUEL COMBUSTION

Process Description

Section 7.2.2 pertains to those processes in which fuel is burned. The major fuels in use are coal, fuel oil, and natural gas. These three fuels will be considered in the following tables. Other fuels, such as wood, will not be considered here, both because the relative quantities consumed are small, and because relatively little information is available about the problem.

Fuels are burned to produce heat. The heat may be utilized for space heating or for power generation, but the process of combustion is the same. Effluent characteristics are dependent upon both the nature of the fuel burned, and the design of the furnace in which burning takes place. Combustion for the disposal or compaction of waste is considered in section 7.2.6

Scrubbers Used

Scrubbers are occasionally used to remove fly ash from flue gas, although other types of control devices are more common. Scrubbers may become more widely used in the future, as control systems are devised for the simultaneous removal of fly ash and gaseous pollutants. Table 7.2-12 gives scrubber fly ash removal data.

Scrubbers are being used more and more frequently to control the gaseous emissions from fuel combustion, especially sulfur oxides. The major processes which have been developed to scrub sulfur oxides from flue gas will be described below. To date, much less effort has been made on scrubbing out gases other than sulfur oxides from flue gases; most notably on nitrogen oxides.

A. Battersea Process

The first process developed to remove SO_x from flue gas was developed for the Battersea Power Station in London in 1929, and is still in use. Here chalk (relatively pure $CaCO_3$) is added to already alkaline Thames River water and reacted counter currently with the flue gas. Manganese sulfate is added to the scrubbing liquor as it flows from the base of the scrubber, to assist in the oxidation of the liquor. Next it passes to a settling tank and an aerator, and then back to the river. Scrubbing liquid is not recycled. Sulfur oxide removal efficiencies have exceeded ninety per cent.

Problems with the Battersea process include processing the large volumes of water required, and loss of plume buoyancy. In addition, the spent scrubbing liquor, with a high concentration of calcium sulphate, may cause scale formation in heat exchangers using this water downstream. In 1957, the cost of installing, operating, and maintaining this process at a modern power plant was estimated to be about $1.10 to $1.40 per ton of coal burned. (Kennaway, 1958)

B. Howden-I.C.I. Cyclic Lime Process

The Howden-I.C.I. Cyclic Lime Scrubbing Process was used at the Fulham Power Station in London prior to World War II. It was the first attempt to develop a scrubbing process utilizing a recirculating scrubber solution. In this approach, lime was continuously added to the circulating scrubbing solution as it emerged from the scrubber - before settling and recirculating.

Disadvantages of the Howden-I.C.I. process included deposition of calcium sulfite within the scrubber, high maintenance costs due to the recirculation of solids unless a detention tank is used through the scrubber, corrosion, high cost of disposing of the non-saleable calcium sulfate sludge, and the potential danger of reducing the capacity of the boilers due to choking of the scrubbers from deposited calcium sulfite. The complete cost of installing a similar scrubber or a power plant was estimated at $2.40 per ton of coal burned, in 1957. (Kennaway, 1958).

C. Limestone Injection - Wet Scrubbing Process

The limestone injection - wet scrubbing process has been tried at several power plants in the United States, beginning in the middle 1960's. In this process, pulverized limestone, $CaCO_3$ and/or pulverized dolomite, a combination of $MgCO_3$ and $CaCO_3$ are fed to the boiler either together with the coal, or slightly downstream of the boiler. The high furnace temperatures calcine the stone to more reactive CaO, (MgO) which combines with SO_2 in the flue gas to form calcium (magnesium) sulfite and sulfate. From 20 to 30 per cent of the SO_2 in the gas is removed in this manner. Coal and limestone are usually fed in proportion of about 8 to 1 by weight.

Next the gas passes through a scrubber which removes fly ash, the reacted sulfite and sulfate salts, and unreacted CaO (MgO). Due to the absorbed CaO (MgO), the scrubbing solution can remove additional unreacted SO_2 from the gas stream. Overall SO_2 removal efficiencies can exceed 90 per cent.

Scrubbers which have been tried include the UOP moving bed scrubber at the Wisconsin Electric Power Company, the Combustion Engineering marble bed scrubber, which has been installed on 125 MW units at the Union Electric Company in St. Louis, and the Lawrence Plant of the Kansas Power and Light Company. On the basis of these tests, the Kansas Power and Light Company is proceeding with plans to install a similar scrubber for a new 430 MW plant, to be completed in 1971. The Office of Air Programs of the Environmental Protection Agency is supervising the construction and operation of scrubbers at the Paducah, Kentucky power plant of the TVA, and at the St. Clair Station of the Detroit Edison Company. No results are available from these tests yet.

Problems with the limestone injection - wet scrubbing systems include sludge disposal plus corrosion and erosion of the boiler tubes, if the stone is injected ahead of this point, i.e., with the coal. Scale builds upin the scrubber and corrosion of the scrubber itself may occur.

D. Magnesium Oxide Scrubbing

The magnesium oxide process, developed by Chemico, contacts flue gas with a solution of magnesium oxide in a low pressure drop venturi scrubber. Utilizing pre-calcined magnesium oxide in the scrubbing solution allows higher sulfur dioxide removal efficiencies than would be the case if uncalcined dolomite were used. Better control of the scrubbing solution, and less fly ash removal are required than is the case when stone is calcined in the boiler directly, as is done in the limestone or dolomite injection process, and the boiler scaling problem due to limestone injection is eliminated. Chemico proposes a recovery plant for breaking down the magnesium sulfite formed in the scrubber to recover magnesium oxide for recycling, and sulfur dioxide for further processing and sale.

Boston Edison Company is installing a magnesium oxide scrubbing process on a 150 MW power generating station. Magnesium oxide scrubbing is more expensive than the limestone injection - wet scrubbing process. However, part of the cost can be recovered as the sulfur removed from the gas stream can be converted to saleable sulfuric acid.

E. Wellman-Lord Process

The Wellman-Lord Process, sometimes called the Beckwell Process, scrubs flue gas with potassium sulfite solution. Absorbed sulfur dioxide forms potassium bisulfite, which precipitates from the scrubbing solution in the form of potassium pyrosulfite. The potassium pyrosulfite can then be heated to yield potassium sulfite and a concentrated stream of sulfur dioxide, amenable to further processing and sale.

Pilot studies of this process were conducted at Gannon station of the Tampa Electric Company. A 25 MW study has been conducted at Crane Station of the Baltimore Gas and Electric Company.

The cost for installing a Wellman-Lord process on a 500 MW coal fired power plant was estimated at between 5 and 6 million dollars according to NAPCA (1969a). Operating costs were envisioned as covered by the sale of recovered sulfur dioxide.

F. Scale in Wet Scrubbing Process

In the wet scrubbing process for the removal of SO_2 from flue gases, the use of lime, limestone chalk, dolomite and magnesium oxide in the scrubbing solution may cause scale formation. Scale can deposit in the scrubber or the auxiliary equipment and may be very difficult to remove once it has settled. Scale composition may vary depending on the material used for the scrubbing. It may contain various hydrates of calcium sulfite and sulfate as well as calcium carbonate, magnesium sulfite and magnesium hydroxide. It should be emphasized here that for easy removal of the sulfate and sulfite from the absorbing liquid precipitation of these salts is advantageous. Otherwise, the salt concentration in the scrubbing liquor increases, decreasing absorption capacity for SO_2 and transferring an air pollution problem into a water pollution one. However, precipitation should occur in a place where the precipitate is easily removed from the system as solid and does not interfere with normal operation.

In principal, scale prevention can be approached in several ways. The Howden I.C.I. approach has been to provide a delay tank following the scrubber into which the make up alkali slurry is added. Precipitation then takes place in this tank and the slurry clarified and filtered. The supernatent is returned to the scrubber for future scrubbing. A second approach would be to use such construction materials or plate the equipment with materials which are conducive to sludge formation rather than scale build up.

In the injection wet scrubbing process a promising approach is to use two scrubbers in series. The first one removes particulate matter and is relatively ineffective to mass transfer, thus removing the calcined limestone from the flue gas. The second scrubber does all of the SO_2 removal. This way the lime suspension can be introduced in the best place in the system. There are many variations to these approaches, all aimed at eliminating scale, scrubbing over 90% of the SO_2 and removing it as sulfite or sulfate salts at the minimum possible cost. Research proceeds now in all directions and there is still no fool-proof method for scale prevention.

G. Other Processes

The previous five sections cover the flue gas scrubbing processes which have been tried in large scale pilot tests. However, many other processes are under development.

A wet-char process developed by Hitachi, Ltd., of Tokyo, absorbes sulfur oxides in a bed of activated carbon, which then catalytically converts the SO_2 to SO_3. At intervals, the adsorption bed is removed from the gas stream, and washed with water, to produce sulfuric acid. Disadvantages include the weak strength of the acid produced, and the cyclic nature of the process.

Scrubbing of flue gas with amines at high temperature has been explored in a study by Arthur D. Little Co. in 1968. This report states that it is conceptually feasible to separate the absorbed sulfur dioxide from the amine by chemical methods. A suitable amine for use in this process is tetraethylene pentamine, which can absorb 70 grams of sulfur dioxide per 100 grams of amine from a gas stream containing 1% sulfur dioxide and 10% moisture at 100° C.

An eutectic mixture of molten lithium, sodium and potassium carbonates has been explored for scrubbing flue gases by Atomics International. Absorption of sulfur dioxide is very rapid - oxygen, water vapor, and fly ash do not interfere with sulfur dioxide removal. The resulting sulfite-carbonate mixture can be regenerated chemically. Absorption takes place at about 430° C, while regeneration needs temperatures of about 200° C higher. Corrosion is a problem which is aggravated by the high operating temperatures necessary. Another problem is access to flue gases at the high temperatures necessary. Advantages include the low volumes of scrubbing solution necessary and release of flue gas at high temperature for good plume rise.

The Klaus process reacts sulfur dioxide in the gas stream with hydrogen sulfide, to produce water and elemental sulfur. The sulfur may be sold to offset the cost of the operation. This process may be applicable if a suitable supply of hydrogen sulfide is available.

Other processes include a formate scrubbing process developed by the Consolidation Coal Company, scrubbing with ammonia as is done in the Fullham-Simon-Carves Process, scrubbing with sodium hydroxide followed by electrolytic reclaimation of the sodium hydroxide as is done in the Stone and Webster/Ionics Inc. process, sodium bicarbonate adsorption as developed by Dow Chemical Company, and others. For further information see NAPCA (1969a).

Tables 7.2-13, -14, -15 give data on the typical emissions from fuel combusion processes.

TABLE 7.2-11

WET SCRUBBING PROCESSES FOR REMOVING SO_2 FROM FLUE GAS

Process Name; Where Used	Costs \$/KW installed - - - - - - \$/ton coal op. cost	Advantages	Disadvantages	Product Disposal Method
Battersea Process Battersea and Bankside Power Stations, London.	25 (1968) - - - - - - 1.15 (1968)	90% efficiency obtained.	Large volumes water required. Loss of plume buoyancy.	Dilute slurry in exit water.
Howden-I.C.I. Cyclic Lime Process. Fulham, Tir John & Swansea Power Stations, England	- - - - - - 1.25 - 1.93 (1965)	Recirculating scrubbing solution.	High maintenance costs. Disposal of sludge. Possibility of reducing boiler capacity due to blockages in scrubber.	Sludge barged to sea and dumped.
Limestone injection-wet scrubbing Wisconsin Electric Power Co. Union Electric Co. (St. Louis), Meramac Plant. Kansas Power & Light Co., Lawrence Plant (2) TVA-Paduca Kentucky Plant. Detroit Edison Co., St. Clair Plant.	12 (1970) - - - - - - 1.32 (1970)	Recirculating scrubbing solution. 90% efficiency possible. Can be added to existing boiler without extensive modifications. Low installed cost.	Sludge disposal. Corrosion and erosion in boiler. Scale and corrosion in scrubber.	Sludge is dumped.

TABLE 7.2-11 (cont'd)

WET SCRUBBING PROCESSES FOR REMOVING SO_2 FROM FLUE GAS

Process Name; Where Used	Costs $/KW installed $/ton coal op. cost	Advantages	Disadvantages	Product Disposal Method
Magnesium Oxide Scrubbing Boston Edison Company	33 (1970) - - - - - - Depends on price of product sale.	Saleable sulfur product recovered. Unlike limestone injection, no scale or corrosion in boiler. High efficiency possible. Can be added to existing plant without extensive modifications. Closed system-little absorbent makeup necessary.	Cost Need buyer for product.	Sold.
Wellman-Lord Process Tampa Electric Co. Gannon Station. Baltimore Gas & Electric Co. Crane Station. Olin-Matheson Chemical Co. Paulsboro, N.J. Plant.	10-12 (1969) - - - - - - Hope to break even.	Saleable sulfur product recovered.	Need buyer for product.	Sold.

TABLE 7.2-12 SCRUBBER PERFORMANCE DATA - Fuel Combustion

GENERAL		SCRUBBER		CARRIER GAS			PARTICLES			POLLUTANT GAS			SOLUTION		COST		
#	Process	Name	Description	m^3/hr	T_i °C	T_e °C	Name	$(g/m^3)_e$	%E	Name	$(ppm)_e$	%E	Composition	m^3/hr	ΔP cm.	Installed $	OP. $/mo.
1	Power Generation	Venturi (3) Units	Rubber Lined Steel	2,530,000 (Total)	132	54	Fly Ash	0.0915	99.7				Water	6130	81.3		
2	Power Generation	Moving Bed	Stainless Steel	850,000			Fly Ash	0.09 to 0.14	99	SO_2	350 min		Lime Slurry 2%				
3	Power Generation	Moving Bed	Fiber-Glass & Steel	1,340			Fly Ash	0.013 to 0.0228	99.6	SO_2		82	$CaCO_3$ Slurry	9.7	15.3		
4	Power Generation	Spray	316 S.S.	327,900	99	49	Fly Ash	0.115	29				Water	181	7.6	75,000	

TABLE 7.2-13
EMISSIONS FROM STATIONARY SOURCES BURNING COAL

TABLE 7.2-13a FLUE GAS AND PARTICLE PROPERTIES+

Coal Feed Location	Gas Temp °C	Dew Pt. °C	Typ. Loading g/m^3	Part. Dens. g/cm^3 (avg.)	Particle Size Distribution 50% under (μm)	Particle Size Distribution 16% under (μm)
Cyclone Furnace	133	38	1.95	2.3	6.4	1.85
Pulverized Coal Furnace.						
a. Vertical Feed	122	38	11	2.3	18	6.0
b. Corner Feed	131	40	7.6	2.3	18	6.0
c. Front wall horizontal feed	122	35	5.7	2.3	18	6.0
d. Horizontally opposed	157	39	9.0	2.3	18	6.0
e. Unspecified	-	-	7.6	2.3	12.5	3.6
Stoker						
a. Spreader	211	41	4.4	2.3	58	14
b. Underfeed	-	-	-	2.3	100	21
Hand Fired	-	-	-	2.3	all <5 micron	

TABLE 7.2-13b PARTICLE EMISSION FACTORS++

Type of Furnace	Grams of particles emitted/Kg coal burned
Cyclone Furnace	1.5A*
Pulverized Coal Furnace	
a. dry bottom	8.5A
b. wet bottom	6.5A
c. wet bottom, with fly ash reinjection.	12A
d. general	8A
Stoker	
a. spreader, no fly ash reinjection	6.5A
b. spreader, with fly ash reinjection	10A
c. all other stokers	2.5A
Hand Fired	5A

TABLE 7.2-13c
POLLUTANT GAS EMISSION FACTORS ++

Pollutant	Power Plant Emission g emitted/ Kg coal burned	Power Plant Emission ppm	Industrial Emissions g emitted/ kg coal	Industrial Emissions ppm	Domestic + Commercial Emissions g emitted/ Kg coal	Domestic + Commercial Emissions ppm
SO_x as SO_2	19S	$\frac{7.13\times10^6 S}{(100-A)(100+E)}$	19S	$\frac{7.13\times10^6 S}{(100-A)(100+E)}$	19S	$\frac{7.13\times10^6 S}{(100-A)(100+E)}$
NO_x as NO_2	10	580	10	580	8	230
HC as CH_4	0.01	6	0.5	30	10	300
CO	0.25	15	1.5	90	50	1450
Aldehydes as HCHO	0.0025	0.15	0.0025	0.15	0.0025	0.15

+Adapted from Midwest Research Institute(1970). ++Adapted from Duprey(1968).

Notes:
S = per cent sulfur in coal
A = per cent ash in coal
E = percent excess air used

Basis of Calculation: Coal composed of ash and sulfur, balance as carbon.

Size of Boilers:	
Power Plant	>4 x 10^7 K cal/hr
Industrial	4 x 10^6 to 4 x 10^7 K cal/hr
Domestic + Commercial	<4 x 10^6 K cal/hr

TABLE 7.2-14a
STATIONARY SOURCES BURNING FUEL OIL

Emission Characteristics							Quantities of Particulates Emitted	
Process	Gas Temp. °C	Dew Pt. °C	Typ. g/M³	Part. Dens. g/cm³	Particle Size Distribution 50% under (μm)	16% under (μm)	Process	Grams of Part. emitted per M³ burned
Horiz. Fired Furnace	157	43	0.07	2.5	90%<	1 μm	Power Pl. Furn.	1200
Tangentially Fired Furn.	132	-	0.07	2.5	90%<	1 μm	Ind. Furn. a. resid.	2760
Pressure Atomizing Furn.	154	37	0.19	2.5	90%<	1 μm	b. distillate	1800
Steam Atomizing Furn.	288	46	0.19	2.5	90%<	1 μm	Domestic	960
Centrifugal Atom. Furn.	189	37	0.19	2.5	90%<	1 μm		

Characteristics data adapted from Midwest Research Institute
Quantity Data adapted from Duprey (1968).

TABLE 7.2-14b
STATIONARY SOURCES BURNING FUEL OIL

Quantities of Gases Emitted

Pollutant	Power Plant Emissions g emitted/M³ oil burned	ppm	Industrial & Commercial Emissions g emitted/M³ oil burn.	ppm	Domestic Emissions g emitted/M³ oil burn.	ppm
SOx as SO_2	19,000S	$\frac{66,300}{(100+E)}S$	19,000S	$\frac{66,100}{(100+E)}S$	19,000S	$\frac{66,100}{(100+E)}S$
NOx as NO_2	12,500	430	8,650	300	1440	50
HC	384	15	240	8	360	13
CO	4.8	0.2	240	8	240	8
Aldehydes As HCHO	72	2.5	240	8	240	8

Notes: S = percent sulfur in oil
E = percent excess air used.

Basis of Calculation:
15° API oil
1,000 BTU/lb heating value
7.58 lb air/10,000 BTU;
0% excess air
8 lb/gal. oil density.

Data adapted from Duprey (1968).

TABLE 7.2-15

STATIONARY SOURCES BURNING NATURAL GAS
EMISSION CHARACTERISTICS AND QUANTITIES

	Power Plant Emissions		Industrial Emmisions		Domestic & Commercial Emissions	
Pollutant	g emitted per m^3 gas burned	ppm	g emitted/ m^3 gas	ppm	g emitted/ m^3 gas	ppm
Particles	0.241	-	0.289	-	0.305	-
SOx as SO_2	0.0064	$\frac{36.6}{100+E}$	0.0064	$\frac{36.6}{100+E}$	0.0064	$\frac{36.6}{100+E}$
NOx as NO_2	6.25	360	3.44	200	1.86	100
HC	-	~ 0	-	~ 0	-	~ 0
CO	-	~ 0	0.0064	0.4	0.0064	0.4
Aldehydes as HCHO	0.016	0.9	0.032	1.8	-	~ 0

Note: E = percent excess air used

Basis of calculation:

1000 BTU/scf heating value
100 BTU/scf combustion air

SECTION 7.2.2 - REFERENCES

Ad Hoc Panel, Control of Sulfur Dioxide from Stationary Combustion Sources, Committee on Air Quality Management, Division of Engineering, National Research Council. "Abatement of Sulfur Oxide Emissions from Stationary Combusion Sources," APTIC No.PB 192 887. (1970).

Atomics International, "Development of a Molten Carbonate Process for Removal of Sulfur Dioxide from Power Plant Stack Gases," Report to NAPCA from contract No. Ph 86-67-126; APTIC No. PB 179 908. (1968).

Beutner, Heinz P., et. al., "Feasibility of a Regenerative High Temperature Amine Absorption Process for the Control of Sulfur Dioxide Emissions from Stack Gases," Report to NAPCA from contract No. Ph 86-68-57; APTIC No. PB 180233. (1968).

Bechtel, "Alkali Scrubbing Test Facility Phase 1B: Preliminary Engineering Installation at TVA, Shawnee Power Station," Report to NAPCA on contract No. Ph 22-68-67, (June, 1969).

Bienstock, D.; J. H. Field and J. G. Myers, "Process Development in Removing Sulfur Dioxide from Hot Flue Gases," U.S. Bureau of Mines Report of Investigations Number 5735. (1961).

Boll, R. H., "A Mathematical Model of SO_2 Absorption by Limestone Slurry," Presented at the Int. Symp. on Limestone Scrubbing for SO_2 Removal Meeting, Pensacola, Florida (March 16-20, 1970).

Clay, C. W., G. G. Poe, and J. M. Craig, "Wet Scrubbing of Sulfur Dioxide from Power Plant Flue Gases," Presented at the 63rd Annual Meeting of the Air Pollution Control Association, St. Louis, (June 14-18, 1970).

Coutant, R. W., R. H. Cherry, H. Rosenberg, J. Genco and A. Levy, "Investigation of the Limestone-SO_2 Wet Scrubbing Process," Report to NAPCA from contract No. Ph-86-68-84, (November 30, 1969).

Coutant, R. W., B. Campbell, R. E. Barrett, and E. H. Lougher, "Investigation of the Reactivity of Limestone and Dolomite for Capturing SO_2 from Flue Gas," report to NAPCA from contract No. PH 86-67-115 (June 27, 1969).

Craig, John M., "Pilot Scale Lime/Limestone Scrubbing with a Doyle-Type Scrubber." Presented at the Int. Symp. on Limestone Scrubbing for SO_2 Removal Meeting, Pensacola, Florida, (March 16-20, 1970).

Eckman, Frank, "Removal of SO_2 with Lime(stone) Slurries," Presented at the Int. Symp. on Limestone Scrubbing for SO_2 Removal Meeting, Pensacola, Florida, (March 16-20, 1970).

Elder, H. W., "Economics of Limestone-Wet Scrubbing," Presented at the Int. Symp. on Limestone Scrubbing for SO_2 Removal Meeting, Pensacola, Florida, (March 16-20, 1970).

Falkenberry, H. L. and A. V. Slack, "Removal of SO_2 from Power Plant Stack Gases by Limestone Injection," Presented at the Symposium on Chemical Reaction Engineering, Part II, 61st Annual Meeting, AIChE, Los Angeles, (December 15, 1968).

Field, J. H., L. M. Brunn, W. P. Haynes and H. E. Benson, "Cost Estimates of Liquid Scrubbing Processes for Removing Sulfur Dioxide from Flue Gases," J. of APCA, 1, 2, pp. 109-114, (1957).

Goldschmidt, K., "Deposit-tests with Lime-flyash-slurry of the Wet Scrubbing Pilot Plant System 'Bischoff'," Presented at the Int. Symp. on Limestone Scrubbing for SO_2 Removal Meeting, Pensacola, Florida, (March 16-20, 1970).

Gustavsson, K. A., "Commercial Installation at Södersjukhuset, a Swedish Hospital in Stockholm," Presented at the Int. Symp. on Limestone Scrubbing for SO_2 Removal Meeting, Pensacola, Florida, (March 16-20, 1970).

Gustavsson, K. A., "Pilot Plant Connected to Bahco's Central Heating Plant," Presented at the Int. Symp. on Limestone Scrubbing for SO_2 Removal Meeting, Pensacola, Florida, (March 16-20, 1970).

Hausberg, Gerhard, "The Removal of SO_2 and Dust from Flue Gas-the Bischoff Process," Presented at the Int. Symp. on Limestone Scrubbing for SO_2 Removal Meeting, Pensacola, Florida, "March 16-20, 1970).

References (cont'd)

Kennaway, T., "The Fulham-Simon-Carves Process for the Recovery of Sulphur from Flue Gas," J. of APCA, 7, 4, pp. 266-274 (1958).

Kittleman, Thomas A., "NAPCA In-House Studies of the Dissolution of CaO and $Ca(OH)_2$," Presented at the Int. Symp. on Limestone Scrubbing for SO_2 Removal Meeting, Pensacola, Florida, (March 16-20, 1970).

Kohl, Arthur L., and Fred C. Riesenfeld, "Gas Purification," McGraw Hill, New York (1960).

Lowell, Phillip S., Delbert M. Ottmers, Jr., Thomas T. Strange, Klaus Schwitzgebel, and David W. DeBerry, "A Theoretical Description of the Limestone Injection-Wet Scrubbing Process," report to NAPCA from contract No. CPA-22-69-138, (June 9, 1970).

Lowell, P. L., "A theoretical Description of the Limestone Injection-Wet Scrubbing Process," Presented at the Int. Symp. on Limestone Scrubbing for SO_2 Removal Meeting, Pensacola, Florida, (March 16-20, 1970).

Martin, J. R., and A. L. Plumley, "The CE Air Pollution Control System," Presented at the Int. Symp. on Limestone Scrubbing for SO_2 Removal Meeting, Pensacola, Florida, (March 16-20, 1970).

McKenna, J. D., "Evaluation of a Two-Stage Particulate Scrubber and Gas Absorber Applied to Power Plant Flue Gas," Presented at the International Symp. on Limestone Scrubbing for SO_2 Removal Meeting, Pensacola, Florida, (March 16-20, 1970).

Midwest Research Institute, "Handbook of Emissions, Effluents, and Control Practices for Stationary Particulate Pollution Source," report to NAPCA from contract No. CPA-22-69-104, (November 1, 1970).

Miller, Daric M., "Experience with Wet Scrubber for SO_2 Removal at the Lawrence Station of the Kansas Power and Light pany," Presented to the Society of Mining Engineers of AIME, Salt Lake City, Utah, (September 19, 1969).

National Air Pollution Control Administration, "Control Techniques for Particulate Air Pollutants," 2nd ed. NAPCA Publication No. 999-AP-51 (1960).

National Air Pollution Control Administration, "Control Techniques for Sulfur Oxide Air Pollutants," 2nd ed., NAPCA Publication No. 999-AP-52, (1969).

National Air Pollution Control Administration, "Compilation of Air Pollutant Emission Factors," NAPCA Publication No. 999-AP-42, (1968).

National Air Pollution Control Administration, "Control Techniques for Nitrogen Oxide Emissions," NAPCA Publication No. 999-AP-67, (1970).

Phillips, J. L., "Limestone-Wet Scrubbing Program National Air Pollution Control Administration", Presented at the Int. Symp. on Limestone Scrubbing for SO_2 Removal Meeting, Pensacola, Florida, (March 16-20, 1970).

Pollock, W. A., J. P. Tomany and Gary Frieling, "Flue Gas Scrubber," Mech. Eng., 89 8, pp. 21-25, (1967).

Pollock, W. A., James Tomany, and Gary Frieling, "Removal of Sulfur Dioxide and Fly Ash from Coal Burning Power Plant Flue Gases," Presented at ASME winter Annual Meeting, New York, (Nov. 27 to Dec. 1, 1966).

Potter, Allen E., "Preliminary Bench-Scale Scrubbing Studies at NAPCA," Presented at the Int. Symp. on Limestone Scrubbing for SO_2 Removal Meeting, Pensacola, Florida, (March 16-20, 1970).

Rabin, E., S. A. Almanula, F. V. Karlson and J. Roberts, "Process Model Development for the Shawnee Test Facility," Presented at the Int. Symp. on Limestone Scrubbing for SO_2 Removal Meeting, Pensacola, Florida, (March 16-20, 1970).

Shah, I. S., and J. E. Radway, "Removal of Oxides of Sulfur from Power Plant Stack Gases by Reaction with Compounds of Calcium," Presented at the Limestone Scrubbing for SO_2 Removal Meeting, Pensacola, Florida, (March 16-20, 1970).

References (cont'd)

Sherwin, R. M., and J. A. Raben, "The Limestone Test Facility at TVA's Paducah Power Plant," Presented at the Int. Symp. on Limestone Scrubbing for SO_2 removal Meeting, Pensacola, Florida, (March 16-20, 1970).

Slack, A. V., "Absorption of Sulfur Dioxide in Limestone Slurry-Small Scale Tests at TVA," Presented at the Int. Symp. on Limestone Scrubbing for SO_2 Removal Meeting, Pensacola, Florida, (March 16-20, 1970).

Stone and Webster Engineering Corp., "Final Report on Sulfur Dioxide Scrubbers, Stone and Webster - Ionics Process," report submitted to Division of Process control Engineering, National Air Pollution Constrol Administration, U.S. Department of H.E.W., 5710 Woester Pike, Cincinnati, (January, 1970).

Tailor, John P. "A Study of the CVX Wet Gas Scrubber and its Application," John P. Tailor and Company, Davenport, Iowa, (1965).

TVA, "Sulfur Oxide Removal from Power Plant-Flue Gas," Report to NAPCA from contract No. TV-29233A, (1962).

TVA, "Sulfur Oxide Removal from Power Plant Stack Gas," Report to NAPCA on project 2438, (May 16, 1969).

Uno, T.; S. Fukui, M. Atsukawa, H. Higashi, H. Yamada and K. Kameri, "Scale-up of a SO_2 Control Process,: Chem. Eng. Prog., 66 1 pp. 61-65, (1970).

Unc, Tsukumo; Seigo Aramaki, and Majahiro Kishi, "Full Scale Studies of the MHI Lime/Limestone Scrubbing Process, Presented at the Int. Symp. on Limestone Scrubbing for SO_2 Removal Meeting, Pensacola, Florida, (March 16-20, 1970).

Walker, A. B., "Mass Transfer Characteristics of Variable Annular Throat Venturi Scrubbers," Presented at the Int. Symp. on Limestone Scrubbing for SO_2 Removal Meeting, Pensacola, Florida, (March 16-20, 1970).

Walker, A. B. and R. M. Hall, "Operating Experience with a Flooded Disk Scrubber - A New Variable Throat Orifice Contactor," J. of APCA, 18, 5 pp. 319-323, (1968).

7.2.3 METALLURGICAL PROCESSES

7.2.3.1 Blast Furnaces

Process Description

A blast furnace is a large reactor in which iron ore, flux and coke and air are combined to form iron, slag, and top gas (blast furnace gas). The top gas is composed of steam, nitrogen, carbon dioxide, and on a dry basis, about 25 percent carbon monoxide, plus entrained particles. Molten iron and slag are tapped from the bottom of the furnace.

Blast furnace gas has sufficient heating value, generally about 900 kcal/m^3 (100 BTU/ft^3) to be burned. It is utilized in blast furnace stoves for preheating air going to the blast furnace, or for the compressors which supply air to the blast furnace. To prevent fouling of the equipment burning the blast furnace gas, entrained particles are removed from the gas. These particles may be recycled to the blast furnace after processing with other fine materials in a sintering plant.

Scrubbers Used

After passing through a primary cleaner, often a settling chamber or a cyclone, blast furnace gas usually goes to a medium pressure drop scrubber, i.e.: one with about 25 cm H_2O pressure drop. Baffled spray towers, packed towers, and baffle plate impingement towers are often used. The gas may be further cleaned by passing through an electrostatic precipitator or venturi scrubber. The dust loading from final treatment is 0.10 to 0.15 g/m^3 or less.

Blast furnaces are operated at relatively high positive pressures, typically 150 cm of H_2O. This pressure may be utilized to move the gas through a venturi scrubber operating at a typical pressure drop of 70 cm H_2O, and leave sufficient pressure to distribute the gas to the stoves and boilers where it is burned. Data from scrubbers used or blast furnaces are given in Table 7.2-16. Typical emissions from blast furnaces are listed in Table 7.2-17.

TABLE 7.2-16 SCRUBBER PERFORMANCE DATA - Blast Furnaces

GENERAL		SCRUBBER		CARRIER GAS			PARTICLES			POLLUTANT GAS			SOLUTION		COST		
#	Process	Name	Description	m³/hr	T_i °C	T_e °C	Name	$(g/m^3)_e$	%E	Name	$(ppm)_e$	%E	Composition	m³/hr	ΔP cm.	Installed $	OP. $/mo.
1	Secondary Clean.	Venturi		133,000			Entrain. dust	0.023 to 0.092	99.6 to 99.8				Water		75		
2	Sec. Clean.	Venturi		133,000			Entrain. dust	0.046 to 0.18	97.4 to 99.0				Water		75		
3	Sec. Clean.	Venturi		145,000			Entrain. dust	0.023 to 0.069	99 to 99.5						75-100		
4	Sec. Clean.	Venturi		76,500			Entrain. dust	0.046 to 0.069	98.5 to 99				Water		75		
5	Sec. Clean.	Venturi		44,000			Entrain. dust	0.25	97.8				Water		30		
6	Sec. Clean.	Venturi		47,500			Entrain. dust	0.25	97.8				Water		30		
7	Sec. Clean.	Impnge Plate					Entrain. dust	0.57	95				Water		15-23		
8	Sec. Clean.	Spray Tower					Entrain. dust	0.286	97.5				Water		2.5-5		
9	Iron Ore Pellet.	Centrif.	2.1m dia. 7m tall	36,500		34	Iron Ore Dust						Water	9.8	13+		
10	Iron Ore Pellet.	Centrif.	2.1m dia. 7.9m t.	33,200		21	Iron Ore Dust	0.082					Water	8.0	13++		
11	Iron Ore Pellet.	Centrif.	3m dia. 9.4m t.	60,000		27	Iron Ore Dust						Water	18	13+++		
12	Iron Ore Pellet.	Centrif.	3.4m dia. 11.9m t.	102,000			Iron Ore Dust						Water	20.4	7.7		
13	Iron Ore Pellet.	Centrif.	3.7m dia. 8.1m t.	110,000			Iron Ore Dust						Water	29	12.8		

\+ Integral 100 HP fan
\++ Integral 60 HP fan
\+++ Integral 200 HP fan

TABLE 7.2-17

CHARACTERISTICS OF EMISSIONS FROM BLAST FURNACES

Process	Gas Temp °C	Dew Point °C	Typical loading g/m³	Particle density g/cm³	Particle Size Dist		g emitted / Kg iron
Blast Furnace	200	35-50	15-25	3.4	highly 15-90%	variable <74 μ	65

Blast Furnace	Gas Composition	range	avg %		range	avg %
	CO	21-42	26	CH_4	0.2-3	2
	CO_2	7-19	18	N_2	50-60	52
	H_2	1.7 - 5.7	3.1	H_2O	-	-

All data adopted from
Midwest Research Institute (1970)

7.2.3.1 - Blast Furnaces - REFERENCES

Basse, Bernard, "Gases Cleaned by the Use of Scrubbers", Blast Furnace and Steel Plant, November 1956. pp. 1307-1312

Jennings, R. F., "Blast Furnace Gas Cleaning," Journal of Iron and Steel Inst., (March, 1950).

Midwest Research Institute, "Handbook of Emissions, Effluents and Control Practices for Stationary Particulate Pollution Sources," NAPCA Project No. CPA 22-69-104, (November, 1970).

Pilpel, N., "Gas Cleaning in the Iron & Steel Industry", Chemical & Process Engineering, (June, 1961).

Sebesta, William, "Ferrous Metallurgical Processes," in Stern III, 2nd Ed., Academic Press, New York (1968).

Singhal, R. K., "Fume Cleaning Systems Used in the Steel Industries" Steel Times, (August, 1969).

Underwood, G., "Removal of Sub-Micron Particles from Industrial Gases, Particularly in the Steel and Electricity Industries," Int. J. Air and Water Pollution, 6, p. 229. (1962).

7.2.3.2 Steel Manufacture

A. Open Hearth Process

Process Description

The open hearth process accounted for about half the steel produced in the US in 1970. In the open hearth process, scrap, limestone and pig iron either cold or molten, and sometimes iron ore, are heated in a reverberatory furnace. A flame with substantial excess air passes over the charge providing heat and oxygen for the refining process. During the refining process, unwanted carbon in the iron combines with oxygen in the ore and the air, and is removed as a gas. The limestone forms a slag which floats on the molten iron and traps impurities. The carbon content of the iron is carefully watched, and the steel is tapped from the furnace when the carbon content reaches the desired level. The refining process takes from eight to ten hours. However, it may be speeded up by oxygen lancing; that is, introducing pure oxygen to the slag-metal interface using lances.

Scrubbers Used

The gases leaving open hearth furnaces are at high temperatures, about 800°C. At times, waste heat boilers are used to salvage heat energy and lower gas temperatures to a level where electrostatic precipitators may be applied. If there is no need for the energy obtainable from waste heat boilers, scrubbers may be used. Scrubbers can handle the hot gases directly, without temperature lowering pretreatment. The fume from open hearth furnaces includes a substantial portion of submicron material. High energy venturi scrubbers have been successfully utilized to remove this fume. Data on scrubbers controlling open hearth fume is in Table 7.2-18, while data describing the fume characteristics is in 7.2-19.

B. Basic Oxygen Furnace (BOF)

Process Description

The basic oxygen process produced about half the steel produced in the US in 1970. It is becoming increasingly popular, as the time to convert iron to steel by this process is much less than that required in the open hearth process.

In the basic oxygen process used in the US, molten iron is added to steel scrap in a large, pear shaped vessel. Relatively pure (95%) oxygen is blown onto the molten metal surface, oxidizing the carbon and impurities, and releasing heat. This heat is sufficient to melt a charge of 30% scrap. No fuel is used with the BOF other than the carbon and impurities in the metal itself. Total processing time averages about 45 minutes for a heat, tap to tap.

Scrubbers Used

Gases coming from the BOF contain from 75 to 90 percent CO, and have heating values of 2000 to 2500 Kcal/m^3 (225 to 280 BTU/ft^3).

Air is usually introduced to the mouth of the BOF to burn these gases and eliminate any explosion hazard. Generally, three volumes of air are used per volume of BOF gas. The combustion products are then cleaned by electrostatic precipitators or venturi scrubbers.

Lottus Engineering Company of Japan, and German patent No. 1,178,874 (1956) awarded to Dr. Kurt Baum, have devised processes in which the BOF gases are scrubbed without prior combustion, the furnace mouth being sealed with nitrogen to keep oxygen content in the gas below the explosive limit. Advantages of this process include reduction of the size of the scrubbing equipment by about 75% (combustion air is eliminated), reducing the heat load on the scrubbing equipment, reducing the power costs for moving gas through the scrubbing system due to the smaller amounts of gas processed, and salvage of the CO rich gas which might be used as fuel elsewhere in the plant. Lottus claims that its oxygen converter gas recovery process costs 50% of an electrostatic cleaning system. It is being operated at the Wakayama Works of Sumitomo Metal Industries, Ltd., and at Yawata Tobata's No. 2 Plant, both in Japan.

C. Electric Arc Furnace

Process Description

In the electric arc process, heat is provided to scrap by the arcing of electricity between carbon electrodes lowered in from the top of the furnace. Careful control of product composition is possible, as no material extraneous to the charge need be added, except that desired to achieve the desired qualities of the finished product.

Scrubbers Used

Emissions from electric arc furnaces may be copious if the scrap melted is dirty. Venturi scrubbers have been successfully applied to controlling the submicron particles emitted. However, low pressure drop scrubbers are evidently not suited to capturing more than about 60 percent of the fume.

TABLE 7.2-18 SCRUBBER PERFORMANCE DATA - Steel Manufacture.

GENERAL		SCRUBBER		CARRIER GAS			PARTICLES			POLLUTANT GAS			SOLUTION		COST		
#	Process	Name	Description	m^3/hr	T_i °C	T_e °C	Name	$(g/m^3)_e$	%E	Name	$(ppm)_e$	%E	Composition	m^3/hr	ΔP cm.	Installed $	OP. $/mo.
1	Sim. O.H. O_2 Lance	Venturi	6.35 cm throat	875	85	48		0.85	98.2				Water	0.49	34.6		
2	Sim. O.H. O_2 Lance	Venturi	6.35 cm throat	875	86	48		0.46	99.0				Water	0.49	34.6		
3	Sim. O.H. O_2 Lance	Venturi	6.35 cm throat	875	wide variations			0.53	99.4				Water	0.49	34.6		
4	Sim. O.H. O_2 Lance	Venturi	6.35 cm throat	515				0.27	99.6				Water	0.585	39.4		
5	Sim. O.H. O_2 Lance	Venturi	6.35 cm throat	515				0.23	99.3				Water	0.585	39.4		
6	Sim. O.H. O_2 Lance	Venturi	6.35 cm throat	600				0.32	99.1				Water	0.721	63.5		
7	O.H. O_2 Lance	Venturi	throat: 214 cm x 30.5 cm	400,000	300 to 800			<0.115	99+				Recirculated Slurry		76		
8	O.H. O_2 Lance	Venturi	throat: 190 cm x 30.5 cm	220,000	760 to 980	75		<0.115	99+				Recirculated Slurry	135-250			
9	Open Hearth	Venturi	throat: 107 cm x 30.5 cm	200,000		75		0.05 to 0.07	95 avg.				Recirculated Slurry	240	84		
10	BOF	Venturi						0.1 max.	99				--				
11	Iron Holding Furnace	Moving Bed	(4 stage)	34,000	71	43			95				Water	34	107	60,000	
12	Electric Arc Furnace	Venturi		2,690		80		1.18	<7 lbs/hr				--				

TABLE 7.2-19

CHARACTERISTICS OF EMISSIONS FROM STEEL MAKING OPERATIONS

Process	Gas Temp °C	Dew Point °C	Typical loading g/m^3	Particle density g/cm^3	Particle Size Dist 50% under (microns)	16% under (microns)	g emitted / Kg steel
Steel Making							
a) Open Hearth no oxygen lance	250-950[1]	50-60	1.1	5.0	5.0		8
with oxygen lance	400[1]-1100[1]	60	3.5	5.0	6.0[2] 2.5[3]	1.7[2] 0.8[3]	10.5
b) Basic Oxygen Furnace	300[1]-1650[1]			5.25	0.095	0.041	20

Gas Composition	Open Hearth	B.O.F.[4]	[5]
CO_2	8-9%	CO_2-0.7 to 13.5	5-16
O_2	8-9%	CO-0-0.3	74-91
SO_2	2-5ppm	N_2-74.5 to 78.9	3-8
SO_3	100-300ppm	O_2 balance	-
NO_x	500-800ppm	-	-
N_2	balance	-	-

(1) Depends on whether or not waste heat boiler is used
(2) Composite for heat
(3) Lime boil only
(4) After combustion with aspirated air
(5) Before combustion with aspirated air

SECTION 7.2.3.2 - REFERENCES

a Open Hearth

Bishop, C. A., W. W. Campbell, D. L. Hunter and W. M. Lightner, "Successful Cleaning of Open Hearth Exhaust Gas with High Energy Venturi Scrubber", JAPCA, 11, 2, p. 83.(1961).

Broman, Carl U., and Ronald R. Iseli, "The Control of Open Hearth Stack Emissions with Venturi Type Scrubber," Blast Furnace and Steel Plant, (February, 1968).

Danielson, John A., "Air Pollution Engineering Manual", NAPCA Publication No. 999-AP-40.(1967).

Gledhill, P. K., P. J. Carnall, and K. H. Sargent, "Oxygen Lancing of Pig Iron and Subsequent Fume Treatment with a Pease-Anthony Venturi Scrubber," Journal of Iron and Steel, 188, (June, 1957).

Johnson, J. E., "Wet Washing of Open Hearth Gas," Iron and Steel Engineer, (February, 1967).

Midwest Research Institute, "Handbook of Emissions, Effluents, and Control Practices for Stationary Particulate Pollution Sources," NAPCA Contract No. CPA 22-69-104, (November, 1970).

Pilpel, N., "Gas Cleaning in the Iron and Steel Industry," Chemical and Process Engineering, (June, 1961).

Sebesta, William, "Ferrous Metallurgical Processes", in Air Pollution III, 2nd edition, ed. Stern, Academic Press, New York.(1968).

Thomas, F. A., "Venturi Gas Scrubbers" Journal of Metals, (March, 1965).

b. Basic Oxygen Process

Editor, "Scrubbing System Removes Dust from Steel Furnace Gas for Pollution Control," Chemical and Engineering News, (August 5, 1963, p. 48), (1963).

Henschen, H. C., "Wet vs. Dry Gas Cleaning in the Steel Industry," JAPCA, 18, 5, p. 338, (1968).

Wheeler, D. H., "Fume Control in L-D Plants," JAPCA, 18, 2, p. 98, (1968).

7.2.3.3 Iron Foundries

Process Description

In the foundry operation, pig iron or scrap is melted and cast into useful form for sale. Melting takes place in either a cupola or an electric furnace.

In the cupola, a cylindrical vessel lined with firebrick, coke (fuel), limestone (flux) and pig iron are charged (introduced). After lighting, the coke burns, supplying heat for melting the iron, which is tapped from the bottom of the cupola.

The electric furnace is of the arc or of the induction type. In the electric arc furnace, heat is generated by passing current between carbon rods positioned above (indirect arc), or just below (direct arc) the slag cover over the metal. In the induction furnace, heat is supplied by passing alternating current through a water-cooled copper coil surrounding the furnace. The metal charge acts as a secondary coil, and develops heat through means of its electrical resistance to the current induced within it.

Scrubbers Used

Emissions from iron melting operations generally include sub-micron condensed iron and silicon oxides, and zinc oxides, if galvanized scrap is being melted. As the boiling point of zinc is 907°C (well below the normal temperatures reached in a foundry furnace, 1650°C), any zinc present can be expected to boil away and cause a pollution problem. Dirty or greasy scrap will also add to emissions. If a cupola is utilized, the combustion products of the coke burned will also be present. The gases emanating from a cupola are rich in carbon monoxide, and are usually gas fired with excess air to obviate an explosion hazard. This firing may be done within the cupola, if it is sufficiently large to ensure proper gas mixing and residence time, or it may be done in an external combustion chamber. In any case, the combustion products will be present, and provide additional volume for the dust collection system to process.

Wet caps, or simple water curtains, are often used at the top of cupolas to remove large particles from the exit gas stream. Venturi scrubbers have been used effectively to clean the submicron particles produced in foundry furnaces. Data for scrubbers used to control foundry furnace emissions are given in table 7.2-20. Emissions from this process are given in table 7.2-21.

TABLE 7.2-20 SCRUBBER PERFORMANCE DATA - Iron Foundries.

GENERAL		SCRUBBER		CARRIER GAS			PARTICLES			POLLUTANT GAS			SOLUTION		COST		
#	Process	Name	Description	m³/hr	T_i °C	T_e °C	Name	$(g/m^3)_e$	%E	Name	$(ppm)_e$	%E	Composition	m³/hr	ΔP cm.	Installed $	OP. $/mo.
1	Cupola	Venturi		14,400 out		88	Cupola Emis.	0.260					Water		50-115	110,000	
2	Cupola	Impingement Plate		143,000			Cupola Emis.						Water				
3	Cupola	Wet Cap			260		Cupola Emis.	0.252					Water	53.5			
4	Cupola	Wet Cap			260		Cupola Emis.	0.252					Water	53.5			
5	Cupola	Wet Cap			260		Cupola Emis.	0.230					Water	53.5			
6	Cupola	Wet Cap			260		Cupola Emis.	0.275					Water	53.5			
7	Cupola	Venturi	S. Steel				Cupola Emis.	0.5					Water		28		
8	Cupola	Venturi					Cupola Emis.	0.30					Water			30,000	
9	Cupola	Impingement Plate		52,400	200	61	Cupola Emis.	0.55	>91.3				Water	28	19	75,000	
10	Cupola	Flooded Disk	1/4" S. S.	170,000		74	Fe_2O_3+ Silica		99				Water	191	107	350,000	
11	Cupola	Venturi	1/4" S. S.	149,000		74	Fe_2O_3+ Silica	0.35	95				Water	191	71	170,000	
12	Iron Casting	Moving Bed	1/4" Mild Steel	85,000	43	32	Silica Dust		99				Water	34	16.5	100,000	
13	Iron Casting	Venturi	1/4" Mild Steel	85,000	43	32	Silica Dust		99				Water	57	20.3	100,000	
14	Charge Hoist	Moving Bed		51,000	ambient		Fe_2O_3+ Silica		99				Water	23	16.5	65,000	
15	Cupola	Venturi		47,500			Iron Oxides	0.115	96				Water	136	114	150,000	
16	Cupola	Venturi		42,500	82		Cupola Emis.	0.33	≤18 lbs./hr				NaOH Solution	85+	92	60,900 (FOB)	

TABLE 7.2-20 cont'd. SCRUBBER PERFORMANCE DATA - Iron Foundries.

GENERAL		SCRUBBER		CARRIER GAS			PARTICLES			POLLUTANT GAS			SOLUTION		COST		
#	Process	Name	Description	m^3/hr	Ti °C	Te °C	Name	$(g/m^3)_e$	%E	Name	$(ppm)_e$	%E	Composition	m^3/hr	ΔP cm.	Installed $	OP. $/mo.
17	Cupola	Venturi		23,800			Cupola Emis.		88.5				Water			45,000 (FOB)	850-1,700
18	Cupola	Venturi		16,100			Cupola Emis.	0.82					Water			144,000	
19	Cupola	Venturi		123,000		70	Cupola Emis.		99.5/5μm				Water			270,540	
20	Cupola	Venturi		58,000			Cupola Emis.						Water			232,716	
21	Cupola	Venturi		373,000		80	Cupola Emis.		99.5/5μm				Water			330,000	2,750
22	Cupola	Moving Bed		48,000		50	Cupola Emis.	0.75 to 1.0					Water		22.8		
23	Cupola	Wet Cap + Venturi		26,300	200 to ven.		Cupola Emis.	0.115	97				Water	57	100	150,000	
24	Cupola	Venturi		41,000	800	66	Cupola Emis.	0.177	93				Water	54	90	95,000	
25	Cupola	Venturi		54,300	70		Cupola Emis.	0.224	92.5				Water	113	107	(FOB) 32,000	
26	Cupola	Venturi		40,500			Eupola Emis.		99.9				Water				
27	Sand Handling	Comb. Venturi, Centrif.	Carbon Steel.	85,000	24	11	Sand, Grit		99.9				Water	21	10	20,000	340

TABLE 7.2-21

TYPICAL EMISSIONS FROM IRON FOUNDRIES

Process	Gas Temp °C	Dew Point °C	Typical loading g/m³	Particle density g/cm³	Particle Size Dist 50% under (microns)	16% under (microns)	g emitted / Kg iron
Cupola Furnace							
Hot Blast	100-800	21	2.7	2.5-3.1	100	7	7.5
Cold Blast	100-800	21	2.7	2.5-3.1	100	7	11.5
Electric Arc							2.5-5
Induction							2.5-5

All data adapted from Midwest Research Institute (1970)

7.2.3.3 - Iron Foundries - REFERENCES

Air Pollution Control Association, "Technical Manual No. 1," Air Pollution Control Association, 4400 5th Avenue, Pittsburgh, Pa, (1963).

American Foundrymen's Society, "Control of Emissions from Metal Melting Operations," American Foundrymen's Society, Golf and Wolf Roads, Des Plaines, Ill,

Basse, Barnard, "Venturi Scrubbers for Cleaning Cupola Gases," APCA Journal, 6, 4, p. 218, (1957).

Brechtelsbauer, O. J., "Cupola Gas Scrubbers," American Foundryman, February, 1955.

Danielson, John A., "Air Pollution Engineering Manual," U.S. Dept. of HEW, Publication No. 999-AP-40, Cincinnati, (1967).

Editor, "Gas Scrubber Installation Successfully Controls Foundry Cupola Emissions," Air Engineering, (March, 1966, p. 8).

Medley, Gene W., "Controlling Foundry Dust," Foundry, (June, 1966, p. 203).

Midwest Research Institute, "Handbook of Emissions, Effluents, and Control Practices for Stationary Particulate Pollution Sources," NAPCA Contract No. CPA 22-69-104, (November 1, 1970).

Sebesta, William, "Ferrous Metallurgical Processes," in Air Pollution, Vol. III, 2nd ed. editor: Stern, A. C., Academic Press, New York, (1968).

Weber, Herbert J., "Methods of Combatting Air Pollution in Ferrous and Nonferrous Foundries," Journal of APCA, 7, 3, p. 178, (1957).

Williamson, Donald, "Venturi Scrubber Beats Pollution Code Deadline," Foundry, (March, 1968, p. 170).

7.2.3.4 Ferroalloys

Process Description

Ferroalloys are usually made in either a cupola or an electric furnace.

Cupola furnaces are usually smaller than pig iron cupolas, and operate at lower temperatures. The rate of air blowing to the furnace is lower also. Ferromanganese is produced in a cupola by charging coke (fuel) limestone (flux), manganese and iron ores. Carbon monoxide formed as a combustion product of the coke, reduces the ores to the desired metallic product.

Silicon chromium and manganese alloys are often produced in a submerged electric arc furnace. The carbon electrodes are submerged more than a meter below the level of the charge, which is comprised of ore, coke, and limestone. Submerged arc furnaces are usually operated on a continuous basis.

Scrubbers Used

In the open furnace, unburned carbon monoxide is oxidised with induced air above the change. This process, of course, results in an increased flow rate of gas to be purified in an air pollution control device which follows. In the closed furnace, the carbon monoxide is withdrawn from the furnace without burning.

Due to the submicron nature of the metallurgical fumes eminating from a ferro alloy furnace, the only scrubbers which have been succesfully applied are venturis. Data on the performance of venturi scrubbers in controlling ferroalloy furnaces is given in Table 7.2-22. Information on the emissions characteristic of these installations is detailed in Table 7.2-23. Efficiencies in the following tables seem high in light of the particle size distribution of the emission.

TABLE 7.2-22 SCRUBBER PERFORMANCE DATA - Ferroalloys.

GENERAL		SCRUBBER		CARRIER GAS			PARTICLES			POLLUTANT GAS			SOLUTION		COST		
#	Process	Name	Description	m³/hr	T_i °C	T_e °C	Name	$(g/m^3)_e$	%E	Name	$(ppm)_e$	%E	Composition	m³/hr	ΔP cm.	Installed $	OP. $/mo.
1	Open, Low Hood	Venturi		333,000	260 to 300		Furnace Dust	0.115	92.3				Water	410	140		
2	Open, Low Hood	Venturi		333,000	250 to 290		Furnace Dust	0.23	98.7				Water	410	145		
3	Open, Low Hood	Venturi		333,000	250		Furnace Dust	0.295	97.9				Water	410	145		
4	Semi-Closed	Venturi		34,000	600 to 650		Furnace Dust	0.059	98.4				Water	17-23	183-203		
5	Furnace	Venturi	Steel	5,100			Furnace Dust		98				Water		100	6,500 (FOB)	

TABLE 7.2-23

CHARACTERISTICS OF EMISSIONS FROM FERROALLOY FURNACES

Process	Gas Temp °C	Dew Point °C	Typical loading g/m³	Particle density g/cm³	Particle Size Dist 50% under (microns)	16% under (microns)	g emitted / Kg product
Blast Furnace	180-400		10-40		0.45	0.1	205
Electric Furnace Open Furnace	35-80[1] 120-290[7]		2.4		0.3	0.1	180[1] 22[2] 97[3] 290[4] 60[5] 100[6]
Semi-Closed Furnace	200-650						

1 Ferrosilicon
2 Ferromanganese
3 Silico Manganese
4 Silicon Metal
5 Silvery Iron
6 Ferrochrome, Ferrophosphorous
7 Miscellaneous Alloys

All Data Adopted from Midwest Research Institute (1970)

7.2.3.4 - Ferroalloy- REFERENCES

Midwest Research Institute, "Handbook of Emissions, Effluents, and Control Practices for Stationary Particulate Pollution Sources," NAPCA Contract No. CPA 22-69-104, (November, 1970).

Parson, R. A., "Control of Emissions from Ferroalloy Furnace Processing," Union Carbide Corp., Niagara Falls, New York, (1969).

Thring, M. W. and R. J. Sarjant, "Dust Problems in the Iron and Steel Industry," Iron and Coal Trades Review, (March 29, 1957).

7.2.3.5 Copper Smelting and Refining

Process Description

Processing copper involves winning the metal from ores containing as little as 1% copper, and refining it to the high degree of purity necessary for many of its uses. There are three fundamental pyrometallurgical copper operations: roasting, smelting, and converting. Concentrated ore, often chalcopyrite ($CuFeS_2$) is first roasted in a vertical, multiple hearth roaster, to drive off sulfur dioxide. This step has often been eliminated in recent years.

The roaster products (or concentrated ore, if roasting is omitted) are then smelted in a large reverberatory furnace. Slag from the converter furnace, which follows, is also charged to the reverberatory unit, to recover the copper present in the slag and take up some of the iron present in the material charged. Copper matte, a mixture of cuprous and ferrous sulfides, forms below the slag and is tapped into ladles for further processing in a converter furnace. Valuable metals such as gold, silver, bismuth and nickel are also concentrated in the matte.

A silicious slag is charged to the converter furnace, along with the copper matte from the reverberatory furnace. Air is blown through tuyeres in the converter. The air oxidises the sulfur in the copper sulfide to SO_2, and releases 98.5-99.5% pure "blister copper". The blister copper is tapped from the bottom of the converter furnace, deoxidised in a holding furnace, and cast into anodes for further purification.

Blister copper anodes are put into a dilute solution of copper sulfate and sulfuric acid, alternately with thin sheets of pure copper. A low electrical potential gradient is set up between the blister copper anodes and the pure copper cathodes, causing copper to be dissolved from the anodes and plated onto the cathodes in pure form. The impurities in the anode, containing the valuable metals, dissolve in the electrolyte or settle to the bottom of the tanks as a black "anode mud" or "slimes". These may then be further processed.

Scrubbers Used

Copper winning and refining produces dust and sulfur dioxide in all stages of operation. Sulfur dioxide from the roasting and converting stages is often sufficiently concentrated (greater than 4 percent) to serve as feed to a sulfuric acid plant. However, the large capital investment necessary, and problems with finding suitable markets for the sulfuric acid produced, often economically preclude the use of acid recovery plants. As copper smelters are not usually constructed near large metropolitan areas, they often dispose of their sulfur oxide wastes by dispersing them through tall stacks. With tightening air pollution control regulations in rural as well as urban areas, copper smelters may have to turn to scrubbers more in the future to limit their gaseous and particulate emissions. Data on emissions from copper smelters is given in Table 7.2-24. Typical emissions from copper smelters are described in Table 7.2-25.

TABLE 7.2-24 SCRUBBER PERFORMANCE DATA - Copper Smelting and Refining.

GENERAL		SCRUBBER		CARRIER GAS			PARTICLES			POLLUTANT GAS			SOLUTION		COST		
#	Process	Name	Description	m³/hr	T_i °C	T_c °C	Name	$(g/m^3)_e$	%E	Name	$(ppm)_e$	%E	Composition	m³/hr	ΔP cm.	Installed $	OP. $/mo.
1	Smelting	Spray Tower		41,300		50		1.63 to 2.62		SO_2/ NO_x						53,000	
2	Re-claim. Smelt.	Spray Tower		12,400 to 13,600				1.1 4.5	+				Water	41			
3	Ore Processing	Centrif	304 S.S.	32,200			Ore Dust						Water	11.5	28		
4	Ore Processing	Centrif	304 S.S.	8,500	ambient		Ore Dust						Water	3.4			
5	Ore Processing	Centrif	304 S.S.	10,200	ambient		Ore Dust						Water	4.1			
6	Ore Processing	Centrif	304 S.S.	11,900	ambient		Ore Dust						Water	5.4			
7	Ore Processing	Centrif		28,000									Water	9.2			
8	Cu ore Spray Drier	Centrif	304 S.S.	119,000									Water	32			

+ Does not meet requirements

TABLE 7.2-25

CHARACTERISTIC EMISSIONS FROM COPPER SMELTING AND REFINING

Process	Gas Temp °C	Dew Point °C	Typical loading g/m³	Particle density g/cm³	Particle Size Dist 50% under (microns)	16% under (microns)	g emitted / Kg copper
Roasting	315-475		14-55			.10	84
Reverberatory Furnace	175-400	28-46	2-14		37		103
Converting Furnace	150-340		12		44		118

Gaseous Emissions

	Roasting	Reverb. Furnace	Conver. Furnace
SO_2	12-14%	1-2%	<6%

Particle Data Adapted from Midwest Research Institute (1970)
Gas Data Adapted from Duprey (1968)

SECTION 7.2.3.5 - REFERENCES

McKee, Arthur G. and Co., "Systems Study for Control of Emissions - Primary Nonferrous Smelting Industry," Volumes I, II, III, NAPCA Contract No. PH 86-65-85, (June, 1969).

Midwest Research Institute, "Handbook of Emissions, Effluents, and Control Practices, for Stationary Particulate Pollution Sources," NAPCA Contract No. CPA 22-69-104, (November, 1970).

NAPCA, "Control Techniques for Sulfur Oxide Air Pollutants," National Air Pollution Control Association Publication No. AP-52, (1969).

Nelson, Kenneth W., "Nonferrous Metallurgical Operations," in Air Pollution, I_I, 2nd ed., editor: A. C. Stern, Academic Press, New York, (1968).

Schwartz, Harry F., Leo E. Kallan and Arnold Stein, "Controlling Atmospheric Contaminants in the Smelting and Refining of Copper-Base Alloys," Air Repair, 5, 1, p. 5, (1955).

Verein Deutscher Ingenieure, "Restriction of Emission: Copper-Ore Mills," CFSTI Number TT 68-50469/7, (1966).

Verein Deutscher Ingenieure, "Restriction of Emission: Copper-Scrap Smelting Plants and Copper Refineries," CFSTI Number TT 68-50469/9, (October, 1966).

7.2.3.6 Aluminum Processing

Process Description

Bauxite, the ore from which aluminum is made, consists mainly of hydrated aluminum oxide. The ore is refined chemically, then calcined to produce pure alumina, Al_2O_3. The calcined alumina is in the form of a fine powder made up of monocrystals of anhydrous alumina, ranging in size up to 100 microns.

The alumina is converted to aluminum metal by an electrolytic process. Alumina is dissolved in a mixture of molten sodium and calcium fluoride salts, within carbon lined "pots". A carbon anode is inserted at the top of the pot. Electric current is passed between the pot and the anode, disassociating the Al_2O_3 to metallic aluminum, which collects at the bottom of the pot, and oxygen which reacts with the carbon anode to form CO or CO_2. Periodically, the metallic aluminum is tapped. Fresh alumina is added to the molten bath to replace that which has decomposed.

Secondary processing of aluminum involves melting of suitable pig or scrap, and casting the melt into a more salable product. Chlorine gas is often used to remove unwanted magnesium from the melt, although sometimes aluminum fluoride is used.

Chlorine gas is usually added rapidly to the melt through lances inserted through the furnace top. Chlorine reacts preferentially with magnesium, forming a liquid or solid dross, which rises to the surface of the bath. Excess chlorine reacts with aluminum to form aluminum chloride, which sublimes at 178°C, significantly below the normal operating temperature for this process.

Scrubbers Used

Dust produced by the alumina calcining kilns is usually controlled by cyclone precleaners followed by electrostatic precipitators or baghouses.

Emissions from aluminum reducing pots are vented to hoods. Included are both particulate and gaseous fluorides which are amenable to control by scrubbers. A simple spray chamber may be used to collect gaseous fluorides, in conjunction with an electrostatic precipitator or baghouse for removing particulates. When scrubbers are used for both particle and gas emission control, the particles are generally more difficult to remove efficiently, and determine the degree of sophistication of the scrubber.

Sufficient fluoride gases may escape the pot ventillating hoods to necessitate scrubbing the ventillation air coming from the pot room.

The aluminum chloride fumes eminating from an aluminum smelter are well suited to collection by scrubbers. Steam resulting from quenching the gases combines with the aluminum chloride to form soluble hydrated aluminum oxide and gaseous hydrochloric acid. Both may be removed in a high efficiency scrubber such as a venturi, using a scrubbing solution containing sodium hydroxide. Some difficulty can be experienced if HCl mist is formed, as this is difficult to collect.

Data on the performance of scrubbers used in the aluminum producing industry is given in Table 7.2-26. Typical emissions from these processes are given in Table 7.2-27.

TABLE 7.2-26 SCRUBBER PERFORMANCE DATA - Aluminum Processing.

GENERAL		SCRUBBER		CARRIER GAS			PARTICLES			POLLUTANT GAS			SOLUTION		COST		
#	Process	Name	Description	m³/hr	T_i °C	T_e °C	Name	$(g/m^3)_e$	%E	Name	$(ppm)_e$	%E	Composition	m³/hr	ΔP cm.	Installed $	OP. $/mo.
1	Al Dross. Reclam.	Venturi		1,700 to 2,100	540		$AlCl_3$, KCl, Na_3AlF_6	9.2	99				NaOH Solu.	9.1	76	4,000 sc. 1,000 fan & duct	
2	Al Alloy Furnace	Venturi		15,300	720	60	$AlCl_3$ $MgCl_2$	0.147							81	29,000	
3	Al Die Casting	Venturi		2,740	50	22	Part./ Oil Mist	0.0148 0.0021	68 98						79		
4	Al Die Casting	Venturi		2,080	42	20	Part./ Oil Mist	0.0074 0.0021	69 85						83		
5	Al Die Casting	Venturi		2,060	47	21	Part./ Oil Mist	0.0099 0.	97.2 100						79		
6	Al Die Casting	Venturi		2,810	48	21	Part./ Oil Mist	0.017/ 0.0004	97.5 99.9						72.5		

TABLE 7.2-27

CHARACTERISTIC EMISSIONS FROM ALUMINUM PROCESSING

Process	Gas Temp °C	Dew Point °C	Typical loading g/m³	Particle density g/cm³	Particle Size Dist 50% under (microns)	16% under (microns)	g part.* emitted / Kg alum. Produced
Primary Processing							
Calcining Kiln	120-380	77-82	230-700		42	5.7	100
Aluminum Reducing Pot							
Soderberg Cell							
-horizontal stud			0.07 -				72
-vertical stud			4.5				42
Pre-bake Cell							32
Materials Handling							5
Secondary Processing							
Chlorine Fluxing	90-790				100% < 1μ		1g/gCl$_2$ used

ppm gases emitted**	Soderberg Cell -horizontal stud-	-vertical stud-	Pre-bake Cell
		300	

* Particles may include

Sodium fluoride-NaF
Aluminum fluoride-AlF_3
Calcium fluoride-CaF_2
Cryolite-Na_3AlF_6
Carbon-C
Aluminum oxide-Al_2O_3

** Gases may include

Carbon tetrafluoride-CF_4
Silicon tetrafluoride-SiF_4
Hexafluoroethane-C_2F_6
Carbon nomoxide-CO
Hydrogen sulfide-H_2S
Hydrocarbons-various

All Data Adopted from Midwest Research Institute (1970).

SECTION 7.2.3.6 - REFERENCES

Danielson, John A., Air Pollution Engineering Manual, Public Health Service Publication No. 999-AP-40, (1967).

Midwest Research Institute, "Handbook of Emissions, Effluents and Control Practices for Stationary Particulate Pollution Sources," NAPCA Contract No. CPA-69-104, (November 1, 1970).

Nelson, Kenneth W., "Nonferrous Metallurgical Operations," in Air Pollution Vol. III, 2nd ed., editor: Arthur C. Stern, Academic Press, New York, (1966).

Tomany, James P., "The Control of Aluminum Chloride Fumes," Paper 68-130 Presented at 61st Annual Meeting of Air Pollution Control Association, June 23-27, (1968).

7.2.3.7 Electroplating

Process Description

Brass, bronze, chrome, copper, cadmium, iron, lead, nickel, tin, zinc and the precious metals can all be electroplated onto a surface. Reasons for electroplating include reducing corrosion, improving wearing qualities, and for decoration.

A cathode, made up of the material to be plated, and an anode are submerged in an electrolytic bath containing ions of the metal to be deposited. A direct current is passed through the electrolyte, depositing the plating metal on the cathode.

Plating baths are usually operated under conditions which decompose the water in the bath into oxygen and hydrogen at the cathode and anode, respectively, leading to vigorous agitation of the bath.

Scrubbers Used

Little air pollution is emitted from the electroplating operation, except in the case of hard chrome plating. In the hard chrome plating operation, current densities through the bath are sufficient to generate substantial agitation due to liberated oxygen and hydrogen. The agitated bath then envolves a fine mist of toxic, corrosive chromic acid mist. Scrubbers are effectively used to eliminate this mist from the plating tank vent system. Liquid used in the scrubber is commonly recycled to the plating tank. This serves the dual purpose of reclaiming the chromic acid mist, and replacing the water electrolytically decomposed at the electrodes.

Surface active agents have been effectively used to lower the surface tension of plating baths. This results in reducing the acid mist generated when bursting bubbles of gas arrive at the surface of the plating tank.

Data on the performance of plating tank scrubbers is given in Table 7.2-28.

TABLE 7.2-28 SCRUBBER PERFORMANCE DATA - Electroplating.

GENERAL		SCRUBBER		CARRIER GAS			PARTICLES			POLLUTANT GAS			SOLUTION		COST		
#	Process	Name	Description	m³/hr	T_i °C	T_e °C	Name	$(g/m^3)_e$	%E	Name	$(ppm)_e$	%E	Composition	m³/hr	ΔP cm.	Installed $	OP. $/mo.
1	Prec. Metal Plating	Packed Bed	p.P	11,600			Acid Mists		>90				Sodium Hydrox.	11.4	4.5		
2	Anodiz. &Stripping	Packed Bed	p.P	55,500					>90				Sodium Hydroxide	52.6	4.5		
3	Chrome Plating	Packed Bed	2.5mx2.5 mx3.2m tall	48,100	21-24		Chrom. Acid Mist	0.00001	99+					27.1		12,500	875
4	Simulated Plating	Fiber Bed (4 unit)	Nylon Fibers	4,250						HCl		99.25	Water	0.227	13.6		
5	Simulated Plating	Packed Bed	F.R.P.	4,250						HCl		99/ 98.8	Water	2.27/ 1.13	11/ 11.8		
6	Simulated Plating	2 Hori. Fiber Bed	F.R.P.	4,250						HCl		96.7	Water	5.9			
7	Simulated Plating	Impinge. Plate		2 230						HCl		96.7	Water	0.91	9.1		
8	Simulated Plating	Mech. Aided								HCl		57		0.34			

SECTION 7.2.3.7 - REFERENCES

Danielson, John A., Air Pollution Engineering Manual, U.S. Dept. HEW. Publication No. 999-AP-40. (1967).

Kempner, Stanley K., E. N. Seiler, and Donald H. Bowman, "Comparison of Comparison of Commercially Available Plating Fume Scrubbers", Paper #69-81, presented at 62nd Annual Meeting of APCA (1969).

7.2.3.8 Nonferrous Salvage Operations

Process Description

This section covers salvage smelting of nonferrous metals other than copper and aluminum, which are covered in Sections 7.2.3.5 and 7.2.3.6 respectively.

Nonferrous metals have appreciable value, and are often smelted to be recast and resold. Scrap for processing is sometimes dirty. Melting dirty scrap leads to emissions of particulate matter as the impurities are burned or evaporated off. Reclaimation of zinc, or zinc containing alloys such as brass, often cause difficulties due to zinc's low boiling point of 906°C. The zinc vaporizes, and condenses as zinc oxide, with a particle size of 0.03 to 0.3 micron diameter.

Scrubbers Used

Venturi scrubbers have been used to control the emissions from nonferrous scrap melting operations. Venturis are able to lower emissions to acceptable levels in terms of weight per hour discharged, or weight concentration of particulate matter in the effluent gas stream. However, they are unable to collect the extremely fine zinc oxide and oil smoke particles which are often emitted. These particles cause a plume opacity problem due to their small size, even when their weight concentration in the gas stream is low. For this reason, where opacity restrictions are tight, scrubbers are usually replaced by a baghouse, which is more readily able to collect the submicron zinc oxide fume produced. Alternate means of control include use of fluxes to cover the molten bath, and bath temperature control. Table 7.2-29 lists the data on the emissions from nonferrous salvage operations. Table 7.2-30 gives the characteristic emissions from nonferrous smelting.

TABLE 7.2-29 SCRUBBER PERFORMANCE DATA - Nonferrous Salvage Operations

GENERAL		SCRUBBER		CARRIER GAS			PARTICLES			POLLUTANT GAS			SOLUTION		COST		
#	Process	Name	Description	m³/hr	T_i °C	T_e °C	Name	$(g/m^3)_e$	%E	Name	$(ppm)_e$	%E	Composition	m³/hr	ΔP cm.	Installed $	OP. $/mo.
1	Zinc Salvage Smelt.	Venturi		3,740	80	36	ZnO	0.0252	98.8				Water	16.3	117		
2	Zinc Salvage Smelt.	Venturi		3,700	64	30	ZnO	0.037	92.1				Water	>16	147		
3	Lead Salvage Smelt.	Venturi		16,000	60	59	$PbSO_4$, PbO	0.0763	99.3				Water	50	105		
4	Brass Salvage Smelt.	Venturi		25,000				0.34					Water*	90.5	86		
5	Brass Salvage Smelt.	Venturi		15,500									Water*	90.5	46		
6	Brass Salvage Smelt.	Venturi		15,500									Water*	90.5	46		

* Settling pond used to clarify water.

TABLE 7.2-30

CHARACTERISTIC EMISSIONS FROM NONFERROUS SMELTING

Process	Gas Temp °C	Dew Point °C	Typical loading g/m³	Particle density g/cm³	Particle Size Dist		g emitted / Kg crushed
					50% under (microns)	16% under (microns)	
Brass Smelt. (Primarily Zinc Oxide)							
Crucible Fur.					0.03 -0.3μ		1.95
Electric Fur.							1.50
Reverberatory Furn.							13.15
Rotary Fur.							10.45
Lead Smelt. (Primarily Zinc Oxide)							
Cupola Fur.					0.3μ		150.0
Pot Fur.							0.05
Reverberatory Furn.							77.0
Zinc Smelt. (Zinc Oxides)							
Sweating Metallic Scrap					0.03 -0.5μ		6.0
Residual Scrap							15.0
Distillation Furn.							22.5 *

* g/Kg Zn present

Data adapted from the Midwest Research Institute (1970)

SECTION 7.2.3.8 - REFERENCES

Danielson, John A., Air Pollution Engineering Manual, Publication AP-40, Air Pollution Control Office of Environmental Protection Agency, (1967).

Duprey, R. L., Compilation of Air Pollutant Emission Factors, Publication AP-42, Air Pollution Control Office of Environmental Protection Agency, (1968).

Nelson, Kenneth W., "Nonferrous Metallurgical Operations" in Air Pollution III, 2nd edition, editor A. C. Stern, Academic Press, New York, (1968).

7 OF 9

PB

213016

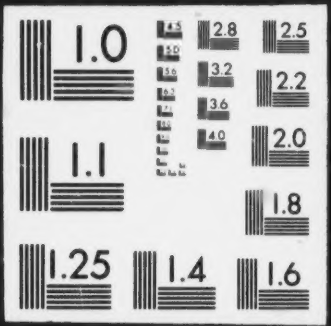

7.2.3.9 Chemical Cleaning, Etching and Milling of Metals

Process Description

Chemical milling was developed as a way to produce intricate metallic parts which could not be formed by mechanical milling. It is usually applied to sheets of metal used in the aircraft and missle industry.

The metallic surface to be milled must first be cleaned. Then a masking agent is applied over the surface. The masking is scribed by the use of a template, and the masking removed from that area which is to be milled. Next the part is submerged in the milling bath. The amount of metal removed is controlled by the temperature and concentration of the milling solution, and length of time the metal is immersed in the bath. Sodium hydroxide is used to mill aluminum, sulfuric acid for titanium, and stainless steel requires aqua regia. The part is removed from the milling bath, rinsed in water, and the masking removed.

Scrubbers Used

Emissions from chemical milling tanks include milling solution mists, milling solution vapors (if the solution has a high vapor pressure, eg. nitric or hydrochloric acid), and hydrogen gas, formed as the solution acts on the metallic surface. Although the emissions are not copious, due to their strongly corrosive properties they can be irritating and damaging even at low concentrations.

Scrubbers are commonly used to control the mists and vapors from chemical milling tanks. Spray plus baffle scrubbers, and packed bed scrubbers are commonly used. Spray plus baffle scrubbers are more popular due to their lower cost. The scrubber must be able to withstand the strongly corrosive climate of the bath. Table 7.2-31 lists data on emissions from the chemical cleaning, etching and milling of metals.

SECTION 7.2.3.9 - REFERENCES

Danielson, John A., "Air Pollution Engineering Manual," publication AP-40, Air Pollution Control Office of the Environmental Protection Agency (1967).

TABLE 7.2-51 SCRUBBER PERFORMANCE DATA - Chemical Cleaning, Etching and Milling of Metals.

GENERAL		SCRUBBER		CARRIER GAS			PARTICLES			POLLUTANT GAS			SOLUTION		COST		
#	Process	Name	Description	m^3/hr	T_i °C	T_e °C	Name	$(g/m^3)_e$	%E	Name	$(ppm)_e$	%E	Composition	m^3/hr	ΔP cm.	Installed $	OP. $/mo.
1	Chem. Milling Al	Packed Bed	F.R.P.	34,700	21-24	20-23		6	67	HF	7,200	66		29.5		12,500 (FOB)	900
2	Chem. Milling Al	Packed Bed	F.R.P.	34,700	21-24	20	H_3BO_4 $H_2Cr_2O_3$ H_3PO_4	$3x10^{-6}$	99+					29.5	5.1	12,500 (FOB)	900
3	Al Cleaning	Spray & Baffle	Ep. Coated 14 ga. steel	25,200	21-24		NaOH	0.0113	51						3.8	13,500	600
4	Chem. Milling Al	Packed Bed		34,000	30		H_2SO_4 Cr_2O_3									10,000	
5	Chem. Milling Al			8,500						NO_x			Water		38		
6	Chem. Milling Al	Spray & Baffle		85,000	54		NaOH Mist						Water			2,300 sc 8,500	
7	Chem. Milling	Cross-Flow Packed Bed	P.V.C.	85,000	38-66		HNO_3 Mist			HF, NO_x	560-1400 NO_x		Water	34	14	25,000sc 35,000f&d 35,000aux	**

**1800 water
130 fan
150 mainten.
200 cleanup & inspection
$2280/mo. total

7.2.3.10 Miscellaneous Metallurgical Industries

Following are data on metallurgical industries not covered in the preceeding sections. A list of contents is below in Table 7.2-32:

TABLE 7.2-32

DATA ON MISCELLANEOUS METALLURGICAL PROCESSES

Process	Number
Aluminum alloy oxidation	1
Lead blast furnace	2
$MgCl_2$ flux manufacture	3
Molybdenite smelting	4
Nodulizing kiln	5
Nonferrous foundry	6
Plutonium manufacture	7
Plutonium manufacture	8
Radioisotope manufacture	9
Radioisotope manufacture	10
Radiocesium manufacture	11
Radiocesium manufacture	12
Uranium burning	13
Uranium ore denitration	14
Uranium ore denitration	15
Uranium ore denitration	16
Uranium oxide carbon burnout	17
Uranium refining	18
Sodium cleaning	19
Zinc galvanizing	20
Zinc galvanizing	21

Table 7.2-33 lists data on the emission from miscellaneous metallurgical processes.

TABLE 7.2-33 SCRUBBER PERFORMANCE DATA - Miscellaneous Metallurgical Industries

GENERAL		SCRUBBER		CARRIER GAS			PARTICLES			POLLUTANT GAS			SOLUTION			COST	
#	Process	Name	Description	m³/hr	T_i °C	T_e °C	Name	$(g/m^3)_e$	%E	Name	$(ppm)_e$	%E	Composition	m³/hr	ΔP cm.	Installed $	OP. $/mo.
1	Al Alloy deoxida.	Packed Tower	M.S. Tar & Ep. Ctd	25,200	21-24		$H_2Cr_2O_4$	$2.3x10^{-6}$	99							12,500	600
2	Lead Blast Furn.	Venturi	Rigidon	11,000	50	35	PbO	0.08	96				Water	11.4	61	35,000	
3	M_gCl_2 Flux Mfg.	Venturi		11,000	660	56	$MgCI_2$, $AlCl_3$, HCl	0.25 in					NaOH sol'n.	11.5	115	22,000	
4	Molybdenite Smelt.			17,000	300-375					SO_x	9600 to 13000		Water+	6.8			
5	Nodulizing Kiln	Venturi		221,000	340	82		0.0039	99.7	F_2			$Ca(OH)_2$ sol'n.				10,000 for lime
6	Nonferrous Foundry	Venturi		85,000	540	71	Cupola Dust	0.0242	99				Water		90	44,000 (FOB)	
7	Plutonium Mfg.	Venturi	p.E.	170	60	27	H_2SO_4 Mist		95							700 sc. 100 duct 400 aux.	
8	Pu Mfg. Calc. Disch.	Water Curtin	S.S.	270	260	99	U_2O_3 Dust	0.18 to 0.28	96							1500 sc. 2000 f&d 4000 aux.	40
9	Radioisotope I_2 Rem.	Packed Bed	2m dia. 5m tall	3,900	43	30				I_2	$2\text{-}6x10^{-10}$	65-90	NaOH or $Hg\text{-}HNO_3$	34	65		
10	Radioisotope Mfg.	Venturi	S.S. PVC Lined	68	22	30				HF, NO_x			NaOH sol'n.	3.35			
11	Radio. Cs Mfg.	Fiber Bed	1.7m dia.	10,200	83	38	Radio-Cs Dust	0.0017	50				NaOH sol'n.	3.6		35,000 scrubber only	
12	Radio. Cs Mfg.	Fiber Bed	20 μm p.P. Fibers	10,200	83	38	Radio-Cs Dust	0.0017	95						137	35,000 sc. 7,500aux.	
13	U Burning	Venturi	304L SS	3,400	85		UO_x Dusts		95				Water	40	5	4600 sc. 1460 aux.	
14	Denitr. of U ore	Centrif	S.S.	255	100	90	U Cpds.		90	NO_x			Water	6.5		3000 sc. 200 f&d 5500 aux.	
15	Denitr. of U Ore	Packed Bed	S.S.	255	870		U Cpds.			NO_x			Water			1000 sc. 2000 f&d 1500 aux.	350
16	Denitr. of U Ore	Spray & Baffle	S.S.	255	760		U Cpds.			NO_x			Water	0.45		750 sc. 2500 f&d 1500 aux.	250

TABLE 7.2-33 cont'd. SCRUBBER PERFORMANCE DATA - Miscellaneous Metallurgical Industries

GENERAL		SCRUBBER		CARRIER GAS			PARTICLES			POLLUTANT GAS			SOLUTION		COST		
#	Process	Name	Description	m³/hr	T_i °C	T_e °C	Name	$(g/m^3)_e$	%E	Name	$(ppm)_e$	%E	Composition	m³/hr	ΔP cm.	Installed $	OP. $/mo.
17	UO_2 carbon burnout	impinge & entrain	rubber lined	1,800	150	60	UO_2 $NH_4P_2O_4$ $UO_2P_2O_7$		90				NaOH sol'n 10%			5,125 sc 5,320 aux	
18	uranium refining	venturi	fiberglass	2,500	75		U		95	Cl_2			NaOH sol'n 10%	16	76	5,550 sc 6,180 f&d 11,245 aux	
19	sodium cleaning	centrifugal	carbon steel	7,630	ambient		Na_2O						water	5.7	22.5	2,500 sc 6,300 other	
20	Zn galvanize	mech. aided		8,500	36		NH_4Cl	0.224	95					1.14			
21	Zn galvanize	packed bed		8,150	60		NH_4Cl		+					5.7	9		

+ Did not meet local emission code

7.2.4 CHEMICAL PROCESSES

7.2.4.1 Petroleum Refining

Process Description

The modern petroleum refinery is complex. Processing oil involves a number of steps, each of which has a potential for air pollution emission. Emissions from petroleum refineries may come either from the processing of the petroleum, or from the combustion of fuels needed for auxiliaries to the refining process.

Petroleum processing emissions include those present in the petroleum itself, and the reaction products which are produced in the refining process. These include hydrocarbons, aldehydes, carbon monoxide, nitrogen oxides, ammonia, mercaptans, hydrogen sulfide, catalyst dust, and others. The magnitude of some of these emissions can be estimated from Table 7.2-34. However, it should be stressed that the values listed in this table are approximate. Large variations exist from refinery to refinery, depending primarily upon crude oil capacity, type of crude oil processed, type and complexity of processing employed, air pollution control measures in use, and the extent to which good housekeeping practices are in force.

Scrubbers Used

Emissions of gaseous hydrocarbons and carbon monoxide are usually controlled by incineration. However, some of the sulfur which enters the refinery in the crude oil is converted to hydrogen sulfide, which is often removed by scrubbing. Three suitable scrubbing procedures are reported by the API (1957). They are:

1. Scrubbing with caustic solution to produce a solution of sodium sulfide and hydrosulfide. This solution may be sold or oxidised by blowing with air. However, the air from the blowing operation should be incinerated, and the effluent water may cause a secondary pollution problem.

2. Scrubbing with various amines (Wood and Storrs, 1938; Blohm and Chapin, 1948), phenolate (Carvlin, 1938), or phosphate (Rosebaugh, 1938) solutions. These solutions absorb hydrogen sulfide at low (<40 C) temperatures, and release it when heated to the boiling point. The scrubbing solution can then be reused. Both absorption and desorption are usually carried out in the bubble-cap towers.

3. Scrubbing with thioarsenate solutions (Gollmar, 1934). Here hydrogen sulfide is absorbed; then the solution is aerated to produce elemental sulfur, which can be filtered out and ultimately sold.

Hydrogen chloride and ammonia may be removed from refinery gases by scrubbing with water. Mercaptans are sometimes removed by scrubbing with alkaline solutions. Particulate emissions from the fluidized bed catalytic cracking process are generally handled by cyclones, sometimes in conjunction with an electrostatic precipitator.

Heat is needed in the refining process. It is provided by boilers and process heaters, which burn oil or natural gas. In addition, pumps and compressors are used to move the petroleum through the refinery. These devices usually operate on natural gas. The emissions from fuel combustion in boilers, heaters, pumps and compressors are small compared with the emissions from the refining operation, and are not normally controlled. They can be estimated using the techniques for fuel combustion, section 7.2.2.

In summary, scrubbers are used in petroleum refineries to salvage products from waste gases, and for air pollution control if necessary. The majority of emissions from refineries are combustible, and are controlled by incineration.

Table 7.2-34

TYPICAL EMISSIONS FROM PETROLEUM REFINERIES

	Pollutant	Uncontrolled Emission	Comments
Fluidized Bed Catalytic Cracking Unit	HC	623 g/m^3 feed	principally methane scrubbing reclaimed in waste heat boiler.
	CO	38,800 g/m^3 feed	
	NO_2	180 g/m^3 feed	
	Aldehydes as HCHO	54 g/m^3 feed	
	NH_3	154 g/m^3 feed	
	Particles	10-60 g/m^3 exhaust gas	usually controlled by cyclones, sometimes with ESP.
Moving Bed Catalytic Cracking Unit	HC	248 g/m^3 feed	
	CO	1080 g/m^3 feed	
	NO_2	14 g/m^3 feed	
	Aldehydes as HCHO	34 g/m^3 feed	
	NH_3	14 g/m^3 feed	
	Particles	4.5-23 g/m^3 exhaust gas	usually controlled by cyclones.
Blowdown System	HC	850 g/m^3 refining capacity	sporadic, may be reduced to 14 g/m^3 by proper venting and/or flame incineration.
Drains	HC	600 g/m^3 waste water	may be reduced to 23 g/m^3 by proper control measures.
Vacuum Jets	HC	370 g/m^3 vacuum distillation capacity	may be reduced to ≈0 with control, usually incineration.
Cooling Towers	HC	17 g/m^3 water cooled	
Valves, Seals, Others	HC	202 g/m^3 refinery capacity	

Data adapted from Duprey (1968).

SECTION 7.2.4.1 - REFERENCES

American Petroleum Institute, Manual on Disposal of Refinery Wastes, Vol. II, 5th ed., New York, (1957).

Blohm, C. L. and W. F. Chapin, "Oil and Gas Journal" 47, 29, p. 75, (1948).

Carvlin, G. M., Refiner Natural Gasoline Mfr. 17, 225, (1938).

Danielson, John A., Air Pollution Engineering Manual, Public Health Service Publication No. 999-AP-40, Cincinnati, (1967).

Duprey, R. L., Compilation of Air Pollutant Emission Factors, Public Health Service Publication No. 999-AP-42, Raleigh, N.C., (1968).

Elkin, Harold F., "Petroleum Refinery Emissions, in Air Pollution, Vol. III, 2nd Ed., editor A. C. Stern, Academic Press, New York, (1968).

Gollwar, H. A., Ind. Eng. Chem. 26, 130, (1934).

Rosebaugh, T. W., Refiner Natural Gasoline Mfr. 17, 245, (1938).

Wood, W. R., and B. D. Storrs, Refiner Natural Gasoline Mfr., 17, 234, (1938).

7.2.4.2 Pulp Manufacture

Process Description

Pulp is extracted from wood, and is used to make paper, cardbord, etc. Over 90 per cent of the paper produced in the United States in 1970 was produced by the Kraft process. Pulp may also be made by the sulfite or the NSSC process. In the Kraft process, wood chips are cooked at a pressure of 8 or 9 atmospheres and 180°C for 3 hours in a solution of sodium sulfide and sodium hydroxide. The cooking process releases the cellulose fiber in the wood for use as pulp.

At the end of the cook, the pressure within the cooking vessel is used to blow the pulp and solution into a blow chamber. Next, the pulp is separated from the chemical cooking solution. Pulp is then washed thoroughly, and ready for use in the paper making process. The rest of the pulp production process is regenerating the chemicals used in cooking the wood chips - a necessity if the process is to function economically.

Spent liquor from the cooking process, so called "black" liquor due to the lignin, waste fibers, and sulfide salts which give it its color, is first concentrated by evaporation usually in multiple effect evaporators. Black liquor is usually brought to the 65% concentration level by direct contact with the recovery furnace flue gases. After concentration, the black liquor is burned in a recovery furnace to produce molten sodium carbide and carbonate. Sometimes the black liquor is passed through air oxidation tower prior to burning. The oxidation tower oxidises some of the malodorous sulfur compounds, both assuaging an odor problem and aiding sulfur recovery.

The molten salts go into a smelt tank, and dissolve to form "green" liquor. The sodium carbonate in the green liquor is then reacted with lime to form sodium hydroxide solution ("white" liquor) and precipitate calcium carbonate. The white liquor produced is now ready for recycling as cooking liquor. The precipitated calcium carbonate, after washing, is sent to a kiln for calcining, to produce the lime necessary for reacting "green" liquor to "white".

Scrubbers Used

A Kraft pulp mill is potentially the source of polluting odors, gases, and particles. Three sources which may be controlled by scrubbers are the recovery furnace, the smelt tank, and the lime kiln.

In the recovery furnace, concentrated black liquor is burned to recover sodium salts. Particles, hydrogen sulfide and odor are emitted. Particulate emissions are usually controlled by an electrostatic precipitator, followed by a scrubber to remove odors and gases. Hot furnace gases, used for direct-contact, final concentration of the black liquor prior to combustion, will strip volatile sulfur compounds from the liquor, and place an additional load on the scrubber following.

Scrubbers of the venturi, cyclonic, or fibrous packing type are often used to control the emissions from the smelt tank. Emissions from the lime calcining kiln are often controlled by scrubbers. Control practices are as detailed in Section 7.2.1.4. Data on scrubbers used in the pulp making process is given in Table 7.2-35. Typical emissions are given in Table 7.2-36 and Table 7.2-37.

.E 7.2-35 SCRUBBER PERFORMANCE DATA - Pulp Manufacture.

GENERAL		SCRUBBER		CARRIER GAS			PARTICLES			POLLUTANT GAS			SOLUTION		COST		
#	Process	Name	Description	m³/hr	T_i °C	T_e °C	Name	$(g/m^3)_e$	%E	Name	$(ppm)_e$	%E	Composition	m³/hr	ΔP cm.	Installed $	OP. $/mo.
1	Black Liquor Sp. Dry	Moving Bed	Spheres	4,250	96	50	Na_2SO_4 Primarily	0.0008	98				Water	3.4	8.9		
2	Black Liquor Sp. Dry	Moving Bed	Spheres	4,250	88	49	Na_2SO_4 Primarily	0.0915	93.7				Water	3.4	8.9		
3	Black Liquor Sp. Dry	Moving Bed	Spheres	4,250	105	51	Na_2SO_4 Primarily	0.0082	98.1				Water	3.4	8.9		
4	Jensson Tower		3 m x 27.5 m	1,000	45	28				SO_2	267	99.85					
5	Recovery Furnace	Venturi		1,700	230 after evap	66		0.02	96.6				Black Liquor Sol'n	3.1 evap/ 1.4 V.	63.5		
6	Recovery Furnace	Venturi		1,700	200 after evap	66		0.066	98.9				Black Liquor Sol'n	3.7 evap/ 3.4 V.	74.6		
7	Recovery Furnace	Venturi		1,700	188 after evap	67		0.382	93.9				Black Liquor Sol'n	5.6 V.	77.8		
8	Recovery Furnace	Venturi		1,700	85 V.	67		0.059	90.3				Water	4.3	42		
9	Recovery Furnace	Venturi		1,700	84 V.	71		0.055	87.4				Black Liquor Sol'n	1.6	61		
10	Recovery Furnace	Venturi		1,700	82	69		0.043	91.8				White Wash	3.2	61		
11	Recovery Furnace	Packed Tower	180cm tallx160 cm dia.	1,700	150				70				Water	9.5	15		
12	Recovery Furnace	Impnge. Plate		1,700					55				Water	0.68	25.4		
13	Recovery Furnace	Spray and Baffles		1,700					85				Water	0.68			
14	Recovery Furnace	Venturi and Baffle		1,700					96				Water	2.27			
15	Recovery Furnace	Impnge & Entrn.		1,700					98				Water	0.227	17.7		

Table 7.2-36

PARTICULATE EMISSIONS FROM KRAFT PULP MANUFACTURING PROCESS

Process	Gas Temp °C	Dew Point °C	Typical loading g/m^3	Particle density g/cm^3	Particle Size Dist 50% under (microns)	Particle Size Dist 16% under (microns)	g emitted / Kg dry pulp
Recovery Furnace	180	56-82	7-18		1	0.48	75
Smelt Tank	70-90		0.4-3.0		90%	< 5 µm	2.5
Lime Kiln	200-500		7-45		95%	<25 µm	22

All data adapted from Midwest Research Institute (1970).

Table 7.2.37

GASEOUS EMISSIONS FROM KRAFT PULP MANUFACTURING PROCESS

(grams per kilogram of dry pulp produced)

Process	Hydrogen Sulfide	Methyl Mercaptan	Dimethyl Sulfide
Digester-blow Chamber	0.05 - 0.35	0.45 - 2.85	0.45 - 1.9
Lime Kiln	0.5	-	-
Recovery Furnace	1.8	2.5	1.5
Multiple Effect Evaporator	0.6	0.02	-
Oxidation Tower	-	-	0.05

Data adapted from Duprey (1968).

SECTION 7.2.4.2 - REFERENCES

Adams, Donald F., "Pulp and Paper Industry", in Air Pollution III, 2nd ed., edited by A. C. Stern, Academic Press, New York, (1968).

Aho, William O., "The Jenssen Exhaust Scrubber - An Effective Air Protection System", TAPPI, 52, 4., (1969).

Blosser, Russel O., "Identification of Potential Air Pollution Problems in the Pulp and Paper Industry," TAPPI, 51, 8.

Blosser, Russel O., and Hal B. H. Cooper, Jr., "Secondary Scrubbing of Kraft Recovery Stack Gases", Presented at Annual Meeting of APCA, 1968, paper No. 68-129. (1968).

Collins, T. T., Jr., "The Scrubbing of Sulphate Recovery Furnace Stack Gases - Part II", Paper Industry & Paper World, September, (1957)

Collins, T. T., Jr., "The Scrubbing of Sulphate Recovery Furnace Stack Gases - Part III", Paper Industry & Paper World, October, (1957)

Collins, T. T. Jr., "The Scrubbing of Sulphate Recovery Furnace Stack Gases", August, 1957. Paper Industry & Paper World.(1957).

Collins, T. T., Jr., C. R. Seaborne, and A. W. Anthony, Jr., "Removal of Salt Cake Fume from Sulphate Recovery Furnace Stack Gases by Scrubbing", (1957).

Duprey, R. L., "Compilation of Air Pollutant Emission Factors", U.S. Department of H.E.W., Publication No. 999-AP-42, (1968).

Environmental Engineering, Inc., Control of Atmospheric Emissions in Wood Pulping Industry, 3 vol., NAPCA Contract No. CPA 22-69-18, March 15, 1970.

Galeano, S. F., and C. I. Harding, "SO_2 Removal and Recovery from Pulp Mill Power Plants", Presented at Annual Meeting of APCA, 1966, Paper No. 66-97., (1966).

Hendrickson, E. R., C. G. Walker, and V. D. Chapnerkar, "Identification of Non-Sulfur Organic Compounds in Stack Gases from Pulp Mills", AIHA Journal, 24, pp. 121-26, (1963).

Landry, Joseph E. and Daniel H. Longwell, "Advances in Air Pollution in the Pulp and Paper Industry", TAPPI, 48, 6, (1965).

Midwest Research Institute, Handbook of Emissions, Effluents and Control Practices for Stationary Particulate Pollution Sources, NAPCA Contract No. CPA 22=69-104, November 1, 1970.

Murray, J. S., "Scrubbing Kraft Recovery Furnace Gases", TAPPI, 43, 11, (1960).

Shah, I. S., "The Two-stage Evaporator-Scrubber and Secondary Scrubbing

Systems for Efficient Heat and Chemical Recovery from Kraft Recovery Furnace Flue Gases," Paper Trade Journal, March 11 and March 18 (1968).

7.2.4.3 Acid Manufacture

A. Sulfuric Acid

Process Description

Sulfuric acid is manufactured by either the contact process or the chamber process. Ninety-five percent of the sulfuric acid manufactured in the U.S. is made by the contact process.

In the contact process, gases containing 7-12% of SO_2 come from the combustion of sulfur in a suitable burner, or are the off gases from a preceeding process such as copper smelting, which liberates a suitable concentration of SO_2. The gases are dried, then catalytically oxidised to SO_3 over a vanadium pentoxide catalyst. The SO_3 is then absorbed in a solution of sulfuric acid and sold.

Scrubbers Used

The effluents from a contact sulfuric acid plant come from the final SO_3 absorption tower. Pollutants include gaseous, unconverted SO_2 and sulfuric acid mist. Sulfuric acid mist is often captured using fiber bed type mist eliminators. For performance data see Table 7.2-38.

B. Hydrochloric Acid

Process Description

Hydrochloric acid is produced by absorbing gaseous hydrogen chloride in water. Most hydrochloric acid (81%) is produced by recovering gaseous hydrogen chloride from the chlorination of organic compounds. Hydrogen chloride gas amenable to further processing to make hydrochloric acid is also produced by reacting sulfuric acid with sodium chloride at high temperatures (10%) and by burning hydrogen and chlorine gases in a reactor (9%).

Scrubbers Used

Some gaseous hydrogen chloride is unabsorbed in the HCl absorbing towers, and released as "tail gas". The tail gas is usually scrubbed in a packed or spray tower. Effluent from the tail gas scrubber is often recycled to the primary HCl absorber. For scrubber performance data see Table 7.2-39.

TABLE 7.2-38 SCRUBBER PERFORMANCE DATA - Sulfuric Acid Manufacturing

GENERAI		SCRUBBER		CARRIER GAS			PARTICLES			POLLUTANT GAS			SOLUTION		COST		
#	Process	Name	Descrip-tion	m³/hr	T_i °C	T_e °C	Name	$(g/m^3)_e$	%E	Name	$(ppm)_e$	%E	Compo-sition	m³/hr	ΔP cm.	Installed $	OP. $/mo.
1	H_2SO_4 Tail Gas Purify	Fiber Bed	Carpenter 20 teflon grid supp	156,000	93	93	H_2SO_4 Mist	0.071	88				H_2SO_4		7.5 - 10	20,000 each pad	
2	H_2SO_4 Tail Gas Purify	Spray Tower	Redwood		77	38				SO_2	300	97	NH_4OH Sol'n	205		340,000	

TABLE 7.2-39 SCRUBBER PERFORMANCE DATA - Hydrochloric Acid Manufacturing

GENERAL		SCRUBBER		CARRIER GAS			PARTICLES			POLLUTANT GAS			SOLUTION		COST		
#	Process	Name	Description	m³/hr	T_i °C	T_e °C	Name	$(g/m^3)_e$	%E	Name	$(ppm)_e$	%E	Composition	m³/hr	ΔP cm.	Installed $	OP. $/mo.
1	HCl tail gas	Packed Tower		2,040	27		HCl Mist	0.015	99.3				Water	1.14			
2	HCl tail gas	Spray Tower		42.5						HCl	985	90	Water	0.68		140 sc. 60 aux. 200 total	
3	HCl tail gas	Packed Tower	100 cm dia x 168 cm tall	102	0	21				HCl		99.9	Water	9.1			
4	HCl tail gas	Spray	Hetron Plastic	42	15	10				HCl	1,000	90	Water	0.7		200	
5	HCl tail gas	Spray	FRP	6,230		49				HCl	0.5-1%	80	Water	340			

C. Nitric Acid

Process Description

Ammonia and air are catalytically reacted at about 750°C and at pressures from 1 to 9 atmospheres. The resulting mixture of NO and H_2O and nitric acid containing condensate are passed through an absorption tower. The absorption tower is also supplied with air to convert the NO to NO_2. Water or weak nitric acid is fed to the top of the tower, while 55 to 65 percent HNO_3 is withdrawn from the bottom.

Scrubbers Used

The chief source of emissions from nitric acid plants is tail gas from the absorption tower. The tail gas contains nitrogen oxide, nitrogen dioxide, and nitric acid mist. According to Heller, Cuffe and Goodwin (1968), nitrogen oxide emissions may be reduced by

(1) Absorption in water if NO_2 content is 2-8% (not usually the case.

(2) Scrubbing with ammonium bicarbonate after treatment with NO_2.

(3) Scrubbing with waste caustic ammonia liquor.

(4) Scrubbing with lime slurry in solution of calcium nitrate and nitrite.

(5) Absorption with dry oxides of lime.

(6) Two-stage absorption in water, and sodium hydroxide solution.

(7) Adsorption in activated carbon or silica gel.

(8) Catalytic reduction to N_2.

D. Phosphoric Acid

Process Description

Phosphoric acid is produced by either of two processes. About 75% of the acid is produced by the wet process, and used in the fertilizer industry. The remaining 25% is produced by the thermal process, and is used in the food industry, or in high grade chemicals.

In the wet process, ground phosphate rock $(Ca_3(PO_4)_2)CaF_2$ is contacted with concentrated sulfuric acid in a series of attack tanks. The product, 30-35% P_2O_5, is rotary filtered to remove the gypsum ($CaSO_4$) formed, and then evaporated to a final strength of 50-55% P_2O_5.

In the thermal process, liquid phosphorous is burned with air to form P_2O_5. The P_2O_5 is hydrated, then absorbed in a spray tower to produce 85% acid. Much of the acid produced by the thermal process is used in the food industry. This acid is treated with NaHS to precipitate the potentially harmful lead and arsenic ions which may be present. The precipitates are removed by filtration.

Scrubbers Used

The chief air contaminants released in the wet process are silicon tetrafluoride and hydrogen fluoride, evolved in the attach tanks. These gases, plus fumes from the rotary filter and storage tanks are processed through a common scrubber, often of the spray type.

Phosphoric acid mist escapes from the absorption tower used in the thermal phosphoric acid production process. Fiber bed type mist eliminators are commonly used to reclaim this mist, as are venturi scrubbers and packed towers. For scrubber performance data see Table 7.2-40. Table 7.2-41 lists data on the emissions from acid manufacturing processes.

TABLE 7.2-40 SCRUBBER PERFORMANCE DATA - Phosphoric Acid Manufacturing.

GENERAL		SCRUBBER		CARRIER GAS			PARTICLES			POLLUTANT GAS			SOLUTION		COST		
#	Process	Name	Description	m³/hr	T_i °C	T_e °C	Name	$(g/m^3)_e$	%E	Name	$(ppm)_e$	%E	Composition	m³/hr	ΔP cm.	Installed $	OP. $/mo.
1	H_3PO_4 wet proc vent	Venturi	Neoprene Lined Steel	8,500	30	70				SiF_4	55	96	Water	108	11.5		
2	H_3PO_4 wet proc vent	Spray + Centri-fugal-2	Rubber Lined Steel	42,500	54	50				SiF_4	5.5	99.8	Pond Water	108	32	110,000	
3	H_3PO_4 wet proc vent	Packed Bed	Rubber Lined Steel	37,500	60	43				SiF_4, NH_3			Water	172	56	15000 sc 40000 - Total	
4	H_3PO_4 condensor	Orifice Plate	Rubber Lined Steel 4-Stages	8,500	121	38	H_3PO_4 Mist		>90	HF	36	99.7	1st stage: H_3PO_4 2nd, 3rd & 4th stage: Pond Water	1st stage: 46 2,3+4 stage: 159 total 205	120	53,000	

TABLE 7.2-41

EMISSIONS FROM ACID MANUFACTURING PROCESSES

Process	Gas Stream			Particulate Emissions					Gaseous Emissions		
	Temp°C	Dew Point °C	Name	Loading g/m3	density g/cm^3	size 50%<	dist.wt. 16%<	g.emit. Kg Acid Prod.	Name	ppm	g.emit. Kg Acid Prod.
Sulfuric Acid Contact Process Absorption Tower	**40-65**	40-65	H_2SO_4 mist	0.45	17-1.8	64(98%	< 3μ)	1	SO_2	1300 5400	10-35
Hydrochloric Acid By-Product Recovery Process	various										
Salt Process	35								HCl		
Thermal Process											
Nitric Acid	30		HNO_3 mist	Trace					NO, NO_2	1000, 6900	28
Phosphoric Acid Wet Process									gas. fluor.	1300	10-30
Thermal Process	56-93	45-85	H_3PO_4 mist	3.5-4.5	1.57-1.68	1.6		67*			

* g/Kg P_2O_5 produced

Particle Data adapted from Midwest Research Institute (1970)
Gaseous Data adapted from Duprey (1968)

SECTION 7.2.4.3 - REFERENCES

Brink, J. A. Jr., W. F. Burggrabe and J. A. Rauscher, "Fiber Mist Eliminators for Higher Velocities," CEP 59, 11 (1964).

Brink, J. A. Jr., "Chapter 15-Part B, Removal of Phosphoric Acid Mists, " in Gas Purification Processes, George Newnes, Ltd., London (1964).

Brink, J. A. Jr., W. F. Burggrabe, and L. E. Greenwell "Mist Eliminators for Sulfuric Acid Plants," CEP 64, 11 (1968)

Chemical Construction Co. "Engineering Analysis of Emissions Control Technology for Sulfuric Acid Manufacturing Processes," NAPCA Contract No. CPA 22-69-81, March (1970).

Danielson, John A. "Air Pollution Engineering Manual," U. S. Dept. H.E.W., Publication No. 999-AP-40 (1967).

Editor, "SO_2 Absorber: Two Scrubs Better Than One," Chemical Engineering, Feb. (1955).

Heller, Austin N., Stanley T. Cuffe, and Don R. Goodwin, "Inorganic Chemical Industry," in Air Pollution III, 2nd ed.; editor: A. C. Stern, Academic Press, New York (1966).

Lawler, "Air Pollution Control by a Sulfur Dioxide Scrubbing System," J. of APCA 7, 1 (1957).

Midwest Research Institute "Handbook of Emissions, Effluents and Control Practices for Stationary Pollution Sources," NAPCA Contract No. CPA 22-69-104 (1970).

NAPCA, "Atmospheric Emissions from Wet-Process Phosphoric Acid Manufacture," Nat'l Air Pollution Control Administration Publication No. AP-57 (1970).

NAPCA, "Atmospheric Emissions from Thermal Process Phosphoric Acid Manufacture," Nat'l Air Pollution Control Administration Publication No. AP-48 (1968).

York, Dr. H., E. W. Poppele, "Wire Mesh Mist Eliminators," CEP, 59, 6 (1963).

7.2.4.4 Fertilizer Manufacture

A. Normal Superphosphate

Process Description

Normal superphosphate is produced by reacting phosphate rock $[Ca_3(PO_4)_2]$ CaF_2 with sulfuric acid, H_2SO_4. Five parts of rock are reacted to four parts of acid, mixed for several minutes, and then dropped into a "den" for curing. Here the slurry solidifies to a porous solid. The solid is then cured for as long as six weeks to allow the acidulation to be completed. The finished superphosphate is either ground as is and bagged for sale, sold as is (run of pile product) or blended with some or all of the following: ammonia, sulfuric acid, phosphoric acid, triple superphosphate, potash, then rotary dried, rotary cooled, and bagged or sold in bulk form.

Scrubbers Used

The acidulation of phosphate rock liberates about one third of the fluoride in the rock as SiF_4 or HF. Fluoride gases and entrained solids are usually vented to a scrubber of the centrifugal, spray chamber, or venturi type. Driers, coolers and granulators may produce fertilizer dust and some gaseous fluorides-emissions are commonly treated in a scrubber.

B. Triple Superphosphate (TSP)

Triple superphosphate is produced by reacting phosphate rock with phosphoric acid. The phosphoric acid is made by reacting phosphate rock with sulfuric acid as described in Section 7.2.4.3. The product contains 40-50 percent P_2O_5, about 250% as much as normal superphosphate. After reacting, the product is cured for 30-60 days to ensure complete acidulation, then sold as is (run of the pile product) or granulated and sold.

Scrubbers Used

Low pressure drop scrubbers, often of the centrifugal or spray chamber type, are used to remove fluoride gases SiF_4 and HF from process vent gases. Normally, emissions from the acid-rock reactor are scrubbed, while emissions from the curing buildings are untreated. If the run of pile product is granulated or mixed, fertilizer dust and fluoride gases SiF_4 and HF are emitted. Control is by cyclones, often followed by a scrubber.

C. Diammonium Phosphate (DAP)

Process Description

Diammonium phosphate $(NH_4)_2HPO_4$ is made by reacting ammonia with phosphoric acid in an acid brick lined reactor tank. The phosphoric acid used is manufactured by reacting sulfuric acid with phosphate rock (see Section 7.2.4.3.) and may contain as much as 1-2% fluoride.

Some sulfuric acid may be added to control product quality. Slurry from the reactor is pumped to an ammoniator, where additional ammonia is added. Diammonium phosphate granules discharged from the ammoniator go to a rotary drier, a screening station, a rotary cooler, and finally to storage.

Scrubbers Used

Product off-gases from the reactor and ammoniator contain ammonia, gaseous fluorides and particulate matter. These gases are scrubbed with acid to recover the ammonia. Dust is generated by the cage mills used to process oversize product from the screening station. This fertilizer dust is collected in a cyclone, often followed by a venturi or impingement plate scrubber.

Table 7.2-42 gives scrubber performance data for fertilizer manufacturing processes. Table 7.2-43 gives typical emissions from phosphate fertilizer manufacturing.

TABLE 7.2-42 SCRUBBER PERFORMANCE DATA - Fertilizer Manufacturing.

GENERAL		SCRUBBER		CARRIER GAS			PARTICLES			POLLUTANT GAS			SOLUTION		COST		
#	Process	Name	Description	m³/hr	T_i °C	T_e °C	Name	$(g/m^3)_e$	%E	Name	$(ppm)_e$	%E	Composition	m³/hr	ΔP cm.	Installed $	OP. $/mo.
1	TSP	Centrifugals Venturi	Rubber Lined	82,000						SiF_4, HF	5.5	99.1	Pond Water	267 Total	43 Total		50 (cleaning)
2	TSPvent from bldg.	Fiberous Packing	Fiberglass	170,000			TSP Dust			SiF_4, HF	0.54	92	Water	150	15		200
3	TSP mfg.	Venturi		64,500						SiF_4 HF	1.8	88	Water	90	56		100 (clean only)
4	Normal Super-Phos. mfg.	Ejector Venturi	10 cm dia (2)	17,000	88	66			99								
5	Fertilizer Drier	Hydro-Filter		51,000	121	82			97								
6	Phos. Rock Drier	Cyclon. Scrubber	Polyurethane coated Steel	119,000	93	72	Phosphate rock	0.018	99.8				Water	125		90,000 scrubber only	
7	Fertilizer Storage	Centrifugal	Steel	41,000	46	24	Phosphate Rock	0.012	99.9				Water		7.6	45,000	
8	Phos. Rock Defluor	Spray Tower	Hetron	1,300,000	149	99	none			SiF_4, HF		100% Conden.	Water	114	nil	12,000	
9	DAP Granulator	Impingement Plate	Acid Brick	30,000	100	100				NH_3, SiF_4, HF			P_2O_5 Sol'n	114	12.5		
10	DAP Tail Gas	Venturi	Rubber Lined Steel	170,000	77	66	DAP Dust	0.17		NH_3 HF + SiF_4	178 }40.5	91.4 NH_3/ 0 SiF_4	P_2O_5 Sol'n	135 - 160	14	250,000	
11	Fertilizer mfg.	Moving Bed		51,000	82	27			97								
12	Fertilizer mfg.	Moving Bed		51,000	121	82			97								
13	DAP mfg.	Packed Bed	Stainless Steel	54,500	120		Fertilizer Dust								38	15,000	
14	Dicalcium Phos.	Centrifugal	Fiberglass	39,000		71	Dicalcium Phos.	0.73	94				Water	202	approx. 7.6		
15	DAP mfg.	Impnge. & Entrn.	Neoprene Lined Steel	98,000	74	57	DAP Dust	0.87	81	NH_3	1,150	81	P_2O_5 Sol'n	34	12.5 - 18		
16	DAP mfg. Convey.	Impnge. & Entrn.	Neoprene Lined Steel	44,400	68	46	DAP Dust			NH_3	195	71	P_2O_5 Sol. 10%	11.4	12.5 - 18		

TABLE 7.2-42 cont'd. SCRUBBER PERFORMANCE DATA - Fertilizer Manufacturing.

GENERAL		SCRUBBER		CARRIER GAS			PARTICLES			POLLUTANT GAS			SOLUTION		COST		
#	Process	Name	Description	m³/hr	T_i °C	T_e °C	Name	$(g/m^3)_e$	%E	Name	$(ppm)_e$	%E	Composition	m³/hr	ΔP cm.	Installed $	OP. $/mo.
17	DAP mfg. Cooler	Impnge & Entrn.	Neoprene Lined Steel	48,000	60	43	DAP Dust			NH_3 F	86 0.78	93 65	P_2O_5 Sol'n	11.4	12.5 - 18		
18	Phos-Rock Defluor	Packed Bed Horiz.	Rubber Lined Steel	49,000	84	38				HF	6.5	99.9	1st pack wk.acid 2nd pack Lime sol	89 364	15.5	90,000	
19	Fertilizer Grind.	Comb. Venturi Centrif.		17,000	33.3	17.2	Agricult. Chem.	0.011	96				Water	6.7	10	5,000	76

TABLE 7.2-43

EMISSIONS FROM PHOSPHATE FERTILIZER MANUFACTURING PROCESSES

Process	Carrier Gas		Particles						Gases		
	gas temp °C	Dew Pt. °C	Name	typical loading g/m^3	density g/cm^3	Size 50%< µm	Dist. 16%< µm	g emit. Kg prod.	Name	Typical ppm	g emit. KgP$_2$O$_5$
Normal Super-phosphate											
1.acid reactor			H_2SiF_6, SiO_2	0.2-0.35				24	SiF_4,HF	6-20	20-38% of total F in rock process
2.rotary drier			fluorides, fertil.dust	1.6-9	1.6-2.5	80	13	52			
3.rotary cooler	95		fertil. dust		2.2	75	12	45			
4.bagger			"		2.2	80	25				
Triple Super-phosphate											
1.acid reactor								24	SiF_4,HF		
2.granulator								0.25			
3.drier			fertil. dust					52			
4.cooler			"					45			
Diammonium Phosphate											
1.reactor			fertil. dust					24	SiF_4,HF		0.05-0.2
2.drier			"					52			
3.cooler			"					45			

Particle data adapted from Midwest Research Institute (1970).
Gas data adapted from Heller, Cuffe and Goodwin (1968)

SECTION 7.2.4.4 - REFERENCES

Heller, Austin, N., Stanley T. Cuffe, and Don R. Goodwin, "Inorganic Chemical Industry," in Air Pollution III, 2nd edition, editor A. C. Stern, Academic Press, New York. (1968).

Midwest Research Institute, "Handbook of Emissions, Effluents and Control Practices for Stationary Particulate Pollution Sources," NAPCA Contract No. CPA 22-69-104, November (1970).

Sachsel, G. F., J. E. Yocum, and F. A. Retzke, "Fume control in a Fertilizer Plant, " J. of APCA, 6, 4 (1957).

7.2.4.5 Asphaltic Pavement Manufacture

Process Description

In the asphaltic pavement manufacturing process, crushed stone is dried, screened, weighed, mixed with asphalt and shipped off to the job site in trucks. Portable asphalt plants may be disassembled and moved from job site to job site. Permanent plants are usually located close to an urban area.

Cold rock aggregate is first fed to a rotary drier, where it is contacted with hot gases from a burner. After moisture has been driven off, the heated aggregate is screened according to size into hot bins. From here on, processing depends on whether the plant is of the batch, or of the continuous type.

In batch plants, the operator weighs desired amounts of each size of stone into a mixing mill. After mixing, hot asphalt is added, and mixing continues until the product is drawn off through a hopper to a waiting truck.

In the continuous process, proper proportions of the different sizes of rock are continuously drawn from the hot bins. The mix is fed to a mill where hot asphalt is on a weir at the end of the mixing chamber. Product continuously moves over the weir, into a waiting truck.

Scrubbers Used

The chief source of emissions from an asphaltic pavement manufacturing plant is the rotary drier used to heat and dry the cold rock aggregate. Cyclones are usually employed as precleaners. Secondary cleaning is usually done by a centrifugal scrubber, although baghouses are also used.

Data on the performance of scrubbers applied to asphalt plant rotary driers is given in Table 7.2-44. Typical emissions from asphalt plants are in Table 7.2-45. Costs for operating asphalt plants are given in Table 7.2-46.

TABLE 7.2-44 SCRUBBER PERFORMANCE DATA - Asphaltic Pavement Manufacture.

GENERAL		SCRUBBER		CARRIER GAS			PARTICLES			POLLUTANT GAS			SOLUTION		COST		
#	Process	Name	Description	m³/hr	T_i °C	T_e °C	Name	$(g/m^3)_e$	%E	Name	$(ppm)_e$	%E	Composition	m³/hr	ΔP cm.	Installed $	OP. $/mo.
1	Asphalt Plant Drier	Centrifugal		80,000	190	38	Rock Dust		99				Water			45,000	
2	Asphalt Plant Drier	Centrifugal		61,000	153	71	Rock Dust	0.083	99.6				Water	26.1	20.3	40,000	
3	Asphalt Plant Drier	Centrifugal		61,000	168	76	Rock Dust	0.078	99.4				Water	26.1	20.3	35,000	
4	Asphalt Plant Drier	Centrifugal		77,800	193	64	Rock Dust	0.092	99.5				Water				
5	Asphalt Plant Drier	Centrifugal		15,900	204		Rock Dust						Water	41		10,000	
6	Asphalt Plant Drier	Centrifugal		35,000		54	Rock Dust	0.75	99.2				Water	35		25,000 Scrubber only	
7	Asphalt Plant Drier	Centrifugal	8 sprays 75x100cm duct	28,000		38	Rock Dust	0.238	97	SO_2 SO_3	15.7 < 5		Water	11.4			
8	Asphalt Plant Drier	Centrifugal	8 sprays 75x100cm duct	32,800		50	Rock Dust	0.344		NO_2	76		Water				
9	Asphalt Plant Drier	Centrifugal		37,100		58	Rock Dust	0.39					Water	32		28,400	670
10	Asphalt Plant Drier	Moving Bed	Spheres	4,250	320		Rock Dust	0.11	98.8				Water	1.6	15		
11	Asphalt Plant Drier	Moving Bed	Mild Steel	40,000	86	52	Rock Dust	0.4	96.5				Water			30,000	
12	Asphalt Plant Drier	Centrifugal	Mild Steel	64,000	142	50	Rock Dust	0.17	99.4				Water			40,000	
13	Asphalt Plant Drier	Centrifugal	Mild Steel	64,000	142	50	Rock Dust	0.17	99.4				Water			40,000	
14	Asphalt Plant Drier	Centrifugal	Steel	56,500	150	60 -80	Rock Dust		98 (est)				Water	91		20,000	
15	Asphalt Plant Drier	Venturi					Rock Dust		99.2				Water				
16	Asphalt Plant Drier	Centrifugal					Rock Dust		98.5				Water			16,850	

TABLE 7.2-44 cont'd. SCRUBBER PERFORMANCE DATA - Asphaltic Pavement Manufacture.

GENERAL		SCRUBBER		CARRIER GAS			PARTICLES			POLLUTANT GAS			SOLUTION			COST	
#	Process	Name	Descrip-tion	m³/hr	T_i °C	T_e °C	Name	(g/m³)_e	%E	Name	(ppm)_e	%E	Compo-sition	m³/hr	ΔP cm.	Installed $	OP. $/mo.
17	Asphalt Plant Drier			40,000		70	Rock Dust		99				Water			60,000	
18	Asphalt Plant Drier	Ven-turi		46,000			Rock Dust		99.3				Water			20,000 (FOB)	
19	Asphalt Plant Drier	Centri-fugal		65,500		38	Rock Dust	0.032					Water	65	19		
20	Asphalt Plant Drier	Centri-fugal		72,500		40	Rock Dust	0.10					Water	18.1	19		
21	Asphalt Plant Drier	Spray Cham-ber		39,200			Rock Dust	0.25					Water	115			
22	Asphalt Plant Drier	Centri-fugal		66,300	120		Rock Dust	0.0117	99.7				Water	50 -84	26	30,000 (FOB)	
23	Asphalt Plant Drier	Centri-fugal		55,400	108		Rock Dust	0.0329	99.5				Water	24	20	23,000 (FOB)	
24	Asphalt Plant Drier	Ven-turi		68,000	150	60	Rock Dust	0.059	98.9				Water	91	50	14,000 (FOB)	
25	Asphalt Plant Drier	Ven-turi		55,000	74		Rock Dust		98				Water	32	50		
26	Asphalt Plant Drier	Centri-fugal	3 m dia.	8,500	93		Rock Dust		95				Water	50	2	44,500 (FOB)	
27	Asphalt Plant Drier	Ven-turi		70,000	120		Rock Dust		99				Water	115	39.5		
28	Asphalt Plant Drier	Moving Bed		80,000	120		Rock Dust		98				Water	51.5	25		
29	Asphalt Plant Drier	Centri-fugal		25,500	66		Rock Dust		99				Water	36.5	35.5		

TABLE 7.2-45

CHARACTERISTIC EMISSIONS FROM ASPHALTIC PAVEMENT MANUFACTURE

Process	Gas Temp °C	Dew pt. Temp. °C	Typical loading* g/m^3	Particle density g/cm^3	Particle 50%under (microns)	Size Dist. 16% under (microns)	g emit. Kg pavement	
Rotary Drier	116	65	68	2.6	18	3.4+	16	+size distribution widely variable.
Bins, Hoppers, etc.	100		159	2.6	11	4.3	8	

Data adapted from Midwest Research Institute (1970).

* prior to cyclone precleaner

TABLE 7.2-46

COSTS INCURRED IN SCRUBBING ASPHALT PLANT ROTARY DRIER EFFLUENT

Mixer capacity, kilograms	m^3/hr gas @20°C	g/m^3 particles		efficiency	installed cost		\$/yr.operating cost
		in*	out		scrubber	total sys.	
6,600	27,200	15	0.114	99.2	26,500	105,000	6,000
6,600	27,200	15	0.114	99.2	26,500	105,000	6,000
6,600	25,500	16	0.121	99.2	25,000	100,000	6,000
6,600	25,500	16	0.121	99.2	25,000	105,000	6,000
6,600	27,200	15	0.114	99.2	26,500	105,000	6,000
8,800	30,600	15.4	0.109	99.3	28,400	108,000	8,000
8,800	30,600	15.4	0.109	99.3	28,400	108,000	8,000
8,800	30,600	15.4	0.109	99.3	28,400	108,000	8,000
11,000	45,900	16.6	0.116	99.3	28,400	108,000	8,000
11,000	45,900	37.6	0.099	99.7	27,700	111,000	10,000
11,000	45,900	37.6	0.099	99.7	27,700	111,000	10,000
13,200	37,400	21.8	0.165	99.2	31,200	120,000	12,000
17,600	51,000	30.3	0.160	99.5	45,000	150,000	16,000
22,000	61,200	28.2	0.185	99.3	60,000	150,000	20,000

All scrubbers are centrifugal type.

* after cyclone precleaner

SECTION 7.2.4.5 - REFERENCES

Aase, Glenn D., "Dust Control of Hot Mix Asphalt Plants", Information Bulletin, Bay Area Air Pollution Control District, San Francisco Co., California (1961).

Danielson, John A. "Air Pollution Engineering Manual", U.S. Dept. of H.E.W. Publication No. 999-AP-40 (1967).

Haynes, S.C., N. M. McGrave, and D. B. Pertis "Visual Clarity in Kiln Discharge Gases," J. of APCA, 5, 3, p. 171 (1955).

Ingels, Ray M., Norman R. Shaffer, and John A. Danielson "Control of Asphaltic Concrete Plants in Los Angeles County," J. of APCA, 10, 1, p.29 (1960).

Midwest Research Institute "Handbook of Emissions, Effluents and Control Practices for Stationary Pollution Sources", NAPCA Contract No. CPA-22-69-104, November (1970).

Sussman, Victor H., "Nonmetallic Mineral Products Industries," in Air Pollution III, 2nd Ed., editor: A. C. Stern, Academic Press, New York, (1968).

7.2.4.6 Chlorine Gas Manufacture

Process Description

Almost all chlorine gas is produced by the electrolytic decomposition of brine in diaphragm cells (67% of total production) and in mercury cells (28% of total production).

A purified solution of 26.5% NaCl is fed continuously to an electrolytic cell. Chlorine is liberated at the graphite anode. In the diaphragm cell, hydrogen gas is produced at the graphite cathode, leaving behind a solution of sodium hydroxide (NaOH), which can then be evaporated to concentrations of 50 or 73 percent and sold. Hydrogen gas can be burned or used in an adjoining chemical process. In the mercury cell, sodium ion forms an amalgam with the continuously fed mercury cathode. The amalgam is then decomposed with water to form sodium hydroxide and hydrogen gas in a neighboring decomposer. High quality sodium hydroxide is assured, as separation of the caustic from the brine solution prevents the presence of heavy metal brine impurities in the product.

Chlorine gas is cooled with water sprays, dried with sulfuric acid, passed through mist eliminators, cooled and compressed to liquid, and sold.

Scrubbers Used

The main source of emissions from the chlorine gas manufacturing process is residual or "blow gas" from the product compressing stage. Chlorine remains in the blow gas due to its vapor pressure at the compressor temperature and pressure. Packed bed scrubbers are commonly used to scrub clean the blow gas before release to the atmosphere. Sodium hydroxide solution produced in the electrolytic cell is often used as a scrubbing solution. Table 7.2-47 lists data on the emissions from chlorine gas manufacturing. See Table 7.2-48 for characteristic emissions from chlorine gas manufacturing.

TABLE 7.2-47 SCRUBBER PERFORMANCE DATA - Chlorine Gas Manufacturing.

GENERAL		SCRUBBER		CARRIER GAS			PARTICLES			POLLUTANT GAS			SOLUTION		COST		
#	Process	Name	Description	m³/hr	T_i °C	T_e °C	Name	$(g/m^3)_e$	%E	Name	$(ppm)_e$	%E	Composition	m³/hr	ΔP cm.	Installed $	OP. $/mo.
1	Blow Gas	Ejector Venturi		565	ambient	80				Cl_2	1%	96				4,500 sc. 145,000 aux.	4,500
2	Blow Gas	Packed Bed	Steel	340	20	20				Cl_2			NaOH Sol'n	16		1,400 sc. 4,100 aux	
3	Blow Gas	Packed Bed	Hetron	340						Cl_2	0-5%		NaOH Sol'n or H_2O	4.5		1,650 sc. 2,100 aux	300 -400
4	Blow Gas	Packed Bed	ARCO 870 R.L. Stl.	340	-40	15 - 20				Cl_2	1%	95 - 96.5		27 - 41	72		
5	Blow Gas	Spray Tower	Rubber Lined Steel	1,700	15	38				Cl_2	60	98.5	NaOH Sol'n	148	<1	40,000	
6	Blow Gas	Packed Tower	Rubber Lined Steel	520	-28	10				Cl_2	0.3%	97	Water	86		20,500 for similar tower. 0.76 m dia.	
7	Blow Gas	Packed Tower	Rubber Lined Mild Steel	35.5	15	15				Cl_2	0.8%	93.3	Water	34		8,000	10
8	Emergency Scrubber	Packed Tower	Steel	340 norm. 2,000 max.	20 - 90	20				Cl_2	5%		Caustic Brine	32		5,500 (1956)	
9	Blow Gas	Packed Tower	Hetron	340	varies					Cl_2	0-2.5%	95	Caustic Brine/ Water	4.5 - 7.0, 0.45		3,750	300
10	Blow Gas	Packed Column	Rubber Lined Steel	340 - 510	-40	15 - 21				Cl_2	0.3 - 5.0%	69 - 98.5	Water	27 - 41	68	5,500 Scrubber only	

TABLE 7.2-48

CHARACTERISTIC EMISSIONS
FROM CHLORINE GAS MANUFACTURING

Process	Pollutant	%Cl_2 in Blow Gas	$\frac{\text{g produced}}{\text{kg } Cl_2\text{gas produced}}$
Diaphragm Cell Plant	Cl_2	5-50%	10-80 (1 to 8% of the total Cl_2 produced)
Mercury Cell Plant	Cl_2	5-50%	20-80 (2 to 8% of the total Cl_2 produced)

Data adapted from Duprey (1968) and from Heller, Cuffe, and Goodwin (1968).

SECTION 7.2.4.6 - REFERENCES

Bryson, H. W. "Oregon State Coll. Eng. Expt. Sta. Circ.," 29, 147-149, (1963).

Duprey, R. L., "Compilation of Air Pollution Emission Factors", U.S. Dept. of H.E.W., Public Health Service Publication, No. 999-AP-42, (1968).

Editor, "Chemical Engineering," 64, 6 (1957).

Editor, "Chemical Age," 80, 635-644, (1958).

Heller, Austin H., Stanley T. Cuffe, and Don R. Goodwin, "Inorganic Chemical Industry", in Air Pollution III, 2nd ed., editor A. C. Stern, Academic Press, New York (1968).

Hooker, T. et.al. U.S. Patent No. 2,750,002 (1956).

Verein Deutsche Ingenieure, Kommission Reinhaltung der Luft "The Restriction of Chlorine Gas Emissions," VDI 2103, p.5 Federation of the Chemical Industry, Frankfurt am Main, (1960).

7.2.4.7 Miscellaneous Chemical Industries

Following are data on scrubbers used in chemical precesses not covered in the preceeding sections. A table of contents is below.

TABLE 7.2-49

DATA ON MISCELLANEOUS CHEMICAL PROCESSES

Process	Number
Alodine color conversion coating	1
Amine removal	2
Ammonia hydrolysis	3
Ammonia dydrolysis	4
Ammonia tail gas	5
Ammonia use	6
Ammonium bifluoride	7
Analytical chemical lab fumes	8
Analytical chemical lab fumes	9
Asphalt roofing manufacturer	10
Banbury Exhaust	11
Basic Lead sulfate	12
Can Spraying	13
Chlorination: organic chemicals	14
Chlorination: organic chemicals	15
Chlorination: organic chemicals	16
Dyestuff manufacture	17
Fluorescent Powder manufacturer	18
Fluorescent powder manufacturer	19
Heavy inorganics mfr.	20
Hexachlorocyclopentadiene mfr.	21
Hexachlorocyclopentadiene mfr.	22
Hexachlorocyclopentadiene mfr.	23
Hydrogen chloride evolution	24
Hydrogen cleaning	25
Hydrogen cooling	26
Hydrogen cooling	27
Monomer removal	28
Paint manufacture	29
Pharmaceuticals	30
Pharmaceuticals	31
Pharmaceuticals	32
Pharmaceuticals	33
Pharmaceuticals	34
Pharmaceuticals	35
Phosphor Spray Reclaimation	36
Pigment cooler	37
Pressurizing gas lines	38

Process	Number
Pressurizing gas lines	39
Resin coating	40
Solvent use	41
Sulfonated naphthelene mfr.	42
Sulfuric acid anodization	43
Sulfuric acid anodization	44
Sulfuric acid anodization	45
Sulfuric acid mixing spent	46
Sulfuric acid mixing spent	47
Tar dipping culvert pipe	48
Varnish, alkyd resins, epoxy resins	49
Vulcanizer	50

Table 7.2-50 lists data on the emissions from miscellaneous chemical industries.

TABLE 7.2-50 SCRUBBER PERFORMANCE DATA - Miscellaneous Chemical Industries.

GENERAL		SCRUBBER		CARRIER GAS			PARTICLES			POLLUTANT GAS			SOLUTION			COST	
#	Process	Name	Description	m³/hr	T_i °C	T_e °C	Name	$(g/m^3)_e$	%E	Name	$(ppm)_e$	%E	Composition	m³/hr	ΔP cm.	Installed $	OP. $/mo.
1	Alodine Color Convers Coating	Packed Bed	Fiberglass	34,000	35		NaOH Mist			H_2				6.8	13	4,160 sc. 4,706 f&d 1,066 aux	
2	Amine Removal	Slatted Tower	Redwood	51,000	ambient					Aliphatic Amines		99	Dilute H_2SO_4	45 - 90	10	25,000 (1953)	
3	NH_3 Hydrolysis	Spray Tower	Mild Steel	2,500	35					NH_3	5.5%	89	NH_4OH	22.7		60,000	1,500
4	NH_3 Hydrolysis	Packed Bed	Mild Steel	850	35					NH_3	5.5%	89	NH_4OH Sol'n			35,000	300
5	NH_3 Tail Gas	Venturi	Mild Steel							NH_3		95	NH_4OH	5.65		12,000	100
6	Ammonia Usage	Packed Tower	1 m tall	715	20	20				Ammonia	0.1%	97.5	Water	7.9		150 scrub. 50 aux.	
7	NH_4HF_2 Rotary Drier	Baffles + Spray		10,200	121	21								6.8	15 - 20		
8	Analyt. Chem. Fumes	Fiber Bed 16 Units	Polypropylene	3,400	20		acid, ethylene diamine mists	0.272 ± 0.136	84				Water			4,500	
9	Analyt. Chem. Fumes	Fiber Bed 16 Units	Polypropylene	3,470	20		acid, ethylene diamine mists	0.287 ± 0.174	78				Water			4,500	
10	Asphalt Roofing	Venturi	316 SS	6,800	150	38		0.104	94.8				Water	0.55	96	4,000 sc 3,000 f&d 5,000 aux	
11	Banbury Exhaust	Comb. Vent. & Centrif	Stainless Steel	5,950	43.3	27.2	Carbon Black + oil	0.015	99				Water	5	76	7,000	250
12	Basic Lead Sulfate	Mechanically Aided	18.8 SS	15,300	92	36	Basic Lead Sulfate		98				Water	1.1		3,500 (FOB)	
13	can mfg Spray Coating	Mechanically Aided	Mild Steel + SS	2,380	ambient		Lacquer Spray		99				Water	0.25		4,000	40
14	Chlorination Vent	Venturi	Tile & Saran Lined Pipe	765	66	21				HCl, Cl_2	3%	90	Lime Slurry 14%	71		4,000	65
15	Chlorination Vent	Packed Tower		470	20					HCl, Cl_2	2.7%	87	Lime Slurry	1.1		2,000 sc 2,000 aux	
16	Chlorinated organic	Packed Tower			ambient					HCl Cl_2		99				136,000	

TABLE 7.2-50 cont'd. SCRUBBER PERFORMANCE DATA - Miscellaneous Chemical Industries.

GENERAL		SCRUBBER		CARRIER GAS			PARTICLES			POLLUTANT GAS			SOLUTION		COST		
#	Process	Name	Description	m³/hr	T_i °C	T_e °C	Name	$(g/m^3)_e$	%E	Name	$(ppm)_e$	%E	Composition	m³/hr	ΔP cm.	Installed $	OP. $/mo.
17	Dye Stuff Mfg.	Mechanically Aided		17,000	ambient		Dyestuff Dust	0.0054	99				Water	1.8			
18	Fluorescent Powder mfg.	Ejector Venturi		15,300	93	24	Fluorescent Powder	0.04 - 0.072	72						12.5		
19	Fluorescent Powder mfg.	Impnge & Entrn.		17,000	93	24	Fluorescent Powder								12.5		
20	"heavy inorganics" mfg	Ejector Venturi		105,000	150	46								410		60000 sc 50000 f&d	
21	hexachlorocyclopentadiene	Packed Towers (3 Units)	Haveg	102	0	21				HCl	varies	99.9	Water	9.1			
22	hexachlorocyclopentadiene	Venturi (2Units)	Aludur	510	ambient					Cl_2			NaOH Sol'n	45		1,300 sc 18,300 aux	
23	hexachlorocyclopentadiene	Venturi	Aludur-scrubber Hetron ducts	510	ambient					Cl_2			Caustic Brine	15.9		18,300 total	
24	HCl evolution	Packed Tower	Fiberglass	17	36					HCl			$Ca(OH)_2$ sol'n	1.9		500 sc 300 pump 200 aux 1200 tot.	
25	Hydrogen clean.	Venturi	Carbon Steel	4,750	6		Mercury	0.00026	99.9				Water	13.6	66	50,000	
26	Hydrogen Cooler	Spray	1.5mdiax 6.1m tall	2,830	90	10				H_2O			NaCl sol'n 25%	62.5		10000 sc 15000 f&d 10000 aux	
27	H_2 Cooler	Spray		2,850	90	15				H_2O	sat. at 15°		NaCl sol'n 25%	64		35,000	
28	Monomer Removal	Packed Tower	Column: steel Packing: ceramic	170	ambient					mixed acryl. monom.	25 - 50	97.5 - 98.3	caustic 2-8%	11.4		25,000	
29	Paint Mfg	Packed Tower	telleret-tes+burl saddle mixture	8,500						Formaldehyde		94		23		17,000	
30	Pharma. Salt removal	Ejector Venturi	Fiberglass	27,200	100	82	$BaSO_4$, HCl, $CaCl_2$	$BaSO_4$ 0.08	86				Water	20.5		18000 sc 15000 f&d 15000 aux	350
31	Pharma. HF removal	Mechanically Aided	PVC	1,450	ambient					HF	35	>90	Water			5,000 sc 750 d 750 aux	
32	Pharma. Calcining	Venturi	304 ELC	510	430	50	NH_4, F	0.115	99.7				Water	2.7	98	9500 sc 6000 f&d 9500 aux	200

TABLE 7.2-50 cont'd. SCRUBBER PERFORMANCE DATA - Miscellaneous Chemical Industries.

GENERAL		SCRUBBER		CARRIER GAS			PARTICLES			POLLUTANT GAS			SOLUTION		COST		
#	Process	Name	Description	m³/hr	T_i °C	T_e °C	Name	$(g/m^3)_e$	%E	Name	$(ppm)_e$	%E	Composition	m³/hr	ΔP cm.	Installed $	OP. $/mo.
33	Antacid Spray Drier	Spray Tower	304 SS	22,800		38	Ant-acid Dust		≈100				Water	7.2	10		
34	antiperspirant Spray Drier	Spray Tower	304 SS	22,800		38	antiperspirant dust		≈100				Water		10		
35	Face Powder Mfg.	Ejector Venturi		8,500	20	20	SiO_2	0.0000 053 $5.3x10^{-6}$	99	HCl, $SiCl_4$ H_2, SiH_4		98	NaOH sol'n 10%	35	100	30,500	
36	Phos. Spray Reclaim	Comb. Vent + Centrif	Stainless Steel	1,870	22	12	Phos.						Water	0.6	23	2,000	22,000
37	Pigment Cooler	Comb. Vent + Centrif		8,500	54	20	Paint Pigment						Water	2.3	18	3,000	70
38	Pressurize Gas	Packed Tower	Raschig Rings	5,100	ambient					N_2O_4	1	>99.9	NaOH sol'n 20%				
39	Pressurize Gas	Packed Towers	mild steel hypalon coated	14,800						Hydrazine	120	99.7	Water	18.2			
40	Resin Coating	Comb. Vent + Centrif	SS	34,000	93	35	Phenol-formaldehyde Resin			Phenol-formaldehyde	0.9/ 4	96/ 98+	Caustic Sol'n 20%	230	25.5	30,000	540
41	Solvent Use	Impingement Plate		3,750	21	21							$KMnO_4$ sol'n	14.6	25		
42	Sulphonated napthelene mfg	Centrifugal		28,200	39		sulfonated napthelene	0.2					Water			150,000	
43	Anodize H_2SO_4	Packed Bed	Fiberglass		35		H_2SO_4 HNO_3, HF mists							36.2	12.5	9410 sc 5792 f&d 2705 aux	
44	Sulfuric acid anodize	Packed Tower	14 ga steel; epoxy coated	25,200	21 - 24		H_2SO_4 Mist	4.75	45 - 55				Water	9.1	3.8	12,000	1,060
45	Sulfuric acid anodize	Spray Baffle	14 ga. steel: epoxy coated	25,200	21 - 24		Chromic acid mist	0.0000 023 $2.3x10^{-6}$	90						3.8	13,500	500
46	mixing spent H_2SO_4	Ejector Venturi	PVC	54						HCl		98	Water	0.6		350	
47	Mixing spent H_2SO_4	Ejector Venturi	PVC	54	ambient					HCl, some Cl_2		98 (est)	Water	0.6		99 sc 250 duct	
48	Tar dipping Culvert Pipe	Spray		35,000		20		0.03									

TABLE 7.2-50 cont'd. SCRUBBER PERFORMANCE DATA - Miscellaneous Chemical Industries.

GENERAL		SCRUBBER		CARRIER GAS			PARTICLES			POLLUTANT GAS			SOLUTION		COST		
#	Process	Name	Description	m^3/hr	T_i °C	T_e °C	Name	$(g/m^3)_e$	%E	Name	$(ppm)_e$	%E	Composition	m^3/hr	ΔP cm.	Installed $	OP. $/mo.
49	Varnish Resins Mfg	Spray	30 cm dia	2,000	66		Raw Material		90				Water				
50	Vulcanizer	Comb. Vent + Centri	Carbon Steel	25,500	22	12	Talc & Oil			H_2S	0	>99.7	Caustic Sol'n 5%	69	19	10,000	190

7.2.5 FOOD AND FEED INDUSTRY

Process Description

The food and feed industry processes farm products into comestibles for animal and human consumption, and other goods. Grains and grain products are often dried in their natural form in rotary driers prior to further processing. Many grains are processed to a slurry form which is then spray-dried.

Processing meat products and meat by-products can often lead to an odor problem. Fish processing, meat packing and rendering of by-products all may lead to odor production.

Scrubbers Used

The emissions from a grain rotary drier are sometimes vented through a cyclone to a scrubber. Scrubbers are particularly suitable if the material to be removed is hygroscopic. Emissions from spray driers can be scrubbed also. The scrubber liquid effluent can sometimes be recycled to the drier.

Odors arise from the decomposition of proteinaceous material. Many are amines, including mono, di- and trimethylamine, fatty acids such as buteric, valeric or caproic acid, or sulfur compounds - mercaptans, thiols and hydrogen sulfide. Odors can often be effectively removed by oxidizing the odorous gas. This can be accomplished by scrubbing the gas with an oxidizing agent such as potassium permangenate. An alternative is condensing the odoriferous compounds out of the gas stream. This can be done in a spray tower. If necessary, the gas may then be incinerated. Interestingly, in some cases it is less expensive to scrub the gas with a water spray and then incinerate the gas, than it is to incinerate the gas directly. This is because cooling the gas in a scrubbing tower condenses out water vapor in the gas stream, which otherwise would have to be heated to high incineration temperature. Precondensing this water vapor results in a lower incinerator fuel bill. Table 7.2-51 lists data on the emissions from the food and feed industry.

TABLE 7.2-51 SCRUBBER PERFORMANCE DATA - Food and Feed Industry.

GENERAL		SCRUBBER		CARRIER GAS			PARTICLES			POLLUTANT GAS			SOLUTION		COST		
#	Process	Name	Description	m³/hr	T_i °C	T_e °C	Name	$(g/m^3)_e$	%E	Name	$(ppm)_e$	%E	Composition	m³/hr	ΔP cm.	Installed $	OP. $/mo.
1	Orange Peel Drier	Centrifugal		29,000		80		0.40		NO_2	13.5						
2	Orange Peel Drier	Centrifugal		27,000		60		0.286									
3	Orange Peel Drier	Centrifugal		36,800		72		0.416									
4	Orange Peel Drier	Centrifugal		59,300		73		0.288									
5	Orange Peel Drier	Centrifugal		67,500		78		0.415									
6	Spray Drier	Spray Tower	304 L SS	42,500	54	35	Whey Residue	0.192	>85						30	8500 sc 3500 f&d 4000 aux	200
7	Rendering	Spray Condenser	304 SS	112,000	ambient					Odor	50 ou	85 - 96		204 total	20.4	60,000	830
8	Rendering	Spray Condenser	304 SS	170,000	ambient					Odor				136		45,000	735
9	Rendering	Packed Tower	packing: plastic Shell: 316 SS	73,000		60				Odor							
10	Rendering	Centrif & Packed Bed	Pall Rings	15,300						Odors			$KMnO_4$ Sol'n 2%	13.5 - 17		8,700	
11	bone meal + tallow mfg.	Spray Tower	SS	73,000	ambient					Odors			Water			68,000	400
12	meat, blood meal + tallow mfg.	Spray Tower	2.4 m dia 9.2m tall	42,500						Odors			$KMnO_4$ Sol'n	67		7,000 sc 6,000 f&d 2,000 aux	
13	meat + bone meal tallow mfg.	Spray & Baffle		170,000						Odors			Soda Ash Sol'n			33000 s&f 10000 d. 20000inst	
14	Bone Steaming	Ejector Venturi	10 cm dia	850	93	71				Odors		97					
15	Bone Char Mfg.	Impingement Plate	46cmdia x 3.8m tall	1,520	116	82			99							5,000 sc 2,000 f&d	
16	Hoof-meal digester	Impnge & Entrn.	10 ga. Mild Steel	6,800	21					NH_3	89	36	Water	5.65	13	19,000	≈300

TABLE 7.2-51 cont'd. SCRUBBER PERFORMANCE DATA - Food and Feed Industry.

GENERAL		SCRUBBER		CARRIER GAS			PARTICLES			POLLUTANT GAS			SOLUTION		COST		
#	Process	Name	Description	m³/hr	T_i °C	T_e °C	Name	$(g/m^3)_e$	%E	Name	$(ppm)_e$	%E	Composition	m³/hr	ΔP cm.	Installed $	OP. $/mo.
17	Vegetable oil processing	Ejector Venturi		27,200						Cl_2+ SO_2			NaOH Sol'n 10%				

SECTION 7.2.5 - REFERENCES

Faith, W. L., "Food and Feed Industries," in Air Pollution, 111, 2nd ed., Editor A. C. Stern, Academic Press, New York, (1968).

Danielson, John A. "Air Pollution Engineering Manual," U. S. Dept. of H.E.W. Public Health Service Publication No. 999-AP-40 (1967).

Anderson, Catherine E. , "Odor Control with Potassium Permanganate, " paper presented 9th Annual Purdue Air Pollution Control Conference, October, (1970).

Anderson, Catherine E., "Odor Control in the Rendering and Food Processing Industries, " paper 71-22, presented Air Pollution Control Association Meeting, Atlantic City, New Jersey, June (1971).

7.2.6 WASTE DISPOSAL

Process Description

Disposal of solid and liquid wastes can lead to air pollution problems. Solid refuse is often burned in incinerators ranging from large, multichamber municipal units, through apartment house incinerators, to small backyard wire-basket burners. All types present an air pollution potential. Lumber processing wastes are often incinerated in conical, screen-topped teepee burners. The disposal of liquid wastes through sewers often presents an odor problem where the sewer lines are vented.

Scrubbers Used

Designing an air pollution collection device to handle the effluent from an incinerator is quite difficult. The quantity of gas to be handled may vary by a factor of four, depending upon the amount of material burned. Temperatures are widely variable. Particle loading is also widely variable, depending primarily upon the nature of the charge and the amount of excess air used. Particle sizes range from large flakes of unburned material larger than a centimeter in diameter, through submicron particles. Finally, the gases are often corrosive due to the presence of HCl in the gas, if chlorine-containing plastics are burned.

Large municipal and industrial incinerators have traditionally provided a secondary chamber, in which exhaust gases could complete combustion and larger particles could settle out, before being exhausted up the stack. Present day standards have shown these chambers to be insufficient. Modern practice is to scrub the incinerator exhaust gases by passing them through a water spray or curtain, followed by a series of wetted baffles. This arrangement removes large particles, greater than 100 microns diameter, but is inefficient on smaller particles present. Scrubbers utilizing a bed with mobile packing have been used to capture the smaller particles emitted.

Apartment house incinerators are often simple fireboxes. Waste is fed through a chute which also serves as the incinerator flue. In the past, these incinerators have often been uncontrolled. Today, many cities are requiring control. Spray chambers followed by a baffle type entrainment separator are common.

The odorous gases eminating from sewer lines at pumping stations, treatment plants, and other points where the lines converge, can be treated by scrubbing in a packed tower utilizing a suitable oxidizing scrubbing liquid such as potassium permangenate or sodium hypochlorite.

Table 7.2-52 gives typical particulate emissions from incinerators while Table 7.2-53 gives typical gaseous emissions. Table 7.2-54 gives scrubber performance data.

TABLE 7.2-52

PARTICULATE EMISSIONS FROM INCINERATORS

Process	Gas Temp °C	Sat. Temp °C	Typical loading g/m³ *	Particle density g/cm³	Particle 50% under (microns)	Size Dist. 16% under (microns)	g emitted / kg burned
Municipal Incinerator	120-800		0.2-2.0 at 12% CO_2 avg:0.9	1.8-3.8	90.0	1.6	8.5
Commercial Incinerator	200-800		0.14-1.2 at 12% CO_2 avg:0.5		22	5	5---single chamber 1.5--multiple chamber
Apartment House Incinerator Flue fed	40-150		0.05-3.7		22	5	14

* Strongly dependent upon operating procedures

Data adapted from the Midwest Research Institute (1970) and Duprey (1968).

TABLE 7.2-53

GASEOUS EMISSIONS FROM INCINERATION

Process	Gas name	Typical ppm	$\frac{\text{g emitted}}{\text{kg burned}}$
Municipal Incinerator	ammonia, NH_3	30	0.15
	aldehydes, HCHO	1-50	0.15
	carbon monoxide, CO	100-4000	0.50
	hydrocarbons, HC	50-250	0.15 as C_6H_{14}
	nitrogen oxides, NO_2	20-100	1.0
	organic acids, CH_3COOH	15	0.3
	sulfur oxides, SO_2	36	1.0
Commercial Incinerator a) multiple chamber	ammonia, NH_3		0.05
	aldehydes, HCHO		0.10
	carbon monoxide, CO	100-4000	5.0
	hydrocarbons, HC	50-250	0.25
	nitrogen oxides, NO_2	10-70	1.0
	organic acids, CH_3COOH		1.5
	sulfur oxides, SO_2		0.5
b) single chamber	ammonia, NH_3		0.2
	aldehydes, HCHO		
	carbon monoxide, CO	550	22.0
	hydrocarbons, HC	850	0.4
	nitrogen oxides, NO_2		1.5
	organic acids, CH_3COOH		1.5
	sulfur oxides, SO_2		1.0
Apartment House Incinerator-Flue Fed	ammonia, NH_3		0.2
	aldehydes, HCHO		1.5
	carbon monoxide, CO		13.5
	hydrocarbons, HC		1.0
	nitrogen oxides, NO_2		0.15
	organic acids, CH_3COOH		12.5
	sulfur oxides, SO_2		0.1

Data adapted from Duprey (1968).

TABLE 7.2-54 SCRUBBER PERFORMANCE DATA - Waste Disposal Processes.

GENERAL		SCRUBBER		CARRIER GAS			PARTICLES			POLLUTANT GAS			SOLUTION		COST		
#	Process	Name	Description	m³/hr	T_i °C	T_e °C	Name	$(g/m^3)_e$	%E	Name	$(ppm)_e$	%E	Composition	m³/hr	ΔP cm.	Installed $	OP. $/mo.
1	Sewage Sludge Drying	Moving Bed	Marble Spheres	100,000	177	35	Fly Ash	0.073	89.7				Water	600			
2	Incinerator	Impnge Plate& Centri		2,200	120		Fly Ash						Water	4.5			
3	Pathol. Waste Incin.	Spray & Baffle	10 ga. HRS Steel				Fly Ash							1.87			
4	Odor from Sewer Line	Packed Bed	3 m tall	136						H_2S, Odors	0.76	92 50	Sodium Carbonate	7.7			
5	Odor from Sewer Line	Packed Bed	3 m tall	136						H_2S, Odors		74 83	$ZnSO_4$ H_2O	7.7			
6	Odor from Sewer Line	Packed Bed	3 m tall	136						H_2S, Odors	0	100 96	NaOCl	7.7			
7	Odor from Sewer Line	Packed Bed	3 m tall	136	ambient				100: H_2S 81: odor	H_2S, Odors	0		$KMnO_4$, Na_2CO_3 buffer.	7.7			
8	Odor from Sewer Line	Packed Bed	3 m tall	136	ambient				<70: H_2S 0 odor	H_2S, Odors			non-foaming detcrg.	7.7			
9	Odor from Sewer Line	Packed Bed	3 m tall	136	ambient				100: H_2S	H_2S, Odors	0		NaOCl Sol'n	2.27			
10	Sewage Sludge Incin.	Centrifugal	316 SS	51,300	80 - 120		Fly Ash	0.305	99				Water	56.6 to 22.7 sc/precool.	17.7	125,000 (Includes Inciner)	
11	Radioactive Waste Incin.	Impingement Plate	316 SS	255	720	80	Radioactive Dust	0.04	90								
12	Biology Lab Ashing Hood	Impingement Plate	SS	5,400			Grease Aerosol			Odors			Water	4.5			

SECTION 7.2.6 - REFERENCES

Achinger, William C., "Study Report on a Pilot Plant Conical Incinerator," U.S. Dept. of H.E.W., Bureau of Solid Waste Management, 5555 Ridge Ave., Cincinnati, Ohio 45213 (1970).

Calhoun, F. P. "Gas Scrubbing for Municipal Incinerators," Paper No. 68-163, presented at 61st annual meeting of Air Pollution Control Association (1968).

Daniels, Leland E. "A Report on the Hartsfield Incinerator Study," U.S. Dept. of H.E.W., Bureau of Solid Waste Management. 5555 Ridge Avenue, Cincinnati, Ohio 45213 (1970).

Danielson, John A., "Air Pollution Engineering Manual," U.S. Dept. H.E.W., Public Health Service Publication No. 999-AP-40 (1967).

DeMarco, Jack, Daniel J. Keller, Jerold Leckman and James L. Newton, "Incinerator Guidelines - 1969," U.S. Dept. of H.E.W., Public Health Service Publication No. 2012 (1969).

Duprey, R. L., "Compilation of Air Pollutant Emission Factors," U.S. Dept. of H.E.W., Public Health Service Publication No. 999-AP-42 (1968).

Eugdahl, Richard B., "Stationary Combustion Sources," in Air Pollution III, 2nd ed. Editor A. C. Stern, Academic Press, New York (1968).

Hahn, Jeffrey L., "Study of the Delaware Co. No. 3 Incinerator in Broomall, Pennsylvania, U.S. Dept. of H.E.W., Bureau of Solid Waste Management, 5555 Ridge Ave., Cincinnati, Ohio 45213 (1970).

Midwest Research Institute "Handbook of Emissions, Effluents, and Control Practices for Stationary Combustion Sources," NAPCA Contract No. CPA-22-69-104, November (1970).

Mitchel, J.N., and S. G. Gillette "Control of Emissions from the Precessing of Noncombustible Municipal Refuse," Air Repair, 5, 1, (1955).

Ongerth, Jerry E., and Morris G. Tucker, "Report on a Study of the Weber County Incinerator in Ogden, Utah," U.S. Dept. of H.E.W., Bureau of Solid Waste Management, 5555 Ridge Avenue, Cincinnati, Ohio 45213 (1970).

Rodger, W. A., and D. C. Hampson,"Operating Characteristics and Economics of a 100 Ft^3/Day In Incinerator for Radioactive Wastes," J. of APCA, 6, 1, (1956).

Stone, Arthur F., "Gas Scrubbing for Municipal Incinerators," Paper No. 68-163, presented at 61st annual meeting of Air Pollution Control Association.(1968).

Verein Deutscher Ingenieure, "Restriction of Emission -Waste Incineration in Plants with Throughput of up to 1500 kg per hr.," Translated from the German and Published with Permission for NAPCA.(1967).

7.2.7 MISCELLANEOUS PROCESSES

In this section data are presented on the performance of scrubbers fitted to unknown and unusual processes. A table of contents is below.

TABLE 7.2-55

DATA ON MISCELLANEOUS PROCESSES

Process	Number
Clean Room	1
Unknown	2
"	3
"	4
"	5
"	6
"	7
"	8
"	9
"	10

Scrubber performance data for these processes are given in Table 7.2-56.

TABLE 7.2-56 SCRUBBER PERFORMANCE DATA - Miscellaneous Processes.

GENERAL		SCRUBBER		CARRIER GAS			PARTICLES			POLLUTANT GAS			SOLUTION		COST		
#	Process	Name	Description	m³/hr	Ti °C	Te °C	Name	(g/m³)e	%E	Name	(ppm)e	%E	Composition	m³/hr	ΔP cm.	Installed $	OP. $/mo.
1	Clean Room Scrub.	Packed Tower	Polypropylene	47,500					>90				NaOH Sol'n				
2		Packed Tower	3 m tall	820	32					N_2O_4	3.02%	90	NaOH sol'n 25%	6.1			
3		Packed Tower	3 m tall	820	32					HF			Water				
4		Venturi + Packing entrn.sep	Porcelain Haveg	51	40	25				H_2S	1%	99	NaOH Sol'n 20%	0.54	2.5	4,500	400
5		Packed Tower	Porcelain 304 SS	850	40	25				H_2S	<1%		NaOH Sol'n 20%	2.3	20.4	5,700	400
6		Centrifugal	SS	2,020	100	40							Water	1.1	14	3,500	100
7		Packed Tower	Porcelain Saddles, SS		40					H_2S	2,000	<80	NaOH Sol'n 20%	17	6.1	6,300	475
8		Spray & Baffles	Haveg	2,720	110	50				SO_2	<5		NaOH Sol'n 20%	6.8	20.3	7,500	350
9		Packed Tower	Porcelain Saddles, Haveg Shell	2,720	90	30				H_2S	2		NaOH Sol'n 20%	3.4	20.3	6,000	325
10		Venturi		18,700		77		0.242					Water				

7.3 GENERALIZATIONS REGARDING SCRUBBER USE

In this section, analyses will be made of the data presented in the preceeding section. Trends in scrubber application and performance will be pointed out.

7.3.1 UNIT PROCESSES TO WHICH SCRUBBERS ARE APPLIED

A unit process is a processing step which is common to several industries. Seven unit processes to which scrubbers are frequently applied are: calciners, fuel burners, crushers, driers, gases, liquid mists, and smelters. For example, the scrubbers applied to the calciners used in the lime, cement, and wood pulp industries, can be considered as a group. Similarly, the liquid mist scrubbers used in the sulfuric acid and electroplating industries can also be considered as a group.

Sections and Tables 7.3-1 through 7.3-7 are devoted to the scrubbers applied to the seven unit processes identified above. In the tables, note that the entries in parentheses refer to the number of scrubbers which were available from the survey (Section 7.2) and were analysed to obtain a datum entry.

7.3.1.1 Calcining Processes

The industrial processes from which data were extracted and developed for the calcining processes section include: limestone calcining, lime sludge calcining, kraft pulp process recovery furnaces, and cement kilns. All utilize a high temperature gas to chemically alter the material being processed. Only particulate emissions are considered here. The scrubbers used to control calcining processes are described in Table 7.3-1.

Venturi scrubbers are most commonly applied to calcining operations, and comprise 70 percent of the scrubbers installed according to the present survey. Simple sprays are also used. The average venturi installation processes less gas, but is more efficient than the average spray. However, venturi systems can also be made to handle large gas flows. Self-induced spray scrubbers are also used. Since only three scrubbers of this type were found in the survey, conclusions should not be hastily drawn as to their performance.

7.3.1.2 Combustion Processes

Data for combustion processes were distilled from information on steam boilers used for power generation, and on waste incinerators. Both processes exhaust products of combustion. Table 7.3-2 gives these data.

No clear trends emerge. Many different types of scrubbers have been tried - no single type emerges as the definite favorite. An insufficient number of scrubbers have been examined to make definite statements as to efficiency capabilities of various types of scrubbers. It may be noteworthy, however, that the single spray scrubber for which data are available, performed relatively poorly.

TABLE 7.3-1

SCRUBBERS USED TO CONTROL PARTICULATE EMISSIONS FROM CALCINING PROCESSES+

		Plate	Packed Tower	Fiber Bed	Spray	Venturi	Centri-fugal	Baffle	Self-Induced	Mech. Aided	Moving Bed	Total
% each type used		(1) 3	(1) 3	(0) 0	(5) 15	(23) 70	(0) 0	(0) 0	(3) 9	(0) 0	(0) 0	(33) 100
Through-put, (m^3/hr)	Low	-	-	-	270	510	-	-	1700	-	-	
	Avg.	(1) 1700	(1) 1700	-	(5) 103,600	(20) 49,400	-	-	(3) 77,200	-	-	
	High	-	-	-	220,000	159,000	-	-	115,000	-	-	
Effic-iency (%)	Low	-	-	-	85	87.4	-	-	96	-	-	
	Avg.	(1) 55	(1) 70	-	(4) 93.5	(20) 95.1	-	-	(3) 96.7	-	-	
	High	-	-	-	98	99.7	-	-	98	-	-	

Notes: Numbers in parentheses refer to number of scrubbers analysed to obtain data entry.

Low and High values are lowest and highest values found in the scrubber survey.

+Includes:
Limestone Calcining
Lime Sludge Calcining
Kraft Pulp Process Recovery Furnace
Cement Kilns

TABLE 7.3-2

SCRUBBERS USED TO CONTROL PARTICULATE EMISSIONS FROM COMBUSTION PROCESSES+

	Plate	Packed Tower	Fiber Bed	Spray	Venturi	Centri-fugal	Baffle	Self-Induced	Mech. Aided	Moving Bed	Total
% each type used	(3) 25	(0) 0	(0) 0	(2) 17	(2) 17	(1) 8	(0) 0	(2) 17	(0) 0	(2) 17	(12) 101
Through-put, (m^3/hr) Low	255	-	-	-	3400	-	-	1800	-	1340	
Through-put, (m^3/hr) Avg.	(3) 2390	-	-	(1) 327,000	(2) 1,265,000	(1) 51,300	-	(2) 2000	-	(2) 425,000	
Through-put, (m^3/hr) High	5400	-	-	-	2,530,000	-	-	2200	-	850,000	
Efficiency (%) Low	27.8	-	-	-	95	-	-	-	-	99	
Efficiency (%) Avg.	(3) 72.5	-	-	(1) 29	(2) 97.3	(1) 99	-	(1) 90	-	(2) 99.3	
Efficiency (%) High	99	-	-	-	99.7	-	-	-	-	99.6	

Notes: Numbers in parentheses refer to number of scrubbers analysed to obtain data entry.

Low and High values are lowest and highest values found in the scrubber survey

+Includes:

Power generation boilers
Waste incinerators

7.3.1.3 Crushers and Mills

Crushers are used to reduce the size of many kinds of ore, stone, as well as finished mineral products. Data on this unit process is given in Table 7.3 -3.

Information on the application of scrubbers to crushing processes is spotty. Centrifugal scrubbers were employed in the preponderence of applications surveyed. However, efficiency data are lacking. Any judgements as to typical efficiencies based on the data in Table 7.3-3 would be rash.

7.3.1.4 Driers

Data on fluidized bed, rotary and spray driers are included in Table 7.3-4. These devices are used to drive the moisture from minerals, manufactured chemicals and foodstuffs.

Several types of scrubbers have been applied. The most popular is the centrifugal, followed by the venturi and the moving bed. Centrifugal scrubbers are apparently applied to smaller installations than those to which venturi scrubbers are applied. Average efficiency for centrifugal and venturi scrubbers is about equal, as is the highest efficiency encountered. Average and highest efficiencies for the moving bed scrubber are slightly less.

TABLE 7.3-3

SCRUBBERS USED TO CONTROL PARTICULATE EMISSIONS FROM CRUSHERS AND MILLS+

	Plate	Packed Tower	Fiber Bed	Spray	Venturi	Centri-fugal	Baffle	Self-Induced	Mech. Aided	Moving Bed	Total
% each type used	(1) 7	(0) 0	(0) 0	(0) 0	(0) 0	(11) 79	(0) 0	(1) 7	(0) 0	(1) 7	(14) 100
Low	-	-	-	-	-	8500	-	-	-	-	
Through-put, Avg.	(1) 30,000	-	-	-	-	(11) 43,000	-	(1) 16,100	-	(1) 4250	
(m^3/hr) High	-	-	-	-	-	110,000	-	-	-	-	
Low	-	-	-	-	-	-	-	-	-	-	
Effic-iency Avg.	-	-	-	-	-	(1) 99.9	-	(1) 95	-	(1) 98.7	
(%) High	-	-	-	-	-	-	-	-	-	-	

Notes: Numbers in parentheses refer to number of scrubbers analysed to obtain data entry.

Low and High values are lowest and highest values found in the scrubber survey.

+Includes:

Ore crushing
Stone crushing
Phosphate rock crushing

TABLE 7.3-4

SCRUBBERS USED TO CONTROL PARTICULATE EMISSIONS FROM DRIERS+

		Plate	Packed Tower	Fiber Bed	Spray	Venturi	Centri-fugal	Baffle	Self-Induced	Mech. Aided	Moving Bed	Total
% each type used		(7) 9	(0) 0	(0) 0	(4) 5	(19) 25	(30) 40	(1) 1	(0) 0	(1) 1	(14) 19	(75) 100
Through-put,	Low	71,500	-	-	21,800	37,400	8500	-	-	-	4250	
	Avg.	(7) 202,000	-	-	(4) 32,000	(13) 150,000	(29) 54,100	(1) 102,000	-	(1) 17,000	(14) 37,100	
(m^3/hr)	High	340,000	-	-	42,500	344,000	119,000	-	-	-	100,000	
Effic-iency	Low	-	-	-	85	91	81	-	-	-	89.7	
	Avg.	-	-	-	(3) 94	(8) 97.8	(17) 97.4	-	-	(1) 99	(12) 96.5	
(%)	High	-	-	-	99	99.7	99.7	-	-	-	98.8	

Notes: Numbers in parentheses refer to number of scrubbers analysed to obtain data entry.

Low and High values are lowest and highest values found in the scrubber survey.

+Includes:
Fluidized Bed Driers
Rotary Driers
Spray Driers

7.3.1.5 Gases

A wide range of polluting gases can be captured through the application of a suitable scrubber. The data presented in Table 7.3-5 reflect the application of scrubbers to the fifteen gases noted on that table.

Almost half of all gas scrubbers are packed towers. Better than a quarter are spray towers. The remaining applications involve every other type of scrubber listed, except for baffle type scrubbers. Packed towers are shown to be capable of high efficiencies. For very large gas flow rates, spray towers and venturi scrubbers have been used.

7.3.1.6 Liquid Mists

Data on scrubbers used to capture liquid mists come from the acid manufacturing and electroplating industries. These data are given on Table 7.3-6.

Packed towers are most frequently used to control liquid mist emissions. They are also apparently the most effective at so doing. Fiber beds and sprays are used for larger installations, and perform with somewhat inferior efficiency.

7.3.1.7 Smelting

Pyrometallurgical processes supply the data which are presented in Table 7.3-7.

The venturi scrubber is by far the most popular type for the control of pyrometallurgical emissions. It is applied to both very small and very large installations. Efficiency is variable, but has reached high values.

Spray scrubbers have been applied, but are decidedly inferior to other types of scrubber in efficiency in this application. Moving bed scrubbers have displayed good efficiency.

TABLE 7.3-5

SCRUBBERS USED TO CONTROL GASES+

		Plate	Packed Tower	Fiber Bed	Spray	Venturi	Centrifugal	Baffle	Self-Induced	Mech. Aided	Moving Bed	Total
% each type used		(3) 4	(33) 46	(2) 3	(18) 30	(10) 14	(1) 1	(0) 0	(1) 1	(2) 3	(1) 1	(71) 102
Throughput, (m^3/hr)	Low	2230	17	4250	42	142	-	-	-	-	-	
	Avg.	(3) 31,400	(32) 8600	(2) 87,000	(17) 34,500	(9) 36,600	(1) 42,500	-	(1) 6800	(1) 1450	(1) 1340	
	High	48,000	51,000	170,000	170,000	170,000	-	-	-	-	-	
Efficiency (%)	Low	71	70	92	89	70	-	-	-	57	-	
	Avg.	(3) 87	(26) 94.6	(2) 94.3	(12) 93.7	(8) 90	(1) 99.8	-	(1) 36	(2) 73	(1) 82	
	High	96.7	99.9	96.7	99.8	99.7	-	-	-	90	-	

Notes: Numbers in parentheses refer to number of scrubbers analysed to obtain data entry.

Low and High values are lowest and highest values found in the scrubber survey.

+Includes:

H_2O
Acrylic monomers
Formaldehyde
HF
N_2O_4
HCl
odors
H_2S
NH_4OH
NH_3
Cl_2
SiF_4
SO_x
Cl_2
I_2

TABLE 7.3-6

SCRUBBERS USED TO CONTROL LIQUID MISTS⁺

		Plate	Packed Tower	Fiber Bed	Spray	Venturi	Centrifugal	Baffle	Self-Induced	Mech. Aided	Moving Bed	Total
% each type used		(0) 0	(11) 65	(3) 18	(3) 18	(0) 0	(0) 0	(0) 0	(0) 0	(0) 0	(0) 0	(17) 101
Throughput, (m^3/hr)	Low	-	2040	3400	25,200	-	-	-	-	-	-	
	Avg.	-	(10) 35,600	(3) 54,200	(3) 45,000	-	-	-	-	-	-	
	High	-	85,000	156,000	85,000	-	-	-	-	-	-	
Efficiency (%)	Low	-	50	78	51	-	-	-	-	-	-	
	Avg.	-	(8) 86.6	(3) 83.3	(2) 70	-	-	-	-	-	-	
	High	-	99.3	88	90	-	-	-	-	-	-	

Notes: Numbers in parentheses refer to number of scrubbers analysed to obtain data entry.

Low and High values are lowest and highest values found in the scrubber survey.

⁺Includes:
Chromic acid
Sulfuric acid
Nitric acid
Hydrochloric acid

TABLE 7.3-7

SCRUBBERS USED TO CONTROL PARTICULATE EMISSIONS FROM SMELTING OPERATIONS+

		Plate	Packed Tower	Fiber Bed	Spray	Venturi	Centri-fugal	Baffle	Self-Induced	Mech. Aided	Moving Bed	Total
% each type used		(3) 4	(1) 1	(0) 0	(8) 11	(54) 76	(0) 0	(0) 0	(0) 0	(1) 1	(4) 6	(71) 99
Through-put,	Low	52,400	-	-	68	500	-	-	-	-	34,000	
	Avg.	(2) 98,000	(1) 8150	-	(3) 20,400	(51) 73,700	-	-	-	(1) 8500	(4) 54,500	
(m^3/hr)	High	143,000	-	-	41,300	400,000	-	-	-	-	85,000	
Effic-iency	Low	91	-	-	68	72.5	-	-	-	-	95	
	Avg.	(2) 93	-	-	(2) 83	(41) 95.5	-	-	-	(1) 95	(3) 98.7	
(%)	High	95	-	-	97.5	99.7	-	-	-	-	99	

Notes: Numbers in parentheses refer to number of scrubbers analysed to obtain data entry.

Low and High values are lowest and highest values found in the scrubber survey.

+Includes:
- Blast Furnaces
- Steel Furnaces
- Iron Foundries
- Ferroalloy Furnaces
- Copper Smelting
- Aluminum Smelting
- Nonferrous Reclaimation Smelting

7.3.2 PROCESSES TO WHICH EACH TYPE OF SCRUBBER IS APPLIED

Ten types of scrubbers are used. They differ in layout, efficiency and performance. Their distinguishing layouts are discussed in Chapter 3, while efficiency and performance are described in Chapter 5.

Scrubbers are frequently applied to the seven unit processes discussed in the preceeding section. This section points out those processes to which each type of scrubber is applied, the relative number of scrubbers used in each process, and the overall popularity of each type of scrubber.

The processes to which each type of scrubber is applied are given in Table 7.3-8. The data were taken from the survey of scrubber users performed in conjunction with this study, and described in Section 7.2.

Plate type scrubbers are most frequently applied to drying processes, although they are also applied to combustion and smelting processes, and for pollutant gas removal.

Packed bed scrubbers are used almost exclusively for collecting pollutant gases, and the collection of liquid mists.

Fiber bed scrubbers, like packed towers, are used to capture pollutant gases and liquid mists.

Spray chambers are used to capture gases. They are also applied to smelting operations (wet caps) and very occasionally to calcining, combustion, drying processes, and for the collection of liquid mists.

Venturi scrubbers are used most frequently on smelting operations. They are also used on calcining and drying processes, and occasionally for pollutant gas collection and for control of combustion processes.

Most centrifugal scrubbers are applied to driers. Some are applied to crushers. Centrifugal scrubbers are seldom used to control processes other than these.

Baffle scrubbers are almost never used. The only application uncovered in the users survey was to a drying process.

Self-induced spray scrubbers are applied to calcining, combustion and crushing processes, and for pollutant gas collection.

Few applications of mechanically aided scrubbers were uncovered in the users survey. Those applications noted were to drying and smelting processes, and for pollutant gas removal.

TABLE **7.3-8**

PROCESSES TO WHICH EACH TYPE OF SCRUBBER IS APPLIED⁺

	Plate	Packed Bed	Fiber Bed	Spray	Venturi	Centri-Fugal	Baffle	Self-Induced	Mech. Aided	Moving Bed
Calcining	(1) 6	(1) 2	(0) -	(5) 13	(23) 21	(0) -	(0) -	(3) 43	(0) -	(0) -
Combustion	(3) 17	(0) -	(0) -	(2) 5	(2) 2	(1) 2	(0) -	(2) 29	(0) -	(2) 9
Crushing	(1) 6	(0) -	(0) -	(0) -	(0) -	(11) 26	(0) -	(1) 14	(0) -	(1) 5
Drying	(7) 39	(0) -	(0) -	(4) 10	(19) 18	(30) 70	(1) 100	(0) -	(1) 25	(14) 64
Gases	(3) 17	(33) 72	(2) 40	(18) 45	(10) 9	(1) 2	(0) -	(1) 14	(2) 50	(1) 5
Liquid Mists	(0) 0	(11) 24	(3) 60	(3) 7	(0) -	(0) -	(0) -	(0) -	(0) -	(0) -
Smelting	(3) 17	(1) 2	(0) -	(8) 20	(54) 50	(0) -	(0) -	(0) -	(1) 25	(4) 18

⁺ Read vertically. Example: 39% of all plate type scrubbers are applied to controlling drying processes.

Numbers in parentheses refer to number of scrubbers reporting the information to the scrubber study.

Moving bed scrubbers are applied most frequently to drying processes. They are also used to control smelting and combustion processes, and for the control of crushers and polluting gases.

7.3.3 SALES OF SCRUBBERS COMPARED WITH OTHER EQUIPMENT

Other types of control equipment than scrubbers are often used on the processes which have been discussed in the preceeding sections. Table 7.3-9 lists the sales in 1967 of all types of air pollution control equipment. This table is adapted from "Industrial Gas Cleaning Equipment Shipments and End Use - 1967", prepared by the U. S. Department of Commerce, Washington, D. C. 20230 (10¢). The figures given are for uninstalled equipment.

TABLE 7.3-9

INDUSTRIAL GAS CLEANING EQUIPMENT - MANUFACTURER'S SHIPMENTS BY INDUSTRY, 1967

(Purchase Price in Thousands of Dollars)

Industry	Total Shipments	Adsorbers & Incinerators	Electrost. Precip.	Fabric Filters	Mech. (Cyclone) Collec.	Scrubbers	
						Gases	Particles
Iron & Steel	24,317	(2)	5,783	4,536	2,300	4,275	7,423
Utilities	18,481	(1)	15,506	(1)	2,476	(1)	(1)
Chemicals	15,870	1,001	1,207	5,344	3,130	1,479	3,704
Rock Products	8,966	(1)	2,760	3,602	1,038	(1)	1,142
Pulp & Paper	6,753	(1)	(1)	122	802	193	989
Mining & Metallurgical	6,160	(1)	(1)	1,855	389	394	825
Refinery	4,098	282	(1)	(1)	(1)	(1)	(1)
All Clear(4)	20,206	2,137	687	4,959	8,408	114	3,901
Exports	5,744	79	(1)	1,081	(1)	72	651
Totals	110,595	3,976	36,509	21,730	22,381	6,770	19,229

Notes:
(1) Not published to avoid disclosure.
(2) Gas incinerators and absorbers purchased by iron & steel companies are included in "all others" category to avoid disclosure.
(3) "Rock Products" includes cement & asbestos.
(4) "ALL other" includes shipments to distributors where end use cannot be identified.

CHAPTER 8

SYSTEM ANALYSIS, COSTS, AND OPTIMIZATION

TABLE OF CONTENTS

8.1 Introduction 8-2

8.2 Design Analysis 8-3
  8.2.1 Effect of Particle Size Distribution on Performance . 8-3
  8.2.2 Effect of Particle Inlet Concentration 8-5
  8.2.3 Design for Integrated Particle Penetration, $\overline{Pt}$ . . . 8-7
    8.2.3.1 Sieve Plate 8-7
    8.2.3.2 Packed Column 8-7
    8.2.3.3 Counter-Flow Spray Chamber 8-8
    8.2.3.4 Venturi Scrubber 8-8
    8.2.3.5 Centrifugal Scrubber 8-9
    8.2.3.6 Secondary-flow Baffle Collector 8-9

8.3 Scrubber Cost Estimation Methods 8-15
  8.3.1 Cost Components 8-15
    8.3.1.1 Initial Costs 8-15
    8.3.1.2 Annual Costs 8-16
    8.3.1.3 Annualized Cost 8-18
    8.3.1.4 Other Costs 8-19
  8.3.2 Purchase Cost Estimation 8-19
    8.3.2.1 Tanks and Towers 8-19
    8.3.2.2 Plate and Packed Column 8-25

8.4 Cost Analysis 8-32
  8.4.1 Introduction 8-32
  8.4.2 Scrubber System Costs According to Stairmand(1965) . 8-32
  8.4.3 Scrubber Purchase Cost - Literature Values 8-34
  8.4.4 Installed Cost of Scrubbers - Survey Results 8-35

8.5 Optimization 8-41
  8.5.1 Introduction 8-41
  8.5.2 Performance Optimization 8-42
    8.5.2.1 Venturi Scrubber 8-42
    8.5.2.2 Cyclone 8-43
    8.5.2.3 Scrubbers in Series and Parallel 8-45

CHAPTER 8

SYSTEM ANALYSIS, COSTS, AND OPTIMIZATION

8.1 INTRODUCTION

In this chapter we change from the close focus on the scrubber and the microscopic processes within it, as exemplified by Chapters 4 and 5, and look broadly at the scrubber system. Since the ultimate test of the system is its ability to perform satisfactorily within cost limitations or at optimum cost, economic data and methods must be introduced.

Also, other factors besides performance will have an influence on the design of a scrubber system. Some of these factors are the size distribution of the particles to be collected (if the scrubber is to be used for particle collection), capital costs, and operating costs of the system. Sometimes the performance of a scrubber system can be optimized from the standpoint of performance or cost through following a suitable optimization procedure.

Section 8.2 shows the influence of particle size distribution on scrubber performance. The equations in Chapter five can be used to predict the collection efficiency of a scrubber on particles of a single, given size. Section 8.2 covers the application of these equations to typical industrial dusts with a range of particle sizes. The way to design a scrubber for achieving a required efficiency on dusts with a size distribution is discussed.

The intelligent evaluation of alternative means of pollution control by scrubbers will involve an economic analysis of the costs which the various alternatives present. Section 8.3 describes the various elements which go into determining what scrubber initial and operating costs will be. Various means of predicting scrubber purchase costs are presented and described, and are compared in several examples.

Information is available in the literature and from the users survey conducted in conjunction with the present study, on the costs of installing and operating most of the kinds of scrubbers identified and discussed in this handbook. This information is presented in Section 8.4.

The optimization of mathematical models is a useful technique for improving the performance of a scrubber system. This topic is discussed in Section 8.5. It may be possible to improve the performance of an existing system through the optimization of performance as controlled by operating parameters. Or, costs of a new or existing installation can be minimized while keeping performance at a fixed level through a suitable optimization procedure. Section 8.5 also discusses the operating characteristics of collection devices operated in series or in parallel.

8.2 DESIGN ANALYSIS

8.2.1 EFFECT OF PARTICLE SIZE DISTRIBUTION ON PERFORMANCE

When dust is produced by a comminution process (milling, grinding, crushing), the particle size distribution is probably log normal. The number and weight size distribution data for most industrial particulate emissions follow the log normal law. Hence, the two well established parameters of the log normal law adequately describe the size distributions of particulate matter. They are the geometric mean weight diameter "d_{pg}" and the geometric standard deviation "σ_g".

Frequently, one uses the geometric mean weight diameter "d_{pg}" to design control equipment for the required efficiency on a given incoming particle load of stated log normal size distribution. It has been commonly assumed that the average penetration, $P\underline{t}_a$, calculated based upon "d_{pg}" is close to the integrated penetration, $\overline{Pt}$, obtained taking into account the size distribution. This can give quite misleading results. In the following we show the relation between the integrated penetration and the average penetration.

The log-normal particle distribution density is:

$$\frac{1}{w_c}\frac{dw}{d(\ln d_p)} = f(d_p) = \frac{1}{\sqrt{2\pi}\ \ln \sigma_g}\exp\left[-\left(\frac{\ln d_p - \ln d_g}{\sqrt{2}\ \ln \sigma_g}\right)^2\right] \qquad (8.2\text{-}1)$$

where, σ_g = mass geometric standard deviation of dust

d_{pg} = mass geometric mean particle diameter

$f(d_p)$ = size frequency

w_c = total weight of particle sample

dw = particle weight corresponding to the interval $d(\ln d_p)$ of particle sizes.

In the practical analysis of particle size data, logarithmic probability paper is often used to plot the percent of particles less or greater than a stated size vs. the logarithm of the stated size. A log normal size distribution will then plot as a straight line. The 50% value of "d_p" is "d_{pg}" and:

$$\sigma_g = \frac{84.3\%\text{ value of } d_p}{50\%\text{ value of } d_p} \qquad (8.2\text{-}2)$$

We have shown that penetration for many types of inertial collection equipment can be expressed, neglecting the contribution of Cunningham correction, as:

$$Pt = \exp\ (-A\ d_p{}^B) \qquad (8.2\text{-}3)$$

Packed towers, centrifugal scrubbers, and sieve plate columns follow the above relationship. For the packed tower and sieve plate column "B" has a value of 2. For centrifugal scrubbers "B" is about 0.67. Venturi scrubbers also follow the above relationship with $B \cong 2$ when the throat inertia parameter is between 1 and 10.

The overall (integrated) penetration, $\overline{Pt}$, of any device on a dust of any type of size distribution will be:

$$\overline{Pt} = \frac{1}{W_c} \int_0^W Pt\ dw \qquad (8.2\text{-}4)$$

The right-hand side of the above equation is the integral of the product of each weight fraction of dust times the penetration on that fraction.

If Equations 8.2-1 and 8.2-3 hold for the particle size distribution and penetration, respectively,

$$\overline{Pt} = \frac{1}{W_c} \int_0^W Pt\ dw = \int_{-\infty}^{+\infty} Pt\ f(d_p)\ d(\ln d_p) \qquad (8.2\text{-}5)$$

Therefore,

$$\overline{Pt} = \int_{\ln(d_p)=-\infty}^{\ln(d_p)=\infty} \frac{1}{(\sqrt{2\pi})\ \ln \sigma_g} \exp\left[-\left(\frac{\ln d_p - \ln d_{pg}}{\sqrt{2}\ \ln \sigma_g}\right)^2 - A\ d_p^{\,B}\right] d(\ln d_p) \qquad (8.2\text{-}6)$$

For convenience we will use the following transformations. Let:

$$z = \frac{\ln d_p - \ln d_{pg}}{\sqrt{2}\ \ln \sigma_g} \qquad (8.2\text{-}7)$$

$$dz = \frac{1}{\sqrt{2}\ \ln \sigma_g}\ d(\ln d_p) \qquad (8.2\text{-}8)$$

Equation 8.2-6, in terms of "z" and "dz", will become

$$\overline{Pt} = \frac{1}{\sqrt{\pi}} \int_{-\infty}^{+\infty} \exp\left[-z^2 - A\ d_{pg}^{\ B} \exp\left(B\ z\ \sqrt{2}\ \ln \sigma_g\right)\right] dz \qquad (8.2\text{-}9)$$

Note that the $-A\ d_{pg}^{\ B}$ term in equation 8.2-9 is equivalent to $\ln(Pt_a)$ as can be seen through equation 8.2-3, where Pt_a is penetration of particles of the mass mean size, d_{pg}.

Equation 8.2-9 was integrated on a digital computer from $z = +3.5\sqrt{2}\ (\sigma_g)$ to $z = +3.5\sqrt{2}\ (\sigma_g)$. The results are given in Figure 8.2-1, relating "$\overline{Pt}$" with "Pt_a" and "σ_g" for $B = 2$. The difference between the mean particle penetration, Pt_a, and the integrated penetration, $\overline{Pt}$, increases as the standard deviation of the incoming dust increases. It is important to note that standard deviations greater than $\sigma_g = 2.5$ require an inertial scrubber to have greater than 99.9% efficiency on the average particle size, "d_{pg}" in order to have an overall efficiency greater than 90%. As can be seen in Table 8.2-1, particulate emissions from various industries can have widely varying standard deviations, but most are above $\sigma_g = 3$.

A more general relationship results when B is not set equal to 2, but is allowed to take on any value. An explanation of this case follows. Particle size "d_p" is called "d_{p50}" when its penetration is 50%. Then Equation 8.2-3 can be written as follows:

$$\ln(2) = A\, d_{p50}^{\,B} \qquad (8.2\text{-}10)$$

Combining the above equation with Equation 8.2-9 results in the following equation:

$$\overline{Pt} = \frac{1}{\sqrt{\pi}} \int_{-\infty}^{+\infty} \exp\left[-z^2 - \ln(2)\left(\frac{d_{pg}}{d_{p50}}\right)^B \exp\left(\sqrt{2}\, z\, B \ln(\sigma_g)\right)\right] dz \qquad (8.2\text{-}11)$$

Figure 8.2-4 is a plot of "$\overline{Pt}$" vs. $(d_{p50}/d_{pg})^B$ with $B \ln(\sigma_g)$ as a parameter. For a required "$\overline{Pt}$" one can find the value of d_{p50} when "d_{pg}", "σ_g", and "B" are given.

8.2.2 EFFECT OF PARTICLE INLET CONCENTRATION

Some of the effects, dependent upon the inlet dust concentration, that are likely to occur in a scrubber are as follows:

1. Turbulent agglomeration of small particles into large ones will aid collection efficiency, as the large agglomerates are more easily collected than the smaller individual particles. Turbulent agglomeration is discussed in Section 4.3 from the theoretical viewpoint. Even the most optimistic viewpoint suggests negligible magnitude of agglomeration in a conventional scrubber and common inlet dust concentrations.

2. Polydispersity of dust may allow one particle to catch another as they move towards the main collecting surface at a particle size dependent velocity. The magnitude of this interaction will depend upon the collection mechanism. This effect has not been investigated and its efficiency is not known.

3. Coating of the collecting surface at heavy dust loading may also alter the collection efficiency. Little theoretical or experimental knowledge is available in this area.

Available useful experimental results pinpointing the effect of particle loading are meager. Harris (1964) shows that as the inlet loading increases, the collection efficiency of an ejector venturi decreases at a given energy input in terms of hp/1000 CFM. The inlet loading ranged from 0.91 g/m³ to 6.9 g/m³. In a cyclone, on the other hand, it is found that the collection efficiency increases with increasing dust load as discussed in Section 5.3-7. It may be that this is due to the particle interaction mentioned above in point 2.

TABLE 8.2-1

PARTICLE SIZE DISTRIBUTIONS

Dust Source	Average Particle Diameter d_{pg} in microns	Standard Deviation σ_g
Coal Drier		
Fluid Bed	200	4.45
Multilouver Drier	28	4.24
Flash Drier	3	4.41
Cascade Drier	28	4.24
Stone Crushing		
Jaw Crushing	200	10
Conveying	10	3.33
Lime Manufacture		
Rotary Kiln	40	11.4
Coal Burning		
Cyclone Furnace	6.4	3.46
Pulv. Coal, vertical corner, frontwall horizontal or horizontally opposed	18	
Pulv. Coal, unspecified	12.5	3.47
Spreader Stoker	58	4.14
Underfeed Stoker	100	4.76
Steel Making		
O.H. composite for heat	6.0	3.53
O.H. Lime Boil only	2.5	3.13
B.O.F.	0.095	2.31
Gray Iron Foundry		
Cupola	100	14.3
Ferroalloy Manufacture		
Blast Furnace	0.45	4.5
Electric Furnace (open)	0.3	3

Note: Data for the particle size distribution were taken from the Midwest Research Institute's report (1970). Their data were plotted on a log probabability graph paper to obtain d_{pg} and σ_g.

Calvert et al. (1971) have evaluated a number of scrubbers at dust loading of about 0.05 g/m^3. The dust loading varied somewhat with all the other conditions remaining constant. They did not specifically intend to evaluate the effect of inlet dust loading. The results of their study indicate an increase in efficiency with increasing dust loading to the scrubber. However, the magnitude of this effect is within the bounds of sampling error.

Ekman and Johnstone (1951) carried out an efficiency study of a venturi scrubber. They varied the inlet loading up to 0.034 g/m^3 for 1.0 micron diameter monodisperse particles of dioctylphthalate. There are no comparative runs at the same operating conditions where only the inlet loading varied and it is difficult to extract the explicit effect of inlet loading. However, Ekman and Johnstone concluded that under the same conditions efficiency increased as the inlet dust loading increased.

8.2.3 DESIGN OF EQUIPMENT FOR DUST WITH LOG-NORMAL SIZE DISTRIBUTION

In section 5.3, equations are presented for predicting scrubber collection efficiency on particles of a single diameter, d_p, as a function of collector geometry and operating variables such as liquid to gas ratio or pressure drop. In this section, the equations from section 5.3 for various scrubbers will be combined with the analysis of section 8.2.1 to obtain collection efficiency on particles with a log-normal size distribution, again as a function of collector geometry and operating variables.

8.2.3.1 Sieve Plate

Section 5.3.2 shows that for a sieve plate, inertial collection efficiency is given by an equation analogous to Equation 8.2.3, with B equal to 2. Therefore, Figure 8.2.4 can be used to determine the collector's required cut diameter, d_{p50}, as a function of overall penetration, "$\overline{Pt}$", dust mass mean diameter, "d_{pg}", and standard deviation, "σ_g". From Figure 5.3.2-2 one can determine the sieve plate's aerodynamic cut diameter, d_{pa50}, as a function of hole size and air velocity. Aerodynamic cut size can be converted to cut size, d_{p50} from Figure 5.6.7-6 if particle density is known.

The above treatment is for a single plate. When more than one plate is used, the size distribution at the exit of the first plate is not log normal, and the above analysis cannot be used.

8.2.3.2 Packed Column

The design or evaluation of an existing design for a packed column can be approached in a manner that is similar to that for a sieve plate column described in Section 8.2.3.1. Equation 5.3.3-4 gives the relationship between the system variables and the packed bed penetration. Neglecting the influence of the Cunningham factor, C', this equation has the same dependence on "d_p" as Equation 8.2-3 with B = 2. Hence, Figure 8.2-4 can be used in conjunction with Figure 5.3.3-2 (a) and (b) for the design. Figures 5.3.3-2 (a) and (b) are plots of "d_{pa50}" vs. packing height with gas velocity as a parameter at various packing diameters.

8.2.3.3 Counter-Flow Spray Chamber

Equation 5.3.5-13 is the design equation for a counter-flow spray chamber. Figures 5.3.5-2 (a), (b), (c), and (d) are plots of predicted counter-flow spray chamber performance, "d_{pa50}" vs. the chamber height with preformed drop diameter as parameter at various gas velocities and liquid to gas volumetric ratios. (d_{p50}/d_{pg}) cannot be related to "$\overline{Pt}$" in a simple manner as was done for equipment behaving according to Equation 8.2-3. One should integrate for penetration over the particle size range as illustrated in Chapter 9 examples.

8.2.3.4 Venturi Scrubber

Equation 5.3.6-5 describes collection monodisperse particles by monodisperse drops in a venturi scrubber. This, however, is not a real situation as there normally exists a particle size distribution and a drop size distribution.

Similar to our approach in 8.2.3.1, effect of particle size distribution can be accounted for if a plot of "$\overline{Pt}$" vs. (d_{p50}/d_{pg}) is prepared for this case with equation 5.3.6-5 describing the collection efficiency for the monodisperse situation.

Equation 5.3.6-5 and Equation 8.2-1 can be combined to yield the following result.

$$\overline{Pt} = \int_{-\infty}^{+\infty} \frac{1}{\sqrt{\pi}} \exp\left[-z^2 + \frac{(\ln 0.5)\ X^2}{b} \times \left\{ \frac{-0.7 - Y\,b + 1.4\,\ln\left(\frac{Y\,b + 0.7}{0.7}\right) + \frac{0.49}{0.7 + Y\,b}}{-0.7 - Y\,X^2 + 1.4\,\ln\left(\frac{Y\,X^2 + 0.7}{0.7}\right) + \frac{0.49}{0.7 + Y\,X^2}} \right\} \right] dz \qquad (8.2\text{-}12)$$

where $X = \dfrac{d_{p50}}{d_{pg}}$

$Y = f\ K_{pt}$

K_{pt} = impaction parameter for d_{pg} at the throat velocity

$b = \exp\ [2\ \sqrt{2}\ z\ \ln \sigma_g]$

z = is defined in Equation 8.2-7

Figures 8.2-5, 8.2-6 and 8.2-7 are plots of "$\overline{Pt}$" vs. (d_{p50}/d_{pg}) with "$f\ K_{pt}$" as parameter for various "σ_g" values. These plots are exact solutions of Equation 5.3.6-5, accounting for log normal particle size distribution as given by Equation 8.2-1. These along with "d_{pa50}" curves in Figure 5.3.6-13 allow venturi scrubber design for a required "$\overline{Pt}$" by a trial and error method, or evaluation of an existing design for given operating conditions. Note that "d_{pa50}" can be converted to "d_{p50}" and vice versa through Figure 4.6.7-6. This approach is illustrated in Section 9.3.4.

8.2.3.5 Centrifugal Scrubber

Cyclone performance equation is of Equation 8.2-3 type. Hence, the design approach given in Section 8.2.1 is applicable here also, to account for the particle size distribution.

Figure 8.2-4 which relates "$\overline{Pt}$" to $(d_{p50}/d_{pg})^B$ with $B \ln \sigma_g$ as a parameter can be used to determine the integrated penetration if cut size, d_{p50}, and B are known. For centrifugal devices:

$$B = \frac{1}{n + 1} \tag{8.2-13}$$

where n is given by equation 5.3.7-8. This value for B comes from equation 5.3.7-3. Figures 5.3.7-7 (a), (b), (c), and (d) are plots of predicted cyclone performance, (Equation 5.3.7-2) for "d_{pa50}" vs. "C" with "u", inlet gas velocity, as parameter, at various cyclone diameters. "C" is the cyclone geometry group and is defined by Equation 5.3.7-3.

8.2.3.6 Secondary-flow Baffle Collector

Equation 5.3.8-4 describes collection of particles by inertial mechanism in a baffle device. Figures 5.3.8-9 (a), (b), (c), and (d) are based on this equation and are plots of "d_{pa50}" vs. the number of baffles with the gas velocity as parameter at various "α" and "h" values. On two of the figures concurrent pressure drop curves are also given.

Equation 5.3.8-4 for "d_{pa50}" becomes:

$$A = \frac{1 - (0.5)^{1/n}}{\left[d_{p50}\right]^2} \tag{8.2-14}$$

Here, n is the number of baffles in series. Combining Equation 8.2-14 with Equation 8.2-5 and using the "z" transformation per Equation 8.2-7 gives:

$$\overline{Pt} = \frac{1}{\sqrt{\pi}} \int_{-\infty}^{+\infty} \exp(-z^2)\left[1 - \left(\left[1 - (0.5)^{1/n}\right]\left[\frac{d_{pg}}{d_{p50}}\right]^2 \exp(2\sqrt{2}\, z \ln \sigma_g)\right)\right]^n dz \tag{8.2-15}$$

Figure 8.2-8 is a plot of "$\overline{Pt}$" vs. (d_{p50}/d_{pg}) with "σ_g" as a parameter.

It was noticed that the curves remain practically the same for the values of "n" greater than 10. At lower values of "n" divergence increases as "n" goes to smaller values. This plot along with the use of Figure 5.3.8-9 permits the design of a secondary flow baffle device.

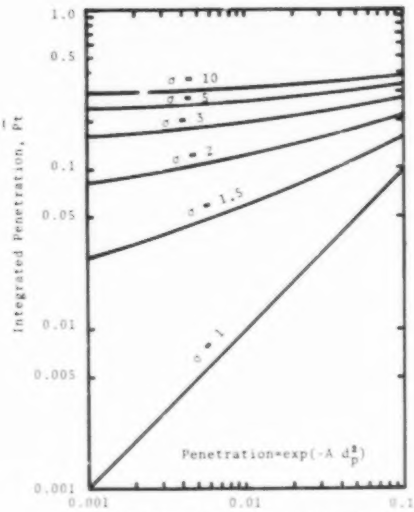

FIGURE 8.2-1

RELATIONSHIP BETWEEN THE PENETRATION BASED ON MEAN PARTICLE SIZE AND THE INTEGRATED PENETRATION

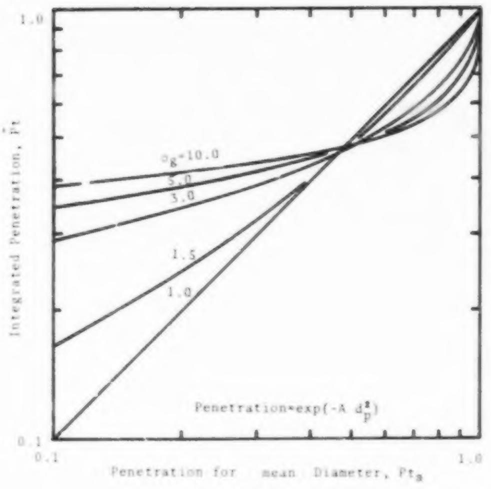

FIGURE 8.2-2

RELATIONSHIP BETWEEN THE PENETRATION BASED ON MEAN PARTICLE SIZE AND THE INTEGRATED PENETRATION.

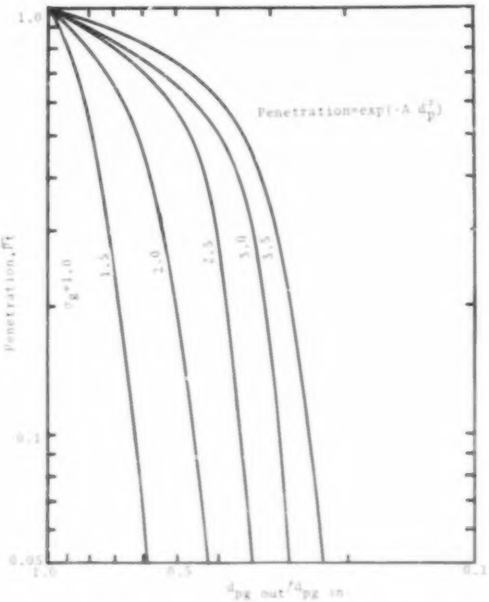

FIGURE 8.2-3

RELATIONSHIP BETWEEN AVERAGE PARTICLE SIZE ENTERING AND LEAVING A COLLECTION DEVICE.

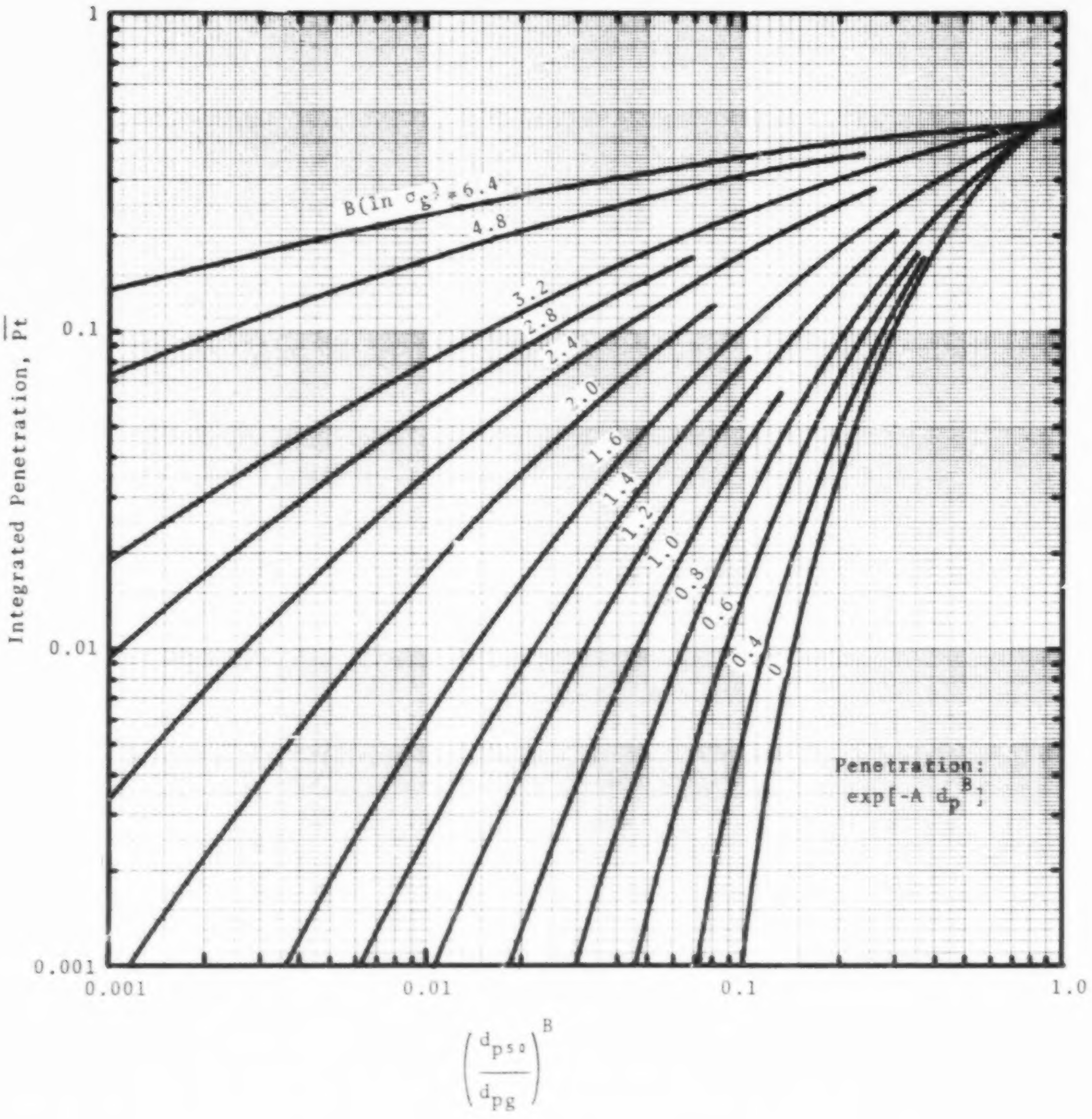

FIGURE 8.2-4

INTEGRATED PENETRATION, $\overline{Pt}$, VS. d_{p50}/d_{pg},

WITH $B(\ln \sigma_g)$ AS PARAMETER

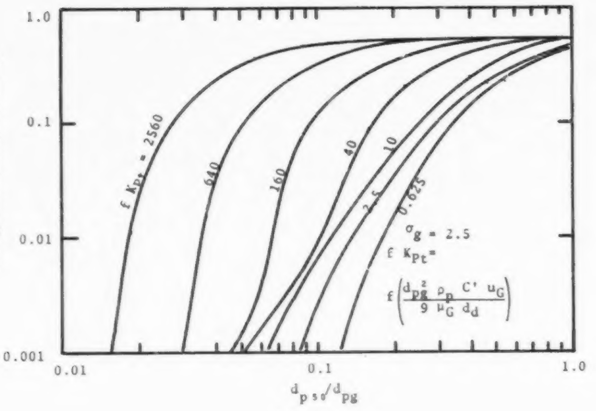

FIGURE 8.2- 5

VENTURI SCRUBBER INTEGRATED PENETRATION,
$\overline{Pt}$, VS. d_{p50}, WITH f K_{Pt} AS PARAMETER, σ_g = 2.5

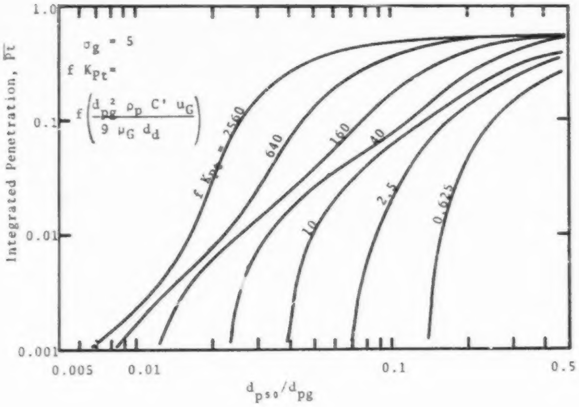

FIGURE 8.2- 6

VENTURI SCRUBBER INTEGRATED PENETRATION,
$\overline{Pt}$, VS. d_{p50}/d_{pg}, WITH f K_{Pt} AS PARAMETER, σ_g = 5.0

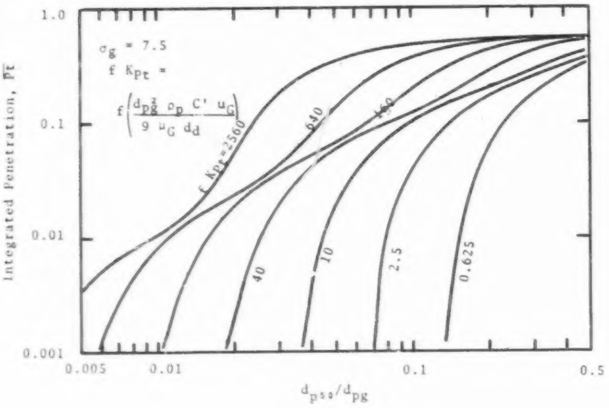

FIGURE 8.2- 7

VENTURI SCRUBBER INTEGRATED PENETRATION, $\overline{Pt}$
VS. d_{p50}/d_{pg}, WITH f K_{Pt} AS PARAMETER, σ_g = 7.5

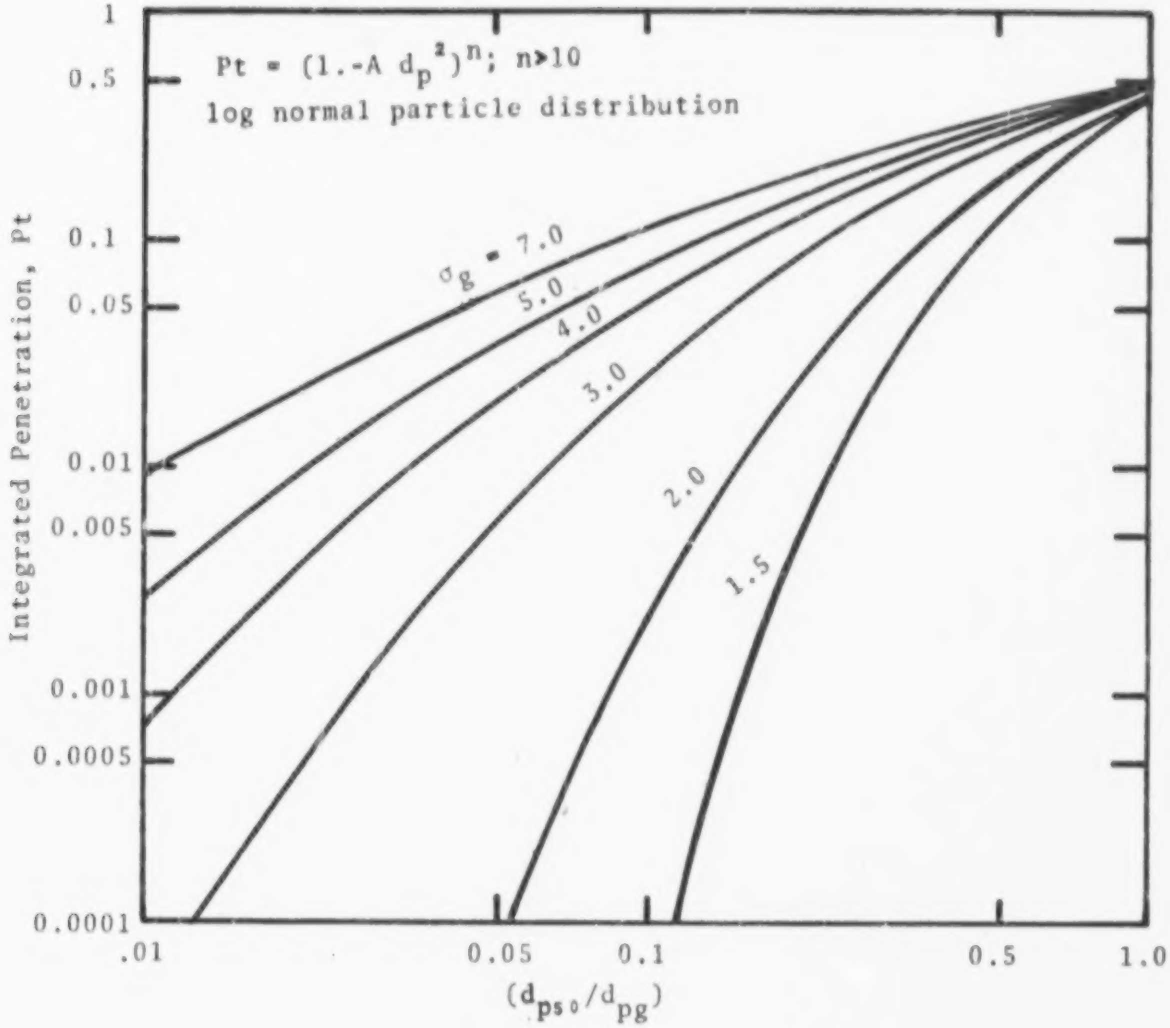

FIGURE 8.2-8

PREDICTED INTEGRATED PENETRATION VS. (d_{ps0}/d_{pg}) WITH "σ_g" AS PARAMETER FOR SECONDARY FLOW BAFFLES, EQUATION (8.2-15)

8.3 SCRUBBER COST ESTIMATION METHODS

Whether one of the wet scrubbers is the optimum gas cleaning method in a given pollution control situation depends upon a detailed cost analysis and the special emission conditions restricting the use of a particular type of control equipment. It is the purpose of this section to provide information on cost components involved in the building, installation and operation of control equipment. Techniques for estimating the costs of installing and operating control equipment are given.

8.3.1 COST COMPONENTS

The cost of installing and operating air pollution equipment is a function of many direct and indirect cost factors. These factors can be grouped into two cost categories -- initial costs and annual costs. It will become apparent that individual cost factors vary widely from one installation to another. For a given control problem it requires examining each contributing factor in turn to prepare a reasonable and useful cost estimate. Such estimates should be prepared for competitive control strategies to select the best option.

8.3.1.1 Initial Costs

The initial costs (or installed cost, or capital cost) includes the cost factors listed in Table 8.3-1.

TABLE 8.3-1

INITIAL COST FACTORS

- Planning and Design
- Scrubber Purchase Cost
    - F.O.B. Wet Scrubber
    - Freight
- Scrubber Auxiliaries*
    - Fan and Motor*
    - Ducting*
    - Liquor and solids handling and treatment*
    - Instrumentation*
- Scrubber Installation Costs
    - Site preparation, including foundations and supports
    - Modifications in existing process
    - Installation*
    - Start-up

The most definable cost component is the FOB cost of "flange-to-flange" control hardware. We have given the method of calculation and final purchase costs of various control devices based upon the size of the device and material of construction in Section 8.3.2. It is difficult to assign values to the other factors listed above, and still be general. Some of them (denoted by asterisk), however, may be grouped together, and their contribution to the initial costs expressed as a percentage of the FOB cost. The NAPCA Report AP-51 (1969) gives the percentages for wet scrubbers listed in Table 8.3-2. Table 8.3-3 gives the expected ranges for installation costs in industrial applications.

TABLE 8.3-2

INSTALLATION COST EXPRESSED AS A PERCENTAGE OF PURCHASE COST

Wet Scrubber Type	Cost Range, Percent			
	Low	Typical	High	Extremely High
Low, medium energy	50	100	200	400
High energy	100	200	400	500

The absence of accurate descriptions has resulted in terms such as low, medium, and high energy scrubbers. A high energy scrubber is commonly taken to be one having a pressure drop of greater than 25 mbar (≈10 in wg). This would result in higher fan and motor costs.

8.3.1.2 Annual Costs

Annual costs include the factors in Table 8.3-4.

TABLE 8.3-4

ANNUAL COST FACTORS

Operating Cost
  Utilities
  Labor
  Supplies and Materials
  Treatment and Disposal

Maintenance Cost
  Labor
  Materials

Plant Overhead
  Space, heat, lights, insurance, etc.

Annual operating cost depends upon the operating policy, which includes:

1. Gas - gas volume (and temperature, affecting the liquor lost), pressure drop across the system, the consumption and cost of electricity, the mechanical efficiency of the fan.

2. Liquor - the scrubbing liquid volume, pumping cost, liquor consumption cost, and effluent and recycle liquor treatment cost.

3. Operating time.

TABLE 8.3-3

EXPECTED COST RANGES FOR SCRUBBER INSTALLATION IN VARIOUS INDUSTRIAL APPLICATIONS*

Source	Cost Range	Remarks
Kraft mills Recovery furnace	Typical	In high collection efficiency installation, ESP followed by low-energy wet collector
Lime Kiln	High	High-energy wet scrubber
Integrated Iron & Steel B.O.F.	High to extreme high	Special duct work & hooding design, cooling & gas conditioning requirements
Electric furnace	High to extreme high	High temperature materials
Sintering	Typical to high	
Phosphate rock preparation kilns	Low to typical	
Phosphate fertilizer mfg. reactor	High	Corrosive gas
Curing building	High to extreme high	Extensive ventilation system, large gas volumes
Granulator	High	Corrosive gas
Sulfuric acid absorber	High to extreme high	Special materials for acid mists
Phosphoric acid absorber	High to extreme high	Special materials for acid mists
Gray Iron cupola	Typical	
Aluminum Ore Electrolytic cells	Typical to high	Corrosion problems; extensive ductwork
Asphalt Batch Dryer	Typical	
Incinerators	Typical to high	Usually installed on roof of building
Coal Thermal Dryers	Typical	

*Costs are for new plants, except open hearth furnaces.

The theoretical annual cost of operation and maintenance for wet collectors can be expressed as follows:

$$OC = Q_G \left[0.438\times10^{-3}\, HK \left(\frac{P}{15.8\ E} + \frac{g\ Q_L}{15.7\ F\ Q_G} + \frac{h\ Q_L}{162\ F\ Q_G}\right) + \frac{Q_L'}{Q_G} HL + M\right] \quad (8.3\text{-}1)$$

where:

OC = \$, annual cost of operation and maintenance

Q_G = design capacity of the wet collector, actual m^3/hr

H = annual operating time, hours (total possible is 8760)

K = power costs, dollars/kilowatt-hour

P = pressure drop across fan, mbar

Q_L/Q_G = liquor circulation, ℓ/m^3

g = liquor pressure at the collector, atm

h = physical height liquor is pumped in circulation system, m

Q_L'/Q_G = make-up liquor consumption, ℓ m^3/hr - (A m^3/hr)

L = liquor cost, dollars/m^3

M = maintenance cost, dollars/yr - (A m^3/hr)

E = fan efficiency, typically 60 percent

F = pump efficiency, typically 50 percent

The maintenance cost will depend upon the maintenance program carried out, with proper replacement of defective and worn parts. Estimates of maintenance and other costs in Equation 8.3-1 are given below in Table 8.3-5.

TABLE 8.3-5
OPERATING AND MAINTENANCE COST FACTORS

	Cost Range		
	Low	Typical	High
Maintenance, \$/m^3/hr	0.017	0.0235	0.0352
Electricity, \$/kwhr	0.005	0.011	0.020
Cost of Liquor in \$/m^3	0.027	0.0675	0.135
Makeup liquor rate, m^3/m^3	0.0375	0.0375	0.0375

8.3.1.3 Annualized Cost

Annualized cost of control is the summation of the annual costs (operating and maintenance), depreciation of the initial investment, and capital charges (taxes, interest, insurance). The initial investment might be amortized using straight-line depreciation over a period of 15 years, i.e. 6.6 percent per year. Capital charges might be equal to 6.6 percent of the initial costs. Therefore, typical depreciation plus capital charges might amount to 13.2 percent of the initial capital cost of the equipment. A typical annualized cost would be, therefore:

Annualized Cost (AC) = 0.132 (initial costs) + Annual Costs (8.3-2)

8.3.1.4 Other Costs

Along with the many individual cost factors mentioned, one must consider the space requirement imposed by the collector. To express it in terms of a dollar value, one needs to know the floor area requirement.

Control equipment space is defined as the enclosed space in cubic meters which the separator needs. Figure 8.3-1 below, shows the volume requirement of various dust separators in $m^3/1,000\ m^3$ of gas cleaned per hour as given by Engels (1970).

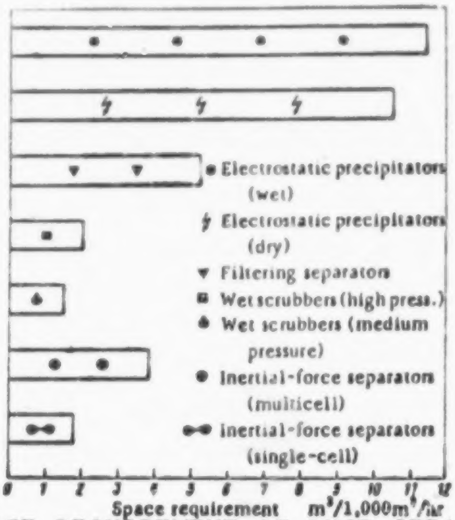

SPACE REQUIREMENT OF DUST SEPARATORS

FIGURE 8.3-1

8.3.2 PURCHASE COST ESTIMATION

Purchase cost is the most definable cost component. Yet one may find a range of prices and estimates in the literature for the same piece of equipment. In this section we present a detailed analysis of how one may estimate purchase cost from the cost of materials, labor and other basic information. Such an estimate provides a means to make an independent check on what should be a reasonable cost for a piece of equipment of a given size and capacity.

8.3.2.1 Tanks and Towers

The purchase cost of tanks and towers for the following dimensions, operating pressures and materials shall be estimated:

Diameter - 0.5 to 5 m (2 to 20 feet)

Height - 1 to 5 diameters

Pressure or Vacuum 150 cm (60") W.C.

Materials - carbon steel, 316 stainless steel, PVC, and fiberglass plastic

Thickness - 0.65 cm (0.25 inch)

We will discuss two different ways of estimating the purchase cost. The first method utilizes a relationship between fabrication cost per unit weight and vessel weight. Cost of nozzles, manhole, etc, is added to arrive at the total cost of the unit. The second method is a more detailed one which takes into account the time required for cutting, rolling, welding etc. to arrive at the fabrication cost.

Method I - Cost based on weight of tank or tower shell

In order to determine the weight of the scrubber shell it is necessary to know its thickness and other dimensions. Tank plate thickness must be sufficient to stand the extremes of pressure mentioned above. A method of tank design for either internal or external pressure is given below.

Design for Internal Pressure

With a given diameter and operating pressure, the minimum thickness due to internal pressure may be determined from the equation:

$$t = \frac{1.2\ P\ D}{30\ S\ E - 18\ P} + C \qquad (8.3.3a)$$

where
t = minimum thickness, cm
S = allowable maximum stress value, atm
E = joint or weld efficiency
C = corrosion allowance
D = diameter, cm
P = design pressure, atm.

In English units this becomes:

$$t = \frac{P\ D}{2\ S\ E - 1.2\ P} + C \qquad (8.3\text{-}3b)$$

where
t = minimum thickness, inches
S = allowable maximum stress value, psi
E = joint or welding efficiency
C = corrosion allowance
D = diameter, in.
P = design pressure, psi

A lower limit on design pressure is given by the constraint that the vessel must be capable of holding a full load of water without bursting. Such a case may happen when a piece of equipment fails or clogs causing the vessel to be filled up with water. It may be that process pressure exceeds this, but it is not usual for air pollution control equipment. Based on the maximum vessel height of 750 cm (25 ft), a pressure of 0.75 atm (10.82 psi) will be exerted by the water on the lower portion of the cylindrical vessel. The minimum thickness needed as calculated from Equation 8.3.3 would be 0.3 cm (.118 inches). This is within the chosen thickness of 0.65 cm (0.25 inches).

Other considerations of process pressure, wind loads, loads due to dead weight of the vessel, temperature and safety factors must be taken into account in the design.

Design for External Pressure (Vacuum)

Representative requirements for the vessel shell in this case calls for either a pressure or vacuum of 150 cm (60") water gauge. This is a fairly high pressure drop for a scrubber and will typify the majority of the cases. Adding a 50% safety allowance, a pressure (internal and external) of 0.22 atm (3.25 psi) will be used in all calculations.

Vacuum design, being more critical due to buckling and collapse, will be the controlling condition. A straightforward method of determining the allowable pressure for a given length, diameter and thickness may be found in Perry (1963) Figure 24-8, and is shown here as Figure 8.3-2.

To use the chart, enter the curve at the bottom with a value of L/D_o, move vertically to the D_o/t value, then horizontally to the material line for the design temperature, and then vertically to read the value of "B". The allowable pressure differential decreases as the diameter increases and as the L/D_o ratio increases.

$$B = P\frac{D_o}{t} \qquad (8.3.4)$$

L = Length, cm
D_o = outside diameter, cm
t = thickness, cm
P = allowable pressure differential, atm.

Example: The following are assumed:

T = 150°C (300°F) maximum
P = 0.22 atm (3.25 psi)
t = 0.65 cm (0.25 inch)
L/D_o = values from 5 to 1

Figure 8.3-2 shows that a column with a diameter of 60 to 120 cm (2 to 4 ft) would operate safely at 0.22 atm vacuum for all values of L/D_o (1 to 5). For vessels with a diameter of 150 cm (5 ft) and up, the allowable pressure differential would be safe only for the lower values of L/D_o.

Stiffeners

To enable one to maintain the designed external pressure, stiffeners may be added. This has the effect of decreasing L/D_O. To calculate the size needed and spacing, we have to choose the desired stiffener shape (angle, flange, channel or I-beam). The stiffeners chosen for the cost computations which follow were angles of equal sides. From the properties of the stiffener chosen, the following information may be obtained.

1. Size and thickness
2. Moment of inertia, I, cm^4 (in^4)
3. Cross-sectional area, As, cm^2 (in^2)
4. Weight per foot of section, Kg/m (lb/ft)

With the above values of "As" known, we assign a value of "L_s" equal to the spacing between the stiffeners, and calculate the "B" value from the equation:

$$B = \frac{P\ D_O}{t + (As/L_s)} \qquad (8.3\text{-}5)$$

where B = atm (psi)
P = allowable pressure differential, atm (psi)
D_C = diameter of shell, cm (in)
t = min. required thickness of shell, cm (in)

With the value of "B" and using Figure 8.3-2, move downward to the material line at the design temperature and then horizontally to read factor A.

The required moment of inertia, I_S, of the stiffener ring about its neutral axis parallel to the axis of the shell is approximately:

$$I_s = \frac{D_O^2\ L_s\ [(t + As/L_s)]\ A}{14}\ cm^4\ (in^4) \qquad (8.3\text{-}6)$$

After substitution of the various values into Equation 8.3-6, a value for "I_S" is obtained. Various stiffener sizes and spacings have to be tried until one identifies an arrangement which is practical, economical, and within the allowable pressure differential.

Once the size and spacing of the stiffeners have been established, the weight of the stiffener ring may be calculated. The weight divided by the spacing between stiffeners gives the stiffener weight per unit length of shell. Now the total shell weight per unit length of shell length can be calculated. The weights of the various components are calculated from the following formulas:

$$\text{Weight of Head} = \frac{\pi d^2}{4}\ t\ \rho_{material} \qquad (8.3\text{-}7)$$

$$\text{Weight of Shell/length of shell} = \pi d\ t\ \rho_{material} \qquad (8.3\text{-}8)$$

$$\text{Weight of stiffener/length of stiffener} = \frac{\pi d\ (\text{wt/length of stiffener})}{L_s} \qquad (8.3\text{-}9)$$

Total shell weight/length of shell
= wt of shell/length + wt of stiffener/length (8.3-10)

Total weight of scrubber = 2 (wt of head)
+ L (total shell weight/length of shell) (8.3-11)

Cost of Towers

Method I

Results of various calculations of the type described above are expressed in Figure 8.3-3, a plot of weight per length of shell and weight of head vs. shell diameter. Figure 8.3-4 is a plot of shell weight vs. height of the vessel with diameter as parameter. Figure 8.3-5 is a plot of shop fabrication cost for vessel shell only in \$/Kg vs. the weight of the shell for carbon steel towers and tanks (Modern Cost Engineering Techniques, 1970). Fabricated cost of carbon steel towers can be calculated by combining values from Figures 8.3-4 and 8.3-5. Figure 8.3-6 gives fabricated cost of towers vs. height of vessel with diameter as parameter. This covers the cost of the vessel shell and heads only and does not include packings, trays, internals and connections.

The cost of manholes and flanged nozzles are given in Figure 8.3-7 as taken from Peters and Timmerhaus (1968). It shows the cost per connection per centimeter of inside diameter, for various tower wall thicknesses.

For vessels made with other types of material, a quick cost estimate may be established by using cost multipliers. It is suitable for comparing costs of vessels fabricated from different materials.

Material	Cost Multiplier
Steel	1.0
Reinforced plastics	1.3
304 Stainless steel	4.0
316 Stainless steel	5.2
Monel	7.0

The internal components of packed columns consist of packings, support plate, and distributor plates. Packing costs are variable and a representative cost can be taken at \$350/m^3 (\$10.00/ft^3). The distributor plate cost will roughly be equal to a bubble-cap tray cost while a support plate of simple construction will carry an average cost of \$50/m^2 (\$5.00/ft^2).

Figure 8.3-8 shows a chart for determining the cost of the different types of trays. Prices used were from How (1960) and are not indicated for diameters larger than 3 meters (10 feet). Costs were found to be approximately \$200/m^2 (\$20.00/ft^2) of tray area.

Auxiliaries for towers include ladders and platforms. Ladders weigh 45 kg/m (30 lbs/ft) of height and a platform weighs 156 kg/m (105 lbs/ft) of circumference. For both of them, the price per kg of steel is \$.478/Kg (\$.217 lb)

Method II

A detailed estimation can be made to arrive at the vessel cost. This is based on the work of How (1960). Two checks will be made to compare estimates by this method with both Method I estimates and cost estimates given in the literature. Consider a vessel 3 m (10 ft) high, and 3m (10 ft) in diameter, as shown in Figure 8.3-9. A detailed cost analysis requires calculation of material cost, labor cost, and shop overhead.

All the necessary materials are listed as square meters of steel plate in Table 8.3-5. The number of man-hours for cutting, rolling, edge preparation, fitting and assembly, welding and cleaning and machining are also listed. Labor required was calculated as per How (1968) in the reference mentioned above. Twenty percent was added to the material to allow for unaccounted for miscellaneous parts. Carbon steel cost was taken as \$.22/kg (\$.10/lb) and labor at \$8.00/hr. The sum of the material and direct labor represents the direct cost. A shop burden overhead of 100% of the total direct labor was added to attain the manufacturing cost. Additional percentage must be added to cover the sale, administrative, engineering expenses and profit.

Comparison

Costs calculated by Method I and Method II are compared with those found in the literature in Table 8.3-7. Table 8.3-6 gives cost details of Method I. The purchased cost of steel storage tanks is shown in Figure 8.3-10, updated to Marshall and Stevens' Index of 285.

FIGURE 8.3-9

DETAILED FABRICATION BY METHOD II

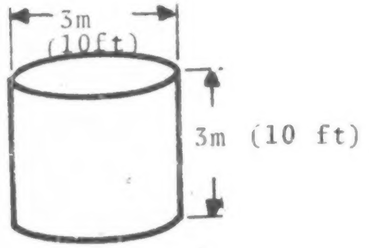

TABLE 8.3-5

Material Area Shell = π 3x3 = 28.3 m^2 (314 ft^2)

Material Area Ends = 2 x $\frac{\pi x 9}{4}$ = 14.2 m^2 (157 ft^2)

Total area = 42.5 m^2 (471 ft^2)

Carbon steel 0.65 cm (1/4 in) plate has weight of 50 Kg/m^2 (10.2 lb/ft^2)

Cost of material = (total area + 20% allowance) x(weight per unit area)
x(cost per unit weight)= $580

Linear edge = 4 πd + 2 H = 37.8 + 6 = 43.8 m (146 ft)

Cutting time = 43.8 mx0.115 hrs/m = 5.1 hrs
Rolling time = = 3.4 hrs
Edge Preparation = 43.8x0.115 = 5.1 hrs
Welding time = (43.8/2)x0.525 = 11.7 hrs
Fitting and assembling = 50.8 = 50.8 hrs

76.1 x $8/hr = $610

Shop Overhead @ 100% $610

$1,800

TABLE 8.3-6

TANK FABRICATION COST - METHOD I

Tank data - 3 m (10 ft) diameter
x 3 m (10 ft) height, 0.65 cm (1/4 in) thickness plate
Weight of shell and ends = 2440 Kg
Material cost (22 /Kg) = $534
Fabrication cost (Figure 8.3-5) = 2440 Kgx0.66 $/Kg = $1610

Fabricated Tank Cost $2,144

TABLE 8.3-7

COST COMPARISON

Size	Capacity m³ (Gallons)	Method I Table 8.3-6	Method II Table 8.3-5	Literature Fig. 8.3-9
3 m (10 ft) dia. 3 m (10 ft) hgt.	22.2 (5,860)	$2,144	$1,800	$3,460
		Fabrication Cost	Fabrication Cost	Purchase Cost

8.3.2.2 Plate and Packed Column

Method I described in 8.3.2.1 was followed to illustrate estimations of plate and packed column cost and to compare it with estimates in the literature. Due to the numerous price estimates that can result from the combinations of various designs, dimensions, sizes and efficiencies of the various components, it was necessary to make some assumptions in order to reach a comparative cost for packed columns and tray towers having the same capacity and dimension and a constant height of equivalent transfer units. The following assumptions were made:

1. Gas velocity = 150 cm/sec (5 ft/sec)
2. Packing height = 3 m (10 ft)
3. Cost of packing = $.36/liter ($10.00/cu ft)
4. Tray stack height = 3 m (10 ft)
5. Tray spacing = 60 cm (24 in)
6. Ratio of height to diameter
   = 7.5 m @ 6 m dia (25 ft @ 20 ft dia)
   = 4.5 m @ 1.5 m dia (15 ft @ 5 ft dia)
7. Diameter of gas inlet and outlet ducts = 0.45 diameter of shell

Table 8.3-8 and Table 8.3-9 show the detailed calculations and costs for several sizes of packed columns and tray towers, respectively. Cost of fabrication was estimated from Figure 8.3-5. Nozzles and manholes of 68 Kg (150 lb) connections were used with prices taken from Figure 8.3-7. Other costs were described in Section 8.3.2.1.

The calculated fabrication costs of the packed columns showed them to be almost equal to the purchased cost, shown in Figure 8.3-10, and compared in Table 8.3-10. Costs in Table 8.3-10 can be arrived at by multiplying the cost per plate by the 5 trays assumed for the tray towers and the cost per unit of packing height by the 3 meters (10 feet) assumed for packed columns. The calculated fabrication costs when compared with reported costs of wet collectors from other sources indicated agreement with reported costs in the high efficiency range. This can be explained by the substantial packing height which we assumed for the example calculation.

TABLE 8.3-10

SUMMARY OF PACKED COLUMN AND TRAY TOWER COSTS

Diameter		Throughput		Fabricated Cost, Packed Column Table 8.3-8	Fabricated Cost, Tray Tower Table 8.3-9	Purchased Cost Figure 8.3-11 M&S - 285.0
m	ft	m^3/m	cfm			
1.5	5	10,000	5,900	$ 4,881		$ 5,600
3	10	40,000	23,600	13,979		14,000
4.5	15	90,000	53,000	28,955		27,500
6	20	160,000	94,300	48,550		50,000
1.5	5	10,000	5,900		$ 6,746	5,250
3	10	40,000	23,600		16,268	13,500
4.5	15	90,000	53,000		30,610	28,000
6	20	160,000	94,300		49,501	49,000

TABLE 8.3-8

PACKED COLUMNS

1. Diameter, m (ft)	1.5 (5)	3 (10)	4.5 (15)	6.1 (20)
2. Height, m (ft)	4.5 (15)	5.6 (18.3)	6.6 (21.7)	7.6 (25)
3. Thickness, cm (in)	0.65 (1/4)	0.65 (1/4)	0.65 (1/4)	0.65 (1/4)
4. m^3/sec and (CFM) at 150 cm/sec (5 ft/sec) gas velocity	10,000 (5,900)	40,000 (23,600)	90,000 (53,000)	160,000 (94,300)
5. Weight of shell and flat heads, Kg and (lbs) (Figure 8.3-4)	1,335 (2,942)	3,810 (8,400)	8,170 (18,000)	14,100 (31,000)
6. Fab. Cost, ¢/Kg for tanks (Figure 8.3-5)	.86	.55	.44	.37
7. Fabrication Cost = (5) (6), $	$1,150	$2,100	$3,600	$5,270
8. Cross sectional area, m^2 and (sq ft)	1.82 (19.6)	7.3 (78.54)	16.4 (176.8)	29.2 (314)
9. Diameter of gas inlet & outlet = .45 D m^2 and (sq ft)	0.685 (2.245)	1.37 (4.5)	2.05 (6.74)	2.75 (9)
10. Cost of two flanged nozzles (Figure 8.3-7 used)	$ 782	$ 1,565	$ 2,350	$ 3,130
11. Manholes, 45.6 cm (18 in) 150 psi (Figure 8.3-7 used)	$ 450	$ 450	$ 900	$ 900
12. Distributor plate @ $215/$m^2$ ($21/sq ft)	$ 435	$ 1,630	$ 3,540	$ 6,280
13. Support plate @ $54 m^2 ($5/sq ft)	$ 100	$ 380	$ 885	$ 1,570
14. Packing volume, m^3 and (cu ft)	5.55 (196.4)	22.2 (785.4)	50 (1,768)	89 (3,140)
15. Packing costs, $354/$m^3$ ($10/cu ft)	$1,964	$ 7,854	$17,680	$31,400
16. Total Fabricated Cost = (7) + (10) + (11) + (12) + (13) + (15)	$4,881	$13,979	$28,955	$48,550

Marshall & Stevens Index = 285

TABLE 8.3-9

TRAY TOWERS

1. Diameter, m and (ft)	1.5 (5)	3 (10)	4.6 (15)	6.1 (20)
2. Height, m and (ft)	4.6 (15)	5.6 (18.3)	6.6 (21.7)	7.6 (25)
3. Thickness, cm and (in)	0.65 (1/4)	0.65 (1/4)	0.65 (1/4)	0.65 (1/4)
4. CFM at 150 cm/sec and (5 ft/sec) gas vel.	10,000 (5,900)	40,000 (23,600)	90,000 (53,000)	160,000 (94,300)
5. Weight of shell and flat heads, Kg and (lbs) (Figure 8.3-4)	1,340 (2,942)	3,820 (8,400)	8,200 (18,000)	14,100 (31,000)
6. Fab. Cost, ¢/Kg and (¢/lb) for tray towers (Figure 8.3-5)	1.52 (.69)	1.19 (.54)	.99 (.45)	.86 (.39)
7. Vessel Cost = (5) (6)	$2,030	$ 4,540	$ 8,100	$12,100
8. Cross sectional area, m² and (sq ft)	1.82 (19.6)	7.1 (78.5)	16.4 (176.8)	29.2 (314)
9. Dia. of gas inlet & outlet = .45 D, m and (ft)	0.685 (2.245)	1.38 (4.5)	2.06 6.74)	2.75 (9)
10. Cost of two flanged nozzles (Figure 8.3-7 used)	$ 782	$ 1,565	$ 2,350	$ 3,130
11. 4 pcs (10 cm) (15 cm) [(4 in) (6 in)] insp. Hole @ $84 + 2 pcs manhole @ ($25) (18)	$1,226	$ 1,226	$ 1,226	$ 1,226
12. Bubble Cap tray, steel	$2,175	$ 8,100	$17,680	$31,400
13. Tower auxiliaries				
Ladder, (44.6 Kg/m) ($.576/Kg) (30 lbs/ft) ($.217/lb)	$ 98	$ 120	$ 142	$ 163
Platform, (156 Kg/m) ($.476/Kg) (105 lb/ft) ($.217/lb)	$ 435	$ 717	$ 1,112	$ 1,482
14. Total Fabricated costs = (7) + (10) + (11) + (12) + (13)	$6,746	$16,268	$30,610	$48,501

Marshall & Stevens Index 285

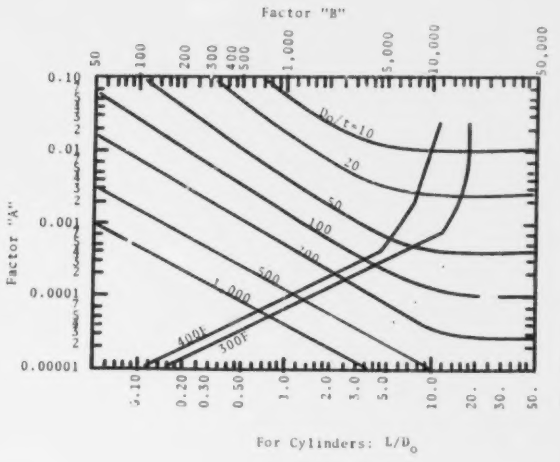

FIGURE 8.3-2

SHELL THICKNESS OF VESSELS UNDER EXTERNAL PRESSURE
FROM: PERRY (1963)

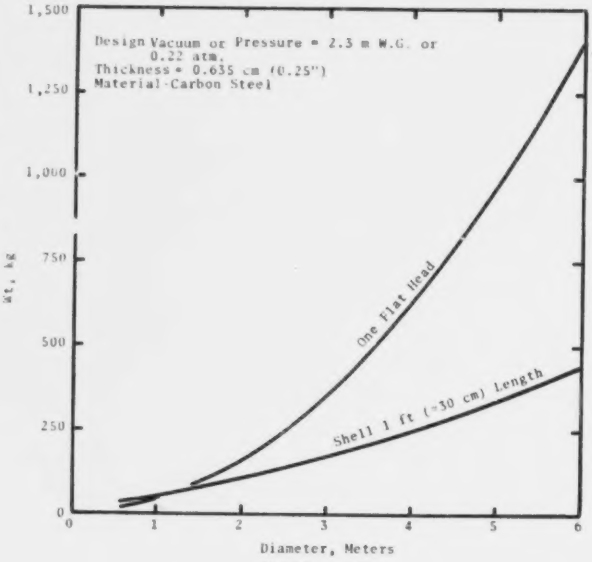

FIGURE 8.3-3

SHELL AND FLAT HEAD WEIGHT VERSUS DIAMETER

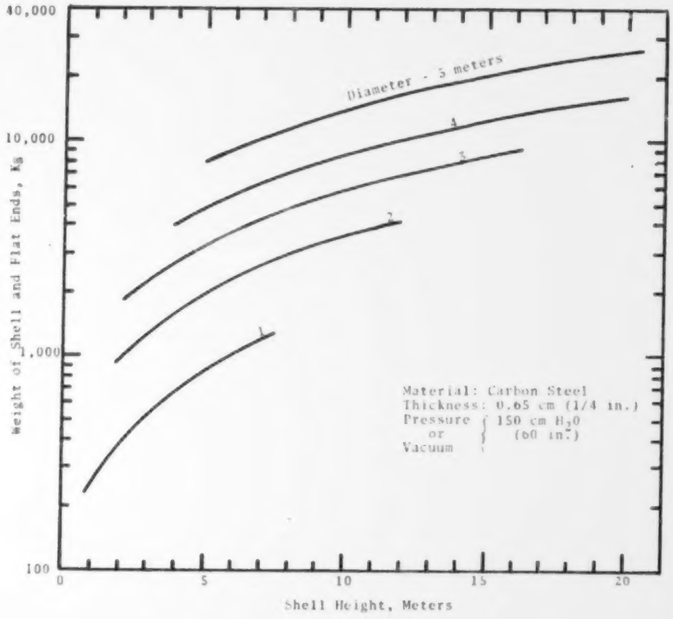

FIGURE 8.3-4

WEIGHT OF SHELL INCLUDING FLAT HEADS VERSUS SHELL HEIGHT WITH DIAMETER AS PARAMETER

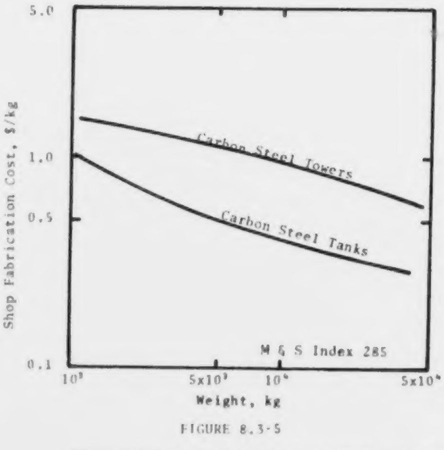

FIGURE 8.3-5

FABRICATION COST OF TOWERS AND TANKS PER "kg" VERSUS THE TOTAL WEIGHT "kg"

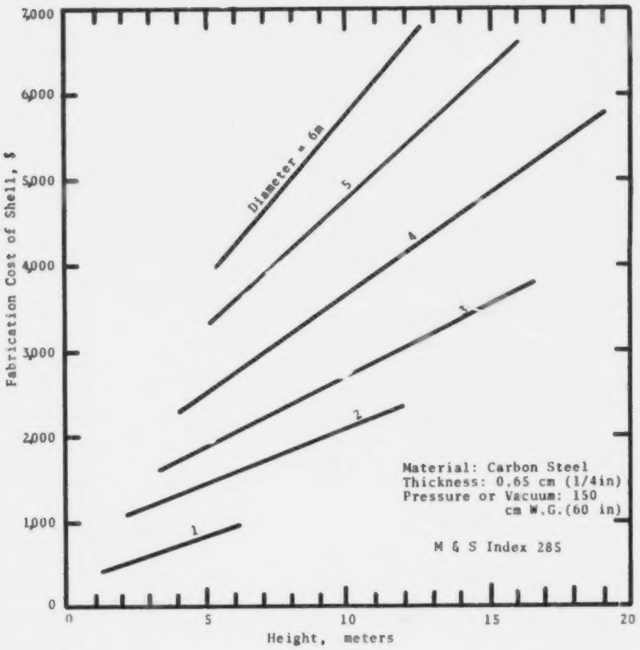

FIGURE 8.3-6

FABRICATION COST OF SHELL VS. HEIGHT WITH DIAMETER AS PARAMETER, FOR CARBON STEEL TANKS

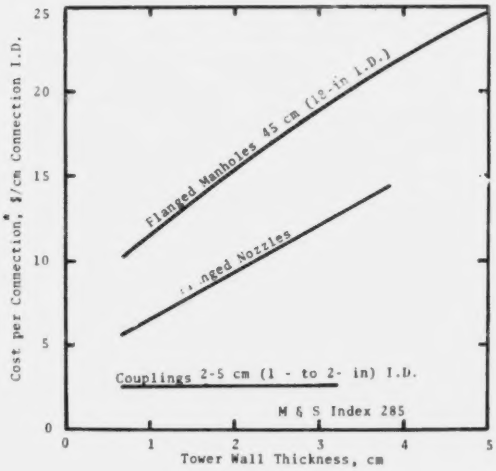

FIGURE 8.3-7

APPROXIMATE INSTALLED COST OF STEEL TOWER CONNECTIONS.
(REF. PLANT DESIGN AND ECONOMICS FOR CHEMICAL ENGINEERS, 1967)

* VALUES APPLY TO 300-LB CONNECTIONS. MULTIPLY COSTS BY 0.9 FOR 150-LB CONNECTIONS AND BY 1.2 FOR 600-LB CONNECTIONS)

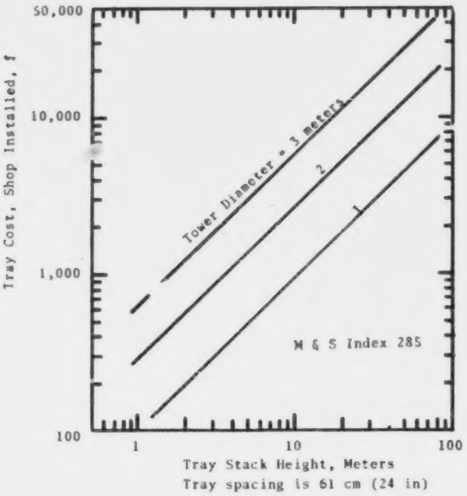

FIGURE 8.3-8

TRAY COST VERSUS TOWER HEIGHT (ADAPTED FROM MODERN COST ENGINEERING TECHNIQUES)

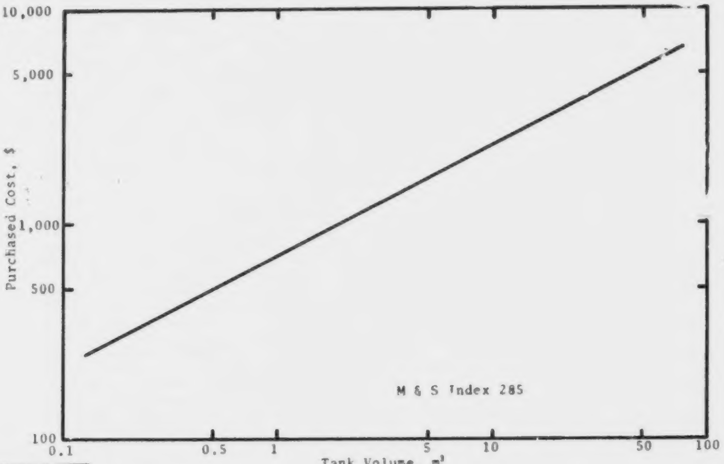

FIGURE 8.3-10

PURCHASED COST OF STORAGE TANK (CARBON STEEL) VERSUS TANK VOLUME (REF. PLANT DESIGN AND ECONOMICS FOR CHEMICAL ENGINEERS 1968)

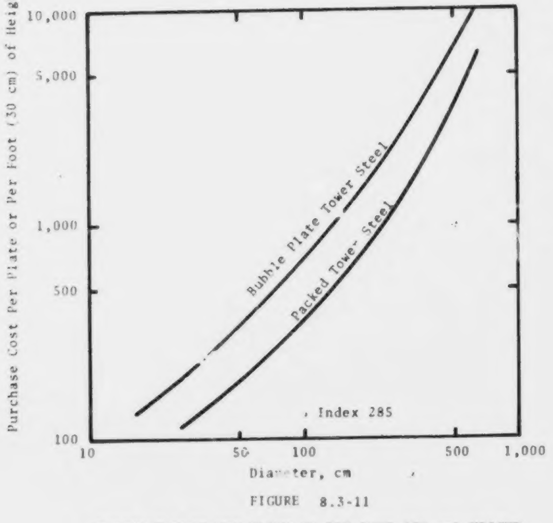

FIGURE 8.3-11

PURCHASE COST PER PLATE OR PER FOOT (30 cm) HEIGHT VERSUS COLUMN DIAMETER FOR BUBBLE CAP AND PACKED TOWER (REF. PLANT DESIGN AND ECONOMICS FOR CHEMICAL ENGINEERS 1968)

8.4 COST ANALYSIS

8.4.1 INTRODUCTION

In this section, cost data taken from the literature, and obtained in the scrubber users' survey detailed in Chapter Seven will be presented. The data obtained from the users' survey will be compared with literature values.

In general, more information is available on the initial purchase cost or installed cost of scrubber systems than is available on their operating costs. This is because operating costs for the scrubber system are usually lumped together with other plant operating costs, and cannot be separated.

Cost analyses in the following sections are those taken from Stairmand (1965) in Section 8.4.2, from standard cost engineering references in Section 8.4.3, and from the survey of scrubber users in Section 8.4.4.

8.4.2 SCRUBBER SYSTEM COSTS ACCORDING TO STAIRMAND (1965)

Stairmand (1965) has compared the installed and operating costs of a number of wet scrubbers. Although his original article gives costs in terms of English currency, Sargent (1969) has expressed these costs in American currency, and brought the costs up to date at the year 1968.

Table 8.4-1 gives Stairmand's cost data for six scrubbers commonly used. Note that an efficiency (experimentally determined) for a "standard" test dust is listed. The size distribution of this test dust is given in Table 8.4-2. The costs are for collectors operating on 100,000 m^3/hr (60,000 cfm) of gas at 20°C (68°F) with an inlet dust loading of 11.5 g/m^3 (5gr/ft^3). The installed cost includes equipment, auxilliaries such as fans, pumps and motors (but does not include solids disposal equipment), site preparation and installation. Installation charges are 100% of all equipment costs except for mechanically aided scrubbers which are 50%. The cost of power is taken at $0.01 per kwh. Efficiencies of fans and motors are assumed 60%. Water cost is $0.019/$m^3$($0.05/1000 gallons) and reported usage converted from Imperial (assumed) to U. S. gallons. The British pound was taken at $2.84 U. S. Prices are adjusted to 1968 with a Marshal and Stevens index of 273.

TABLE 8.4-1

OVER-ALL COST OF GAS CLEANING

Collector Type	Efficiency on Standard Dust, %	Average Pressure Drop		Installed Cost, $	Power Cost $/yr	Water Required		Water Cost $/yr	Maintenance $/yr	Total Annual Cost, $/yr	Total Annual Cost	
		mbar	in w.g.			ℓ/m³	Gal/ 1,000 cu ft				¢/(yr) (m³/hr)	¢/(yr) (cfm)
Impingement and Entrainment	93.6	15.5	6.1	66,700	5,640	0.093	0.7	1,010	700	14,020	13.7	23.3
Spray Chamber	94.5	3.5	1.4	139,000	4,760	2.9	21.7	31,250	1,000	50,910	50	84.8
Impingement Scrubber	97.9	15.5	6.1	82,200	5,800	0.48	3.6	5,190	1,000	20,210	20	33.7
Mechanically Aided Scrubber	98.5	----	---	136,000	45,400	0.8	6.0	8,640	700	68,340	83	141
Low energy venturi	99.7	51	20.0	107,000	18,820	1.1	8.4	12,100	1,000	42,620	42	71.2
High energy venturi	99.9	80	31.5	117,000	29,740	1.1	8.4	12,100	1,000	54,540	53.5	91.0

TABLE 8.4-2

SIZE DISTRIBUTION OF TEST DUST USED TO DEVELOP EFFICIENCIES LISTED IN TABLE 8.4-1

Particle Size range Microns	Particle Size Midpoint of Range, Microns	Fraction of Total Dust in Range, wt %
<2 1/2	1 1/4	12
2 1/2 -5	3 3/4	8
5-7 1/2	6 1/4	6
7 1/2-10	8 3/4	4
10-15	12 1/2	8
15-20	17 1/2	7
20-30	25	10
30-40	35	10
40-60	50	15
60-75	67 1/2	10
75-104	89 1/2	7
104-150	127	3

Stairmand (1965) also presented the annualized cost versus efficiency graph as shown in Figure 8.4-1. Annual capital charges were taken as 10% of the total capital cost. Annual operating time was taken as 8000 hours. Other costs are as noted in the preceeding paragraph. Other types of collection equipment than scrubbers are also listed for purposes of comparison. "The heavy straight line can be regarded," according to Stairmand," as an overall 'value line' in the sense that it indicates the average cost of gas cleaning to the efficiencies shown. If the point for any particular deduster lies well below this line we can regard this as an indication that this equipment represents a good value for the money, while points above the line generally indicate an uneconomic choice." It should be noted that this economic comparison is based on the economic conditions listed above regarding costs of power, water, etc. In situations where these costs are altered, where special materials of construction are necessary, or where other factors enter into consideration, the picture presented here may be altered.

8.4.3 SCRUBBER PURCHASE COST - LITERATURE VALUES

As is explained in Section 8.3, the purchase cost of a scrubber depends on many factors, including type of scrubber, materials of construction, and gas processing capacity.

Figures 8.4-2 through 8.4-4 are plots of scrubber purchase cost against gas flow, with type of scrubber as parameter. These data were taken from Sargent (1969), with a Marshal and Stevens price index of 273. Mild steel construction is assumed. Costs for other materials of construction can be developed by multiplying the price for mild steel by an appropriate factor as listed on page 8-23.

Figure 8.4-2 plots purchase cost versus gas throughput for impingement and entrainment, centrifugal, and gravity spray scrubbers. Figure 8.4-3 is a similar plot for high and low energy venturi scrubbers and for submerged nozzle (impingement and entrainment) scrubbers. Figure 8.4-4 is for dynamic (mechanically aided) scrubber and for cyclones.

Figures 8.4-5 and 8.4-6 are taken from Dallavalle (1960) with Marshal and Stevens index of 180. They are plots of purchase cost expressed as $ per cubic meter of gas processed per hour, versus gas throughput in cubic meter per hour. Figure 8.4-5 is for water spray scrubbers, both "light" and "heavy" duty, while Figure 8.4-6 is for cyclones, again both "light" and "heavy" duty. Note that in both figures, the cost per unit of gas processed increases markedly for small gas processing units.

8.4.4 INSTALLED COST OF SCRUBBERS - SURVEY RESULTS

During the survey of scrubber users, detailed more completely in Chapter Seven, information was gathered on the installed costs of industrial scrubbing systems. It was decided that the most effective means of displaying this data would be in the form of graphs which express installed cost versus gas flow (throughput), for the various types of scrubbers for which data was available. Installed cost as used here means purchase cost plus installation cost as discussed in section 8.3.1-1.

Although ten different kinds of scrubbers were identified in Chapter Three and are discussed in Chapter Five, it was found through the scrubber survey that Fiber Bed scrubbers, Baffle and Secondary Flow Scrubbers and Mechanically Aided Scrubbers are infrequently used. Insufficient data was obtained for these scrubbers to enable plotting a cost versus throughput figure. The figures developed for the remaining seven types of scrubbers are given in Figures 8.4-7 through 8.4-12, and are described below. Figure 8.4-11 combines data for impingement plate scrubbers and impingement and entrainment scrubbers.

Each figure includes a plot of the lines given in the NAPCA (1969) AP-51 report. These lines are purported to be for high and low installed costs for scrubbers.

Figure 8.4-7 expresses installed costs for packed bed scrubbers. Virtually all of these scrubbers were used for gas removal (mass transfer) operations rather than for particle collection. The costs observed were generally within the range predicted by the NAPCA report. Note that there were no really large installations using packed beds; all were found to be under 100,000 m^3/hr (60,000 cfm).

Figure 8.4-8 gives the installed costs for spray scrubbers. Included are both spray towers and ejector venturis in accordance with the definition of spray scrubbers given in Chapter Three. Note that the cost of spray scrubbers appears to be roughly constant, despite considerable variations in throughput. The NAPCA report seriously underestimates the cost of spray scrubbers processing small throughputs of gas. This may be because many of the smaller spray scrubbers are ejector venturis requiring auxilliary equipment (pumps primarily) which are quite expensive. The larger installations are simple gravity spray towers.

Figure 8.4-9 gives the installed cost of venturi scrubbers. Most venturis are operated at high pressure drops, and therefore require expensive blowers. Many costs encountered, as shown in Figure 8.4-9, are considerably above even the high installed cost line given in the NAPCA report. Some installations reported costs as much as five times the reported "high" cost given in the NAPCA report. Also notable is the large spread in installed cost for applications processing the same gas throughput. Based on the data shown in Figure 8.4-9, the cost of a venturi system processing 20,000 m^3/hr of gas (12,000 cfm) might range from 10,000 to 150,000 dollars, depending on the nature of the gas stream to be cleaned and the degree of cleanup required.

Figure 8.4-10 gives the installed cost of centrifugal scrubbers. These scrubbers fall neatly within the brackets of high and low costs given in the NAPCA report. The spread in data for applications processing the same gas throughput is considerable. The data shows that an installation processing 40,000 m^3/hr of gas might have an installed cost ranging from about 10,000 to 50,000 dollars, which a typical value being about 25,000 dollars.

Figure 8.4-11 presents the installed cost data for impingement plate and impingement and entrainment scrubbers. The data cluster quite well around the "high" cost line of the NAPCA report, and represent a good cross-section of various sized installations.

Figure 8.4-12 gives the installed cost of moving bed scrubbers. All data are for moderate sized scrubbers between about 35,000 and 80,000 m^3/hr (20,000 - 45,000 cfm). The data seem to cluster around the "high" cost line of the NAPCA report. The spread in the data is such that a 40,000 m^3/hr (23,000 cfm) moving bed scrubber might cost between 30,000 and 60,000 dollars.

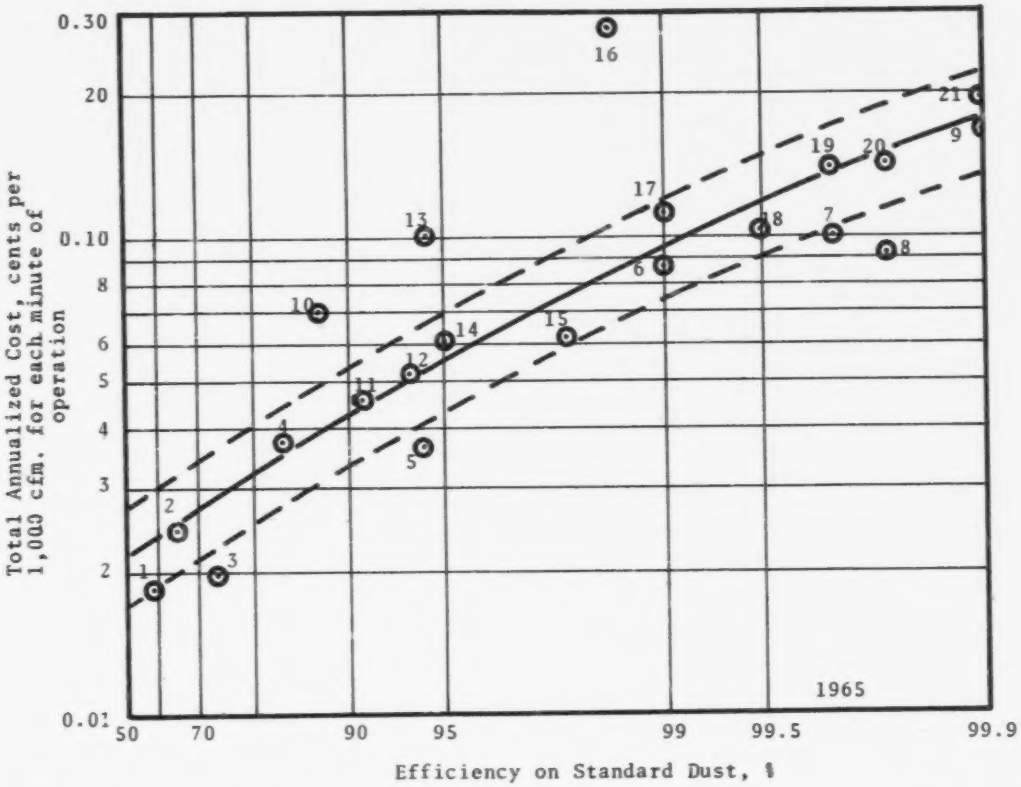

FIGURE 8.4-1

TOTAL COST OF VARIOUS AIR POLLUTION CONTROL DEVICES VERSUS EFFICIENCY ON STANDARD DUST

1. Inertial Collector
2. Medium Efficiency Cyclone
3. Cellular Cyclone
4. High Efficiency Cyclone
5. Tubular Cyclone
6. Electrostatic Precipitator
7. Shaker-type Fabric Filter
8. Low Velocity Fabric Filter
9. Reverse jet Fabric Filter
10. Impingement and Entrainment Scrubber (a)
11. Irrigated Cyclone
12. Impingement and entrainment scrubber (b)
13. Spray tower (counter current)
14. Moving bed scrubber
15. Impingement plate scrubber
16. Mechanically aided scrubber
17. Irrigated electrostatic precipitator
18. Annular throat scrubber-low energy
19. Venturi scrubber - medium energy
20. Annular throat scrubber - medium energy
21. Venturi scrubber - high energy.

To Convert ¢/1,000 ft^3 to ¢/1,000 m^3, multiply by 35.3

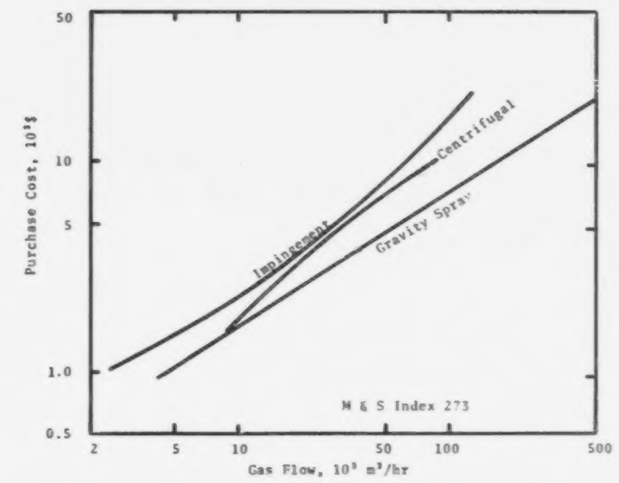

FIGURE 8.4.2
MANUFACTURER's PRICE VS. GAS FLOW FOR SCRUBBERS
(AFTER G. D. SARGENT, 1969)

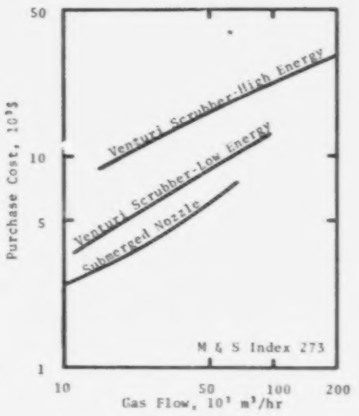

FIGURE 8.4-3

MANUFACTURER'S PRICE VS. GAS FLOW FOR SCRUBBERS

(AFTER G. D. SARGENT, 1969)

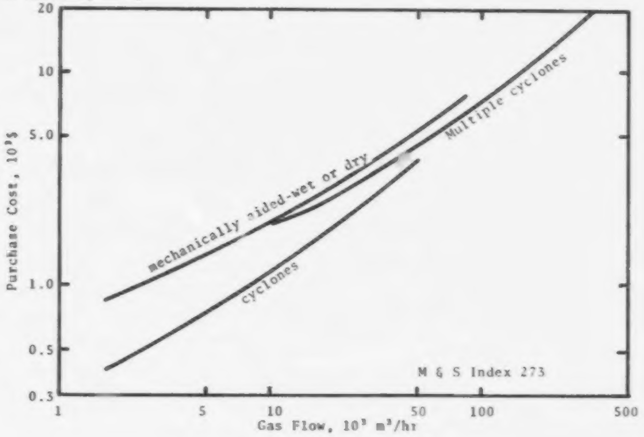

FIGURE 8.4-4

MANUFACTURER'S PRICE VS. GAS FLOW FOR SCRUBBERS
(AFTER G. D. SARGENT, 1969)

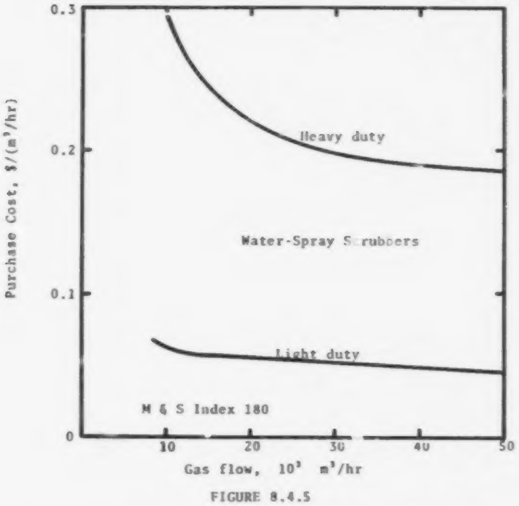

FIGURE 8.4.5

MANUFACTURER'S PRICE VS. GAS FLOW FOR SCRUBBERS
(AFTER J. M. DALLAVALLE 1960)

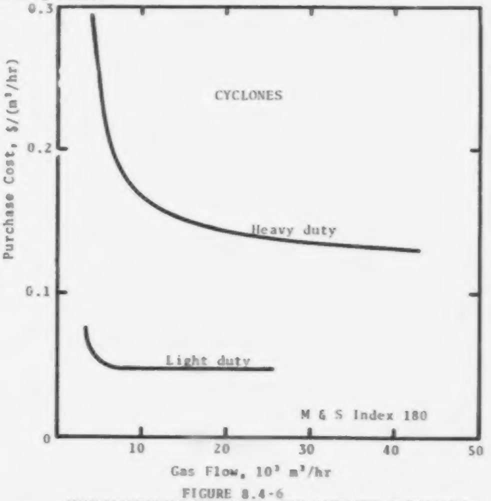

FIGURE 8.4-6
MANUFACTURER'S PRICE VS. GAS FLOW FOR SCRUBBERS
(AFTER J. M. DALLAVALLE 1960)

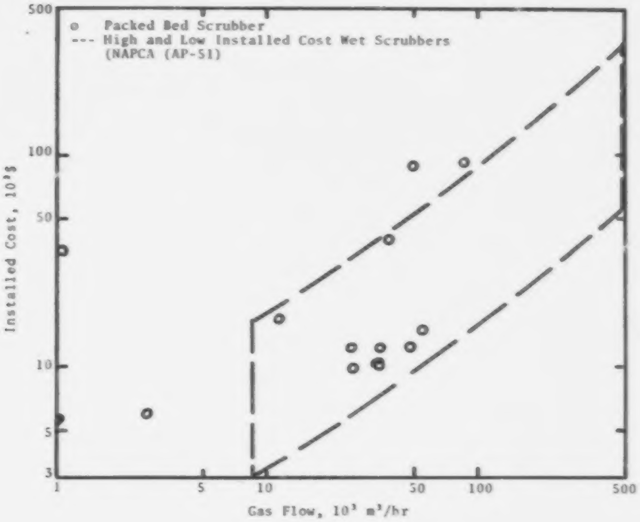

FIGURE 8.4-7
SURVEY RESULTS INSTALLED COST OF PACKED BED SCRUBBERS

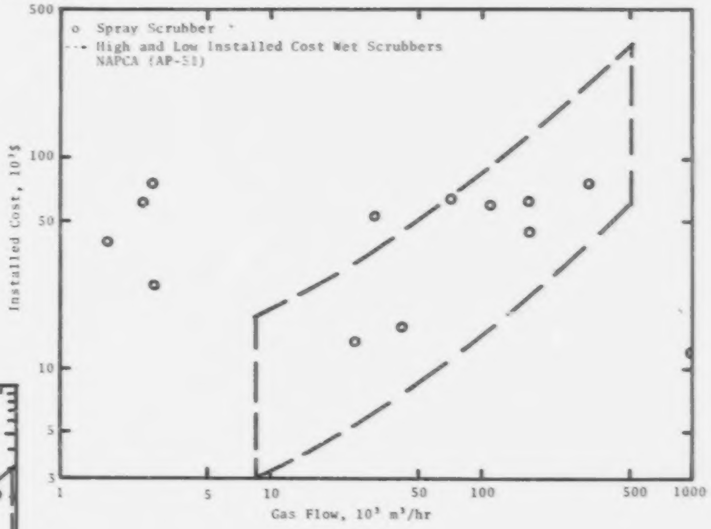

FIGURE 8.4-8

SURVEY RESULTS INSTALLED COST OF SPRAY SCRUBBER VS. GAS FLOW

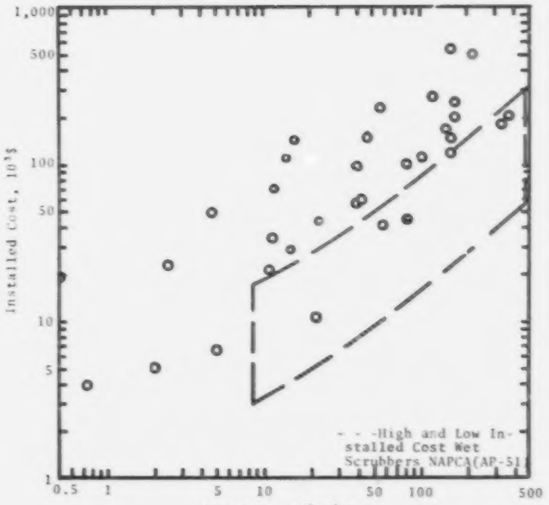

FIGURE 8.4-9

SURVEY RESULTS INSTALLED COST OF VENTURI VS. GAS FLOW

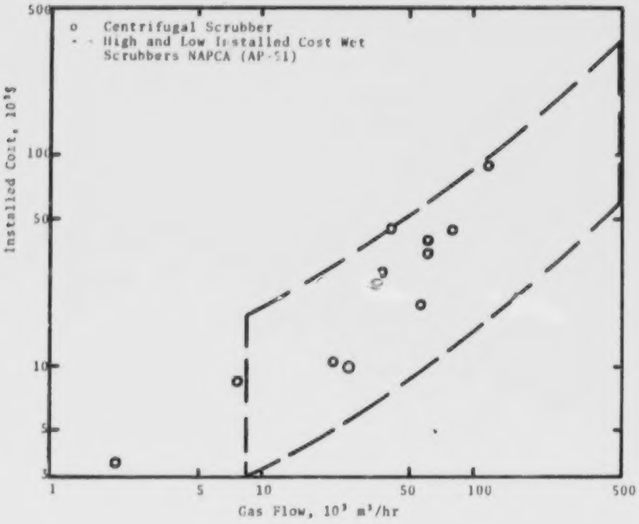

FIGURE 8.4-10

SURVEY RESULTS INSTALLED COST OF CENTRIFUGAL SCRUBBER

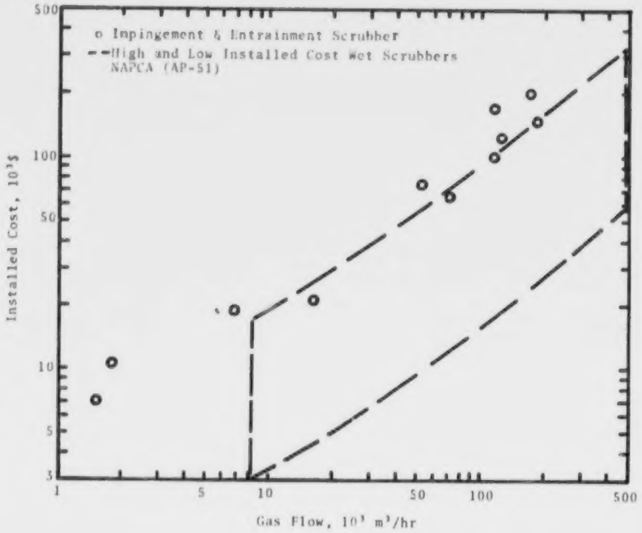

FIGURE 8.4-11

SURVEY RESULTS INSTALLED COST OF IMPINGEMENT AND ENTRAINMENT SCRUBBER VS. GAS FLOW

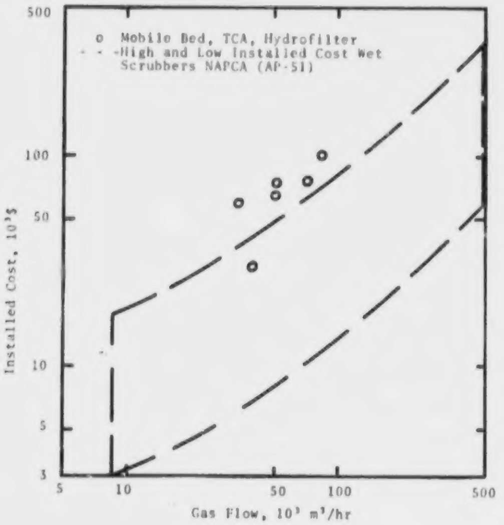

FIGURE 8.4-12

SURVEY RESULTS INSTALLED COST OF MOBILE BED SCRUBBERS VS. GAS FLOW

8.5 OPTIMIZATION

8.5.1 INTRODUCTION

In the area of scrubber design the problem of optimization occurs in a multitude of ways. Irrespective of the particular form that the problem assumes, the nature of the problem is the same. Out of a multiplicity of potential solutions, the designer is required to find that particular solution judged to be the "best" by some preassigned criterion of optimality.

It is well to define some of the terms used in optimization which we will refer to in our discussions later.

1. Unimodal Function - A function with one peak, either maximum or minimum.
2. Multimodal Function - A function with more than one peak.
3. Objective Function - A function of the design variables the value of which provides a basis for choice between alternative acceptable designs. The objective function may be related to cost, performance, pressure drop or some other criterion.
4. Preassigned Parameters - Those quantities describing the scrubber system that are fixed at the outset and not varied by the optimization procedure.
5. Design variables - Those quantities describing the scrubber system that are varied by the optimization procedure.
6. Constraints - A bound or constraint among the variables. Most design equations are valid within the limitation of the inherent assumptions and/or the experimental validity of design variables range. Constraints limit the domain in which the search is to take place.

A rather general class of scrubber optimization may now be stated concisely as follows:

Given the preassigned parameters, find the vector of design variables $(\vec{D})$ such that the objective function M $(\vec{D})$ is minimized (or maximized) subject to a collection of inequality constraints on the design variables.

$h_j\ (\vec{D}) \leq 0;\ j = 1, 2, \ldots j$

Where the functions $h_j\ (\vec{D})$ are such that (1) unsatisfactory behavior subject to limitations placed is precluded; (2) the design vector $(\vec{D})$ is subject to further restrictions based upon considerations such as fabrication limitations and geometric realizability.

Optimization Technique

There are many optimization techniques to evaluate the objective function once the problem is defined. The crudest and mathematically least sophisticated (but often the best) method is the basic search. This is a case study technique where all possible solutions are examined and the best one selected. Although exhaustive, time consuming and expensive it may be the best where the functions are unimodal and the number of design variables small. Following the guidelines set by experience and intuition, within the operational area guarded by the inequality constraints, this approach was found very useful in some of the optimizations carried out here.

8.5.2 PERFORMANCE OPTIMIZATION

The problem of performance optimization, where performance is the objective function, can be viewed in many ways. Depending upon the combinations of preassigned variables, design variables, and constraints, numerous answers result. Some situations of interest are examined here which, while providing useful answers, also illustrate how to formulate a problem and method of arriving at the solution.

8.5.2.1 Venturi Scrubber

A problem of interest is to find the maximum particle collection efficiency at a given air pressure drop in a venturi scrubber. Mathematical functions describing the relationship between variables is given by Equations 5.3.6-5 and 5.3.6-10. We may define the problem in optimization terminology as follows:

1. Objective Function - Find the minimum of penetration "Pt" for a given particle size, d_p, and constant pressure drop.

2. Preassigned Parameters - Preassigned variables are particle size "d_p" and pressure drop through venturi, "ρ_L", "μ_G", and "f".

3. Design Variables - Volumetric liquid to gas ratio, Q_L/Q_G, and "u_G" are the design variables.

4. Constraints - One of the constraints is in the form of an equality as described by Equation 5.3.6-1 for the Sauter mean drop diameter size. We may also constrain the range of gas velocity in the venturi throat and the liquid to gas volumetric ratio. Let them be as follows:

$$5{,}000 \text{ cm/sec} \leq u_G \tag{8.5-1}$$

$$u_G \leq 15{,}000 \text{ cm/sec} \tag{8.5-2}$$

$$0.25 \ \ell/\text{m}^3 \leq \frac{Q_L}{Q_G} \tag{8.5-3}$$

$$\frac{Q_L}{Q_G} \leq 4.0 \ \ell/\text{m}^3 \tag{8.5-4}$$

A visual direct optimization is possible for three different particle sizes with the help of Figures 5.3.6-10, 5.3.6-11 and 5.3.6-12. Preassigned variables are as assumed in the preparation of those figures. Let a pressure drop of 50 cm W.C. be the constant pressure drop. The figures are plots of penetration vs. "u_G" with Q_L/Q_G in ℓ/m^3

and "ΔP" as parameters. Optimum results are given in the following tabulation.

TABLE 8.5-1

OPTIMIZATION OF VENTURI SCRUBBER

Figure	Pressure Drop cm W.G.	d_{pa} $\mu m\ \sqrt{g/cm^3}$	u_G m/sec	(Q_L/Q_G) ℓ/m^3	Optimum Penetration
5.3.6-10	50	0.5	110 to 150	0.35 to 0.2	0.85
5.3.6-11	50	1.0	70	0.1	0.53
5.3.6-12	50	2.0	50	0.2	0.073

8.5.2.2 Cyclone

Optimization of a cyclone for performance at a given pressure drop is a much more complex task and brings out many interesting problems a designer may encounter. Optimization will give as accurate a result as the equations describe the real situation. Equation 5.3.7-2 describes the performance of a cyclone. We have already exercised designers' judgement and preferred Equation 5.3.7-2 over the equations given in Table 5.3.7-1. Discussion in Section 5.3.7 comments on selection of this performance equation. Table 5.3.7-2 presents some of the pressure drop equations. Note that some of the pressure drop equations do not include all the cyclone geometry design variables involved in describing the performance of a cyclone. If the performance equation contains a variable not involved in the pressure drop equation, that variable will allow increasing efficiency without a corresponding penalty in pressure drop. The pressure drop equation after Shepherd and Lapple (1939) was used (see Table 5.3.7-2).

It is normally true that the pressure drop and penetration do not have the same functionality in a set of variables. This very fact makes possible a best choice of common design variables which optimizes objective function for a given set of preassigned variables. Those variables that are independent and not common to both the equations must be preassigned or constrained, otherwise a lack of penalty may give an ambiguous result.

1. Objective Function - Find the maximum collection efficiency, E, for a given particle collection problem and constant pressure drop.

2. Preassigned Parameters - Preassigned variables are "d_p", "ρ_p", "Δ_p", "d_c", "Q_G", "ρ_G" and "μ_G". Let $h = 5\ d_c$; $h_s = 3\ d_c$; $b_e = 0.375\ d_c$; $\rho_G = 1.2\text{x}10^{-3} g/cm^3$; $\mu_G = 1.8\text{x}10^{-4}$ poise.

3. Design Variables - "a", "b", "d_e" and "S" are design variables.

4. Constraints - Natural length of the cyclone, ℓ, as defined by Equation 5.3.7-5 should not protrude through the bottom of the cyclone.

Hence,

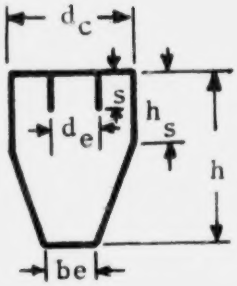

FIGURE 8.5-1

CYCLONE GEOMETRY NOMENCLATURE

$$h > S + \ell \tag{8.5.5}$$

The inlet height, a, and width, b, are constrained as follows:

$$a \leq S \tag{8.5-6}$$

$$b \leq \frac{d_c - d_e}{2} \tag{8.5-7}$$

For the efficiency optimization, Equation 5.3.7-2 expressing cyclone efficiency can be rearranged to:

$$E = 1 - \exp\left[-2\ CP\ SIP\right] \tag{8.5-8}$$

where:

$$CP = \left[\frac{C\ Q_G}{a\ b\ d_c}\ (n + 1)\right]^{1/(2n+2)} \tag{8.5-9}$$

and:

$$SIP = \left[\frac{d_p^2\ \rho_p}{18\ \mu_G}\right]^{1/(2n+2)} = \tau^{1/(2n+2)} \tag{8.5-10}$$

Here, "τ" is the particle "relaxation time", raised to a power, and is independent of the cyclone geometry to be optimized. For particles of any properties, and hence "τ", best efficiency will be achieved when "CP" is maximized.

For given values of gas throughout, Q_G, cyclone diameter, d_c, and pressure drop, ΔP, the value of "CP" was optimized on a digital computer. Results are given in Figures 8.5-2, 3, and 4, as plots of cyclone diameter "d_c" versus "CP" with inlet gas velocity and throughout as parameters for pressure drops of 7.5 cm (3 in), 12.5 cm (5 in) and 17.5 cm (7 in) of water, respectively. Using these figures, the optimum "CP" value and inlet velocity can be found.

The "CP" value determined can be used in conjunction with Equations 8.5-8 and 10 to find an optimum cyclone's efficiency on any particle.

The optimization results can be used in two ways. They can be used to design an optimized cyclone to achieve a specified efficiency, for a given particle. They can also be used to determine the best (i.e., most efficient) cyclone for a given gas throughput.

First, consider the problem of achieving a specified efficiency or a given particle. This may be done by using any of a number of combinations of cyclone diameter and pressure drop. To start, assume a pressure drop and diameter. Then calculate vortex exponent, "n", for the diameter chosen, using Equation 5.3.7-8. Next calculate the SIP value corresponding to the particles to be collected, from Equation 8.5-10. With required efficiency, "E", and SIP at hand, calculate the required value for "CP" from Equation 8.5-8. Now enter Figure 8.5-2, 3 or 4 (depending on the pressure drop chosen). Opposite the "CP" value required, and for the throughput to be used, read the optimized cyclone's diameter, "d_c". Hopefully, it will be close to the diameter initially assumed. If not, use the diameter just determined to calculate a new value of "n" and "CP", as outlined above. When the assumed and calculated values of "d_c" agree, note the corresponding value of inlet gas velocity from the figure. Now go to Figure 8.5-6, a plot of geometry coefficient, "C", versus dimension ratios, and determine the optimized cyclones' dimension ratios. This completes the cyclone design. A similar procedure for a different pressure drop will result in a different cyclone design. A series of designs for a series of pressure drops can be made, to determine the cyclone with lowest annualized cost.

Next, consider the problem of determining the cyclone with best efficiency for a given throughput, "Q_G". First, assume a pressure drop. Then refer to Figure 8.5-2, 3 or 4, depending on the pressure drop chosen. Enter the appropriate "Q_G" line, and it will be seen that a range of inlet velocities may be used. Generally, it will be prudent to limit inlet velocity to less than about 40 m/sec. Reentrainment of collected dust increases with increasing gas velocity. However, the effect of reentrainment and its subsequent effect on efficiency have not been thoroughly studied or quantified. Limiting velocity to under 40 m/sec hopefully will keep reentrainment to acceptable levels. For a velocity of 40 m/sec or less, locate the corresponding value of "CP". A grade efficiency curve (particle size versus efficiency) can now be constructed using the value of "CP" determined through the use of Equations 8.5-8 and 8.5-10. The dimensions of the cyclone can be determined once the pressure drop and inlet velocity are established, as was explained in the preceeding paragraph. Optimized cyclones can be determined for pressure drops of 7.5, 10.5 and 17.5 cm W.C. by using Figures 8.5-2, 3 and 4, respectively.

8.5.2.3 Scrubbers in Series and Parallel

Optimization may not necessarily be on an individual unit. It may be over a grid of units arranged in series or parallel or a combination thereof. The question may arise as to whether a series or a parallel strategy is advantageous. This is a form of optimization and the formulation of the problem can be carried out according to the format presented in the introduction and illustrated subsequently. The following background is necessary to evaluate these strategies.

Scrubbers in Series

When scrubbers are placed in series, end to end, the penetration through them on particles of one size is the product of individual penetrations on particles of that size:

$$Pt_{(1-n)} = Pt_1\ Pt_2\ \ldots\ Pt_n \qquad (8.5\text{-}11)$$

Corresponding pressure drop will be:

$$\Delta P_T = \Delta P_1 + \Delta P_2 + \ldots + \Delta P_n \qquad (8.5\text{-}12)$$

where: $Pt_{(1-n)}$ = total penetration through "n" scrubbers in series on particles of one diameter

ΔP_T = total pressure drop through "n" scrubbers in series

If the units in series are similar and have the same penetration on particles of one diameter then the above equation becomes:

$$Pt_{(1-n)} = Pt_1^{\,n} \qquad (8.5\text{-}13)$$

and

$$\Delta P_T = n\ \Delta P \qquad (8.5\text{-}14)$$

Scrubbers in Parallel

Input gas flow may be divided into "n" parts and processed through "n" scrubbers in parallel. Let f_1, f_2, ..., f_n be fractions of gas going through scrubbers, 1, 2, ..., n and $f_1 + f_2 + \ldots + f_n = 1$. Then:

$$Pt_{(\frac{1}{n})} = f_1\ Pt_1 + f_2\ Pt_2 + \ldots + f_n\ Pt_n = \sum_1^n f\ Pt \qquad (8.5\text{-}15)$$

If the penetration through each unit is the same, then:

$$Pt_{(\frac{1}{n})} = Pt\ (f_1 + f_2 + \ldots + f_n) = Pt \qquad (8.5\text{-}16)$$

where $Pt_{(\frac{1}{n})}$ = total penetration through "n" scrubbers in parallel.

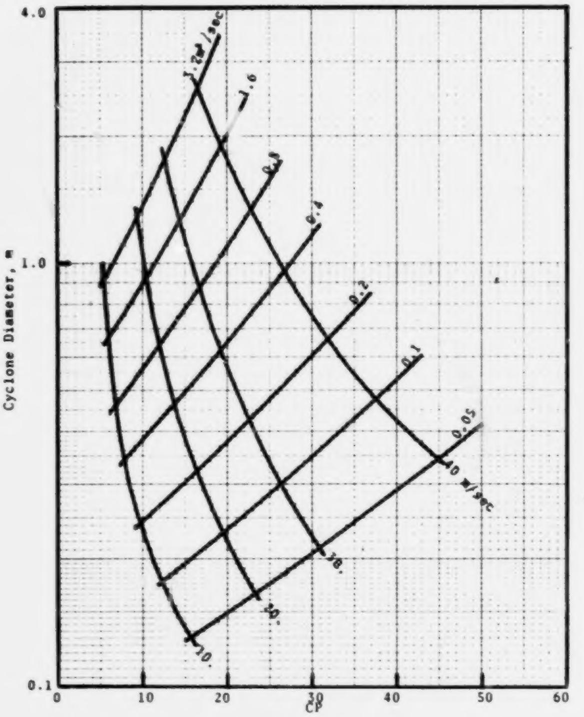

FIGURE 8.5-2

CYCLONE DIAMETER VERSUS CP WITH INLET VELOCITY AND THROUGHPUT AS PARAMETERS, PRESSURE DROP IS (3") W.C.
7.5 cm

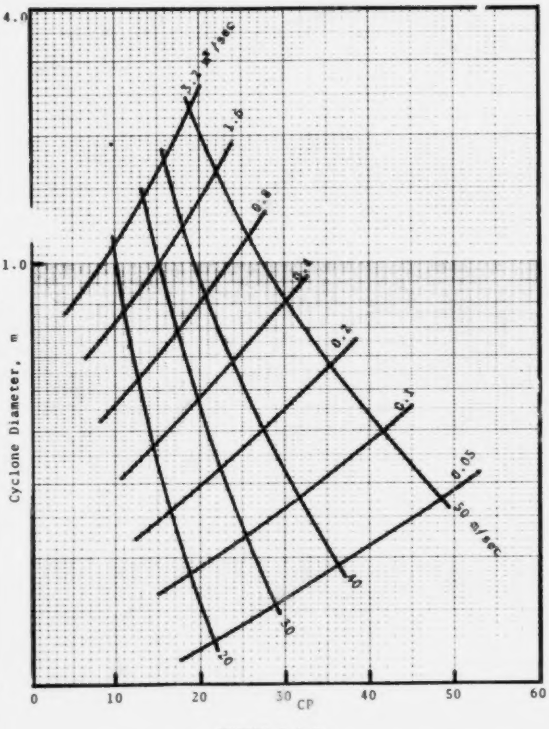

FIGURE 8.5-3

CYCLONE DIAMETER VERSUS CP WITH INLET VELOCITY AND THROUGHPUT AS PARAMETERS. PRESSURE DROP IS 12.5 cm(5") W.C.

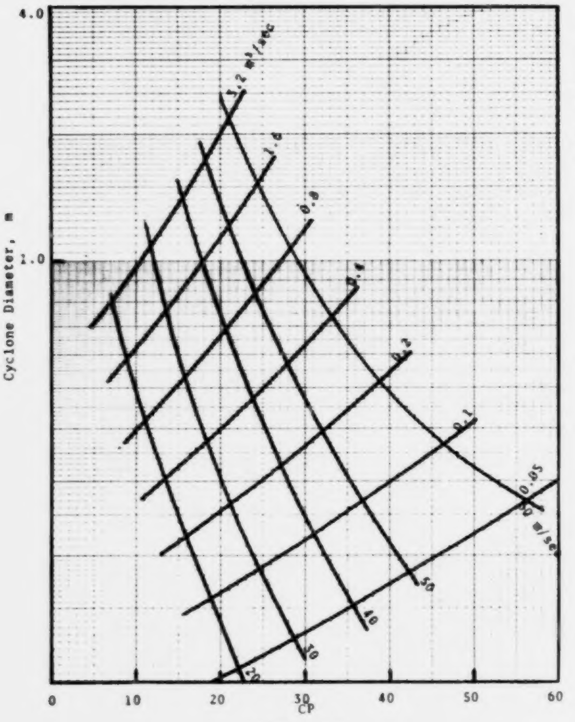

FIGURE 8.5-4

CYCLONE DIAMETER VERSUS CP WITH INLET VELOCITY AND THROUGHPUT AS PARAMETERS. PRESSURE DROP: 17.5 cm (7") W.C.

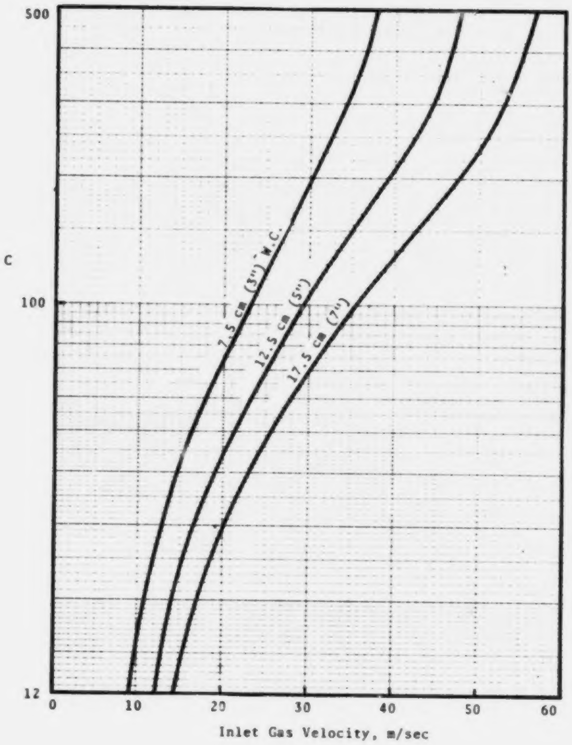

FIGURE 8.5-5

"C" VERSUS INLET GAS VELOCITY WITH
PRESSURE DROP AS
PARAMETER
FOR CYCLONES

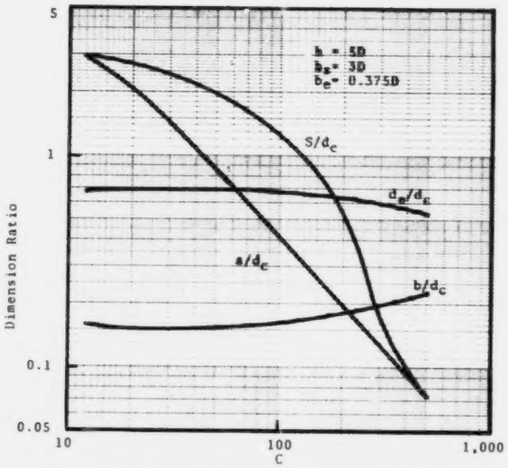

FIGURE 8.5-6

OPTIMUM DIMENSION RATIOS VERSUS
CYCLONE GEOMETRY COEFFICIENT, "C"

CHAPTER 8 - NOMENCLATURE

LATIN

A = area, m^2 or cm^2
A = constant
b = $\exp[2\sqrt{z}\ \ln \sigma_g]$
b_e = cyclone dust exit diameter, m or cm
B = constant
C = cyclone geometry coefficient
d = diameter, m or cm
d_c = cyclone diameter, m or cm
d_e = cyclone gas exit duct diameter, m or cm
d_p = particle diameter, cm or μm
d_{pa} = aerodynamic particle diameter, μm $(g/cm^3)^{1/2}$
d_{pg} = geometric mean particle diameter, cm or μm
d_{p50} = particle size collected with 50% efficiency , cm or μm
E = device efficiency
f = velocity ratio factor
$f(d_p)$ = size frequency distribution
°F = degrees Farenheit
h = total height of cyclone, m or cm
h_s = height of cylindrical portion of cyclone, m or cm
I = moment of inertia, m^4 or cm^4
K_{Pt} = impaction parameter for d_{pg} at the throat velocity
K_p = inertia parameter
ℓ = "natural length" of cyclone, m or cm
L = length, m or cm
n = vortex exponent (see Equation 5.3.7-8)

CHAPTER 8 - NOMENCLATURE

LATIN

n = number of baffles in series

P = total pressure, atm

Pt = penetration (t not subscripted)

$\overline{Pt}$ = penetration integrated through particle size distribution (see Equation 8.2.5)

Pt_a = penetration based on "average size" method

Pt_c = penetration based on "cut size" method

Q_G = volume per unit time of gas processed, m^3/hr or cm^3/sec

Q_L = volume per unit time of liquid processed, ℓ/m^3

S = depth of cyclone gas exit duct, m or cm

t = thickness, cm

T = absolute temperature, °K

u_G = gas velocity, m/sec or cm/sec

w = weight, kg or g

w_c = total weight of particle sample, kg or g

X = d_{p50}/d_{pg}

Y = $f\ K_{Pt}$

z = defined in Equation 8.2-7

GREEK

τ = particle "relaxation time"

μ_G = viscosity of gas, poise

ρ_p = density of particle, g/cm^3

σ_g = standard deviation

REFERENCES - CHAPTER 8

Calvert, S. and K. L. Legatski, "A Comprehensive State-of-the-Art Evaluation for All Types of Dust Collection Equipment That May be Applicable in Underground Coal Mines," Contract No. S0100231, U.S. Bureau of Mines Open File Report 4-71, Dec. (1970).

Dallavalle, J. M., "How to Estimate Dust Collector Costs",in Cost Engineering in the Process Industries, C. H. Chilton, ed., McGraw Hill, New York (1960).

Ekman, F. O. and H. F. Johnstone, Ind. Eng. Chem. 43, 1358 (1951).

Engels, Lothar-Hans, "Expenditure and Performance of Various Processes for Dust Control - A Cost Evaluation", Staub 30, 3, p.23-28 March (1970).

Harris, L. S., "Energy and Efficiency Characteristics of the Ejector Venturi Scrubber", paper 64-35 presented at the 57th Annual Meeting of the Air Pollution Control Association, Houston, Texas, June (1964).

How, Harlan, "Short-Cut Estimation of Welded Process Vessels", in Cost Engineering in the Process Industries, C. H. Chilton, ed., McGraw Hill, New York (1960).

Midwest Research Institute, "Handbook of Emissions, Effluents and Control Practices for Stationary Particulate Pollution Sources", NAPCA Contract CPA 22-69-104, November 1970.

NAPCA, "Control Techniques for Particulate Air Pollutants", NAPCA Publication Number AP-51, Washington, D.C. (1969).

Perry, Robert H. ed. "Chemical Engineers Handbook", 4th edition, McGraw Hill, New York (1963).

Peters, Max S., and Klaus P. Timmerhaus, "Plant Design and Economics for Chemical Engineers", 2nd edition, McGraw Hill, New York, (1968).

Sargent, Gordon D. in "Modern Cost Engineering Techniques", Herbert Popper, editor, McGraw Hill, New York (1970).

Stairmand, C. J., "Removal of Grit, Dust and Fume from Exhaust Gases from Chemical Engineering Processes, The Chem. Eng. pp. 310-326 (Dec. 1965).

CHAPTER 9

DESIGN EXAMPLES

TABLE OF CONTENTS

9.1 Introduction 9-2

9.2 General Approach 9-2

9.3 Example Calculations 9-3

9.3.1 Particle Separation Calculations. 9-3

9.3.1.1 Plates 9-4
9.3.1.2 Packed Beds. 9-9
9.3.1.3 Fiber Bed. 9-11
9.3.1.4 Preformed Sprays 9-14
9.3.1.5 Gas Atomized Spray 9-19
9.3.1.6 Centrifugal. 9-21
9.3.1.7 Secondary Flow 9-23
9.3.1.8 Impingement and Entrainment. 9-25

9.3.2 Mass Transfer Calculations. 9-26

9.3.3 Mass Transfer With Chemical Reaction Calculations . 9-27

9.3.4 Example Problem: Coal Dryer Exhaust 9-27

9.3.5 Example Problem: Application of Diffusiophoresis and Particle Growth to a Rock Wool Cupola 9-33

9.3.6 Example Problem: Phosphoric Acid Plant Fluoride Scrubbing 9-40

9.4 Trouble Shooting 9-50

References 9-61

Nomenclature 9-58

CHAPTER 9

DESIGN EXAMPLES

9.1 INTRODUCTION

This chapter is for the purposes of clarifying the design methods, enabling the reader to check his calculation method for computational errors, and for tying a few loose ends. Most of the examples center on the scrubber performance itself and a few are fairly extensive. Mass transfer examples have been presented in Chapter 5 in many instances, for more effective relationship to the text, but they are listed under 9.3.2 to ensure that the reader can find them.

Some discussion of "trouble shooting", (i.e. the solution of operating problems) is given in Section 9.4. Recognition of the sorts of possible difficulties one may encounter has an obvious beneficial effect on the design of scrubbers. Thus the last part of this chapter serves as a reminder of the many factors besides scrubber efficiency to consider in system design, selection, operation, and maintenance.

9.2 GENERAL APPROACH

The design or the evaluation of a scrubber system may range from a quick check on a crucial point to a complete project development. To aid in the visualization and organization of the design work, the following outline of a general approach is presented. It is a fairly complete sequence of steps necessary for the design of a scrubber process.

I. Background information
   A. Process description
   B. Flow sheet showing stream compositions and quantities if available.
   C. Effluent description, composition and quantity.

II. Objective
   A. Air pollution regulation limit(s).
   B. Emission concentration or rate limit(s).
   C. Constraints on control method, other than performance requirement.

III. Method of Approach
   A. Explore any alternatives which are available either for process change or control.
   B. Gather what background knowledge exists for a scrubbing process.
      1. Process and equipment which have been tried or used.
      2. Data useful for scrubber design.
   C. Choose potentially suitable approach(es) for preliminary design review.

IV. Detailed design for each alternative

- A. Definition of the process
  - 1. Flow sheet for control process
  - 2. Equilibrium considerations
  - 3. Material balance
  - 4. Process conditions
  - 5. Heat balance
- B. Equipment sizing
  - 1. Set performance requirements (efficiency, cut diameter, or N.T.U.)
  - 2. Predict equipment performance for design conditions (such as cut diameter, HTU or stage efficiency)
  - 3. Compute capacity based parameters (e.g., diameter based on flooding)
- C. Predicted performance over range of design conditions
- D. Auxiliaries
- E. Materials of construction
- F. Power requirement
- G. Labor and maintenance
- H. Liquid supply and cost
- I. Liquid and solid waste disposal and costs
- J. Sampling and analysis
- K. Controls
- L. Health and Safety
- M. Overall costs
  - 1. Capital
  - 2. Operating
  - 3. Annualized

V. Conclusions

What process is best, if any, or what processes seem equally good.

- A. Optimization procedure
- B. Uncertainties
- C. Adaptability to possible new requirements or modifications.

9.3 EXAMPLE CALCULATIONS

9.3.1 PARTICLE SEPARATION CALCULATIONS

The problem of designing a scrubber for particle separation will be illustrated for the control of stone dust from an asphalt plant dryer. This dust is reported (MRI, 1970) as having quite a wide size distribution, as shown in 7.2.4.5 by σ_g=5.0 for d_{pg}=18 microns. Figure 9.3-1 is a log-probability plot of this size distribution. A typical plant (Danielson, 1967) has a capacity of 136 metric tons/hr and a flue gas rate of 34,000 am^3/hr (150 pound tons/hr and 20,000 acfm). Other conditions are: gas temperature = 116°C, dew point = 65°C, particle density = 2.6 g/cm^3, and uncontrolled emission rate = 2,310 Kg/hr.

If the Bay Area APCD process weight limit were used, the emission could not exceed 25 Kg/hr (55 lb/hr). The maximum penetration would be 25/2,310 = 0.0108; corresponding to about 99% efficiency. The use of Figure 5.3.1-4, estimated overall penetration vs. d_{p50}/d_{pg} with "σ_g" parameter, gives the cut diameter, $d_{p50} = 0.021 \quad 18 \approx 0.38$ microns. This corresponds to an aerodynamic cut diameter as shown below: (Figure 4.6.7-6 is a plot of this relationship)

$$d_{pa50} = d_{p50}\,(\rho_p\,C')^{1/2} = 0.38\left[(2.6)\left(1+\frac{.16}{.38}\right)\right]^{1/2} = 0.73\ \mu m\ (g/cm^3)^{1/2}$$

Several types of scrubbers will be investigated to see whether they could meet this performance and under what conditions. Some devices which would not ordinarily be considered for such a difficult job will be taken up, for the purpose of illustrating the computations. Quite often a pre-cleaner of moderate efficiency would be used to reduce the dust loading in the high-efficiency collector. This will be neglected in the examples given, because it would not substantially change the performance requirement for the high-efficiency unit.

9.3.1.1 Plates

Design methods are given in 5.3.2.2 and 5.3.2.3 for impingement and sieve (perforated) plates, which will be taken up here, sieves first.

Outline of Approach Shown for Sieve Plate

1. Determine the possible operating range of gas velocity between weeping and flooding. Assume reasonable parameters for the first trial. (We compute weeping velocity through 0.3 cm holes = 840 cm/sec and superficial velocity for flooding = 204 cm/sec).

2. Compute parameters required to achieve the required cut diameter of 0.73 μm $(g/cm^3)^{1/2}$. (The required cut diameter can be achieved in "N" stages if $N\,u_h/d_h = 4\times10^4\ [cm^{-1}]$).

3. Explore the possibilities for different combinations of plate and flow parameters to give the required cut diameter. (We conclude that 4 stages would be better than fewer stages with higher ratios of u_h/d_h).

4. Compute the pressure drop and column diameter required. (We compute a pressure drop of 48 cm W.C. and a column diameter of 3.7 m).

5. Check the possible contribution of collection by particle diffusion. (We estimate a negligible effect because of the small percentage of dust smaller than 0.1 μm).

The weeping velocity is taken from Equation 5.2.2-4, as modified below:

$$u_h^2 = \left(\frac{u_s}{f_h}\right)^2 = 10g\,d_h\left(\frac{\rho_L}{\rho_G}\right)\left(\frac{\mu_W}{\mu_L}\right)^{0.16}\exp\left[-4\left(\frac{L}{G}\right)^{0.25}\left(\frac{\rho_G}{\rho_L}\right)^{0.125}\right] \qquad (9.3\text{-}1)$$

Where: u_h = gas velocity in hole (cm/sec).

The gas density is computed on the basis of 25% (mole) H_2O, corresponding to the 65°C dew point, which leads to an average molecular weight of $(.75)30+(.25)\ 18 = 27$. At 116°C and 760 mm Hg, the gas density is 850 g/m^3 (0.053 lb/ft^3). If L/G corresponds to the common water to gas ratio of 1 ℓ/m^3, it will have a value of $(1{,}000/850) \approx 1$. Taking the viscosity of the liquid to be the same as pure water, $(\mu_W/\mu_L) = 1$. If the hole diameter is about 0.3 cm (1/8") the computed hole velocity is 840 cm/sec (27.5 ft/sec).

Flooding velocity is computed according to Equation 5.2.2-3 and Table 5.2.2-1 (compute "K" from tabulated "ψ") as given below:

$$u_{s,max} = K \left(\frac{\rho_L - \rho_G}{\rho_G}\right)^{1/2} = 6.0 \left(\frac{1{,}000 - 0.85}{0.85}\right)^{1/2} = 204 \text{ cm/sec} (6.7 \text{ ft/sec}) \qquad (9.3\text{-}2)$$

The next step is to compute penetration for velocities ranging between weeping and flooding. To compute the cut diameter for a given velocity/hole size combination, or visa-versa one can use Equation 4.6.4-1, as follows for "N" plates in series;

$$N \ln(Pt) = -40F^2\ K_p\ N = \ln 0.5 = -0.693 = -40F^2 N \left(\frac{d_{pa}^2\ u \text{x} 10^{-8}}{9\ \mu_G\ d_h}\right) \qquad (9.3\text{-}3)$$

For this example, we will not compute the effect of diffusional collection, considering it to be a safety factor which can be accounted for later.

The froth density, F, may be approximated from Figure 4.4.1-3 for a superficial gas velocity of 100 cm/sec (3.3 ft/sec) to be about 0.4. Figure 9.3-2 presents the relationship between K_p, d_{pa}, and u_h/r_h in convenient form and either it or Equation 4.6.2-5 can be used to obtain values of $N(u_h/d_h)$ corresponding to $d_{pa_{50}} = 0.73\ \mu m\ (g/cm^3)^{1/2}$.

$$NK_p = \frac{0.693}{40(0.4)^2} = N \left[\frac{(.73)^2\ u_h\ 10^{-8}}{9(2.15 \text{x} 10^{-4}) d_h}\right] = N \left(\frac{u_h}{d_h}\right) \quad (2.75 \text{x} 10^{-6})$$

So:

$$N(u_h/d_h) = \frac{0.108 \text{x} 10^6}{2.75} \simeq 4.0 \text{x} 10^4 \ (\text{sec}^{-1}) \qquad (9.3\text{-}4)$$

Alternatively, Figure 9.3-2 shows $(u/r_c) = 6.5\text{x}10^4$ for $d_{pa} = 0.73\ \mu m\ (g/cm^3)^{1/2}$ and $K_p = 0.108$. This corresponds to $N(u_h/d_h) = 6.5/2)\text{x}10^4$ for $NK_p = 0.108$. It is necessary to introduce a gas viscosity correction because Figure 9.3-2 is for standard air with 0.018 centipoise viscosity while the gas (estimated as air) at 116°C has a viscosity of 0.0215 centipoise. As Equation 4.6.2-5 indicates, the corrected $(u_h/d_h) = (2.15/1.8)\ 3.25\text{x}10^4 = 3.9\text{x}10^4$. This checks the computed value within the error of reading the plot. The interpolation line (dashed) in Figure 9.3-2 is used for finding parameter values between the powers of 10, as illustrated by the construction for this example.

Note that the relationship between overall penetration and cut diameter as given in Figure 5.3.1-4 is approximate for this type of collector, because penetration is proportional to $\exp\ [-d_p{}^2]$, only for the first stage. Particles emerging from the first stage are not normally distributed anymore.

Figure 5.3.2-9 can also be used for determining performance cut diameter for one stage, although the necessary velocity for this example would be off-scale for F=0.4.

We can now explore the consequences of using various combinations of N, u_h, and d_h. If one used u_h=3,000 cm/sec (about 100 ft/sec), which exceeds the weeping velocity, and d_h=0.3 cm, then N=4 plates. Because the pressure drop for the dry plate varies as $(u_h)^2$, it will probably be better to use 4 stages rather than 1 stage at 4 times the velocity (thus having 4 times the single dry plate pressure drop rather than 16 times). Furthermore, the hole velocity is higher than usual practice and the hole diameter is smaller. Considering possible problems with either blowing the liquid away from the holes, or plugging small holes, it is prudent to use more stages rather than a higher (u_h/d_h).

Pressure drop for the dry sieve plate can be estimated by the method of Perry's Handbook (1963, page 18-12, equation 18-14). Also see Section 5.3.2.3). This is an orifice pressure drop equation and the coefficient of discharge, a function of plate thickness and percent free area, can be approximated as C_o = 0.7 for this type of plate. In C.G.S. units the pressure drop is given by:

$$\frac{\Delta Pd}{\rho_{H_2O}} = \left(\frac{u_h}{C_o}\right)^2 \left(\frac{\rho_G}{2g\ \rho_{H_2O}}\right) = \left(\frac{3{,}000}{0.7}\right)^2 \left[\frac{8.5\text{x}10^{-4}}{2(980)}\right] = 8.0 \text{ mbar} \approx 8 \text{ cm W.C.} \tag{9.3-5}$$

The total pressure drop per plate will be approximately the sum of the dry plate and the foam head contributions. Assuming that the foam density is 0.4 and the height is 10 cm, the total pressure drop would be about = 8.0 + 10(0.4) = 12 mbar (4.7 in W.C.), and the total pressure drop for a four plate tower would be four times as much, 48 mbar (18.8 in W.C.).

Column diameter can be estimated on the basis of the foam density desired, so long as the superficial gas velocity is below the flooding velocity. Equation 4.4.1-10 can be solved for a foam density of about 0.4.

$$-\ln(1-h_g) = 0.184\ v_s \sqrt{\rho_g} + 0.45 = -\ln\ (0.4) = 0.915 =$$

$$= 0.184\ v_s\ (8.5\text{x}10^{-4})^{1/2} + 0.45 = 5.3\text{x}10^{-3}\ v_s + 0.45$$

$$v_s = \frac{0.465}{5.3\text{x}10^{-3}} = 88 \text{ cm/sec } (2.91 \text{ ft/sec}) \tag{9.3-6}$$

If "v_s" is 88 cm/sec and the hole velocity, v_h = 3,000 cm/sec, the gross percent free area would be (88/3,000) 100≈2.9%. This is lower than for the usual sieve plate, but not excessively so. For this superficial velocity the plate area would be 34,000/3,600 (0.88) = 10.7 m², corresponding to a diameter of 3.7 m.

Diffusion

Diffusional collection can be accounted for at this point, although for the dust size distribution chosen for the example it will not have much effect on overall collection efficiency. Equation 4.6.4-10 can be solved to indicate the contribution of diffusion alone. If foam height is taken as 10 cm, bubble radius as 0.23 cm, and bubble rise velocity as 30 cm/sec, we have:

$$\ln Pt_D = -1.87(10)\left[\frac{Dp}{(0.23)^3\ 30}\right]^{0.5} = -31\ (Dp)^{0.5} \qquad (9.3\text{-}7)$$

Thus if $Dp = 10^{-6}$ cm^2/sec corresponding to a particle diameter of 0.4 μm, $Pt_D = 0.97$ and if $Dp = 10^{-5}$ cm^2/sec corresponding to dp=0.1 μm $Pt_D = 0.91$. The overall effect of diffusion and inertia can be calculated by means of Equation 5.3.2-11, if desired. It is obvious that for this example, where 1% of the dust is smaller than 0.43 μm and 0.06% smaller than 0.1 μm, diffusion could account for only a few hundredths percent of the total dust.

Impingement Plate

Impingement plate design, as discussed in 5.3.2.2, should ideally be based on the conservative basis of what can be rationalized, rather than undefined test data. This implies that one can have more confidence in what can be predicted for collection from jets than in the performance data given in figures 5.3.2-3, -4, and -5. As a first estimate, one could use the sieve plate design to approximate the performance of an impingement plate. A more specific approach is to predict performance based on impaction from round jets. The steps involved in the following example are:

1. Estimate velocity and hole size to provide the required cut diameter, based on impaction from round jets. (We compute $u_h/r_h = 1.44\text{x}10^5$ [sec^{-1}]).

2. Compare velocity to hole size ratio with customary values for impingement plates. (The necessary ratio is ten times higher than usual.)

3. Determine whether velocity and hole size can be adjusted enough to give the required performance. Also check the possibility of using more than one stage. Because the performance can not accurately be estimated by the cut diameter approach for "N" stages, use the graphical integration method of determining penetration. (We find that with $u_h/r_h = 2.86\text{x}10^4$ the penetration for one stage is 0.032 and for four stages is 0.029.

First, see what velocity and hole size would be required for $d_{pa_{50}}$=0.73 μm(g/cm^3)$^{1/2}$. The value of "K_p" for 50% penetration, $K_{p_{50}}$ is about 0.2, as shown in Figure 4.6.7-4 and as discussed in 4.6.7.2. Using Figure 9.3-2 for convenience (and adding a gas viscosity correction), one finds $u/r_c(=u_h/r_h)$ of $1.2\text{x}10^5$ for $\mu_G=1.8\text{x}10^{-4}$ poise. For $\mu_G=2.15\text{x}10^{-4}$ poise, $u_h/r_h=(2.15/1.8)\ 1.2\text{x}10^5$ $=1.44\text{x}10^5$ sec^{-1}. What does this lead to?

If a standard type of impingement plate were used, the gas velocity based on hole area would be about 1,500 cm/sec (50'/sec) and the velocity of the gas jet at the vena contracta would be about (1,500/.75 = 2,150 cm/sec (72 ft/sec). Perforation diameter usually is 3/16" = 0.475 cm. Thus the "standard" u_h/r_h = 2,150/0.238≈9x10³; nearly 10^4 sec^{-1}. This is over an order of magnitude lower than needed for d_{pa50} = 0.73, μm $(g/cm^3)^{1/2}$.

The velocity might be doubled and the hole diameter decreased to 0.3 cm, so that (u_h/r_h) would become (4,300/0.15) = 2.86x10⁴ sec^{-1}. This would be 2.4x10⁴ at std. viscosity and d_{pa50} = 1.6 μm $(g/cm^3)^{1/2}$ (at K_{p50} = 0.2). Figure 5.3.2-7 can also be used to find performance cut diameter as a function of hole velocity and diameter.

Some other values for several particle sizes are tabulated below for (u_h/r_h) = 2.4x10⁴. Values of $\sqrt{K_{p50}}$ at various penetrations are taken from Figure 4.6.7-4 at β = 1.0. The ratio of $(K_p/K_{p50})^{0.5}$ = (d_{pa}/d_{pa50}), so the diameters at various penetrations can be calculated from d_{pa50}. For "N" stages of impaction, the penetration is equal to that for 1 stage raised to the N'th power.

Pt	0.1	.3	.5	.8	.9	.95	.99
$K_p^{0.5}$	0.5	0.46	0.44	0.42	.4	0.37	.35
$(K_p/K_{p50})^{0.5}$	1.14	1.045	1.0	0.955	0.91	0.84	.8
d_{pa}	1.83	1.67	1.6	1.53	1.46	1.34	1.27
Pt^2	0.01		0.25	.64	0.81	0.90	.98
Pt^3	0.001		0.125	.51	0.73	0.86	.97
Pt^4	0.0001		0.0625	.41	0.66	0.815	.96
d_p	1.05	0.96	0.92	0.88	0.84	0.77	.73
$Fr<d_p$	0.04	.035	0.032	0.03	0.028	0.026	.023

The last two rows in the computation table are d_p, actual particle size at ρ_p=2.6 g/cm³, and $Fr<d_p$, the weight fraction of dust smaller than each value of "d_p". By plotting penetration for a given "d_p" against the $Fr<d_p$, it is possible to compute overall penetration by means of a graphical integration (see 5.3.1).

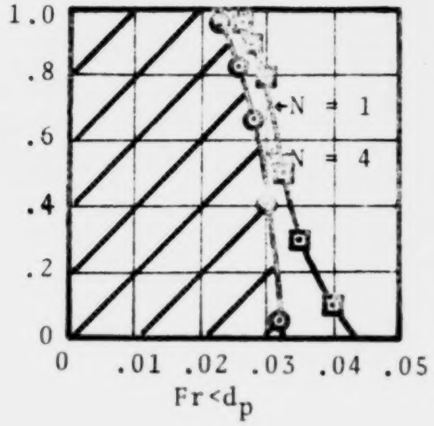

The plot shown here is for N=1 and N=4 stages. The area under the curve (hatched) is the integral for four stages.

$$\int_{d_p=0}^{\infty} Pt\ f\ (d_p)\ d\ (d_p) \quad (9.3\text{-}8)$$

The area under the curve has a value of about 0.029 = $\overline{Pt}$. Also plotted in this figure is the penetration vs. Fr<d_p relationship for one plate instead of four in series. If one plate instead of four is used, overall penetration increases from 0.029 to 0.032. The last three plates, then, do very little collecting as all together they capture only 0.3% of the dust.

Adding additional plates beyond four will have a similarly small effect. This is due to the sharp "cut" effect of a jet impactor at its cut size. If the particle size-penetration relationship for the collector did not increase as steeply at the cut particle size, the addition of more plates would have more of an effect on overall penetration.

Pressure drop for this velocity should be 4x that for standard operation because it should vary as about the square of velocity. It should also be about the same as previously computed for a single sieve plate at the same velocity of 3,000 cm/sec; ΔP = 12 mbar (4.7" W.C.). A column of four impingement plates will than have a total pressure drop of 4 x 12 = 48 mbar (18.8" W.C.).

The penetration predictions made above were based on collection from round jets and this is not nearly as efficient as the performance curves shown in Figures 5.3.2-3, -4, and -5. One might accept these figures as being correct and compute penetrations by the graphical integration method. However, the performance claimed is so good that one hesitates to believe it. For example Figure 5.3.2-5 shows a cut diameter of about 0.35 μm for dust with a density of 2.7, which corresponds to an aerodynamic cut diameter of about 0.7 μm $(g/cm^3)^{1/2}$.

If we now look at figure 5.3.6-13 we see that a venturi would come nowhere near this cut size at a pressure drop of 4 cm W.C. Because the predicted pressure drop shown in Figure 5.3.6-13 is that required for the acceleration of water drops, we can assume that it will also be a measure of the Q_L/Q_G resulting from the atomization of liquid on the impingement plate. Thus the cut diameter corresponding to about 2,000 cm/sec and 4 cm W.C. for a venturi would approximate that for an impingement plate and would be perhaps 2.0 μm $(g/cm^3)^{1/2}$. We are unable to resolve the question of whether impingement plates are capable of efficiency as good as shown in Figure 5.3.2-5 or not, so one would have to rely on a realistic test to settle the issue.

9.3.1.2 Packed Beds

A packed bed might be used to collect particles of the sizes coming from the asphalt plant drier. However, packed beds are usually used for liquid mists rather than solid particles, to preclude plugging problems within the bed. To counteract particle buildup within the packed bed, it can be washed with liquid either continuously or discontinuously. Since equilibrium considerations are not involved, the contact may be co-, counter-, or cross-current.

In the example below we will explore the possibility of using a packed bed by means of the following steps:

1. Find the required separation cut size as in previous examples. ($d_{pa_{50}}$=0.73).

2. Estimate packed bed characteristics from Figure 5.3.3-2a. (A 300 cm deep bed of 2.5 cm packing with porosity of 0.75 would provide the required performance at an air velocity of 450 cm/sec).

3. Select packing with appropriate characteristics (2.5 cm Raschig Rings would do).

4. Determine bed diameter from flow rate and velocity (we compute 2.72 m).

Section5.3.3, which describes particle collection in packed beds, shows that penetration bears the following relationship to particle size (see Equations 5.3.3-4 and 5.3.3-5):

$$Pt \ \alpha \ \exp(-d_p^2) \qquad (9.3\text{-}9)$$

As was discussed in Section 9.3-1, the stone dust has a log-normal distribution, with d_{pg} = 18 µm and σ_g = 5. For equipment such as packed beds, whose performance is described by Equation 9.3-9, operating on log-normal dust, Figure 5.3.1-4 shows it will be necessary to achieve a particle cut size, d_{p50}, of 0.38 µm. Figure 5.3.1-4 is a plot of overall penetration (taken as 1% here) versus d_{p50}/d_{pg} with σg as parameter. The 0.38 µm cut size corresponds to an aerodynamic cut size, d_{pa50} of 0.73 µm $(g/cm^3)^{1/2}$.

With aerodynamic cut size established, the height of the packed bed can be found from Figure 5.3.3-2a, a plot of d_{pa50} versus bed height, with packing diameter and gas velocity as parameters. The figure shows that for the aerodynamic cut size necessary, the bed height should be about 300 cm (10 ft). Velocity could be 450 cm/sec (15 ft/sec), and 2.5 cm (1 inch) packing material with bed porosity of 0.75 should be used. Table 5.3.3-1 shows that Raschig rings might fit these requirements. Alternatively, one could use a lower velocity and a deeper bed, or a lower velocity and smaller packing. If Figures 5.3.3-2 a and b do not include the desired range of variables, one can useEquation 5.3.3-4 as illustrated in 5.3.3.

The problem states that 34,000 m³/hr 20,000 acfm) of gas are to be processed. Since gas velocity was established at 450 cm/sec, the diameter of a suitable tower can be found:

$$d = \sqrt{\frac{4Q_G}{V_G}} = \sqrt{\frac{4 \ 30{,}000 \ \frac{m^3}{hr}}{4.5 \ \frac{m}{sec} x 3{,}600 \ \frac{sec}{hr}}} = 2.72 \text{ m (9 ft)} \qquad (9.3\text{-}10)$$

The specifications for a suitable packed tower, and the key figure or equation from which they were calculated are summarized below:

Item	Size	Source
Necessary Particle "Cut Diameter"	0.38 μm	Figure 5.3.1-4
Necessary Particle "Aerodynamic Cut Dia."	0.73 μm $(g/cm^3)^{1/2}$	Figure 4.6.7-6
Bed Height	300 cm	Figure 5.3.3-2a
Gas Velocity	450 cm/sec	Figure 5.3.3-2a
Packing Material	2.5 cm (1 inch) Raschig Rings	Figure 5.3.3-2a Table 5.3.3-1
Bed Diameter	2.7 m (9 ft)	Equation 9.3-10

9.3.1.3 Fiber Bed

A fiber bed, like the packed bed discussed in the previous section, is usually used to collect liquid mists and low concentrations of solid particles. This is because the fibers have a tendency to clog as collected material accumulates, resulting in loss of efficiency and buildup of pressure drop. A liquid washing over the fibers helps remove collected particles from the bed; however, this might not be sufficient to remove all particles collected. A fiber bed for the effluent from an asphalt plant drier would have to include provision for easy access to and replacement of the fiber bed elements.

Section 5.3.4 describes the methods which can be used to calculate the particle collection efficiency of a fiber bed collector. Figures 5.3.4-2 through 5.3.4-5 are plots of single fiber efficiency, η_s, against particle diameter, for various gas velocities through the bed, and various fiber diameters. As the stone dust to be collected is relatively coarse, large, strong collecting fibers should be used. Figure 5.3.4-5 is a single fiber efficiency plot for 256 μm (0.01 in) fibers, which should be suitable. Screen made of 0.011 in. wire is commonly available and would be a low cost material to consider for fabrication into panels. Choose a velocity through the bed of 25 cm/sec, as this is the highest velocity plotted. Higher velocities result in both better collection efficiency (for large particles) and a smaller bed.

The figure is for particles of density of 1 g/cm^3, while the density of the rock dust is about 2.6. Collection efficiency on the more dense rock particles will be higher than the figure predicts, and add a "bonus" or "safety factor" to the design. The temperature of the effluent gas will be higher than the 300°K for which the figure was made, and tend to lower efficiency as can be seen through the appropriate equations in Section 5.3-4. This effect should be more than compensated for the the "safety factor" due to increased particle density.

Remembering that penetration is one minus efficiency, Equation 5.3.4-1 shows that collection of particles of a given size will be:

$$Pt = \exp(-\eta_s S) \qquad (5.3.4\text{-}1)$$

where "S" is the "solidarity factor" given by:

$$S = \frac{4\ell\alpha}{\pi d_f} = 1.49\ell \qquad (5.3.4\text{-}2)$$

for a bed solid fraction (α) of 0.03, and where bed thickness, ℓ, is in centimeters.

Combining Equations 5.3.4-1 and 5.3.4-2 finds:

$$Pt = \exp[-1.49\ell\ \eta_s] \qquad (9.3\text{-}11)$$

Single fiber efficiency, η_s, is related to particle diameter through Figure 5.3.4-5, while cumulative weight of particles is related to particle size through Figure 9.3-1. It is now necessary to solve for bed depth, ℓ, by trial and error. First select a value for "ℓ", then calculate its penetration versus particle size relationship via Equation 9.3-11, getting values of "η_s" from Figure 5.3.4-5. Then compute the overall penetration of the collector on the size distribution of particles in a manner similar to that done for plate scrubbers in Section 9.3.1.1. If the overall penetration is greater than 1%, choose a larger value for "ℓ", and repeat the same steps, until a suitable value for "ℓ" is found. The steps in the trial and error solution are described below. As a first approximation for "ℓ", assume a particle cut diameter of about 0.5 μm will be necessary. This fixes "η_s" at 0.0013. If this is the case, then "ℓ" can be calculated:

$$0.5 = 1 - \exp(-1.49\ \ell\ 0.0013)$$

$$\ell = 350\text{ cm}$$

Trial and Error Steps for Calculating Bed Depth, "ℓ"

ℓ	d_p (μm)	η_s	Pt	$Fr<d_p$	Overall Pt
350	0.5	0.0015	0.4580	0.014	0.024
	1.0	0.0021	0.3350	0.038	
	2.0	0.0070	0.0260	0.088	
	3.0	0.0160	0.0002	0.135	
	4.0	0.0300	~ 0	0.177	
700	0.5	0.0015	0.210	0.014	0.009
	1.0	0.0021	0.112	0.038	
	2.0	0.0070	0.007	0.088	
	3.0	0.0160	~ 0	0.135	
	4.0	0.0300	~ 0	0.177	

A plot of "Pt" versus $Fr< d_p$ is given below. To collect 99% of the dust, it is necessary to have a fiber bed about seven meters (23 ft) long.

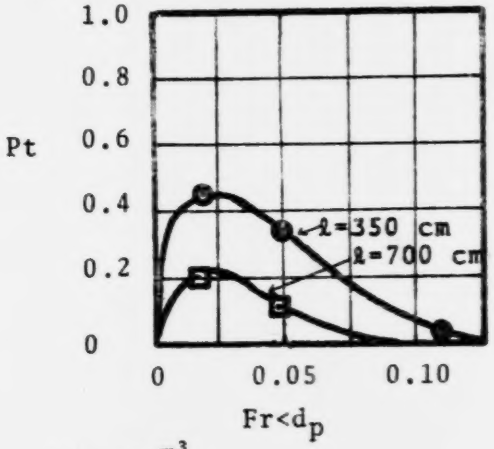

The area of the bed can be calculated, as the throughput (34,000 m^3 /hror 20,000 acfm) is known, as is the gas velocity, 25 cm/sec (900 m/hr).

$$A = \frac{Q_G}{V_G} \quad \frac{34{,}000 \ \frac{m^3}{hr}}{900 \ \frac{m}{hr}} = 38 \ m^2 \qquad (9.3\text{-}12)$$

A square bed, 6.2 m (29 ft) on a side will do. The overall dimensions are then 6.2 x 6.2 x 7 m; this is a huge unit, and further demonstrates the inapplicability of a fiber bed with low gas velocity for this application. If smaller fibers could have been used (and higher velocities) the bed would have been much smaller.

If a bed of 100 μm (4 mil.) diameter fibers and a gas velocity of 600 cm/sec (20 ft/sec) were used, the required penetration could be achieved, in a much smaller bed. Because the fiber Reynolds number would be 24, which is in the transition region, collection efficiencies will have to be computed by a different method than in the preceeding (laminar flow) case Section 4.6.3 should be consulted and Equation 4.6.3-1 with Figure 4.6.3-1 used for finding inertial efficiencies and Equation 4.6.3-5 used for interception. The efficiencies for impaction and interception are added to yield "η_S", which is then used in Equation 5.3.4-1, as before.

Some computational steps are tabulated below.

d_{pa}	0.5	0.8	1.	2	4
η_p	0.0007	0.01	0.032	0.32	0.82
η_I	0.0044	0.0093	0.012	0.023	.01
η_{pI}	0.005	0.02	0.033	0.34	0.83

Use of the graphical integration technique for solving Equation 9.3-11 yields overall penetrations of 0.022 for a 10 cm deep bed and 0.011 for a 20 cm bed. Thus, a fiber bed somewhat deeper than 20 cm (take 25 cm or 10 in) and with a porosity of 97% would do the job.

9.3.1.4 Preformed Sprays

Two types of preformed spray scrubbers will be considered; counter-flow and cross-flow. Design methods are given in Section 5.3.5 and some performance cut diameter predictions are given in Figures 5.3.5-1 and 5.3.5-2. It can be seen from the performance figures that spray chambers do not appear to have the capability of achieving a $d_{pa50}=0.73$. Nevertheless, we will go through the design calculations and explore the possibilities for finding better operating conditions than used in preparing Figures 5.3.5-1 and -2.

The computational steps shown below are as follows:

1. Compute or estimate the gas phase conditions as affected by simultaneous heat and mass transfer with the liquid. (We assume that the gas rapidly approaches saturation at the inlet liquid temperature).

2. Assume a drop size and water rate. (For illustration, we chose 200 and 400 μm drop diameters and $Q_L/Q_G = 1\ \ell/m^3$)

3. For counter-flow, assume a chamber height. (We chose 3 m as an arbitrary starting point).

4. Assume gas velocities to suit the spray drop diameters and the corresponding settling velocities. (We used 50 cm/sec for 200 μm dia drops and 120 cm/sec for 400 μm dia drops).

5. Assume what fraction of the spray will be effective because of wall losses. There is no rational method of computation available. (We assume an ultra-conservative value of 10% utilization, a probable value of >20%, and perform computations for these and for 30% and 100% utilization).

6. Compute penetration for several particle sizes based on inertial impaction. Compute efficiencies for single drops based on a compensation for the "N_{Re}" of the falling drop. (Results are tabulated).

7. Compute overall penetration for the dryer dust size distribution by means of the graphical integration technique. (Results are plotted for 400 μm dia drops at 10, 20, 30, and 100% spray utilization and for 200 μm dia drops at 10% utilization).

8. Perform a similar set of calculations for a cross-flow spray scrubber. (Assume that the gas reaches the cocurrent equilibrium temperature. Arbitrarily choose a gas velocity of 1 m/sec, so the corresponding cross-sectional area is 7.67 m² and we assume a height of 3 m for the spray to fall).

9. Estimate performance for cross-flow based on inertial impaction. (We compute overall penetration = 0.2 for 400 μm drops, the dryer dust size distribution, and 20% utilization of spray).

10. Compute pressure drop for counter-flow based on the weight of liquid holdup and for cross-flow based on the rate of momentum transfer to the spray. (We find a pressure drop of 0.85 cm W.C. for 400 μm dia. spray, assuming 100% utilization and the other conditions of the example for counter-flow. For cross-flow we compute 0.01 cm W.C.)

11. Estimate the effect of Brownian diffusion. A particle diameter of 0.1 μm is used for a starting point because if diffusion will not do much at this size there is no point in making computations for larger particles. (We compute Pt = 0.982 for 0.1 μm dia particles and abandon any further computation).

Counter-Flow

For pre-formed spray scrubbers the gas-liquid contact time is long. In the case of counter-flow, it can be assumed that the gas temperature will approach the inlet liquid temperature and that the outlet gas will be saturated at that temperature.

We will assume that nozzles can be selected such that the spray size is near the optimum of about 500 μm diameter. Because of the uncertainty of the drop size distribution, however, we will compute penetrations for d_d = 0.02 and 0.04 cm. As a first trial, we will pick $Q_L/Q_G = 1$ (ℓ/m³) ≈(7.5 gal/MCF) and a chamber height of Z = 3.0 m (≈10 ft). Drop terminal settling velocities and "N_{Re}" can be taken from Figure 4.6.2-4 because the gas density and viscosity will be nearly standard. For $d_d = 0.02$, $u_t = 72$ cm/sec and a gas velocity $u_G \approx 50$ cm/sec is chosen in order to have as high a throughput as possible without getting so close to terminal velocity that performance is sensitive to "u_G". For $d_d = 0.04$, $u_t = 162$ cm/sec and "u_G" is chosen = 120 cm/sec.

Penetration is given by Equation 5.3.5-13. Note that only a fraction of the water is effective; the remainder strikes the scrubber walls. To be ultra-conservative, assume that only 10% of the spray is effective. This is about half that we estimate for the mass transfer studies of Pigford and Pyle (1958) on an 80 cm (31") diameter column. Even 20% would probably be too low for as large a cross-section as would be needed here. However, as will be seen, we can easily determine the effect of better use of water. Unfortunately, we have no way of predicting the wall losses with any confidence.

$$-\ln Pt = \frac{3\ (0.1)\ Q_L\ u_t\ \eta_p\ Z}{4\ Q_G\ r_d\ (u_t - u_G)} = \frac{3\ \ 0.1\ (10^{-3})\ u_t\ (300)}{4\ (72-50)} \left(\frac{\eta_p}{r_d}\right)$$

$$-\ln (Pt) = 0.0735 \left(\frac{\eta_p}{r_d}\right) \text{ for } r_d = 0.01 \text{ cm (i.e., 200 μm dia drops)} \qquad (9.3\text{-}13)$$

$$\text{and } -\ln Pt = 0.09 \left(\frac{\eta_p}{r_d}\right) \text{ for } r_d = 0.02 \text{ cm (i.e., 400 μm dia drops)} \qquad (9.3\text{-}14)$$

Values of (η_p/r_d) can be taken from Figure 4.6.2-5, or computed as described in Section 4.6.2. Drop N_{Re} for settling drops are so low that the collection efficiency must be adjusted from that given for potential flow. The Langmuir interpolation formula is used.

Computation steps and values obtained for Equations 9.3-13 and -14 for the two drop sizes with 10% water effectiveness are shown in the tables below. The plot of "Pt" vs. weight fraction undersize ($Fr<d_p$) is used for the graphical integration method as described in 5.3.1. Lines are shown for r_d=0.01 cm with 10% utilization of spray and for r_d=0.02 cm with 10%, 20%, 30% and 100% utilization. Note that Lx2 means 20% utilization, Lx3 means 30%, and Lx10 means 100%. The apparent (input) liquid to gas ratio is $Q_L/Q_G = 1\ \ell/m^3$ in all cases.

The overall penetrations computed by graphical integration are:

r_d (cm)	% Spray Utilization	$\overline{Pt}$
0.01	10	0.17
0.02	10	0.16
0.02	20	0.12
0.02	30	0.11
0.02	100	0.07

Note that Figure 5.3.5-1 (d) shows a cut diameter of about 2.7 μm $(g/cm^3)^{1/2}$ for $Q_L/Q_G = \ell/m^3$, d_d = 0.05 cm, Z = 300 cm. and u_G = 90 cm/sec. These conditions are close to those used in this example, so it is interesting to compare the cut diameter found for 100% utilization. The plot shown below indicates $\overline{Pt}$ = 0.5 for $Fr<d_p \approx 0.07$. If we look at Figure 9.3-1, we find that this fraction undersize corresponds to about 1.7 μm. Conversion of this to aerodynamic diameter yields 2.8 μm· $(g/cm^3)^{1/2}$, which is nearly identical with the performance cut diameter shown by Figure 5.3.5-1.

For r_d = 0.01 cm

d_{pa}	2	3		6	8	10
η_p/r_d	0	0.3	2.	10	19	28
0.0735 η_p/r_d	0	0.022	1.47	.735	1.4	2.06
Pt	1.	0.98	0.86	0.48	.25	0.13

For r_d = 0.02

d_{pa}	2	3	4	6	8	10
η_p/r_d	0	0.85	3	12	18	23.5
0.09 η_p/r_d	0	.0765	0.27	1.08	1.62	2.1
Pt	1.0	0.93	0.76	0.34	0.2	0.12
d_p	1.17	1.8	2.4	3.7	4.9	6.2
$Fr<d_p$	0.045	0.076	0.11	0.165	0.21	0.25

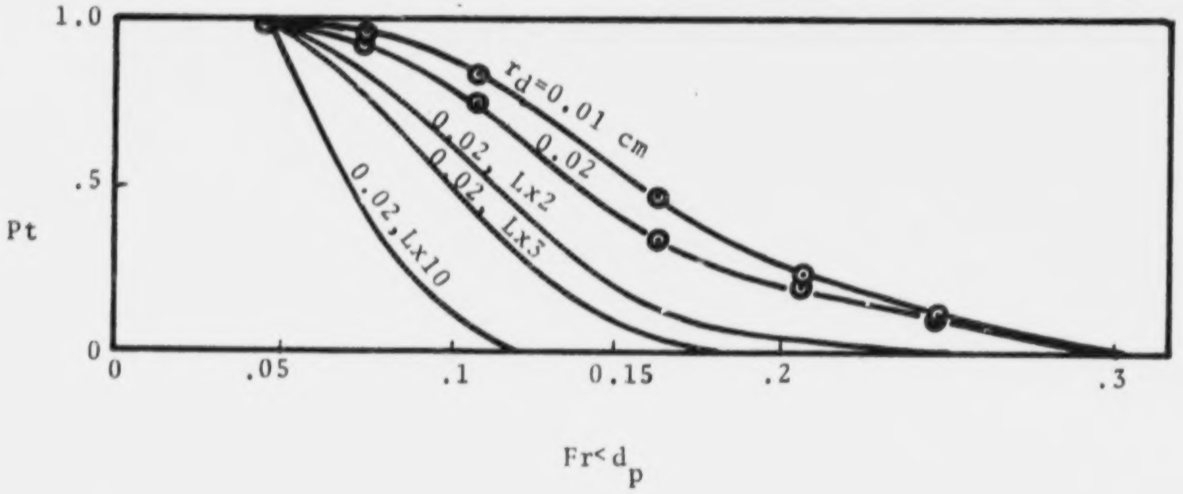

Cross-Flow

A cross-flow spray might use about the same water rate (Q_L/Q_G=1.0 ℓ/m^3) as chosen before. To get some idea of the scrubber cross-sectional area, and therefore height, we need to know gas flow rate at temperature and gas velocity. If the water enters at 38°C (100°F), the gas will rapidly reach its adiabatic saturation temperature of 68°C (154°F) and shortly reach the cocurrent equilibrium temperature of 43°C (110°F). If in countercurrent flow it could eventually reach the inlet water temperature. We will assume that it is at 43°C throughout the chamber. Thus the gas flow rate becomes 34,000 (316/389)/3,600=7.67 m^3/sec (271 C.F.S.).

If a gas velocity of 1 m/sec is used, the chamber could be 2.77 m x 2.77 m square. Take h=300 cm, for illustration. Penetration is given by Equation 5.3.5-23. Assume that spray utilization is 20%, rather than 10% as for counter-flow, because the drop velocity is higher (=u_t) than for counter-flow and the drops have less time to move sideways to the wall.

$$-\ln Pt = \frac{3\ (0.2)\ Q_L\ h\ \eta_p}{4\ Q_G\ r_d} = 0.15\times10^{-3}\ (300)\left(\frac{\eta_p}{r_d}\right) = 0.045\left(\frac{\eta_p}{r_d}\right) \qquad (9.3\text{-}15)$$

For r_d = 0.02, integration of the penetration computed by Equation 9.3-15 over the entire dust distribution, as for the counter-flow case gives $\overline{Pt}$ = 0.2. While variation of liquid rate and chamber size are possible, they will only produce limited results, (using 5 times the liquid rate chosen would decrease overall penetration to about 0.12). Efficiency is basically tied to the efficiency of the falling drop and the only thing which can be done is to use an optimum drop size if possible. The effect of increased liquid rate is to "sharpen" the cut between the particle sizes which are either completely removed or not removed.

We can compare the performance cut diameter shown in Figure 5.3.5-2(a) with the results of the present computations. If we assume 100% spray utilization and evaluate Equation 9.3-15 for Pt=0.5, we find $(\eta_p/r_d) \approx 3.1$. Inspection of the table of computations for counter-flow with r_d=0.02 cm shows that this ratio of single drop efficiency to drop radius occurs for an aerodynamic particle diameter of 4 μm $(g/cm^3)^{1/2}$. Figure 5.3.5-2(a) is for the same Q_L/Q_G and it shows a performance cut diameter of 3.6 for 500 μm drop diameter and 4.3 for 200 μm drop diameter.

As also noted above for counter-flow, the performance cut diameter predictions of plots such as 5.3.5-2 are quite reliable approximations to the results of detailed calculations. For the example being illustrated, a spray chamber will not give the required performance, but might make a good pre-cleaner. Flux force effects such as diffusio-, thermo-, and electro-phoresis can change this situation. Two other points remaining to be touched on are the prediction of pressure drop and of Brownian diffusional collection.

Pressure Drop

Pressure drop for a vertical counter-flow spray may be predicted as that required to support the liquid holdup. The volume fraction liquid holdup is given by:

$$Hd = \frac{Q_L}{u_d A} = \frac{Q_L}{(u_t - u_G)\ A} = \left(\frac{Q_L}{Q_G}\right) \frac{u_G}{(u_t - u_G)} = \frac{10^{-3}\ m^3/m^3\ (50)\ cm/sec}{(72-50)\ cm/sec} \simeq$$

$$\simeq 2.3x10^{-3} \text{ for } r_d = 0.01 \text{ and } = \frac{120x10^{-3}}{(162-120)} = 2.8x10^{-3} \text{ for } r_d = 0.02 \qquad (9.3\text{-}16)$$

The "head" of a column of drops supported by gas flow is Hd ρ_L $(g/cm^2\text{-}cm)$. Thus, for r_d=0.01 the pressure drop is $2.3x10^{-3}$ $(g/cm^2\text{-}cm)$ or cm H_2O/cm height (or ft H_2O ft height), even if we neglect the spray which has reached the wall. The total pressure drop for a 3 m high column is 300 x 2.3 x 10^{-3} = 0.69 g/cm² (or cm H_2O). For the r_d=0.02, total ΔP = 0.85 cm H_2O.

Cross-flow pressure drop is computed on the basis of the rate of change of momentum of spray in the horizontal direction. It is given by:

$$\Delta P = \left(\frac{u_G}{A}\right) \left(\frac{dM}{dt}\right) = \frac{u_G\ Q_L\ \rho_L}{A}\ (dyne/cm^2) \approx \frac{Q_L\ (u_G)^2\ \rho_L}{Q_G} =$$

$$= 10^{-3}\ (100)^2\ (1.0) = 10\ dyne/cm^2 \simeq 0.01\ cm\ W.C. \simeq 0.01\ mbar \qquad (9.3\text{-}17)$$

Diffusion

Diffusional collection in a countercurrent spray chamber is described by Equations 5.3.5-15 through 5.3.5-18, depending on N_{Re} and N_{Sc}. Let us first compute the dimensionless parameters. Figure 4.6.2-4 gives "N_{Re}" for r_d = 0.01 cm and 0.02 cm at terminal settling velocity as 9.6 and 4.3, respectively. Next, we compute the "N_{Sc}", using particle diffusivities taken from Figure 4.3.3-3, gas viscosity of 0.018 centipoise, and gas density of $1.2x10^{-3}$ g/cm³ so that $N_{Sc} = 1.8x10^{-4}/1.2x10^{-3}\ Dp$.

For a 0.1 μm diameter particle and a 0.02 cm radius drop, $D_p = 7 \times 10^{-6}$ cm²/sec, $N_{Sc} = 2 \times 10^4$, and $N_{Pe} = (N_{Re}\ N_{Sc}) = 4.3 \times 2 \times 10^4 = 8.6 \times 10^5$.

Using Equation 5.3.5-16 the penetration due to diffusion is as follows for $Q_L/Q_G = 10^{-3}$ m³/m³, and assuming for simplicity, 100% utilization of the spray;

$$Pt = \exp\left[-\frac{3\ Q_L\ D_p\ Z\ N_{Pe}^{1/3}}{2\ Q_G\ (u_t - u_G)\ r_d^2}\right] = \exp\left[-\frac{3(10^{-3})7 \times 10^{-6}(300)(8.6 \times 10^5)^{1/3}}{2\ (162-120)\ (0.02)^2}\right]$$

$$Pt = \exp\ (-0.0178) = 0.982 \qquad (9.3\text{-}18)$$

9.3.1.5 Gas Atomized Spray

A gas atomized spray scrubber such as a venturi is a frequent choice for collecting the emission from an asphalt plant drier. Venturis are able to handle heavy loading of dust without difficulty, and can achieve the low penetration desired.

Venturi design can be done either by means of the suitable equations or by the cut diameter approach. Because of the complex effect of liquid/gas ratio, however, the cut diameter method must be based on a specific relationship between overall penetration and the cut/mean diameter ratio. This example will illustrate the use of the specific cut diameter approach to venturi design. The main steps involved are:

1. Compute the inertial parameter for the mean particle diameter, an arbitrarily chosen gas velocity (in the throat), a drop diameter corresponding to an arbitrarily chosen Q_L/Q_G, and the fluid and particle parameters. Since the solution is trial and error, this step will be repeated several times. (We started with u_G=150 m/sec, Q_L/Q_G = 1 ℓ/m³, air and water properties assumed suitable, and dryer dust size distribution.)

2. Choose a value for "f", depending on whether the particle is hydrophilic or not. If hydrophilic, use f=0.4 and if hydrophobic, use f=0.25. (We assumed that the dust is hydrophobic, to be conservative, and used f=0.25).

3. Find the required cut/mean diameter ratio by means of Figure 8.2-7 (for σ_g=5) from the computed value of "f K_{pt}" and the necessary $\overline{Pt}$ = 0.01. (Computation results are tabulated below).

4. Next find the performance cut diameter for the assumed conditions by means of Figure 5.3.6-13. As usual, performance cut diameter has to match the required cut diameter if the scrubber is adequate. This is the test in the trial and error method. If the cut diameters do not match, another trial is necessary. (Several iterations are described in the table).

5. Compute pressure drop for each of the solutions. For each suitable pair of "u_G" and Q_L/Q_G there will be a pressure drop. Generally the optimum will be the minimum pressure drop because fan

power cost is greater than liquid handling cost. (Results are shown in the second table below).

The stone dust has a log-normal size distribution, with mass mean diameter, d_{pg} of 18 μm, and σ_g=5, as has been discussed in Section 9.3.1. Venturi penetration is a function of the group "f K_{pt}" as can be seen from Equation 5.3.6-5, where:

$$f\ K_{pt} \ = \ f\left(\frac{d_{pa}{}^2\ u_G}{9\ \mu_G\ d_d}\right) \tag{9.3-19}$$

The performance of a venturi is determined if the gas velocity through the throat, u_G, and liquid to gas throughput, (Q_L/Q_G), are specified. Drop diameter, d_d, must be known, but this is determined once "u_G" and (Q_L/Q_G) are fixed. The parameter "f" depends on wettability and is assumed to be 0.25, corresponding to non-wettable particles.

To get "u_G" and (Q_L/Q_G), a trial and error solution for (Q_L/Q_G) is necessary. To do this, refer to the following figures:

Figure	Plot	Parameter
8.2-7	$\overline{Pt}$ vs. d_{p50}/d_{pg}	f K_{pt} (at d_{pg})
5.3.6-13	d_{pa50} vs. Q_L/Q_G	u_G
5.3.6-2	d_d vs. u_G	Q_L/Q_G
4.6.7-6	d_{pa} vs. d_p	ρ_p

Starting the trial and error, first choose a value of "u_G". Then pick (Q_L/Q_G), which determines "d_d" from Figure 5.3.6-2. Now Figure 8.2-7 will give the value of "d_{p50}" necessary for the overall penetration desired (here 0.01) and the "u_G" and "dd" selected.

Finally, after converting "d_{p50}" into "d_{pa50}", Figure 5.3.6-13 is used to check to see if the required separation "d_{pa50}" necessarily is the same as the performance "d_{pa50}" which results from the "u_G" and Q_L/Q_G selected. If not, go back and pick another value of (Q_L/Q_G) until the required and performance values of "d_{pa50}" check with each other. The trial and error is illustrated by the table below. Note that a separate solution exists for each velocity. Also note that the higher the Q_L/Q_G, the closer the required cut diameter comes to the 0.73 which is based on the assumption that "Pt" varies as $(\exp\text{-}d_p{}^2)$.

u_G(m/sec)	Q_L/Q_G (ℓ/m³)	d_d(cm) (Fig.5.3.6-2)	required d_{p50} (μm) (Fig.8.2-7)	required d_{pa50} (Fig.4.6.7-6)	performance d_{pa50} (Fig.5.3.6-13)
150	1.0	0.0064	0.260	0.53	0.49
	0.8	0.0055	0.225	0.47	0.54
	0.9	0.0060	0.252	0.51	0.51
100	1.0	0.0080	0.279	0.56	0.72
	1.5	0.0092	0.297	0.58	0.61
	2	0.0106	0.306	0.60	0.55
	1.7	0.0100	0.300	0.59	0.58
75	2	0.0125	0.325	0.64	0.76
	3	0.0240	0.378	0.72	0.72

The three solutions above will have different pressure drops. The trend is toward higher water usage with lower pressure drop. The best solution will depend upon the economic situation of the plant at which the equipment is to be installed, i.e. the local cost of power and of water. The alternative solutions are listed below. Pressure drops are from Figure 5.3.6-14.

u_G(m/sec)	Q_L/Q_G(ℓ/m³)	ΔP
150	0.9	200 mbar (79 in W.C.)
100	1.7	175 mbar (69 in W.C.)
75	3	160 mbar (63 in W.C.)

9.3.1.6 Centrifugal

Centrifugal scrubbers are frequently used to control the emissions from asphalt plant driers. However, they have trouble meeting regulations as stringent as those required in the present example.

A typical centrifugal scrubber might be of the type pictured in Figure 5.3.7-4, combining centrifugal action with a spray of drops directed outwards from a centrally located spray manifold. Equation 5.3.7-19 applies.

$$Pt = \exp\left[-2\,(C\,\psi)^{\frac{1}{2n+2}} - \frac{3}{4}\,\frac{Q_L}{Q_G}\,\frac{(r_2-r_s)}{r_d}\,\eta_p\right] \qquad (5.3.7\text{-}19)$$

Use an inlet velocity of 15 m/sec or 54,000 m/hr (50 ft/sec). Assume the entrance duct is square. Then "a" and "b", the height and width of the inlet will be, respectively,

$$b = a = \sqrt{ab} = \sqrt{\frac{Q_G}{u_G}} = \sqrt{\frac{34{,}000}{54{,}000}}\ \text{m} = 80\ \text{cm} \qquad (9.3\text{-}20)$$

Next, assume the diameter of the unit will be about three times the inlet width:

$$d_c = 80 \times 3 = 240 \text{ cm} \qquad (9.3\text{-}21)$$

Letting the gas exit, d_e, be half the main body diameter, and overall height be twice the main body diameter yields:

$$d_e = 1/2 \times 240 = 120 \text{ cm} \qquad (9.3\text{-}22)$$

$$h = 2 \times 240 = 480 \text{ cm} \qquad (9.3\text{-}23)$$

For a cylindrical vessel, "C" can be calculated from:

$$C = \frac{4\, d_c^2}{a\, b} \left[\frac{\pi (d_c^2 - d_e^2)}{4} \left(h - \frac{a}{2} \right) \right] \qquad (9.3\text{-}24)$$

From Equations 9.3-24 and 5.3.7-8, "C" and "n" are, respectively, 39.5 and 0.76. From Equation 5.3.7-6, "ψ" will be:

$$\psi = \left(\frac{\rho_p\, d_p^2\, u_G}{18\, \mu_G\, d_c} \right) (n + 1) = 8.8 \times 10^4\, d_p^2 \qquad (9.3\text{-}25)$$

where "d_p" is in centimeters.

Assume initially that a (Q_L/Q_G) of 0.8 ℓ/m³ (6 gal/mcf) will be sufficient. This can be adjusted later, if the penetration resulting from this ratio is too high. Assume that 200 μm radius droplets are sprayed outward from the central spray manifold. Assume also that Equation 4.6.2-11 can be used to predict single droplet efficiency, η_p, and that drops move at a constant velocity of 10 m/sec relative to the gas.

Collection efficiency on particles of various sizes can now be calculated by substituting the appropriate values into Equation 5.3.7-19. Results are presented below.

d_p (μm)	η_p	Pt	$Fr<d_p$	
0.5	0.016	0.50	0.014	Q_L/Q_G=0.8 ℓ/m³
0.707	0.049	0.414	0.023	
1.0	0.132	0.29	0.037	
2.0	0.485	0.055	0.088	
4.0	0.81	0.010	0.176	
0.5	0.016	0.46	0.014	Q_L/Q_G=2.0 ℓ/m³
0.707	0.049	0.32	0.023	
1.0	0.132	0.141	0.037	
1.5	0.316	0.025	0.062	
2.0	0.485	0.004	0.088	

For the lower water to air ratio of 0.8 ℓ/m³ (6 gal/mcf), the plot of "Pt" versus Fr<d_p has an area of 0.03, corresponding to an overall penetration of 3.0%. Since the maximum permissible penetration is 1.0%, this mode of operation will be unacceptable. A similar trial was made for a water to air ratio of 2.0 ℓ/m³ (15 gal/mcf). Despite the increase in water usage, overall penetration is still unacceptable at 1.9%.

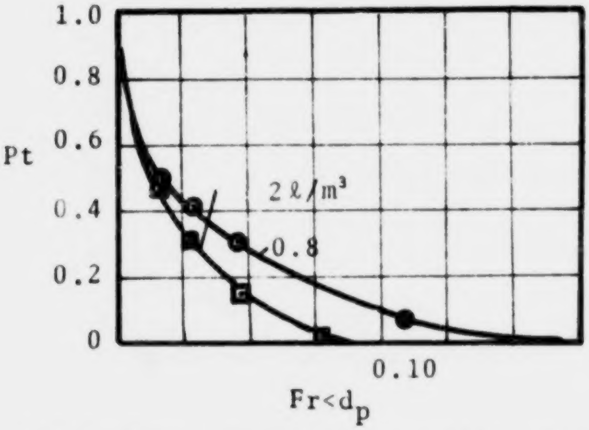

In summary, despite operating at a very high water to air ratio, calculations show that it will still be impossible to meet the desired penetration of 1%.

9.3.1.7 Secondary Flow

A secondary flow collector might be used to collect dust such as that which comes from an asphalt plant drier. It would be necessary to provide a way to remove collected particles from the collection plates. This might be done by washing them continuously with a liquid. A multi-slot plate arrangement as shown in Figure 5.3.8-8, will be considered.

The design of a secondary flow collectors is made easier with the help of the following figures:

Figure	Plot	Parameter
8.2-9	Pt vs. d_{p50}/d_{pg}	σ_g
4.6.7-6	d_{pa} vs. d_p	ρ_p
5.3.8-9	"n" vs. d_{pa50}	u_G

Figure 8.2-8 shows that in order to achieve the penetration of 0.01 which is desired, the value of d_{p50}/d_{pg} should be about 0.025, as the value of "σ_g" for asphalt plant drier dust is 5. Since d_{pg} is 18 µm, the value of cut size, d_{p50}, necessary will be 0.45 µm. This is equivalent to an aerodynamic cut size of 0.82 µm $(g/cm^3)^{1/2}$ as can be seen from Figure 4.6.7-6, remembering that "ρ_p" is 2.6.

It is now necessary to design the secondary flow collector, equipped with the knowledge that an aerodynamic cut diameter of 0.82 µm $(g/cm^3)^{1/2}$ is required. Figure 5.3.8-9 is a plot of aerodynamic cut diameter against the number of baffles to be used in the collector, with gas velocity and pressure drop as parameters. Plots "a" through "d" are for different geometric arrangements.

To avoid possible problems with plugging, and to decrease the influence of drops passing through the slots in the baffle plates on the gas flow patterns within the collector, let the slot width be 0.6 cm. Slot width for the multi-slot arrangement is equal to 2(h) in the single baffle (Figure 5.3.8-7) arrangement. Figure 5.3.8-9 will predict cut diameters properly if "h" is half of the slot width for multi-slots. The design requires knowledge of the factor "α" in order to determine the number of baffles. For the multi-slot arrangement, the value is about 3.5 for a variety of configurations. An approximate design would result from taking the number of baffles associated with an "α" value of 3.0 (Figure c). For a velocity of 18 m/sec, and "α" of 3.0, Figure 5.3.8-9 c (for standard air properties) shows that about 110 baffles in series would be needed. To employ the gas viscosity of 2.15centipoise and the "α" value of 3.5, use Equations 5.3.8-6 and 5.3.8-7, as shown below:

$$\eta = \frac{\pi\, d_{pa}{}^{2}\, \bar{u}}{12\, \mu_G\, h\, \alpha^2} = \frac{\pi\,(0.82\text{x}10^{-4})^2\,(1{,}800)}{12(2.15\text{x}10^{-4})(\frac{0.6}{2})(3.5)^2} = 0.00405 \qquad (5.3.8\text{-}7)$$

and

$$Pt = (1 - \eta)^N = (1 - 0.00405)^N = 0.5 \qquad (5.3.8\text{-}6)$$

So

$N = 171$ baffles in series for $Pt = 0.5$ @ $d_{pa} = 0.82$

Cross-Sectional Area

To find the size, or cross-sectional area of the collector, let us first determine the fractional free area for flow. The ratio of distance between slots to slot width ranged from about 6/1 to 12/1 in the studies by Calvert and Taheri. Assume a ratio of 9/1, so that "f_h", the open (slot) area, is 10% of the total cross-sectional area. From the flow rate and slot velocity we can find area as follows:

$$Q_G = \bar{u}\, A\, f_h$$

so

$$A = \frac{34{,}000 \text{ m}^3/\text{hr}}{65{,}000 \text{ m/hr } (0.1)} = 5.25 \text{ m}^2$$

If the scrubber were square, its dimensions would be 2.3 m x 2.3 m (7.5 ft x 7.5 ft).

Scrubber length can be found if we assume that baffle spacing is half the distance between slots. Since slot width is 0.6 cm and distance between slots is 9 (0.6) = 5.4 cm, the distance bewween baffles is 2.7 cm (1.06"). Baffled section length would be 171 (2.7) = 460 cm (15 ft). Some additional length would be necessary for inlet and outlet transitions and liquid inlets and outlets.

Both area and length could be reduced to about 70% of these values if the ratio of baffle to slot width were reduced to 6/1. Since this type of scrubber has not been used in a field installation, to our knowledge, any design would be speculative so far as plugging and other practical problems are concerned.

9.3.1.8 Impingement and Entrainment

The performance of impingement and entrainment scrubbers is described in Section 5.3.9. An impingement and entrainment collector might be a good selection for the control of dust from an asphalt plant drier, if it is able to reach sufficiently high efficiencies. As discussed in 5.3.9, scrubbers in this category range from low velocity (and efficiency) devices to high energy loss, high efficiency equipment such as the Doyle Scrubber. Because all impingement and entrainment (I & E) type scrubbers involve cocurrent flow and the atomization of liquid to some degree by the gas, they share a common collection mechanism with venturis. Accordingly, the performance of I & E scrubbers is described mathematically by the same equations as gas-atomizing scrubbers. The only distinction is that at low gas velocities the atomization is better (smaller drops formed) than predicted by an extrapolation of equation 5.3.6-1 below 75 m/sec.

The approach used below is along the following lines:

1. Select an appropriate velocity and pressure drop range for the required performance. (We select a Doyle type for consideration and assume the highest gas velocity and pressure drop would be used; $u_G = 72$ m/sec, $\Delta P = 30$ cm W.C.).

2. Determine Q_L/Q_G from the gas velocity and pressure drop. (We find $Q_L/Q_G = 0.6 \ell/m^3$.).

3. Determinethe predicted performance cut diameter as for a gas-atomized scrubber at the same velocity and Q_L/Q_G. (We find a performance $d_{pa50} = 1.4\ \mu m\ (g/cm^3)^{1/2}$).

4. Compute "f K_{pt}" for the mean dust diameter and other properties, as in example 9.3.1.5. (We assume f = 0.25 as for hydrophobic particles and find f $K_{pt} = 100$).

5. Compute the overall penetration which would result from a performance $d_{pa50} = 1.4$, $d_{pg} = 18$, and f $K_{pt} = 100$, and $\sigma_g = 5$. (We find that $\overline{Pt}$ would be 0.025 rather than the 0.01 required).

The efficiency of an impingement and entrainment scrubber is given in Equation 5.3.9-16:

$$Pt = \exp\left[\frac{4\ \Delta P_d\ r_d}{55\ u_G\ \mu_G} F\ (K_{pt},\ f)\right] \qquad (5.3.9\text{-}16)$$

Substitution of Equation 5.3.9-3 for "ΔP_d" into Equation 5.3.9-16 yields the same equation as was developed previously for efficiency in a venturi scrubber:

$$Pt = \exp\left[\frac{2\ Q_L\ u_G\ \rho_L\ d_d}{55\ Q_G\ \mu_G} F\ (K_{pt}, f)\right] \qquad (5.3.6\text{-}5)$$

Pressure drop in a Doyle type of impingement and entrainment scrubber is generally less than 30 cm W.C. as discussed in Section 5.3.9. Gas velocity ranges from 27 to 72 m/sec. Figure 5.3.6-13 applies to devices whose performance is described by Equation 5.3.6-5 above, including both venturi and impingement and entrainment scrubbers, shows that the predicted performance aerodynamic cut diameter for pressure drop of 30 cm W.C. and gas velocity of 7,200 cm/sec will be about 1.4 μm $(g/cm^3)^{1/2}$. Figure 5.3.6-14 shows that for u_G=7,200 cm/sec and ΔP = 30 cm W.C., Q_L/Q_G is about 0.6 ℓ/m³. This corresponds to a drop diameter of about 85 μm, according to Figure 5.3.6-2.

Figure 8.2-7 relates overall penetration to d_{p50}/d_{pg} for log normal dusts where "σ_g" is 5. Values of "f K_{pt}" are parameter. For the present situation, and assuming f = 0.25:

$$f\ K_{pt} = 0.25 \left[\frac{(1.8)^2\ (2.6)\ 7{,}200\times10^{-6}}{9(2.15\times10^{-4})\ 0.08}\right] \simeq 100$$

Figure 4.6.7-6 is used to convert the d_{pa50} determined above into d_{p50} of 0.8 μm. Hence the value of d_{p50}/d_{pg} for the asphalt plant drier will be 0.8/18 = 0.045. Figure 8.2-7 shows that for this value of d_{p50}/d_{pg}, and f K_{pt} of 100, overall penetration will be about 2.5%, in excess of the 1% maximum permissible. Since this represents nearly the best possible performance for an impingement and entrainment collector, the conclusion is drawn that this type of scrubber is probably incapable of collecting the asphalt plant dust with the required efficiency. It is conceivable that higher velocity and pressure drop would bring it close to the required performance.

9.3.2 MASS TRANSFER CALCULATIONS

The problem of designing a scrubber for mass transfer occurs when it is desired to remove a polluting gas from an effluent gas stream. The calculations which must be made to design mass transfer scrubbers will vary according to the type of scrubber to be designed.

Section 5.2 is devoted to explaining the equations to be used in designing mass transfer equipment. For most types of scrubbers discussed, a sample calculation is given. The sample calculation illustrates the use of the design equations, and is done for an industrial sized gas purification problem.

To avoid repetition of the design examples given in Section 5.2, additional calculations illustrating the use of mass transfer design equations will not be given here. The reader is referred to the listing below of the types of mass transfer equipment discussed in Section 5.2, and fully described there with design examples.

Section	Topic
5.2.2	Plate Column Scrubbers
5.2.3	Packed Column Scrubbers
5.2.4	Fibrous-Packed Scrubbers
5.2.5	Pre-Formed Spray Scrubbers
5.2.6	Gas Atomized Spray Scrubbers
5.2.7	Centrifugal Scrubbers
5.2.8	Moving Bed Scrubbers

9.3.3 MASS TRANSFER WITH CHEMICAL REACTION CALCULATIONS

Chemical reaction of the pollutant gas with the liquid phase or slurry is often used in an industrial scrubber to enhance the mass transfer characteristics of the scrubber being used. Section 4.2.6, "Mass Transfer with Chemical Reaction", discusses the various models of behavior which have been identified and when each applies. Example calculations demonstrating the utility of chemical reaction in mass transfer are given in this section.

The basic information on mass transfer with chemical reaction given in Section 4.2.6 can be applied to the common industrial scrubbers discussed in detail in Section 5.2. The performance of a scrubber functioning either with or without mass transfer can be calculated. Note that either completely dissolved (single phase), partially dissolved (soluble slurry), or insoluble (insoluble slurry) reactants may be used.

9.3.4 EXAMPLE PROBLEM: COAL DRYER EXHAUST

In the coal industry certain high grade metallurgical coals are dried in flash dryers or fluid bed dryers. The proportion of coal of the size less than about 0.6 cm (1/4 inch) being mined is increasing because of the use of continuous mining machines. It is this fine coal that retains moisture in the wet beneficiation plants. This has the effect of increasing the use of thermal driers for the removal of moisture from the coal prior to its sale and use.

The metallurgical coal is beneficiated at the mine head where the shale or refuse is separated by techniques such as heavy media separation, flotation, jigging or riffle tables.

The fine coal from flotation (-28 mesh) is partly dewatered in continuous disc filters after which it still contains 25% moisture; it is then mixed with a coarser 0.6 cm (1/4") x 28 mesh fraction and passes to the fluid bed dryers where the two fractions are dried together.

In the fluid bed drier, hot gas passes through a bed of coal which is to be dried, driving the moisture from the coal. Small coal particles are entrained in the drying gas stream, and pass out from the drier with the gas to the air pollution control equipment which is fitted. Details on the quantity and properties of the emissions from coal driers are given in Section 7.2.1.1.

Fluid bed dryers are fitted with dust arresting equipment which is a combination of first stage dry cyclones for the coarse coal dust and fly ash followed by a second stage of wet scrubbing. The type of equipment used for wet scrubbing varies widely. Such devices as spray towers and impingement scrubbers are used, but with the tightening of regulations as to the dust emission permitted either some more sophisticated scrubber, or ones with higher energy input will have to be used to reach the limits imposed by law. Generally speaking, the laws are aimed at the production of a clear exhaust from the dryer plant stack. The threshold of discoloration appears to be at about 0.115 g/cm³ (0.05 grains per cubic foot) calculated at the stack gas temperature.

Drying Plant

A typical coal beneficiation plant dryer will process from about 54 to 360 metric tons/hr (60 to 400 English tons/hr) of coal which is a mixture of 30% 28 mesh and less and 70% 0.6 cm (1/4") x 28 mesh from 18% moisture to 4% moisture. The heat source is pulverized coal burned in an external furnace. On the large sizes of dryer the gas volume can reach 340,000 m³/hr (200,000 SCFM) at the scrubber exhaust and the inlet gas to the scrubber can contain as much as 5 to 30 g/m³ (2 to 10.0 grains/ft³) of dust measured at the dryer exit temperature, which is normally about 50-60°C (130-140°F) and about 95% saturated with water vapor.

The furnace exhaust is diluted with tempering air to cool it to 400 - 500°C (800 - 900°F) before it enters the fluid bed.

Effluent Description

The effluent from the drier can be assumed to be air at 60°C (140°F), 95% saturated and containing 460 g/m³ (200 grains/ft³) of entrained dust. The dust has a density of 1.35 g/cm³, and a log-normal size distribution with mass median particle diameter of 200 μm and standard deviation, σ_g, of 4.5. This information was taken from Table 7.2-2, "Typical Coal Dust Emissions from Thermal Coal Driers".

A cyclone precleaner will be used to remove coarse material from the gas stream before passing it to the scrubber. A typical cyclone would have a "cut" diameter of d_p = 4 μm, and the value of "B", the power to which particle diameter is raised in the efficiency equation (see Equation 8.2-3) of 0.70.

For a value of $(d_{p50}/d_{pg})^B$ of $(4/200)^{0.7}$ = 0.065, and $B \ln \sigma_g$ of 0.7 ln (4.5) = 1.05. Figure 8.2-4 shows that the penetration of dust through the cyclone precleaner will be 0.021 corresponding to an exit dust loading of 0.021 x 460 = 9.6 g/m^3 (4.2 grain/ft^3). For the purpose of illustration, assume the dust coming from the cyclone has a log-normal size distribution, with d_{pg} = 8 µm and σ_g = 3.

Object

The object of the scrubbing device is to remove sufficient dust as to render the exhaust gas tail invisible once the steam plume from the stack has dispersed. This, as stated earlier, is at a concentration less than 0.115 g/m^3 (0.05 grains/cu ft) based on the wet gas volume at temperature of the exhaust.

Method of Solving the Problem

There are not many alternatives to explore in solving this dust pollution problem. One way which comes to mind immediately is not to use wet beneficiation methods but rather to use dry methods. Dry methods are advantageous in ways other than reduction of pollution problems in that less extensive cleaning of bituminous coals renders the product less corrosive to the gas side of boiler tubes. Leaving some alkaline earth compounds in the fly ash is beneficial to the boiler tubes. Dry beneficiation is also reported to be of lowest initial capital investment and maintenance cost, but to study all aspects of the coal cleaning economics is beyond the scope or intent of this study.

Segregating or variation of the quantity of fine coal passing to a fluid bed dryer has been studied in a cursory manner, but no difference could be detected, over a short time interval, in the quantity of fines emitted from the cyclones in the drying plant. This may not be the case with other less friable coals.

Another possibility that comes to mind, if the coarser coal does not dust in the fluid bed, is to treat the minus 28 mesh coal, which is 30% of the total, in a spray dryer instead of a fluid bed dryer. It may even be possible to use a small quantity of binder so that the product from the dryer would be in the form of non dusting agglomerates. In this way a great deal of the dust load could be removed from the exhaust and expensive scrubbing equipment would not be needed. In addition the complication and expense of recovering fine dust from the liquid effluent from the wet scrubber would be avoided. Spray dryers are probably more efficient thermally than fluid bed or flash dryers.

According to the MRI Report (1970), a variety of equipment is used to clean the final exhaust on a coal drying plant. These generally can be categorized as low pressure drop wet scrubbers, although half the plants in existence only have dry cyclones. Much of the equipment could not be expected to be efficient at one micron. About 4-5% of the dryers have high energy scrubbers which in effect mean venturi scrubbers or possibly spray towers with high pressure water sprays.

Low energy wet scrubbers will give an effluent containing about 0.35 g/m³ (0.15 grains of dust per standard cubic foot) but they are reported to vary from 0.11 to 0.9 g/m³ (0.05 to 0.42 grains/scf).

A high energy scrubber will give residual concentration of less than 0.115 g/m³ (0.05 grains per scf) and can probably be adjusted by changing the water rate to give a pressure drop consistent with attaining the required concentration in the exhaust without wasting power on excessive pressure drop. In this example a venturi scrubber will be designed to meet the required penetration. Possibly pre-chilling of the gas stream with a fine mist of cold water might help to sensitize the dust and cause growth on the particles, although there could be a danger of the prewetted dust building up on duct walls. In the calculations which follow no pre-wetting will be assumed.

Design of the Scrubber

To achieve the emission level required, 0.115 g/m³, the venturi scrubber to be designed will have to have a penetration of 0.115/9.6 = 0.012. This is to be achieved on a dust of mass median diameter of 8 μm and standard deviation of 3, as noted above.

The design of the scrubber will be completed when gas velocity through the throat (hence throat diameter), water usage rate, and pressure drop have been determined. A preliminary design can be made to tentatively set the design variables. The preliminary design can then be checked by a more accurate, exact design procedure.

Preliminary Design

The preliminary design uses Figure 5.3.1-4, a plot of overall penetration versus d_{p50}/d_{pg} with "σ_g" as parameter for devices where: $Pt \propto \exp(-d_p^2)$. Since for a venturi, penetration is only approximated by this relationship, the design is only approximate.

Figure 5.3.1-4 shows that for the penetration of 0.012 desired, and for $\sigma_g = 3$, the value of d_{p50}/d_{pg} required is 0.07, corresponding to a particle cut size of 0.56 μm, as d_{pg} is 8 μm. Figure 4.6.7-6, a plot of "d_{pa}" versus "d_p" with "ρ_p" as parameter, shows that since "ρ_p" is 1.4 g/cm³, "d_{pa50}" should be 0.72 μm (g/cm³)$^{1/2}$.

Now turning to Figure 5.3.6-13, a plot of "d_{pa50}" for venturi scrubbers against operating conditions, it appears that for the d_{pa} necessary, the following combinations of velocity and pressure drop will work:

u_G m/sec	Q_L/Q_G ℓ/m³	ΔP cm of W.G.
150	0.53	130
125	0.68	110
100	1.0	100
75	2.5	150

Any of these combinations of "u_G" and (Q_L/Q_G) should give the required overall penetration. However, notice that operation below 100 m/sec increases water usage rate, pressure drop, and size of equipment.

Final Design

The final design must involve a trial and error solution for (Q_L/Q_G) once a value of "u_G" is specified. A first trial for (Q_L/Q_G) can be made based on the results of the preliminary design. The following figures will be used:

Figure	Plot	Parameter
8.2-6	$\overline{Pt}$ vs. d_{p50}/d_{pg}	f K_{pt} (at d_{pg})
5.3.6-13	d_{pa50} vs. Q_L/Q_G	u_G
5.3.6-2	d_d vs. u_G	Q_L/Q_G
4.6.7-6	d_{pa} vs. d_p	ρ_p

First, pick a value of "u_G". Then choose a value of (Q_L/Q_G), a good initial trial being that calculated in the preliminary design. Then "d_d" can be determined from Figure 5.3.6-2. Now f K_{pt} can be calculated from:

$$f\ K_{pt} = f\left(\frac{d_{pg}{}^2 \rho_p u_G}{9\ \mu_G\ d_d}\right) \qquad (9.3.-29)$$

and Figure 8.2-6 can be used to get the value of "d_{p50}" required to meet the penetration requirement of 0.012. Conversion of "d_{p50}" to "d_{pa50}" is made by Figure 4.6.7-6. Finally, the required value of "d_{pa50}" can be compared with the performance value, as found from Figure 5.3.6-13 for the "u_G" and (Q_L/Q_G) selected. If the required and performance values of "d_{pa50}" are not the same, choose another value for (Q_L/Q_G) and repeat the above procedure. The results of this procedure for several values of "u_G" are presented below.

u_G m/sec	Q_L/Q_G ℓ/m³	d_d (Figure 5.3.6-2)	required d_{p50} (Fig.8.2-6) μm	required d_{pa50} (Figure 4.6.7-6)	performance d_{pa50} (Fig. 5.3.6-13)
150	0.53	0.0045	0.66	0.82	0.72
	0.4	0.0041	0.70	0.90	0.95
	0.42	0.0042	0.69	0.89	0.90
100	1.0	0.0080	0.81	1.05	0.72
	0.8	0.0071	0.80	1.0	0.80
	0.6	0.0064	0.79	0.98	0.98
75	2.5	0.0160	1.0	1.25	0.72
	0.6	0.080	0.91	1.15	1.25
	0.7	0.085	0.88	1.18	1.20

Results of the preliminary and final designs are plotted below:

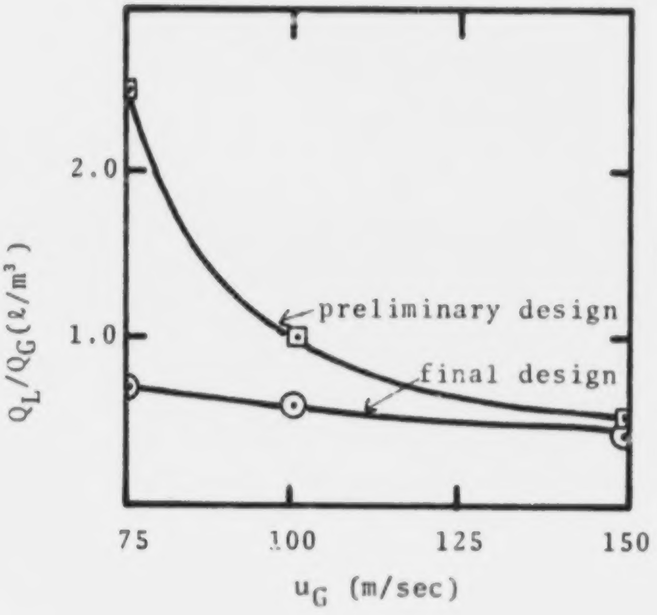

There is a substantial discrepancy between the preliminary design results and the final design results. This is due to two factors. First, as mentioned above, the preliminary method assumes no limiting influence of liquid rate, whereas the final method accounts for the effect of Q_L/Q_G on penetration. Second, the final method used Figure 8.2-6 to get "d_{pa50}" required. This figure was made for log normal dust with standard deviation of 2.5 instead of the 3 specified in the present problem.

Final design results show that lowering gas velocity (and raising the water to gas ratio required) has the effect of lowering pressure drop. However, it is also true that lowering velocity will increase the size of the equipment required. The best choice for the designer will depend upon the relative costs of water, power, and equipment.

For the rest of the analysis presented here, it will be assumed that economics points to a gas velocity of 125 m/sec, and a liquid to gas ratio of 0.5 ℓ/m^3. To account for inaccuracies built into the design method and equations used, and to be on the safe side, design the venturi to operate with a higher than "necessary" liquid to gas ratio - say 0.75ℓ/m^3 (5.65 gal/mcf).

The throat size of the venturi can now be determined from the gas velocity through the throat and the total flowrate of gas to be processed:

$$d = \sqrt{\frac{4}{\pi}\frac{Q_G}{u_G}} = \sqrt{\frac{4 \quad 340,000 \ \frac{m^3}{hr}}{\pi \quad 125 \times 3,600 \ \frac{m}{hr}}} = 0.98 \text{ m} \qquad (9.3\text{-}30)$$

The water consumption rate can be calculated, since (Q_L/Q_G) and "Q_G" are known:

$$\frac{Q_L}{Q_G} Q_G = 7.5\text{x}10^{-4}(340,000) = 255 \text{ m}^3\text{/hr (1,100 gpm)} \qquad (9.3\text{-}31)$$

In summary, the following design for the venturi should do the job:

u_G = 125 m/sec (410 ft/sec)
Q_L/Q_G = 0.75 ℓ/m^3 (5.65 gal/mcf)
Q_G = 255 m^3/hr (1,100 gpm)
throat diameter = 1 m (39 inches)
ΔP = 115 cm W.G. (45 inches W.G.)

9.3.5 EXAMPLE PROBLEM: APPLICATION OF DIFFUSIOPHORESIS AND PARTICLE GROWTH TO A ROCK WOOL CUPOLA

Introduction

This design example illustrates a case where performance of a wet scrubber was evaluated and improved. We chose a relatively simple example which demonstrates improved performance through beneficial utilization of thermo- and diffusiophoresis. Additional improvement to that demonstrated can be achieved by forming conditions which are conducive to particle growth.

Process Description

The rock wool manufacturing process involves melting slag and other additives in two cupolas, the North and the South. Figure 9.3-3 describes the system. Coke is the major source of heat and is added at the rate of 400 lbs/charge (182 kg/charge). Additional fuel is natural gas, used at the rate of 6 million BTU/hr cupola (1.51×10^9 cal/hr cupola) together with 3,500 CFM (5940 m^3/hr) of air. The flue gas coming out of the cupola contains enough particulate matter to cause a visible plume. The flue gas temperature varies in a cycle corresponding to the cupola charging cycle. The lowest gas temperature, at the beginning of the cycle when the cupola is charged, is 270°F (132 °C), it climbs gradually to 600°F (315 °C) in 16 minutes. Then when the fire "breaks", temperature rises immediately to 800°F (426 °C) in the South cupola and to 1100 °F (593 °C) in the North cupola. The temperature remains constant for 3-4 minutes to the end of the cycle. The hot gases, at constantly varying temperature and flow rate, enter a cyclone where part of the dust is collected, then flows into a venturi scrubber.

When both cupolas are operating two venturi scrubbers are used, when only the South cupola works, only one venturi is used. 12-15,000 ACFM (20,000 - 25,000 m^3/hr) of air at 110-140 °F (43-60 °C) measured at the blower inlet flows through the South venturi and 130 GPM (30 m^3/hr) water at 110-140 °F (43-60 °C) is sprayed into it. The rate of water evaporation in the South venturi is ≈2 GPM (0.45 m^3/hr). Water is sprayed into the North venturi at the same rate of 130 GPM (30 m^3/hr) and at the same temperature as in the South, the air flow rate to the North venturi is also 12-15,000 ACFM (20,000- 25,000 m^3/hr) at 110-140°F (43-60 °C) measured at the North blower inlet venturi. When both venturi scrubbers are working 7-8 GPM (1.6-1.8 m^3/hr) of water evaporates.

The two venturis are followed by entrainment separators and blowers which emit the flue gas into the atmosphere through two short chimneys. Since the exhaust gas did not meet the Air Pollution Control District specifications the operator increased pressure drop across the venturis up to 75" (190 cm) water but there was still a visible plume on occasions. The water leaving the venturis and the entrainment separators, flows into a settling pond and then is recirculated.

Process Analysis

When analyzing the process let us start with the cyclone and then look at the venturi scrubbers. Collection efficiency of a cyclone can be improved slightly by spraying water into it. This also helps in keeping the particles from reentraining into the gas stream. If we are not going to change the dimensions of the cyclone, then this is the only improvement here.

When looking at the venturi it becomes immediately evident that the high rate of water evaporation (7-8 GPM) decrease drop collection efficiency, because the Stephan flow forces particles away from the evaporating drops. The temperature gradient on the other hand is in the right direction and helps the collection. Gravitational forces are negligible and there is no electrical field present.

So the change that comes to mind is spraying water into the cyclone to prevent reentrainment, and cool the gas and increase its relative humidity. To have diffusiophoresis helping rather than hindering, the flue gas should be supersaturated when entering the venturi. Spraying water into the cyclone may not be enough to insure supersaturation so it may be better to spray water or steam ahead of the cyclone, in the duct close to the cupola and spray again in the cyclone if required.

Calculating Process Modifications

Calculations will be carried out for the case when only the South cupola and South venturi are working.

1. Present humidity of the flue gases. Water in the flue gases may come from three sources: as a combustion product, dampness of the charge, and humidity of the air used for combustion. Reactions in the cupola do not lead to the production of water and the temperature is too low for water to be consumed through the water gas reactions.

Assuming the air is at 80°F (26.7°C) and 65% humidity. From the psychrometric chart for air water, there is 0.0148 lbs water/lb dry air and the specific volume is $13.601 + 0.65 \cdot 0.486 = 13.917$ ft^3/lb dry air (870 cm^3/gm).

$$\text{lbs water in air/min} = \frac{(3{,}500)\ (0.0148)}{13.917} = 3.72 \text{ lbs water/min}$$

(1.69 kg water/min)

The quantity of water coming from burning of natural gas is calculated from the following:

For natural gas let us assume 1,000 BTU/ft^3 (8,900 cal/ℓ) and a composition of 80% CH_4 and 20% C_2H_6. Burning of methane yields two moles water per mole methane and ethane yields three moles water per mole of gas.

$$\text{Natural gas used} \quad \frac{6\text{x}10^6}{10^3\ 60} = 100 \text{ CFM } (170 \text{ m}^3/\text{hr})$$

$$\text{Methane} \quad \frac{100\ (0.8)\ 28.3}{22.4} = 101 \text{ mole}$$

$$\text{Ethane} \quad \frac{100\ (0.2)\ 28.3}{22.4} = 25.3 \text{ mole}$$

$$\text{Water produced} \frac{[101\ (2) + 25.3\ (3)]\ 18}{454} = 11 \text{ lb water/min } (5 \text{ kg/min})$$

Total quantity of water in flue gas $11+3.72 = 14.72$ lbs/min (6.7 kg/min)

From measurements the quantity of flue gas coming out of the cupola is 9,200 ACFM (15,650 m³/hr) at 400 °F (200°C). The ratio of air to water in the flue gas is:

$$\text{CFM water} = \frac{14.72\ (454)\ 0.082\ (477.7)}{18\ (28.32)} = 513\ \text{CFM}\ (9\ \text{m}^3/\text{hr})$$

$$\frac{\text{lbs dry flue gas}}{\text{min}} = \frac{(9{,}200-513)\ (28.32)\ 29}{0.082\ (477.7)\ 454} = 402\ \text{lbs}\ (182\ \text{kg})$$

$$\frac{\text{lbs water vapor}}{\text{lbs dry flue gas}} = \frac{14.72}{402} = 0.0367$$

2. Quantity of water needed to saturate the flue gas.

It will take more water to saturate the hotter flue gas than the cooler. So we shall calculate quantity of water needed for the hotter gas which will also suffice for the cooler part of the cycle.

For adiabatic cooling assuming the water is sprayed at the adiabatic saturation temperature (see also 4.2.8)

$$(t_g - t_{as}) = (Y'_{as} - Y'_i)\ \frac{\lambda as}{C_{si}}$$

Since 800 °F (426 °C) and 0.0367 lbs water/lbs dry air is outside most psychrometric charts, this equation has to be solved by a trial and error method using psychrometric tables (Perry, pp 15-16). For the first trial let us choose

$$t_{as} = 150°\text{F then, } (800-150) = 650 = (0.2125-0.0367)\ \frac{1012}{0.251} = 682$$

2nd trial

$$t_{as} = 149°\text{F } (800-149) = 651 = (0.2055-0.0367)\ \frac{192}{0.257} = 664$$

3rd trial

$$t_{as} = 148°\text{F } (800-148) = 652 = (0.1989-0.0367)\ \frac{1012}{0.257} = 639$$

The saturation temperature is 148.5°F (64.7°C) and the saturation humidity is 0.2022 lbs water/lbs dry air.

$$\text{Quantity of water to evaporate} = \frac{402\ (0.1655)}{8.28} \approx 8\ \text{GPM}\ (1.82\ \text{m}^3/\text{hr})\ \text{at} \approx 149°\text{F}\ (65°\text{C})$$

If the water is available at a lower temperature, the heat should be compensated for in the calculation. For the case of flue gas at 270 °F (132 °C) we can use a chart and t_{as} = 118 °F (47.8 °C) the final humidity is 0.078 lb water/lb dry air, and only 2 GPM (3.4 m³/hr) are needed.

3. Heat Transfer Calculations.

The next question is do we have enough heat transfer capacity to evaporate the water, again let us check for the higher temperatures. The water is sprayed into the gas stream and moved together with it so let us calculate "ΔT" from the equations for cocurrent heat transfer.

$$\Delta_T = \frac{\Theta_1 - \Theta_2}{\ln \frac{\Theta_1}{\Theta_2}}$$

Much will depend upon "Θ_2" which is the temperature difference at the cold end, let us assume it to be 5°F (2.78°C).

$$\Theta_1 = 800-148 = 652°\text{F}\ (344.4°\text{C})$$

$$\Delta_T = \frac{652-5}{2.3 \log \frac{652}{5}} \quad \frac{647}{(2,3)(2,1153)} = 133°\text{F}\ (74°\text{C})$$

The heat transfer area and drop size distribution can be estimated from the characteristics of the nozzle chosen. Let us choose a nozzle such that d_{av} = 0.0028 ft (850 μm) then heat transfer area can be calculated from drop surface area.

$$A = \frac{3\ Q}{r} = \frac{(8)(3)(2)}{7.481\ (2.8\text{x}10^{-3})} = 2{,}140\ \text{ft}^2/\text{min}\ (249\ \text{m}^2/\text{min})$$

The area available for heat transfer can be estimated from the time the drops stayed in the duct, which depends on the gas flow rate and the drop rate of acceleration. One should also consider the decrease of drop area due to evaporation. Thus estimated drop area is arbitrarily assumed to be ≈ 0.3 of the calculated.

Heat transfer coefficient, h, can be estimated from Treybal (1955), Figure 3.11.

$$N_{Re}\ N_{pr}^{\ 2/3} = \frac{d_d\ \bar{u}\ \rho_G}{\mu_G} \left(\frac{C_p\ \mu_G}{k_G}\right)^{2/3} =$$

$$\frac{2.8\text{x}10^{-3}\ (1.257\text{x}10^{5})\ 4.23\text{x}10^{-2}}{6.46\text{x}10^{-2}} \left[\frac{0.24\ (6.46\text{x}10^{-2})}{2.46\text{x}10^{-2}}\right]^{2/3} = (230)(0.631)^{2/3} = 168$$

From the figure $\frac{hd\ \rho_L}{k_G}\ 10^{-3} = 0.0095$

$$h = \frac{(9.5)\ 2.46\text{x}10^{-2}}{2.8\text{x}10^{-3}} = 83.5\ \frac{\text{BTU}}{\text{hr}\ °\text{F}\ \text{ft}^2} \left(40.7\ \frac{\text{cal}}{\text{hr}\ °\text{C}\,\text{cm}^2}\right)$$

$Q_{trans} = h \cdot A \cdot \Delta T = 83.5(0.3)2140(133) = 7.15 \times 10^6$ BTU/hr (5×10^5 cal/sec)

$Q_{ev} = 8(8.345)60(990) = 3.95 \times 10^6$ BTU/hr (2.76×10^5 cal/sec)

Under these assumptions, there is enough heat transfer capacity to evaporate the water needed to make the flue gas saturated.

4. Predicted Effect of Particle Collection in the Venturi.

Saturating or supersaturating the flue gas before entering the venturi scrubber and using water colder than 149°F (65°C) in the venturi will cause condensation of water vapors on the drops. Thus diffusiophoresis will help in particle collection by the drops in the venturi.

It is interesting to calculate the magnitude of this effect. The gas flow rate into the venturi will increase due to the water vapors and decrease due to lower temperature. Let us start by calculating new gas flow rate assuming no change in temperature and composition after water injection in the duct is completed.

ACFM = $402 \cdot 16.343$ = 6580 at 118°F (11,200 m^3/hr at 48°C) - beginning of cycle.

ACFM = $402 \cdot 30.28$ = 8160 at 148.5°F (13,900 m^3/hr at 65°C) - end of cycle.

The water recirculating through the venturi will get warm due to the condensation of water vapors. If no heat is removed, the water will eventually reach the air temperature and no diffusiophoresis will take place any more. It is thus necessary to cool the venturi water. This can be done either by bleeding a known fraction and adding city water which is at 55-65°F (13-18°C) or by installing a water cooler in the system. In any event we would like to keep the water temperature lower than 118°F to provide for the worse case. Let us choose a water temperature of 100°F.

Drop diameter in the venturi is found from Nukiyama and Tanasawa's correlation as plotted in Figure 5.3.6-2. For a 12" diameter venturi, the throat velocity is:

V_{g1} = 140 fps (42.6 m/sec) V_{g2} = 175 fps (53.5 m/sec)

$Q_L/Q_G|_1$ = 130/6.58 = 19.7 gal/MCF (2.62 ℓ/m^3)

$Q_L/Q_G|_2$ = 130/8.16 = 16 gal/MCF (2.13 ℓ/m^3)

d_{s1} = 210 μm = $6.9\text{x}10^{-4}$ ft

d_{s2} = 180 μm = $5.9\text{x}10^{-4}$ ft

The diffusiophoretic velocity of the particles can be calculated from equation 4.3.3-32. To estimate vapor pressure gradient assume that the temperature gradient and vapor concentration gradient at the drop surface are of the same shape and that the main resistance to heat transfer lies in heat conduction through the air envelope around the drop. It can be shown that:

$$\frac{dp}{dx} \approx \frac{\Delta p_v}{\frac{d_d}{2}} \quad \text{for low velocities}$$

The diffusiophoretic velocities for the two cases are:

$$v_{D1} = \frac{\sqrt{18}}{\frac{83}{760}\sqrt{18} + \frac{677}{760}\sqrt{29}} \; \frac{0.258}{677} \left[\frac{83-49.1}{1.05\text{x}10^{-2}}\right] = 0.965 \text{ cm/sec} = 1.9 \text{ft/min}$$

$$v_{D2} = \frac{\sqrt{18}}{\frac{185}{760}\sqrt{18} + \frac{575}{760}\sqrt{29}} \; \frac{0.258}{575} \left[\frac{185-49.1}{9\text{x}10^{-2}}\right] = 5.58 \text{ cm/sec} = 10.9 \text{ ft/min}$$

If it is assumed that the particles flux due to diffusiophoresis is additive to the flux due to inertial collection, then the added collection should be applied to those particles which are not being removed in the present system. The collection in a venturi scrubber due to diffusiophoresis alone is given in Section 5.3.5. Substituting the values in the equation gives for the beginning of the cycle:

$$E_1 = 1 - \exp\left[-\frac{(0.935)(2.62)\ 10^{-3}(0.965)2.1\text{x}10^{-2}}{1.8\text{x}10^{-4}}\right] = 0.24$$

and for the end of the cycle

$$E_2 = 1 - \exp\left[-\frac{(0.935)2.13\text{x}10^{-3}\ (5.58)1.8\text{x}10^{-2}}{1.8\text{x}10^{-4}}\right] = 0.67$$

As an estimate we can expect 24-67% collection of the particles presently escaping the collector due to the additional mechanisms.

Before ending, two more subjects should be checked. The first is, could the present equipment handle the new gas volumetric flow rate, and the second, should we expect air supersaturation and particle growth? With regard to the first question, the answer is simple: since the gas volume decreases due to the cooling effect, much more than the water vapor adds to the volume. We should thus expect a lower frictional pressure drop. Also since we increase collection efficiency of the smaller particles we may be able to reduce throat velocity without causing a visible plume. The second question is much more difficult to answer. If we spray water only in the duct the way it was described before, we should not expect much supersaturation, condensation and particle growth. If however cold water is sprayed also into the cyclone, we may cause supersaturation and particle growth through water vapor condensation on the particles. The rate of particle growth can be calculated from Equation 4.3.4-21.

$$r \frac{dr}{dt} = \frac{M\ D}{\rho_L\ R_g\ T} (P_\infty - P_o) \left[\frac{1}{\dfrac{D}{r v \alpha} + 1} \right]$$

where $(p_\infty - p_o)$ is the difference in vapor pressure between the bulk of the gas and the particle's surface, or the degree of supersaturation. As a result of this parabolic relationship between particle radius and time, the particles will grow and become more uniform in size as the condensation proceeds. To calculate actual particle growth, one needs particle size distribution and the degree of supersaturation.

9.3.6 EXAMPLE PROBLEM: PHOSPHORIC ACID PLANT FLUORIDE SCRUBBING

Process Description

Phosphoric acid manufacturing operations are discussed in brief form in Chapter 7. The 30% phosphoric acid produced, is first concentrated and then goes forward to be processed further to triple superphosphate, di-ammonium phosphate, merchant grade phosphoric acid, or superphosphoric acid.

In the phosphoric acid plant, phosphate rock containing 3 to 4% of fluorine is digested with sulfuric acid which is recycled at 180°F (82°C) in a reactor having about 8 hours residence time. The products of the reaction are phosphoric acid, gypsum and hydrofluoric acid. The hydrofluoric acid reacts with silica in the rock and is partly evolved as silicon tetrafluoride, SiF_4, the remainder going forward to subsequent processes.

In the past, gases from the reactors were often emitted to the atmosphere. In modern practice fluoride scrubbers are always provided and the resultant fluosilicic acid is recovered for sale or is neutralized.

In phosphate rock digestion the gases evolved from reaction of the rock with sulfuric acid consist of CO_2, HF, SiF_4, and steam. The CO_2 evolved strips SiF_4 out of the acid and traces of HF according to the vapor pressure of these components in equilibrium with the concentration in the liquid phase in the reactor. To prevent these gases escaping to the air, the reactor is kept under a slight negative pressure by a fan, and a scrubber is placed between the fan and the reactor.

Assuming 600 ton/day (545 metric ton/day) P_2O_5 digestor, the rock consumed would be 2,000 ton/day (1,820 metric ton/day) containing approximately 3.5% of F, 4% CO_2, and 4% SiO_2.

The evolution of CO_2 would thus be 80 tons/day (72.5 metric ton/day). Of the 70 tons/day F (63.5 metric tons/day) released, 5% is evolved in the reactor, i.e., 3.5 tons/day (3.18 metric tons) measured as F, but this appears as SiF_4 due to the excess silica present in the reactor.

Reactor Temperature	180°F (82°C)
From Duhring Lines, Equivalent Water Temp.	168°F (76°C)
Vapor Pressure of Water over 30% P_2O_5	295 mm Hg
SiF_4 Evolved in Reactor	400 lb/hr (182 kg/hr)

GASES EVOLVED IN REACTOR

	Tons/Day	Lb/Hr	Lb Moles/Hr	Mole %	Partial Pressure
CO_2	80	6,667	152.0	59.7	453.7
SiF_4	4.8	400	3.8	1.5	11.3
H_2O		1,778	98.8	38.8	295
TOTAL		8,845	254.6	100.0	760

Volume of reactor gases measured at 32°F (0°C) and 760 mm Hg:

$$254.6 \ \frac{\text{lb moles}}{\text{hr}} \times \frac{359 \text{ ft}^3}{\text{lb mole}} = 91{,}400 \text{ ft}^3/\text{hr} \ (2{,}590 \text{ m}^3/\text{hr})$$

By good reactor design it should be possible to control the ingress of air through agitator seals and manhole covers. We will assume that the reactor gases become diluted with an equal volume of saturated air before reaching the scrubber. Also, for the sake of the example, we will assume that the scrubber only cleans the gases from the reactor and does not treat the gases from other parts of the plant. To mix streams together before entering the scrubber dilutes the fluoride content of the stream and results in a requirement for a greater number of transfer units than would otherwise be needed by separate treatment of the reactor gases before mixing with the more dilute gases. With dilution by 91,400 cu ft/hr (2,590 m³/hr) of wet air saturated at 90°F (32°C), but measured at 32°F (0°C) and 760 mm Hg the dilution air is as follows:

	% Vol	Cu ft/hr	Cu ft/hr at 90°F
Air	95.25	87,059	
Water Vapor	4.75	4,341	
	100.0	91,400	102,175 (2,900 m^3/hr)

The gases entering the scrubber will be, therefore:

GAS ENTERING SCRUBBER

	lb mole/hr	lb/hr	cu ft/hr at 32°F & 760 mm Hg	Partial Pressure mm Hg	lb/hr of 'F'
Air	242.5	6,984	87,059	361.9	
CO_2	152.5	6,667	54,568	226.8	
SiF_4	3.8	400	1,364	5.7	289
H_2O	110.9	1,996	39,810	165.5	
TOTAL	509.2	16,047	182,801	760.0	

Saturation Temperature 144°F (63°C)

Total Volume at 144°F (63°C)

$182,801 \times \frac{604}{492}$ 224,414 cu ft/hr (6,350 m^3/hr)

Design of the Scrubber

The air pollution limits for gaseous fluorides vary from one district to another within the U.S.A. The most stringent regulations, however, to which this design will conform, are in terms of the absolute quantity of fluorine per day or per ton of P_2O_5 per day which is permitted to be discharged to the atmosphere.

In Florida, where the laws governing fluoride emissions are the most stringent, the permitted emission of fluoride for plants constructed after May 1, 1964 is less than 0.4 lb F/ton (0.2 g/Kg) of phosphoric acid design capacity for a complete chemical complex. That is the evoluation includes all the manufacturing facilities for di-ammonium phosphate or triple superphosphate, for phosphoric acid concentration or any other phosphate processing at the same site. For phosphoric acid production alone the accepted fluoride emission is 0.05 lb F /ton (0.025 g/Kg) of P_2O_5 daily design capacity. Therefore for the particular size plant which we have assumed of 600 tons/day (546 metric tons/day) P_2O_5 the allowable emission is 30 lb F/day (13.6 Kg/day).

In selecting the scrubbing system, several points should be borne in mind. The system should have as low a pressure drop as possible. As some particulate matter may be entrained in the gas stream, it is important that the scrubber selected be able to process the gas without plugging due to collected particles. For the present problem, a two stage scrubbing system will be designed.

The first stage or primary system is simply a set of high pressure pond water sprays in a duct to absorb a large proportion of the highly soluble SiF_4. The walls of the duct will be running with water to prevent the SiO_2 from sticking or building up. This type of arrangement cannot block with solids which will be washed out of the water drains to the water pond.

The second stage is a cyclonic empty spray tower containing high pressure sprays operating on pond water. Adequate water drains are provided to avoid blockage and to prevent backup of water into the scrubbing vessel. The cyclonic stage will help remove particulate matter entrained in the gas stream which gets through the first stage.

This design is used with a view to saving power costs. Venturi scrubbers are efficient for solids removal but the high pressure drop of 10 to 30 inches (25 to 75 cm) water gauge for about 1.5 to 2.0 transfer units implies the use of high speed corrosion resistant expensive suction fans and results in very high power costs. Furthermore, for the sake of simplicity, as mentioned previously, it is assumed that this scrubber is designed only to handle the gases from the phosphoric acid reactor itself and not for the gypsum filter vent hood or the other seal tanks or filtrate tanks within the phosphoric acid plant, from which more particles might come.

If an even greater removal of fluroide is required it can be achieved by adding an extra stage operating on clean water and for very low concentrations a packed section should be used. To use a cross-flow packed scrubber in the early stages of the gas cleaner would be to invite high maintenance and downtime in order to clean the packing.

The SiF_4 in the reactor gases passing to the scrubber will not hydrolyze to SiO_2 and HF in the vapor phase below a temperature of 195°F (90°C). As soon as the SiF_4 is absorbed in water, however, in dilute solution the SiF_4 will hydrolyze according to the equation:

$$3SiF_4 + (x+2)\ H_2O \ = \ 2H_2SiF_6 + SiO_2(H_2O)_x$$

The H_2SiF_6 does not hydrolyze further, in any significant amount,to HF and SiO_2.

The equilibrium data for the vapor pressure of HF and SiF_4 over pond water and the effects of temperature are not available. Pond water is normally at a concentration of about 0.9% H_2SiF_6. The equilibrium vapor pressure of SiF_4 and HF over pond water is given by Teller and Reeve (A.V. Slack "Phosphoric Acid Part II") as

$p\ SiF_4 = 0.00007$ mm Hg

$p\ HF = 0.00080$ mm Hg

presumably this is at an ambient temperature of about 90°F, (32°C).

With the large volumes of water used in the proposed scrubber, the concentration of H_2SiF_6 or HF in the scrubbing solution will not change. The only effect of the dilute acid will be to leave a residual concentration of HF in the effluent gas which could be further reduced by means of scrubbing with clean water.

To achieve the maximum outlet emission rate of 30 lb/day (13.6 kg/day) of F, when 3.5 tons per day of "F" are being evolved, a minimum "F" removal efficiency of 6,970/7,000 = 0.9957 or ≈99.6% is required. The overall design efficiency of fluoride or SiF_4 removal will be chosen as 99.8%.

Heat Balance for Stage 1

In the stage 1 sprays, heat will be transferred due to the process described below. To determine the outlet temperature of the stage 1 contactor, and set a reasonable liquid flow rate, a heat balance over stage 1 can be carried out. First assume a liquid throughout of 40 gpm (150 ℓ/min). This can be altered later, if the heat balance shows it should be increased or decreased.

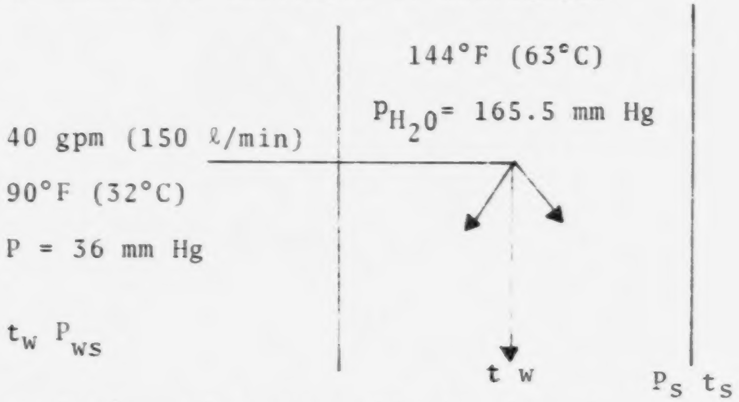

The heat load on the water side is given by:

$$40\ (60)\ 8.33\ (t_w - 90)\ \text{Btu/hr}$$

On the gas side the heat to the water is:

(heat of absorption of SiF_4) + (latent heat from water condensation) + (sensible heat from inert gas) + (sensible heat from water vapor)

$$=(0.918)\ (400)\ (3{,}200)+(1{,}070)\left[(110.9)\ (18)-\frac{(18)\ (395)\ (Ps)}{760 - Ps}\right]$$

+ sensible heat

$$= 1{,}175{,}040 + 2{,}135{,}934 - \frac{7{,}607{,}700\ Ps}{760 - Ps} + \text{sensible heat}$$

where 0.918 is the fraction of the fluorides removed in the first scrubber as calculated later.

It can be seen by inspection that the water rate chosen is too small because if the water emerged at the same temperature as the inlet gas then:

$$(40)\ (60)\ (8.33)\ [144 - 90] = 1{,}079{,}568 \text{ Btu/hr}$$

This is just sufficient to remove the heat of absorption of SiF_4 without cooling the gas at all. This is just possible but it would be advisable to use more water than this. Try a water throughput of twice as much, 80 gpm (300 ℓ/min).

The heat balance for the co-current spray contactor of stage 1 can now be expressed as follows:

$$(80)\ (60)\ (8.33)\ [t_w - 90] = \text{heat transfer}$$

This equals the heat removed from gas which is

$$(0.918)\ (400)\ (3{,}200) + 1{,}070\left[(110.9)\ (18) - \frac{(18)\ (395)\ (Ps)}{760 - Ps}\right]$$

$$+ \text{ sensible heat removed}$$

$$Ps = P_{ws} + y$$

and if "y" is negligible, $Ps = P_{ws}$, the expression becomes:

$$(0.983)\ (400)\ (3{,}200) + 1{,}070\ \left[(110.9)\ (18) - \frac{(18)\ (395)\ (P_{ws})}{760 - P_{ws}}\right] +$$

$$(13{,}651)\ (0.24)\ (144 - t_w) + \left[(110.9)\ (18) - \frac{(18)\ (395\ P_{ws})}{760 - P_{ws}}\right]$$

$$\left[\frac{0.45}{2}\ (144 - t_w)\right]$$

This reduces to:

$$39{,}985\ (t_w - 90) = 3{,}392{,}248 - \frac{7{,}607{,}700\ P_{ws}}{(760 - P_{ws})} + 3{,}276\ (144 - t_w) +$$

$$449 - \frac{1{,}560\ P_{ws}}{760 - P_{ws}}\ (144 - t_w)$$

"t_w" and "P_{ws}" are directly related by the vapor pressure tables for water.

SOLUTION OF EQUATION

t_w °F	P_{ws} mm Hg	L.H.S. of Equation Btu/hr	R.H.S. of Equation Btu/hr
130	115	1,599,360	2,084,065
140	149	1,999,200	1,550,395
135	130	1,799,280	1,870,047

:

The exit temperature from the stage 1 scrubber will be 136°F (57°C). The selected water throughput of 80 gpm (300 ℓ/min) seems reasonable.

Mass Transfer for Stage 1

Two spray sets will be inserted in a vertical duct, each set having one upward directed spray and one downward spray. The sprays will operate at 50 psig (3.4 afm) in order to obtain a good droplet surface area for absorption of the SiF_4.

From Figure 5.2.5-1 (also consult Kohl and Riesenfeld, 1960) one would expect to be able to obtain 2 or 3 gas-phase transfer units in this type of spray tower. We can either assume that the relationship in the figure is suitable or we can estimate "N_{OG}" from basic relationships, as follows. Because of the high solubility of fluorides, we can assume gas-phase control and that $K_G \approx k_G$ in equation 5.2.5-6.

$$N_{OG} = K_G a \ P \ Z/G_M \approx k_G a \ P \ Z/G_M \qquad (5.2.5\text{-}6)$$

Figure 4.5.1-1 shows a value of $k_G \approx 6\text{x}10^{-4}$ gmol/sec - cm² - atm for drops of 400 to 500 μm diameter falling in air, for D_G = 0.1 cm²/sec. This is close enough to the present case, despite the slight differences in gas density, viscosity and diffusivity, in view of the many uncertainties involved.

For a countercurrent scrubber, the drop surface area per unit volume of scrubber can be estimated by the use of Figure 4.5.1-3. This shows a value of a 0.15 cm²/cm³ for drops ranging from 400 to 500 μm diameter, for an upward air velocity of about 100 cm/sec, and for (Q_L/Q_G) = 1 ℓ/m³.

If a cocurrent, downward flow is to be used, we must first compute the drop holdup and then the area to volume ratio. Figure 4.6.2-4 shows a terminal settling velocity of about 200 cm/sec for drops of 400 to 500 μm diameter. Equation 5.3.5-21 provides a way of computing A_d, total drop area in the scrubber, from which we can compute "a".

$$A_d = \frac{3 \ Q_L \ Z}{u_d \ r_d} \qquad (5.3.5\text{-}21)$$

and

$$a = \frac{A_d}{A \ Z} = \frac{3 \ Q_L \ Z}{u_d \ r_d \ A \ Z} = \frac{3 \ Q_L \ u_G}{r_d \ Q_G \ u_d}$$

If we take $(Q_L/Q_G) = 1.8\text{x}10^{-3}$ cm³/cm³, corresponding to Q_L=300 ℓ/min, r_d = 0.02 cm, and u_G = 300 cm/sec (10 ft/sec), we compute as follows:

u_d = drop velocity relative to duct = 200 + 300 = 500 cm/sec

and,

$$a = \frac{3 \ (1.8\text{x}10^{-3}) \ 300}{2\text{x}10^{-2}(500)} = 0.16 \text{ cm}^2/\text{cm}^3$$

To compute "N_{OG}" we still need to find "G_M", as follows:

$$G_M = u_G \rho_M = 300 \left[\frac{273°K}{22{,}400\ (336°K)}\right] = 300(3.62x10^{-5}) = 0.0108$$

therefore,

$$N_{OG} = \frac{6x10^{-4}\ (0.16)\ (1\ atm)\ Z}{(0.0108)} = 9x10^{-3}\ Z$$

If column height = 1,000 cm (33 ft), and if all of the spray is effective,

N_{OG} = 9

We might estimate that ≈30% of the spray hits the wall and provides negligible transfer, so that N_{OG} = 2.7

Note that increasing (Q_L/Q_G) will increase "N_{OG}" proportionately and smaller drops will not only have larger surface area but also slower settling velocity, so they will stay in the scrubber longer. On the other hand, higher drop concentration increases agglomeration and wall losses.

Clearly, with all of the uncertainties about drop size, coefficient, wall losses, etc., it does not pay to be very precise in computations. The best we can do is make an estimate and then add a large safety factor.

Due to the precipitation of SiO_2 which can coat the spray droplets a conservative figure of 2.5 transfer units should be taken.

With sprays the most effective absorption occurs near the spray nozzle itself, where the water film breaks up into individual droplets. As the spray drops travel through the gas the circulation within the drop and oscillations of the drop itself aid absorption, but if the drop becomes coated with a film of SiO_2 as can occur with SiF_4 absorption, the only effective part is near the spray nozzle. Therefore, it would be best to employ a number of spray nozzles in series to produce the greatest effective interfacial area.

For soluble gas

$$N_{OG} = \ln \frac{y_1 - y^*}{y_2 - y^*}$$

N_{OG} = number of overall gas phase transfer units = 2.5

y_1 = concentration of soluble constituent in the inlet gas = 5.7 mm Hg.

y_2 = concentration of soluble constituent in the exit gas. (unknown)

y^* = equilibrium concentration of the soluble component over the liquid, ≈0

In this case the equilibrium concentration is assumed to remain the same throughout the scrubber and is so small as to be negligible. Therefore for this case:

$$2.5 = \ln \frac{5.7}{y_2} \; ; \; y_2 = 0.468 \text{ mm Hg}$$

The percentage removal of SiF_4 in one stage is:

$$\left[\frac{5.7 - 0.468}{5.7}\right] 100 = 91.8\%$$

First Stage Drainage Pipe

Care should be taken in the design of the first stage drain pipe to prevent flooding and carry-over to the second stage. The drain should be designed as a free running downcomer to ensure that the liquid does not back up into the gas space.

Design of Sprays

To distribute the 80 gpm (1.8 ℓ/m³) liquid load, four sprays each delivering 20 gpm can be used.

Second Stage Design

The gas to the second stage will be at 136°F (57°C) and will be 209,000 cu ft/hr (5,930 m³/hr) measured at 136°F (57°C). This will enter the cyclonic type scrubbing chamber at 50 ft/sec (1,500 cm/sec).

$$\text{Inlet Area} = \frac{209,000}{50 \times 3,600} = 1.61 \text{ ft}^2 \quad (0.15 \text{ m}^2)$$

The vessel should be designed like a slot inlet cyclone where normally the slot height is twice the width and the vessel diameter is four times the slot width.

The slot inlet size should be 9" x 18" (23 cm x 46 cm). The cyclonic vessel diameter is 36" (92 cm). The height will be 4 vessel diameters 12' 0" (3.65 m).

Expected Performance

For a cyclonic scrubber, Equation 5.2.7-1 applies:

$$N_{OG} = \frac{8,140\, Q_L\, d_c\, P}{G_M^{0.8}\, A_i\, d_d\, N_{Sc}^{2/3}} + \frac{0.0581\, A_W\, P}{G_M^{0.37}\, A_i\, N_{Sc}^{2/3}} \qquad (5.2.7\text{-}1)$$

the units to be used in this equation are given in Section 5.2-7.

As was discussed above, the outlet concentration of SiF_4 from the second stage will have a maximum partial pressure of 0.01 mm Hg. Since the outlet partial pressure from the first stage (inlet to second stage) was calculated to be 0.463 mm Hg, the number of transfer units required in the second stage will be:

$$N_{OG} = \ln \frac{0.468}{0.010} = 3.8$$

All terms in Equation 5.2.7-1 are known except Q_L, the liquid rate, and Schmidt number, N_{Sc}. Liquid rate can be adjusted to 3.8, give the required number of transfer units, and Schmidt number can be calculated:

$$N_{Sc} = \frac{\mu_G}{\rho_G \; D_G} = 1.24$$

where:

$\mu_G = 1.1 \times 10^{-4}$ poise
$\rho_G = 6.5 \times 10^{-4}$ g/cm^3
$D = 0.134$ cm^2/sec

Here the viscosity and density terms were taken as those for air at 140°F (60°C), and diffusivity for SiF_4 was calculated from Equation 10.2-22.

To calculate the value of "Q_L" necessary, the following values were substituted into Equation 5.2.7-1:

$N_{Sc} = 1.24$

$d_c = 0.92$ m (3 ft)

$P = 1$ atm

$G_M = 1{,}550 \frac{\text{kgmole}}{\text{hr m}^2}$ $(316 \frac{\text{lb mole}}{\text{hr ft}})$

$A_i = 0.15$ m^2 (1.61 ft^2)

$d_d = 595$ µm assuming 1/6" (0.42 cm) orifice at 67 psig (4.5 atm)

$A_w = (\pi)(0.92)(4 \times 0.92) = 10.6$ m^2 (113 ft^2)

$N_{OG} = 3.8$

The value for "G_M" was found by assuming the same molar flow rate enters the second stage scrubber as entered the first (509 lb-mole/hr) dividing by the inlet area (1.61 ft^2). This neglects the water vapor and SiF_4 transferred out in the first stage, but yields results sufficiently accurate for the present analysis. The calculated value of "Q_L" necessary is 17.6 m^3/hr or 78 gpm. As was true with the first stage, to allow for heat effects, more liquid than this should be used. Additional liquid also provide a "safety factor" to make sure the performance of the scrubbing system meets design speicifications. Design the liquid supply system to the second stage scrubber to handle 30 m^3/hr (132 gpm).

If we use 1/6 inch (0.42 cm) diameter nozzles, solid core type at 60 psig (4 atm) the flow through each would be 6 gpm (1.4 m^3/hr). The number of nozzles would be:

$$\frac{30\ m^3/hr}{1.4\ m^3/hr} = 21.4$$

Use 22 nozzles.

9.4 TROUBLE SHOOTING

Introduction

The discussion of trouble shooting and operating problems in this section is divided into categories according to scrubber type. Before discussing problems associated with different types of scrubbers, general difficulties which might be encountered in the operation of all types of scrubbers will be discussed. Many of these problems are common to the operation of any type of chemical plant or equipment.

Start Up of New Installations

One of the most important points about starting up new equipment is to have aclear and definite plan. Once this has been set and the general outlines in order, attention to details assumes real significance. During construction of the equipment take precautions to prevent nuts, bolts, pieces of wood and debris from falling into pipework from where it can work its way into automatic valves or pumps or cause blockage of nozzles, orifice plates or pipework.

Follow the maker's instructions on pumps, valves and instruments. Ensure that oil levels are correct, that the impellers are free, that the pumps or fans rotate in the correct direction, that alignment is correct. Make certain that valve and damper positions are indicated correctly and that they are able to move as intended.

It is recommended that the internals of all towers, scrubbers, pipework be inspected and washed out before being put into service, and where practicable, operation on water to check out equipment should be carried out. When making internal checks, as well as looking for foreign matter check internal dimensions of weirs, seal pots, seal downcomer pipes, spray nozzle orifices, to make sure the equipment is according to the drawings and is correctly assembled. Even go to the extent of climbing through equipment with a flashlight, measuring tape and drawings.

Initial Operating Problems with New Installations

Initial operating problems with scrubbers occur from either the mechanical equipment itself or from the mass-transfer process. Common equipment problems are incorrect installation of scrubber components, incorrect matching of equipment capacities, incorrect sizing of equipment components, and poor selection of materials of construction. Some more specific examples of what can happen from mechanical problems are described under the appropriate scrubber category. A thorough check of scrubbing equipment against specifications is recommended if a mechanical problem is suspected.

One of the most common problems associated with start up is that the quantity of gas to be scrubbed is increased over design with a consequent drop in concentration of material to be removed. This can happen because the scrubbing system was designed for average operating conditions rather than extreme conditions or that air inspiration into the system through blower seals and openings is greater than expected. Consequently, it is of the utmost necessity to check the inlet gas quantity and composition of the gas to be scrubbed if poor scrubbing efficiency is initially suspected. Also cut down on unnecessary leakage of air through hatch covers, blower flanges, inspection ports, etc. At the same time, the scrubbing liquor quantity and quality should also be checked.

Another problem that is fairly prevalent in start up is that design temperature conditions cannot be met. For some mass-transfer operations which are dependent on viscosity, surface tension, or chemical reaction rates; changes in temperature can have drastic effects on scrubbing efficiency. In those cases where heat is required, the addition of a heat exchanger in the scrubber liquor line may be of benefit in reaching design temperatures. In most cases, however, the cause of not reaching design operating temperature can be determined and corrected at less cost than addition of a heating or cooling system to a scrubber.

Plate-type Scrubbers

Flooding

Excessive entrainment may rapidly decrease scrubbing efficiency. It usually occurs when the maximum liquor and/or gas rate exceeds maximum design rates. It can also occur from priming, when foaming on one tray reaches the tray above. Flooding can occur due to by-passing of the vapor through the downcomer, when the pressure drop through a plate exceeds the liquid head available in the downcomer, especially if the liquid in the downcomer is frothy. These problems are usually associated with exceeding maximum design operating rates and may be alleviated by decreasing gas and/or liquor rates if the system upstream of the scrubber permits this. If flooding occurs at lower than design gas or liquid rates it may be caused by foaming.

Some of the more common mechanical problems occurring with plate-type scrubbers which decrease scrubber efficiency are listed below:

1. Plate Sealing. Faulty sealing of the plate to the column I.D. can cause excessive liquid by-passing through the plate with little gas-liquid contacting. Excessive gas by-passing can also occur.

2. Tray Levelling. Non-level tray installation can result in excessive liquid and/or gas by-passing. This problem occurs mostly from faulty installation.

3. Faulty Installation. Another common initial operating problem depending on plate-type is the installation of plates upside down. Careful checking during installation prior to operation alleviates this kind of problem.

4. Corrosion. Gas by-passing up downcomers can occur if corrosion is a problem. The gas-liquid interface and turbulence at the liquid level makes the downcomer especially susceptible to corrosion.

5. Dirt. Solids accumulation can occur in quiescent areas of plates and decrease tray effectiveness. The usual symptoms are a gradual decrease in scrubber capacity before flooding occurs.

6. Bottom Liquid Outlets. These seem to be susceptible to trouble. Liquid can back up due to a restriction at the outlet pipe, especially with rubber lined pipe where the internal bore at the outlet spigot may be far less than the nominal bore.

7. Gas Inlet. It has been known for liquid to back up in an absorber base and because the gas inlet was horizontal or came upwards into the absorber, the absorber liquor poured down the gas main into process equipment or blowers situated upstream in the process.

8. Pressure Tappings. Make sure that adequate pressure and sample points are allowed for in the design. It should be possible to take differential pressure readings across different sections of a scrubber as a check on its performance. These tappings can also be used for temperature measurements or sampling.

9. Liquor Recycling. When liquid is recycled from the base of an absorber, and if the liquid is hot, special care must be taken with the head over the pump suction to avoid boiling in the pump suction cavitation. Vibration due to cavitation can be so bad as to cause severe damage to pumps and couplings.

10. Overflows. Overflow pipes from absorber sumps can become gas locked thus restricting the flow until the head builds up sufficiently to cause a surge of liquid. This cycling effect can severely upset the absorber or connected equipment.

11. Superheated Gas. Extremely hot gas impinging on a downcomer can cause bubbling or boiling within the downcomer which will cause flooding on the plate above.

Packed Scrubbers

Generally speaking, packed columns are used on duty in which the flows remain steady and which are subject only to small changes during operation.

Problems which can be encountered are as follows:

1. Liquid Mal-Distribution. This seems to be fairly common, the usual fault is that insufficient liquid feed points are provided at the column top. This may be due to the designer trying to avoid restricting the gas flow with the liquid distributor.

2. Heat Shock on Packing. If a hot gas enters the base of a packed absorber, the sudden heating and cooling effects on a ceramic packing can cause its disintegration. With a hot dusty gas the broken packing

catches the dust and causes severe blocking problems at the absorber base. Carbon packings are resistant to heat shock due to the low coefficient of expansion of carbon.

De-superheating or saturating of the gas with water or with absorber product by spraying solution with the hot gas stream will reduce heat shock effects. It will also prevent drying out of the packing and keep it cleaner.

3. Plastic Packings and Temperature. If reliance is placed on quenching a hot gas to below the melting point of a plastic packing one can be almost certain that the packing will be melted due to a fault or breakdown in the quench system. One rule in design is that if you can visualize damage to a system due to failure of one part of the system, you can be sure that the damage will occur.

If there is a chance of melting the packing use a different type of packing.

4. Rubber Lined Packed Towers. If these are operated at temperatures above ambient using ceramic or carbon packing, the lining should be protected with the tile brick or acid proof concrete, to prevent the ceramic packing from gradually pushing its way into the softened rubber. This also gives protection to the surface of the rubber from sudden escalations of temperature due to faulty operation.

5. Methods of Packing. With small absorbers the absorber can be filled with water and the packing poured gently into the water. With larger towers the packing should be lowered in a container and spread out evenly over the surface of the packing in the tower.

Poor performance can occur if the packing is poured in across a sloping surface of packing in a column. Apart from the possibility of breakage with ceramics, an inclined stratification will take place, resulting in channeling and reduced performance.

The recommendations of the manufacturers of tower packing should be carefully adhered to. Some excellent catalogues are available describing methods of packing absorption columns.

6. Support Plates. With flat beam support plates it is difficult to obtain sufficient free cross-sectional area at the plate, and the environs of the support plate are prone to flooding. For this reason a few layers of stacked partition rings are used as the grid upon which saddles or raschig rings are dumped. If rings are dumped directly on the grid they protrude between the grids and reduce the free cross-sectional area.

7. Packing Hold Down Devices. With plastic packing it is especially necessary to restrain the packing material to prevent it from being carried out of the column. It is not unknown when hold down devices fail for plastic packing to rain from the stack.

Even with ceramic or carbon packing hold down plates are advisable, otherwise packing pieces will lift or bump causing the pieces to grind together and chip or wear.

Sieve Plate Columns

General problems which might be encountered in sieve plate columns are similar to those of plate columns. Downcomers and weirs are similar in design; the importance of inspection before putting the equipment to work, and the careful checking of mechanical details on site is very important.

Troubles to be avoided by means of good design are as follows,

1. Tower Cross Section. Use of too small a tower cross section thus creating difficulties in fitting the required internals into the available area. After the weirs and calming sections and downcomers have been fitted the hole spacing can become too cramped, especially with a carbon sieve plate, thus weakening the carbon plate. It is then subject to mechanical damage by people walking on the plate during installation.

2. Downcomers. A case of incorrect siting of downcomers has been experienced, on a rectangular tray, which apparently led to the formation of dry areas on the tray with consequent inefficiencies.

3. Hole size. Half inch holes appear to be the best size to use. At 3/4" diameter excessive weeping occurs which can subsequently lead to blocking of the holes due to deposits, if the liquid stream is dirty. Sieve trays have a good capability of handling dirty liquid streams.

Spray Towers

Spray scrubbers are normally associated with removal of highly soluble or reactive gases or are used for the removal of coarse dust from gases, that is dust above about five microns in diameter. They frequently have tangential inlets.

1. Demisting. The use of fine mesh demisters or spray arresters is to be avoided in dusty applications since eventually they will become blocked. Knock out pots or baffle boxes are more reliable.

2. Solid Deposits. Spray towers or cyclonic spray scrubbers or combined venturi and cyclonic spray scrubbers are used on highly soluble and reactive gases like SiF_4. This reacts with water to form SiO_2, especially just within the inlet duct of the scrubber. These solids must be removed mechanically or by liquid flush or a continuous spray. Sometimes for certain deposits, an acid wash may be effective in removing the solids and avoiding blockage.

Solids removal by use of sprays requires that the scrubbing liquor be capable of keeping the solids suspended without excessive wear in circulating equipment or lines except where solids separation occurs. If problems occur with excess wear or settling, attention to the solids' characteristics and handling of the slurry should result in finding acceptable solutions.

With spray scrubbers, misting can be a problem not so much from the quantity of mist as from its quality. Because of short retention times and parallel flow, mist character will be similar to that of the inlet gases. Acid vapors which are spray scrubbed will tend to result in an acid mist in the carryover. For this reason, attention should be paid to providing a mist eliminator, or if this is impractical, sufficient residence time at high gas velocity to coalesce the mist produced from the spray. This latter technique may work for HCl mists but probably not on SO_3 or sulfuric mist.

Venturi and Orifice Scrubbers

These are generally high velocity inertial type scrubbers for the removal of dust or acid mists. Problems encountered can be:

1. Sudden Loss of Efficiency. This can be very apparent with acid mist scrubbers where sub-micron mists form a highly visible cloud. The first particles to penetrate the scrubber if the gas flow is reduced are the finest ones with the greatest specific surface. These will form an opaque cloud.

A disadvantage of some types of high velocity inertial or impingement scrubber is the difficulty of adjusting the scrubber to the optimum pressure drop. For this reason variable throat scrubbers are advantageous or else a design where the liquid flow can be varied over wide limits in order to maintain the same gas pressure drop.

2. Incomplete Throat Coverage. With some designs, especially with a short throat, insufficient liquid injection points are provided leaving spaces through which unscrubbed gas can by-pass. The use of liquid weirs within the venturi, with the gas atomizing the liquid before the throat is said to avoid liquid distribution problems.

3. Orifice Scrubbers. The disadvantage of a multi-orifice plate scrubber is the difficulty of adjusting the pressure drop to the best value. This can be done by inserting plugs in the orifices though more refined mechanical adjustment devices have been used.

Demisters and Fine Fibre Filters

The main problem with fine fibre filters is their susceptibility to blockage by solids, although there are some particular designs where a replaceable felt cloth can be used, where the blockage is not so serious.

On the metallic knitted mesh spray arresters which are used at the end of a sulfuric acid plant the materials of construction of the wire used is important. This is believed to be alloy 20 wire which is resistant to 98% sulfuric, the life being dependent on the temperature of the exhaust. Some sulfuric acid plants produce sub-micron mist which must be removed by means of fine fibre mist eliminators such as the Brinks filters which are extremely efficient on sub-micron particles. The tendency to form fine mist in a sulfuric acid plant appears to depend on the design of the plant and is not inherent in all plants.

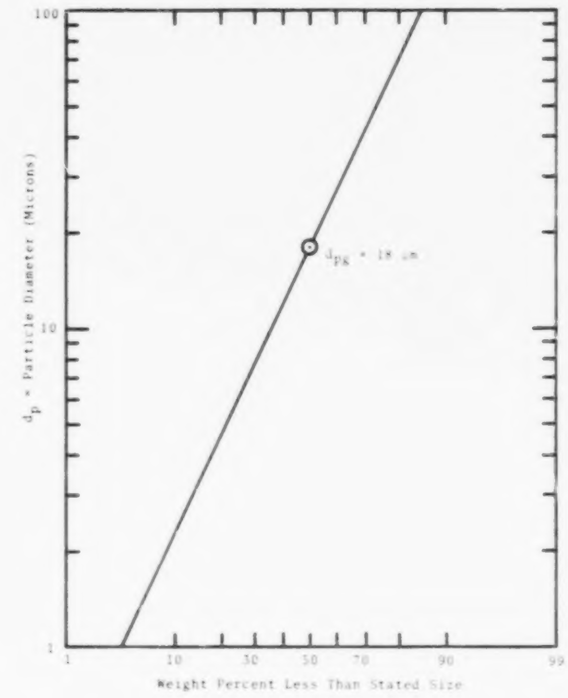

FIGURE 9.3-1

PARTICLE DIAMETER VS. WEIGHT PERCENT UNDERSIZE FOR ASPHALT PLANT DRYER DUST WITH d_{pg}=18 μm and σ_g=5.0

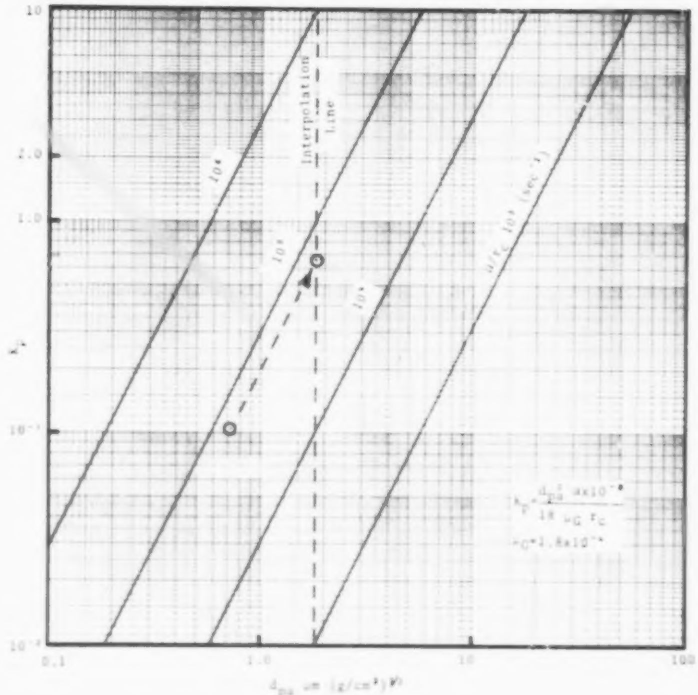

FIGURE 9.3-2

INERTIAL IMPACTION PARAMETER VS. PARTICLE AERODYNAMIC DIAMETER WITH VELOCITY/COLLECTOR RADIUS AS PARAMETER

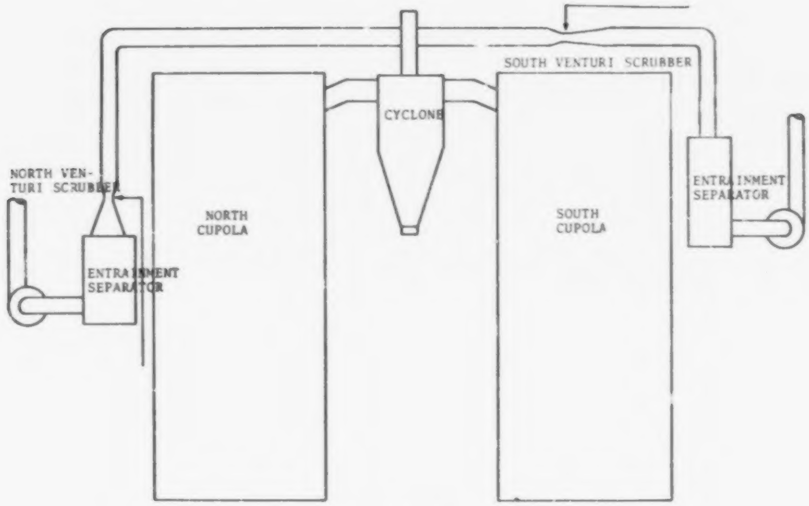

FIGURE 9.3-3

SCHEMATIC DESCRIPTION OF THE CUPOLA AIR POLLUTION CONTROL SYSTEM

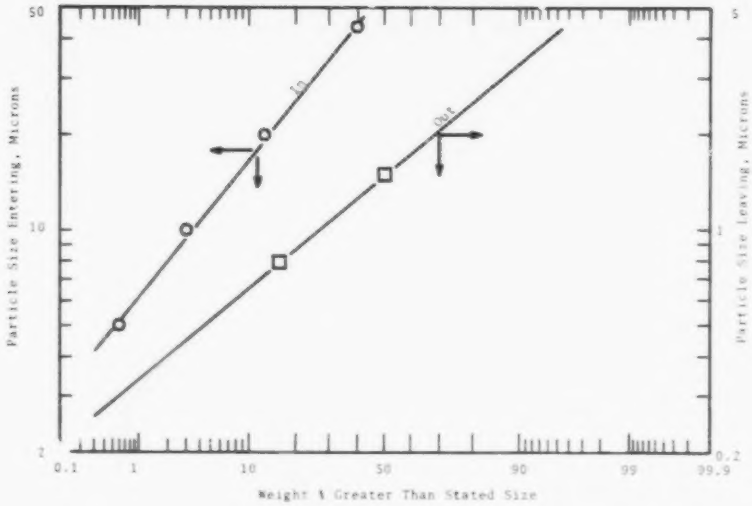

FIGURE 9.3-4

SIZE DISTRIBUTIONS INTO AND FROM ROCK WOOL CUPOLA SCRUBBER

CHAPTER 9 NOMENCLATURE

LATIN

a = inlet height

A = cross-sectional area of bed or tower

A_i = inlet area

A_w = wetted wall area

b = inlet width

C = centrifugal scrubber geometry coefficient

C' = Cunningham correction factor

C_o = orifice discharge coefficient

d = diameter

d_d = drop diameter

d_e = exit duct diameter

d_f = fiber diameter

d_{pa} = aerodynamic particle diameter size collected with 50% efficiency

d_p = particle size collected with 50% efficiency

D = gas diffusivity

D_p = particle diffusivity

f = velocity ratio factor; ≈0.25

f_h = ratio of hole or slot open area to toal cross-section of column, Fraction.

F = froth density

$Fr<d_p$ = fraction of dust (by weight) smaller than d_p

G_M = molar gas flow rate

h = overall height

Hd = liquid holdup

K_p = inertia parameter

K_{pt} = inertia parameter evaluation at throat velocity

CHAPTER 9 NOMENCLATURE

LATIN

ℓ = bed depth

M = momentum

n = vortex exponent

N = no. of plates or stages

N_{OG} = number of overall gas-phase transfer units

N_{Pe} = Peclet number

N_{Re} = Reynolds number

N_{Sc} = Schmidt number

P = total pressure

Pt = penetration

$\overline{Pt}$ = penetration over a particle size distribution

Q_c = liquid throughput

Q_G = gas throughput

r_d = drop radius

r_n = radius of hole

S = single solidarity factor

t = time

$\bar{u}$ = average gas velocity through slots, cm/sec

u_d = drop velocity

u_G = gas velocity

u_h = velocity of gas through hole, cm/sec

$u_{s,max}$ = maximum superficial gas design for flooding, cm/sec

u_t = drop terminal velocity

v_g = gas velocity

v_s = superficial velocity

CHAPTER 9 NOMENCLATURE

LATIN

y = concentration of pollution in vapor phase

Z = height

GREEK

α = solid fraction in fiber bed

ΔP = pressure drop

η_p = single drop efficiency due to impaction

η_s = single fiber efficiency

μ_G = gas viscosity

ρ_L = liquid density

ρ_G = gas density

ρ_p = particle density

Ψ = centrifugal scrubber process. coefficient

σ_g = standard deviation of dust

CHAPTER 9 REFERENCES

Biales, G. A., Chem. Eng. Prog. 60, #10, p. 71 (1964).

Danielson, John A., ed., "Air Pollution Engineering Manual", Public Health Service Publication 999-AP-40 (1967).

Eckert, J.S., Chem. Eng. Prog. 61, #9, p. 89 (1965).

Fair, James R., Chemical Engineering, 107, July 5, (1965).

Kohl, Arthur L., and Fred C. Riesenfeld, "Gas Purification Processes", McGraw Hill, New York (1960).

McLaren, D.B., and J. C. Upchurch, Chemical Engineering, 77, #13, p. 139 (1970).

Midwest Research Institute, "Handbook of Emission Properties", APCO Contract CPA 22-69-104, May 1 (1971).

Perry, John H., editor, Chemical Engineers' Handbook, 4th edition, McGraw Hill, New York (1963).

CHAPTER 10

PHYSICAL AND CHEMICAL DATA

TABLE OF CONTENTS

10.1 Introduction 2

10.2 Estimation Methods 3

10.3 Explanatory Notes. 12

10.4 Physical and Chemical Data 15

Nomenclature 30

References 32

CHAPTER 10

PHYSICAL AND CHEMICAL DATA

10.1 INTRODUCTION

The information presented in this chapter is intended to be useful in a preliminary design of a scrubber system. For a more detailed design the engineer should refer to original sources of data and may need to use more sophisticated estimation methods than are presented here. A valuable reference is "The Properties of Gases and Liquids", Reid and Sherwood (1966).

The data are organized by chemical systems (e.g., H_2S - H_2O is a chemical system), rather than by properties. CGS units are to be assumed unless other units are stated explicitly. Liquid composition is expressed either as mole fraction or as concentration in moles per liter. The nomenclature is defined fully at the end of the chapter.

10.2 ESTIMATION METHODS

When experimental overall equilibrium data are unavailable for a scrubber system of interest the equilibrium relation can often be estimated. The equilibrium for ammonia over SO_2 solutions as developed by Johnstone (1935) is given as an example. The physical equilibrium is

$$H' = \frac{p_{NH_3}}{[NH_4OH]} \qquad (10.2\text{-}1)$$

and the important chemical equilibria are

$$K_b = \frac{[NH_4^+][OH^-]}{[NH_4OH]} \qquad (10.2\text{-}2)$$

$$K_w = [H^+][OH^-] \qquad (10.2\text{-}3)$$

$$K_2 = \frac{[H^+][SO_3^=]}{[HSO_3^-]} \qquad (10.2\text{-}4)$$

combining these equilibrium expressions gives

$$p_{NH_3} = \frac{H'K_w}{K_bK_2} \; \frac{[NH_4^+][SO_3^=]}{[HSO_3^-]} \qquad (10.2\text{-}5)$$

The total concentrations of sulfite and of ammonia can be written

$$s = [H_2SO_3] + [HSO_3^-] + [SO_3^=] \qquad (10.2\text{-}6)$$

$$a = [NH_4OH] + [NH_4^+] \qquad (10.2\text{-}7)$$

electroneutrality requires that

$$[H^+] + [NH_4^+] = [HSO_3^-] + 2[SO_3^=] + [OH^-] \qquad (10.2\text{-}8)$$

In the practical range of pH 4 to 8, $[H^+]$, $[OH^-]$, $[H_2SO_3]$, and $[NH_4OH]$ are negligible in the above equations, and so

$$s \simeq [HSO_3^-] + [SO_3^=] \qquad (10.2\text{-}9)$$

$$a \simeq [NH_4^+] \simeq [HSO_3^-] + 2[SO_3^=] \qquad (10.2\text{-}10)$$

$$[HSO_3^-] = 2s - a \qquad (10.2\text{-}11)$$

$$[SO_3^=] = a - s \qquad (10.2\text{-}12)$$

The result is

$$p_{NH_3} = \frac{H'K_w}{K_bK_2} \; \frac{a(a - s)}{2s - a} \qquad (10.2\text{-}13)$$

When no overall equilibrium data are known, the coefficient $H'K_w/K_bK_2$ (which is a function of temperature) can be calculated from estimates of the individual constants. Alternatively, the group $H'K_w/K_bK_2$ can be determined from one or two experimental equilibrium points; in this way a derivation such as the above is useful in interpolating and extrapolating limited data to other concentrations.

In some design situations, for example a rigorous analysis of simultaneous diffusion and chemical reaction, the true Henry's constant is required. If a gas reacts in aqueous solution, the true Henry's constant can be estimated from the apparent Henry's constant and the appropriate chemical equilibrium, as is shown in the following example for SO_2 dissolved in water. H', the apparent Henry's law constant (based on concentration instead of mole fraction) is defined by

$$p_{SO_2} = H's \qquad (10.2\text{-}14)$$

$$s \equiv [H_2SO_3] + [HSO_3^-] \qquad (10.2\text{-}15)$$

From the equilibrium data

$$K = \frac{[H^+][HSO_3^-]}{[H_2SO_3]} = 1.7 \times 10^{-2} \text{ at } 25°C \qquad (10.2\text{-}16)$$

and electroneutrality requires that

$$[H^+] = [HSO_3^-] \qquad (10.2\text{-}17)$$

we get

$$s = \frac{p_{SO_2}}{H'} = [H_2SO_3] + \sqrt{K[H_2SO_3]} \qquad (10.2\text{-}18)$$

This equation can be solved for $[H_2SO_3]$, and then the true Henry's law constant (neglecting the reaction between SO_2 and water to form H_2SO_3) can be estimated

$$H \simeq \frac{p_{SO_2}}{[H_2SO_3]} \qquad (10.2\text{-}19)$$

Density data are usually available for aqueous solutions of a single solute. The same is not true of multicomponent aqueous solutions, and estimation of the density composition dependence for such solutions is difficult unless partial molar volumes are known. For scrubber design purposes, available density data for the several aqueous solutions of solute 1, 2, etc. can be fitted by the least squares method to give

$$\rho_L = \rho_L(\text{water}) + a_1x_1 + a_2x_2 + \cdots + a_nx_n \qquad (10.2\text{-}20)$$

where 1, 2, ... n are the solutes, and a_1, a_2 ... a_n are coefficients.

In the absence of experimental data on the effect of temperature on solution density, use can be made of the temperature dependence of water, i.e.

$$\rho_L(\text{solution at } t) = \frac{\rho_L(\text{water at } t)}{\rho_L(\text{water at } t_o)} \cdot \rho_L(\text{solution at } t_o) \qquad (10.2\text{-}21)$$

where "t_o" is the closest temperature for which the solution density is known.

For estimating gas-phase diffusivities, Reid and Sherwood (1966) suggest the empirical correlation of Fuller, Schettler, and Giddings:

$$D_{12} = \frac{0.001\, T^{1.75}\, (1/M_1 + 1/M_2)^{1/2}}{P\, [(\Sigma V)_1^{1/3} + (\Sigma V)_2^{1/3}]^2} \qquad (10.2\text{-}22)$$

"T" is temperature in °K, "P" is pressure in atmospheres, "M" is molecular weight, and "ΣV" is the sum of diffusion volume contributions given in Table 10.2-1 (adapted from Reid and Sherwood). Estimates obtained from this correlation are almost always accurate to within 10%.

Reid and Sherwood (1966) suggest the Othmer-Thakar method for aqueous non-electrolyte solutions at infinite dilution around 20°C:

$$D_A = \frac{14\text{x}10^{-5}}{\mu_L^{1.1}\, V_A^{0.6}} \qquad (10.2\text{-}23)$$

"μ_L" is the viscosity of water at the temperature of interest in centipoises, and "V_A" is the molar volume of the solute obtained by adding the group contributions given in Table 10.2-1 (from Reid and Sherwood).

The temperature dependence of liquid-phase diffusivities of non-electrolytes can be estimated from

$$\frac{D\mu_L}{t + 273} = \text{constant} \qquad (10.2\text{-}24)$$

where "μ" is the viscosity of the solution, or of water, if the solution is dilute.

Estimation methods for liquid-phase diffusivities are much less well developed.

Chemical Equilibrium

Chemical equilibrium constants at 25°C can be calculated from standard chemical potentials tabulated in various sources, by the following equation,

$$\log_{10} K = \frac{-\Sigma\ \nu\phi^\circ}{1{,}363} \qquad (10.2\text{-}25)$$

where the "ν's" are the stoichiometric coefficients of the equilibrium equation; by convention "ν" is positive for products and negative for reactants. For illustration, consider the equilibrium

TABLE 10.2-1

VOLUME CONTRIBUTIONS TO DIFFUSIVITY

	Gas-phase (Fuller et al.)	Liquid-phase (Othmer-Thakar)
Simple molecules		
N_2	17.9	31.2
O_2	16.6	25.6
Air	20.1	29.9
CO	18.9	30.7
CO_2	26.9	34.0
SO_2	41.1	44.8
NO		23.6
N_2O	35.9	36.4
NH_3	14.9	25.8
H_2O	12.7	18.9
H_2S		32.9
Cl_2	37.7	48.4
Br_2	67.2	53.2
Atoms		
C	16.5	14.8
H	1.98	3.7
O	5.48	7.4
O in acid		12.0
O with S, P, or N		8.3
N	5.69	
N=		15.6
N primary amine		10.5
N secondary amine		12.0
Cl	19.5	24.6
F		8.7
S	17.0	25.6
3 - member ring		-6.0
4 - member ring		-8.5
5 - member ring		-11.5
6 - member ring		-15.0
Aromatic ring	-20.2	
Heterocyclic ring	-20.2	

	NH_4OH	$\rightarrow$ NH_4^+	$+$ OH^-
ν	-1	+1	+1
$\phi°$,cal/mol	-63,050	-19,000	-37,595

$$\log K = -(63{,}050 - 37{,}595 - 19{,}000)/1{,}363$$

$$K = 1.86 \times 10^{-5}$$

The literature value at 25°C is the same.

For some oxidation-reduction reactions a chemical equilibrium constant can be calculated by combining Nernst equations for the appropriate half-cell reactions. For a simple example, consider

$$2\ NO(g) + 1/2\ O_2(g) + H_2O \rightarrow 2\ HNO_2\ (aq.) \qquad (10.2\text{-}26)$$

Nitrogen oxide oxidation:

$$NO + H_2O = HNO_2 + H^+ + e^- \qquad (10.2\text{-}27)$$

$$E_N = 1.004 - 0.0591 \log_{10} \frac{[HNO_2][H^+]}{p_{NO}} \qquad (10.2\text{-}28)$$

Oxygen reduction:

$$O_2 + 4H^+ + 4e^- = 2\ H_2O \qquad (10.2\text{-}29)$$

$$-E_O = -1.228 + \frac{0.0591}{4} \log_{10} p_{O_2} [H^+]^4 \qquad (10.2\text{-}30)$$

Combining equations 10.2-29 and 10.2-27 to get eq. 10.2-26, and after some algebra,

$$\log K = \log \frac{[HNO_2]^2}{p_{NO}^{\ 2}\ p_{O_2}^{\ 1/2}} = \frac{2}{0.0591} (1.228 - 1.004) \qquad (10.2\text{-}31)$$

$$K = 3.7 \times 10^7$$

The temperature dependence of an equilibrium constant is given by

$$\frac{\partial \ln K}{\partial T} = \frac{\Delta H}{Rg\ T^2} \qquad (10.2\text{-}32)$$

where "ΔH" is the heat of reaction and "T" is absolute temperature. If "ΔH" is known, "K" can be calculated from "K_{25}" the value at 25°C, by

$$\log K/K_{25} = \frac{-\Delta H}{2.3Rg} \left(\frac{1}{T} - \frac{1}{298}\right) \qquad (10.2\text{-}33)$$

If K is known at two temperatures, ΔH can be calculated from

$$\Delta H = \frac{2.3R_g \log K_2/K_1}{(1/T_1 - 1/T_2)} \qquad (10.2\text{-}34)$$

Reaction Rate

Estimation of a reaction rate constant is not necessary if the absorption is known to take place in the instantaneous or surface reaction regime; the ionization (dissociation) of any acid gas in water, the hydration of NH_3, and most acid-base reactions have such rapid kinetics that scrubbing processes involving these reactions are almost always diffusion-controlled. Order-of-magnitude rate constants are shown below for some industrially important classes of reactions.

	Reaction	Approx. k
First order ($k = sec^{-1}$)		
	Acid gas dissociation in water	10^6 to 10^8
Second order ($k = \frac{\ell}{mol\text{-}sec}$)		
	$H^+ + OH$	1.4×10^{11}
	H^+ + anion	10^{10} to 10^{11}
	OH^- + amine	10^{10}
	OH^- + metal cation	10^{10} to 10^{11}
	OH^- + acid	10^{10}
	OH^- + amine cation	3×10^{10}

For a reversible reaction, if the forward and reverse reaction rate expressions correspond directly to the stoichiometry of the equilibrium, the forward rate constant can be calculated if the equilibrium constant and the rate constant for the reverse reaction are known.

$$A + B \rightleftarrows C \qquad (10.2\text{-}35)$$

$$\vec{R} = \vec{k}[A][B] \qquad (10.2\text{-}36)$$

$$\overleftarrow{R} = \overleftarrow{k}[C] \qquad (10.2\text{-}37)$$

At equilibrium $\vec{R} = \overleftarrow{R}$, hence

$$\frac{[C]}{[A][B]} \qquad K = \vec{k}/\overleftarrow{k} \qquad (10.2\text{-}38)$$

$$\vec{k} = K\overleftarrow{k} \qquad (10.2\text{-}39)$$

Density

In many scrubbing applications the density of the gas stream is the same as air. Perry's Handbook (1963) gives the compressibility factor $Z = PV/R_g T$ for various gases as a function of temperature and pressure. The density is then

$$\rho_{air} = \frac{0.3529\ P}{Z\ T} \qquad (10.2\text{-}40)$$

where "ρ" is in g/cm³, "P" is in atm, and "T" is in °K.

For other gases, the density can be estimated with sufficient accuracy for design purposes by using a generalized compressibility factor chart such as the one given in Chapter 3 of Perry's Handbook (1963). The compressibility factor is given as a universal function of reduced temperature T/T_c and reduced pressure P/P_c. The density is then

$$\rho = \frac{M\ P}{Z(T_r, P_r) R_g\ T} \qquad (10.2\text{-}41)$$

Values of the critical constants for the gas are required in using such generalized correlations; in the rare case where the gas mixture is not dilute enough to use simply the critical constants of the major component, pseudo-critical constants can be estimated as discussed below.

Viscosity

The viscosity of air is shown in Figure 10.2-1 as a function of temperature and pressure. The temperature dependence is from the tabulated data in Hodgman (1959) and in Fishenden and Saunders (1950), while the pressure effect was estimated from the correlation of Carr et al. (1955), reproduced in Perry (1963). The pressure effect is negligible except at very high pressures and low temperatures. For other gases, Reid and Sherwood (1966) recommend the empirical relations of Stiel and Thodos (1961). For nonpolar gases at low pressures:

$$\mu_G = 3.4 \times 10^{-6} \frac{M^{1/2} P_c^{\ 2/3}}{T_c^{\ 1/6}} T_r^{\ 0.94} \qquad T_r \leq 1.5 \qquad (10.2\text{-}42)$$

$$\mu_G = 1.778 \times 10^{-6} \frac{M^{1/2} P_c^{\ 2/3}}{T_c^{\ 1/6}} (4.58 T_r - 1.67)^{5/8} \qquad T_r > 1.5 \qquad (10.2\text{-}43)$$

where $T_r \equiv T/T_c$, T_c is in °K, P_c is in atm, M is molecular weight, and "μ" is in poise. (These equations are not valid for halogen gases; see Stiel & Thodos (1961).) The group $(\mu_G T_c^{\ 1/6})/(M^{1/2} P_c^{\ 2/3})$ is plotted against "T_r" in Figure 10.2-2; combining both Equations 10.2-42 and 10.2-43. If any viscosity data are available for the gas those data should be used in conjunction with the temperature dependence indicated in Equations 10.2-42 and 10.2-43 for extrapolation purposes. The correction for high pressures may be estimated from the correlation of Carr et al. (1955) given in Perry (1963); the increase in viscosity is about 10% for the highest pressures and lowest temperatures likely to be encountered in a scrubber system.

Example:

Estimate the viscosity of air at 200°C and low pressures. The critical constants are 132°K and 36.4 atm, and "M" is 28.97 g/mol.

$T_r = 473.2/132 = 3.58$

$$\mu_G = 1.778 \times 10^{-6} \quad \frac{28.97^{1/2} \times 36.4^{2/3}}{132^{1/6}} \quad (4.58 \times 3.58 - 1.67)^{5/8}$$

$$= 2.51 \quad 10^{-4} \text{ poise.}$$

The observed value from Figure 10.2-1 is 2.57×10^{-4} poise.

When the minor components of a gas stream have an appreciable effect on its properties, generalized correlations such as the ones described above can be applied through the use of "pseudo-critical" constants for the gas mixture. Simple, reasonably accurate pseudo-critical constants are:

$$T_{c,\ mix} \equiv \sum_i y_i\, T_{ci} \qquad (10.2\text{-}44)$$

$$V_{c,\ mix} \equiv 1/8 \sum_i \sum_j y_i y_j\, (V_{ci}{}^{1/3} + V_{cj}{}^{1/3})^3 \qquad (10.2\text{-}45)$$

$$Z_{c,\ mix} \equiv \sum_i y_i\, Z_{ci} \qquad (10.2\text{-}46)$$

$$P_{c,\ mix} \equiv (Rg\ T_{c,\ mix}\ Z_{c,\ mix})/(V_{c,\ mix}) \qquad (10.2\text{-}47)$$

Example:

How does the calculated viscosity of an air stream, containing 20% SO_2 by volume, differ from the viscosity of pure air at 200°C?

The critical constants are

	T_c	V_c	P_c	M
Air	132°K	86.6 cm³/mol	36.4 atm	28.97
SO_2	430.7°K	122 cm³/mol	77.8 atm	64.07

The pseudo-critical constants for the mixture are then

$$T_{c,\ mix} = 0.8 \times 132 + 0.2 \times 430.7 = 191.7°K \qquad (10.2\text{-}48)$$

$$V_{c,mix}\ 1/8\ [(0.8)\ (0.8)\ (2\text{x}86.6^{1/3})^3 + (2)\ (0.8)\ (0.2)\ (86.6^{1/3} + 122^{1/3})^3 + $$
$$+ (0.2)\ (0.2)\ (2\text{x}122^{1/3})^3\ ] = 93.42 \text{ cm}^3/\text{mol} \qquad (10.2\text{-}49)$$

$$Z_{c,\ mix} = \frac{(0.8)\ (36.4)\ (86.6)}{82.06\ (132)} + \frac{(0.2)\ (77.8)\ (122)}{82.06\ (430.7)} = 0.2865 \qquad (10.2\text{-}50)$$

$$P_{c,\ mix} = \frac{(82.06)\ (191.7)\ (0.2865)}{93.42} = 48.24 \text{ atm} \qquad (10.2\text{-}51)$$

$$M_{mix} = (0.8)\ (28.97) + (0.2)\ (64.07) = 35.99 \qquad (10.2\text{-}52)$$

$$T_r = 473.2/191.7 = 2.47 \qquad (10.2\text{-}53)$$

$$\mu_G = 1.778 \times 10^{-6} \left[\frac{35.99^{1/2}\ (48.24^{2/3})}{191.7^{1/6}}\right] [4.58\ (2.47) - 1.67]^{5/8} \qquad (10.2\text{-}54)$$

$\mu_G = 2.43 \times 10^{-4}$ poise for the mixture.

The value calculated above for pure air is 2.51×10^{-4}, and the experimental value is 2.57×10^{-4} poise.

10.3 EXPLANATORY NOTES

The first section under each chemical system, titled "Equilibrium", gives information relating the partial pressure of the gaseous component being scrubbed to its concentration in the liquid phase. If the scrubbed component A is chemically inert in the liquid phase (e.g., CO in water) the equilibrium is properly defined by Henry's law constant. In addition, however, for several important systems the observed equilibrium data are described adequately by an "apparent" Henry's constant, $H' \equiv p_A/x_{\text{total A}}$, even though "A" reacts and consequently exists in more than one form in the liquid. For example, in the scrubbing of H_2S with water, the true Henry's constant would be

$$H_x = p_{H_2S}/x_{H_2S} \tag{10.3-1}$$

while the apparent Henry's constant is

$$H'_x = p_{H_2S}/(x_{H_2S} + x_{HS^-} + x_{S^=}) = p_{H_2S}/\Sigma_S \tag{10.3-2}$$

It is easy to show from chemical equilibrium considerations that for this example

$$H'_x = p_{H_2S}/x_{H_2S}(1 + \frac{K_1}{[H^+]} + \frac{K_1K_2}{[H^+]^2}) \tag{10.3-3}$$

where K_1 and K_2 are the equilibrium constants for the ionization of H_2S in water and are defined by

$$K_1 = \frac{[H^+][HS^-]}{H_2S} \tag{10.3-4}$$

$$K_2 = \frac{[H^+][S^=]}{[HS^-]} \tag{10.3-5}$$

This result shows that in such cases the apparent Henry's constant depends on the pH, and thus values of apparent "H'_x" given for an equilibrium over water cannot be used at other pH's without modification. (See the section on estimation methods.) To provide an idea of the ranges commonly encountered, apparent Henry's constants for several important gases scrubbed with water are shown in Figure 10.3-1.

In cases where absorption is greatly enhanced by chemical reaction with another component, the equilibrium is not expressed as apparent Henry's law constant. Rather, the equilibrium expression given in the Data section is based on the true Henry's constant, the chemical equilibria among the species present and experimental data.

Several aspects of gas-liquid absorption are worth recalling here. The gas and the liquid are usually assumed to be at physical equilibrium (true Henry's constant) at the gas-liquid interface. The degree of attainment of physical equilibrium elsewhere in the liquid phase depends on diffusion rates, while the degree of attainment of chemical equilibrium depends on both reaction and diffusion rates. (For a discussion of mass transfer accompanied by chemical reaction see Chapter 4.) In other words, equilibrium is not always attained in an operating scrubber, especially if the scrubber operates in the diffusional or fast reaction regime (see Chapter 4).

Since many scrubber liquids are dilute aqueous solutions, the liquid density is often taken as unity. However, this assumption can lead to serious design inaccuracies for some industrially important scrubber operations where the liquid is a concentrated solution, and density information should be used if it is available. In addition to its value in determining material balances, the liquid density is useful in converting concentrations in the liquid phase between moles per liter and mole fraction.

$$c_A = \frac{1000\ x_A\ \rho_L}{\overline{M}} \tag{10.3-6}$$

where "ρ_L", the liquid density, is a function of "x_A" and temperature, and $\overline{M}$ is the average molecular weight of the solution, defined by $\overline{M} \equiv \sum_i x_i M_i$. The inverse is

$$x_A = \frac{\sum_{i \neq A} x_i M_i}{1000\ \rho/c_A - M_A} \tag{10.3-7}$$

Data on diffusivities of gases are scarce, and where they exist, the temperature dependence has rarely been determined. Some of the values given in the Data section were obtained through estimation procedures and have uncertainties of 20% or more for liquid-phase diffusivities.

Chemical equilibrium data are presented in the form of ratios between the various species in the chemical system. Brackets [ ] indicate concentrations in moles per liter; partial pressures are in atmospheres. When ratios have been calculated from standard chemical potentials or other semi-theoretical estimation methods, the equilibria refer to activities, and the ratios as given imply ideal solutions, i.e. all activity coefficients = 1. The ratios can be used to determine the concentration of each species in the solution, as shown in the following example, using H_2S:

$$\begin{aligned} c_{\text{total } H_2S} &= [H_2S] + [HS^-] + [S^=] \\ &= [H_2S] + \frac{[HS^-]}{[H_2S]} \cdot [H_2S] + \frac{[S^=]}{[H_2S]} \cdot [H_2S] \end{aligned} \tag{10.3-8}$$

at pH 6, for example and 25°C

$$c_{\text{total } H_2S} = [H_2S](1 + 0.1 + 0) = 1.1\ [H_2S] \tag{10.3-9}$$

$$\%\ H_2S = \frac{[H_2S]}{c_{\text{total } H_2S}} = \frac{1}{1.1} = 90.9\% \tag{10.3-10}$$

$$\% \text{ HS}^- = \frac{[\text{HS}^-]}{c_{\text{total H}_2\text{S}}} = \frac{0.1}{1.1} = 9.1\% \qquad (10.3\text{-}11)$$

Similarly, at pH 10, % H_2S = 0.1%, % HS^- = 99.9%. For a given temperature, these results can be calculated for several pH values and plotted as shown for example in Figure 10.3-2. Such a plot (or the calculation on which it is based) is useful in establishing what effect changes in pH has on the absorption equilibrium. A practical example is the absorption of H_2S in buffered bicarbonate solutions. Here H_2S absorption is greatly increased over scrubbing with water, in part because the higher pH of the buffer solution drives the equilibrium toward ionization of the H_2S into HS^-, thus reducing the concentration of H_2S in solution and allowing more gaseous H_2S to dissolve in the liquid. See the example in Chapter 4.

Kinetic rate data are also not plentiful, especially for the faster chemical reactions occurring in some industrial scrubbing systems. Fortunately, if the reaction is fast enough the absorption is liquid-diffusion or even gas-diffusion controlled, and in that case an order-of-magnitude estimate for the rate constant is all that is required to demonstrate that the reaction is in the instantaneous or surface regime (see Chapter 4).

10.4 PHYSICAL AND CHEMICAL DATA

CARBON MONOXIDE - WATER

Equilibrium - Henry's constant is

$$\ln H = 10.489 + 0.0220\ t - 0.000137\ t^2 \qquad (10.4\text{-}1)$$

H in atmospheres/mole fraction. Reproduces data in Perry (1963) within 2%. Range 0-100°C.

Liquid density - Use density of water.

Diffusivity - for CO in water,

$$D_A = 2.0 \times 10^{-5}\ \text{cm}^2/\text{sec at } 25°\text{C} \qquad (10.4\text{-}2)$$

roughly estimated by Othmer-Thakar method (see section on estimation methods). Rough temperature dependence is

$$D_A \simeq \frac{6.1 \times 10^{-10}\ (t + 273)}{\mu_L} \qquad (10.4\text{-}3)$$

"μ_L" is viscosity of water in poise.

CARBON MONOXIDE - CUPROUS AMMONIUM - WATER

Equilibrium - Partial pressure (atmospheres) of CO over cuprous ammonium salt solutions is

$$p_{CO} = \frac{H'\ R}{(1-R)(c_{NH_3} - Rc_{Cu^+})} \qquad (10.4\text{-}4)$$

$R \equiv$ moles CO absorbed/mole Cu^+

c_{Cu^+} is total cuprous ion concentration, mol/ℓ; c_{NH_3} is free NH_3 concentration, mol/ℓ. When the anion is formate, H' is given by

$$H' = \exp[22.61 + 0.092I - 6800/(t + 273)] \qquad (10.4\text{-}5)$$

$$I \equiv (\Sigma\ c_i\ \nu_i^2)/2 = (c_{Cu^+} + 4c_{Cu^{++}} + c_{HCOO^-} + c_{NH_4^+})/2 \qquad (10.4\text{-}6)$$

(Kohl and Riesenfeld, 1960)

Liquid density - Tabular data in Perry (1963) in the range of -15°C to +25°C for aqueous NH_3 solutions is reproduced within 1% by

$$\rho_L = A + Bx_{NH_3} + Cx_{NH_3}^2 \qquad (10.4\text{-}7)$$

$$A = 0.9996 + 0.029 \times 10^{-3}\ t - 0.556 \times 10^{-5}\ t^2 \qquad (10.4\text{-}8)$$

$$B = -0.3694 - 2.70 \times 10^{-3}\ t + 5.04 \times 10^{-5}\ t^2 \qquad (10.4\text{-}9)$$

$$C = 0.2054 + 1.90 \times 10^{-3}\ t - 8.41 \times 10^{-5}\ t^2 \qquad (10.4\text{-}10)$$

The effect of the other components on the density of the scrubbing liquid at 25°C is roughly

$$\rho_L = 1.0023 + 0.172\ x_{NH_3} + 0.475\ x_{HCOOH} + 3.214\ x_{Cu} \qquad (10.4\text{-}11)$$

based on data for solutions of NH_4OOCH, $Cu(OOCH)_2$, and of HCOOH (International Critical Tables, 1928).

Diffusivity - For CO in water,

$$D_A = 2.0 \times 10^{-5}\ cm^2/sec \text{ at } 25°C \qquad (10.4\text{-}12)$$

roughly estimated by Othmer-Thakar method (see section on estimation methods). Very rough temperature dependence due to lack of a better correlation is:

$$D_A = \frac{6.1 \times 10^{-10}\ (t + 273)}{\mu_L} \qquad (10.4\text{-}13)$$

For $Cu(NH_3)_2^+$ complex in water,

$$D_B = 1.1 \times 10^{-5}\ cm^2/sec \text{ at } 25°C \qquad (10.4\text{-}14)$$

This value was also estimated by the Othmer-Thakar method and must be considered to be very approximate.

Chemical equilibrium - The equilibrium for the main reaction, the complexing of CO,

$$Cu(NH_3)_2^+ + CO + NH_3 \rightleftarrows Cu(NH_3)_3CO^+ \qquad (10.4\text{-}15)$$

is implied in the Henry's law expression given above. Other relevant equilibria are tabulated below for the side reactions

$$2\ Cu^+ = Cu + Cu^{++} \qquad (10.4\text{-}16)$$

$$4\ Cu^+ + O_2 + 2\ H_2O = 4\ Cu^{++} + 4\ OH^- \qquad (10.4\text{-}17)$$

$$2\ Cu^{++} + HCOOH + 2OH^- = 2\ Cu^+ + CO_3^= + 2\ H_2O \qquad (10.4\text{-}18)$$

These are estimated from standard chemical potentials in Pourbaix (1966).

TABLE 10.4-1

EQUILIBRIUM CONSTANTS AT 26°C AFTER POURBAIX (1966)

pH	$\frac{[Cu^{++}]}{[Cu^+]^2}$	$\frac{[Cu^{++}]}{[Cu^+]p_{O_2}^{1/4}}$	$\frac{[Cu^+]^2[CO_3^=]}{[Cu^{++}]^2p_{CO}}$	$\frac{[Cu^+]^2p_{CO_2}}{[Cu^{++}]^2[HCOOH]}$
4	1.6×10^6	1.6×10^{14}	3.2×10^6	9×10^3
6	1.6×10^6	1.6×12^{12}	3.2×10^{14}	9×10^{-1}
8	1.6×10^6	1.6×10^{10}	3.2×10^{22}	9×10^{-5}
10	1.6×10^6	1.6×10^8	3.2×10^{30}	9×10^{-9}

Kinetics - The complexing reaction is very rapid and probably takes place in the surface reaction regime (Kohl and Riesenfeld, 1960).

HYDROGEN CHLORIDE - WATER

Equilibrium - Vapor pressure of HCl over aqueous HCl solutions cannot be described by Henry's constant. The equilibrium for dilute solutions is shown in Figure 10.4-1. (Note that the partial pressure shown is in mm Hg.) (International Critical Tables, 1928).

Liquid density - The data in Perry's Handbook (1963) for aqueous HCl solutions are reproduced within less than 1% by

$$\rho_L = A + Bx_A + Cx_A^2 \qquad (10.4\text{-}19)$$

$$A = 1.0007 - 0.685 \times 10^{-4}\ t - 0.356 \times 10^{-5}\ t^2 \qquad (10.4\text{-}20)$$

$$B = 1.045 - 37.84 \times 10^{-4}\ t + 3.722 \times 10^{-5}\ t^2 \qquad (10.4\text{-}21)$$

$$C = -0.738 + 55.29 \times 10^{-4}\ t - 10.65 \times 10^{-5}\ t^2 \qquad (10.4\text{-}22)$$

Range 0-100°C, $x_A < 0.11$.

Diffusivity

$$D_{A,L} = 2.1 \times 10^{-5}\ \text{cm}^2/\text{sec}$$

Rough temperature dependence is

$$D_{A,L} = 10^{-9}\ (t + 273)/\mu_L \qquad (10.4\text{-}23)$$

The concentration dependence is approximately

$$D(c) = D_{A,L} + 1.08 \times 10^{-3}\ c \qquad (10.4\text{-}24)$$

where "c" is in mol/cm³. The range of experimental data used in arriving at these estimation equations is t = 0-15°C, c < 0.01 mol/cm³ (International Critical Tables, 1929).

The estimated diffusivity of HCl in air at 25°C and atmospheric pressure is

$$D_{A,G} = 0.175\ \text{cm}^2/\text{sec}$$

(See section on estimation methods.)

Chemical equilibrium

pH	$\frac{[Cl^-]}{p_{HCl}}$
2	2×10^{8}
4	2×10^{10}
6	2×10^{12}

"p" is partial pressure in atm; concentrations in mol/ℓ. Ratios at 25°C, from Pourbaix (1966).

Kinetics - The dissociation of HCl is extremely fast and occurs in the surface regime.

HYDROGEN SULFIDE - WATER

Equilibrium - Henry's constant is

$$\ln H_x = 10.2071 + 0.3105\ t - 0.000140\ t^2 \qquad (10.4\text{-}25)$$

H_x in atm/mole fraction total S, "t" in °C. Error less than 5%, 0-100°C, International Critical Tables, (1928).

Liquid density - Same as water, since H_2S is so slightly soluble.

Diffusivity - in water

$D_A = 1.61 \times 10^{-5}\ cm^2/sec$ at 25°C

Perry et al. (1963). Temperature dependence is approximately

$$D_A = \frac{4.8 \times 10^{-10}\ (t + 273)}{\mu_L} \qquad (10.4\text{-}26)$$

Chemical equilibrium

$$\frac{[H^+][HS^-]}{[H_2S]} = 9.1 \times 10^{-8} \text{ at } 18°C \qquad (10.4\text{-}27)$$

$$\frac{[H^+][S^=]}{[HS^-]} = 1.2 \times 10^{-15} \text{ at } 18°C \qquad (10.4\text{-}28)$$

Chemical equilibrium

TABLE 10.4-2

EQUILIBRIUM CONSTANTS AT 25°C

	25°C			18°C	
pH	$\frac{[H_2S]}{PH_2S}$	$\frac{[HS^-]}{PH_2S}$	$\frac{[S^=]}{PH_2S}$	$\frac{[HS^-]}{[H_2S]}$	$\frac{[S^=]}{[H_2S]}$
4	0.10	0.0001		0.00091	
6	0.10	0.01		0.091	
8	0.10	1.	0.000001	9.1	0.0000011
10	0.10	100.	0.0129	910.	0.011
12	0.10	10000.	129		

"p" is partial pressure in atm; concentration in mol/ℓ. Ratios at 25°C calculated from data of Purbaix (1966). Ratios at 18°C from data in Hodgman (1959).

Kinetics

$k = 4.4 \times 10^{5}$ sec^{-1} for

$H_2S \rightarrow H^+ + HS^-$

in aqueous solution at 25°C, calculated from the second order constant given by Caldin (1964). Instantaneous reaction regime applies (Astarita, 1967).

HYDROGEN SULFIDE - AMMONIA - WATER

Equilibrium - H_2S in aqueous ammonia solutions does not obey Henry's law. The partial pressure of H_2S over a solution containing "S" moles H_2S/liter and "A" moles NH_3/liter is

$$p = \frac{S^2}{(A-S)\exp(a + 0.205S)} \qquad (10.4\text{-}29)$$

a is 4.10, 2.71 and 1.58 at 20, 40 and 60°C; p in atmospheres (Kohl and Riesenfeld (1960)).

Liquid density - based on aqueous ammonia solutions, a crude estimate is

$$\rho_L = 0.999 + 0.5\, x_{H_2S} - 0.38\, x_{NH_3} \qquad (10.4\text{-}30)$$

at 15.5°C.

Diffusivity - for H_2S,

$D_A = 1.61 \times 10^{-5}$ cm^2/sec at 25°C

(Perry et al., 1963). Temperature dependence is approximately

$$D_A = \frac{4.8 \times 10^{-10}\,(t + 273)}{\mu_L} \qquad (10.4\text{-}31)$$

TABLE 10.4-3

DIFFUSIVITY OF AMMONIA IN WATER

t, °C	C_{Bo}, mol/cm³	D_B, cm²/sec
5	0.0007	1.24×10^{-5}
8	0.001	1.36×10^{-5}
12		1.64×10^{-5}
15		1.77×10^{-5}
5	0.0035	1.24×10^{-5}

(International Critical Tables, 1929). Temperature dependence is approximately

$$D_A = \frac{7.0 \times 10^{-10}\ (t + 273)}{\mu_L} \qquad (10.4\text{-}32)$$

Chemical Equilibrium

$$\frac{[H^+]\ [HS^-]}{[H_2S]} = 9.1 \times 10^{-8} \text{ at } 18°C \qquad (10.4\text{-}33)$$

$$\frac{[H^+][S^=]}{[HS^-]} = 1.2 \times 10^{-15} \text{ at } 18°C \text{ (Hodgman, 1959)} \qquad (10.4\text{-}34)$$

$$\frac{[HN_3][H^+]}{[NH_4^+]} = 2.2 \times 10^{-10} \text{ at } 20°C \text{ (Danckwerts, 1970)} \qquad (10.4\text{-}35)$$

Chemical equilibrium

TABLE 10.4-4

EQUILIBRIUM CONSTANTS AT 25°C

pH	$\frac{[NH_4OH]}{p_{NH_3}}$	$\frac{[NH_4^+]}{p_{NH_3}}$
4	56.2	
6	56.2	100,000.
8	56.2	1,000.
10	56.2	10.
12	56.2	0.1

"p" is partial pressure in atm; concentrations in mol/ℓ. Ratios at 25°C, calculated from data cited by Scott and McCarthy (1967) and Pourbaix (1966). For H_2S at 18°C, see "Hydrogen sulfide - water". Hodgman (1959) gives ammonia equilibrium at other temperatures.

Kinetics

$k = 4.4 \times 10^5\ sec^{-1}$ for

$H_2S \rightarrow H^+ + HS^-$

in aqueous solution at 25°C, calculated from the second order constant given by Caldin (1964). Instantaneous reaction regime applies (Astarita, 1967).

HYDROGEN SULFIDE - MONOETHANOLAMINE - WATER

Equilibrium - H_2S in solutions of MEA does not obey Henry's law. The vapor pressure data cited in Perry (1963) can be represented by

$$p = \frac{R^2}{(1-R)(R+1/x_{MEA})} \exp(-2.566 + 0.068\ t - 10^{-4}\ t^2) \qquad (10.4\text{-}36)$$

where $R \equiv x_{H_2S}/x_{MEA}$, p in atmospheres, t in °C. Error in "p" less than 15% in range 60-140°C.

Liquid density - Data plotted by Kohl and Riesenfeld (1960) for MEA solutions can be represented by

$$\rho_L = A + Bx_{MEA} + Cx_{MEA}^2 \qquad (10.4\text{-}37)$$

$$A = 1.0017 - 1.9 \times 10^{-4}\ t - 2.3 \times 10^{-6}\ t^2 \qquad (10.4\text{-}38)$$

$$B = 0.1492 - 14.2 \times 10^{-4}\ t + 3.8 \times 10^{-6}\ t^2 \qquad (10.4\text{-}39)$$

$$C = 0.0645 - 2.7 \times 10^{-4}\ t + 16.4 \times 10^{-6}\ t^2 \qquad (10.4\text{-}40)$$

Applicable range 0-100°C, $x_{MEA} < 0.25$.

Diffusivity - for H_2S in water,

$D_A = 1.61 \times 10^{-5}$ cm^2/sec at 25°C

(Perry et al., 1963). Temperature dependence is roughly

$$D_A = \frac{4.8 \times 10^{-10}\ (t + 273)}{\mu_L} \qquad (10.4\text{-}41)$$

The viscosity of MEA solutions at 27°C is approximately

$$\mu_L = 0.00924 + 0.0350\ x_{MEA} + 0.69\ x_{MEA}^2 \qquad (10.4\text{-}42)$$

for $x_{MEA} < 0.25$, based on data plotted by Kohl and Riesenfeld (1960).

For MEA in water at low concentrations,

$D_B = 1.2 \times 10^{-5}$ cm^2/sec at 25°C

roughly estimated by Othmer-Thakar method (see section on estimation methods).

Chemical Equilibrium

TABLE 10.4-5
EQUILIBRIUM CONSTANTS

	18°C		20°C
pH	$\frac{[HS^-]}{[H_2S]}$	$\frac{[S^=]}{[H_2S]}$	$\frac{[RNH_3^+]}{[RNH_2]}$
8	9.1	0.0000011	65.
10	910.	0.011	0.65
12	91,000.	110.	0.0065

H_2S ratios at 25°C calculated from data in Pourbaix (1966); 18°C ratios from data in Hodgman (1959). MEA ($\equiv RNH_2$) equilibrium is from Danckwerts (1970).

Kinetics

$k = 4.4 \times 10^5 \text{ sec}^{-1}$ for

$H_2S \rightarrow H^+ + HS^-$

in aqueous solution at 25°C, calculated from the second order constant given by Caldin (1964). Instantaneous reaction regime applies unless the MEA solution has a high loading of CO_2 (Astarita, 1967).

NO - WATER

Equilibrium - Henry's constant is:

$$\log_{10} H'_x = 1.2405 + 2535/T - 469800/T^2 \qquad (10.4\text{-}43)$$

in the range 0 - 80°C. H'_x in atm, T in °K. Maximum deviation from data of International Critical Tables (1928) is 0.6% at 80°C.

Liquid density - Solubility is so low that density of pure water is sufficiently accurate for design.

Diffusivity - for NO in water;

$D_{A,L} = 2.4 \times 10^{-5} \text{ cm}^2/\text{sec}$ at 25°C

roughly estimated by Othmer-Thakar method. Rough Temperature dependence is

$$D_{A,L} = \frac{7.1 \times 10^{-10} (t + 273)}{\mu_L} \qquad (10.4\text{-}44)$$

where μ_L is viscosity of water in poise.

For NO in air;

$D_{A,G} = 0.20 \text{ cm}^2/\text{sec}$ at 25°C and 1 atm

estimated by the method of Fuller et al. The temperature dependence can be estimated through the same method.

NITRIC OXIDE - SULFURIC ACID - WATER

Equilibrium - Henry's constant is:

$$\ln H'_x = 11.1429 + 2.8356\, x_B - 8.2611\, x_B^2 \qquad (10.4\text{-}45)$$

at 18°C. "x_B" is mole fraction of H_2SO_4 in the NO-free scrubbing solution. "H'_x" in atmospheres/mole fraction. Calculated "H'_x" is within 5% of data of International Critical Tables (1928) for $p_A = 1$ atm and $x_B < 0.62$.

Liquid density - Tabular data in Perry (1963) for aqueous H_2SO_4 solutions is reproduced within 1% by

$$\rho_L = A + Bx_B + Cx_B^2 \qquad (10.4\text{-}46)$$

$$A = 1.0055 - 0.143 \times 10^{-3}\, t - 0.309 \times 10^{-5}\, t^2 \qquad (10.4\text{-}47)$$

$$B = 3.423 - 8.805 \times 10^{-3}\, t - 5.038 \times 10^{-5}\, t^2 \qquad (10.4\text{-}48)$$

$$C = -4.982 + 26.20 \times 10^{-3}\, t - 16.08 \times 10^{-5}\, t^2 \qquad (10.4\text{-}49)$$

Range 0-100°C, $x_B < 0.6$.

Diffusivity - For NO in water at low concentrations,

$D_A = 2.4 \times 10^{-5}$ cm^2/sec at 25°C

roughly estimated by Othmer-Thakar method (see section on estimation methods). Rough temperature dependence is

$$D_A = \frac{7.2 \times 10^{-10}\,(t + 273)}{\mu_L} \qquad (10.4\text{-}50)$$

μ_L is viscosity in poise.

TABLE 10.4-6

DIFFUSIVITY OF H_2SO_4 IN WATER AT 20°C

c_B, mol/ℓ	x_B	D_B, cm^2/sec
0.1	0.002	1.73×10^{-5}
0.25	0.005	1.63×10^{-5}
0.5	0.009	1.62×10^{-5}
0.75	0.014	1.60×10^{-5}
1.0	0.018	1.58×10^{-5}
1.5	0.028	1.56×10^{-5}
2.0	0.038	1.50×10^{-5}

(International Critical Tables, 1929). Temperature dependence is roughly

$$D_B = \frac{5.4 \times 10^{-10}\,(t + 273)}{\mu_L} \qquad (10.4\text{-}51)$$

at low concentrations. μ_L is viscosity of water in poise.

Chemical equilibrium - Data are scarce. Better than 80% removal of flue gas is achieved at 25°C when scrubbed with 92% H_2SO_4 (x_B = 0.68) at a space velocity of 500 hr^{-1}. Lower removal at higher temperatures. Lower removal for NO/NO_2 ratio different from 1 (Ganz, 1956).

SULFUR DIOXIDE - WATER

Equilibrium - Henry's constant is:

$$\ln H'_x = 2.518 + 0.04263\ t - 0.0001235\ t^2 \qquad (10.4\text{-}52)$$

based on partial pressure of SO_2 and mole fraction of SO_2 (as SO_2, H_2SO_3, and HSO_3^-). H'_x in atmospheres/mole fraction total dissolved SO_2; "t" in °C. Less than 5% error in "x" for $P_A \leq 1$ atm, 10-130°C (International Tables, 1928).

Liquid density

$$\rho_L = 0.9987 + 1.649\ x \quad (g/cm^3) \qquad (10.4\text{-}53)$$

for aqueous solutions at 15.5°C, $x \leq 0.03$ (International Critical Tables, 1928). For other temperatures, use

$$\rho_{Lt} = \frac{\rho(H_2O,\ t)}{0.999023}\ \rho_{L15.5} \qquad (10.4\text{-}54)$$

Diffusivity - $D_A = 1.7 \times 10^{-5}\ cm^2/sec$ at 25°C (Perry et al., 1963). Temperature dependence is approximately

$$D_A = \frac{5 \times 10^{-10}\ (t + 273)}{\mu_L} \qquad (10.4\text{-}55)$$

μ_L is the viscosity of water in poise.

Chemical Equilibrium

TABLE 10.4-7

EQUILIBRIUM CONSTANTS

pH	25°C $\frac{[H_2SO_3]}{p_{SO_2}}$	25°C $\frac{[HSO_3^-]}{p_{SO_2}}$	25°C $\frac{[SO_3^=]}{p_{SO_2}}$	50°C $\frac{[H_2SO_3]}{p_{SO_2}}$	50°C $\frac{[HSO_3^-]}{p_{SO_2}}$	50°C $\frac{[SO_3^=]}{p_{SO_2}}$
2	1.23	1.60	0.00001	0.56	0.43	10^{-6}
4	1.23	160.	0.10	0.56	43.	0.0182
6	1.23	16,000	1000	0.56	4300	182.
8	1.23	1,600,000	10,000,000	0.56	430,000	1,820,000
10	1.23	2×10^8	10^{11}			

"p" is partial pressure in atm; concentrations in mol/ℓ. Ratios calculated from data given by Lowell et al. (1970) and Scott and McCarthy (1967).

Kinetics

$k = 1.06 \times 10^8\ sec^{-1}$ for dissociation

$H_2SO_3 \rightarrow H^+ + HSO_3^-$

at 25°C in aqueous solution of ionic strength 0.9 (Betts and Voss, 1970). Caldin (1964) and Lowell et al. (1970) cite the value

$k = 3.4 \times 10^6\ sec^{-1}$ for the hydration

$SO_2(aq.) + H_2O \rightarrow H^+ + HSO_3^-$

at 20°C. Instantaneous reaction regime will apply in most cases.

SULFUR DIOXIDE - AMMONIA - WATER

Equilibrium - SO_2 in aqueous NH_3 solutions does not obey Henry's law. Vapor pressure of SO_2 in atmospheres is given by

$$p_{SO_2} = \frac{(2S - A)^2}{A - S} \exp\left(6.871 - \frac{5455}{t + 273}\right) \tag{10.4-56}$$

where "S" is total dissolved SO_2 in moles/100 moles H_2O, and "A" is total dissolved NH_3 in moles/100 moles H_2O. Less than 10% error in p_{SO_2} in applicable ranges 35 - 90°C; $5.8 < A < 22.4$; $S < A$ and $2S > A$ (Perry et al., 1963). "S" and "A" are related to mole compositions by

$$S = \frac{100\ x_{SO_2}}{1 - x_{NH_3} - x_{SO_2}} \tag{10.4-57}$$

$$A = \frac{100\ x_{SO_2}}{1 - x_{NH_3} - x_{SO_2}} \tag{10.4-58}$$

Liquid density

$$\rho_L = 0.9987 + 1.649\ x_{SO_2} - 0.38\ x_{NH_3} \text{ at } 15.5°\text{C}. \tag{10.4-59}$$

This approximation is based on the empirical relations

$$\rho_{15.5} = 0.9987 + 1.649\ x_{SO_2} \text{ and } \rho_{15.6} = 0.9986 - 0.38\ x_{NH_3}. \tag{10.4-60}$$

Diffusivity - For SO_2:

$D_A = 1.7 \times 10^{-5}$ cm²/sec at 25°C

(Perry et al., 1963). Temperature dependence is roughly

$$D_A = \frac{5 \times 10^{-10}\ (t + 273)}{\mu_L} \tag{10.4-61}$$

μ_L is viscosity of water in poise.

TABLE 10.4-8

DIFFUSIVITY OF NH_3 IN WATER

t, °C	C_{Bo}, mol/cm³	D_B, cm²/sec
5	0.0007	1.24×10^{-5}
8	0.001	1.36×10^{-5}
12		1.64×10^{-5}
15		1.77×10^{-5}
5	0.0035	1.24×10^{-5}

(International Critical Tables, 1928). Temperature dependence is roughly

$$D_B = \frac{7 \times 10^{-10}\ (t + 273)}{\mu_L} \qquad (10.4\text{-}62)$$

μ_L is viscosity of water in poise.

Chemical equilibrium

TABLE 10.4-9

EQUILIBRIUM CONSTANTS

pH	$\frac{[NH_4OH]}{p_{NH_3}}$	$\frac{[NH_4^+]}{p_{NH_3}}$
4	56.2	
6	56.2	100,000
8	56.2	1,000.
10	56.2	10.
12	56.2	0.1

"p" is partial pressure in atm; concentrations in mol/ℓ. Ratios at 25°C, calculated from data cited by Scott and McCarthy (1967), Pourbaix (1966), and Lowell et al. (1970). Temperature dependence of ammonia equilibrium is given in Hodgman (1959). For SO_2 at 50°C, see "Sulfur dioxide - water".

Kinetics

$k = 1.06 \times 10^8\ \text{sec}^{-1}$ for dissociation

$H_2SO_3 \rightarrow H^+ + HSO_3^-$

at 25°C in aqueous solution of ionic strength 0.9 (Betts and Voss, 1970). Caldin (1964) and Lowell et al. (1970) cite the value

$k = 3.4 \times 10^6\ \text{sec}^{-1}$ for the hydration

$SO_2(aq.) + H_2O \rightarrow H^+ + HSO_3^-$

at 20°C. Instantaneous reaction regime will apply in most cases.

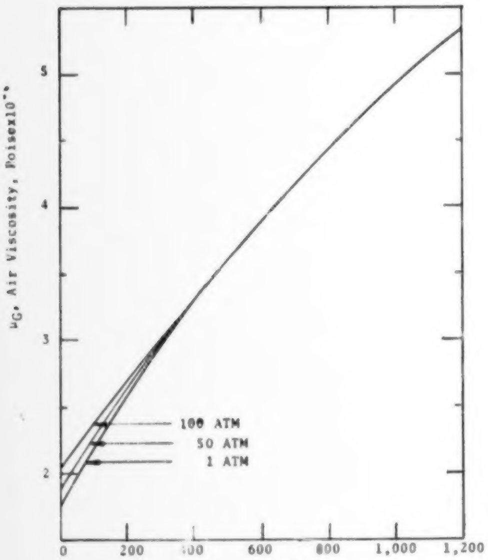

FIGURE 10.2-1

VISCOSITY OF DRY AIR

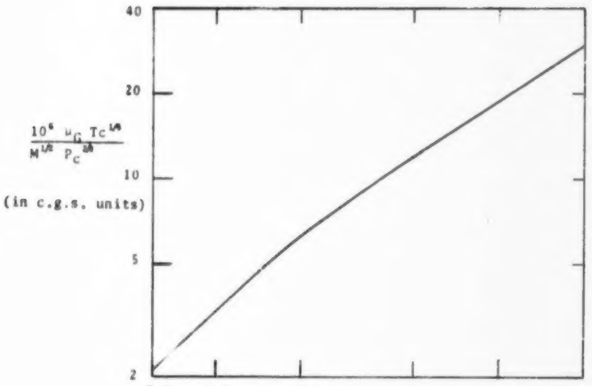

FIGURE 10.2-2

REDUCED VISCOSITY OF NONPOLAR GASES

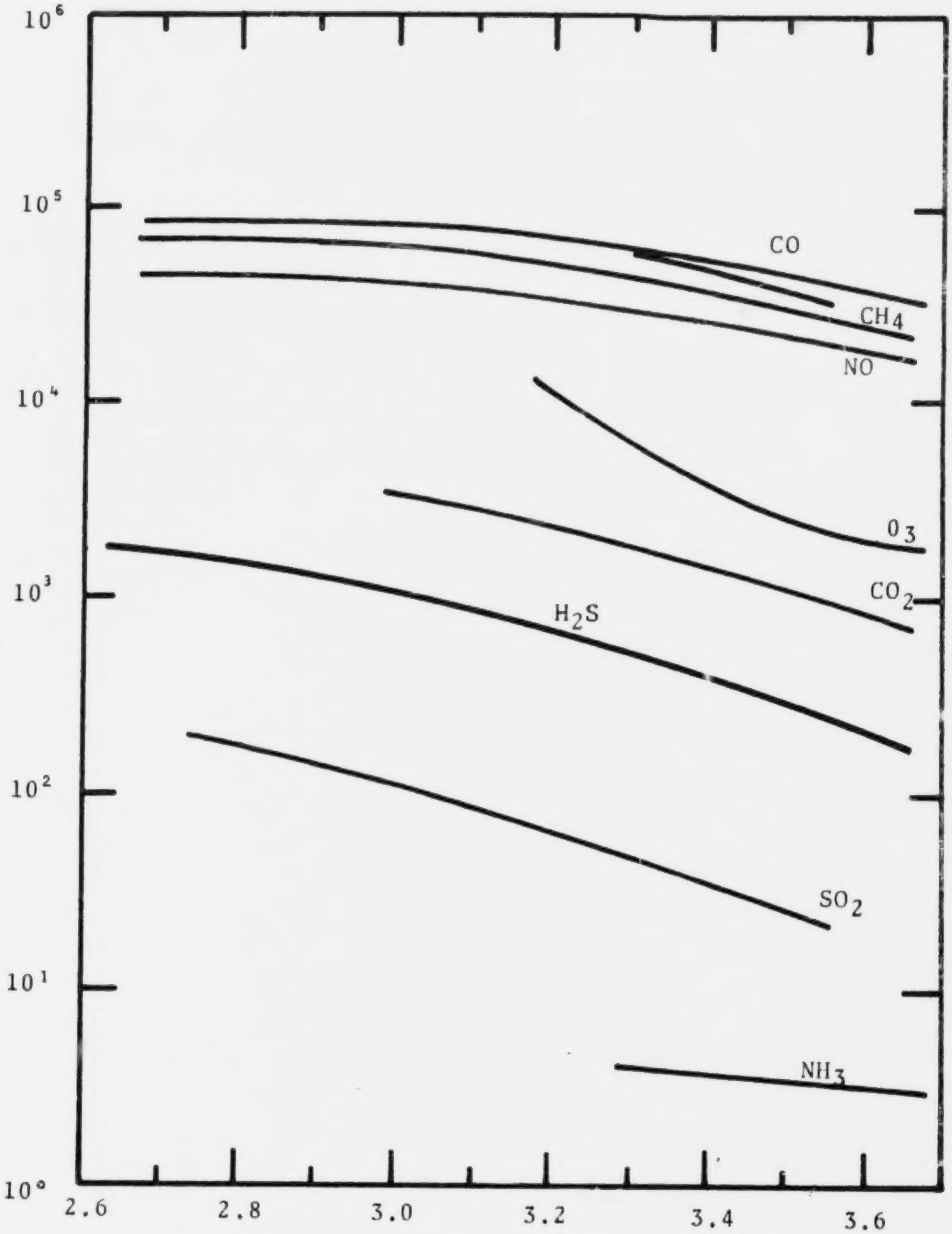

FIGURE 10.3-1

APPARENT SATURATION HENRY'S LAW CONSTANTS
FOR GASES IN DISTILLED WATER.
INTERNATIONAL CRITICAL TABLES (1928)

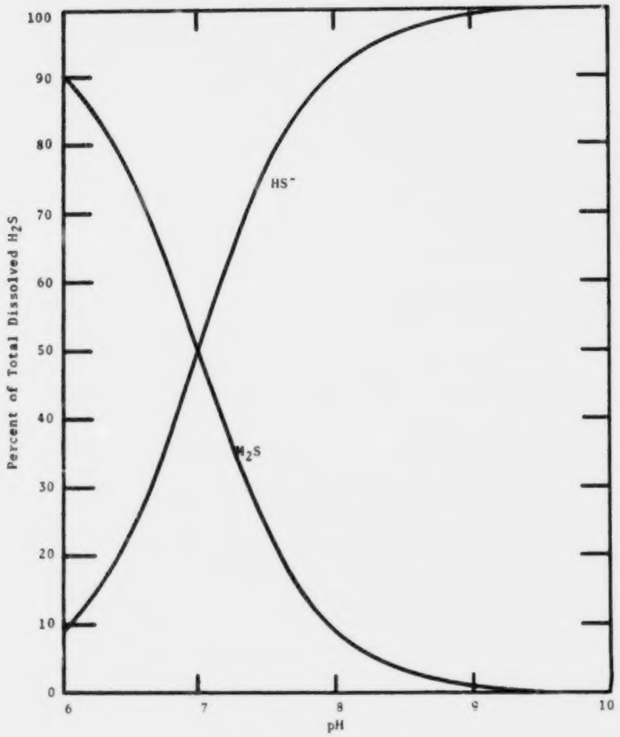

FIGURE 10.3-2

CHEMICAL SPECIES AT EQUILIBRIUM IN AQUEOUS H_2S SOLUTION AT 25°C. CALCULATED FROM DATA TABULATED IN 10.4-2

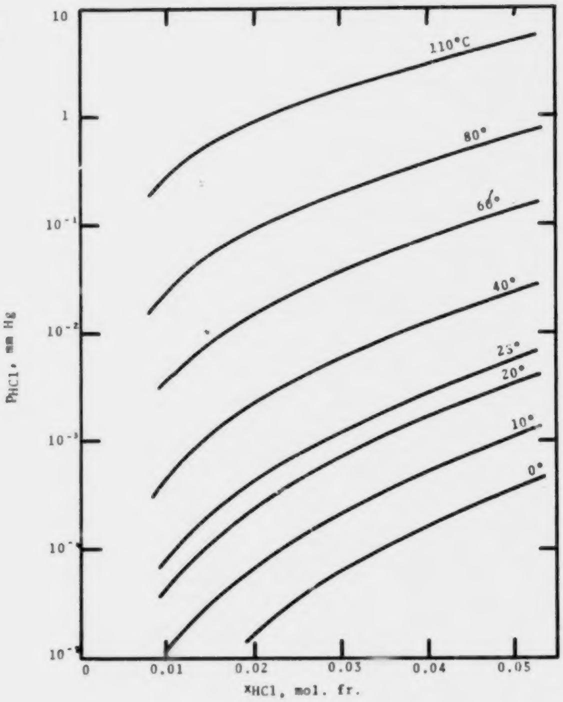

FIGURE 10.4-1

PARTIAL PRESSURE OF HCl OVER AQUEOUS HCl SOLUTIONS

NOMENCLATURE - CHAPTER 10

a = total ammonia, mol/ℓ

c = concentration, mol/ℓ

D = diffusivity, cm^2/sec

E = half-cell potential, volts

H'_x = apparent Henry's law constant (mole fraction basis), atm

H' = apparent Henry's law constant (concentration basis), atm-ℓ/mol

H'' = true Henry's law constant (mole fraction basis), atm

H = true Henry's law constant (concentration basis), atm-ℓ/mol

ΔH = heat of reaction, cal/mol

K = chemical equilibrium constant

k = reaction rate constant, sec^{-1} or ℓ/mol-sec

M = molecular weight, g/mol

p = partial pressure, atm

P = total pressure, atm

Rg = gas constant, 1.987 cal/mol °K or 82.06 atm-cm^3/mol °K

R = reaction rate, mol/ℓ-sec

s = total sulfite, mol/ℓ

T = absolute temperature, °K

t = temperature, °C

Vm = molar volume, cm^3/mol

x = mole fraction in liquid

y = mole fraction in gas

Z = compressibility factor $Z = \frac{PV}{Rg\ T}$

μ = viscosity, poise (except where noted) (must be subscripted)

ν = stiochiometric coefficients of the equilibrium equation

ρ = density, g/cm (must be subscripted)

ϕ° = standard chemical potential, cal/mol

[ ] = concentration, mol/ℓ

→ = forward reaction

← = reverse reaction

Subscripts

A = scrubbed component

c = critical property

G = gas phase

L = liquid phase

mix = mixture property

r = reduced property

w = water

REFERENCES - CHAPTER 10

Astarita, G., "Mass Transfer with Chemical Reaction", Elsevier, New York (1967).

Betts, R. H., Voss, R. H., Can J. Chem. 48, 2035 (1970).

Caldin, E. F., "Fast Reactions in Solution", Wiley, New York (1964).

Carr, N. L., Parent, J. D., Peck, R. E., Chem. Eng. Progress Symp. Ser., No. 16, 51, 91 (1955).

Danckwerts, P. V., "Gas-Liquid Reactions," McGraw-Hill, San Francisco (1970).

Fishenden, M., Saunders, O. A., "An Introduction to Heat Transfer", Clarendon Press, Oxford (1950).

Ganz, S. N., J. Appl. Chem. USSR 29, 1107 (1956).

Hodgman, C. D., ed., "Handbook of Chemistry and Physics," Chemical Rubber Publishing Co., Cleveland (1959).

International Critical Tables, vol. III (1928), vol. V (1929), McGraw-Hill, New York.

Johnstone, H. F., Ind. Eng. Chem. 27, 587 (1935).

Kohl, A. L. Riesenfeld, F. C., "Gas Purification," McGraw-Hill, New York (1960).

Lowell, P. S., et al., "Theoretical Description of Limestone Injection Wet Scrubbing Process", Contract CPA-22-69-138 Final Report, Natl. Air Pollution Control Administration, June, 1970.

Perry, R. H., Chilton, C. H., Kirkpatrick, S. D., "Chemical Engineers' Handbook", McGraw-Hill, San Francisco (1963).

Pourbaix, M. J. N., "Atlas of Electrochemical Equilibria in Aqueous Solutions", Pergamon, New York (1966).

Reid, R. C., Sherwood, T. K., "The Properties of Gases and Liquids", McGraw-Hill, San Francisco (1966).

Scott, W. D., McCarthy, J. L., I&EC Fundamentals 6, 40 (1967).

Stiel, L. I., Thodos, G., A.I.Ch.E.J. 7, 611 (1961).

CHAPTER 11

MATERIALS DATA

TABLE OF CONTENTS

11.1 Introduction 11-2

11.2 General Conditions 11-2
  - 11.2.1 Temperature. 11-2
  - 11.2.2 Velocity 11-3
  - 11.2.3 State of Oxidation 11-3
  - 11.2.4 Effect of Impurities 11-3

11.3 Plastics 11-3

11.4 Chemicals. 11-4
  - 11.4.1 Sulfuric Acid. 11-4
  - 11.4.2 Hydrochloric Acid and Metal Chlorides 11-5
  - 11.4.3 Hydrofluoric Acid and Fluorides 11-6
  - 11.4.4 Phosphoric Acid. 11-7
  - 11.4.5 Nitric Acid and Nitrates 11-7
  - 11.4.6 Sulfur Dioxide or Sulfurous Acid 11-8
  - 11.4.7 Salt Solutions 11-8

11.5 Miscellaneous Solutions and Gases. 11-8
  - 11.5.1 Wet Chlorine and Hypochlorites of Calcium or Sodium 11-8
  - 11.5.2 Sea Water 11-9
  - 11.5.3 H_2S Containing Gases 11-9
  - 11.5.4 Hydrofluosilicic Acid. 11-9

References 11-10

CHAPTER 11

MATERIALS DATA

11.1 INTRODUCTION

In Chapter 11 a limited amount of data is presented, to help the designer of scrubbing equipment with the selection of materials of construction. Engineering materials commonly required in the design of scrubbers are reviewed, with indications of other references where more detailed information and charts can be obtained.

The section on Materials of Construction is arranged in the form of chemical systems, which may be commonly encountered in a scrubbing problem. The preponderance of scrubbing applications involves acidic gases, and as encountered in scrubbing applications they will be dilute. In addition to chemical systems, a general preamble is presented, in discussing the other factors affecting corrosion, such as: velocity effects, temperature, aeration, oxidation and reduction. A short survey of plastic materials is included.

11.2 GENERAL CONDITIONS

When choosing construction materials certain salient operating conditions should be considered. A metal will behave very differently in the same acid, depending on conditions of: velocity, temperature, aeration, whether the conditions are reducing or oxidizing, and upon the presence of impurities. Traces of ions, such as ferric or cupric in acids, can have a very beneficial effect and reduce corrosion rates of stainless steels and titanium alloys dramatically, Cotton (1970). On the other hand, traces of chloride or fluoride in sulfuric acid can have disastrous results on the resistance of stainless steels, causing severe pitting.

In the selection of materials for different environments, testing in pure media should be regarded only as an approximate guide to narrow the choice. Wherever possible, tests should be done using plant liquors, or test coupons should be inserted in the actual streams in the plant or pilot plant. Testing in pure media can give very different results from media containing the usual gamut of impurities.

11.2.1 TEMPERATURE

Corrosion rates generally increase with increase in temperature. This is due to reduction in viscosity, increased mobility of ions and increased reaction rates. However, in some cases such as that of Monel, the corrosion is accelerated by the presence of oxygen; increasing the acid temperature in this case eventually results in boiling out dissolved oxygen, when the corrosion rapidly diminishes. In 6% H_2SO_4 at 80°C, Monel has a corrosion rate of 114 mpy (0.114 inches penetration per year) whereas at 101°C the rate of corrosion falls off to about 2 mpy (Shellmoller and Laque (1961). The skin temperature of alloy steam coils has an important bearing on the corrosion rate in aggressive environments. The rate can greatly increase if excessive steam pressures are used (Shellmoller and Laque 1961).

11.2.2 VELOCITY

Often the corrosion resistance of an alloy depends on the existence of an adhering oxide layer on the surface. Too high a velocity or local impingement of liquid on the surface, can remove or erode the surface layer which cannot be renewed because the oxide film is washed away as it forms. For example, a low tin bronze in sea water flowing at 0.3 to 0.6 m/sec (1 to 2 ft/sec) corroded at the rate of 0.0002 ipy but at 6 m/sec (20 ft/sec) velocity the corrosion rate increased to 0.037 ipy, Uhlig (1966). For this reason nickel based alloys are now being used at high velocities in sea water, Niederberger et al. (1970), but at low velocities some suffer local attack under deposits.

11.2.3 STATE OF OXIDATION

Under reducing conditions Monel Alloy 400 (Ni - 66%, Fe - 1.35%, Cu - 31.5%, C - 0.12%, Si - 0.15%, Mn - 0.90%) is very resistant to boiling 15% sulfuric acid. That is why monel hooks are used for pickling wire in boiling 15% sulfuric acid. Under oxidizing conditions, or in the presence of oxidizing ions, very rapid corrosion would occur.

The reverse is true of 304 and 316 stainless steels which are resistant to oxidizing media but are attacked by acids under reducing conditions.

11.2.4 EFFECT OF IMPURITIES

Pure titanium is dissolved by hydrochloric acid above 5% concentration, but if ferric ions or cupric ions are present in the solution, the corrosion will be inhibited. The inclusion of a small quantity of palladium in the titanium also confers much greater acid resistance.

11.3 PLASTICS

A separate section is necessary to cover plastics, due to their peculiar properties which make them especially useful as construction materials for scrubbers.

Plastics have a unique combination of properties, having strength with lightness, flexibility and resistance to corrosion over wide ranges of conditions. Very large structures are now being made of plastic materials, such as stacks, 18 meter (60 ft) high and 1.35 meter (4 ft 6 inches) in diameter made from PVC/glass reinforced, 30 hp suction fans with PVC casings and polypropylene impellers and others. A very large installation in Chile by N.V. Hooker Chemical S.A., including among others a complete scrubber unit made of FRP (Figerglass Reinforced Plastic) is reported in British Chemical Engineering (1968). In the same reference, a description is given of an effluent pipeline four miles long of polypropylene reinforced with fiberglass, resistant to sea water and an alkaline effluent from a Nylon plant. Polypropylene packing is particularly useful for scrubbing columns for air pollution control, where resistance to a wide variety of chemicals is needed, though care must be taken to avoid temperature escalations. Polypropylene is slightly better in this respect than polyethylene since its melting point is 168°C (335°F) whereas the melting point of high density polyethylene is 127°C (260°F). The respective heat distortion temperatures under a load of 4.5 atm (66 psi) stress are 127°C (260°F) and 65-77°C (150-170°F) for polyethylene.

The qualitative characteristics of various resins and plastics are as follows:

	Aqueous Strong Mineral Acids		Aqueous Alkalis	Solvents
	Oxidizing	Reducing		
ABS Resins	B	A	A	Alcohols O.K.
Polycarbonates	A	A	-	Soluble in chlorinated hydrocarbons
Acrylics	B	B	B	D
Alkyds	B	B	D	A
Chlorinated Polyether	A	A	A	-
Epoxy	B	B	A	-
PTFE	A	A	A	A

A - Excellent

B - Limited resistance

D - Destroyed

11.4 CHEMICALS

11.4.1 SULFURIC ACID

Concentrated Sulfuric

For hot 98% sulfuric acid mist at 90°C as found in the tail gases of contact plants, the knit mesh de-misters are made of Carpenter 20 wire, (C - 0.07%, Cr - 29%, Ni - 20%, Cu - 3.25%, Mo - 2.25%, Balance Fe).

For very fine sulfuric acid mist removal, Teflon filament and glass fiber are used, such as in a "Brink" demister.

Dilute Sulfuric Acid

Mixtures of dilute sulfuric acid containing metal salts are encountered in many applications, such as pickle bath exhaust gas scrubbers, scrubbers on evaporator gases from dryers or from the exhaust of kilns - such as those of the sulfate TiO_2 process, and in many hydrometallurgical processes.

Commonly used materials are:

Metals (less than 20 ipy)	Lead and antimonial lead
	Alloy "20" (max. 5% H_2SO_4 at boiling)
	Alloy R 55
	High Silicon Iron
Non-Metallics	Acid-proof Brick
	Fiberglass Reinforced Plastics
	Hard Rubber-Lined Steel
	Haveg

One can use steel vessels with hard rubber linings up to 82°C (180°F). At higher temperatures the lining can be protected with a layer of tile, or acid proof brick set in acid proof cement - such as a phenolic or furan cement.

Pumps can be ceramic-lined, rubber-lined (up to say 65°C (150°F), or of Alloy R 55. Additionally, tanks can be of fiberglass reinforced plastic, or plastic-lined such as PVC or polypropylene. A new cheap form of construction for acid resisting large plastic tanks, such as high density polyethylene, polypropylene or polybutene, is helically wound extruded tanks. Maximum volume is about 19 m^3 (5,000 gallons) Binder and Sutton (1970).

Certain special grades of stainless steel can be used in sulfuric but only with extreme caution, such as stainless 254 which is a grade approaching alloy "20" in composition. The presence of even small traces of chloride in sulfuric acid solutions can cause pitting of stainless and severe roughening of the surface. Probably fluoride would have the same effect.

11.4.2 HYDROCHLORIC ACID AND METAL CHLORIDES

Very few metals withstand hydrochloric acid at any temperature. Tantalum, which is extremely expensive, has good resistance to all strengths and temperatures.

Titanium is excellent with dilute acid, say below 5%, up to 65°C (150°F). For added resistance to free HCl, titanium with paladium 0.2% is used, Cotton (1970). The conditions for titanium must be oxidizing; it has good resistance to cold dilute HCl in the presence of small concentrations of ferric chloride, but the pure acid can attack it quickly.

In general, non-metallic materials should be used for HCl, if cool enough, such as stoneware, ceramics, carbon and graphite, and plastics or fiberglass reinforced plastics. For high temperatures rubber-lined steel, additionally protected with carbon brick set in furan cement, is an excellent form of construction.

For oxidizing metal chloride solutions with low free acid, titanium pumps can be used for extreme duties, or rubber lined pumps for lower pressures and temperatures. Also, at elevated temperatures or in boiling acids, fluorinated ethylene propylene (FEP) pumps can be used. At low temperatures PVC or PVDC (Polyvinylidene chloride) are good materials to use in chloride service.

In packed towers, under conditions of fluctuating temperature, carbon raschig rings should be used, as these are more resistant to temperature shock than ceramic rings and they will withstand extremes of temperature.

For dry hydrochloric acid gas, or even HCl gas in mixtures of air and steam, steel can be used up to about 300°C, provided the steel is kept above the dew point of the gas. Extreme caution should be used in the design of steel ducts for such conditions, because, should the gas fall below the dew point rapid corrosion will occur.

11.4.3 HYDROFLUORIC ACID AND FLUORIDES

Any ceramic material containing silica is attacked by HF or H_2SiF_6 as is silicon iron.

Care must be exercised in specifying rubber linings for use with HF or H_2SiF_6 becuase many grades have silica in them as a filler. This would be leached out by free HF and render the rubber porous.

Metals

Monel is the alloy with outstanding resistance to HF over a wide range of concentration and temperature. However, aeration, as one might expect in a scrubber, or oxidizing salts, accelerate the corrosion of Monel. Copper is more sensitive to oxidizing conditions than Monel. Lead behaves in a similar way to low concentrations in that it is good in an air free environment.

Non-Metals

Wet dilute hydrofluoric acid is similar to HCl in that metals are better avoided. Rubber-lined pumps or Teflon pumps, rubber-lined pipework, especially butyl and neoprene or Saran and a variety of plastics have good resistance.

For gases containing HF or fluorides at high temperature, and under oxidizing conditions, high alumina refractories are resistant to the atmosphere.

11.4.4 PHOSPHORIC ACID

Corrosion by phosphoric acid depends on the method of manufacture of the acid. Made by the burning of phosphorus and the absorption of P_2O_5 in water, the acid is pure; when manufactured by the "wet" process, the acid contains a wide variety of impurities including sulfuric acid, fluorides, iron, aluminum and silicon.

Generally, rubber-lined and carbon brick lined equipment, is used as well as graphite for heat exchangers, alloy "20" for pumps. Stainless 316 (low carbon) is a commonly used material of construction for the acid from 30% P_2O_5 to 54%. Since the composition of the acid depends on the original rock from which it was made, care should be taken in the use of stainless steels. For instance, traces of chloride can have a profound influence and so could the ratio of iron to aluminum in the acid, because of the formation of fluoride complexes. It has been reported, Chemical Engineering Deskbook Issue (1972), that Hastelloy alloy G can replace graphite tubes in phosphoric acid evaporators.

For pure acid made by the combustion of phosphorus process, 316L, low carbon stainless steel is used.

Plastics are reported to be used in phosphoric acid service. A. V. Slack (1968) gives an excellent description of the properties of plastic materials in general, with special reference to their use in fertilizer manufacture. Baked on PVC coatings have been used successfully as linings for phosphoric acid rail cars. Also PVC rotary dip feeders are used for sulfuric and phosphoric acids.

Other materials which have excellent resistance to phosphoric acid are fluorocarbons to 149°C (300°F), polyethylene to 49°C (120°F), chlorinated polyether to 110°C (230°F), ABS to 82°C (180°F). Also, polypropylene lined fiberglass is used, polyester resins reinforced can be used for ducting.

11.4.5 NITRIC ACID AND NITRATES

Metals

With nitric acid the choice of materials to use is limited. Stainless steel with not less than 15% chromium should be used, or cast high silicon alloys. Stainless steel 18-8 (type 304) and type 430 are used for a wide variety of conditions. Duriron has excellent resistance to nitric acid but poor mechanical properties. Durimet 20 and Carpenter 20 are also excellent materials of construction especially for boiling weak nitric acid.

Non-Metals

Teflon has the best resistance and is completely unaffected. Butyl rubber is good to 65°C (150°F), Fontana and Greene (1967), and Penton is good as are epoxy resins. Generally, plastics are not used as pipework for nitric acid because stainless steel type 304 has such good resistance to a wide variety of concentrations and temperatures, and some plastics could suffer oxidation.

For mixtures of nitric acid and HF which are used for pickling stainless, carbon has a good resistance. The oxidation of carbon by nitric acid appears to be inhibited by the fluoride.

11.4.6 SULFUR DIOXIDE OR SULFUROUS ACID

Sulfurous acid can be extremely aggressive and careful choice of the correct grade of stainless steel is necessary, for handling solutions of SO_2 in water. Only the molybdenum containing 18-8 (type 316) will withstand sulfurous acid; even columbium-stabilized stainless steel is very rapidly attacked by the solution, especially with added sulfuric acid and at high velocity. Four-inch 18-8 stainless steel pipe, columbium-stabilized, has been known to corrode through at sharp bends, with 3% SO_2 solution at about 71°C (160°F) in two days.

11.4.7 SALT SOLUTIONS

Solutions of acid salts such as nitrates, chlorides, and sulfates will behave much as their parent acids, only they are generally less aggressive. As stated earlier, the state of oxidation of the metal ions in the solution can have a profound influence on the choice of material.

Solutions of alkaline salts, such as many sodium salts, can be handled to the boiling point with steel or cast iron. Alkaline ammonium salts can be handled in aluminum alloys and nickel cast irons; copper alloys must be avoided. Of course, rubber-lined steel and a variety of plastics will also handle most salt solutions except highly oxidizing solutions.

11.5 MISCELLANEOUS SOLUTIONS AND GASES

11.5.1 WET CHLORINE AND HYPOCHLORITES OF CALCIUM OR SODIUM

Titanium has excellent resistance to wet chlorine, below the dew point, over a wide temperature range (it is not suitable for dry chlorine, zirconium is used). Some filament-reinforced fiberglass plastics are used on wet chlorine service. Polyester resins have good resistance to wet chlorine. There is a wide variety of proprietary unpublished information on the resistance of plastic lining to aggressive environments. It is best to consult with specialist manufacturers to obtain detailed practical information. For a wide choice of manufacturers of plastics consult Materials in Design Engineering (1966).

11.5.2 SEA WATER

Steel has good resistance to sea water when totally immersed. Corrosion rates are about 5 mpy but in the air, where splashed with sea water, corrosion rates rise to three to four times this value. Austenitic nickel case iron is also a good material, showing corrosion rates of about 2 mpy. Copper, bronze and aluminum brass are all excellent materials to use. Stainless steels are subject to chloride pitting.

Plastics are excellent constructional materials for use in sea water, both fiberglass reinforced and thermoplastic materials such as polyethylene, polypropylene, PVC and ABS.

11.5.3 H_2S CONTAINING GASES

Hydrogen sulfide and gases containing hydrogen sulfide and carbon dioxide, or hydrogen sulfide and carbon disulfide are encountered in scrubber use.

Generally speaking, nickel based alloys should be avoided in the presence of sulfur bearing gases. Iron based alloys have the best resistance, such as 316L stainless steel. Plastic or rubber-lined equipment can also be used. Wet hydrogen sulfide in air behaves in a similar manner to wet SO_2 and a low carbon stainless containing molybdenum should be used. Other steels may be subject to crevice attack and pitting.

Scrubbers employing ethanolamines for H_2S and CO_2 are usually made of steel, if no air is present. The steel re-boilers on the ethanolamine strippers can be subject to corrosion and alloys may be used. However limiting steam pressures and temperatures on the metal will control corrosion of steel tubes.

Where air is present in the H_2S containing gas, organic absorbents are avoided because of degradation of the organic by the oxygen. So scrubbing is done with caustic or potassium or sodium carbonate. Wet H_2S can be corrosive; probably the best materials are butyl rubber-lined steel and plastics.

11.5.4 HYDROFLUOSILICIC ACID

Very dilute hydrofluosilicic acid, as found in some phosphate plant emissions, can be handled in rubber-lined equipment with 316L pipework and alloy "20" pumps. At 29°C (85°F) stainless 316 is reported to have a corrosion rate of 0.003 ipy and alloy "20" 0.0014. If free HF is present the corrosion rate increases to an impossible extent for stainless 316, but alloy "20" still has useful resistance. For example, at 60°C (140°F) not more than 0.025 ipy with 10% H_2SiF_6, some free HF and phosphoric acid has been observed.

CHAPTER 11 - REFERENCES

Anon., British Chemical Eng. Equipment Supplement 13, p.119, (1968).

Binder, G., Sutton, N., Brit. Chem. Eng. 15, 1332, (1970).

Climax Molybdenum Company, "A Guide to Corrosion Resistance", 1600 Huron Parkway, Ann Arbor, Michigan, 48105.

Cotton, J. B., Chem. Eng. Prog. 66, #10, 57-62, (1970).

Deskbook Issue, Chem. Eng. 77, #22 (1970).

Fontana, M. G., Greene, N. D., "Corrosion Engineering", p.249 & p.268, McGraw-Hill Book Corp., New York (1967).

Nelson, G. A., editor, "Corrosion Data Survey", National Association of Corrosion Engineers, Houston, Texas, (1967).

Niederberger, R. B., Ferrara, R. J., Plummer, F. A., Materials Protection and Performance 9, #8, 18-22, (1970).

Materials in Design Engineering-Materials Selector Issue, 64, #5, Reinhold Publishing Corporation, New York (1966).

Shellmoller, C. M., Laque, F. L., "Factors in the Choice of Corrosion-Resisting Materials of Construction", Interscience Publishers, Inc., New York (1961).

Slack, V. A., ed., "Phosphoric Acid", Pt. 2, Marcel Dekker, Inc., New York (1968).

Uhlig, H. N., "The Corrosion Handbook", p.401, John Wiley & Sons, Inc., New York, (1966).

CHAPTER 12

LIQUID AND SOLID WASTE DISPOSAL

TABLE OF CONTENTS

12.1 Introduction. 12-2

12.2 Industry Survey 12-3

12.3 Sedimentation 12-5

12.4 Coagulation and Flocculation. 12-8
    12.4.1 Coagulation 12-8
    12.4.2 Flocculation. .12-8

12.5 Filtration. 12-10

12.6 Neutralization and Chemical Precipitation 12-13

12.7 Ion Exchange. 12-15

12.8 Desalting 12-17

12.9 Disposal of Liquid. 12-19

12.10 Disposal of Solids. .12-21

12.11 Economics 12-22
    Nomenclature. 12-24
    References 12-26

CHAPTER 12

LIQUID AND SOLID WASTE DISPOSAL

12.1 INTRODUCTION

The objective of all wet scrubbers is to accomplish transfer of matter, be it particulate or gaseous, from a gaseous stream, mainly air, into a liquid stream, usually water. Thus, all wet scrubbers require liquid treatment and disposal to one degree or another. Liquid and solid waste disposal were described briefly in Chapter 6 as part of the scrubber auxiliaries. In this chapter the major water treatment unit operations will be reviewed and methods of liquid and solid waste disposal discussed. It is not the purpose of this chapter to give an in depth review; it is aimed more as a guide and a list of selected references.

The degree of treatment required will depend upon the methods of disposal or recycle and state and federal regulations. Once required effluent quality is known one can design a treatment plant, or establish a treatment method, employing customary engineering methods.

For scrubbers removing particulate matter some form of sedimentation, or for finer particles,coagulation and flocculation followed by sedimentation, may be all the treatment required. In other cases straining or deep sand filtration will be the more economical way to remove particulate matter.

In the many cases where scrubbers are used to absorb gaseous pollutants other methods such as neutralization, chemical precipitation or ion exchange are resorted to. Here the pollutant is preferentially removed from the scrubbing liquid, or its harmful action neutralized, so as to comply with effluent quality requirements.

A different case is when, due to liquid evaporation in the scrubber or due to other reasons, the dissolved salt concentration in the liquid effluent exceeds the limits set by the standards. In such cases various desalting methods are employed. Some of these methods, such as reverse osmosis, electrodialysis, evaporation and freezing, are mentioned in short.

Liquid effluent treatment and disposal are an essential part of every wet scrubber and add to its capital and operating costs. However, in the majority of the cases the treatment required is a simple one, such as a plain sedimentation tank, which does not add much to the scrubber economics.

To get an overall view let us start by examining the various treatment and disposal methods as reported by industry in response to our questionnaire.

12.2 INDUSTRY SURVEY

In the industry survey we had conducted, several questions were included, aimed at obtaining information on: 1) Liquid treatment methods. 2) Liquid waste disposal method. 3) Solid waste disposal method. We got back 72 questionnaries which contained partial or full answers to the above questions. Table 12.2-1 gives a breakdown of the various unit operations reported in the industry survey. Out of 35 replies to the first question, only three went through a complex treatment process that included more than one unit operation, and all three were chemical industries. Fourteen, the largest portion, did not do more than neutralize the liquid effluent, 8 filtered it and 6 passed it through some sort of a settling device. Continuous bleeding, oxidation, dilution and evaporation were reported in one instance each.

Table 12.2-2 lists the various methods of liquid waste disposal with or without prior treatment. Out of 55 replies on the method of liquid waste disposal, the majority, 17, recycle the liquid waste back to the process. Fifteen pond the liquid waste, 11 dump it into the city sewer and 7 sent it to be treated in the plant treatment plant. The rest gave other methods of disposal.

In Table 12.2-3 the various methods used for solid waste disposal are listed. Ponding takes first place while transferring the solid waste to a refuse dump takes second place. Radioactive waste materials require special methods of disposal and these are marked in the tables.

TABLE 12.2-1

WATER TREATMENT METHODS USED IN TREATING SCRUBBER EFFLUENT (INDUSTRY SURVEY)

Unit of Operation	No. of Plants
Special separation processes	3
Settling	6
Neutralization	14
Continuous Bleeding	1
Oxidation	1
Filtration	8
Dilution	1
Evaporation	1
Total	35

TABLE 12.2-2

LIQUID WASTE DISPOSAL METHODS APPLIED TO WET SCRUBBER EFFLUENTS (INDUSTRY SURVEY)

Method of Waste Disposal	No. of Plants
Recycle to process	17
Ponding	15
To city sewer	11
To plant treatment plant	7
Pump to open field	2
Permanent storage*	3
Total	55

*The permanent storage applies to radioactive waste.

TABLE 12.2-3

SOLID WASTE DISPOSAL METHODS APPLIED TO WET SCRUBBER EFFLUENTS(INDUSTRY SURVEY)

Method of Solid Waste Disposal	No. of Plants
Ponding	5
To city sewer	2
Back to process	2
To refuse dump	4
Buried*	4
Burned	1
Trucked to animal farm	1
Total	19

*Burial applies to radioactive waste

12.3 SEDIMENTATION

Sedimentation is defined as the removal by gravitational settling of suspended particles heavier than water. When the solids are separated from the fluid by gravitational settling and natural aggregation alone, the operation is called plain sedimentation. When chemicals or other substances are added to induce or accelerate aggregation and settling, the operation is called coagulation. However, when chemicals are added to precipitate dissolved substances out of solution, the operation is called chemical precipitation.

The basic equations governing sedimentation are the same for air and water and have already been discussed in some detail in Chapter 4.3. Here the discussion is limited to the various aspects of sedimentation tanks and basin design.

Gravitational sedimentation of a spherical particle in water is described by Stokes' equation for $N_{Rep} \leq 1$ and particle concentration smaller than ~2,500 mg per ℓ of suspended solids of density 1. In more concentrated suspensions, the sedimentation of one particle is hindered by its neighbors and the sedimentation velocity decreases.

For convenience of discussion, let us start by considering an ideal settling tank and then examine various deviations from ideal behavior. Following Hazen (1904) derivation, let us simplify the picture by assuming that the basin is divided into four parts: Inlet zone, settling zone, outlet zone and a bottom zone where the removed solids accumulate. The following simplifying assumptions are made:

1. Sedimentation takes place in the tank exactly as in a quiescent container of the same depth.

2. Flow in the tank is steady and the concentration of particles when entering the settling zone is uniform.

3. Particles settling to the bottom zone are not re-suspended.

Designating the volume of the settling zone by "V" and the liquid volume flow rate by "Q_L" then the average residence time is $\bar{t} = V/Q_L$. If the height of the settling zone is "h_s" then all the particles having a settling velocity $u_t > h_s\bar{t} = u_{to}$ will reach the bottom and be collected. If the concentration of the particles possessing a settling velocity $u_t \leq u_{to}$ is "c_o", then the proportion of these particles removed due to the fact that they start at a height $h < h_s$ is:

$$\frac{c}{c_o} = \frac{h}{h_s} = \frac{u_t}{u_{to}} \qquad (12.3\text{-}1)$$

For an ideal rectangular basin where the horizontal velocity is constant

$$u_{to} = \frac{h_s}{\bar{t}} = \frac{h_s\,Q_L}{V} = \frac{Q_L}{A} \qquad (12.3\text{-}2)$$

where "A" is the basin surface area. For a circular tank

$$-\frac{dh}{dr} = \frac{u_t}{u} = \frac{2\ \pi r\ h_s}{Q_L}\ u_t \qquad (12.3\text{-}3)$$

Integrating Equation 12.3-3 for particles that settle in the tank one gets

$$\frac{h}{h_s} = \frac{u_t\ \pi}{Q_L}(r_o^2 - r_i^2) = \frac{u_t\ A}{Q_L} \qquad (12.3\text{-}4)$$

where "r_i" is the radius of the inlet zone, "r_o" is the radius of the inlet plus settling zones, and "A" is the surface area of the tank. Substituting Equation 12.3-2 for a rectangular tank, or 12.3-6 for a circular tank, into Equation 12.3-1, one gets:

$$\frac{c}{c_o} = \frac{u_t}{(Q/A)} \qquad (12.3\text{-}5)$$

The settling velocity "u_t" in Equation 12.3-5 is a function of the particle size, shape and density, and will vary from one particle to another. Thus if one has a frequency distribution curve, of particle settling velocity vs. frequency, one can integrate equation 12.3-5 for all particles possessing a settling velocity $u_t < u_{to}$, add to it the fraction of particles possessing a settling velocity $u_t \geq u_{to}$ and obtain the fraction removed in an ideal settling tank.

Basin Characteristics

It is time now to examine some of the factors contributing to basin non-ideality, of which currents is one. Currents can be set up by the inertia of the incoming liquid, by temperature and density differences and by outside forces such as winds. Under disturbing currents, Fair et al. (1968) give the following equation, which better describes the efficiency of the settling basin

$$\frac{c}{c_o} = 1 - \left[1 + \frac{n\ u_{to}}{(Q_L/A)}\right]^{-\frac{1}{n}} \qquad (12.3\text{-}6)$$

where "n" is a coefficient describing the basin efficiency. The best possible performance is when n=0, and the basin performs poorly when n=1.

In an ideal basin displacement is steady and uniform, while all real basins suffer from short-circuiting to one degree or another. The extent of short-circuiting can be evaluated experimentally by injecting a tracer into the inlet and monitoring its concentration at the outlet. Modal, median and mean flowing-through periods, identify the central tendency of the time concentration distribution, since in the absence of short-circuiting they all coincide, their percentiles reflect its variance. Morrill (1932) suggested the ratio of the 10 percentile to the 90 percentile period as a parameter of the volumetric efficiency of a settling tank. If the time concentration curve does not reproduce itself reasonably well in repeated tests, flow through the tank is not stable and tank performance may be erratic.

An important consideration in the design of a settling tank is the prevention of bottom scouring. Fair et al. (1968) give for the scouring velocity of discrete particles, with density not close to one, the following equation:

$$u = \left[\frac{8\,a}{f}\, g \left(\frac{\rho_p}{\rho_L} - 1\right) d_p\right]^{1/2} \qquad (12.3\text{-}7)$$

thus the liquid displacement velocity should be smaller than "u". The limiting value for the ratio of length to height is then

$$\left(\frac{\ell}{h}\right)_{\text{lim.}} = \frac{u\, t_d}{u_{to}\, \bar{t}} \qquad (12.3\text{-}8)$$

Substituting for "u" from Equation 12.3-7 and for "u_{to}" from the general particle settling equation

$$\left(\frac{\ell}{h}\right)_{\text{lim.}} = \left(\frac{\bar{t}_d}{\bar{t}}\right) \left(\frac{6\,a}{f}\, C_D\right)^{1/2} \qquad (12.3\text{-}9)$$

where $(t_d/\bar{t}) = 1$ for ideal tank, a = 0.04 for unigranular sand and 0.06 or more for non-uniform sticky materials. "f" the friction factor, can be estimated from

$$f = 0.039\, N_{Re}^{-0.17} \qquad (12.3\text{-}10)$$

In conclusion, it should be mentioned that as in the case of aerosols, agglomeration can be enhanced by gentle stirring, thus increasing sedimentation rate. It is best to base the design of the settling tank on experimental results. However when the tank receives a suspension composed of discretely settling particles of known size and density, theoretical calculation will approach reality quite closely.

12.4 COAGULATION AND FLOCCULATION

12.4.1 COAGULATION

When colloidal particles come in contact and coalesce or adhere to one another, the process is called coagulation. In this paragraph we shall distinguish between chemical coagulation and flocculation, which is more of a "physical coagulation". Chemical coagulation is brought about by the addition of a chemical which decreases colloid stability and enmesh, or otherwise combine, with the colloid to form a rapidly settling floc. Flocculation occurs when the coagulation rate is increased by physical means, such as stirring or agitation (see Section 4.3.4.2 and 4.3.4.3). This is somewhat of an arbitrary classification, but it proves useful in visualizing matters. Coagulation and flocculation can thus be employed together, first adding the chemical, then a fast mixing to achieve good distribution, and finally slow stirring or agitation to enhance floc growth.

Stability of colloidal suspensions is attributed to the electric double layer formed at the interface between the aqueous and non-aqueous medium and to the creation of a diffuse layer in the aqueous phase. For a colloid to settle it has to grow in size, which is usually accomplished through the meeting and coalescence of several particles. When two colloidal particles with charges of the same sign approach one another, they are at first repulsed by the electrostatic force. However, at smaller distances attractive Van der Walls forces tend to draw the two particles together. To approach each other, the particles must surmount an energy hill. Only if the kinetic energy of the particles is large enough or the energy hill made small enough, can the colloid coagulate.

Chemical coagulants act in various ways to decrease colloid stability. Some neutralize the electric charge as predicted by the Schulze-Hardy rule, and some combine with the colloidal particles through hydrogen bridging, complex formation, and physical capture. Chemicals most often used are ferric and aluminum salts and polyelectrolytes. The latter are linear or branched chain polymers of small identical subunits which contain ionizable groups. The rate and efficiency of coagulation depend upon many variables; among them are the metal ion concentration, the pH of the medium, and the concentration of the colloidal substance. It is recommended to determine the type and optimum concentration of the chemical to be used through a "jar test". This test is described in many books on water and waste water treatment, e.g. Standard Methods for the Examination of Water and Wastewater (1970), Water Quality and Treatment (1971).

Coagulation can be improved by the addition of coagulant aids. These are substances that increase the critical mass of the colloids. Occasionally coagulant aids may reduce coagulant dosage by speeding the kinetics of the process.

12.4-2 FLOCCULATION

Flocculation, as defined earlier, is the stirring or agitation of wastewater containing flocs, aimed at increasing floc size and density. The stirring should always be gentle to prevent floc breakup. In chemical coagulation followed by flocculation, stirring or agitation may commence just as soon as the coagulating chemical has been added.

Flocculator performance depends on the substance to be removed, the additives introduced to promote removal, the detention time, the hydraulics of the flocculator and the useful power input. In most cases, when designing a new flocculator, it is best to check a flocculator already in operation and translate its operation mode to the specific problem at hand. Jar test data are also helpful in designing a flocculator.

Many commercial flocculator designs are available. In essence they all try to achieve fast mixing, a slow agitation and floc settling. As an example, consider an upflow clarification tank. A typical tank can be divided into four zones: sludge, inlet, flocculation and outlet. Inlet and sludge zones are in close contact. The flocculation zone which follows is occupied in part or as a whole by a cloud of floc. The hydraulic design of the upflow clarifier is aimed at achieving floc growth by increasing the useful power input, positioning of the flocculation zone surface and regulating the intensity of floc shear to prevent floc breakup. Hydraulic control is exerted by proper dissipation of hydraulic power and adjustment of residence time in the flocculation zone. Further discussion of flocculators can be found in Fair, Geyer and Okun book (1968), Water Quality Treatment (1971), Clark and Viessman (1965), and many others.

12.5 FILTRATION

Liquid solid separation by filtration can be accomplished either by solid accumulation in front of a filter medium, where a filter cake is built and stops the suspended particles, or by retention inside a deep porous bed - where the suspension flows through the porous medium in which the particles are retained. The second type is usually referred to as granular or deep filters; it is the one most used in water and wastewater treatment. However, we shall start with surface filtration or straining.

The conditions under which filtration is carried out are varied and the choice of the most suitable type of equipment will depend on a large number of factors. Whatever type of equipment is used for surface filtration, a filter cake gradually builds up on the medium and the resistance to flow increases progressively throughout the operation. Because the particles forming the filter cake are normally small and the rate of filtrate flow is low, streamline conditions are almost always obtained. The pressure drop through the cake is described by Kozeny equation, Coulson and Richardson (1955).

$$\frac{1}{A}\frac{dV}{dt} = \frac{\varepsilon^3 \ \Delta P}{5(1-\varepsilon)^2 \ a^2 \ \mu_L \ \ell} \qquad (12.5\text{-}1)$$

The quantity $r = \frac{5(1-\varepsilon)^2 \ a^2}{\varepsilon^3}$ is a property of the particles forming the cake and should be constant for a given material. One can distinguish between two cases: a) filtration at a constant rate. b) filtration at a constant pressure. For the first case

$$\frac{dV}{dt} = \frac{V}{t} = \text{constant} \qquad (12.5\text{-}2)$$

$$\frac{V}{t} = \frac{A \ \Delta P}{r \ \mu_L \ \ell} \qquad (12.5\text{-}3)$$

Let us now define "v" as the volume of cake deposited by the passage of unit volume of filtrate, then

$$\ell = \frac{v \ V}{A} \qquad (12.5\text{-}4)$$

Substituting Equation 12.5-4 into Equation 12.5-3 and rearranging gives

$$\frac{t}{V} = \frac{r \ \mu_L \ v}{A^2 \ \Delta P} V \qquad (12.5\text{-}5)$$

For constant pressure, substituting Equation 12.5-4 into Equation 12.5-1 and integrating yields

$$\frac{t}{v} = \frac{r \ \mu_L \ v}{2 \ A^2 \ \Delta P} V \qquad (12.5\text{-}6)$$

Following this line of reasoning equations can be derived for more complicated cases, such as: starting with constant volume filtration and changing to a constant pressure, considering pressure drop through the filter cloth, considering compressible cake, etc. A broader discussion of filtration can be found in many chemical engineering textbooks, like Coulson and Richardson (1955), Foust et al. (1960) and in Perry's Handbook.

In many cases, filtration efficiency is low at the beginning, until enough filter cake builds up. During this period unclear filtrate is recycled and filtered again. If the slurry is dilute and the solid particles settle readily in the fluid, it may be desirable to effect a preliminary concentration in a thickener. The thickened suspension is then fed from the thickener to the filter, and the quantity of material to be handled is thereby reduced.

The theoretical treatment shows that the nature of the filter cake has a very pronounced effect on the rate of flow of filtrate and that it is, in general, desirable that the particles forming the filter cake should have as large a size as possible. More rapid filtration is therefore obtained if a suitable agent is added to the slurry to cause coagulation. If the solid material is formed in a chemical reaction by precipitation, the particle size can generally be controlled to a certain extent by the conditions of formation.

Filter aids are extensively used where the filter cake is relatively impermeable to the flow of filtrate. Filter aids are materials which pack to form beds of very high voidages and therefore are capable of increasing the porosity of the filter cake, if added to the slurry before filtration. Apart from economic considerations, there is an engineering aspect leading to an optimum quantity of filter aid which should be added. Whereas the presence of the filter aid reduces the specific resistance of the filter cake, it also results in the formation of a thicker cake. The actual quantity used will therefore depend on the nature of the material. Filter cakes incorporating filter aid are usually very compressible and care should therefore be taken to ensure that the good effect of the filter aid is not destroyed by employing too high a filtration pressure. (Coulson and Richardson, 1955).

In granular filters, impurities are filtered all the way down to the last layer of active grains. When flowing through the porous medium, the particles are brought into contact with the available retention sites; they stop there or are carried away by the stream. The deep filtration is therefore the result of two major mechanisms: the contacting of particles with the retention sites and the fixing of particles on these sites. A set of three differential equations describe the filtration inside the porous bed. A simplified version of these equations (see Herzig et al., 1970) is:

$$\frac{\partial\sigma}{\partial t} = -u \frac{\partial c}{\partial Z} \qquad \text{local material balance} \qquad (12.5\text{-}7)$$

$$\frac{\partial c}{\partial Z} = -\lambda c \qquad \text{kinetic equation} \qquad (12.5\text{-}8)$$

$$\frac{\partial\sigma}{\partial Z} \qquad \frac{b}{u}\,\sigma \qquad (12.5\text{-}9)$$

In these equations, "σ" is the volume of deposited particles per unit filter volume, "u" is the suspension approach velocity, "c" is the volume fraction of particles in suspension, "λ" is the filtration coefficient and "b" is the clogging rate constant which is a function of "σ". Many expressions, most of them experimental or semi-experimental, can be found in the literature for "λ". Still in most cases it is best to determine "λ" experimentally for the operating conditions expected.

Pressure drop for this case can also be calculated from the Kozeny equation 12.5-1. In constant rate filtration, the pressure drop across the filter increases with clogging. Several models have been proposed but none of them adequately predicts the pressure drop. It is thus recommended to use the Kozeny equation for pressure drop estimation; exact pressure drop values should be determined experimentally.

12.6 NEUTRALIZATION AND CHEMICAL PRECIPITATION

In many cases, the gases scrubbed, or the particulate collected, are either basic or acidic. The scrubbing solution requires neutralization before it can be disposed of. Sometimes partial or full neutralization is accomplished in the scrubber, for reasons described in Chapters 4.2 and 5.2. In other cases partial or full neutralization is done outside the scrubber. A case in point is SO_2 scrubbing with lime, where the scrubbing solution enters the scrubber alkaline and leaves it acidic. Lime is then added in a special tank where precipitation of $CaSO_3$ and $CaSO_4$ takes place.

Acid wastes are undesired in wastewater conduits as well as in streams. Lime (CaO) is normally the cheapest available acid-neutralizing substance, but calcareous and dolomitic limestone may perform satisfactorily in preliminary reactions. Soda ash (Na_2CO_3) is a more expensive, but often a more convenient neutralizer than lime, since required equipment can be kept simple. The equipment includes weighing and mixing devices for adding and dissolving calculated quantities of alkaline chemicals, provides sufficient contact time for reactions to be completed, hasten slow reactions by hydraulic or mechanical stirring, and exercise control over the process by measuring the pH of the effluent. Alkaline wastewaters may also have to be neutralized. They are normally treated with sulfuric acid. Within a given plant, waste acids and waste alkalis can be conjoined for neutralization. However, one or the other may be present in excess, and reaction times may be long. The final pH must lie within a range acceptable to the receiving stream. Some industrial wastewaters may have to be treated with much acid or alkali.

We can not go into too much detail here, because neutralization depends upon the specifics of the process and the results sought. It would be best to refer to such books as Water and Wastewater Treatment by Fair, Geyer and Okun (1968), Degremont - Water Treatment Handbook (1965), Industrial Water Pollution Control by Eckenfelder (1966), "Theories and Practices of Industrial Waste Treatment" by Nemerow (1963) and many others.

Precipitation is the opposite of dissolution. Understandably therefore, precipitation can often be based on the low of mass action and available equilibrium constants. However, conformance of this kind does not necessarily assure either stoichiometric completion of the precipitation reaction or the adequacy of added stoichiometric amounts. Amounts greater than calculated from equilibrium constants and the thermodynamic considerations may have to be called upon to attain wanted performance because of supersaturation or kinetic considerations. As a rule, precipitants should be chosen from among: chemicals normally occurring in natural waters, relatively insoluble and safe that do not produce toxic residues. Most multivalent cations in water can be precipitated in predictable amounts as carbonates or hydroxides. Carbonates and phosphates, on the other hand, can be precipitated in predictable amounts as salts of calcium, iron or aluminum.

Quantitative evaluation of the systemic relations determining the equilibrium concentrations of a solution is subject to exact and systematic treatment without a priori assumptions. A convenient schedule comprises (1) enumeration of all the chemical species that will exist in the solution at equilibrium; (2) establishment of the various reaction equilibria; and (3) selection of the equilibrium constants that identify the equilibrium concentrations of the solute components. For precise calculations, values for temperatures other than the normal reference temperature of 25°C must be employed. For "n" unknowns (i.e. "n" species), "n" equations are needed to define the problem. Required information generally comprises the necessary mass-law relationships and two equations describing the constitution of the solution; equations describing a concentration and an electroneutrality condition are examples.

In many cases chemical precipitation is but one stage in the removal process. Coagulation and sedimentation or filtration codetermine the overall removal rate, or the efficiency of removal of these constituents. Again the reader is referred to the references given above for further discussion, data and worked up examples of chemical precipitation.

12.7 ION EXCHANGE

Ion exchange is the reversible interchange of ions between a solid ion exchange medium and a liquid solution. Ion exchange fosters the concentration, isolation and recovery of ionic materials from dilute solutions. In industry, both cation and anion exchangers are employed to deionize or demineralize process water, reduce quantity and strength of wastewaters and reclaim byproducts which are worth reclaiming. For example, cation exchangers can recover and concentrate copper, zinc, and chromic acid from dilute solutions, anion exchange resins can concentrate cyanide and fatty acids, and ion exchange can play an important role in decontamination of radioactive wastes.

To be effective, solid ion exchangers must contain ions of their own, be insoluble in water and provide enough space in their porous structure for ions to pass freely in and out of the solid. Cation exchangers have a negatively charged framework, but their pores contain cations that maintain electroneutrality. Anion exchangers carry just the opposite electrical charges.

Synthetic ion exchange resins act as a large many-charged ions arranged in a three dimensional network. The charges of the polymeric ion are neutralized by small ions of opposite charge within the network, where they are held in place by electrostatic forces without being bound to the ion exchange matrix. Thus they are able to change places with ions in solution.

The exchange capacity of an ion exchanger is expressed by the number of equivalents of ions necessary to maintain electroneutrality within the solid phase, for a given weight or volume of ion exchange material. The exchange capacity is determined by "titrating" all the exchangeable ions.

The design of ion exchange processes is based on a knowledge of ion exchange equilibria, or "selectivity coefficients" which governs the distribution of ions between an aqueous phase and the ion exchange phase. The selectivity coefficients provide a semi-quantitative interpretation of the ion exchange equilibrium and characterize the relative selectivities of an ion exchanger for specific ions. In the exchange of monovalent ions by other monovalent ions, the selectivity coefficients are close to unity, while for the displacement of monovalent by bivalent ions it reaches 20 - 40. Thus dilute Ca^{++} solution in contact with a Na^+ cation exchanger will replace practically all of the Na^+. While for regeneration, i.e. replacing the Ca^{++} by Na^+, concentrated solutions of Na^+ are required. Exchange reactions are generally slower than electrolyte reactions and are diffusion controlled.

Ion exchange is usually done in cylindrical containers with the treated solution flowing down the column. If the concentration of the exchangeable ion in the solution leaving the exchanger is plotted vs. quantity treated, the curve rises from zero at the point where some of the removed ion penetrates the column, this point is defined as the breakthrough point. The area enclosed by the breakthrough curve is a measure of the total exchange capacity of the bed. The breakthrough capacity is influenced by exchanger particle size, column dimensions, flow rate, temperature and solution composition.

The breakthrough curve usually deteriorates with time due to air pockets, deposits of colloidal substances and fouling of the organic ion exchange material.

More information on ion exchange can be found in: Kunin (1958); Kunin (1960); Treybal (1955); Fair, Geyer and Okun (1968; and Degrimont Handbook (1965).

12.8 DESALTING

The increase in total dissolved salts of the scrubbing water due to partial evaporation and collection of salt particles, is a problem faced by scrubber operators mainly in semi-arid regions, where increased salt concentration in the aquifers is of growing concern. In these cases and where partial or full desalting is advantageous, attention should be paid to the various desalting techniques now available. In the last section ion exchange, which can be employed for preferential removal of certain cations or anions, or to achieve complete demineralization, has been discussed. Here several of the other desalting methods will be described in short.

Electrodialysis

Electrodialysis involves removing the inorganic ions from water by impressing an electrical potential across the water, resulting in the migration of cations and anions to the cathode and anode, respectively. By alternately placing anionic and cationic permeable membranes a series of concentrating and diluting compartments result. The amount of electric current required for the demineralization is proportional to the number of ions removed from the diluting compartments. To minimize membrane fouling and maintain long runs, it is essential that turbidity suspended solids, colloids, and trace organics be removed prior to the electrodialysis cell. Large organic ions and colloids are attracted to the membranes by electrical forces and result in fouling of the membranes. This results in an increase in electrical resistance which, at constant stack voltage, decreases the current and hence the demineralizing capacity of the equipment. Turbidity in the feed has a major effect on membrane fouling. Conventional methods of coagulation, filtration, and adsorption would be employed to decrease turbidity.

Reverse Osmosis

Reverse osmosis can be employed for the removal or concentration and recovery of ions such as chromate and phosphates and for the selective rejection of organic compounds. In reverse osmosis, water containing dissolved materials is placed in contact with a suitable membrane at a pressure in excess of the osmotic pressure of the solution. Under these conditions water with a small amount of dissolved material permeates the membrane and the dissolved materials are concentrated. The membranes are a specially prepared cellulose acetate.

High concentrations of soluble material can cause a scale, and suspended solids can form a fouling layer. This is reduced by moving water past the membrane surface at a velocity sufficient to cause turbulence. The area of transfer is significant. DuPont has employed hollow fibers in a size range of 25 to 250 μ as the membrane media. Treatment units 30.5 cm by 2.13 m (12 in by 7 ft) will contain 15 to 80 million hollow fibers with surface areas of 4,650 to 7,440 m^2 (50,000 to 80,000 ft^2). Acidification of the feed may be necessary to prevent calcium carbonate scale formation. Total dissolved salt removal of 95% with substantial removals of COD, phosphate and ammonia have been reported.

Distillation

Removal of the water by distillation, concurrently increasing the salt concentration, is the oldest desalting process and is now the most widely used for sea water desalting. In this process the efficiency of energy production and utilization is the controlling factor. Hence plant design is directed to tapping the most economic sources of heat energy and to exploiting the most efficient process of heat transfer.

Three types of evaporators are most widely used. These are: the multiple effect evaporator, multistage flash evaporator, and vapor compression still. For an adequate description of the processes, equipment and cost, the reader is referred to the various publications of the Office of Saline Water.

Freezing

Water can be desalted by freezing, since the ice crystals, due to their crystalline structure, will reject the salt ions. However, even though the ice crystals formed are essentially pure water, the yield of product water is decreased because some of it must be used to wash salt from the ice surfaces. There are many variations to the freezing processes and again the reader is referred to the many publications of the Office of Saline Water for further information.

12.9 DISPOSAL OF LIQUID

In most cases, the best method of liquid disposal is recycle to plant or to the scrubber. However, if the contaminant removed in the scrubber is not of value so that the scrubbed solution is not recycled to the process, it will call for some kind of treatment to bring the liquid to a workable degree of purity. Recycling for further scrubber use is a preferred method of liquid disposal and is used especially in areas where water is scarce and relatively expensive.

In general, one can count five methods of liquid disposal on top of recycling. These are: 1. Disposal into receiving waters, like rivers, lakes or sea. 2. Disposal into an aquifer either by spreading or injecting directly into the aquifer. 3. Disposal into a pond which accomplishes further treatment or evaporates the liquid. 4. Disposal into the company or city sewer. 5. Permanent storage.

In the following each one of these methods will be discussed briefly. For more detailed information the reader is referred to the bibliography. The choice between the various disposal methods will depend upon economic considerations, the geography and climate of the area, and upon state or federal water pollution control regulations.

Disposal into a body of receiving water is now controlled by state agencies which determine the quality of the effluent. In some cases, where the plant is located near a large body of water it may still be economical to pump the water, use it once through and dispose of it. However, such places are getting more and more scarce. In most cases, disposal is done after treatment in compliance with state quality criteria and utilizing outlets which enhance dispersion of the effluent in the receiving waters.

Disposal into an aquifer is usually done by spreading the water over infiltration ponds. The ground soil has some purification power, however this power varies with the soil's physical and chemical properties. Much research work is now being done in this field, however the stage has not yet been reached where positive and definite predictions of soil purifying power and holding capacity can be made. It is for this reason that water quality control agencies usually do not view this method favorably, though it is used quite extensively. Another variation that has been in use during the last decade, is the injection of liquid effluent into confined salty aquifers. Here again more and more questions are being raised with regard to the final fate of the injected effluent. The use of this method depends upon the availability of the right aquifer in the neighborhood.

Disposal by ponding may mean either final disposal into a sealed pond from where the water evaporates, or use of the pond as a treatment step. Ponds may achieve various degrees of treatment and accordingly a wide variety of ponds are discussed in the literature. The simplest treatment is settling which was discussed earlier. During a long stay, a microbial and algae population usually develop in the pond. The kind of population depends on the nutrients entering the pond. While the bacteria decomposes the more complex compounds, the algae consume nitrates, phosphates, CO_2, and other simple compounds, generate oxygen and increase the pH. In sunny weather the high pH causes the precipitation of heavy metal ions, provided they do not poison the population. At the same time, the long stay of the effluent in the pond brings about stripping of gases which are in excess and dissolution of gases which are present at a high partial pressure in the atmosphere. Thus the effluent coming out of the pond may be suitable for recycle or final disposal into an aquifer or a stream.

There is a price tagged to the disposal into the company or city sewer. Many cities are converting now to charges based on quantity and quality of the effluent discharged into the city sewer. However, in many cases the mere fact of the larger scale of treatment plants, make these methods attractive. One should always remember that most cities would not accept effluent which is harmful to their biological treatment plant, thus a pretreatment at the plant site may be required.

Disposal by permanent storage is the method most commonly used for radioactive and highly toxic materials. In this case the liquid effluent is usually first concentrated by means of evaporation, extraction, or other methods, and later stored in closed containers and put in a safe storage place.

For further information on liquid disposal, also see Fair, Geyer and Okun (1968); Escritt (1956); Klein (1959-66); Pearson (1960); Eckenfelder (1966) and Amphlett (1961).

12.10 DISPOSAL OF SOLIDS

Sludge may be disposed of in any one of the states in which it is produced, i.e. wet, partially dewatered, or granular. Waste slurries and sludges are normally deposited on land or discharged into the sea. Only rarely are they introduced into flowing streams or standing bodies of fresh water. Stable industrial slurries can be mounded on close-by cheap land. Putrescible or other noxious wastes must be buried or covered with earth, as in sanitary land fills. The danger of soluble components leaching from them into surface streams or underground aquifers must not be overlooked.

For most convenient handling and conservation of space, waste solids may be dewatered. Combustion destroys putresible solids and further simplifies disposal. Objectionable features of disposal on land are odorous and dusty dumps, marshes of non-drying sludge and potential harm to persons or to animals by corrosive contact or toxicity.

For the engineering aspects of sludge, characteristics, texture, movement, concentration, digestion, etc., the reader is referred to the reference list at the end of this chapter.

12.11 ECONOMICS

Cost of scrubber effluent treatment and disposal depends on many factors such as: the kind and degree of treatment required, the size of the treatment plant, the corrosivity of the effluent, the method of disposal for the liquid and solid and on the need and availability of land and manpower. It is always advisable to compare treatment and disposal costs with the alternative of disposing of the effluent through the city sewer. Maystre and Geyer (1970) surveyed 221 cities in the U.S. for the charge they levy on industrial sewage and tabulated their findings.

Figures 12-1 to 12-6 after Eckenfelder (1970) show the costs in 1967 prices of the following unit operations: equalization basins, neutralization facilities, oil separators, primary clarifiers, lagoons, aerated lagoons and vacuum filters. To get present day capital cost one should sum the costs of the individual unit operations which make up the chosen treatment process. Then use either the ENR Construction Cost Index or the Federal Water Pollution Control Administration Cost Index to convert the capital cost to todays prices. The capital cost computed this way should be increased by 30 to 35 percent to compensate for contractor's profit, contingencies, omissions, miscellaneous, piping, land acquisition and engineering.

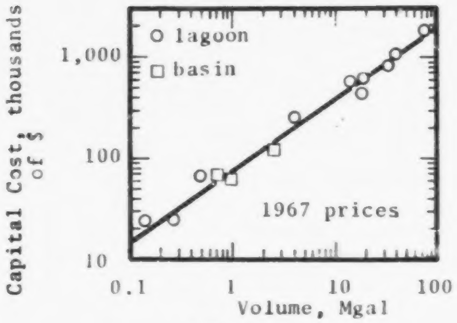

FIGURE 12-1

COST VS. VOLUME OF AERATED LAGOONS AND EQUALIZATION BASINS
ECKENFELDER (1970)

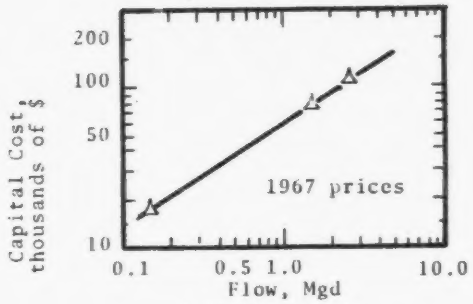

FIGURE 12-2

CAPITAL-COST RELATIONSHIP, NEUTRALIZATION FACILITIES
ECKENFELDER (1970)

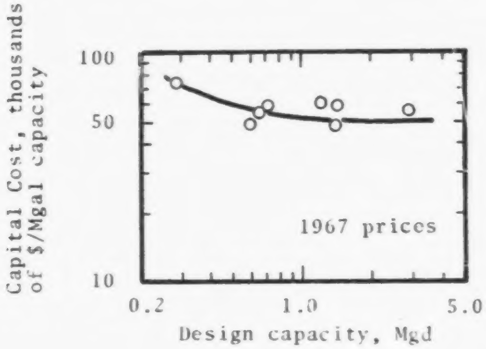

FIGURE 12-3

CAPITAL-COST RELATIONSHIP OIL SEPARATORS
ECKENFELDER (1970)

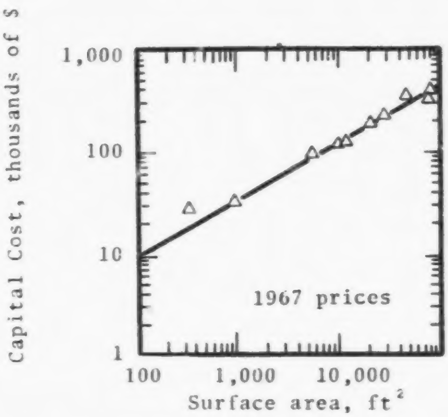

FIGURE 12-4

COST VS. SURFACE AREA, PRIMARY CLARIFIER
ECKENFELDER (1970)

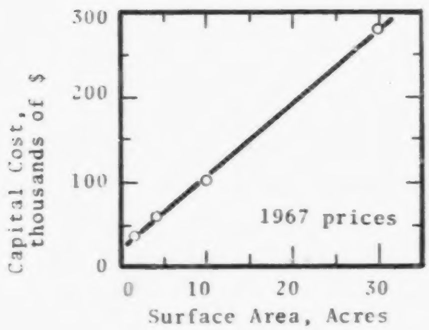

FIGURE 12-5

CAPITAL-COST RELATIONSHIP FOR LAGOONS
ECKENFELDER (1970)

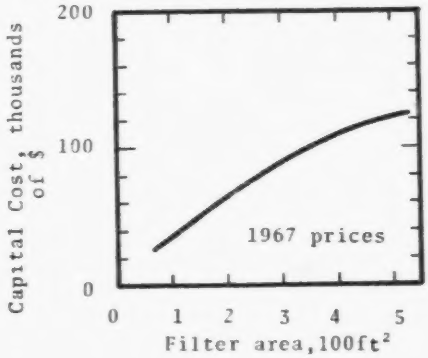

FIGURE 12-6

CAPITAL-COST RELATIONSHIP, VACUUM FILTERS.

ECKENFELDER (1970)

NOMENCLATURE - CHAPTER 12

LATIN

a, b = constants

a = specific surface, cm^{-1}

A = area, cm^2 or m^2

c = particle mass concentration, g/cm^3 or kg/m^3

C_D = drag coefficient

d = diameter (must be subscripted), cm or m

f = friction factor, see Equation 12.3-10

g = acceleration of gravity, 980.7 cm/sec^2

h = height, cm or m

ℓ = length, cm or m

N_{Re} = Reynolds number, $(d\ u\ \rho_G)/(\mu_G)$ (must be subscripted)

ΔP = pressure drop, dyn/cm^2

Q_L = liquid volume flow, cm^3/sec or m^3/sec

r = radial distance (with subscript for particle or collector) cm or m

t = time, sec

u = velocity along x axis, cm/sec or m/sec

v = volume of cake deposited by the passage of unit volume of filtrate, cm^3 or m^3

V = volume, cm^3 or m^3

Z = distance in z direction, cm or m

GREEK

ε = fraction void volume space

λ = filtration coefficient

μ = viscosity (must be subscripted), poise

ρ = density (must be subscripted) kg/m^3; g/cm^3

ρ_p = particle density, g/cm^3 or kg/m^3

σ = volume of deposited particles per unit filter volume

SUBSCRIPTS

L = liquid phase

p = particle

s = settling zone

t = terminal velocity

CHAPTER 12 - REFERENCES

Amphlett, C.B., "Treatment and Disposal of Radioactive Wastes", Pergamon, New York (1961).

Besselievre, E.B., "Industrial Waste Treatment", McGraw Hill Book Co., New York (1952).

Clark, J.W., Viessman, W., Jr., "Water Supply and Pollution Control", International Textbook Company, Scranton, Pennsylvania (1965).

Coulson, J.M., Richardson, J.F., "Chemical Engineering", McGraw-Hill Book Co., New York (1955).

Degrémont, "Water Treatment Handbook", 3rd ed., H. K. Elliott, London (1965).

Eckenfelder, W.W., Jr., "International Water Pollution Control", McGraw-Hill Book Co., New York (1966).

Eckenfelder, W.W., Jr., "Water Quality Engineering", Barnes and Nobel, Inc., New York (1967).

Escritt,L.B., "Sewerage and Sewage Disposal", Contractor's Record, London (1956).

Fair, G.M., Geyer, J.C., Okun, D.A., "Water and Wastewater Engineering", Vol. 2, John Wiley and Sons, New York (1968).

Faust, A.S., Wenzel, L.A., Clumb, C.W., Maus, L., Anderson, L.B., "Principles of Unit Operations", Wiley, New York (1960).

Gurnham, C. F., ed., "Industrial Wastewater Control", Vol. 2, Academic Press, New York (1965).

Hazen, A., Trans. Am. Soc. Civil Eng. 53, 63 (1904).

Herzig, J. P., Leclerc, D.M., LeFogg, P., Ind. & Eng. Chem. 62, 8-35 (1970).

Klein, L., "River Pollution", 3 vols., Butterworths, London (1959-66).

Kunin, R., "Ion Exchange Resins", 2nd ed., Wiley, New York (1958).

Kunin, R., "Elements of Ion Exchange", Reinhold, New York (1960).

McKee, J.E., Wolf, H.W., "Water Quality Criteria", State Water Quality Control Board, Resources Agency of California, Sacramento (1963).

Maystre, Y., Geyer, J.C., Journal W.P.C.F., Vol. 42, 1277-1291 (1970).

Morrill, A.B., J.A.W.W.A. 24, 1442 (1932).

CHAPTER 12 - REFERENCES

Nemerow, N.L., "Theories and Practices of Industrial Waste Treatment", Addison-Wesley, Reading, Mass. (1963).

Pearson, E.A., ed., "Waste Disposal in the Marine Environment", Pergamon, New York (1960).

Perry, R. H., Ed., "Chemical Engineers Handbook", 4th ed., McGraw-Hill Book Co., New York (1963).

Rich, L.G., "Unit Operations of Sanitary Engineering", Wiley, New York (1961).

Salle, A.J., "Fundamental Principals of Bacteriology", McGraw-Hill, Book Co., New York (1961).

Sawyer, C.N., "Chemistry for Sanitary Engineers", McGraw-Hill Book Co., New York (1960).

"Standard Methods for the Examination of Water and Wastewater", 13th ed., American Public Health Association (1970).

"The Economics of Clean Water", Vol. 1, F.W.P.C.A., U.S. Department of the Interior (1970).

Treybal, R.E., "Mass Transfer Operations", McGraw-Hill, New York (1955).

"Water Quality and Treatment", American Water Works Association, 3rd ed., McGraw Hill Book Co., New York (1971).

CONVERSION FACTORS

To Go From	To	Multiply by
atmospheres	centimeters H_2O	1,033
atmospheres	dyne/square cm	1.01×10^6
atmospheres	inches H_2O	406.8
atmospheres	pounds/square inch	14.7
centimeters	inches	0.394
centimeters	feet	0.0328
centimeters	microns	10^4
centimeters/second	feet/minute	1.97
cubic centimeters	cubic inches	0.0610
cubic centimeters	cubic feet	3.53×10^{-5}
cubic centimeters/second	cubic feet/minute	0.00212
cubic centimeters/second	gallons/minute	0.01585
cubic feet	cubic centimeters	28,317
cubic feet	cubic meters	0.0283
cubic feet/minute	cubic centimeter/second	472
cubic feet/minute	cubic meter/hour	1.7
cubic meter	gallon	264
cubic meter	cubic feet	35.3
cubic meter/cubic meter	gallons/1,000 cubic feet	7,550
cubic meter/hour	cubic feet/minute	0.59
cubic meter/hour	gallons/minute	4.4
dyne	gram cm/sec^2	1
dyne/square centimeter	atmospheres	9.87×10^{-7}
dyne/square centimeter	centimeter H_2O	0.00102

CONVERSION FACTORS (cont'd)

To Go From	To	Multiply by
dyne/square centimeter	inches H_2O	$4.015x10^{-4}$
dyne/square centimeter	gram/square centimeter	$1.02x10^{-3}$
dyne/square centimeter	pounds/square inch	$1.45x10^{-5}$
foot	centimeter	30.48
foot	meter	0.3048
foot/minute	centimeter/second	0.508
gallons	cubic meter	$3.78x10^{-3}$
gallons/minute	cubic meter/hour	0.227
gallons/1,000 cubic feet	cubic meter/cubic meter	$1.33x10^{-4}$
gallons/1,000 cubic feet	liter/cubic meter	0.133
grain	pound	$1.43x10^{-4}$
grain	gram	0.0648
grain/cubic foot	gram/cubic meter	2.29
gram	grain	15.4
gram	pound	$2.2x10^{-3}$
gram/cubic meter	grain/cubic foot	0.437
inch	centimeter	2.54
inches H_2O	atmosphere	0.00246
inches H_2O	dynes/square centimeter	2,491
inches H_2O	pounds/square inch	0.0361
micron	centimeter	10^{-4}
micron	foot	$3.28x10^{-6}$
meter	foot	3.28
milligrams/cubic foot	grams/cubic meter	$3.53x10^{-2}$
milligrams/cubic meter	grains/cubic foot	$4.37x10^{-4}$

CONVERSION FACTORS (cont'd)

To Go From	To	Multiply by
pounds	grams	454
pounds/square inch	atmospheres	0.068
pounds/square inch	centimeters H_2O	70.3
pounds/square inch	dynes/square centimeter	6.89×10^4
pounds/square inch	inches H_2O	27.68
pounds/ton	grams/kilogram	0.5
lb/1000 lb gas at 273°K	grams/cubic meter	1.38
square centimeter	square inch	0.155
square inch	square centimeter	6.45
square foot	square centimeter	929

All gallons are U.S. liquid gallons.